frontiers
RESEARCH TOPICS

INTERVAL TIMING AND TIME-BASED DECISION MAKING

Hosted by
Warren H. Meck, Valerie Doyere
and Agnes Gruart

frontiers in
INTEGRATIVE NEUROSCIENCE

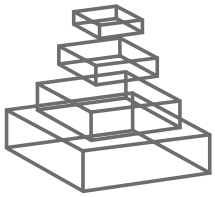

frontiers

Cover image provided by Ibbl sarl, Lausanne CH

ISSN 1664-8714
ISBN 978-2-88919-034-8
DOI 10.3389/978-2-88919-034-8

ABOUT FRONTIERS

Frontiers is more than just an open-access publisher of scholarly articles: it is a pioneering approach to the world of academia, radically improving the way scholarly research is managed. The grand vision of Frontiers is a world where all people have an equal opportunity to seek, share and generate knowledge. Frontiers provides immediate and permanent online open access to all its publications, but this alone is not enough to realize our grand goals.

FRONTIERS JOURNAL SERIES

The Frontiers Journal Series is a multi-tier and interdisciplinary set of open-access, online journals, promising a paradigm shift from the current review, selection and dissemination processes in academic publishing.
All Frontiers journals are driven by researchers for researchers; therefore, they constitute a service to the scholarly community. At the same time, the Frontiers Journal Series operates on a revolutionary invention, the tiered publishing system, initially addressing specific communities of scholars, and gradually climbing up to broader public understanding, thus serving the interests of the lay society, too.

DEDICATION TO QUALITY

Each Frontiers article is a landmark of the highest quality, thanks to genuinely collaborative interactions between authors and review editors, who include some of the world's best academicians. Research must be certified by peers before entering a stream of knowledge that may eventually reach the public - and shape society; therefore, Frontiers only applies the most rigorous and unbiased reviews.
Frontiers revolutionizes research publishing by freely delivering the most outstanding research, evaluated with no bias from both the academic and social point of view.
By applying the most advanced information technologies, Frontiers is catapulting scholarly publishing into a new generation.

WHAT ARE FRONTIERS RESEARCH TOPICS?

Frontiers Research Topics are very popular trademarks of the Frontiers Journals Series: they are collections of at least ten articles, all centered on a particular subject. With their unique mix of varied contributions from Original Research to Review Articles, Frontiers Research Topics unify the most influential researchers, the latest key findings and historical advances in a hot research area!
Find out more on how to host your own Frontiers Research Topic or contribute to one as an author by contacting the Frontiers Editorial Office: researchtopics@frontiersin.org

INTERVAL TIMING AND TIME-BASED DECISION MAKING

Hosted By
Warren H. Meck, Duke University, USA
Valerie Doyere, CNRS, France
Agnes Gruart, University Pablo de Olavide, Seville, Spain

Artwork kindly provided by Sarah Le Ridou and Glenn Dallérac

The perception of time is crucial for everyday activities from the sleep–wake cycle to playing and appreciating music, verbal communication, to the determination of the value of a particular behavior. With regard to the last point, making decisions is heavily influenced by the duration of the various options, the duration of the expected delays for receiving the options, and the time constraints for making a choice. Recent advances suggest that the brain represents time in a distributed manner and reflects time as a result of temporal changes in network states and/or by the coincidence detection of the phase of different neural populations. Moreover, intrinsic oscillatory properties of neural circuits could determine timed motor responses. This Research Topic, partly an emergence of a Satellite EBBS meeting sponsored by the COST-Action TIMELY, will discuss how time in the physical world is reconstructed, distorted and modified in brain networks by emotion, learning and neuropathology. This Research Topic on Timing contains up-to-date reviews regarding the relationship between time and decision-making with respect to the underlying psychological and physiological mechanisms responsible for anticipation and evaluation processes.

Table of Contents

frontiers in
INTEGRATIVE NEUROSCIENCE

EDITORIAL
published: 30 March 2012
doi: 10.3389/fnint.2012.00013

Interval timing and time-based decision making

Warren H. Meck[1], Valérie Doyère[2] and Agnès Gruart[3]*

[1] *Duke University, Durham, NC, USA*
[2] *CNRS, Université Paris-Sud, Orsay, France*
[3] *University Pablo de Olavide, Seville, Spain*
**Correspondence: agrumas@upo.es*

The importance of time perception and timed performance is revealed in everyday activities from the sleep–wake cycle to verbal communication, playing, and appreciating music, the exquisite temporal control of both voluntary and involuntary behavior, and choice. With regard to the last point, making decisions is heavily influenced by the duration of the various options, the duration of the expected delays for receiving the options, and the time constraints for making a choice. Recent advances suggest that the brain represents time in a distributed manner and reflects time as a result of temporal changes in network states and/or by the coincidence detection of the phase of different neural populations. Moreover, the oscillatory properties of neural circuits can be shown to influence the acquisition of conditioned responding and the timing of motor responses. This Research Topic on "*Interval Timing and Time-Based Decision Making*" emerged from a symposium sponsored by the European COST-Action on Time In MEntaL activity: theoretical, behavioral, bioimaging, and clinical perspectives (TIMELY) that was a satellite of the European Brain and Behaviour Society meeting held in Seville, Spain (September 9, 2011). The focus of that TIMELY symposium was on "Neurobiology of Time Perception: From Normality to Dysfunction" and was organized by Valérie Doyère, Argiro Vatakis, and Elzbieta Szelag. The current volume contains 58 state-of-the-art original research, opinion, and review articles exploring the relationships between time and decision making with respect to the underlying psychological and biological mechanisms. The overall goal is to examine how time in the physical world is reconstructed, distorted, and modified in brain networks by emotion, learning, and neuropathology.

The contributions to the Research Topic have been divided by the co-editors into nine main categories in order to organize the breadth of coverage, from animal to human research. These categories were selected based upon research strategy and experimental techniques, and include the following:

(1) Perception, representation, and categorization
(2) Emotional distortions
(3) Decision making and learning
(4) Development of timing and counting
(5) Neuroimaging and pathophysiology
(6) Temporal conditioning and neurophysiology
(7) EEG/ERP analyses and the role of the supplementary motor area
(8) Molecular, neuropharmacological, and neuroendocrine mechanisms
(9) Neural-network models

As papers often may belong to more than a single category, we apologize if some authors feel they have been "misplaced," but we tried to maintain equilibrium among the different categories without being unfaithful to the authors' main message.

It has been a great pleasure to be involved in this Research Topic as much progress has been made in exploring the temporal horizons of the mind and brain in the past few years. Much more work needs to be done and many issues remain to be addressed before we fully understand the functional and neural mechanisms of interval timing. We would like to thank all of the authors, reviewers, and Frontiers staff for helping to make this Research Topic possible and we look forward to further explorations of interval timing and time-based decision making.

Received: 14 March 2012; accepted: 14 March 2012; published online: 30 March 2012.
Citation: Meck WH, Doyère V and Gruart A (2012) Interval timing and time-based decision making. Front. Integr. Neurosci. ***6****:13. doi: 10.3389/fnint.2012.00013*

frontiers in
INTEGRATIVE NEUROSCIENCE

REVIEW ARTICLE
published: 18 October 2011
doi: 10.3389/fnint.2011.00066

Moments in time

Marc Wittmann*

Department of Empirical and Analytical Psychophysics, Institute for Frontier Areas in Psychology and Mental Health, Freiburg, Germany

Edited by:
Valerie Doyere, Centre National de la Recherche Scientifique, France

Reviewed by:
Valtteri Arstila, University of Turku, Finland
Bruno Mölder, University of Tartu, Estonia

****Correspondence:***
Marc Wittmann, Institute for Frontier Areas in Psychology and Mental Health, Wilhelmstr. 3a, 79098 Freiburg, Germany.
e-mail: wittmann@igpp.de

It has been suggested that perception and action can be understood as evolving in temporal epochs or sequential processing units. Successive events are fused into units forming a unitary experience or "psychological present." Studies have identified several temporal integration levels on different time scales which are fundamental for our understanding of behavior and subjective experience. In recent literature concerning the philosophy and neuroscience of consciousness these separate temporal processing levels are not always precisely distinguished. Therefore, empirical evidence from psychophysics and neuropsychology on these distinct temporal processing levels is presented and discussed within philosophical conceptualizations of time experience. On an elementary level, one can identify a *functional moment*, a basic temporal building block of perception in the range of milliseconds that defines simultaneity and succession. Below a certain threshold temporal order is not perceived, individual events are processed as co-temporal. On a second level, an *experienced moment*, which is based on temporal integration of up to a few seconds, has been reported in many qualitatively different experiments in perception and action. It has been suggested that this segmental processing mechanism creates temporal windows that provide a logistical basis for conscious representation and the experience of *nowness*. On a third level of integration, continuity of experience is enabled by working memory in the range of multiple seconds allowing the maintenance of cognitive operations and emotional feelings, leading to *mental presence*, a temporal window of an individual's experienced presence.

Keywords: temporal integration, time perception, the present, psychophysics

The contents of consciousness are phenomenally present – now. This temporal aspect of phenomenal consciousness – its *nowness* – is inherent in all our experiences: I see, hear, feel, and think at the present moment (Metzinger, 2004; Droege, 2009). What is experienced is experienced *now*. Conscious experience is not static and unchanging; the passage of time is often described by a stream or a flow. Phenomenological analysis has pointed to these two complementary (or seemingly paradoxical) aspects of experience: the feeling of a present moment and the passage of time (James, 1890, chapter XIV; Husserl, 1928). The unity of the present is related to our sense of *nowness*. The experience of the passage of time constitutes itself through an event that is first anticipated, then experienced and eventually remembered. Taken together, phenomenal consciousness consists of an island of presence in the continuous flow of time related to what is happening right now (Metzinger, 2004).

A debate exists in the philosophical literature surrounding a presumed puzzle of how it is possible to have a temporal experience, to perceive duration, when our experiences are confined to the present moment. If perception is really limited to a present moment then we cannot perceive motion, change, the passage of time (Le Poidevin, 2007). This puzzle is based on the assumption that an observer perceives static snapshots of the world that somehow have to be integrated to form unified experiences over time (Kelly, 2005). A present moment, in this line of thought, is like a mathematical point on a continuum, an isolated and duration-less instant in time. Accordingly, distinct and duration-less present moments of experience have to be connected to create phenomenal continuity over time, this conception of time essentially being a cinematographic metaphor. An alternative account of how we perceive change and succession, the flow of time, is that our experiences actually possess inherent temporal properties, i.e., we experience whole intervals in time (Kiverstein, 2010); succession, rhythmic grouping and motion can be directly perceived as constituents of present experience (Stern, 1897). Our momentary experience is embedded in a temporal field reaching both into the past and into the future (Stern, 1897; Lloyd, 2004, 2011). Present experience contains traces of what has just happened and what is anticipated, or in Husserl (1928) terms, the tripartite structure of present experience involves *retention*, *impression*, and *protention*. The perceived present represents its history and possible future, this tripartite structure being an implicit aspect of any conscious experience (Lloyd, 2004, 2011). According to this conception, our present experience is characterized as stretched across time. In different terms, the present moment – as the "specious present" – has duration (James, 1890, chapter XIV). Various conceptualizations have been put forward concerning the experience of an extended present moment. The "retentionalist" view assumes that the contents of momentary experience, although the moment itself is without extension, represent temporally extended intervals; the "extensionalist" position assumes that experiences themselves are defined by temporally extended "chunks." These models are not

discussed here, but a thorough comparison of the intricate details can be found in Dainton (2010).

The philosophical debate concerning the present moment is mirrored by empirical research in psychology and the neurosciences on the issue of temporal integration of events that constitutes the "psychological present." In fact, recent philosophical contributions refer to the neuroscientific literature of how the brain might integrate events over time; by interpreting empirical findings tentative estimates of characteristic times are provided that are supposed to underlie the experience of the present moment (Pockett, 2003; Kelly, 2005; Callender, 2008; Droege, 2009; Dainton, 2010). The goal of this article is to provide a systematic overview of empirical findings in psychophysics and neuroscience pertaining to temporal integration processes. This article does not aim at contributing to the question concerning the legitimacy of merging phenomenology with neuroscience – bridging the subjective and the objective perspective of the world, essentially the neurophenomenological approach (Varela, 1999; Thompson, 2007). It may be read as presenting knowledge of empirically identified levels of temporal integration that could potentially be assigned to phenomenal experiences of the present moment. However, this is not a philosophical paper but a review of the empirical literature which can be seen as a complementary attempt (from the viewpoint of cognitive neuroscience and psychophysics) to summarize and structure the body of literature on temporal integration as potential correlates of the present moment.

In many independent conceptualizations, perception, cognition, and motor behavior are thought to happen in discrete windows or processing epochs (White, 1963; Pöppel, 1970, 1997; Dehaene, 1993; VanRullen and Koch, 2003). Related specifically to the perception of time, these temporal units have been attributed to a physiological pacemaker or "internal clock" emitting regular pulses (Treisman, 1963). However, it is important to note that the theoretical approach presented here is not primarily concerned with "psychological time" or "explicit judgment of duration." Although empirical findings from research on time perception will be integrated as evidence pertaining to the presented conceptions, the discussed levels of temporal integration are thought to underlie mental processing in general as particularly related to the "present moment." According to these conceptions, successive events are fused into functional units forming *snapshots of experience* or *psychological presents* (Ruhnau, 1995; van Wassenhove, 2009). Essentially, temporal experience has no "null point," which would correspond to zero physical duration (Wackermann, 2007). Psychophysical investigations reveal thresholds and minimal durations necessary for certain temporal experiences. Departing from the taxonomy by Pöppel (1997) three different temporal processing levels will be discerned which are assumed to temporally integrate events on different time scales. Each level is discussed to be related to different aspects of the conceptions of a present moment and experienced presence.

THE FUNCTIONAL MOMENT

The fundamental notion that perception and action are based on discontinuous processing of information in discrete units is characterized by the idea of co-temporality, i.e., events within such a time unit have no before–after relation (Ruhnau, 1995). This is demonstrated by the analysis of psychophysical experiments assessing the perception of successiveness of two events. The sensory systems have different temporal resolutions for the detection of successiveness or non-simultaneity. The highest temporal resolution (the lowest threshold of detection) is observed in the auditory system, where two short acoustic stimuli which are only 2–3 ms apart are detected as non-simultaneous. The visual and the tactile system have a lower temporal resolution with respect to non-simultaneity with thresholds of some tens of milliseconds; inter-modal stimulation leads to the highest thresholds (Exner, 1875; Lackner and Teuber, 1973; Kirman, 1974; Lotze et al., 1999). The detection of non-simultaneity of two short events, however, is not perceptually sufficient to indicate their temporal order. Although we may be aware that two events did not occur simultaneously, we can still be unable to tell which one of the two stimuli occurred first. The temporal order threshold, which defines the inter-stimulus interval between two events at which an observer can reliably indicate the temporal order is more comparable across senses and lies roughly at 20–60 ms, to some extent depending on physical stimulus properties (Hirsh and Sherrick, 1961; Fink et al., 2006a; Miyazaki et al., 2006; Szymaszek et al., 2009). A similar minimal threshold of at least 20 ms is necessary for the identification of temporal order of onset between two longer complex acoustic events, adding to the notion that the temporal-order threshold marks a fundamental limit of temporal perception (Pastore and Farrington, 1996).

Temporal order is a primary experiential temporal datum, connecting subjective experience with the objective order of events (Wackermann, 2007, 2008). Ultimately, the notion of time is based on the elementary temporal relation of two events, *A* and *B*, which can be judged in their temporal order, "*A* occurs before *B*" or "*A* occurs after *B*." For example, music and spoken language are only meaningful if the correct temporal order of individual components is detected. The inversion of temporal order would lead to a different and new experience. For this reason, experienced temporal order as retrieved from memory appears in the same temporal order as when it was perceived (Mach, 1911). Below the experimentally assessed threshold of some tens of milliseconds the temporal order of events cannot be reliably detected. Elements that are perceived as non-simultaneous can be inter-changed without a noticeable effect for an observer. This has, for example, lead to the idea that temporal information within a segment of the speech signal not exceeding the *functional moment* might not be relevant for decoding spoken language (Kiss et al., 2008). The relation between the perception of speech and the perception of temporal order has repeatedly been demonstrated in studies with neurological patients suffering from aphasia and with adolescents who have language-learning impairments (Wittmann and Fink, 2004). These individuals have difficulties in discriminating consonants, which requires the ability to detect temporal order of speech signal components, because they have increased auditory temporal order thresholds (Wittmann et al., 2004; Fink et al., 2006b).

Based on the empirical findings of discrete processing in perception and action it has therefore been suggested that the brain creates a-temporal system states during which incoming information is treated as co-temporal, and which are on the one hand responsible for binding intra- and inter-modal information and

on the other hand create the experience of temporal order (Pöppel et al., 1990; Ruhnau, 1995; Pöppel, 1997). The idea that perceptual information as well as motor commands might be processed in discrete packets, at regular moments in time (Dehaene, 1993; VanRullen and Koch, 2003; van Wassenhove, 2009), is in accordance with the conception of a *functional moment*, a snapshot of perception. Findings of several independent empirical approaches in neuroscience have lead to the suggestion that temporal building blocks in sensory and cognitive processing exist – responsible for creating discrete functional units in time as well as binding spatial features into perceptual wholes. These temporal units have been related to rhythmic brain activity of thalamo-cortical loops, the "gamma" band with a frequency of around 40 Hz (Joliot et al., 1994; Basar-Eroglu et al., 1996; Fries et al., 2007; Ehm et al., 2011). However, periodicities in the alpha band (around 10 Hz) as well as the theta band (4–8 Hz), and potentially related to functional integration on a time scale of 100 ms and above (see below), may additionally contribute to temporal integration phenomena (VanRullen and Koch, 2003; van Wassenhove, 2009).

It is important to note that basic temporal integration mechanisms uniting disparate events into perceptual segments have been identified on different time scales and also in more complex inter-sensory perceptual tasks. For example, a time frame of about 200 ms determines the integration of auditory–visual input in speech processing when probing for the McGurk effect – an illusory fusion percept created when lip movements are incongruent to heard syllables (van Wassenhove et al., 2007). The fusion percept was reported if the onset of lip movement and syllable did not exceed this time lag. Temporal integration in a time frame of around 250 ms was reported in sensory–motor processing distinguishing maximum tapping speed from a personal, controlled motor speed (Peters, 1989; Wittmann et al., 2001). With repetitive finger movements such as with maximum tapping speed, when inter-tap intervals are around 150 ms, movements are too fast to be represented as individual button presses within an ordered sequence. Only when the movement slows down and inter-tap intervals exceed at least 250 ms individuated button presses are experienced as following each other. Stimulus durations of 200–300 ms (and minimum inter-onset intervals) are a necessary prerequisite for the establishment of temporal order representation for the detection of the correct sequence of four acoustic or visual events (Warren and Obusek, 1972; Ulbrich et al., 2009). When stimuli are shorter, or the inter-onset between stimuli is smaller, subjects cannot reliably report the temporal order of the presented sequence. An interpretation of these finding is that if two or more stimulus onsets fall within one window of temporal integration then temporal order cannot be experienced as the onsets are treated as co-temporal.

Regarding this approximate time range, it has been proposed that anterior insular cortex function may provide the continuity of subjective awareness by temporally integrating a series of elementary building blocks – successive moments of self-realization informed by the interoceptive system (Craig, 2009). The continuous processing from moment to moment would advance with a frame rate of about 8 Hz, these temporal building blocks of perception lying in the range of 125 ms (Picard and Craig, 2009). Neural microstates with average duration of 125 ms as derived from electrophysiological recordings have been discussed as potential "atoms of thought," constituting critical time windows within which neural events are functionally integrated (Lehmann et al., 1998). In combining the two kinds of *functional moments* presented here, endogenous cortical rhythms in the gamma and theta range involved in speech perception and production have been related to corresponding left- and right-hemispheric neural activation. Speech would be processed by the left auditory cortex, integrating the signal into 20–60 ms segments which would correspond to phoneme length; at the same time speech would be processed in the right auditory cortex, integrating the signal into segments of 100–300 ms corresponding to syllabic analyzes (Poeppel, 2003; Giraud et al., 2007). In the context of findings of various temporal integration phenomena it has moreover been proposed that mental processing is organized in multiple ranges of discrete periods which are all multiples of an absolutely smallest quantal period estimated to lie at approximately 4.5 ms (Geissler and Kompass, 2003).

It has to be noted that research has identified further integration phenomena, all being on comparable time scales (Fraisse, 1984). For example, a temporal integration window of 100–150 ms duration has been suggested to operate for perceptual grouping mechanisms of target and distractor tones in sensori-motor processing (Repp, 2004). Using the paradigm of mismatch negativity of magnetic brain responses a window of integration of 160–170 ms was estimated to bind successive auditory input into an auditory percept (Yabe et al., 1998). Further integration levels below 1 s as related to the processing of static stimuli as well as associated with motion perception are not presented, but see Fraisse (1984) and Dainton (2010). Potentially, many other kinds of basic *functional moments* may exist.[1] What these divergent findings have in common is that on a temporally fine grained level in the range of tens of milliseconds as well as of hundreds of milliseconds temporal integration phenomena occur that are the basis for the experience of temporal unity of events (below the threshold) and of succession and temporal order (above the threshold). Below the reported thresholds of around 30 ms (when two short events are presented) or of thresholds ranging between 100 and 300 ms (when a stream of events is presented) temporal integration provides *functional moments* of experienced co-temporality. One could argue that these *functional moments*, within which events are fused together, are not experienced as having duration. Although the sensation of non-simultaneity implies two temporally separated events, one could nevertheless say that the experience of duration necessitates a clearly demarcating onset *A* and offset *B* defining an interval (with the inherent temporal order *A* before *B*). In this sense one can state that below the temporal order threshold, when two events have no clear temporal relation, subjective duration between the two stimuli is not experienced; the *functional moment* has no perceivable duration.

THE EXPERIENCED MOMENT

Despite the possibly discrete nature of underlying processes in perception and cognition, our phenomenal experience is nevertheless

[1] On the level of the *functional moment* the concepts of prediction (van Wassenhove et al., 2005) and postdiction (Eagleman and Sejnowski, 2000) could be discussed.

characterized as evolving continuously (VanRullen and Koch, 2003). Only in rare neurological disorders or under the influence of pharmacological agents such as LSD individuals occasionally report of perceiving a series of discrete stationary images (Dubois and VanRullen, 2011). However, we typically do not perceive static snapshots of the world but perceived events are embedded in an ongoing stream of experience. Music and language are only conceivable as consisting of extended moments, melodies, and phrases, which inter-connect individual musical and linguistic elements (Wittmann and Pöppel, 2000). Even when we focus on an individual note in a musical piece or a word in a spoken sentence, these acoustic events can only be understood in its temporal relation to the preceding and the following musical or language structure. It is impossible to ignore the temporal context of what we perceive. Lloyd (2004, 2011) has an intuitive example for temporality in music: when we hear Paul McCartney land on "Jude," the "Hey" is still somehow present although no longer sensed (Husserl's *retention*). A listener familiar with the *Beatles*, when she hears the "Hey" cannot help but already hear the "Jude." The "Jude" is somehow present but it is actually only anticipated (Husserl's *protention*). In phenomenological terms, what we perceive at present is strongly intertwined with what has just happened and what is about to happen (Lloyd, 2004, 2011; Kiverstein, 2010).

When listening to a metronome at moderate speed, we do not hear a train of individual beats, but automatically form perceptual gestalts as an accent is perceived on every *n*th beat (1–2, 1–2, or 1–2–3, 1–2–3). These temporal units are mental constructs – physically speaking, they do not exist (Pöppel, 2009). If the metronome is too fast, the inter-beat intervals are very short, a fast train of beats is perceived that cannot be experienced as containing temporally separated events with an ordered temporal structure. Subjective accentuation is not possible. If on the other hand the metronome is too slow, inter-beat intervals are too long, only individual beats which are not related to each other are perceived (1–1–1 etc.). This lower and upper range of the metronome speed at which accentuated temporal structures can be heard defines the temporal limits of perceptual grouping on this time scale. Empirical evidence suggests that these mental units comprising several individual beats have a lower limit of around 250 ms and an upper limit of approximately 2 s (Szelag et al., 1996; von Steinbüchel et al., 1999; London, 2002). Further empirical observations revealed through a systematic variation of duration indicate that empty intervals marked by two acoustic events larger than 150–250 ms and shorter than 2 s are perceived as qualitatively different than intervals beyond these temporal boundaries (Benussi, 1913; Nakajima et al., 1980). For example, two sound bursts separated by an interval below 150 ms were perceived as one double-peaked sound; between 150 ms and 2 s the two sound bursts were clearly separated from each other but subjects still felt a relation between them and they tried to automatically synchronize their body movements to the stimulus pair; with intervals larger than 2 s subjects reported that the two sounds were difficult to relate to each other and synchronization of body movements was not attempted (Nakajima et al., 1980). Whereas findings of qualitative as well as quantitative differences between intervals below and above 2 s are predominantly found by presenting empty intervals that are marked by two sounds (for a psychophysical study see Getty, 1975), also regarding filled intervals it has been shown that duration up to 2–3 s is differently processed than duration exceeding 3 s (Ulbrich et al., 2007). However, results are not as clear cut as with empty intervals and "break points" are not always found (Noulhiane et al., 2008; Lewis and Miall, 2009). Temporal segmentation has been reported in further investigations in sensory–motor control. Subjects can synchronize their motor actions to a sequence of presented tones with inter-stimulus intervals of above 250 ms (Peters, 1989). However, this synchronization ability can only be maintained when inter-tone intervals do not exceed durations of about 2–3 s. With longer intervals precise anticipation of tones – effortless timing of behavior – breaks down (Mates et al., 1994). In a further analysis of this type of timing behavior, time ranges between 0.45 and 1.5 s seemed to be processed automatically, i.e., not strongly affected by secondary task fulfillment, whereas concomitant processing of a secondary task affected intervals in the range between 1.8 and 3.6 s (Miyake et al., 2004).

Also the phenomenon of perceptual bi-stability suggests itself for studying temporal constraints of conscious experience as one can easily tap into the subjective percepts (Leopold et al., 2002; van Ee, 2005). The temporal analysis of bi-stable perception has been suggested as primary experimental approach for the understanding of the dynamics of mental states (Atmanspacher and Filk, 2010). In essence, an ongoing competition between the neural representations of the two aspects of an ambiguous figure, such as the Necker cube, has to be resolved leading to the experience of one of the two perspectives at a given point in time. During continuous presentation, one aspect lasts on average for around 3 s before a switch in perspectives occurs, with some inter-individual variability and variance attributable to stimulus characteristics of the particular ambiguous figure (Gómez et al., 1995; von Steinbüchel et al., 1999; Meng and Tong, 2004; Kornmeier et al., 2007). Given its temporal dynamics, the spontaneous switching rate has been discussed as stemming from the discussed temporal segmentation mechanism related to the subjective present (Varela, 1999; Franck and Atmanspacher, 2009; Pöppel, 2009).

The *experienced moment* can be related to more elementary units of perception. For example, it has been proposed that the temporal integration mechanism of around 3 s, evoking our feeling of *nowness*, integrates successive processing units of around 30 ms, *functional moments* (Pöppel, 1997, 2009; Szelag et al., 2004). In another line of research that treats bi-stable perception as evolving from unstable two-state systems it was proposed that different mental processing stages have temporal properties matching the found temporal integration levels of 30, 300, and 3 s (Atmanspacher et al., 2004; Atmanspacher and Filk, 2010). In combining the empirical findings, temporal integration of a few seconds has been suggested to provide the logistical basis for the subjective present (Pöppel, 1978, 2009; Fraisse, 1984; Szelag et al., 2004). Whereas the duration of the *functional moment* is not perceived, an *experienced moment* relates to the experience of an extended now. According to this conception, the *experienced moment* has duration.

MENTAL PRESENCE

A temporal interval with duration exceeding about 3 s is experienced as being qualitatively different than shorter duration. When two events are separated by an interval of, say, 6 s, the experience of "emptiness" evolves, events are not bound together and the length of the interval separating the two becomes the focus of attention (Wackermann, 2007). A pause in a conversation, if it reaches 6 s, might be felt as disturbingly long. In that sense, duration longer than 3 s leads to the predominant experience of an extended temporal interval. On the other side of the spectrum, what is the maximum time interval an observer can directly experience? It is well possible to judge the duration of 1 h, i.e., pressing a button every time one thinks that an hour has passed (Aschoff, 1998). However, it is impossible to maintain a 1-h time interval continuously in the focus of awareness (Wackermann, 2007). During such a period of 1 h a multitude of experiences accumulates that later can be retrieved from memory forming temporal cues that can be used to judge duration retrospectively (Zakay and Block, 1997). But then the question remains what the upper limit of integration in prospective time perception might be, that is, of the perception of duration as presently and continuously experienced? More generally formulated and more importantly, what are the temporal boundaries of perception that allow us to hold events in present experience, in *mental presence*? Whereas the *experienced moment* forms an elementary unit, a temporally unified percept, *mental presence* involves the experience of a perceiving and feeling agent ("my self") within a window of extended presence, a phenomenon that is based on working memory function. "Working memory provides a temporal bridge between events – both those that are internally generated and environmentally presented – thereby conferring a sense of unity and continuity to conscious experience" (Goldman-Rakic, 1997). An *experienced moment* happens *now*, for a short but extended moment. *Mental presence* encloses a sequence of such moments for the representation of a unified experience of presence.

Reports from neurological case studies with individuals who suffer from anterograde amnesia after bilateral damage to the hippocampus indicate that these patients live within a moving temporal window of presence that does not reach beyond their short-term or working memory span, incapable of storing incidents into episodic long-term memory (Scoville and Milner, 1957). These patients can hold information for a limited time in memory, they perform short tasks accurately and seemingly behave normal; but already after a few minutes they can not recall what has just happened (for a striking description of a patient with anterograde amnesia, see Sacks, 1986). Due to their neurological impairment, patients with anterograde amnesia can act adequately within the temporal constraints of their functioning working memory, which accordingly must be a temporal constraint for *mental presence*, the continuous awareness of oneself as presently perceiving and acting within an environment. These clinical cases emphasize the functioning of short-term memory in healthy humans and how it can be interpreted as forming temporal boundaries of present awareness.

Experimental investigations of short-term memory show how the number of correct recalls of presented syllables decreases with increasing interval length between stimulus presentation and recall – in the range of multiple seconds – if the rehearsal of syllables is prevented (Peterson and Peterson, 1959; Baddeley, 1990). The capacity of short-term retention is defined as gradual loss of memorized elements as time passes. The typical retention functions described by logarithmic and exponential fits decrease rapidly at first and then levels out on a plateau (Rubin and Wenzel, 1996). One could state that the time frame provided by short-term memory (related, working memory) creates a temporal horizon of experience which in humans contains descriptive–narrative elements created by our capacity for language (Varela, 1999). Within this temporal horizon *mental presence* unfolds integrating mental processes and enabling conscious experience of a narrative self that has personal identity and continuity over time (Gallagher, 2000). *Mental presence* is bound to the ability of maintaining mental representations in an active state for a certain period of time. It depends on the integration of multiple mental operations that lead to intentional behavior – created by ongoing activity of a global workspace, integrating activity from multiple distributed and specialized brain areas (Baars, 1988; Dehaene and Naccache, 2001). Essentially, it is working memory, a system of limited attentional capacity, supplemented by visuospatial, episodic, and phonologic storage systems, which holds information for temporal storage and manipulation (Baddeley, 2003).

In duration reproduction tasks, individuals have to reproduce temporal intervals by pressing a key to indicate that a second comparison stimulus has reached the duration of a previously presented stimulus. The mean of reproduced intervals is accurate for shorter intervals of up to 3 s but with increasing interval lengths are progressively under-reproduced relative to physical time (Eisler and Eisler, 1992; Wackermann, 2005; Ulbrich et al., 2007; Wittmann et al., 2010). The negative curvature of the duration reproduction function results in an asymptotic upper limit of duration accessible to experience, i.e., a temporal horizon of experienced time in the range of roughly 10^2 s (Wackermann, 2007). Note, that the negative curvature in duration reproduction performance is found in those studies where subjects are instructed or discouraged from counting (Rattat and Droit-Volet, 2011). Without chronometric counting, the immediate experience of duration is limited by an ultimate temporal horizon of reproducibility due to memory-loss of duration representation over time; temporal resolution of duration blurs with increasing interval length (Wackermann, 2007, 2008).[2] It is tempting to suggest that a healthy individual's short-term memory span is related to the upper limit of prospective time perception; the limits of temporal experience, of perceiving duration continuously, would

[2]A famous patient with anterograde amnesia, H.M., as studied by Richards (1973) was supposedly found to show an impaired performance in duration reproduction at longer time intervals. This claim, however, is not substantiated by the available data (Wackermann, personal communication). When plotting the behavioral data of H.M. as absolute values, extracted by Eisler and Eisler (2001), and not as log–log plots one can see a perfect asymptotic curve for stimulus durations ranging from 1 to 300 s. A parametric fit using the 'dual klepsydra model' (Wackermann and Ehm, 2006) revealed that parameter κ, reflecting the progressive under-reproduction of duration, with 0.011 s^{-1} is in a typical range of adult subjects (Wackermann, 2005). That is, H.M. was able to time his behavior adequately within the time range of his *mental presence*.

thereafter rely on the basic temporal properties of working memory. In fact, decay of memory traces has been discussed to underlie the experience of duration. Since memory strength decreases with time, memory trace decay could actually function as a "clock" (Staddon, 2005). That way, the same processes would underlie forgetting as well as time perception. This memory-loss component is an intrinsic feature of the "dual klepsydra model" (Wackermann and Ehm, 2006; Wackermann, 2008), where subjective duration is represented by the state of a lossy accumulator. This accumulator receives inflow for the build-up of duration presentation of a stimulus that has to be judged. A simultaneous outflow reflects the loss of representation leading to typical responses in psychophysical tasks, indicative of "subjective shortening" of stored duration over time.

There is no absolute, fixed temporal boundary of *mental presence*. The reports of a limiting value in the order of magnitude of 10^2 s in the ability to reproduce duration indicate that the representation of increasing duration becomes more and more compressed. The duration reproduction curve becomes increasingly flatter, i.e., with increasing temporal intervals differences in physical duration are represented with decreasing resolution (Wackermann, 2007).

That is, the reported limits in duration reproduction and short-term memory do not point to absolute and static boundaries – correspondingly, *mental presence* has no fixed duration – but to a gradual dissolving of representation with increasing duration. Related to this temporal characteristic, *mental presence* is related to the fact that once attended objects slowly phase out of experience over time; that is, the phenomenally experienced sliding window of *mental presence* co-occurs with the constant loss of memory contents. The moving window of presence is related to the constant sequential input of a sequence of perceived events, which each fade out of working memory one after the other after some time. *Mental presence* is a temporal platform of multiple seconds within which an individual is aware of herself and the environment, where sensory–motor perception, cognition, and emotion are interconnected features of representation leading to phenomenal experience.

CONCLUSION

Facing the puzzle of how we can perceive duration of events if our perception is bound to the present moment, more than 1600 years ago St. Augustine gave an answer (Flasch, 1993). Although the present (*praesens tempus*) has no extension as it passes away in a moment (*in puncto praeterit*), an observation nevertheless has extension (*distentio*) through temporally lasting attention (*attentio*) which encompasses the anticipation of events (*expectatio*) that eventually fade into memory (*memoria*); here, anticipation and memory are part of an extended present where attention lasts for some time (Confessions, book XI; section XXVIII.37 in Flasch, 1993). Moreover, conscious experience involving a sense of self may only be understood as an entity that is extended over time (Zahavi, 2005; Wittmann, 2009; Stolzenberg, 2010). It is obvious that St. Augustine's conception of time has strong similarities to Husserl (1928) tripartite structure of present experience. Although a variety of philosophical models concerning the present moments exists, important in the present context is the common insight that the present moment is experienced as extended. Also our everyday language use implies that what is happening at the present moment typically has duration.[3]

Present experience on the level of content is a continuously evolving phenomenon and individual events are embedded in an extended temporal field (Stern, 1897; Lloyd, 2004, 2011). A suddenly occurring short stimulus of a few milliseconds might actually be perceived as a point in time. Moreover, psychophysical investigations in which stimulus properties are systematically varied reveal thresholds of experience below which no temporal relationship is perceived. In these limiting cases disclosed by psychophysics one can actually speak of *functional moments* without perceivable duration because temporal order, a primary experiential datum, is not detected. This single momentary event is nevertheless part of a continuous and extended experience. For example, if a short tone with a lower pitch is followed by another short tone with a slightly higher pitch, the impression of a single tone rising in pitch can be elicited (Fink et al., 2006a). Within different modalities, the rapid serial appearance of two or more stimuli at different positions can give the impression of apparent motion (Exner, 1875; Kirman, 1974). That is, the common cases of perception, in accordance with the phenomenological analysis of our *Lebenswelt*, suggest that subjective time provides a frame of reference within which moments are stretched out over time.

The integration level of the experienced moment is the basic operational platform within which temporality can evolve. The unit that the first two words in the Beatles lyrics "Hey Jude" form, as short as the overall duration may seem, involves anticipation and memory which are activated while the "Hey" passes over to "Jude" (Lloyd, 2004, 2011). After having heard "Hey Jude" some people might even anticipate the ". . .don't make it bad." Then, however, the two verses may already fall into two different experienced moments. The break between the two subunits "Hey Jude" and ". . .don't make it bad" points to a general principle in poems and in music where *caesurae* form boundaries between which individual verses are recited; across different languages and cultures the duration of these lyrical and musical units seems not to exceed 3 s (Pöppel, 1988; Turner and Pöppel, 1988). Beyond the experienced moment successive events are less strongly bound together. "Hey Jude" is a stronger bounded unit than "Hey Jude, don't make it bad." And with increasingly longer intervals temporally separate components within these units will become less strongly connected; retention and protention are temporally limited in the way that they cover only what has just happened and is about to happen in the range of a few seconds, working memory span forming a boundary of present experience as *mental presence*. The discussed examples in literature of experienced temporality refer to situations concerning temporal integration in the several seconds range. Husserl (1928, p. 383) discusses the situation of hearing a melody which is only possible because individual tones are integrated to form a perceptual whole. Kelly (2005) presents the example of hearing a steady high C produced by an opera singer

[3]When J. W. Goethe's Faust proclaims: "When, to the Moment then, I say: Ah, linger on, thou art so fair!" ("Werd ich zum Augenblicke sagen: Verweile doch! Du bist so schön!"), he definitely refers to an extended moment that he would like to see prolonged indefinitely.

who holds that note for some time – for the listener subjectively going on for a long time – that is, for several seconds.

Different from this phenomenological notion of *retention* and *protention* is the conception of time perspective as a fundamental cognitive dimension partitioning human experience into past, present, and future (Zimbardo and Boyd, 1999). Past and future in this context can span decades, as far as long-term memory reaches back in time and as far as we plan our future. Through this partitioning of time, the notion of a presence becomes meaningful since the explicit representation of the present perspective is only possible through its distinction from past and future (Droege, 2009). Within the realm of the *mental presence* an individual can be considered fully operational as she tracks current conditions, compares them with memories of past incidences, and makes plans for the future. The past and the future as presently experienced can also be explicitly judged in relation to subjective time. When judging the past, we typically perceive the decades of our lives to speed up as we get older (Wittmann and Lehnhoff, 2005). Related to the future, we constantly generate predictions about how long it will take for some events to occur, these temporal estimates eventually leading to decisions regarding options with different delays (Wittmann and Paulus, 2009). For example, a person who chooses to save money opts for a momentary loss of money that otherwise would be available now in order to gain a future greater benefit.

A fundamental question remains of how lower-level temporal units are bound together forming higher-level units; a variety of concepts has been rigorously discussed by Dainton (2010). Independent of how the sequential units of lower-level units might be related to each other, potentially overlapping each other or following in direct succession, continuity of experience has been considered to stem from an ongoing semantic connection across individual segments, which masks the discontinuity of the sequential units (Pöppel, 1997; Droege, 2009). Regarding specifically the continuity of experience across *experienced moments*, working memory related to semantic and episodic content might bind together the sequence of temporal segments of *nowness* that leads to the experience of *mental presence*. The *experienced moment* is defined as what is occurring *now* as immediate experience. It is also a prerequisite for interpersonal communication between two individuals made possible by synchronizing the moments of individuals, thereby creating shared moments of presence for effortless interaction – an essential feature in music, conversation, and dance (Wittmann and Pöppel, 2000). However, the experience of a self acting in its environment, remembering the past and planning the future necessitates an integration interval – as has been related to *mental presence* – exceeding the postulated 3-s time window of the *experienced moment*. Continuity of experience only unfolds as *mental presence*, which is a floating window of feeling present and acting at present.

ACKNOWLEDGMENTS

This work has been supported by the European project COST ISCH Action TD0904 "Time In MEntaL activitY: theoretical, behavioral, bioimaging, and clinical perspectives (TIMELY; www.timely-cost.eu)." Over the years, the author's research was supported by the Bundesministerium für Bildung und Forschung, Germany, the Max Kade Foundation, New York, The National Institute on Drug Abuse, Bethesda, and the Kavli Institute for Brain and Mind, San Diego. I would like to thank Jirí Wackermann, Jürgen Kornmeier, Harald Atmanspacher as well as the two reviewers for helpful comments on the manuscript.

REFERENCES

Aschoff, J. (1998). Human perception of short and long time intervals: its correlation with body temperature and the duration of wake time. *J. Biol. Rhythms* 13, 437–442.

Atmanspacher, H., and Filk, T. (2010). A proposed test of temporal nonlocality in bistable perception. *J. Math. Psychol.* 54, 314–321.

Atmanspacher, H., Filk, T., and Römer, H. (2004). Quantum Zeno features of bistable perception. *Biol. Cybern.* 90, 33–40.

Baars, B. J. (1988). *A Cognitive Theory of Consciousness.* Cambridge: Cambridge University Press.

Baddeley, A. (1990). *Human Memory. Theory and Practice.* Boston: Allyn and Bacon.

Baddeley, A. (2003). Working memory: looking forward and looking back. *Nat. Rev. Neurosci.* 4, 829–839.

Basar-Eroglu, C., Strueber, D., Schuermann, M., Stadler, M., and Basar, E. (1996). Gamma-band responses in the brain: a short review of psychophysiological correlates and functional significance. *Int. J. Psychophysiol.* 24, 101–112.

Benussi, V. (1913). *Psychologie der Zeitauffassung.* Heidelberg: Carl Winters Universitätsbuchhandlung.

Callender, C. (2008). The common now. *Phil. Issues* 18, 339–361.

Craig, A. D. (2009). How do you feel – now? The anterior insula and human awareness. *Nat. Rev. Neurosci.* 10, 59–70.

Dainton, B. (2010). "Temporal consciousness," in *The Stanford Encyclopedia of Philosophy*, ed. E. N. Zalta. Available at: http://plato.stanford.edu/archives/fall2010/entries/consciousness-temporal

Dehaene, S. (1993). Temporal oscillations in human perception. *Psychol. Sci.* 4, 264–270.

Dehaene, S., and Naccache, L. (2001). Towards a cognitive neuroscience of consciousness: basic evidence and a workspace framework. *Cognition* 79, 1–37.

Droege, P. (2009). Now or never: how consciousness represents time. *Conscious. Cogn.* 18, 78–90.

Dubois, J., and VanRullen, R. (2011). Visual trails: do the doors of perception open periodically? *PLoS Biol.* 9, e1001056. doi:10.1371/journal.pbio.1001056

Eagleman, D. M., and Sejnowski, T. J. (2000). Motion integration and postdiction in visual awareness. *Science* 287, 2036–2038.

Ehm, W., Bach, M., and Kornmeier, J. (2011). Ambiguous figures and binding: EEG frequency modulations during multistable perception. *Psychophysiology* 48, 547–558.

Eisler, H., and Eisler, A. D. (1992). Time perception: effects of sex and sound intensity on scales of subjective duration. *Scand. J. Psychol.* 33, 339–358.

Eisler, H., and Eisler, A. D. (2001). Subjective time in a patient with neurological impairment. *Psychologica* 28, 193–206.

Exner, S. (1875). Experimentelle Untersuchung der einfachsten psychischen Prozesse. III. Abhandlung. *Pflug. Arch. Ges. Physiol.* 11, 403–432.

Fink, M., Ulbrich, P., Churan, J., and Wittmann, M. (2006a). Stimulus-dependent processing of temporal order. *Behav. Processes* 71, 344–352.

Fink, M., Churan, J., and Wittmann, M. (2006b). Temporal processing and context dependency of phoneme discrimination in patients with aphasia. *Brain Lang.* 98, 1–11.

Flasch, K. (1993). *Was ist Zeit? Augustinus von Hippo. Das XI. Buch der Confessiones.* Frankfurt am Main: Vittorio Klostermann.

Fraisse, P. (1984). Perception and estimation of time. *Annu. Rev. Psychol.* 35, 1–36.

Franck, G., and Atmanspacher, H. (2009). "A proposed relation between intensity of presence and duration of nowness," in *Recasting Reality. Wolfgang Pauli's Philosophical Ideas and Contemporary Science*, eds H. Atmanspacher and H. Primas (Berlin: Springer), 211–225.

Fries, P., Nikolic, D., and Singer, W. (2007). The gamma cycle. *Trends Neurosci.* 30, 309–316.

Gallagher, S. (2000). Philosophical conceptions of the self: implications for cognitive science. *Trends Cogn. Sci.* 4, 14–21.

Geissler, H.-G., and Kompass, R. (2003). "Invariants in mental timing: from taxonomic relations to task-related modelling," in *Time and Mind II*, ed H. Helfrich (Göttingen: Hogrefe & Huber), 185–207.

Getty, D. J. (1975). Discrimination of short temporal intervals: a comparison of two models. *Percept. Psychophys.* 18, 1–8.

Giraud, A.-L., Kleinschmidt, A., Poeppel, D., Lund, T. E., Frackowiak, R. S. J., and Laufs, H. (2007). Endogenous cortical rhythms determine cerebral specialization for speech perception and production. *Neuron* 56, 1127–1136.

Goldman-Rakic, P. (1997). Space and time in the mental universe. *Nature* 386, 559–560.

Gómez, C., Argandoa, E. D., Solier, R. G., Angulo, J. C., and Vázquez, M. (1995). Timing and competition in networks representing ambiguous figures. *Brain Cogn.* 29, 103–114.

Hirsh, I. J., and Sherrick, C. (1961). Perceived order in different sense modalities. *J. Exp. Psychol.* 62, 423–432.

Husserl, E. (1928). *Vorlesungen zur Phänomenologie des inneren Zeitbewußtseins.* Halle: Max Niemeyer Verlag.

James, W. (1890). *The Principles of Psychology*. London: MacMillan.

Joliot, M., Ribary, U., and Llinás, R. (1994). Human oscillatory brain activity near 40 Hz coexists with cognitive temporal binding. *Proc. Natl. Acad. Sci. U.S.A.* 88, 4966–4970.

Kelly, S. (2005). "The puzzle of temporal experience," in *Cognition and the Brain: The Philosophy and Neuroscience Movement*, eds A. Brook and K. Akins. (Cambridge: Cambridge University Press), 208–238.

Kirman, J. H. (1974). Tactile apparent movement: the effects of number of stimulators. *J. Exp. Psychol.* 103, 1075–1080.

Kiss, M., Cristescu, T., Fink, M., and Wittmann, M. (2008). Auditory language comprehension of temporally reversed speech signals in native and non-native speakers. *Acta Neurobiol. Exp. (Wars)* 68, 204–213.

Kiverstein, J. (2010). Making sense of phenomenal unity: an intentionalist account of temporal experience. *R. Inst. Philos. Suppl.* 85, 155–181.

Kornmeier, J., Ehm, W., Bigalke, H., and Bach, M. (2007). Discontinuous presentation of ambiguous figures: how interstimulus-interval durations affect reversal dynamics and ERPs. *Psychophysiology* 44, 552–560.

Lackner, J. R., and Teuber, H.-J. (1973). Alterations in auditory fusion threshold after cerebral injury in man. *Neuropsychologia* 11, 409–415.

Le Poidevin, R. (2007). *The Images of Time. An Essay on Temporal Representation.* Oxford: Oxford University Press.

Lehmann, D., Strik, W. K., Henggeler, B., Koenig, T., and Koukkou, M. (1998). Brain electric microstates and momentary conscious mind states as building blocks of spontaneous thinking: I. Visual imagery and abstract thoughts. *Int. J. Psychophysiol.* 29, 1–11.

Leopold, D. A., Wilke, M., Maier, A., and Logothetis, N. K. (2002). Stable perception of visually ambiguous patterns. *Nat. Neurosci.* 5 605–609.

Lewis, P. A., and Miall, R. C. (2009). The precision of temporal judgement: milliseconds, many minutes, and beyond. *Philos. Trans. R. Soc. Lond. B Biol. Sci.* 364, 1897–1905.

Lloyd, D. (2004). *Radiant Cool. A Novel Theory of Consciousness.* Cambridge, MA: The MIT Press.

Lloyd, D. (2011). Neural correlates of temporality: default mode variability and temporal awareness. *Conscious. Cogn.* doi: 10.1016/j.concog.2011.02.016. [Epub ahead of print].

London, J. (2002). Cognitive constraints on metric systems: some observations and hypotheses. *Music Percept.* 19, 529–550.

Lotze, M., Wittmann, M., von Steinbüchel, N., Pöppel, E., and Roenneberg, T. (1999). Daily rhythm of temporal resolution in the auditory system. *Cortex* 35, 89–100.

Mach, E. (1911). *Die Analyse der Empfindungen und das Verhältnis des Physischen zum Psychischen*, 6th Edn, Jena: Verlag von Gustav Fischer.

Mates, J., Müller, U., Radil, T., and Pöppel, E. (1994). Temporal integration in sensorimotor synchronization. *J. Cogn. Neurosci.* 6, 332–340.

Meng, M., and Tong, F. (2004). Can attention selectively bias bistable perception? Differences between binocular rivalry and ambiguous figures. *J. Vis.* 4, 539–551.

Metzinger, T. (2004). *Being No One. The Self-Model Theory of Subjectivity*. Cambridge : MIT Press.

Miyake, Y., Onishi, Y., and Pöppel, E. (2004). Two types of anticipation in synchronization tapping. *Acta Neurobiol. Exp. (Wars)* 64, 415–426.

Miyazaki, M., Yamamoto, S., Uchida, S., and Kitazawa, S. (2006). Bayesian calibration of simultaneity in tactile temporal order judgment. *Nat. Neurosci.* 9, 875–877

Nakajima, Y., Shimojo, S., and Sugita, Y. (1980). On the perception of two successive sound bursts. *Psychol. Res.* 41, 335–344.

Noulhiane, M., Pouthas, V., and Samson, S. (2008). Is time reproduction sensitive to sensory modalities? *Eur. J. Cogn. Psychol.* 21, 18–34.

Pastore, R., and Farrington, S. (1996). Measuring the difference limen for identification of order of onset for complex auditory stimuli. *Percept. Psychophys.* 58, 510–526.

Peterson, L. R., and Peterson, M. J. (1959). Short-term retention of individual verbal items. *J. Exp. Psychol.* 58, 193–198.

Peters, M. (1989). The relationship between variability of intertap intervals and interval duration. *Psychol. Res.* 51, 38–42.

Picard, F., and Craig, A. D. (2009). Ecstatic epileptic seizures: a potential window on the neural basis of self-awareness. *Epilepsy Behav.* 16, 539–546.

Pockett, S. (2003). How long is "now"? Phenomenology and the specious present. *Phenomenol. Cogn. Sci.* 2, 55–68.

Poeppel, D. (2003). The analysis of speech in different temporal integration windows: cerebral lateralization as 'asymmetric sampling in time.' *Speech Commun.* 41, 245–255.

Pöppel, E. (1970). Excitability cycles in central intermittency. *Psychol. Res.* 34, 1–9.

Pöppel, E. (1978). "Time perception," in *Handbook of Sensory Physiology*, eds R. Held, W. Leibowitz, and H.-L. Teuber (Berlin: Springer), 713–729.

Pöppel, E. (1988). The measurement of music and the cerebral clock: a new theory. *Leonardo* 22, 83–89.

Pöppel, E. (1997). A hierarchical model of temporal perception. *Trends Cogn. Sci.* 1, 56–61.

Pöppel, E. (2009). Pre-semantically defined window for cognitive processing. *Philos. Trans. R. Soc. Lond. B Biol. Sci.* 364, 1887–1896.

Pöppel, E., Schill, K., and Steinbüchel, N. V. (1990). Sensory integration within temporally neutral system states: a hypothesis. *Naturwissenschaften* 77, 89–91.

Rattat, A.-C., and Droit-Volet, S. (2011). What is the best and easiest method of preventing counting in different temporal tasks? *Behav. Res. Methods* doi:10.3758/s13428-011-0135–133. [Epub ahead of print].

Repp, B. H. (2004). On the nature of phase attraction in sensorimotor synchronization with interleaved auditory sequences. *Hum. Mov. Sci.* 23, 389–413.

Richards, W. (1973). Time reproductions by H. M. *Acta. Psychol.* 37, 279–282.

Rubin, D. C., and Wenzel, A. E. (1996). One hundred years of forgetting: a quantitative description of retention. *Psychol. Rev.* 103, 734–760.

Ruhnau, E. (1995). "Time-gestalt and the observer," in *Conscious Experience*, ed. T. Metzinger (Paderborn: Ferdinand Schöningh), 165–184.

Sacks, O. (1986). *The Man Who Mistook his Wife for a Hat.* London: Picador.

Scoville, W. B., and Milner, B. (1957). Loss of recent memory after bilateral hippocampal lesions. *J. Neurol. Neurosurg. Psychiatr.* 20, 11–21.

Staddon, J. E. R. (2005). Interval timing: memory, not a clock. *Trends Cogn. Sci.* 9, 312–314.

Stern, L. W. (1897). Psychische Präsenzzeit. *Z. Psychol. Physiol. Sinnesorg.* 13, 325–349.

Stolzenberg, J. (2010). "Zeit und Selbst," in *Zum Problem der Zeiterfahrung bei Aristoteles, Augustinus, Husserl und Heidegger*, eds K. Crone, R. Schnepf, and J. Stolzenberg (Berlin: Suhrkamp Verlag), 275–301.

Szelag, E., Kanabus, M., Kolodziejczyk, I., Kowalska, J., and Szuchnik, J. (2004). Individual differences in temporal information processing in humans. *Acta Neurobiol. Exp. (Wars)* 64, 349–366.

Szelag, E., von Steinbüchel, N., Reiser, M., Gilles de Langen, E., and Pöppel, E. (1996). Temporal constraints in processing of nonverbal rhythmic patterns. *Acta Neurobiol. Exp. (Wars)* 56, 215–225.

Szymaszek, A., Sereda, M., Pöppel, E., and Szelag, E. (2009). Individual differences in the perception of temporal order: the effect of age and cognition. *Cogn. Neuropsychol.* 26, 135–147.

Thompson, E. (2007). *Mind in Life: Biology, Phenomenology, and the Sciences of Mind.* Cambridge, MA: Harvard University Press.

Treisman, M. (1963). Temporal discrimination and the difference interval: Implications for a model of the "internal clock." *Psychol. Monogr.* 77, 1–31.

Turner, F., and Pöppel, E. (1988). "Metered poetry, the brain, and time," in *Beauty and the Brain. Biological Aspects of Aesthetics*, eds I. Rentschler, B. Herzberger, and D. Epstein. (Basel: Birkhäuser), 71–90.

Ulbrich, P., Churan, J., Fink, M., and Wittmann, M. (2007). Temporal reproduction: further evidence for two processes. *Acta Psychol. (Amst)* 125, 51–65.

Ulbrich, P., Churan, J., Fink, M., and Wittmann, M. (2009). Perception of temporal order: The effects of age, sex, and cognitive factors. *Aging Neuropsychol. Cogn.* 16, 183–202.

van Ee, R. (2005). Dynamics of perceptual bi-stability for stereoscopic slant rivalry and a comparison with grating, house-face, and Necker cube rivalry. *Vision Res.* 45, 29–40.

van Wassenhove, V. (2009). Minding time – an amodel representational space for time perception. *Philos. Trans. R. Soc. Lond. B Biol. Sci.* 364, 1815–1830.

van Wassenhove, V., Grant, K. W., and Poeppel, D. (2005). Visual speech speeds up the neural processing of auditory speech. *PNAS* 102, 1181–1186.

van Wassenhove, V., Grant, K. W., and Poeppel, D. (2007). Temporal window of integration in auditory-visual speech perception. *Neuropsychologia* 45, 598–607.

VanRullen, R., and Koch, C. (2003). Is perception discrete or continuous? *Trends Cogn. Sci.* 7, 207–213.

Varela, F. J. (1999). Present-time consciousness. *J. Consciousness Stud.* 6, 111–140.

von Steinbüchel, N., Wittmann, M., and Szelag, E. (1999). Temporal constraints of perceiving, generating, and integrating information: clinical indications. *Restor. Neurol. Neurosci.* 14, 167–182

Wackermann, J. (2005). "Experience of time passage: phenomenology, psychophysics, and biophysical modelling," in *Endophysics, Time, Quantum and the Subjective*, eds R. Buccheri, A. C. Elitzur, and M. Saniga (Singapore: World Scientific Publishing), 189–208.

Wackermann, J. (2007). Inner and outer horizons of time experience. *Span. J. Psychol.* 10, 20–32.

Wackermann, J. (2008). Measure of time: a meeting point of psychophysics and fundamental physics. *Mind Matter* 6, 9–50.

Wackermann, J., and Ehm, W. (2006). The dual klepsydra model of internal time representation and time reproduction. *J. Theor. Biol.* 239, 482–493.

Warren, R. M., and Obusek, C. J. (1972). Identification of temporal order within auditory sequences. *Percept. Psychophys.* 12, 86–90.

White, C. T. (1963). Temporal numerosity and the psychological unit of duration. *Psychol. Monogr.* 77, 1–37.

Wittmann, M. (2009). The inner experience of time. *Philos. Trans. R. Soc. B* 364, 1955–1967.

Wittmann, M., Burtscher, A., Fries, W., and von Steinbüchel, N. (2004). Effects of lesion size and location on temporal-order judgment in brain-injured patients. *Neuroreport* 15, 2401–2405.

Wittmann, M., and Fink, M. (2004). Time and language – critical remarks on diagnosis and training methods of temporal-order judgement. *Acta Neurobiol. Exp. (Wars)* 64, 341–348.

Wittmann, M., and Lehnhoff, S. (2005). Age effects in perception of time. *Psychol. Rep.* 97, 921–935.

Wittmann, M., and Paulus, M. P. (2009). Temporal horizons in decision making. *J. Neurosci. Psychol. Econ.* 2, 1–11.

Wittmann, M., and Pöppel, E. (2000). Temporal mechanisms of the brain as fundamentals of communication – with special reference to music perception and performance. *Musicae Scientiae Special Issue* 1999–2000, 13–28.

Wittmann, M., Simmons, A. N., Aron, J. L., and Paulus, M. P. (2010). Accumulation of neural activity in the posterior insula encodes the passage of time. *Neuropsychologia* 48, 3110–3120.

Wittmann, M., von Steinbüchel, N., and Szelag, E. (2001). Hemispheric specialisation for self-paced motor sequences. *Cogn. Brain Res.* 10, 341–344.

Yabe, H., Tervaniemi, M., Sinkkonen, J., Huotilainen, M., Ilmoniemi, R. J., and Näätänen, R. (1998). Temporal window of integration of auditory information in the human brain. *Psychophysiology* 35, 615–619.

Zahavi, D. (2005). *Subjectivity and Selfhood: Investigating the First-Person Perspective*. Cambridge, MA: MIT Press.

Zakay, D., and Block, R. A. (1997). Temporal cognition. *Curr. Dir. Psychol. Sci.* 6, 12–16.

Zimbardo, P. G., and Boyd, J. N. (1999). Putting time in perspective: a valid, reliable individual-difference metric. *J. Pers. Soc. Psychol.* 77, 1271–1288.

Conflict of Interest Statement: The author declares that the research was conducted in the absence of any commercial or financial relationships that could be construed as a potential conflict of interest.

Received: 07 June 2011; paper pending published: 11 July 2011; accepted: 02 October 2011; published online: 18 October 2011.

*Citation: Wittmann M (2011) Moments in time. Front. Integr. Neurosci. **5**:66. doi: 10.3389/fnint.2011.00066*

frontiers in
INTEGRATIVE NEUROSCIENCE

OPINION ARTICLE
published: 31 January 2012
doi: 10.3389/fnint.2012.00003

Why the transitivity of perceptual simultaneity should be taken seriously

Valtteri Arstila*

Department of Behavioral Sciences and Philosophy, University of Turku, Turku, Finland
**Correspondence: valtteri.arstila@utu.fi*

A relation is transitive if and only if from the fact that A has a relation to B, and B has a relation C, it necessarily follows that A also has a relation to C. As a relation fulfilling this requirement, consider simultaneity understood as two events occurring at the same time and only at the same time (thus this is not a case of mere partial temporal overlap): If A and B share all the same temporal properties, and B and C share them too, then it is impossible for A and C not to share them too. Accordingly, the simultaneity of the time of events is a transitive relation. On the other hand, "to be non-simultaneous (asynchronous)" is not a transitive relation because A and C can be simultaneous although both of them are non-simultaneous with B.

Perceptual simultaneity refers to our perception or judgment that two or more things are simultaneous (or at least that we cannot tell their temporal order). While the transitivity of the simultaneity of time of events is virtually always accepted, philosopher Kelly (2005) has argued that perceptual simultaneity is an intransitive relation. If successful, and the conclusions drawn from this claim were sound, Kelly's (2005) argument would pose a serious challenge to certain theories of consciousness and views on neural synchrony (Elliott et al., 2006). Instead of elaborating on these consequences, and how they follow from the possible intransitivity of perceptual simultaneity, I will argue that the argument itself rests on an assumption that requires justification. Accordingly, it should remain an open question whether perceptual simultaneity is a transitive or intransitive relation, and addressing this question would be a fruitful empirical endeavor.

Kelly's argument takes the imprecision of perceptual simultaneity as its starting point. It is indeed a well-known fact that when two stimuli are presented in a short temporal asynchrony, we judge them to be simultaneous. Depending on the nature of the stimuli, this window of simultaneity – temporal extension during which we cannot tell the temporal order of asynchronous stimuli – can range from few milliseconds to tens of milliseconds. Based on this imperfection of our perceptual processes, Kelly's argument focuses on situations where subjects are shown three or more asynchronous stimuli. One way to present it goes as follows.

Let us assume that a subject is shown three brief asynchronous stimuli (A, B, and C) such that the onset asynchrony between A and B is three quarters of the temporal window of simultaneity, and that this holds for B and C too. Accordingly, A and B, and B and C are judged to be simultaneous. But the onset asynchrony between A and C is 50% longer than the window of simultaneity. Hence, A and C are not perceptually simultaneous. Given that the relation of perceptual simultaneity holds between A and B, and between B and C, but not between A and C, perceptual simultaneity turns out to be an intransitive relation.

To make this more concrete, let us assume that the temporal window of simultaneity is 40 ms (although the exact number has no bearing on the success of the argument, this is close the lower limit of the estimations for visual simultaneity threshold). In this case A and B, and B and C could be presented 30 ms apart, and they are perceptually simultaneous. Nevertheless, A and C appear 60 ms apart, which makes them perceptually asynchronous.

The previous line of reasoning rests, however, on (at least thus far unjustified) assumption because the intransitivity of perceptual simultaneity does not follow by logical necessity from the imperfection of our perceptual processes to determine temporal relations between stimuli. To see this, consider Kelly's argument again. In order for the argument to get off the ground, three comparisons need to be established: while we perceive A and B as simultaneous, we also perceive B and C as simultaneous and A and C as non-simultaneous. For this to take place, the argument needs to entail that we can successfully make a number of simultaneity comparison that cover the same episodes of experiencing. If it turned out, for example, that the episode of experiencing B cannot be part of two simultaneity comparisons, one for A and B and the other for B and C, then the simultaneity of one of them cannot be established and at least one of the premises of the argument for intransitivity would lose its grounding. Kelly's argument is therefore based on a hidden *assumption of parallelity* according to which two or more simultaneity comparisons can partly cover the same moments of experiencing. (Because the simultaneity comparisons are done based on the information still lingering in our consciousness rather than, say, based on our memory of yesterday's events, the assumption of parallelity amounts roughly to the idea that we can do more than one simultaneity comparison before the information disappears.) If one holds the assumption opposite to the one that Kelly is making – *the assumption of seriality* according to which simultaneity comparisons cannot cover the same moments of experiencing – then there is no argument for the intransitivity.

It thus remains an open question whether perceptual simultaneity is transitive or not. Nevertheless, in addition to the general principle that one should not adopt any assumptions – especially those that may have significant consequences – without testing them, two experiments suggest that the assumption of parallelity along with the intransitivity of perceptual simultaneity may not hold. It is worth noticing that the following cases concern only visual modalities, and whether they can be extended to apply to other sensory modalities as well as to crossmodal simultaneity is an open question.

First, the issue whether the visual judgments of simultaneity are transitive or not has been explicitly tested by Corwin and Boynton (1968). Based on their results, they concluded that "[w]ithin the experimental

variability obtained, the transitivity relation was confirmed" (Corwin and Boynton, 1968, p. 560). Subsequently, their study provides support for the assumption of seriality and against the assumption of parallelity.

Second, rather than testing transitivity directly, one can also wonder what happens when more than two asynchronous stimuli are presented. An indication to this can be found from a study done by Lichtenstein (1961), where subjects were presented flashes in four locations with varying asynchronies between them (and then the cycle began again). The results showed that despite large onset asynchronies (up to 95 ms), all four flashes were perceived to be simultaneous. More precisely, they appeared to pulsate together in a manner that "no time difference among any of the pulsating dots is discernible" (Lichtenstein, 1961, p. 56). That is, adding more asynchronous stimuli to the comparison appeared to make the temporal window of simultaneity considerably wider than it is usually for visual stimuli. On the other hand, the pulsation of stimuli implies that after a critical period of time, one temporal window of simultaneity ends and another begins – meaning that perceptual contents are part of only one perceptual simultaneity comparison at a time as suggested by the assumption of seriality.

There are thus one explicit and one indirect reason to think that the transitivity and the assumption of seriality might be true. Such evidence is hardly conclusive, however, and therefore it remains an open question whether this is the case or not. In addition of merely settling the issue of transitivity, addressing this question would also be a fruitful way for testing the theoretical models of simultaneity judgments – something that would be lost if we simply assumed that perceptual simultaneity is transitive or intransitive. This is because the models put forward to explain our simultaneity judgments usually imply that perceptual simultaneity is either a transitive or an intransitive relation. Let me finish with examples of this.

When thinking about perceptual simultaneity, some psychologists have postulated an existence of a comparator that compares the arrival times of sensory messages produced by presented stimuli. It has a temporal resolution, a limit below which it cannot separate the temporal order of the stimuli and if the difference of sensory messages produced by some stimuli is below this threshold, the comparator regards them as simultaneous. It is worth noticing that the idea of comparator can be either understood literally (Efron, 1963) or merely as a useful theoretical construct to account our performance in simultaneity judgment tasks (Ulrich, 1987). Thus, even if there is no real simultaneity-comparator in the brain, the following models can be understood as providing different theoretical accounts of the key factors influencing how we come about judging that two stimuli are simultaneous.

One example of how this comparator could function originates from von Baer (1862) and was later revived by Stroud (1955). According to this *discrete moment hypothesis*, one temporal window of simultaneity (one perceptual moment) follows another in discrete fashion – when one temporal window ends, another one begins immediately. Everything that occurs (or is registered) within one perceptual moment is considered simultaneous, while everything outside of this perceptual moment is non-simultaneous. Because "belonging to a single perceptual moment" determines the perceptual simultaneity, and this relation is transitive, on this model perceptual simultaneity is also a transitive relation. The same also applies to the *triggered moment hypothesis* that resembles Stroud's proposal with the exception that here the comparator begins to do its task only when it has been triggered by a stimulus – temporal windows of simultaneity do not follow each other automatically in the absence of stimuli. Lichtenstein's (1961) results, in turn, suggest that the window of simultaneity is partly determined by the properties of the stimuli. Accordingly, they imply a model that is likely to be a version of the triggered model hypothesis. Unlike in other models discussed here though, the window of simultaneity is flexible. Thus it could be called *triggered flexible moment hypothesis*. Nevertheless, as mentioned above, here the perceptual simultaneity is a transitive relation. Allport (1968) *traveling moment hypothesis*, on the other hand, maintains that there is only one continuously moving perceptual moment. Because the perceptual moment moves continuously, two different perceptual moments can partly cover the same episode of experiencing in Allport's model. Consequently, this model is compatible with the assumption of parallelity and if it were correct, then perceptual simultaneity would turn out to be an intransitive relation. At this point it remains an open question which one of these models, if any, explain the empirical data best. For this reason, the issue of transitivity of perceptual simultaneity should be taken seriously because it would provide an additional way to separate these and similar models.

To sum up, all means of "measuring" are somewhat imprecise and our ability to determine asynchronies is not an exception. Accordingly, we can never know whether two events occurred exactly at the same time or not. Nevertheless, the intransitivity of perceptual simultaneity does not follow by logical necessity from this imperfection because it requires further that the assumption of parallelity is true – that two or more simultaneity comparisons can (partly) cover the same moments of experiencing. Moreover, the two discussed empirical studies bearing relevance on the matter suggest that that perceptual simultaneity may not be a transitive relation after all and thus that the assumption of parallelity is not true. On the other hand, as this evidence is not conclusive, conducting more research on the topic would be valuable.

ACKNOWLEDGMENTS

I am very grateful for Dr. Christine Falter for the countless stimulating discussions on the topic. I also want to thank the participants of "Neurobiology of Time Perception: from normality to dysfunction" satellite meeting at EBBS on Seville for their constructive and helpful comments. This work was supported by the Academy of Finland and a European Cooperation in Science and Technology (COST) action on Time in Mental Activity (TIMELY; TD0904).

REFERENCES

Allport, D. A. (1968). Phenomenal simultaneity and the perceptual moment hypothesis. *Br. J. Psychol.* 59, 395–406.

Corwin, T. R., and Boynton, R. M. (1968). Transitivity of visual judgments of simultaneity. *J. Exp. Psychol.* 78, 560–568.

Efron, R. (1963). The effect of handedness on the perception of simultaneity and temporal order. *Brain* 86, 261–284.

Elliott, M. A., Shi, Z., and Kelly, S. D. (2006). A moment to reflect upon perceptual synchrony. *J. Cogn. Neurosci.* 18, 1663–1665.

Kelly, S.D. (2005), "The puzzle of temporal experience," in *Cognition and the Brain: The Philosophy*

and Neuroscience Movement, eds A. Brook and K. Akins (Cambridge: Cambridge University Press), 218–248.

Lichtenstein, M. (1961). Phenomenal simultaneity with irregular timing of components of the visual stimulus. *Percept. Mot. Skills* 12, 47–60.

Stroud, J. (1955). "The fine structure of psychological time," in *Information Theory in Psychology*, Vol. 138, ed. H. Quastler (Glencoe, IL: Free Press), 623–631.

Ulrich, R. (1987). Threshold models of temporal-order judgments evaluated by a ternary response task. *Percept. Psychophys.* 42, 224–239.

von Baer, K. E. (1862). *Welche Auffassung der lebenden Natur ist die richtige? und Wie ist diese Auffassung auf die Entomologie anzuwenden?* Berlin: A. Hirschwald.

Received: 18 October 2011; accepted: 10 January 2012; published online: 31 January 2012.

*Citation: Arstila V (2012) Why the transitivity of perceptual simultaneity should be taken seriously. Front. Integr. Neurosci. **6**:3. doi: 10.3389/fnint.2012.00003*

frontiers in
INTEGRATIVE NEUROSCIENCE

ORIGINAL RESEARCH ARTICLE
published: 28 March 2012
doi: 10.3389/fnint.2012.00014

Perception of duration in the parvocellular system

Guido M. Cicchini*

Visual Psychophysics, Institute of Neuroscience, Consiglio Nazionale delle Ricerche, Pisa, Italy

Edited by:
Warren H. Meck, Duke University, USA

Reviewed by:
Virginie Van Wassenhove, Cognitive Neuroimaging Unit, France
Alan Johnston, University College London, UK

****Correspondence:***
Guido M. Cicchini, Visual Psychophysics, Institute of Neuroscience, Consiglio Nazionale delle Ricerche, Via Moruzzi, 1 - 56124 Pisa, Italy.
e-mail: cicchini@in.cnr.it

Both theoretical and experimental evidence suggests that duration perception is mediated preferentially by the color-blind but high temporally sensitive luminance pathway. In this experiment we tested whether color modulated stimuli and high spatial frequency luminance modulated stimuli, which are known to be relayed mostly by the slow parvocellular system, are able to elicit reliable sense of duration. We show that ramped color modulated stimuli seem to last less than luminance modulated stimuli matched for visibility. The effect is large, about 200 ms and is constant at all durations tested (range 500–1100 ms). However, high spatial frequency luminance stimuli obtain duration matches similar to those of low spatial frequency luminance modulated stimuli. The results at various levels of contrast and temporal smoothing indicate that equiluminant stimuli have higher contrast thresholds to activate the mechanisms which time visual stimuli. Overall the results imply that both the magnocellular and the parvocellular systems access reliably the timing mechanisms with a difference only in the way these are engaged.

Keywords: parvocellular, magnocellular, duration, distributed clocks, motion

INTRODUCTION

Despite subjective time is a perceptual dimension that transcends each sensory modality, recent evidence is showing that the estimation of brief temporal intervals is computed by multiple parallel temporal units deeply rooted in sensory processes (Buonomano and Merzenich, 1995; Ivry and Spencer, 2004; Mauk and Buonomano, 2004; Johnston et al., 2006; Johnston, 2010). Psychophysical results indicate that one first division for temporal processing regards events the modality which signals the event. Intervals in different modalities are processed with different sensitivities (Goodfellow, 1934; Grondin, 1993; Burr et al., 2009; Cicchini et al., 2012), undergo selective distortions (Yarrow et al., 2001; Morrone et al., 2005, 2010; Johnston et al., 2006; Binda et al., 2009), and can be calibrated one with the other (Fujisaki et al., 2004; Miyazaki et al., 2006; Stetson et al., 2006; van Wassenhove et al., 2008). In addition it is now becoming clear that even within the same modality multiple clocks exist. For instance, in vision adaptation to drifting gratings distorts events only in the adapted location (Johnston et al., 2006; Ayhan et al., 2009); similarly, if an interval is defined by two flashes in the same location, it is estimated correctly even when attention is draw away (Cicchini and Morrone, 2009). Not least perceived timing depends on very basic stimulus features (such as speed, contrast, size), indicating that the network for temporal processing extends to and is in partial overlap with purely sensory processes (Roelofs and Zeeman, 1951; Brown, 1995; Terao et al., 2008; Cicchini and Morrone, 2009). All of these notions go hand in hand with the concept that even small neuronal ensembles, not specialized for temporal processing, are able to encode the passage of time (Buonomano and Merzenich, 1995; Yamazaki and Tanaka, 2005; Karmarkar and Buonomano, 2007).

Within vision a further parcellation seems to occur. Among the multiple parallel visual channels, those that support temporal processing should be the ones best suited for visual transients. Consistently moving and flickering stimuli are perceived as lasting longer than static stimuli (Roelofs and Zeeman, 1951; Brown, 1995; Kanai et al., 2006; Kaneko and Murakami, 2009) and adaptation to high speed gratings induces a decrease of duration (Johnston et al., 2006; Burr et al., 2007; Ayhan et al., 2009).

The demand for fast and reliable temporal information about the environment seems to be met at retino-cortical level by the existence of the magnocellular visual pathway. Neurons along the magnocellular pathway have relatively large receptive fields and fast response properties (Livingstone and Hubel, 1988). These cells have also diphasic impulse response functions which are well suited to capture changes in visual stimuli and relay temporal information with good temporal resolution. The spatial frequency selectivity of magnocellular neurons is bandpass with a peak just below 1 cpd and a cut-off spatial frequency that ranges between 2 and 6 cpd depending on the temporal frequency of the stimulus (Derrington and Lennie, 1984) and its eccentricity (Alitto et al., 2011). Indeed, the selectivity for low spatial frequencies and high temporal frequencies suggests that the magnocellular information is crucial to perceive motion and rapid changing events (Livingstone and Hubel, 1988; Levitt et al., 2001; Leonova et al., 2003).

The other main subcortical pathway, the parvocellular one, seems much less suited for temporal processing with slower peak responses and low pass temporal characteristics. In agreement with physiology reaction times and VEP, responses to luminance modulated stimuli are faster than responses to equiluminant stimuli equated for contrast (Burr et al., 1998; Burr and Corsale, 2001; McKeefry et al., 2003). In terms of spatial selectivity neurons in the parvocellular pathway extend well beyond the frequencies of the magnocellular system and respond to up to 15–20 cpd for color and luminance defined gratings with a peak of sensitivity at around 10 cpd. Parvocellular neurons afferents are the most common input to visual cortex making up to 80% of visual afferent signals

and their putative role is to support finer aspects of visual analysis for tasks that are not demanding of high temporal resolution (Ingling Jr. and Martinez-Uriegas, 1983; Kaplan and Benardete, 2001; Gegenfurtner and Kiper, 2003).

All these lines of evidence indicate that magnocellular transmission has a primary role in mediating the fine temporal aspects of visual processing including onsets and offsets and when magnocellular transmission is impaired (like after adaptation or in dyslexia) temporal compression is expected (Johnston et al., 2006, 2008; Johnston, 2010; Ayhan et al., 2011).

In this study I tried to extend this notion by investigating perceived duration of stimuli relayed by the parvocellular pathway. I found that equiluminant stimuli are perceived as much shorter than luminance modulated stimuli with a constant difference at all durations in the range 500–1100 ms. Further experiments estimated the visibility threshold at which timing starts and stops and confirm that equiluminant and luminance modulated stimuli differ only in the way they engage timing mechanism but they share the mechanism which integrates the passage of time.

These results have been published in abstract form (Cicchini and Tomassini, 2008).

MATERIALS AND METHODS

PARTICIPANTS

Overall nine right-handed participants aged 20–32 (two men, seven women) took part in these experiments. All had normal or corrected-to-normal vision, and had no reported hearing deficits. The experimental procedures were approved by the Ethics Committee of Università Vita-Salute San Raffaele. All the subjects but the author were naive to the purpose of the experiment and gave informed consent to participate to the study.

APPARATUS

Subjects sat 57 or 228 cm away from a calibrated Silicon Graphics 21″ CRT Trinitron monitor running at a resolution of 800 × 600 pixels at a frame rate of 100 Hz. Stimuli were generated through a VSG 2/5 Graphics Card (Cambridge Research Systems) controlled via Matlab software and the VSG routines. The red phosphor had CIE coordinates of $x = 0.56$, $y = 0.34$, while the green phosphor had coordinates $x = 0.3$ and $y = 0.55$. Experiments were run in a dimly lit room.

EQUILUMINANCE

For each subject equiluminance point was determined via standard flicker photometry reversing at 15 Hz a 1 cpd Gabor patch with the maximum possible red gun modulation and a variable green to red luminance ratio. The subject adjusted the amplitude of the green color component until the percept of minimum flicker was obtained. The procedure was repeated five times and the green–red ratio yielding minimum flicker were averaged.

STIMULI

The stimuli for the time judgments were gratings windowed by a Gaussian of 3° of standard deviation presented at fixation. Achromatic stimuli were obtained putting in phase the red and green profiles of the underlying sinusoid. Color modulation was obtained putting in antiphase the two calibrated sinusoids. Overall three types of stimuli were employed, Achromatic 1 cpd, Chromatic 1 cpd, Achromatic of 8 cpd. The first type of stimulus should excite preferentially the magnocellular system, the latter two the parvocellular system.

TEMPORAL SMOOTHING

Since perception of duration is altered by the presence of changes and transitions, care was taken to ensure that both luminance and colored patches had a smooth onset and offset. For this reason the square wave temporal profile of the stimuli with a given nominal duration was smoothed with a Gaussian temporal window. In most experiments the Gaussian window had a σ of 100 ms. In one experiment, which tested directly the effect of stimulus ramping, the smoothing constant assumed values between 50 and 180 ms. Also with these shorter constants, the stimuli never yielded the percept of a brisk transient and duration matches were always made upon perceptually similar stimuli.

Throughout the paper stimuli are described in terms of their nominal duration (i.e., the duration of the underlying square wave). This quantity does not correspond necessarily to the time the stimulus exceeds detection threshold. A stimulus with a contrast barely above detection thresholds remains visible for less than the nominal duration. If the stimulus has a contrast of twice visibility thresholds, time above threshold equals nominal duration. At higher contrasts the time the stimulus is above threshold is longer than nominal duration (see **Figure 3A**). Indicatively at a contrast of 15 times the visibility threshold (which is a common choice throughout the work) a Gabor of nominal duration 1000 ms is above detection threshold for 1212 ms.

VISIBILITY THRESHOLDS

Visibility thresholds were measured with a standard 2 IFC procedure where two 3-s blocks (one empty, one containing a target stimulus) were presented in random order and subjects had to indicate which of the two contained a target. The target stimulus lasted 600 ms and was smoothed in time with a σ of 100 ms. Contrast was varied by a QUEST routine and data were fitted by a psychometric function. The point of passage through the 75% correct responses was taken as the visibility threshold for that type of stimulus.

Visibility thresholds serve as a unit for standardizing stimuli across subjects. All contrasts used in the paper are expressed in terms of "visibility" which is "multiples of the detection contrast." Visibility as such is a normalized physical quantity and bears no implication on the perceived contrast and or salience of the stimulus.

DURATION COMPARISON

In the duration comparison subjects were asked to compare the duration of two smoothed Gabors presented sequentially at fixation. One of the two stimuli, the "reference," was an achromatic Gabor of 1 cpd, 15 times the visibility level and had a fixed duration throughout an experimental session. The other stimulus, the "test," had visibility, color and spatial frequency which changed with the experimental condition. The duration of the "test" varied on every trial following a QUEST routine (Watson and Pelli, 1983) curtailed at 200 and 3000 ms. Duration matches have been

performed with several durations of the reference (from 500 to 1000 ms) and for each, a separate psychometric function has been drawn.

Each trial begun with a variable foreperiod (from 1000 to 2500 ms) in which only a small black fixation dot (1 pixel) was present at the center of a uniform yellow screen. Reference and test were then presented in random order separated by a pause of 1000–2500 ms. At the end of the second stimulus the subjects indicated which of the two stimuli had been presented longer. Each experimental session comprised about 40 trials and, on average, 200 trials per condition were collected.

The point of subjective equality (PSE) of the reference and test stimulus duration was estimated from the median of the best fitting cumulative Gaussian psychometric function. This value corresponds to how long the test stimulus has to be presented for in order to equate the reference stimulus. If the test stimulus is underestimated the match is obtained at longer exposures and matching durations are higher. The precision (i.e., JND) in the duration task was calculated as the difference between the third and first quartiles divided by 2.

Standard errors of PSE and JND were calculated via a bootstrap procedure which re-sampled with re-emission 500 times the set of stimulus–responses. The standard deviation of the re-sampled values yields an estimate of the standard error of the measurement (Efron and Tibshirani, 1994).

AUDIOVISUAL TEMPORAL ORDER JUDGMENT

In a separate experiment subjects were asked to compare the onset (or offset) of the test stimulus with respect to a brief auditory stimulus (a brief burst of white noise windowed by a Gaussian envelope of 5 ms standard deviation). In the case of the onset AVTOJ the pause preceding the stimulus ranged between 1000 and 2500 ms. In the case of the temporal offset judgment the duration of the grating varied at random between 500 and 1200 ms. The time between the auditory stimulus and the nominal beginning or end of the visual stimulus were selected by a QUEST routine. At least 60 trials were collected per condition and data were analyzed via fitting a cumulative Gaussian distribution and taking the median of the best fitting distribution.

MODELING CONTRAST DEPENDENCE

Duration matches for luminance modulated and equiluminant stimuli have been fitted with a simple clock model that is engaged when the stimulus attains a certain contrast. The clock's threshold is a free parameter and it has been assumed that the luminance and the color modulated stimuli may trigger timing with a separate threshold. Thus the whole dataset has been fitted with two free parameters.

The data fitting procedure analyzes first the achromatic dataset calculating first how much time the reference stimulus (15 times visibility) exceeds threshold and then how much time the test stimuli (of various contrasts) spend above threshold. The difference between the two values gives an estimate of how subjective duration should vary as function of contrast. The procedure is repeated for several candidate thresholds and the best fitting threshold for achromatic dataset is selected. The threshold for achromatic stimuli intrinsically provides also an estimate of how much time the reference stimulus (1 cpd Achromatic, 15 times visibility) engages the clock.

Data fitting is then performed on equiluminant stimuli calculating how much time a clock is engaged as function of visibility and assuming that this value is compared to the recorded duration of the achromatic reference. Predictions for several thresholds for color stimuli are compared and the best fitting value is chosen.

RESULTS

PERCEIVED DURATION IN THE MAGNOCELLULAR AND PARVOCELLULAR SYSTEMS

Figure 1 shows the results when subjects had to compare the duration of a color modulated stimulus to that of a reference luminance modulated stimulus. **Figures 1A,B** present the data for two illustrative subjects at various reference durations (red symbols). In both subjects the data points lie above the diagonal indicating that subjects needed a longer presentation of the color modulated stimulus to match the duration of a reference luminance modulated stimulus. This corresponds to a temporal underestimation of the color modulated stimulus. **Figure 1C** shows results for four subjects at two representative durations (500 and 1000 ms). On average the effect was 195 ms at 500 ms and 174 ms at 1000 ms [$F(3) = 13.6$, $p < 0.05$] and was not proportional to the base interval duration [$F(3) = 0.14$, $p > 0.7$].

Figures 1D–F report the precision of the temporal judgments as function of stimulus duration. JNDs increase with stimulus duration, complying with Weber's law for temporal judgments. On average color modulated stimuli yielded less precise judgments by 31 ms [$F(3) = 9.9$, $p = 0.05$]. This effect however is similar at the two base durations [28 ± 8 ms at 500 ms, 33 ± 8 ms at 1000 ms, $F(3) = 0.15$, $p > 0.7$] speaking against the idea that the increase of noise in the judgment is caused by the recruitment of a more noisy temporal integrator.

Interestingly the effect did not generalize to other stimuli relayed by the parvocellular pathway such as 8 cpd achromatic Gabors. **Figure 2** reports the results in a different subject pool which confirmed the effect with color modulated stimuli [185 ms across all durations, $t(4) = 9.9$ and 14.7 for the two base durations, both t-test $p < 0.01$] but found a much weaker effect for 8 cpd achromatic gratings (9 ms at 500 ms and 20 ms at 1000 ms, both t-test $p > 0.10$).

This suggests that some stimuli relayed by the parvocellular pathway are able to engage effectively temporal duration mechanisms.

CONTRAST THRESHOLD FOR TEMPORAL MARKERS

All the effects encountered so far are independent of stimulus duration and seem to indicate that the differences in perceived duration of equiluminant stimuli arise in the process of engaging and disengaging the timing mechanisms. In the remainder of the paper I present three complementary experiments that estimated the contrasts thresholds at which timing starts and stops.

Effect of stimulus visibility

The first technique was to measure perceived duration as function of contrast and comparing perceptual data with the predictions of a simple threshold model.

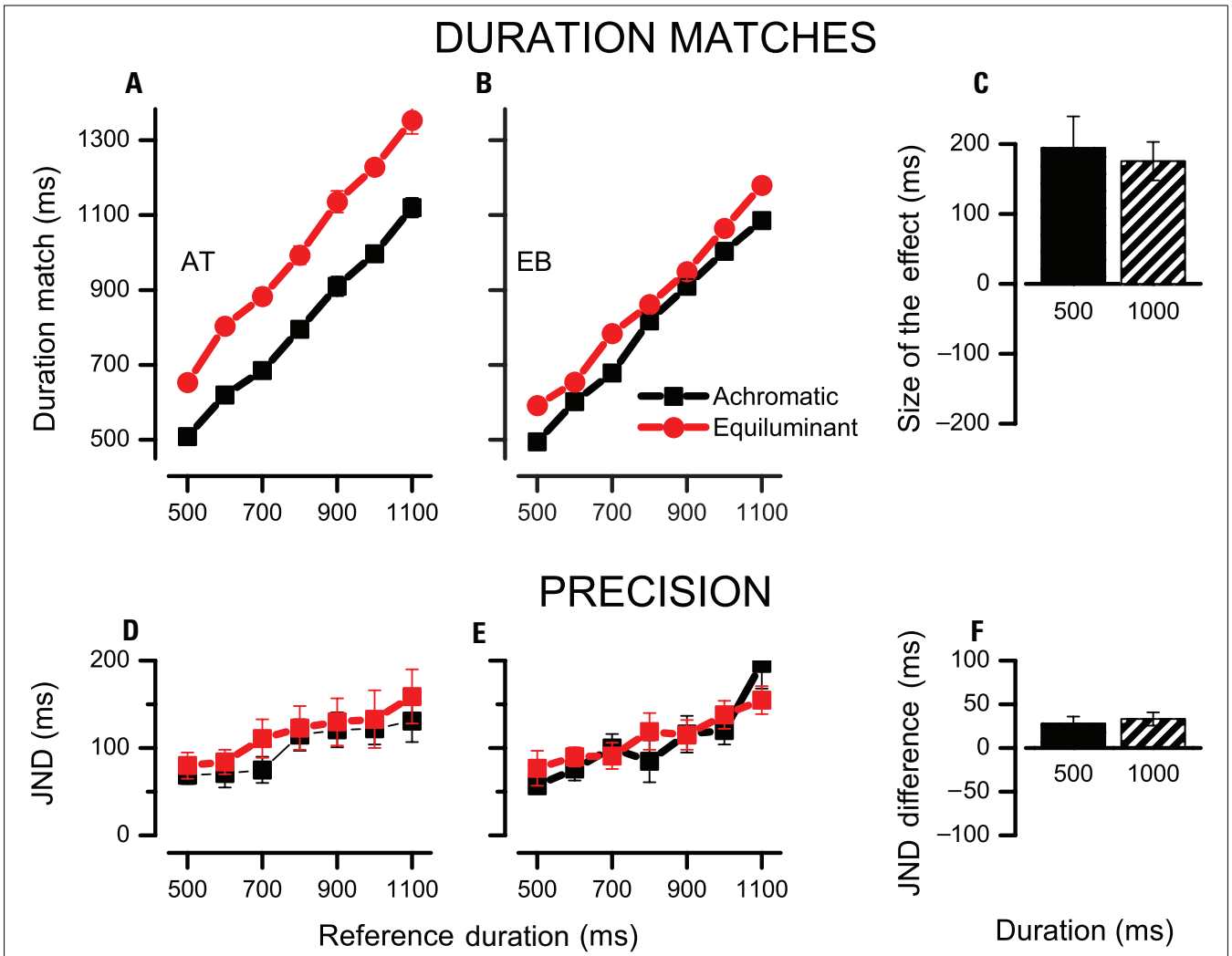

FIGURE 1 | Duration judgments for equiluminant and achromatic low spatial frequency stimuli. (A,B) Duration of the test stimulus required to match the reference stimulus in duration is plotted for several reference durations (red for equiluminant, black for achromatic, both low spatial frequency). Data lying above the diagonal indicate that the test stimulus was underestimated and required a longer presentation duration to yield a match. **(C)** Difference between equiluminant and achromatic matches at two reference durations averaged across four subjects. **(D,E)** JNDs of the duration judgment as function of reference duration. **(F)** Difference between the JNDs of achromatic and equiluminant judgments for 500 and 1000 ms intervals. Positive values indicate higher JNDs for achromatic stimuli. For individual data points error bars indicate the standard error calculated via bootstrap, for average data, bars indicate SEM.

Figure 3A illustrates how the interval recorded by a clock varies as function of visibility and the clock threshold. High contrast stimuli pass more time above threshold than low contrast stimuli. Due to temporal smoothing, the modulation can be quite large, up to several hundred milliseconds especially at higher clock thresholds (see dashed lines).

Figures 3B,C data points show duration matches for achromatic and color modulated stimuli of 1 cpd at various visibility levels (i.e., multiples of detection contrast). At lower contrasts both achromatic and color modulated stimuli require longer presentations indicating that lowering the contrast decreases perceived duration.

Figures 3B,C overlay on raw data the predictions of models which start timing at different visibility levels. Interestingly a simple model which starts timing at detection (gray curves) captures just coarsely the relationship between duration and visibility levels ($R^2 = 0.73$ and 0.84). Models which assume higher thresholds fare better ($R^2 = 0.98$ and 0. 99). The thresholds which fit best the achromatic dataset assume that timing is engaged at 3.3 and 2.5 visibility contrast for the subjects GMC and OS respectively (black curves). Best fitting values for equiluminant stimuli are obtained assuming that clock thresholds are 7.3 and 8.2 times detection thresholds ($R^2 = 0.96$ and 0.95).

In the case of equiluminant stimuli the model captures well human performance only between moderate and high contrasts. This is because a threshold model predicts that when contrast approaches the clock threshold, a very dramatic decrease of perceived duration should be found. Indeed at contrasts

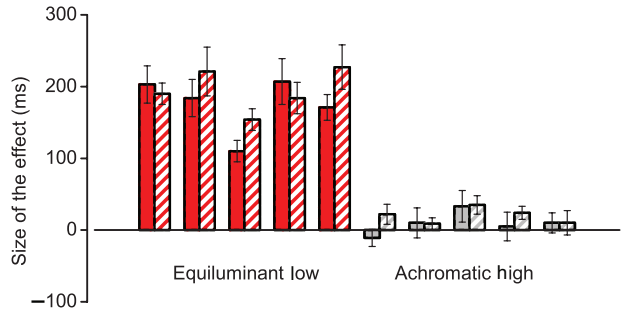

FIGURE 2 | Duration bias for stimuli relayed in the parvocellular pathway. Difference between test stimulus and reference stimulus matches for two types of stimuli relayed by the parvocellular pathway. Positive values indicate an underestimation of the test stimulus. Red bars are individual data for equiluminant low spatial frequency stimuli and gray bars for achromatic high spatial frequency stimuli. Solid and hatched bars refer to matches obtained with reference stimuli of 500 and 1000 ms respectively. Error bars indicate bootstrap standard errors.

lower than clock threshold, such a model predicts that subjects should not even be able to do the task. In these suboptimal conditions it is likely that alternative timing strategies may come into play.

It is also interesting to compare the data to a model which assumes that equiluminant and achromatic stimuli are timed with the same criteria (i.e., thresholds) and that all the difference relies on a fixed bias. Such fits can be obtained adding 220 and 280 ms to the luminance curves but provide just rough fits to the data ($R^2 = 0.68$ and 0.63 for the two subjects).

Effect of temporal smoothing

The data presented so far indicate that the timing mechanisms may be triggered at different visibility levels depending on the type of stimulus. Here we try to reinforce this conclusion with a technique that does not require the collection over a large range of contrast and potentially different levels of salience.

This technique exploits a basic property of smoothed stimuli whereby a stimulus that has a peak contrast twice the clock's threshold engages the clock for the same time independently of temporal smoothing. This invariance point is flanked by two regions with opposite behaviors. At lower contrasts (**Figure 4A**), the stimulus with more temporal smoothing (orange) engages the clock for very little and should be perceived as shorter. At higher contrasts (i.e., above two clock thresholds, **Figure 4B**) the stimulus with more smoothing engages the clock for more time and is perceived as longer. Indeed the transition from a region where more smoothing is more time to a region where more smoothing is less time indicates that the indifference point has been crossed. Interestingly the estimate remains valid even if a low pass perceptual stage adds onto the temporal smoothing embedded in the stimulus.

Figures 4C,D present the results for luminance modulated stimuli for two subjects. In both subjects a stimulus contrast of three visibility limens is below the invariance point of twice the clock' threshold and the stimuli with less temporal smoothing are those which are perceived as longer. However as soon as the contrast is increased to five or six visibility limens, the stimuli with higher temporal smoothing begin to be perceived as longer indicating that the threshold has been exceeded. Spline interpolation among the data points indicate that point where the two curves cross (i.e., the invariance point) amounts to 4.26 and 5.82 for the two subjects, indicating that clock threshold for achromatic stimuli is between 2 and 3 visibility thresholds.

The results for the color modulated stimuli are presented in **Figures 4E,F**. In this case the critical value corresponding to twice the clock's threshold is higher: 10.8 and 12.5 for subjects GMC and OS. This indicates that the clock's threshold for colored stimuli is comprised between five and six visibility thresholds, a much larger value than luminance stimuli threshold.

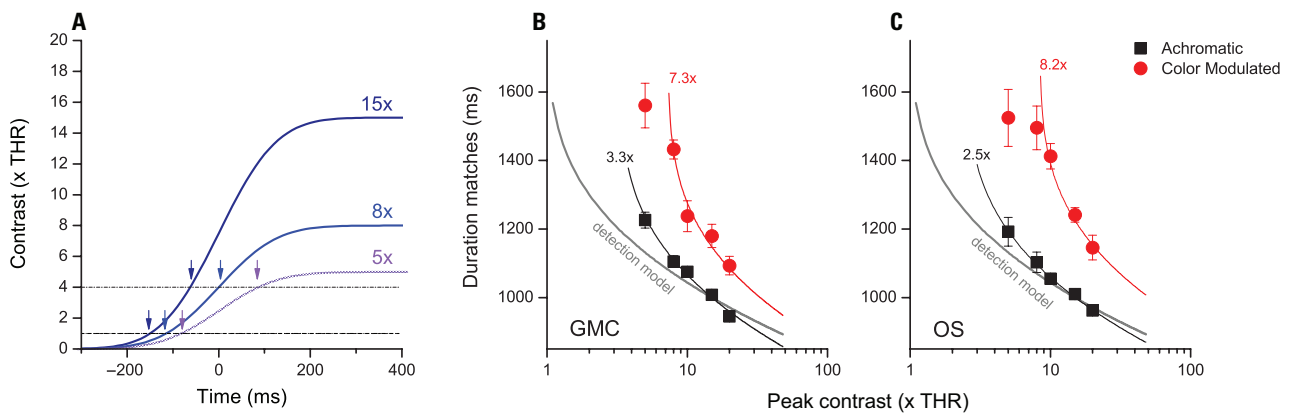

FIGURE 3 | Matching durations as function of stimulus contrast. **(A)** Illustration of how timed interval varies as function of visibility and clock contrast threshold. Blue lines illustrate the temporal profile of stimuli of different contrast (from 15× visibility thresholds to 5×). Dashed and dash-dot lines illustrate two sample clock thresholds (1× and 4×). Arrows indicate the moment at which timing is engaged. **(B,C)** Duration estimates that match the duration of a 1000-ms achromatic reference stimulus are shown for achromatic (black) and color modulated (red) test stimuli. The solid gray line indicates the predictions from a model where timing starts at detection. Continuous black and red lines indicate best fits provided by a model with separate thresholds for achromatic and color modulated stimuli.

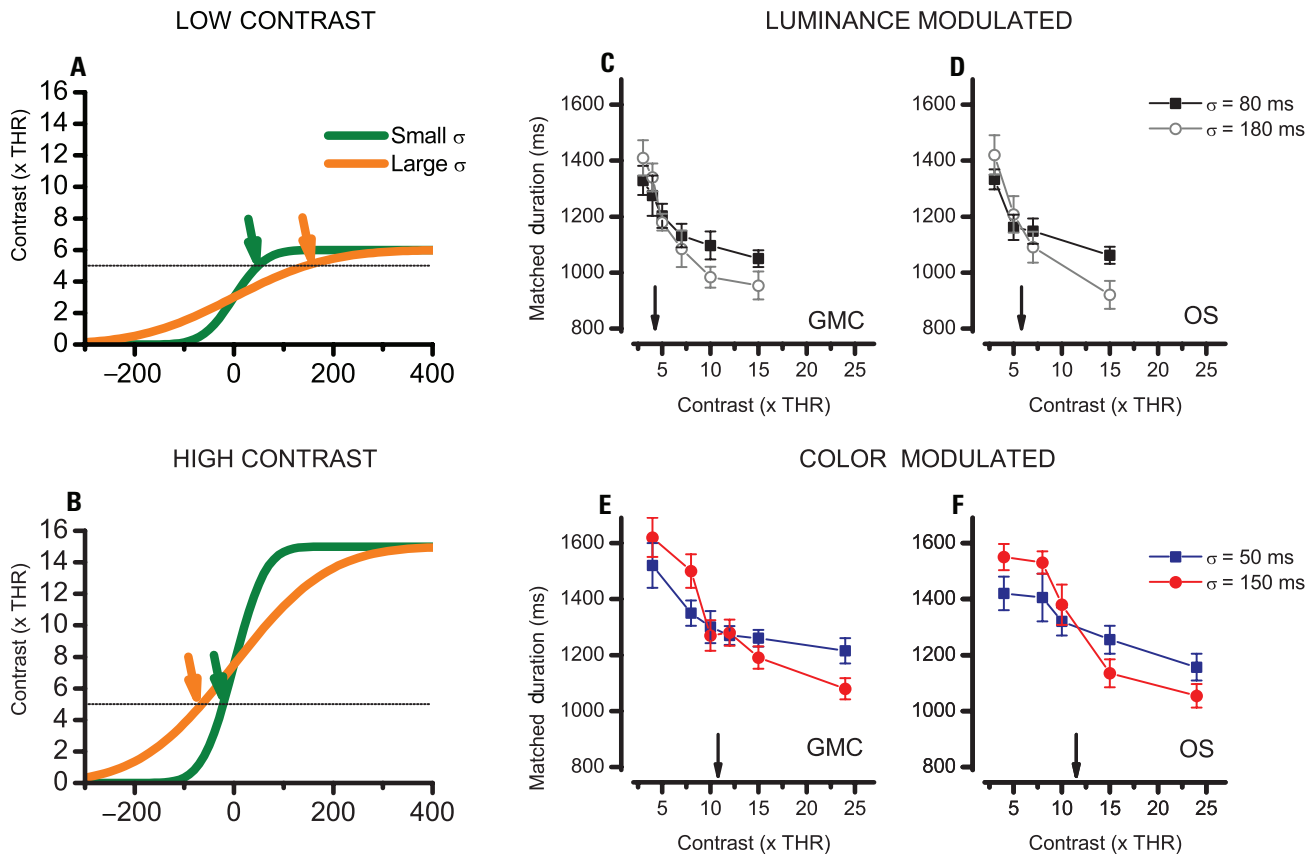

FIGURE 4 | Perceived duration for stimuli with different temporal smoothing. (A,B) Onset profiles of two stimuli with different smoothing constants (green, $\sigma = 50$ ms; orange, $\sigma = 150$ ms) along with a hypothetical clock threshold of four visibility thresholds (dashed). **(A)** Test stimulus with low contrast (six visibility thresholds). **(B)** Stimulus of high contrast (15 visibility thresholds). In the case of high contrast, stimuli which have a higher smoothing constant (orange) exceed threshold for more time than stimuli with less smoothing. The effect reverses when peak contrast is just barely above the clock's threshold. **(C–F)** Duration matches for two stimuli with different temporal smoothing measured at various peak contrasts. The arrows indicate a peak contrast at which duration is invariant of temporal smoothing which corresponds to twice the clock threshold. **(C,D)** Data for 1 cpd achromatic stimuli in two subjects. **(E,F)** Data for 1 cpd color modulated stimuli in two subjects.

Audiovisual temporal order judgment

One last procedure to assess the properties of the mechanism which start and stop the integration of time has been a multimodal judgment where the subjects compare the timing of the onset or offset of the visual stimulus to a reference brief auditory tone. **Figure 5A** shows the average PSE for the Onset Audio Visual TOJ and **Figure 5B** shows the results for the Offset AVTOJ for two subjects. The data indicate that the onset of luminance modulated stimulus is timed much earlier than the onset of the color modulated stimulus. On the other hand the offset of the two stimuli yield similar estimated timings.

Although a direct comparison with duration matching experiments is not possible this result indicates that the difference in processing the temporal markers is in the same ballpark as the duration compression. On a face value the temporal distortion seems asymmetric and somewhat questions the idea of a common threshold for onset and offset detection. However, it must be considered that the color modulated stimuli are relayed via a channel that has sluggish dynamics and this may introduce a delay in the overall response. To illustrate the point I have simulated the response to a 1000-ms stimulus of two filters having the dynamics of the luminance and color pathways as inferred from the literature (Burr and Morrone, 1996; **Figure 5C**, continuous black and red lines). Interestingly, when we employ the thresholds inferred from previous procedures one obtains a pattern of results similar to the experimental data. The onset of colored stimuli is delayed both due to a sluggish response and to a higher clock threshold. At the offset the two factors work against each other and predict similar perceived offsets for luminance and colored stimuli (**Figure 5C**, arrows).

DISCUSSION

In this work I have explored the mechanisms that mediate the duration of stimuli relayed via the parvocellular pathway. In a first set of data I reported that color modulated stimuli last less than luminance modulated stimuli of equal visibility. The effect is quite large with an average difference of 185 ms in favor of luminance modulated stimuli. At odds with other forms of duration compression like those induced by attentional decrement or by adaptation (Johnston et al., 2006; Cicchini and Morrone, 2009)

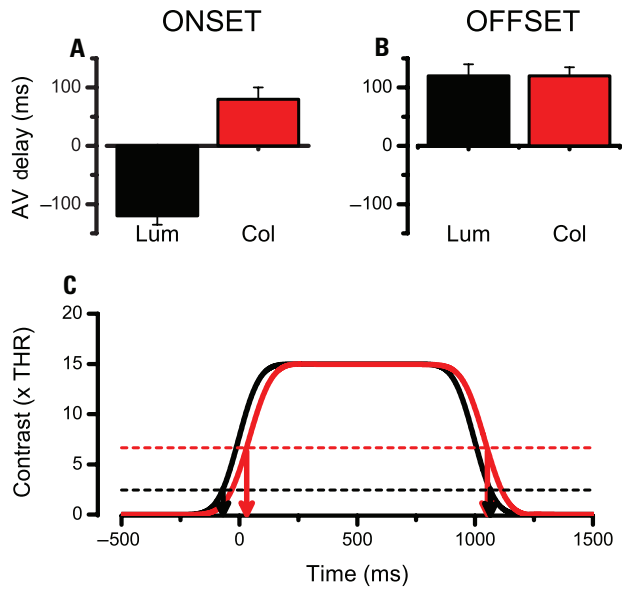

FIGURE 5 | Perceived onset and offset of the visual stimulus as measured with an AVTOJ. (A,B) Average perceived onset and offset of a luminance modulated stimulus (black) or a color modulated stimulus (red) for two subjects. Positive values indicate that a sound had to be presented after the visual event to be perceived as simultaneous. Hence positive values correspond to the visual event to be perceived after its nominal occurrence. **(C)** Illustration of how a higher threshold for color modulated stimuli combined with more sluggish relay of visual information predicts a great effect at the onset and a very small effect at the offset (see text for more details).

the bias is constant at all durations tested. This suggests that the difference arises more in the mechanisms that delimit the stimulus than those that integrate the passage of time.

The effect seems to be specific for color modulated stimuli and does not occur for other stimuli conveyed by the parvocellular system such as high spatial frequency luminance modulated gratings. This indicates that both the magnocellular and the parvocellular systems are able to produce reliable temporal estimates provided that they are engaged by suitable stimuli.

These conclusions presented here bear upon the assumption that 1 cpd equiluminant gratings and 8 cpd achromatic gratings are able to excite exclusively the parvocellular pathway. At present some controversy exists on the possibility to obtain such selective responses. In particular monkey recordings show that gratings of 8 cpd drifting at 4 Hz, even if not optimally, may still drive a subpopulation of 5–10% of magnocellular neurons (Levitt et al., 2001; Alitto et al., 2011). One main difference between those studies and the present one is temporal frequency: in most neurophysiological recordings a temporal frequency of 4 Hz is employed, here the stimulus which is sustained and filtered by a temporal Gaussian has a spectrum well contained below 2 Hz. Physiological data on such fine conditions are scarce, but some evidence indicates that at lower temporal frequencies, spatial cut-off frequencies of magnocellular neurons is lower with responses stopping at about 2–3 cpd (see Figure 13 in Derrington and Lennie, 1984). In addition studies in humans show that achromatic contrast sensitivity is mediated by magnocellular neurons only up to 2 cpd and by parvocellular neurons from 4 cpd onward (Leonova et al., 2003). In any case, even considering the highest spatial cut-off frequencies, it is quite clear that 8 cpd luminance gratings are much less optimal than 1 cpd gratings in engaging the magnocellular system and if duration perception were mediated only by magnocellular neurons one should still have expected a large difference between 1 and 8 cpd.

One of the most prominent differences between magnocellular and parvocellular responses are their temporal impulse response functions (Morrone et al., 2005; Schutz et al., 2009). In particular, the parvocellular neurons have high temporal integration constants and operate as low pass temporal filters. However, simple simulations show that the stimulus which is filtered with longer constants (i.e., the parvocellular) is more smeared in time and thus it should be perceived as longer. This indicates that by itself temporal smoothing cannot explain the results reported here.

One simple explanation for the difference in perceived duration for the two types of stimuli is to postulate that the measurement of duration is engaged at different visibility levels for the two stimuli. In the paper the three techniques employed all suggest that timing of color modulated stimuli starts at higher visibility levels than timing of luminance modulated stimuli.

The first evidence is based on the dependence of perceived duration upon stimulus visibility. Data collected in a wide range of contrasts indicated that perceived duration decreases at lower contrasts consistent with the idea that timing starts only at a given visibility level. Best fitting curves for the 1 cpd achromatic and the 1 cpd color modulated stimulus yield different clock thresholds, about two detection thresholds for the achromatic and six detection thresholds for the equiluminant stimulus. This model not only predicted well the experimental data (average $R^2 = 0.95$) but also fared better than a model assuming a constant bias between the two types of stimuli ($R^2 = 0.65$).

A second technique exploited the property that when the contrast of the stimuli is twice that necessary for timing, the duration estimates are the same regardless of smoothing of the onset and of offset. This procedure yields reliable clock thresholds estimates which are independent of temporal smoothing (even those introduced by visual analysis), stimulus type and visual salience. Also in this case the threshold for color modulated events was estimated to be three times that for achromatic stimuli.

Finally I employed audiovisual temporal order judgment. These results indicated that the decrease of perceived duration of the color modulated stimuli can be ascribed to a mislocalization of the event markers. The difference is not symmetrical and resides mostly at the onset of visual stimuli. This is probably because at stimulus onset the sluggish response to colored stimuli adds up to the effect of a higher threshold.

Overall the simple hard threshold model has been quite successful in predicting perception of duration in a variety of tasks. Whereas in general perceived duration may depend on factors such as alertness, stimulus complexity and the like, these data indicate that the difference in duration of achromatic and chromatic stimuli depends almost entirely by way the onset and the offset of the stimulus are timed.

Interestingly the effect reported here shares many similarities with reaction times to equiluminant stimuli (Burr et al., 1998; Burr and Corsale, 2001; McKeefry et al., 2003). Reaction times to equiluminant stimuli are about 200 ms slower than to luminance modulated stimuli of equal visibility, very similarly to what happens for the onset of visual stimuli. Burr and Corsale (2001) have proposed an explanation for these differences based on different gain mechanisms along the magnocellular and parvocellular pathways with the former saturating at lower contrast values and the latter proceeding more linearly. Indeed a difference in gain at low visibility levels is compatible with the idea that achromatic stimuli engage the clock at low visibility levels whilst equiluminant stimuli do not engage the clock up to higher contrasts.

The bulk of these results indicates that luminance modulated stimuli are more effective in engaging temporal mechanisms. This division does not correspond to the division of visual afferents into magnocellular and parvocellular pathways and is well modeled assuming different contrast thresholds for timing the two types of stimuli.

ACKNOWLEDGMENTS

This research was supported by the ERC grants FP6-MEMORY and FP7-STANIB. The author would like to thank Alice Tomassini and Ottavia Silva for help in data collection and Maria Concetta Morrone for helpful discussions on the experimental design. Special thanks go to David Murphy and Eckart Zimmermann for reading an early version of the manuscript.

REFERENCES

Alitto, H. J., Moore, B. D. T., Rathbun, D. L., and Usrey, W. M. (2011). A comparison of visual responses in the lateral geniculate nucleus of alert and anaesthetized macaque monkeys. *J. Physiol.* 589, 87–99.

Ayhan, I., Bruno, A., Nishida, S., and Johnston, A. (2009). The spatial tuning of adaptation-based time compression. *J. Vis.* 9, 2.1–2.12.

Ayhan, I., Bruno, A., Nishida, S., and Johnston, A. (2011). Effect of the luminance signal on adaptation-based time compression. *J. Vis.* 11, 22.

Binda, P., Cicchini, G. M., Burr, D. C., and Morrone, M. C. (2009). Spatiotemporal distortions of visual perception at the time of saccades. *J. Neurosci.* 29, 13147–13157.

Brown, S. (1995). Time, change, and motion: the effects of stimulus movement on temporal perception. *Percept. Psychophys.* 57, 105–116.

Buonomano, D. V., and Merzenich, M. M. (1995). Temporal information transformed into a spatial code by a neural network with realistic properties. *Science* 267, 1028–1030.

Burr, D., Silva, O., Cicchini, G. M., Banks, M. S., and Morrone, M. C. (2009). Temporal mechanisms of multimodal binding. *Proc. Biol. Sci.* 276, 1761–1769.

Burr, D., Tozzi, A., and Morrone, M. C. (2007). Neural mechanisms for timing visual events are spatially selective in real-world coordinates. *Nat. Neurosci.* 10, 423–425.

Burr, D. C., and Corsale, B. (2001). Dependency of reaction times to motion onset on luminance and chromatic contrast. *Vis. Res.* 41, 1039–1048.

Burr, D. C., Fiorentini, A., and Morrone, C. (1998). Reaction time to motion onset of luminance and chromatic gratings is determined by perceived speed. *Vis. Res.* 38, 3681–3690.

Burr, D. C., and Morrone, M. C. (1996). Temporal impulse response functions for luminance and colour during saccades. *Vis. Res.* 36, 2069–2078.

Cicchini, G. M., Arrighi, R., Cecchetti, L., Giusti, M., and Burr, D. C. (2012). Optimal encoding of interval timing in expert percussionists. *J. Neurosci.* 32, 1056–1060.

Cicchini, G. M., and Morrone, M. C. (2009). Shifts in spatial attention affect the perceived duration of events. *J. Vis.* 9, 9.1–9.13.

Cicchini, G. M., and Tomassini, A. (2008). Perception of duration in the parvocellular system. *Perception* 37, 69.

Derrington, A. M., and Lennie, P. (1984). Spatial and temporal contrast sensitivities of neurones in lateral geniculate nucleus of macaque. *J. Physiol.* 357, 219–240.

Efron, B., and Tibshirani, R. J. (1994). *An Introduction to the Bootstrap.* New York: Chapman & Hall/CRC.

Fujisaki, W., Shimojo, S., Kashino, M., and Nishida, S. (2004). Recalibration of audiovisual simultaneity. *Nat. Neurosci.* 7, 773–778.

Gegenfurtner, K. R., and Kiper, D. C. (2003). Color vision. *Annu. Rev. Neurosci.* 26, 181–206.

Goodfellow, L. D. (1934). An empirical comparison of audition, vision, and touch in the discrimination of short intervals of time. *Am. J. Psychol.* 46, 243–258.

Grondin, S. (1993). Duration discrimination of empty and filled intervals marked by auditory and visual signals. *Percept. Psychophys.* 54, 383–394.

Ingling, C. R. Jr., and Martinez-Uriegas, E. (1983). The relationship between spectral sensitivity and spatial sensitivity for the primate r-g X-channel. *Vis. Res.* 23, 1495–1500.

Ivry, R. B., and Spencer, R. M. (2004). The neural representation of time. *Curr. Opin. Neurobiol.* 14, 225–232.

Johnston, A. (2010). "Modulation of time perception by visual adaptation," in *Attention and Time*, eds. K. Nobre and J. Coull (New York, NJ: Oxford University Press), 187–200.

Johnston, A., Arnold, D. H., and Nishida, S. (2006). Spatially localized distortions of event time. *Curr. Biol.* 16, 472–479.

Johnston, A., Bruno, A., Watanabe, J., Quansah, B., Patel, N., Dakin, S., and Nishida, S. (2008). Visually-based temporal distortion in dyslexia. *Vis. Res.* 48, 1852–1858.

Kanai, R., Paffen, C. L., Hogendoorn, H., and Verstraten, F. A. (2006). Time dilation in dynamic visual display. *J. Vis.* 6, 1421–1430.

Kaneko, S., and Murakami, I. (2009). Perceived duration of visual motion increases with speed. *J. Vis.* 9, 14.

Kaplan, E., and Benardete, E. (2001). The dynamics of primate retinal ganglion cells. *Prog. Brain Res.* 134, 17–34.

Karmarkar, U. R., and Buonomano, D. V. (2007). Timing in the absence of clocks: encoding time in neural network states. *Neuron* 53, 427–438.

Leonova, A., Pokorny, J., and Smith, V. C. (2003). Spatial frequency processing in inferred PC- and MC-pathways. *Vis. Res.* 43, 2133–2139.

Levitt, J. B., Schumer, R. A., Sherman, S. M., Spear, P. D., and Movshon, J. A. (2001). Visual response properties of neurons in the LGN of normally reared and visually deprived macaque monkeys. *J. Neurophysiol.* 85, 2111–2129.

Livingstone, M., and Hubel, D. (1988). Segregation of form, color, movement, and depth: anatomy, physiology, and perception. *Science* 240, 740–749.

Mauk, M. D., and Buonomano, D. V. (2004). The neural basis of temporal processing. *Annu. Rev. Neurosci.* 27, 307–340.

McKeefry, D. J., Parry, N. R., and Murray, I. J. (2003). Simple reaction times in color space: the influence of chromaticity, contrast, and cone opponency. *Invest. Ophthalmol. Vis. Sci.* 44, 2267–2276.

Miyazaki, M., Yamamoto, S., Uchida, S., and Kitazawa, S. (2006). Bayesian calibration of simultaneity in tactile temporal order judgment. *Nat. Neurosci.* 9, 875–877.

Morrone, M. C., Cicchini, M., and Burr, D. C. (2010). Spatial maps for time and motion. *Exp. Brain Res.* 206, 121–128.

Morrone, M. C., Ross, J., and Burr, D. (2005). Saccadic eye movements cause compression of time as well as space. *Nat. Neurosci.* 8, 950–954.

Roelofs, C. O., and Zeeman, W. P. C. (1951). Influence of different sequences of optical stimuli on the estimation of duration of a given interval of time. *Acta Psychol.* 8, 89–128.

Schutz, A. C., Braun, D. I., and Gegenfurtner, K. R. (2009). Improved visual sensitivity during smooth pursuit eye movements: temporal and spatial characteristics. *Vis. Neurosci.* 26, 329–340.

Stetson, C., Cui, X., Montague, P. R., and Eagleman, D. M. (2006). Motor-sensory recalibration leads to an illusory reversal of action and sensation. *Neuron* 51, 651–659.

Terao, M., Watanabe, J., Yagi, A., and Nishida, S. (2008). Reduction of stimulus visibility compresses apparent time intervals. *Nat. Neurosci.* 11, 541–542.

van Wassenhove, V., Buonomano, D. V., Shimojo, S., and Shams, L. (2008). Distortions of subjective

time perception within and across senses. *PLoS ONE* 3, e1437. doi: 10.1371/journal.pone.0001437

Watson, A. B., and Pelli, D. G. (1983). QUEST: a Bayesian adaptive psychometric method. *Percept. Psychophys.* 33, 113–120.

Yamazaki, T., and Tanaka, S. (2005). Neural modeling of an internal clock. *Neural Comput.* 17, 1032–1058.

Yarrow, K., Haggard, P., Heal, R., Brown, P., and Rothwell, J. C. (2001). Illusory perceptions of space and time preserve cross-saccadic perceptual continuity. *Nature* 414, 302–305.

Conflict of Interest Statement: The author declares that the research was conducted in the absence of any commercial or financial relationships that could be construed as a potential conflict of interest.

Received: 29 June 2011; paper pending published: 18 July 2011; accepted: 14 March 2012; published online: 28 March 2012.

Citation: Cicchini GM (2012) Perception of duration in the parvocellular system. Front. Integr. Neurosci. ***6****:14. doi: 10.3389/fnint.2012.00014*

frontiers in
INTEGRATIVE NEUROSCIENCE

ORIGINAL RESEARCH ARTICLE
published: 12 September 2011
doi: 10.3389/fnint.2011.00051

Perceived duration of visual and tactile stimuli depends on perceived speed

Alice Tomassini[1]*, Monica Gori[1], David Burr[2,3], Giulio Sandini[1] and Maria Concetta Morrone[1,4,5]

[1] *Department of Robotics, Brain and Cognitive Sciences, Istituto Italiano di Tecnologia, Genova, Italy*
[2] *Dipartimento di Psicologia, Università Degli Studi di Firenze, Florence, Italy*
[3] *Istituto di Neuroscienze del Consiglio Nazionale delle Ricerche, Pisa, Italy*
[4] *Dipartimento di Scienze Fisiologiche, Facolta' di Medicina, Universita'di Pisa, Pisa, Italy*
[5] *Fondazione Stella Maris, Pisa, Italy*

Edited by:
Warren H. Meck, Duke University, USA

Reviewed by:
Christine M. Falter, University of Oxford, UK
Simon Grondin, Université Laval, Canada

****Correspondence:***
Alice Tomassini, Department of Robotics, Brain and Cognitive Sciences, Istituto Italiano di Tecnologia, Via Morego, 30, Genova, 16163, Italy.
e-mail: alice.tomassini@iit.it

It is known that the perceived duration of visual stimuli is strongly influenced by speed: faster moving stimuli appear to last longer. To test whether this is a general property of sensory systems we asked participants to reproduce the duration of visual and tactile gratings, and visuo-tactile gratings moving at a variable speed (3.5–15 cm/s) for three different durations (400, 600, and 800 ms). For both modalities, the apparent duration of the stimulus increased strongly with stimulus speed, more so for tactile than for visual stimuli. In addition, visual stimuli were perceived to last approximately 200 ms longer than tactile stimuli. The apparent duration of visuo-tactile stimuli lay between the unimodal estimates, as the Bayesian account predicts, but the bimodal precision of the reproduction did not show the theoretical improvement. A cross-modal speed-matching task revealed that visual stimuli were perceived to move faster than tactile stimuli. To test whether the large difference in the perceived duration of visual and tactile stimuli resulted from the difference in their perceived speed, we repeated the time reproduction task with visual and tactile stimuli matched in apparent speed. This reduced, but did not completely eliminate the difference in apparent duration. These results show that for both vision and touch, perceived duration depends on speed, pointing to common strategies of time perception.

Keywords: time perception, multisensory integration, vision, touch, motion

INTRODUCTION

Any sensory experience, regardless of the modality of the stimulus – visual, auditory, or tactile – is defined within a temporal interval. Stimuli of different sensory modalities are all mapped along the same temporal dimension, allowing us to order events in time as well as to judge their relative duration. The most immediate and intuitive comprehension of time is therefore that of a universal dimension that transcends each specific sensory modality. The idea that our brain is endowed with a unique and centralized clock has dominated the research on time perception for many years (Treisman, 1963; Gibbon et al., 1997). Emerging evidence suggests, however, that the analysis of temporal information may have modality-specific components (e.g., Gamache and Grondin, 2010) and may be intimately embedded within local sensory processing. It has been shown that perceived time can be distorted by means of local sensory adaptation both in the visual (Johnston et al., 2006; Burr et al., 2007) and, most recently, in the tactile domain (Tomassini et al., 2010; Watanabe et al., 2010). Moreover, modality-specific temporal distortions have been documented around the time of saccadic eye movements (Morrone et al., 2005). Multiple and distributed mechanisms, though likely constrained by similar computational principles, may thus underlie timing functions within different sensory modalities.

That no dedicated system exists for perceiving time, at least in the sub-second range, would also explain the ease with which many non-temporal, low-level properties of the stimuli – such as visibility (Terao et al., 2008), size (Xuan et al., 2007), temporal frequency (Kanai et al., 2006; Khoshnoodi et al., 2008), and speed (Kaneko and Murakami, 2009) – can alter perceived time. The strong influence of stimulus motion on apparent duration has long been recognized (Lhamon and Goldstone, 1975; Brown, 1995), although its neural bases and functional significance remain unknown. So far, the relationship between these two perceptual attributes has been uniquely studied within the visual system, showing that faster moving stimuli appear to last longer.

This motion-induced temporal illusion is well suited to investigate the properties of timing mechanisms within and across sensory modalities. Recent evidence suggests that visual and tactile motion processing share much in common (e.g., Pei et al., 2011): for example visual and tactile motion are subject to similar illusions (Harrar and Harris, 2007; Watanabe et al., 2007; Bicchi et al., 2008), show cross-modal interactions (Bensmaia et al., 2006; Craig, 2006; Konkle et al., 2009), multisensory facilitation (Gori et al., 2011), and seem to have partially overlapping neural substrates (Hagen et al., 2002; Ricciardi et al., 2004).

One remarkable feature, that has no counterpart in the spatial domain, is that not only do different sensory modalities show different temporal resolutions (as in space) but they can also provide different estimates for the temporal properties of sensory events (Grondin, 2003; van Erp and Werkhoven, 2004). It is well

known, for example, that auditory tones are perceived to last longer than visual flashes of the same physical length (Walker and Scott, 1981; Wearden et al., 1998; Harrington et al., 2011). Given the importance of accurate timing for multiple perceptual, motor, and cognitive functions, a relevant but poorly investigated question is how the brain deals with these inter-sensory discrepancies in temporal estimates and ultimately provides a combined percept of event duration.

THE BAYESIAN FRAMEWORK FOR MULTISENSORY INTEGRATION

In recent years the Bayesian statistical approach has been successful in providing a quantitative prediction of the effects of inter-sensory signal combination in many perceptual domains (Ernst and Banks, 2002; Ernst and Bülthoff, 2004). Optimal Bayesian integration of multiple sensory signals requires each source of information to be weighted by its relative reliability so that the most probable, though sometimes erroneous, perceptual estimate is obtained with the less uncertainty (see Eqs 1–4 in the Materials and Methods). The so-called "ventriloquist effect" illustrates clearly how the most precise information, in this case that provided by vision, drives the final percept with the sound being attracted toward the location of the visual stimulus (just like the ventriloquist's voice seems to come from the mouth of the puppet; Alais and Burr, 2004). By virtue of its higher spatial acuity, vision usually dominates audition in the spatial domain; the reverse is however true in the temporal domain. Many cases show that auditory stimuli can strongly influence the perceived timing of visual (Shams et al., 2000; Aschersleben and Bertelson, 2003; Morein-Zamir et al., 2003; Recanzone, 2003) and tactile events (Bresciani et al., 2005). Although this is in line with what optimal ''Bayesian" integration would predict on the basis of the greater temporal precision of the auditory system, it is not clear whether this model provides a good quantitative description of the data. While most studies reporting auditory dominance in temporal judgments have not assessed this issue directly, two recent studies, testing audio–visual integration in a temporal bisection task (Burr et al., 2009) and audio–tactile temporal order judgments (Ley et al., 2009), provide conflicting results. Evidence as to whether the Bayesian cue-combination theory is a good explanatory framework in the temporal domain, like it is in the spatial domain, remains thus inconclusive.

In this study we test whether speed-dependency of apparent duration is a general property of sensory systems. That apparent duration depends on speed for both vision and touch would suggest that timing mechanisms share common operating principles across different modalities. Our results show that the duration of tactile events also depends on speed, pointing to a general principle. We also studied bimodal visuo-tactile gratings, to investigate how vision and touch are combined to yield an estimate of duration. The results show that the two modalities do interact with each other, but the advantage gained from the bimodal fusion is quantitatively suboptimal.

MATERIALS AND METHODS

Visual, tactile, and visuo-tactile motion stimuli were provided by physical wheels (diameter 10.5 cm; width 3 cm) etched with a corrugated grating of alternating ridges and grooves of equal width, of spatial frequency 3 c/cm (**Figure 1A**). The wheels were spatially aligned to give the appearance of a common object and driven at specific velocities by two independently controlled motors (**Figure 1B**). The velocity of the wheels was calibrated by means of a visual tracking system (NDI Optotrack Certus system), showing only minor deviations (3%) from the ideal constant velocity stimuli.

Subjects, seated at 57 cm from the stimuli, observed the front wheel through a small aperture (visual condition) and touched with their right index finger the second wheel, concealed from view (tactile condition). In the bimodal condition participants observed and touched the two wheels simultaneously (**Figure 1C**). The gratings were oriented horizontally (perpendicular to the long axis of the finger) and the direction of the motion could be either up-to-down (distal-to-proximal relative to the finger) or down-to-up (proximal-to-distal) depending on the trial (always coherent in the bimodal condition).

Participants were required to reproduce the duration of the moving stimuli by pressing a button on a keyboard with their left index finger after each stimulus presentation. The next stimulus started 1 s after the end of the reproduction phase.

The stimuli were presented for three different durations, 400, 600, and 800 ms, with speed varied between 3.5, 5, 7.5, 10, 12.5, and 15 cm/s. Data were collected in separate sessions of 90 trials, with different durations and speeds intermingled within each session.

FIGURE 1 | Illustration of the stimuli. (A) Physical wheel etched with a sinewave profile of 3 c/cm. **(B)** Setup with two arms driven at specific speeds by independent computer-controlled motors. **(C)** In the visual condition subjects observed the front wheel in motion through a small window; in the tactile condition they touched with their right index finger the second wheel occluded to vision by a shield; in the bimodal condition they observed and touched the two wheels simultaneously.

Although this procedure may result in what is called "regression toward the mean," reducing the real effect of speed on duration, we chose to randomize both durations and speeds so as to encourage subjects to attend to the stimuli and avoid stereotyped responses. No feedback was provided about the physical duration of the stimuli. Six subjects, one author and five naïve to the goals of the experiment, participated in the experiment; each subject completed a minimum of four sessions per condition (visual, tactile, and visuo-tactile). Participants did not receive any training. The average and variance of the reproduced durations across trials were calculated separately for each subject, stimulus modality, duration, and speed.

The second part of the experiment involved a cross-modal speed-matching task. The experimental apparatus and stimuli were the same as described above. Three subjects (one author and two naïves from the previous group) were asked to judge the relative speed of two moving stimuli, one visual and the other tactile, presented in succession in random order for 600 ms each. The direction of the movement was randomized on a trial-by-trial basis, but was always the same for the two stimuli within each trial.

The speed of one stimulus (the probe) was varied from trial to trial by means of the QUEST algorithm (Watson and Pelli, 1983) to generate a psychometric function; the other stimulus (the standard) had fixed speed. Two different conditions were intermingled within the same experimental session, with the probe being either tactile or visual. Three separate sessions of 40 trials each (half trials with visual probes and half with tactile probes) were run for four different standard speeds, 3.5, 7.5, 10, and 15 cm/s (except for subject MG who did not complete the 10 cm/s condition), chosen among the speed values used in the time reproduction task. Data for each condition were fitted with cumulative Gaussian functions estimated by means of the maximum likelihood method; the point of subjective equality (PSE) and the differential threshold were derived from the median and SD of the psychometric function, respectively. SEs for the PSEs and SDs were estimated by bootstrap.

The PSE indicated the speed of the visual (tactile) probe for which it was perceived as fast as the tactile (visual) standard. We thus repeated the time reproduction task (in the same three subjects) with new speed values, determined for each subject and stimulus modality according to the PSEs found in the cross-modal speed-matching task, so that the stimuli for both modalities were matched in perceived speed to those previously used. In the bimodal condition, the cross-modal speed-matching was obtained by using the standard speeds (3.5, 5, 7.5, 10, 12.5, and 15 cm/s) for the visual stimuli and appropriately changing the speeds of the tactile stimuli so as to match the visual speeds. Since PSEs were known for four of the six standard speeds, the other values were estimated by interpolation with the best-fitting linear function. The experiment required about 9 h testing for the three subjects who completed all the conditions and 4 h for the other subjects.

The results for the bimodal condition were modeled within the Bayesian framework (Ernst and Banks, 2002; Alais and Burr, 2004). According to optimal "Bayesian" integration the perceived duration of the combined visuo-tactile stimuli results from a weighted sum of the estimates of duration provided separately by each modality. Assuming that the visual and tactile estimates are statistically independent, the combined estimate of event duration, $\widehat{D}_{VT}$, is given by the following equation:

$$\widehat{D}_{VT} = w_V \widehat{D}_V + w_T \widehat{D}_T \tag{1}$$

where $\widehat{D}_V$ is the visual estimate and $\widehat{D}_T$ the tactile estimate, calculated as the average reproduced duration across trials, for each stimulus duration and speed. The weights, w_V and w_T, sum to unity and are inversely related to the variances for vision (σ_V^2) and touch (σ_T^2), respectively:

$$w_V = \frac{1/\sigma_V^2}{1/\sigma_T^2 + 1/\sigma_V^2} \tag{2}$$

$$w_T = \frac{1/\sigma_T^2}{1/\sigma_V^2 + 1/\sigma_T^2} \tag{3}$$

since the variance of the reproduced duration did not change systematically with stimulus speed, σ_V^2 and σ_T^2 were computed averaging variances across speeds, separately for each duration.

The model predicts that the variance for the combined estimate, σ_{VT}^2, is always less than the unimodal variances, σ_V^2 and σ_T^2, with the greatest improvement in precision ($\sqrt{2}$) when $\sigma_V^2 \cong \sigma_T^2$:

$$\sigma_{VT}^2 = \frac{\sigma_V^2 \sigma_T^2}{\sigma_V^2 + \sigma_T^2} \leq \min\left(\sigma_V^2, \sigma_T^2\right) \tag{4}$$

RESULTS

Figure 2 reports the individual reproduced durations as a function of speed for the 400, 600, and 800 ms visual (left column) and tactile (right column) stimuli. Duration reproduction is rather biased, so reproduced duration differs from the physical duration of the stimuli, with considerable variation between subjects. Regardless of the individual bias in the reproduction, the visual stimuli are always perceived to last longer (264 ± 40 ms on average) than the tactile stimuli. In most cases, the difference in perceived duration between visual and tactile stimuli grows with stimulus duration (**Figure 3**).

For both modalities apparent duration increases linearly with log speed. However, the speed-dependency was stronger for the tactile than for the visual stimuli, as can be observed in **Figure 4A**. To analyze better the relationship between perceived duration and speed, data were normalized by dividing them by the reproduced duration obtained for the stimuli moving at 7.5 cm/s. In this way we preserved only the information regarding the relative change in apparent duration, unaffected by systematic biases in the reproduction. The slopes of the normalized reproduced duration versus speed functions (calculated by linear regression) for touch are plotted against the slopes for vision. Tactile slopes are much greater than the visual slopes as indicated by the points lying above the equality line. A repeated-measures analysis of variance (ANOVA) with two within-subjects factors (modality and duration) was conducted on the slopes, leading to a significant difference between visual and tactile slopes [main effect of factor modality; $F(1,5) = 10.183$; $p = 0.024$], but neither to a significant effect of stimulus duration [$F(2,10) = 1.06$; $p = 0.427$], nor to a significant interaction between stimulus modality and duration [$F(2,10) = 0.427$; $p = 0.679$].

Importantly, the slopes for the visual modality correlate positively with the slopes for the tactile modality [$r = 0.584(16)$, p(one-tailed) $= 0.005$], suggesting that similar mechanisms are

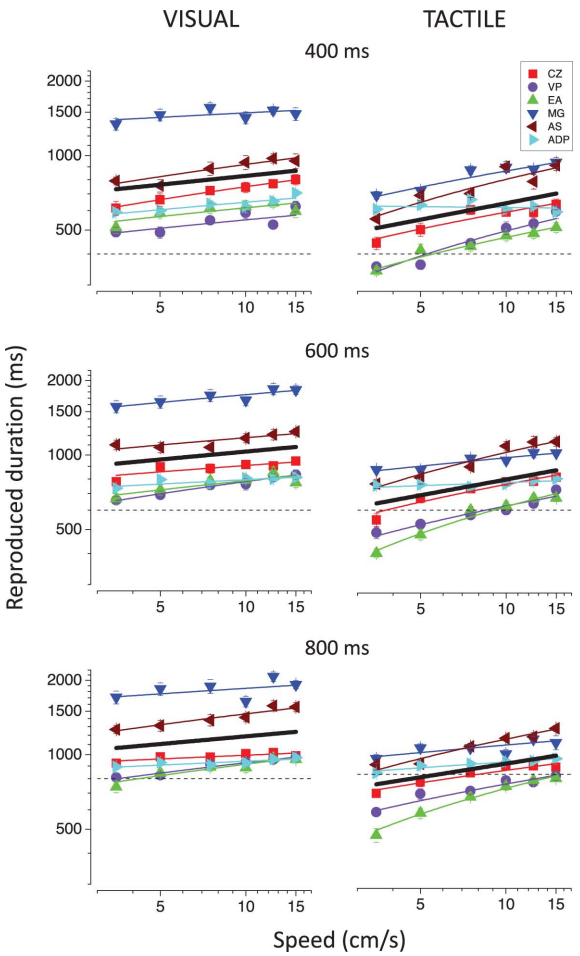

FIGURE 2 | Individual reproduced durations as a function of speed for the visual (left column) and the tactile (right column) stimuli. Different colors represent different subjects. The black solid lines represent the best-fitting linear functions for the average reproduced durations. The results for the 400, 600, and 800 ms durations are reported in the upper, middle, and lower panels, respectively. The dashed lines indicate the actual physical durations of the stimuli.

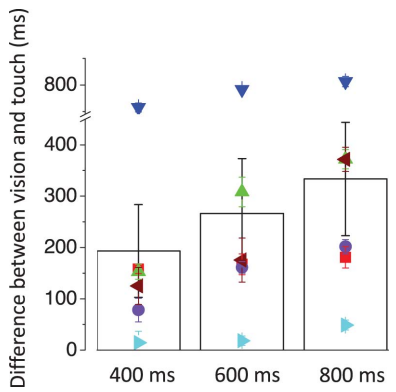

FIGURE 3 | Difference between the reproduced durations for the visual and tactile stimuli as a function of stimulus duration. The symbols represent the individual data and the bars represent the averages across subjects.

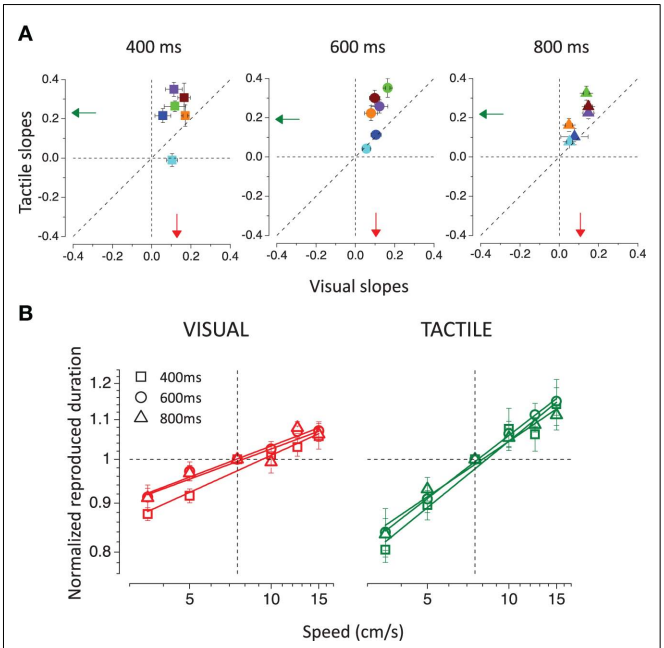

FIGURE 4 | (A) Tactile slopes plotted against visual slopes. The slopes were calculated, separately for each subject and condition, from the linear regression of the normalized reproduced durations (divided by the reproduced duration obtained for the 7.5-cm/s moving stimuli) as a function of speed. Different colors represent different subjects. The vertical and horizontal dashed lines indicate absence of dependence on speed, the diagonal shows equal dependence for vision and touch. The arrows show the averages for the visual (in red) and for the tactile (in green) conditions. **(B)** Normalized reproduced durations averaged across subjects are plotted as a function of speed for the visual (on the left) and tactile (on the right) stimuli. Different stimulus durations (400, 600, and 800 ms) are represented by different symbols.

driving the time expansion of both visual and tactile stimuli. **Figure 4B** shows average results for each stimulus duration in the visual and tactile conditions. The increasing linear functions have very similar slopes within each modality, indicating that the same relationship between apparent duration and speed applies to all stimulus durations, but they are always steeper for the tactile than for the visual stimuli.

To evaluate the relative contributions of vision and touch to the final combined percept we took advantage of the large differences in perceived duration between visual and tactile stimuli (in some cases up to 400–800 ms), leading to two clearly distinct unimodal duration estimates. We thus employed bimodal stimuli comprising visual and tactile stimuli moving at the same physical velocity for the same duration. The results for each subject are reported in **Figure 5A** for the 600 ms stimuli (comparable results were obtained for the other two durations tested; individual data not shown). In all cases except one, the apparent duration of bimodal stimuli lies between the unimodal estimates, as the Bayesian account predicts. Importantly, only one subject (CZ) shows a clear improvement in the precision of the reproduction

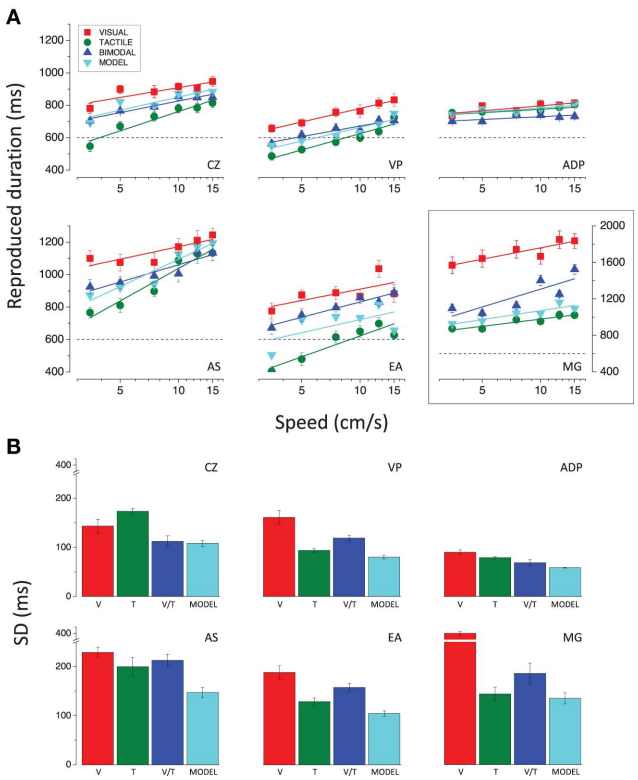

FIGURE 5 | (A) Reproduced durations for the 600 ms stimuli, plotted as a function of speed for all conditions. The results for the subject MG have been plotted on a different scale to encompass her wider range of duration estimates. **(B)** SDs of the reproduction averaged across speeds relative to the 600 ms visual (red bar), tactile (green bar), and bimodal (blue bar) stimuli and predicted for bimodal stimuli according to the Bayesian model (cyan bar); results for all subjects.

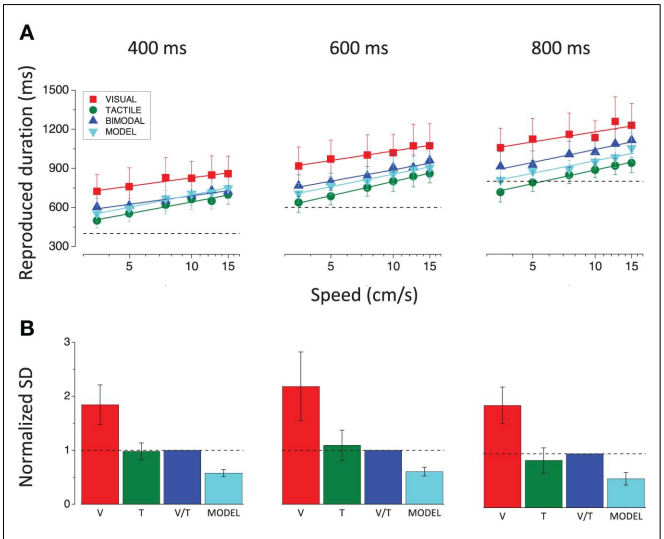

FIGURE 6 | (A) Reproduced durations averaged across subjects, plotted as a function of speed, separately for the three stimulus durations (400, 600, and 800 ms). The dashed lines indicate the actual physical durations of the stimuli. **(B)** Average normalized SDs for all conditions and stimulus durations. The variances for all speeds and subjects were first divided by the bimodal variance, then summed and square-rooted to yield the SDs. The dashed lines show the normalized bimodal SDs.

for the bimodal stimuli as predicted by Eq. 4 (see Materials and Methods). As shown in **Figure 5B**, the bimodal SDs for all other subjects are never better than the best unimodal case, and worse than what predicted by the model.

To quantify the goodness of model fit, we performed a linear regression between the bimodal data and the model predictions (see Eq. 1 in the Materials and Methods) for all subjects. We tested whether the best-fitting linear function is significantly different from the ideal fit (equality line with intercept equal to 0 and slope equal to 1) by looking at the 95% confidence intervals for the intercept and slope. The duration estimates for the bimodal stimuli do not deviate significantly from the predicted estimates. However, since the confidence intervals are quite large, the absence of a significant difference between the bimodal and predicted estimates can be affirmed with high uncertainty.

Figure 6 shows results averaged across subjects, separately for the three durations. As was evident in the single-subject results, the bimodal duration reproductions fall between the unimodal reproductions, close to the model predictions. The strong test of optimal integration is an improvement in thresholds (SDs). The lower bar graphs show average normalized thresholds for all conditions: the variances for all speeds and subjects were first divided by the bimodal variance (to eliminate inter-subject variability), then summed and square-rooted to yield the thresholds of **Figure 6B**. The predicted SDs are significantly lower than the bimodal SDs, indicating suboptimal integration [$t(35) = 6.3$, $p < 0.0001$ for 400 ms; $t(35) = 5.5, p < 0.0001$ for 600 ms; $t(35) = 6.5, p < 0.0001$ for 800 ms; two tailed paired t-tests].

Figure 2 shows that not only does the duration of both visual and tactile stimuli depend on speed, but visual stimuli tend to be perceived as lasting longer than tactile stimuli. As perceived duration varies strongly with stimulus speed, the difference in perceived duration of visual and tactile stimuli could arise from differences in their perceived speed. To examine this possibility, we first measured relative speed perception between vision and touch. The cross-modal speed-matching task (see Materials and Methods for details) revealed that visual stimuli appear to move faster than tactile stimuli. Visual (red symbols) and tactile (green symbols) PSEs for the three subjects who completed the task are plotted in **Figure 7A** as a function of tactile and visual standard speeds, respectively. The dashed line indicates equal perceived speed between vision and touch. Visual PSEs lie below the equality line, and tactile above, indicating overestimation of visual speed relative to tactile speed.

We then repeated the time reproduction task with higher speeds for touch and lower speeds for vision (specified by the PSEs), so that the new visual and tactile stimuli were matched in perceived speed to those previously used. **Figure 7B** reports the results for visual and tactile stimuli matched in physical (filled symbols) and perceived speed (red open symbols match with green filled symbols and green open symbols with red filled symbols). After speed-matching, the difference in apparent duration between visual and tactile stimuli is reduced but not completely eliminated. For two

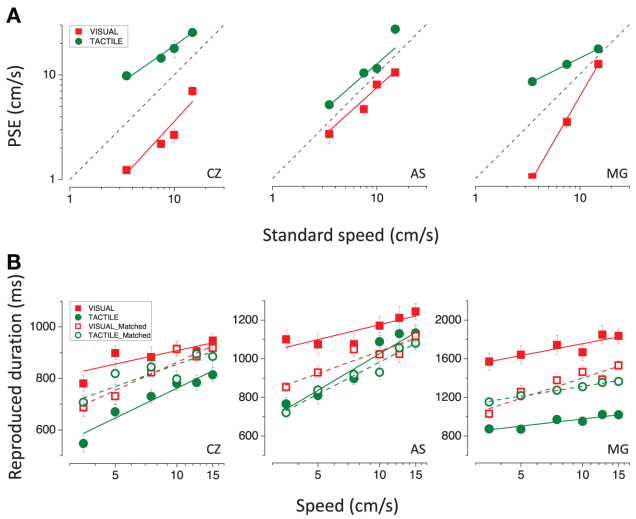

FIGURE 7 | (A) Point of subjective equalities for the visual (in red) and tactile (in green) stimuli as a function of tactile and visual standard speeds (3.5, 5, 7.5, 10, 12.5, 15 cm/s), respectively. The dashed line represents the equality line. **(B)** Reproduced durations plotted as a function of speed for the 600 ms visual (in red) and tactile (in green) moving stimuli. Filled symbols represent the results for the visual and tactile stimuli moving at the same physical speeds (standard speeds). Red open symbols represent the results for the visual stimuli matched in perceived speed to the tactile stimuli moving at the standard speeds (filled green symbols); green open symbols represent the results for the tactile stimuli matched in perceived speed to the visual stimuli moving at the standard speeds (filled red symbols); results for all subjects.

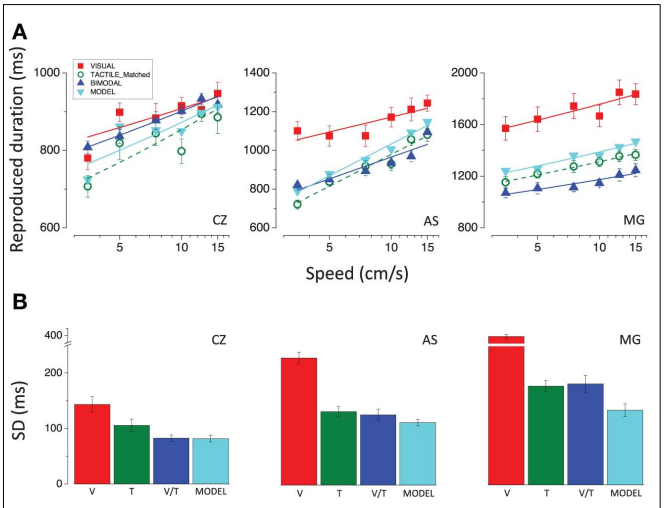

FIGURE 8 | (A) Reproduced durations as a function of speed relative to the 600 ms stimuli. The green open symbols represent the reproduced durations for the tactile stimuli moving at the same perceived speed as the visual stimuli (red filled symbols). Blue symbols represent the results for the bimodal stimuli (visuo-tactile speed-matched stimuli) and the cyan symbols represent the results for the bimodal stimuli predicted according to Bayesian integration. **(B)** SDs of the reproduction averaged across speeds relative to the 600 ms visual (red bar), tactile (green bar), and bimodal (blue bar) stimuli and predicted for bimodal stimuli according to the Bayesian model (cyan bar); results for all subjects.

subjects out of three (CZ and MG) perceived speed explains exactly half of the difference in perceived duration between vision and touch, as indicated by the open symbols lying halfway between the filled symbols. Subject AS shows an asymmetrical pattern of results: speed-matching did not affect tactile apparent duration (green open symbols overlap with green filled symbols), whereas it produced a remarkable decrease (more than half of the difference between vision and touch) in visual apparent duration. These findings appear quite surprising if one considers the strong speed-dependency of tactile apparent duration shown by the same subject, unless we hypothesize that she changed her response criterion in the second part of the experiment, shortening all reproduction times (this would also be consistent with the greater reduction in perceived duration reported by AS after visual speed-matching compared with what reported by the other two subjects).

The results for the bimodal speed-matched stimuli (**Figure 8**) do not allow us to draw different conclusions with respect to those already discussed for bimodal stimuli consisting of physically identical visual and tactile stimuli. Both before and after speed-matching the results for the subject CZ indicate that vision and touch are combined in an optimal way to yield an estimate of event duration, as shown by the good fit of the model. Bimodal duration estimates and precision of the reproduction deviate little from what predicted by optimal integration for the subject AS, while they are completely inconsistent with the model for the subject MG.

DISCUSSION

We used a time reproduction task to measure the apparent duration of visual, tactile, and visuo-tactile stimuli moving at various speeds. The study yielded three main results. Firstly, we show that motion induces temporal dilation in the tactile modality as previously shown in the visual modality: faster stimuli appear to be longer. Secondly, visual stimuli appear to last longer and to move faster than tactile stimuli of the same duration and speed. Thirdly we model the results with the Bayesian theory of optimal integration, and find an adequate fit for the duration estimates but not for their precision.

Unlike prior investigations in vision (Kanai et al., 2006; Kaneko and Murakami, 2009), our experiment was not designed to evaluate the differential role of speed, temporal frequency, and spatial frequency in time dilation; we did not manipulate the spatial frequency of the stimuli (3 c/cm for touch; 3 c/deg for vision) and consequently the temporal frequency and speed always covaried. We found that also for the tactile modality, apparent duration increases with increasing speed (and temporal frequency, in agreement with Khoshnoodi et al., 2008). Speed-dependency for touch is stronger than for vision. This might be explained by the different spatial and temporal tuning properties of the two sensory systems, which determine a different sensitivity to stimulus motion in the range of speeds considered. The maximum speed tested (15 cm/s, 45 Hz) is actually quite low compared with the high temporal resolution (up to 400 Hz) of the tactile system, while it approaches the upper limit of sensitivity for visual motion. This may account for the more rapid saturation of the effect in the visual modality, reflected in the

lower slopes of the increasing linear functions describing speed dependence.

The functional architectures of early visual and tactile sensory processing show several important similarities. Although the two systems have different temporal resolutions, both are equipped with low-pass and band-pass temporal channels that yield sustained and transient neural responses. Several lines of evidence indicate that motion processing also shares similar properties and possibly common neural substrates between vision and touch (Konkle et al., 2009; Gori et al., 2011; Pei et al., 2011). Recently, compelling evidence has linked the encoding of duration in the sub-second range to the early sensory machinery for temporal analysis. It has been shown that perceived time can be locally altered by means of visual motion (or flicker) adaptation (Johnston et al., 2006; Burr et al., 2007) and the same result has been also extended to the tactile modality (Watanabe et al., 2010). Here we report that time dilation induced by motion is a common finding across vision and touch. All this fits well with the suggestion that timing functions may be realized by multiple, modality-specific mechanisms, operating according to similar computational principles and rooted in the early sensory function.

Vision and touch yield different duration reproductions for stimuli moving at the same physical speed, with tactile reproductions being in general slightly more accurate (closer to the actual physical duration) and precise (showing less inter-trial variability) than visual reproductions. As visual stimuli appear to last longer than tactile stimuli (∼200 ms), we tested whether this inter-sensory difference in perceived duration could result from differences in perceived speed. The cross-modal speed-matching task revealed that visual stimuli are perceived to move faster than the tactile stimuli, but this does not explain entirely the difference in perceived duration, which persists, although to a lesser extent, after the stimuli are matched in perceived speed. That the apparent duration may change depending on stimulus modality is not a new finding in the timing literature (Goldstone and Lhamon, 1974; Walker and Scott, 1981). Differences in apparent duration have been previously reported for auditory and visual stimuli and generally interpreted within the "internal clock theory" as modality-specific differences in the pulse rate of the pacemaker (e.g., Wearden et al., 2006). The difference that we observe between vision and touch increases proportionally with stimulus duration, ruling out explanations based on effects at onset and offset (Penney et al., 2000; Burle and Casini, 2001).

The reasons for these modality effects in the perception of duration are not clear at present, but certainly pose the problem of how the brain handles inter-sensory conflicts when multimodal events have to be timed. We tried to tackle this issue examining duration reproduction for bimodal visuo-tactile stimuli. The results show that both vision and touch contribute to the final duration percept, as indicated by the bimodal estimates lying between the unimodal estimates. The bimodal durations were statistically indistinguishable from the quantitative predictions of optimal fusion (weighted average of the unimodal estimates). However, the bimodal precision was far from being "optimal," not showing the theoretical improvement. One reason for the lack of improvement in thresholds may be that our experimental design involved temporal reproduction, and a full model would have to consider that the reproduction task might have introduced its own noise, and this would affect the predictions. In effect, as this noise occurs after the fusion of visual and tactile signals, it would add to all threshold estimates, and dilute any advantage that may have been gained from the bimodal fusion.

The encoding of duration cannot rely on specific sense organs, nor seems to be subserved by a specifically dedicated pathway. Our sense of time is continuously subject to numerous distortions (for a review see Eagleman, 2008), probably reflecting the fact that time analysis is interconnected with the processing of other contents of the external world, suggesting that this inherent plasticity of the system is functionally more relevant than having a stable and exact metric of time.

ACKNOWLEDGMENTS

This work was partially supported by the IDEA-ERC project STANIB, ASI Italian Space Agency and the PRIN2009 grant from the Italian Ministry for Universities and Research.

REFERENCES

Alais, D., and Burr, D. (2004). The ventriloquist effect results from near-optimal bimodal integration. *Curr. Biol.* 14, 257–262.

Aschersleben, G., and Bertelson, P. (2003). Temporal ventriloquism: crossmodal interaction on the time dimension 2. Evidence from sensorimotor synchronization. *Int. J. Psychophysiol.* 50, 157–163.

Bensmaia, S. J., Killebrew, J. H., and Craig, J. C. (2006). Influence of visual motion on tactile motion perception. *J. Neurophysiol.* 96, 1625–1637.

Bicchi, A., Scilingo, E. P., Ricciardi, E., and Pietrini, P. (2008). Tactile flow explains haptic counterparts of common visual illusions. *Brain Res. Bull.* 75, 737–741.

Bresciani, J. P., Ernst, M. O., Drewing, K., Bouyer, G., Maury, V., and Kheddar, A. (2005). Feeling what you hear: auditory signals can modulate tactile tap perception. *Exp. Brain Res.* 162, 172–180.

Brown, S. W. (1995). Time, change, and motion: the effects of stimulus movement on temporal perception. *Percept. Psychophys.* 57, 105–116.

Burle, B., and Casini, L. (2001). Dissociation between activation and attention effects in time estimation: implications for internal clock models. *J. Exp. Psychol. Human Percept. Perform.* 27, 195–205.

Burr, D., Banks, M. S., and Morrone, M. C. (2009). Auditory dominance over vision in the perception of interval duration. *Exp. Brain Res.* 198, 49–57.

Burr, D., Tozzi, A., and Morrone, M. C. (2007). Neural mechanisms for timing visual events are spatially selective in real-world coordinates. *Nat. Neurosci.* 10, 423–425.

Craig, J. C. (2006). Visual motion interferes with tactile motion perception. *Perception* 35, 351–367.

Eagleman, D. M. (2008). Human time perception and its illusions. *Curr. Opin. Neurobiol.* 18, 131–136.

Ernst, M. O., and Banks, M. S. (2002). Humans integrate visual and haptic information in a statistically optimal fashion. *Nature* 415, 429–433.

Ernst, M. O., and Bülthoff, H. H. (2004). Merging the senses into a robust percept. *Trends Cogn. Sci. (Regul. Ed.)* 8, 162–169.

Gamache, P., and Grondin, S. (2010). Sensory-specific clock components and memory mechanisms: investigation with parallel timing. *Eur. J. Neurosci.* 31, 1908–1914.

Gibbon, J., Malapani, C., Dale, C. L., and Gallistel, C. R. (1997). Toward a neurobiology of temporal cognition: advances and challenges. *Curr. Opin. Neurobiol.* 7, 170–184.

Goldstone, S., and Lhamon, W. T. (1974). Studies of auditory-visual differences in human time judgment: 1. Sounds are judged longer than lights. *Percept. Mot. Skills* 39, 63–82.

Gori, M., Mazzilli, G., Sandini, G., and Burr, D. (2011). Cross-sensory facilitation reveals neural interactions between visual and tactile motion in humans. *Front. Psychol.* 2:55. doi: 10.3389/fpsyg.2011.00055

Grondin, S. (2003). "Sensory modalities and temporal processing," in *Time and Mind II*, ed. H. Helfrich (Göttingen: Hogrefe & Huber), 61–77.

Hagen, M. C., Franzen, O., McGlone, F., Essick, G., Dancer, C., and Pardo, J. V. (2002). Tactile motion activates the human middle temporal/V5 (MT/V5) complex. *Eur. J. Neurosci.* 16, 957–964.

Harrar, V., and Harris, L. R. (2007). Multimodal ternus: visual, tactile and visuo-tactile grouping in apparent motion. *Perception* 36, 1455–1464.

Harrington, D. L., Castillo, G. N., Fong, C. H., and Reed, J. D. (2011). Neural underpinnings of distortions in the experience of time across senses. *Front. Integr. Neurosci.* 5:32. doi: 10.3389/fnint.2011.00032.

Johnston, A., Arnold, D. H., and Nishida, S. (2006). Spatially localized distortions of event time. *Curr. Biol.* 16, 472–479.

Kanai, R., Paffen, C. L. E., Hogendoorn, H., and Verstraten, F. A. J. (2006). Time dilation in dynamic visual display. *J. Vis.* 6, 1421–1430.

Kaneko, S., and Murakami, I. (2009). Perceived duration of visual motion increases with speed. *J. Vis.* 9, 1–12.

Khoshnoodi, M. A., Motiei-Langroudi, R., Omrani, M., Diamond, M. E., and Abbassian, A. H. (2008). Effect of tactile stimulus frequency on time perception: the role of working memory. *Exp. Brain Res.* 185, 623–633.

Konkle, T., Wang, Q. I., Hayward, V., and Moore, C. I. (2009). Motion aftereffects transfer between touch and vision. *Curr. Biol.* 19, 745–750.

Ley, I., Haggard, P., and Yarrow, K. (2009). Optimal integration of auditory and vibrotactile information for judgments of temporal order. *J. Exp. Psychol. Human Percept. Perform.* 35, 1005–1019.

Lhamon, W. T., and Goldstone, S. (1975). Movement and the judged duration of visual targets. *Bull. Psychon. Soc.* 5, 53–54.

Morein-Zamir, S., Soto-Faraco, S., and Kingstone, A. (2003). Auditory capture of vision: examining temporal ventriloquism. *Cogn. Brain Res.* 17, 154–163.

Morrone, M. C., Ross, J., and Burr, D. (2005). Saccadic eye movements cause compression of time as well as space. *Nat. Neurosci.* 8, 950–954.

Pei, Y. C., Hsiao, S. S., Craig, J. C., and Bensmaia, S. J. (2011). Neural mechanisms of tactile motion integration in somatosensory cortex. *Neuron* 69, 536–547.

Penney, T. B., Gibbon, J., and Meck, W. H. (2000). Differential effects of auditory and visual signals on clock speed and temporal memory. *J. Exp. Psychol. Human Percept. Perform.* 26, 1770–1787.

Recanzone, G. H. (2003). Auditory influences on visual temporal rate perception. *J. Neurophysiol.* 89, 1078–1093.

Ricciardi, E., Vanello, N., Dente, D., Sgambelluri, N., Scilingo, E. P. Gentili, C., Sani, L., Positano, V., Santarelli, F. M., Guazzelli, M., Haxby, J. V., Landini, L., Bicchi, A., and Pietrini, P. (2004). "Perception of visual and tactile flow activates common cortical areas in the human brain," in *Proceedings of the EuroHaptics 2004* (Germany: Technische Universitat Munchen), 290–292.

Shams, L., Kamitani, Y., and Shimojo, S. (2000). What you see is what you hear. *Nature* 408, 788.

Terao, M., Watanabe, J., Yagi, A., and Nishida, S. (2008). Reduction of stimulus visibility compresses apparent time intervals. *Nat. Neurosci.* 11, 541–542.

Tomassini, A., Gori, M., Burr, D., Sandini, G., and Morrone, C. (2010). The spatial selectivity of neural timing mechanisms for tactile events. *J. Vis.* 10, 1410.

Treisman, M. (1963). Temporal discrimination and the indifference interval. Implications for a model of the 'internal clock'. *Psychol. Monogr.* 77, 1–31.

van Erp, J. B. F., and Werkhoven, P. J. (2004). Vibro-tactile and visual asynchronies: sensitivity and consistency. *Perception* 33, 103–111.

Walker, J. T., and Scott, K. J. (1981). Auditory-visual conflicts in the perceived duration of lights, tones and gaps. *J. Exp. Psychol. Human Percept. Perform.* 7, 1327–1339.

Watanabe, J., Amemiya, T., Nishida, S., and Johnston, A. (2010). Tactile duration compression by vibrotactile adaptation. *Neuroreport* 21, 856–860.

Watanabe, J., Hayashi, S., Kajimoto, H., Tachi, S., and Nishida, S. (2007). Tactile motion aftereffects produced by appropriate presentation for mechanoreceptors. *Exp. Brain Res.* 180, 577–582.

Watson, A. B., and Pelli, D. G. (1983). QUEST: a Bayesian adaptive psychometric method. *Percept. Psychophys.* 33, 113–120.

Wearden, J. H., Edwards, H., Fakhri, M., and Percival, A. (1998). "Why sounds are judged longer than lights": application of a model of the internal clock in humans. *Q. J. Exp. Psychol. B* 51, 97–120.

Wearden, J. H., Todd, N. P., and Jones, L. A. (2006). When do auditory/visual differences in duration judgments occur? *Q. J. Exp. Psychol.* 59, 1709–1724.

Xuan, B., Zhang, D., and Chen, X. (2007). Larger stimuli are judged to last longer. *J. Vis.* 7, 1–5.

Conflict of Interest Statement: The authors declare that the research was conducted in the absence of any commercial or financial relationships that could be construed as a potential conflict of interest.

Received: 09 June 2011; paper pending published: 26 June 2011; accepted: 23 August 2011; published online: 12 September 2011.

*Citation: Tomassini A, Gori M, Burr D, Sandini G and Morrone MC (2011) Perceived duration of visual and tactile stimuli depends on perceived speed. Front. Integr. Neurosci. **5**:51. doi: 10.3389/fnint.2011.00051*

frontiers in
INTEGRATIVE NEUROSCIENCE

OPINION ARTICLE
published: 08 August 2011
doi: 10.3389/fnint.2011.00034

The sensory representation of time

Domenica Bueti*

Functional Electrical Neuroimaging Laboratory, Department of Clinical Neurosciences, Centre Hospitalier Universitaire Vaudois and Université de Lausanne, Lausanne, Switzerland
**Correspondence: domenica.bueti@gmail.com*

Time is embedded in many aspects of our sensory experience; sensory events unfold in time and often acquire particular meaning because of their specific temporal structure. The speed of a moving object, the words pronounced by a speaker and the tactile exploration of a texture, are all examples of temporally structured sensory experiences. Despite the ubiquitousness of the temporal dimension of our sensory experience, the understanding of the neural mechanisms underlying the temporal representation of sensory events, that is the capacity to estimate duration in milliseconds/seconds range, remains a controversial and complex issue. The controversy relates to the effective involvement of sensory-specific brain regions in the processing of temporal information. The complexity arises from the neurophysiological mechanisms underlying the representation of time in these areas and the functional interplay between sensory-specific and amodal temporal mechanisms (Harrington et al., 2011).

The idea that we time sensory signals via a single "centralized" and "amodal" clock dominated the field of temporal cognition over the last 30 years. More recently the universality of timing mechanisms has been challenged by new theoretical positions and a growing body of empirical data (Buhusi and Meck, 2005). From a theoretical perspective the challenge comes from "distributed" timing models. This is a broad class of models, which – although different regarding the neurophysiological mechanisms proposed for time processing – collectively share the idea that we have multiple timing mechanisms "distributed" across brain areas or circuits; and that the engagement of each single mechanism depends on the psychophysical task, sensory modality, and lengths of temporal intervals (Ivry and Richardson, 2002; Durstewitz, 2003; Matell and Meck, 2004; Buonomano and Maass, 2009). The idea that sensory-specific timing mechanisms exist is supported by studies showing that the ability to discriminate temporal information depends on the modality of the signals. For example, temporal discrimination thresholds are lower for auditory compared to visual signal durations (Grondin, 1993; Grondin et al., 2005; Merchant et al., 2008); and the capacity to keep in memory multiple intervals improves if the temporal signals belong to different modalities and therefore rely on different memory resources (Gamache and Grondin, 2010). The existence of independent sensory-specific clocks is also suggested by the observation that the perceived duration of a sensory event can be distorted by modality-specific properties of the stimuli such as visual adaptation (Johnston et al., 2006; Ayhan et al., 2009), spatial, and temporal frequency (Kanai et al., 2006; Kaneko and Murakami, 2009); or by the observation that such distortions are limited to a single sensory domain, like in case of saccadic eye movements causing compression of the perceived duration of visual but not of auditory stimuli (Morrone et al., 2005; Burr et al., 2011). From the neurophysiological point of view, electrophysiological recordings in animals as well as neuroimaging and magnetic stimulation studies in humans suggest that both modality-specific and supramodal mechanisms underlie the estimation of temporal intervals (Ghose and Maunsell, 2002; Shuler and Bear, 2006; Bosco et al., 2008; Bueti et al., 2008b; Sadeghi et al., 2011). For example, it has been demonstrated that the extrastriate visual area MT/V5 is necessary for temporal discrimination of visual, but not of auditory durations (Bueti et al., 2008a) and that duration estimation to predict expected visual and auditory events involves secondary as well as primary visual and auditory cortices (Ghose and Maunsell, 2002; Shuler and Bear, 2006; Bueti and Macaluso, 2010; Bueti et al., 2010).

Taken together these behavioral and neurophysiological data highlight the functional contribution of sensory-specific cortices and support the existence of modality-specific timing mechanisms. However, *how* temporal information is actually represented in these cortices and what is the neurophysiological mechanism behind it, remain unclear. A few interesting theoretical hypotheses have been advanced. "Intrinsic" timing models for example, describe time as a general and inherent property of neural dynamics. A consequence of this assumption is that any area of the brain is in principle able to encode time. Temporal computations according to these models rely on inherent temporal properties of neural networks like short-term synaptic plasticity [i.e., state-dependent networks (SDNs) model; Buonomano and Maass, 2009] or arise either from the overall magnitude of neural activity (Eagleman, 2008) or from the linear ramping of neuronal firing rate (Durstewitz, 2003; Reutimann et al., 2004). "Intrinsic models" of temporal coding are particularly suitable to describe the functional organization of sensory timing mechanisms because they assume that time is encoded by the same circuits encoding other stimulus properties such as color or motion in the visual modality. However the explanatory power of some of these models, like for example the SDNs model, is constrained to durations of a few hundred milliseconds (i.e., <500 ms; Buonomano et al., 2009; Spencer et al., 2009); this is indeed a strong limitation, given that most of the neurophysiological evidence in favor of modality-specific timing mechanisms deal with durations from hundreds of milliseconds to a few seconds. An alternative possibility is that temporal computations in sensory cortices engage wider and specialized temporal circuit (s), where time signals from sensory cortex are sent to "dedicated" timing areas where these signals are integrated and used to guide action for example (Coull et al., 2011). In this latter case the relationship between sensory-specific and sensory independent timing areas need to be elucidated. Many cortical (parietal, premotor, prefrontal, and insular cortices) and subcortical (basal ganglia and cerebellum) brain structures have indeed been implicated in the processing of temporal information independently

from the sensory modality of the stimuli (see Spencer et al., 2003; Coull et al., 2004; Koch et al., 2008; Wiener et al., 2010 for a review; Wittmann et al., 2010). Although there is only a partial agreement regarding the relevance of all these structures to time processing, the challenge is now to explore whether these areas have dissociable or interchangeable/overlapping functional roles and therefore whether these areas support the same or different temporal mechanisms compared to sensory-specific areas. A very special case of multimodal timing area is represented by the auditory cortex, a sensory-specific area. It has been recently demonstrated indeed that the auditory cortex is important for temporal discrimination not only of auditory but also of somatosensory and visual stimuli (Bolognini et al., 2009; Kanai et al., 2011). The supramodal involvement of auditory areas in temporal tasks has been associated with a strategic use of auditory-based mental representations for time estimation (Franssen et al., 2006). An interesting hypothesis, suggested by Kanai and colleagues, is that given the dominance of the auditory system over vision in temporal tasks (Walker and Scott, 1981; Burr et al., 2009), visual information is converted into an auditory code for temporal computation(Kanai et al., 2011). This hypothesis is interesting because offers new insight into the relationship between visual and auditory timing systems and highlights a possible link between modality independent and modality-specific temporal mechanisms.

It is therefore clear that the study of the functional architecture of sensory timing mechanisms poses a few more theoretical and experimental challenges. A few important questions are still open. It is, for example, unclear whether the organizational principles that apply to space also apply to time and whether the temporal dimension of visual stimuli is processed by the same or distinct networks compared to those for space. Is time coding in visual cortex retinotopic specific? Do we encode all possible temporal intervals at each retinotopic position? In which context do sensory-specific temporal mechanisms work? Is temporal information encoded in sensory cortices automatically or does it require explicit attention? Are sensory areas engaged only during duration encoding or are also active during working memory maintenance?

The already complex scenario of the neural representation of time is getting even more intricate. From the idea of a *single* "amodal" mechanism we moved into the idea of *multiple* "modality-specific" and "modality independent" temporal mechanisms (Wiener et al., 2011). The challenge is now to find out the functional architecture of these mechanisms as well as the interaction between them. As a concluding remark, I would like to emphasize that the focus of the majority of studies exploring the neural correlates of temporal processing has been so far to identifying the key components of internal timing networks (i.e., the "where" of timing mechanisms). The result of this approach has been, for example, an exponential increase of the number of neuroimaging studies on this topic that has lead to a substantial disagreement regarding the structures that are relevant to time processing (Wiener et al., 2010 for a review). It is time to adopt new experimental approaches that pose more mechanistically oriented questions about the underlying timing mechanisms while at the same time attempting to link computational models and neurophysiology (Portugal et al., 2011).

ACKNOWLEDGMENT

Thanks to Micah M. Murray for his helpful comments on an earlier version of the manuscript.

REFERENCES

Ayhan, I., Bruno, A., Nishida, S., and Johnston, A. (2009). The spatial tuning of adaptation-based time compression. *J. Vis.* 9, 1–12.

Bolognini, N., Miniussi, C., Savazzi, S., Bricolo, E., and Maravita, A. (2009). TMS modulation of visual and auditory processing in the posterior parietal cortex. *Exp. Brain Res.* 195, 509–517.

Bosco, G., Carrozzo, M., and Lacquaniti, F. (2008). Contributions of the human temporoparietal junction and MT/V5+ to the timing of interception revealed by transcranial magnetic stimulation. *J. Neurosci.* 28, 12071–12084.

Bueti, D., Bahrami, B., and Walsh, V. (2008a). Sensory and association cortex in time perception. *J. Cogn. Neurosci.* 20, 1054–1062.

Bueti, D., Van Dongen, E. V., and Walsh, V. (2008b). The role of superior temporal cortex in auditory timing. *PLoS ONE* 3, e2481. doi: 10.1371/journal.pone.0002481

Bueti, D., Bahrami, B., Walsh, V., and Rees, G. (2010). Encoding of temporal probabilities in the human brain. *J. Neurosci.* 30, 4343–4352.

Bueti, D., and Macaluso, E. (2010). Auditory temporal expectations modulate activity in visual cortex. *Neuroimage* 51, 1168–1183.

Buhusi, C. V., and Meck, W. H. (2005). What makes us tick? Functional and neural mechanisms of interval timing. *Nat. Rev. Neurosci.* 6, 755–765.

Buonomano, D. V., Bramen, J., and Khodadadifar, M. (2009). Influence of the interstimulus interval on temporal processing and learning: testing the state-dependent network model. *Philos. Trans. R. Soc. Lond. B Biol. Sci.* 364, 1865–1873.

Buonomano, D. V., and Maass, W. (2009). State-dependent computations: spatiotemporal processing in cortical networks. *Nat. Rev. Neurosci.* 10, 113–125.

Burr, D., Banks, M. S., and Morrone, M. C. (2009). Auditory dominance over vision in the perception of interval duration. *Exp. Brain Res.* 198, 49–57.

Burr, D. C., Cicchini, G. M., Arrighi, R., and Morrone, M. C. (2011). Spatiotopic selectivity of adaptation-based compression of event duration. *J. Vis.* 11, 21. [Author reply 21a].

Coull, J. T., Cheng, R. K., and Meck, W. H. (2011). Neuroanatomical and neurochemical substrates of timing. *Neuropsychopharmacology* 36, 3–25.

Coull, J. T., Vidal, F., Nazarian, B., and Macar, F. (2004). Functional anatomy of the attentional modulation of time estimation. *Science* 303, 1506–1508.

Durstewitz, D. (2003). Self-organizing neural integrator predicts interval times through climbing activity. *J. Neurosci.* 23, 5342–5353.

Eagleman, D. M. (2008). Human time perception and its illusions. *Curr. Opin. Neurobiol.* 18, 131–136.

Franssen, V., Vandierendonck, A., and Van Hiel, A. (2006). Duration estimation and the phonological loop: articulatory suppression and irrelevant sounds. *Psychol. Res.* 70, 304–316.

Gamache, P. L., and Grondin, S. (2010). Sensory-specific clock components and memory mechanisms: investigation with parallel timing. *Eur. J. Neurosci.* 31, 1908–1914.

Ghose, G. M., and Maunsell, J. H. (2002). Attentional modulation in visual cortex depends on task timing. *Nature* 419, 616–620.

Grondin, S. (1993). Duration discrimination of empty and filled intervals marked by auditory and visual signals. *Percept. Psychophys.* 54, 383–394.

Grondin, S., Roussel, M. E., Gamache, P. L., Roy, M., and Ouellet, B. (2005). The structure of sensory events and the accuracy of time judgments. *Perception* 34, 45–58.

Harrington, D. L., Castillo, G. N., Fong, C. H., and Reed, J. D. (2011). Neural underpinnings of distortions in the experience of time across senses. *Front. Integr. Neurosci.* 5:32. doi: 10.3389/fnint.2011.00032

Ivry, R. B., and Richardson, T. C. (2002). Temporal control and coordination: the multiple timer model. *Brain Cogn.* 48, 117–132.

Johnston, A., Arnold, D. H., and Nishida, S. (2006). Spatially localized distortions of event time. *Curr. Biol.* 16, 472–479.

Kanai, R., Lloyd, H., Bueti, D., and Walsh, V. (2011). Modality-independent role of the primary auditory cortex in time estimation. *Exp. Brain Res.* 209, 465–471.

Kanai, R., Paffen, C. L., Hogendoorn, H., and Verstraten, F. A. (2006). Time dilation in dynamic visual display. *J. Vis.* 6, 1421–1430.

Kaneko, S., and Murakami, I. (2009). Perceived duration of visual motion increases with speed. *J. Vis.* 9, 14.

Koch, G., Costa, A., Brusa, L., Peppe, A., Gatto, I., Torriero, S., Gerfo, E. L., Salerno, S., Oliveri, M., Carlesimo, G. A., and Caltagirone, C. (2008). Impaired reproduction of second but not millisecond time intervals in Parkinson's disease. *Neuropsychologia* 46, 1305–1313.

Matell, M. S., and Meck, W. H. (2004). Cortico-striatal circuits and interval timing: coincidence detection of oscillatory processes. *Brain Res. Cogn. Brain Res.* 21, 139–170.

Merchant, H., Zarco, W., and Prado, L. (2008). Do we have a common mechanism for measuring time in the hundreds of millisecond range? Evidence from multiple-interval timing tasks. *J. Neurophysiol.* 99, 939–949.

Morrone, M. C., Ross, J., and Burr, D. (2005). Saccadic eye movements cause compression of time as well as space. *Nat. Neurosci.* 8, 950–954.

Portugal, G. S., Wilson, A. G., and Matell, M. S. (2011). Behavioral sensitivity of temporally modulated striatal neurons. *Front. Integr. Neurosci.* 5:30. doi: 10.3389/fnint.2011.00030

Reutimann, J., Yakovlev, V., Fusi, S., and Senn, W. (2004). Climbing neuronal activity as an event-based cortical representation of time. *J. Neurosci.* 24, 3295–3303.

Sadeghi, N. G., Pariyadath, V., Apte, S., Eagleman, D. M., and Cook, E. P. (2011). Neural correlates of subsecond time distortion in the middle temporal area of visual cortex. *J. Cogn. Neurosci.* doi: 10.1162/jocn_a_00071. [Epub ahead of print].

Shuler, M. G., and Bear, M. F. (2006). Reward timing in the primary visual cortex. *Science* 311, 1606–1609.

Spencer, R. M., Karmarkar, U., and Ivry, R. B. (2009). Evaluating dedicated and intrinsic models of temporal encoding by varying context. *Philos. Trans. R. Soc. Lond. B Biol. Sci.* 364, 1853–1863.

Spencer, R. M., Zelaznik, H. N., Diedrichsen, J., and Ivry, R. B. (2003). Disrupted timing of discontinuous but not continuous movements by cerebellar lesions. *Science* 300, 1437–1439.

Walker, J. T., and Scott, K. J. (1981). Auditory-visual conflicts in the perceived duration of lights, tones and gaps. *J. Exp. Psychol. Hum. Percept. Perform.* 7, 1327–1339.

Wiener, M., Matell, M. S., and Coslett, H. B. (2011). Multiple mechanisms for temporal processing. *Front. Integr. Neurosci.* 5:31. doi: 10.3389/fnint.2011.00031

Wiener, M., Turkeltaub, P., and Coslett, H. B. (2010). The image of time: a voxel-wise meta-analysis. *Neuroimage* 49, 1728–1740.

Wittmann, M., Simmons, A. N., Aron, J. L., and Paulus, M. P. (2010). Accumulation of neural activity in the posterior insula encodes the passage of time. *Neuropsychologia* 48, 3110–3120.

Received: 25 July 2011; accepted: 26 July 2011; published online: 08 August 2011.

Citation: Bueti D (2011) The sensory representation of time. Front. Integr. Neurosci. ***5****:34. doi: 10.3389/fnint.2011.00034*

frontiers in
INTEGRATIVE NEUROSCIENCE

ORIGINAL RESEARCH ARTICLE
published: 08 September 2011
doi: 10.3389/fnint.2011.00050

Temporal and spatial categorization in human and non-human primates

Juan Carlos Mendez, Luis Prado, German Mendoza and Hugo Merchant*

Instituto de Neurobiología, Universidad Nacional Autónoma de México Campus Juriquilla, Queretaro, México

Edited by:
Warren H. Meck, Duke University, USA

Reviewed by:
Domenica Bueti, Centre Hospitalier Universitaire Vaudois and University of Lausanne, Switzerland
Dustin Merritt, Duke University, USA

***Correspondence:**
Hugo Merchant, Instituto de Neurobiología, Universidad Nacional Autónoma de México Campus Juriquilla, Boulevard Juriquilla No. 3001, Queretaro, Mexico.
e-mail: hugomerchant@unam.mx

It has been proposed that a functional overlap exists in the brain for temporal and spatial information processing. To test this, we designed two relative categorization tasks in which human subjects and a Rhesus monkey had to assign time intervals or distances to a "short" or "long" category according to varying prototypes. The performance of both species was analyzed using psychometric techniques that showed that they may have similar perceptual, memory, and/or decision mechanisms, specially for the estimation of time intervals. We also did a correlation analysis with human subjects' psychometric thresholds and the results imply that indeed, temporal and spatial information categorization share neural substrates. However, not all of the tested distances and intervals correlated with each other, suggesting the existence of sub-circuits that process restricted ranges of distances and intervals. A different analysis was done on the monkey data, in which the influence of the previous categorical prototypes was measured on the task currently being performed. Again, we found a significant interaction between previous and current interval and distance categorization. Overall, the present paper points toward common or at least partially overlapped neural circuits for temporal and spatial categorization in primates.

Keywords: time and space, categorization, psychophysics, Rhesus monkeys

INTRODUCTION

Moment by moment our brain is presented with uncountable stimuli that contain spatial and temporal information. The processing of these magnitudes is basic for successful behavior and it has been proposed that common neural mechanisms are used for their measurement. Evidence supporting this hypothesis, sometimes referred to as A Theory of Magnitude or ATOM (Walsh, 2003), comes from very different sources. Elapsed time is widely represented graphically in spatial coordinates and our language contains many metaphors that speak of time as a spatial magnitude and vice versa (Casasanto and Boroditsky, 2008; Vallesi et al., 2008). Also, patients with brain lesions affecting spatial processing show accompanying deficits in temporal estimation (Basso et al., 1996) and the opposite case, enhanced magnitude processing, has also been reported in synesthetes (Teuscher et al., 2010; Cohen Kadosh et al., 2011). This suggests that indeed, similar neural circuits are engaged when time and space are quantified. Among the structures that have been involved in these circuits are the prefrontal cortex and the posterior parietal cortex, particularly in the right hemisphere (Bueti and Walsh, 2009).

However, some challenges have been made to this theory (Correa and Nobre, 2008). An issue that has not been addressed is the degree of overlap in the processing of these magnitudes. If time and space are regarded as similar dimensions by the brain, then particular time intervals should be equivalent to particular distances and vice versa. While much research has been done regarding the neural mechanisms behind the quantification of different time scales (Gibbon et al., 1997; Buonomano and Karmarkar, 2002; Buhusi and Meck, 2005), there are, to our knowledge, no reports of separate substrates for the processing of distinct spatial scales. At least four different mechanisms have been proposed to account for timing in different ranges, from microseconds to circadian rhythms. Do all of these timing mechanisms also process spatial magnitudes? If so, which range of distances is quantified by them? An issue that has already been investigated is the influence that one magnitude exerts over the other. Casasanto and Boroditsky (2008) tested human subjects on six different tasks that required subjects to reproduce either the length or the duration of visual stimuli. They found that the spatial features of the stimuli had a significant influence on subjects' temporal estimates, but not the other way around. These results imply that there is an asymmetrical dependence in which temporal processing requires some degree of spatial representation. On the other hand, Rhesus monkeys did not seem to present this bias, since they were equally affected by irrelevant temporal or spatial information in their magnitude estimations (Merrit et al., 2010).

In the present work, we designed two categorization tasks in which time intervals in the millisecond range or distances in the millimeter range had to be categorized as "short" or "long" according to previously acquired prototypes. These tasks were performed by human subjects and one rhesus monkey. The rationale behind our approach is that categorization tasks are well characterized and allow the analysis of various psychophysical measures. Furthermore, categorization is one of the most common perceptual mechanisms in humans and consists in mentally grouping environmental stimuli into clusters known as categories. In the middle of a category lies a representative element, known as prototype, which has the greatest percentage of relevant features that characterize the category. Also, categories have limits or boundaries beyond which similar elements are not considered as members (Kéri, 2003). In fact, investigators have long hypothesized that the assignment of a particular stimulus to a category may be done either by comparing

it to the prototype, the boundaries, or to the members in the category (Ashby and Maddox, 2005). Importantly, categorization is a relative and dynamic process, since the same object can be part of different and even opposed groups depending on the current context (Maddox, 2002; Roy et al., 2010). Many species are capable of categorization and Rhesus monkeys have been trained to perform different categorization tasks (Merchant et al., 1997; Romo et al., 1997; Freedman et al., 2001; Smith et al., 2004). The aim of this research was two-fold: first, we wanted to determine the similarities and differences in spatial and temporal categorization between both species. Second, we studied whether different psychophysical measures supported the notion of a common or a partially overlapped mechanism for magnitude processing. Our results point that both species do share some mechanisms for temporal and spatial categorization and that these magnitudes influence each other. They also propose that a particular range of time intervals may be considered as equivalent to specific distances.

MATERIALS AND METHODS

HUMAN SUBJECTS

Participants

Twenty-five human subjects [13F, 12M; age 25.36 ± 3.49 years (mean $\pm$ SD)] with normal or corrected vision volunteered for this study. All subjects were right-handed and gave written consent before commencement of experiments. The study complied with the Declaration of Helsinki and was approved by the National University of Mexico Institutional Review Board.

Materials

We programmed two categorization tasks using Visual Basic (Microsoft Visual Basic 6.0, 1998) for the presentation of stimuli and behavioral data collection. All the tasks were performed in front of a computer monitor (HP 7540, 160 Hz refresh rate) with the chin and the forehead placed in a custom-made headrest that kept the subject's eyes approximately 56 cm from the center of the monitor. A joystick (H000E-NO-C, CTI electronics, Stratford, CT, USA) was manipulated by the subject to control the position of the cursor.

Tasks

All subjects were tested on the Temporal (TCT) and Spatial (SCT) Categorization Tasks. In both tasks, subjects had to categorize eight different stimuli as "short" or "long," the first four values being considered as "short" (see **Table 1**). In the case of SCT, subjects had to categorize eight different distances between two vertical bars, whereas in TCT they had to categorize eight different time intervals between the first and the second appearance of the bars. The temporal sequence of a trial was the same for both tasks (**Figure 1**). A circle appeared in the center of the screen with the cursor, represented by a small red dot, under it. The subject decided when to begin the trial by placing and maintaining the cursor inside the central circle. After a variable delay ($500 + \Delta$ 1,000 ms), two parallel bars ($8^\circ \times 0.7^\circ$ of visual angle) separated by a particular distance appeared briefly (50 ms) above the central circle, disappeared for a particular interval, and reappeared in the same position. In the SCT, the interval was kept constant in all the trials (669 ms) but the distance between the bars varied from trial to trial and could be any of the eight distances. In the TCT the opposite happened: the distance was kept constant (6° of visual angle), but the interval varied from one trial to the next. To help distinguish between tasks, the stimuli and the central circle were yellow in SCT and green in TCT. In both tasks, after a 1-s delay, two response circles were presented above the central circle. The leftmost circle represented the "short" category, whereas the rightmost represented the "long" category. The subject had to move the cursor to the response circle that matched the category of the stimulus, that is, the category of the trial's distance in the SCT or the interval in the TCT, based on previously acquired prototypes and boundaries (see below). Subjects were instructed to maintain their gaze in a fixation point located inside the central circle during trial execution.

In order to categorize the stimuli, subjects first had to acquire a criterion. To accomplish this, the first 24 trials were part of the "Training Phase" in which only the shortest and the largest distances or intervals, corresponding to the category prototypes, were presented in an alternate fashion. We expected that in this way, subjects generated a mental implicit value, that is the distance or the interval midway between the two prototypes presented, which would serve as a limit or boundary between categories (see **Table 1**). The correct response circle was highlighted to the subject with a green outline while the incorrect one had a red outline. When the subject placed the cursor inside the correct circle, the word "correct" appeared under the central circle. Otherwise, the word "incorrect" would be read. The 96 trials that followed were

Table 1 | Time and distance values used in TCT and SCT in human subjects.

Intervals for TCT (ms)			Distances for SCT (visual angle)		
T1 (350)	**T2 (685)**	**T3 (1195)**	**S1 (2.85)**	**S2 (4.8)**	**S3 (6.9)**
200			1.8		
250			2.1		
319			2.7		
331			2.8		
369			2.9		
381			3		
450	450		3.7	3.7	
500	500		4	4	
	619			4.6	
	669			4.7	
	706			4.9	
	756			5.1	
	870	870		5.7	5.7
	920	920		6	6
		981			6.6
		1169			6.8
		1231			7.1
		1419			7.3
		1470			7.9
		1520			8.2

The value in parentheses for each set corresponds to the implicit value, which was never actually presented to the subjects. Note that in each set, two values are shared with another block (shaded in gray). However, in one set these values belong to the "short" category and in the other block those same values belong to the "long" category.

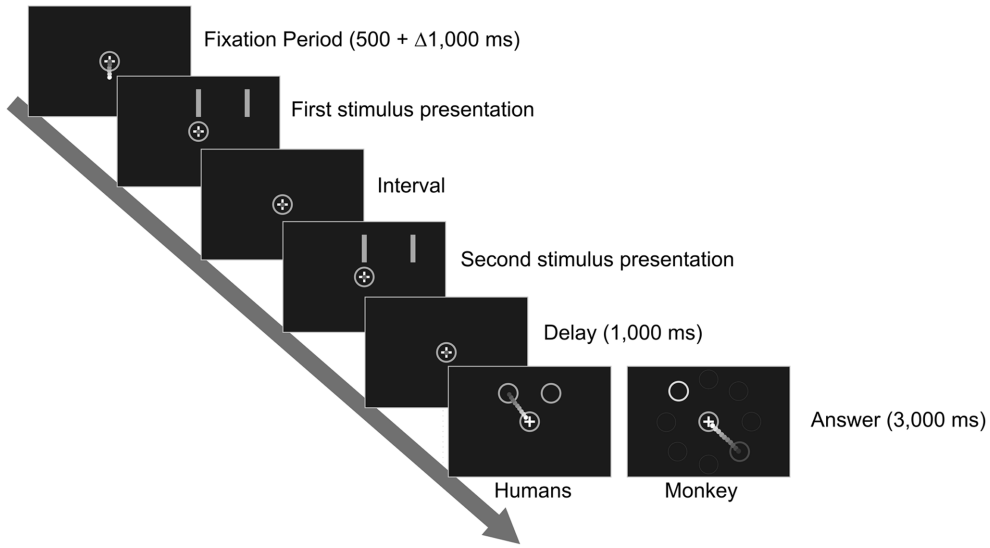

FIGURE 1 | Sequence of events in a trial of the Categorization Tasks. In SCT the distance between the bars changes from trial to trial but the interval is the same in all trials. In TCT the interval varies from trial to trial but the distance between the bars remains constant. Humans reported their decision by introducing the cursor inside the leftmost circle if they categorized the stimulus as "short" or inside the rightmost circle if they categorized it as "long." The monkey moved the cursor toward the circle with an orange outline if its decision was "short" and toward the circle with a blue outline if its decision was "long." Depicted are the eight possible positions that the response circles could adopt in the monkey response configuration. In a particular trial only the two response circles were visible.

regarded as part of the "Testing Phase," in which the eight values were presented randomly from trial to trial. Each value appeared 12 times and the 96 trials constitute one block. In this phase, both response circles had a green outline, so the only information available to the subject to solve the task was the distance or the interval. No feedback was provided during this phase.

We captured the relative nature of the categorization process in the following way: We created three different sets containing eight stimuli values each, for both tasks (labeled S1, S2, and S3 for the SCT and T1, T2, and T3 for the TCT). The values in these sets were arbitrarily defined after preliminary tests with human subjects in which the aim was to obtain sigmoid-shaped psychometric curves. Only one set of stimuli was used in a particular block of trials (see **Table 1**). The three sets used on each task represent a continuum across the space or time spectrum and, importantly, were partially overlapped: the two shortest and the two longest values of the middle set were exactly the same as the two longest values of the first set and the two shortest values of the third set, respectively. This means that one particular value could be correctly categorized either as "short" or as "long" depending on the context, that is on the particular set being used in that block. All subjects did both tasks with the three sets for a total of six blocks. The order in which the tasks were performed was assigned randomly for each subject but they decided how many sessions they needed to complete them (two or three).

Analysis

Subroutines written in Matlab (MathWorks v. 7.6.0.324) and the SPSS statistical package (version 17, SPSS Inc., Chicago, IL, USA, 2008) were used for statistical analyses. The psychophysical relative threshold was calculated for each subject and for each block of trials from the subject's psychometric curve, where the probability of long-interval categorization was plotted as a function of the stimulus magnitude. A logistic function was fitted to these data, and the relative threshold was computed as half the subtraction of the interval or the distance at $0.75p$ and at $0.25p$. The psychophysical relative threshold is a measure of the amount of change that a stimulus must have in the studied dimension to be detected by the subject. In addition, the point of subjective indifference (PSE) was calculated as the interval or distance at $0.5p$ in the psychometric curves. Then, the constant error was defined as the difference between the PSE minus the implicit interval or distance.

The relative thresholds of each subject on each of the six blocks were used in a correlation analysis. The rationale behind this analysis is that if a common system is being used to solve these tasks, then a subject's performance must be very similar throughout the six blocks. The level of statistical significance to reject the null hypothesis was $\alpha = 0.05$.

MONKEYS

Participant

One male Rhesus monkey (*Macaca mulatta*, 5.5 kg) was tested. All the experimental procedures were approved by the National University of Mexico Institutional Animal Care and Use Committee and conformed to the principles outlined in the Guide for Care and Use of Laboratory Animals (NIH, publication number 85–23, revised 1985).

Materials

The monkey performed the tasks using the same instruments as humans. It was seated in a primate chair with its head restrained

by a head halo. The position of its gaze was monitored throughout the experiments with an infrared eye scanner (ISCAN, Inc., Woburn, MA, USA).

Tasks

The monkey performed TCT and SCT. The sequence of events in a trial was almost identical to the one described for humans with one exception: in this case, the outline of one response circle was now orange and was associated with the "short" category, whereas the other circle's outline was blue and was associated with the "long" category. In this way, the response circles' position could be varied on each trial without losing the stimulus–response association. Each circle could occupy one of eight possible locations around the central circle (see **Figure 1**). This manipulation was implemented to dissociate possible relationships between the categorization process and the motor implementation of the decision communication in future neurophysiological experiments. During the "Training Phase," the color of the stimulus bars matched the color of the correct target, forcing the monkey to make a color-category association. Again, only the extreme values were presented during this phase, helping the monkey to create a mental implicit value. In the "Testing Phase" the color of the stimulus bars was always the same as the central circle's, that is yellow in SCT and green in TCT, regardless of the stimulus category. Correct trials were rewarded in both phases with drops of juice, with a greater amount delivered in the Testing Phase because of the greater difficulty of these trials. Also, in TCT, reward was adjusted to be proportional to the set of values being categorized in order to avoid a preference for the shorter intervals: blocks performed with T2 gave the monkey more juice than T1 blocks, but less juice than T3 blocks. It is important to mention that the values used in TCT were the same as the ones used by humans. However, the values used in SCT were slightly larger (**Table 2**).

Table 2 | Distance values used in SCT with the monkey.

Distances for SCT (visual angle)		
S1 (3.9)	**S2 (5.9)**	**S3 (8)**
2.8		
3.1		
3.7		
3.8		
4		
4.1		
4.7	4.7	
5	5	
	5.6	
	5.7	
	6	
	6.1	
	6.7	6.7
	7	7
		7.6
		7.8
		8.1
		8.3
		8.9
		9.2

*The value in parentheses for each set corresponds to the implicit value, which was never actually presented. Again, each block shares two values with another block (shaded in gray). However, in one block they belong to the "short" category and in the other to the "long" category. Time interval values (not shown) were the same as for humans (see **Table 1**).*

Training

The monkey was trained using classical conditioning techniques with drops of juice as a reward for every correct trial. Food was provided *ad libitum* in its cage but water was only available during training sessions. Body weight was strictly controlled and extra water was provided if needed. The monkey was trained 6 days a week for sessions of 2–3 h of duration in which it consumed around 200 ml of juice (see Zarco et al., 2009). We first determined hand dominance by placing the monkey in the primate chair in front of the computer monitor with the joystick at arm-reaching distance and rewarding joystick grasping, which it did preferentially with its right hand. After that, training proceeded with its left arm restrained and the following increasingly complex behaviors were sequentially rewarded: First, the monkey had to move and maintain the cursor inside a yellow central circle. Then, it had to move the cursor to a response circle that appeared at random positions in the periphery. The color of this circle could be either blue or orange from trial to trial. The next step was waiting inside the central circle for the presentation of the two-bar stimulus, which also varied randomly in color between blue and orange, before moving to the single response circle. Even though the stimulus was irrelevant at this time, its' color and that of the response circle always matched. The distance between the bars and their color were also co-varied, so when the color was orange, the distance was short (1.8° of visual angle, the shortest distance of set S1) and when the color was blue, the distance was long (8.2° of visual angle, the longest distance of set S3). Learning this took around 1 month.

A new level of difficulty was introduced by presenting the two response circles, orange and blue, simultaneously with a 1-s delay after stimulus presentation in pseudorandom positions around the central circle. The stimulus then became relevant, since the monkey had to remember its color and take the cursor to the response circle that matched it. This task was essentially the same as the "Training Phase" of SCT. The monkey learned this rule after approximately 5 months of training.

Once this had been achieved, we surgically implanted three head posts for skull fixation to a halo that maintained the monkey's head in the same position during training (see Merchant et al., 2001 for details in the surgery). This allowed us to train the monkey to fixate its gaze in a window centered in the middle of the monitor. If the monkey exited this window before the presentation of the response circles, the trial was aborted and the fixation point flashed briefly. The diameter of this window was systematically reduced until the monkey performed the tasks with a 4° diameter window. We then introduced testing trials in which the color of the bars was the same as the central circle's and the only

information available to solve the task was the distance between them. The monkey had to take the cursor to the orange circle if the distance was short and to the blue circle if the distance was long. This task was essentially the same as the "Testing Phase" of SCT and it was done initially with the two extreme distances mentioned above. Once the monkey had learned the rule, we progressively shortened the difference between the "short" and "long" distances, added intermediate distances, and used different "short" and "long" prototypes for particular blocks of trials until the monkey was performing SCT with the three different value sets. However, after several weeks of training, the monkey rarely did the task using S1 values with a performance above chance. This forced us to increase slightly the distances tested (**Table 2**). Reaching a stable performance with blocks above 70% of correct trials took around 6 months. Once this task had been learned, training in TCT was started from the "Training Phase." The central circle was now green and only two extremely different intervals (200 and 1520 ms) were presented from trial to trial. Again, when the short interval was presented, the stimulus bars were orange and when the long-interval was presented, the bars were blue. Training then proceeded in the same fashion as for SCT, with the progressive introduction of testing trials and the three different sets of intervals. In the end, around 2 years were needed for the monkey to perform the two tasks.

Analysis

As for humans' data, subroutines written in Matlab (MathWorks v. 7.6.0.324) and the SPSS statistical package (version 17, SPSS Inc., Chicago, IL, USA, 2008) were used for the statistical analyses. Again, the psychophysical relative threshold was used as a measure of the monkey's sensitivity. The PSE and the constant errors were also obtained as described for humans. In this case, the thresholds and constant errors were calculated for 19 blocks in the TCT and seven blocks in the SCT where the three set of stimuli showed a performance above 70% of correct trials and were computed in the same way as for humans. The level of statistical significance to reject the null hypothesis was $\alpha = 0.05$.

RESULTS

HUMAN AND MONKEY PERFORMANCE

Twenty-five human subjects and one monkey were tested on two relative categorization tasks in which either time intervals or distances in the millisecond and millimeter range respectively, were categorized as "short" or "long" according to previously instructed prototypes. **Figure 2A** shows the psychometric curves of both species for the three sets of values of TCT, in which the same stimuli were categorized by human subjects and the monkey. It can be seen that the curves are very similar across species, following the typical sigmoid shape characteristic of psychometric functions. Also, the slope of these curves decreases as a function of the values being categorized which implies that the scalar property is present in temporal categorization. This is more evident in **Figure 2C**, where the relative thresholds of the three curves are plotted as a function of the implicit value of the corresponding set of stimuli. Indeed, an ANOVA was carried out using the thresholds as dependent variable and the species as factors, and the results showed no significant differences in the timing thresholds between human subjects and monkeys [$F(1,130) = 2.22$, $p = 0.138$]. In addition, linear regressions between the timing threshold and the three implicit intervals were performed for each human subject and for each behavioral run in the monkey. Then, we performed ANOVAs where the slope or the intercept of such regressions were the dependent variable and the specie was the factor. The results showed no significant differences between species in neither the slope [$F(1,42) = 1.73$, $p = 0.196$] nor the regression intercept [$F(1,42) = 0.001$, $p = 0.978$], suggesting that the psychometric behavior in humans and Rhesus monkeys was very similar for interval categorization.

The scenario was different for spatial categorization. **Figure 2B** shows the psychometric curves for SCT of both species. Again, both species present sigmoid-shaped curves, but the slope is evidently steeper for humans than for monkeys, especially for the larger distances. As shown in **Figure 2D**, the relative thresholds were larger in the monkey than in human subjects [ANOVA, $F(1,94) = 133.9$, $p < 0.0001$]. However, as was the case in TCT, the spatial relative thresholds also showed an increase as a function of the implicit distance, and therefore, we performed linear regressions between these parameters for each human subject and across behavioral runs in the monkey. The corresponding ANOVAs showed a significant increase in the regression slope [ANOVA, $F(1,30) = 9.43$, $p = 0.005$] and intercept [ANOVA, $F(1,30) = 6.73$, $p = 0.015$] in the monkey with respect to human subjects. These results indicate that the categorization of distances between spatial stimuli was not as precise in macaques as in humans, at least for the range tested in the present study. Nevertheless, Weber's law is evident in both species.

On the other hand, we compared the constant error between species for the SCT and TCT (**Figures 2E,F**). Positive and negative constant errors are associated with under- and overestimation, respectively. For the TCT this measure was close to zero across implicit intervals in human subjects, whereas it showed a linear decrease as a function of the implicit interval in the monkey. The ANOVA showed marginal differences between species [$F(1,130) = 3.88$, $p = 0.051$]. In contrast, during the SCT the constant error showed a linear decrease as a function of implicit distance in both species with no significant differences between humans and monkeys [$F(1,94) = 1.99$, $p = 0.161$]. Overall, the constant error across implicit values was very close to zero for both species and tasks, which means that their estimation of the implicit value was very accurate.

To summarize, these findings suggest that the neural mechanisms for temporal categorization are similar between human subjects and macaques. Both species showed similar relative thresholds and a similar increase in temporal variability as a function of the implicit interval, following the scalar property of interval timing. In contrast, the monkeys showed larger relative thresholds for the SCT that could be due to differences in the processing of spatial information, the memory storage of spatial prototypes, or the decision process.

HUMAN SPACE–TIME INTERACTIONS

Previous studies have found that individual differences in the variability of execution of different timing are correlated (Keele et al.,

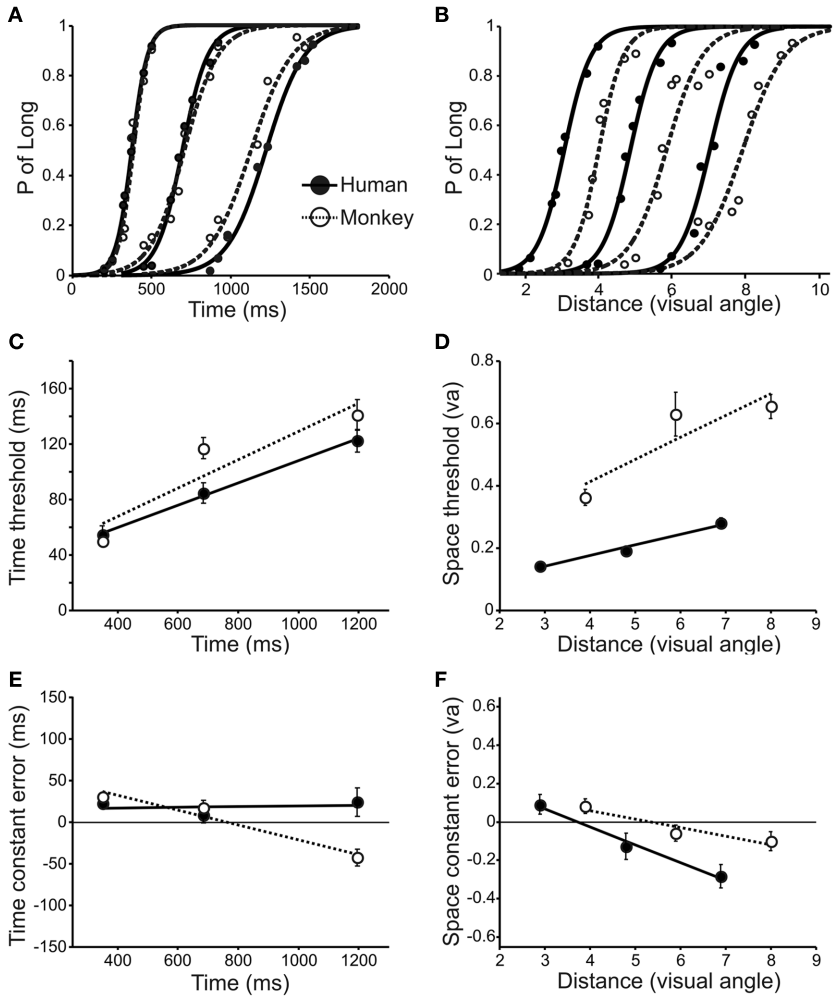

FIGURE 2 | (A,B) Psychometric curves of the human subjects and the monkey for the three sets of values used in TCT **(A)** and SCT (**B**). **(C,D)** Relative thresholds during TCT **(C)** and SCT **(D)** as a function of the implicit values used in both species. **(E,F)** Constant error as a function of implicit values during TCT **(E)** and SCT **(F)**; the horizontal line at zero corresponds to perfect accuracy. For thresholds and constant errors the lines correspond to the best linear regression models. Human subjects are depicted in solid lines and filled circles and the monkey in dotted lines and open circles.

1985; Spencer and Zelaznik, 2003; Merchant et al., 2008). This means that subjects that are good timers in one behavioral context are good timers in another one. Thus, the existence of significant intra-subject correlations in the temporal variability across different timing tasks has been taken as an indication of a common timing mechanism. In the present paper we used the individual variation in the thresholds for temporal and spatial categorization in order to determine whether there was a common magnitude mechanism across tasks. Correlations were carried out on the Z-scored relative threshold in order to analyze the precision of individual subjects between pairs of tasks.

Figure 3 shows the correlation matrix obtained from the comparison of the psychophysical relative thresholds of all the subjects in all the tasks. Three important results stem from this analysis: First, the three TCT sets were significantly correlated with each other (Pearson R T1–T2 = 0.694; T2–T3 = 0.348; T1–T3 = 0.454), a result that goes in accordance with the timing literature that proposes that at a single neural mechanism deals with time

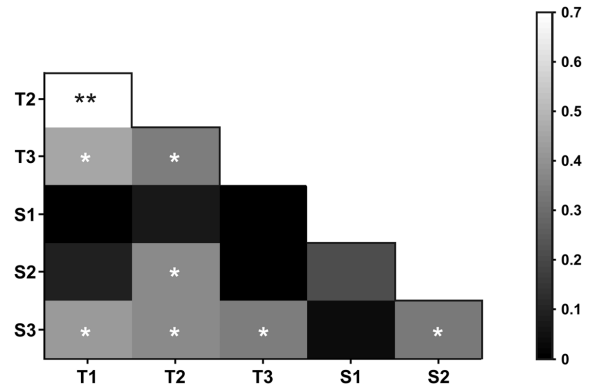

FIGURE 3 | Correlation matrix showing the Pearson *R* value in a grayscale (inset, right) for all possible pairwise block comparisons. Asterisks indicate significant correlations ($*p \leq 0.05$, $**p \leq 0.01$).

processing in the hundreds of milliseconds range (Gibbon et al., 1997). In contrast, in the case of SCT only S2 and S3 correlated significantly with each other ($R = 0.338$). Importantly, these were also the sets that correlated with the sets used for TCT. S2 correlated with T2 ($R = 0.378$) and S3 correlated with all three TCT sets (T1–S3 = 0.421; T2–S3 = 0.378; T3–S3 = 0.344). Blocks done with S1 values did not correlate with any other of the SCT or the TCT blocks.

These results support the hypothesis that at least in some scales temporal and spatial processing may be supported by common neural circuits. Furthermore, the fact that only some sets of distances correlated with each other and with the sets of intervals used, suggests that there may be sub-circuits specialized for the processing of narrow sub-ranges of distances and intervals which would be considered as equivalent magnitudes.

MONKEY SPACE–TIME INTERACTIONS

Due to the long training period in the monkey, it was impossible to use the individual differences in the performance variability between tasks to test whether a common magnitude mechanism exists across multiple Rhesus monkeys. Instead, we took advantage of the thousands of trials performed by the monkey in the SCT and TCT. The approach followed was to evaluate the effects of the set of values used in the previous block over the categorization performance of the current block during its initial and final trials within the SCT and TCT blocks, and then to determine the space–time interactions on this measure of categorization carryover. For this purpose, we first computed the normalized value of the difference in the number of correct trials between long minus short stimuli for the 20 initial test trials in the current block. A negative value of this normalized categorization bias indicates that the previous block-prototypes had an underestimation effect on the initial execution of the current block, whereas a positive value indicates an overestimation effect from the previous to the current categorization block. Indeed, **Figure 4A** shows that when the previous block was larger than the current one, there was a significant underestimation of the current block stimuli (t-test, $p < 0.05$), whereas when the previous was smaller than the current block there was a significant overestimation on the current block (t-test, $p < 0.05$). These effects were similar within the TCT (filled circles) and SCT (open circles) and were more evident between the sets T1 and T3, and between S1 and S3 (P>> and P<<, respectively) as shown in **Tables 1** and **2**. In contrast, when the normalized categorization bias was computed for the last 20 trails of the current block no significant under- or overestimation carryover effect was observed (**Figure 4B**). These results suggest that the previous short and long prototypes, within spatial or temporal categorization, had an initial influence on the current categorization performance, generating a bias that was congruent with the magnitude of the previous minus current block difference. The results also suggest that the influence of previous categorization prototypes was washed-out during task performance using newly instructed prototypes.

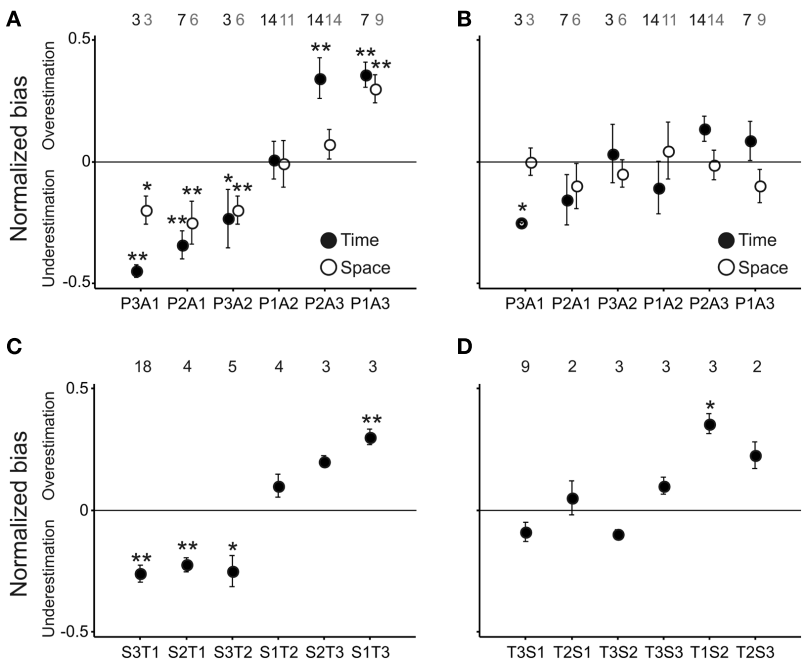

FIGURE 4 | Normalized categorization bias as a function of the difference between the previous and current blocks of stimuli. (A) Normalized bias for the initial 20 trials of the current block for TCT (solid circle) and SCT (open circle). **(B)** Normalized bias for the last 20 trials of the current block for TCT (solid circle) and SCT (open circle). In both **(A,B)** the ordinate labels correspond to the notation P*n*A*n*, where P is for previous and A for actual stimulus, and *n* is the set number. **(C)** Normalized bias for the initial 20 trials of the current block, when the current was TCT and the previous SCT (i.e., S3–T1 corresponds to a current T1 and a previous S3). **(D)** Normalized bias for the initial 20 trials of the current block, when the current was SCT and the previous TCT. The number of runs analyzed for each combination is depicted on top of each panel; for **(A,B)** the black and gray numbers correspond to TCT and SCT, respectively. $^{*}p \leq 0.1$, $^{**}p \leq 0.05$.

The next step was to evaluate whether the normalized categorization bias showed the same under/overestimation between the spatial and temporal categorization performance. The results showed that when the previous block was SCT and the current was TCT, there was congruent under- and overestimation on the initial 20 trials of the current block, with significant effects for the extreme magnitudes (S3 and T1, S1 and T3, t-test, $p < 0.05$; **Figure 4C**). These cross-magnitude carryover effects were smaller when the previous block was TCT and the current was SCT (**Figure 4D**).

These findings support the notion of a common magnitude mechanism across space and time, where the storage in memory of categorical prototypes from a previous block of trials of space has an influence on the current categorization performance of time. Consequently, it is possible that the memory representation of categorical prototypes has a similar neural representation for the two magnitudes.

DISCUSSION

Many previous papers have addressed the ability of Rhesus monkeys to categorize a wide variety of stimuli, from concrete objects (Freedman et al., 2001) to abstract entities (Romo et al., 1997; Freedman and Assad, 2006). In the same line, the first important result of our work is that the monkey was able to categorize time intervals and distances. In fact, its performance in TCT was comparable to humans'. This implies that their timing, memory, and decision mechanisms may be very similar to ours, at least for the processing of single intervals. In this respect, results from our own laboratory (Zarco et al., 2009) have pointed out that monkeys are capable of producing timed movements, but their performance is significantly better when single, rather than multiple intervals, are generated. In turn, this may be a consequence of the ecological significance of timing for both species. While humans need to explicitly time multiple intervals for complex behaviors, such as dance or language, monkeys rarely process more than one interval.

The monkey was not as good in the SCT as it was in TCT. It required a distance of a minimum of 2.8° of visual angle to have a performance above 70%, whereas humans had no problem categorizing distances below 2°. This may also be related to the environment in which the two species live, with humans manipulating tools, discriminating letters, and handling objects much smaller than monkeys do. Of course, a possibility exists that this particular monkey was not good at categorizing distances. However, preliminary results with a second monkey show a similar trend. Yet, the monkey was able to correctly categorize the spatial magnitude and, in the same way as humans, presented an increase in the relative threshold which means it is in accordance with Weber's law.

The constant errors, a measure of the accuracy of the categorization, showed that both species performed well in their estimation of the implicit values for each set. However, a tendency to underestimate the smaller values and to overestimate the larger ones was found for both tasks in monkeys, but only for SCT in humans. It has been argued the constant error is adjusted constantly as a function of the previous tasks, which reflects the influence of the global context on the current state of the system (Jones and McAuley, 2005). In this regard, it is possible that our experimental design accounts for some of the observed differences: the monkey performed at least six blocks per session, which would be sufficient for the constant error to be adjusted and minimized around the middle values. In contrast, humans normally performed only two or three blocks per session which would prevent the influence of previous blocks.

Another relevant finding is that there is a correlation between distance and interval categorization in humans. These results are in accordance with the hypothesis of an overlapped neural mechanism for the processing of these two magnitudes. However, not all the distances and intervals that we tested shared the same behavior. Categorization of distances below 3.7° of visual angle did not correlate with categorization of larger distances nor with any of the intervals. Conversely, larger distances not only correlated with each other but also with the time intervals used. This points toward possible subsets of the hypothetical magnitude processing circuits, each of which would be responsible for the quantification of different subscales. In this regard, distances in the 3.7–8.2° range may share the same neural substrate for estimation as intervals around 200 and 1520 ms. However, the degree of overlap may not be that straightforward. Distances between 3.7° and 6° only correlated with larger distances and with intervals between 450 and 920 ms. While more research is needed to support this notion, this result goes in hand with findings describing progressively wider tuning curves for the processing of bigger magnitudes (Nieder and Merten, 2007; Bartolo and Merchant, 2009; Merchant et al., 2011). In this sense, circuits that quantify larger distances would also be used to measure a broader range of intervals. Results obtained by Casasanto and Boroditsky (2008) may be considered as complementary to ours. They analyzed the influence that distances in the 7° to 27° range and intervals between 1,000 and 5,000 ms had on the estimation of each other. One of their results implies that for the 3,000 ms interval performance was best when presented together with a distance of 27° (800 pixels at the viewing distance and monitor resolution reported).

Finally, we investigated the carryover effect of the previous prototypes on the initial categorical performance with different current sets of values for the monkey. Within the spatial or temporal magnitudes the carryover found suggests an interference of the memory representation of the previous over the current prototypes. This interference might be due to the competition for the same neural substrates between the memory representation of the prototypes within each magnitude. In fact, a large set of studies in motor control have suggested that the interference between movement parameters in adaptation tasks of position-dependent visuomotor rotations (Tong et al., 2002) and velocity-dependent force fields (Brashers-Krug et al., 1996; Shadmehr and Brashers-Krug, 1997) are an evidence of shared neural resources for the encoding of these parameters. In addition, as in these motor adaptation tasks, we found a washout effect of the previous over the current block performance, emphasizing the dynamic and labile nature of the working memory representation of categorical prototypes. More importantly, the results also showed a cross-magnitude carryover effect of the previous

spatial prototype on the initial performance of the current set of temporal stimuli but not the other way around. This is a similar finding to Casasanto and Boroditsky's (2008) for human subjects but not for monkeys (Merrit et al., 2010). They attribute this space–time asymmetry in humans to a metaphorical representation of more abstract entities, such as time, with entities that can be perceived through the senses, such as space. They also propose several explanations for the absence of this asymmetry in monkeys, among them language-related differences and the lack of mental time-travel abilities. However, the fact that we found a greater influence of space on temporal categorization in the trained monkey implies that this asymmetry may be rooted in the neural circuits for magnitude processing, irrespective of language or other complex abilities. Of course, our results come from only one monkey and more animals need to be tested in these and similar tasks. Nevertheless, these data support the hypothesis of a common or partially overlapping neural mechanism for the working memory storage of categorical information of time and space. Hence, the present findings increase the list of psychophysical approaches to study the nature of common neural underpinnings of complex variables, such as time and space, using categorization behavior (Wright et al., 1997; Nagarajan et al., 1998).

To conclude, using different analytical approaches in human subjects and monkeys we have found evidence that implies that the primate brain uses a common or partially overlapping mechanism to represent categorical information about space and time. In addition, the results showed that the categorization abilities of a Rhesus monkey are similar to human subjects', especially for interval durations. Hence, the present paper indicates that the Rhesus monkey is a good animal model for studying the basis of spatial and temporal categorization. Indeed, the final goal of our research program is the neurophysiological study of the brain signals behind these highly complex cognitive abilities.

ACKNOWLEDGMENTS

We thank Raúl Paulín for his technical assistance and the Graduate Program in Biomedical Sciences of the Universidad Nacional Autónoma de México. Supported by CONACYT: 053944 and 244466, PAPIIT: IN200511-22. Funding source: TIMELY COST ISCH TD0904.

REFERENCES

Ashby, F. G., and Maddox, W. T. (2005). Human category learning. *Annu. Rev. Psychol.* 56, 149–178.

Bartolo, R., and Merchant, H. (2009). Learning and generalization of time production in humans: rules of transfer across modalities and interval durations. *Exp. Brain Res.* 197, 91–100.

Basso, G., Nichelli, P., Frassinetti, F., and Di Pellegrino, G. (1996). Time perception in a neglected space. *Neuroreport* 7, 2111–2114.

Brashers-Krug, T., Shadmehr, R., and Bizzi, E. (1996). Consolidation in human motor memory. *Nature* 382, 252–255.

Bueti, D., and Walsh, V. (2009). The parietal cortex and the representation of time, space, number and other magnitudes. *Philos. Trans. R. Soc. B Biol. Sci.* 364, 2369–2380.

Buhusi, C. V., and Meck, W. H. (2005). What makes us tick? Functional and neural mechanisms of interval timing. *Nat. Rev. Neurosci.* 6, 755–765.

Buonomano, D. V., and Karmarkar, U. R. (2002). How do we tell time? *Neuroscientist* 8, 42–54.

Casasanto, D., and Boroditsky, L. (2008). Time in the mind: using space to think about time. *Cognition* 106, 579–593.

Cohen Kadosh, R., Gertner, L., and Terhune, D. B. (2011). Exceptional abilities in the spatial representation of numbers and time: insights from synesthesia. *Neuroscientist* 17, 1–8.

Correa, A., and Nobre, A. C. (2008). Spatial and temporal acuity of visual perception can be enhanced selectively by attentional set. *Exp. Brain Res.* 189, 339–344.

Freedman, D. J., and Assad, J. A. (2006). Experience-dependent representation of visual categories in parietal cortex. *Nature* 443, 85–88.

Freedman, D. J., Riesenhuber, M., Poggio, T., and Miller, E. K. (2001). Categorical representation of visual stimuli in the primate prefrontal cortex. *Science* 291, 312–316.

Gibbon, J., Malapani, C., Dale, C. L., and Gallistel, C. (1997). Toward a neurobiology of temporal cognition: advances and challenges. *Curr. Opin. Neurobiol.* 7, 170–184.

Jones, M. R., and McAuley, J. D. (2005). Time judgments in global temporal contexts. *Percept. Psychophys.* 67, 398–417.

Keele, S. W., Pokorny, R. A., Corcos, D. M., and Ivry, R. (1985). Do perception and motor production share common timing mechanisms: a correctional analysis. *Acta Psychol. (Amst)* 60, 173–191.

Kéri, S. (2003). The cognitive neuroscience of category learning. *Brain Res. Rev.* 43, 85–109.

Maddox, W. T. (2002). Toward a unified theory of decision criterion learning in perceptual categorization. *J. Exp. Anal. Behav.* 78, 567–595.

Merchant, H., Bartolo, R., Mendez, J. C., Perez, O., Zarco, W., Mendoza, G. (2011). "What can be inferred from multiple-task psychophysical studies about the mechanisms for temporal processing?" in *Time and Time Perception*, ed. A. Vatakis (Berlin: Springer LNCS/LNAI series), 207–229.

Merchant, H., Battaglia-Mayer, A., and Georgopoulos, A. P. (2001). Effects of optic flow in motor cortex and area 7a. *J. Neurophysiol.* 86, 1937–1954.

Merchant, H., Zainos, A., Hernández, A., Salinas, E., and Romo, R. (1997). Functional properties of primate putamen neurons during the categorization of tactile stimuli. *J. Neurophysiol.* 77, 1132–1154.

Merchant, H., Zarco, W., and Prado, L. (2008). Do we have a common mechanism for measuring time in the hundreds of millisecond range? Evidence from multiple-interval timing tasks. *J. Neurophysiol.* 99, 939–949.

Merrit, D. J., Casasanto, D., and Brannon, E. M. (2010). Do monkeys think in metaphors? Representations of space and time in monkeys and humans. *Cognition* 117, 191–202.

Nagarajan, S. S., Blake, D. T., Wright, B. A., Byl, N., and Merzenich, M. (1998). Practice related improvements in somatosensory interval discrimination are temporally specific but generalize across skin location, hemisphere, and modality. *J. Neurosci.* 18, 1559–1570.

Nieder, A., and Merten, K. (2007). A labeled-line code for small and large numerosities in the monkey prefrontal cortex. *J. Neurosci.* 27, 5986–5993.

Romo, R., Merchant, H., Zainos, A., and Hernández, A. (1997). Categorical perception of somesthetic stimuli: psychophysical measurements correlated with neuronal events in primate medial premotor cortex. *Cereb. Cortex* 7, 317–326.

Roy, J. E., Riesenhuber, M., Poggio, T., and Miller, E. K. (2010). Prefrontal cortex activity during flexible categorization. *J. Neurosci.* 30, 8519–8528.

Shadmehr, R., and Brashers-Krug, T. (1997). Functional stages in the formation of human long-term motor memory. *J. Neurosci.* 17, 409–419.

Smith, J. D., Washburn, D. A., and Minda, J. P. (2004). Category learning in rhesus monkeys: a study of the Shepard, Hovland, and Jenkins (1961) tasks. *J. Exp. Psychol. Gen.* 3, 398–414.

Spencer, R. M., and Zelaznik, H. N. (2003). Weber (slope) analyses of timing variability in tapping and drawing tasks. *J. Mot. Behav.* 35, 371–381.

Teuscher, U., Brang, D., Ramachandran, V. S., and Coulson, S. (2010). Spatial cueing in time-space synesthetes: an event-related brain potential study. *Brain Cogn.* 74, 35–46.

Tong, C., Wolpert, D.M., and Flanagan, J. R. (2002). Kinematics and dynamics are not represented independently in motor working memory: evidence from an interference study. *J. Neurosci.* 22, 1108–1113.

Vallesi, A., Malcolm, A. B., and Schallice, T. (2008). An effect of spatial–temporal association of response codes: understanding the cognitive representations of time. *Cognition* 107, 501–527.

Walsh, V. (2003). A theory of magnitude: common cortical metrics of time, space and quantity. *Trends Cogn. Sci. (Regul. Ed.)* 7, 483–488.

Wright, B. A., Buonomano, D. V., Mahncke, H. W., and Merzenich, M. M.

(1997). Learning and generalization of auditory temporal-interval discrimination in humans. *J. Neurosci.* 17, 3956–3963.

Zarco, W., Merchant, H., Prado, L., and Mendez, J. C. (2009). Subsecond timing in primates: comparison of interval production between human subjects and Rhesus monkeys. *J. Neurophysiol.* 102, 3191–3202.

Conflict of Interest Statement: The authors declare that the research was conducted in the absence of any commercial or financial relationships that could be construed as a potential conflict of interest.

Received: 25 June 2011; paper pending published: 09 July 2011; accepted: 21 August 2011; published online: 08 September 2011.

*Citation: Mendez JC, Prado L, Mendoza G and Merchant H (2011) Temporal and spatial categorization in human and non-human primates. Front. Integr. Neurosci. **5**:50. doi: 10.3389/fnint.2011.00050*

frontiers in
INTEGRATIVE NEUROSCIENCE

ORIGINAL RESEARCH ARTICLE
published: 09 August 2011
doi: 10.3389/fnint.2011.00033

Emotion and time perception: effects of film-induced mood

Sylvie Droit-Volet[1]*, Sophie L. Fayolle[1] and Sandrine Gil[2]

[1] *Laboratoire de Psychologie Sociale et Cognitive, CNRS, UMR 6024, Université Blaise Pascal, Clermont-Ferrand, France*
[2] *Centre de Recherche sur la Cognition et l'Apprentissage, CNRS, UMR 6234, University of Poitiers, Poitiers, France*

Edited by:
Valerie Doyere, CNRS, France

Reviewed by:
Ullrich Wagner, Charité - University Medicine Berlin, Germany
Jason Tipples, University of Hull, UK

***Correspondence:**
Sylvie Droit-Volet, Laboratoire de Psychologie Sociale et Cognitive, CNRS, UMR 6024, Université Blaise Pascal, 34 Avenue Carnot, 63037 Clermont-Ferrand, France.
e-mail: sylvie.droit-volet@univ-bpclermont.fr

Previous research into emotion and time perception has been designed to study the time perception of emotional events themselves (e.g., facial expression). Our aim was to investigate the effect of emotions *per se* on the subsequent time judgment of a neutral, non-affective event. In the present study, the participants were presented with films inducing a specific mood and were subsequently given a temporal bisection task. More precisely, the participants were given two temporal bisection tasks, one before and the other after viewing the emotional film. Three emotional films were tested: one eliciting fear, another sadness, and a neutral control film. In addition, the direct mood experience was assessed using the Brief Mood Introspective Scale that was administered to the participants at the beginning and the end of the session. The results showed that the perception of time did not change after viewing either the neutral control films or the sad films although the participants reported being sadder and less aroused after than before watching the sad film clips. In contrast, the stimulus durations were judged longer after than before viewing the frightening films that were judged to increase the emotion of fear and arousal level. In combination with findings from previous studies, our data suggest that the selective lengthening effect after watching frightening films was mediated by an effect of arousal on the speed of the internal clock system.

Keywords: time perception, timing, emotion, mood, fear, sadness

INTRODUCTION

In everyday life, the experience of a mood changes our relationship with time. When we are sad and depressed we have the feeling that the flow of time slows down. Every hour seems like an eternity, as if time had stopped. In contrast, the feeling of stress seems to accelerate the flow of time. One hour seems nothing. Although these mood-related fluctuations in our experience of time have often been described, they have rarely been experimentally studied. Finally, we do not know whether these explicit judgments concerning the passage of time correspond to a reality experienced in our bodies or brains.

It may seem strange to speak about the reality of time since humans are not equipped with any specific sensory receptor enabling them to capture temporal information (for recent reviews, see Coull et al., 2011; Van Wassenhove et al., 2011). Nevertheless, the brain is inherently capable of processing time. Whatever the model of the temporal neural machinery (e.g., oscillators, climbing neurons, pulses), the subjective duration of events is thought to be based on cerebral units accumulated in time (e.g., Durstewitz, 2004; Matell and Meck, 2004; Karmarkar and Buonomano, 2007). Researchers have therefore posited the existence of an internal clock-like system that provides the raw material for the representation of time. According to the analogical internal clock models (Treisman, 1963; Gibbon et al., 1984), this clock consists of a pacemaker and an accumulator. At the beginning of the stimulus to be timed, a switch controlled by attention closes, and the pulses emitted by the pacemaker flow into the accumulator. The subjective duration thus depends on the number of pulses accumulated. When more pulses are accumulated, time is judged to be longer. Two main mechanisms have therefore been suggested to account for fluctuations in the passage of time: (1) an attention-based mechanism and (2) an arousal-based mechanism (Droit-Volet and Meck, 2007; Droit-Volet and Gil, 2009). In the case of the first mechanism, when attention is distracted away from the processing of time, the switch connecting the pacemaker to the accumulator opens, and some pulses are lost. The duration is therefore judged relatively shorter because fewer pulses have been accumulated. A shortening effect is therefore observed as the amount of attention devoted to time decreases. In the case of the second mechanism, a lengthening rather than a shortening effect occurs. When the level of arousal increases, the pacemaker is thought to speed up in line with the physiological activation of the organism. More pulses are emitted and the duration is judged longer. The mathematics underpinning the internal clock models predicts that the attention-based mechanism would result in an additive effect, with an attentional effect on switch closure latency that remains constant whatever the length of the stimulus duration. In contrast, the arousal-based speeding-up of the internal clock would result in a multiplicative effect accompanied by a lengthening effect that is relatively greater for long than for shorter stimulus durations (Penton-Voak et al., 1996; Penney et al., 2000; Droit-Volet and Wearden, 2002). This has been verified in experiments which have used at least two different duration ranges (a short and a longer one) and manipulated the level of dopamine in the brain through the administration of psychostimulant drugs (methamphetamine,

cocaine, caffeine; e.g., Maricq et al., 1981; Meck, 1983; Rammsayer, 1989, 2009).

As of some 10 years ago, researchers started to systematically investigate the mechanisms involved in the time distortions that are seen to occur in the presence of emotions. Unlike the pioneering psychologists who invented original situations without, however, perfectly controlling the emotional environment (e.g., Falk and Bindra, 1954; Langer et al., 1961; Thayer and Schiff, 1975), these researchers have used material taken from tested, validated databases of normative stimuli to elicit emotions in the laboratory (Coan and Allen, 2007). Studies of the perception of time have used images from the well-known International Affective Picture System (IAPS; Angrilli et al., 1997; Lang et al., 2008; Grommet et al., 2010). Pouthas and her collaborators also used sounds from the International Affective Digital Sounds (IADS; Bradley and Lang, 1999; Noulhiane et al., 2007; Mella et al., 2011). In our laboratory, we have mainly used emotional facial expressions (Droit-Volet et al., 2004; Effron et al., 2006; Gil et al., 2007; Gil and Droit-Volet, 2011a,b), which have since been used by other researchers (Tipples, 2008, 2011; Bar-Haim et al., 2009; Doi and Shinohara, 2009; Lee et al., 2011). These studies using different emotional stimuli have systematically shown that the presentation duration of negative high-arousing emotional stimuli was judged longer than that of neutral control stimuli. They thus logically explained this lengthening effect in terms of these emotional stimuli that physiologically activated the central nervous system, and accelerated the mechanisms which underpin the internal clock.

However, these different studies have investigated the judgment of the presentation duration of emotional stimuli rather than the effect of emotional states (mood) *per se* on the perception of time, i.e., on the perception of the duration of a neutral, non-affective stimulus. In the case of the processing of emotional stimuli, the non-temporal characteristics of the stimuli might interfere with the processing of time. As far as emotional sounds are concerned, the parameters of sounds (melodic contour, tempo, loudness, etc.) have been shown to affect the perception of time irrespective of their emotional dimension. For example, when listening to a piece of music, a feeling of happiness is induced when the music is played at a fast tempo in a major key compared to the feeling a sadness that results from hearing the music played at a slow tempo in a minor key (Peretz et al., 1998). Tempo is thus a critical factor influencing the experience of emotion. More specifically, when tempo is controlled, no effect of emotional valence on the perception of time is observed (Droit-Volet et al., 2010a). It is therefore difficult, on the basis of the temporal judgments, to distinguish between what is produced by the elicited emotion and the non-temporal characteristics of sound since the two are closely interlinked. This methodological problem is reduced in the case of emotional visual stimuli, or at least in the case of facial expressions. An angry face is indeed a threatening stimulus which in itself automatically activates the specific fear system related to defensive mechanisms that have their roots in human evolutionary history (Darwin, 1998; Ohman and Mineka, 2001). Recently, Tipples (2011) found that the magnitude of the overestimation of the presentation duration of angry faces depends on the level of threat experienced by individuals. However, the problem is that the arousal effect produced by the perception of an image of angry face is rapid and short-lived. The biological process of activation therefore occurs very quickly. In a temporal reproduction task, Bar-Haim et al. (2009) showed that the significant temporal overestimation of fearful faces disappeared after 2 s, "as if time perception returns to its baseline state." In these experimental conditions, it is therefore difficult to verify the existence of a multiplicative effect which would support the clock speed hypothesis but would require the use of two duration ranges, one longer than the other, in order to be tested.

The emotional stimuli used in the studies described above therefore have only a limited ability to produce intense forms of emotion which persist over time, with the result that it is only possible to study the effects of emotion on the perception of very short durations. The only studies that have elicited intense, long-lived emotions are probably the animal-based studies that have used fear conditioning paradigms based on the administration of electric shocks (e.g., Meck, 1983; Meck and MacDonald, 2007). In the experiment conducted by Meck (1983) using the temporal bisection task, rats were initially trained to discriminate between a short and a long anchor stimulus duration. They were then tested with probe durations (intermediate or similar values) in a footshock and a no-footshock condition. The results showed that the rats responded "long" more often in the footshock condition than in the no-footshock control condition, thus shifting the psychometric function toward the left and lowering the point of subjective equality (bisection point, BP). The BP is the stimulus duration judged to be long and short with equal frequency (proportion of long responses equal to 0.50). Meck (1983) therefore concluded that the footshock stress increased the speed of the animals' internal clock. In a recent study conducted among human adults, Droit-Volet et al. (2010b) employed a similar bisection task with an aversive sound (a 50-ms burst of 95 dB white noise with instantaneous rise time) heard at the end of the stimulus (blue circle) to be estimated. The emotional effects of this sound had already been tested in the participants on the basis of self-reports and electrophysiological measures (skin conductance response). In line with Meck's results, the authors found that the participants responded more often "long," with a leftward shift of the psychometric function and a lower BP value, on the trials in which the participants expected the aversive sound at the end of the stimulus duration compared to trials in which they expected either a non-aversive sound or no sound. This experiment thus clearly confirms that, in the same way as in animals, fear distorts time perception in human adults by inducing a lengthening effect. This finding is entirely consistent with the works on fear showing that threatening stimuli elicit fear reactions which automatically trigger a wide variety of behavioral and physiological responses (heart rate, muscle contraction), because the organism must be prepared to react as fast as possible for its survival (LeDoux, 2000; Phelps and LeDoux, 2005; Delgado et al., 2006; Phelps, 2006). One of the bodily changes observed in reaction to fear thus consists of a speeding-up of the internal clock (Droit-Volet et al., 2010). However, in these studies, the time distortions were the result of reactions to a detected or expected threatening stimulus which interfered with the processing of time and not the result of the effect of a diffuse emotional state on time judgments in a neutral situation devoid of emotional stimuli.

The originality of the present study therefore lies in the attempt to examine the effect of mood experience on participants' subsequent time judgment of neutral events. We used an emotion elicitation technique that had not previously been employed in studies of time perception, namely emotional film clips. We used three types of films from the recent database of films validated by Schaefer et al. (2011): films eliciting fear (1) or sadness (2) and neutral control films (3). The selected emotional films were used because they both elicit negative emotions. However, one was high-arousing (frightening film) and the other low-arousing (sad film; Izard, 1991). Before and after the presentation of the films, the participants performed a bisection task. The bisection task administered before the film was designed to provide baseline values. Two duration ranges (200/800 and 400/1600 ms) were used in order to try to identify the mechanisms underlying the effect of emotion on time perception (arousal/multiplicative effect or attention/additive effect) In addition, each participant's mood was assessed at the beginning and the end of each experimental session to identify changes in the mood experience produced by the film and verify whether their mood had dissipated. Our assumption was that after viewing a film, the perception of time would not change when the film was neutral. By contrast, stimulus durations would be judged longer (leftward shift of psychometric function and lower BP) after than before the high-arousing, fear-inducing film, and shorter (rightward shift of psychometric function and higher BP) after than before the sadness-inducing film that decreases the arousal level.

MATERIALS AND METHODS

PARTICIPANTS

Forty-five psychology students (Mean age = 19.46, SD = 1.31, 40 women and 5 men) participated in order to fulfill a course requirement and signed a written consent form as required by the Clermont-Ferrand Sud-Est VI Statutory Ethics Committee (CPP).

MATERIALS

The experiment took place in an isolated room at Blaise Pascal University. The participants were seated in front a PC, with a 17″ screen, that controlled the experimental events via E-prime software. Two loudspeakers were placed on either side of the computer. The stimulus to be timed was always a blue circle presented in the center of the computer screen. The response (long or short) consisted of pressing the "*S*" and "*L*" keys of the computer keyboard. The films consisted of excerpts taken from the Schaefer et al. (2011) validated database of emotional films. The films were selected as a function of the discrete emotion elicited (fear, sadness, neutrality) and the intensity of this emotion. The film clips were: The Blair (No. 55, code 65), Scream 1 (No. 16, code 26), and Shining (No. 28, code 38) for the emotion of fear; City of Angels (No. 36, code 46), Philadelphia (No. 62, code 72), and Dangerous Mind (No. 52 code 62), for sadness; and four excerpts of TV weather news and four excerpts of stock market news for the neutral condition. In each emotional condition, two different sequences of film clips were created to form a sequence of 9 min in length. The direct experience of mood produced in the participants by viewing these films was assessed using the French version of the Brief Mood Introspective Scale (BMIS; Mayer and Gaschke, 1988) with 18 mood-adjective scales (e.g., calm/calme, nervous/nerveux, aroused/excité, sad/triste, happy/joyeux, frightened/apeuré)(Niedenthal and Dalle, 2001). In the BMIS, the participants rated the intensity of their experience of each of the mood adjectives on a 4-point scale: (XX) definitely do not feel, (X) do not feel, (V) slightly feel, and (VV) definitely feel.

PROCEDURE

The participants were assigned to one of two duration conditions: 200/800 or 400/1600-ms. In the 200/800 condition, the short (*S*) anchor stimulus duration was 200 ms and the long (*L*) anchor stimulus duration 800 ms. The probe durations were 200, 300, 400, 500, 600, 700, and 800 ms. In the 400/1600-ms, *S* and *L* were 400 and 1600 ms and the probe durations 400, 600, 800, 1000, 1200, 1400, and 1600 ms. In each duration condition, the participants completed three emotion sessions as a function of film content (fear, sad, neutral). The sessions were presented with a new random order for each participant, with a 15-min inter-session interval during which the participants were free to leave the experimental room.

Each session consisted of two bisection tasks, a baseline bisection task given before film presentation (pre-film), which was followed by a test bisection task administered after film presentation (post-film). In the bisection task performed before the film, the participants were first presented with *S* and *L* once. They then performed the bisection task with eight blocks of seven trials (56 trials), with one trial being administered for each probe duration. For each probe duration, they therefore had to indicate whether it was more similar to *S* or to *L* by pressing the corresponding button. The durations within each block were presented randomly. The inter-trial interval was also randomly chosen between 500 and 1500 ms. The participants started the trial after the word "ready/prêt" was presented, immediately followed by a 200-ms interval and then the stimulus to be timed (blue circle). The procedure used for the post-film bisection task was exactly the same as that used in the pre-film bisection task, except that it was divided into two series of four blocks of trials, with emotional films being presented for 9 min before each series of blocks. In addition, the participants completed the BMIS at the start and end of each session, i.e., before and after viewing the emotional films.

RESULTS

ASSESSMENT OF EMOTIONS

Table 1 presents the mean mood ratings expressed by the participants on the 4-point scales for the 18 adjectives of the BMIS that was completed just before the pre-film bisection task and after the post-film bisection task. For each emotional condition taken separately, viewing the emotional films significantly changed the participants' mood as indicated by the overall ANOVAs on mood experience ratings with mood adjectives and the bisection task (before vs. after the film) as within-subjects factors. There was indeed a significant interaction between the mood adjectives and the bisection phases in each emotional condition [Fear, $F(17, 748) = 19.74$, Sadness, $F(17, 748) = 15.52$, and Neutral, $F(17, 748) = 8.19$, $p < 0.05$]. As shown in **Table 1**, in the fear condition, the participants felt less calm and more aroused or nervous after than before watching frightening movies [paired

Table 1 | Mean rate (*M*) and SEM of experienced mood on 4-point scales for 18 mood adjectives of the French version of the Brief Mood Introspective Scale (BMIS) given before and after the film, for each emotional content of the films (fear, sadness, and neutral).

	Fear				Sadness				Neutral			
	Before		After		Before		After		Before		After	
	M	SEM	*M*	SEM	*M*	SEM	*M*	SEM	*M*	SEM	*M*	SEM
Lively	2.44	0.12	2.42	0.13	2.49	0.14	2.07**	0.13	2.53	0.13	2.09**	0.13
Happy	2.78	0.11	2.44**	0.11	2.87	0.12	2.4**	0.10	2.84	0.12	2.6**	0.12
Sad	1.47	0.10	1.67	0.10	1.36	0.08	2.38**	0.13	1.53	0.10	1.36	0.09
Tired	2.51	0.13	2.4	0.14	2.4	0.14	2.53	0.14	2.42	0.14	2.78*	0.13
Caring	2.47	0.12	2.42	0.12	2.51	0.11	2.31*	0.12	2.6	0.11	2.4*	0.12
Content	2.76	0.12	2.22**	0.11	2.78	0.12	2.24**	0.12	2.8	0.12	2.69	0.13
Gloomy	1.4	0.11	1.58	0.12	1.31	0.09	2**	0.13	1.53	0.12	1.51	0.11
Aroused	1.58	0.09	1.96**	0.13	1.78	0.10	1.31**	0.07	1.62	0.12	1.53	0.11
Drowsy	1.96	0.14	1.6*	0.11	1.87	0.14	2.04	0.14	1.93	0.14	2.56**	0.14
Grouchy	1.29	0.07	1.49	0.11	1.24	0.08	1.2	0.07	1.29	0.08	1.4	0.10
Peppy	2.16	0.14	2.36	0.14	2.2	0.14	1.87**	0.14	2.27	0.15	1.78**	0.10
Nervous	1.49	0.10	2.31**	0.15	1.58	0.12	1.49	0.11	1.59	0.11	1.42	0.10
Calm	3.27	0.11	1.82**	0.11	3.13	0.12	3.11	0.11	2.98	0.12	3.07	0.12
Loving	2.62	0.14	2.16**	0.14	2.58	0.14	2.53	0.13	2.58	0.14	2.31*	0.15
Fedup	1.4	0.10	1.73	0.14	1.47	0.13	1.4	0.11	1.38	0.10	1.96**	0.15
Active	1.96	0.12	2.29*	0.12	2.11	0.12	1.78**	0.11	1.87	0.13	1.67*	0.11
Worried	1.31	0.10	2.09**	0.13	1.38	0.10	1.58*	0.11	1.44	0.10	1.29*	0.08
Frightened	1.11	0.05	2.22**	0.14	1.09	0.04	1.18	0.07	1.09	0.07	1.14	0.03

**Difference between the base line and the test significant at $p < 05$, and ** at $p < 0.01$.*

sample t-test, $t(44) = 9.57$, $t(44) = 2.78$, $t(44) = 5.144$, respectively, all $p < 0.05$]. They also reported being more frightened and worried [$t(44) = 7.77$, $t(44) = 5.48$, $p < 0.05$]. Watching sad films also caused the participants to feel sadder and gloomier and less happy [$t(44) = 8.17$, $t(44) = 6.05$, $t(44) = 5.72$, $p < 0.05$]. This also reduced the feeling of arousal [$t(44) = 3.32$, $p < 0.05$], although the participants reported that they remained calm between the two bisection tasks [$t(44) = 0.19$, $p > 0.05$]. Neutral films also changed the individuals' moods. However, it affected neither the arousal and calmness dimensions [$t(44) = 0.68$, $t(44) = 0.71$, $p > 0.05$], nor the specific emotions of fear and sadness [$t(44) = 1.21$, $t(44) = 1.83$, $p > 0.05$]. It simply made the participants feel more tired, less lively and less happy [$t(44) = 3.08$, $t(44) = 3.67$, $t(44) = 2.88$, respectively, $p < 0.05$]. In other words, they were more dispirited when they completed their reports, $t(44) = 3.83$, $p < 0.05$. In sum, watching the emotional films elicited the expected discrete emotions, i.e., fear and sadness, in the participants. These emotions were associated with an increase and a decrease in arousal level respectively, although the magnitude of the difference in arousal between the pre- and post-film bisection tasks was larger for the frightening films.

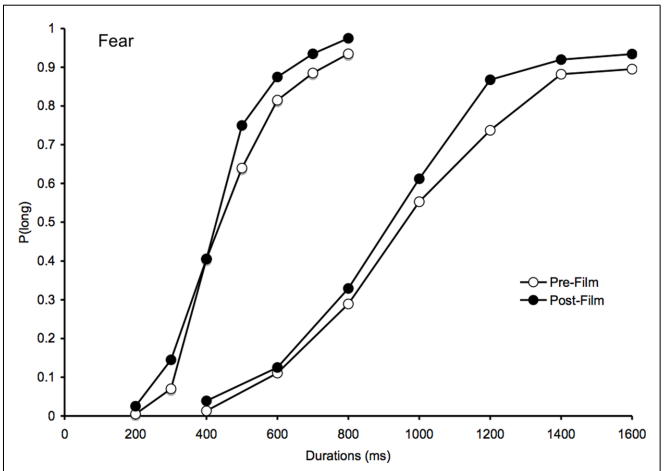

FIGURE 1 | Psychometric function for fear. Proportion of long responses plotted against probe durations (ms) for the bisection task before and after viewing the frightening films in the 200/400 and the 800/1600-ms duration range.

TEMPORAL BISECTION

For each emotional condition (fear, sadness, neutral), the psychometric functions were represented by plotting the proportion of long responses [p(long)] against the comparison durations in the 200/800 and the 400/1600-ms duration range for the two bisection tasks, i.e., before and after the presentation of the films (**Figures 1–3**). To account for the leftward or the rightward shift of the psychometric function for the post-film bisection task compared to that for the pre-film bisection task, we calculated the BP. As reported in introduction, the BP is the point of subjective equality, [$t(p(\text{long}) = 0.50$]. A decrease in the BP value reveals a time distortion in the form of a lengthening effect which is consistent with a leftward shift of the psychometric function. In contrast, an increase in the BP indicates a shortening effect associated with a

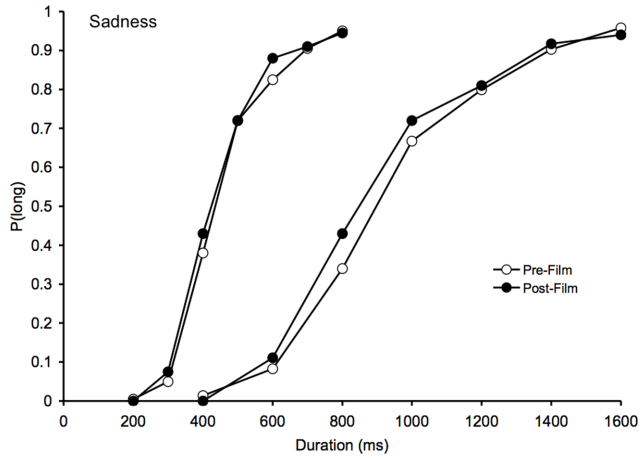

FIGURE 2 | Psychometric function for sadness. Proportion of long responses plotted against probe durations (ms) for the bisection task before and after viewing the sad films in the 200/400 and the 800/1600-ms duration range.

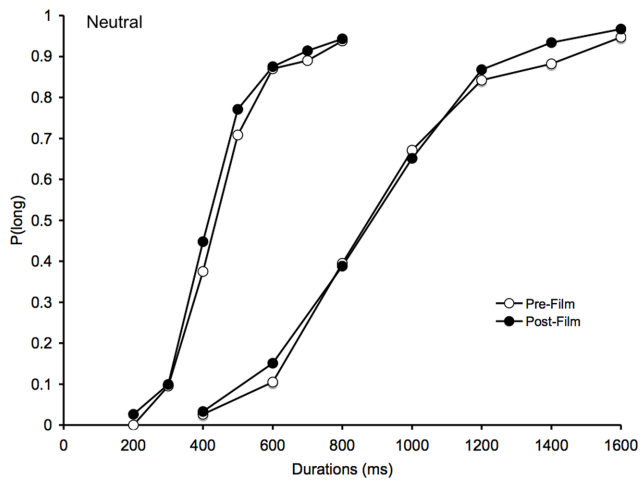

FIGURE 3 | Psychometric function for neutral. Proportion of long responses plotted against comparison durations (ms) for the bisection task before and after viewing the neutral films in the 200/400 and the 800/1600-ms duration range.

rightward shift of the psychometric function. This measures was derived from the slope and intercept parameters obtained by fitting a logistic function to the individual subject data. In the case of one participant, the fit was not significant in any emotional condition, and it was not significant in one of the three conditions for three other participants. The results for these participants were therefore excluded from the subsequent analyses. **Table 2** presents the BP obtained in this way.

An initial omnibus ANOVA was performed on the BP with duration range as between-subjects factor (200/800 vs. 400/1600) and two within-subjects factors: (1) the bisection task (pre- and post-film) and (2) the emotion (fear, sadness, neutral). The

Table 2 | Mean (*M*) and SEM for bisection point (BP) and Weber ratio (WR) for the films inducing fear and sadness as well as for the neutral films before and after viewing the films.

	Fear			
	BP		**WR**	
	M	**SEM**	***M***	**SEM**
200/800				
Pre-film	494	34	0.20	0.05
Post-film	446	35	0.14	0.03
400/1600				
Pre-film	1045	38	0.17	0.05
Post-film	910	39	0.17	0.03
	Sadness			
	BP		**WR**	
	M	**SD**	***M***	**SD**
200/800				
Pre-film	499	27	0.14	0.03
Post-film	481	31	0.16	0.03
400/1600				
Pre-film	996	31	0.12	0.03
Post-film	964	37	0.12	0.03
	Neutral			
	BP		**WR**	
	M	**SD**	***M***	**SD**
200/800				
Pre-film	483	25	0.15	0.02
Post-film	462	28	0.14	0.03
400/1600				
Pre-film	949	28	0.15	0.02
Post-film	918	31	0.20	0.03

ANOVAs on p(long) are not presented because the results were similar to those found for the BP. The ANOVA on the BP suggested the presence of time distortions as a function of task, i.e., pre- or post-film, and emotion. Indeed, there was a significant interaction between the timing of the task and the emotion, $F(2, 80) = 3.24$, $p < 0.05$, which subsumed a significant task effect, $F(1, 40) = 13.91$, $p < 0.05$, and no significant emotion effect, $F(2, 80) = 0.63$, $p > 0.05$. The effect of duration range was also significant, $F(1, 40) = 228.99$, $p < 0.05$, but duration range did not interact with any other factors (all $p > 0.05$). In the case of the pre-film bisection task, no significant effect of emotion, $F(2, 82) = 1.19$, $p > 0.05$, was found, thus indicating that there were no differences between the emotion conditions before the participants viewed the films. Consequently, to examine how the mood induced by a type of film modifies time perception, we compared the bisection performance before the film with that after the film for each emotional film taken separately. To do this we

ran an ANOVA on the BP with task time as within-subjects factor and duration range as a between-subjects factor for each type of emotional induction.

For the fear-inducing film (**Figure 1**), there was a clear leftward shift of the psychometric function after the film compared to the psychometric function before the film. This suggests that the comparison durations were judged longer after the participants had watched fear-inducing films that increased their arousal levels as the BMIS scores indicated. In line with this leftward shift of the psychometric functions, the ANOVA on the BP showed a significant main effect of task, $F(1, 41) = 20.05$, $p < 0.05$, indicating that the BP was lower after than before the frightening film (**Table 2**). There was also a significant task × duration interaction, $F(1,41) = 4.55$, $p < 0.05$, which subsumed a significant main effect of duration, $F(1, 41) = 110.75$, $p < 0.05$. For each duration range, the BP was indeed lower after than before the film [200/400, $F(1, 23) = 9.55$; 800/1600, $F(1, 18) = 10.52$, both $p < 0.05$]. The probe durations were thus judged longer after the frightening films, when the participants had experienced fear and were more aroused or nervous. In line with this suggestion, for the post-film bisection task, there was a significant correlation between the BP value and the subjective individual feeling of being more nervous/nerveux after viewing the frightening films ($R = 0.32$, $p < 0.05$): The more nervous the participants reported being in the BMIS after the film, the smaller their BP value was. The correlation between the BP value and the aroused/excité adjective did not reach significance, probably related to the French word "excité" that did not verbally describe as well as the word "nerveux" the subjective mood experienced by the participants after viewing a frightening film. In addition, and in accordance with the hypothesis of a clock rate mechanism (multiplicative effect), the magnitude of the difference in the BPs between the pre-film and post-film bisection tasks was larger for the long than for the shorter duration range. When we calculated the difference in the BPs between these two bisection tasks, the one-way ANOVA did indeed reveal a significant effect of duration that indicates that the task-related difference was larger in the 400/1600 than in the 200/800-ms duration condition [133.65 vs. 43.38, $F(1, 41) = 4.55$, $p < 0.05$].

With regard to the sad film clips, the assessment of mood experience using the BMIS suggested that these films did indeed induce sadness in the participants and reduce their arousal level. However, as **Figure 2** suggests, this change in mood did not significantly modify the participants' time perception. The ANOVA on the BP found neither a significant effect of task, $F(1, 41) = 2.08$, $p > 0.05$, nor any significant task × duration interaction, $F(1, 41) = 0.09$, $p > 0.05$. There was only a significant main effect of duration, $F(1, 41) = 163.72$, $p < 0.05$, thus indicating that the BP value was higher in the 400/1600 than in the 200/800-ms duration condition.

As expected, for the neutral films, the psychometric functions obtained after the neutral films were also similar to those obtained before the neutral films (**Figure 3**). Consequently, the effect of task on the BP was not significant [$F(1, 41) = 2.08$, $p > 0.05$], and neither was the effect of the task × duration interaction [$F(1, 41) = 1.44$, $p > 0.05$]. There was only a significant main effect of duration for the BP, $F(1, 41) = 163.72$, $p > 0.05$.

We performed the same analyses on the Weber ratio (WR; **Table 2**), which is an index of sensitivity to time. It is the Difference Limen [$t(p(\text{long}) = 0.75 - t(p(\text{long}) = 0.25)/2$] divided by the BP. A high WR value indicates that participants' temporal discrimination varies and that they find it more difficult to discriminate between two durations. The omnibus ANOVA on the WR did not show any significant effect (all $p > 0.05$). This is verified in the ANOVA conducted for the sad film [task, $F(1, 41) = 0.06$, duration, $F(1, 41) = 1.29$, task × duration, $F(1, 41) = 0.057$, all $p > 0.05$] and for the neutral film [task, $F(1, 41) = 1.11$, duration, $F(1,41) = 1.05$, task × duration $F(1,41) = 1.44$, all $p > 0.05$]. This indicates that Weber's Law continued to hold and that the sensitivity to time did not vary after viewing the neutral film and the sad films despite the reduction in arousal reported in the BMIS questions for the sadness.

For the fear-inducing film, in line with the general ANOVA, the ANOVA on the WR showed neither a significant main effect of emotion, $F(1,41) = 1.11$, $p > 0.05$, or of duration, $F(1,41) = 0.02$, $p > 0.05$, nor any significant emotion × duration interaction, $F(1, 41) = 1.12$, $p > 0.05$. This suggests that the scalar property of time continued to apply, with a constant WR being observed across the different durations. However, for the frightening film associated with a leftward shift of the psychometric function, this also confirms that the leftward shift of the psychometric functions in response to fear was proportional (multiplicative) rather than absolute (additive) in nature. This proportional shift was confirmed by the good superimposition of the psychometric functions when plotted on a relative scale by dividing the probe durations by the mean group BP (**Figure 4**). Overall, these different results suggest that, in the present experiment which used emotional films, the internal clock system ran faster when the participants experienced a fearful and arousing mood that caused the stimulus durations to be judged longer.

DISCUSSION

The originality of the present study lies in the fact that it attempts to investigate the effect of mood experience on the time perception of neutral events rather than to investigate the estimation of the duration of emotional events. We therefore showed our participants validated emotional films that lasted for long periods (9 min) in order to modify their general mood. Our results demonstrated that viewing emotional films for periods of several

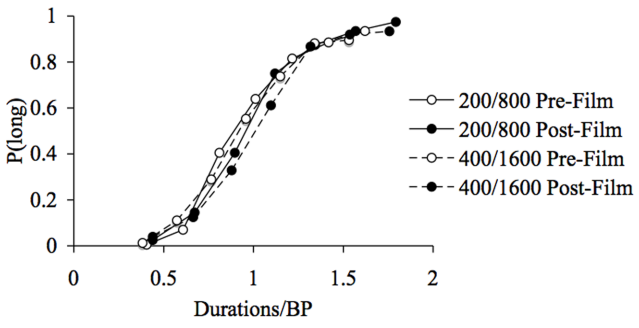

FIGURE 4 | Superimposition of psychometric functions for fear. Proportion of long responses plotted against probe durations divided by the bisection point (BP) for the pre- and post-film bisection task in the 200/400 and the 800/1600-ms duration range.

minutes changed the participants' mood, and that the mood experience may affect the perception of time in a subsequent temporal task. Three types of emotional films were used: frightening, sad, and neutral control films. In line with other studies which have used emotional films (Rottenberg et al., 2007), our results showed that viewing the frightening films increased the participants' feeling of fear and their arousal level. In contrast, viewing sad films induced sadness and decreased the level of arousal, while viewing neutral films did not significantly change the arousal dimension or the discrete emotions. The participants were simply bored by watching excerpts of TV weather or stock market news. However, and more originally, our results showed that the mood elicited by the films affected time judgments in a subsequent temporal task in which no emotional stimuli were present. The stimulus to be timed was simply a blue circle of the type often used in studies of time perception in humans. However, our results showed that the perception of time was distorted only following the induction of fear rather than of sadness.

Our study showed that the mood of fear produced by the frightening films had a lengthening effect on time perception, with the result that the stimulus durations were judged longer after than before viewing these emotional films. Indeed, our results indicated that the psychometric functions were shifted toward the left in the post-compared to the pre-film bisection tasks, with a significant lowering of the BP being observed. In addition, our results demonstrated that the fear-related effect on the perception of time was not due to simply watching a film, independently of the elicited emotion. Indeed, the neutral films did not affect time perception. In sum, a clear distortion of time was produced by the mood of fear induced by the films. Furthermore, this time distortion was not associated with an impairment of temporal discrimination. Indeed, our findings showed that variability in time discrimination did not change between the experimental conditions as indicated by the fact that the WR values were similar in the different conditions. They also showed that Weber's law holds whatever the emotional condition, with a constant WR being observed for the different stimulus duration ranges. Overall, these results are entirely consistent with those found in temporal studies using other negative highly arousing emotional stimuli (aversive sounds, faces, pictures; for a recent review, see Droit-Volet, in press). As in these earlier studies, we may thus assume that the lengthened time experience observed in response to the frightening films in our study was due to the automatic activation of the nervous system by the emotion of fear. Since the internal clock system depends on the dynamic functioning of the brain, when its rate increases in response to the emotion of fear, it produces more time units for the representation of time, and time is judged longer. In line with this idea, our results suggested a significant correlation between the subjective individual feeling of being more nervous after viewing the frightening films, on the one hand, and the magnitude of the lengthening effect, on the other. The more nervous the participants reported feeling after the frightening films, the lower the associated BP values were. According to the mathematics of the internal clock models, a clock rate-based mechanism requires a multiplicative effect in which the magnitude of the temporal overestimation is proportional to the duration values, i.e., it is greater for the long than for the shorter stimulus durations. This is confirmed by our data that showed a larger leftward shift of the psychometric function in response to fear in the 400/1600 than in the 200/800-ms duration conditions, and a greater difference between the BP values in the pre- and post-film bisection tasks in the long than in the shorter duration conditions. Furthermore, in the fear condition, when the psychometric functions for the two duration ranges were plotted against a relative scale (Probe durations/BP), they superimposed well. Overall, these different results support the idea that viewing frightening films speeds up the internal clock system and consequently lengthens the experience of time.

Unlike the emotion of fear, sadness did not modify time perception in the present bisection task despite the fact that the participants reported being sadder and less aroused after than before viewing the sad films in the BMIS. The mood of sadness is considered to be a low-arousal emotion inducing a slowing down of mental and motor activity (Izard and Ackerman, 2000). Consequently, on the basis of our results, we can suggest that a low-arousal emotion, i.e., an emotion that is not arousing, does not affect time perception. This is consistent with studies of emotions that have found that the durations of low-arousal stimuli were less overestimated that those of high arousal stimuli (Angrilli et al., 1997). Using negative low-arousal pictures from the IAPS, Gil and Droit-Volet (submitted) recently found that negative low-arousal pictures had few effect on time estimation compared to neutral pictures. Nevertheless, we might have expected that the decrease in arousal after the sad film would result in a slowing down of the internal clock system that, in turn, would have shortened the perceived duration. It is possible that, in our experiment, the magnitude of the decrease in arousal in the participants when viewing the sad films was insufficient to produce a significant physiological slowing down of the internal clock system. This type of slowing down may be observed to a greater extent during a major depressive episode associated with a real loss of energy (Hoffer and Osmond, 1962; Wyrick and Wyrick, 1977; Gil and Droit-Volet, 2009) or in response to the administration of sedative drugs (e.g., Rammsayer, 1989; Lustig and Meck, 2005). In a laboratory situation, it is therefore difficult to slow down the internal clock using external stimuli that significantly affect temporal behavior. Although several studies have used periodic clicks to accelerate the internal clock with click rates of between 5 and 25 Hz (Treisman et al., 1990; Ortega and López, 2008; Wearden, 2008), none have successfully attempted to slow down the internal clock by using lower click frequencies. In addition, these click rate effects have been observed in "relative" conditions, in which the clock slows down after having been accelerated, rather than in an "absolute" condition, i.e., following the measurement of a baseline clock rate. In this latter condition, Wearden (2008) was nevertheless able to manipulate the slowing down of the internal clock by designing a particularly boring experiment with long intervals between each trial. In these specific conditions, a significant rightward shift of time estimates was observed in the boring compared but to the non-boring experiment in both a temporal generalization and a temporal verbal estimation task but not in a temporal bisection task. In sum, it is very difficulty, but not impossible, to slow down the general nervous system and its internal clock by means of external emotional stimuli.

This difficulty in finding emotional stimuli that can slow down the internal clock system is due to the fact that human beings are genetically predisposed to produce automatic behavioral reactions rather than to reduce their rate of action when events occur in the environment. The motivation for action is thus one of the main factors explaining the acceleration of the internal clock mechanisms in response to emotion. Time distortions thus indirectly allow us to identify the fundamental adaptive function of emotions (Frijda, 1986). Fear is an emotional state of readiness for action. As argued by Droit-Volet (in press), a threatening stimulus triggers a cascade of physiological reactions: the pupils dilate, the heart accelerates, blood pressure increases, the muscles contract. The whole body is mobilized to react, i.e., to escape or to attack as quickly as possible. Consequently, without disrupting the processing of time, the internal clock runs faster, thus ensuring that the individual is prepared to react earlier to incoming events. In contrast, sadness is a poorly understood emotion, an obscure emotion in Lazarus' (1991) words. Its function is not clearly identified, all the more so since it often co-exists alongside other emotions (guilt, anger). In addition, the nature of the feeling of sadness depends on its source (dull pain, grief, frustration, empathy with others), as well as on its intensity and duration, with prolonged periods of sadness resulting in depression (Freed and Mann, 2007). Nevertheless, sadness is thought to be "linked to a loss, such as the death of someone we love, the failure of a central life value or role, or the loss of the positive regard of another" (Lazarus, 1991, p. 247). This loss therefore involves a certain degree of disengagement. In line with this behavioral description of emotions, neuroscientific studies using neuroimaging techniques have shown a clear relationship between the emotion of fear, the amygdala of the basal ganglia, and the dopaminergic system (LeDoux, 2005). The dopaminergic system is known to be involved in the detection of incoming events that are potentially dangerous and lead to a specific motor reaction. As Nieoullon and Coquerel (2003) explained, Dopa is a gatekeeper allowing stimuli to access high-order voluntary motor regions of the brain. More specifically, as reported above, time judgments have been shown to be highly sensitive to arousal effects and to the administration of dopaminergic drugs. In contrast, except in the case of major depression, little is known in the neuroscientific domain about episodes of sadness lasting several minutes. In the case of sadness, it seems that no specific neuroanatomical structures are involved, although the induction of a sad mood seems to involve the anterior cingulate cortex (Barrett, 2006; Freed and Mann, 2007). This probably explains why sadness had no effect on time in the present study. Whatever the case, the perception of time in the presence of sadness is particularly intriguing and various exploratory experiments are now required in order to gain a better understanding of individuals' relation to time in the emotional state of sadness.

ACKNOWLEDGMENTS

This work was supported by the European Cooperation in Science and Technology (COST; TIMELY) and by a Partner University Fund between France and United-States on Emotion and Time. It was also supported by a grant from the Agence Nationale de la recherche (ANR) Emotion(s), Cognition, Comportement from France.

REFERENCES

Angrilli, A., Cherubini, P., Pavese, A., and Manfredini, S. (1997). The influence of affective factors on time perception. *Percept. Psychophys.* 59, 972–982.

Bar-Haim, Y., Kerem, A., Lamy, D., and Zakay, D. (2009). When time slow down: the influence of threat on time perception in anxiety. *Cogn. Emot.* 24, 1–9.

Barrett, L. F. (2006). Are emotion natural kinds. *Assoc. Psychol. Sci.* 1, 28–57.

Bradley, M. M., and Lang, P. J. (1999). *International Affective Digitized Sounds (IADS): Stimuli, Instructions Manual and Affective Ratings.* (Tech. Rep. No. B-2). Gainesville, FL: University of Florida, Center for Research in Psychophysiology.

Coan, J. A., and Allen, J. J. B. (2007). *Handbook of Emotion Elicitation and Assessment.* Oxford: Oxford University Press.

Coull, J. T., Cheng, R. K., and Meck, W. H. (2011). Neuroanatomical and neurochemical substrates of timing. *Neuropsychopharmacology* 36, 3–25.

Darwin, C. (1998). *The Expression of the Emotions in Man and Animals.* Oxford: Oxford University Press. [Original work published 1872].

Delgado, M. R., Olsson, A., and Phelps, E. A. (2006). Extending animal models of fear conditioning to humans. *Biol. Psychol.* 73, 39–48.

Doi, H., and Shinohara, K. (2009). The perceived duration of emotional face is influenced by the gaze direction. *Neurosci. Lett.* 457, 97–100.

Droit-Volet, S., Bigand, E., Ramos, D., and Bueno, J. L. O. (2010a). Time flies with music whatever its emotional valence. *Acta Psychol. (Amst.)* 135, 226–236.

Droit-Volet, S., Mermillod, M., Cocenas-Silva, R., and Gil, S. (2010b). The effect of expectancy of a threatening event on time perception in human adults. *Emotion* 10, 908–914.

Droit-Volet, S., Brunot, S., and Niedenthal, P. M. (2004). Perception of the duration of emotional events. *Cogn. Emot.* 18, 849–858.

Droit-Volet, S., and Gil, S. (2009). The time-emotion paradox. *J. Philos. Trans. R. Soc. Lond. B Biol. Sci.* 364, 1943–1953.

Droit-Volet, S., and Meck, W. H. (2007). How emotions colour our time perception. *Trends Cogn. Sci. (Regul. Ed.)* 11, 504–513.

Droit-Volet, S., and Wearden, J. H. (2002). Speeding up an internal clock in children? Effects of visual flicker on subjective duration. *Q. J. Exp. Psychol.* 55B, 193–211.

Droit-Volet, S. (in press). "What emotions tell us about time," in *Subjective Time: The Philosophy, Psychology, and Neuroscience of Temporality,* eds D. Llyod and V. Arstila (Cambridge, MA: MIT Press).

Durstewitz, D. (2004). Neural representation of interval time. *Neuroreport* 15, 745–749.

Effron, D. A., Niedenthal, P. M., Gil, S., and Droit-Volet, S. (2006). Embodied temporal perception of emotion. *Emotion* 6, 1–9.

Falk, J. L., and Bindra, D. (1954). Judgment of time as a function of serial position and stress. *J. Exp. Psychol.* 39, 327–331.

Freed, P. J., and Mann, J. J. (2007). Sadness and loss: toward a neurobiopsychosocial model. *Am. J. Psychiatry* 164, 1, 28–34.

Frijda, N. H. (1986). *The Emotions.* New York: Cambridge University Press.

Gibbon, J., Church, R. M., and Meck, W. (1984). "Scalar timing in memory," in *Annals of the New York Academy of Sciences, 423: Timing and Time Perception*, eds J. Gibbon and L. Allan (New York: New York Academy of Sciences), 52–77.

Gil, S., and Droit-Volet, S. (2009). Time perception, depression and sadness. *Behav. Processes* 80, 169–176.

Gil, S., and Droit-Volet, S. (2011a). Time flies in the presence of angry faces, depending on the temporal task used! *Acta Psychol. (Amst.)* 136, 354–362.

Gil, S., and Droit-Volet, S. (2011b). Time perception in response to ashamed faces in children and adults. *Scand. J. Psychol.* 52, 138–145.

Gil, S., Niedenthal, P. M., and Droit-Volet, S. (2007). Anger and time perception in children. *Emotion* 7, 219–225.

Grommet, E. K., Droit-Volet, S., Gil, S., Hemmes, N. S., Baker, A. H., and Brown, B. (2010). Effects of a fear cue on time estimation in human observers. *Behav. Processes* 86, 88–93.

Hoffer, A., and Osmond, H. (1962). The relationship between mood and time perception. *Psychiatr. Q. Suppl.* 36, 87–92.

Izard, C. E. (1991). *The Psychology of Emotions.* New York: Plenum.

Izard, C. E., and Ackerman, B. (2000). *Motivational, Organizational and Regulatory Functions of Discrete Emotions. Handbook of Emotions,* 2nd Edn. New York: Guilford Press.

Karmarkar, U. R., and Buonomano, D. V. (2007). Timing in the absence of clocks: encoding time in neural network states. *Neuron* 53, 427–438.

Lang, P. J., Bradley, M. M., and Cuthbert, B. N. (2008). *International Affective Picture System (IAPS): Affective Ratings of Pictures and Instruction Manual.* Technical Report A-8. Gainesville, FL: University of Florida.

Langer, J., Wapner, S., and Werner, H. (1961). The effect of danger upon the experience of time. *Am. J. Psychol.* 74, 94–97.

Lazarus, R. S. (1991). *Emotion and Adaptation.* New York: Oxford University Press.

LeDoux, J. E. (2000). Emotion circuits in the brain. *Annu. Rev. Neurosci.* 23, 155–184.

LeDoux, J. E. (2005). Fear and the brain. Where have we been and where are we going. *Biol. Psychiatry* 44, 1229–1238.

Lee, K-H., Seelam, K., and O'Brien, T. (2011). The relativity of time perception produced by facial emotion stimuli. *Cogn. Emot.* doi:10.1080/02699931.2010.544455. [Epub ahead of print].

Lustig, C., and Meck, W. H. (2005). Chronic treatment with haloperidol induces deficits in working memory and feedback effects of interval timing. *Brain Cogn.* 58, 9–16.

Maricq, A. V., Roberts, S., and Church, R. M. (1981). Methamphetamine and time estimation. *J. Exp. Psychol. Anim. Behav. Process.* 7, 18–30.

Matell, M. S., and Meck, W. H. (2004). Cortico-striatal circuits and interval timing: coincidence-detection of oscillatory processes. *Brain Res. Cogn. Brain Res.* 21, 139–170.

Mayer, J. D., and Gaschke, Y. N. (1988). The experience and meta-experience of mood. *J. Pers. Soc. Psychol.* 55, 102–111.

Meck, W. H. (1983). Selective adjustment of speed of internal clock and memory processes. *J. Exp. Psychol. Anim. Behav. Process.* 9, 171–201.

Meck, W. H., and MacDonald, C. J. (2007). Amygdala inactivation reverses fear's ability to impair divided attention and make time still. *Behav. Neurosci.* 121, 707–720.

Mella, N., Conty, L., and Pouthas, V. (2011). The role of physiological arousal in time perception: psychophysiological evidence from an emotion regulation paradigm. *Brain Cogn.* 75, 2, 182–187.

Niedenthal, P. M., and Dalle, N. (2001). Le mariage de mon meilleur ami: emotional response categorization during naturally-induced emotional states. *Eur. J. Soc. Psychol.* 31, 737–742.

Nieoullon, A., and Coquerel, A. (2003). Dopamine: a key regulator to adapt action, emotion, motivation and cognition. *Curr. Opin. Neurol.*16, 3–9.

Noulhiane, M., Mella, N., Samson, S., Ragot, R., and Pouthas, V. (2007). How emotional auditory stimuli modulate time perception. *Emotion* 7, 697–704.

Ohman, A., and Mineka, S. (2001). Fears, phobias, and preparedness. Toward an evolved module of fear and fear learning. *Psychol. Rev.* 108, 483–522.

Ortega, L., and López, F. (2008). Effects of visual flicker on subjective time in a temporal bisection task. *Behav. Processes* 78, 380–386.

Penney, T., Gibbon, J., and Meck, W. (2000). Differential effects of auditory and visual signals on clock speed and temporal memory. *J. Exp. Psychol. Hum. Percept. Perform.* 26, 1770–1787.

Penton-Voak, I. S., Edwards, R., Percival, K., and Wearden, J. H. (1996). Speeding up an internal clock in humans? Effects of click trains on subjective duration. *J. Exp. Psychol. Anim. Behav. Process.* 22, 307–320.

Peretz, I., Gagnon, L., and Bouchard, B. (1998). Music and emotion: perceptual determinants, immediacy, and isolation after brain damage. *Cognition* 68, 111–141.

Phelps, E. A. (2006). Emotion and cognition: insights from studies of the human amygdala. *Annu. Rev. Psychol.* 57, 27–53.

Phelps, E. A., and LeDoux, J. E. (2005). Contributions of the amygdala to emotion processing: from animal models to human behavior. *Neuron* 48, 175–187.

Rammsayer, T. (1989). Dopaminergic and serotoninergic influence on duration discrimination and vigilance. *Pharmacopsychiatry* 22, 39–43.

Rammsayer, T. (2009). Effects of pharmacologically induced dopamine-receptor stimulation on human temporal information processing. *Neuroquantology* 7, 103–113.

Rottenberg, J., Ray, R. B., and Gross, J. J. (2007). "Emotion eliciting films," in *Handbook of Emotion Elicitation and Assessment*, eds J. A. Coan and J. J. B. Allen (Oxford: Oxford University Press), 9–28.

Schaefer, A., Nils, F., Sanchez, X., and Philippot, P. (2011). Assessing the effectiveness of a large database of emotion-eliciting films: a new tool for emotion researchers. *Cogn. Emot.* 24, 1153–1172.

Thayer, S., and Schiff, W. (1975). Eye-contacts, facial expression, and the experience of time. *J. Soc. Psychol.* 95, 117–124.

Tipples, J. (2008). Negative emotionality influences the effects of emotion on time perception. *Emotion* 8, 127–131.

Tipples, J. (2011).When time stands still: fear-specific modulation of temporal bias due to threat. *Emotion* 11, 74–80.

Treisman, M. (1963). Temporal discrimination and the indifference interval: implications for a model of the "internal clock." *Psychol. Monogr.* 77, 1–13.

Treisman, M., Faulkner, A., Naish, P. L. N., and Brogan, D. (1990). The internal clock: evidence for a temporal oscillator underlying time perception with some estimates of its characteristic frequency. *Perception* 19, 705–748.

Van Wassenhove, V., Wittmann, M., Craig, A. D., and Paulus, M. P. (2011). Psychological and neural mechanisms of subjective time dilation. *Front. Neurosci.* 5:56. doi: 10.3389/fnins.2011.00056

Wearden, J. H. (2008). Slowing down an internal clock: implications for accounts of performance on four timing. *Q. J. Exp. Psychol.* 61, 263–274.

Wyrick, R. A., and Wyrick, L. C. (1977). Time experience during depression. *Arch. Gen. Psychiatry* 34, 1441–1443.

Conflict of Interest Statement: The authors declare that the research was conducted in the absence of any commercial or financial relationships that could be construed as a potential conflict of interest.

Received: 30 May 2011; paper pending published: 16 June 2011; accepted: 22 July 2011; published online: 09 August 2011.
Citation: Droit-Volet S, Fayolle SL and Gil S (2011) Emotion and time perception: effects of film-induced mood. Front. Integr. Neurosci. ***5****:33. doi: 10.3389/fnint.2011.00033*

frontiers in
INTEGRATIVE NEUROSCIENCE

ORIGINAL RESEARCH ARTICLE
published: 16 November 2011
doi: 10.3389/fnint.2011.00073

Subjectivity of time perception: a visual emotional orchestration

Anna Lambrechts[1], Nathalie Mella[2], Viviane Pouthas[3] and Marion Noulhiane[4]*

[1] *INSERM Cognitive Neuroimaging Unit (U992), CEA/DSV/I2BM/NeuroSpin, Gif-sur-Yvette, France*
[2] *Department of Psychology, University of Geneva, Geneva, Switzerland*
[3] *Groupe Cogimage CRICM, UPMC/INSERM UMRS975/CNRS UMR7225, Paris, France (retired)*
[4] *UMR 663 Epilepsies de l'Enfant et Plasticité Cérébrale - INSERM Paris Descartes University Hôpital Necker Enfant Malade, France /CEA/DSV/I2BM/NeuroSpin, Gif-sur-Yvette, France*

Edited by:
Valerie Doyere, Centre National de la Recherche Scientifique, France

Reviewed by:
Annett Schirmer, National University of Singapore, Singapore
Kwang-Hyuk Lee, University of Sheffield, UK

***Correspondence:**
Marion Noulhiane, UMR663 INSERM Université Paris Descartes - Epilepsies de l'Enfant et Plasticité Cérébrale Hôpital Necker Enfant Malade / CEA NeuroSpin, I2BM, DSV, CEA, Bat 145, PC 156 - 91191 Gif Sur Yvette, France.
e-mail: marion.noulhiane@parisdescartes.fr

The aim of the present study was to examine how visual emotional content could orchestrate time perception. The experimental design allowed us to single out the share of emotion in the specific processing of content-bearing pictures, i.e., real-life scenes. Two groups of participants had to reproduce the duration (2, 4, or 6 s) of content-deprived stimuli (gray squares) or differentially valenced content-bearing stimuli, which included neutral, pleasant, and unpleasant pictures (International Affective Pictures Systems). Results showed that the effect of content differed according to duration: at 2 s, the reproduced duration was longer for content-bearing than content-deprived stimuli, but the difference between the two types of stimuli decreased as duration increased and was not significant for the longest duration (6 s). At 4 s, emotional (pleasant and unpleasant) stimuli were judged longer than neutral pictures. Furthermore, whatever the duration, the precision of the reproduction was greater for non-emotional than emotional stimuli (pleasant and unpleasant). These results suggest a dissociation within content effect on timing in the visual modality: relative overestimation of all content-bearing pictures limited to short durations (2 s), and delayed overestimation of emotional relative to neutral pictures at 4 s, as well as a lesser precision in the temporal judgment of emotional pictures whatever the duration. Our results underline the relevance for time perception models to integrate two ways of assessing timing in relationship with emotion: accuracy and precision.

Keywords: subjective time, content, emotional valence

INTRODUCTION

The literature on time perception contains many examples showing that subjective time is greatly modulated by stimulus features. A well-known effect is the sensory modality effect, i.e., the duration of light and sound are judged differently. Evidence suggests that auditory stimuli are judged longer and with greater precision than visual stimuli of equal duration and these findings have generally been interpreted in the framework of the scalar expectancy theory (Gibbon et al., 1984; Penney and Tourret, 2005; Droit-Volet et al., 2007; Noulhiane et al., 2008). This latter considers the model of an internal clock composed of three stages (1) a clock, i.e., a switch opening at the beginning of a temporal event and closing at the end of it, and a pacemaker generating pulses, (2) an accumulator stocking pulses throughout the event, (3) a comparator computing the difference between the accumulated number of pulses in working memory and a known duration in reference memory. In this interpretation the modality effect is mainly located at the clock stage: either because the pacemaker is faster in the auditory modality (Wearden et al., 1998, 2006; Droit-Volet et al., 2004b), or because the switch flickers more in the visual modality, more pulses are accumulated with sounds than lights therefore auditory signals seem longer than visual stimuli of equivalent duration (Collier and Logan, 2000; Penney et al., 2000; Droit-Volet et al., 2007). Another effect involves the sensory material filling the interval to be timed. In the auditory modality, a clear distinction is made between empty and filled intervals: empty intervals are bounded by two brief tones, whereas filled intervals contain a continuous tone with a beginning and an end. Psychophysical studies indicate greater accuracy in the timing of empty intervals (Rammsayer and Lima, 1991; Grondin, 1993). In addition, an increasing number of studies show that numerical and spatial content can interfere with temporal estimation, i.e., the number and the size of objects presented, or the magnitude of task-irrelevant Arabic numbers appearing alongside the stimulus modulate temporal judgment: the larger the number or size, the longer the subjective duration (Roitman et al., 2007; Casasanto and Boroditsky, 2008; Oliveri et al., 2008; Bueti and Walsh, 2009). A last feature of interest concerns the influence of emotion on time perception.

A recent upsurge in the number of studies on the research of time perception involves the probing of emotional stimuli on perceived duration. These studies are probably inspired by everyday knowledge of how in unpleasant situations we experience a slower passage of time and overestimate duration. This aspect of time perception, although part of everyday experience, had been neglected in research over the past few decades. Only recently, a body of evidence has been accumulated that is indicative of the intricate

interplay between mood states and perceived duration. That is, in psychophysical experiments auditory or visual stimuli that have emotional content are often overestimated when compared to neutral stimuli. Studies using emotional visual stimuli such as facial expressions or standardized emotional pictures from International Affective Pictures Systems (IAPS, Lang et al., 1997), or standardized emotional sounds from International Affective Digital Sounds (Bradley and Lang, 2007), indicate that duration perception is highly dependent on emotional content. For instance, Angrilli et al. (1997) proposed that emotion should not be considered as a whole but as the combination of two factors: valence (i.e., the sign of the emotional value) and intensity (i.e., the magnitude of the emotional value). They designed a paradigm to disentangle the effect of each component on time perception. Participants were presented with pleasant and unpleasant pictures, both moderately and highly arousing, alongside neutral pictures from the IAPS. Pictures appeared for 2, 4, or 6 s. Participants were asked to perform a prospective timing task, either by indicating the perceived duration of the picture presentation on an analog scale or by pressing a button to reproduce the duration. The analysis showed an interaction between the two components of emotion regardless of the timing method: duration of highly arousing pleasant pictures was more underestimated than that of highly arousing unpleasant pictures whereas duration of low-arousing pleasant pictures was less underestimated than that of low-arousing unpleasant pictures. However, no clear comparison with neutral stimuli, which were used as fillers, was performed. Yet durations seem subjectively different when timing stimuli with an emotional valence than when timing stimuli with a neutral valence (e.g., Watts and Sharrock, 1984; Droit-Volet et al., 2004a; Gil et al., 2007; Noulhiane et al., 2007). Overall, duration of all emotional pictures is overestimated in comparison with that of neutral pictures. In the framework of an internal pacemaker model researchers postulated that such emotional overestimation was mainly due to an arousal-related acceleration of the internal pace in such situations. Thus overestimation is greater for highly arousing emotions (for instance, angry faces are the most overestimated, followed by happy and then sad faces; Droit-Volet and Gil, 2009). Attention is also believed to impact timing: when attention is diverted from the timing task, i.e., by a concurrent task or by emotional information, it can delay the switch closure or produce a flickering which both lead to a fewer number of accumulated pulses, and therefore an underestimation of duration (Droit-Volet and Gil, 2009; Lui et al., 2011). Although there is increasing interest in the subjective experience of time and how it is modulated by emotional states, to our knowledge, no study has compared stimuli with a content (i.e., ecological stimuli, capturing some of the complexity of real-life scenes) and those without (e.g., a picture of a square or a pure tone). The existence of such a valence rating as neutral is somewhat controversial since it is not clear whether there is such an emotional category or whether neutral stimuli simply have a low-value valence or emotional intensity. The use of content-deprived stimuli would provide a higher contrast between emotional and non-emotional pictures – and thus would test the heuristic value of timing model to determine the influence of emotion. Finally, the impact of emotions on subjective time has been largely investigated in short-time scale subjective duration (i.e., sub-second to second range), with most findings assuming an internal pacemaker devoted to time. Studies using longer scales are still scarce and do not systematically reinforce the internal pacemaker theory. Alternative concepts favor the idea of duration-dependant timing processes (Vierordt, 1868; Fraisse, 1984; Pöppel, 2009; Wittmann and van Wassenhove, 2009).

The aim of the present study was to investigate how visual emotional content influences time perception. By content we will refer hereafter to the property for a picture to be realistic, i.e., to contain representation of real-life objects or scenes, as opposed to abstract signs or shapes. We used a temporal reproduction paradigm involving stimuli of gradual content-related emotional valence (content-deprived, content-bearing neutral, pleasant, and unpleasant pictures). Two groups of participants were presented with three standard durations (2, 4, and 6 s) of visual stimuli: (1) Group 1 had to encode the duration of a content-deprived stimulus, i.e., a gray square (no-content task); (2) Group 2 had to encode the duration of content-bearing stimuli from the IAPS, i.e., pictures rated for neutral, pleasant, and unpleasant emotional valence (content task). We assumed that the duration of content-deprived stimuli would be judged shorter than that of content-bearing stimuli. We also expected that neutral stimuli would be judged shorter than emotional ones (positive or negative valence).

MATERIALS AND METHODS

PARTICIPANTS

Thirty-four right-handed participants with no history of neurological or psychiatric disorder volunteered for this study. Seventeen performed the no-content task (Group 1) and seventeen performed the content task (Group 2). All participants were recruited in a population of young adults (age range 20 to 35 years old) with a higher-education profile (**Table 1**). Two independent groups assumed no interference between tasks. In accordance with the Declaration of Helsinki, all participants gave their informed consent.

MATERIALS

The experiment was conducted using an IBM compatible computer with a module controlling a shutter for the presentation of visual stimuli. A specifically designed program controlled both the presentation of the standard durations and the recording of the participants' responses (reproduced durations) with an accuracy of ±0.5 ms. Stimuli were displayed in the center of the screen against a black background, at a viewing distance of 0.5 m.

The two tasks were adapted from previous studies using either emotional content-bearing stimuli in the visual modality (Angrilli et al., 1997), content-deprived stimuli in the visual modality or emotional stimuli in the auditory modality (Noulhiane et al., 2007, 2008). For the no-content task, the stimulus was a gray

Table 1 | Demographic data of participants.

	Total number	Age (mean±SD, years)	Educational level (mean±SD, years)
Group 1	17 (female, 8)	30.3 ± 5	15.27 ± 2.3
Group 2	17 (female, 8)	25.2 ± 3	16.94 ± 0.97

10×10 cm square of uniform luminance. For the content task, 36 pictures were selected from the IAPS (neutral: 1390, 5120, 5531, 5731, 7002, 7010, 7224, 7234, 7500, 7595, 7640, 7830; pleasant: 1340, 1463, 1500, 2170, 4659, 4670, 5480, 5629, 5831, 8080, 8180, 8190; unpleasant: 1052, 1111, 1300, 3550, 6260, 7361, 9250, 9320, 9520, 9584, 9592, 9921), with three 12-item groups of different valence: pleasant (mean $\pm$ SD $= 7.57 \pm 0.43$), unpleasant (2.84 ± 1.13), and neutral (5.57 ± 0.66). In both tasks, the duration reproduction paradigm involved three standard durations: 2, 4, and 6 s. During the no-content task each duration was presented 10 times in random order. During the content task, three series were created by selecting four pictures from each group (pleasant, unpleasant, and neutral), each picture appearing once for each duration (2, 4, or 6 s), adding up to 36 (picture, duration) stimuli in each list. Every participant was presented with the three lists in pseudo-random order (108 trials in all).

PROCEDURE AND DESIGN

Each trial started with a stimulus presented for a randomly selected standard duration. Participants were instructed to pay attention to the duration of the stimulus in order to reproduce it. They were told to avoid chronometric counting strategies. When the stimulus disappeared, a gray square was displayed on the screen in both tasks. Participants were asked to press the spacebar until they judged that the time elapsed equaled the duration of the picture presentation. The reproduced duration was recorded. A random 2–3 s time gap was introduced after presentation of the stimulus and during the inter-trial interval to prevent participants from having an implicit evaluation of the fixed time period. Before the experiment, the participants were trained with five trials using content-deprived or neutral pictures in the no-content and content tasks respectively.

A control experiment was performed to verify that the emotions elicited by the pictures were stable over time for all durations used. Stimuli were presented for 2, 4, and 6 s in random order. Ratings of valence levels were collected from 12 young adults (six women, aged 27 ± 3.43 years, and six men, aged 27 ± 3.77 years) who did not participate in the main experiment. Participants were asked to rate the self-assessment Manikin. Rated scores computed for the three durations showed that subjective valence ratings matched those of the IAPS, whatever the duration. Moreover, one-way analyses of variance (ANOVA) performed on rated scores for each valence with duration as a factor revealed no significant effect of duration (all $ps > 0.1$). In sum, emotional valence does not vary within this range of duration (**Table 2**).

STATISTICAL ANALYSES

Accuracy of temporal performance was examined by computing a T-corrected score with the following formula: [T-corrected = (T estimated – T standard)/T standard]. Negative values indicate that the reproduced duration was shorter than the standard, and positive values indicate that it was longer. Precision of temporal performance was examined by computing the coefficient of variation (CV) with the following formula: [CV = SDs of mean reproduction time/mean reproduction time]. Paired t-tests were performed to compare results across duration (3) and content (4). Bonferroni corrections were applied for all analyses ($p < 0.005$). Some results did not reach significance after correction ($p < 0.05$), but they are still presented hereafter for discussion. These results are however to be taken with caution.

RESULTS

T-CORRECTED

Student paired t-test scores (**Figure 1**) comparing durations within the same content showed no difference in the no-content task between 2, 4, and 6 s. Within the content-bearing stimuli on the opposite, duration had a larger influence: all pairs of durations for each content condition were found significantly different (all $ps < 0.005$), showing that 4 s-pictures were underestimated with respect to 2 s-pictures, and 6 s-pictures were underestimated with respect to both 2- and 4 s-pictures for all content conditions. Overall, the longer the duration, the more underestimated it is. Note that "underestimation" is used relatively between durations.

Table 2 | Rated scores from IAPS and those from 12 participants computed for the three durations.

Duration/content	IAPS score	Rated score (±SD)	Student test, $t(11)$; p
2 s Pleasant	7.58	6.22 ± 0.62	2.02; NS
2 s Unpleasant	2.84	2.68 ± 0.38	0.40; NS
2 s Neutral	5.57	4.73 ± 0.66	1.22; NS
4 s Pleasant	7.58	6.29 ± 0.54	2.22; NS
4 s Unpleasant	2.84	2.49 ± 0.43	0.75; NS
4 s Neutral	5,57	4.62 ± 0.77	1.17; NS
6 s Pleasant	7.58	6.31 ± 0.60	1.94; NS
6 s Unpleasant	2.84	2.49 ± 0.39	0.84; NS
6 s Neutral	5.57	4.72 ± 0.81	1.01; NS

Student unpaired t-tests showed that scores were matched to IAPS scores whatever the duration. One-way ANOVAS performed for each valence with duration as a factor showed no main effect of duration [pleasant: $F(2,22) = 2.22$, $p = 0.13$; unpleasant: $F(2,22) = 0.94$, $p = 0.40$; neutral: $F(2,22) = 0.65$, $p = 0.53$]: emotional valence does not vary with duration. Rated scores for emotional valence.

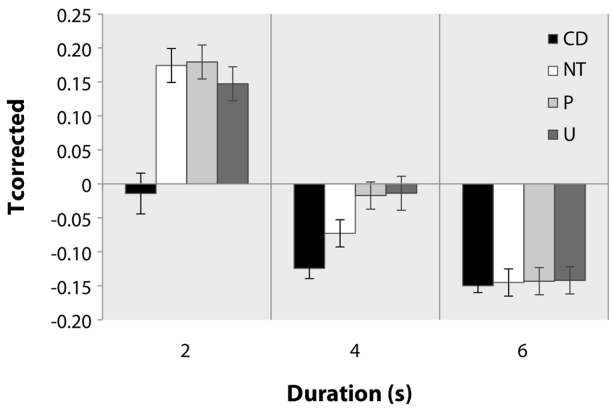

FIGURE 1 | T-corrected (averaged across participants) for each standard duration (2, 4, 6 s) in content-deprived (CD), neutral (NT), pleasant (P), and unpleasant (U) conditions (error bars denote SR of the mean).

Comparison of subjective durations to their actual standards showed that 2 s-stimuli are overestimated, 4 s-stimuli are quite accurately reproduced, and 6 s-stimuli are underestimated.

Student paired t-test scores between content conditions showed that at 2 s, content-deprived stimuli were judged shorter than neutral and pleasant content-bearing pictures [$t(16) = -2.24$, $p = 0.039$ and $t(16) = -2.18$, $p = 0.044$, respectively]. There was no difference between any of the content conditions at 2 s. At 4 s, there was no difference between content-deprived and any of the content-bearing conditions. The neutral pictures were judged shorter than the pleasant and the unpleasant ones [$t(16) = -2.27$, $p = 0.037$ and $t(16) = -2.12$, $p = 0.050$, respectively]. No difference was found between pleasant and unpleasant pictures. Finally, at 6 s, no difference between content-deprived and content-bearing stimuli was found, nor between any of the content-bearing conditions.

COEFFICIENT OF VARIATION

Student paired t-tests (**Figure 2**) showed that CVs were smaller at 6 s than at 2 s [$t(16) = 4.85$, $p < 0.001$] and at 4 s than at 2 s for unpleasant content only [$t(16) = 4.38$, $p < 0.001$]. Over all contents the variability in response is however little influenced by duration. Within duration, Student independent t-tests showed that both content-deprived and content-bearing neutral pictures had smaller CVs than pleasant and unpleasant pictures for all durations (all ps < 0.001). No difference was found between content-deprived and neutral content-bearing pictures. These results showed that emotional pictures are judged with greater variability than both content-deprived and neutral pictures, even though the effect slowly diminishes with duration.

DISCUSSION

This study aimed at investigating the influence of visual emotional content on time perception. Participants reproduced 2, 4, and 6 s durations in a task contrasting stimuli of varying emotional valence (content-bearing neutral, pleasant, and unpleasant pictures) with content-deprived stimuli (gray squares).

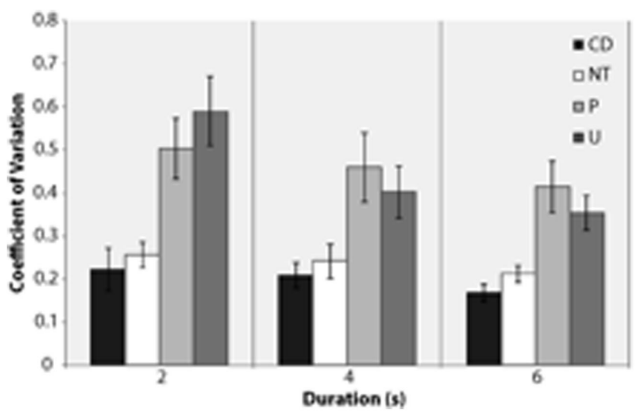

FIGURE 2 | Coefficient of variation (averaged across participants) for each standard duration (2, 4, 6 s) in content-deprived (CD) and content-bearing [neutral (NT), pleasant (P), unpleasant (U)] conditions. (Note error bars denote SR of the mean.)

The main results revealed that content affected both the accuracy and precision of the responses, and that this effect generally diminished with time.

The measures of response accuracy (T-corrected) showed that for a 2 s duration, all content-bearing stimuli were judged to last longer than content-deprived ones; at 4 and 6 s, no more significant differences were found. In the framework of the internal clock model, this content-related effect can be explained by an attentional mechanism, a gray square capturing presumably less attention than a content-bearing picture (Zakay, 2005). According to this theory, enhanced attention paid to content-bearing pictures would both fasten internal pacing and reduce the switch flickering, making duration appear longer (Tse et al., 2004; Zakay, 2005; New and Scholl, 2009). This hypothesis is drawn in parallel to the idea that emotional stimuli capture attentional resources more easily than non-emotional ones (Droit-Volet and Meck, 2007). Our results revealed thus that not only emotional but more generally content-bearing stimuli (even neutrally valenced) are still more susceptible to capture attention than content-deprived stimuli. Using a gray square, we did not investigate the specific input of arousal. In future studies, this aspect would however need to be examined by controlling the arousal level induced by the presentation of content-deprived stimuli, for instance by mean of physiological measures (e.g., skin conductance response, heart rate). Additionally it should be noted that we chose to increase the contrast between content-deprived and content-bearing stimuli by using a simple one-color shape on the one hand, and complex multicolored scenic pictures on the other hand. These features are possible confounds that should be controlled for in future studies by using for instance scrambled versions of the content-bearing pictures as content-deprived stimuli. However in this context, the relevance of the IAPS was to provide a battery of pictures rated for emotion on a 1–9 linear scale (Lickert scale, 1 = highly unpleasant, 9 = highly pleasant). "Neutral" pictures could thus still elicit emotion in some participants (as reflected by interindividual variability, see Lang et al., 1997), whereas by using geometrical squares we made sure that the stimuli elicited no emotion at all. Our experimental design separated the content conditions into two tasks executed by two different groups. Although this methodological point could be considered as a limit, this allowed us to ensure the gray square during the reproduction phase did not trigger any change in the pacemaker rate in the content-deprived task as it could have if it had been contextualized by a majority of content-bearing pictures, had the task been intermixed. Nevertheless, futures studies should control this aspect by having the same participants perform the two tasks in a counter-balanced order, or by intermixing content-deprived and content-bearing stimuli with an equal number of trials in each condition.

Overall, we found that for any content-bearing stimulus, the longer the duration, the shorter it is judged relative to the standard. This effect of duration is consistent with Vierordt's (1868) law; in a series of durations, the shortest are over-reproduced and the longest are under-reproduced, reproduction of sample durations below and above the mean of the series shifting progressively toward the central value. Yet an interesting result is that the effect of stimulus content on time processing decreases as the duration to be processed increases. We propose that the attentional effect drawn

by content-bearing stimuli is limited in time: attention reflects the ability to quickly allocate neural resources to the processing of a relevant stimulation. Once the latter has been processed and the appropriate answer has been produced, attentional level decreases, leading the internal pace to return to its initial speed. This lowering of content-induced activation with time could appear at odds with the literature on activation and timing. Studies have generally reported a greater activation effect for longer than for shorter times, the effect being multiplicative (Burle and Casini, 2001). As in our previous study (Noulhiane et al., 2007), the present results show the reverse pattern. However, most studies have tested the influence of activation on the processing of durations shorter than 2 s, which was the lowest limit of our range. Moreover in the emotional context, these studies have usually used facial emotional expressions which constitute particular and unique stimuli for humans as they involved social interactions and categorical emotions (happiness, sadness, fear...). One may then posit that the pacemaker rate increases within the duration of the content effect, driven either by attention, arousal or complexity processing, and then gradually returns to its baseline. Future studies in the subsecond range using emotional scenes of real-life could clarify this point.

Focusing on the emotional valence, our results surprisingly show that emotion has a delayed effect on time reproduction: at 2 s pleasant and unpleasant pictures were not judged differently from the neutral pictures; however at 4 s they were judged longer than neutral pictures. At 6 s, no difference was observed anymore. This result suggests that the difference in pace between non-emotional and emotional scenes is not so big that we can notice the difference after a 2 s-accumulation, but in 4 s the difference is bigger and reaches significance. As mentioned above, the pace then progressively returns to its baseline level, so that at 6 s no emotional-driven difference is noticeable again. This result differed from those reported by Lui et al. (2011), where the authors introduced either an emotional or neutral picture from the IAPS in-between the reference (S1) and the probe (S2) for durations ranging from 1100 to 2300 ms in a reproduction task. They found that the duration of S2 was underestimated after an emotional stimulus compared to a neutral stimulus, in agreement to an acceleration of the pacemaker triggered by emotion. However the presentation of the task-irrelevant picture happened 1300 ms before the presentation of S2, overruling any latency in the emotional effect on the pacemaker, which could explain the presence of an emotional effect below 2 s. It is also in contradiction with what was observed in the auditory modality within the same duration range as in the present study, where the effect of emotion happened early and decreased with time (Noulhiane et al., 2007). Such discrepancy raises a broader issue about the relationship between timing, emotion and sensory modality: namely, this questions whether the intrinsically dynamic aspect of auditory stimuli facilitates the extraction of emotional information in comparison to static visual stimuli, and whether this would result in a delay of emotional effect between auditory and visual modalities. Future studies using emotional cross-modality paradigm could refine this question.

The effect of stimuli content appeared also on the precision: the CVs were slightly reduced with the length of duration for any content. This effect could not be explained by the use of chronometric counting since the high values reflect timing processing (all CVs > 0.15; Wearden, 1991). Focusing on emotional valence, the variability of judgments (CVs) was greater for emotional (both pleasant and unpleasant) than non-emotional (both neutral and content-deprived) pictures, for all three standard durations. This suggests that emotional valence, and not content, reduces the precision of temporal judgments. To respond appropriately to a picture, it is more important to decipher emotional valence, and probably the nature of the conveyed emotion, than to evaluate the exact duration of its presentation. In line with the internal clock model, we hypothesize that emotion induces a greater flickering of the switch. This flickering adds a random factor that increases the variability of the final estimation. Note that this does not contradict the fact that more pulses are accumulated since, according to our attentional hypothesis, the pacemaker is still running faster than for content-deprived stimuli. The findings obtained on precision finally support the recent proposal that timing is a self-referential processing highly dependent of our emotional state (Craig, 2009): the reduced precision in the estimation of emotional stimuli duration may lie in the extreme variability one may observe in the experience of emotion. According to Craig's (2009) model, our sense of time is based on the succession of global emotional moments that are intrinsically linked to the interoceptive information integrated in the insular cortex. Considering that emotional stimuli are probably not equivalent in the generation of emotion within an individual – even in the same hedonic category – the internal state resulting in the exposition of such stimuli may vary across trials. As a result time estimates of such stimuli would also vary.

Finally, our data extend future perspective to elucidate mechanisms of time processing in link with content. For instance, the temporal overestimation of content-bearing stimuli could reflect a usual timing effect which has yet to be elucidated in current neural timing models: the difference in number and complexity between content-deprived and content-bearing pictures affects the temporal judgement (Ornstein, 1969; Schiffman and Bobko, 1974; Fraisse, 1984). Recent models propose that the passage of time can be encoded in the evolving patterns of activity in neural networks (Buonomano and Mauk, 1994; Buonomano and Merzenich, 1995; Mauk and Buonomano, 2004; Buhusi and Meck, 2005; Karmarkar and Buonomano, 2007; Ivry and Schlerf, 2008). This kind of model is all the more exciting that so far the clock model has found little support in physiology whereas this new approach is based on neural dynamics. These models suggest that the duration assigned to a stimulus reflects the change in distribution of neural activity following the stimulus presentation. To date, this hypothesis was essentially investigated with events of short-time scale subjective durations (e.g., in the time scale of tens to hundreds of milliseconds, Eagleman and Pariyadath, 2009). There is not enough evidence to indicate that similar mechanisms come into play in duration judgments at longer time scales while certain principles observed at brief time scales appear to hold at longer ones. Furthermore, these models have not to date investigated emotional stimuli. Future studies should determine their validity in wider ranges of duration and for the specific case of emotion.

In conclusion, this study shows that content modulates time perception in the visual modality. Interestingly, our results suggest

a dissociation in the content effect on timing: relative overestimation of all content-bearing pictures for short durations (2 s) and delayed effect of emotion at 4 s, alongside less precision in the temporal judgment of emotional pictures, whatever their duration. This double susceptibility of timing toward emotion should be taken into consideration in future studies.

ACKNOWLEDGMENTS

We would like to address a special thank to Viviane Pouthas for her input and expertise, and for bringing us together on this project. More generally we thank her for her life-long contribution to the scientific development of her students which she did with kindness and constant support.

REFERENCES

Angrilli, A., Cherubini, P., Pavese, A., and Mantredini, S. (1997). The influence of affective factors on time perception. *Percept. Psychophys.* 59, 972–982.

Bradley, M. M., and Lang, P. J. (2007). The International Affective Digitized Sounds Affective Ratings of Sounds and Instruction Manual. *Emotion* 18. University of Florida, Gainesville, FL.

Bueti, D., and Walsh, V. (2009). The parietal cortex and the representation of time, space, number and other magnitudes. *Philos. Trans. R. Soc. Lond. B Biol. Sci.* 364, 1831–1840.

Buhusi, C. V., and Meck, W. H. (2005). What makes us tick? Functional and neural mechanisms of interval timing. *Neuroscience* 6, 755–765.

Buonomano, D. V., and Mauk, M. D. (1994). Neural Network model of the cerebellum: temporal discrimination and the timing of motor responses. *Neural Comput.* 6, 38–55.

Buonomano, D. V., and Merzenich, M. (1995). A neural network model of temporal code generation and position-invariant pattern recognition. *Neural Comput.* 11, 103–116.

Burle, B., and Casini, L. (2001). Dissociation between activation and attention effects in time estimation: implications for internal clock models. *J. Exp. Psychol. Hum. Percept. Perform.* 27, 195–205.

Casasanto, D., and Boroditsky, L. (2008). Time in the mind: using space to think about time. *Cognition* 106, 579–593.

Collier, G. L., and Logan, G. (2000). Modality differences in short-term memory for rhythms. *Mem. Cognit.* 28, 529–538.

Craig, A. D. (2009). Emotional moments across time: a possible neural basis for time perception in the anterior insula. *Philos. Trans. R. Soc. Lond. B Biol. Sci.* 364, 1933–1942.

Droit-Volet, S., Brunot, S., and Niedenthal, P. M. (2004a). Perception of the duration of emotional events. *Cogn. Emot.* 18, 849–858.

Droit-Volet, S., Tourret, S., and Wearden, J. H. (2004b). Perception of the duration of auditory and visual stimuli in children and adults. *Q. J. Exp. Psychol.* 57A, 797–818.

Droit-Volet, S., and Gil, S. (2009). The time-emotion paradox. *Philos. Trans. R. Soc. Lond. B Biol. Sci.* 364, 1943–1953.

Droit-Volet, S., and Meck, W. H. (2007). How emotions colour our perception of time. *Trends Cogn. Sci.* 11, 504–513.

Droit-Volet, S., Meck, W. H., and Penney, T. B. (2007). Sensory modality and time perception in children and adults. *Behav. Processes* 74, 244–250.

Eagleman, D. M., and Pariyadath, V. (2009). Is subjective duration a signature of coding efficiency? *Philos. Trans. R. Soc. Lond. B Biol. Sci.* 364, 1841–1851.

Fraisse, P. (1984). Perception and estimation of time. *Annu. Rev. Psychol.* 35, 1–36.

Gibbon, J., Church, R. M., and Meck, W H. (1984). Scalar timing in memory. *Ann. N. Y. Acad. Sci.* 423, 52–77.

Gil, S., Niedenthal, P., and Droit-Volet, S. (2007). Anger and time perception in children. *Emotion* 7, 219–225.

Grondin, S. (1993). Duration discrimination of empty and filled intervals marked by auditory and visual signals. *Percept. Psychophys.* 54, 383–394.

Ivry, R. B., and Schlerf, J. E. (2008). Dedicated and intrinsic models of time perception. *Trends Cogn. Sci. (Regul. Ed.)* 12, 273–280.

Karmarkar, U. R., and Buonomano, D. V. (2007). Timing in the absence of clocks: encoding time in neural network states. *Neuron* 53, 427–438.

Lang, P. J., Bradley, M. M., and Cuthbert, B. N. (1997). "Motivated attention: affect, activation, and action," in *Attention and Orienting: Sensory and Motivational Processes*, eds P. J. Lang, R. F. Simons, and M. T. Balaban (Hillsdale, NJ: Erlbaum), 97–135.

Lui, M. A., Penney, T. B., and Schirmer, A. (2011). Emotion effects on timing: attention versus pacemaker accounts. *PLoS ONE* 6, e21829. doi:10.1371/journal.pone.0021829

Mauk, M. D., and Buonomano, D. V. (2004). The neural basis of temporal processing. *Annu. Rev. Neurosci.* 27, 307–340.

New, J. J., and Scholl, B. J. (2009). Subjective time dilation: spatially local, object-based, or a global visual experience? *J. Vis.* 9, 1–11.

Noulhiane, M., Mella, N., Samson, S, Ragot, R., and Pouthas, V. (2007). How emotional auditory stimuli modulate time perception. *Emotion* 7, 697–704.

Noulhiane, M., Pouthas, V., and Samson, S. (2008). Is time reproduction sensitive to sensory modalities? *Eur. J. Cogn. Psychol.* 21, 18–34.

Oliveri, M., Vicario, C. M., Salerno, S., Koch, G., Turriziani, P., Mangano, R., Chillemi, G., and Caltagirone, C. (2008). Perceiving numbers alters time perception. *Neurosci. Lett.* 438, 308–311.

Ornstein, R. E. (1969). *On the experience of time.* Hammandsworth, UK: Penguin.

Penney, T. B., Gibbon, J., and Meck, W. H. (2000). Differential effects of auditory and visual signals on clock speed and temporal memory. *Perception* 26, 1770–1787.

Penney, T. B., and Tourret, S. (2005). Les effets de la modalité sensorielle sur la perception du temps Modality effects in short interval timing. *Psychol. Fr.* 50, 131–143.

Pöppel, E. (2009). Pre-semantically defined temporal windows for cognitive processing. *Philos. Trans. R. Soc. Lond. B Biol. Sci.* 364, 1887–1896.

Rammsayer, T. H., and Lima, S. D. (1991). Duration discrimination of filled and empty auditory intervals: cognitive and perceptual factors. *Percept. Psychophys.* 50, 565–574.

Roitman, J. D., Brannon, E. M., Andrews, J. R., and Platt, M. L. (2007). Nonverbal representation of time and number in adults. *Acta Psychol. (Amst)* 124, 296–318.

Schiffman, H. R., and Bobko, D. J. (1974). Effects of stimulus complexity on the perception of brief temporal intervals. *J. Exp. Psychol.* 103, 156–159.

Tse, P. U., Intriligator, J., and Rivest, J. (2004). Attention and the subjective expansion of time. *Perception* 66, 1171–1189.

Vierordt, K. (1868). *Der Zeitsinn nach Versuchen.* Tübingen, Germany: Laupp.

Watts, F. N., and Sharrock, R. (1984). Questionnaire dimensions of spider phobia. *Behav. Res. Ther.* 22, 575–580.

Wearden, J. (1991). Do humans possess an internal clock with scalar timing properties? *Learn. Motiv.* 22, 59–83.

Wearden, J. H., Edwards, H., Fakhri, M., and Percival, A. (1998). Why "sounds are judged longer than lights": application of a model of the internal clock in humans. *Psychology* 51B, 97–120.

Wearden, J. H., Todd, N. P. M., and Jones, L. A. (2006). When do auditory/visual differences in duration judgements occur? *Exp. Psychol.* 59, 1709–1724.

Wittmann, M., and van Wassenhove, V. (2009). The experience of time: neural mechanisms and the interplay of emotion, cognition and embodiment. *Philos. Trans. R. Soc. Lond. B Biol. Sci.* 364, 1809–1813.

Zakay, D. (2005). Attention et jugement temporel Attention and duration judgment. *Psychol. Fr.* 50, 65–79.

Conflict of Interest Statement: The authors declare that the research was conducted in the absence of any commercial or financial relationships that could be construed as a potential conflict of interest.

Received: 15 June 2011; accepted: 12 October 2011; published online: 16 November 2011.

Citation: Lambrechts A, Mella N, Pouthas V and Noulhiane M (2011) Subjectivity of time perception: a visual emotional orchestration. Front. Integr. Neurosci. ***5****:73. doi: 10.3389/fnint.2011.00073*

frontiers in
INTEGRATIVE NEUROSCIENCE

MINI REVIEW ARTICLE
published: 05 October 2011
doi: 10.3389/fnint.2011.00058

How emotions change time

Annett Schirmer*

Department of Psychology, National University of Singapore, Singapore

Edited by:
Warren H. Meck, Duke University, USA

Reviewed by:
Antonio Pereira, Federal University of Rio Grande do Norte, Brazil
Jason Tipples, University of Hull, UK
Jessica Lake, Duke University, USA

***Correspondence:**
Annett Schirmer, Department of Psychology, Faculty of Arts and Social Sciences, National University of Singapore, 9 Arts Link, Block AS4, Level 2, Singapore 117570.
e-mail: schirmer@nus.edu.sg

Experimental evidence suggests that emotions can both speed-up and slow-down the internal clock. Speeding up has been observed for to-be-timed emotional stimuli that have the capacity to sustain attention, whereas slowing down has been observed for to-be-timed neutral stimuli that are presented in the context of emotional distractors. These effects have been explained by mechanisms that involve changes in bodily arousal, attention, or sentience. A review of these mechanisms suggests both merits and difficulties in the explanation of the emotion-timing link. Therefore, a hybrid mechanism involving stimulus-specific sentient representations is proposed as a candidate for mediating emotional influences on time. According to this proposal, emotional events enhance sentient representations, which in turn support temporal estimates. Emotional stimuli with a larger share in ones sentience are then perceived as longer than neutral stimuli with a smaller share.

Keywords: interval-timing, insula, affective, temporal, speed

INTRODUCTION

Being able to time is essential for a range of tasks including driving a car, cooking a meal, or having a conversation (Schirmer, 2004; Buhusi and Meck, 2005). Although we typically learn and complete these tasks with little effort, there are instances in which cars collide, meals overcook, and conversations desynchronize. Thus, it seems that, although accurate on average, our sense of time is not fixed but varies within and across individuals.

Prominent among the factors that influence our sense of time are emotions (for reviews see Droit-Volet and Meck, 2007; Craig, 2009a; Droit-Volet and Gil, 2009). Evidence for this comes from a range of paradigms some of which will be shortly reviewed here. One paradigm entails the presentation of stimuli for which participants subsequently estimate or reproduce the duration. With a few exceptions (e.g., Noulhiane et al., 2007), to-be-timed emotional stimuli elicit longer estimates and reproduction times than to-be-timed neutral stimuli (Angrilli et al., 1997; Noulhiane et al., 2007; Doi and Shinohara, 2009). A second popular paradigm is called duration bisection. In the training phase of this paradigm, participants learn to discriminate two anchor durations, one short and one long. In the test phase, participants perceive probe stimuli ranging in duration from the short to the long anchor and judge whether these stimuli are more similar to the short or the long anchor. Again, with a few exceptions (Gil et al., 2009; Droit-Volet et al., 2010), emotional test stimuli are judged more similar to the long anchor than neutral stimuli (Effron et al., 2006; Gil et al., 2007; Grommet et al., 2011). Finally, researchers have examined the relationship between emotion and subjective time using a duration discrimination paradigm with intermediate emotional or neutral distractors (Lui et al., 2011). Here participants are presented with two successive stimuli (i.e., S1/S2) and indicate whether the second stimulus was shorter or longer than the first. Participants are more likely to judge S2 as shorter when it was preceded by an emotional as compared to neutral distractor.

Together, this literature confirms the popular perception that emotions both speed-up and slow-down our sense of time. Moreover, it suggests that emotional events are generally perceived as longer than they really are, which may be conceptualized as a speeding up of subjective temporal pulses. It also suggests that neutral events occurring in the context of a distracting, emotional one are perceived as shorter then they really are, which may be conceptualized as a slowing down of subjective temporal pulses. Different mechanisms have been proposed to explain these effects and the remainder of this paper will focus on reviewing and contrasting them.

AROUSAL MODULATES TIME

The first mechanism draws on a popular timing model derived from scalar expectancy theory (SET; Gibbon et al., 1984). This model entails a clock stage comprising a pacemaker and an accumulator, both of which are connected by a switch. The pacemaker emits pulses that are collected by the accumulator when the switch is in a closed state. Delayed closing or flickering of the switch causes pulses to be lost (Penney, 2003). The clock stage is followed by a memory stage. During this stage, pulses from the accumulator enter working memory and are compared with previously stored durations. The result of this comparison informs temporal decisions and associated behavioral responses.

Research in both non-human animals and humans suggests that bodily arousal affects timing at the clock stage. For example, rats injected with the psychostimulant methamphetamine, a drug which enhances dopaminergic activity, treat a given duration as longer than do rats injected with saline (Meck, 1983). In contrast, rats injected with the dopamine antagonist haloperidol treat the duration as shorter than do the control rats (Meck, 1983). In humans, changes in physiological arousal as assessed by self-report and psychophysiological markers have been shown to concur with changes in perceived time. Relative overestimations

have been found in conjunction with a putative increase in bodily arousal (Angrilli et al., 1997; Droit-Volet et al., 2011; Mella et al., 2011), whereas relative underestimations have been found with a putative decrease in bodily arousal (Wearden et al., 1999). As these effects typically represent a simple shift in the timing function, researchers assume that arousal positively correlates with pacemaker rate. Moreover, because emotions frequently increase physiological arousal, emotion effects on timing have been proposed to be mediated by the arousal/pacemaker link (Droit-Volet and Meck, 2007; Droit-Volet and Gil, 2009).

Although compelling, this proposal is not without problems. First, the concept of arousal and its relationship to an internal clock are poorly defined. Implicit in the published work is the understanding that arousal equates with sympathetic activation as determined by increased heart-rate, breathing, or skin conductance (e.g., Droit-Volet et al., 2011). However, this and other possible conceptualizations are not clearly spelled out. Moreover, it is assumed that this arousal somehow feeds back to the internal clock supported by the dopaminergic system. Yet, how this feedback occurs is still unclear. Second, available evidence for a relationship between emotional arousal and duration estimates is at best indirect. Although studies have shown corresponding differences in arousal measures and duration judgments elicited by emotional versus neutral stimuli, they never actually correlated the two at an individual or trial level. Moreover, even if such a correlation were found, effects of arousal on attention and working memory (Brennan and Arnsten, 2008; Advokat, 2010) offer an alternative causal link. Third, there appears to be a mismatch between the time-course of emotion-induced arousal and timing effects reported in the literature. The latter have been observed primarily for short stimuli (∼2–3 s) and seem to dissipate for longer stimuli (Noulhiane et al., 2007; Mella et al., 2011). In comparison, emotion-induced increases in physiological arousal are relatively sluggish with heart-rate and skin conductance taking between 3 and 6 s to peak (Bradley et al., 2001; Schirmer and Escoffier, 2010). Moreover, heart-rate for example typically decreases for the first 3 s through parasympathetic activation (Bradley et al., 2001). During this time, one should observe a slow-down in time keeping if heart-rate or sympathetic activation translate into pacemaker rate. Finally, the arousal model fails to fully accommodate existing data (Droit-Volet and Meck, 2007; Droit-Volet and Gil, 2009). Not all emotions lead to an increase in physiological parameters linked to arousal (e.g., sadness; Levenson et al., 1990) but may nevertheless elicit temporal overestimation (Lee et al., 2011). Furthermore, situations in which the timing stimulus is neutral, but presented in the context of an emotionally arousing distractor, fail to produce temporal overestimations (Lui et al., 2011). Given these problems, the arousal/pacemaker link may not or may not fully explain the relationship between emotions and time.

ATTENTION MODULATES TIME

A second putative mechanism by which emotions may shape our experience of time is linked to the cognitive resources allocated to stimulus processing. Two possibilities of how stimulus processing may affect timing will be discussed here. The first concerns the amount of attention individuals dedicate to time. In reference to the SET timing model, mentioned above, it assumes that the clock stage (Macar et al., 1994; Droit-Volet, 2003) and/or memory stage (Buhusi and Meck, 2009) share attentional resources with other ongoing mental processes such that greater resource allocation to the temporal dimension of a stimulus results in fewer temporal pulses being lost. Support for this notion comes from studies that manipulated participant attention to time. For example, Macar et al. (1994) presented participants with stimuli for which they had to subsequently judge both duration and intensity. On some trials, participants were cued to focus all or most of their attention on the duration task, whereas on other trials, they were cued to focus all or most of their attention on the intensity task. Compared to the former, the latter trials were more likely to result in temporal underestimations of the target suggesting that pulses from a putative pacemaker were lost.

In line with this, some researchers reported underestimation of emotional relative to neutral stimuli in timing tasks. For example, participants underestimated the duration of appetizing and disgusting food pictures relative to neutral food pictures and this was interpreted to reflect a diversion of attention from the temporal dimension of the pictures to their emotional dimension (Gil et al., 2009). As such, the first attentional mechanism introduced here has some explanatory power. Moreover, unlike the arousal mechanism, it makes clear statements as to the underlying processes and has the advantage that temporal distortions can be explained by processes occurring during rather than after temporal encoding. Yet, its problem is that it discords with the overwhelming number of studies that find overestimation for emotional as compared to neutral stimuli. Given the greater significance of emotional relative to neutral events, the former should always, not just in the case of disgust, divert attention away from time and produce temporal underestimations.

A second variant of the cognitive resource mechanism addresses this problem. It assumes that it is the stimulus processing itself that contributes to timing and that attentional resources directed toward or away from the stimulus determine timing accuracy (Hicks et al., 1977; Ornstein, 1997). This proposal fits most over- and underestimation effects reported in the literature. Overestimations of emotional relative to neutral stimuli could be explained by the former recruiting more cognitive resources and having greater ability to sustain attention than the latter. Underestimations of neutral stimuli presented in an emotional as compared to neutral context could be explained by the former being more distracting than the latter, thereby leaving fewer resources for the processing of the timing stimulus (Lui et al., 2011). Nevertheless, this proposal is not without problems. For example, it cannot explain why presentation durations of appetizing foods are underestimated relative to neutral foods (Gil et al., 2009) and, more importantly, it conflicts with the evidence that attention to non-temporal stimulus dimensions typically impairs timing (Macar et al., 1994).

SENTIENT PROCESSING MODULATES TIME

A third proposal for how emotions influence time evokes the concept of sentience – often equated with being aware or conscious of one's self (Craig, 2009a; Wittmann, 2009). Specifically, it holds that external and internal sensory signals including information from the muscles, skeletal system, and internal organs are

integrated in the brain and enable self-awareness. As we experience ourselves across moments or time, the proposal makes sentience the basis for temporal perception and the mediator in the relationship between emotions and time. Emotion-induced bodily changes, such as heart-rate decelerations or accelerations, presumably increase sentience and thereby sensitivity to the passage of time. Different lines of theoretical and experimental work substantiate this possibility.

Vierordt, a nineteenth century pioneer of timing research, raised the "self" as a potential origin for the emergence of time (Vierordt, 1868). Furthermore, James (1981) argued for a reliance of temporal perception on sensation and noted that perceived durations tend to have an "emotional feeling." He also famously speculated about a critical role of bodily feedback for emotion. Although heavily criticized at the time, recent emotion theory has turned back to James and leveraged on his ideas. Important with respect to the present paper is Damasio's somatic marker hypothesis, which holds that an emotional event triggers bodily changes whose feedback to the brain critically contributes, not just to the emotional experience, but also to the processing of the event and event-related decision making (Damasio, 1996). In extension of this, some researchers interested in the processing of time now hold that there is a relationship between sentient processing and subjective time (Effron et al., 2006; Craig, 2009a; Wittmann, 2009).

Experimental support for this assertion is steadily accumulating. For example, researchers have identified a correlation between self-awareness and temporal estimates. Individuals who are experimentally deprived of visual, tactile, and/or auditory stimulation and whose primary sensory experiences therefore come from within report that the hours pass more slowly than usual (Schulman et al., 1967). Furthermore, it was demonstrated that both bodily change and awareness of one's current bodily state positively predict temporal estimates in interval-timing tasks (Meissner and Wittmann, 2011). Individuals with a more pronounced decrease in heart-rate during temporal encoding and a better accuracy at guessing their own heart-rate were less likely to underestimate a given temporal duration.

Neuroimaging studies further substantiate the link between sentient processing and time. Sentient processing has been associated with the insular cortex. This structure receives input from all senses including the somatosensory sense, which apart from its role in touch informs about visceral, skeletal, and muscular states. The insula has therefore been proposed as the seat for self-awareness or consciousness (Craig, 2009a,b). Although, temporal processing has been largely linked to striatal and prefrontal structures (Buhusi and Meck, 2005), the insula has been implicated as well (Pouthas et al., 2005; Livesey et al., 2007; Wittmann et al., 2010; for a review see Wittmann, 2009). For example, Pouthas et al. (2005) isolated insula activation both when comparing a timing task with a control task and when comparing the timing of long with short durations. Wittmann et al. (2010) further tested the relationship between insular activation and time. They found that this activation increased linearly with the encoded stimulus duration. Based on this and the intricate connections between insula and striatum (Chikama et al., 1997), one may venture that the insula's sentient computations support temporal perception and potentially mediate the relationship between emotions and time.

One such possible mediation could entail an influence of emotion-induced bodily changes on sentient processing. Specifically, such changes might heighten sentient processing and self-awareness thereby contributing to an increased sensitivity to the passage of time (Wittmann, 2009). Evidence in support of this possibility is currently only indirect but nevertheless promising. First, researchers have shown that both bodily change and sentience positively predict the duration of temporal estimates. But more importantly, there seems to be a correlation between both predictors. Individuals with a greater reduction in heart-rate during timing trials tended to be better at guessing their own heart-rate prior to the timing task (Meissner and Wittmann, personal communication). A second line of support, for a link between bodily changes and sentient processing comes from the emotion literature. As demonstrated repeatedly, emotional stimuli elicit greater bodily changes than neutral stimuli (Bradley et al., 2001) such that bodily changes may well account for associated differences in the perception of time. Furthermore, meta-analyses find the insula more strongly activated for emotional as compared to neutral events, particularly when individuals focus on how they feel (Phan et al., 2004; Lee and Siegle, 2009). Thus, one may infer that emotion-induced bodily changes enhance sentient representations in the insula and that these representations are further enhanced if bodily changes become the focus of attention. Lastly, a study by Effron et al. (2006) speaks to the relationship between bodily states, sentience, and time. These authors asked participants to perform a temporal bisection task with emotional and neutral facial expressions in the test phase. In one condition, participants were prevented from automatically embodying the facial expression by holding a pen in their mouth. In another condition, participants could move their face freely. Relative overestimations for emotional as compared to neutral expressions were only found in the latter condition suggesting that bodily representations are critical for emotion effects on time.

Like the attentional proposal, the sentient proposal has a few advantages over the arousal proposal. First, it outlines a concrete mechanism and brain substrate by which emotions influence time. As such, the proposal can be tested relatively easily. Second, it ties emotion-induced temporal distortions to processes that occur while, not after, participants encode time. Specifically, while the arousal proposal evokes sympathetic activations that often peak after the timing stimulus has lapsed, the sentient proposal allows for any bodily changes to affect time. Hence, also parasympathetic changes, such as heart-rate decelerations that occur after the onset of a timing stimulus, can affect temporal estimates. Nevertheless, the sentient proposal is not without problems. Specifically, if one assumes that emotional stimuli lead to bodily changes and thus potentially heighten sentient processing and temporal awareness, such stimuli should consistently produce longer temporal estimates than neutral stimuli. However, emotional events may both speed-up and slow-down subjective time relative to neutral events and thus, by itself, this proposal also fails as an adequate explanation.

MODEL INTEGRATION

As usual, where there is conflict, reconciliation may be attempted through a compromise of existing proposals. Such a compromise could take different forms. One possibility is that the various mechanisms identified here all support the relationship between emotions and time and that their respective contributions vary across situations and, perhaps, individuals. For example, their contributions may depend on the particular emotion that is evoked by a timing stimulus or distractor. Fear relevant stimuli might accelerate an internal clock by increasing bodily arousal, capturing an individual's attention (Pourtois et al., 2006), and enhancing sentient processing. Disgust relevant stimuli, on the other hand, may decelerate an internal clock by biasing our attention away from both the stimulus and its temporal dimension (Curtis et al., 2004) in-spite of up-regulating sentient processing (Wicker et al., 2003). Likewise different mechanisms may be at play depending on whether emotional stimuli are the context or focus of the timing task and depending on stimulus duration. With respect to the latter factor, one could envision emotion effects on attention to be more acute during initial as compared to continued stimulus processing thus leading to a drop-off of emotion effects for the timing of longer stimuli.

Despite its ability to accommodate the data, the possibility of situation-specific timing mechanisms is unsatisfying. It seems too flexible to have true explanatory power and thus one may attempt to reconcile the literature by proposing a fourth, hybrid mechanism with a more general utility. In light of the preceding discussion it seems that the stimulus and the sentient processing mechanisms are well suited for this. Specifically, all one needs to do is accept the idea that sentient processing is stimulus-specific; that we experience ourselves not independently from our environment but in relationship to the various stimuli and events we encounter. Thus, we create stimulus-specific sentient and ultimately temporal representations.

Although speculative, this notion is not too far fetched because there is already evidence that we can assign different temporal values to equally long and temporarily overlapping stimuli (Penney et al., 2000). Specifically, two concurrent stimuli of equivalent duration, but differing in modality may be perceived as of different duration, thereby raising the possibility of different (i.e., stimulus-specific) sentient representations. In the context of emotions, such representations could account for both relative over and underestimations observed in interval-timing studies. As mentioned before, overestimations would result for emotional as compared to neutral timing stimuli due to an increase in sentient processing. Underestimations would result for neutral timing stimuli presented in the context of emotional as compared to neutral distractors. Here, sentient representations emerging from the timing stimulus would be relatively weaker than the sentient representations emerging from the emotional distractor, making the former seem shorter than it really is.

The hybrid model proposed here (**Figure 1**) fairs better than the arousal, attention, or sentient model alone in accommodating the existing data. Moreover, by making emotions relevant for timing it solves the issue that attention to non-temporal neutral information (e.g., intensity) impairs timing, whereas attention to non-temporal emotional information does not. It holds that attending to emotions is similar to attending to time. Nevertheless, the model is at present highly speculative. It rests on a few assumptions that have not yet been tested or for which existing evidence is still equivocal. For example, the assumption that emotion-induced bodily changes enhance self-awareness awaits investigation. This could be done by relating objective physiological measures to self-reports of cardiac or respiratory activity and to temporal judgments. Specifically, one could test whether self-reports mediate the relationship between bodily change and subjective time. Furthermore, the idea of stimulus-specific sentient representations needs further investigation. The evidence cited above merely suggests that we can perceive concurrently presented same-duration stimuli as differently long. Whether and in what way this is linked to different sentient representations and whether emotions could differently moderate those are still open issues.

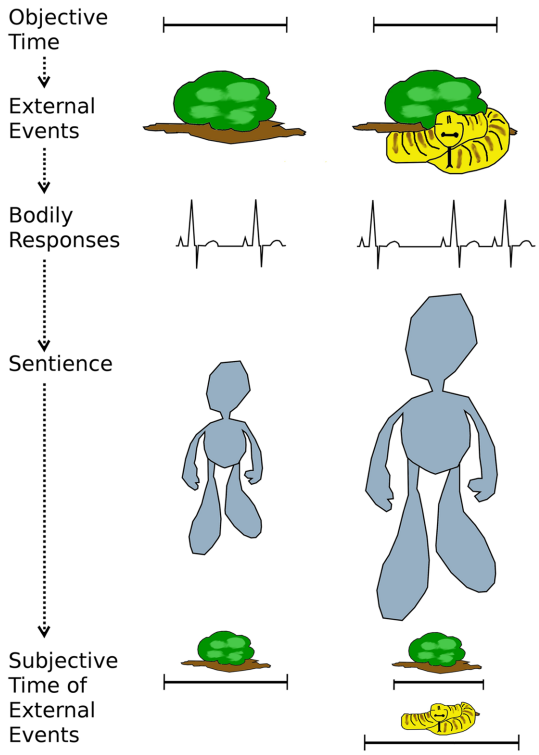

FIGURE 1 | Illustrated is a potential mechanism by which emotions may influence the perceived duration of external events. Depending on their emotional significance, environmental stimuli may trigger bodily changes, which in turn may increase self-awareness or sentience – a potential contributor to the perception of time. Depending on their contribution to bodily and sentient changes, concurrent environmental stimuli may be perceived as relatively longer (e.g., snake) or shorter (e.g., shrub) than their objective duration.

CONCLUSION

Emotion-induced subjective changes in time are a ubiquitous everyday phenomenon that is well documented in the literature.

Different proposals have been put forth to explain how emotions impact time. Of these proposals, a hybrid that combines sentient and stimulus processing seems to best accommodate existing experimental data as it can account for why we sometimes experience events to last longer *and* shorter than they really are. According to this proposal, such events trigger bodily changes that increase our sense of "being" across time. The subjective duration of objects that concur with such events then depends on how much they share in sentience or awareness. Salient objects that capture and hold attention would be overestimated relative to other, less salient objects. Thus, differences in perceptual salience would translate into differences in mnemonic salience as the more important stimuli would receive greater temporal weights. As such these objects may more readily influence present and future behaviors.

ACKNOWLEDGMENTS

I would like to thank Trevor Penney and Marc Wittmann for commenting on an earlier version of this manuscript. This work was supported by the NUS Yong Investigator Award (WBS R581-000-066-101) and the A*Star SERC grant (0921570130).

REFERENCES

Advokat, C. (2010). What are the cognitive effects of stimulant medications? Emphasis on adults with attention-deficit/hyperactivity disorder (ADHD). *Neurosci. Biobehav. Rev.* 34, 1256–1266.

Angrilli, A., Cherubini, P., Pavese, A., and Mantredini, S. (1997). The influence of affective factors on time perception. *Percept. Psychophys.* 59, 972–982.

Bradley, M. M., Codispoti, M., Cuthbert, B. N., and Lang, P. J. (2001). Emotion and motivation I: defensive and appetitive reactions in picture processing. *Emotion* 1, 276–298.

Brennan, A. R., and Arnsten, A. F. T. (2008). Neuronal mechanisms underlying attention deficit hyperactivity disorder: the influence of arousal on prefrontal cortical function. *Ann. N. Y. Acad. Sci.* 1129, 236–245.

Buhusi, C. V., and Meck, W. H. (2005). What makes us tick? Functional and neural mechanisms of interval timing. *Nat. Rev. Neurosci.* 6, 755–765.

Buhusi, C. V., and Meck, W. H. (2009). Relative time sharing: new findings and an extension of the resource allocation model of temporal processing. *Philos. Trans. R. Soc. Lond. B Biol. Sci.* 364, 1875–1885.

Chikama, M., McFarland, N. R., Amaral, D. G., and Haber, S. N. (1997). Insular cortical projections to functional regions of the striatum correlate with cortical cytoarchitectonic organization in the primate. *J. Neurosci.* 17, 9686–9705.

Craig, A. D. B. (2009a). Emotional moments across time: a possible neural basis for time perception in the anterior insula. *Philos. Trans. R. Soc. Lond. B Biol. Sci.* 364, 1933–1942.

Craig, A. D. B. (2009b). How do you feel – now? The anterior insula and human awareness. *Nat. Rev. Neurosci.* 10, 59–70.

Curtis, V., Aunger, R., and Rabie, T. (2004). Evidence that disgust evolved to protect from risk of disease. *Proc. R. Soc. B Biol. Sci.* 271, S131–S133.

Damasio, A. R. (1996). The somatic marker hypothesis and the possible functions of the prefrontal cortex. *Philos. Trans. R. Soc. Lond. B Biol. Sci.* 351, 1413–1420.

Doi, H., and Shinohara, K. (2009). The perceived duration of emotional face is influenced by the gaze direction. *Neurosci. Lett.* 457, 97–100.

Droit-Volet, S. (2003). Alerting attention and time perception in children. *J. Exp. Child. Psychol.* 85, 372–384.

Droit-Volet, S., Bigand, E., Ramos, D., and Bueno, J. L. O. (2010). Time flies with music whatever its emotional valence. *Acta Psychol. (Amst.)* 135, 226–232.

Droit-Volet, S., Fayolle, S. L., and Gil, S. (2011). Emotion and time perception: effects of film-induced mood. *Front. Integr. Neurosci.* 5:33. doi:10.3389/fnint.2011.00033

Droit-Volet, S., and Gil, S. (2009). The time-emotion paradox. *Philos. Trans. R. Soc. Lond. B Biol. Sci.* 364, 1943–1953.

Droit-Volet, S., and Meck, W. H. (2007). How emotions colour our perception of time. *Trends Cogn. Sci. (Regul. Ed.)* 11, 504–513.

Effron, D. A., Niedenthal, P. M., Gil, S., and Droit-Volet, S. (2006). Embodied temporal perception of emotion. *Emotion* 6, 1–9.

Gibbon, J., Church, R. M., and Meck, W. H. (1984). Scalar timing in memory. *Ann. N. Y. Acad. Sci.* 423, 52–77.

Gil, S., Niedenthal, P. M., and Droit-Volet, S. (2007). Anger and time perception in children. *Emotion* 7, 219–225.

Gil, S., Rousset, S., and Droit-Volet, S. (2009). How liked and disliked foods affect time perception. *Emotion* 9, 457–463.

Grommet, E. K., Droit-Volet, S., Gil, S., Hemmes, N. S., Baker, A. H., and Brown, B. L. (2011). Time estimation of fear cues in human observers. *Behav. Processes* 86, 88–93.

Hicks, R. E., Miller, G. W., Gaes, G., and Bierman, K. (1977). Concurrent processing demands and the experience of time-in-passing. *Am. J. Psychol.* 90, 431–446.

James, W. (1981). *The Principles of Psychology*. Cambridge, MA: Harvard University Press.

Lee, K.-H., Seelam, K., and O'Brien, T. (2011). The relativity of time perception produced by facial emotion stimuli. *Cogn. Emot.* PMID: 21432628. [Epub ahead of print].

Lee, K. H., and Siegle, G. J. (2009). Common and distinct brain networks underlying explicit emotional evaluation: a meta-analytic study. *Soc. Cogn. Affect. Neurosci.* Available at: http://www.ncbi.nlm.nih.gov/pubmed/19270039 [Accessed July 14, 2011].

Levenson, R. W., Ekman, P., and Friesen, W. V. (1990). Voluntary facial action generates emotion-specific autonomic nervous system activity. *Psychophysiology* 27, 363–384.

Livesey, A. C., Wall, M. B., and Smith, A. T. (2007). Time perception: manipulation of task difficulty dissociates clock functions from other cognitive demands. *Neuropsychologia* 45, 321–331.

Lui, M. A., Penney, T. B., and Schirmer, A. (2011). Emotion effects on timing: attention versus pacemaker accounts. *PLoS ONE* 6, e21829. doi:10.1371/journal.pone.0021829

Macar, F., Grondin, S., and Casini, L. (1994). Controlled attention sharing influences time estimation. *Mem. Cognit.* 22, 673–686.

Meck, W. H. (1983). Selective adjustment of the speed of internal clock and memory processes. *J. Exp. Psychol. Anim. Behav. Process.* 9, 171–201.

Meissner, K., and Wittmann, M. (2011). Body signals, cardiac awareness, and the perception of time. *Biol. Psychol.* 86, 289–297.

Mella, N., Conty, L., and Pouthas, V. (2011). The role of physiological arousal in time perception: psychophysiological evidence from an emotion regulation paradigm. *Brain Cogn.* 75, 182–187.

Noulhiane, M., Mella, N., Samson, S., Ragot, R., and Pouthas, V. (2007). How emotional auditory stimuli modulate time perception. *Emotion* 7, 697–704.

Ornstein, R. E. (1997). *On the Experience of Time*. Boulder, CO: Westview Press.

Penney, T. B. (2003). "Modality differences in interval timing: attention, clock speed, and memory," in *Functional and Neural Mechanisms of Interval Timing*, ed. W. Meck (Boca Raton, FL: CRC Press), 209–234.

Penney, T. B., Gibbon, J., and Meck, W. H. (2000). Differential effects of auditory and visual signals on clock speed and temporal memory. *J. Exp. Psychol. Hum. Percept. Perform.* 26, 1770–1787.

Phan, K. L., Wager, T. D., Taylor, S. F., and Liberzon, I. (2004). Functional neuroimaging studies of human emotions. *CNS Spectr.* 9, 258–266.

Pourtois, G., Schwartz, S., Seghier, M. L., Lazeyras, F., and Vuilleumier, P. (2006). Neural systems for orienting attention to the location of threat signals: an event-related fMRI study. *Neuroimage* 31, 920–933.

Pouthas, V., George, N., Poline, J.-B., Pfeuty, M., Vandemoorteele, P.-F., Hugueville, L., Ferrandez, A.-M., Lehéricy, S., Lebihan, D., and Renault, B. (2005). Neural network involved in time perception: an fMRI study comparing long and short interval estimation. *Hum. Brain Mapp.* 25, 433–441.

Schirmer, A. (2004). Timing speech: a review of lesion and neuroimaging findings. *Brain Res. Cogn. Brain Res.* 21, 269–287.

Schirmer, A., and Escoffier, N. (2010). Emotional MMN: anxiety and heart rate correlate with the ERP signature for auditory change detection. *Clin. Neurophysiol.* 121, 53–59.

Schulman, C. A., Richlin, M., and Weinstein, S. (1967). Hallucinations and disturbances of affect, cognition, and physical state as a function of sensory deprivation. *Percept. Mot. Skills* 25, 1001–1024.

Vierordt, K. (1868). *Der Zeitsinn nach Versuchen*. Tubingen: H. Laupp.

Wearden, J. H., Pilkington, R., and Carter, E. (1999). "Subjective lengthening" during repeated testing of a simple temporal discrimination. *Behav. Processes* 46, 25–38.

Wicker, B., Keysers, C., Plailly, J., Royet, J. P., Gallese, V., and Rizzolatti, G. (2003). Both of us disgusted in my insula: the common neural basis of seeing and feeling disgust. *Neuron* 40, 655–664.

Wittmann, M. (2009). The inner experience of time. *Philos. Trans. R. Soc. Lond. B Biol. Sci.* 364, 1955–1967.

Wittmann, M., Simmons, A. N., Aron, J. L., and Paulus, M. P. (2010). Accumulation of neural activity in the posterior insula encodes the passage of time. *Neuropsychologia* 48, 3110–3120.

Conflict of Interest Statement: The author declares that the research was conducted in the absence of any commercial or financial relationships that could be construed as a potential conflict of interest.

Received: 21 July 2011; paper pending published: 09 August 2011; accepted: 14 September 2011; published online: 05 October 2011.

*Citation: Schirmer A (2011) How emotions change time. Front. Integr. Neurosci. **5**:58. doi: 10.3389/fnint.2011.00058*

frontiers in
INTEGRATIVE NEUROSCIENCE

OPINION ARTICLE
published: 19 September 2011
doi: 10.3389/fnint.2011.00055

Unpredictability and uncertainty in anxiety: a new direction for emotional timing research

Jessica I. Lake[1,2]* and Kevin S. LaBar[1,2]

[1] *Center for Cognitive Neuroscience, Duke University, Durham, NC, USA*
[2] *Department of Psychology and Neuroscience, Duke University, Durham, NC, USA*
**Correspondence: jessica.lake@duke.edu*

Interest in the relationship between emotion and time perception has noticeably increased in the past few years (Buhusi and Meck, 2005; Droit-Volet and Meck, 2007; Craig, 2009; Droit-Volet et al., 2011). Most of this recent work has used emotional stimuli, such as faces (e.g., Droit-Volet et al., 2004; Tipples, 2008), pictures (e.g., Angrilli et al., 1997; Grommet et al., 2011), and sounds (e.g., Noulhaine et al., 2007) to understand how emotion can change the subjective experience of short intervals of time. Efforts have largely focused on determining what these findings reveal about how time can be distorted and identifying the mechanisms responsible for flexibly modulating these distortions. In this issue, Schirmer (2011) reviews various theories that attempt to explain the mechanisms underlying emotional influences on time perception and proposes a hybrid theory to better support findings in the field. Further research will be necessary to support or contradict the proposed mechanistic influences of emotion on timing. While the value of this work is clear, it is equally important to address how timing research can inform affective science and affective disorders, a question that has thus far received little attention within the field. Specifically, a better understanding of how time is perceived in anxiety-provoking contexts could be important in fully appreciating the processes underlying the experience of anxiety.

Many of the first studies of time perception and anxiety analyzed estimates of elapsed time under stressful conditions (e.g., Langer et al., 1961; Hare, 1963; Watts and Sharrock, 1984; Loftus et al., 1987). While these studies consistently reported overestimation of time and were ecologically relevant, they were limited in that they relied on small numbers of trials and retrospective reports, which have been argued to reflect memory, rather than timing, processes *per se* (Zakay, 1990). Using standardized emotional stimuli such as pictures and film clips, more recent studies have added support to the idea that increased fear and anxiety are correlated with the overestimation of time intervals (e.g., Droit-Volet et al., 2011; Grommet et al., 2011). At the same time, recent work on anxiety and related disorders has focused on the role of ambiguity (e.g., Nader and Balleine, 2007; Shankman et al., 2011; Zweifel et al., 2011). Using work on timing and time perception to address the influence of ambiguity on anxiety could provide a unique perspective from which to further advance our understanding of these clinical disorders.

Anxiety is defined as a state of prolonged fear or arousal in response to a threat that is ambiguous or unspecific (Lang et al., 2000). Ambiguity refers to a situation or context in which a threat may take various forms, and different predictions and behaviors based on these predictions may subsequently occur (Whalen, 1998). Temporal unpredictability (ambiguity in *when* an event will occur) and probabilistic uncertainty (ambiguity in *how likely* an event is to occur) are two types of threat ambiguity. Human and non-human animal studies suggest that both unpredictability and uncertainty modulate anxiety-like behaviors and activity in brain regions associated with anxiety (Hsu et al., 2005; Rosen and Donley, 2006; Herry et al., 2007).

Most studies showing an increase in anxiety associated with temporal unpredictability have used paradigms involving anticipation of negative emotional events (e.g., Grillon et al., 2006). Note that this approach contrasts with typical time perception studies in which emotion is manipulated phasically through alterations in the sensory features of a stimulus whose duration is to be timed. In Grillon et al. (2004), anxiety was operationally defined as the magnitude of a startle response (Brown et al., 1951) during cue-free periods within an aversive conditioning paradigm (context-potentiated startle). Context-potentiated startle was greater when surrounding cues were not predictive of when aversive events occurred (i.e., aversive events were perceived as occurring randomly) compared to cue-free periods within the context of cues that reliably predicted the temporal occurrence of aversive events. Simply cuing previously unpredictable shocks also reduces context-potentiated startle responses (Fonteyne et al., 2010). Together, these findings suggest that temporal unpredictability increases anxiety levels. The aversive nature of unpredictability is further supported by studies showing that animals prefer to receive predictable over unpredictable shocks (Gliner, 1972; Badia et al., 1979). Unpredictability on its own (i.e., without an explicit association with an aversive stimulus) may also be anxiogenic. In a translational study examining both a mouse model and healthy human participants, Herry et al. (2007) found that manipulating the unpredictability of neutral tones increased anxiety-like behaviors. Furthermore, this study implicated the amygdala, a structure commonly associated with fear and anxiety (e.g., LaBar et al., 1998; Davis et al., 2010; Tye et al., 2011), in the monitoring of unpredictability. Across species evidence of sustained activity in the amygdala was interpreted as reflecting modified habituation processes to allow individuals to remain prepared for action in the face of unpredictability.

In addition to temporal unpredictability, probabilistic uncertainty also seems to modulate anxiety. While different relationships between the probability of aversive events and anxiety have been proposed when those probabilities are known to the subject (e.g., Epstein and Roupenian, 1970; Bankart and Elliott, 1974; Loewenstein et al., 2001), increased anxiety levels are evident when subjects are unaware of event contingencies. Sarinopoulos et al. (2010) found that, in retrospective estimates, healthy participants overestimated how often a cue that ambiguously predicted negative stimuli (50% chance of negative

stimulus presentation following cue) was followed by an aversive event. In this study, increased activity in the amygdala and insula was found during ambiguous cues relative to cues that perfectly predicted negative stimuli. The magnitude of this difference was further correlated with the degree of overestimation in retrospective reports. Ambiguous cues are also associated with increased skin conductance responses (Grupe and Nitschke, 2011). These results suggest that, like unpredictability, individuals find uncertain probabilities aversive. Neuroeconomic studies have also provided evidence supporting the role of the amygdala (e.g., Hsu et al., 2005) and insula (e.g., Preuschoff et al., 2008) in the processing of decisions under uncertainty.

While time perception research has shown that subjective time is sensitive to fear and anxiety (e.g., Campbell and Bryant, 2007; Bar-Haim et al., 2010), there is a paucity of research directly addressing the function of ambiguity in time distortions. Based on the work cited above showing that anxiety is influenced by different types of ambiguity, we predict that the experience of time may also be sensitive to manipulations of threat ambiguity and, specifically of interest here, to manipulations of unpredictability and uncertainty. Fearful and angry faces, which are both considered social indicators of threat, tend to be overestimated in time (Droit-Volet et al., 2004; Bar-Haim et al., 2010; Tipples, 2011, but see Tipples, 2008). Temporal overestimation of fearful faces is further modulated by individual differences in trait anxiety (Bar-Haim et al., 2010, but see Tipples, 2011). The overestimation of fearful faces is particularly relevant in considering the influence of ambiguity on time perception. Whalen (1998) proposed that fearful facial expressions are ambiguous stimuli in experimental designs because the source of threat resulting in the expressed fear is unknown to participants. Findings indicating that fearful faces increase time estimates therefore provide preliminary support for the idea that threat ambiguity can influence time perception.

In Droit-Volet et al. (2010), participants judged a probe duration that began after a neutral cue or a cue that predicted an aversive event. Probe durations were overestimated following the threat cue compared to the neutral cue and a longer anticipation period prior to the delivery of the aversive event resulted in an even greater overestimation of time. These findings suggest that the magnitude of time distortion was correlated with the degree of anticipatory anxiety experienced by the participants. In this study, the cues predicting an aversive event were always temporally predictable and 100% reinforced. Manipulating unpredictability and uncertainty in a similar paradigm by varying the anticipation period within participants or altering reinforcement probabilities could reveal more about the relationship between anxiety and time. If unpredictability and uncertainty increase aversiveness (Herry et al., 2007; Sarinopoulos et al., 2010), it may be predicted that these anxiety-provoking contexts would also increase distortions of subjective time.

While the evidence provided above implicates both temporal unpredictability and probabilistic uncertainty in increased anxiety, these two types of ambiguity may be functionally dissociable across clinical populations. Grillon et al. (2008) found that panic disorder patients showed greater context-potentiated startle in a temporally unpredictable aversive condition compared to a predictable condition with temporally cued (but probabilistically uncertain) aversive sounds. Similar results were found for post-traumatic stress disorder patients using a comparable study paradigm (Grillon et al., 2009). The authors predicted these results based on the idea that both disorders are characterized by anxiety resulting from the unpredictability of aversive events. Interestingly, Grillon et al. (2009) found that generalized anxiety disorder (GAD) patients did not show the same pattern of anxiety-like responses, suggesting that the anxiety experienced by GAD patients might be qualitatively different. It is important to consider that while the predictable condition in this study was temporally invariant, a probabilistic reinforcement rate was used such that the cue did not perfectly predict the aversive stimulus. It is therefore possible that GAD patients had an enhanced aversive response to the probabilistic uncertainty associated with this cue. Indeed, GAD patients showed the highest context-potentiated startle in the predictable condition, though this finding was not statistically significant. The hypothesis that GAD patients find probabilistic uncertainty aversive is indirectly supported by Krain et al. (2008), who found that adolescent GAD patients with high *intolerance of uncertainty* (IU) scores showed greater activity in the amygdala than controls when contrasting "pure" uncertainty (50% probability of a correct response) with other task conditions. These patients also rated the 50% probability condition as more anxiety-provoking than control participants. IU is believed to correlate with worry (Dugas et al., 1997), a characteristic feature of GAD, according to the *Diagnostic and Statistical Manual of Mental Disorders – 4th edn* (American Psychiatric Association, 1994). Interestingly, while IU may be positively correlated with probabilistic uncertainty, it was found to be *negatively* correlated with context-potentiated startle responses in a temporally unpredictable context (Nelson and Shankman, 2011). College students with higher IU scores showed decreased context-potentiated startle responses. Because high IU scores are associated with GAD, this supports Grillon et al. (2009) and the idea that GAD is not associated with increased context-potentiated startle during temporal unpredictability. Probabilistic uncertainty and temporal unpredictability may, therefore, differentially modulate anxiety and distinguish different anxiety-related disorders. Further work with these clinical populations is necessary and could have important implications for nosology and treatment.

While studies have demonstrated time distortions in non-anxious patient populations (Meck, 1996, 2005; Berlin and Rolls, 2004; Melgire et al., 2005; Penney et al., 2005; Allman and Meck, 2011), examinations of how time may be distorted in individuals with anxiety disorders are lacking. It is likely that time is distorted to a greater extent during periods of increased threat and anxiety in clinical populations suffering from anxiety disorders than in healthy controls. It is also predicted, based on current research on unpredictability and uncertainty, that these two forms of threat ambiguity may differentially influence time distortions across clinical groups and could help further characterize the differences between certain anxiety-related populations. For example, panic and post-traumatic stress disorder patients might show greater time distortions resulting from unpredictable stimuli, whereas GAD patients might show greater distortions resulting from probabilistic uncertainty. Such findings would indicate

that time perception is intimately related to the way in which anxiety is experienced and how individuals respond to aversive events.

Taking this idea a step further, the hypothesis that time distortions are yoked to the experience of anxiety could potentially open the door to new therapies focused on using cognitive strategies to reduce these distortions and, as a result, reduce feelings of anxiety. A study by Mella et al. (2011) provides preliminary evidence that paying attention to time rather than emotion can reduce physiological arousal as a form of emotion regulation. Future work could address the potential for attending to time in reducing the aversiveness of ambiguous stimuli. This therapeutic direction would represent a novel treatment in the control of anxiety disorders.

Finally, research on ambiguity and time perception could increase our understanding of anxiety even further if future studies combined neuroimaging techniques with psychological studies of behavior. Only a few studies have examined the neural correlates of anxiety and time perception (Meck and MacDonald, 2007; Gan et al., 2009). The findings of Meck and MacDonald (2007), in particular, indicate that the amygdala may be critical for distortions in timing arising from the threat of an aversive event. Other researchers have suggested the importance of the insula in the relationship between emotion and time (Craig, 2009; Schirmer, 2011). Research showing that these brain regions mediate the effects of unpredictability and uncertainty on time distortions would help in better understanding the biological mechanisms underlying the experience of anxiety.

It is suggested here that researchers in the field of timing and time perception consider how the study of emotional timing may benefit not just the field of time perception, but that of emotion and affective disorders as well. Addressing the influence of ambiguity on anxiety and how different aspects of ambiguity interact with time perception could help improve our understanding of the mechanisms underlying the experience of anxiety, how these processes become impaired in clinical populations, and potential treatment avenues (Meck et al., 2008; Allman and Meck, 2011; Coull et al., 2011; Gu et al., 2011). While the present paper only addresses the potential influence of unpredictability and uncertainty on time distortions in the context of the anticipation of aversive events, it is equally likely that these components of ambiguity may also influence time during the anticipation of positive events, an additional avenue for future research. Overall, there is great promise in bridging psychological and neurobiological disciplines by addressing current topics in the field of emotion to increase the value and applicability of time perception research.

ACKNOWLEDGMENT

This work was supported by a National Science Foundation Graduate Fellowship to Jessica I. Lake.

REFERENCES

Allman, M. J., and Meck, W. H. (2011). Pathophysiological distortions in time perception and timed performance. *Brain* doi: 10.1093/brain/awr210. (in press).

American Psychiatric Association (APA). (1994). *DSM-IV: Diagnostic and Statistical Manual of Mental Disorders*, 4th Edn. Washington, DC: American Psychiatric Press.

Angrilli, A., Cherubini, P., Pavese, A., and Manfredini, S. (1997). The influence of affective factors on time perception. *Percept. Psychophys.* 59, 972–982.

Badia, P., Harsh, J., and Abbott, B. (1979). Choosing between predictable and unpredictable shock conditions: data and theory. *Psychol. Bull.* 86, 1107–1131.

Bankart, C. P., and Elliott, R. (1974). Heart rate and skin conductance in anticipation of shocks with varying probability of occurrence. *Psychophysiology* 11, 160–174.

Bar-Haim, Y., Kerem, A., Lamy, D., and Zakay, D. (2010). When time slows down: the influence of threat on time perception in anxiety. *Cogn. Emot.* 24, 255–263.

Berlin, H. A., and Rolls, E. T. (2004). Time perception, impulsivity, emotionality, and personality in self-harming borderline personality disorder patients. *J. Pers. Disord.* 18, 358–378.

Brown, J. S., Kalish, H. I., and Farber, I. E. (1951). Conditioned fear as revealed by magnitude of startle response to an auditory stimulus. *J. Exp. Psychol.* 41, 317–328.

Buhusi, C. V., and Meck, W. H. (2005). What makes us tick? Functional and neural mechanisms of interval timing. *Nat. Rev. Neurosci.* 6, 755–765.

Campbell, L. A., and Bryant, R. A. (2007). How time flies: a study of novice skydivers. *Behav. Res. Ther.* 45, 1389–1392.

Coull, J. T., Cheng, R. K., and Meck, W. H. (2011). Neuroanatomical and neurochemical substrates of timing. *Neuropsychopharmacology* 36, 3–25.

Craig, A. D. (2009). Emotional moments across time: a possible neural basis for time perception in the anterior insula. *Philos. Trans. R. Soc. Lond. B Biol. Sci.* 364, 1933–1942.

Davis, M., Walker, D. L., Miles, L., and Grillon, C. (2010). Phasic vs sustained fear in rats and humans: role of the extended amygdala in fear vs anxiety. *Neuropsychopharmacology* 35, 105–135.

Droit-Volet, S., Brunot, S., and Niedenthal, P. (2004). Perception of the duration of emotional events. *Cogn. Emot.* 18, 849–858.

Droit-Volet, S., Fayolle, S. L., and Gil, S. (2011). Emotion and time perception: effects of film-induced mood. *Front. Integr. Neurosci.* 5:33. doi: 10.3389/fnint.2011.00033

Droit-Volet, S., and Meck, W. H. (2007). How emotions colour our perception of time. *Trends Cogn. Sci. (Regul. Ed.)* 11, 504–513.

Droit-Volet, S., Mermillod, M., Cocenas-Silva, R., and Gil, S. (2010). Expectancy of a threatening event on time perception in human adults. *Emotion* 10, 908–914.

Dugas, M. J., Freeston, M. H., and Ladouceur, R. (1997). Intolerance of uncertainty and problem orientation in worry. *Cogn. Ther. Res.* 21, 593–606.

Epstein, S., and Roupenian, A. (1970). Heart rate and skin conductance during experimentally induced anxiety: the effect of uncertainty about receiving a noxious stimulus. *J. Pers. Soc. Psychol.* 16, 20–28.

Fonteyne, R., Vervliet, B., Hermans, D., Baeyens, F., and Vansteenwegen, D. (2010). Exposure to the context and removing the unpredictability of the US: two methods to reduce contextual anxiety compared. *Biol. Psychol.* 85, 361–369.

Gan, T., Wang, N., Zhang, Z., Li, H., and Luo, Y. (2009). Emotional influences on time perception: evidence from event-related potentials. *Neuroreport* 20, 839–843.

Gliner, J. A. (1972). Predictable vs. unpredictable shock: preference behavior and stomach ulceration. *Physiol. Behav.* 9, 693–698.

Grillon, C., Baas, J. M. P., Cornwell, B., and Johnson, L. (2006). Context conditioning and behavioral avoidance in a virtual reality environment: effect of predictability. *Biol. Psychiatry* 60, 752–759.

Grillon, C., Baas, J. P., Lissek, S., Smith, K., and Milstein, J. (2004). Anxious responses to predictable and unpredictable aversive events. *Behav. Neurosci.* 118, 916–924.

Grillon, C., Lissek, S., Rabin, S., McDowell, D., Dvir, S., and Pine, D. S. (2008). Increased anxiety during anticipation of unpredictable but not predictable aversive stimuli as a psychophysiologic marker of panic disorder. *Am. J. Psychiatry* 165, 898–904.

Grillon, C., Pine, D. S., Lissek, S., Rabin, S., Bonne, O., and Vythilingham, M. (2009). Increased anxiety during anticipation of unpredictable aversive stimuli in posttraumatic stress disorder but not in generalized anxiety disorder. *Biol. Psychiatry* 66, 47–53.

Grommet, E. K., Droit-Volet, S., Gil, S., Hemmes, N. S., Baker, A. H., and Brown, B. L. (2011). Time estimation of fear cues in human observers. *Behav. Processes* 86, 88–93.

Grupe, D. W., and Nitschke, J. B. (2011). Uncertainty is associated with biased expectancies and heightened responses to aversion. *Emotion* 11, 413–424.

Gu, B. M., Cheng, R. K., Yin, B., and Meck, W. H. (2011). Quinpirole-induced sensitization to noisy/sparse periodic input: temporal syhchronization as a component of obsessive-compulsive disorder. *Neuroscience* 179, 143–150.

Hare, R. D. (1963). The estimation of short temporal intervals terminated by shock. *J. Clin. Psychol.* 19, 378–380.

Herry, C., Bach, D. R., Esposito, F., Di Salle, F., Perrig, W. J., Scheffler, K., Luthi, A., and Seifritz, E. (2007). Processing of temporal unpredictability in human and animal amygdala. *J. Neurosci.* 27, 5958–5966.

Hsu, M., Bhatt, M., Adolphs, R., Tranel, D., and Camerer, C. F. (2005). Neural systems responding to degrees of uncertainty in human decision-making. *Science* 310, 1680–1683.

Krain, A. L., Gotimer, K., Hefton, S., Ernst, M., Castellanos, X., Pine, D. S., and Milham, M. P. (2008). A functional magnetic resonance imaging investigation of uncertainty in adolescents with anxiety disorders. *Biol. Psychiatry* 63, 563–568.

LaBar, K. S., Gatenby, J. C., Gore, J. C., LeDoux, J. E., and Phelps, E. A. (1998). Human amygdala activation during conditioned fear acquisition and extinction: a mixed-trial fMRI study. *Neuron* 20, 937–945.

Lang, P. J., Davis, M., and Öhman, A. (2000). Fear and anxiety: animal models and human cognitive psychophysiology. *J. Affect. Disord.* 61, 137–159.

Langer, J., Wapner, S., and Werner, H. (1961). The effect of danger upon the experience of time. *Am. J. Psychol.* 74, 94–97.

Loewenstein, G. F., Weber, E. U., Hsee, C. K., and Welch, N. (2001). Risk as feelings. *Psychol. Bull.* 127, 267–286.

Loftus, E. F., Schooler, J. W., Boone, S. M., and Kline, D. (1987). Time went by so slowly: overestimation of event duration by males and females. *Appl. Cogn. Psychol.* 1, 3–13.

Meck, W. H. (1996). Neuropharmacology of timing and time perception. *Brain Res. Cogn. Brain Res.* 3, 227–242.

Meck, W. H. (2005). Neuropsychology of timing and time perception. *Brain Cogn.* 58, 1–8.

Meck, W. H., and MacDonald, C. J. (2007). Amygdala inactivation reverses fear's ability to impair divided attention and make time stand still. *Behav. Neurosci.* 121, 707–720.

Meck, W. H., Penney, T. B., and Pouthas, V. (2008). Cortico-striatal representation of time in animals and humans. *Curr. Opin. Neurobiol.* 18, 145–152.

Melgire, M., Ragot, R., Samson, S., Penney, T. B., Meck, W. H., and Pouthas, V. (2005). Auditory/visual duration bisection in patients with left or right medial-temporal lobe resection. *Brain Cogn.* 58, 119–124.

Mella, N., Conty, L., and Pouthas, V. (2011). The role of physiological arousal in time perception: psychophysiological evidence from an emotion regulation paradigm. *Brain Cogn.* 75, 182–187.

Nader, K., and Balleine, B. (2007). Ambiguity and anxiety: when a glass half full is empty. *Nat. Neurosci.* 10, 807–808.

Nelson, B. D., and Shankman, S. A. (2011). Does intolerance of uncertainty predict anticipatory startle responses to uncertain threat? *Int. J. Psychophysiol.* 81, 107–115.

Noulhaine, M., Mella, N., Samson, S., Ragot, R., and Pouthas, V. (2007). How emotional auditory stimuli modulate time perception. *Emotion* 7, 697–704.

Penney, T. B., Meck, W. H., Roberts, S. A., Gibbon, J., and Erlenmeyer-Kimling, L. (2005). Interval-timing deficits in individuals at high risk for schizophrenia. *Brain Cogn.* 58, 109–118.

Preuschoff, K., Quartz, S. R., and Bossaerts, P. (2008). Human insula activation reflects risk prediction errors as well as risk. *J. Neurosci.* 28, 2745–2752.

Rosen, J. B., and Donley, M. P. (2006). Animal studies of amygdala function in fear and uncertainty: relevance to human research. *Biol. Psychol.* 73, 49–60.

Sarinopoulos, I., Grupe, D. W., Mackiewicz, K. L., Herrington, D., Lor, M., Steege, E. E., and Nitschke, J. B. (2010). Uncertainty during anticipation modulates neural responses to aversion in human insula and amygdala. *Cereb. Cortex* 20, 929–940.

Schirmer, A. (2011). How emotions change time. *Front. Integr. Neurosci.* (in press).

Shankman, S. A., Robison-Andrew, E. J., Nelson, B. D., Altman, S. E., and Campbell, M. L. (2011). Effects of predictability of shock timing and intensity on aversive responses. *Int. J. Psychophysiol.* 80, 112–118.

Tipples, J. (2008). Negative emotionality influences the effects of emotion on time perception. *Emotion* 8, 127–131.

Tipples, J. (2011). When time stands still: fear-specific modulation of temporal bias due to threat. *Emotion* 11, 74–80.

Tye, K. M., Prakash, R., Kim, S., Fenno, L. E., Grosenick, L., Zarabi, H., Thompson, K. R., Gradinaru, V., Ramakrishnan, C., and Deisseroth, K. (2011). Amygdala circuitry mediating reversible and bidirectional control of anxiety. *Nature* 471, 358–362.

Watts, F. N., and Sharrock, R. (1984). Fear and time estimation. *Percept. Mot. Skills* 59, 597–598.

Whalen, P. (1998). Fear, vigilance, and ambiguity: initial neuroimaging studies of the human amygdala. *Curr. Dir. Psychol. Sci.* 7, 177–188.

Zakay, D. (1990). "The evasive art of subjective time measurement: some methodological dilemmas," in *Cognitive Models of Psychological Time*, ed. R. A. Block (Hillsdale, NJ: Lawrence Erlbaum), 59–84.

Zweifel, L. S., Fadok, J. P., Argilli, E., Garelick, M. G., Jones, G. L., Dickerson, T. M. K., Allen, J. M., Mizumori, S. J. Y., Bonci, A., and Palmiter, R. D. (2011). Activation of dopamine neurons is critical for aversive conditioning and prevention of generalized anxiety. *Nat. Neurosci.* 14, 620–628.

Received: 15 August 2011; accepted: 29 August 2011; published online: 19 September 2011.

*Citation: Lake JI and LaBar KS (2011) Unpredictability and uncertainty in anxiety: a new direction for emotional timing research. Front. Integr. Neurosci. **5**:55. doi: 10.3389/fnint.2011.00055*

frontiers in
INTEGRATIVE NEUROSCIENCE

ORIGINAL RESEARCH ARTICLE
published: 27 September 2011
doi: 10.3389/fnint.2011.00056

Optimal temporal risk assessment

Fuat Balcı[1,2]*, David Freestone[3], Patrick Simen[2†], Laura deSouza[2], Jonathan D. Cohen[2,4] and Philip Holmes[2,5,6]

[1] *Department of Psychology, Koç University, Istanbul, Turkey*
[2] *Princeton Neuroscience Institute, Princeton University, Princeton, NJ, USA*
[3] *Department of Psychology, Brown University, Providence, RI, USA*
[4] *Department of Psychology, Princeton University, Princeton, NJ, USA*
[5] *Program in Applied and Computational Mathematics, Princeton University, Princeton, NJ, USA*
[6] *Department of Mechanical and Aerospace Engineering, Princeton University, Princeton, NJ, USA*

Edited by:
Warren H. Meck, Duke University, USA

Reviewed by:
Barry Setlow, University of Florida, USA
Diego A. Golombek, Universidad Nacional de Quilmes, Argentina

****Correspondence:***
Fuat Balcı, Department of Psychology, Koç University, Rumeli Feneri Yolu 34450, Sariyer, Istanbul, Turkey.
e-mail: fbalcı@ku.edu.tr

†Present address:
Patrick Simen, Department of Neuroscience, Oberlin College, Oberlin, OH 44074, USA

Time is an essential feature of most decisions, because the reward earned from decisions frequently depends on the temporal statistics of the environment (e.g., on whether decisions must be made under deadlines). Accordingly, evolution appears to have favored a mechanism that predicts intervals in the seconds to minutes range with high accuracy on average, but significant variability from trial to trial. Importantly, the subjective sense of time that results is sufficiently imprecise that maximizing rewards in decision-making can require substantial behavioral adjustments (e.g., accumulating less evidence for a decision in order to beat a deadline). Reward maximization in many daily decisions therefore requires optimal temporal risk assessment. Here, we review the temporal decision-making literature, conduct secondary analyses of relevant published datasets, and analyze the results of a new experiment. The paper is organized in three parts. In the first part, we review literature and analyze existing data suggesting that animals take account of their inherent behavioral variability (their "endogenous timing uncertainty") in temporal decision-making. In the second part, we review literature that quantitatively demonstrates nearly optimal temporal risk assessment with sub-second and supra-second intervals using perceptual tasks (with humans and mice) and motor timing tasks (with humans). We supplement this section with original research that tested human and rat performance on a task that requires finding the optimal balance between two time-dependent quantities for reward maximization. This optimal balance in turn depends on the level of timing uncertainty. Corroborating the reviewed literature, humans and rats exhibited nearly optimal temporal risk assessment in this task. In the third section, we discuss the role of timing uncertainty in reward maximization in two-choice perceptual decision-making tasks and review literature that implicates timing uncertainty as an important factor in performance quality. Together, these studies strongly support the hypothesis that animals take normative account of their endogenous timing uncertainty. By incorporating the psychophysics of interval timing into the study of reward maximization, our approach bridges empirical and theoretical gaps between the interval timing and decision-making literatures.

Keywords: decision-making, interval timing, optimality, psychophysics, reward maximization, risk assessment, uncertainty

INTRODUCTION

Evolution appears to have favored at least two well-regulated neurobiological time-keeping mechanisms that are shared by many organisms. One of these mechanisms, *circadian timing*, captures periods with approximately 24-h cycles. Many events in nature, on the other hand, are non-periodic, and capturing their temporal structure requires a flexible time-keeping apparatus that can be started and stopped as required. To that end, a stopwatch-like mechanism enables many organisms, with high accuracy but limited precision, to time intervals between arbitrary events that range from seconds to minutes. This ability is referred to as *interval timing*.

Timing intervals allows organisms to organize their relevant activities around critical times (Drew et al., 2005), keep track of reward rates (RRs; Gallistel et al., 2007), or prefer rewards that occur after a short rather than a long delay (Gibbon and Church, 1981; Cui, 2011). Importantly, these apparently simple time-dependent decisions and inferences are inevitably made under endogenous timing uncertainty, and thus entail temporal risk assessment. In this paper, we will evaluate whether humans and animals take normative account of their endogenous timing uncertainty when making decisions. Here, endogenous timing uncertainty specifically refers to an agent's inherent scale-invariant response time variability (imprecision) around a target time interval.

Across species and within individuals, temporal judgments in a wide range of tasks conform to Weber's Law, suggesting that endogenous timing uncertainty is proportional to the represented time interval: i.e., the standard deviation (SD) of time estimates is proportional to the target time intervals. This time scale invariance property appears ubiquitous in animal timing (Gibbon, 1977). Consequently, different individuals across species capture and exploit the temporal structure of their environment under similar scale-invariant temporal precision constraints irrespective of the signal modality or the behavioral goal (e.g., choice, avoidance, approach).

It is evident that representing time intervals can serve to maximize reward. For instance, when making choices between two options that deliver identical rewards, but at different delays, the option with the shorter delay (with the higher RR) is chosen. The temporal discounting curve – a curve which shows how preferences change as delay increases –is hyperbolic (Rachlin, 2006). Traditionally, researchers have tended to overlook the role of subjective time in generating the hyperbolic discounting curve, but more recently, some have proposed a strong role for subjective time (Takahashi, 2006; Ray and Bossaerts, 2011). In particular, Cui (2011) derived a mathematical expression for a hyperbolic discounting curve whose only assumption is Weber's law for timing. These studies support our contention that representing time intervals and the underlying endogenous uncertainty of those intervals, is likely an important contributor to temporal discounting. It is less evident how different levels of that endogenous timing uncertainty affect reward maximization in these, and other, types of decisions. For instance, when one has to withhold responding for a minimum duration before acquiring a potential reward, how does timing uncertainty interact with the optimal (reward-maximizing) temporal decision strategy? And to what extent does temporal uncertainty come into play in maximizing reward in two-choice perceptual discrimination tasks?

In this paper, we will discuss a number of scenarios in which reward maximization depends not only on the temporal task structure but also on the level of uncertainty in its representation. We will formally evaluate human and animal performance in these tasks within the framework of optimality, and demonstrate that organisms ranging from mice to humans behave nearly optimally in these dissimilar tasks. In the first section of the paper, we review and discuss experimental data supporting the hypothesis that rats account for their endogenous timing uncertainty when making time-related decisions. In this section, we also perform a new, secondary data analysis on an existing data set. In the second section, we review and discuss data supporting the hypothesis that humans and non-human animals can *optimally* incorporate their endogenous timing uncertainty in their time-related decisions. In this section, we also present new human and rat datasets collected from the differential reinforcement of low rates of responding task (DRL) and evaluate their performance within the framework of optimality. In the third section, we discuss recently published data from a perceptual decision-making task suggesting that humans use time and timing uncertainty to maximize rewards, even when the task has no obvious temporal component. Together, these results strongly suggest that humans and rodents exercise nearly optimal temporal risk assessment.

ENDOGENOUS TIMING UNCERTAINTY AND TIMING BEHAVIOR

If animals can account for their endogenous timing uncertainty in modifying their behavior, then individuals with more precise timing should be expected to be more confident in their time-related choices and responses. For example, anticipating a temporally deterministic reward, actors should respond at a higher rate around the critical interval when their timing uncertainty is low, and at a lower rate when their uncertainty is high.

Foote and Crystal's (2007) experiment with rats lends indirect support for this prediction. In their study, rats were trained to categorize a series of durations as either short or long based on a 4-s bisection point between the two durations (Stubbs, 1976). Correct categorizations resulted in a reward. Because of endogenous timing uncertainty, any duration close to the bisection point is harder to discriminate as short or long. Foote and Crystal (2007) modified this task by adding a sure reward option; responses on this option were always rewarded (regardless of the duration), but the reward magnitude was smaller. This allowed a test of whether rats took account of their temporal precision, because when a rat is less certain about its temporal judgment, it should choose the small but sure reward. This was indeed what they observed; while the rats almost always chose short or long for extreme durations (i.e., 2 and 8 s), a subgroup of rats often chose the small but sure reward for the more ambiguous durations (close to the bisection point). This finding suggests that rats may have taken into account their endogenous temporal uncertainty when deciding to choose short, long, or neither. On the other hand, rats in this experiment might simply have learned the differential reinforcement of different time intervals rather than accounting for their timing uncertainty (Jozefowiez et al., 2010).

An alternative way of testing this hypothesis without reinforcing the intermediate durations is to assess the relative response rates emitted for each probe interval in a bisection task. In such a design, subjects seeking to maximize rewards should exhibit a higher response rate on the "short" operandum for the short target interval and a higher response rate on the "long" operandum for the long target interval. These response rates should decrease as the target interval gets longer or shorter, respectively. Yi (2009) modified the bisection task by introducing a 10-s response period following the offset of the timing signal and, in a subset of trials, rewarding the rats for their correct responses (for reference intervals) on a random-interval schedule during the response period. This allowed the characterization of short and long response rates for different intervals. Response rate as a function of probe intervals qualitatively confirmed this response rate prediction.

We performed a secondary data analysis to conduct a different test of this hypothesis using published data (Church et al., 1998) from rats engaged in a "peak procedure" task (Catania, 1970). In the peak procedure, subjects are presented with a mixture of reinforced discrete fixed interval (FI) trials and non-reinforced "peak" trials that last longer than the FI trials. In the FI trials, subjects are reinforced for their first response after the FI elapses since the onset of a conditioned stimulus. No reinforcement is delivered in the peak trials, and responding typically falls off after the expected time of the reward. We examined the relation between temporal

precision and timed-response rate in this data, using response rate as a behavioral index of confidence for temporal judgments (Blough, 1967; Yi, 2009). For this analysis, we used the dataset of Church et al., 1998; Experiment 1), in which three groups of rats (five rats per group) were trained on the peak procedure. The Church et al. (1998) experiment used 30, 45, and 60 s schedules for 50 sessions of the peak procedure, with a single schedule for each group of rats. We analyzed data from the last 20 sessions, by which point performance had stabilized.

When responses are averaged across many peak trials, the resulting response curve approximates a bell curve (with a slight positive skew) that peaks at the reinforcement availability time (Roberts, 1981). In individual peak trials, however, responding switches between states of high and low rates of responding (Church et al., 1994), following a "break–run–break" pattern. Specifically, subjects abruptly increase the response rate about midway through the FI (*start time*) and they abruptly decrease the response rate after the FI elapses with no reinforcement (*stop time*). The length of the run period (*stop time minus start time*) is used as an index of temporal precision, with shorter periods indicating lower timing uncertainty. Subjects with higher uncertainty about the time of reinforcement availability initiate responding earlier (*earlier start times*) and terminate it later (*later stop times*). Within a run period, subjects respond approximately at a constant rate, which we used as an index of the rat's confidence in their estimate of reinforcement availability time in that given trial. Under our timing uncertainty hypothesis, if timing precision fluctuates across trials, then rats should respond at a higher rate in trials in which they exhibit shorter run periods. A detailed description of modeling single-trial responding is presented in the Appendix.

In our analyses, we applied a log transformation to normalize the dependent variables. We first established that response rates were approximately constant within a run period by regressing inter-response times (IRTs) on their order within the run period (e.g., 1st, 2nd, 3rd... IRT) separately for each subject (mean $R^2 = 0.02 \pm$ SEM 0.01). Overall response rate (defined over the entire peak trial) was also independent of the run period length (mean $R^2 = 0.03 \pm$ SEM 0.01). In order to test our prediction, we then regressed the response rates within a run period on the run period length. Supporting our hypothesis, rats exhibited lower response rates in longer run periods (mean $R^2 = 0.17 \pm$ SEM 0.03). This was a statistically reliable relation in all rats after Holm–Bonferroni correction for multiple comparisons. Note that although we tried to minimize it through our choice of measures, a level of analytical dependence might still exist between these measures (e.g., response rate and run period length). Thus, these results should be interpreted with special caution.

These findings from different tasks suggest that rats took account of their endogenous timing uncertainty in organizing their time-dependent responding with two different behavioral goals. (1) In the case of temporal discrimination, when a given duration proved difficult to discriminate due to timing uncertainty, a subset of rats chose not to categorize that duration, and instead settled for a smaller but sure reward. (2) On a similar task, rats exhibited higher response rates for intervals that were closer to the short and long references (i.e., easier conditions). (3) In the case of peak responding, rats responded less vigorously for a temporally deterministic reinforcement when they appeared less certain about the reinforcement availability time. These results constitute qualitative support for the role of temporal uncertainty in shaping timed choice behavior. With the research that we are about to describe, we will further argue that humans and rodents not only appear to represent their endogenous timing uncertainty, but that they also appear to behave nearly optimally in assessing temporal risk: that is, they adapt to different levels of uncertainty in a way that tends to maximize rewards.

OPTIMAL TEMPORAL RISK ASSESSMENT

In Foote and Crystal's task, taking account of timing uncertainty is adaptive. Many natural tasks pose similar problems with respect to the dependence of reward maximization on timing uncertainty. For example, consider a foraging experiment in which two patches are far apart (imposing travel cost), and both deliver reward on a FI schedule (i.e., the first response following the FI is rewarded). After visiting a patch, it can suddenly and unpredictably stop delivering rewards without a signal (unsignaled patch depletion). Once a patch depletes, the critical decision is when to stop exploiting the current patch and move onto the other one.

In this example, representing the fixed inter-reward interval allows detection of reward omissions during a given visit to a patch. Here, a subject with perfectly accurate and precise timing would stop exploiting the current patch (Brunner et al., 1992) as soon as the patch is depleted – i.e., as soon as the fixed inter-reward interval elapses with no reward. Despite being accurate however, animal timing abilities are imprecise, and thus the optimal time to stop exploiting a given patch depends on the level of timing uncertainty: the likelihood that a timed duration has exceeded a given value (i.e., the FI), given a subject's level of noise in time estimation, will grow at different rates for different levels of timing uncertainty.

Figure 1 depicts this sort of dependency by a cumulative normal distribution with the schedule as its mean (accurate timing) and a SD that reflects the subject's endogenous timing uncertainty (limited precision timing). When the cumulative distribution function (*cdf*) reaches, say, 0.95 (well past the schedule), the subject stops exploiting the current patch. When there is very little temporal uncertainty (implying a nearly step-like sigmoidal function), the *cdf* will reach this threshold earlier, leading to an earlier termination of patch exploitation. When there is high timing uncertainty however, it will take longer to reach the same threshold and the subject will stop exploiting later (**Figure 1**). Brunner et al. (1992) and Kacelnik and Brunner (2002) tested starlings in this task and found that the average termination time on the current patch after its unsignaled depletion was a constant proportion of the FI schedule (approximately 1.5·FI: ∼95% of the cdf for a CV of 0.25; see also Davies, 1977). This observation suggests that starlings not only adopted an exploitation strategy with a termination time longer than the FI schedule, but that this latency was modulated by scale-invariant endogenous timing uncertainty.

We now discuss temporal decision-making scenarios for which optimal decisions depend explicitly on the level of timing uncertainty. For these tasks, we formalize optimality as a function of the level of timing uncertainty and then compare the performance of

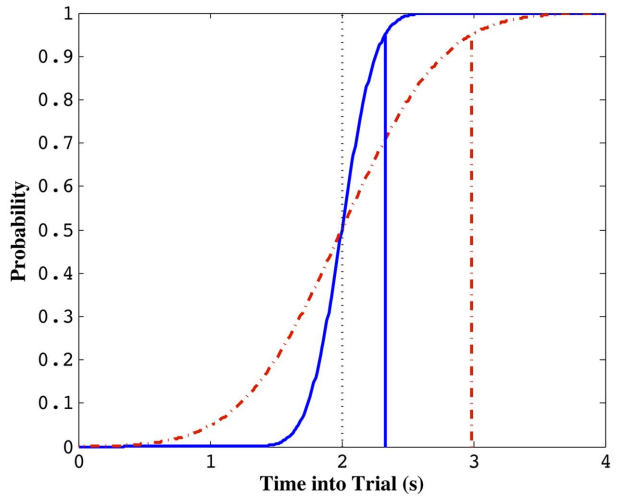

FIGURE 1 | Standard normal cumulative distribution functions with the same mean (i.e., 2 s) but different coefficients of variation (CV, σ/μ). Solid curve illustrates the normal cdf for a CV of 0.1 and the dotted curve illustrates the normal cdf for a CV of 0.3. The probability of a random variable taking on a value shorter than the trial time, indicated by vertical solid and dotted lines, respectively, is 0.95. Note that this value is much lower for the simulated subject with smaller timing uncertainty (solid curve).

humans and rodents to optimal performance given the observed level of timing uncertainty.

WHEN TO SWITCH FROM A RICH TO A POOR PROSPECT

Using a task similar to that of Brunner et al. (1992; see also Balcı et al., 2008), Balcı et al. (2009) investigated the extent to which humans and mice behave normatively in incorporating estimates of endogenous timing uncertainty into temporal decisions made in the face of additional, exogenous uncertainty. In their experiment, subjects tried to anticipate at which of two locations a reward would appear. On a randomly scheduled fraction of the trials, it appeared with a short latency at one location; on the complementary fraction, it appeared after a longer latency at the other location. Switching prematurely on short trials or failing to switch in time on the long trials yielded either no reward, or yielded a penalty, depending on the payoff matrix. The exogenous uncertainty was experimentally manipulated by changing the probability of a given trial type (short or long). For humans, the payoff matrix was also manipulated by changing the magnitude of rewards and penalties associated with different consequences (e.g., switching early on a short trial). Mice received equal rewards and no penalty.

The optimal response policy in this "switch task" is to begin each trial assuming that the reward will occur at the short location, and when the short interval elapses with no reinforcement, to switch to the long location. The trial time at which the subject leaves the short option for the long one is called the "*switch latency.*" Switch latencies were normally distributed, to a close approximation. The mean of the best-fitting normal distribution was assumed to represent the subject's target switch latency, and the coefficient of variation ($CV = \sigma/\mu$) was taken to reflect endogenous timing uncertainty.

The expected gain (EG) for a given target switch latency is the sum of the relative values of the options. The relative value is the gain for a given option weighted by the probability of attaining it. In this case, it is the payoff matrix weighted by the probability of the corresponding consequences determined jointly by endogenous timing uncertainty and exogenous uncertainty (i.e., probability of a short trial). Equation 1 defines the EG for an estimate of target switch point ($\hat{t}$) and endogenous timing uncertainty ($\hat{\omega}$) :

$$\begin{aligned} EG\left(\hat{t}\right) = {} & g\left(\sim T_S\right) p\left(T_S\right) \Phi\left(T_S, \hat{t}, \hat{\omega}\hat{t}\right) \\ & + g\left(T_S\right) p\left(T_S\right) \left(1 - \Phi\left(T_S, \hat{t}, \hat{\omega}\hat{t}\right)\right) \\ & + g\left(T_L\right) \left(1 - p\left(T_S\right)\right) \Phi\left(T_L, \hat{t}, \hat{\omega}\hat{t}\right) \\ & + g\left(\sim T_L\right) \left(1 - p\left(T_S\right)\right) \left(1 - \Phi\left(T_L, \hat{t}, \hat{\omega}\hat{t}\right)\right) \end{aligned} \quad (1)$$

where $\hat{\omega} = \hat{\sigma}/\hat{t}$, $\hat{t}$ is the subject's temporal criterion for switching, T_S and T_L are the short and long referents, $p(T_S)$ is the probability of a short trial, and g denotes the payoff matrix [e.g., $g(T_S)$ reflects the payoff for a correct short trial and $g(\sim T_S)$ reflects the loss for an incorrect short trial]. Φ is the normal cdf with mean $\hat{t}$ and SD $\hat{\omega}\hat{t}$, evaluated at T_S or T_L.

Figure 2 depicts the dependence of optimal switch latencies on the timing uncertainty for a given payoff matrix and on two exogenous probability conditions. For equally probable durations, the optimal switch latency (t_o, the t that maximizes the EG in Eq. 1) approaches the short target interval T_S as the timing uncertainty ω increases, due to scalar timing noise. Different combinations of the probability of a short trial $p(T_S)$, and the payoff matrix g, result in different EG surfaces (gain for each combination of t and ω). **Figures 2A,B** depict the normalized EG surface for $p(T_S) = 0.5$ and $p(T_S) = 0.9$, respectively, with a penalty for early and late switches. Balcı et al. (2009) compared the empirical target switch latencies $\hat{t}$ to optimal switch latencies $\hat{t}_o$ for the estimated level of timing uncertainty $\hat{\omega}$ by experimentally manipulated exogenous uncertainty $p(T_S)$, and the payoff matrix g. They found that both mice and humans performed nearly optimally in this task, achieving 99 and 98% of the maximum possible expected gain (MPEG), respectively. The average slopes of the orthogonal regression between empirical and optimal target switch latencies were 0.81 and 1.05 for human and mouse subjects, respectively (**Figure 3A**: Humans; B: Mice). These values were significantly different from 0 (both $ps < 0.05$) but not from 1 (both $ps > 0.5$). These results indicate that subjects tracked the optimal target switch latencies.

In line with reports reviewed earlier, these findings showed that humans and mice adapted performance to account for their endogenous timing uncertainty. It further demonstrated that subjects performed nearly optimally in adapting to exogenous uncertainty and to payoffs along with their endogenous uncertainty: i.e., they planned their timed responses such that they nearly maximized their expected earnings. This experiment thus lends strong support to the hypothesis that both humans and rodents can optimally assess temporal risk in certain contexts.

However, this work addresses only decisions about temporal intervals between a stimulus and a reward in a discrete-trial paradigm. Many natural tasks, on the other hand, are better characterized as free-response paradigms. Unlike discrete-trial tasks,

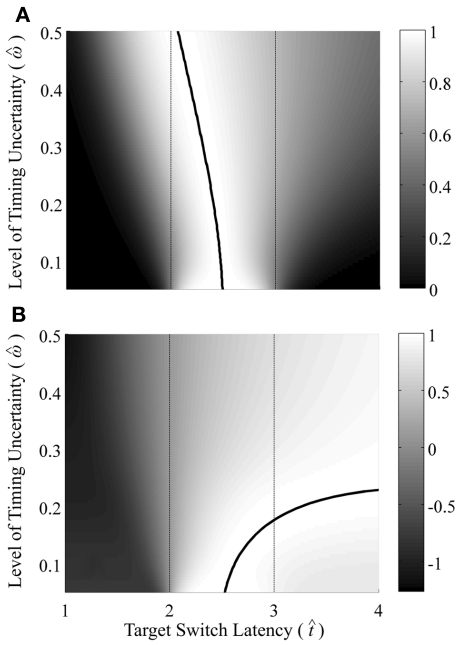

FIGURE 2 | Expected gain surface (normalized by the maximum expected gain for different levels of timing uncertainty) as a function of target switch latency and the level of timing uncertainty ($\hat{\omega}$). Shades of gray indicate the percentage of normalized maximum expected gain for the corresponding parameter values, $\hat{t}$ and $\hat{\omega}$. **(A)** is for equally probable short (2 s) and long (3 s) target intervals $p(T_S) = 0.5$. The ridge of this surface (bold black curve) shows the optimal switch latencies for different levels of timing uncertainty. **(B)** is for a higher probability of the short target interval, $p(T_S) = 0.9$. For both cases note the dependence of optimal target switch latencies on the level of timing uncertainty (*y*-axis). Also note the differences in optimal target switch latencies for two different exogenous uncertainty conditions.

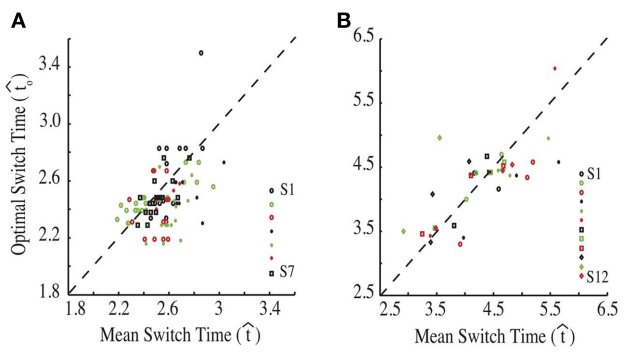

FIGURE 3 | Empirical performance of human and mouse subjects as a function of optimal performance, calculated for the critical task parameters and subjects' estimated level of endogenous timing uncertainty. Dashed line denotes the identity line. S: subject. Reprinted from Balcı et al. (2009). **(A)** Humans; **(B)** Mice.

these tasks impose tradeoffs between the speed and accuracy of decisions that are analogous to speed–accuracy tradeoffs in perceptual decision-making (see The Drift–Diffusion Model – An Optimal Model for Two-Choice Decisions). A prototypical timing task with this property is the differential reinforcement of low rates of responding (DRL) task. This task poses an interesting, naturalistic problem in which reward maximization depends on achieving the optimal level of patience, which is equivalent to finding the optimal tradeoff between two time-dependent quantities (as we now describe). In the following section, we will use reward rate (RR) in place of "EG" since we will evaluate the performance in free-response rather than discrete-trial protocols.

OPTIMAL TRADEOFF BETWEEN TWO TIME-DEPENDENT QUANTITIES (NEW EXPERIMENT)

In the DRL task, subjects are taught to space each successive response so that it occurs after a fixed minimum interval (or "withhold duration") since the last response. Each response immediately starts a new trial and only those responses emitted after the minimum withhold duration are rewarded. For instance, in a DRL 10 s schedule, subjects are reinforced for responding after at least 10 s following the previous response. If they respond sooner, then the trial timer restarts with no reward. Reward maximization in this simple task depends on the optimal tradeoff between two time-dependent quantities with opposing effects on the rate of reward: the probability of reward, $p(R)$, and the average IRT. The reward probability increases as IRTs increase (serving to increase the RR), but with sufficiently long IRTs, the mean inter-reward interval increases as well. The RR is the probability of reward divided by the average time between responses (see Eq. 2):

$$\mathrm{RR} = \frac{p\,(\mathrm{R})}{\mathrm{IRT}} \tag{2}$$

Importantly, the optimal tradeoff between $p(R)$ and IRT that maximizes RR depends on the subject's endogenous timing uncertainty (see also Wearden, 1990). Equation 3 defines the RR in the DRL task assuming inverse Gaussian (Wald) distributed IRTs. This assumption accurately describes our DRL data, and it is consistent with a recently developed random walk model of interval timing (Rivest and Bengio, 2011; Simen et al., 2011). In this model, a noisy representation of time rises at a constant rate (on average) as time elapses. Responses are emitted when this increasing quantity crosses a single, strictly positive threshold (this model is described in more detail in the discussion). Our inverse Gaussian assumption also accurately describes other human and animal datasets from paradigms in which subjects emit a single response or a target interval can be estimated (see Simen et al., 2011). For the DRL procedure, the expected RR for a given, normalized target IRT ($\hat{t}$) and a given level of timing uncertainty ($\hat{\omega}$) is:

$$\mathrm{RR}\left(\hat{t}\right) = t^{-1}\left(1 - \mathrm{waldcdf}\left(T, \hat{t}, \hat{\lambda}\right)\right) \tag{3}$$

Here, T is the DRL schedule, $\hat{t}$ is the schedule-normalized mean IRT (i.e., the average target withhold duration divided by the DRL schedule), and $\hat{\lambda} \geqslant 0$ is the Wald distribution's shape parameter, which captures the noisiness of the underlying random walk (the Wald cumulative distribution function – waldcdf in Eq. 3 – is defined in the Appendix). The timing uncertainty equals the

coefficient of variation, or SD divided by the mean, of this IRT distribution.

Figure 4 shows the normalized EG surface for the DRL task as defined by Eq. 3. The ridge of the surface (dark solid line) denotes the optimal IRTs as a function of timing uncertainty ($\hat{\omega}$). As the coefficient of variation increases, the optimal IRT diverges from the DRL schedule in a negatively accelerating fashion.

Methods

To assess the optimality of rat and human DRL performance, we tested rats in a new experiment for 42 sessions with 7, 14, 28, and 56 s DRL schedules[1] (∼12 rats per group), and humans in single session experiments with DRL schedules that ranged between 5 and 15 s (varied across participants). Methodological details of these experiments are presented in the Appendix. Rats exhibited two types of responses: timed and untimed. This created a mixture distribution for the IRTs that was best fit by an exponential-Wald mixture distribution. The IRTs that were best fit by the exponential component were considered to be untimed responses, which occurred relatively quickly after the previous response. The IRTs that were best fit by the Wald component were considered to be timed responses.

Results

Human performance. **Figure 4A** depicts the performance of humans (asterisks). It suggests that humans tracked the modulation of optimal IRTs as a function of temporal uncertainty. Statistical analyses corroborated these observations. The median performance of humans provided 98% [interquartile interval (IQI) 4%] of the MPEG. Similar estimates of nearly maximal EG were obtained when we used an independent estimate of endogenous timing uncertainty from a temporal reproduction task with parametric feedback on each trial (see Appendix for details). Optimal IRTs were significant predictors of the empirical IRTs, $R^2 = 0.56$, $F(1,13) = 16.29$, $p < 0.01$. When one outlier was excluded from the dataset (using 2 SD as the exclusion criterion), this relation became even stronger and more reliable, $R^2 = 0.71$, $F(1,12) = 29.45$, $p < 0.001$. During debriefing this outlier participant reported that s/he was not engaged in the task. Humans' earnings were significantly larger than what they would have earned if they had aimed at the schedule, $t(14) = 11.06$, $p < 0.0001$, and their empirical IRTs were significantly longer than the minimum withhold duration, $t(14) = 3.96$, $p < 0.01$. When data were fit with an exponential–Gaussian mixture distribution instead, the median earnings were 99% of the MPEG.

Rat performance. Median performance of rats for 7 and 14 s DRL schedules were 98% (IQI 3%) and 96% (IQI 5%) of the MPEG. **Figures 4B,C** show that rats' average withhold durations tracked the optimal duration. Corroborating this observation, optimal IRTs were significant predictors of empirical IRTs for both 7 and 14 s schedules, $R^2 = 0.60$, $F(1,10) = 14.68$, $p < 0.01$ and $R^2 = 0.38$, $F(1,9) = 5.60$, $p < 0.05$, respectively. The earnings of rats were significantly larger than they would have been if they had aimed for the DRL schedule itself for 7 s [$t(11) = 18.97$, $p < 0.0001$], and 14 s [$t(10) = 6.84$, $p < 0.0001$]. Empirical IRTs were significantly longer than the minimum withhold duration for 7 s [$t(11) = 11.42$, $p < 0.0001$], and 14 s [$t(10) = 7.30$, $p < 0.0001$]. When data were fit with an exponential–Gaussian mixture distribution instead, median proportions of the MPEG were 99% for both schedules.

In a theoretical work, Wearden (1990) conducted essentially the same analysis as ours to characterize the optimal target IRTs in the DRL task. He showed that linear "overestimation" of the DRL was the optimal strategy, and that the degree of overestimation depended on the level of timing uncertainty. His reanalysis of a pigeon dataset (Zeiler, 1985) from a DRL-like

[1]Rat performance in DRL 28 and 56 s schedules did not reach steady state performance, and thus was not included in the analysis.

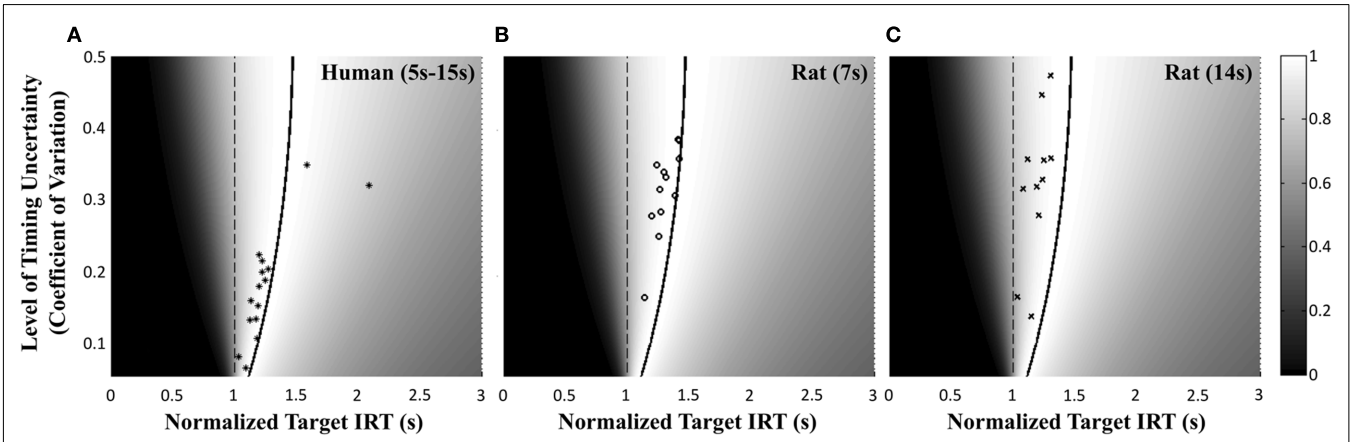

FIGURE 4 | Normalized expected reward rate surface as a function of the normalized target IRT and the level of timing uncertainty. Shades of gray denote the proportion of normalized MPEG, which decreases from light to dark. The solid black curve is the ridge of the normalized expected reward rate surface and denotes the optimal IRT for different levels of timing uncertainty. The dashed vertical black line shows the normalized DRL schedule (in actuality ranging from 5 to 15 s). Each symbol corresponds to the performance of a single rat or human subject in the novel experiment. **(A)** (Asterisks) shows the human data (DRL 5–15 s), **(B)** (circles) shows the rat data (DRL 7 s) and **(C)** (crosses) shows the rat data (DRL 14 s). Data points were clustered near and to the left of the ridge of the expected reward rate surface.

task revealed nearly optimal "overestimation" of the scheduled reinforcement availability time. Wearden's reanalysis of human DRL data from Zeiler et al. (1987), with target intervals ranging from 0.5 to 32 s, also revealed very nearly optimal performance. Our secondary analyses of two independent, published datasets from rats corroborated our and Wearden's observations from rats, pigeons, and humans. We compared the performance of control group rats in Sanabria and Killeen (2008 – 5 s DRL), and Orduña et al. (2009 – 10 s DRL) to the optimal performance computed for their estimated levels of timing uncertainty. Rats in these experiments achieved 93, and 94% of the MPEG for 5 and 10 s schedules, respectively, under an exponential-Wald fit. These values reached 96% for both datasets, when exponential–Gaussian mixture distributions were fit to the data instead.

Other examples can be found in the literature in which IRT distributions peak long after the DRL schedule at least for schedules up to 36 s. These data qualitatively corroborate our observations [e.g., Fowler et al., 2009 (Figure 2A); Stephens and Cole, 1996 (Figure 4A), Cheng et al., 2008, (Figures 5 and 6), Sukhotina et al., 2008 (Table 1 and Figure 3)]. With longer DRL schedules (e.g., DRL 72 s), on the other hand, subjects perform pronouncedly sub-optimally [e.g., Balcells-Olivero et al., 1998 (Figure 1), Fowler et al., 2009 (Figure 2B), Paterson et al., 2010 (Figures 1–4)]. In line with our observations with 28 and 56 s DRL schedules, the sub-optimal performance in longer schedules might simply be due to the need for longer training. Wearden (1990) alternatively argued that the "underestimation" of the DRL schedules might be due to a satisficing strategy to obtain a certain satisfactory rate of reinforcement, an adaptive response bias the extent of which also depends on the level of endogenous timing uncertainty (Wearden, 1990, Figure 4). Overall, in line with our findings from the discrete-trial switch task, human and rat performance in the free-response DRL task suggests that these species can assess temporal risk optimally when timing uncertainty is a determinant of the optimal tradeoff between waiting and responding.

In the DRL task, subjects are not rewarded (thereby suffering an opportunity cost) for responding prior to the minimum response–withholding duration. On the other hand, being late is also commonly "penalized" in nature, as in the case of losing a precious resource to a competitor by virtue of not claiming it early enough. In the next section, we describe a task with this characteristic, in which reward maximization requires avoiding late responses, and we re-evaluate human performance data from Simen et al. (2011) within the framework of optimality.

BEAT-THE-CLOCK TASK

In the beat-the-clock (BTC) task (Simen et al., 2011), participants are asked to press a key just before a target interval elapses, but not afterward. The reward for responding grows exponentially in time, increasing from approximately 0 cents immediately after the cue appears to a maximum of 25 cents at the target interval. Thus responding as close to the target interval as possible is adaptive. Failing to respond prior to the target interval is not rewarded (imposing an opportunity cost). Response times collected in the BTC task were best fit by a Gaussian distribution, with the mean reflecting the target response time and the CV reflecting endogenous timing uncertainty. Equation 4 defines the EG for a given target response time $\hat{t}$, timing uncertainty $\hat{\omega}$, and schedule T.

$$\mathrm{EG}\left(\hat{t}\right) = \int_{x=0}^{T} p\left(t|\hat{t},\,\hat{\omega}\right) g\left(t\right)\, dt \tag{4}$$

where t is a possible response time, $\hat{t}$ is the target response time, p is the probability of responding at t given the subject's mean ($\hat{t}$) and coefficient of variation ($\hat{\omega}$), and g is the exponentially increasing reward function that drops to zero after the deadline. The optimal aim point t_o is the one that maximizes EG for a given level of timing uncertainty $\hat{\omega}$. We performed a secondary data analysis on this dataset, originally presented in Simen et al. (2011). **Figure 5** depicts the dependence of optimal aim points on psychologically plausible levels of timing uncertainty and shows that human participants tracked the optimal target times.

Consistent with **Figure 5**, optimal target times were significant predictors of empirical target times [$R^2 = 0.76$, $F(1,15) = 47.67$, $p < 0.0001$). Participants earned 99% median (IQI 3%) of the MPEG for their level of timing uncertainty. The proportion of earnings was 99% median (IQI 2%) of the MPEG when the timed responses were assumed to be Wald distributed, instead. As in the switch and DRL tasks, these results suggest a nearly optimal human capacity for taking endogenous timing uncertainty into account when planning timed responses – in this case, in scenarios in which late responding is maladaptive.

In three different temporal decision-making tasks that impose different time constraints on the problem of reward maximization, we have demonstrated that optimal performance depends on endogenous timing uncertainty. We have further demonstrated that humans, rats, and mice incorporate their endogenous timing uncertainty nearly optimally in their temporal risk assessment, at least for supra-second target durations.

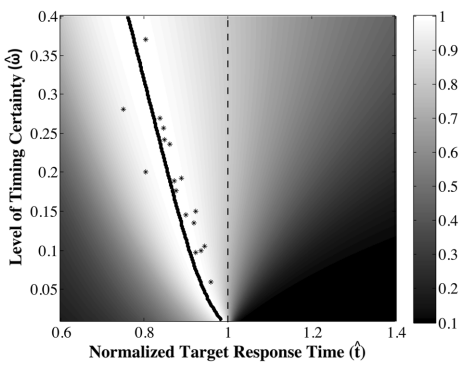

FIGURE 5 | Normalized expected gain surface as a function of normalized aim point and level of timing uncertainty. Shades of gray denote the proportion of normalized MPEG, which decreases from light to dark. The black curve is the ridge of the expected gain surface and denotes the optimal aim points for psychologically plausible levels of endogenous timing uncertainty. Each point (asterisk) corresponds to the performance of a single subject and points are clustered around the curve of the optimal aim points. Figure is redrawn based on the data presented in Simen et al. (2011).

OPTIMALITY IN THE SUB-SECOND RANGE

The characterization of temporal risk assessment in the switch, DRL, and BTC tasks pertains exclusively to decisions about supra-second intervals. There is, however, substantial evidence that different neural circuits might underlie supra-second and sub-second intervals (e.g., Breukelaar and Dalrymple-Alford, 1999; Lewis and Miall, 2003). Thus, there is reason to believe that optimality of temporal risk assessment might be exclusive to supra-second interval timing. Using a simple temporal reproduction task with humans, however, Jazayeri and Shadlen (2010) showed that optimal temporal risk assessment also applies to sub-second target durations.

In their task, participants were asked to reproduce time intervals that were sampled from different underlying distributions (including sub-second intervals). When reproductions fell within a temporal window of the target interval, participants received positive feedback. The resulting reproductions of target intervals were observed to regress to the mean of the encountered intervals, and thus the reproduction of the same interval could change depending on the underlying distribution of intervals experienced. Importantly, Jazayeri and Shadlen (2010) demonstrated that a reward-maximizing model that took account of the statistics of the target interval distribution and incorporated knowledge of scale-invariant endogenous timing uncertainty accounted for the performance of the participants. Their findings demonstrate that humans take normative account of endogenous timing uncertainty to maximize reward, even in the case of sub-second target durations. Temporal decision-making with sub-second target intervals is more common in simple motor planning tasks, which we discuss next.

OPTIMAL MOTOR TIMING

Hudson et al. (2008) reported an experiment in which human participants were asked to touch a computer screen at a particular time (e.g., 650 ms) to earn monetary reward. A small time window around this target interval served as the reward region (e.g., 650 ± 50 ms). There was also a penalty region, which imposed monetary costs. Lastly, there was a region in which neither reward or penalty occurred. The temporal position of the penalty region was manipulated. Sometimes it perfectly straddled the reward region (and anything outside the reward region was penalized). Sometimes it was adjacent to the reward region on one side but not the other (thus aiming toward the other side was a good strategy). The participant's task was to maximize the monetary reward during the course of the experiment.

There were two sources of variance: (1) the participants' own timing uncertainty (ω) and (2) experimentally added exogenous noise (α) that was applied to every temporal aim point (drawn from a Gaussian with $\mu = 0$ and $\sigma = 25$ ms). Empirical data suggested that participants incorporated both endogenous and exogenous temporal uncertainties (ω and α) as they aimed at a time that very nearly compensated for both the timing uncertainty and the payoff matrix (i.e., the temporal positions of the reward and penalty regions). Thus, consistent with earlier reports, these findings showed that humans can take nearly normative account of their endogenous timing uncertainty and that they can also learn to take account of experimentally introduced temporal noise in planning their movement times. Analogous nearly optimal timing of single isolated movements was also reported in other studies (e.g., Battaglia and Schrater, 2007; Dean et al., 2007).

Further work (Wu et al., 2009), however, discovered a bound for optimal performance in these tasks and showed that optimality of timed motor planning does not hold when subjects are asked to allocate time across two options to complete a sequence of movements under stringent time pressure (i.e., 400 ms). Specifically, they observed that subjects spent more time than optimal on the first target, even when the payoff for the second target was five times larger. Based on this finding, Wu et al. (2009) claimed that the optimality of motor timing is restricted to isolated, single movements, and fails in the context of a sequence of movements. One important feature of their task that should be considered, however, is the very stringent response deadline imposed on the completion of the movement sequence (although subjects could take as much time as they wanted before initiating the trial). These findings overall suggest that except in the case of a sequence of movements made under a strict response deadline, humans exercise optimal motor timing with sub-second target intervals.

In the last two sections, we described decision-making scenarios that were explicitly temporal in nature, both with sub-second and supra-second target durations. In these tasks, subjects made explicit judgments about time intervals and exhibited optimal temporal risk assessment. The adaptive role of interval timing is however not at all limited to explicitly temporal decision-making. It also plays a crucial but understudied role in reward maximization in perceptual decision-making. In free-response paradigms for instance, timing uncertainty interacts with two-choice performance because reward maximization requires subjects to keep track of RRs and thus inter-reward times. In the case of time-pressured decisions (i.e., with response deadlines), interval timing is even more directly instrumental for reward maximization, since optimality then requires taking account of the deadline, as well as uncertainty in its representation. In the next section, we discuss the role of interval timing in perceptual two-choice decision-making tasks.

INTERVAL TIMING AND REWARD MAXIMIZATION IN NON-TEMPORAL DECISION-MAKING

The likely connection between RR estimation and time estimation suggests that endogenous timing uncertainty should translate into uncertainty about RRs. As we describe below, within the framework of optimality, this dependence generates a prediction that a decision-maker with higher timing uncertainty will respond more slowly than optimal (favoring accuracy over RR) in free-response two-choice tasks (Bogacz et al., 2006). Under this hypothesis, Bogacz et al. (2006) and Balcı et al. (2011) argued that such "sub-optimally" *conservative* responding in these paradigms might in fact reflect an adaptive bias in decision threshold setting in response to endogenous timing uncertainty. Our analysis and discussion of optimal temporal risk assessment in these tasks will heavily rely on the drift–diffusion model (DDM) of two-choice decisions, which we describe next.

THE DRIFT–DIFFUSION MODEL – AN OPTIMAL MODEL FOR TWO-CHOICE DECISIONS

The sequential probability ratio test (SPRT; Barnard, 1946; Wald, 1947) is an optimal statistical procedure for two-alternative hypothesis testing in stationary environments that provide an unlimited number of sequential data samples. The SPRT minimizes the number of samples for any given level of accuracy, and maximizes accuracy for any given number of samples (Wald and Wolfowitz, 1948). In an SPRT-based model of choice reaction time in two-choice tasks, Stone (1960) proposed that decision-makers computed the likelihood ratio of the two hypotheses when sampling a noisy signal, equating the total sample count with the decision time. In the DDM this discrete sequence of samples is generalized to a continuous stream, in which the time between samples is infinitesimal (Ratcliff, 1978; Ratcliff and Rouder, 1998).

The DDM assumes that the difference between the evidence supporting the two hypotheses is the decision variable, that this variable is integrated over time, and that when the integrated evidence crosses one of two decision thresholds – one $(+z)$ above and one $(-z)$ below the prior belief state – the corresponding decision is made. The first crossing of a threshold is identified as the decision time. The DDM in its most simplified form, is given by a first order stochastic differential equation in which x denotes the difference between the evidence supporting the two different alternatives at any given time t; it can be interpreted as the current value of the log-likelihood ratio:

$$dx = Adt + \sigma dW,\ x(0) = 0 \quad (5)$$

Here, Adt represents the average increase in x during the tiny interval dt, and σdW represents white noise, Gaussian distributed with mean 0 and variance $\sigma^2 dt$ (see Ratcliff and McKoon, 2008 for a detailed description of the DDM).

In the DDM, the clarity of the signal is represented by the drift A (the signal-to-noise ratio is A/σ). Speed–accuracy tradeoffs arise in the DDM because of the threshold parameter z: Due to noise, lower thresholds lead to faster but less accurate decisions and vice versa. The pure form of the DDM in Eq. 5 (e.g., Ratcliff, 1978) often provides reasonably good fits to behavioral data, and benefits from extremely simple, analytically tractable predictions regarding RR maximization (Bogacz et al., 2006). Versions of the DDM with additional parameters (e.g., Ratcliff and Rouder, 1998) are needed for fitting a broader range of data, especially data with unequal mean RTs for errors and correct responses.

OPTIMAL TWO-CHOICE DECISION-MAKING AND INTERVAL TIMING

The pure DDM (i.e., a model without the additional variability parameters used in the model of Ratcliff and Rouder, 1998) prescribes a parameter-free optimal performance curve that relates decision time to error rate (Bogacz et al., 2006). Optimal performance, however, requires decision thresholds that are a function of the response-to-stimulus interval (RSI). Better estimation of the RSI by participants with more precise timing abilities may therefore result in better decision-making performance. Deviations from optimal performance may thus derive from timing uncertainty. The shape of the function relating the expected RR to the decision threshold in the DDM suggests why this may be the case. Specifically, this function is an asymmetric hill, whose single peak defines the optimal threshold. For a given level of deviation from the optimal threshold, setting the threshold too high earns a higher expected RR than setting it too low by the same amount [Balcı et al., 2011 (Figures 7 and 10), Bogacz et al., 2006 (Figure 15)]. Thus, if decision-makers are to minimize loss in RR due to endogenous timing uncertainty in RR estimates, they should err toward overestimating instead of underestimating the optimal threshold. The behavioral manifestation of overestimating a threshold is longer response times coupled with greater accuracy (which in model fits appears to suggest a suboptimal, "conservative," emphasis on accuracy over speed, and thus RR).

In a single session of two-alternative forced choice tasks, human participants have indeed been shown to set their decision thresholds higher than the optimal decision threshold (Bogacz et al., 2010). Balcı et al. (2011) replicated this finding (but also showed that this deviation decreased nearly to zero with sufficient practice) and observed that deviations from optimality during early training could be accounted for by participants' timing uncertainty (assessed independently). Balcı et al. (2011) quantified deviation from optimality in two different ways: (1) deviations between optimal and observed RTs; and (2) deviations between optimal and fitted thresholds. For both measures, Balcı et al. (2011) reported that the regression of deviations from optimality on CVs revealed a significant relationship $F(1,15) = 12.1$, $p < 0.01$ ($R^2 = 0.45$) and $F(1,14) = 22.57$, $p < 0.001$ ($R^2 = 0.62$; excluding one outlier based on a 2 SD rule), respectively (see **Figure 6**). They also reported that this relationship held even after first accounting for suboptimal performance by another model that included a parameter representing a self-imposed penalty for errors (Maddox and Bohil, 1998; Bogacz et al., 2006).

Zacksenhouse et al. (2010) recently analyzed the data presented in Bogacz et al. (2010) using a decision strategy that maximized the minimal RR achievable for a given level of timing uncertainty. This decision strategy fit the Bogacz et al. (2010) dataset better than an optimally parameterized DDM, and better than the alternative models that contained an assumed penalty for errors. Conservative

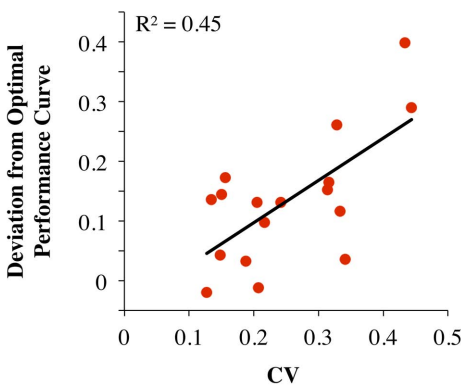

FIGURE 6 | Deviation from the optimal performance curve of the pure DDM as a function of CV redrawn based on the data presented in Balcı et al. (2011). Solid line is the linear regression line fit to the data.

decision thresholds can therefore be viewed as an intrinsic, adaptive bias in response to endogenous timing uncertainty, a dynamic that underlies nearly optimal performance in the switch, BTC, and DRL tasks. These findings suggest the importance of timing uncertainty in shaping behavior and determining how much reward is earned even in non-temporal decision-making.

TWO-CHOICE DECISION-MAKING UNDER TIME PRESSURE

Interval timing plays a more direct role in two-choice decisions when a response deadline sets an upper bound for rewarding responses and/or for viewing time. Frazier and Yu (2008) showed that optimal performance in these scenarios requires subjects to start collapsing decision thresholds so that by the time the deadline is reached, the decision threshold converges on the starting point of the accumulation process (see also Rapoport and Burkheimer, 1971; Latham et al., 2007; Rao, 2010). This strategy ensures that a decision is made prior to the response deadline while maximizing accuracy for a given response time. According to this model, for a given level of timing uncertainty, subjects should start collapsing decision thresholds earlier for shorter response deadlines. Conversely, for a given response deadline, subjects with higher timing uncertainty should start collapsing decision thresholds earlier compared to subjects with lower timing uncertainty. We are currently testing these two specific predictions with human subjects. Preliminary results do not fully support the notion of optimal, within-trial modulation of response thresholds. Nevertheless, they do suggest some amount of threshold modulation within and across trials in response to changing deadlines. They further suggest a relation in the expected direction between the level of subjects' timing uncertainty and the degree of accuracy reduction in their conditional accuracy (or micro speed–accuracy tradeoff) curves in response deadline conditions (i.e., accuracy levels in each of a set of binned RTs, which should be flat for the pure DDM with a fixed threshold, but which must decrease for RT bins near the deadline if thresholds collapse).

Discussion

Time is a defining feature of behavior. By incorporating the well-characterized psychophysics of interval timing into the study of reward maximization, we have demonstrated that temporal intervals and uncertainty in their representation are critical factors in both temporal and non-temporal decisions. The findings we reviewed show that humans and animals come close to maximizing their earnings in simple timing and decision-making tasks, which suggests that they can normatively compensate for their endogenous timing uncertainty in their decision-making. Subjects nearly maximized the reward earned in scenarios that spanned sub-second and supra-second target durations, in the presence and absence of speed–accuracy tradeoffs (i.e., free-response vs. fixed viewing time), and explicitly temporal and perceptual decisions.

These findings contrast with the assertions of classical decision-making research that has repeatedly shown that humans are irrational decision-makers about probabilistic prospects (e.g., Kahneman and Tversky, 1979). Here, we have shown that when uncertainty is endogenous and specifically temporal in nature, humans in fact make nearly optimal decisions. Supporting this view, a series of experiments on motor planning have also shown that humans decide (plan their motor end-points) optimally when confronted with other ubiquitous sources of endogenous uncertainty, such as motor noise (e.g., Trommershäuser et al., 2008). These results suggest that when the origin of uncertainty is endogenous, as in interval timing or motor planning, the resulting uncertainty is accounted for by mechanisms that organize and adapt behavior optimally in response to environmental statistics. We note, however, that these findings do not necessarily indicate that endogenous uncertainty is explicitly represented via a domain-general, metacognitive ability. They simply show that humans and other animals can make decisions that are adapted to endogenous timing uncertainty in a way that tends to maximize rewards. Depending on the task representation (avoiding being early or late), the level of timing uncertainty can be implicitly translated into a response bias signal that in turn partially determines the temporal characteristics of behavior. In fact, the task representation might simply determine the direction, whereas the timing uncertainty might determine the magnitude, of the response bias.

An important observation with humans is that reward maximization in perceptual decision-making (i.e., dot motion discrimination) requires extensive training (e.g., Simen et al., 2009; Balcı et al., 2011), whereas optimal performance in temporal decision-making appears within a single session: i.e., in the switch task (Balcı et al., 2009), DRL (current experiment), and BTC (Simen et al., 2011). This difference is possibly due to the relatively extensive exposure of humans to temporal intervals compared to the specific visual stimuli (e.g., dot motion patterns) typically used in perceptual decision-making tasks. Time, after all, is a fundamental quantity that factors critically into the outcome of almost all human and animal behavior. The ubiquity of time experience may have allowed animals to establish a veridical, scale-invariant model of their endogenous timing uncertainty, which can be used normatively in decision-making. Estimating the signal-to-noise ratios of novel stimuli (e.g., dot motion stimuli), on the other hand, requires extensive new training, which is likely the primary factor in the delayed achievement of optimal performance in perceptual decision-making. Timing might therefore appear to be a special case in which optimal decisions are made in single session experiments simply due to the degree of previous experience. Consistent with this interpretation, when timing uncertainty also has an exogenous source, human participants require some additional experience before exhibiting optimal performance (Hudson et al., 2008).

In addition to addressing the optimality of temporal risk assessment, a reward maximization framework also offers a novel, principled resolution to a psychophysical controversy in the domain of interval timing: namely the location of the point of subjective equality (PSE) between different durations. The PSE is the time interval that is subjectively equidistant to two other intervals, which subjects are equally likely to categorize as short or long. The PSE for animals is often found to be close to the geometric mean of the referents (e.g., Church and Deluty, 1977) but closer to the arithmetic mean for humans (e.g., Balcı and Gallistel, 2006). This inconsistency has been a source of theoretical controversy because of its implications regarding the subjective time scale – i.e., whether it is logarithmic or linear (Montemayor and Balcı, 2007; Yi, 2009). The optimality-based account of temporal

discrimination (switch or bisection) performance offers a principled account of the location(s) of the PSE; it quantitatively predicts this difference based on cross-species differences in the level of endogenous timing uncertainty on a linear subjective time scale.

The switch task is essentially a free-operant variant of the temporal bisection task, in which subjects can emit responses throughout the trial rather than just a single, terminal choice after an experimenter-determined probe interval elapses. In fact, in temporal bisection trials, animals move from the short to the long response option as the elapsed time approaches and exceeds the PSE (Machado and Keen, 2003). This suggests that despite the retrospective nature of the temporal bisection task, animals make real-time judgments about the elapsing interval in this task, just as in the case of the switch task. Balcı and Gallistel (2006) further showed that in temporal bisection tasks, human participants set a single criterion between the referents and judge intervals as short or long relative to that criterion (see also Allan, 2002; Penney et al., 2008).

Based on the parallels between decision strategies employed in both temporal discrimination tasks, the expected reward function of the switch task also applies to the temporal bisection task. Accordingly, when **Figure 2A** is evaluated for the temporal bisection task, where the short and long target intervals refer to the short and long reference durations, it predicts that PSEs are closer to the geometric mean for higher endogenous timing uncertainty (as in animals) and closer to the arithmetic mean for lower endogenous timing uncertainty (as in humans). This account, based on the same principles, also predicts the effect of task difficulty (short/long ratio) on the location of the PSE in humans (Wearden and Ferrara, 1996): more difficult task conditions mimic higher timing uncertainty and easier task conditions mimic lower, and the PSE moves across conditions accordingly.

Finally, for the rat DRL dataset, we only considered what are referred to as "timed responses" for our optimality analysis (see also Wearden, 1990). Wearden (1990) showed that untimed short responses (responses occurring almost immediately after the preceding response) did not exert much cost on the reward earned in the DRL task. For instance, 75% of untimed mostly short responses (uniformly distributed between 0.25 and 0.75 s) resulted in 92% of the reward that could be obtained without any untimed short responses for a DRL 20 s schedule, mean IRT of 20 s, and CV of 0.3. We further argue that particularly given their low cost regarding reward earned, untimed short responses could in fact constitute an optimal strategy in the long run for non-stationary environments. For instance, these responses would enable subjects to detect a shift to a richer schedule (DRL20 → DRL10 s) and thus adjust responding accordingly. On the other hand, the detection of this change would be more difficult and/or delayed for a subject who exclusively exploits the DRL schedule (i.e., emitting only timed responses).

Despite our claim about the ability of humans and non-human animals to account for their endogenous timing uncertainty, we have not proposed a mechanistic account of this ability. What are the possible mechanisms by which organisms infer and represent their timing uncertainty? We assume that this ability relies on keeping track of the discrepancies between the time of maximal expectancy of an event and the actual time of its occurrence over many instances. The stochastic ramp and trigger (SRT) model of Simen et al. (2011) allows keeping track of such experiential discrepancies. The SRT model approximates a drift–diffusion process with a single, fixed threshold, and a noise coefficient proportional to the square root of the drift (see also Rivest and Bengio, 2011). This model, which contains the Behavioral Theory of Timing of Killeen and Fetterman (1988) as a special case (where accumulation is effectively a pulse counting process), exploits the same mechanism used to account for response times in decision-making. In the simplest terms, the model times an interval by accumulating a quantity at a constant rate until it crosses a threshold, call it z. This accumulation is perturbed by the addition of normally distributed random noise with mean 0. Time intervals of duration T are timed by setting the accumulation rate (the "drift") equal to the threshold divided by T, and simple learning rules can tune the drift to the right value after a single exposure to a new duration. The resulting threshold crossing times exhibit scalar invariance and predict response time distributions that account for human and animal empirical data.

Importantly, as in models of decision-making (e.g., Simen et al., 2006), adjustments can be made in the intended time of responding relative to T by setting a response threshold that is either higher or lower than the timing threshold. Optimality requires that it be higher for the DRL task, and lower for the BTC task. Although this threshold-adjustment approach to optimizing timed performance appears to be novel in the timing literature, it is standard fare in the literature on perceptual decision-making. Thus, both the underlying model (the drift–diffusion process) and the techniques for adapting its speed–accuracy tradeoffs (via threshold-adjustment) emerge as potentially common computational principles in two distinct psychological domains.

The SRT model allows keeping track of discrepancies from veridical times. When ramping activity hits the threshold prior to the occurrence of the event (early clock), the organism can time the interval between the threshold crossing and the event. Likewise, when ramping activity fails to hit the threshold at the time of the event (late clock), the organism can now time the interval between the event and projected threshold crossing. When these values are divided by the target interval (threshold/drift), it indicates the scale-invariant measure of endogenous timing uncertainty. Simen et al. (2011) in fact used these values to adjust the clock speed to time veridical intervals in their model (see also Rivest and Bengio, 2011, where the same learning rules were proposed). The same mechanism can be conveniently used to keep track of timing noise through experience.

How this function might be embedded in the neural circuitry (i.e., corticostriatal loops) that have been implicated in interval timing is an important question that deserves special attention. In parallel to the striatal beat frequency model (Matell and Meck, 2004), different roles can be assigned to different brain regions within the SRT framework. For instance, the clock role can be assigned to the cortex and the effective role of decision threshold to the striatum. Within this scheme, it is possible that the reinforcement contingent dopamine activity serves as a teaching signal, which, via long-term synaptic plasticity (i.e., LTP and LTD), changes the excitability of the striatal medium-spiny neurons that are innervated by cortical glutamatergic and nigral dopaminergic

input. This activity might effectively set the decision thresholds in the direction and magnitude that maximizes the RR. In cases where the reward function depends on endogenous timing uncertainty, dopamine activity would thus inherently serve as a signal of the interaction between endogenous timing uncertainty and task structure. In tasks like the DRL and BTC, brain regions involved in inhibitory control (e.g., orbitofrontal cortex) would also be assumed to factor into this process. This framework however suffers a critical problem, namely: "If the striatal neurons are 'trained' to respond specifically at intervals that maximize the reward (which are systematically shorter and longer than the critical interval), how do they represent the veridical critical temporal intervals?" This question suggests that the adaptive response bias signal should perhaps be assigned to an independent process controlled by an independent structure such as the orbitofrontal cortex. This scheme allows that task representation to be coded independently from the critical task parameter values.

There are two interesting issues, which should motivate and guide future research seeking a more comprehensive understanding of temporal risk assessment ability. One of these questions regards the correspondence between the temporal risk assessment performance of participants across multiple tasks. Considerable overlap between performances would constitute strong evidence for the assertion that the ability to account for timing uncertainty is an inherent (i.e., not entirely task-dependent) property of organisms. The second question regards the possible relation between decision-making performance under endogenous uncertainty (e.g., timing uncertainty) and exogenous uncertainty (e.g., discrete probability of reward delivery). Balcı et al. (2009) observed close to optimal performance in a task that involved both kinds of uncertainties. However, it would be informative to test the same subjects in independent tasks in which the reward function depends exclusively on either endogenous or exogenous uncertainty in a given task.

In this paper, we have presented both published and novel datasets that support the claim that humans and other animals can take approximately normative account of their endogenous timing uncertainty in a variety of timing and decision-making tasks. This notion contrasts with the now-traditional view of humans as irrational decision-makers under uncertainty, a difference that may be driven by differences in the origin of the uncertainty (i.e., endogenous vs. exogenous uncertainty) and by the ways in which estimates of this uncertainty are acquired (i.e., by experience or by explicit description). Or it may be that timing is simply so critical for reward-maximizing behavior that the resulting selective pressure on animals' timing abilities dominates the costs of maintaining those abilities.

ACKNOWLEDGMENTS

The authors would like to thank Russell Church, Federico Sanabria, Peter Killeen, Vladimir Orduna, Lourdes Valencia-Torres, and Arturo Bouzas for making their data available to us. This work was supported by an FP7 Marie Curie PIRG08-GA-2010-277015 to FB, the National Institute of Mental Health (P50 MH062196, Cognitive and Neural Mechanisms of Conflict and Control, Silvio M. Conte Center), the Air Force Research Laboratory (FA9550-07-1-0537), and the European project COST ISCH Action TD0904, TIMELY.

REFERENCES

Allan, L. G. (2002). Are the referents remembered in temporal bisection? *Learn. Motiv.* 33, 10–31.

Balcells-Olivero, M., Cousins, M. S., and Seiden, L. S. (1998).Holtzman and Harlan Sprague–Dawley rats: differences in DRL 72-sec performance and 8-hydroxy-di-propylaminotetralin-induced hypothermia. *J. Pharmacol. Exp. Ther.* 286, 742–752.

Balcı, F., Freestone, D., and Gallistel, C. R. (2009). Risk assessment in man and mouse. *Proc. Natl. Acad. Sci. U.S.A.* 106, 2459–2463.

Balcı, F., and Gallistel, C. R. (2006). Cross-domain transfer of quantitative discriminations: Is it all a matter of proportion? *Psychon. Bull. Rev.* 13, 636–642.

Balcı, F., Papachristos, E. B., Gallistel, C. R., Brunner, D., Gibson, J., and Shumyatsky, G. P. (2008). Interval timing in the genetically modified mouse: a simple paradigm. *Genes Brain Behav.* 7, 373–384.

Balcı, F., Simen, P., Niyogi, R., Saxe, A., Hughes, J., Holmes, P., and Cohen, J. D. (2011). Acquisition of decision-making criteria: reward rate ultimately beats accuracy. *Atten. Percept. Psychophys.* 73, 640–657.

Barnard, G. A. (1946). Sequential tests in industrial statistics. *J. R. Stat. Soc.* 8(Suppl.), 1–26.

Battaglia, P. W., and Schrater, P. R. (2007). Humans trade off viewing time and movement duration to improve visuomotor accuracy in a fast reaching task. *J. Neurosci.* 27, 6984–6994.

Blough, D. S. (1967). Stimulus generalization as a signal detection in pigeons. *Science* 158, 940–941.

Bogacz, R., Hu, P. T., Holmes, P., and Cohen, J. D. (2010). Do humans produce the speed accuracy tradeoff that maximizes reward rate? *Q. J. Exp. Psychol.* 63, 863–891.

Bogacz, R., Shea-Brown, E., Moehlis, J., Holmes, P., and Cohen, J. D. (2006). The physics of optimal decision making: a formal analysis of models of performance in two-alternative forced choice tasks. *Psychol. Rev.* 113, 700–765.

Breukelaar, J. W., and Dalrymple-Alford, J. C. (1999). Effects of lesions to the cerebellar vermis and hemispheres on timing and counting in rats. *Behav. Neurosci.* 113, 78–90.

Brunner, D., Kacelnik, A., and Gibbon, J. (1992). Optimal foraging and timing processes in the starling, *Sturnus vulgaris*: effect of intercapture interval. *Anim. Behav.* 44, 597–613.

Catania, A. C. (1970). "Reinforcement schedules and psychophysical judgments: a study of some temporal properties of behavior," in *The Theory of Reinforcement Schedules*, ed. W. N. Schoenfeld (New York: Appleton-Century-Crofts), 1–42.

Cheng, R.-K., MacDonald, C. J., Williams, C. L., and Meck, W. H. (2008). Prenatal choline supplementation alters the timing, emotion, and memory performance (TEMP) of adult male and female rats as indexed by differential reinforcement of low-rate schedule behavior. *Learn. Mem.* 15, 153–162.

Church, R. M., and Deluty, M. Z. (1977). Bisection of temporal intervals. *J. Exp. Psychol. Anim. Behav. Process.* 3, 216–228.

Church, R. M., Lacourse, D. M., and Crystal, J. D. (1998). Temporal search as a function of the variability of interfood intervals. *J. Exp. Psychol. Anim. Behav. Process.* 24, 291–315.

Church, R. M., Meck, W. H., and Gibbon, J. (1994). Application of scalar timing theory to individual trials. *J. Exp. Psychol. Anim. Behav. Process.* 20, 135–155.

Cui, X. (2011). Hyperbolic discounting emerges from the scalar property of interval timing. *Front. Integr. Neurosci.* 5:24. doi: 10.3389/fnint.2011.00024

Davies, N. B. (1977). Prey selection and the search strategy of the spotted flycatcher (*Muscicapa striata*). *Anim. Behav.* 25, 1016–1033.

Dean, M., Wu, S.-W., and Maloney, L. T. (2007). Trading off speed and accuracy in rapid, goal-directed movements. *J. Vis.* 7, 1–12.

Drew, M. R., Zupan, B., Cooke, A., Couvillon, P. A., and Balsam, P. D. (2005). Temporal control of conditioned responding in goldfish. *J. Exp. Psychol. Anim. Behav. Process.* 31, 31–39.

Foote, A., and Crystal, J. (2007). Metacognition in rats. *Curr. Biol.* 17, 551–555.

Fowler, S. C., Pinkston, J., and Vorontsova, E. (2009). Timing and space usage are disrupted by amphetamine in rats maintained on DRL 24-s and DRL 72-s schedules of reinforcement. *Psychopharmacology (Berl.)* 204, 213–225.

Frazier, P., and Yu, A. J. (2008). Sequential hypothesis testing under stochastic deadlines. *Adv. Neural Inf. Process. Syst.* 20, 465–472.

Gallistel, C. R., King, A. P., Gottlieb, D., Balcı, F., Papachristos, E. B., Szalecki, M., and Carbone, K.S. (2007). Is matching innate? *J. Exp. Anal. Behav.* 87, 161–199.

Gibbon, J. (1977). Scalar expectancy theory and Weber's law in animal timing. *Psychol. Rev.* 84, 279–325.

Gibbon, J., and Church, R. M. (1981). Time left: linear versus logarithmic subjective time. *J. Exp. Psychol. Anim. Behav. Process.* 7, 87–108.

Hudson, T. E., Maloney, L. T., and Landy, M. S. (2008). Optimal movement timing with temporally asymmetric penalties and rewards. *PLoS Biol.* 4, e1000130. doi: 10.1371/journal.pcbi.1000130

Jazayeri, M., and Shadlen, M. N. (2010). Temporal context calibrates interval timing. *Nat. Neurosci.* 13, 1020–1026.

Jozefowiez, J., Staddon, J. E., and Cerutti, D. T. (2010). The behavioral economics of choice and interval timing. *Psychol. Rev.* 116, 519–539.

Kahneman, D., and Tversky, A. (1979). Prospect theory: an analysis of decisions under risk. *Econometrica* 47, 263–291.

Kacelnik, A., and Brunner, D. (2002). Timing and foraging: Gibbon's scalar expectancy theory and optimal patch exploitation. *Learn. Motiv.* 33, 177–195.

Killeen, P. R., and Fetterman, J. G. (1988). A behavioral theory of timing. *Psychol. Rev.* 95, 274–295.

Latham, P. E., Roudi, Y., Ahmadi, M., and Pouget, A. (2007). Deciding when to decide. *Abstr. Soc. Neurosci.* 33, 740.10.

Lewis, P. A., and Miall, R. (2003). Brain activation patterns during measurement of sub- and supra-*second intervals. Neuropsychologia* 41, 1583–1592.

Machado, A., and Keen, R. (2003). Temporal discrimination in a long operant chamber. *Behav. Process.* 62, 157–182.

Maddox, W. T., and Bohil, C. J. (1998). Base-rate and payoff effects in multidimensional perceptual categorization. *J. Exp. Psychol. Learn. Mem. Cogn.* 24, 1459–1482.

Matell, M. S., and Meck, W. H. (2004). Cortico-striatal circuits and interval timing: coincidence detection of oscillatory processes. *Brain Res. Cogn. Brain Res.* 21, 139–170.

Montemayor, C., and Balcı, F. (2007). Compositionality in language and arithmetic. *J. Theor. Philos. Psychol.* 27, 53–72.

Orduña, V., Valencia-Torres, L., and Bouzas, A. (2009). DRL performance of spontaneously hypertensive rats: dissociation of timing and inhibition of responses. *Behav. Brain Res.* 201, 158–165.

Paterson, N. E., Balcı, F., Campbell, U., Olivier, B., and Hanania, T. (2010). The triple reuptake inhibitor DOV216,303 exhibits limited antidepressant-like properties in the differential reinforcement of low-rate 72-sec responding assay, likely due to dopamine reuptake inhibition. *J. Psychopharmacol.* doi: 10.1177/0269881110364272 [Epub ahead of print].

Penney, T. B., Gibbon, J., and Meck, W. H. (2008). Categorical scaling of duration bisection in pigeons (*Columba livia*), mice (*Mus musculus*), and humans (*Homo sapiens*). *Psychol. Sci.* 19, 1103–1109.

Rachlin, H. (2006). Notes on discounting. *J. Exp. Anal. Behav.* 85, 425–435.

Rao, R. P. N. (2010). Decision making under uncertainty: a neural model based on partially observable Markov decision processes. *Front. Comput. Neurosci.* 4:146. doi: 10.3389/fncom.2010.00146

Rapoport, A., and Burkheimer, G. J. (1971). Models for deferred decision making. *J. Math. Psychol.* 8, 508–538.

Ratcliff, R. (1978). A theory of memory retrieval. *Psychol. Rev.* 83, 59–108.

Ratcliff, R., and McKoon, G. (2008). The diffusion decision model: theory and data for two-choice decision tasks. *Neural Comput.* 20, 873–922.

Ratcliff, R., and Rouder, J. N. (1998). Modeling response times for two-choice decisions. *Psychol. Sci.* 9, 347–356.

Ray, D., and Bossaerts, P. (2011). Positive temporal dependence of the biological clock implies hyperbolic discounting. *Front. Neurosci.* 5:2. doi: 10.3389/fnins.2011.00002

Rivest, F., and Bengio, Y. (2011). Adaptive drift-diffusion process to learn time intervals. arXiv:1103.2382v1 [q-bio.NC].

Roberts, S. (1981). Isolation of an internal clock. *J. Exp. Psychol. Anim. Behav. Process.* 7, 242–268.

Sanabria, F., and Killeen, P. R. (2008). Evidence for impulsivity in the spontaneously hypertensive rat drawn from complementary response-withholding tasks. *Behav. Brain Funct.* 4, 7.

Simen, P., Balcı, F., deSouza, L., Cohen, J. D., and Holmes, P. (2011). A model of interval timing by neural integration. *J. Neurosci.* 31, 9238–9253.

Simen, P., Cohen, J. D., and Holmes, P (2006). Rapid decision threshold modulation by reward rate in a neural network. *Neural Netw.* 19, 1013–1026.

Simen, P., Contreras, D., Buck, C., Hu, P., Holmes, P., and Cohen, J. D. (2009). Reward-rate optimization in two-alternative decision making: empirical tests of theoretical predictions. *J. Exp. Psychol. Hum. Percept. Perform.* 35, 1865–1897.

Stephens, D. N., and Cole, B. J. (1996). AMPA antagonists differ from NMDA antagonists in their effects on operant DRL and delayed matching to position tasks. *Psychopharmacology (Berl.)* 3, 249–259.

Stone, M. (1960). Models for choice-reaction time. *Psychometrika* 25, 251–260.

Stubbs, D. A. (1976). Response bias and the discrimination of stimulus duration. *J. Exp. Anal. Behav.* 25, 243–250.

Sukhotina, I. A., Dravolina, O. A., Novitskaya, Y., Zvartau, E. E., Danysz, W., and Bespalov, A. Y. (2008).Effects of mGlu1 receptor blockade on working memory, time estimation, and impulsivity in rats. *Psychopharmacology (Berl.)* 196, 211–220.

Takahashi, T. (2006). Time-estimation error following Weber-Fechner law may explain subadditive time-discounting. *Med. Hypotheses* 67, 1372–1374.

Trommershäuser, J., Maloney, L. T., and Landy, M. S. (2008). Decision making, movement planning, and statistical decision theory. *Trends Cogn. Sci. (Regul. Ed.)* 12, 291–297.

Wald, A. (1947). *Sequential Analysis.* New York: Wiley.

Wald, A., and Wolfowitz, J. (1948). Optimum character of the sequential probability ratio test. *Ann. Math. Stat.* 19, 326–339.

Wearden, J. H. (1990). Maximizing reinforcement rate on spaced responding schedules under conditions of temporal uncertainty. *Behav. Process.* 22, 47–59.

Wearden, J. H., and Ferrara, A. (1996). Stimulus range effects in temporal bisection by humans. *Q. J. Exp. Psychol.* 49B, 24–44.

Wu, S.-W., Dal Martello, M. F., and Maloney, L. T. (2009). Sub-optimal tradeoff of time in sequential movements. *PLoS ONE* 4, e8228. doi: 10.1371/journal.pone.0008228

Yi, L. (2009). Do rats represent time logarithmically or linearly? *Behav. Process.* 81, 274–279.

Zacksenhouse, M., Holmes, P., and Bogacz, R. (2010). Robust versus optimal strategies for two-alternative forced choice tasks. *J. Math. Psychol.* 54, 230–245.

Zeiler, M. D. (1985). Pure timing in temporal differentiation. *J. Exp. Anal. Behav.* 43, 183–193.

Zeiler, M. D., Scott, C. K., and Hoyert, M. K. (1987). Optimal temporal differentiation. *J. Exp. Anal. Behav.* 47, 191–200.

Conflict of Interest Statement: The authors declare that the research was conducted in the absence of any commercial or financial relationships that could be construed as a potential conflict of interest.

Received: 01 June 2011; paper pending published: 30 June 2011; accepted: 29 August 2011; published online: 27 September 2011.

*Citation: Balcı F, Freestone D, Simen P, deSouza L, Cohen JD and Holmes P (2011) Optimal temporal risk assessment. Front. Integr. Neurosci. **5**:56. doi: 10.3389/fnint.2011.00056*

APPENDIX

PEAK RESPONDING SINGLE-TRIAL ANALYSIS

The single-trial analysis involved modeling each individual trial as a three-state system (break–run–break) with a period of low responding followed by a period of high responding followed by a final period of low responding (Church et al., 1994). An exhaustive search of the parameter space with 1-s bins yielded the best fits for a start time (transition from low to high rate of responding) and stop time (transition from high to low rate of responding). From these, start and stop times were calculated. Trials with bad fits were defined as those in which the single-trial analysis resulted in start times that occurred later than the criterion interval and stop times that were earlier than the criterion interval or three times longer than the fixed interval. These trials were excluded from the analysis.

DRL METHODS

Subjects

Humans. Fifteen adults (7 males and 8 females), aged 18–30 years, were recruited via announcements posted online and around the Princeton University campus. The experiment was approved by the Institutional Review Panel for Human Subjects of Princeton University and all participants provided written consent for their participation.

Rats. Forty-eight male Sprague Dawley rats (Taconic Laboratories, Germantown, NY, USA) were used in this experiment. The rats were kept in a colony room on a 12:12 light–dark cycle (lights off at 8:30 a.m.). Dim red lights provided illumination in the colony room and testing rooms. Upon arrival, the rats were 8 weeks of age and weighed between 75 and 100 g. During the first week, the rats were on a free-feeding schedule. After a week, their daily food (FormuLab 5008) was rationed to 16 g per day. During the experimental session, the rats were fed 45-mg Noyes pellets (Improved Formula A) as a reward. Water was available *ad libitum* in both the home cage and the testing chamber. The rats were previously used in an experiment that used lights and sounds as stimuli. They were previously trained on a Fixed Interval procedure with gaps. All procedures were approved by the Brown University Institutional Animal Care and Use Committee.

Stimuli and apparatus

Humans. The visual stimulus consisted of a white square on black background. The display was generated in MATLAB on a Macintosh computer, using the Psychophysics Toolbox extension (Brainard, 1997; Pelli, 1997). Responses were collected with a standard computer keyboard.

Rats. Twenty-four experiment chambers (Med Associates, dimensions 25 cm × 30 cm × 30 cm) were situated in two separate experiment rooms (12 in each room). Each chamber was contained in a sound-attenuating box (Med Associates, dimensions 74 cm × 38 cm × 60 cm) with a fan for ventilation. Each experimental chamber was equipped with a pellet dispenser (Med Associates, ENV-203) on the front wall that delivered the reward into a food cup. A head entry into this cup interrupted a photo beam (Med Associates, ENV-254). On both sides of the food cup, there were two retractable levers. On the opposite wall, a water bottle protruded into the chamber allowing *ad libitum* access to water during the session. A lick on the spout of the water bottle completed an electric circuit. Four Gateway Pentium III/500 computers running Med-PC for Windows (version 1.15) controlled the experiments and recorded the data. The interruption of the photo beam and the completion of the lick and lever circuits were recorded in time-event format with 2-ms accuracy.

Procedure

Rat experiment. In each of the 42 sessions, the rats were placed in the box and a lever was inserted (counterbalanced across rats). Rats were rewarded for spacing their lever presses (the time between lever presses or IRT) by at least the DRL schedule. Any IRT shorter than the DRL schedule was not rewarded. There were four groups, each with a different DRL schedule. The DRL schedules were 7, 14, 28, and 56 s. There were 12 rats in each group. The session lasted 1-h. The amount of reward per session for an optimal animal ranged from about 60 (DRL 56) to about 515 food pellets (DRL 7).

Human experiment. Humans were tested in single session experiments with one of the following DRL schedules per session: 5, 8, 10, 12, 15 s. Subjects were told that they would earn money for each response after a minimum withhold interval since their last response and that any earlier response would reset the trial clock with no monetary reward. They were also told how much they would earn per correct response, that the session time was fixed and that they should try to make as much money as possible. Trial-based monetary gain in DRL blocks was parameterized such that if the participant always responded at the DRL schedule, s/he would earn at most around $20 per session. This equated the reward rate for different schedules/participants. Thus, monetary gain per response increased with longer DRL schedules. Participants were also explicitly instructed not to count, tap, or adopt any rhythmic activity in order to time the intervals.

At the beginning of the session, participants were presented with the minimum withhold duration for three times. This duration was signaled by a white square presented on a black ground. Following demonstrations of the target interval, participants familiarized themselves with this interval by reproducing it for around 50 times over two blocks. During this familiarization phase, in each trial a white square appeared in the middle of the screen and participants were asked to press the space key when they thought the target interval elapsed. Once the space key was hit, the square disappeared and participants were given feedback on a fixed length horizontal line about how far their reproduction was from the target interval in that trial. The reproduction discrepancy was signaled by the horizontal distance between two vertical lines, one representing the target (white) and the other (red) reproduction in that particular trial. This distance was normalized by the DRL schedule, so that the same number of pixels corresponded to the same proportion of discrepancy. Following two blocks of reproduction, participants were presented with eight, 5 min-long blocks of DRL testing (one schedule per subject).

Before the first DRL block, participants were told that the actual experiment was about to start and were again reminded of the DRL task rules (see above). Test blocks started with the appearance of a white square in the middle of the screen. Participants could respond at any time and as often as they chose during the

trial. If a response was emitted at or after the minimum withholding duration since the previous response, the square turned green, and was accompanied by a brief auditory feedback (beep) and presentation of the money earned in that trial. If the response was emitted prior to the minimum withholding duration, the square turned red and was accompanied by a brief buzzer. Following feedback, the square turned white again. Cumulative earning was presented at all times on top of the screen during the test blocks.

A secondary task was used during familiarization and DRL testing in order to prevent explicit counting. At the beginning of each block, participants were presented with a four-digit number and at the end of each block they were presented with a single digit number. Participants were asked if the four-digit set contained that single digit. At the end of the session, earning from the timing trials was multiplied by the proportion of correct recollections in the working memory task. At the beginning of the experiment, participants were told about the secondary task and that their earning from timing trials would be weighted by their performance in the working memory task.

One of the participants reported that s/he was not engaged in the task during testing. We include this participant in graphical depictions and analyses for completeness. However, we also report results based on the analysis of data after excluding this participant.

WALD CUMULATIVE DISTRIBUTION FUNCTION

$$\text{waldcdf}(T,\hat{t},\hat{\lambda}) = \Phi\left(\sqrt{\frac{\hat{\lambda}}{T}}\left(\frac{T}{\hat{t}} - 1\right)\right) + \exp\left(\frac{2\hat{\lambda}}{\hat{t}}\right)\Phi\left(-\sqrt{\frac{\hat{\lambda}}{T}}\left(\frac{T}{\hat{t}} + 1\right)\right),\ \hat{\omega} = \sqrt{\frac{\hat{t}}{\hat{\lambda}}}.$$

where Φ is the standard Gaussian distribution cdf.

REFERENCES

Brainard, D. H. (1997). The psychophysics toolbox. *Spat. Vis.* 10, 433–436.
Pelli, D. G. (1997). The video toolbox software for visual psychophysics: transforming numbers into movies. *Spat. Vis.* 10:437–442.

frontiers in
INTEGRATIVE NEUROSCIENCE

ORIGINAL RESEARCH ARTICLE
published: 28 October 2011
doi: 10.3389/fnint.2011.00071

Temporal decision making in simultaneous timing

Florian Klapproth*

Languages, Culture, Media and Identities Research Unit, University of Luxembourg, Luxembourg

Edited by:
Warren H. Meck, Duke University, USA

Reviewed by:
Catalin V. Buhusi, Medical University of South Carolina, USA
Claudette Fortin, Université Laval, Canada

****Correspondence:***
Florian Klapproth, Languages, Culture, Media and Identities Research Unit, University of Luxembourg, Building III, Office 007, Route de Diekirch, L-7201 Walferdange, Luxembourg.
e-mail: florian.klapproth@uni.lu

With two experiments it was examined whether one or two clocks operate the timing of two intervals presented simultaneously. The target interval always preceded the distracter interval, and was longer than it. Thus, the distracter was completely embedded within the target interval. The participants used the method of temporal production. The stimuli to be judged differed in modality which allowed for testing the hypothesis of modality-specific internal clocks that operate in parallel and independent from one another when two stimuli were presented at the same time. The main results of this study were as follows. First, production times of the target interval increased proportionally with production times of the distracter interval. Second, the auditory distracter interval was on average produced in less time than the visual distracter interval. Third, a target interval that was accompanied by an auditory distracter interval was on average produced in less time than a target interval that was accompanied by a visual distracter interval. The results obtained support the hypothesis of multiple clocks being involved in the timing of different intervals presented simultaneously.

Keywords: simultaneous timing, temporal judgment, temporal decision making, modality, dual-clock hypothesis, multiple timers

INTRODUCTION

Decision making involves the selection of at least two options which may differ regarding any attribute that is salient to the decision maker. Temporal decision making is a special case of choices made between alternatives differing in duration (Klapproth, 2008). Examples of temporal decision making in real live are numerous and ubiquitous, be it the judgment of the duration of a boring situation (often accompanied by the hope of an early ending of that situation) or the estimation of cooking time in order to prevent a meal from getting burnt. Several models have been proposed to explain and predict human and non-human temporal judgments. Most of these models rely on assumptions concerning an internal clock that in some aspects resembles a physical clock. For example, both the physical clock and the "mental" clock emit "pulses" at a regular pace (like the finger or the digits of a clock), both do in some way record the elapsed time by either storing the emitted pulses (mental clock) or adding seconds to the next minute (physical clock), and both need some form of energy (current in case of a physical clock and attention in case of a mental clock) to make them work. Moreover, as with the physical clock, the mental clock is prone to errors (although to a much larger degree). The latter attribute has provoked a lot of research since errors in judgments of time seem to obey some principles. One principle asserts that estimates of real duration are, on average, accurate, that is, if a subject makes several estimates of a given duration, then the mean time measured by the mental clock corresponds to the time measured by the physical clock. A second principle is a form of Weber's Law which means that SDs of temporal judgments grow proportionally with the mean of time estimations.

Most prominent theories that explain regularities in human and non-human temporal judgments with reference to mental clocks are the scalar-timing theory (Gibbon et al., 1984; Gibbon, 1991) and modifications of it. The scalar-timing theory posits three stages of processing temporal information that are involved in temporal judgments: a clock, consisting of a pacemaker which generates pulses at a regular pace (with random error), which are recorded and added by an accumulator; a memory which stores pulses transferred from the accumulator for a longer while; and a comparison process through which a judgment is made by relating the to be judged duration to a reference duration stored in memory. Modifications of scalar-timing theory (or of its information-processing model) have altered the decision rule as to which sameness or differences of durations are examined (e.g., Wearden, 1992), have added attention as a factor that is supposed to affect temporal judgments (e.g., Block and Zakay, 1996), or have proposed the clock to be sensitive to physiological or physical properties (like, for example, stimulus modality, cf. Penney et al., 1998; Wearden et al., 1998).

One model that is able to explain variations in attention and clock speed is the attentional-gate model proposed by Block and Zakay (1996) and Zakay and Block (1996, 1998). Like the scalar-timing model, the attentional-gate model is composed of a pacemaker that emits pulses at a constant rate, a cognitive counter, and a decision-making stage. An additional component is the attentional-gate. The attentional-gate is assumed to explain the influence of a person's attentional resource allocation to timing. The more attention is allocated to the timing process, the wider (metaphorically speaking) is the gate, thus allowing more pulses to be counted within a given period of time. Conversely, limiting attention for the timing of events will result in fewer pulses counted. Limitation of attention may be achieved by dividing attentional resources between attending to external events and

attending to time (Zakay and Block, 1997). How accuracy in timing declines when processing demands are increased has often been investigated by the use of so-called dual-task procedures. In timing experiments, examples of tasks that were executed in order to distract attention from the timing were card sorting (Hicks et al., 1976), memory scanning (Fortin and Rousseau, 1998), or listening to music (Brown et al., 1992).

Models of temporal decision making have initially been developed to describe and explain judgments of single durations, that is, durations of stimuli that occur in succession rather than in parallel. However, we know from everyday life and from a growing body of research that humans and even non-human animals are able to estimate the durations of more than one stimulus simultaneously (cf. Curtis and Rule, 1977; Rule et al., 1983; Meck and Church, 1984; Rule and Curtis, 1985; Brown and West, 1990; van Rijn and Taatgen, 2008).

Most authors who aimed at explaining effects of simultaneous timing referred to limited attentional resources. If a timing device necessitates attention to be operated, timing of two intervals simultaneously might lead to a conflict in sharing attentional resources in order to monitor these intervals. Sharing attention means that less attention is devoted to the timing of either interval, resulting in judgmental biases compared to single-stimulus timing. According to the attentional-gate model (e.g., Block and Zakay, 1996), withdrawing attention from a timing task will result in less accurate temporal judgments. However, their model might allow for more precise predictions on how simultaneous timing will alter temporal judgments. The model predicts that if attention is distracted from the main timing task, fewer pulses will be accumulated during a certain period of time which will result in a shortening of perceived time. However, with temporal productions, the opposite pattern is likely to occur. Because perceived time is shortened, more time will be needed to accumulate the number of pulses that defines the mental equivalent of that duration. In other words, when people are required to produce a time interval and are to fulfill another task in parallel, time productions should become longer, compared to people who are engaged in the time-production task only (see for example, Hemmes et al., 2004; Brown and Merchant, 2007). This should also be true when two timing tasks are conducted concurrently. That is, if attention is divided between both timing tasks, each task will be provided with fewer attentional resources, resulting in longer time productions, than if it would be done solely.

Concerning the internal clock in simultaneous timing, some authors suggest the existence of one central pacemaker but different counters, each for every signal to be timed (e.g., Church, 1984; van Rijn and Taatgen, 2008). If one clock operates the timing of two parallel events, simultaneous timing has to be converted into sequential timing. This might be done by dividing the stream of stimuli into segments that are defined by stimulus onsets and offsets. For example, suppose the duration of two stimuli has to be judged, and both stimuli overlap to a certain degree. The first stimulus to be judged starts at t_1, and while the stimulus is being presented, the second stimulus occurs at t_2. Suppose further that the second stimulus is completely embedded within the first one. That is, presentation of the second stimulus will end at t_3, and finally the first stimulus will end at t_4. When judging the duration of both stimuli, one can divide the duration of the stimuli into three segments, which are the segment t_1t_2, the segment t_2t_3, and the segment t_3t_4. The duration of the first stimulus can then be judged by adding all segments, whereas the duration of the second stimulus might be judged by judging the segment t_2t_3.

Others propose that timing different intervals simultaneously necessitates multiple independent clocks which generate pulses that are switched into multiple accumulators. First hints referring to the existence of multiple clocks come from studies where rats were trained on a peak procedure in which three levers were individually associated with different durations initiated by the onset of a single signal (Matell et al., 2004, 2006; Buhusi and Meck, 2009). The responses of the rats showed that they were able to time the durations quite independently from each other, suggesting the use of independent clocks rather than a single clock.

If each of both concurrent stimuli is timed by a separate and independent pacemaker, judging both durations might be affected by different pacemaker speeds. Pacemaker speed has been discussed to be governed by stimulus modality (Penney et al., 1998; Wearden et al., 1998), referring to the fact that intervals marked by auditory signals are judged – on average – as being longer in duration than intervals marked by visual signals when both intervals are in fact the same (e.g., Goldstone and Goldfarb, 1964; Goldstone, 1968; Goldstone and Lhamon, 1974; Sebel and Wilsoncroft, 1983; Stubbs et al., 1984). According to the attentional-gate model, auditory stimulation increases the frequency of the pacemaker, resulting in a larger number of pulses being accumulated within a given time period. Thus, compared to time intervals presented by visual signals of equal length, time intervals presented by auditory signals should be judged as being longer in duration.

In this study, the method of temporal production was used to examine effects of concurrent timing on timing performance. In temporal production, participants are presented with a stimulus, and their task is to stop its presentation after a pre-specified time has elapsed. Usually, mean time productions vary linearly, and approximately accurately, with the time the participants are asked to produce, with more variance in judgments the longer the time produced is (Wearden and McShane, 1988; Wearden, 2003). In simultaneous temporal production, two (or more) durations have to be produced in parallel. This is achieved when the stimuli which have to be terminated overlap in part or in total. In the experiments of this study, the target interval was accompanied by a distracter interval, which was always shorter than the target interval and completely embedded within it.

Temporal productions have frequently been used for eliciting temporal judgments, especially within the dual-task paradigm in order to show interference effects between the timing task and the distracter task (e.g., Fortin and Breton, 1995; Hemmes et al., 2004; Brown and Merchant, 2007). However, when individual temporal productions are transformed into relative frequencies, distributions of these frequencies tend to be slightly skewed, although the fit to the normal distribution has been shown to be generally good (Wearden and McShane, 1988).

Two hypotheses were tested with this study, each pertinent to a single possible source of variance in simultaneous temporal judgments. First, it was hypothesized that if attentional resources needed to judge stimulus duration are limited and must be divided

in case of the timing of two concurrent stimuli, temporal judgments in simultaneous timing should be altered in relation to the overlap of the two durations. During overlap, fewer pulses would be accumulated within a time period for each interval to be judged than if only a single interval has to be estimated. Therefore, it would take more time to reach the critical number of pulses that reflect the time to be produced. Accordingly, production times of the target interval should vary as a function of production times of the distracter interval: the longer the distracter interval is produced, the longer should be the production times of the target interval.

The second hypothesis was concerned with the question of whether one or two clocks are needed if two durations have to be judged concurrently. If the stimuli presented in different modalities would be timed by different and independent clocks, one would expect modality-dependent effects on clock speed to occur. More precisely, if one stimulus is presented within the visual modality and the other stimulus is presented within the auditory modality, the speed of the clock timing the visual interval should be lower than the speed of the clock timing the auditory interval (cf. Penney et al., 1998; Wearden et al., 1998). Hence, in case of two independent clocks, productions of the *distracter* interval should be shorter in the VIS–AUD condition than in the VIS–VIS condition (and shorter in the AUD–AUD condition than in the AUD–VIS condition) since clock speed in the auditory modality is assumed to be higher than in the visual modality. Moreover, if mean productions of the distracter interval presented within the visual modality are longer than mean productions of the distracter interval presented within the auditory modality, the duration of the overlap of the target interval and the distracter interval should be longer in the VIS–VIS condition than in the VIS–AUD condition (and accordingly longer in the AUD–VIS condition than in the AUD–AUD condition). The longer the overlap, the longer should be the production time for the target interval. Hence, mean productions of the *target interval* should be longer in the VIS–VIS condition than in the VIS–AUD condition, and longer in the AUD–VIS condition than in the AUD–AUD condition. **Figure 1** illustrates the hypotheses stated above.

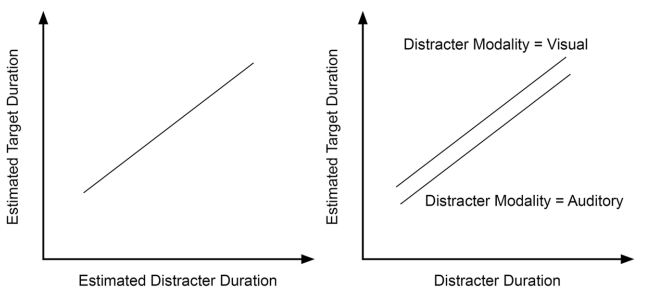

FIGURE 1 | Illustration of the hypotheses of this study. Left panel: Illustration of Hypothesis 1 which states that estimated target duration grows proportionally with estimated distracter duration; right panel: Illustration of Hypothesis 2 which asserts that estimated target duration grows proportionally with the announced distracter duration, but is longer in case of a visual distracter stimulus than in case of an auditory distracter stimulus.

MATERIALS AND METHODS

In both experiments, the participants had to simultaneously produce two time intervals which had different onsets. The target interval was the longer of both intervals, and the durations chosen for the target interval were 9, 10, or 11 s. The second interval, the distracter interval, was shorter than the target interval and was always embedded within the target interval. The conditions realized differed regarding the modality of the target interval and of the distracter interval. In Experiment 1, the target interval was presented visually, and the distracter was either presented auditorily or visually. In Experiment 2, the distracter was again either auditory or visual, but the target interval was presented auditorily. Thus, four conditions were realized in total. In Experiment 1, the conditions were VIS–VIS and VIS–AUD, and in Experiment 2 the conditions were AUD–AUD and AUD–VIS.

In this study, control trials in which participants judged only a single duration were omitted. The major reason for this decision was that comparisons between single-stimulus timing and simultaneous timing might be confounded with an effect of the mere presentation of a second stimulus. Suppose that in simultaneous timing the target duration is produced longer than the same duration in single-stimulus timing. This effect might be due to the attention that is distracted from timing the target duration in order to judge the distracter duration in parallel. However, detecting the distracter stimulus might also capture attention, irrespectively of its duration (cf. Ivry and Hazeltine, 1995). Hence, variance in judging the target interval in simultaneous timing could be an effect of both the concurrent timing of the distracter stimulus and attending to its mere presentation. In this study, duration-independent variance due to the mere presentation of the distracter stimulus was kept constant by comparing conditions only differing in duration of the distracter stimulus. Therefore, the hypotheses according to effects of the production of the distracter duration on the production of the target duration were tested by varying the production times of the distracter duration.

PARTICIPANTS

With Experiment 1, temporal judgments of 40 participants (22 women, 18 men) were examined. Mean age of all participants was 30.3 years (SD = 4.6). In Experiment 2, 21 women and 19 men participated. Mean age of all participants was 29.7 years (SD = 7.2). The participants were randomly assigned to the conditions. The participants attended voluntarily and gave their consent for participation in the experiments.

STIMULI AND APPARATUS

The target stimulus in Experiment 1 was a white square (3 cm × 3 cm) presented on a dark background on the left side of the computer monitor screen. In Experiment 2, the target stimulus was a sine tone of 300 Hz, presented via headphones. The distracter intervals were presented either visually or auditorily. The visual distracter stimulus was the same as the target stimulus, but presented on the right side of the screen. The auditory distracter stimulus was a 500-Hz sine tone, presented via headphones.

All visual experimental events (including the instructions) were presented on a 15″ computer screen (50 Hz refresh rate), and

were controlled by the software "Experimental Run Time System" [ERTS], version 3.00, from BeriSoft, Frankfurt, Germany, running on a Pentium-II-Computer. The software allows for precise timing of stimuli and responses in the milliseconds range. The distance between the participants and the screen was about 70 cm.

In both experiments, white digits were presented on dark background to the participants on the monitor prior to onset of the target and distracter durations on each trial. These digits announced the durations (in seconds) to be produced. The digits were either "9," "10," or "11" for the target duration (presented on the left side of the screen), and "2," "4," or "6" for the distracter duration (presented on the right side of the screen).

PROCEDURE

The participants were tested individually in a moderately illuminated and quiet room. After each participant took her/his seat in front of the monitor, she/he was informed about the purpose of the experiment. Then, the participant received instructions presented on the computer screen.

Both the target interval and the distracter interval to be produced were symbolized as digits presented at the beginning of each trial. The digit on the left side represented the target duration, the digit on the right side the duration of the distracter. Presentation of the digits was aborted by the participant's key press.

Two seconds after abortion of the presentation of the digits, the production task started in Experiment 1 with a white square presented on the left side of the monitor, and in Experiment 2 with the presentation of a 300-Hz sine tone. Presentation of the target stimulus indicated the participants to begin with the production of the target interval. After a randomly chosen inter-onset interval (IOI), the stimulus indicating the beginning of the production of the distracter interval started, which was either a second square appearing on the right side of the monitor (Condition VIS–VIS and Condition AUD–VIS), or a tone presented via headphones (Condition AUD–AUD and Condition VIS–AUD). The production times of the target intervals were announced to be 9, 10, or 11 s, the production times of the distracter interval were announced to be 2, 4, or 6 s.

After the time had elapsed that was judged to be the same as previously announced, the participants pressed the ALT key for the target interval and the ALT-R key for the distracter interval. By pressing either key, the respective stimulus disappeared. After that, a new trial began following an inter-trial interval of 3 s.

The participants were instructed to conduct the production task by the following instruction (here an example of the VIS–VIS condition is used; the original instructions were given in German). In order to prevent the participants from using a simple arithmetic as a strategy for timing the simultaneous stimuli, they were encouraged not to count when producing the durations.

> You will now be presented with two digits that will appear on the computer monitor screen. One digit will appear on the left side of the screen, and one will appear on the right side of the screen. These digits represent the durations (in seconds) you will have to produce then. By pressing the space bar, the digits will disappear. Please keep the digits in mind.
>
> After disappearance of the digits, a white square will be presented on the left side of the screen. Please wait for the time that was previously indicated by the left digit until you have to press the ALT key to terminate the appearance of the left square.
>
> While the left square is being presented, a second square will occur on the right sight of the screen. Please wait for the time that was previously indicated by the right digit until you have to press the ALT-R key to terminate the appearance of the right square.
>
> Please do not count when judging the durations.

Each participant judged every possible combination of the target duration and the distracter duration three times, resulting in a total of 27 trials per participant. The onset of both durations was temporally displaced, with the onset of the distracter duration occurring later than the onset of the target duration. The IOI was chosen randomly, with a minimum IOI = 1.5 s and a maximum IOI = 2.5 s (mean IOI = 2.0 s).

RESULTS

EXPERIMENT 1

A first step toward the analyses of the data obtained was to inspect the frequency distributions of the temporal productions in order to evaluate their appropriateness for being entered into parametric analyses. Therefore, frequencies of times produced were grouped into bins of 0.50 s width, and histograms were plotted. A Gaussian curve was fitted to the frequency distributions, with the same mean and the same SD as the frequency distribution. **Figure 2** shows the distributions for both the target durations (upper panel) and the distracter durations (lower panel).

As can be seen, the distributions were unimodal and slightly shifted to the left, which is also indicated by a mean being somewhat larger than the median value. However, Kolmogorov–Smirnov tests conducted for each distribution to test for deviances from normality yielded significant deviations in most cases (almost all p-values were smaller than $p = 0.01$). Therefore, square-root transformations of raw production times were conducted, which yielded values that were better described by a normal distribution that the raw values. In fact, only one out of four p-values were smaller than $p = 0.05$, the remaining three p-values were larger than $p = 0.10$.

With Experiment 1 the hypothesis was tested that the duration needed for producing the target interval should be linearly related to the productions of the distracter interval. This hypothesis was tested by regression analysis, with the square root of the temporal productions of the target time as criterion, and the square root of the temporal productions of the distracter time as predictor. **Figure 3** shows the scatter plots obtained from Experiment 1 wherein the square root of the production times of the target interval (plotted on the ordinate) are related to the square root of the production times of the distracter interval (plotted on the abscissa). It is clearly visible that a linear relationship well describes the connection between both durations. Regression analyses yielded a slope of $B_1 = 0.39$ and an intercept of $B_0 = 2.50$ for Condition VIS–VIS, and a slope of $B_1 = 0.38$ and an intercept of $B_0 = 2.37$ for Condition VIS–AUD. Both linear trends were highly significant ($p < 0.001$).

Moreover, Experiment 1 aimed at answering the question of how many clocks were involved in the production of two intervals in parallel. If one clock would be sufficient, one would expect that temporal productions of the target interval should not differ

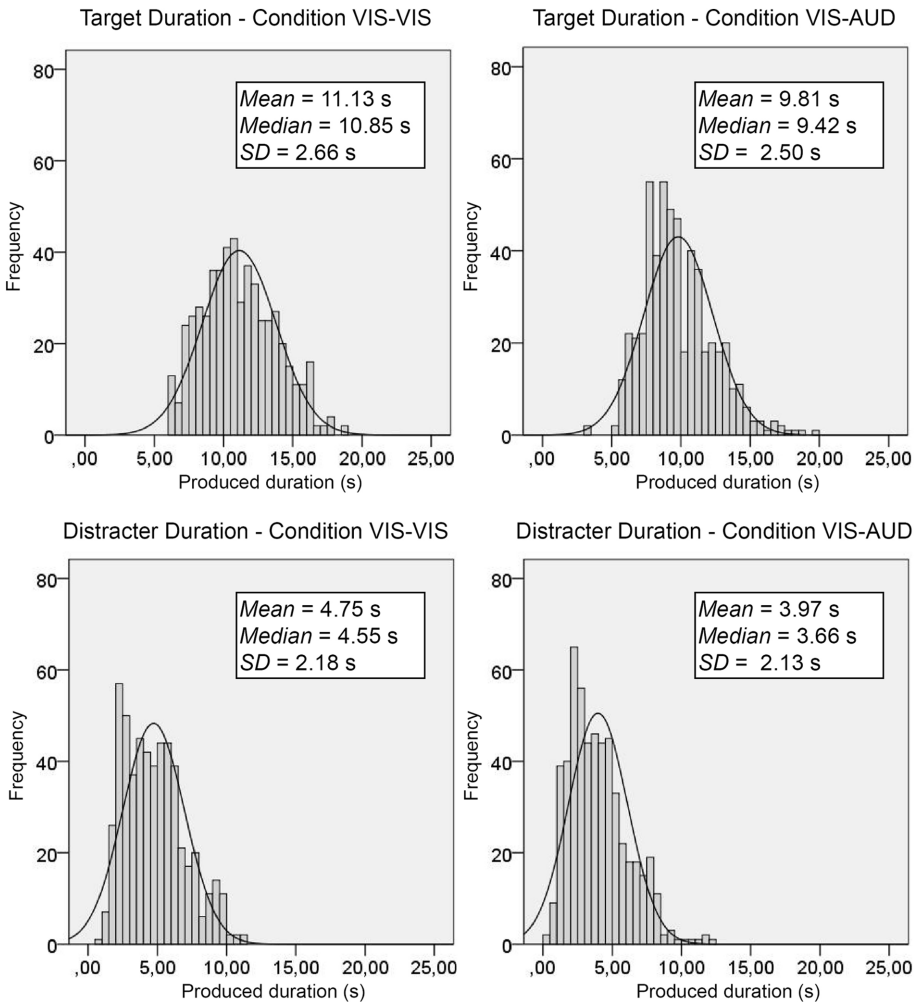

FIGURE 2 | Histograms for times produced in Experiment 1. Upper panel: Frequency distributions for the target durations. Lower panel: Frequency distributions for the distracter durations. Each distribution is accompanied with a Gaussian curve with the same mean and the same SD as the frequency distribution. Additionally, the means, the medians, and the SDs of the frequency distributions are depicted in the figure.

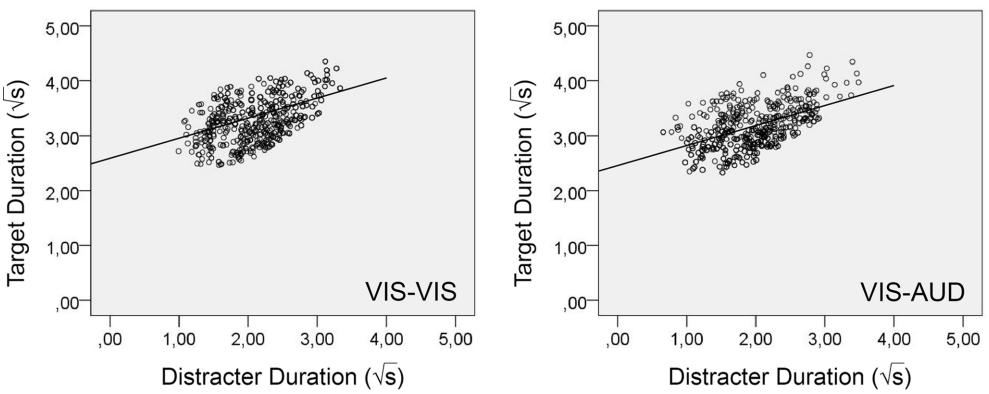

FIGURE 3 | Scatter plots showing the relationship between the square root of the production times of the distracter interval (abscissa) and the square root of the production times of the target interval (ordinate) obtained from Experiment 1. Left panel: Data obtained from Condition VIS–VIS; Right panel: Data obtained from Condition VIS–AUD. The straight line indicates the least-square regression line.

between both conditions. However, if one clock would operate the timing of the target interval and another clock would operate the timing of the distracter interval, each clock should be triggered by stimulus modality. For the bimodal condition, this would mean that the (auditory) distracter interval was timed by a clock that was assumed to be "faster" than the clock timing the (visual) target interval. If this were true, two consequences should follow. The first consequence is related to the production time of the distracter intervals. If clock speed was altered due to stimulus modality, then the auditory distracter interval should on average be produced in less time than the visual distracter interval because the "auditory" clock is supposed to emit pulses at a faster rate than the "visual" clock.

As a second consequence, the mean production times of the target interval should be shorter in Condition VIS–AUD than in Condition VIS–VIS due to a shorter overlap of the target and the distracter duration.

To test the second hypothesis, regression analysis was run, with the square root of estimated target time as the criterion, and both the square root of the announced distracter duration and distracter modality as predictors. If the hypothesis holds, regression analysis should reveal a linear trend, a positive regression weight for distracter duration (since the longer the distracter was announced to be produced, the longer should the target be produced), and a negative regression weight for modality (since target productions should be shorter with an auditory than with a visual distracter). Indeed, regression analysis confirmed the hypothesis. Estimated target time was a function of both distracter time ($B_1 = 0.08$, $p = 0.004$) and distracter modality ($B_2 = -0.20$, $p < 0.001$), with an intercept of $B_0 = 3.36$, $p < 0.001$. The linear trend was shown to be significant, $F(2,\ 1075) = 40.36$, $p < 0.001$. **Figure 4** displays temporal productions of the target interval, estimated by regression analysis.

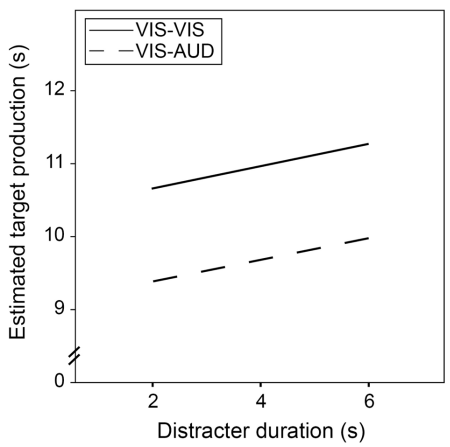

FIGURE 4 | Temporal productions of the target interval in Experiment 2, estimated by linear regression analysis. The straight line indicates estimations of temporal productions in case the distracter stimulus was presented visually, the interrupted line indicates temporal productions in case the distracter stimulus was presented auditorily. Note that temporal estimates and distracter times were displayed as untransformed values to yield better comprehensibility.

EXPERIMENT 2

Analyses of results of Experiment 2 were the same as those conducted in Experiment 1. First, the frequency distributions of the production times were plotted (see **Figure 5**). As in Experiment 1, the distributions were in part skewed. Kolmogorov–Smirnov tests yielded significant deviations in most cases (almost all p-values were smaller than $p = 0.01$). After square-root transformation, Kolmogorov–Smirnov tests identified only in one case a slight deviation from normality ($p = 0.02$), the remaining three p-values were larger than $p = 0.25$.

Second, scatter plots were obtained with the transformed estimates (**Figure 6**) which show the square root of the production times of the target interval (plotted on the ordinate) related to the square root of the production times of the distracter interval (plotted on the abscissa).

Both inspection of the scatter plots and regression analyses show a clear linear relationship between production times of the target interval and production times of the distracter interval, indicating again a proportional effect of the duration of the distracter interval on the duration of the target interval. Regression analyses yielded a slope of $B_1 = 0.53$ and an intercept of $B_0 = 2.21$ for Condition AUD–VIS, and a slope of $B_1 = 0.61$ and an intercept of $B_0 = 1.97$ for Condition AUD–AUD. Both linear trends were again highly significant ($p < 0.001$).

To examine whether stimulus modality affected the production times of both the distracter stimuli and the target stimuli, regression analysis was run, with the square root of estimated target time as the criterion, and the square root of the announced distracter duration and distracter modality as predictors. Again, regression analysis confirmed the hypothesis. Estimated target time was a function of both the distracter time ($B_1 = 0.18$, $p < 0.001$) and distracter modality ($B_2 = -0.23$, $p < 0.001$), with an intercept of $B_0 = 3.23$, $p < 0.001$. The linear trend was significant, $F(2,\ 1077) = 42.69$, $p < 0.001$. **Figure 7** displays temporal productions of the target interval, estimated by regression analysis.

DISCUSSION

With this study, it was examined whether one or two clocks operate the timing of two intervals which were presented simultaneously. The target interval always preceded the distracter interval, and was longer than it. Thus, the distracter interval was completely embedded within the target interval. The participants used the method of temporal production, that is, they monitored the duration of both stimuli and pressed a button when they judged a match between a criterion which was announced prior to stimulus presentation, and the actual stimulus duration. The stimuli to be judged differed in modality which allowed for testing the hypothesis of modality-specific internal clocks that operate in parallel and independent from one another when two stimuli were presented at the same time.

The distributions of the production times of this study resembled those obtained in previous studies (e.g., Wearden and McShane, 1988). The distributions were slightly skewed, with more productions made at intervals shorter than the mean than made at intervals longer than the mean. Since skewness of data might affect estimates of parametric statistical analyses, production times were square-root transformed. Transformation of the data actually

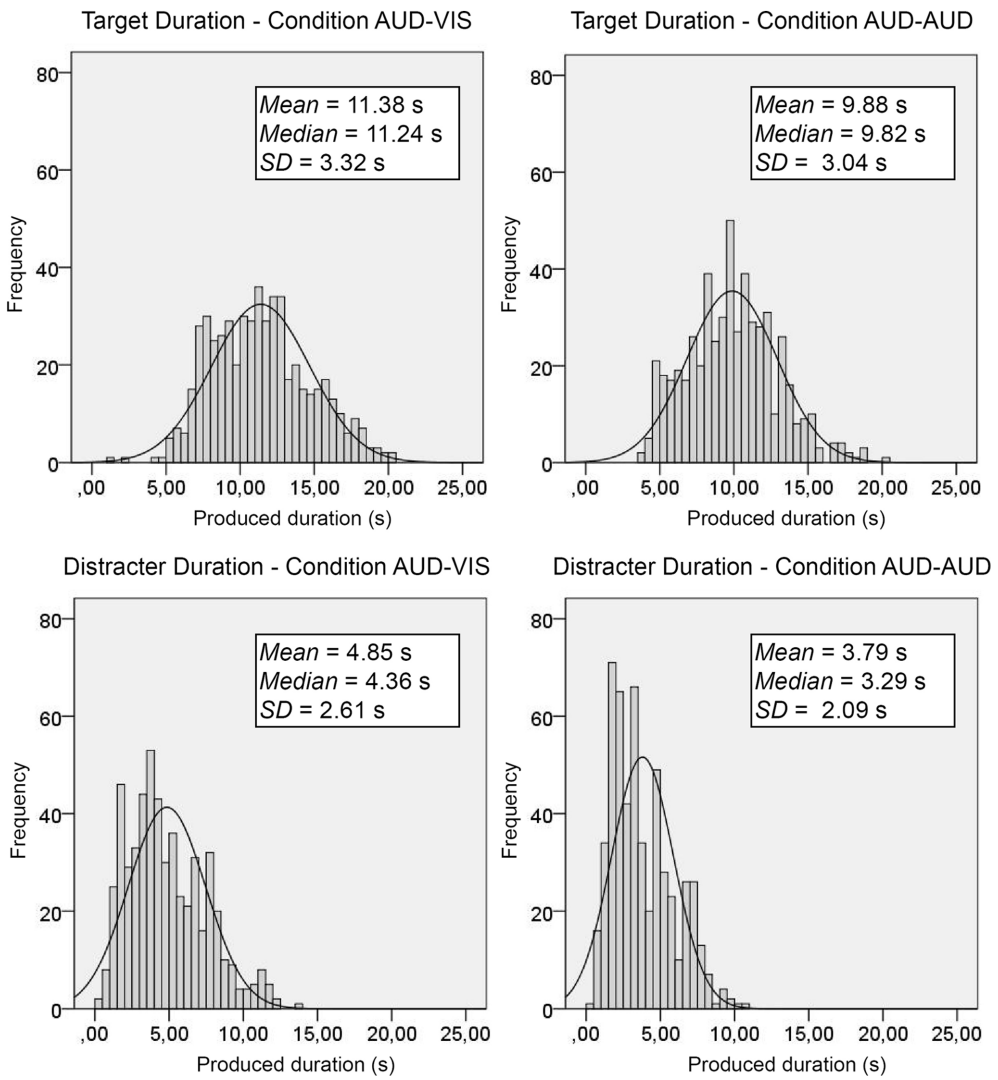

FIGURE 5 | Histograms for times produced in Experiment 2. Upper panel: Frequency distributions for the target durations. Lower panel: Frequency distributions for the distracter durations. Each distribution is accompanied with a Gaussian curve with the same mean and the same SD as the frequency distribution. Additionally, the means, the medians, and the SDs of the frequency distributions are depicted in the figure.

yielded a better fit to normality than did untransformed data. The following discussion of the results is done with regard to the transformed data, although it might be generalized to untransformed data as well.

The main results of this study were as follows. First, production times of the target interval varied proportionally with production times of the distracter interval. On average, productions of the target interval increased with increasing productions of the distracter interval. This result corresponds to predictions made by the attentional-gate model proposed by Block and Zakay (1996) which assumes that – due to limited attentional resources – doing two tasks in parallel will affect performance on either task. Moreover, a linear relationship between production of the target and production of the distracter points to a constant amount of attention per time unit that misses in temporal judgment when the duration of two stimuli has to be judged concurrently. This result is furthermore in contradiction to the assumption of a single clock that operates the timing of two stimuli presented in parallel by dividing both durations into a succession of segments.

It may be argued that prolongation of the distracter duration occurred in part due to a tendency of the participants not to end the production of the target interval before production of the distracter interval had been finished because the participants knew that one interval (the target) was always longer than the other (the distracter). However, it should be noted that there was no explicit requirement given in the instructions to wait with finishing the production of the target interval until production of the distracter interval had been done. Moreover, as the IOI between the presentation of the target stimulus and the presentation of the distracter stimulus randomly varied, the participants were not able to infer

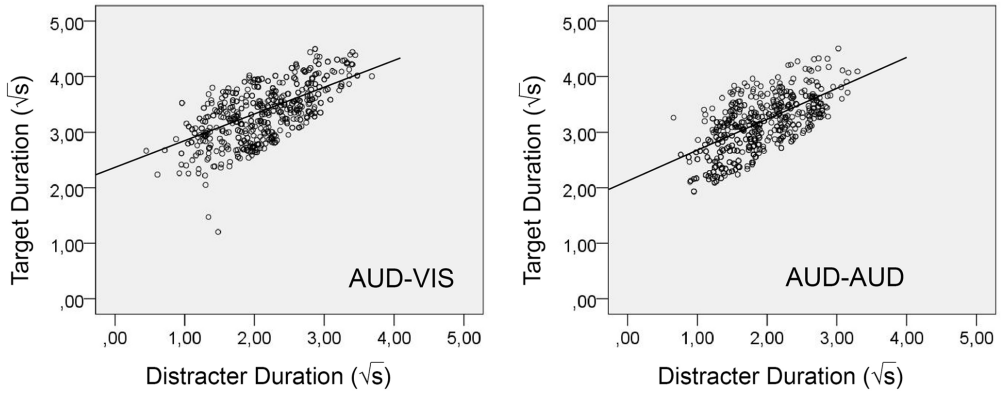

FIGURE 6 | Scatter plots showing the relationship between the square root of the production times of the distracter interval (abscissa) and the square root of the production times of the target interval (ordinate) obtained from Experiment 2. Left panel: Data obtained from Condition AUD–AUD; right panel: Data obtained from Condition AUD–VIS. The straight line indicates the least-square regression line.

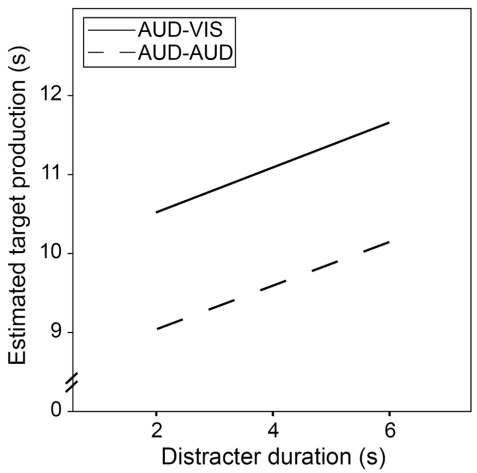

FIGURE 7 | Temporal productions of the target interval in Experiment 2, estimated by linear regression analysis. The straight line indicates estimations of temporal productions in case the distracter stimulus was presented visually, the interrupted line indicates temporal productions in case the distracter stimulus was presented auditorily. Note that temporal estimates and distracter times were displayed as untransformed values to yield better comprehensibility.

that production of the distracter interval should always be embedded within production of the target interval. Moreover, inspection of the scatter plots might suggest that producing a short distracter resulted in a shortening of the target production. Shortening in this sense means that a short distracter would lead to a target that is produced in less time than when no distracter is presented. If this were true, a contradiction to Zakay's and Block's attentional-gate model would have been found since this model assumes always a prolongation of the target production if a distracter duration is to be judged in parallel. The reason for the assumed prolongation is that according to the model doing two tasks in parallel leaves fewer attentional resources for the single task so that each single task has to be done with attentional deficits. Hence, if less attention is devoted to timing, longer instead of shorter temporal productions should result. However, if a shortening effect in the sense described above was actually present in this study it could hardly be detected because there was no condition realized wherein only one duration was to be judged.

Second, if one clock would operate the timing of the target interval and another clock would operate the timing of the distracter interval, it was expected that each clock should be triggered by stimulus modality separately. For the bimodal conditions realized in this study, this would mean that the distracter interval was timed by a clock that was assumed to be either "faster" than the clock timing the target interval, if the target was a light and the distracter was a sound, or "slowed down," if the target was a sound and the distracter was a light. According to this hypothesis, two findings were expected. First, if clock speed was altered due to stimulus modality, then the auditory distracter interval should on average be produced in less time than the visual distracter interval because the "auditory" clock is supposed to emit pulses at a faster rate than the "visual" clock (Penney et al., 1998; Wearden et al., 1998) Second, the produced duration of the target stimulus should be shorter when accompanied by an auditorily presented distracter than when accompanied by a visually presented distracter.

The actual outcomes matched the expected ones. As regression analyses have shown, target durations were produced in less time when distracter stimuli were presented auditorily rather than visually. Moreover, production times of the target interval grew proportionally with the announced duration of the distracter stimulus.

This study brought evidence in favor of a timing device in humans that is able to estimate two durations in parallel by the use of separate and independent clocks. Timing, however, appeared to be affected by limited attention since it was found that temporal estimates of one stimulus varied proportionally with temporal estimates of the second stimulus. The attentional-gate model offers a straightforward explanation of this proportional effect. It assumes a gate that allows pulses emitted by the pacemaker to be stored and accumulated in a counter if attention is devoted to the timing task. If, however, attention is detached from the timing

task, fewer pulses are accumulated. This assumption can easily be adapted to simultaneous timing. Whenever two timing tasks have to be executed in parallel, attention has to be divided between both timing tasks, therefore less attention is devoted to the timing of a stimulus in simultaneous timing, compared to timing single durations.

A quantitative modeling of simultaneous timing may be achieved when the slopes and the intercepts obtained in this study, and differences of slopes and intercepts between the conditions realized, are analyzed and interpreted. The slope reflects the impact of the duration produced for the distracter stimulus on the duration produced for the target stimulus. The larger the slope, the larger was the impact of the distracter duration on the target duration. If the distracter duration would have had no effect on the target duration, a slope of (or near to) zero would be expected. The intercept represents an estimate of the target duration, if one would assume that there was no effect of the distracter on the target. It is an additive constant that best predicts the nominal average value for the target duration (which actually was 10 s). The value of the slope points to the amount of prolongation of the target duration. For example, in Condition VIS–VIS of Experiment 1, mean slope was 0.39. This value means that the square root of the production of the target time increased by 0.39 times the square root of the production of the distracter time. If the production time for the distracter was, for example, 4 s, the additional time the square root of the target was produced was on average $\sqrt{4} \times 0.39$ s. Inserting the values into the regression equation obtained will, of course, easily yield the untransformed production times.

With respect to the attentional-gate model, the slope may be interpreted as the amount to which attention was detached from the timing of the target interval. If the slope would be zero, attention would be fully devoted to the target interval. On the contrary, if the slope would be one, all attention would be withdrawn from the timing of the target interval, since producing 1 s of the distracter would result in an additional 1 s of the target. Hence, in case of a slope that equals one, timing both the distracter and the target could be well described by the stop mode suggested by Meck and Church (1983). In the stop mode, participants behave as if they retain the pulses accumulated prior to the distracter, and proceed with the timing of the target after producing the distracter had been finished.

One might speculate about the reason why the slopes obtained from Experiment 1 were smaller than those obtained from Experiment 2. A possible explanation refers to differences in clock speed that have been assumed for the visually and auditorily displayed target intervals, and the role attention might play in timing. There is some evidence that information being active in working memory is processed serially instead of simultaneously (e.g., Sternberg, 1966; Schneider and Shiffrin, 1977). For example, in a dual-count task in which subjects were required to keep two running counts in working memory, they switched between these counts in order to update both running counts (Garavan, 1998). If attention is necessary for counting the pulses that are emitted by the pacemaker, one can assume analogously that attention has to be switched from one counter to the other counter in order to keep the counts in working memory, in case of two counters being involved in timing. Consequently, since switching needs some time, the pace with which attention switches between both counters should have an effect on the outcome of the timing process. Suppose that switching from one counter to the other counter takes the same time than to emit one pulse from the pacemaker. In this case, attention would only capture every second pulse, thus doubling the "normal" production time would result. In case the attentional switch is twice as fast as the pacemaker rate, every pulse will be monitored, and counted. In Experiment 1, the target stimulus was visual, whereas in Experiment 2 it was auditory. If a clock timing an auditory stimulus is faster than a clock timing a visual one, more pulses would be left during the attentional switch in the auditory modality than in the visual modality. Accordingly, the slope would be larger in audition than in vision.

The results obtained are in line with the hypothesis of multiple clocks timing different overlapping stimuli. Nonetheless it is unknown whether there exist components of the clock that might be shared when judging time intervals in parallel. For example, it seems plausible that only one reference memory is needed two judge more than one interval simultaneously. Further research should address this issue. Moreover, within this study only simultaneous temporal judgments were realized. This experimental design did not allow for comparisons between simultaneous and single time productions. With respect to a possible shortening of target productions when being accompanied with short distracter durations, it might be worth to extend this design by including direct comparisons between single and parallel temporal productions.

ACKNOWLEDGMENT

This research paper was financially supported by the Fonds National de la Recherche Luxembourg. (Grant number: FNR/11/AM4/67).

REFERENCES

Block, R. A., and Zakay, D. (1996). "Models of psychological time revisited," in *Time and Mind*, ed. H. Helfrich (Göttingen: Hogrefe & Huber Publishers), 171–195.

Brown, S. W., and Merchant, S. M. (2007). Processing resources in timing and sequencing tasks. *Percept. Psychophys.* 69, 439–449.

Brown, S. W., Stubbs, D. A., and West, A. N. (1992). "Attention, multiple timing, and psychophysical scaling of temporal judgments," in *Time, Action, and Cognition*, eds F. Macar, V. Pouthas, and W. J. Friedman (Dordrecht: Kluwer Academic Publishers), 129–140.

Brown, S. W., and West, A. N. (1990). Multiple timing and the allocation of attention. *Acta Psychol. (Amst.)* 75, 103–121.

Buhusi, C. V., and Meck, W. H. (2009). Relativity theory and time perception: single or multiple clocks? *PLoS ONE* 4, 1–6. doi:10.1371/journal.pone.0006268

Church, R. M. (1984). "Properties of the internal clock," in *Timing and Time Perception. Annals of the New York Academy of Sciences*, Vol. 423, eds J. Gibbon and L. Allan (New York: New York Academy of Sciences), 566–582.

Curtis, D. W., and Rule, S. J. (1977). Judgment of duration relations: simultaneous and sequential presentation. *Percept. Psychophys.* 22, 578–584.

Fortin, C., and Breton, R. (1995). Temporal interval production and processing in working memory. *Percept. Psychophys.* 57, 203–215.

Fortin, C., and Rousseau, R. (1998). Interference from short-term memory processing on encoding and reproducing brief durations. *Psychol. Res.* 61, 269–276.

Garavan, H. (1998). Serial attention within working memory. *Mem. Cognit.* 26, 263–276.

Gibbon, J. (1991). Origins of scalar timing. *Learn. Motiv.* 22, 3–38.

Gibbon, J., Church, R. M., and Meck, W. H. (1984). "Scalar timing in memory," in *Timing and Time Perception. Annals of the New York Academy of Sciences*, Vol. 423, eds J. Gibbon and L. Allan (New York: New York Academy of Sciences), 52–77.

Goldstone, S. (1968). Production and reproduction of duration: intersensory comparisons. *Percept. Mot. Skills* 26, 755–760.

Goldstone, S., and Goldfarb, J. L. (1964). Auditory and visual time judgment. *J. Gen. Psychol.* 70, 369–387.

Goldstone, S., and Lhamon, W. T. (1974). Studies of auditory-visual differences in human time judgment: 1. Sounds are judged longer than lights. *Percept. Motor Skills* 39, 63–82.

Hemmes, N. S., Brown, B. L., and Kladopoulos, C. N. (2004). Time perception with and without a concurrent nontemporal task. *Percept. Psychophys.* 66, 328–341.

Hicks, R. E., Miller, G. W., and Kinsbourne, M. (1976). Prospective and retrospective judgments of time as a function of amount of information processed. *Am. J. Psychol.* 89, 719–730.

Ivry, R. B., and Hazeltine, R. E. (1995). Perception and production of temporal intervals across a range of durations: evidence for a common timing mechanism. *J. Exp. Psychol. Hum. Percept. Perform.* 21, 3–18.

Klapproth, F. (2008). Time and decision making in humans. *Cogn. Affect. Behav. Neurosci.* 8, 509–524.

Matell, M. S., Bateson, M., and Meck, W. H. (2006). Single-trial analyses demonstrate that increases in clock speed contribute to the methamphetamine-induced horizontal shifts in peak-interval timing functions. *Psychopharmacology (Berl.)* 188, 201–212.

Matell, M. S., King, G. R., and Meck, W. H. (2004). Differential modulation of clock speed by the administration of intermittent versus continuous cocaine. *Behav. Neurosci.* 118, 150–156.

Meck, W. H., and Church, R. M. (1983). A mode control model of counting and timing processes. *J. Exp. Psychol. Anim. Behav. Process.* 9, 320–334.

Meck, W. H., and Church, R. M. (1984). Simultaneous temporal processing. *J. Exp. Psychol. Anim. Behav. Process.* 10, 1–29.

Penney, T. B., Allan, L. G., Meck, W. H., and Gibbon, J. (1998). "Memory mixing in duration bisection," in *Timing of Behavior: Neural, Computational, and Psychological Perspectives*, eds D. A. Rosenbaum and C. E. Collyer (Cambridge, MA: MIT Press), 165–193.

Rule, S. J., and Curtis, D. W. (1985). Ordinal properties of perceived average duration: simultaneous and sequential presentations. *J. Exp. Psychol. Hum. Percept. Perform.* 11, 509–516.

Rule, S. J., Mahon, M. L., and Curtis, D. W. (1983). Composition rule for perceived duration of simultaneous events. *Percept. Psychophys.* 34, 569–572.

Schneider, W., and Shiffrin, R. M. (1977). Controlled and automatic human information processing: I. Detection, search, and attention. *Psychol. Rev.* 84, 1–66.

Sebel, A. J., and Wilsoncroft, W. E. (1983). Auditory and visual differences in time perception. *Percept. Mot. Skills* 57, 295–300.

Sternberg, S. (1966). High-speed scanning in human memory. *Science* 153, 652–654.

Stubbs, D. A., Dreyfus, L. R., and Fetterman, J. G. (1984). "The perception of temporal events," in *Timing and Time Perception. Annals of the New York Academy of Sciences*, Vol. 423, eds J. Gibbon and L. Allan (New York: New York Academy of Sciences), 30–42.

van Rijn, H., and Taatgen, N. A. (2008). Timing of multiple overlapping intervals: how many clocks do we have? *Acta Psychol. (Amst.)* 129, 365–375.

Wearden, J. H. (1992). Temporal generalization in humans. *J. Exp. Psychol. Anim. Behav. Process.* 18, 134–144.

Wearden, J. H. (2003). "Applying the scalar timing model to human time psychology: progress and challenges," in *Time and Mind I: Information Processing Perspectives*, ed. H. Helfrich (Göttingen: Hogrefe & Huber Publishers), 21–39.

Wearden, J. H., Edwards, H., Fakhri, M., and Percival, A. (1998). Why "sounds are judged longer than lights": application of a model of the internal clock in humans. *Q. J. Exp. Psychol.* 51B, 97–120.

Wearden, J. H., and McShane, B. (1988). Interval production as an analogue of the peak procedure: evidence for similarity of human and animal timing processes. *Q. J. Exp. Psychol.* 40B, 363–375.

Zakay, D., and Block, R. A. (1996). "The role of attention in time estimation processes," in *Time, Internal Clocks and Movement*, eds M. A. Pastor and J. Artieda (Amsterdam: Elsevier), 143–164.

Zakay, D., and Block, R. A. (1997). Temporal cognition. *Curr. Dir. Psychol. Sci.* 6, 12–16.

Zakay, D., and Block, R. A. (1998). "New perspective on prospective time estimation," in *Time and the Dynamic Control of Behavior*, eds V. de Keyser, G. d'Ydewalle, and A. Vandierendonck (Seattle: Hogrefe & Huber Publishers), 129–141.

Conflict of Interest Statement: The author declares that the research was conducted in the absence of any commercial or financial relationships that could be construed as a potential conflict of interest.

Received: 15 June 2011; paper pending published: 30 June 2011; accepted: 08 October 2011; published online: 28 October 2011.

Citation: Klapproth F (2011) Temporal decision making in simultaneous timing. Front. Integr. Neurosci. ***5****:71. doi: 10.3389/fnint.2011.00071*

frontiers in
INTEGRATIVE NEUROSCIENCE

OPINION ARTICLE
published: 06 June 2011
doi: 10.3389/fnint.2011.00024

Hyperbolic discounting emerges from the scalar property of interval timing

Xu Cui*

Department of Psychiatry and Behavioral Sciences, Stanford University, Stanford, CA, USA
**Correspondence: cuixu@stanford.edu*

Ten dollars today is more attractive than the same amount of money tomorrow and is consistent with the well known proverb, "a bird in the hand is worth two in the bush." We all know that the value of a reward is discounted over time. How the value discounts over time and what is the rationale for such discounting, however, is less clear. Classical economic theory has assumed an exponential form of discounting which has been repeatedly shown insufficient for explaining the data(Frederick and Loewenstein, 2002). Hyperbolic discounting, with a faster discount rate in the beginning than in the distant future, is found to fit the data better empirically. Consequently, it is of great interest to understand why people and other animals discount future rewards hyperbolically.

In the past, a number of explanations have been offered. Not surprisingly these explanations can be categorized into either *value-based models* or *time-based models*. In *value-based* models, hyperbolic discounting emerges when discount rates are assumed to be stochastic (Farmer and Geanakoplos, 2009), or there is uncertainty of the risk that the future reward will not be realized (Sozou, 1998), or there is uncertainty of the timing of the realization (Dasgupta and Maskin, 2005). In *time-based models*, hyperbolic discounting can be shown to result from the perceptual distortion of time (Takahashi, 2005; Kim and Zauberman, 2009). Recently, Ray and Bossaerts (2011) offered another time-based explanation beginning with the crucial observation that subjective or psychological time is different from objective or physical time. They argued that the discounting function is indeed exponential with respect to the subject's internal clock, but it appears to be hyperbolic to observers who use objective time – the measurement of which isn't dependent upon biological systems and their inherent variability. Specifically, they made three assumptions:

1 Increment of psychological time is stochastic and auto-correlated (i.e., the internal clock is positive quadrant dependent).
2 Increment of psychological time is stationary.
3 Value discounting over psychological time is exponential.

Ray and Bossaerts performed both analytical proof and numeric simulation. When the auto-correlation of psychological time increments is reduced to 0, the discounting function becomes the classical exponential form; when the auto-correlation is non zero (e.g., 0.3), the discounting function becomes hyperbolic. Thus, hyperbolic discounting naturally emerges when psychological time advances in a self-correlated way – i.e., if the current increment is large, it's likely that the next increment is also large.

This explanation is quite interesting and unlike other subjective time-based models (e.g., Takahashi, 2005; Kim and Zauberman, 2009) in which psychological time is a concave function of physical time, the psychological time in this model is actually synchronized with the physical time on average. This is an important property because experiments have shown that while we have uncertainty in estimating time intervals, the average of our estimates is actually quite accurate (Church et al., 1994; Rakitin et al., 1998; Buhusi and Meck, 2005).

On the other hand, the representation of psychological time in this model does not follow the scalar property (or Weber's law) of timing and time perception, which has been demonstrated in numerous studies – including those involving optimal foraging (see Gibbon et al., 1984, 1997; Bateson, 2003 for reviews). The scalar property of interval timing means that the coefficient of variation of time estimates is a constant, thereby producing timescale invariance (Gibbon, 1977). Based on numeric simulation, the coefficient of variation in the Ray and Bossaerts (2011) model is decreasing over time.

Here we demonstrate that hyperbolic discounting can be shown to result from the scalar property of time perception alone, without the assumption of internal exponential discounting over time. In a nutshell, Weber's law states that the incremental amount of change required for a stimulus to be perceptually differentiated or noticeable is proportional to the current stimulus magnitude. Time perception is well known to abide by Weber's law across a wide range of durations (Buhusi and Meck, 2005; Grondin, 2010 – but see Lewis and Miall, 2009). We reason that if the change in duration is not noticeable, then the change of the corresponding reward value should not be noticeable either. Otherwise people can detect the difference of time based on the difference of value.

Let's assume that both the perception of value and time follow Weber's law with Weber fractions a and b, respectively. Imagine that a subject perceives the value of reward is V at time t. As time advances, the perceived value decreases. Consider a delay τ in time where the subject just perceives a noticeable change in time. With the scalar property of time perception, we have

$$\tau = bt$$

The delay also causes the perceived value to decrease. As the delay τ is a barely noticeable change, the change of value V, denoted as Δ, should also be barely noticeable (see **Figure 1**). That is:

$$\Delta = V(t) - V(t+\tau) = aV(t)$$

Combining the two equations together we get:

$$V(t) - V(t+bt) = aV(t)$$

We want to find an explicit form of $V(t)$ satisfying the above condition. One solution is:

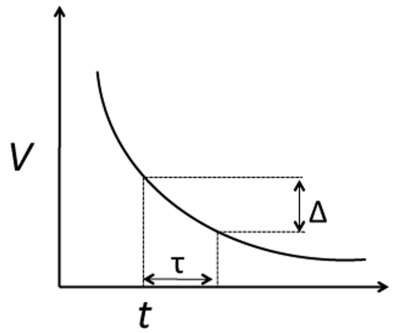

FIGURE 1 | A "just noticeable" change in time will result in a "just noticeable" change in the corresponding value.

$$V(t) = (1-a)^{\ln(t)/\ln(1+b)}$$

This discounting function is hyperbolic, as the discount rate, |dV/dt/*V*|, is a decreasing function of *t*. This model has two advantages: (1) the free parameters, *a* and *b*, have psychological meaning and can be independently measured – see Meck, 2006; (2) the model does not assume any form of discounting to start with. However, it should be emphasized that the assumptions made in this model, i.e., Weber's law in time and value perception, are only valid within certain time ranges. Particularly, in the sub-second range, time perception typically does not always follow Weber's law so clearly (see Gibbon, 1977; Grondin, 2010).

ACKNOWLEDGMENT

We thank Professor Warren Meck for his thoughtful comments and thorough revisions.

REFERENCES

Bateson, M. (2003). "Interval timing and optimal foraging," in *Functional and Neural Mechanisms of Interval Timing*, ed. W. H. Meck (Boca-Raton, FL: CRC Press), 113–141.

Buhusi, C. V., and Meck, W. H. (2005). What makes us tick? Functional and neural mechanisms of interval timing. *Nat. Rev. Neurosci.* 6, 755–765.

Church, R. M., Meck, W. H., and Gibbon, J. (1994). Application of scalar timing theory to individual trials. *J. Exp. Psychol. Anim. Behav. Process.* 20, 135–155.

Dasgupta, P., and Maskin, E. (2005). Uncertainty and hyperbolic discounting. *Am. Econ. Rev.* 95, 1290–1299.

Farmer, J. D., and Geanakoplos, J. (2009). *Hyperbolic Discounting is Rational: Valuing the Far Future with Uncertain Discount Rates.* Cowles Foundation Discussion Paper No. 1719. Available at http://ssrn.com/abstract=1448811

Frederick, S., and Loewenstein, G. (2002). Time discounting and time preference: a critical review. *J. Econ. Lit.* 40, 351–401.

Gibbon, J. (1977). Scalar expectancy theory and Weber's law in animal timing. *Psychol. Rev.* 84, 279–325.

Gibbon, J., Church, R. M., and Meck, W. H. (1984). Scalar timing in memory. *Ann. N. Y. Acad. Sci.* 423, 52–77.

Gibbon, J., Malapani, C., Dale, C. L., and Gallistel, C. R. (1997). Toward a neurobiology of temporal cognition: advances and challenges. *Curr. Opin. Neurobiol.* 7, 170–184.

Grondin, S. (2010). Timing and time perception: A review of recent behavioral and neuroscience findings and theoretical directions. *Atten. Percept. Psychophys.* 72, 561–582.

Kim, B. K., and Zauberman, G. (2009). Perception of anticipatory time in temporal discounting. *J. Neurosci. Psychol. Econ.* 2, 91–101.

Lewis, P. A., and Miall, R. C. (2009). The precision of temporal judgement: milliseconds, many minutes, and beyond. *Philos. Trans. R. Soc. Lond. B Biol. Sci.* 364, 1897–1905.

Meck, W. H. (2006). Neuroanatomical localization of an internal clock: A functional link between mesolimbic, nigrostriatal, and mesocortical dopaminergic systems. *Brain Res.* 1109, 93–107.

Rakitin, B. C., Gibbon, J., Penney, T. B., Malapani, C., Hinton, S. C., and Meck, W. H. (1998). Scalar expectancy theory and peak-interval timing in humans. *J. Exp. Psychol. Anim. Behav. Process.* 24, 15–33.

Ray, D., and Bossaerts, P. (2011). Positive temporal dependence of the biological clock implies hyperbolic discounting. *Front. Neurosci.* 5:2. doi: 10.3389/fnins.2011.00002

Sozou, P. D. (1998). On hyperbolic discounting and uncertain hazard rates. *Proc. R. Soc. Lond. B Biol. Sci.* 265, 2015–2020.

Takahashi, T. (2005). Loss of self-control in intertemporal choice may be attributable to logarithmic time-perception. *Med. Hypotheses* 65, 691–693.

Received: 16 May 2011; accepted: 21 May 2011; published online: 06 June 2011.

Citation: Cui X (2011) Hyperbolic discounting emerges from the scalar property of interval timing. Front. Integr. Neurosci. 5:24. doi: 10.3389/fnint.2011.00024

frontiers in
INTEGRATIVE NEUROSCIENCE

ORIGINAL RESEARCH ARTICLE
published: 17 October 2011
doi: 10.3389/fnint.2011.00062

Effects of accuracy feedback on fractal characteristics of time estimation

***Nikita A. Kuznetsov*[1]* and *Sebastian Wallot*[2]**

[1] *Perceptual-Motor Dynamics Laboratory, Department of Psychology, CAP Center for Cognition, Action and Perception, University of Cincinnati, Cincinnati, OH, USA*
[2] *Department of Psychology, CAP Center for Cognition, Action and Perception, University of Cincinnati, Cincinnati, OH, USA*

Edited by:
Warren H. Meck, Duke University, USA

Reviewed by:
Warren H. Meck, Duke University, USA
Espen Alexander Fürst Ihlen, Norwegian University of Science and Technology, Norway

***Correspondence:**
Nikita A. Kuznetsov, Perceptual-Motor Dynamics Laboratory, Department of Psychology, CAP Center for Cognition, Action and Perception, University of Cincinnati, Cincinnati, OH, USA.
e-mail: kuznetna@mail.uc.edu

The current experiment investigated the effect of visual accuracy feedback on the structure of variability of time interval estimates in the continuation tapping paradigm. Participants were asked to repeatedly estimate a 1-s interval for a prolonged period of time by tapping their index finger. In some conditions, participants received accuracy feedback after every estimate, whereas in other conditions, no feedback was given. Also, the likelihood of receiving visual feedback was manipulated by adjusting the tolerance band around the 1-s target interval so that feedback was displayed only if the temporal estimate deviated from the target interval by more than 50, 100, or 200 ms respectively. We analyzed the structure of variability of the inter-tap intervals with fractal and multifractal methods that allow for a quantification of complex long-range correlation patterns in the timing performance. Our results indicate that feedback changes the long-range correlation structure of time estimates: Increased amounts of feedback lead to a decrease in fractal long-range correlations, as well to a decrease in the magnitude of local fluctuations in the performance. The multifractal characteristics of the time estimates were not impacted by the presence of accuracy feedback. Nevertheless, most of the data sets show significant multifractal signatures. We interpret these findings as showing that feedback acts to constrain and possibly reorganize timing performance. Implications for mechanistic and complex systems-based theories of timing behavior are discussed.

Keywords: time estimation, 1/*f* noise, multifractal, accuracy feedback, embodied cognition

INTRODUCTION

Human performance on virtually all tasks exhibits variability from trial to trial (Bernstein, 1967). Studying the variability of human performance provides a window into the organization of perceptual-motor (Riley and Turvey, 2002), motor (Slifkin and Newell, 1998), and cognitive systems (Van Orden et al., 2011). One of the first attempts to understand the nature of variability of discrete human movements was made by Wing and Kristofferson (1973) using tasks that required continuous estimation of a constant time interval by tapping the index finger. They hypothesized that two independent processes determine the inter-tap interval (ITI) at tap j (ITI_j) by the following relation:

$$\mathrm{ITI}_j = C_j + \left(D_j - D_{j-1}\right), \quad (1)$$

where C_j is a timing motor command from a central cognitive timer to the motor periphery that executes it with a neuromuscular delay (D_i) compounded with the delay on the previous tap. Both C and D were assumed to be independent, uncorrelated white noise processes. Because of the subtraction of the two motor delays from consecutive trials, their model predicted that a continuous sequence of temporal interval estimates should yield a negative lag-1 autocorrelation. This prediction was verified in studies of Vorberg and Wing (1996), as well as Wing (1980) for series of about 100 estimates (cf. Delignières and Torre, 2011).

However, Gilden et al. (1995) presented results that failed to corroborate this prediction in long-term continuous temporal estimation. In their study, participants first heard several examples of a temporal interval (ranging from 0.3 to 10 s) and then continued tapping at the presented pace until they had tapped 1000 times. Power spectral analysis of time series of ITIs revealed a pattern of long-range correlated variation called 1/*f* noise which possesses positive autocorrelation structure, not the negative lag-1 autocorrelation predicted by the Wing and Kristofferson's (1973) model. They extended the two-component model of Wing and Kristofferson by treating the cognitive timer (C) as a source of 1/*f* noise. Further studies confirmed the presence of positive long-range correlations in the ITIs through the use of autoregressive fractionally integrated moving average (ARFIMA) modeling (Lemoine et al., 2006). The finding was also replicated by Holden et al. (2011) and Kiefer et al. (2009). Processes with long-range correlations that conform to 1/*f* noise are statistical fractals because the larger patterns of variability repeat themselves on smaller scales (Brown and Liebovitch, 2010).

Most recently, Ihlen and Vereijken (2010) reported results that suggested that ITIs in continuous time estimation exhibit intermittent fluctuations – an even more intricate pattern of variability than what is expected from a fractal signal. Intermittency is a special kind of inhomogeneity of variance in time that manifests itself in periods of relatively low variability interspersed with periods of relatively high variability. Presence of intermittency implies that

different moments of the observed time series of ITIs require different fractal exponents – they are multifractal (Mandelbrot, 1997; Ihlen and Vereijken, 2010).

The current paper extends this line of work by studying the effects of different task constraints aimed at manipulating the strength of $1/f^{\alpha}$ noise in the ITI variability as well as examining related changes in multifractality of these response series. The strength of $1/f$ noise in cognitive measures is typically defined by the distance of the α exponent from the ideal pink noise ($\alpha = 1$). In the sections below, we first describe $1/f$ noise and multifractality in greater detail and then present our logic for the experimental hypotheses.

FRACTAL VARIABILITY IN COGNITIVE AND TIMING PERFORMANCE

$1/f$ noise is a specific kind of variability different in quality from random (white) noise – it is an example of a fractal structure because fluctuations of the measured quantity on large time scales are effectively repeated on smaller time scales (Holden, 2005; Brown and Liebovitch, 2010). This type of variability is frequently expressed in terms of Fourier decomposition: $1/f$ noise is characterized by a power–law relationship between the power (P) and frequency (f) content of the time series of the type $P = 1/f^{\alpha}$ on a log–log plot (Eke et al., 2000, 2002; Holden, 2005). The scaling exponent α identified in a variety of tasks of cognitive psychology lies typically between 0 and 1 – the range of fractional Gaussian noise. However, α is usually close to 1. $1/f^{\alpha}$ noise processes with $\alpha = 1$ are termed pink noise. Pink noise has been found in numerous measurements of human performance (Gilden, 2001) as well as in many other biological signals (Werner, 2010).

The observation of $1/f$ noise in cognitive performance spurred a debate about its significance not only for timing, but also for cognition and psychological measurement in general (Van Orden et al., 2003, 2005, 2010; cf. Wagenmakers et al., 2004, 2005; Torre and Wagenmakers, 2009). Currently, there are two major perspectives on the occurrence of $1/f$ noise in cognitive measurements (Diniz et al., 2010). From the *mechanistic* perspective, this kind of noise is simply a statistical characteristic of the observed data that should be incorporated into already existing models of interval timing by assigning it to one of the components in these models (e.g., Delignières et al., 2008; Torre and Delignières, 2008), effectively expanding the models' error terms. From the *complexity* perspective, the appearance of $1/f$ noise suggests that the cognitive system maintains itself in a state of criticality similarly to other physical systems (Bak, 1996; Jensen, 1998). From this perspective, there is no particular cognitive component that causes $1/f$ noise to occur – instead it is an emergent property that stems from the interactions across the many spatio-temporal scales of organization of an organism – it is a signature of interaction-dominant dynamics (Van Orden et al., 2003, 2005). The defining characteristic of this view is that the interactions among the components play a greater role in explaining the behavior than the dynamics of individual components themselves (Turvey, 2007, p. 690). From the perspective of interaction–dominance the idea of an independent central timer would be an oversimplification, since timing behavior is the result of the inextricable interaction between the participant and the environmental regularities. This debate about the organization of cognition as component- or interaction-dominant mirrors the debate about the organization of timing as being either event-based or continuous (see Schöner, 2002) – and the interpretation of the role of $1/f$ noise lies at its center.

Initially, many measured signals such as heart rate (Ivanov et al., 1999), human gait (West and Scafetta, 2003), and simple response tasks (Ihlen and Vereijken, 2010) were thought to be a monofractal $1/f$ noise but have recently been reclassified as multifractal – the variability in these signals cannot be fully accounted for by a single scaling exponent α. Multifractality in a time series can either due to due to very heavy tail of the distribution of responses, generating many instances of high magnitude values, due to the temporal sequences in which periods of low variability are irregularly interspersed with periods of relatively high variability, or due to a combination of the two (Kantelhardt et al., 2002). Mandelbrot (1997) pointed out that monofractal analysis based on Fourier power spectrum decomposition is "blind" to such dynamics because it assumes a single stable scaling relation between the frequency and magnitude of fluctuations. Continuation tapping seems to exhibit a moderate degree of multifractality that is more pronounced in some participants than others (Ihlen and Vereijken, 2010).

We consider that proper experimental control over the α exponent in $1/f$-type fluctuations and of the magnitude of multifractality is the next challenge in understanding the long-term organization of timing behavior. We propose that thinking about different kinds of constraints imposed on the actor during temporal estimation tasks may provide a heuristic framework for the understanding of changes in the scaling exponents and potentially multifractal characteristics as well. Newell (1986) suggested that any behavioral performance results from the coordination between the degrees of freedom of the organism, constrained by the intrinsic characteristics of the actor (e.g., properties of the neuro-muscular apparatus), constraints of the task at hand, and the environment (Newell, 1986). Within the continuous time estimation paradigm, we reasoned that accuracy feedback about every produced time estimate is a kind of task constraint that limits the possible coordination patterns of the actor during behavioral performance. In the case of continuous time interval estimation, accuracy feedback constrains the participant's timing responses so that they remain closer to the level of the target interval required by the task instructions. Certain responses that would result in a greater deviation from the target interval become less likely – the range of possible behaviors is narrowed through feedback. Thus, the observed final behavior is a result of the coordination of the degrees of freedom available to the participant under the given constraints from the neuro-muscular system, task, and the environment.

EXPERIMENT AND HYPOTHESES

The specific aim of this experiment was to test the effects of increasing external constraints on the long-term structure of responses in continuous time interval estimation. We manipulated external task constraints by changing the likelihood of receiving accuracy feedback about the produced temporal estimates. This manipulation has been used in previous studies of classical scalar timing models (Wearden and McShane, 1988) and seems to affect the magnitude of response variability. This suggests that participants

may employ different strategies for interval estimation depending on such external constraints. However the effects of this feedback manipulation on the long-range correlation or multifractal structure of the temporal estimates have not been investigated.

Continuous time estimation without feedback produces the clearest and strongest signatures of $1/f^{\alpha}$ noise as compared to a variety of other cognitive tasks (Kello and Van Orden, 2009; Holden et al., 2011). Perhaps this is so because the time estimation task typically places only minimal constraints on the actor (Gilden, 2001). Since unperturbed temporal estimation has been found to yield $1/f$ noise, we expected that the no-feedback condition in our experiment would similarly reveal a clear signature of $1/f$ noise. Accuracy feedback constitutes a source of constraint and perturbation to the performance dynamics of time estimation and more frequent feedback should result in increasingly perturbed dynamics quantified by α (Kloos and Van Orden, 2010; Holden et al., 2011; Van Orden et al., 2011). Thus, we expected that the time series of ITIs with full accuracy feedback delivered on every trial would be closer to white noise ($\alpha = 0$) as compared to the estimates produced without feedback. In addition, we manipulated the likelihood of receiving feedback by changing the tolerance thresholds for feedback delivery centered on the 1-s target interval. In different conditions, accuracy feedback was provided if participants over- or under-estimated the 1-s interval by either 50, 100, or 200 ms. Trial-by-trial feedback of this kind will be unsystematic as it is contingent on the irregular trial performance itself. A higher tolerance for deviation (e.g., $\pm$200 ms) leads to fewer occurrences of feedback and therefore constitutes a less frequent source of perturbation. Lower tolerance (e.g., $\pm$50 ms) should lead to more frequent trial perturbations and progressively whiter, more uncorrelated performance (α closer to 0).

Our secondary goal was to provide preliminary evidence for the effects of external task constrains on the multifractal characteristics of long-term behavioral responses using the methodological framework for multifractal analysis of cognitive measurements proposed by Ihlen and Vereijken (2010). First, we quantified the effects of task constraints on the local α exponent of the ITI time series, $\alpha(t)$, that was calculated from wavelet variance. If feedback acts as a constraint on the changing scaling properties of the time estimates, then it could be expected that $\alpha(t)$ would fluctuate less with frequent accuracy feedback deliveries because this constraint favors a stable organization of behavior with respect to the task and could be accomplished by simple error correction. Second, we estimated the multifractal spectrum of scaling exponents – a generalization of $1/f^{\alpha}$ power–law to higher moments of variability of response series (Ihlen and Vereijken, 2010). The prediction that more frequent feedback perturbations will yield whiter $1/f$ signals has not been extrapolated to multifractal analysis – it is hard to visualize how higher moments of the variability might behave under such circumstances. Typically multifractals show intermittency where the magnitude of the variability of the dependent variable changes over time (Ihlen and Vereijken, 2010). Larger width of the multifractal spectrum suggests presence of stronger intermittency – greater differences between the relatively quiescent and variable periods of the performance. We did not have specific expectations about changes in the multifractal spectrum width with respect to the task constraints. On the one hand, multifractality may decrease with more frequent feedback because participants will be able to make more precise and systematic corrections, effectively eliminating inhomogeneities in the variability of timing. On the other hand, even with frequent feedback, participants may show local periods where they are producing more variable temporal estimates at some times during task performance. Accordingly, our goal was to provide an initial insight into the relationship between accuracy feedback and multifractality during time estimation.

MATERIALS AND METHODS

PARTICIPANTS

Six undergraduate students (two male, four female) participated in the experiment and were compensated with $5 per session. Five were students of the University of Cincinnati and one was an acquaintance of the authors. The mean age was 21.2 years, ranging from 19 to 27 years. The IRB of the University of Cincinnati approved the study.

PROCEDURE

Participants listened to 20 metronome beats of the 1-s interval to be estimated and then immediately began performing the time estimation task. Participants were asked to press the keyboard space bar each time they thought a 1-s interval had passed for a total of 1050 interval estimates. The task was performed without breaks and took approximately 20 min. There were five conditions that every participant completed on five separate days: Time estimation without any accuracy feedback, with feedback only if the response exceeded either the 200, 100, or 50-ms band around the 1-s target interval, and with feedback after every trial. The order of the conditions was counterbalanced as a Latin square between participants. The condition without the accuracy feedback was similar to continuation tapping experiments conducted before (Gilden et al., 1995; Chen et al., 2002; Wagenmakers et al., 2004; Torre and Delignières, 2008). In the accuracy feedback condition, participants saw visual feedback specifying the error of their current time estimate in milliseconds. For example, if a participant hit the space bar 250 ms after 1 s had passed since the previous press, feedback on the screen would read "250 ms late." Participants wore noise-reducing headphones to minimize distractions. However, they were able to hear the sound of their own button presses.

MATERIALS AND EQUIPMENT

We used the Psychophysics Toolbox for Matlab (Brainard, 1997) to collect the time of each key press during the experiment. Time estimates were recorded from the presses of the spacebar of a millisecond-accurate keyboard (Apple A1048, Empirisoft). We defined one time interval estimate (ITI) as the time from the beginning of one space bar press to the next one.

DATA ANALYSIS

Monofractal analysis

We conducted power spectral density (PSD) analysis using Welch's windowed method (Matlab's "pwelch" function) to examine changes in the monofractal structure of variability of ITIs. We

first removed any time interval estimates lower than 200 ms and greater than 2000 ms because these are likely to be spurious presses not related to 1-s interval estimation[1]. We also removed linear and quadratic trends from the data to avoid classifying a given time series that merely exhibited a simple trend as fractal. The number of removed data points across all participants and conditions ranged from 2 to 8 with a median of 3.5 per trial. Participant 4 had more trials removed compared to other participants (range 15–52; median 16) because he frequently pressed the response key faster than 200 ms.

Power spectral density was applied to the time series of ITIs using a 128-point Hamming window with 50% overlap and 128-point NFFT Fourier transform length. We calculated the slope of the linear relationship between the log-transformed frequency and log-transformed power of the signal for up to 1/4 of the total number of estimated frequencies as a measure of the spectral scaling exponent α (the absolute value of the slope was computed). Only the lowest 25% of the frequencies were used because the scaling relation typically breaks down at frequencies higher than that in continuation timing data (Lemoine et al., 2006). Slopes (α) close to 1 suggest the presence of long-range correlated $1/f^{\alpha}$ noise. Slopes close to 0 indicate uncorrelated (white) noise.

Wavelet variance PSD estimate: α(t)

We calculated the trial-dependent changes in the scaling exponent $a(t)$ using the methodology proposed by Ihlen and Vereijken (2010). The time series of the ITIs were first decomposed into a set of wavelet coefficients defined for a set of discrete dyadic scales ranging from 2 to 64 trials using the maximal overlap discrete wavelet transform (MODWT) with the eighth order least-asymmetric waveform (for a description of MODWT see Ihlen and Vereijken, 2010 or Percival and Walden, 2000). Then the variance of the wavelet coefficients at each scale was calculated in 100 trial windows over the length of the whole time series. Because wavelet scales are closely related to signal frequencies, the estimate of wavelet variance over the defined scales is frequently used as an alternative method to define the PSD function of the response series. Using this relation, a linear fit between $\log_{10}$(scale) and $\log_{10}$(wavelet variance) gave an estimate of the $\alpha(t)$ for a particular window. We used mGn_modwt_estim function from the toolbox developed by E. Ihlen to conduct this analysis[2].

Multifractal spectrum

Multifractal spectrum provides an additional insight into the nature of changes in the scaling exponent. The MODWT-based method to estimate $\alpha(t)$ described above assumes that $\alpha(t)$ changes smoothly over the trials, whereas the analysis of multifractality in terms of the multifractal spectrum assumes that $\alpha(t)$ is a random variable defined by its distribution. Both analyses are therefore complimentary because they give some idea about the variability in the fractal properties. We followed the methodological framework for multifractal analysis described in Ihlen and Vereijken (2010) to estimate the multifractal spectrum of the ITIs. We used the continuous wavelet transform (CWT) to analyze ITI variability (for a description of CWT see Percival and Walden, 2000). A Morlet wavelet (wavenumber 6) at scales corresponding to a range of 2 to 64 trials was chosen for the mother wavelet. The spacing between the resolved scales was set to 1/16 of a trial. **Figure 1B** provides an example of the CWT of one of the time series recorded in the experiment in the no-feedback condition (**Figure 1A**). We then calculated the log-transformed average of the absolute wavelet coefficients for each wavelet scale Δt across the duration of all trials to estimate the linear scaling relation (ζ) between $\log_2$(average wavelet coefficient at scale Δt) and $\log_2(\Delta t)$. Using an additional parameter q, one can emphasize smaller or larger wavelet coefficients by raising each one of them present at a Δt scale to the q-th power to obtain a general function $\zeta(q)$ specifying the range of scaling exponents between $\log_2$(average wavelet coefficient at scale Δt) raised to the power of q and $\log_2(\Delta t)$. We used q-values in the range 0.1–3. The results of these calculations are plotted in **Figure 1C**.

As a last step, we calculated the multifractal spectrum using the $\zeta(q)$ results. The Hölder exponent h and the multifractal spectrum $D(h)$ were obtained through the Legendre transformation of:

$$\begin{aligned} h &= \frac{d\zeta(q)}{dq} \\ D(h) &= qh - \zeta(q). \end{aligned} \tag{2}$$

The width $h_{\max} - h_{\min}$ of the multifractal spectrum $D(h)$ defines the amplitude difference between the variability in the intermittent and in the laminar periods of the observed time series (see **Figure 1D**; Ihlen and Vereijken, 2010). If $h_{\max} - h_{\min}$ is close to zero, then the time series can be assumed to be monofractal (intermittent periods are absent). On the other hand, if $h_{\max} - h_{\min}$ is greater than zero, then the time series may be multifractal. Larger $h_{\max} - h_{\min}$ are associated with a greater degree of multifractality.

Two types of comparisons are of interest when the multifractal spectrum of time estimation data is computed. The first type of comparison is whether the width of the multifractal spectrum ($h_{\max} - h_{\min}$) changes with the application of accuracy feedback. The second type of comparison is the surrogate analysis, where the multifractal spectrum of the time series of ITIs with the original ordering is compared to the same time series with randomized ordering of the data points. Ihlen and Vereijken (2010) proposed to conduct surrogate tests to distinguish between multifractality due to multiplicative interactions between temporal scales and multifractality due to $1/f^{\alpha}$ power–law and a non-Gaussian probability density function. To test whether observed multifractal structure is not just a function of the power spectrum and the probability density, we shuffled the phases of the time series of temporal estimates while their probability density function and scaling relation (α) were kept constant using the inverse amplitude-adjusted Fourier transform (IAAFT; Ihlen and Vereijken, 2010). We generated 30 such surrogate data series for each response time series

[1]There are guidelines for outlier removal when using monofractal analyses (Holden, 2005). Removal of outliers according these criteria obscures the degree of intermittent structure in the performance leading to a sharp decrease in the range of multifractality (i.e., markedly less pronounced intermittency). Therefore, we attempted to minimize the number of removed observations.

[2]www.ntnu.edu/inm/geri/software

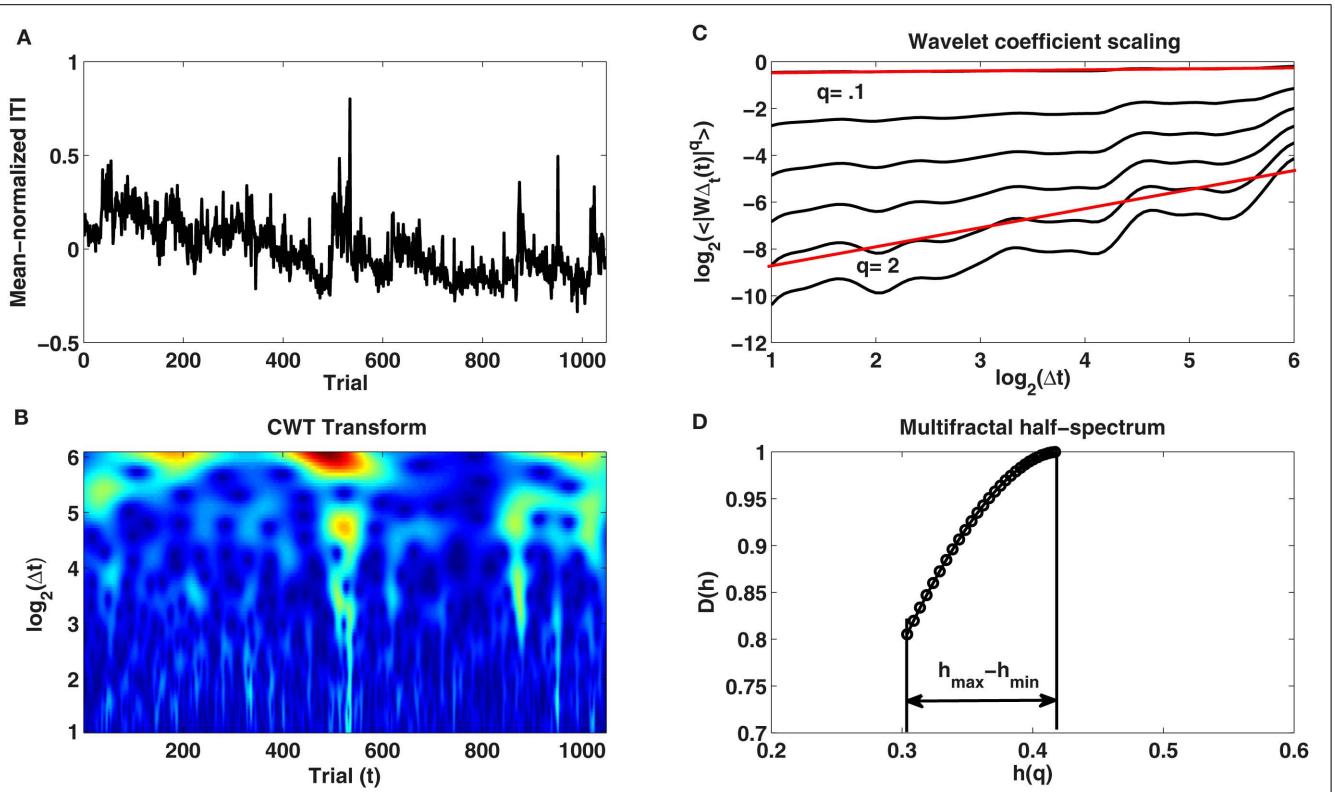

FIGURE 1 | (A) Shows the time series of mean-normalized inter-tap intervals produced by participant 3 in the no-feedback condition over the 1048 trials. **(B)** Illustrates the continuous wavelet transform (CWT) of this ITI time series for scales Δt ranging from 2 to 64 trials. **(C)** Depicts the linear relationship between the averaged absolute wavelet coefficients $<|W_{\Delta t}(t)|^q>$ calculated across trials (t) at each scale (Δt) and different wavelet scales (Δt) on log–log plot for different q-values (see text). **(D)** Shows the multifractal spectrum $D(h)$ and its width ($h_{max} - h_{min}$) estimated with the CWT.

of the experiment. Multifractality due to multiplicative interactions between the time scales of time estimates (phase couplings between the scales) is present when the observed multifractal spectrum ($h_{\max} - h_{\min}$) is greater than the 95% confidence interval calculated from the $h_{\max} - h_{\min}$ of the surrogates. If the observed spectrum is within or below the 95% confidence interval then the observed time series is either monofractal or multifractal due to a broad non-Gaussian distribution of response times. Such broad distribution is indicative of singular outlying events that introduce inhomogeneity of variance as opposed to intermittent periods of lower and higher variability. Monofractality is only present if the 95% confidence interval and the observed $h_{\max} - h_{\min}$ are close to zero. This analysis was conducted using the functions from the multifractal analysis toolbox developed by E. Ihlen[3].

RESULTS

FREQUENCY OF ACCURACY FEEDBACK

The frequency of received accuracy feedback changed reliably between the five conditions, $F(4, 20) = 184.75$, $p < 0.001$. In the full-feedback condition, participants received feedback on every trial (100.0%), and in the no-feedback condition, participants received feedback on none of the trials (0.0%). In the three conditions between full-feedback and no-feedback, participants received feedback on 50.3% (SD = 15.6%) of the trials with a 50-ms window around the target interval, 24.3% (SD = 8.0%) of the trials with a 100-ms window around the target interval, and 4.5% (SD = 4.2%) of the trials with a 200-ms window around the target interval.

AVERAGE INTERVAL LENGTH AND SD OF TIME ESTIMATION

Table 1 shows the average time intervals estimated, as well as the average SD of interval estimates, for each condition. A repeated-measures ANOVA revealed differences in the average time interval estimation due to differences in the feedback condition, $F(4, 20) = 3.69$, $p < 0.05$. Planned contrasts revealed that the no-feedback condition led to relatively faster estimates than all other conditions. There was no difference in the average SD of time interval estimation due to differences in the frequency of feedback received, $F(4, 20) = 0.76$, $p = 0.56$.

MONOFRACTAL CHARACTERISTICS OF TIME ESTIMATION

The overall time estimate data are presented in **Figure 2** and the results of power spectral analysis of these data are given in **Figure 3**. A repeated-measures ANOVA revealed that scaling exponents changed from values close to idealized pink noise to values closer to idealized white noise the more often participants received feedback, $F(4, 20) = 5.07$, $p < 0.01$. Within-participant contrasts

[3]www.ntnu.edu/inm/geri/software

revealed a roughly linear increase in α exponents with as the amount of feedback received decreased, $F(1, 5) = 18.18$, $p < 0.01$.

CHANGES IN $\alpha(t)$

A repeated-measures ANOVA showed that the range of the scaling exponents $\alpha(t)$ differed across the feedback conditions, $F(4, 20) = 5.87$, $p < 0.01$ (see **Figure 4**). *Post hoc* corrected t-tests showed that the range of variability of $\alpha(t)$ during time estimation without feedback was greater than in all feedback conditions which were similar to one another ($p > 0.05$).

MULTIFRACTAL SPECTRUM

We were interested in whether the width of the multifractal spectrum differed between the different feedback conditions and whether there were differences in the width of the multifractal spectrum between the original time series and their phase-shuffled surrogates. A repeated-measures ANOVA revealed no differences in the width of the multifractal spectrum among feedback conditions, $F(4, 20) = 0.66$, $p = 0.62$. To investigate differences between the original time series data and their surrogates, we counted the number of observed multifractal widths that were larger than the 95% confidence interval of the phase-shuffled surrogates as an indication of multifractality due to interaction of processes across the different time scales examined in the wavelet analysis. There were 22 such response series. We also counted the number of cases falling within the 95% confidence interval, as well as the number of cases that lay outside of the 95% confidence interval but close to zero multifractal width ($h_{max} - h_{min}$). There were six series in the former group and only two in the latter (participant 4 full-feedback; participant 2 50 ms feedback). These individual results are illustrated in **Figure 5**. Overall group results averaged over all feedback conditions are presented in **Figure 6** together with the multifractal spectra for the simulated ideal white and pink noises.

There was no significant Pearson correlation between the $h_{max} - h_{min}$ and the scaling exponents α ($r = 0.12$, $p = 0.50$). We also examined correlation with the high frequency slope (highest 75% of the frequencies) and found no correlation as well ($r = -0.11$, $p = 0.53$).

Table 1 | Averages and average SD of time interval estimates.

Feedback	Average intervals	Average SD
Full (100.0%)	971 ms (SD = 45 ms)	89 ms (SD = 30 ms)
50 ms window (50.3%)	988 ms (SD = 22 ms)	89 ms (SD = 25 ms)
100 ms window (24.3%)	973 ms (SD = 15 ms)	88 ms (SD = 7 ms)
200 ms window (4.2%)	982 ms (SD = 45 ms)	90 ms (SD = 20 ms)
No (0.0%)	921 ms (SD = 73 ms)	104 ms (SD = 32 ms)

DISCUSSION

The presented experiment examined the role of environmental task constraints in the form of accuracy feedback on the organization of long-term the pattern of ITI in repetitive timing behavior. We manipulated the likelihood of receiving accuracy feedback for participants and interpreted this as a measure of the strength

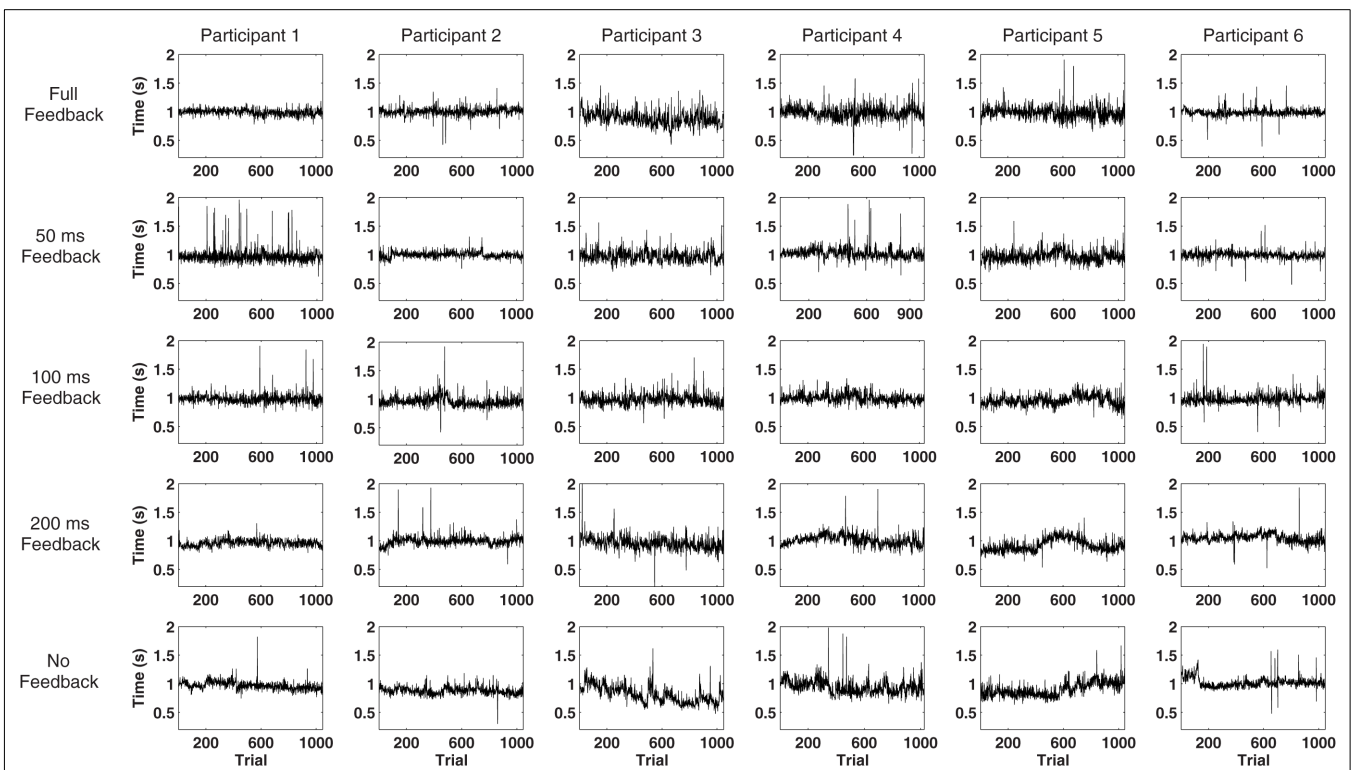

FIGURE 2 | Illustration of the individual response series in each one of the experimental conditions.

of the external constraints on their performance. More frequent instances of accuracy feedback were hypothesized to result in a greater constraint on the task performance and to decrease the strength of the long-range correlations in the series of estimated time intervals. Results of the PSD analysis showed that spectral exponents α in all conditions were in the range of fractional Gaussian noises ($0 < \alpha < 1$), but were closest to 1 when no feedback was provided (in line with Gilden et al., 1995; Delignières et al., 2004; Lemoine et al., 2006). However, when participants were given accuracy feedback on each trial, the structure of variability of the time estimates moved closer to uncorrelated white noise. In general,

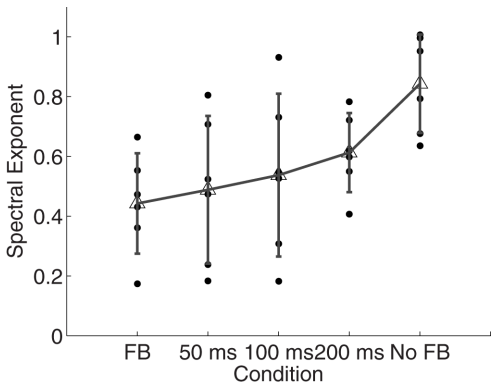

FIGURE 3 | Spectral exponents of the time estimates. Spectral exponents α closer to 0 imply presence of white noise whereas values closer to 1 suggest pink noise. Individual points represent observations from individual participants. Error bars plot within-condition SD.

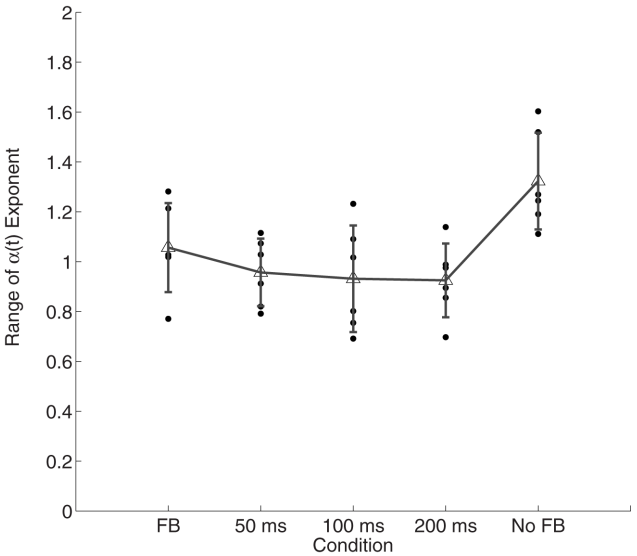

FIGURE 4 | Range of variability in $\alpha(t)$ as function of accuracy feedback. Individual points represent observations from individual participants. Error bars plot within-condition SD.

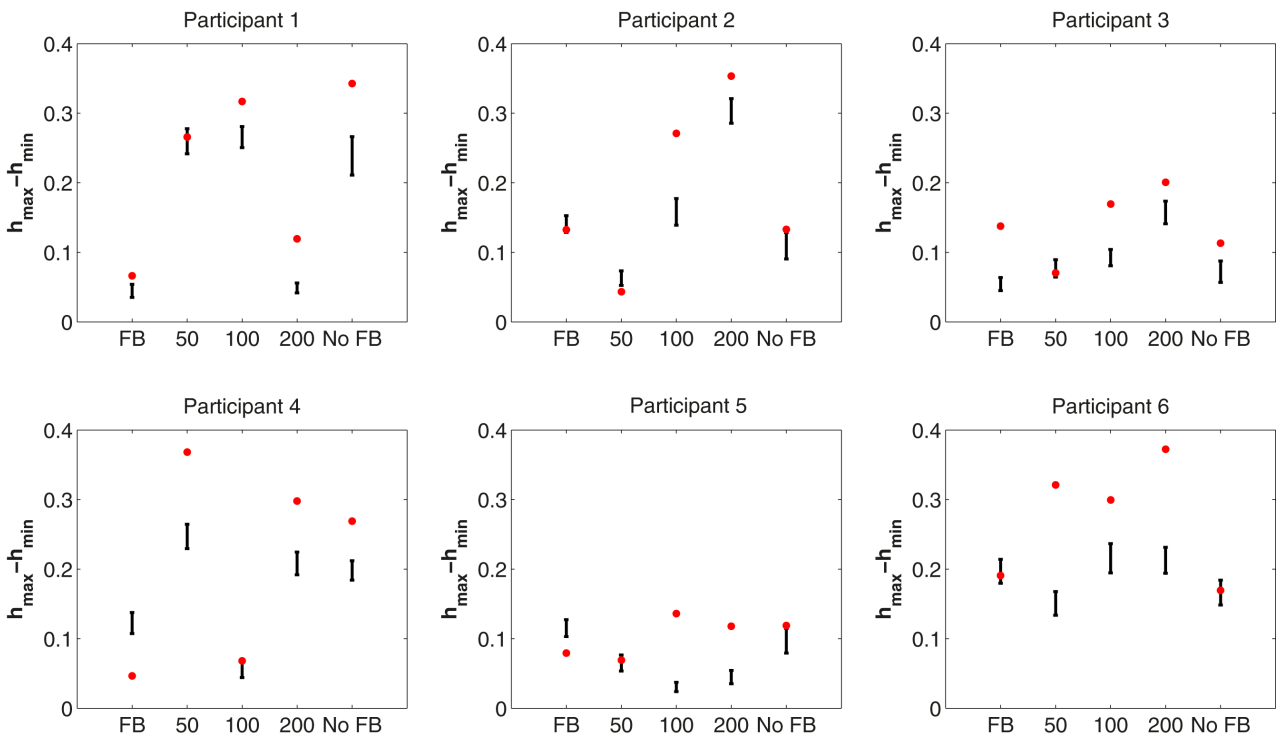

FIGURE 5 | Results from the multifractal analysis of ITI response series for each participant and each condition. The width of the multifractal spectrum width ($h_{max} - h_{min}$) is shown by a red dot. Ninety-five percentage confidence interval for the 30 surrogate time series from each response series is illustrated. Multifractal spectrum width for a pure simulated $1/f$ noise without phase couplings is close to zero.

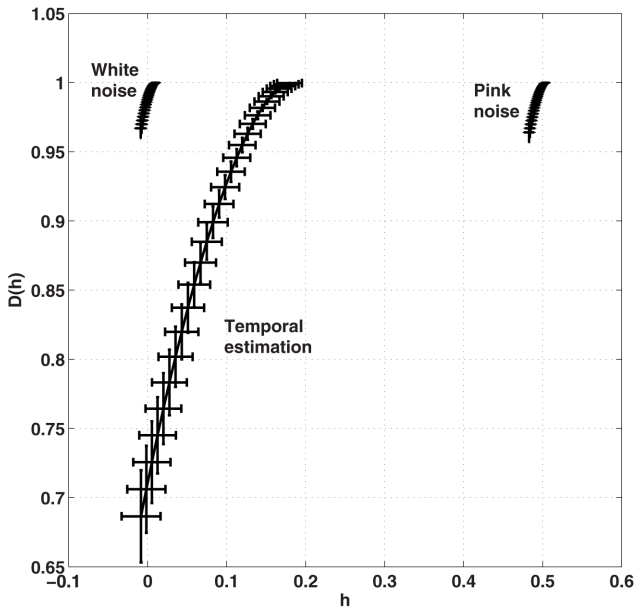

FIGURE 6 | Average multifractal width of the ITIs averaged across all participants and all conditions is presented in Figure 5. Results of the multifractal analysis of the simulated $1/f$ noises ($\alpha = 0$; white noise and $\alpha = 1$; pink noise) are provided for a comparison with the multifractal width of the observed time series of ITIs. Horizontal and vertical error bars indicate SE across 30 experimental response series and 30 simulations of each noise process, respectively.

spectral exponents progressively decreased with more stringent accuracy feedback. These findings corroborate the hypothesis that increased constraints on the performance may lead to a different organization of the control systems that underlie long-term timing behavior (Newell, 1986; Van Orden et al., 2011).

Furthermore, the variability of ITI was more complex than expected from a pure monofractal model in most of our participants. We considered two aspects of this complexity in relation to the feedback manipulation: slow changes in the local α exponent, $\alpha(t)$, and the different scaling regimes in the wavelet variance using the methodology of Ihlen and Vereijken (2010). We expected that more frequent accuracy feedback would decrease the shifts between different serial dependency regimes and but did not make any explicit predictions for the changes in the multifractal structure.

LOCAL α EXPONENT α(*t*)

We observed that the range of the $\alpha(t)$ exponent fluctuations was the greatest in the unconstrained temporal estimation, but sharply decreased as soon as any feedback was introduced. This finding suggests that a single scaling exponent may not be appropriate to characterize the variability of unconstrained time estimation – instead α appears to slowly fluctuate throughout the trial. Since changes in scaling properties are indicative of changes in the organization of behavior, participants in the no-feedback condition might have tapped into many more different modes of behavioral organization during the performance on a particular trial. Frequent feedback appears to have kept the participants' performance much more stable in that regard. Perhaps a less constrained task allowed participants to explore more modes of organization in the no-feedback condition during the time course of the task. Different modes of behavioral organization could lead to different locally constraining patterns on the performance, while transitions from one mode to another are effectively unstable periods. Feedback effectively delimits the number of modes that are explored, thereby delimiting the changes of the local $\alpha(t)$.

The concept of "behavioral organization" can also be interpreted in much broader terms than a change in the cognitive strategy. Maybe behavioral organization as indexed by changes of the $\alpha(t)$ exponent captures more subtle properties of changes in the activity of the neuro-muscular system of our participants. For example, Mikkelsen (unpublished dissertation) found that the resting state fMRI was not well characterized by a single Hurst exponent, but rather by an unstable, changing set of Hurst exponents. One interpretation of this finding could be that the resting state is not so much a single state in the sense of the word, but rather a constant drifting between multitudes of states as a by-product of the coordination patterns within the neural networks in the absence of strong environmental constraints. Likewise, in the relatively unconstrained no-feedback time estimation task, $\alpha(t)$ might similarly capture the constant need of coordinating the upkeep of performance with a simultaneous drift between states of neuronal activation, indexing a form of metastability (Kelso, 1995; Kello et al., 2010).

Since we did not observe a linear decrease in the range of fluctuations of the local Hurst exponent, but rather an abrupt drop in the range of variability in $\alpha(t)$ from the no-feedback condition to the conditions that contained feedback (see **Figure 4**), the slightest bit of information from the environment might have sufficed to tip this balance and qualitatively reorganize timing behavior and stabilize the range of available behavioral organizations. Nevertheless, it has to be noted that changes in persistent and anti-persistent fluctuations are more pronounced in almost all of the data sets – also those produced under feedback conditions – compared to what would be expected from a clear monofractal signal alone. However, whether this is a distinct property of the performance or simply a result of their multifractality cannot be conclusively answered.

MULTIFRACTAL SPECTRUM

In terms of the multifractal spectrum analysis, our results show that time estimation performance is more multifractal than suggested by Ihlen and Vereijken (2010) when they reanalyzed the data from the Wagenmakers et al. (2004) time estimation study. This could be due to the different outlier treatment procedures – their data did not have observations beyond 3 SD from the mean whereas we only eliminated very fast (<200 ms) and very slow (>2000 ms) responses. We also conducted the analysis with the removal of the outliers. In this case, the strength of multifractality was much weaker. However, we decided to keep the "outlying" trials because these would be legitimately expected if time estimation is an intermittent process.

There was no correlation between the scaling exponents α and the multifractal width suggesting that these indices are sensitive to different aspects of the timing performance. Intermittent dynamics were present in most of the time series recorded in this experiment. One interpretation is that the intermittency is

an intrinsic property of repetitive human performance that is not specifically affected by the local constraints of the task. There was no clear effect of accuracy feedback on the multifractal structure. The width of the multifractal spectrum was greater than what would be expected from a pure $1/f$ noise in 28 series out of 30 (the 95% confidence interval of $h_{max} - h_{min}$ of pure monofractals is in the range 0.032–0.036), but there was no change in the multifractal width ($h_{max} - h_{min}$) as a function of accuracy feedback. Surrogate analysis with phase-shuffled time series showed that 22 out of 30 response series revealed multifractal structure due to multiplicative interaction across scales (their obtained $h_{max} - h_{min}$ were greater than the IAAFT surrogates; see **Figure 5**). Six response series showed multifractality due to a broad probability density distribution (their obtained $h_{max} - h_{min}$ were within the 95% confidence interval of the IAAFT surrogates). Only two were monofractal (participant 4 full-feedback; participant 2 50 ms feedback).

What does the evidence of multiplicative interactions in more than half of the response series suggest? One tentative conjecture is that timing performance relies on a set of interdependent processes that concurrently operate across multiple time scales and mutually influence each other. This conjecture is based on the intuitions provided by the model of multiplicative cascades introduced into the cognitive literature by Ihlen and Vereijken (2010). We elaborate on this in the section on the possible organization of the timing system, but before that we would like to describe the mechanistic and complex systems account of cognitive function to discuss how our results fit into these two accounts, and where they seem to be problematic.

MECHANISTIC ACCOUNT

Mechanistic accounts of human timing behavior take a variety of forms: Shifting strategy models (Wagenmakers et al., 2004), error correction models (Pressing, 1998), or autoregressive models (Ward, 2002). What unites these different models is the aim to localize component effects that cause the observed timing behavior. In the case of timing behavior, mechanistic accounts have to plausibly localize the source of $1/f$ fluctuations in one or several encapsulated independent components within the nervous system (Diniz et al., 2010). A classic example of a mechanistic account is the model of discrete event timing by Wing and Kristofferson (1973) that we described in the introduction. The model postulates that there are two independent component processes in discrete event timing: Cognitive central timer and motor error. Gilden et al. (1995) extended this model by endowing the cognitive timer with the $1/f$ structure while keeping the source of motor error as differenced white noise. They argued that the spontaneous emergence of $1/f$ noise in the cognitive timer was due to complex non-linear interactions within the cognitive system. However, it is not immediately apparent why the principles of complex non-linear interaction do not similarly lead to the spontaneous emergence of $1/f$ in the motor system. This is especially puzzling because the movement system itself has been conceptualized as a complex interactive system (Kelso, 1995; Turvey, 2007) and also given that many motor tasks such as precision pointing (Wijnants et al., 2009) or walking on a treadmill (Hausdorff et al., 1996; cf. Delignières and Torre, 2009) show $1/f$ scaling as well. In our opinion, if one wants to make a strong case for localized mechanistic models of $1/f$ noise in human performance, there needs to be a reasonable set of principles for breaking the system into truly independent components and an additional set of principles to define why one independent part of the system would operate in a fractal or a non-fractal regime.

This criticism would apply to other mechanistic models as well. For example, another mechanistic modeling strategy is to capture the structure of temporal estimates by positing several *ad hoc* negative feedback processes with short term-correlations operating on different time scales (Madison and Delignières, 2009) – this model could probably mimic our monofractal results, but it would have to be *post hoc* parameterized anew, every time changes of the monofractal exponent occur (Van Orden et al., 2005; Kello et al., 2008). Thus, an additional theory about the parameterization of the model would be necessary as well. A third mechanistic model that could potentially apply is the model based on switching between time estimation strategies (Wagenmakers et al., 2004). The gist of the model is that participants use different time estimation strategies (counting silently, tapping foot, etc.) during the task; each employed strategy leads to a bout of short-range correlated measurements and strategies follow one another serially. Fewer strategy shifts could have occurred with more frequent feedback in our task. As the number of strategies decreases, the long-range correlations in the time series decrease. It is possible that the cognitive timer uses fewer time estimation strategies. However, as with the model of Madison and Delignières (2009), the re-parameterization problem would have to be solved first.

Mechanistic models seem to be paralleled by the hypothesis of fixed localization of function in the nervous system (Anderson, 2010, but see Diniz et al., 2010), where a single region in the brain encapsulates a specific function. For example, timing is typically said to result from the activity of distributed neuronal networks that act as a causal controller of the observed timing behavior. As new aspects of timing behavior are uncovered, the neural timer has to be enhanced with additional capabilities so as to explain the full complexity of timing behavior (Schöner, 2002). This also leads to additional mechanisms (added network members) that have to be considered in order to explain timing behavior more properly (Buhusi and Meck, 2009). This is why mechanistically oriented models of the nervous system functioning develop theoretically in the same way as the mechanistic psychological models we discussed. Their theoretical basis in the explanation of behavior by using a set of isolable, independent functions implemented in independent neuronal networks makes them natural travel companions.

Lastly, none of the listed mechanistic models in their current form can capture the observed multifractal structure (inhomogeneity of variance) of the time estimates because these models are based on independently contributing stationary processes (Ihlen and Vereijken, 2010). The complexity explanation (Van Orden et al., 2003, 2005) offers a different explanation of $1/f$ noise and multifractality in the time estimates.

COMPLEX SYSTEMS ACCOUNT

What separates the complex systems account from the mechanistic account is the reluctance to separate the system into independent

components. As we stated above, one needs to have a principled rule for the dissection of components – this is a formidable task in a functionally and anatomically integrated biological system. This problem disappears in the complex systems account because the components are not thought to be causal to behavior. Instead, the whole system can be treated as single entity that is organized and defined by complex non-linear interactions between the components. Presence of long-range correlations and multifractality are statistical features that might reflect coordination and metastability – two characteristic processes suggested as universally present in complex systems (Van Orden et al., 2003, 2005; Kello et al., 2007; Kello and Van Orden, 2009). From the complexity perspective, it is not possible to identify single components that propagate their influence via concatenated, additive, linear causal effects and suggests a different kind of thinking from the component-dominant dynamics in dealing with the cognitive system.

The complexity account would suggest that cognitive activity implicated in the timing behavior tends to spontaneously self-organize toward a state of criticality (Van Orden et al., 2003, 2005). Systems maintaining themselves in this state emit $1/f$ signals (Bak, 1996). Within this account the clearest $1/f$ noise signals are expected to appear when the behavioral measurement least interferes with the measured performance in experiments, because the system is allowed to reveal its own intrinsic dynamics. From the complexity perspective, weakening of the fractal pattern (lower α) with more extensive accuracy feedback most likely occurred due to the perturbation of the coupling between the intrinsic actor characteristics and the task demands. Natural behavioral tendencies of the neuro-muscular system can either be promoted or inhibited by the behavioral contingencies. In either case, the overall organization of the observed behavior that results from this interaction is likely to show different long-term fractal properties. Also, this coupling might be viewed as change in the state of response preparedness of the neuro-muscular system due to the change in neuronal activity via perception of feedback (Järvilehto, 1998).

One advantage of the explanation at this level is that similar general principles apply to a range of different phenomena in seemingly unrelated complex systems (West and Deering, 1995). For example, long-term measurements of stride lengths show $1/f$ patterns in normal walking, but become more uncorrelated with metronome pacing (Hausdorff et al., 1996). The same phenomenon appears in rhythmic movements while synchronizing with a metronome (Chen et al., 1997).

However, observation of $1/f$ noise is not strong enough evidence that the cognitive system works on the principles of self-organized criticality (SOC) because multiple processes not based on the SOC principle can mimic the presence of $1/f$ fluctuations (Wagenmakers et al., 2005; Torre and Wagenmakers, 2009; Ihlen and Vereijken, 2010). As such, our monofractal results do not speak to the idea that the timing system organized on the principles of SOC directly. However, we consider that SOC is a valuable heuristic framework of thinking about the overall organization of human behavior because it allows seeing commonalities between the dynamics of performance across many perceptual-motor and cognitive tasks (Kello et al., 2010). One additional positive feature of criticality at the neural level would be that it allows for a rapid propagation of signals in the nervous system (Linkenkaer-Hansen et al., 2001; Ihlen and Vereijken, 2010; Wallot and Van Orden, under review).

At the same time, there are some assumptions of the typical physical sand pile SOC models that do not fit the characteristic of biological systems. First, it is required that the events produced by the SOC systems are independent from one another in time (Aschwanden, 2011). If we consider events to be the observed behavioral outcomes (e.g., finger taps in our case), then clearly, all human behavior exhibits interdependencies between the produced events and therefore does not fit that assumption. Second, the power–law behavior emitted by the physical SOC systems is typically stationary in time, whereas the power–laws produced by living complex systems fluctuate. Even in our data we have observed the alpha exponent, $\alpha(t)$, to fluctuate in time for every participant; furthermore, the average α changed with the introduction of feedback. All these considerations suggest that biological systems show a higher level of complexity than one would expect from the simpler sand pile-type SOC systems. One possible reason is that the inputs to these physical SOC are typically assumed to be random, whereas biological systems usually do not receive randomly structured stimulation – they actively orient their perceptual systems to the behaviorally relevant aspects of the environment (Gibson, 1966; Järvilehto, 1998). There is computational evidence to suggest that changes in the input regime lead to different dynamics of the critical states of the sand pile surface (Zhang, 2000).

Additionally, what really seems to distinguish the biological SOC systems from their physical counterparts, such as piles of sand and rice, is their ability to change the relevant parameters of the interaction between the elements constituting the system (Kloos and Van Orden, 2010; Van Orden et al., 2011). Some of the early empirical studies examining the presence of the SOC behavior were conducted using grains of sand. The observed distribution of avalanches was only scale-invariant for small piles (80 grains and less) and lost its scale-invariant behavior due to the inertia of the sand, which favored large periodic avalanches – a behavior clearly different from the power–laws. However, later research using a different element – rice – found consistent evidence for the assembly of critical states and the consequent power–law behavior of the avalanches (Frette et al., 1996; summarized in Jensen, 1998). It may be that the inertia and the shape of the physical elements play a role of a control parameter in tuning an SOC system such that criticality becomes possible after some value of inertia, size, or their ratio, but that remains to be tested.

POSSIBLE ORGANIZATION OF THE TIMING SYSTEM

We observed a wide multifractal spectrum due to multiplicative interactions in 22 out of 30 response series of interval production by our participants. The multiplicative cascading model introduced by Ihlen and Vereijken (2010) can account for such empirical observations: Within the model, each individual measurement is a result of a multiplicative interaction between the processes operating at many time scales of the measured behavior. Based on the framework of thinking provided by this model, we conjecture that the timing system spans the boundary of the brain and body and non-trivially includes the environment – timing performance is embodied and situated (Järvilehto, 1998; Haselager et al., 2008) contra to the view that the timing system operates only at the neural level. A non-trivial interaction between the nervous system, the body and the environment entails that the neural activity only partially feeds into the structure of the variability

of temporal estimates and is not its sole determinant. The evidence for interaction-dominant multifractality suggests that the regularities found in the slower time scales of the task and environment matter essentially and that the structure of variability of the observed timing behavior most likely emerges as a property of the coordination among all these levels. At the neural level, there is coordination across multiple time scales of the neural firing patterns ranging from relatively slow alpha rhythms to very high frequency theta oscillations (Linkenkaer-Hansen et al., 2001; cf. Buzsaki, 2006). At the same time, there are oscillations occurring at the behavioral scales (such as heart beats and breathing) that are much slower than the neural fluctuations and also feed in to the subjective perception of time (Münsterberg, 1866; Stetson et al., 1992). The task regularities provide another constraint on the timing system (Jazaheri and Shadlen, 2010) and, of course, the environmental fluctuations on the order of day–night cycles also contribute (Block, 1990). Multifractality in the observed timing behavior therefore may be an expression of the coupling between these all these oscillations. As Castillo et al. (2011) put it: "The observed timing of physiology and behavior is an outcome of the coordination of the body, not the other way around."

CONCLUSION

This experiment examined the effect of accuracy feedback on the long-term correlation structure of the time interval estimates in the continuation time estimation task. We found that the degree of $1/f$ noise scaling decreased with accuracy feedback in a manner consistent with the complexity explanation of long-range correlations in cognitive measurements (Kloos and Van Orden, 2010). We also found that continuous time estimation with or without accuracy feedback contained multifractal structure that was in some response series due to the interaction across scales of the cognitive system and in other series due to the non-Gaussian distribution of the response times. The identification of multifractality shows that repeated time estimates possess a level of complexity that is not expected from previous componential models of timing that posit a single or a few fixed timing structures. Furthermore, our results show evidence that changes in feedback qualitatively alter timing performance suggesting that the overall organization of the timing behavior depends on the intrinsic dynamics of the body, task, and the environment.

ACKNOWLEDGMENTS

We thank Guy Van Orden and Michael Riley for helpful discussions of the manuscript. We would like to thank Espen Ihlen for the guidance on the multifractal analyses. We also would like to thank Anna Haussmann for proofreading the manuscript. Preparation of this article was supported by NSF grants to Guy Van Orden (BCS #0642716; BCS #0843133; DHB #0728743).

REFERENCES

Anderson, M. L. (2010). Neural reuse: a fundamental organizational principle of the brain. *Behav. Brain Sci.* 33, 245–313.

Aschwanden, M. (2011). *Self-Organized Criticality in Astrophysics: The Statistics of Nonlinear Processes in the Universe*. Berlin: Springer-Verlag.

Bak, P. (1996). *How Nature Works. The Since of Self-Organized Criticality*. New York, NY: Copernicus.

Bernstein, N. A. (1967). *The Co-Ordination and Regulation of Movements*. Oxford: Pergamon Press.

Block, R. A. (1990). "Models of psychological time," in *Cognitive Models of Psychological Time*, ed. R. A. Block (Hillsdale, NJ: Erlbaum), 1–35.

Brainard, D. H. (1997). The psychophysics toolbox. *Spat. Vis.* 10, 433–436.

Brown, C., and Liebovitch, L. (2010). *Fractal Analysis*. Los Angeles, CA: Sage.

Buhusi, C. V., and Meck, W. H. (2009). Relativity theory and time perception: single or multiple clocks? *PLoS ONE* 4, e6268. doi: 10.1371/journal.pone.0006268

Buzsaki, G. (2006). *Rhythms of the Brain*. New York, NY: Oxford University Press.

Castillo, R. D., Van Orden, G. C., and Kloos, H. (2011). "The embodiment of time estimation," in *Time and Time Perception 2010*, eds A. Vatakis, A. Esposito, M. Giagkou, F. Cummins, and G. Papadelis (Heidelberg: Springer-Verlag), 196–206.

Chen, Y., Ding, M., and Kelso, J. A. S. (1997). Long memory processes (1/fα type) in human coordination. *Phys. Rev. Lett.* 79, 4502–4504.

Chen, Y., Repp, B., and Patel, A. (2002). Spectral decomposition of variability in synchronization and continuation tapping: comparisons between auditory and visual pacing and feedback conditions. *Hum. Mov. Sci.* 21, 515–532.

Delignières, D., Lemoine, L., and Torre, K. (2004). Time intervals production in tapping and oscillatory motion. *Hum. Mov. Sci.* 23, 87–103.

Delignières, D., and Torre, K. (2009). Fractal dynamics of human gait: a reassessment of the 1996 data of Hausdorff et al. *J. Appl. Physiol.* 106, 1272–1279.

Delignières, D., and Torre, K. (2011). Event-based and emergent timing: dichotomy or continuum? A reply to Repp and Steinman (2010). *J. Mot. Behav.* 43, 311–318.

Delignières, D., Torre, K., and Lemoine, L. (2008). Fractal models for event-based and dynamical timers. *Acta Psychol. (Amst.)* 127, 382–397.

Diniz, A., Wijnants, M. L., Torre, K., Barreiros, J., Crato, N., Bosman, A. M. T., Hasselman, F., Cox, R. F. A., Van Orden, G. C., and Delignières, D. (2010). Contemporary theories of 1/f noise in motor control. *Hum. Mov. Sci.* 30, 889–905.

Eke, A., Herman, P., Bassingthwaighte, J. B., Raymound, G. M., Percival, D. B., Cannon, M., Balla, I., and Ikrenyi, C. (2000). Physiological time series: distinguishing fractal noises from motions. *Eur. J. Physiol.* 439, 403–415.

Eke, A., Herman, P., and Kozak, L. R. (2002). Fractal characterization of complexity in temporal physiological signals. *Physiol. Meas.* 23, R1–R38.

Frette, V., Christensen, Malthe-Sørenssen, A., Feder, J., Jøssang, T., and Meakin, P. (1996). Avalanche dynamics in a pile of sand. *Nature* 379, 49–52.

Gibson, J. J. (1966). *The Senses Considered as Perceptual Systems*. Boston: Houghton Mifflin.

Gilden, D. L. (2001). Cognitive emissions of 1/f noise. *Psychol. Rev.* 108, 33–56.

Gilden, D. L., Thornton, T., and Mallon, M. (1995). 1/f noise in human cognition. *Science* 267, 1837–1839.

Haselager, P., van Dijk, J., and van Rooj, I. (2008). "A lazy brain? Embodied embedded cognition and cognitive neuroscience," in *Handbook of Cognitive Science: An Embodied Approach*, eds P. Calvo and T. Gomila (Oxford: Elsevier), 273–287.

Hausdorff, J. M., Purdon, P. L., Peng, C.-K., Ladin, Z., Wei, J. Y., and Goldberger, A. L. (1996). Fractal dynamics of human gait: stability of long-range correlations in stride interval fluctuations. *J. Appl. Physiol.* 80, 1448–1457.

Holden, J. G. (2005). "Gauging the fractal dimension of response times from cognitive tasks," in *Contemporary Nonlinear Methods for Behavioral Scientists*, eds M. A. Riley and G. C. Van Orden, 267–318. Available at: http://www.nsf.gov/sbe/bcs/pac/nmbs/nmbs.jsp [Retrieved April 8, 2011].

Holden, J. G., Choi, I., Amazeen, P. G., and Van Orden, G. C. (2011). Fractal 1/*f* dynamics suggest entanglement of measurement and human performance. *J. Exp. Psychol. Hum. Percept. Perform.* 37, 935–948.

Ihlen, E. A. F., and Vereijken, B. (2010). Interaction-dominant dynamics in human cognition: beyond $1/f^{\alpha}$ fluctuation. *J. Exp. Psychol. Gen.* 139, 426–463.

Ivanov, P. C., Amaral, L. A. N., Goldberger, A. L., Havlin, S., Rosenblum, M. G., Struzik, Z. R., and Stanley, H. E. (1999). Multifractality in human heartbeat dynamics. *Nature* 399, 461–465.

Järvilehto, T. (1998). The theory of the organism-environment system: I. Description of the theory. *Integr. Physiol. Behav. Sci.* 33, 321–334.

Jazaheri, M., and Shadlen, M. N. (2010). Temporal context calibrates interval timing. *Nat. Neurosci.* 13, 1020–1026.

Jensen, H. J. (1998). *Self-Organized Criticality*. Cambridge: Cambridge University Press.

Kantelhardt, J. W., Zschiegner, S. A., Koscielny-Bunde, E., Havlin, S., Bunde, A., and Stanley, H. E. (2002). Multifractal detrended fluctuation analysis of nonstationary time series. *Physica A* 316, 87–114.

Kello, C. T., Anderson, G. G., Holden, J. G., and Van Orden, G. C. (2008). The pervasiveness of 1/f scaling in speech reflects the metastable basis of cognition. *Cogn. Sci.* 32, 1217–1231.

Kello, C. T., Beltz, B., Holden, J. G., and Van Orden, G. C. (2007). The emergent coordination of cognitive function. *J. Exp. Psychol. Gen.* 136, 551–568.

Kello, C. T., Brown, G. D. A., Ferrer-i-Cancho, R., Holden, J. G., Linkenkaer-Hansen, K., Rhodes, T., and Van Orden, G. C. (2010). Scaling laws in cognitive sciences. *Trends Cogn. Sci. (Regul. Ed.)* 14, 223–232.

Kello, C. T., and Van Orden, G. C. (2009). Soft-assembly of sensorimotor function. *Nonlinear Dynamics Psychol. Life Sci.* 13, 57–78.

Kelso, J. A. S. (1995). *Dynamic Patterns: The Self-Organization of Brain and Behavior*. Cambridge, MA: MIT Press.

Kiefer, A., Riley, M. A., Shockley, K., Villard, S., and Van Orden, G. C. (2009). Walking changes the dynamics of cognitive estimates of time intervals. *J. Exp. Psychol. Hum. Percept. Perform.* 35, 1532–1541.

Kloos, H., and Van Orden, G. C. (2010). Voluntary behavior in cognitive and motor tasks. *Mind Matter* 8, 19–43.

Lemoine, L., Torre, K., and Delignières, D. (2006). Testing for the presence of 1/f noise in continuation tapping data. *Can. J. Exp. Psychol.* 60, 247–257.

Linkenkaer-Hansen, K., Nikouline, V. V., Palva, M. J., and Ilmoniemi, R. J. (2001). Long-range temporal correlations and scaling behavior in human brain oscillations. *J. Neurosci.* 21, 1370–1377.

Madison, G., and Delignières, D. (2009). Auditory feedback affects the long-range correlation of isochronous serial production: support for a closed-loop or memory model of timing. *Exp. Brain Res.* 193, 519–527.

Mandelbrot, B. B. (1997). *Fractals and Scaling in Finance*. New York: Springer-Verlag.

Münsterberg, H. (1866). "Beiträge zur experimentellen Psychologie," in *The Principles of Psychology*, Vol. 1, ed. W. James (New York: Henry Holt and Co), 620–627.

Newell, K. M. (1986). "Constraints on the development of coordination," in *Motor Development in Children: Aspects of Coordination and Control*, eds M. Wade and H. Whiting (Dordrecht: Martinus Nijhoff), 341–360.

Percival, D. B., and Walden, A. T. (2000). *Wavelet Methods for Time Series Analysis*. New York, NY: Cambridge University Press.

Pressing, J. (1998). Error correction processes in temporal pattern production. *J. Math. Psychol.* 42, 63–101.

Riley, M. A., and Turvey, M. T. (2002). Variability and determinism in motor behavior. *J. Mot. Behav.* 34, 99–125.

Schöner, G. (2002). Timing, clocks, and dynamical systems. *Brain Cogn.* 48, 31–51.

Slifkin, A. B., and Newell, K. M. (1998). Is variability in human performance a reflection of system noise? *Curr. Dir. Psychol. Sci.* 7, 170–177.

Stetson, D. A., Albers, J. W., Silverstein, B. A., and Wolfe, R. A. (1992). Effects of age, sex, and anthropometric factors on nerve conduction measures. *Muscle Nerve* 15, 1095–1104.

Torre, K., and Delignières, D. (2008). Unraveling the finding of 1/f noise in self-paced and synchronized tapping: a unifying mechanistic model. *Biol. Cybern.* 99, 159–170.

Torre, K., and Wagenmakers, E. J. (2009). Theories and models of $1/f^{\beta}$ noise in human movement science. *Hum. Mov. Sci.* 28, 297–318.

Turvey, M. T. (2007). Action and perception at the level of synergies. *Hum. Mov. Sci.* 26, 657–697.

Van Orden, G. C., Holden, J. G., and Turvey, M. T. (2003). Self-organization of cognitive performance. *J. Exp. Psychol. Gen.* 132, 331–350.

Van Orden, G. C., Holden, J. G., and Turvey, M. T. (2005). Human cognition and 1/f scaling. *J. Exp. Psychol. Gen.* 134, 117–123.

Van Orden, G. C., Kello, C. T., and Holden, J. G. (2010). Situated behavior and the place of measurement in psychological theory. *Ecol. Psychol.* 22, 24–43.

Van Orden, G. C., Kloos, H., and Wallot, S. (2011). "Living in the pink: intentionality, wellbeing, and complexity," in *Philosophy of Complex Systems. Handbook of the Philosophy of Science*, ed. C. A. Hooker (Amsterdam: Elsevier), 639–684.

Vorberg, D., and Wing, A. (1996). "Modeling variability and dependence in timing," in *Handbook of Perception and Action*, Vol. 2, eds H. Heuer and S. W. Keele (London: Academic Press), 181–262.

Wagenmakers, E. J., Farrel, S., and Ratcliff, R. (2004). Estimation and interpretation of 1/f-noise in human cognition. *Psychon. Bull. Rev.* 11, 579–615.

Wagenmakers, E. J., Farrell, S., and Ratcliff, R. (2005). Human cognition and a pile of sand: a discussion on serial correlations and self-organized criticality. *J. Exp. Psychol. Gen.* 135, 108–116.

Ward, L. (2002). *Dynamical Cognitive Science*. Cambridge, MA: MIT Press.

Wearden, J. H., and McShane, B. (1988). Interval production as an analogue of the peak procedure: evidence for similarity of human and animal timing processes. *Q. J. Exp. Psychol. B* 40, 363–375.

Werner, G. (2010). Fractals in the nervous system: conceptual implications for theoretical neuroscience. *Front. Physiol.* 1:15. doi: 10.3389/fphys.2010.00015

West, B. J., and Deering, B. (1995). *The Lure of Modern Science: Fractal Thinking*. Singapore: World Scientific.

West, B. J., and Scafetta, N. (2003). A nonlinear dynamical model of human gait. *Phys. Rev. E* 67, 051917.

Wijnants, M. L., Bosman, A. M. T., Hasselman, F., Cox, R. F. A., and Van Orden, G. C. (2009). 1/f scaling in movement time changes with practice in precision aiming. *Nonlinear Dynamics Psychol. Life Sci.* 13, 79–98.

Wing, A. M. (1980). "The long and short of timing in response sequences," in *Tutorials in Motor Behavior*, eds G. E. Stelmach and J. Requin (Amsterdam: North Holland), 469–486.

Wing, A. M., and Kristofferson, A. B. (1973). Response delays and the timing of discrete motor responses. *Percept. Psychophys.* 14, 5–12.

Zhang, S. (2000). $1/f^{\alpha}$ fluctuations in a ricepile model. *Phys. Rev. E* 61, 5983–5986.

Conflict of Interest Statement: The authors declare that the research was conducted in the absence of any commercial or financial relationships that could be construed as a potential conflict of interest.

Received: 01 June 2011; paper pending published: 27 June 2011; accepted: 27 September 2011; published online: 17 October 2011.

Citation: Kuznetsov NA and Wallot S (2011) Effects of accuracy feedback on fractal characteristics of time estimation. Front. Integr. Neurosci. ***5****:62. doi: 10.3389/fnint.2011.00062*

frontiers in
INTEGRATIVE NEUROSCIENCE

ORIGINAL RESEARCH ARTICLE
published: 24 October 2011
doi: 10.3389/fnint.2011.00065

Left hand dominance affects supra-second time processing

Carmelo Mario Vicario*[1]*, *Sonia Bonní*[2] *and *Giacomo Koch*[2]

[1] *Scuola Internazionale superiore di Studi Avanzati, Trieste, Italy*
[2] *Istituto di Ricovero e Cura a Carattere Scientifico, Santa Lucia Foundation, Rome, Italy*

Edited by:
Warren H. Meck, Duke University, USA

Reviewed by:
Martin Wiener, University of Pennsylvania, USA
Deborah Lynn Harrington, VA San Diego Healthcare System, USA

***Correspondence:**
Carmelo Mario Vicario, Cognitive Neuroscience Sector, Scuola Internazionale Superiore di Studi Avanzati, via Bonomea 265, 34136 Trieste, Italy.
e-mail: cvicario@sissa.it;
Giacomo Koch, Istituto di Ricovero e Cura a Carattere Scientifico, Santa Lucia Foundation, via Ardeatina 306, 00179 Rome, Italy.
e-mail: g.koch@hsantalucia.it

Previous studies exploring specific brain functions of left- and right-handed subjects have shown variances in spatial and motor abilities that might be explained according to consistent structural and functional differences. Given the role of both spatial and motor information in the processing of temporal intervals, we designed a study aimed at investigating timing abilities in left-handed subjects. To this purpose both left- and right-handed subjects were asked to perform a time reproduction of sub-second vs. supra-second time intervals with their left and right hand. Our results show that during processing of the supra-second intervals left-handed participants sub-estimated the duration of the intervals, independently of the hand used to perform the task, while no differences were reported for the sub-second intervals. These results are discussed on the basis of recent findings on supra-second motor timing, as well as emerging evidence that suggests a linear representation of time with a left-to-right displacement.

Keywords: left-handers, motor timing, time line, temporal accuracy

INTRODUCTION

The literature exploring brain functions of left and right-handed subjects has shown variances in spatial and motor abilities that might be explained by consistent structural and functional differences.

In terms of visuo-spatial skills it is thought that in right-handed subjects, the right hemisphere has a prominent role in orienting attention toward the ipsi and contralateral space (Heilman et al., 1987). This leads to an over-representation of the left hemispace in comparison to the right hemispace (Kinsbourne, 1970). In left-handed subjects, instead, this spatial unbalance seems to be almost absent (Sampaio and Chokron, 1992; Luh, 1995). A possible explanation for this difference may be obtained from the hemispheric activation model (Bradshaw et al., 1986; McCourt et al., 2001; Failla et al., 2003), which proposes that left-handed subjects have more equitably distributed visuo-spatial functions across cerebral hemispheres compared to right-handed subjects (McGlone and Davidson, 1973; Burnett et al., 1982; Vogel et al., 2003).

Nevertheless, the behavioral studies supporting this theoretical framework are rather contrasting. In the important study of Luh (1995) researchers reported a larger leftward bias in left-handed subjects than in right-handed subjects. However, the participants were only required to use their dominant hand to give the response (the right hand for right-handed subjects vs. the left hand for left-handed subjects). Similarly, Scarisbrick et al. (1987) provided evidence for an over-representation of the left hemispace in left-handed people. These authors asked right- and left-handed subjects to perform a visual line bisection task with each hand. The data reported that left-handed subjects using their left hand deviated significantly further left than right-handed subjects using their left hand.

Other interesting results were found in studies with children. Van Vugt et al. (2000) asked two groups of children (left-handed vs. right-handed) to bisect lines presented on the left, on the right or in the central position of a computer screen. According to the result reported by Scarisbrick et al. (1987) and Luh (1995), left-handed children showed a leftward bisection error in all hemispaces, while right-handed children displayed a left bias in the left hemispace, a right bias in the right hemispace, and no bias when the lines were presented in the center. On the other hand, there are at least two studies reporting different results. In the work of both Bradshaw et al. (1987) and Dellatolas et al. (1996) it was shown that left-handed subjects bisected horizontal lines toward the left of the objective midpoint when using the left hand, and more toward the right when using their right hand. A reversed pseudoneglect (rightward bias) was also more recently found in adult left-handed participants. Brodie and Dunn (2005) reported that left-handed participants only displayed a reversed pseudoneglect when using their preferred hand (left hand) and adopting a scan direction from right to left. Furthermore, a recent study of Begliomini et al. (2008) provides indirect evidence for a visuo-spatial function difference between these groups by reporting a different activity corresponding to the intraparietal sulcus (IPS), which represents a key area when attention as well as spatial updating are involved (Dehaene et al., 2003). In particular, a higher bilateral IPS activity was evident for right-handers compared to left-handers when using the right hand during a visuo-grasping task.

These anatomo-functional findings suggest that left- and right-handed people differ in their visuo-spatial functions, although several factors such as manual response, the allocation of visual attention (scan direction), and even the type of task performed by

participants can critically affect the neural pattern and its' related behavioral outcome.

Differences between left and right-handers also emerge from studies that compare the motor cortical organization of these two groups. In a seminal study (Kimura, 1993) 10 right-handed and five left-handed subjects were instructed to make repetitive opposition movements of the thumb on each of the remaining four fingers when studied with functional magnetic resonance imaging (fMRI). Results showed a hemispheric asymmetry in the functional activation of the motor cortex during contralateral and ipsilateral movements which was significantly higher in right-handed subjects.

Similarly, Solodkin et al. (2001) reported that left-handers activated larger volumes and a larger number of brain areas than right-handers, and showed significantly less brain lateralization during a sequential movement task. A lower lateralization index was furthermore reported when left-handed subjects were asked to perform unimanual/bimanual tool-use pantomimes (Vingerhoets et al., 2011).

On the other hand, Begliomini et al. (2008) showed an increased activity corresponding to the right premotor cortex (PMC) of left-handed individuals (compared to the right-handed) when performing a grasping task with their left hand.

All these findings demonstrate consistent visuo-spatial and motor functional differences when comparing right- and left-handed individuals.

It has been proposed that time may be represented along a left-to-right oriented mental time line, by analogy with numbers and other magnitudes, and that spatial attention plays a role in constructing this representation (Vicario et al., 2009). Moreover there is a large number of neuroimaging studies documenting a PMC engagement during the execution of several timing tasks.

We designed a research protocol aimed at exploring whether spatial and motor specificities documented in left-handed subjects could affect their ability in detecting temporal intervals. Numerous studies have already shown that a temporal underestimation may follow a leftward manipulation of the spatial attention, and that vice-versa a temporal overestimation may follow a rightward manipulation of the spatial attention (Vicario et al., 2007, 2008, 2009, 2011. Frassinetti et al., 2009. Oliveri et al., 2009). On the basis of such findings, we predicted that left-handed subjects would show a greater underestimation than right-handed subjects, in accordance with studies documenting a larger leftward bias of this group during the execution of visuo-spatial tasks (Scarisbrick et al., 1987; Luh, 1995).

In order to investigate such processes, we submitted our participants to a motor timing task, according to the evidence reporting important differences in the cortical organization of motor and sensorimotor regions of left-handed and right-handed subjects (Solodkin et al., 2001; Begliomini et al., 2008). This agrees with the suggestion of some potential role of sensorimotor regions in motor timing tasks (Vicario et al., 2010, 2011; Bengtsson et al., 2005; Lewis and Miall, 2006; Jantzen et al., 2007; Wiener et al., 2010).

Hence, we used a task engaging explicit time processing activity (Coull and Nobre, 2008) in the form of a motor response, in which subjects were asked to represent the timed duration within a sustained motor act (time reproduction task).

MATERIALS AND METHODS

PARTICIPANTS

Fourteen left-handed (five males, nine females; mean age = 26 ± 3.3 SD) and fourteen right-handed (five males, nine females; mean age = 26 ± 3.3 SD) subjects participated in the experiment. All participants reported normal or corrected-to-normal vision and no neurological abnormalities. They were selected according to the Standard Handedness Inventory (Briggs and Nebes, 1975). Participants responded to this scale by indicating whether they use their right, left, or either hand for 12 common actions. We calculated the score for each subject by assigning a number from one to five to each response of the handedness Inventory (left = 1; usually left = 2; no preference = 3; usually right = 4; always right = 5). In order to maximize the effects of handedness on the temporal performance, we excluded ambidextrous participants and participants totalizing an inventory score >1.2 and <4.8 (left-handed participants: mean = 1.005 ± 0.022 SD, min–max range 1–1.083; right-handed participants: mean = 4.981 ± 0.049 SD, min–max range 4.83–5). All subjects gave their written informed consent prior to their inclusion in the study and were naive in relation to its purpose. Subjects were compensated with 10€ for their participation, and specific information concerning the study was provided only after the subject had terminated all experimental sessions.

APPARATUS AND STIMULI

We used E-prime 1.2 software to create the visual stimuli and conduct the experiment. We used a version of the time reproduction task previously used by other authors (Jones et al., 2004; Koch et al., 2007; Vicario et al., 2010). Subjects sat at a distance of 60 cm opposite the monitor configured to a refresh rate of 100 Hz. Subjects were asked to fixate a black cross of 0.2° in diameter, centrally located on the screen. After 500 ms, the black circle (test stimulus; size: 0.8° × 0.1°) appeared in the same location of the fixating cross; after a specified period, it disappeared. Immediately after the black circle disappeared, subjects were instructed to reproduce the interval they had just perceived by keeping the space bar on the computer keyboard pressed down with the index finger of their dominant hand. During such time they fixated a white screen. When they had judged that the same amount of time had elapsed, they had to release the space bar. Each session consisted in two separate and consecutive blocks. Following a study design previously adopted by other authors (Jones et al., 2004), we chose to challenge subjects in the reproduction of five different time intervals within each of the two blocks, in order to minimize the chance of a learning process throughout the performance of the task. Therefore, one block consisted of 50 trials in which subjects estimated five sub-second intervals (500, 600, 700, 800, 900 ms) each of which was presented for 10 repetitions in a randomized order; while the other block consisted of 50 trials in which subjects estimated five supra-second intervals (1500, 1600, 1700, 1800, 1900 ms) with again 10 repetitions of each presented in randomized order. The reference stimulus was presented immediately before the test stimulus in each of the 50 trials of each block, and in both blocks the inter-trial interval was 2000 ms. The presentation order of the sub-second and the supra-second blocks

was counterbalanced within subjects in each group. Each block also consisted of two counterbalanced sessions in which participants were separately asked to perform the task by using their left or their right hand. Therefore our participants performed a total of four sessions. The performance of each subject on this task was analyzed as the mean difference expressed in milliseconds between groups. We did not test longer intervals to limit the length of the session, maintain a constant level of attention in participants, and to discourage subjects from adopting counting procedures to help themselves during the perception or reproduction of time intervals. No feedback concerning the quality of their performance was given to the subjects during the inter-trial interval.

DATA ANALYSIS

The reproduction performance in the time reproduction task was analyzed using ANOVA for repeated measures, with BLOCK (sub-second vs. supra-second) as the between-subject factor, and GROUP (left-handed subjects vs. right-handed subjects), MANUAL RESPONSE (left hand vs. right hand), and INTERVALS (500–900 vs. 1500–1900 ms) as within-subject factors. Reaction times (RTs) trials that fell 2.5 SDs above or below each individual mean for each experimental condition were excluded as outlier trials (sub-second block: Left-handers 2.29%; Right-handers 2.42%; supra-second block: Left-handers 2.57%; Right-handers 2.86%). Two tailed t-test analysis showed any significant between groups difference (Sub-second block $t = -0.210, p = 0.836$; Supra-second block $t = -0.353$, $p = 0.729$). The mean response times were fit with a linear regression ($y = ax + y0$), and the slope and intercept values obtained for both groups were compared. Finally, as a measure of variability, we used the coefficient of variation (CV; SD/mean response time).

Post hoc comparisons were performed using the Newman–Keuls *post hoc* test, and for all statistical analyses, a p value of <0.05 was considered to be significant. Data analysis was performed using Statistica software, version 8.0, StatSoft, Inc., Tulsa, USA.

RESULTS

The three-way ANOVA for repeated measures on the accuracy did not detect a significant main effect of GROUP on the time reproduction task [$F(1, 13) = 3.8$, $p = 0.074$]. Likewise there was no effect of the main factor MANUAL RESPONSE [$F(1, 13) = 2.1$, $p = 0.175$] and interaction terms BLOCK × MANUAL RESPONSE [$F(2, 26) = 2.4$, $p = 0.143$], GROUP × MANUAL RESPONSE [$F(2, 26) = 1.0$, $p = 0.337$], GROUP × INTERVALS [$F(2, 26) = 0.1$, $p = 0.996$] MANUAL RESPONSE × INTERVALS [$F(2, 26) = 0.2, p = 0.937$], BLOCK × GROUP × MANUAL RESPONSE [$F(3, 39) = 0.6$, $p = 0.451$] BLOCK × GROUP × INTERVALS [$F(3, 39) = 0.8$, $p = 0.508$], BLOCK × MANUAL RESPONSE × INTERVALS [$F(3, 39) = 0.4$, $p = 0.773$], GROUP × MANUAL RESPONSE × INTERVALS [$F(3, 39) = 2.1, p = 0.097$], and BLOCK × GROUP × INTERVALS × MANUAL RESPONSE [$F(4, 52) = 1.5, p = 0.227$]. There was, instead, a significant main effect of the within-subject factor BLOCK [$F(1, 13) = 323.7$, $p < 0.001$], INTERVALS [$F(1, 13) = 129.1$, $p < 0.001$], and the interaction terms BLOCK × INTERVALS [$F(2, 26) = 3.2$, $p = 0.020$] and GROUP × BLOCK [$F(2, 26) = 4.8$, $p = 0.046$]. *Post hoc* tests showed that left-handed subjects underestimated temporal durations only for the supra-second range of intervals ($p = 0.008$) when compared to right-handed subjects; whereas the reproduction performance did not differ between the two groups for the sub-second range of intervals ($p = 0.982$; **Figure 1**).

A further one-tailed t-test analysis was performed only for the supra-second block, in order to asses a possible role of the hand used to generate the temporal response.

WITHIN-SUBJECT ANALYSIS

Left-handed group: left hand $M = 1308.2\,\text{ms} \pm 52.70$ vs. right hand $M = 1239.2\,\text{ms} \pm 54.55$ $t = 0.909$, $p = 0.186$; right-handed group: left hand $M = 1442.5\,\text{ms} \pm 57.76$ vs. right hand $M = 1427.4\,\text{ms} \pm 80.13$; $t = 0.152$, $p = 0.440$.

BETWEEN-SUBJECT ANALYSIS

Left hand: left-handed $M = 1308.2\,\text{ms} \pm 52.70$ vs. right-handed $M = 1442.5\,\text{ms} \pm 57.76$, $t = -1.71$, $p = 0.048$; right hand: left-handed $M = 1239.2\,\text{ms} \pm 54.55$ vs. right-handed $M = 1427.4\,\text{ms} \pm 80.13$, $t = -1.94$, $p = 0.032$.

The *within-subject* analysis did not show significant differences among the analyzed conditions, while the between-subject analysis showed that left-handers underestimated time with both their left and right hand.

Since we obtained a significant difference for the supra-second block, we tried to fit the accuracy for the supra-second intervals range with a linear regression model and looked for differences in slope or intercept (**Figure 2**).

The ANOVA performed on the slope scores did not detect a significant main effect of GROUP [$F(1, 13) = 0.8$, $p < 0.373$] and HAND [$F(1, 13) = 0.8$, $p < 0.361$] and the interaction term GROUP × BLOCK [$F(1, 13) = 2.5, p = 0.137$]. Likewise the ANOVA performed on the intercept scores did not detect a significant main effect of GROUP [$F(1, 13) = 0.04$, $p < 0.836$] and HAND [$F(1, 13) = 1.84$, $p < 0.198$] and the interaction term GROUP × BLOCK [$F(1, 13) = 0.20, p = 0.658$].

Finally, the ANOVA for repeated measures on the CV scores for both groups did not detect a significant interaction for the factors BLOCK × GROUP [$F(1, 13) = 0.4$, $p = 0.503$], BLOCK × GROUP × MANUAL RESPONSE [$F(1, 13) = 0.7$, $p = 0.797$]. However we detected a significant main effect of GROUP [$F(1, 13) = 7.7$, $p = 0.015$], which indicated lower variability of the left-handers (0.228 ± 0.013) compared to the right-handers (0.256 ± 0.012). Likewise there was a main effect for the MANUAL RESPONSE [$F(1, 13) = 17.0$, $p < 0.001$], BLOCK [$F(1, 13) = 53.8$, $p < 0.001$], INTERVALS [$F(1, 13) = 63.0$, $p < 0.001$] factor, and the interaction effect BLOCK × MANUAL RESPONSE [$F(1, 13) = 42.7$, $p < 0.001$], GROUP × MANUAL RESPONSE [$F(1, 13) = 47.5$, $p < 0.001$], BLOCK × INTERVALS [$F(1, 13) = 30.7$, $p < 0.001$], GROUP × INTERVALS [$F(1, 13) = 25.7$, $p < 0.001$], MANUAL RESPONSE × INTERVALS [$F(1, 13) = 4.3$, $p < 0.004$], and the interaction terms BLOCK × GROUP × INTERVALS [$F(1, 13) = 6.0$, $p < 0.001$], BLOCK × MANUAL RESPONSE × INTERVALS [$F(1, 13) = 7.7$, $p < 0.001$], GROUP × MANUAL

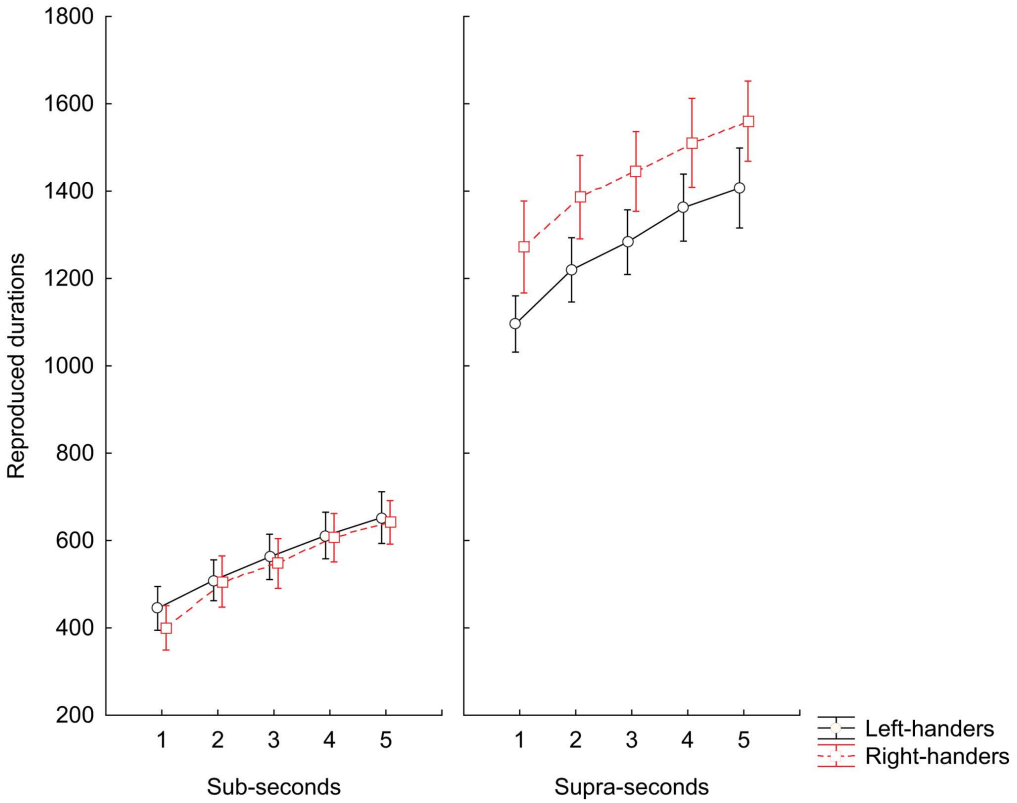

FIGURE 1 | Time reproduction task. Means of median RT values during reproduction of sub-second and supra-second intervals for left-handed subjects and right-handed subjects participants. The vertical bars indicate SE mean.

RESPONSE × INTERVALS [$F(1, 13) = 11.8$, $p < 0.001$], and BLOCK × GROUP × INTERVALS × MANUAL RESPONSE [$F(1, 13) = 12.1$, $p = 0.001$].

Post hoc analysis on the interaction factors BLOCK × GROUP × INTERVALS × MANUAL RESPONSE, when using the *left hand*, reported that right-handers were more variable than left-handers in reproducing almost all sub-second intervals (600 ms, $p = 0.003$; 700 ms, $p = 0.004$; 800 ms, $p < 0.001$); however the accuracy pattern was inverted at 900 ms in which case left-handers were more variable than right-handers ($p < 0.001$); any difference was reported when participants reproduced intervals at 500 ms.

We observed that right-handers were also more variable than left-handers in reproducing 1500 ms ($p < 0.001$), but more accurate at 1700 ms ($p < 0.003$) and at 1900 ms ($p < 0.001$). Any significant differences was reported for 1600 and 1800 ms. (see **Figure 3** for further details).

A similar pattern of higher variability of the right-handers was reported when using their *right hand* in reproducing sub-second intervals such as 500 ms ($p < 0.001$); 600 ms ($p < 0.001$), and 700 ms ($p < 0.001$). Any difference was reported in reproducing 800 and 900 ms. Our right-handers were more variable than left-handers even when asked to reproduce supra-second intervals (1500 ms, $p < 0.001$; 1600 ms, $p < 0.001$; 1700 ms, $p < 0.001$; 1800 ms, $p < 0.001$). However, any difference was reported at 1900 ms (see **Figure 4** for further details).

DISCUSSION

The aim of the present work was to assess the ability of left-handed subjects to reproduce temporal intervals within the sub-second and the supra-second duration ranges. The rationale of our study was based on previous findings that reported substantial differences in the processing of visuo-spatial and motor information between left-handed and right-handed groups (Scarisbrick et al., 1987; Peters, 1991; Sampaio and Chokron, 1992; Luh, 1995; Rushworth et al., 1997; Solodkin et al., 2001; Begliomini et al., 2008; Vingerhoets et al., 2011). During processing of the supra-second intervals left-handed participants sub-estimated the duration of the intervals, independently of the hand used to perform the task, while no differences were reported for the sub-second intervals. The CV analysis showed that the performances of left-handed participants were significantly less variable than right-handed participants. This result was particularly evident for the timing of sub-second intervals, though we did not detect a significant difference between groups when comparing the raw data of this temporal range. Left-handed subjects were also less variable in the timing of supra-second intervals when using their right hand to generate the temporal response.

On the other hand, for the timing of supra-second intervals the parameters of variability were much more flexible between groups when subjects were asked to use their left hand to reproduce the temporal intervals. This result may imply that the hemispheric

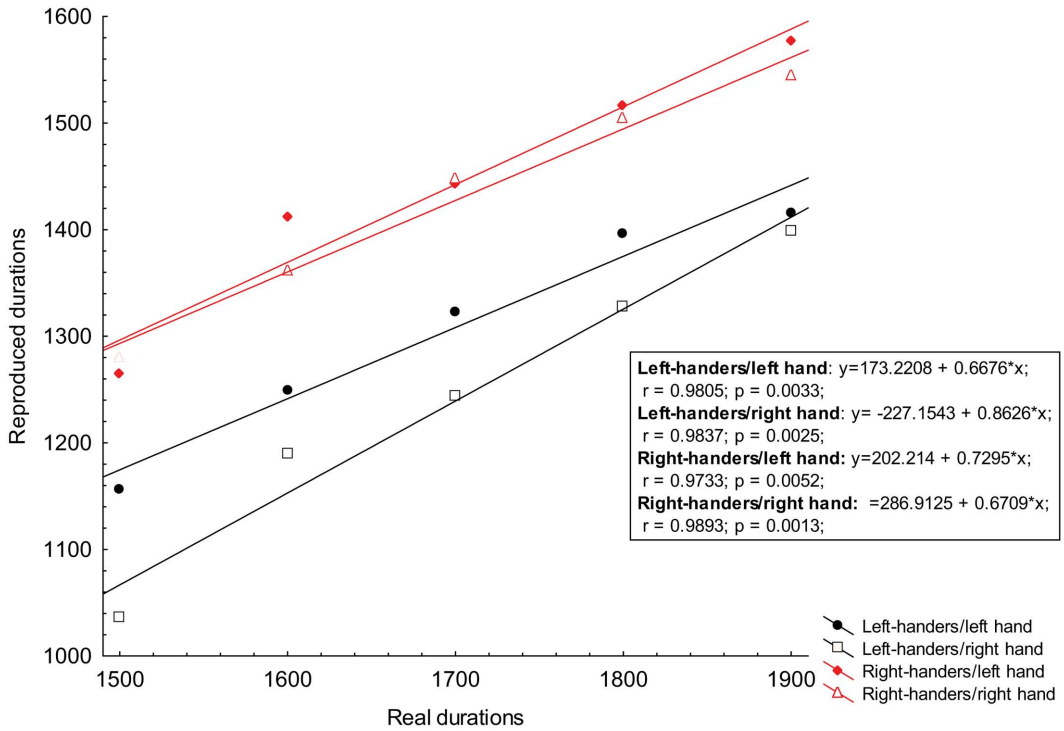

FIGURE 2 | The obtained reproduction scores for supra-second intervals were plotted against references durations and then fit with a linear regression. The ordinate represents the reproduced time for both left-handers and right-handers groups performing the task with their left and right hand; The abscissa represents the real durations of reference stimuli. Both scores are expressed in milliseconds. Equations derived from each linear regression, correlation, and *R* square for each condition are displayed in the graph.

activation associated to the limb used for generating the response has different effects on the timing variability itself.

The present findings could be related to the different underlying neural circuits that are thought to be involved in the processing of sub-second and supra-second time intervals, although there are several common neural activation mechanisms involved in both temporal domains (Koch et al., 2009; Wiener et al., 2010, 2011). In particular, when subjects are required to quickly estimate the passage of sub-second time intervals or perform sub-second motor timing tasks, and when time is computed in relation to precise salient events, it is thought that the neural activity of the cerebellum and the superior temporal gyrus is most crucial. Conversely, the parieto-frontal circuits mainly in the right hemisphere seem to be the most implicated processing of supra-second time intervals (included motor timing tasks), and when time is processed in conjunction with other cognitive functions (Koch et al., 2009).

In the group of left-handed subjects the time reproduction of supra-second intervals was biased toward a sub-estimation pattern. On the other hand, left-handed subjects did not differ from controls (right-handed subjects) in the reproduction of sub-second intervals. Data from the CV analysis suggest that the variability cannot be responsible of the current sub-estimation pattern found in the left-handed participants. In fact, although the sub-estimation pattern founded in our left-handed participants can be explained in terms of a minor temporal precision (given the greater temporal gap from the real durations), the lower variability found in the performance of left-handers indicates a potential difference in the clock speed between these two groups for the timing of supra-second durations. This view is furthermore corroborated by the absence of a difference in accuracy when reproducing sub-second intervals in presence of a significant difference in the CV.

A prediction deriving from the hemispheric activation model is that the selective activation of one hemisphere by a unimanual response could result in an enhancement of the spatial representation contralateral to the cerebral hemisphere activated. Thus, in accordance with previous studies on left-handed subjects, (e.g., Bradshaw et al., 1987) who showed a leftward bias when bisecting a line with their left hand and a rightward bias when bisecting a line with their right hand, it is reasonably likely to expect a similar bias on temporal performance, depending of the hand used for responding. However, the GROUP × MANUAL RESPONSE factor was not significant. Since we did not test visuo-spatial skills in our participants, we cannot exclude a leftward bias dominance in our left-handed participants independently from the hand used for generating the temporal response. This suggestion is confirmed by the between-subject *t*-test analysis for accuracy reported in the current study.

Therefore the attentional orientation bias of the right hemisphere toward the left hemispace seems to be accentuated in left-handed subjects in relation to the frequency of use of their

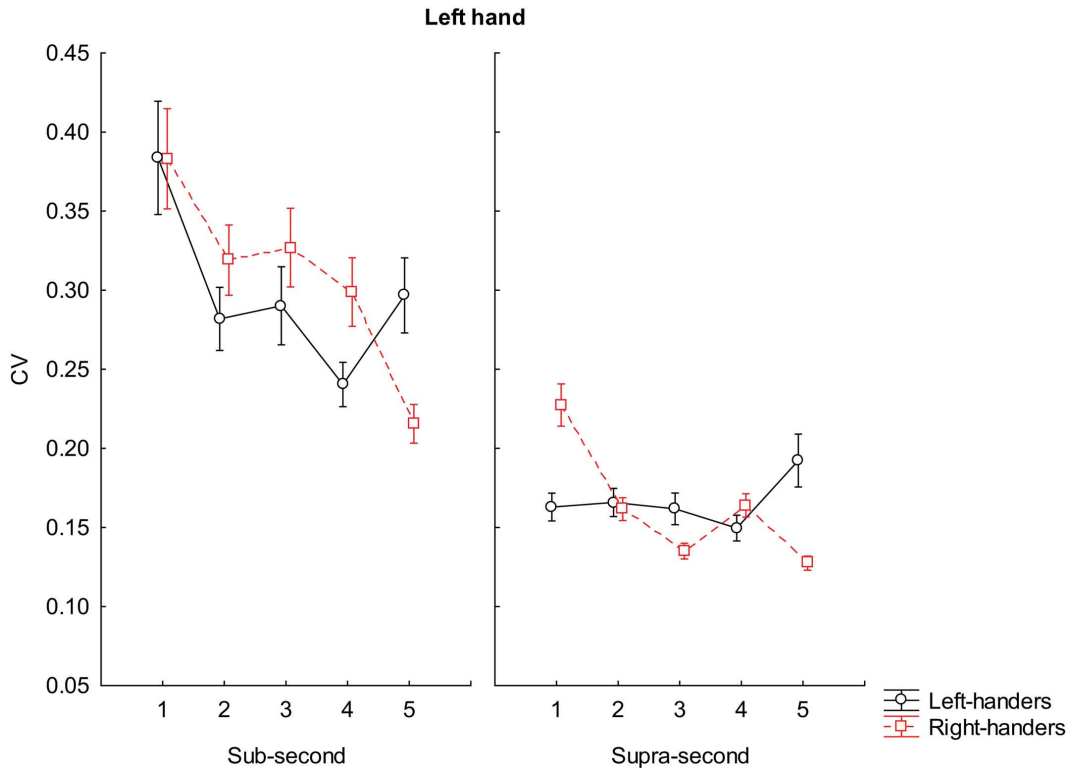

FIGURE 3 | Coefficient of variation scores during reproduction of sub-second and supra-second intervals with left hand. The vertical bars indicate SE mean.

left hand in their everyday activities. This could, in turn, account for the current temporal underestimation.

Indirect evidence supporting the possible impact of the attentional orientation bias of the right hemisphere toward the left hemispace on time originates from an important study by Polzella et al. (1977). The authors of the study found that the mean judged duration of patterns flashed to the left visual field was significantly less than the mean judged duration of patterns flashed to the right visual field.

In a recent study Vicario et al. (2007) tested the effects of left vs. rightward optokinetic stimulation on time comparison tasks of stimuli presented in a central position. The main results showed that directing attention toward the right hemispace induces time overestimation, while directing it toward the left hemispace time underestimation compared to baseline (Oliveri et al., 2009). In this setting, we might hypothesize that the spatial attention leftward bias reported in the studies exploring the performance of left-handed subjects in a line bisection task (Scarisbrick et al., 1987; Luh, 1995; Van Vugt et al., 2000), is responsible for the above-mentioned temporal sub-estimation.

An alternative – not mutually exclusive – explanation for the result we observe could be given by the functional and/or structural differences in motor and sensorimotor regions between the two groups we tested. Motor timing performance seems to depend on the degree of co-activation between the basal ganglia and the supplementary motor area (SMA), the dorsolateral prefrontal cortex, and the cerebellum (see Witt et al., 2008 for a meta analysis). Together with other brain regions, the right SMA activity seems to be particularly related to the processing of supra-second motor timing tasks (Wiener et al., 2010). A possibility is that the current timing pattern would be related to the functional specificities concerning the SMA of left-handed subjects, as reported by Solodkin et al. (2001). In the context of this discussion, a different explanation could be referred to the functional differences across other regions involved in the motor control. For example, there is a large number of neuroimaging studies documenting the engagement of PMC during the execution of several timing tasks. It was recently shown (Begliomini et al., 2008) that the right PMC activity is increased in left-handed individuals (compared to the right-handed) who were asked to perform a grasping task.

The superiority of right-handed subjects in motor tasks such as finger-tapping, which is likely related to the superiority in the neural processing of their left hemisphere, emerges from at least two neuropsychological studies (Peters, 1991; Rushworth et al., 1997); thus the sub-estimation bias of our left-handed group could be interpreted in terms of a lower accuracy as a consequence of the lower motor control of this group.

The language dominance hemisphere view is also in agreement with the results of the first report of lateralized differences on perceptual timing (Efron, 1963). In his study, the author showed that for right-handers, the sensation of subjective simultaneity

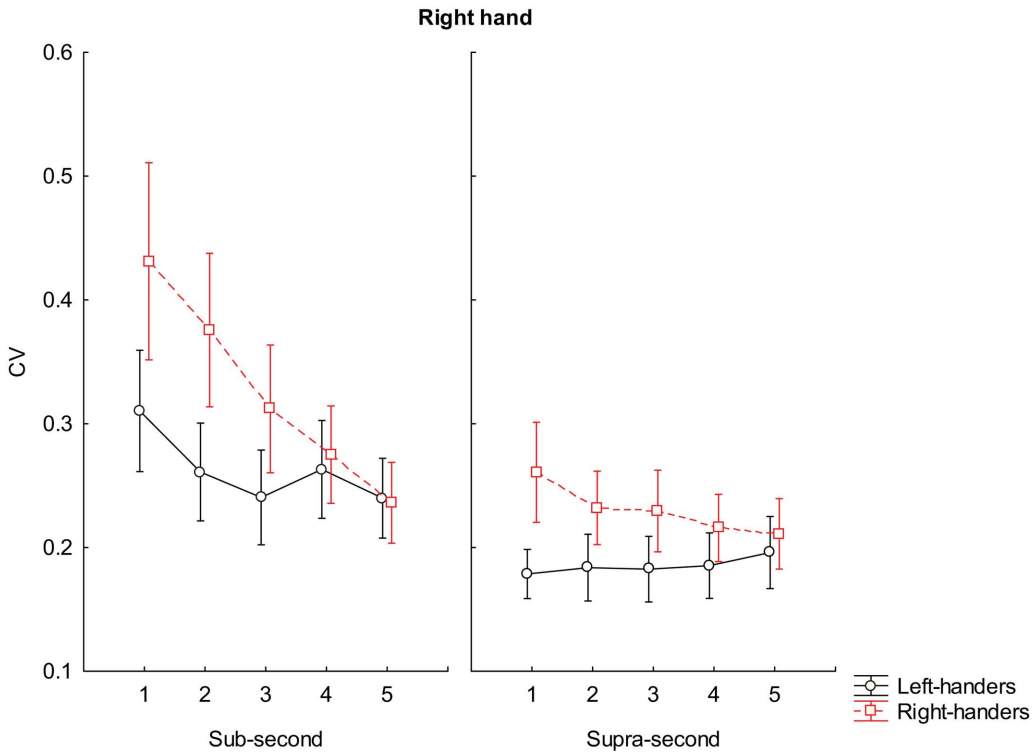

FIGURE 4 | Coefficient of variation scores during reproduction of sub-second and supra-second intervals with right hand. The vertical bars indicate SE mean.

of a pair of lateralized stimuli (brief light flashes and cutaneous shocks were used) was felt when the stimulus delivered to the left visual field or left index finger preceded the stimulus delivered to the right side by 3–4 ms. Instead, the point of subjective simultaneity for a group of left-handers did not differ from zero.

Although the hemispheric difference reported above can differentially impact the current results, other factors, such as scanning strategies and the manual response may influence the final timing outcome.

All these studies could be useful in explaining the alteration of the temporal performance in left-handed subjects as well as the direction of the bias toward sub-estimation.

To the best of our knowledge, our study is the first to explore and report differences in explicit timing tasks between left- and right-handed subjects. However, our study presents an important limitation, given our subjects performed only a time reproduction task, which do not allow an investigation of the perceptual domain that is pertinent of a different timing paradigms such as a time discrimination task.

REFERENCES

Begliomini, C., Nelini, C., Caria, A., Grodd, W., and Castiello, U. (2008). Cortical activations in humans grasp-related areas depend on hand used and handedness. *PLoS ONE* 3, e3388. doi:10.1371/journal.pone.0003388

Bengtsson, S. L., Ehrsson, H. H., Forssberg, H., and Ullen, F. (2005). Effector independent voluntary timing: behavioural and neuroimaging evidence. *Eur. J. Neurosci.* 22, 3255–3265.

Bradshaw, J. L., Bradshaw, J. A., Nathan, G., Nettleton, N. C., and Wilson, L. E. (1986). Leftwards error in bisecting the gap between two points: stimulus quality and hand effects. *Neuropsychologia* 24, 849–855.

Bradshaw, J. L., Nettleton, N. C., Wilson, L. E., and Bradshaw, C. S. (1987). Line bisection by left-handed preschoolers: a phenomenon of symmetrical neglect. *Brain Cogn.* 6, 377–385.

Briggs, G. G., and Nebes, R. D. (1975). Patterns of hand preference in a student population. *Cortex* 11, 230–238.

Brodie, E. E., and Dunn, E. M. (2005). Visual line bisection in sinistrals and dextrals as a function of hemispace, hand, and scan direction. *Brain Cogn.* 58, 149–156.

Burnett, S. A., Lane, D. M., and Dratt, L. M. (1982). Spatial ability and handedness. *Intelligence* 6, 57–68.

Coull, J. T., and Nobre, A. C. (2008). Dissociating explicit timing from temporal expectation with fMRI. *Curr. Opin. Neurobiol.* 18, 137–144.

Dehaene, S., Piazza, M., Pinel, P., and Cohen, L. (2003). Three parietal circuits for number processing. *Cogn. Neuropsychol.* 20, 487–506.

Dellatolas, G., Coutin, T., and Agostini, M. (1996). Bisection and perception of horizontal lines in normal children. *Cortex* 32, 705–715.

Efron, R. (1963). Temporal perception, Aphasia and D'e J'a vu. *Brain* 86, 403–424.

Failla, C. V., Sheppard, D. M., and Bradshaw, J. L. (2003). Age and responding-hand related changes in performance of neurologically normal subjects on the line-bisection and chimeric-faces tasks. *Brain Cogn.* 52, 353–363.

Frassinetti, F., Magnani, B., and Oliveri, M. (2009). Prismatic lenses shift time perception. *Psychol. Sci.* 20, 949–954.

Heilman, K. M., Bowers, D., Valenstein, E., and Watson, R. T. (1987). "Hemispace and hemispatial neglect," in *Neurophysiological and Neuropsychologial Aspects of Spatial Neglect*, ed. M. Jeannerod (Amsterdam: Elsevier), 115–150.

Jantzen, K. J., Oullier, O., Marshall, M., Steinberg, F. L., and Kelso, J. A. (2007). A parametric fMRI investigation of context effects in sensorimotor timing and coordination. *Neuropsychologia* 45, 673–684.

Jones, C. R., Rosenkranz, K., Rothwell, J. C., and Jahanshahi, M. (2004). The right dorsolateral prefrontal cortex is essential in time reproduction: an investigation with repetitive transcranial magnetic stimulation. *Exp. Brain Res.* 158, 366–372.

Kimura, D. (1993). *Neuromotor Mechanisms in Human Communication.* New York: Oxford University Press.

Kinsbourne, M. (1970). The cerebral basis of lateral asymmetries in attention. *Acta Psychol.* 33, 193–201.

Koch, G., Oliveri, M., and Caltagirone, C. (2009). Neural networks engaged in milliseconds and seconds time processing: evidence from transcranial magnetic stimulation and patients with cortical or subcortical dysfunction. *Philos. Trans. R. Soc. Lond. B Biol. Sci.* 364, 1907–1918. [Review].

Koch, G., Oliveri, M., Torriero, S., Salerno, S., Lo Gerfo, E., and Caltagirone, C. (2007). Repetitive TMS of cerebellum interferes with millisecond time processing. *Exp. Brain Res.* 179, 291–299.

Lewis, P. A., and Miall, R. C. (2006). Remembering the time: a continuous clock. *Trends Cogn. Sci. (Regul. Ed.)* 10, 401–406.

Luh, K. E. (1995). Line bisection and perceptual asymmetries in normal individuals: what you see is not what you get. *Neuropsychology* 9, 435–448.

McCourt, M. E., Freeman, P., Tahmahkera-Stevens, C., and Chaussee, M. (2001). The influence of unimanual response on pseudoneglect magnitude. *Brain Cogn.* 45, 52–63.

McGlone, J., and Davidson, W. (1973). The relation between cerebral speech laterality and spatial ability with special reference to sex and hand preference. *Neuropsychologia* 11, 105–113.

Oliveri, M., Koch, G., Salerno, S., Torriero, S., Lo Gerfo, E., and Caltagirone, C. (2009). Representation of time intervals in the right posterior parietal cortex: implications for a mental time line. *Neuroimage* 46, 1173–1179.

Peters, M. (1991). Laterality and motor control. *Ciba Found. Symp.* 162, 300–308.

Polzella, D. J., daPolito, F., and Hinsman, C. (1977). Cerebral asymmetry in time perception. *Percept. Psychophys.* 21, 187–192.

Rushworth, M. F., Nixon, P. D., Renowden, S., Wade, D. T., and Passingham, R. E. (1997). The left parietal cortex and motor attention. *Neuropsychologia* 35, 1261–1273.

Sampaio, E., and Chokron, S. (1992). Pseudoneglect and reversed pseudoneglect among left-handers and right-handers. *Neuropsychologia* 30, 797–805.

Scarisbrick, D. J., Tweedy, J. R., and Kuslansky, G. (1987). Hand preference and performance effects on line bisection. *Neuropsychologia* 25, 695–699.

Solodkin, A., Hlustik, P., Noll, D. C., and Small, S. L. (2001). Lateralization of motor circuits and handedness during finger movements. *Eur. J. Neurol.* 8, 425–434.

Van Vugt, P., Fransen, I., Creten, W., and Paquier, P. (2000). Line bisection performances in 650 normal children. *Neuropsychologia* 35, 703–715.

Vicario, C. M., Caltagirone, C., and Oliveri, M. (2007). Optokinetic stimulation affects temporal estimation in healthy humans. *Brain Cogn.* 64, 68–73.

Vicario, C. M., Martino, D., Pavone, E. F., and Fuggetta, G. (2011). Lateral head turning affects temporal memory. *Percept. Mot. Skills* 113, 3–10.

Vicario, C. M., Martino, D., Spata, F., Defazio, G., Giacchè, R., Martino, V., Rappo, G., Pepi, A. M., Silvestri, P. R., and Cardona, F. (2010). Time processing in children with Tourette's syndrome. *Brain Cogn.* 73, 28–34.

Vicario, C. M., Pecoraro, P., Turriziani, P., Koch, G., Caltagirone, G., and Oliveri, M. (2008). Relativistic compression and expansion of experiential time in the left and right space. *PLoS ONE* 3, e1716. doi:10.1371/journal.pone.0001716

Vicario, C. M., Rappo, G., Pepi, A., and Oliveri, M. (2009). Timing flickers across sensory modalities. *Perception* 38, 1144–1151.

Vingerhoets, G., Acke, F., Alderweireldt, A. S., Nys, J., Vandemaele, P., and Achten, E. (2011). Cerebral lateralization of praxis in right- and left-handedness: same pattern, different strength. *Hum. Brain Mapp.* doi:10.1002/hbm.21247. [Epub ahead of print].

Vogel, J. L., Bowers, C. A., and Vogel, D. S. (2003). Cerebral lateralization of spatial abilities: a meta-analysis. *Brain Cogn.* 52, 197–204.

Wiener, M., Lohoff, F. W., and Coslett, H. B. (2011). Double dissociation of dopamine genes and timing in humans. *J. Cogn. Neurosci.* 23, 2811–2821.

Wiener, M., Turkeltaub, P., and Coslett, H. B. (2010). The image of time: a voxel-wise meta-analysis. *Neuroimage* 49, 1728–1740.

Witt, S. T., Laird, A. R., and Meyerand, M. E. (2008). Functional neuroimaging correlates of finger-tapping task variations: an ALE meta-analysis. *Neuroimage* 42, 343–356.

Conflict of Interest Statement: The authors declare that the research was conducted in the absence of any commercial or financial relationships that could be construed as a potential conflict of interest.

Received: 18 July 2011; paper pending published: 29 July 2011; accepted: 30 September 2011; published online: 24 October 2011.

Citation: Vicario CM, Bonní S and Koch G (2011) Left hand dominance affects supra-second time processing. Front. Integr. Neurosci. ***5****:65. doi: 10.3389/fnint.2011.00065*

frontiers in
INTEGRATIVE NEUROSCIENCE

ORIGINAL RESEARCH ARTICLE
published: 28 September 2011
doi: 10.3389/fnint.2011.00044

Temporal sensitivity changes with extended training in a bisection task in a transgenic rat model

Bruce L. Brown[1,2], Sophie Höhn[3,4], Alexis Faure[3,4], Stephan von Hörsten[5], Pascale Le Blanc[3,4], Nathalie Desvignes[3,4], Nicole El Massioui[3,4] and Valérie Doyère[3,4]*

[1] Department of Psychology, Queens College, Flushing, NY, USA
[2] Department of Psychology, Graduate Center, City University of New York, New York, NY, USA
[3] Centre de Neurosciences Paris-Sud, Université Paris-Sud, UMR 8195, Orsay, France
[4] CNRS, Orsay, France
[5] Experimental Therapy, Franz Penzoldt Center, Friedrich-Alexander University, Erlangen-Nürnberg, Germany

Edited by:
Warren H. Meck, Duke University, USA

Reviewed by:
Rosario Moratalla, Consejo Superior de Investigaciones Científicas, Spain
Toshimichi Hata, Doshisha University, Japan

***Correspondence:**
Valérie Doyère, Centre de Neurosciences Paris-Sud, CNRS-UMR 8195, Université Paris-Sud, Bat. 446, 91405 Orsay, France.
e-mail: valerie.doyere@u-psud.fr

The present study investigated temporal perception in a Huntington disease transgenic rat model using a temporal bisection procedure. After initial discrimination training in which animals learned to press one lever after a 2-s tone duration, and the other lever after a 8-s tone duration for food reward, the bisection procedure was implemented in which intermediate durations with no available reinforcement were interspersed with trials with the anchor durations. Bisection tests were repeated in a longitudinal design from 4 to 8 months of age. The results showed that response latencies evolved from a monotonic step-function to an inverted U-shaped function with repeated testing, a precursor of non-responding on trials with intermediate durations. We inferred that temporal sensitivity and incentive motivation combined to control the transformation of the bisection task from a two-choice task at the outset of testing to a three-choice task with repeated testing. Changes in the structure of the task and/or continued training were accompanied by improvement in temporal sensitivity. In sum, the present data highlight the possible joint roles of temporal and non-temporal factors in the temporal bisection task, and suggested that non-temporal factors may compensate for deficits in temporal processing.

Keywords: temporal bisection, temporal discrimination, latency, sensitivity, non-sensory factors, transgenic rat model, Huntington disease

INTRODUCTION

The temporal bisection procedure has been used extensively to study temporal perception in animals. The procedure is a variant of the classical psychophysical method of constant stimuli. It entails an initial conditional discrimination training phase in which one response is rewarded following a short-duration stimulus, while the other response is rewarded following a long-duration stimulus. In a subsequent test phase, the short and long anchor stimuli are presented in addition to intermediate test durations, which are assumed to encompass an interval of uncertainty within which stimuli are indiscriminable from each other (Woodworth and Schlosberg, 1954). A virtue of the method is that it can provide separate measures of the point of subjective equality (PSE), difference limen and Weber fraction that are extracted from the resulting psychometric function. Variations in these measures are assumed to reflect the operations of fundamental mechanisms of temporal perception.

The original purpose of the current study was to investigate temporal perception in a Huntington disease (HD) transgenic rat model. In this model, the striatum is one of the primary structures affected, with the first motor symptoms appearing around 6 months of age and striatal neurodegeneration detectable from 8 months onward (von Horsten et al., 2003; Nguyen et al., 2006). As prefronto-striatal circuits are thought to play a critical role in temporal processing (Buhusi and Meck, 2005), we sought to track the concomitant deterioration in timing behavior over the course of 4–8 months in homozygous models and wt controls. While deficits in timing behavior have been observed at 4 months (Höhn et al., 2011), the data reported here suggest that non-temporal factors may counteract deficits in temporal processing.

MATERIALS AND METHODS

The procedure and apparatus have been reported elsewhere (see Höhn et al., 2011). Details specific to the present study are reported here.

ANIMALS

A cohort of nine wild type (wt) and 12 transgenic (tgHD) rat models for HD was imported at 3 months old (von Horsten et al., 2003). Subjects were housed in pairs in a temperature- and humidity-controlled colony room (23°C, 41% humidity), with a light–dark cycle of 12:12 (lights on at 08:00 AM). After 2 weeks of adaptation, daily food rations were progressively reduced until rats reached 80% of their initial weight before the start of training, and the rats were maintained at 85% of normative weight afterward. All experiments were carried out in accordance with the recommendations of the EEC (86/609/EEC) and the French National Committee (87/848) for care and use of laboratory animals.

APPARATUS

Four operant Skinner boxes (31 cm W × 25 cm D × 31 cm H) in soundproof ventilated chambers (background noise 65 dB) were controlled with the Graphic State program (Coulbourn Instruments, Harvard Apparatus, USA). On the left panel were a pellet dispenser for delivery of 45 mg grain-based precision pellets in a food cup, and two 4-cm retractable response levers. A speaker was located on the opposite side of the box and permitted delivery of an auditory stimulus (1 kHz, 80 dB). At the beginning of each session, a red house light was illuminated.

BEHAVIORAL PROCEDURES

After an initial training phase for temporal discrimination, bisection tests were run monthly in a longitudinal design from 4 to 8 months. The temporal discrimination and the bisection test procedures were identical to those reported previously (Callu et al., 2009; Höhn et al., 2011). Animals were run in six cohorts of four transgenic and wt rats, and were fed in their home cage at the end of the experimental session.

Pretraining

At 3 months of age, rats were magazine trained in one session (30 pellets delivered on a variable time 60 s schedule). The next 2 days, they were trained on a continuous reinforcement schedule for each lever separately until 50 reinforcements were earned.

Temporal discrimination training

Reponses to one of two levers (left vs. right) were reinforced following one of two tone durations (2 vs. 8 s). Two blocks of 40 trials, for a total of 80 trials, were presented with equal probability for each tone duration in each of 17 sessions. The relation of tone duration and reinforced response location was counterbalanced between groups. The levers were retracted immediately after a response or after 5 s. The inter-trial interval (ITI) was 30 s on average (range 20–40 s).

Bisection tests

Rats were then tested in a psychophysical choice procedure with five intermediate durations (2.5, 3.2, 4, 5, and 6.3 s) on non-reinforced trials (12 trials each duration), in addition to the two training anchor durations (2 and 8 s, 60 trials each) with reinforcement available. The mean ITI was 30 s. Four to six bisection sessions were run each month, from 4 to 8 months, followed by one session of discrimination training.

DATA ANALYSIS

Response location and latency were recorded for each trial. Analysis of latency included only trials with a response. Bisection data were calculated as proportion of responses on the lever assigned as correct for the long-duration stimulus on all trials with response. The bisection function relating proportion "long" responses to stimulus duration is typically sigmoidal in shape. The stimulus value corresponding to $p(\text{"Long"}) = 0.5$ typically falls at the geometric mean of the anchor durations PSE. The slope of the function in the vicinity of the PSE reflects temporal sensitivity. The bisection function was analyzed with the pseudo-logistic model (PLM; Killeen et al., 1997) fit for each rat on the averaged curve obtained at each month, using Prism software; With the assumption that scalar variance dominated (Allan, 2002; Callu et al., 2009), the fits were good (median proportion of variance accounted for =0.997 and 0.995 for wt and tgHD groups, respectively). The PSE and the temporal sensitivity parameter (gamma) were estimated for each rat using the following formula (Allan, 2002, Eq. 5):

$$P(R_L) = \left[1 + \exp\left(\frac{T_{1/2} - t}{\frac{\sqrt{3}}{\pi}\gamma t}\right)\right]^{-1}$$

Gamma, which is proportional to the Weber fraction, increases as temporal sensitivity decreases.

Contrast analyses of variance (ANOVAs; Rouanet et al., 1990) with an alpha level of 0.05 were used for statistical assessments.

RESULTS

RESPONSE LATENCY AND PERCENT RESPONSE

As reported elsewhere for these animals (Höhn et al., 2011), performances during initial temporal discrimination training were similar for wt and tgHD rats. At 4 months, tgHD rats showed a typical bisection curve, with similar PSE but poorer sensitivity (higher gamma) than wt. Both groups showed a decrease in response latency with increasing stimulus duration.

During the 25 bisection test sessions that were conducted over a 5-month period, both wt and tgHD rats progressively learned not to respond following intermediate durations, with no available reinforcement, while responding was maintained on trials with the anchor durations. The latter trend was evidenced in a sharp decrease in the mean percent of trials with a response (percent response) as intermediate values approached the 4-s geometric mean of the anchor duration values, and an increase in mean response latency which peaked near the geometric mean of the anchor durations (**Figures 1A,B**). On the final session, the minimum percent response on a given intermediate duration varied between 0 and 100% for tgHD rats, and between 16.67 and 100% for wt rats. Four of 12 tgHD and five of nine wt rats still responded on at least 95% of trials on average for the intermediate durations. Performance was analyzed for these subgroups of animals who had stopped responding or not (with a criterion of 95%) on the final session. On the 4-month test, in addition to the decrease in latency with stimulus duration previously reported (Höhn et al., 2011), an ANOVA indicated that mean latency for subgroup "stop" significantly exceeded that for subgroup "no-stop" [137 ms; $F(1,17) = 6.43, p < 0.05$], with no effects involving genotype (Fs < 1). In order to characterize the development of performance patterns that foreshadowed the cessation of responding, the difference in latency was calculated between the test session immediately prior to cessation of responding for each animal and the 4-month test (**Figure 1C** right panel). For the percent response measure (**Figure 1C** left panel), the difference calculation was based on the 4-month test and the last (25th) test session. Similar inverted U-shaped curves for latency and U-shaped curves for percent response were obtained for wt and tgHD rats

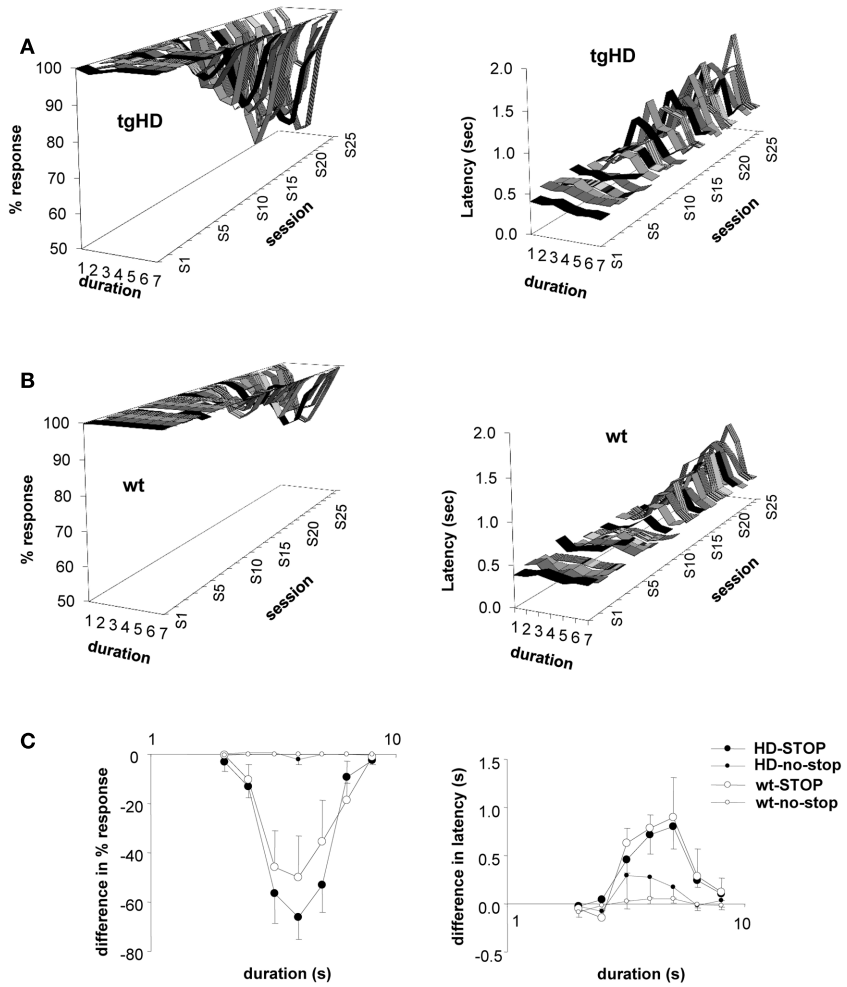

FIGURE 1 | Increased response latency for intermediate durations leads to cessation of responding. Percent responses (left) and response latencies (right) across signal durations and sessions during temporal bisection tests for tgHD **(A)** and wt **(B)** rats. In **(C)** left panel, mean (±SEM) difference in percent responses between the last test session and the 4-months tests for subgroups of animals that stopped responding or not to intermediate durations (with a criterion of 95%). In **(C)** right panel, mean (±SEM) difference in response latencies between the 4-months tests and (a) the last test session prior to stopping responding (95% criterion) for subgroups of animals that stopped responding or (b) the last test session for the no-stop subgroups. For both panels, data are shown as a function of both genotype and duration.

which stopped responding. In genotype × subgroup × duration ANOVAs for both dependent measures, there were no significant effects involving genotype (all Fs < 1). Curves for the stop subgroup differed significantly from the curves of the no-stop subgroup [subgroup × duration interaction, $F(6,102) = 4.63$ and $F(6,102) = 14.21$, ps < 0.001, for response latency and percent response, respectively]. While the stop and no-stop subgroups did not differ at the two anchor durations [$F(1,17) = 1.59$ and $F < 1$ for response latency and percent response, respectively], they differed significantly at the middle three intermediate durations [$F(1,17) = 12.29$ and $F(1,17) = 25.31$; $p < 0.01$ for response latency and percent response]. Thus, the greater effect of duration on latency for the stop subgroup compared to the no-stop subgroup was associated with subsequently observed differences in the tendency to cease responding to non-reinforced intermediate durations.

TEMPORAL SENSITIVITY AND PERCENT RESPONSE

The foregoing findings represent the acquisition of a temporal discrimination between intermediate and anchor durations in the bisection protocol. One factor that may control the speed of acquisition of that discrimination is temporal sensitivity. Considering tgHD rats only, which showed a large variability between animals in temporal sensitivity at 4 months (Höhn et al., 2011), there was a significant positive correlation between gamma measured at 4 months and the session number at which the percent response measure fell below 95% [**Figure 2A**, $r(10) = 0.60$, $p < 0.04$]. The significant correlation held when considering both wt and tgHD rats [z-scores, $r(19) = 0.50$, $p < 0.03$]. Thus, better temporal sensitivity at 4 months predicted faster acquisition of the tendency to stop responding on intermediate durations. Owing to stable high levels of responding to the anchor durations throughout testing, this tendency reflected the acquisition

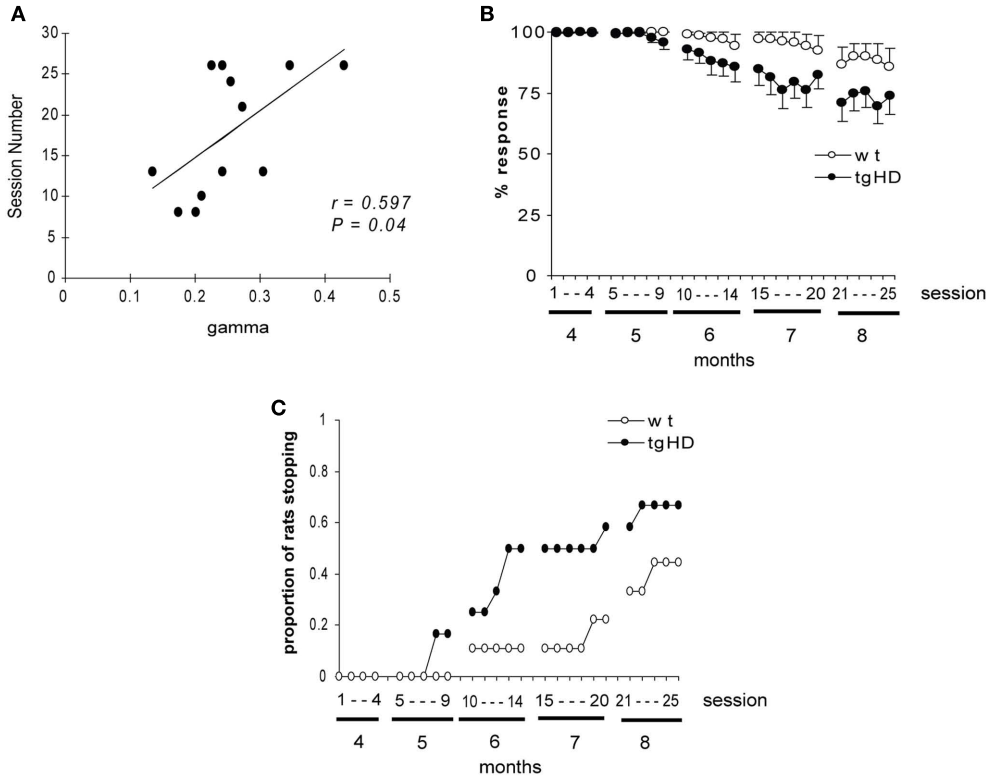

FIGURE 2 | During the course of bisection testing, tgHD animals stop responding to intermediate stimulus durations earlier than wt animals do. (A) Correlation between the session number at which the rats stop responding to intermediate durations (criterion < 95%) and gamma measured at 4 months, for tgHD rats. **(B)** Mean (±SEM) percent responses to intermediate durations on the 25 sessions of testing in months 4–8 for tgHD (filled symbols) and wt (empty symbols) rats. **(C)** Proportion of rats in each group stopping to respond across the 25 sessions of testing.

of a discrimination between intermediate durations and anchor durations.

As mentioned above, tgHD rats showed on average poorer sensitivity at 4 months than wt, and therefore would be expected to be slower in learning the discrimination. The opposite was observed, however, as tgHD rats stopped responding to intermediate durations earlier than wt rats as shown in **Figure 2B** [significant group × session interaction, $F(24,456) = 1.87$, $p < 0.01$]. A trend toward faster learning was also observed when calculating the proportion of animals in each group that stopped responding, for each of the 25 test sessions (**Figure 2C**), although the difference in proportion observed during sessions 13 to 18 was only marginally significant (Fisher Exact Test, $p = 0.07$). Thus, other factors in addition to temporal sensitivity combine to govern temporal performance in the bisection task.

TEMPORAL BISECTION FUNCTION

The fact that animals progressively stopped responding to intermediate durations precluded the analysis of the bisection curves for these animals with repeated testing. Fewer than 50 percent of the total number of animals (four tgHD and five wt) were responding at 8 months, whereas more than 50% were still responding at 7 months. When restricting the analysis to animals that were responding at the 7-month testing phase (wt, $n = 7$; tgHD, $n = 6$), the analysis of this subset confirmed that at 4 months of age tgHD rats showed poorer sensitivity, but similar PSE, compared to wt rats [**Figures 3A,B**, $F(1,11) = 8.12$, $p < 0.02$, and $F < 1$, for gamma and PSE, respectively]. Interestingly, both PSE and gamma decreased with repeated testing across the 4 months [$F(3,33) = 3.38$, $p < 0.03$, $F(3,33) = 8.39$, $p < 0.001$, respectively]. Furthermore, while PSE did not change differentially between genotypes (no group × test month interaction, $F < 1$), gamma tended to decrease more rapidly in tgHD than in wt rats. Both groups showed a significant decrease in gamma across months [$F(3,18) = 3.80$ and $F(3,15) = 5.61$; ps < 0.05, for wt and tgHD groups respectively]. However, a marginally significant group × test month interaction [$F(3,33) = 2.80$, $p = 0.055$], in addition to the fact that gamma for tgHD was significantly lower than for wt at 7 months of age [$F(1,11) = 6.28$, $p < 0.03$] show that temporal sensitivity improved faster for the tgHD than for wt rats. These data indicate that PSE and gamma were differentially sensitive to repeated testing.

DISCUSSION

INCREASED RESPONSE LATENCY FOR INTERMEDIATE DURATIONS LEADS TO CESSATION OF RESPONDING

On initial test sessions, both groups showed a decrease in response latency with increasing test stimulus duration (Höhn et al., 2011),

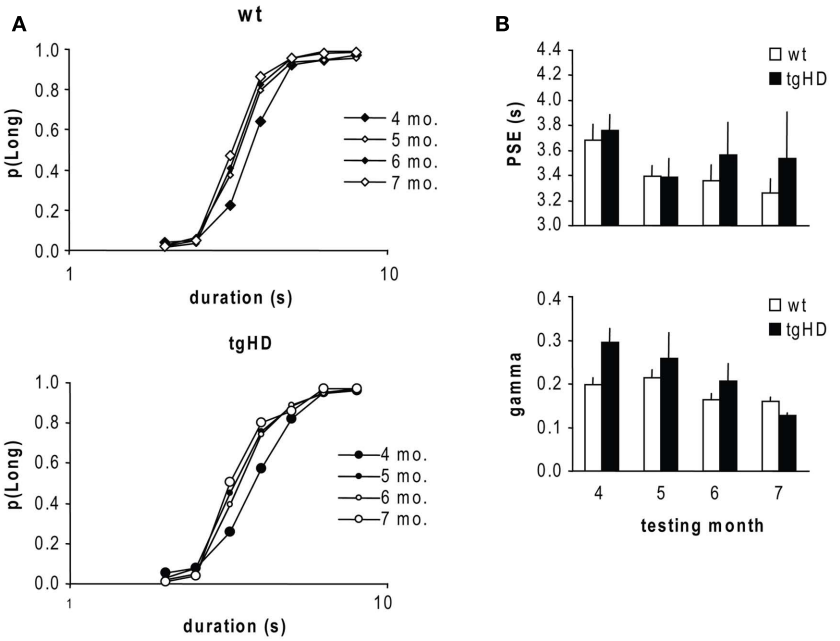

FIGURE 3 | Repetition of bisection testing sharpens temporal sensitivity. (A) Evolution of bisection curves for test months 4–7 for subgroups of animals that were responding at 7 months (top, wt rats; bottom, tgHD rats). **(B)** Mean (+SEM) PSE (top) and gamma (bottom) values estimated from the bisection curves for test months 4–7 represented in **(A)**.

replicating previously reported findings (Callu et al., 2009). The present data demonstrate that in rats, an inverted U-shaped function of response latency emerges as the animals learn to discriminate the intermediate durations from the anchors, and that it leads to cessation of responding to intermediate durations with continued testing. The inverted U-shaped function has been reported previously with both rat and human subjects (Maricq and Church, 1983; Meck, 1983; Rodríguez-Gironés and Kacelnik, 1998). Maricq and Church suggested that elevated latencies for intermediate durations in rats reflect either response conflict or discrimination learning between anchor vs. intermediate durations signaling availability vs. non-availability of reinforcement, respectively. The present data support the latter view, as the inverted U-shaped function was absent during initial test sessions, and was followed by the selective reduction in probability of responding to the intermediate test durations. Thus, intermediate durations used in the present study were discriminatively different from the anchors as indicated by performance in well-trained animals, suggesting that the bisection task functionally shifted from a two- to a three-alternative (two anchors and intermediate durations) discrimination task with repeated testing.

REPETITION OF BISECTION TESTING SHARPENS TEMPORAL SENSITIVITY

Point of subjective equality decreased and temporal sensitivity increased with repeated testing in the present study. The changes in both variables may be unrelated, but a decision–theoretic account, the PLM (Killeen et al., 1997), predicts a decrease in the PSE, from the arithmetic mean of the anchor durations to the harmonic mean as a limit, as gamma decreases. The change in PSE was also accompanied by the emergence of a behavioral discrimination between anchor and intermediate stimulus durations. It is not clear how that discrimination is related to the assumptions of PLM, but it is possible that judgments of "short" vs. "not short" (intermediate and long) that emerge with training may determine the location of the criterion in that model, or response bias in a scalar expectancy theory (SET) account (Gibbon, 1981; Allan and Gibbon, 1991) of the indifference point in the bisection task.

The improvement in temporal sensitivity could also be related to the change in the functional properties of the discrimination task. The introduction of new, intermediate durations in the test phase represents an increase in discrimination difficulty, which has been shown to decrease Weber fraction in humans (see Ferrara et al., 1997). Alternatively, temporal sensitivity may increase as a result of repeated exposure to the test stimuli in the absence of a change in task structure, consistent with the sharpening of stimulus generalization gradients with pre-exposure to the training stimulus (Honey, 1990) or increased amounts of training (Brown, 1970).

The foregoing phenomena may be taken to represent the acquisition of stimulus control, that is, the establishment of behavioral control by specific differences in the properties of stimuli along one or more continua. Thus, animals may learn to identify relevant stimulus dimensions, and change their behavior accordingly, only with repeated discrimination training. Alternatively, stimulus control may be established immediately upon the initial exposure to the discriminative stimuli, with increased training serving only to bring behavior under sharper control by the prevailing contingencies of reinforcement. Thus, sharpening of psychometric

functions in the present study may reflect the effect of repeated exposure to the contingencies of reinforcement on performance, while stimulus differences are fully discriminated early in training (Balsam et al., 2002; Drew et al., 2005). In support of this idea are the results of Droit-Volet and Izaute (2009) who manipulated the availability of a third "I do not know" response in the temporal bisection procedure in human observers. Adults who were given that response option exhibited sharper bisection functions (smaller Weber fractions) immediately in a single test session compared to control subjects with only the two standard response options. Thus, temporal sensitivity may depend upon available response options in both rats and humans, with difference in rate of emergence reflecting the use of verbal vs. contingency-based instructions.

TEMPORAL AND NON-TEMPORAL FACTORS GOVERN THE TEMPORAL PERFORMANCE

Initial measures of sensitivity to temporal properties of stimuli between tgHD and wt rats predicted a difference in speed of acquisition of a temporal discrimination that was opposite to the one observed, that is, at 4 months, the tgHD rats had poorer sensitivity (higher gamma) than wt, but the tgHD rats stopped responding to the intermediate duration sooner than wt. Thus, it is likely that other factors in addition to temporal sensitivity combine to govern temporal performance in the bisection task. Superior learning capacities in tgHD rats could be one factor, as increased prefronto-striatal plasticity has been reported in presymptomatic tgHD rats (Höhn et al., 2011). However, initial learning of the simple 2 vs. 8 s discrimination was similar for tgHD and wt rats, although a more challenging discrimination task might have revealed a difference in temporal learning. In addition, Höhn et al. (2011) reported that at 10 months, the same tgHD rats were inferior to wt in learning a discrimination reversal. Therefore, superior learning is not a likely factor, and increased plasticity in young adult tgHD rats may be an index of compensatory mechanisms secondary to dysfunctional networks. Another factor may reside in age-related neurodegeneration in transgenic animals. The monotonic continuous decrease in percent response observed across sessions (**Figure 2B**), however, more likely reflects learning through repetition rather than an age-related effect (which would be expected to produce decreases between but not within months). Yet another factor may be greater sensitivity to non-reinforcement in tgHD rats, as responses to intermediate durations were never reinforced. In a separate study (Faure et al., 2011), using a runway task in which the sucrose reinforcement was suddenly changed to a lower or a higher concentration (i.e., a less or more rewarding value) tgHD rats were more reactive than wt rats to changes in reward values. It is therefore likely that incentive motivation is a factor in the speed of discrimination learning between anchor (reinforcement) and intermediate (no reinforcement) durations.

CONCLUSION

Our data highlight the dynamic properties of the temporal bisection procedure. A number of factors have been shown to modulate performance in that procedure in animals and humans, including pharmacological agents (e.g., Meck, 1983; Santi et al., 2001), temporal and non-temporal stimulus properties (e.g., Church and Deluty, 1977; Penney et al., 2000), arousal/emotion (e.g., Droit-Volet and Wearden, 2002; Grommet et al., 2011), lesion (e.g., Meck et al., 1984; Breukelaar and Dalrymple-Alford, 1999), and disease (e.g., Smith et al., 2007; Carroll et al., 2008). The present study shows that repetition or amount of training/testing is another relevant variable (see also Machado and Keen, 2003). Repetition resulted in a sharpening of the bisection function and discrimination between anchor durations and intermediate test durations, both of which were more pronounced in tgHD rats. This difference was correlated with responsiveness to motivational factors, reflecting higher sensitivity to changes in reward values.

Transgenic Huntington disease animals exhibit poorer temporal sensitivity at 4 months than wt animals, as shown in two different ways in Höhn et al. (2011). We show here that higher temporal sensitivity was correlated with earlier stopping to respond to intermediate non-reinforced durations during the course of bisection testing. The fact that tgHD animals stopped earlier than wt animals, in contrast to what would be expected from their poorer initial temporal sensitivity, shows that the speed with which stopping to respond occurs does not reflect only temporal sensitivity. We hypothesize that sensory factors and non-sensory (motivational) factors may play competing roles in temporal bisection performance, and that an enhanced sensitivity to non-reinforcement can offset lower levels of temporal sensitivity to produce more rapid expression of the discrimination between anchor vs. intermediate stimulus durations. While initial bisection testing provides a valid measure of temporal sensitivity (gamma), repeated testing in the bisection task provides an opportunity for motivational factors (reinforcement vs. non-reinforcement) to exert their effect on the tendency to respond vs. not respond.

Changes in temporal performance after genetic or other biological manipulations may be related to non-sensory (motivational) factors in addition to sensory (temporal) factors, and control of these factors may be critical in determining underlying mechanisms. Inasmuch as the role of motivational factors in timing performance has been inferred in different timing protocols including both the peak interval procedure (e.g., Ward et al., 2009) and the bisection procedure in this report, the isolation of temporal control of behavior may require more sophisticated measures in the general case. A technical solution to the presumed motivational confound encountered in the present study would be to use narrow anchor duration ranges that closely encompass the interval of uncertainty, as assumed in the method of constant stimuli, thus preserving response tendencies along all test durations. Owing to the joint effects of both anchor stimulus range and repeated stimulus exposure, assessment of temporal sensitivity may require continued adjustments in stimulus range until stable performance is observed.

Sharpening of the bisection function with repetition may reflect an increase in temporal sensitivity apart from the influence of non-temporal factors. At an empirical level it is not known whether repeated exposure to the reinforcement contingencies involving the anchor durations or repeated exposure to the test durations was critical, as these variables were confounded in the present

study. From the perspective of temporal information processing theory (SET, Gibbon et al., 1984), variation in temporal sensitivity could be related to variability in the perception of the anchor stimuli or in memory representation (Allan and Gerhardt, 2001), or possibly in the decision mechanism (Penney et al., 2008). A challenge for future research is the dissociation among these mechanisms as accounts of the effects of repeated training/testing upon performance in the bisection task.

ACKNOWLEDGMENTS

This work was supported by grants from Agence Nationale de la Recherche (ANR) and a Partner University Fund grant awarded to Valérie Doyère, and by a PSC-CUNY grant awarded to Bruce L. Brown by the Research Foundation of CUNY (Grant 61336-00 39). Sophie Höhn was supported by Ministry of Research (MRT). The publication of this paper is sponsored by the COST Action TIMELY.

REFERENCES

Allan, L. G. (2002). The location and interpretation of the bisection point. *Q. J. Exp. Psychol.* 55B, 43–60.

Allan, L. G., and Gerhardt, K. (2001). Temporal bisection with trial referents. *Percept. Psychophys.* 63, 524–540.

Allan, L. G., and Gibbon, J. (1991). Human bisection at the geometric mean. *Learn. Motiv.* 22, 39–58.

Balsam, P. D., Drew, M. R., and Yang, C. (2002). Timing at the start of associative learning. *Learn. Motiv.* 33, 141–155.

Breukelaar, J. W., and Dalrymple-Alford, J. C. (1999). Effects of lesions to the cerebellar vermis and hemispheres on timing and counting in rats. *Behav. Neurosci.* 113, 78–90.

Brown, B. L. (1970). Stimulus generalization in salivary conditioning. *J. Comp. Physiol. Psychol.* 71, 467–477.

Buhusi, C. V., and Meck, W. H. (2005). What make us tick? Functional and neural mechanisms of interval timing. *Nat. Rev. Neurosci.* 6, 755–765.

Callu, D., El Massioui, N., Dutrieux, G., Brown, B. L., and Doyère, V. (2009). Cognitive processing impairments in a supra-second temporal discrimination task in rats with cerebellar lesion. *Neurobiol. Learn. Mem.* 91, 250–259.

Carroll, C. A., Boggs, J., O'Donnell, B. F., Shekhar, A., and Hetrick, W. P. (2008). Temporal processing dysfunction in schizophrenia. *Brain Cogn.* 67, 150–161.

Church, R. M., and Deluty, M. Z. (1977). Bisection of temporal intervals. *J. Exp. Psychol. Anim. Behav. Process.* 3, 216–228.

Drew, M. R., Zupan, B., Cooke, A., Couvillon, P. A., and Balsam, P. D. (2005). Temporal control of conditioned responding in goldfish. *J. Exp. Psychol. Anim. Behav. Process.* 31, 31–39.

Droit-Volet, S., and Izaute, M. (2009). Improving time discrimination in children and adults in a temporal bisection task: The effects of feedback and no forced choice on decision and memory processes. *Q. J. Exp. Psychol.* 62, 1173–1188.

Droit-Volet, S., and Wearden, J. (2002). Speeding up an internal clock in children? Effects of visual flicker on subjective duration. *Q. J. Exp. Psychol. B.* 55, 193–211.

Faure, A., Höhn, S., von Hörsten, S., Delatour, B., Raber, K., Leblanc, P., Desvignes, N., Doyère, V., and El Massioui, N. (2011). Altered emotional and motivational processing in the transgenic rat model for Huntington's disease. *Neurobiol. Learn. Mem.* 95, 92–101.

Ferrara, A., Lejeune, H., and Wearden, J. H. (1997). Changing sensitivity to duration in human scalar timing: an experiment, a review, and some possible explanations. *Q. J. Exp. Psychol. B* 50B, 217–237. [See Wearden and Ferrara (1995). QJEP. 49, 24–44].

Gibbon, J. (1981). On the form and location of the psychometric bisection function for time. *J. Math. Psychol.* 24, 58–87.

Gibbon, J., Church, R. M., and Meck, W. H. (1984). Scalar timing in memory. *Ann. N. Y. Acad. Sci.* 423, 52–77.

Grommet, E. K., Droit-Volet, S., Gil, S., Hemmes, N. S., Baker, A. H., and Brown, B. L. (2011). Time estimation of fear cues in human observers. *Behav. Processes* 86, 88–93.

Höhn, S., Dallérac, G., Faure, A., Urbach, Y., Nguyen, H. P., Riess, O., von Hörsten, S., Le Blanc, P., Desvignes, N., El Massioui, N., Brown, B. L., and Doyère, V. (2011). Behavioral and in vivo electrophysiological evidence for presymptomatic alteration of prefronto-striatal processing in the transgenic rat model for Huntington disease. *J. Neurosci.* 31, 8986–8997.

Honey, R. C. (1990). Stimulus generalization as a function of stimulus novelty and familiarity in rats. *J. Exp. Psychol. Anim. Behav. Process.* 16, 178–184.

Killeen, P. R., Fetterman, J. G., and Bizo, L. A. (1997). "Time's causes," in *Time and Behaviour: Psychological and Neurobehavioral Analyses*, eds C. M. Bradshaw and E. Szabadi (Amsterdam: Elsevier), 79–131.

Machado, A., and Keen, R. (2003). Temporal discrimination in a long operant chamber. *Behav. Process.* 62, 157–182.

Maricq, A. V., and Church, R. M. (1983). The differential effects of haloperidol and methamphetamine on time estimation in the rat. *Psychopharmacology (Berl.)* 79, 10–15.

Meck, W. H., Church, R. M., and Olton, D. S. (1984). Hippocampus, time, and memory. *Behav. Neurosci.* 98, 3–22.

Meck, WH. (1983). Selective adjustment of the speed of internal clock and memory processes. *J. Exp. Psychol. Anim. Behav. Process.* 9, 171–201.

Nguyen, H. P., Kobbe, P., Rahne, H., Wörpel, T., Jäger, B., Stephan, M., Pabst, R., Holzmann, C., Riess, O., Korr, H., Kántor, O., Petrasch-Parwez, E., Wetzel, R., Osmand, A., and Von Hörsten, S. (2006). Behavioral abnormalities precede neuropathological markers in rats transgenic for Huntington's disease. *Hum. Mol. Genet.* 15, 3177–3194.

Penney, T., Gibbon, J., and Meck, W. (2000). Differential effects of auditory and visual signals on clock speed and temporal memory. *J. Exp. Psychol. Hum. Percept. Perform.* 26, 1770–1787.

Penney, T. B., Gibbon, J., and Meck, W. H. (2008). Categorical scaling of duration bisection in pigeons (*Columba livia*), mice (*Mus musculus*), and humans (*Homo sapiens*). *Psychol. Sci.* 19, 1103–1109.

Rodríguez-Gironés, M. A., and Kacelnik, A. (1998). "Response latencies in temporal bisection: implications for timing models," in *Time and the Dynamic Control of Behavior*, eds V. De Keyser, G. d'Ydewalle, and A. Vandierendonck (Seattle: Hogrefe & Huber), 51–70.

Rouanet, H., Bernard, J.-M., and Le Roux, B. (1990). *Analyse Inductive des Données: Statistique en Sciences Humaines.* Paris: Dunod.

Santi, A., Coppa, R., and Ross, L. (2001). Effects of the dopamine D2 agonist, quinpirole, on time and number processing in rats. *Pharmacol. Biochem. Behav.* 68, 147–155.

Smith, J. G., Harper, D. N., Gittings, D., and Abernethy, D. (2007). The effect of Parkinson's disease on time estimation as a function of stimulus duration range and modality. *Brain Cogn.* 64, 130–143.

von Horsten, S., Schmitt, I., Nguyen, H. P., Holzmann, C., Schmidt, T., Walther, T., Bader, M., Pabst, R., Kobbe, P., Krotova, J., Stiller, D., Kask, A., Vaarmann, A., Rathke-Hartlieb, S., Schulz, J. B., Grasshoff, U., Bauer, I., Vieira-Saecker, A. M., Paul, M., Jones, L., Lindenberg, K. S., Landwehrmeyer, B., Bauer, A., Li, X. J., and Riess, O. (2003). Transgenic rat model of Huntington's disease. *Hum. Mol. Genet.* 12, 617–624.

Ward, R. D., Kellendonk, C., Simpson, E. H., Lipatova, O., Drew, M. R., Fairhurst, S., Kandel, E. R., and Balsam, P. D. (2009). Impaired timing precision produced by striatal D2 receptor overexpression is mediated by cognitive and motivational deficits. *Behav. Neurosci.* 123, 720–730.

Woodworth, R. S., and Schlosberg, H. (1954). *Experimental Psychology.* New York: Holt.

Conflict of Interest Statement: The authors declare that the research was conducted in the absence of any commercial or financial relationships that could be construed as a potential conflict of interest.

Received: 13 June 2011; paper pending published: 14 July 2011; accepted: 09 August 2011; published online: 28 September 2011.

Citation: Brown BL, Höhn S, Faure A, von Hörsten S, Le Blanc P, Desvignes N, El Massioui N and Doyère V (2011) Temporal sensitivity changes with extended training in a bisection task in a transgenic rat model. Front. Integr. Neurosci. 5:44. doi: 10.3389/fnint.2011.00044

frontiers in
INTEGRATIVE NEUROSCIENCE

ORIGINAL RESEARCH ARTICLE
published: 13 October 2011
doi: 10.3389/fnint.2011.00061

Learning of temporal motor patterns: an analysis of continuous versus reset timing

Rodrigo Laje[1,2], Karen Cheng[1] and Dean V. Buonomano[1,3]*

[1] *Department of Neurobiology, University of California, Los Angeles, CA, USA*
[2] *Departamento de Ciencia y Tecnología, Universidad Nacional de Quilmes, Bernal, Argentina and CONICET, Argentina*
[3] *Department of Psychology and Brain Research Institute, University of California, Los Angeles, CA, USA*

Edited by:
Warren H. Meck, Duke University, USA

Reviewed by:
Patrick Simen, Oberlin College, USA
Uma R. Karmarkar, Harvard Business School, USA

***Correspondence:**
Dean V. Buonomano, Departments of Neurobiology and Psychology, University of California, 695 Young Drive, Gonda – Room 1320, Los Angeles, CA 90095-1761, USA.
e-mail: dbuono@ucla.edu

Our ability to generate well-timed sequences of movements is critical to an array of behaviors, including the ability to play a musical instrument or a video game. Here we address two questions relating to timing with the goal of better understanding the neural mechanisms underlying temporal processing. First, how does accuracy and variance change over the course of learning of complex spatiotemporal patterns? Second, is the timing of sequential responses most consistent with starting and stopping an internal timer at each interval or with continuous timing? To address these questions we used a psychophysical task in which subjects learned to reproduce a sequence of finger taps in the correct order and at the correct times – much like playing a melody at the piano. This task allowed us to calculate the variance of the responses at different time points using data from the same trials. Our results show that while "standard" Weber's law is clearly violated, variance does increase as a function of time squared, as expected according to the generalized form of Weber's law – which separates the source of variance into time-dependent and time-independent components. Over the course of learning, both the time-independent variance and the coefficient of the time-dependent term decrease. Our analyses also suggest that timing of sequential events does not rely on the resetting of an internal timer at each event. We describe and interpret our results in the context of computer simulations that capture some of our psychophysical findings. Specifically, we show that continuous timing, as opposed to "reset" timing, is consistent with "population clock" models in which timing emerges from the internal dynamics of recurrent neural networks.

Keywords: timing, temporal processing, time estimation and production, human psychophysics, recurrent networks, neural dynamics, computational modeling

INTRODUCTION

The nervous system processes and tracks time over a range of at least 12 orders of magnitude: from our ability to discriminate whether sounds arrive at our left or right ear first (microseconds), to the governing of our circadian rhythms (hours and days). In between these extremes, on the order of milliseconds and seconds, lie what might be considered the most sophisticated forms of timing: those that are required for complex sensory and motor tasks, including speech, or music, perception, and production. It is clear that, unlike the clocks on our wrists or walls that can be used to track milliseconds or months, the brain uses fundamentally different mechanisms to time across different scales (Lewis et al., 2003; Mauk and Buonomano, 2004; Buhusi and Meck, 2005; Buonomano, 2007; Grondin, 2010). For example, the axonal delay lines that contribute to sound localization (Jeffress, 1948; Carr, 1993) have nothing to do with the transcription/translation feedback loops that govern circadian rhythms (King and Takahashi, 2000; Panda et al., 2002). Indeed, while significant progress has been made toward understanding the mechanisms underlying timing in the extremes of biological temporal processes, less progress has been made toward elucidating the mechanism, or more likely mechanisms, underlying timing the in range of hundreds of milliseconds to a few seconds. It is this range, with particular attention to the motor domain, which will be the focus of the current paper.

As in many other areas of sensory perception, Weber's Law has maintained a dominant presence in the field of temporal processing. Specifically, that the SD of motor responses or the precision of sensory discrimination varies linearly with absolute interval. In other words, the coefficient of variation (CV, or Weber's fraction), defined as the SD over mean time, should be constant. This linear relationship is often referred to as the scalar property (Gibbon, 1977).

There is excellent evidence that Weber's law holds true over certain time scales in some paradigms (Gibbon, 1977; Meck and Church, 1987; Allan and Gibbon, 1991; Church et al., 1994; Hinton and Rao, 2004; Jazayeri and Shadlen, 2010). However it is also clear that, at least in its simplest form, Weber's law does not universally hold true. For example, Lewis and Miall (2009) recently reported that in a time reproduction task over a range of 68 ms to 16 min there was a progressive decrease in the CV; they concluded "this finding joins other recent reports in demonstrating a systematic violation of the scalar property in timing data." Indeed, many studies have stressed that even within narrow time ranges both sensory

(Getty, 1975; Hinton and Rao, 2004) and motor (Ivry and Hazeltine, 1995; Bizo et al., 2006; Merchant et al., 2008) timing violates Weber's law. However, these data seem to be well accounted for by a generalized form of Weber's law (Getty, 1975; Ivry and Hazeltine, 1995; Bizo et al., 2006; Merchant et al., 2008), in which the variance increases as T^2 plus a time-independent (residual or noise) variance component. The time-dependent component of the variance is often interpreted as reflecting the properties of some "internal clock," while the independent term is often viewed as reflecting with motor variability. Few, if any, studies have explicitly quantified how these different components change with learning. Here we show that both components change during learning.

Interestingly the majority of studies that have explicitly quantified the relationship between variance and time have done so using independent intervals. That is, the variance of distinct intervals, such as the production of 0.5, 1, and 2 s intervals, is analyzed in separate trials. Here we use a spatiotemporal (or purely temporal) pattern reproduction task, in which the accuracy and precision to multiple consecutive responses within a pattern can be obtained within the same trial. We first confirm that even within a fairly narrow range of a few seconds, the standard version of Weber's law (constant CV) is violated; however, the generalized version where variance increases in proportion to T^2 captures the data well. Additionally, this task allowed us to address a specific question relating to the timing of consecutive intervals. Consider a temporal task such as pressing a sequence of keys on a piano at the appropriate times. Does this task rely on timing all consecutive events in relation to the sequence onset time ($t = 0$), or on resetting and restarting an internal timer at each event – and thus essentially consist of timing consecutive intervals in isolation? Based on expected differences in the variability signature of consecutive responses we conclude that the "internal timer" is not reset during each event.

Finally, based on a previously presented model, we demonstrate how recurrent neural networks that do not exhibit any periodic clock-like activity can generate complex spatiotemporal patterns. The model is consistent with non-resetting timing mechanisms; however, we also highlight the need for this and other models to quantitatively account for the experimentally observed variance characteristics.

MATERIALS AND METHODS

TASKS

The basic task used in this work resembles playing a melody on a piano, by pressing the correct keys in the correct order and target times. Two versions of the task were used: a spatiotemporal pattern reproduction (STPR) task (Experiment 1), where the subjects used four fingers to press the corresponding keys on a computer keyboard; and a Temporal Pattern Reproduction (TPR) task (Experiment 2) where the subjects used only one finger and one key. In the STPR version, each of four rectangles on a computer screen is assigned a corresponding computer key and finger: keys F-D-S-A were assigned to fingers 2 (index) through 5 (pinky) of the left hand. Subjects learned a spatiotemporal pattern consisting of a sequence of key presses; the spatial component corresponds to the order in which each key must be pressed, and the temporal component to the time each key must be pressed in relation to $t = 0$. Each trial consisted of an *exposure* component followed by a *training/testing* component. The exposure component is similar to a "temporal" serial reaction time task (Nissen and Bullemer, 1987; Shin and Ivry, 2002): the subject is instructed to press the appropriate key in response to every flashed rectangle. Stimuli were presented in "open-loop" mode, i.e., the events continue independent of if and when the subject responds. After the exposure component, the training/testing component begins with an onset cue, and then the subject is required to reproduce the entire spatiotemporal pattern on their own as accurately as possible; in this phase the rectangles appear only if and when the subject presses one of the four keys. The beginning of the pattern ($t = 0$) was initiated by the subject by pressing the space bar with the thumb. The response time of each key press in relation to $t = 0$ is recorded to calculate the variance, root-mean-square error (RMSE), and mean of the response times for further analysis. Feedback on the training/testing component is provided at the end of each trial in the form of a performance index, and an image of a "raster" that illustrates the target and produced patterns. In the TPR version of the task only one key/finger was used to reproduce the entire pattern (i.e., a purely temporal pattern with no spatial component). In this task, in an attempt to minimize previous experience all subjects used their pinky finger (left hand).

GENERAL PROCEDURE

During the test subjects sat in front of a computer monitor with a keyboard in a quiet room. Stimulus presentation and behavioral response collection were controlled by a personal computer using custom-written code in Matlab and PsychToolBox. As the overall performance measure to track learning we used the RMSE between the response times and the target times.

WEBER'S GENERALIZED LAW

We fit the "Weber generalized law" (Eq. 1) to our data; and to provide a comparison we also performed fits using a related equation with the same number of degrees of freedom where variance was a linear function of T (Eq. 2; Ivry and Hazeltine, 1995). Specifically:

$$\sigma^2 = k\,T^2 + \sigma^2_{\text{indep}} \quad \text{(Generalized Weber's law)} \tag{1}$$

$$\sigma^2 = k\,T + \sigma^2_{\text{indep}} \tag{2}$$

where σ^2 represents the total variance, σ^2_{indep} the time-independent variance, and k (in Eq. 1) approximates the square root of the conventional Weber fraction at long intervals. Both equations predict a decreasing CV as a function of absolute time T, although to differing degrees.

SLOPE AND INTERCEPT OF THE GENERALIZED WEBER'S LAW

For every day and every subject classified as a learner (see Experiment 1), we performed a linear regression between the variance of each response time and the mean absolute response times squared throughout the pattern. The fitted slope and intercept of the linear regression were the estimates for the parameters k and σ^2_{indep} in the equation for the generalized Weber's law above (Eq. 1).

RESET VERSUS CONTINUOUS TIMING

To examine the Reset versus Continuous timing hypotheses we fit two different functions to the data. Consider the responses to a

temporal pattern composed of six consecutive intervals $t_1 \ldots t_6$, so that the absolute timing of each response is $T_1 \ldots T_6$, with $T_1 = t_1$, $T_2 = t_1 + t_2, \ldots, T_6 = t_1 + t_2 + \ldots + t_6$. The Reset Timing hypothesis assumes that the variance at each response along the pattern adds to the accumulated variance from previous responses, so that the variance at any time T (coincident with a response) along the pattern is

$$\sigma^2_{\text{reset}}(T) = \begin{cases} k\, t_1^2 + \sigma^2_{\text{indep}} & \text{if } T = T_1 \\ k\left(t_1^2 + t_2^2\right) + \sigma^2_{\text{indep}} & \text{if } T = T_2 \\ \cdots & \cdots \\ k\left(t_1^2 + t_2^2 + \ldots + t_6^2\right) + \sigma^2_{\text{indep}} & \text{if } T = T_6 \end{cases}$$

where we conservatively assumed that the time-independent variance σ^2_{indep} adds only once (i.e., a "weak" form of resetting; we also tested a "strong" form of resetting, where the constant term σ^2_{indep} is added at every event as well, with poorer results). On the other hand, the Continuous Timing hypothesis assumes that all responses within a pattern are timed in absolute time T with respect to the beginning of the pattern, and thus the variance at any time T in the pattern is simply $\sigma^2_{\text{cont}}(T) = k\, T^2 + \sigma^2_{\text{indep}}$, in other words continuous timing predicts that the variance should obey Weber's generalized law. For instance, at the last response (time T_6), the Continuous timing yields $\sigma^2_{\text{cont}} = k\, T_6^2 + \sigma^2_{\text{indep}} = k(t_1 + t_2 + \ldots + t_6)^2 + \sigma^2_{\text{indep}}$. We found that in some cases the fitting with the Reset model yielded negative values for the time-independent variance, a non-meaningful value; therefore the fitting procedure was constrained so that this parameter was positive. No constraint was needed when fitting with the Continuous model.

EXPERIMENT 1: LEARNING AND THE GENERALIZED WEBER

Participants

Subjects were 12 undergraduate students from the UCLA community who were between the ages of 18 and 21. Subjects were paid for their participation. All experiments were run in accordance with the University of California Human Subjects Guidelines.

Procedure

Subjects were trained on the STPR task for three consecutive days, in four blocks of 20 trials per day (about 30 min). Each subject was trained on one target pattern. Each target pattern was generated from a random sequence of six key presses (four possible keys), separated by six random intervals between 200 and 800 ms (each target pattern was used for two subjects). The key sequence was constrained to ensure that consecutive key presses were never assigned to the same finger, and all fingers were used at least once.

Analysis

The CV was calculated as the ratio between the SD and the mean of the response times for each response of the pattern, for every day and every subject. To test the hypothesis that the CV is not constant, we performed a linear regression between the CV and the mean response time and then averaged the slopes across subjects. To eliminate potential outliers we discarded the top and bottom 2% of the response times of each interval from a given subject on a given day.

Learning

Since one goal of this experiment was to characterize changes in the time-dependent and independent variance with learning, we classified each subject as a learner if his/her learning curve complied with the following two conditions: 1. a significantly negative slope ($p < 0.001$); 2. a significant improvement in performance (RMSE) between the first and last blocks (one-tailed Student-t-test, $p < 0.01$). Four out of 12 subjects were classified as non-learners, and removed from learning analysis.

EXPERIMENT 2: CONTINUOUS VERSUS RESET TIMING

Participants

Subjects were 10 undergraduate students from the UCLA community between the ages of 18 and 21 paid for their participation.

Procedure

Subjects were trained on the TPR task for five consecutive days, in eight blocks of 20 trials per day (about 45 min). Each subject was trained on a periodic and "complex" pattern. Again, each pattern consisted of six intervals. In the periodic pattern, the interval between consecutive events was always 500 ms; for each complex target pattern, intervals were randomly chosen from a uniform distribution between 200 and 800 ms. The presentation order of the two types of targets (periodic versus complex) was counterbalanced between subjects. To remove potential outliers in the response times we eliminated the top and bottom 4% of the responses.

POPULATION CLOCK MODEL AND NUMERICAL SIMULATIONS

Network model

The model used the general random recurrent network model composed of firing-rate (non-spiking) units (Sompolinsky et al., 1988; Jaeger and Haas, 2004; Sussillo and Abbott, 2009). The network was composed of $N = 1800$ recurrent units, three input units, and four output units (see **Figure 6A**); the recurrent connectivity is represented by a sparse $N \times N$ matrix $\mathbf{W}$; non-zero elements in $\mathbf{W}$ are drawn independently from a Gaussian distribution with zero mean and variance $= g^2/(p \cdot N)$, where $g = 1.35$ is the synaptic strength factor, and $p = 0.1$ is the connection probability. The activity of each recurrent unit is represented by variable x_i (vector notation: $\mathbf{x} \equiv \{x_i\}$), whose dynamics is governed by a firing-rate model with a time constant $\tau = 10$ ms. Network-to-output connectivity is represented by an all-to-all $4 \times N$ matrix $\mathbf{W}_{\text{out}}$, (the only connections subject to training), with values initially drawn from a Gaussian distribution with zero mean and variance $1/N$; output units z_i are linear readouts of the activity of the network: $\mathbf{z} = \mathbf{W}_{\text{out}}\mathbf{x}$, where $\mathbf{r} = \tanh(\mathbf{x})$ are the firing rates. Output-to-network feedback connectivity ($N \times 4$ matrix $\mathbf{W}_{\text{fb}}$) is all-to-all, with matrix elements drawn from a uniform distribution between -1 and 1. Input-to-network connectivity ($N \times 3$ matrix $\mathbf{W}_{\text{in}}$) is all-to-all, with matrix elements drawn from a Gaussian distribution with zero mean and variance 1; input units are represented by variables y_i with no autonomous dynamics other than externally imposed by the experimenter; input baseline is zero, input pulses have duration 100 ms and height 2. All recurrent units have a noise input current with amplitude $= 0.01$. The equations

governing the time evolution of the network were:

$$\tau \frac{d\mathbf{x}}{dt} = -\mathbf{x} + \mathbf{W}\,\mathbf{r} + \mathbf{W}_{\text{in}}\,\mathbf{y} + \mathbf{W}_{\text{fb}}\,\mathbf{z} + \mathbf{I}_{\text{noise}}$$
$$\mathbf{r} = \tanh(\mathbf{x})$$
$$\mathbf{z} = \mathbf{W}_{\text{out}}\,\mathbf{r}$$

Learning algorithm

Training was performed with the FORCE learning rule (Sussillo and Abbott, 2009), applied to the output connectivity $\mathbf{W}_{\text{out}}$. Target functions were flat with a Gaussian-like peak (half width of 50 ms) at the target times, the baseline was 0.15 with a peak amplitude of 1. The inputs corresponded to a brief 100 ms pulse starting at $t = 0$ ms. After training, activation of the input units elicited the corresponding output pattern.

RESULTS

EXPERIMENT 1: TIMING OF CONSECUTIVE RESPONSES DOES NOT FOLLOW WEBER'S LAW

Most studies on timing and Weber's law have focused on isolated intervals rather than multiple time points within a pattern. Here we used a STPR task in which subjects were required to reproduce a spatiotemporal pattern, and thus generate a response at multiple time points within a single trial. Each subject was trained on a single target pattern for three consecutive days. A sample outcome of the task for a single subject (Day 3) is displayed in **Figure 1A**.

Our first observation is that the scalar property – the basic form of Weber's law – is violated when subjects are timing spatiotemporal patterns. That is, the SD of the response time along the spatiotemporal pattern is not proportional to the mean response time, as demonstrated by plotting the normalized fits to the

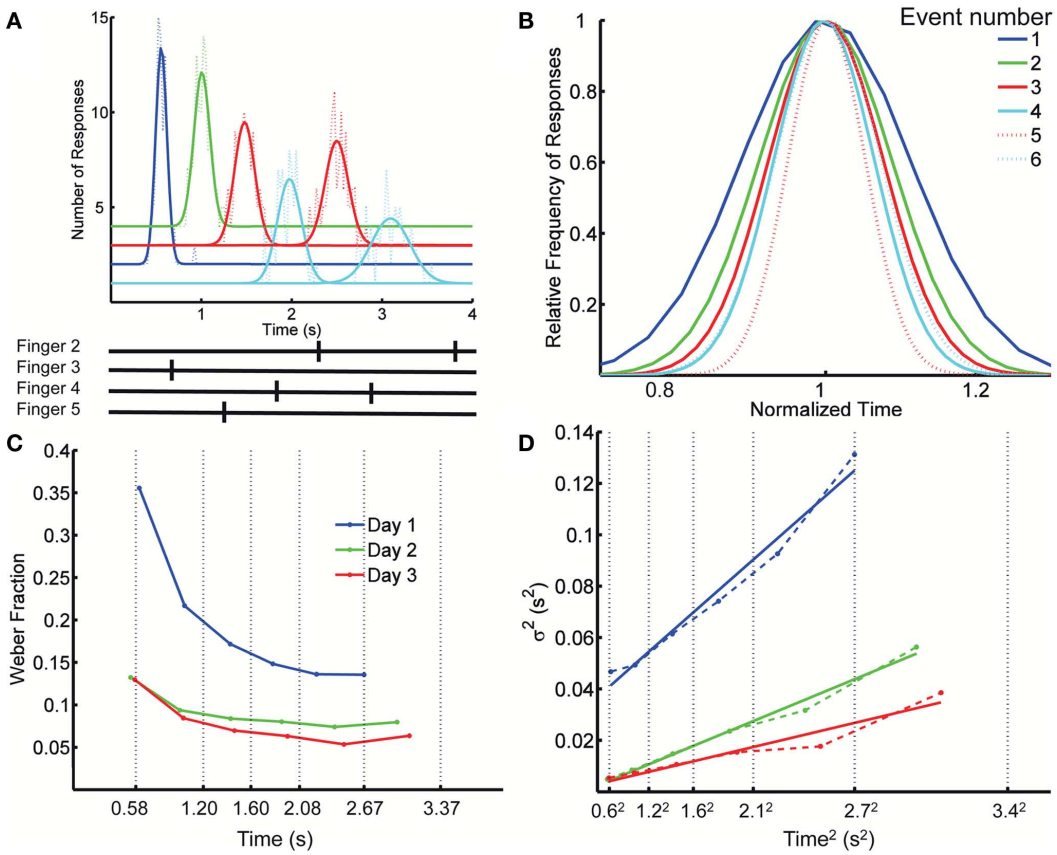

FIGURE 1 | Spatiotemporal Pattern Reproduction task data. **(A)** Top panel: Distribution of response times for each key press (dotted lines), with Gaussian fits (solid lines), for a complex pattern from one subject; Bottom panel: the target pattern. Colors cyan, blue, red, and green, correspond to fingers 2 (index) through 5 (pinky). A systematic anticipation is noticeable at the longer responses in this subject. Although some subjects tended to produce early responses and others late, across subjects there was a tendency to anticipate the target time, particularly at the last responses in the pattern. On the last day of training the difference between the response time and target time at the first element in the pattern was (mean ± SD) 25 ± 75 ms ($p = 0.26$), whereas for the last element it was −230 ± 320 ms ($p = 0.03$). The spatial error rate (trials with incorrect finger presses) decreased rapidly over the first few blocks: in the first block, on average, 33% of the trials had a spatial error; this fell to 8% in the second block, and 0.9% by the last block (12). **(B)** Overlaid normalized Gaussian fits from **(A)**. Each distribution has the *x* axis divided by its mean and their y values divided by their peak value. Dotted lines correspond to the second response of a given finger. **(C)** Weber fraction (=coefficient of variation) as a function of mean response time. Same subject, all 3 days. Vertical dotted lines indicate the target times. **(D)** Variance as a function of mean response time squared (dashed lines), and linear fits according to the generalized Weber's law (Eq. 1, solid lines).

response distributions of the consecutive responses (**Figure 1B**). **Figure 1C** plots the CV of each response as a function of its time in the pattern for the same subject on each day, revealing a clear decrease in CV over time. Across the 12 subjects, on any given day, there was a significant decrease in the CV as revealed by a significant negative slope in relation to absolute time for all 3 days ($p < 0.007$).

This result indicates that the standard version of Weber's law does not account for the changes in precision as a function of absolute time. The generalized version of Weber's law (see Materials and Methods), however, robustly captured the relationship between precision and time of the response (**Figure 1D**). To provide a direct comparison for the generalized Weber fit, we also fit an equation where variance changes linearly with T instead of T^2 (see Materials and Methods; Ivry and Hazeltine, 1995). Although both fits were quite good, the goodness of fit using Weber's generalized law, as measured by the determination coefficient R^2 between the fit and the data, was significantly better (mean R^2 of 0.907 and 0.867, respectively; $p = 0.0002$ two-tailed paired t-test after Fisher transformation). It is also worth noting that for all 3 days the residuals were significantly smaller with the generalized Weber fit compared to a standard Weber fit ($p < 0.001$).

To the best of our knowledge these results are the first to show that "standard" Weber's law does not hold for the timing of consecutively produced intervals. Yet, this result is consistent with previous results demonstrating violations in Weber's law for individual intervals (Getty, 1975; Ivry and Hazeltine, 1995; Merchant et al., 2008; Lewis and Miall, 2009).

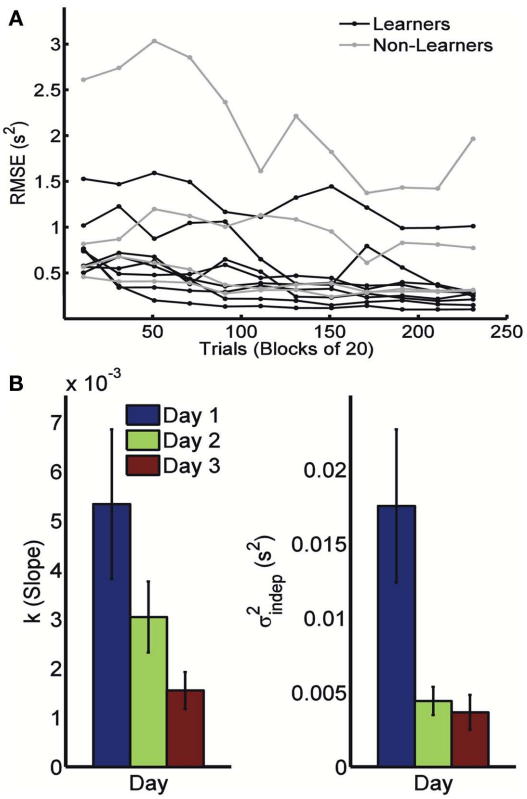

FIGURE 2 | Learning in the spatiotemporal pattern reproduction task. **(A)** Learning curves. Performance of all subjects over 3 days of training. RMSE: root-mean-square error between response times and target times, averaged in blocks of 20 trials. Statistically significant learners are in black, non-learners in gray. Some subjects classified as non-learners had very low RMSE values, but did not exhibit any significant improvement in performance from the first to last block, and were thus classified as "non-learners" (see Materials and Methods). **(B)** Mean slope k and mean intercept σ^2_{indep} across the 3-days of training. Error bars represent the SEM. There was a significant decrease in both k and σ^2_{indep} across training days ($p = 0.013$ and 0.011, respectively).

LEARNING ALTERS BOTH SOURCES OF VARIANCE

Because timing in the STPR task was well accounted for by the generalized Weber's law, we next examined how learning affected the time-dependent and time-independent variance sources. **Figure 2A** shows the learning curves for each of the 12 subjects across 3 days (four blocks of 20 trials each day). We defined performance as the error (RMS) between the response time and target times of each event. Learning of spatiotemporal patterns was observed for 8 out of the 12 subjects (see Materials and Methods).

In order to determine how, and if, the parameters k and σ^2_{indep} change with learning we fit Weber's generalized law to the data of each of the learners on each of the 3-days of training. We found that slope k and intercept σ^2_{indep} both changed with learning (one-way, repeated-measures ANOVA; k: $F_{2,6} = 6.04$, $p = 0.013$; σ^2_{indep}: $F_{2,6} = 6.29$, $p = 0.011$).

EXPERIMENT 2: RESETTING VERSUS CONTINUOUS TIMING

An important question regarding the timing of patterns in which multiple responses are produced within a trial, is whether the internal timer is reset or not at each new interval during the production of the pattern. To examine this issue we trained 10 subjects in the TPR task (i.e., a purely temporal version of the previous task) in which every subject had to learn two different patterns: one periodic (six consecutive, equal intervals of 500 ms) and the other complex (a non-periodic pattern composed of six consecutive random intervals in the range 200–800 ms). The use of a purely temporal task as opposed to the spatiotemporal task used in Experiment 1 was important to rule out any potential variance generated by the spatial component (i.e., switching fingers).

The two contrasting hypotheses we tested are depicted in **Figure 3**. Under "Reset Timing" the timing of consecutive intervals is done independently, and thus the variance of the response time at each next event in the pattern adds to the accumulated variance from the previous responses (based on the result above, and those of others, we are assuming that the timing of any given interval is governed by Weber's generalized law). In the case of a perfectly periodic pattern, this leads to a characteristic sublinear behavior when plotting the variance versus a time squared horizontal axis; for a complex pattern, in the reset mode the variance depends on the particular intervals of a pattern (see Materials and Methods for details). On the contrary, under "Continuous Timing," for either periodic or complex patterns, the temporal pattern is processed in absolute time from its onset. Thus the variance at every event when timed from the onset of the pattern should follow the generalized form of Weber's law, that is a straight line

in a variance × time squared plot. These two qualitatively different behaviors of the variance can be tested by comparing the fit of the two models to the experimental data. We examined timing in both a periodic and complex task because we hypothesized that reset timing might be more likely to be used during periodic patterns.

In **Figure 4A** we show the experimental data from one subject after fitting the reset and continuous equations. The predicted variance under the Resetting hypothesis is decelerating, a trait not observed in the experimental data. The Continuous timing fit appears to better account for the variance in both the periodic and the complex pattern. To quantify this, we performed a repeated-measures two-way ANOVA with factors Model (Continuous versus Reset) and Training Day (1 through 5) on the Pearson correlation coefficient R (Fisher-transformed) between each model's prediction and the experimental data (see Materials and Methods). The difference between Continuous and Reset models was significant for both the periodic and the complex patterns, with the Continuous producing a better fit than the Reset (periodic: mean $R^2 = 0.934$ for the Continuous, mean $R^2 = 0.876$ for the Reset, $F_{1,9} = 49.9$, $p < 10^{-4}$; complex: mean $R^2 = 0.891$ for the Continuous, mean $R^2 = 0.859$ for the Reset, $F_{1,9} = 11.2$, $p = 0.009$; **Figure 4B**). There was no effect of training (periodic: $F_{4,36} = 1.2$, $p = 0.31$; complex: $F_{4,36} = 1.0$, $p = 0.41$) or interaction (periodic: $F_{4,36} = 1.3$, $p = 0.28$; complex: $F_{4,36} = 0.4$, $p = 0.78$), suggesting that the quality of the fits did not change with training.

We also performed this same analysis with the spatiotemporal data in Experiments 1, with similar results. The Continuous model produced significantly better fits than the Reset model (mean $R^2 = 0.907$ and 0.869, respectively; $p = 0.01$). This result suggests that the mechanism for timing consecutive intervals in

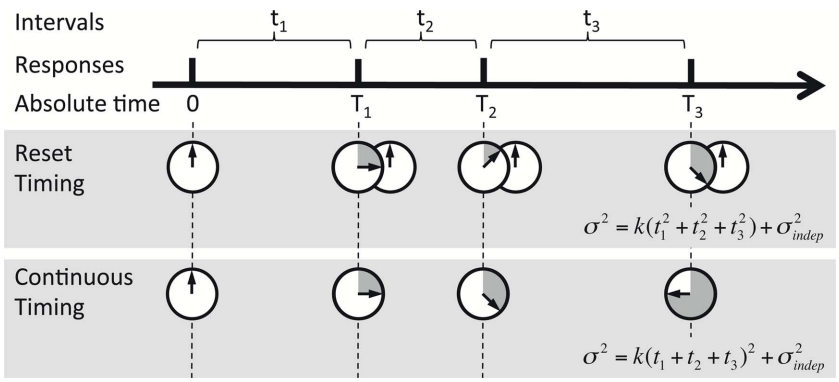

FIGURE 3 | Reset versus continuous timing. Timing of a temporal pattern (thick black line) could be achieved by timing every interval t_n in isolation and resetting the timer at each response (Reset timing), or by timing continuously in absolute time T since the beginning of the pattern (Continuous timing). The predicted variance at every point in the sequence is different, since in Reset timing the variance at each new response adds to the previous variance, whereas in Continuous timing the variance is a function of absolute time squared (note that $T_3 = t_1 + t_2 + t_3$).

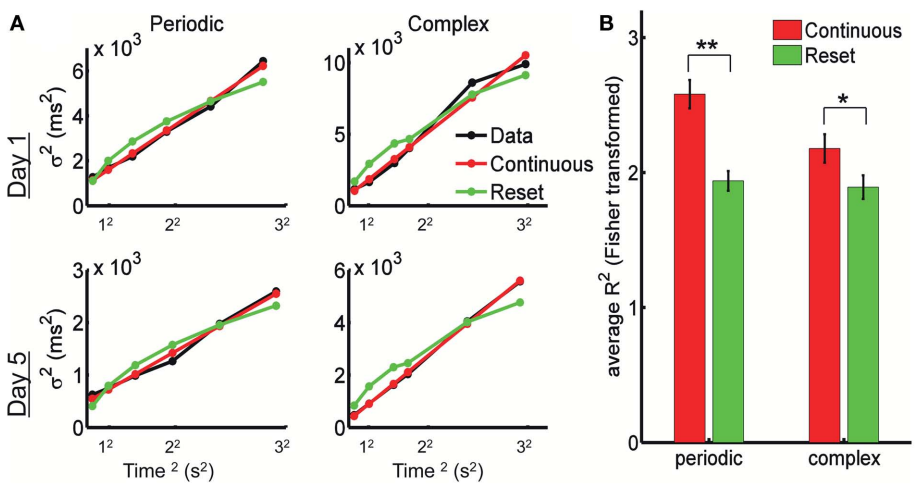

FIGURE 4 | The psychophysical data is best fit by continuous timing. (A) Example of fits for Reset and Continuous timing from one subject: variance as a function of mean response time squared. Left column: periodic pattern; right column: complex pattern. Top row: training day 1; bottom row: training day 5. **(B)** Goodness of fit for Reset and Continuous: average R^2 after Fisher transformation with SE bars. (**) $p < 0.0001$, (*) $p = 0.009$.

a sequence does not change because of the presence of a spatial component. And interestingly, contrary to our expectations there is no significant difference between the quality of the Continuous for the temporal and spatiotemporal tasks ($p = 0.61$). Additionally, we verified that as in Experiment 1, the variance data was best fit by the generalized Weber equation. For the periodic patterns, the mean R^2 was 0.934 and 0.878 for the generalized Weber (Eq. 1) and linear with T equation (Eq. 2), respectively ($p < 10^{-5}$). For the complex patterns, the same mean R^2 values were 0.891 and 0.854 ($p = 10^{-4}$). The learning analysis for the data from Experiment 2 showed a very similar decreasing behavior of k and σ^2_{indep} as a function of training day, for both the periodic and the complex patterns.

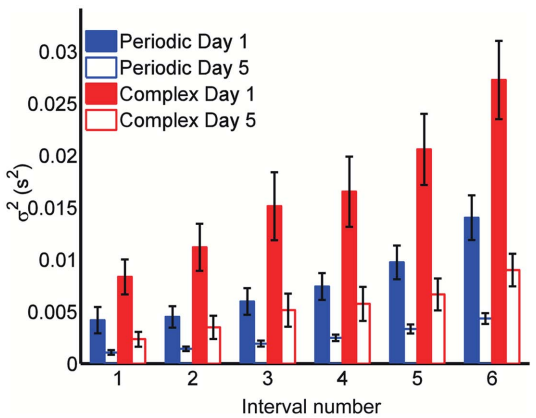

FIGURE 5 | Variance is smaller for periodic patterns. Mean variance at each response for the first and last days of training. Although both periodic and complex patterns had the same total duration (3 s), the variance of the response times at the last response is smaller for the periodic pattern.

Although these results suggest the Reset Timing should be rejected for both the periodic and the complex patterns and both the spatiotemporal and purely temporal tasks, it is interesting to note that the variance of the responses were consistently smaller for the periodic patterns (**Figure 5**). For example, although the target time of the last event of both the periodic and complex patterns was the same for all subjects and patterns (3 s), the variance was approximately double in the complex condition (both on Day 1 and 5). These observations suggest different modes or mechanisms of timing in the periodic and complex tasks (see Discussion).

MODEL: POPULATION CLOCK BASED ON RECURRENT NETWORK DYNAMICS CAN REPRODUCE TIMED PATTERNS

A number of previous models have proposed that the brain's ability to tell time derives from the properties of neural oscillators operating in a clock-like fashion, through accumulation/integration of pulses emitted by a pacemaker. However, few studies have proposed detailed explanations of how these models account for the generation of multiple complex spatiotemporal patterns of the type studied in Experiment 1.

An alternate hypothesis to clock models suggest that timing emerges from the internal dynamics of recurrently connected neural networks, and that time is inherently encoded in the evolving activity pattern of the network – a population clock (Buonomano and Mauk, 1994; Buonomano and Laje, 2010). Here we focus on a population clock model that is well suited to account for the timing of complex spatiotemporal patterns, and is consistent with the results presented above suggesting that timing of patterns does not rely on a reset strategy. Since our psychophysical results above show that both spatiotemporal and temporal patterns are better accounted for by Continuous timing, in this section we focused on the more general problem of spatiotemporal pattern generation.

We implemented a population clock model in the form of a firing-rate recurrent neural network model (Buonomano and Laje,

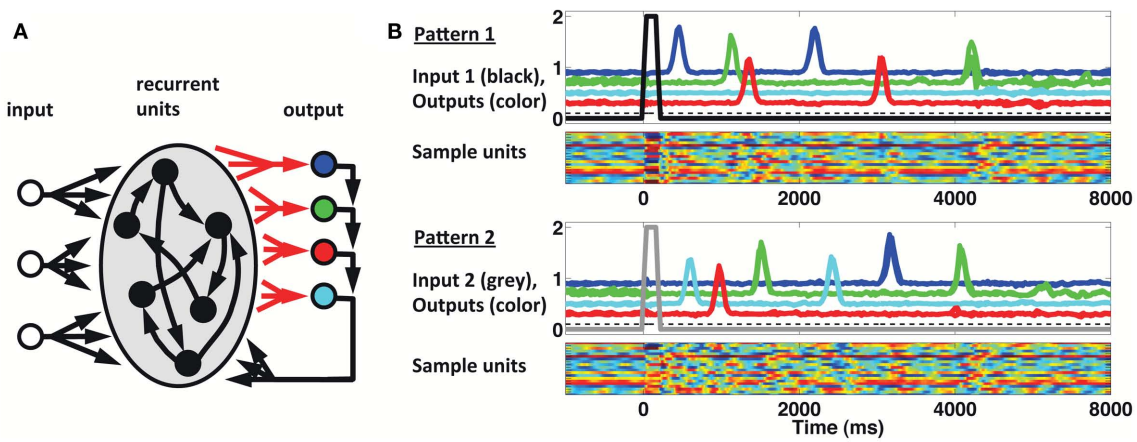

FIGURE 6 | Population clock model based on recurrent network dynamics. (A) Network architecture. The four output units are meant to represent the four fingers. Only the readout connections (depicted in red) are subject to training. **(B)** Reproduction of two complex spatiotemporal patterns (each with three different runs overlaid) after adjusting the weights of the recurrent units onto the readout units. Output traces are shifted vertically for visual clarity. Each pattern is triggered by a brief activation (100 ms) of the corresponding input unit at $t = 0$ (black thick trace, Pattern 1; gray thick trace, Pattern 2). The dashed black trace represents a (third) constant input to the recurrent network. Colored rasters represent a subset (20) of the recurrent units. In these units activity ranges from −1 (blue) to 1 (red).

2010). The network, displayed in **Figure 6A**, is composed of 1800 sparsely connected units, each with a time constant of 10 ms (see Materials and Methods). As shown in **Figure 6B**, a brief input can trigger a complex spatiotemporal pattern of activity within the recurrent network; and this pattern can be used to generate multiple, complex spatiotemporal output patterns several seconds in duration. Different output patterns can be triggered by different brief input stimuli. The results shown are from a network with three inputs and four outputs (each output represents a finger). Input 1 (tonic) sets the network outputs in a state of low-level activity, while Inputs 2 and 3 (pulsed) act as "go" signals for patterns 1 and 2, respectively. The four output units feedback to the network, and the corresponding four sets of output weights are subject to training with the FORCE learning algorithm (Sussillo and Abbott, 2009). The network is trained to reproduce the desired target pattern every time the corresponding "go" signal is activated. In this scenario learning takes place by adjusting the weights on to the readout units. To simulate the responses used in our STPR task (discrete, pulse-like finger movements) the target response is simulated as a smooth but rapidly ascending and descending waveform.

Our numerical simulations reveal that the variance signature exhibited by the model is strongly dependent on the parameters of the model (including the synaptic strength factor g, and the strength of the feedback, see Rajan et al., 2010). In the simulation presented here on average variance increased approximately linearly with T^2 (with a large degree of variation between simulations). However, variance values were much smaller than those observed experimentally: a Weber fraction of around 1% (compare with the experimental Weber fraction on the order of 10–30% in **Figure 1C**). It is well known that the dynamics of recurrent networks is highly complex and prone to chaotic activity (Sompolinsky et al., 1988; Jaeger and Haas, 2004; Rajan et al., 2010), while outside the scope of the current study it is clear that it will be necessary to better understand the dynamics of these systems to determine if they can quantitatively account for the experimentally observed variance signature (see Discussion).

Qualitatively the population clock framework shown in **Figure 6** elegantly accounts for both the spatial and temporal aspects of complex spatiotemporal patterns. That is, the spatial pattern, the timing, and the order of the fingers are all encoded in a multiplexed fashion in the recurrent network plus the readout. Furthermore, the model is most consistent with "continuous" timing, and thus with the experimental data. Specifically, while a feedback loop from the output units to the recurrent network could be used to implement reset timing, such a reset signal would necessarily bring the network to the same state every time that finger was used during a pattern. Consider the production of an aperiodic temporal pattern, and now suppose that the output pulse "resets" the network state through the feedback loop. Resetting to the same state would trigger the same neural trajectory, making the same output fire again leading to a periodic loop. Although the same motor response can be triggered by many different internal states (a many-to-one mapping), every time that motor response is generated it would erase the previous history of the recurrent network through the reset command. However, a reset strategy could potentially be implemented if additional assumptions were incorporated, such as buffers that kept track of the ordinal position of each response. Lastly it should be pointed out that, since recurrent networks seem to exhibit a range of different variance signatures depending on model parameters, it is theoretically possible that in some regimes the model could emulate a reset timing variance signature without actually being reset.

DISCUSSION

WEBER VERSUS GENERALIZED WEBER

The great majority of timing studies that have quantified changes in temporal precision as a function of the interval being timed have examined each interval independently – that is, timing of 500 and 1000 ms intervals would be obtained on separate trials (for reviews see, Gibbon et al., 1997; Ivry and Spencer, 2004; Mauk and Buonomano, 2004; Buhusi and Meck, 2005; Grondin, 2010). Here we examined scaling of temporal precision during a sequential reproduction task in which subjects were required to time different absolute temporal intervals within the same trials. Consistent with a number of previous studies (Getty, 1975; Ivry and Hazeltine, 1995; Hinton and Rao, 2004; Bizo et al., 2006; Merchant et al., 2008; Lewis and Miall, 2009), we established that in consecutive timing, precision also does not follow the standard version of Weber's law; in other words, the Weber fraction calculated as the CV decreased with increasing intervals (**Figure 1**).

Consistent, again, with a number of previous studies we found that the variance of consecutively timed motor responses were well accounted for by the generalized version of Weber's law – specifically, that variance increases with absolute time squared (Getty, 1975; Ivry and Hazeltine, 1995; Bizo et al., 2006; Merchant et al., 2008). Weber's law is, of course, a specific instance of the generalized law in which the intercept (the time-independent variance) is equal to zero. Thus previous results conforming to Weber's law are likely to represent instances in which the non-temporal variance is relatively small compared to the temporal variance. Indeed, most of the studies supporting Weber's law have not explicitly examined whether the reported data would not be significantly better fit by Weber's generalized law.

EFFECTS OF LEARNING

The fact that the data was very well fit by Weber's generalized law allowed us to ask whether learning of spatiotemporal patterns altered the time-dependent and/or independent sources of variance. Traditionally, the time-dependent portion of the variance is interpreted as reflecting the properties of a clock or timing device. The time-independent variance is often taken to reflect the noise in the motor response or "internal" noise that non-specifically alters sensory and/or motor aspects of any psychophysical task. It is not immediately clear which of the potential sources of variance would be expected to underlie the improved performance that occurs with practice. We observed that both σ^2_{indep} and the slope k (which approximates the traditional Weber fraction at long intervals) change over the course of learning (**Figure 2**). Visually, σ^2_{indep} seemed to change and asymptote more rapidly thank k (**Figure 2**), this was not statistically significant however. Nevertheless, in future experiments it will be of interest to determine if both sources of variance can change independently during learning. We interpret σ^2_{indep} as reflecting an amalgam of internal noise sources including

both motor and attentional factors, and speculate that some of the improvements in σ^2_{indep} are likely to reflect attentional components that would generalize across different temporal patterns.

As mentioned, the coefficient k of the time-dependent term is often interpreted as reflecting the property of an internal clock; more specifically, as capturing the variation in the generation of pulses of a hypothetical pacemaker. Within this framework one might interpret the improvement in k as a decrease in the variability of a pacemaker. We have previously argued that motor (and sensory) timing does not rely on an internal clock, but rather as exemplified in **Figure 6**, on the dynamics of recurrently connected neural networks (Mauk and Buonomano, 2004; Buonomano and Laje, 2010). Within *this* framework we would interpret the decrease in k as reflecting less cross-trial variability in the neural trajectory (see below). However, it remains far from clear what the decrease in k truly reflects at the neural level.

RESET VERSUS CONTINUOUS TIMING

The use of consecutively timed responses during the STPR task, as opposed to the timing of independent intervals, raises an important question: when timing multiple consecutive intervals does the internal timer – whatever its nature – operate continuously throughout the entire pattern, or does it "reset" at each event (**Figure 3**)? To use a stopwatch analogy, if you need to time two consecutive intervals, one of 1 s and the second of 1.5 s, do you start a stopwatch at $t = 0$ ms, generate a response at 1 s, then wait until it hits 2.5 s and generate another, or do you reset/restart the stopwatch at 1 s, and generate a second response at 1.5 s?

This question relates to previous studies that have examined the effects of subdividing on timing. Specifically, to generate a multi-second response, it is typically reported that "counting" (which generates subintervals), improves precision (Fetterman and Killeen, 1990; Hinton and Rao, 2004; Hinton et al., 2004; Grondin and Killeen, 2009). One interpretation of this result is that since timing precision increases as a function of absolute time squared T^2, total variance is less if the total interval T is subdivided into $t_1 + t_2$, because $k\,t_1^2 + k\,t_2^2 < k(t_1 + t_2)^2$. In other words, counting may be superior because in essence the internal timer is being reset during each subinterval.

To address the question of whether the internal timer is reset during a pattern we examined whether temporal precision is best fit by continuous or reset assumptions during the reproduction of both periodic and complex temporal patterns. Our results reveal that both fits were actually pretty good ($R^2 > 0.86$), and that the difference between both models can be surprisingly subtle and potentially easily missed. Nevertheless, our findings clearly indicate that for both periodic and complex stimuli the fits using the continuous model produced significantly smaller residuals. These results suggest that the neural mechanisms underlying timing appear to accumulate variance over the course of a pattern in a manner consistent with continuous operation of a timing device. We initially expected that there may be a difference between periodic and complex patterns, specifically, that precision during periodic patterns would more likely be consistent with a reset mechanism. However, this expectation was not supported, as the continuous fits were significantly better for both the periodic and complex patterns.

Nevertheless, consistent with studies showing that counting, and thus presumably periodic subdividing, improves performance, we did observe a significant decrease in total variance of the last event, which was the same for the periodic and complex patterns (3 s). Interestingly there was also difference for the first event between both tasks (500 ms in the periodic patterns, and on average 598 ms in the complex patterns; **Figure 5**). It is noteworthy that by the end of training, the absolute precision of a few subjects was comparable in the periodic and complex tasks, raising the possibility that comparable precision can be achieved in periodic and complex patterns.

These results raise somewhat of a conundrum: timing of a 3-s response is indeed better if the previous five responses were equally spaced compared to an aperiodic pattern; however, the improvement does not appear to be a result of resetting during the periodic task. Are different circuits responsible for the periodic and complex timing? Is periodic timing less flexible, thus allowing for better precision? We cannot speak directly to these questions here; however, in the sensory domain it has been suggested that there may be different neural circuits for periodic and non-periodic timing (Grube et al., 2010; Teki et al., 2011). Still, it remains a possibility that given the relatively small, but significant, difference in the quality of the fits between the reset and continuous timing equations, we were not able to pick out subtle differences between them. It is also possible that, since our subjects were reproducing both patterns in alternation, they were nudged toward using similar "continuous" strategies. Finally, less precise timing in complex conditions might simply reflect non-specific factors relating to the task requirements, e.g., increase attentional and memory load.

MODELS OF TIMING

A critical challenge to any model of timing is to provide a mechanistic description of its postulated underpinning in biologically plausible terms. A number of models have proposed that the brain's ability to tell time derives from the properties of neural oscillators operating in a clock-like fashion, yielding an explicit, linear metric of time (Creelman, 1962; Treisman, 1963). Others have proposed a population of neural elements oscillating at different frequencies, with a readout mechanism that detects specific beats or coincidental activity at specific points in time (Miall, 1989; Matell and Meck, 2004). Still others propose that time might be directly encoded in the activity of neural elements with differing time constants of some cellular or synaptic property (for a review see, Mauk and Buonomano, 2004). As a general rule, many models of timing have focused primarily on the timing of single isolated intervals, as opposed to the generation of multiple complex spatiotemporal patterns as examined here. Indeed, it is not immediately clear how the clock models based on the integration of events from a pacemaker can account for generating different temporal patterns in a flexible fashion. For this reason, here we have focused on network models, which in our opinion can elegantly capture the spatial, timing, and order components of complex motor tasks.

In addition to being implemented at the levels of neurons, any model must of course also account for the behavioral and psychophysical data. Indeed, one of the strengths of psychophysical studies is to test and constrain mechanistic models of timing. The

neural mechanism of timing remains debated, but it is increasingly clear that there are likely multiple areas involved, and that different neural mechanisms may underlie timing on the scale of milliseconds and seconds (for reviews see, Buonomano and Karmarkar, 2002; Mauk and Buonomano, 2004; Buhusi and Meck, 2005; Ivry and Schlerf, 2008; van Wassenhove, 2009; Grondin, 2010). One biologically based model of timing suggests that dynamic changes in the population of active neurons encode time. This model, first proposed in the context of the cerebellum (Buonomano and Mauk, 1994; Mauk and Donegan, 1997; Medina et al., 2000), and later in recurrent excitatory circuits (Buonomano and Merzenich, 1995; Buonomano and Laje, 2010) has been referred to as a population clock (Buonomano and Karmarkar, 2002). In the motor domain, any time-varying neural activity requires either continuous input or internally generated changes in network state. This class of models is most consistent with Continuous timing (see Results). Specifically, since timing relies on setting a particular neural trajectory in motion, different points in time (as well as the ordinal position and the appropriate finger) are coded in relation to the initial state at $t = 0$ (**Figure 6**) – resetting the network, in contrast, can erase information about ordinal position and finger pattern embedded in the recurrent network.

In vivo electrophysiological studies have lent support to the notion of a population clock, including reports of neurons that fire at select time intervals or in a complex aperiodic manner (Hahnloser et al., 2002; Matell et al., 2003; Jin et al., 2009; Long et al., 2010; Itskov et al., 2011). In the experimental and theoretical studies the temporal code of a population clock can take various forms: First, time might be encoded in a feed-forward chain, where each neuron essentially responds at one time point (Hahnloser et al., 2002; Buonomano, 2005; Liu and Buonomano, 2009; Fiete et al., 2010; Long et al., 2010; Itskov et al., 2011); Second, the code can be high dimensional, where at one point in time is encoded in the active population response of many neurons, and each neuron can fire at multiple time points (Medina and Mauk, 1999; Medina et al., 2000; Lebedev et al., 2008; Jin et al., 2009; Buonomano and Laje, 2010). Indeed, some of these studies have shown that a linear classifier (readout unit) can be used to decode time based on the profiles of the experimentally recorded neurons, thus effectively implementing a population clock (Lebedev et al., 2008; Jin et al., 2009; Crowe et al., 2010).

While experimental data showing that different neurons or populations of neurons respond at different points in time supports the notion that time is encoded in the dynamics of neural network – in the neural trajectories – at the theoretical level it has been challenging to generate recurrent excitatory networks capable of producing reliable ("non-chaotic") patterns. While recent progress has been made in both physiological learning rules that may account for the formation of neural trajectories (Buonomano, 2005; Liu and Buonomano, 2009; Fiete et al., 2010) and the circuit architecture that might support them (Jaeger and Haas, 2004; Sussillo and Abbott, 2009; Itskov et al., 2011), these models have not explicitly captured the variance characteristics (Weber's generalized law) observed psychophysically. This holds true for the model presented in **Figure 6** (which tends to exhibit very little variance; or, as the noise is increased, variance that scales too rapidly). Thus, while this class of models is consistent with the notion that the internal timer does not reset during the production of patterns, future models must accurately capture the known relationship between precision and absolute time.

ACKNOWLEDGMENTS

We would like to acknowledge the European project COST ISCH Action TD0904 TIMELY, the Pew Charitable Trusts, and CONICET (Argentina).

REFERENCES

Allan, L. G., and Gibbon, J. (1991). Human bisection at the geometric mean. *Learn. Motiv.* 22, 39–58.

Bizo, L. A., Chu, J. Y., Sanabria, F., and Killeen, P. R. (2006). The failure of Weber's law in time perception and production. *Behav. Processes* 71, 201–210.

Buhusi, C. V., and Meck, W. H. (2005). What makes us tick? Functional and neural mechanisms of interval timing. *Nat. Rev. Neurosci.* 6, 755–765.

Buonomano, D. V. (2005). A learning rule for the emergence of stable dynamics and timing in recurrent networks. *J. Neurophysiol.* 94, 2275–2283.

Buonomano, D. V. (2007). The biology of time across different scales. *Nat. Chem. Biol.* 3, 594–597.

Buonomano, D. V., and Karmarkar, U. R. (2002). How do we tell time? *Neuroscientist* 8, 42–51.

Buonomano, D. V., and Laje, R. (2010). Population clocks: motor timing with neural dynamics. *Trends Cogn. Sci. (Regul. Ed.)* 14, 520–527.

Buonomano, D. V., and Mauk, M. D. (1994). Neural network model of the cerebellum: temporal discrimination and the timing of motor responses. *Neural Comput.* 6, 38–55.

Buonomano, D. V., and Merzenich, M. M. (1995). Temporal information transformed into a spatial code by a neural network with realistic properties. *Science* 267, 1028–1030.

Carr, C. E. (1993). Processing of temporal information in the brain. *Annu. Rev. Neurosci.* 16, 223–243.

Church, R. M., Meck, W. H., and Gibbon, J. (1994). Application of scalar timing theory to individual trials. *J. Exp. Psychol. Anim. Behav. Process.* 20, 135–155.

Creelman, C. D. (1962). Human discrimination of auditory duration. *J. Acoust. Soc. Am.* 34, 582–593.

Crowe, D. A., Averbeck, B. B., and Chafee, M. V. (2010). Rapid sequences of population activity patterns dynamically encode task-critical spatial information in parietal cortex. *J. Neurosci.* 30, 11640–11653.

Fetterman, J. G., and Killeen, P. R. (1990). A componential analysis of pacemaker-counter timing systems. *J. Exp. Psychol. Hum. Percept. Perform.* 16, 766–780.

Fiete, I. R., Senn, W., Wang, C. Z. H., and Hahnloser, R. H. R. (2010). Spike-time-dependent plasticity and heterosynaptic competition organize networks to produce long scale-free sequences of neural activity. *Neuron* 65, 563–576.

Getty, D. J. (1975). Discrimination of short temporal intervals: a comparison of two models. *Percept. Psychophys.* 18, 1–8.

Gibbon, J. (1977). Scalar expectancy theory and Weber's law in animal timing. *Psychol. Rev.* 84, 279–325.

Gibbon, J., Malapani, C., Dale, C. L., and Gallistel, C. R. (1997). Toward a neurobiology of temporal cognition: advances and challenges. *Curr. Opin. Neurobiol.* 7, 170–184.

Grondin, S. (2010). Timing and time perception: a review of recent behavioral and neuroscience findings and theoretical directions. *Atten. Percept. Psychophys.* 72, 561–582.

Grondin, S., and Killeen, P. R. (2009). Tracking time with song and count: different Weber functions for musicians and nonmusicians. *Atten. Percept. Psychophys.* 71, 1649–1654.

Grube, M., Cooper, F. E., Chinnery, P. F., and Griffiths, T. D. (2010). Dissociation of duration-based and beat-based auditory timing in cerebellar degeneration. *Proc. Natl. Acad. Sci. U.S.A.* 107, 11597–11601.

Hahnloser, R. H. R., Kozhevnikov, A. A., and Fee, M. S. (2002). An ultra-sparse code underlies the generation of neural sequence in a songbird. *Nature* 419, 65–70.

Hinton, S. C., Harrington, D. L., Binder, J. R., Durgerian, S., and Rao, S. M. (2004). Neural systems supporting timing and chronometric counting: an FMRI study. *Cogn. Brain Res.* 21, 183–192.

Hinton, S. C., and Rao, S. M. (2004). "One-thousand one... one-thousand two...": chronometric counting violates the scalar property in interval timing. *Psychon. Bull. Rev.* 11, 24–30.

Itskov, V., Curto, C., Pastalkova, E., and Buzsáki, G. (2011). Cell assembly sequences arising from spike threshold adaptation keep track of time in the hippocampus. *J. Neurosci.* 31, 2828–2834.

Ivry, R. B., and Hazeltine, R. E. (1995). Perception and production of temporal intervals across a range of durations – evidence for a common timing mechanism. *J. Exp. Psychol. Hum. Percept. Perform.* 21, 3–18.

Ivry, R. B., and Schlerf, J. E. (2008). Dedicated and intrinsic models of time perception. *Trends Cogn. Sci. (Regul. Ed.)* 12, 273–280.

Ivry, R. B., and Spencer, R. M. C. (2004). The neural representation of time. *Curr. Opin. Neurobiol.* 14, 225–232.

Jaeger, H., and Haas, H. (2004). Harnessing nonlinearity: predicting chaotic systems and saving energy in wireless communication. *Science* 304, 78–80.

Jazayeri, M., and Shadlen, M. N. (2010). Temporal context calibrates interval timing. *Nat. Neurosci.* 13, 1020–1026.

Jeffress, L. A. (1948). A place theory of sound localization. *J. Comp. Physiol. Psychol.* 41, 35–39.

Jin, D. Z., Fujii, N., and Graybiel, A. M. (2009). Neural representation of time in cortico-basal ganglia circuits. *Proc. Natl. Acad. Sci. U.S.A.* 106, 19156–19161.

King, D. P., and Takahashi, J. S. (2000). Molecular genetics of circadian rhythms in mammals. *Annu. Rev. Neurosci.* 23, 713–742.

Lebedev, M. A., O'Doherty, J. E., and Nicolelis, M. A. L. (2008). Decoding of temporal intervals from cortical ensemble activity. *J. Neurophysiol.* 99, 166–186.

Lewis, P. A., and Miall, R. C. (2009). The precision of temporal judgement: milliseconds, many minutes, and beyond. *Philos. Trans. R. Soc. B Biol. Sci.* 364, 1897–1905.

Lewis, P. A., Miall, R. C., Daan, S., and Kacelnik, A. (2003). Interval timing in mice does not rely upon the circadian pacemaker. *Neurosci. Lett.* 348, 131–134.

Liu, J. K., and Buonomano, D. V. (2009). Embedding multiple trajectories in simulated recurrent neural networks in a self-organizing manner. *J. Neurosci.* 29, 13172–13181.

Long, M. A., Jin, D. Z., and Fee, M. S. (2010). Support for a synaptic chain model of neuronal sequence generation. *Nature* 468, 394–399.

Matell, M. S., and Meck, W. H. (2004). Cortico-striatal circuits and interval timing: coincidence detection of oscillatory processes. *Cogn. Brain Res.* 21, 139–170.

Matell, M. S., Meck, W. H., and Nicolelis, M. A. (2003). Interval timing and the encoding of signal duration by ensembles of cortical and striatal neurons. *Behav. Neurosci.* 117, 760–773.

Mauk, M. D., and Buonomano, D. V. (2004). The neural basis of temporal processing. *Annu. Rev. Neurosci.* 27, 307–340.

Mauk, M. D., and Donegan, N. H. (1997). A model of Pavlovian eyelid conditioning based on the synaptic organization of the cerebellum. *Learn. Mem.* 3, 130–158.

Meck, W. H., and Church, R. M. (1987). Cholinergic modulation of the content of temporal memory. *Behav. Neurosci.* 101, 457–464.

Medina, J. F., Garcia, K. S., Nores, W. L., Taylor, N. M., and Mauk, M. D. (2000). Timing mechanisms in the cerebellum: testing predictions of a large-scale computer simulation. *J. Neurosci.* 20, 5516–5525.

Medina, J. F., and Mauk, M. D. (1999). Simulations of cerebellar motor learning: computational analysis of plasticity at the mossy fiber to deep nucleus synapse. *J. Neurosci.* 19, 7140–7151.

Merchant, H., Zarco, W., and Prado, L. (2008). Do we have a common mechanism for measuring time in the hundreds of millisecond range? evidence from multiple-interval timing tasks. *J. Neurophysiol.* 99, 939–949.

Miall, C. (1989). The storage of time intervals using oscillating neurons. *Neural Comput.* 1, 359–371.

Nissen, M. J., and Bullemer, P. (1987). Attentional requirements of learning: evidence from performance measures. *Cogn. Psychol.* 19, 1–32.

Panda, S., Hogenesch, J. B., and Kay, S. A. (2002). Circadian rhythms from flies to human. *Nature* 417, 329–335.

Rajan, K., Abbott, L. F., and Sompolinsky, H. (2010). Stimulus-dependent suppression of chaos in recurrent neural networks. *Phys. Rev. E Stat. Nonlin. Soft Matter Phys.* 82, 011903.

Shin, J. C., and Ivry, R. B. (2002). Concurrent learning of temporal and spatial sequences. *J. Exp. Psychol. Learn. Mem. Cogn.* 28, 445–457.

Sompolinsky, H., Crisanti, A., and Sommers, H. J. (1988). Chaos in random neural networks. *Phys. Rev. Lett.* 61, 259–262.

Sussillo, D., and Abbott, L. F. (2009). Generating coherent patterns of activity from chaotic neural networks. *Neuron* 63, 544–557.

Teki, S., Grube, M., Kumar, S., and Griffiths, T. D. (2011). Distinct neural substrates of duration-based and beat-based auditory timing. *J. Neurosci.* 31, 3805–3812.

Treisman, M. (1963). Temporal discrimination and the indifference interval: implications for a model of the 'internal clock.' *Psychol. Monogr.* 77, 1–31.

van Wassenhove, V. (2009). Minding time in an amodal representational space. *Philos. Trans. R. Soc. Lond. B Biol. Sci.* 364, 1815–1830.

Conflict of Interest Statement: The authors declare that the research was conducted in the absence of any commercial or financial relationships that could be construed as a potential conflict of interest.

Received: 29 June 2011; paper pending published: 09 July 2011; accepted: 25 September 2011; published online: 13 October 2011.

Citation: Laje R, Cheng K and Buonomano DV (2011) Learning of temporal motor patterns: an analysis of continuous versus reset timing. Front. Integr. Neurosci. ***5****:61. doi: 10.3389/fnint.2011.00061*

frontiers in
INTEGRATIVE NEUROSCIENCE

REVIEW ARTICLE
published: 27 September 2011
doi: 10.3389/fnint.2011.00054

Decision-making in the ventral premotor cortex harbinger of action

Jose L. Pardo-Vazquez[1], Isabel Padron[1,2], Jose Fernandez-Rey[2] and Carlos Acuña[1]*

[1] *Laboratorios de Neurociencia, Facultad de Medicina, Departamento de Fisiología, and Complejo Hospitalario Universitario, Universidad de Santiago de Compostela, Santiago de Compostela, Spain*

[2] *Grupo de Procesos Cognitivos y Conducta, Facultad de Psicología, Universidad de Santiago de Compostela, Santiago de Compostela, Spain*

Edited by:
Agnes Gruart, University Pablo de Olavide, Spain

Reviewed by:
Ranulfo Romo, Universidad Nacional Autónoma de México, Mexico
Emilia Iannilli, University Hospital Dresden, Germany

***Correspondence:**
Carlos Acuña, Laboratorios de Neurociencia, Facultad de Medicina, Departamento de Fisiología, Universidad de Santiago de Compostela, c/San Francisco, 1, Santiago de Compostela E-15705, Spain.
e-mail: carlos.acuna.castroviejo@usc.es

Although the premotor (PM) cortex was once viewed as the substrate of pure motor functions, soon it was realized that it was involved in higher brain functions. By this it is meant that the PM cortex functions would better be explained as motor set, preparation for limb movement, or sensory guidance of movement rather than solely by a fixed link to motor performance. These findings, together with a better knowledge of the PM cortex histology and hodology in human and non-human primates prompted quantitative studies of this area combining behavioral tasks with electrophysiological recordings. In addition, the exploration of the PM cortex neurons with qualitative methods also suggested its participation in higher functions. Behavioral choices frequently depend on temporal cues, which together with knowledge of previous outcomes and expectancies are combined to decide and choose a behavioral action. In decision-making the knowledge about the consequences of decisions, either correct or incorrect, is fundamental because they can be used to adapt future behavior. The neuronal correlates of a decision process have been described in several cortical areas of primates. Among them, there is evidence that the monkey ventral premotor (PMv) cortex, an anatomical and physiological well-differentiated area of the PM cortex, supports both perceptual decisions and performance monitoring. Here we review the evidence that the steps in a decision-making process are encoded in the firing rate of the PMv neurons. This provides compelling evidence suggesting that the PMv is involved in the use of recent and long-term sensory memory to decide, execute, and evaluate the outcomes of the subjects' choices.

Keywords: premotor ventral cortex, decision-making, working memory, outcomes, event-related potentials

GENERAL

The discovery that the neuronal activity of the premotor (PM) cortex correlates with all the events that lead to a behavioral decision and with the outcomes of that decision has represented a major advance in our knowledge of the role of this area of the frontal cortex (Hernandez et al., 2002; Romo et al., 2004; Pardo-Vazquez et al., 2008, 2009; Lemus et al., 2009; Acuña and Pardo-Vazquez, 2011). These findings were preceded by clinical and experimental lesions in subhuman primates that ascribe the premotor cortex (PM or area 6 of Brodmann) a causative role in the so-called "syndrome of the premotor cortex," which included, forced grasping, spasticity, increase in tendon reflexes, and vasomotor disturbances in the upper extremity, contralateral to the lesion (review in Kennard et al., 1934). Jacobsen (1931) noted that a chimpanzee trained in feeding-box problems, after a fugitive paralysis resulting from ablation of PM cortex had passed, appeared unable to organize the necessary manipulations and had to relearn them. On commenting on the "syndrome of premotor cortex" Walshe went on to call its characteristic symptom "an intellectual deficit" because the subject has "forgotten how" to perform certain taught movements (Walshe, 1935).

Although these findings were difficult to interpret because the lesions involved adjacent cortical areas, they also gave some hints that suggested the PM was involved in higher-order aspects of motor control. More conclusive evidence came with the introduction of methodological and technical approaches combining operant conditioning with electrophysiological recordings in monkeys. These studies suggested the involvement of PM in planning and execution of complex movements, motor set, preparation for and sensory guidance of movements, reorganization of movements, and learning (Roland et al., 1980; Halsband and Passingham, 1982; Weinrich et al., 1984; Halsband and Freund, 1990; Mitz et al., 1991; Passingham, 1993; Kurata and Hoffman, 1994; Wise et al., 1997) as well as in complex relations with the immediate extrapersonal space (revised in Rizzolatti and Luppino, 2001) and perceptual decision-making (Romo et al., 2004; Pardo-Vazquez et al., 2008, 2009; Lemus et al., 2009). Additionally, conjunction analysis of fMRi data has suggested the involvement of the PM cortices in processing trigeminal information (Iannilli et al., 2007). These results can suggest functional heterogeneity and, in fact, the PM is architectonically heterogeneous and several subdivisions have been proposed on histological or hodological grounds (e.g., Matelli et al., 1985; Luppino and Rizzolatti, 2000; Petrides et al., 2005; Graziano and Aflalo, 2007) although a precise correlation between anatomy and function is not totally clear at the present time. This paper is focused on the ventral premotor (PMv)

cortex where these clinical and experimental studies have led to the proposition that its neural apparatus together with its system connections generates the appropriate signals to decide, act, and record whether the behavioral outcomes were correct or incorrect. Moreover, in order to understand the PMv function we will refer not only to the PMv itself but we will also compare the results obtained in this area with those from other PM subdivisions as well as from other cortical or subcortical areas.

THE PREMOTOR CORTEX AND THE CONTROL OF MOVEMENT

Luria (1980) described that lesions of the PM cortex produced contrasting disturbances; on the one hand they produced disturbance "in automatic intellectual operations" such as the correct understanding of written texts, and, on the other hand, in the integration of complex motor acts. The "syndrome of the premotor cortex" was defined as a clinical entity, which included impairment of skilled movements of the fingers and vasomotor disturbances (Kennard et al., 1934). Interestingly, all manifestations of the condition can be reproduced experimentally in subhuman primates by lesions more or less restricted to the PM area and these symptoms are clinically different from those of the motor-area syndrome; for instance, lesions of the primary motor cortex (M1) or of the cortico-spinal fibers originating in M1 cause paresis, predominantly of finger movements (Denny-Brown and Botterell, 1948; Fulton, 1949; Travis, 1955; Fries et al., 1993). These symptoms can be due to disruption of connections of the PM with both the motor cortex and the motoneuronal pools in the spinal cord (Preuss et al., 1996; Cerri et al., 2003; Shimazu et al., 2004).

From then on many studies have focused on the motor-related properties of the PM cortex. Most of the work has been performed in the PMd, some included the PMd and PMv and some were unspecified. The role of the premotor medial (PMm) cortex in motor preparation has also been studied; it was found that this cortical area is involved in initiating hand movements both when they were self-initiated or externally timed (Romo and Schultz, 1987, 1992). Single extracellular unit recordings in the PM cortex support the hypothesis that the PMv is more involved than the PMd in the selection of an action or motor execution under visual guidance, while the PMd would be more involved in the preparation of movements (Weinrich et al., 1984; Passingham, 1993; Kurata and Hoffman, 1994; Wise et al., 1997; Rizzolatti and Fadiga, 1998). It has also been suggested that in the monkeys that perform in visuospatial tasks the PM plays a role in the selection of motor programs based on environmental context, thereby playing a role in motor learning (Halsband and Freund, 1990; Mitz et al., 1991; Di-Pellegrino and Wise, 1993). In fact, the PM lesions impaired monkeys' ability to associate visual information with particular movements, which is also in line with the proposal that the PM plays a role in the visual guidance of movements (Halsband and Passingham, 1982; Mushiake et al., 1991; Kurata and Hoffman, 1994). Brain imaging studies confirmed the involvement of the PMv in both temporal sequencing and visual guidance of movements (Schubotz and Von Cramon, 2001; Schubotz et al., 2003).

Based on cytoarchitectural and histochemical data the monkey's agranular frontal cortex was divided in seven areas (F1–F7; Matelli et al., 1985; Rizzolatti et al., 1998) of which, areas F4 (caudally) and F5 (rostrally) correspond to the PMv. There are anatomical and functional differences between PMd and PMv but their correlation is still largely unclear because only in a few cases have both areas been studied with the same experimental paradigm. The hodology of the monkey's PM cortex also confirmed the histological sectors and suggested different functions (Kurata, 1991; Rizzolatti and Luppino, 2001). F5 receives somatosensory inputs from the second somatic sensory area (SII), the PF (7b), and the anterior intraparietal (AIP) area (Godschalk et al., 1984; Matelli et al., 1986; Luppino et al., 1999), and visual inputs from the superior temporal sulcus (STS) through the inferior parietal lobe (area PF; Markowitsch et al., 1987; Wise et al., 1997; Rizzolatti and Matelli, 2003). Accordingly, Graziano et al. (1997) found that neurons in area F5 respond to both visual and tactile stimulation, and to proprioceptive inputs. Area F4 receives visual and somatosensory information from the MST and MT of the STS, and from the PEc and PFG of the posterior parietal cortex, respectively, through the ventral intraparietal (VIP) area; accordingly, microstimulation and single unit recordings in F4 have been correlated with arm and face movements (Rizzolatti et al., 1998). Based on the connectivity of the PM cortex, Rizzolatti and Luppino (2001) differentiate the parieto-dependent and the prefronto-dependent areas. The main extrinsic input to the parieto-dependent areas (F1, F2, F4, F5) is from the parietal cortex and the intrinsic connections are with F1. These areas send fibers directly to the spinal cord contributing to the cortico-spinal tract. Altogether, these studies suggest that F1, F2, and F3 use somatosensory information while F5 uses somatosensory and visual information for action or sensory–motor transformations. Other functional differences between PMd and PMv were reported but without precise correlation with the parcelation of the PM cortex. For example, neurons in PMv reflect processes in extrinsic coordinates more often than neurons in M1 do (Kakei et al., 2001), and effector independent activity is more frequent in PMv than in PMd (Hoshi and Tanji, 2002). On the other hand, neurons in PMv present premovement activity less frequently than neurons in PMd do (Boudreau et al., 2001; Hoshi and Tanji, 2002). Hepp-Reymond et al. (1994, 1999) found PMv neurons whose activity co-varied with an external force in a precision grip task, a result consistent with the hypothesis that the PMv might participate in processing of movement dynamics. Movement dynamics, which are widely represented across the motor areas of the frontal lobe, are less precisely represented in the PMd and PMv, thereby revealing areal specialization (Xiao et al., 2006). These findings are seen as a physiological counterpart to the anatomical findings of distinct PMv connectivity (He et al., 1993; Luppino et al., 1993; Boussaoud et al., 2005).

REORGANIZATION OF MOVEMENTS AND MOTOR LEARNING

These experiments highlighted differences between areas suggesting that the contribution of the PMv to motor planning and movement dynamics appears minimal but that they may play a role in planning visually guided movements, more specifically during conditional motor learning. This is exemplified by studies that have shown that the PM dorsal and ventral neurons respond differently to identical stimuli that instruct different actions (Boussaoud and Wise, 1993). Therefore, the PMv is involved in more than basic motor control. The studies that suggested that the

PM areas can contribute to the functional recovery, reorganization, and motor learning of hand movements can be traced to the early ones of Jacobsen (1931). Based on the fact that lesions affecting non-primary motor areas cause predominantly higher-order motor disorders such as apraxia, other studies were focused on the role of the PM cortex in the reorganization of movements (Freund and Hummelshein, 1985; Halsband and Freund, 1990; Halsband et al., 1993; Passingham, 1993; Seitz et al., 1998; Carey et al., 2002; Fridman et al., 2004). In this line it was found that temporal interference with muscimol in PMd/PMv provokes deficits in the use of non-spatial visual information to guide action (Kurata and Hoffman, 1994) and that after recovery of the MI cortex ibotenic acid lesions, injection of muscimol in the premotor (PMd/PMv) cortex of the affected side suppressed the recovery of the motor deficit (Liu and Rouiller, 1999). Also, Frost et al. (2003) demonstrated reorganization in the hand representation of primate ipsi-lesional PMv cortex associated with functional recovery. Particularly interesting are the studies that showed that PM lesions in monkeys made them unable to relearn a visual conditional motor task although they can see the cue or use the information from the cue (Halsband and Passingham, 1982, 1985; Petrides and Milner, 1982; Petrides, 1986). Patients with PM lesions were impaired in conditional motor learning when they have to recall a movement from memory on the basis of a sensory cue (Halsband and Freund, 1990). These results are consistent with the hypothesis that the PM cortex of the affected hemisphere can reorganize to control basic parameters of movement usually assigned to M1 function (Liu and Rouiller, 1999; Frost et al., 2003). Furthermore, learning-dependent changes in activity during a visual conditional task suggest for this area a role in the selection of movements on the basis of arbitrary associations (Mitz et al., 1991) in agreement with the proposal that PM plays a role in retrieval of movements from memory based on environmental context (Passingham, 1988). This view is supported by (a) reports of trans-cranial magnetic stimulation (TMS) of the PM cortex, which interfere with timing and motor learning and off-line consolidation (Schluter et al., 1998; Del Olmo et al., 2007; Boyd and Linsdell, 2009) and (b) by fMRi studies that show that recall from memory of an established motor skill shifts the activity from prefrontal regions to the PM, posterior parietal, and cerebellar cortices probably to stabilize the representation of the motor skill (Shadmehr and Holcomb, 1997; Amiez et al., 2006). Finally, a variety of studies made with fMRi, PET, TMS, and event-related potential (ERP) have shown increased activity in the PMv during training and learning and in selecting stimulus guided movements (Lang et al., 1992; Deiber et al., 1997; Shadmehr and Holcomb, 1997; Grafton et al., 1998; Schluter et al., 1998; Passingham and Toni, 2001; Kelly and Garavan, 2005) but not when performance was automatic, in agreement with the proposal for self-monitoring of ongoing movements (Hoshi and Tanji, 2000).

COMPLEX SENSORY–MOTOR INTERACTIONS

The experimental findings that the monkey's PMv could be involved in complex sensory–motor integrations come from the work of Rizzolatti and Craighero (2004). They described in area F5 neuronal activity related to complex movements and interactions between subjects, mirror neurons, and suggested that these processes are better revealed once the monkeys have understood the rationale of the behavior, which suggests a learning process. These qualitative studies have shown responses related to specific actions such as grasping or holding-tearing, which led to a proposal that the AIP-F5 circuit plays a role in visuomotor transformations for object grasping and manipulation while the VIP-F4 circuit will be involved in encoding the peripersonal space and in transforming the object location into appropriate movements (Jeannerod et al., 1995; Rizzolatti et al., 1998; Rizzolatti and Luppino, 2001; Rizzolatti and Craighero, 2004). The executive control attributed to the prefrontal cortex can be exerted on the PM cortex through the dense anatomical connections as well as with other cortical and subcortical structures such as the basal ganglia (e.g., Pandya and Barnes, 1987; Lu et al., 1994; Fuster, 1997). Therefore, the importance of the PM in higher-order aspects of the cerebral control of movement became evident.

As has been summarized, the role proposed for the PM in general and for the PMv in particular in different aspects of movement control has been obtained with different experimental approaches. Among them, the behavioral paradigms used have been conditional motor tasks, association tasks, or visual instructed delay tasks. In designing the tasks what was in mind was to reveal the participation of PM in movement planning, control, or execution, in the broad sense. These tasks have in common perception of sensory stimuli, motor decisions based on comparison of these stimuli and delay periods between them in which memory traces of these stimuli have to be maintained in working memory. Although all these findings obtained with the these tasks suggested a role for the PMv in cognitive processes that can range from perception to action the first experimental evidence came from the work of Romo et al. in the PMv and PMm cortices (Hernandez et al., 2002; Romo et al., 2004). They used an experimental approach that has proved very fruitful in studying the function of the posterior parietal and frontal cortices (Evarts, 1966; Fuster and Alexander, 1971; Mountcastle et al., 1975) and has allowed an identification of neurons in the PMv cortex that supports both perceptual decisions (Romo et al., 2004; Pardo-Vazquez et al., 2008, 2009; Lemus et al., 2009; Roca-Pardiñas et al., 2011) and correct and error monitoring (Pardo-Vazquez et al., 2008, 2009; Acuña et al., 2010).

PERCEPTION, DECISION-MAKING, WORKING MEMORY, AND PERFORMANCE MONITORING

The physiological and clinical data gathered during the last few years, including the pattern of connections of the PMv cortex, suggest that the PMv could participate in the processes that link sensory perception with motor reports, including the maintenance of information in working memory. In fact, as has been reviewed, the PMv receives inputs from sensory areas, association areas related to working memory and decision-making, and subcortical areas implied in behavioral monitoring, and sends projections to motor-related areas of the frontal cortex, subcortical structures, and spinal cord (Godschalk et al., 1984; Schell and Strick, 1984; Markowitsch et al., 1987; Keizer and Kuypers, 1989; Dum and Strick, 1991; He et al., 1993; Hoover and Strick, 1993; Lu et al., 1994; Ghosh and Gattera, 1995; Luppino et al., 1999; Rouiller et al., 1999; Mcfarland and Haber, 2002; Boussaoud et al.,

2005; Dancause et al., 2006; Borra et al., 2008). To study the participation of the PMv cortex in these processes, it was necessary to design behavioral tasks that include the putative cognitive steps that link perception with action. Perceptual decisions fulfill this prerequisite, as they require subjects to use the available sensory information to make a judgment and communicate it by a simple behavioral action. One kind of perceptual decision task, the two alternative-forced choice (2AFC) task, has the added advantage of allowing the study of neuronal correlates of maintenance of sensory information in working memory. In fact, since the pioneer works of Fuster and Kubota (Fuster and Alexander, 1971; Kubota and Niki, 1971) the tonic elevated neuronal firing rate during the delay period of a memory task is considered to be a neuronal correlate for the internal representation and storage of perceptual or motor information. Although the neuronal activity obtained in the PMv during the delay period of conditional motor tasks has not been explicitly described as working memory (e.g., Weinrich and Wise, 1982; Kurata and Wise, 1988) some could be memory-related activity. Learning-dependent changes in activity (Mitz et al., 1991) and spatial attention/memory and intention related activity have also been described in the PM cortex (Boussaoud, 2001).

PREMOTOR VENTRAL CORTEX AND PERCEPTUAL DECISIONS

The PM cortex was associated to perceptual decisions, for the first time, by Romo et al. (1993, 1997), who recorded the activity of single neurons from the PMm cortex while monkeys performed in a somatosensory categorization task. Later, the function of the PM cortex has been studied by recording the activity of single neurons from this area while monkeys (*Macaca mulatta*) performed perceptual discrimination tasks of different sensory modalities, including somatosensory (Romo et al., 2004), visual (Pardo-Vazquez et al., 2008, 2009; Acuña et al., 2010; Roca-Pardiñas et al., 2011), and auditory (Lemus et al., 2009). In these tasks, subjects have to choose between different behavioral responses based on the comparison of two stimuli. Romo et al. (2004) followed this approach for the first time, using a discrimination task in which the monkeys had to compare the frequencies of two vibrotactile stimuli (S1 and S2) applied sequentially to the monkeys' fingertips and separated by a fixed delay period. They found that the PMv neurons encode all the cognitive steps necessary to solve the perceptual decision: the frequency of the first stimulus when it is presented and also when it is maintained in working memory; the frequency of the second stimulus; the comparison between the two stimuli and the motor commands expressing the result of the comparison. By recording the activity of these PMv neurons in a control task, the authors also ruled out a purely motor explanation of their findings (Romo et al., 2004).

The role of the PMv cortex in visual perceptual decisions has been studied with two variants of an orientation discrimination task (**Figures 1A,B**; Pardo-Vazquez et al., 2008, 2009; Acuña et al., 2010; Acuña and Pardo-Vazquez, 2011). In the continuous discrimination (CD) task, monkeys have to perceive the orientation of two lines (S1 and S2) showed sequentially and separated by a fixed delay. Then, they have to compare the orientation of S2 with the orientation of the memory trace left by S1 and decide whether S2 was oriented to the left or to the right of S1. Finally, they have to communicate the result of their decision by making an eye movement toward one of the response targets. If the response is correct, the monkeys are rewarded. In the fixed discrimination with implicit reference (FDIR) task, the first stimulus is not presented – it is implicit – and remains unchanged in a block of trials. At the beginning of each block, monkeys have to retrieve the correct implicit S1 from long-term memory (LTM) by trial and error. From then on the decision process continues as in the CD task (Vazquez et al., 2000; Pardo-Vazquez et al., 2009).

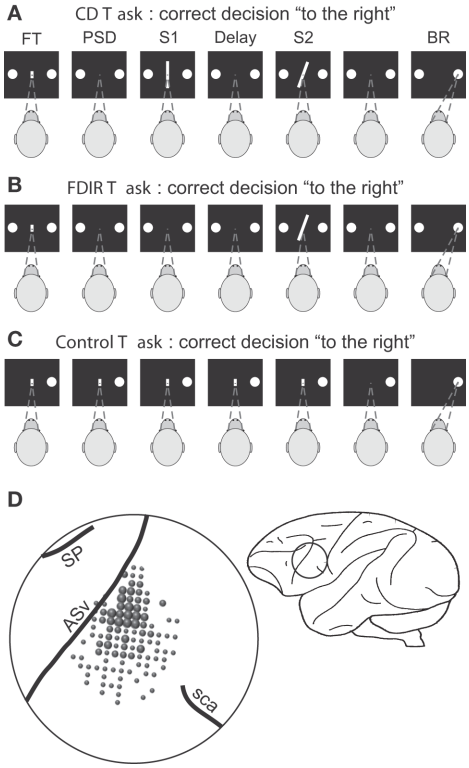

FIGURE 1 | Sequence of events during the two discrimination and the control tasks and localization of the recording area. (A) Continuous discrimination (CD) task: the fixation target (FT) and two circles appeared simultaneously in the center and at both sides of the monitor screen, respectively; the monkey initiated the trial by fixating the FT; fixation had to be maintained during the trial, otherwise it was aborted; when the FT disappeared and after a variable prestimulus delay (PSD; 100–300 ms), two stimuli (S1 and S2), each of 500 ms duration, appeared in sequence separated by a delay of 1 s; once the second stimulus had disappeared, the monkey made an eye movement (behavioral response, BR) to one of the two circles to indicate whether the orientation of the second stimulus was to the left or to the right of the first; correct discriminations were rewarded. **(B)** Fixed discrimination with implicit reference (FDIR) task: same temporal sequence and stimuli set as in the CD task, except that S1 was not shown (i.e., it was implicit) and had to be recovered from long-term memory by trial and error; the implicit stimulus changed from block to block of about 90 trials each and only S2 changed trial by trial. **(C)** Control task: the FT and one of the circles appeared simultaneously; the monkey had to maintain fixation until the FT had disappeared and made an eye movement to the circle; the duration of the trial was the same as that of the CD task. The interval between trials changed randomly in the three tasks between 1.5 and 3.5 s. **(D)** Sketch of the brain showing the localization of the recording area. ASv, *arcuate sulcus ventralis*; SP, *sulcus principalis*; sca, *sulcus subcentralis anterior*. Adapted with permission from Pardo-Vazquez et al. (2008, 2009).

To perform the comparison, the orientation of S1 has to be available during the presentation of S2 (i.e., the comparison or decision period). Therefore, S1 has to be maintained in working memory until S2 is presented. If the PMv neurons encode the sensory evidence used to reach a decision, it is expected that their firing rate will represent the orientation of S1 during the decision period. Besides, if these neurons have a role in the discrimination process, it is expected that they will represent the comparison of the two stimuli and/or the final choice (i.e., whether S2 was oriented to the left or to the right of S1). The dependency between the firing rate and (a) the orientation of S1, (b) the difference between S2 and S1 (S2–S1), and (c) the choice [sign(S2–S1)] was assessed by means of stepwise linear regression (SLR) analysis on single neurons recorded in the PMv (**Figure 1D**). The use of a sliding window of 100 ms moving in 20 ms steps allowed for the study of the dynamic representation of the discrimination process throughout the trial. This analysis showed that the PMv neurons participate in encoding different components of the perceptual decision and that these representations evolve in time during both visual discrimination tasks (**Figure 2**; Pardo-Vazquez et al., 2008, 2009). Firstly, it has been found that neurons from the PMv encode the orientation of S1 in the CD task. These representations are not limited to the time interval during which the stimulus is presented but are also observable during the delay period and especially during the presentation of S2 (**Figure 2A**). Therefore, the PMv neurons encode the orientation of S1 during its presentation and also maintain it in working memory until the presentation of S2, when the comparison is made. Similar results were found in the FDIR task in which the orientation of S1 had to be recovered from LTM (**Figure 2B**): there are PMv neurons encoding the orientation of the implicit S1 from the beginning of the trial until the presentation of S2, when this information is used to compare the orientation of both stimuli. Secondly, it has been found that PMv neurons encode, during the first 200–300 ms of the comparison period, the difference between S2 and S1 in the CD and FDIR tasks. This result suggests that these neurons use the information about the orientation of S1 to compare it with the orientation of the second stimuli. Thirdly, there are PMv neurons that encode the choice, during the comparison period, in both the CD and FDIR tasks. This suggests that the activity of the PMv neurons is very close to the behavioral choices, as will be discussed later. Finally, it is worth noting that some PMv neurons encode the whole process that links sensory information with the behavioral action in the two variants of the discrimination task. The example neuron shown in **Figure 3** encodes the orientation of S1 at the beginning of the decision period (i.e., when the second stimulus is presented and the comparison can be made); after a few tens of milliseconds the same neuron encodes the comparison of S2 and S1, and finally, this neuron also encodes the choice.

The results obtained in the somatosensory and visual discrimination tasks were confirmed in an auditory task (Lemus et al., 2009). Therefore, the PMv neurons encode the same information regardless of the sensory modality: somatosensory, auditory, or visual. There are neurons that represent the sensory features of the first stimulus, its memory trace, the comparison of the two stimuli and the choice. However, there is a difference between the results obtained in the somatosensory and auditory modalities and those obtained in the visual discrimination tasks: the PMv neurons encode the sensory features of the second stimulus in the somatosensory and auditory tasks but not in the visual tasks (Romo et al., 2004; Pardo-Vazquez et al., 2008, 2009; Lemus et al., 2009). These discrepancies may be explained by the temporal differences between the stimuli used; the orientation of the lines in the visual tasks can be perceived as soon as the stimulus is presented while the frequency of the somatosensory and auditory stimuli has to be integrated over time.

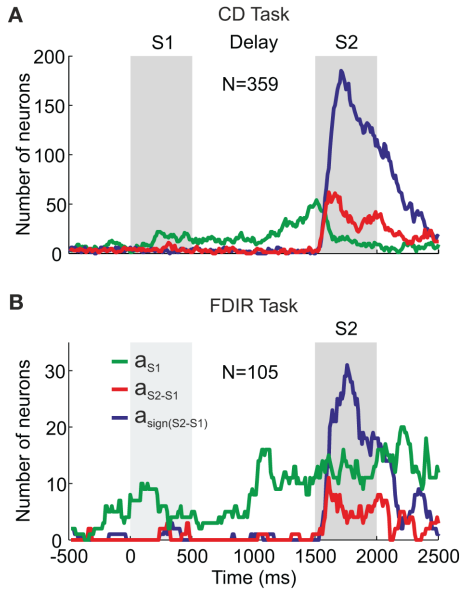

FIGURE 2 | Representation of the discrimination process in the PMv cortex. Number of neurons with significant SLR coefficients as a function of time with respect to the S1 onset during the CD **(A)** and FDIR **(B)** tasks. a_{S1}, a_{S2-S1}, $a_{sign(S2-S1)}$, SLR coefficients associated to the orientation of S1, the difference in orientation between S2 and S1 and the choice ("to the left" or "to the right"), respectively. Adapted with permission from Pardo-Vazquez et al. (2008, 2009).

DISCRIMINATION CAPABILITY OF SINGLE NEURONS FROM THE PMv CORTEX

Another relevant issue regarding the role of the PMv cortex in perceptual decisions is the number of neurons that are needed to perform the discriminations. On the one hand, if the discrimination capability of each PMv neuron were lower than the behavioral performance, this would mean that the information about the decision has to be carried out by combining the activity of a great number of neurons. On the other hand, if each neuron had a similar discrimination capability to that behaviorally observed, a small group of neurons would be able to perform the comparison. The capability of single neurons from the PMv cortex to discriminate the orientation has been studied using trial-to-trial methodology based on signal detection theory (SDT; Green and Swets, 1966; Macmillan and Creelman, 1991). Sensitivity (d') was used as the index of discrimination capability and was estimated for both behavioral and neuronal data (Acuña and Pardo-Vazquez,

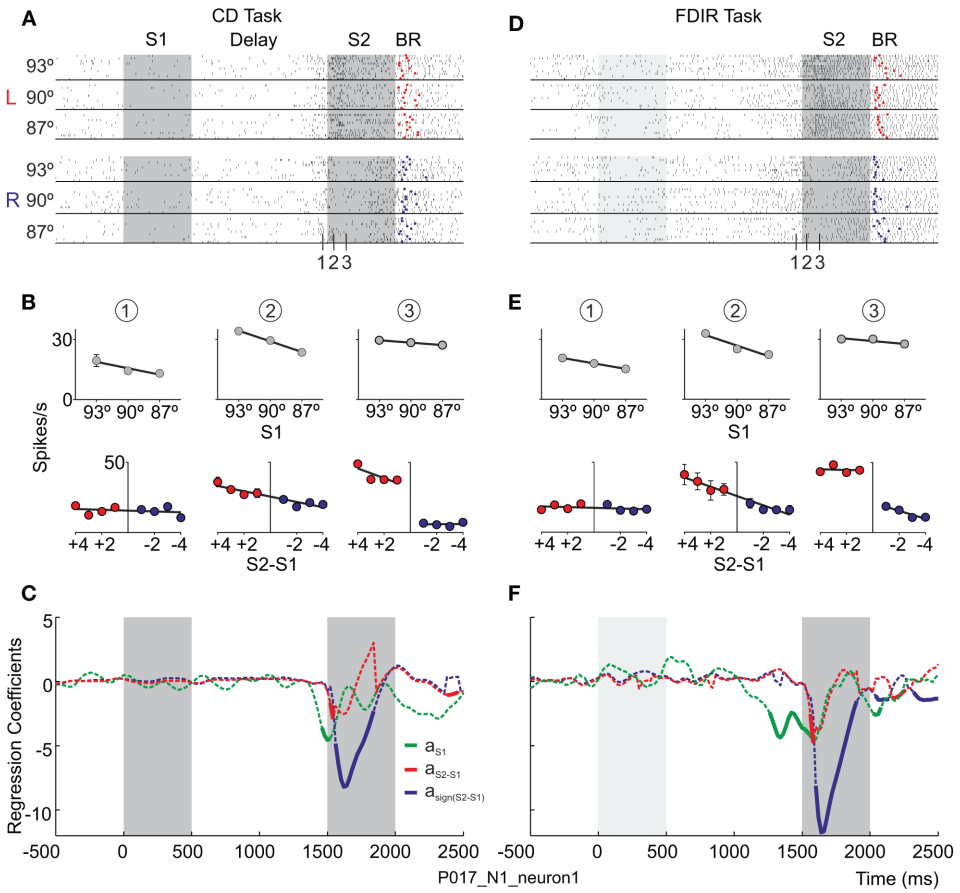

FIGURE 3 | The temporal evolution of neural activity depends on the trace left by the first stimuli – regardless of whether it was recently shown in the visual world or retrieved from LTM – on the comparison between the first and the second stimuli and on the choice. (A,D) Response of the same neuron during the CD and FDIR tasks, respectively, sorted by S1 (93˚, 90˚ and 87˚) and the choice (L, to the left; R, to the right). Raster plot: each line represents a trial and each tick an action potential. Trials were randomly presented. Red and blue dots signal the behavioral response (BR) in each trial, to the left and to the right, respectively. **(B,E)** Temporal evolution of the average firing rates fitted as a function of: S1 and the relative orientation of S2 (S2–S1) during the delay (1) and the comparison (2 and 3) periods. **(C,F)** Stepwise Linear Regression coefficients, a_{S1}, a_{S2-S1}, and $a_{sign(S2-S1)}$, as a function of time; continuous traces indicate significant coefficients. Adapted with permission from Pardo-Vazquez et al. (2009).

2011). The main finding was that the sensitivity of a group of neurons from the PMv is close to the behavioral sensitivity (**Figure 4**). This suggests that subjects could obtain knowledge about their behavioral choices from the activity of a small number of neurons.

CHOICE-RELATED SIGNALS IN THE PMv

The fact that neuronal sensitivity is close to behavioral sensitivity does not imply the existence of a trial-to-trial covariation between the neural activity and the behavioral choices (Newsome et al., 1989). The analysis of the trial-to-trial covariation between the behavioral responses of the monkeys and the choices derived from the activity of single neurons (i.e., the neuronal choices) showed that, for some neurons, the coherence between behavioral and neuronal choices was close to 100% (**Figure 5**; Acuña and Pardo-Vazquez, 2011). The relationship between neuronal activity in the PM cortex and behavioral choices trial-to-trial has also been studied in somatosensory and auditory discrimination tasks. The activity of the PMv neurons predicts the behavioral choices in about 75 and 90% of the trials in the somatosensory (Romo et al., 2004) and auditory (Lemus et al., 2009) tasks, respectively. In the PMd cortex the percentage of predicted behavioral responses is about 60% and in the PMm it is about 70%.

Temporal evolution of the choice-related activity in the PMv cortex

One of the main goals of studying the neural bases of decision-making is to understand how the neurons encode the decision in their firing rates and how these representations emerge and change in time as a function of different behavioral parameters of the discriminations. This question was addressed in the PMv cortex by assessing the optimal parameters (size and position) of the encoding window as a function of the difficulty (Acuña and Pardo-Vazquez, 2011; **Figures 6A,B**). This analysis showed that the percentage of coherence between neuronal and behavioral choices was higher than 85% for most PMv neurons (**Figure 6C**). The main results of the assessment of the optimal encoding window were that: (a) the PMv neurons encode the choices in a short time window (about 20 ms) during the first 200–300 ms of the decision period (when S2 is presented) and (b) the optimal

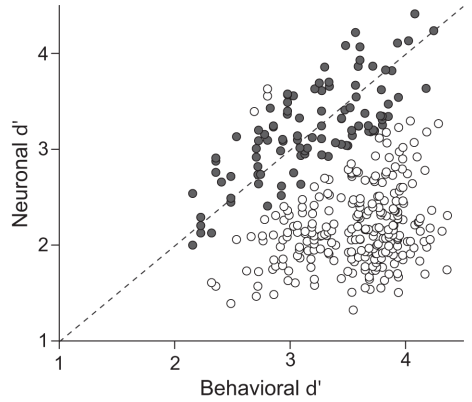

FIGURE 4 | The sensitivity of individual neurons from the PMv cortex is close to the behavioral sensitivity of the monkeys. Comparison of the neuronal and behavioral sensitivities for the 359 neurons with decision-related activity; solid circles correspond to neurons for which the ratio between behavioral and neuronal *d'* is between 0.8 and 1.2 ($n = 102$, 28%); open circles correspond to neurons for which the ratio between behavioral and neuronal *d'* is lower than 0.8 or higher than 1.2 ($n = 256$, 72%). Adapted with permission from Acuña and Pardo-Vazquez (2011).

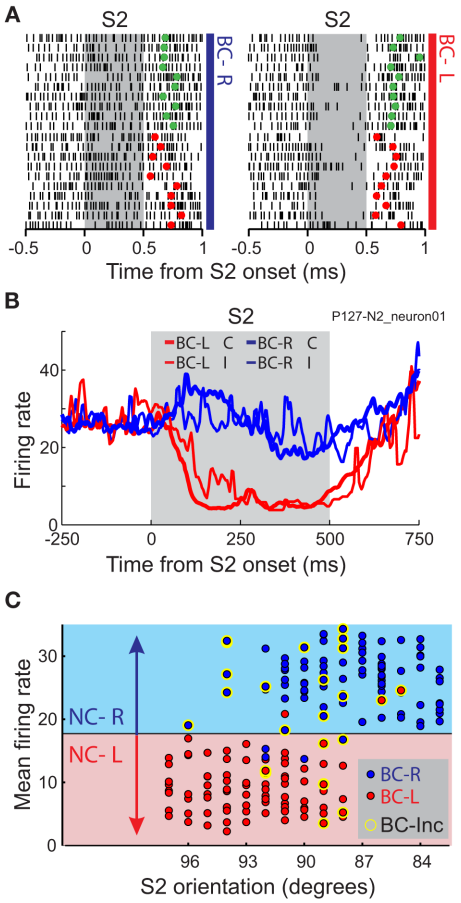

FIGURE 5 | The firing rate of individual neurons represents the behavioral choice of the monkeys both in correct and in incorrect trials. (A) Raster plot representing the activity of one neuron recorded during the CD task during the comparison period (S2). Trials are sorted by the behavioral choice of the monkeys to the left (BC-L) and to the right (BC-R) and by the correctness of the behavioral choice (Green and red dots, correct and incorrect behavioral choices, respectively). Trials were randomly presented. **(B)** Mean firing rate of the neuron in A, during the comparison period, for correct and incorrect behavioral choices to the left (BC-L C, BC-L I) and to the right (BC-R C, BC-R I). **(C)** For the same neuron, mean firing rate as a function of the orientation of S2 and the behavioral choice [red and blue dots represent trials in which the behavioral choices were to the left (BC-L) and to the right (BC-R), respectively] during comparison period (S2). The firing rate in each trial is compared against different criteria to categorize neuronal responses as "to the left" or "to the right." The criterion (horizontal black line) is chosen to maximize the coherence between the neuronal and the behavioral choices. Red and blue background colors indicate the neuronal choices derived from the mean firing rate during the comparison period, to the left (NC-L) and to the right (NC-R), respectively. Yellow halos signal incorrect behavioral choices (BC-Inc). Adapted with permission from Acuña and Pardo-Vazquez (2011).

parameters of the encoding window depend on the difficulty of the discrimination (**Figure 7**). The PMv neurons represent the easy discriminations earlier and within smaller encoding windows than the difficult ones. It is worth noting that to reveal the neuronal correlations of behavior each neuron should be analyzed individually both in the temporal evolution of its activity and in the size of the encoding windows. Given that the difficulty level of the decision affects the accuracy and timing of the behavioral choices, the parameters of the encoding window should also be adjusted to the difficulty level. Therefore, when using windows of fixed size or position for the analysis, the information encoded in the neuronal activity could be underestimated under certain conditions. In the somatosensory task it was found that the covariation between neuronal activity and behavioral choices during the stimulus presentation was higher for easier discriminations (Romo et al., 2004), while the level of coherence is almost equal for all difficulty levels in the CD task (Acuña and Pardo-Vazquez, 2011). There is no reason to expect this dependency between the choice-related activity and the difficulty of the task, and this discrepancy could be related to the analytical procedure, as the covariation between neuronal activity and behavioral choices was analyzed with a fixed duration window in the somatosensory task.

THE MOTOR COMPONENT OF THE TASK CANNOT EXPLAIN THE STRONG CHOICE-RELATED SIGNAL

As the PMv neural activity has been associated with movement execution (Wise, 1985; Kakei et al., 2001), it could be possible that the neuronal activity, which was close to the behavioral choices, represented the motor component of the task. This possibility was ruled out by applying the same analyses to a subset of PMv neurons that were also recorded in a control task (**Figure 1C**). In this task, the motor component is the same as in the CD task but no discrimination (and therefore no perceptual decision) has to be made. The results obtained in the control task were significantly different from those obtained in the CD task for both the sensitivity and the coherence (**Figures 6A,B**). This suggests that the choice-related activity of the PMv neurons does not represent the motor component of the discrimination task and that the choice itself is encoded in the activity of the PMv neurons (Acuña and

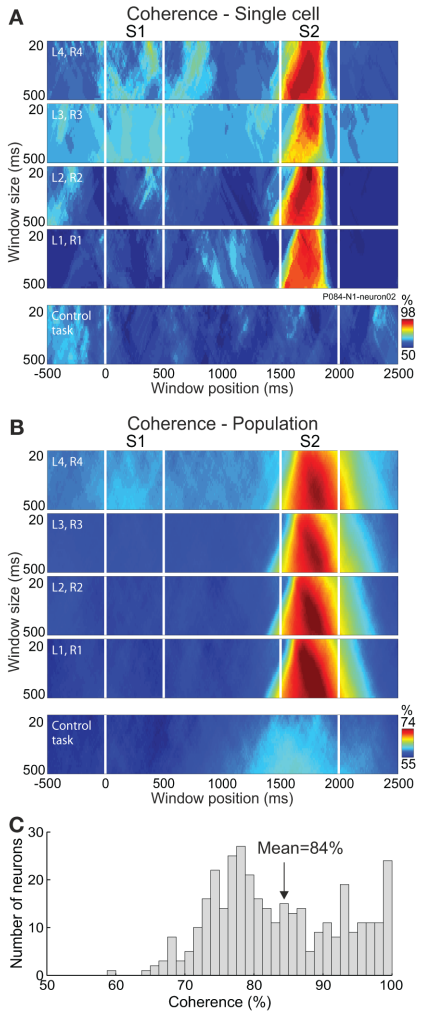

FIGURE 6 | The activity of PMv neurons predicts the behavioral choices of the monkey. CD task: four upper tiers of each panel; Control task: lower tier of each panel. **(A)** For one example neuron each tier depicts the percentage of coherence between the neuronal and behavioral choices (color code) as a function of window position (−500 to 2500 ms from S1 onset, in steps of 5 ms; abscissa) and window size (20 to 500 ms, in 20-ms steps; ordinate) for each level of difficulty [from the most difficult (L1, R1) to the easiest (L4, R4)] in the CD and control tasks. **(B)** Percentage of coherence averaged across the 179 neurons that were recorded in both the CD and the control tasks. **(C)** Distribution of the percentage of coherence for the 359 neurons with decision-related activity. Adapted with permission from Acuña and Pardo-Vazquez (2011).

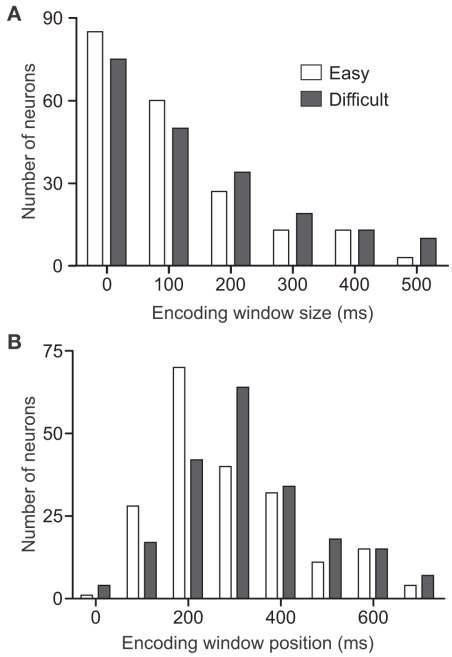

FIGURE 7 | The window size and position that maximize the coherence between neuronal and behavioral choices depend on the difficulty of the discrimination. Distributions of optimal window size **(A)** and optimal window position **(B)** as a function of the difficulty level for the 201 neurons for which the coherence between the behavioral and the neuronal choices is equal to or higher than 80%. Adapted with permission from Acuña and Pardo-Vazquez (2011).

Pardo-Vazquez, 2011). This result confirms that found by Romo et al. (2004) in the somatosensory discrimination task.

PREMOTOR VENTRAL CORTEX AND THE EVALUATION OF THE DECISION PROCESS

Depending on task demands, decisions may be postponed for later report and, in this case, they have to be maintained in working memory. Does PM cortex participate in maintaining these postponed decisions in working memory? Romo et al. have addressed this question in the PMm and PMv cortices during a postponed decision report period (Lemus et al., 2007, 2009). They have found that the activity of PMm neurons encodes both the result of the sensory evaluation (i.e., the choice) and past sensory information used to reach a decision during the somatosensory discrimination task (Lemus et al., 2007). Similar results were found in the PMv using the auditory discrimination task (Lemus et al., 2009; **Figure 8**). The main conclusions are that maintaining in WM the original information about the stimuli could serve to continuously update the postponed decision report and that during this period it is possible that the perceptual decision is evaluated and even corrected. This interpretation is consistent with the finding that behavioral performance is better when the decision report is postponed than when the decision is reported immediately after S2.

These neural representations have been studied along the cerebral cortex in a recent study (Hernandez et al., 2010), in which the activity of single cells from different cortical areas was recorded in monkeys performing a somatosensory discrimination task. It was found that perceptual decisions arise from the activity of neurons distributed across brain circuits and that these circuits represent the information necessary to evaluate the process.

PERFORMANCE MONITORING IN INDIVIDUAL NEURONS DURING PERCEPTUAL DECISIONS

The consequences of the behavioral decision affect all the components of the process and can modify future decisions (Gold and Shadlen, 2007); the decision process does not finish when

the monkeys make a choice and execute the behavioral response. Therefore, the neural correlates of this stage of the decision process can be addressed by studying the neuronal activity after the behavioral responses in decision-related areas. As the PMv receives inputs from areas that encode information about the outcomes of previous decisions (Kurata, 1991; Hoover and Strick, 1993; Ghosh and Gattera, 1995; Takada et al., 2004; Boussaoud et al., 2005; Clower et al., 2005; Dancause et al., 2006), this issue was addressed in the choice-related PMv neurons, i.e., those that showed decision-related activity during the presentation of S2 (Pardo-Vazquez et al., 2008, 2009). In both the CD and the FDIR tasks neurons encoded: (a) the previous choices only, (b) the outcomes (correct or incorrect) only and (c) the previous choices and their outcomes (**Figure 9**). An important difference between the FDIR and the CD task is that, while in the former the correct orientation of S1 had to be retrieved by trial and error, in the later the stimulus is presented in each trial. Therefore, in the FDIR task the information about the retrieved S1 has to be combined with the information about the outcome of the decision while in the CD task this combination is not necessary and consequently, the representation of the orientation of S1 is not useful in this task. The PMv neurons reflect this difference in task requirements: after the behavioral response, and the feedback about the correctness of the previous choice, the PMv neurons encode the orientation of S1 that was compared with the orientation of S2 in the FDIR task but not in the CD task (**Figure 9**). Thus, the activity of the PMv neurons represents the information necessary to evaluate the previous decision process. We wish to emphasize that the fact that these neurons continued to mull over the past information used to reach a behavioral action suggests that the PMv neurons represent the information necessary to evaluate the previous decision process. This evaluation is necessary to learn from errors and adjust further behavior.

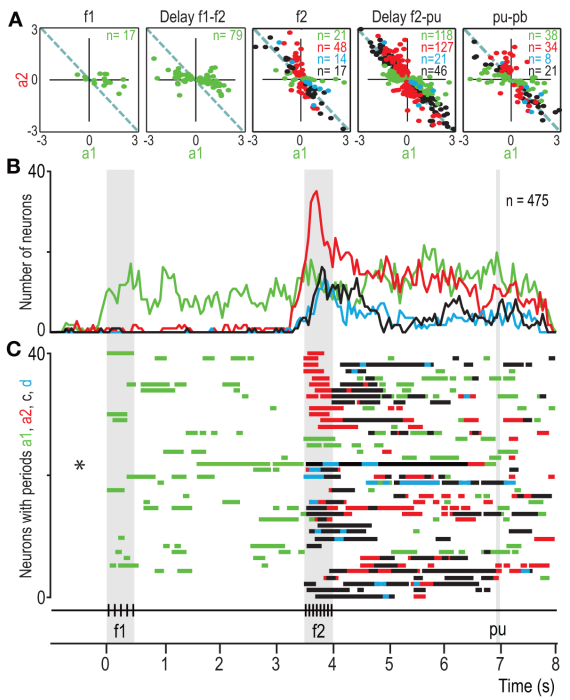

FIGURE 8 | Dynamics of PMv population responses during the acoustic flutter discrimination task. (A) Values of *a*1 and *a*2 coefficients for all neurons selected plotted B. For each point, at least one coefficient is significantly different from zero; *a*1 and *a*2 are the regression coefficients associated with the frequency of the first and second stimuli, respectively. Different plots are for various times in A; *n* = number of neurons. **(B)** Number of neurons with significant coefficients as a function of time. Green and red traces correspond to *a*1 and *a*2, respectively. Blue trace corresponds to neurons with both significant *a*1 and *a*2 coefficients of opposite signs, but significantly different magnitudes; these are partially differential (d) responses. Black trace corresponds to neurons with both significant *a*1 and *a*2 coefficients of opposite signs and statistically equal magnitude; these are fully differential (c) or categorical responses encoding *f*2–*f*1. **(C)** Bar graphs of 40 randomly selected neurons from the 475 neurons that contributed to **(B)**. These bars indicate periods of responses encoding *f*1 (green bars), *f*2 (red bars), partially differential *f*2–*f*1 (blue bars), and fully differential or categorical responses encoding *f*2–*f*1 (black bars). Each line of bars represents the dynamics of the responses of one single neuron during the discrimination task. The dynamics of these coefficients was analyzed using a sliding window of 200 ms duration moving in steps of 100 ms. pu, probe up; ku, key up; pb, push-button. Adapted with permission from Lemus et al. (2009).

PERFORMANCE MONITORING IN HUMANS: EVIDENCE FROM EVENT-RELATED POTENTIALS

Given the importance of detecting errors, the neural bases of the system that encodes the outcomes of previous decisions have also been studied in humans using ERPs. In these studies two components of the ERPs related to error detection have been described. The first component, called error-related negativity (ERN; Gehring et al., 1993) or error negativity (Ne; Falkenstein et al., 1991), is defined as a negative deflection in the electric potential with a fronto-central scalp distribution that peaks about 80–100 ms after an erroneous response has been made. One property of the ERN is that it can be elicited following presentation of error feedback. This waveform, called the feedback error-related negativity (FRN), is a fronto-central negative deflection that occurs at approximately 250–350 ms after negative feedback stimuli (Miltner et al., 1997; Gehring and Willoughby, 2002; Holroyd and Coles, 2002). The second component, called error positivity (Pe; Falkenstein et al., 1991, 1995) is defined as a slow positive wave that usually follows the ERN, with centroparietal distribution, which peaks about 200–450 ms after an incorrect response. Source analyses and neuroimaging data have shown that these components are generated in the activity of neurons from the anterior cingulate cortex (ACC; Van Veen and Carter, 2002; Dehaene et al., 2004; Herrmann et al., 2004). Other localizations such as the basal ganglia and prefrontal cortex may also be involved in their generation (Gehring and Knight, 2000; Falkenstein et al., 2001).

During the last years the functional role of these ERPs has been studied using different behavioral tasks, including a visual discrimination task that is equivalent to the CD task.

The error-related potentials FRN and a positive deflection, that here we will refer to it as feedback related positivity (FRP), can be observed in **Figure 10**. (Pardo-Vazquez, Padron, Fernandez-Rey and Acuña, Unpublished results). As both the ERPs and single cell data were obtained in equivalent tasks, it is possible to compare the temporal evolution of the outcomes-related

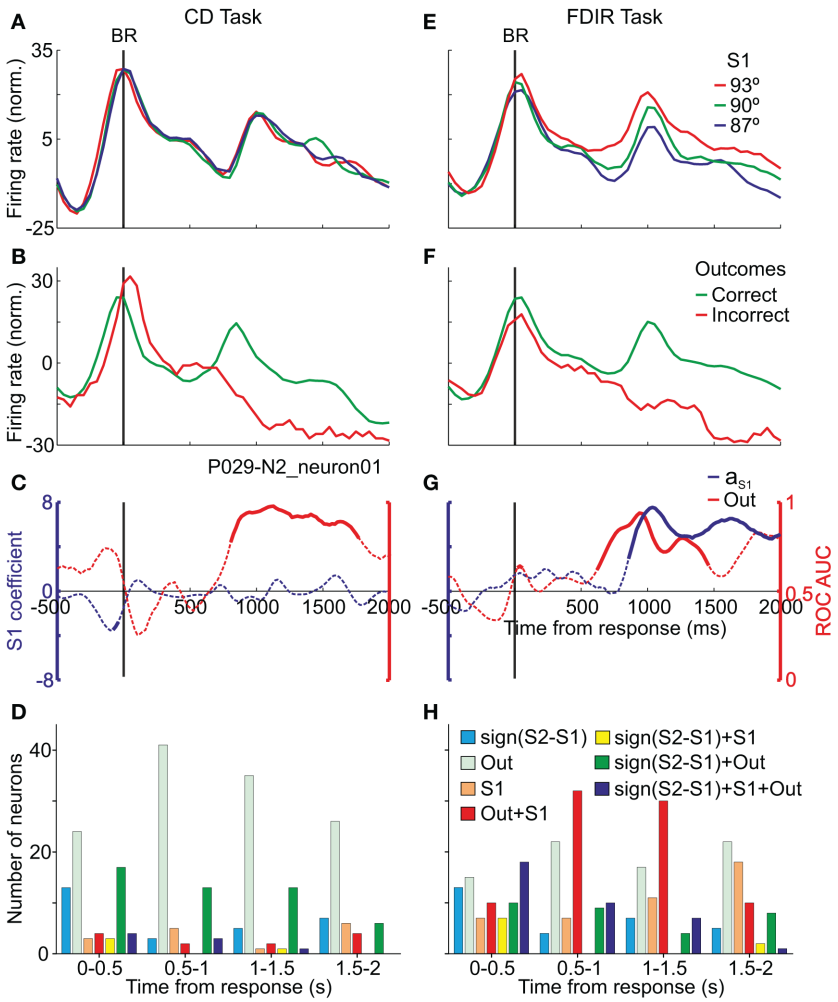

FIGURE 9 | After the monkey gave the behavioral response (BR) the same neuron encoded the outcomes (Out) and the memory traces of S1 depending on the task. (A,E) Averaged firing rates sorted by S1; the memory traces are encoded in the FDIR task only. **(B,F)** Averaged firing rates sorted by correct and incorrect outcomes; in both tasks the same neuron differentiated correct from incorrect trials. **(C,G)** ROC AUC for correct vs. incorrect trials and SLR a_{S1} coefficient, as a function of time; continuous traces indicate significant values. **(D,H)** Number of neurons that carried significant information (ROC and SLR analysis) about the components of the decision in CD and FDIR task. Time intervals taken from the behavioral response. The same neurons can be represented in more than one time period. Adapted with permission from Pardo-Vazquez et al. (2009).

activity. The difference between correct and incorrect trials is significant at 300–500 ms after the feedback is presented, both in the individual neurons recorded in the PMv cortex and in the humans' ERPs. Therefore, it is possible that the FRN and FRP are originated, at least in part, in the activity of those PMv neurons that encode the outcomes of previous decisions. Moreover, the results obtained in individual neurons of subhuman primates show that the brain encodes multiple types of information after the behavioral response and feedback presentation, including not only the outcomes of previous decisions but also the decisions themselves and the sensory information used to reach the decisions (Pardo-Vazquez et al., 2009). These complex neural representations have been revealed, in individual neurons, by the experimental manipulation of different behavioral variables of perceptual decision tasks. Therefore, this approach emerges as a promising method for revealing the contribution of the different cognitive processes that take place after the behavioral responses to the EEG activity.

ROLE OF THE PMv CORTEX IN MAINTAINING INFORMATION IN WORKING MEMORY

Taken together, the results obtained with perceptual discrimination tasks emphasize the role of the PM cortex in working memory and the representation of multiple features of the task during different time periods (Romo et al., 2004; Pardo-Vazquez et al., 2008, 2009; Lemus et al., 2009). The PMv neurons maintain in working memory information from different sources and for different purposes. These representations depend on task demands and also on the cognitive processes involved in each stage within the behavioral tasks (Pardo-Vazquez et al., 2009). The activity of PMv neurons represents, in different sensory modalities, the memory traces of sensory information, recently shown or recovered

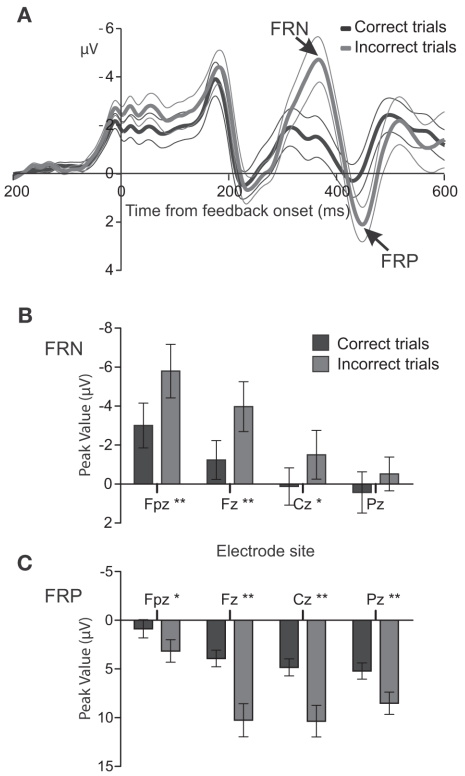

FIGURE 10 | Event-related potentials show significant differences between correct and incorrect decisions. **(A)** Feedback-locked ERPs [mean ± (2×SEM)] at electrode Fpz following correct (black line) and incorrect (gray line) trials in a visual discrimination task ($n = 13$). Zero on abscissa indicates the feedback onset. Note that negative voltages are plotted upward by convention. **(B,C)** Mean peak amplitudes (±SEM) of the FRN and FRP at electrodes Fpz, Fz, Cz, and Pz for correct (black bars) and error (gray bars) trials. Significance was established using a two-tailed t-test at $p < 0.01$ (*) and $p < 0.001$ (**).

from LTM, during the task period in which this information is used to reach a decision (Romo et al., 2004; Pardo-Vazquez et al., 2008, 2009; Lemus et al., 2009). During the postponed decision report, when the decision has to be maintained in WM until it is reported, the PMv neurons maintain a memory trace of the decision (Lemus et al., 2009). Similar results were obtained in the PMm neurons (Lemus et al., 2007). Behavioral data suggests that this task period may be used to evaluate the sensory information used to decide and, eventually, to correct the decision; it has been found that the activity of the PM neurons represents, during this period, the memory traces of the stimuli used to decide (Lemus et al., 2009). Finally, after the behavioral response, when the whole decision process is evaluated, the activity of the PMv neurons represents all the information needed for such evaluation, including the working memory traces of the previous decision and of the information used to decide (Pardo-Vazquez et al., 2008, 2009).

FUNCTION OF THE PREMOTOR CORTEX REVISITED

Early studies on the function of PM cortex were focused on motor aspects of behavior and used behavioral tasks designed to analyze the role of this area in the preparation and execution of movements (Wise, 1985; Passingham, 1993). Recent findings on the role of the PM cortex in decision-making have provided us with alternative interpretations about some of the motor functions attributed to this area, namely sensory guidance of movements (Petrides, 1982, 1985; Halsband and Passingham, 1985), maintenance of movements in working memory (Passingham, 1988), and associative learning (Sasaki and Gemba, 1982; Petrides, 1985, 1986; Halsband and Freund, 1990; Mitz et al., 1991).

The selection of movements based on sensory information has mainly been studied with conditional motor tasks and the main conclusion of these studies was that the PM cortex represents the selected movement when sensory information guides this selection (Wise, 1985; Passingham, 1993). Conditional motor tasks can also be interpreted as a form of perceptual decision as the subjects have to select the correct movement based on the available sensory information. Some of the results obtained with perceptual discrimination tasks indicate that the role of PM cortex goes far beyond representing the selected movement. Firstly, there are PMv neurons that represent the sensory evidence the monkeys use to reach a decision (Romo et al., 2004; Pardo-Vazquez et al., 2008, 2009; Lemus et al., 2009). Secondly, when the task implies the comparison of two stimuli presented sequentially, there are PMv neurons that represent not only the sign of the difference between the stimuli (i.e., the choice) but also its magnitude (Pardo-Vazquez et al., 2008; Acuña et al., 2010). Thirdly, when the same PMv neurons were evaluated in a motor task used as control (in which the motor component was the same as in the discrimination task but no discrimination was necessary) most of the neurons showed no significant differences as a function of the monkeys' movement (Pardo-Vazquez et al., 2008; Acuña et al., 2010).

The participation of the PM cortex in working memory has been studied with conditional motor tasks in which the subjects had to select one movement based on a sensory cue and to execute the movement immediately or after a delay period (Wise and Mauritz, 1985; Passingham, 1988). It has been found that neurons in the PM cortex show directional movement selectivity both in the conditions of the immediate and delayed tasks. From these results it has been concluded that the primary role of PM cortex would be to select the behavioral response and, once selected, hold it in memory until it was necessary (Passingham, 1988). The design of this kind of tasks makes it difficult to interpret the role of PM cortex in working memory; as in the behavioral tasks used each sensory cue is related to one movement, it could also be the case that PM neurons encode the sensory information during its presentation and maintain it in working memory during the delay or, as suggested by data from Lemus et al. (2009), these neurons could maintain both the decision and the sensory information. We favor this last interpretation because it is supported by the recent evidence that PM cortex participates in encoding both sensory and decision-related information and maintaining it in working memory (Romo et al., 2004; Pardo-Vazquez et al., 2008, 2009; Lemus et al., 2009).

Finally, early studies, both with lesions and single cell recordings, have also shown that the PM cortex participates in associative learning (Sasaki and Gemba, 1982; Petrides, 1985, 1986; Halsband and Freund, 1990; Mitz et al., 1991). It has been found that subjects

with lesions in the PM area show learning deficits in association tasks. Commonly, subjects learn how to solve the task by trial and error and this implies that subjects have to relate the actions with their consequences. The results recently obtained while monkeys performed in discrimination tasks could help us to understand the role of PMv in learning (Pardo-Vazquez et al., 2008, 2009; Lemus et al., 2009; Acuña et al., 2010). There are neurons in PMv that encode previous decisions, their outcomes (Pardo-Vazquez et al., 2008; Acuña et al., 2010) and also the information used to reach a decision (Pardo-Vazquez et al., 2009; Acuña et al., 2010). The participation of the PMv in the evaluation of the decision process and of its consequences suggests that this area could be essential for shaping behavior on the basis of experience, through a learning process. Therefore, subjects with PM cortex lesions do not have the representations needed to evaluate the consequences of previous actions and the associative learning will be impaired.

An obvious question, in dealing with the PMv (F5/F4) area is the relationship between the neuronal activity obtained with discrimination tasks (Romo et al., 2004; Pardo-Vazquez et al., 2008, 2009; Lemus et al., 2009) and the neuronal activity obtained during action observation (i.e., mirror activity) in F5 and F4 (reviewed in Rizzolatti and Sinigaglia, 2010). It is difficult to establish a direct relationship because of the different ways of obtaining the data and the uncertainty of the recording places. Albeit speculative, the encoding of a decision-making and evaluating process in the firing rate of the PMv neurons described here could also be embedded in the firing rate of the neurons active during action observation. Should this be the case, the encoding of the relevant sensory information (either current or from LTM) for deciding and acting and then evaluating that chosen action, might be at the service of action observation and communication.

ACKNOWLEDGMENTS

Work supported by grants from Ministerio de Ciencia e Innovación (MICINN) Spain to Carlos Acuña and Dirección Xeral de Investigación, Desenvolvemento e Innovación, Xunta de Galicia (INCITE) Spain to Carlos Acuña and Jose Fernandez-Rey. Work of Jose L. Pardo-Vazquez and Isabel Padron supported by INCITE post-doc and pre-doc grants, respectively.

REFERENCES

Acuña, C., and Pardo-Vazquez, J. L. (2011). Ventral premotor cortex neuronal activity matches perceptual decisions. *Eur. J. Neurosci.* 33, 2338–2348.

Acuña, C., Pardo-Vazquez, J. L., and Leboran, V. (2010). Decision-making, behavioral supervision and learning: an executive role for the ventral premotor cortex? *Neurotox. Res.* 18, 416–427.

Amiez, C., Kostopoulos, P., Champod, A. S., and Petrides, M. (2006). Local morphology predicts functional organization of the dorsal premotor region in the human brain. *J. Neurosci.* 26, 2724–2731.

Borra, E., Belmalih, A., Calzavara, R., Gerbella, M., Murata, A., Rozzi, S., and Luppino, G. (2008). Cortical connections of the macaque anterior intraparietal (AIP) area. *Cereb. Cortex* 18, 1094–1111.

Boudreau, M.-J., Brochier, T., Pare, M., and Smith, A. M. (2001). Activity in ventral and dorsal premotor cortex in response to predictable force-pulse perturbations in a precision grip task. *J. Neurophysiol.* 86, 1067–1078.

Boussaoud, D. (2001). Attention versus intention in the primate premotor cortex. *Neuroimage* 14, S40–S45.

Boussaoud, D., Tanne-Gariepy, J., Wannier, T., and Rouiller, E. M. (2005). Callosal connections of dorsal versus ventral premotor areas in the macaque monkey: a multiple retrograde tracing study. *BMC Neurosci.* 6, 67. doi: 10.1186/1471-2202-6-67

Boussaoud, D., and Wise, S. P. (1993). Primate frontal cortex: neuronal activity following attentional versus intentional cues. *Exp. Brain Res.* 95, 15–27.

Boyd, L. A., and Linsdell, M. A. (2009). Excitatory repetitive transcranial magnetic stimulation to left dorsal premotor cortex enhances motor consolidation of new skills. *BMC Neurosci.* 10, 72. doi: 10.1186/1471-2202-10-72

Carey, J. R., Kimberley, T. J., Lewis, S. M., Auerbach, E. J., Dorsey, L., Rundquist, P., and Ugurbil, K. (2002). Analysis of fMRI and finger tracking training in subjects with chronic stroke. *Brain* 125, 773–788.

Cerri, G., Shimazu, H., Maier, M. A., and Lemon, R. N. (2003). Facilitation from ventral premotor cortex of primary motor cortex outputs to macaque hand muscles. *J. Neurophysiol.* 90, 832–842.

Clower, D. M., Dum, R. P., and Strick, P. L. (2005). Basal ganglia and cerebellar inputs to 'AIP'. *Cereb. Cortex* 15, 913–920.

Dancause, N., Barbay, S., Frost, S. B., Plautz, E. J., Stowe, A. M., Friel, K. M., and Nudo, R. J. (2006). Ipsilateral connections of the ventral premotor cortex in a new world primate. *J. Comp. Neurol.* 495, 374–390.

Dehaene, S., Molko, N., Cohen, L., and Wilson, A. J. (2004). Arithmetic and the brain. *Curr. Opin. Neurobiol.* 14, 218–224.

Deiber, M. P., Wise, S. P., Honda, M., Catalan, M. J., Grafman, J., and Hallett, M. (1997). Frontal and parietal networks for conditional motor-learning: a positron emission tomography study. *J. Neurophysiol.* 78, 977–991.

Del Olmo, M. F., Cheeran, B., Koch, G., and Rothwell, J. C. (2007). Role of the cerebellum in externally paced rhythmic finger movements. *J. Neurophysiol.* 98, 145–152.

Denny-Brown, D., and Botterell, E. H. (1948). The motor functions of the agranular motor cortex. *Res. Publ. Assoc. Res. Nerv. Ment. Dis.* 27, 235–345.

Di-Pellegrino, G., and Wise, S. P. (1993). Visuospatial versus visuomotor activity in the premotor and prefrontal cortex of a primate. *J. Neurosci.* 13, 1227–1243.

Dum, R. P., and Strick, P. L. (1991). The origin of corticospinal projections from the premotor areas in the frontal lobe. *J. Neurosci.* 11, 667–689.

Evarts, E. V. (1966). Pyramidal tract activity associated with a conditioned hand movement in the monkey. *J. Neurophysiol.* 29, 1011–1027.

Falkenstein, M., Hielscher, H., Dziobek, I., Schwarzenau, P., Hoormann, J., Sunderman, B., and Hohnsbein, J. (2001). Action monitoring, error detection, and the basal ganglia: an ERP study. *Neuroreport* 12, 157–161.

Falkenstein, M., Hohnsbein, J., and Hoormann, J. (1995). Event-related potential correlates of errors in reaction tasks. *Electroencephalogr. Clin. Neurophysiol. Suppl.* 44, 287–296.

Falkenstein, M., Hohnsbein, J., Hoormann, J., and Blanke, L. (1991). Effects of crossmodal divided attention on late ERP components. II. Error processing in choice reaction tasks. *Electroencephalogr. Clin. Neurophysiol.* 78, 447–455.

Freund, H.-J., and Hummelshein, H. (1985). Lesions of premotor cortex in man. *Brain* 108, 697–733.

Fridman, E. A., Hanakawa, T., Chung, M., Hummel, F., Leiguarda, R. C., and Cohen, L. G. (2004). Reorganization of the human ipsilesional premotor cortex after stroke. *Brain* 127, 747–758.

Fries, W., Danek, A., Scheidtmann, K., and Hamburger, C. (1993). Motor recovery following capsular stroke. Role of descending pathways from multiple motor areas. *Brain* 116(Pt 2), 369–382.

Frost, S. B., Barbay, S., Friel, K. M., Plautz, E. J., and Nudo, R. J. (2003). Reorganization of remote cortical regions after ischemic brain injury: a potential substrate for stroke recovery. *J. Neurophysiol.* 89, 3205–3214.

Fulton, J. F. (1949). *Physiology of the Nervous System.* New York: Oxford University Press.

Fuster, J. (1997). *The Prefrontal Cortex: Anatomy, Physiology, and Neuropsychology of the Prefrontal Lobe.* Philadelphia: Lippincott-Raven.

Fuster, J. M., and Alexander, G. E. (1971). Neuron activity related to short-term memory. *Science* 173, 652–654.

Gehring, W. J., Goss, B., Coles, M. G. H., Meyer, D. E., and Donchin, E. (1993). A neural system for error detection and compensation. *Psychol. Sci.* 4, 385–390.

Gehring, W. J., and Knight, R. T. (2000). Prefrontal-cingulate interactions in action monitoring. *Nat. Neurosci.* 3, 516–520.

Gehring, W. J., and Willoughby, A. R. (2002). The medial frontal cortex and the rapid processing of monetary gains and losses. *Science* 295, 2279–2282.

Ghosh, S., and Gattera, R. (1995). A comparison of the ipsilateral cortical projections to the dorsal and ventral subdivisions of the macaque premotor cortex. *Somatosens. Mot. Res.* 12, 359–378.

Godschalk, M., Lemon, R. N., Kuypers, H. G., and Ronday, H. K. (1984). Cortical afferents and efferents of monkey postarcuate area: an anatomical and electrophysiological study. *Exp. Brain Res.* 56, 410–424.

Gold, J. I., and Shadlen, M. N. (2007). The neural basis of decision making. *Annu. Rev. Neurosci.* 30, 535–574.

Grafton, S. T., Fagg, A. H., and Arbib, M. A. (1998). Dorsal premotor cortex and conditional movement selection: a PET functional mapping study. *J. Neurophysiol.* 79, 1092–1097.

Graziano, M. S., and Aflalo, T. N. (2007). Mapping behavioral repertoire onto the cortex. *Neuron* 56, 239–251.

Graziano, M. S., Hu, X. T., and Gross, C. G. (1997). Visuospatial properties of ventral premotor cortex. *J. Neurophysiol.* 77, 2268–2292.

Green, D. M., and Swets, J. A. (1966). *Signal Detection Theory and Psychophysics.* New York: Wiley.

Halsband, U., and Freund, H. J. (1990). Premotor cortex and conditional motor learning in man. *Brain* 113(Pt 1), 207–222.

Halsband, U., Ito, N., Tanji, J., and Freund, H. J. (1993). The role of premotor cortex and the supplementary motor area in the temporal control of movement in man. *Brain* 116(Pt 1), 243–266.

Halsband, U., and Passingham, R. (1982). The role of premotor and parietal cortex in the direction of action. *Brain Res.* 240, 368–372.

Halsband, U., and Passingham, R. E. (1985). Premotor cortex and the conditions for movement in monkeys (*Macaca fascicularis*). *Behav. Brain Res.* 18, 269–277.

He, S. Q., Dum, R. P., and Strick, P. L. (1993). Topographic organization of corticospinal projections from the frontal lobe: motor areas on the lateral surface of the hemisphere. *J. Neurosci.* 13, 952–980.

Hepp-Reymond, M., Kirkpatrick-Tanner, M., Gabernet, L., Qi, H. X., and Weber, B. (1999). Context-dependent force coding in motor and premotor cortical areas. *Exp. Brain Res.* 128, 123–133.

Hepp-Reymond, M. C., Husler, E. J., Maier, M. A., and Ql, H. X. (1994). Force-related neuronal activity in two regions of the primate ventral premotor cortex. *Can. J. Physiol. Pharmacol.* 72, 571–579.

Hernandez, A., Nacher, V., Luna, R., Zainos, A., Lemus, L., Alvarez, M., Vazquez, Y., Camarillo, L., and Romo, R. (2010). Decoding a perceptual decision process across cortex. *Neuron* 66, 300–314.

Hernandez, A., Zainos, A., and Romo, R. (2002). Temporal evolution of a decision-making process in medial premotor cortex. *Neuron* 33, 959–972.

Herrmann, M. J., Rommler, J., Ehlis, A. C., Heidrich, A., and Fallgatter, A. J. (2004). Source localization (LORETA) of the error-related-negativity (ERN/Ne) and positivity (Pe). *Brain Res. Cogn. Brain Res.* 20, 294–299.

Holroyd, C. B., and Coles, M. G. (2002). The neural basis of human error processing: reinforcement learning, dopamine, and the error-related negativity. *Psychol. Rev.* 109, 679–709.

Hoover, J. E., and Strick, P. L. (1993). Multiple output channels in the basal ganglia. *Science* 259, 819–821.

Hoshi, E., and Tanji, J. (2000). Integration of target and body-part information in the premotor cortex when planning action. *Nature* 408, 466–470.

Hoshi, E., and Tanji, J. (2002). Contrasting neuronal activity in the dorsal and ventral premotor areas during preparation to reach. *J. Neurophysiol.* 87, 1123–1128.

Iannilli, E., Gerber, J., Frasnelli, J., and Hummel, T. (2007). Intranasal trigeminal function in subjects with and without an intact sense of smell. *Brain Res.* 1139, 235–244.

Jacobsen, C. F. (1931). A study of cerebral function in learning. The frontal lobes. *J. Comp. Neurol.* 52, 271–340.

Jeannerod, M., Arbib, M. A., Rizzolatti, G., and Sakata, H. (1995). Grasping objects: the cortical mechanisms of visuomotor transformation. *Trends Neurosci.* 18, 314–320.

Kakei, S., Hoffman, D. S., and Strick, P. L. (2001). Direction of action is represented in the ventral premotor cortex. *Nat. Neurosci.* 4, 1020–1025.

Keizer, K., and Kuypers, H. G. (1989). Distribution of corticospinal neurons with collaterals to the lower brain stem reticular formation in monkey (*Macaca fascicularis*). *Exp. Brain Res.* 74, 311–318.

Kelly, A. M. C., and Garavan, H. (2005). Human functional neuroimaging of brain changes associated with practice. *Cereb. Cortex* 15, 1089–1102.

Kennard, M. A., Viets, H. R., and Fulton, J. F. (1934). The syndrome of the premotor cortex in man: impairment of skilled movements, forced grasping, spasticity, and vasomotor disturbance. *J. Nerv. Ment. Dis.* 80, 93.

Kubota, K., and Niki, H. (1971). Prefrontal cortical unit activity and delayed alternation performance in monkeys. *J. Neurophysiol.* 34, 337–347.

Kurata, K. (1991). Corticocortical inputs to the dorsal and ventral aspects of the premotor cortex of macaque monkeys. *Neurosci. Res.* 12, 263–280.

Kurata, K., and Hoffman, D. S. (1994). Differential effects of muscimol microinjection into dorsal and ventral aspects of the premotor cortex of monkeys. *J. Neurophysiol.* 71, 1151–1164.

Kurata, K., and Wise, S. P. (1988). Premotor and supplementary motor cortex in rhesus monkeys: neuronal activity during externally- and internally-instructed motor tasks. *Exp. Brain Res.* 72, 237–248.

Lang, W., Beisteiner, R., Lindinger, G., and Deecke, L. (1992). Changes of cortical activity when executing learned motor sequences. *Exp. Brain Res.* 89, 435–440.

Lemus, L., Hernandez, A., Luna, R., Zainos, A., Nacher, V., and Romo, R. (2007). Neural correlates of a postponed decision report. *Proc. Natl. Acad. Sci. U.S.A.* 104, 17174–17179.

Lemus, L., Hernandez, A., and Romo, R. (2009). Neural encoding of auditory discrimination in ventral premotor cortex. *Proc. Natl. Acad. Sci. U.S.A.* 106, 14640–14645.

Liu, Y., and Rouiller, E. M. (1999). Mechanisms of recovery of dexterity following unilateral lesion of the sensorimotor cortex in adult monkeys. *Exp. Brain Res.* 128, 149–159.

Lu, M. T., Preston, J. B., and Strick, P. L. (1994). Interconnections between the prefrontal cortex and the premotor areas in the frontal lobe. *J. Comp. Neurol.* 341, 375–392.

Luppino, G., Matelli, M., Camarda, R., and Rizzolatti, G. (1993). Corticocortical connections of area F3 (SMA-proper) and area F6 (pre-SMA) in the macaque monkey. *J. Comp. Neurol.* 338, 114–140.

Luppino, G., Murata, A., Govoni, P., and Matelli, M. (1999). Largely segregated parietofrontal connections linking rostral intraparietal cortex (areas AIP and VIP) and the ventral premotor cortex (areas F5 and F4). *Exp. Brain Res.* 128, 181–187.

Luppino, G., and Rizzolatti, G. (2000). The organization of the frontal motor cortex. *News Physiol. Sci.* 15, 219–224.

Luria, A. R. (1980). *Higher Cortical Functions in Man.* New York: Basic Books, Consultants Bureau.

Macmillan, N. A., and Creelman, C. D. (1991). *Detection Theory. A User's Guide.* Cambridge: Cambridge University Press.

Markowitsch, H. J., Irle, E., and Emmans, D. (1987). Cortical and subcortical afferent connections of the squirrel monkey's (lateral) premotor cortex: evidence for visual cortical afferents. *Int. J. Neurosci.* 37, 127–148.

Matelli, M., Camarda, R., Glickstein, M., and Rizzolatti, G. (1986). Afferent and efferent projections of the inferior area 6 in the macaque monkey. *J. Comp. Neurol.* 251, 281–298.

Matelli, M., Luppino, G., and Rizzolatti, G. (1985). Patterns of cytochrome oxidase activity in the frontal agranular cortex of the macaque monkey. *Behav. Brain Res.* 18, 125–136.

Mcfarland, N. R., and Haber, S. N. (2002). Thalamic relay nuclei of the basal ganglia form both reciprocal and nonreciprocal cortical connections, linking multiple frontal cortical areas. *J. Neurosci.* 22, 8117–8132.

Miltner, W., Braun, C., and Coles, M. (1997). Event-related brain potentials following incorrect feedback in a time-estimation task: evidence for a "generic" neural system for error detection. *J. Cogn. Neurosci.* 9, 788–798.

Mitz, A. R., Godschalk, M., and Wise, S. P. (1991). Learning-dependent neuronal activity in the premotor cortex: activity during the acquisition of conditional motor associations. *J. Neurosci.* 11, 1855–1872.

Mountcastle, V. B., Lynch, J. C., Georgopoulos, A., Sakata, H., and Acuña, C. (1975). Posterior parietal association cortex of the monkey: command functions for operations within extrapersonal space. *J. Neurophysiol.* 38, 871–908.

Mushiake, H., Inase, M., and Tanji, J. (1991). Neuronal activity in the primate premotor, supplementary, and precentral motor cortex during visually guided and internally determined sequential movements. *J. Neurophysiol.* 66, 705–718.

Newsome, W. T., Britten, K. H., and Movshon, J. A. (1989). Neuronal correlates of a perceptual decision. *Nature* 341, 52–54.

Pandya, D. D., and Barnes, C. L. (1987). "Architecture and connections of the frontal lobe," in *The Frontal Lobes Revisited,* ed. E. Perecman (New York: The IRBN Press), 41–72.

Pardo-Vazquez, J. L., Leboran, V., and Acuña, C. (2008). Neural correlates of decisions and their outcomes in the ventral premotor cortex. *J. Neurosci.* 28, 12396–12408.

Pardo-Vazquez, J. L., Leboran, V., and Acuña, C. (2009). A role for the ventral premotor cortex beyond performance monitoring. *Proc. Natl. Acad. Sci. U.S.A.* 106, 18815–18819.

Passingham, R. E. (1988). Premotor cortex and preparation for movement. *Exp. Brain Res.* 70, 590–596.

Passingham, R. E.(1993). *The Frontal Lobes and Voluntary Action.* Oxford: Oxford University Press.

Passingham, R. E., and Toni, I. (2001). Contrasting the dorsal and ventral visual systems: guidance of movement versus decision making. *Neuroimage* 14, S125–S131.

Petrides, M. (1982). Motor conditional associative-learning after selective prefrontal lesions in the monkey. *Behav. Brain Res.* 5, 407–413.

Petrides, M. (1985). Deficits on conditional associative-learning tasks after frontal- and temporal-lobe lesions in man. *Neuropsychologia* 23, 601–614.

Petrides, M. (1986). The effect of periarcuate lesions in the monkey on the performance of symmetrically and asymmetrically reinforced visual and auditory go, no-go tasks. *J. Neurosci.* 6, 2054–2063.

Petrides, M., Cadoret, G., and Mackey, S. (2005). Orofacial somatomotor responses in the macaque monkey homologue of Broca's area. *Nature* 435, 1235–1238.

Petrides, M., and Milner, B. (1982). Deficits on subject-ordered tasks after frontal- and temporal-lobe lesions in man. *Neuropsychologia* 20, 249–262.

Preuss, T. M., Stepniewska, I., and Kaas, J. H. (1996). Movement representation in the dorsal and ventral premotor areas of owl monkeys: a microstimulation study. *J. Comp. Neurol.* 371, 649–676.

Rizzolatti, G., and Craighero, L. (2004). The mirror-neuron system. *Annu. Rev. Neurosci.* 27, 169–192.

Rizzolatti, G., and Fadiga, L. (1998). Grasping objects and grasping action meanings: the dual role of monkey rostroventral premotor cortex (area F5). *Novartis Found. Symp.* 218, 81–95.

Rizzolatti, G., and Luppino, G. (2001). The cortical motor system. *Neuron* 31, 889–901.

Rizzolatti, G., Luppino, G., and Matelli, M. (1998). The organization of the cortical motor system: new concepts. *Electroencephalogr. Clin. Neurophysiol.* 106, 283–296.

Rizzolatti, G., and Matelli, M. (2003). Two different streams form the dorsal visual system: anatomy and functions. *Exp. Brain Res.* 153, 146–157.

Rizzolatti, G., and Sinigaglia, C. (2010). The functional role of the parieto-frontal mirror circuit: interpretations and misinterpretations. *Nat. Rev. Neurosci.* 11, 264–274.

Roca-Pardiñas, J., Cadarso-Suárez, C., Pardo-Vazquez, J. L., Leboran, V., Molenberghs, G., Faes, C., and Acuña C. (2011). Assessing neural activity related to decision-making through flexible odds ratio curves and their derivatives. *Stat. Med.* 30, 1695–1711.

Roland, P. E., Larsen, B., Lassen, N. A., and Skinhoj, E. (1980). Supplementary motor area and other cortical areas in organization of voluntary movements in man. *J. Neurophysiol.* 43, 118–136.

Romo, R., Hernandez, A., and Zainos, A. (2004). Neuronal correlates of a perceptual decision in ventral premotor cortex. *Neuron* 41, 165–173.

Romo, R., Merchant, H., Zainos, A., and Hernandez, A. (1997). Categorical perception of somesthetic stimuli: psychophysical measurements correlated with neuronal events in primate medial premotor cortex. *Cereb. Cortex* 7, 317–326.

Romo, R., Ruiz, S., Crespo, P., Zainos, A., and Merchant, H. (1993). Representation of tactile signals in primate supplementary motor area. *J. Neurophysiol.* 70, 2690–2694.

Romo, R., and Schultz, W. (1987). Neuronal activity preceding self-initiated or externally timed arm movements in area 6 of monkey cortex. *Exp. Brain Res.* 67, 656–662.

Romo, R., and Schultz, W. (1992). Role of primate basal ganglia and frontal cortex in the internal generation of movements. III. Neuronal activity in the supplementary motor area. *Exp. Brain Res.* 91, 396–407.

Rouiller, E. M., Tanne, J., Moret, V., and Boussaoud, D. (1999). Origin of thalamic inputs to the primary, premotor, and supplementary motor cortical areas and to area 46 in macaque monkeys: a multiple retrograde tracing study. *J. Comp. Neurol.* 409, 131–152.

Sasaki, K., and Gemba, H. (1982). Development and change of cortical field potentials during learning processes of visually initiated hand movements in the monkey. *Exp. Brain Res.* 48, 429–437.

Schell, G. R., and Strick, P. L. (1984). The origin of thalamic inputs to the arcuate premotor and supplementary motor areas. *J. Neurosci.* 4, 539–560.

Schluter, N. D., Rushworth, M. F., Passingham, R. E., and Mills, K. R. (1998). Temporary interference in human lateral premotor cortex suggests dominance for the selection of movements. A study using transcranial magnetic stimulation. *Brain* 121(Pt 5), 785–799.

Schubotz, R. I., and Von Cramon, D. Y. (2001). Functional organization of the lateral premotor cortex: fMRI reveals different regions activated by anticipation of object properties, location and speed. *Brain Res. Cogn. Brain Res.* 11, 97–112.

Schubotz, R. I., Von Cramon, D. Y., and Lohmann, G. (2003). Auditory what, where, and when: a sensory somatotopy in lateral premotor cortex. *Neuroimage* 20, 173–185.

Seitz, R. J., Hoflich, P., Binkofski, F., Tellmann, L., Herzog, H., and Freund, H. J. (1998). Role of the premotor cortex in recovery from middle cerebral artery infarction. *Arch. Neurol.* 55, 1081–1088.

Shadmehr, R., and Holcomb, H. H. (1997). Neural correlates of motor memory consolidation. *Science* 277, 821–825.

Shimazu, H., Maier, M. A., Cerri, G., Kirkwood, P. A., and Lemon, R. N. (2004). Macaque ventral premotor cortex exerts powerful facilitation of motor cortex outputs to upper limb motoneurons. *J. Neurosci.* 24, 1200–1211.

Takada, M., Nambu, A., Hatanaka, N., Tachibana, Y., Miyachi, S., Taira, M., and Inase, M. (2004). Organization of prefrontal outflow toward frontal motor-related areas in macaque monkeys. *Eur. J. Neurosci.* 19, 3328–3342.

Travis, A. M. (1955). Neurological deficiencies after ablation of the precentral motor area in *Macaca mulatta. Brain* 78, 155–173.

Van Veen, V., and Carter, C. S. (2002). The anterior cingulate as a conflict monitor: fMRI and ERP studies. *Physiol. Behav.* 77, 477–482.

Vazquez, P., Cano, M., and Acuña, C. (2000). Discrimination of line orientation in humans and monkeys. *J. Neurophysiol.* 83, 2639–2648.

Walshe, F. M. R. (1935). On the "syndrome of the premotor cortex" (Fulton) and the definition of the terms "Premotor" and "Motor": with a consideration of Jackson's views on the cortical representation of movements. *Brain* 58, 49–80.

Weinrich, M., and Wise, S. P. (1982). The premotor cortex of the monkey. *J. Neurosci.* 2, 1329–1345.

Weinrich, M., Wise, S. P., and Mauritz, K. H. (1984). A neurophysiological study of the premotor cortex in the rhesus monkey. *Brain* 107, 385–414.

Wise, S. P. (1985). The primate premotor cortex: past, present, and preparatory. *Annu. Rev. Neurosci.* 8, 1–19.

Wise, S. P., Boussaoud, D., Johnson, P. B., and Caminiti, R. (1997). Premotor and parietal cortex: corticocortical connectivity and combinatorial computations. *Annu. Rev. Neurosci.* 20, 25–42.

Wise, S. P., and Mauritz, K. H. (1985). Set-related neuronal activity in the premotor cortex of rhesus monkeys: effects of changes in motor set. *Proc. R. Soc. Lond. B Biol. Sci.* 223, 331–354.

Xiao, J., Padoa-Schioppa, C., and Bizzi, E. (2006). Neuronal correlates of movement dynamics in the dorsal and ventral premotor area in the monkey. *Exp. Brain Res.* 168, 106–119.

Conflict of Interest Statement: The authors declare that the research was conducted in the absence of any commercial or financial relationships that could be construed as a potential conflict of interest.

Received: 01 June 2011; paper pending published: 18 July 2011; accepted: 26 August 2011; published online: 27 September 2011.

*Citation: Pardo-Vazquez JL, Padron I, Fernandez-Rey J and Acuña C (2011) Decision-making in the ventral premotor cortex harbinger of action. Front. Integr. Neurosci. **5**:54. doi: 10.3389/fnint.2011.00054*

frontiers in
INTEGRATIVE NEUROSCIENCE

REVIEW ARTICLE
published: 06 March 2012
doi: 10.3389/fnint.2012.00007

Developmental neuroscience of time and number: implications for autism and other neurodevelopmental disabilities

Melissa J. Allman[1]*, Kevin A. Pelphrey[2] and Warren H. Meck[3]

[1] *Kennedy Krieger Institute, The Johns Hopkins University School of Medicine, Baltimore, MD, USA*
[2] *Yale Child Study Center, Yale School of Medicine, New Haven, CT, USA*
[3] *Department of Psychology and Neuroscience, Duke University, Durham, NC, USA*

Edited by:
Valerie Doyere, Centre National de la Recherche Scientifique, France

Reviewed by:
Catherine Jones, University of Essex, UK
Mark Yates, University of Melbourne, Australia

****Correspondence:***
Melissa J. Allman, Kennedy Krieger Institute, The Johns Hopkins University School of Medicine, 707 N. Broadway, Baltimore, MD, USA.
e-mail: allman@kennedykrieger.org; mjallmanjohns@gmail.com

Estimations of time and number share many similarities in both non-humans and man. The primary focus of this review is on the development of time and number sense across infancy and childhood, and neuropsychological findings as they relate to time and number discrimination in infants and adults. Discussion of these findings is couched within a mode-control model of timing and counting which assumes time and number share a common magnitude representation system. A basic sense of time and number likely serves as the foundation for advanced numerical and temporal competence, and aspects of higher cognition—this will be discussed as it relates to typical childhood, and certain developmental disorders, including autism spectrum disorder. Directions for future research in the developmental neuroscience of time and number (NEUTIN) will also be highlighted.

Keywords: timing and time perception, temporal cognition, counting, numerical cognition, mode-control models, cortico-striatal circuits

INTRODUCTION

The interval timing and numerical abilities identified in non-human animals, human infants, and children may represent biological and developmental precursors of adults' highly developed computational abilities (Buhusi and Cordes, 2011; Lustig, 2011; Williams, 2011). For instance, at the perceptual level, non-humans and infants appear capable of making magnitude estimates of duration, numerosity and area (i.e., that a given stimulus is presented for "more" time than another, or contains "more" elements—this basic ability is the focus of our review). The ability to imagine events in the future (which must by implication, require some form of internal time sense) has been postulated to be related to our ability to "anticipate future mental processes and motivational and emotional states" (Pezzulo and Rigoli, 2011:1), and adults at least appear able to comprehend metaphysical and higher concepts of time and space (e.g., imagining the size of the galaxy, or how long it has been around). It seems parsimonious to suppose that the basic ability to represent time, space and numerosity is a basic developmental "building block" for math ability, and abstract mental representations and concepts of metaphysical time and space (see Casasanto and Boroditsky, 2008).

The processing of sensory information according to its spatial, temporal, and numerical properties is a requirement of the central nervous system. Navon (1978) "considered the issue of how we apprehend stimuli that vary along several dimensions. We may often overlook some aspects, and sometimes be unable to ignore others" (1978:3). He suggested that time occupies the dominant dimension, followed by space. In non-humans and humans, there are a variety of interaction effects between our estimates of time, space, and number, and these have been taken as support for mode-control models of (sensory) time and number perception (e.g., Meck and Church, 1983), and those that suppose our ability to make sense of time, space, and numerosity develops from a single magnitude processing system (A Theory of Magnitude, ATOM; Walsh, 2003). In fact, in humans at least, they are most likely component processes in a cognitive system: a "raw substrate" magnitude estimate of time and number is likely processed by some ordinal magnitude comparator (which is recruited to make "how much" or "more than and less than" judgments) that apparently deals with many different dimensions (time, space, numerosity, loudness and luminance, and even emotional expression; e.g., see Smith and Sera, 1992; Holmes and Lourenco, 2009). Although ATOM assumes that "time and quantity estimation operate on similar and partly shared accumulation principles" of the type described in the mode-control model, these two forms of account (Meck and Church, 1983; Walsh, 2003) may be theoretically dissociated at the developmental level—for instance, the mode-control model assumes numerosity is the product of an internal (primitive) count, which is "built in," and according to ATOM, numerosity is acquired by learning associations between magnitudes of different dimensions, as "specializations for time, space and quantity develop from a single magnitude system operating from birth" (2003:484). ATOM does not describe the nature of a shared accumulation system as the mode-control model does. ATOM grounds the ontogeny of multi-dimension magnitude estimation abilities on the basis of the need for action, and the translation from sensory to motor, and this is germane to infant development (i.e., Piaget's sensorimotor stage from 0 to 2 years). It is reasoned in ATOM that the infant is born with a "one-bit" magnitude system, and number sense is mapped onto the magnitude system, which is argued to have a spatial basis (given its emphasis for action).

The primary focus of our review is how we develop the ability to integrate (or "stitch together") representations of duration and numerosity magnitudes, operating at the level of processing incoming sensory input, couched within the influential "mode-control" approach (Meck and Church, 1983). This assumes the substrate for time and number judgments can be represented by an "accumulated" magnitude, and there is quantitative equivalence between an estimate of number and a unit of time (Meck et al., 1985)—space (area) will also be discussed but to a lesser extent (but see Gallistel, 1989). Accordingly, we refer to "time" (time sense) as the ability to estimate duration magnitude in the seconds to minutes range, and "number" (number sense) as the ability to estimate non-symbolic numerosity (i.e., number of dots in an array).

There are three main areas of coverage in this review:

1. We discuss animal findings relating to the neuroscience of time and number sense (NEUTIN), and comparable human studies of time, space, and number magnitude estimation in infants and adults. We also highlight cross-dimensional interaction effects (e.g., between time, space, and number) in non-humans and humans.
2. We review the "mini-evolution" of the development of time and number sense in infancy and childhood. We also comment on the correspondence between number sense and more advanced numerical abilities (symbolic representations of number, counting, math ability), and how children are considered to develop higher-order concepts of time, speed, distance and space.
3. Children with developmental disabilities, particularly those with difficulties as they relate to time and number abilities (developmental dyscalculia, autism, attention-deficit hyperactivity disorder, Down and Williams syndrome) will also be discussed. Studying the atypical development of NEUTIN has the potential to developmentally tease apart the aforementioned accounts, but also to improve understanding of these disorders and their therapeutic and educational remediation. With the exception of Williams and Down syndrome (which have a genetic basis), the disorders included in this review are characterized on the basis of observable behavioral (rather than biomedical) features, and as such, it is useful to know the extent of sensitivity and adaption to time, numerosity and space in these populations—as these types of impairments might contribute to clinical symptoms (and have a "knock-on" effect in development; see also Williams, 2011).

BASIC APPROACH TO TEMPORAL AND NUMERICAL INTEGRATION

The psychological process of actively representing time and number magnitude estimations (see Meck et al., 1985), and the form this integration may take, is expected to be among the premier topics to unite systems, cellular, computational, and cognitive neuroscience for the foreseeable future (Meck, 2003). Temporal processing has been a topic of interest since the dawn of modern experimental psychology—perhaps as a function of its ties to philosophy and physics involving the investigation of absolute vs. relative time perception (Myers, 1971; Wackermann, 2008; Buhusi and Meck, 2009a,b; Lustig, 2011) as well as the impressive ability of humans and other animals to learn and adapt to the temporal and numerical qualities of environmental events (Skinner, 1938; Gibbon, 1977; Gibbon et al., 1997). The mode-control model (for time and number) is related to "scalar expectancy theory" (SET; for time only, Gibbon et al., 1984). These types of accounts were stimulated by studies of rodents (and pigeons) operating on fixed-interval schedules (an event occurs at a fixed period in time). With training, rats and pigeons demonstrate "expectancy" (or anticipation) of an event around the time it is scheduled (Church and Gibbon, 1982; Roberts and Boisvert, 1998), and the accuracy of their temporal expectancies (duration judgment) can be neuropsychologically manipulated (e.g., by pharmacological agents, task load, sensory qualities; e.g., see Meck, 1983, 1996). Their behavioral expectancies conform to the scalar property (discussed in the next section). Animals also appear to perform "superstitious behaviors" (Skinner, 1948) or sequences of actions to "count" (or parse) the passage of time (Killeen and Fetterman, 1988). Rats, pigeons, and monkeys can also discriminate the number of entities in a set when non-numerical dimensions (such as surface area, density, perimeter, duration, and rate) are strictly controlled for, and their performance reflects the use of similar analog representations of number to those of adult humans (e.g., Fetterman and MacEwen, 1989; Brannon and Terrace, 1998, 2000; Emmerton, 1998). These animals can also be trained to press a lever a specific number of times (fixed-ratio schedules), and appear sensitive to the rate of reinforcement (rate is defined as number divided by time)—there is also evidence that certain animals can perform simple arithmetic reasoning (addition, subtraction; see Gallistel and Gelman, 2000 for a fuller discussion).

MODE-CONTROL MODEL OF MECK AND CHURCH (1983)

The mode-control model of counting and timing (see **Figure 1**; Meck and Church, 1983) was developed to account for such findings, and provides a unified theory of numerosity and timing by positing the existence of a functioning isomorphism (formal correspondence) between number and duration. It assumes a similar functional network operates to process either time or number (see; Meck et al., 1985; Church and Broadbent, 1990; Meck, 1997; Carey, 1998, 2001; Gelman and Cordes, 2001; Nieder et al., 2002; Nieder and Miller, 2003, 2004a,b; Pessoa and Desimone, 2003). In this account, "pulses" are accumulated (or integrated) to provide a given estimate of magnitude, and this is then compared to some stored (or remembered) criterion tally (of a given duration or number). Rats show similarities in their discrimination of continuous (time) or segmented (number) signals such that 1-s segmented signal is equivalent to 200 ms of continuous signal (this has been referred to as a "quantal unit"; Meck et al., 1985). This type of organization (in particular, the required comparison between current and stored magnitude estimates) may also facilitate arithmetic processing of basic time and number magnitudes (see Gallistel and Gelman, 2000), as an alternative to cross-dimensional statistical learning process that are proposed in ATOM (Walsh, 2003).

The way the integration mechanism is applied in the model is that at the onset of a relevant stimulus pulses are directed into an

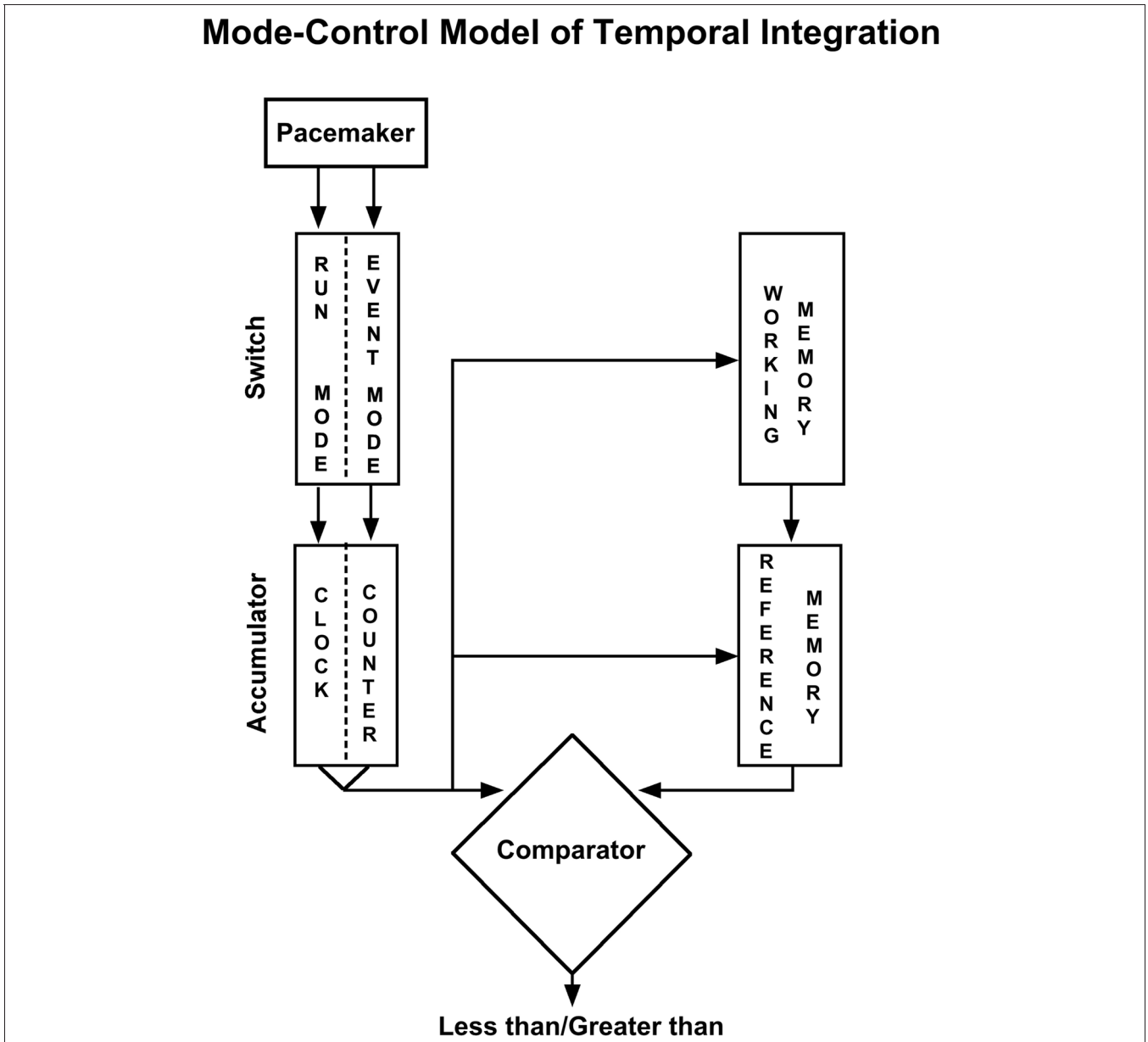

FIGURE 1 | The information-processing "mode-control" model of timing and counting. A pacemaker emits pulses which are gated into an accumulator; it is a counter if operating in the event mode, and a clock if operating in the run mode (see text for details). The current accumulator value can be held in working memory and compared to a previous accumulator value stored in reference memory. A decision process determines the appropriate response [adapted from Meck and Church (1983)].

accumulator by a "mode switch" that allows pulses to flow (into the accumulator) in one of three different modes (run and stop modes for time, and an event mode for number) depending on the nature of the stimulus (see, Church and Meck, 1984; Meck et al., 1985; Broadbent et al., 1993; Meck, 1997). There is no mode nor accumulation process detailing the comparable process for space (although this is not to say the model might not be able to be adapted to do so). "An animal may be said to be timing if the duration of an event serves as a discriminative stimulus; an animal may be said to be counting if the number of events serves as a discriminative stimulus" (Meck and Church, 1983: 320).

A word of caution should be given here to the term "counting." As it relates to the mode-control model, "counting" refers to non-symbolic numerosity accumulation. In the human literature, "counting" typically refers to related symbolic number representations (and related cognitive processes; e.g., Wynn, 1990). We shall highlight the development of symbolic counting abilities in children later.

EVENT MODE

The magnitude estimation of number occurs in the event mode, when the mode-control model is assumed to be a model of

(non-symbolic) counting. In this mode, discrete numerosities are represented by the linear magnitude of a "batch" of pulses from a pacemaker accumulated upon stimulus onset. (Borrowing the analogy of Gallistel and Gelman, 2000; akin to adding a discrete cupful of liquid to a container all at once; n.b. in the experiments by Meck and Church, 1983, 1985, number was signaled by a series of pulses).

RUN MODE

The magnitude estimation of time occurs in run mode. In the model time is represented as the linear magnitude of pacemaker pulses that are accumulated over the course of stimulus duration. (Akin to pouring liquid in from a continuous free-flowing source).

TEMPORAL INTEGRATION

Represents the numerosity of events or objects collected in the accumulator (a total tally) and thus constitutes this model's proposed numeron, just as this same temporal integration process represents duration when pulses are gated through the switch in the run mode. (Akin to the scale on the container measuring how much liquid it contains; see Gallistel and Gelman, 2000).

A further point to note, is that according to mode-control models, if timing pulses are counted when a "neural network" is running (i.e., the ON signal is true) then percentage of time the "neural network" is in use can be calculated by comparing the total count with the elapsed time. This calculation is simple even though the "neural network" may start and stop many times during the monitoring. In order to do this, the counter must have a switch input, as well as its normal count input. You connect the neural network's ON signal to the switch and a source of clock pulses to the normal count input, making the measurements within the counter.

FOUR PHYLOGENIC SIMILARITIES IN TIME AND NUMBER SENSE THAT THE MODE-CONTROL MODEL CAN ACCOUNT FOR

The mode-control model is successful as it can accommodate four fundamental phylogenic (and ontogenetic) similarities common to both time and number sense (e.g., Meck et al., 1985; Fetterman, 1993; Roberts, 1995, 2002; Roberts et al., 1995, 2000; Roberts and Boisvert, 1998), which we shall outline. Another strength of this model (see also, Gibbon, 1977; Gibbon et al., 1984) is that the shape of obtained time and number psychophysical discrimination functions correspond to functioning of the various aspects of the model (**Figure 1**; see Allman and Meck, 2012 for a fuller discussion), and these types of indices are informative with respect to the typical and atypical development of NEUTIN. For example, on a bisection task (where two "anchor" exemplars are trained, and intermediates are classified) non-humans and humans reveal a subjective mid-point between the geometric and arithmetic mean of the "anchor" (smallest and largest) stimuli (durations, numerosities, line length; see, Church and Deluty, 1977; Meck, 1983; Allan and Gibbon, 1991; Wearden, 1991; Wearden and Ferrara, 1995, 1996; McCormack et al., 1999; Melgire et al., 2005; Droit-Volet et al., 2008; Penney et al., 2008; Kopec and Brody, 2010).

1. Both time and number transfer to novel stimuli, and operate simultaneously in a similar manner. Rats trained to press one lever in response to a "short," 2-s, 2-pulse tone sequence and another lever in response to a "long" 8-s, 8-pulse tone sequence reveal they have represented both time and number properties of these compound stimuli (second/pulse). For instance, rats' will continue to use the "short" response when presented with a novel 4-s, 2-pulse sequence and use the "long" response for a novel 4-s, 8-pulse tone sequence. Similarly, they will respond "short" in response to a new 2-s, 4-pulse sequence and "long" to a new 8-s, 4-pulse sequence. In other words, there appears a correspondence and "meaning" to their nature (Meck and Church, 1983).
2. Magnitude estimations of time and number are transferable to an equivalent extent, such that the contents of an accumulator in the "event" (count) mode can be compared to a stored value in "run" (time) mode. Timing and counting in rats also transfers to a similar extent between different stimulus modalities (i.e., auditory to cutaneous) suggesting that amodal estimates of time and number can be extracted from many types of events (Meck and Church, 1983).
3. Certain pharmacological agents; particularly those that modulate dopaminergic, glutamatergic and cholinergic systems, can influence time and number estimations in equivalent ways. The produced magnitude estimate is modulated in a dose-dependent manner by administration of indirect dopamine agonists such as amphetamine and cocaine, which produces an overestimation of both duration and number. Dopamine antagonists (e.g., haloperidol) have the opposite effect, effectively producing an underestimation of time and number (e.g., Meck, 1983, 1996; Meck and Church, 1987; Meck and Williams, 1997; Matell et al., 2004, 2006; Lustig and Meck, 2005; Cheng et al., 2006, 2008).
4. Time and number have identical discriminability and appear bound to the scalar property. For instance, rats reveal equivalent sensitivity to a proportional 4:1 ratio of counts and times (Meck and Church, 1983). This reflects the use of analog mental representations that obey the psychophysical tenets of Weber's law, found in other forms of perception (Moyer and Landauer, 1967; Buckley and Gilman, 1974). "The 'scalar property' refers to the fact that the variance (or 'noisiness') of a cardinal memory magnitude representation is proportional to the objective magnitude (bigger = noisier). When mental magnitudes have scalar variability, the discriminability of values obeys Weber's law, because the degree of overlap between representations remains constant when the ratio of the means is held constant. Thus the amount by which two scalar quantities must differ in order to meet a constant criterion of discriminability is proportional to their magnitude" (Weber's law; Whalen et al., 1999:130). Thus "the overlap between two [magnitude] distributions with scalar variability is determined by the ratio of their means" (Cordes et al., 2001:698). The mode-control model accommodates the scalar property at the level of memory distribution (rather than through variance in the pulse accumulation process).

NON-SYMBOLIC "SENSE" OF NUMBER AND TIME

The mode control model is specifically designed to explain time and number magnitude estimates in animals (see Meck and Church, 1983; Meck et al., 1985), but may provide a useful frame of reference for understanding the development of non-symbolic counting and timing processes in non-verbal infants, young children, and adults (e.g., Gallistel and Gelman, 1992; Wynn, 1992, 1995, 1996, 1998; Broadbent et al., 1993; Roberts and Mitchell, 1994; Roberts, 1995; Meck, 1997; Breukelaar and Dalrymple-Alford, 1998; Wynn and Chiang, 1998; Dehaene et al., 1999; Xu and Spelke, 2000; Spelke, 2000; Wynn et al., 2002; Brannon and Roitman, 2003; Xu, 2003; Cordes et al., 2007).

IN INFANCY

Evidence of a primitive time and number sense in early development includes reports that very young infants (and in some cases, newborns) can discriminate small numbers of syllables and tones (Bijeljac-Babic et al., 1993; van Marle and Wynn, 2006), simple dots (Starkey and Cooper, 1980; Antell and Keating, 1983), moving objects and collections of objects (van Loosbroek and Smitsman, 1990; Wynn et al., 2002), can enumerate heterogeneous arrays of objects as well homogeneous arrays (e.g., Strauss and Curtis, 1981; Feigenson, 2005), and can discriminate between numerosity with the same precision in all modalities (Feigenson, 2007). Infants have also been shown to represent small numerical quantities across modalities (Jordan and Brannon, 2006), and discriminate between large numerosities (Lipton and Spelke, 2003). It even appears that "nuisance" task-irrelevant sensory information may improve infants' numerical precision (Jordan et al., 2008). Infants also show interchangeability between numerosities of different dimensions such as between two-or three drumbeats and two-or three objects, even when duration is controlled for (Starkey et al., 1983; Kobayashi et al., 2004; Feron et al., 2006; Izard et al., 2009). Collectively these studies suggest that an innate form of abstraction exists between different types of the same numerical magnitude in early life.

As it relates to time sense, infants possess sensitivity to temporal rhythm (Trehub and Thorpe, 1989) and are able to synchronize and adapt their sucking behavior (and other forms of motor activity) with the tempo of an external stimulus (Bobin-Bègue et al., 2006). There is also evidence to suggest that infants attend to the temporal features of stimuli in their environment (Clifton, 1974; Jusczyk et al., 1983). For example, by 2 months of age, infants are sensitive to the duration of sounds that differ by less than 1-s (Jusczyk et al., 1983), and similar results have been obtained for speech sounds (Eimas and Miller, 1980).

Lourenco and Longo (2010) revealed that 9-month-old infants can (bi-directionally) transfer learned associations (a mapping between stimulus color and relative magnitude) between greater/lesser durations, size and numerosity. This points to a (at least partly) shared general magnitude representation system, and is consistent with both the mode-control model (although it was not adapted for space) and ATOM. These findings reveal, "representations of magnitude information are (at least partially) abstracted from the specific dimensions" (Lourenco and Longo, 2010:873). They lean away from the mode-control model as findings suggest, "the relation between number and time is only one type of association in a more general system of magnitude representation" (Lourenco and Longo, 2010:79).

Perhaps the most striking support for the mode-control approach is evidence from young infants that magnitude estimates of time and number show scalar variability. Recall that in the mode-control model, ratio dependency (a larger ratio difference is easier to discriminate) is explained due to (a decrease in) the noisiness of stored time and number magnitude estimations (i.e., their spread is reduced, so they overlap less). ATOM acknowledges that the scalar property is a quality of multisensory perception. Intriguingly, the scalar property is also a quality of early social interactions for the infant (e.g., Stern and Gibbon, 1978; Jaffe et al., 2001). Like our other senses, it appears time and number sense is based on ratio (rather than absolute) differences (in magnitude). Furthermore, this appears to be honed during the first year of life (e.g., there are quantitative developmental changes between 6- and 10-months of age in both time and number sense). These findings endorse a common system of magnitude representation between time and number (in the context of the mode-control model; Church and Meck, 1983; Gallistel and Gelman, 2000).

For instance, Xu and Spelke (2000) as well as Xu et al. (2005) report that 6-month-old infants can discriminate visual numerical arrays that differ by a 1:2 ratio (e.g., 8 vs. 16 dots) even when contour length (density, surface area, etc) is controlled for, but these infants do not discriminate visual arrays that differ by a 2:3 ratio (e.g., 16 vs. 24 dots). Although this pattern of results has also been obtained when numerosity is signaled by sequences of tones (which must be integrated across time, Lipton and Spelke, 2003), and actions (Wood and Spelke, 2005) a recent study in 6-month olds has revealed numerical sensitivity to ratios including 2:3, 1:3, 1:4, but only if tested under certain arrangements (Libertus and Brannon, 2010). Moreover, individual differences in preference for a numerically changing display are stable, and the sensitivity to detect (ratio) numerical change at 6-months of age is predictive of numerical change detection scores at 9-months of age (Libertus and Brannon, 2010). Cordes and Brannon (2009) examined the ability of 7-month-old infants to compare small and large number sets under a variety of ratio conditions (e.g., 1:2 and 1:4), and report that small and large number sets could both be discriminated given a fourfold, but not a twofold change in number. In contrast, Wood and Spelke (2005) report that 1:2 ratio dependence in 6-month olds holds for larger numbers of actions (greater than 4), but not for small numbers of actions (less than 4). We shall extend our discussion of small vs. large numbers in a later section.

There are a handful of studies that have behaviorally assessed duration discrimination thresholds in infants between 4- and 10-months of age (Brannon et al., 2004a, 2008; van Marle and Wynn, 2006; Provasi et al., 2011). For example, van Marle and Wynn (2006) revealed 6-month-old infants can discriminate between durations of 2- and 4-s, but not between 3-s and 4.5-s. That is to say, typical 10-month-old infants can discriminate between durations (time) that differ according to a 1:2 ratio, as 6-month olds can, in addition to a 2:3 ratio, which 6-month-old infants cannot (as is the case for number, see Brannon et al., 2007).

Support for the idea that other dimensions (i.e., space) are also represented as noisy magnitudes, and perhaps a shared representational currency is provided by Brannon et al. (2006). These authors report that 6-month infants reveal the same ratio-dependency when discriminating size/area (i.e., 1:2, but not 2:3) as for time and number. To-date, it is unknown whether precision for area similarly increases with age (e.g., by 10 months). In addition, Möhring et al. (2012) revealed the same 1:2–2:3 ratio improvements between infants 6- and 10-months of age when discriminating different speeds (time/distance).

Given that psychophysical functions superimpose (with scalar variability), it appears young infants possess similar subjective sensitivity for different dimensions (i.e., time, number, area, line-length, speed), which supports the idea that all quantities (continuous or not) are represented by analog magnitudes with scalar variability, and the ability to represent magnitudes improves according to a developmental trajectory set into motion in early life.

IN CHILDHOOD

Sensitivity for time and number sense, perhaps not surprisingly, continues to improve during childhood (we shall go on to discuss findings as they relate to time and number in children separately). For instance, Halberda and Feigenson (2008) revealed a marked improvement in the performance of 3-and 6-old year-old children during number discrimination from a 3:4 ratio to 5:6 with increasing age (adults were as high as 10:11), and between the ages of 5–7 years, children become able to discriminate number with increasing precision (e.g., see, Huntley-Fenner and Cannon, 2000; Huntley-Fenner, 2001). Four-year-old children can accurately select the visual array of dots that corresponds numerically to a sequence of sounds while younger children cannot (Mix et al., 1996). Siegler and Booth (2004) report age-related changes between 6 and 8 years of age in children's representation of the "mental number line" (described in more detail later). Specifically, younger children reveal logarithmic spacing and older children linear spacing between numbers. Logarithmic spacing (noise independent of magnitude) is inconsistent with the scalar property (noise proportional to magnitude), and aforementioned non-human and infant findings demonstrating simple arithmetic reasoning (see Gibbon and Church, 1981; Brannon et al., 2001).

Droit-Volet et al. (2003) employed a bisection task with 5-and 8-year-old children (and adults), which required selective attention to either time or number when they were both simultaneously presented (ignore one dimension). They report that for younger children, number interferes with time, but time does not interfere with number (an effect attenuated in older children; but present in adults, Dormal et al., 2006). Droit-Volet and colleagues subsequently examined time, number and line-length, with number and line-length presented sequentially (through time) and non-sequentially (Droit-Volet et al., 2008). During non-sequential presentation, the obtained psychophysical functions for number and line-length were comparable in both 5- and 8-year olds, but there was a relatively larger subjective mid-point, and index of reduced sensitivity, for timing functions from all children. Moreover, when number and line-length were presented sequentially, these dimensional differences disappeared. They interpreted their results in the context of the mode-control model and the pulse accumulation process for time, which is suited to sequential magnitude estimation. They contend that this type of processing demands attentional and working memory abilities (and are themselves components of these models; **Figure 1**) and this system is "tapped into" during sequential presentation of other dimensions (e.g., line-length, however the model is not presently designed to accommodate such dimensions).

DEVELOPMENT OF TEMPORAL COMPETENCE IN CHILDHOOD

Correspondences between age-related changes in sensitivity to different dimensions suggests that between the ages of 5- and 8-years old, sensitivity for time lags behind sensitivity for number (Droit-Volet et al., 2003); time appears to be a dimension that younger children may find less salient and less likely to attend to (Gautier and Droit-Volet, 2002). In fact, it is historically considered in developmental psychology (Piaget, 1946; Fraisse, 1967; Ornstein, 1969) that children are not equipped with temporal abilities; instead these derive from superior abilities in the processing of other dimensions (e.g., speed, number; although studies highlighted in this review have since rebutted this).

For instance, the timing functions obtained with 3-, 5- and 8-year-old children reveal (the scalar property, and) temporal judgments become more precise across development, which may be related to attentional and working memory function (see, Droit-Volet and Wearden, 2001; McCormack et al., 2004; Rattat and Droit-Volet, 2005; Wearden, 2005; Droit-Volet and Meck, 2007; Droit-Volet et al., 2007).

Theoretical and computer modeling (in the context of scalar expectancy theory; Gibbon et al., 1984) of temporal magnitude data from children, tends to support the notion that various components of the mode-control model, particularly "reference memory" and attention, undergo age-related changes (see Droit-Volet and Wearden, 2001; Droit-Volet et al., 2001; Droit-Volet, 2002, 2003a,b). As such, the development of psychological variables closely associated with "timing ability" (e.g., attention, memory), may also play a role in the development of timing performance across childhood and old age (e.g., Lustig and Meck, 2001, 2011; Lustig et al., 2005). Modeling of the timing functions from children (interpreted within the context of scalar expectancy theory) has also suggested that younger children make more random responses than older children (i.e., between 3- and 8-years old; Droit-Volet and Wearden, 2001).

Recently, Zélanti and Droit-Volet (2011) revealed discriminations between relatively small temporal magnitudes are easier than larger ones, and there are age-related improvements (between 5- and 9-years of age), with temporal sensitivity improving earlier for the short than for the long durations. Age-related improvements for "shorter" durations were predictive of the development of the span of short-term memory, whereas improved competence for "longer" durations was related to the development of attention and executive functions. However only age, and no cognitive abilities, were found to predict individual differences in time discrimination between the shortest and longest durations.

It has also been reported the psychophysical timing functions of children aged 3-, 5- and to a lesser extent 8- year olds, become flatter (less sensitive) when interval timing is either interrupted or tested after a (e.g., 24-h) retention delay. Rattat and Droit-Volet (2005) also reveal an interruption task tends to lengthen the subjective magnitude estimation, particularly in 5-year olds, which they attributed to stored representations of trained temporal magnitudes in memory. Furthermore, temporal estimations in children are inflated if the stimulus is bigger or brighter (Levin, 1977, 1979, 1982). This represents known properties of the psychophysiological modulation of time perception in adults (Gibbon et al., 1997; Buhusi and Meck, 2005). Children also tend to overestimate time on perception tasks, and under-reproduce a given duration, and their duration judgments are less stable (see Block et al., 1999).

It has been proposed that children under the age of 8 years, do not tend to spontaneously count while timing (Wilkening et al., 1987), and Clément and Droit-Volet (2006) report that temporal magnitude estimations of 5-year olds display the scalar property in both counting and non-counting conditions, but by 8-years and adulthood, counting during timing results in a violation the scalar property (see also, Hinton and Rao, 2004). This finding can be explained according to the mode-control approach. "Counting is a multistep process, with the number of steps proportional to the numerosity counted. If there is some probability of error (either skipping an item or counting it twice) at every step, then the more steps there are, the greater the expected accumulation of miscounts. The variability in counts from this source should, however. . .grow in proportion to the square root of the numerosity. . .discriminations should get relatively better as numerosities increase. That is, the discrimination of 30 from 20 should be more accurate than the discrimination of 3 from 2, contrary to Weber's law" (Cordes et al., 2001:699).

Lustig and Meck (2011) demonstrated that 8-year-old children (and younger and older adults), showed "typical" sensory modality asymmetry for durations signaled by either "sights" or "sounds." Usually it is found that a magnitude estimation for time can be influenced by the modality, such that a given stimulus duration (i.e., 5-s) is perceived as a longer if it is signaled by a sound rather than a light (Wearden et al., 1998; Penney et al., 2000). It is assumed by the mode-control model that the clock runs faster for auditory stimuli as they capture and hold attention relatively automatically—thus they are more efficient at holding the switch closed, allowing larger pulse accumulations (see **Figure 1**)—whereas attending to visual stimuli requires controlled attention (Meck, 1984). In addition, a memory distribution (of a given duration) may be composed of "mixed-modality" memories, such that there might be a bias by skew of over-represented modality (see Chen and Yeh, 2009; Gu and Meck, 2011). Lustig and Meck (2011) report children tend to overestimate auditory stimuli compared to adults (they are comparable for visual stimuli). "Auditory stimuli are disadvantaged relative to visual stimuli in children's long-term memory and age-related declines in attention" (Lustig and Meck, 2011:2). In a separate study, Droit-Volet et al. (2004) report that 5-year olds have greater variability in their judgments of visual stimuli than auditory ones, indicating improved developmental temporal sensitivity for "sounds" rather than "sights."

It has also been reported that although 3-year-old children can "time" an event, they have difficulty timing the duration between events (Droit, 1994). Young children are also found to base their ability to estimate duration through action (Droit, 1995) or an external "ticking" clock (Droit, 1994), but this is reduced by around age five, and they seem aware of temporal rules governing their behavior (Droit et al., 1990; Pouthas et al., 1990). It has also been reported that 3-year olds produce more accurate temporal magnitude estimates when they are asked to press harder than press longer, and press for longer and harder when asked to press harder. Droit-Volet and Rattat (1999) reveal five-and-a-half-year olds are able to transfer a target duration across different actions, but 3 year-olds cannot, suggesting children do not dissociate time from action, or develop abstract concepts of time, until around 5 years of age. This is consistent with ATOM which emphasizes a single magnitude system arose from the need for action. According to Droit-Volet (1998) "children's feeling that something is resisting them through their action may be the first step toward the understanding of duration" (1998:247).

THE DEVELOPMENT OF NUMERICAL ABILITY AND SYMBOLIC NUMBER ACROSS INFANCY AND CHILDHOOD

As has been discussed, there is much evidence to support the idea that a primitive time and number sense (at least) is ontogenetically "built in," but there is much debate as to the form this may play in numerical development. In fact, preverbal counting may be a precursor to verbal counting abilities, as the basic number sense may provide the basis for the verbal system and arithmetic computation (Gallistel and Gelman, 1992). There are some comparative findings with non-humans to suggest that animals can learn to map symbolic Arabic digits (1–9) to objects and appropriately make use of this knowledge through symbolic labeling (e.g., see, Matsuzawa, 1985; Washburn and Rumbaugh, 1991; Brannon and Terrace, 1998, 2000; Pepperberg, 2006). "A more controversial question is whether there is ontogenetic continuity in numerical cognition" (Brannon, 2002:224). We shall now highlight children's development of counting and symbolic number representation.

The mode-control approach has been influential in the debate surrounding the foundations of numerical thinking and verbal counting ability during human development (e.g., Gallistel, 1990; Starkey et al., 1990; Wynn, 1990; Gallistel and Gelman, 1992; Dehaene et al., 1999; Grondin et al., 1999; Whalen et al., 1999; Brannon et al., 2001). Instead of using the representational convention whereby (symbolic) numbers are used to represent linear magnitudes, the mode-control model supposes the nervous system uses numerosity magnitudes to represent symbolic number. Accordingly, numerate individuals are presumed to have learned to map magnitudes of basic number sense to number words and numerals (i.e., from non-symbolic to symbolic; see Gallistel and Gelman, 2000). ATOM supposes, "when we later learn about [symbolic] number, the scaling mechanisms used for [all continuous] dimensions with action-relevant magnitude information will be co-opted in development for the scaling of [symbolic discrete] number" (Bueti and Walsh, 2009:1836).

IN INFANCY

Although the aforementioned findings support the notion that the ability to represent and compare numerosity appears early in development, other studies suggest that infants attend to continuous spatial dimensions such as surface area and contour length rather than number *per se* (Clearfield and Mix, 1999; Feigenson et al., 2002), challenging the notion that numerical representation is present in infancy (see, Mix et al., 2002; Newcombe, 2002). An alternative view is numerical competence in infancy is the product of an automated system for tracking and reasoning about *small* numbers of (non-numerical) "object files" or object-tracking mechanisms (e.g., Kahneman et al., 1992; Trick and Pylyshyn, 1994). By this form of account, object-file representations (rather than analog magnitudes) form the foundation of the verbal counting system (see, Carey, 1998, 2001; Spelke, 2000; Le Corre and Carey, 2007, 2008).

In support of this view, Feigenson et al. (2002) report that 10- and 12-month-old infants use object-file (size) rather than numerical ratio to track sequentially hidden objects, as they can compare representations of objects, and make ordinal "more" or "less" judgments—but only when the magnitudes were relatively small and within the limits (of about four items) of the "object-file" system (i.e., 1 vs. 2, or 2 vs. 3; but not 4 vs. 6). However Brannon (2002) has revealed that the ability to make ordinal number judgments develops between 9- and 11-months of age, even for numerosities that exceed the bounds of the object-file system (see also Dehaene and Changeux, 1993). Discrepancies between small and large numerosities may also reflect different conditions that direct young infants attention to number (Xu, 2003; Feigenson et al., 2004; Wood and Spelke, 2005).

The "magic number four" has been taken as evidence that infants ability to numerate small numbers is related to "subitizing" (Trick and Pylyshyn, 1994), and that symbolic (verbal) representations of number provide the basis for developing a (non-symbolic) understanding of numerosity (rather than the other way around, as supposed by the mode-control model). Of course, this type of account is at odds with aforementioned findings that infants can discriminate between large numerosities (with a large ratio difference), and can successfully reason about the "magical disappearance" of a large number (specifically, a collection) of objects (Chiang and Wynn, 2000).

Essentially, the dichotomy between small and larger numbers speaks to the issue of whether they are represented by the same or different cognitive system (see Buhusi and Cordes, 2011; Hyde, 2011), and was first addressed by Jevons (1871): are numerosities less than the "magic number four" processed as individual entities (subitizing, effectively filling in pockets of space), while larger numbers are represented through the approximate number system? (ANS; Feigenson et al., 2004). Alternatively, all magnitudes (small and large; as proposed by the mode-control model) may be represented by a single system, such as ANS (Gallistel and Gelman, 2000; Cordes et al., 2001; Cordes and Brannon, 2009), with the accumulated magnitude representing a cardinal value. However it has been cautioned that "accurate theories of numerical cognition must take seriously the notion that, under many conditions, small numbers are represented as arrays of numerically distinct individuals, not as sets with approximate cardinal values" (Hyde and Spelke, 2012:13). Of course, if numerosities below the "magic number" are integers rather than real-valued magnitudes, they should violate scalar variability.

McCrink and Wynn (2004) examined infants' numerical computation explicitly using large numbers, and found that 9-month olds appear to conduct arithmetic operations (addition and subtraction) over estimates of numerical magnitude, further supporting the idea that number sense supports numerical manipulations and operations.

IN CHILDHOOD

A puzzling inconsistency is that infants are often purported to possess numerical abilities that young children do not seem capable of when tested in explicit choice paradigms (Huttenlocher et al., 1994; Mix et al., 1996, 2002; Newcombe, 2002). For example, Huttenlocher et al. (1994) showed that children younger than 3 years of age could not predict the numerical outcome of a nonverbal addition and subtraction task. Four-year-old children could accurately select the visual array of dots that corresponded numerically to a sequence of sounds while younger children performed at chance. These accounts of numerical development suggest that children gradually develop the ability to form and manipulate abstract representations of number.

Cantlon et al. (2010) report that 3-year-old children appear to represent analog numerical magnitudes when enumerating sets of objects, even those within the "magic number four" subitizing range, and numerical judgments were influenced by area. These authors observed ratio-dependence (scalar variance) for numbers both within and beyond the "magic number four" subitizing range. Young children in this study also appeared to preferentially attend to number over area.

Piaget (1952) reports abstract knowledge of arithmetic requires considerable learning (i.e., is not "built-in") and does not emerge until a child is between 4 and 7 years of age, but studies have since revealed young children (between one-and-a-half-year to four years of age) master number conversion (e.g., see Gelman and Gallistel, 1978; Starkey, 1992), and preschool children possess an abstract representation of number and simple addition (Brannon and Van de Walle, 2001; Barth et al., 2005).

Spelke (2000) attributes the acquisition of mathematical skills to object knowledge (permanence through space and time) and numerosity, and it has been asserted that children must "possess a magnitude-based estimation system for representing numerosities that also supports procedures for numerical computation" (McCrink and Wynn, 2004:776). Despite the infamous (debunked) "clever Hans" demonstrations—the horse that apparently had mastered symbolic calculation—it has been revealed in children at least, that basic number sense (and numerosity estimation) is related to math ability and the development of mathematical intelligence (e.g., Carey, 1998, 2001; Gallistel and Gelman, 2000; Gelman and Gallistel, 2004).

Booth and Siegler (2006, 2008) report an association between 5-year-old children's school math achievement and linear (as opposed to logarithmic) sequencing of symbolic (Arabic) numbers along a spatial schematic number line—this suggests the spatial arrangement of numerical representations affects math abilities (Siegler and Ramani, 2009). The ability to quickly make

ordinal comparisons between symbolic numbers also appears to be related to arithmetic calculation in older children (6–10-year olds; e.g., De Smedt et al., 2009).

Recently, Libertus et al. (2011a) reported that the acuity (sensitivity) of preschoolers' number sense was predictive of school math ability, even prior to the onset of formal mathematics instruction, and controlling for age and verbal skills. There are other studies that report stable individual differences in school-based math ability (verbal counting, ordinal comparison, arithmetic) in young children early into their formal education (Jordan et al., 2006, 2007, 2008, 2009). Collectively, these studies provide evidence that a primitive number sense lays the foundation for more advanced numerical abilities.

By 3 years of age, children appear to have mastery of some parts of the one to ten count sequence (Wynn, 1992), and between the ages of three-and-a-half and four and-a-half children are skilled with the decade count order (10, 20, 30, etc; Fuson, 1992). Also, behavioral response times reveal marked age-related changes and improves between the ages of 2 and 7 years (Huntley-Fenner and Cannon, 2000; Huntley-Fenner, 2001). By the age of 5 years, not all children have developed the ability to link symbolic symbols with non-symbolic quantities (Lipton and Spelke, 2005).

A related line of research examines how counting typically becomes related to determining numerosity (cardinal word principle)—this may be related to one-to-one correspondence between items and number tags (Gelman and Gallistel, 1978; Mix et al., 2011). In other words, children need to learn how count, but also why we count (and that the last count represents a magnitude estimate). The fact that small numerosities (<4) can be determined without counting ("subitizing") may be at the root of developing this knowledge. The representation of the words "one," "two, "three, "four" is progressive, but for other number words the child needs to understand the equivalence between the order of the words in the counting list and the successive numbers that are related by the function "+1" (see Carey, 2004). In much the same way, two, 2, and ●● are equivalent in their "two-ness."

Wynn (1990) revealed that children aged between 2- and 3-years old generalize counting such that they can count sounds, actions and objects. This is informative as the number of objects might be determined by counting them in any order, but actions and sounds must be counted in a certain order (i.e., when they occur). If asked "how many" after counting, children younger than 3-years of age are unable to produce an estimation of magnitude that corresponds to the last number counted, whereas children older than 3-years can. Moreover, if required to "give-a-number" (i.e., perform an action a certain number of times), children over 3-years of age will count as they perform the task, whereas younger children do not (they tend to give only one or two; see also Zur and Gelman, 2004).

It has been postulated that acquiring symbolic language enables children to become able to make conceptual inferences (e.g., see Spelke, 2011), by allowing them to selectively attend to relevant information (e.g., Sandhofer and Smith, 1999). This has led some researchers to propose that the numerical concepts demonstrated by infants are not obviously related to the later numerical concepts exhibited by preschool children as they begin to count verbally (Mix, 1999; Mix et al., 2002; Newcombe, 2002; Rousselle et al., 2004). In a study of how children judge the numerical equivalence of arrays of objects, Mix (1999) found that children gradually develop the ability to identify numerical equivalence. Children between 3- and 4-years of age could recognize numerical equivalence among homogeneous arrays in which elements were similar to one another, but could not reliably recognize numerical equivalence among heterogeneous arrays, which was only found in 5-year olds. The ability to identify numerical equivalence for heterogeneous arrays was correlated with children's verbal counting ability, independent of age. Mix (1999) argues that number words allow children to acquire abstract number concepts, even within the context of a nonverbal matching task (see also Mix et al., 1996)—children become better able to ignore superficial object features as they master the verbal counting system because number words embody abstract numerical categories. In other words, children gradually develop the ability to represent number as they acquire linguistic and symbolic knowledge. Previous studies of numerical cognition that required verbal identification of the number of objects in an array have obtained similar results (Von Gast, 1957; Siegel, 1974).

Since Piaget (1952) studies using the number conservation task, it is well known that children before the age of 6 or 7 years will judge the number of counters in two parallel rows to be equal if the counters are arranged opposite to each other (i.e., in one-to-one correspondence), but a longer (or shorter) row (e.g., created by spreading out/pushing together the counters) is consistently judged to have more (or less counters, respectively; see also Mix et al., 2011). In ATOM, Walsh (2003:486) points out "is perhaps maladaptive for an infant brain *not* to use a common metric [for different magnitudes] as it is difficult for an older child to unbind these three elements [time, space, and quantity]," and is highly dependent upon the ability to learn associations between them.

MAGNITUDE ESTIMATION IN ADULTHOOD

As it relates to number (and time) sense, it is found in both non-humans and adults, that the speed and accuracy of estimates of magnitude can be influenced by distance and size effects (see Rumbaugh et al., 1987; Washburn, 1994; Brannon and Terrace, 2000; Brannon and Roitman, 2003). Of course, this relates to ratio-dependence (the scalar property); the ability to discriminate two numbers improves as the numerical *distance* between them increases, and sensitivity worsens as numerical *size* increases. These effects are obtained for both non-symbolic and symbolic number. Typically it is observed that temporal estimation in adults conforms to the scalar property, to both short and large durations (for a review see, Meck, 2003; Buhusi and Meck, 2005).

In a seminal paper, Moyer and Landauer (1967) report that during a task of symbolic Arabic number discrimination, "decision time was an approximately linear inverse function of the numerical distance between the two stimulus digits" (as for other dimensions) and when describing the data, "a reasonable fit is of the same general class as those usually found to describe . . . differences between physical quantities such as pitch and line-length" (Moyer and Landauer, 1967:1520).

When required to press a response key a certain number of times, there is scalar variability of adults pressing for small and

large numbers, both within and beyond the subitizing range, however this effect is abolished when participants are asked to verbally count their presses out loud (Cordes et al., 2001). Whalen et al. (1999) report proportionality (scalar variability) between the number of taps generated following a specific request (i.e., 7–25).

As it pertains to the "two process" theories of number development, Revkin et al. (2008) report disproportionately higher sensitivity for numbers in the subitizing range (1–4) than for larger numbers in adults (see also, Trick and Pylyshyn, 1994). The authors reconcile the violation of Weber's law by suggesting "that in the small-number range, variables other than the ratio between stimuli (possibly variables relating to spatial arrangement or to other perceptual factors) boost number discriminability" and this "seems hard to separate from the original subitizing hypothesis" (Revkin et al., 2008:613). In adults, Dormal and Pesenti (2007) found that space influences number judgments, but number does not influence spatial judgments, and Roitman et al. (2007) report "short/few" and "long/many" classifications transfer between time and number, with improved sensitivity for number. Temporal judgments can also be biased by spatial-numerical associations of response code (SNARC-type) effects (Dehaene, 1997). Human findings have revealed: greater Arabic digits (Oliveri et al., 2008); larger stimuli (Xuan et al., 2007); visualized forwards motion (Vicario et al., 2007); visuomotor shifts to the right (Frassinetti et al., 2009) and greater distances (DeLong, 1981; Sarrazin et al., 2004) are associated with longer estimated durations (see also, Nicholls et al., 2011b). Secondary tasks tend to disrupt temporal magnitude estimates, but only mental arithmetic is impaired by a temporal task (Brown, 1997). It has also been recently reported that adults' ability to estimate time is somewhat predictive of their mathematical intelligence (Kramer et al., 2011).

Numerical magnitudes (i.e., 1–10) appear spatially organized from left to right, and this phenomenon is referred to as the *mental number line* (see de Hevia et al., 2008), and is believed to correspond to the orienting of visual attention. It has been considered that the mere presentation of symbolic digits can impose a spatial attentional bias (i.e., left for a small number), and this shift modulates time judgments (Oliveri et al., 2008). It has been recently reported that it is the process of comparing size differences between numerical cues, rather than the size of the number itself, which appears to bias time estimation (Vicario, 2011). The subjective mid-point during number bisection has also been found to vary as a function of spatial attention to the mental number line, i.e., presenting stimuli in near and far space (Longo and Lourenco, 2010), turning one's head to the left or right also modulates (smaller or larger, respectively) random number generation (Loetscher et al., 2008), and the left and hand rights respond faster (during an odd/even number discrimination) to smaller and larger numbers (respectively, Dehaene et al., 1993). Space and number effects are also found when there is no lateralized (left/right) response (Casarotti et al., 2007) or if events are presented in an orthogonal arrangement (Nicholls et al., 2008; see also Nicholls et al., 2011a). It is not beyond the scope of possibility that (SNARC-type) spatial mappings might be related to a cultural bias (i.e., in the Western world) to read across (and scale) from left to right, and the correspondence to left-lateralized language systems.

It has been suggested that spontaneous cross-modal interaction effects might not be as profuse in adulthood as during infancy and childhood (see Walsh, 2003; Izard et al., 2009)—it might make developmental sense to be equipped with a general magnitude estimator to facilitate comparing functionally equivalent co-varying quantities (e.g., to learn relations between size, weight and length). Any such effects are also taken as support for a general magnitude system, one in which unidirectional asymmetries exist between different dimensions. However, it is important to note that stimulus magnitude effects (intensity, size, number, emotional valence) are precisely known to bias interval time perception, and pulse accumulation, and so caution should be taken before attributing them to a more generalized process. This is particularly important from a developmental perspective, when the attempt is essentially to establish "which comes first?" (see also, Ansari, 2008).

DIFFERENCES IN DEVELOPMENTAL DISABILITIES

Various findings examining the relative development of time and number sense in pediatric developmental disorder populations have emerged. These may shed light on some of the questions surrounding the typical development of NEUTIN. For instance, Spaepen et al. (2011) report that deaf individuals (who live in a remote Nicaraguan culture) who lack a language for number (i.e., no sign language) employ gestures to represent number, but have markedly reduced accuracy in "how many" and "give a number" type tasks for large numerosities (i.e., over three).

DEVELOPMENTAL DYSCALCULIA

Problems with mathematics may readily present in educational environments with academic demands, and thus (at-risk) school-aged children may be identified as having mathematics disorder or developmental dyscalculia. This is one of the most well defined disabilities as it may thus relate to number sense. This is a disorder of numerical competence and arithmetical skill, such as retrieval of antithetic facts and dependence on finger counting when attempting number problems, in children of normal intelligence with no neurological injuries (see Temple, 1992).

Children who experience difficulties with mathematics reveal differences on number-comparison tasks with both symbolic and non-symbolic stimuli. This may suggest problems linking symbolic and approximate, to non-symbolic numerical representations. For example, Rousselle and Noël (2007) tested number magnitude estimates in children with mathematic learning disabilities. They report impairments in Arabic number comparison, number writing and trans-coding of tokens into Arabic numerals (symbolic number), but intact abilities for addition and subtraction (non-symbolic number). Furthermore, those with mathematical disability revealed a propensity to represent number magnitude over physical size (on a Stroop task), and they report a larger numerical distance effect. Ashkenazi et al. (2009) report a larger numerical distance and size effects for double-digit numbers, and interpret their findings to difficulties with subitizing and counting in this population (see Henik et al., 2011).

Ashkenazi and Henik (2010) administered a physical line and symbolic number bisection task to adults with developmental dyscalculia, and revealed affected individuals show a greater (than typical) tendency to underestimate the subjective mid-point (and reveal an absence of a typical bias for line bisection). They discuss their findings within the context of differences in the development of the mental number line, and an over-reliance on logarithmic (rather than linear) spacing (see also Geary et al., 2007).

Collectively, these findings were taken as evidence that children with mathematics disabilities do have a basic number sense (numerosity) but may experience problems relating numerical magnitudes to symbols (see also Landerl et al., 2004; Butterworth, 2010).

WILLIAMS AND DOWN SYNDROME

It has been revealed that young children (around 3 years old) with Williams syndrome (WS) are able to enumerate small numbers in dot arrays, but only when they differ by the 1:2 but not 2:3 ratio-requirement (Van Herwegen et al., 2008). O'Hearn et al. (2011) examined individuals with WS on a visual counting task, and asked them "how many?" (cardinality principle) with a rapidly presented array of dots. Those with WS revealed comparatively normal performance in the counting task, but were only able to (rapidly) accurately enumerate a (comparatively) smaller magnitude, even when arrays were presented for a longer period. These findings were taken as evidence for a limited subitizing system in WS (i.e., a "magic number three"). Ansari et al. (2005) reported the ability of children with WS to understand cardinality was predicted by their verbal language scores. That is, affected children may use language (rather than visuo-spatial skills, as is typical) to develop the cardinality principle (for a review, see O'Hearn and Luna, 2009). It has also been reported that individuals with WS may experience specific difficulties with the "mental number line" (number-space interaction effects) as they are less accurate on tasks such as "is five closer to nine or six?" (O'Hearn and Landau, 2007; see also, Krajcsi et al., 2009).

In an attempt to examine whether numerosity relies upon approximate estimates of magnitude (visuo-spatial) and symbolic number upon verbally mediated language processes, Paterson et al. (2006) made direct comparisons between WS (characteristically aspects of language are spared, but spatial abilities are impaired) and Down syndrome (DS; spatial spared, aspects of language impaired). On a task displaying small numbers of objects, they report infants with DS are impaired in their ability to discriminate small numerosities, but infants with WS are not. On a non-symbolic numerical distance task (using dot arrays) with affected older children and adults, they report those with WS do not reveal an expected distance effect, but those with DS do, suggestive of impaired analog numerical magnitude representation in WS (but not DS). They also report WS impairments on a variety of other tasks, particularly those that require mental manipulation of numbers, such as putting them in order (rote counting was generally in tact). This pattern was interpreted as a problem linking non-symbolic and symbolic forms of number in WS.

Children with Down syndrome display difficulties on counting and cardinal number tests (i.e., reporting "how many"; Gelman and Cohen, 1988), and may be less likely to notice violations of counting principles (Porter, 1999). For example, Nye et al. (2001) required children with DS to verbally count items in a set, and select a certain number of items (i.e., cardinality). Children with DS produced shorter count sequences and could count smaller sets. Camos (2009) required children with DS to enumerate large numerosities (dot arrays) that they were able to do with a 1:2 ratio, but not a 2:3 ratio (comparison participants showed age-related ratio improvements).

ADHD AND AUTISM SPECTRUM DISORDER

It has been reported (Zentall et al., 1994) that children with attention deficit hyperactivity disorder (ADHD) reveal lower (and slower) problem solving for math concepts on timed arithmetic tests, and the authors attributed these findings to difficulties with spatio-temporal organization. Kaufmann and Neurk, 2008 (see also 2006) tested 9- to 12-year-old children with ADHD on a variety of number tasks, including; placing an Arabic digit on an analogue scale, number discrimination at a range of distances, counting, non-symbolic (dot) enumeration (so-called "core" number abilities) and simple and complex mental and written calculation; and report particular difficulties with the first two in children with ADHD, particularly when numerical distance is small (the remainder were not affected). There is a variety of evidence to suggest individuals with ADHD also experience pathophysiological differences in temporal processing (see Barkley et al., 1997; Gooch et al., 2011; Allman and Meck, 2012). For instance, Valko et al. (2010) report impairments on reproduced temporal magnitude estimates (in the supra-seconds range) and temporal discrimination (in the sub-seconds range), and age-related changes between children and adults with ADHD.

The question of whether there is disordered processing of the temporal quality of information in autism spectrum disorder, and the extent to which this may impact the autistic behavioral phenotype, is beginning to be studied (Allman, 2011; Falter and Noreika, 2011), but has much anecdotal and clinical support. Although in their infancy, there are at least some empirical grounds (see also Szelag et al., 2004; Martin et al., 2009; Allman et al., 2011; Kwakye et al., 2011; but see Wallace and Happé, 2008; Jones et al., 2009a) and published commentaries supporting the temporal deficit hypothesis of autism (Boucher, 2001; Wimpory, 2002; Allman and DeLeon, 2009; Allman, 2011).

For example, Allman et al. (2011) report the timing functions across a wide age range (7–17 years) of affected individuals, and reveal (using a bisection task) potentially characteristic differences in the location of the subjective mid-point—which is found to be somewhat predictive of diagnostic communication and working memory impairment for shorter durations. They also reveal poorer temporal sensitivity for longer durations. These authors make modeling comparisons with previous reports from typically developing children (Droit-Volet and Wearden, 2001) and report that those with autism spectrum disorder appear to have more variable temporal memories, to an extent comparable with typically developing 5 year olds; and were likely to truncate (shorten) the "anchor" durations, to an extent that was comparable with typically developing 3 year olds. This lends support to the claim that time sense may be developmentally delayed in affected individuals, and may even contribute to diagnostic symptoms.

Assuming this is indeed the case in autism spectrum disorder, it might be conjectured that there may be relative differences and/or insensitivities in the "run" and "event" modes in the magnitude accumulation system (in a mode-control model). Presumably, given the shared mechanism but different mode of representation between basic time and number estimation, a fault operating in one mode (i.e., run) might produce a compensatory over-reliance upon using the other mode (i.e., event). Of course, we might also expect both time and number sense to be impaired if there are central problems in the function of the integration system, or if magnitude estimation is a more "generalized" process (i.e., ATOM).

If an atypically developing child finds it difficult to make sense of events according to their temporal properties, an adaptive strategy might be to use their numerical (or other stimulus) properties instead. As it pertains to oddities with number, it is common for children with autism spectrum disorder to have preoccupations for symbolic numbers; assigning numbers as labels for objects, events and animate beings; knowing how many parts there are to objects or events, and their order or calendrical quality. To-date it is unknown whether there is preserved number sense (i.e., ANS) and typical magnitude interaction effects (i.e., "mental number line") in this disorder, and like Williams syndrome, perhaps these individuals "over" rely upon rote formal instruction, and symbolic numerical processing (although individuals may also have language problems, unlike in WS). Although not characteristic of the disorder *per se*, for a review of mathematical ability in autism spectrum disorders see Chiang and Lin (2007) and Jones et al. (2009b).

Intriguingly with respect to posited deficits in temporal processing in autism spectrum disorder, and an compensation on symbolic number (or other dimensions), it is not uncommon for affected individuals to have unusual interests in timetables, calendars, and routines, which might serve as useful "external" temporal supports (e.g., Lalli et al., 1994). There is evidence that children and teenagers with autism spectrum disorder reveal impairments in higher-order temporal cognition (Boucher et al., 2007), including the ability to 1) think about past or future changes of think about a current situation; 2) understand that entities change over time but are still the same thing; 3) comprehend that successive events are part of a unitary process, which is not attributable to non-temporal cognitive factors such as inabilities with inferencing or generativity, motivation or attention. Parents of children with autism spectrum disorder (like parents of children with attention-deficit hyperactivity disorder) tend to describe them as having a "poor" sense of time (Barkley et al., 1997; Allman et al., 2011). At face value, these studies endorse a developmental association between a basic time sense and higher concepts and adaptability to time.

It is curious to wonder whether differences with time (and number) are somehow related to the outstanding skills of savants, which fall into five categories; mathematics (human calculator), calendar calculating and music (external representations of time), art and mechanical or spatial skills; particularly as these relate to different analog modes of stimulus representation (i.e., number, time, and length; see Droit-Volet et al., 2008; also González-Garrido et al., 2002; Thioux et al., 2006).

NEUROSCIENCE OF TIME AND NUMBER ABILITY (NEUTIN)

Although researchers have identified particular brain areas that function as neural integrators, and thus would likely serve good candidates for the supposed pulse accumulation process (of the type described by the mode-control model), a full explanation of how neurons integrate time and number is still lacking (Matell et al., 2003, 2011; Matell and Meck, 2004; Meck, 2006a,b; Meck et al., 2008; Coull et al., 2011). As it relates to making magnitude estimates, the basal ganglia, prefrontal cortex and inferior and posterior parietal cortex are usually recruited on tasks examining number and time magnitude estimation (Breukelaar and Dalrymple-Alford, 1999; Casini and Ivry, 1999; Rao et al., 2001; Macar et al., 2002; Hinton et al., 2004; Buhusi and Meck, 2005; Pouthas et al., 2005; Jahanshahi et al., 2006) and these findings tend to support comparative findings from animals (Schubotz et al., 2000; Schubotz and von Cramon, 2001). Although, as we have highlighted, there is much support for the idea that magnitudes of different dimensions (at least partly) share a common basis, they can be dissociated in adults with left-and right lateralized parietal lesions, who reveal selective impairments with number and time. For instance Cappelletti et al. (2011) report a patient with left lesion displayed otherwise intact temporal processing that was influenced by irrelevant numbers, which themselves could not be adequately processed; and a patient with a right lesion revealed impaired time estimation that could be modulated by preserved numerical processing (neither patient showed numerical processing could be influenced by time). The same patient with the right parietal lesion had previously been reported to show impaired temporal processing (a tendency to underestimate duration), but intact spatial and numerical processing and number-time interaction effects (i.e., small numbers perceived as shorter, long numbers perceived as longer; Cappelletti et al., 2009).

Evidence from electrophysiological recordings in animals reveals neurons (single cells) with periodical firing patterns, those tuned to specific magnitudes, and neurons with monotonically increasing firing as a function of increases in magnitude, for both time and number (e.g., see Nieder et al., 2002; Matell et al., 2003; Nieder, 2004; Nieder and Miller, 2004b; Dehaene and Brannon, 2010). For instance, Nieder et al. (2002) revealed individual neurons in monkey prefrontal cortex appear to code for specific cardinal numerosities, and revealed *size* and *distance* effects (at least partly accounted for by the mode-control model). It is also revealed that neurons in the intraparietal sulcus (IPS) are active before those in prefrontal cortex, suggesting number might be represented in the parietal cortex and sent to PFC for further processing (e.g., number related responses). In monkeys trained to perform a temporal comparison task, neurons in intraparietal regions were tuned to the temporal durations of the comparison stimuli (Leon and Shadlen, 2003).

ATOM (Walsh, 2003; Bueti and Walsh, 2009) supposes the parietal cortex is the "seat" of the generalized magnitude system, as this region is often recruited during spatial (Sereno et al., 2001; Pinel et al., 2004), numerical (Dehaene et al., 1999; Piazza et al., 2007) and temporal (Maquet et al., 1996; Leon and Shadlen, 2003) processing. This shared neural basis (parietal cortex) of the representation of number (numerical value) and size (size of

digits; see Dehaene et al., 2003; Fias et al., 2003; Pinel et al., 2004; Kadosh et al., 2005) is undoubtedly reflected in behavioral similarities between magnitude estimation judgments between time and number, and other quantities (i.e., line length). It is often found that number (with its symbolic connotations to language) and number tasks that require calculation (held to use verbal coding), involve left or bilateral parietal cortex, while time and space activates the right parietal cortex. In other words, "dimensions may have become lateralized from one another due to their output—number requires verbal representations, and time and space are more important for coordinating action" (Walsh, 2003:485). Cohen and Dehaene (1996) have suggested both (left and right) inferior parietal cortices are necessary for analogue magnitude representation.

As it relates to time sense, the striatal beat frequency (SBF) model (Matell and Meck, 2004) is a neurobiological instantiation of the pulse accumulator model of scalar expectancy theory (Gibbon et al., 1984; see Meck et al., 2008; Coull et al., 2011). Oscillatory neural inputs from the activity of large areas of cortex constitute the time code, and patterns of oscillatory activity are detected by striatal medium spiny neurons (input cells of the basal ganglia). The memory stage of the model (of the type described by the mode-control model) is attributed to the adjustment of cortico-striatal weights (which become "tuned"), and is assumed to depend upon the same neural representation of a specific stimulus as working memory (see Lustig and Meck, 2005; Lustig et al., 2005). From a computational perspective, it has recently been proposed that "chains of integrators constructed from mechanisms exhibiting a range of intrinsic time constraints (ranging from slow protein synthesis to rapidly ramping neural firing rates) may. . .perform interval timing" (Simen et al., 2011:1). In this account, magnitude estimates of time (in the seconds-to-minutes range) are mediated by chains of leaky accumulators.

IN INFANCY

Recall that time and number discrimination in infancy shows ratio-dependent improvements between 6- and 10-months of age (e.g., Brannon et al., 2007; Cordes and Brannon, 2009; Cantlon et al., 2010). The same pattern of results has also been found in electrophysiological recordings from infant brains. For instance, Libertus et al. (2009) demonstrated 7-month-old infants are able to detect novel numerosities (following habituation to a standard number). The magnitude of the "spike" of the deviant-triggered ("odd-ball") amplitude produced in the brain to the unexpected change in numerosity (or duration, to be discussed) constitutes an event-related potential (ERP). These authors report that the ERP varied in accordance to changes in number—specifically, the greater the relative difference between numerosities (1:3 ratio vs. 1:2 ratio) rather than their absolute difference, the bigger the ERP. Additionally, Hyde and Spelke (2011) recorded ERP's from 6- to 7.5-month-old infants and also obtained evidence that representation of large numerosities in infants are approximate and ratio-dependent. Specifically, large numbers evoked a (mid-latency parietal) ERP that was dependent upon stimulus numerosity, whereas small numbers evoked an (occipital-temporal) ERP that was dependent upon the cardinal value of stimuli (i.e., not ratio-dependent). This finding was interpreted as support for the idea that there might be different cognitive systems for small and large numerosities.

In a recent study, Libertus et al. (2011b) observed that following steady-state repetition of the same numerosity, a proportional change in numerosity produced a proportion change in electrophysiological entrainment (Weber's law). Moreover, neural entrainment predicted infants' number discrimination measured behaviorally 2 months later. Hyde et al. (2010) showed the latency of the ERP after a change in shape (space) occurred much later (i.e., after 5–8 s) compared to when number was changed (i.e., after 2–5 s) in 6-month-old infants. Further, they report a right lateralized response to number changes (see also Izard et al., 2008). This is in contrast to other reports that have found bilateral activity (Cantlon et al., 2006). As it may relate to the development of a "two-part" number system and the "magic number four," Hyde and Spelke (2011) report that 6-month olds display patterns of electrical brain activity which follows the scalar property (i.e., the ERP scaled with the ratio between numbers), but only for the processing of larger, but not smaller numbers (i.e., those in the subitizing range).

In relation to time sense, Brannon et al. (2008) employed a timing-interval oddball paradigm coupled with electrophysiological recording in 10-month-old infants, and examined the amplitude to an time-interval triggered ("odd-ball") spike to deviations in duration, comparing infants' performance with a group of adults. The peak magnitude of the ERP has been shown to vary as a function of the standard to deviant ratio in both infants and adults (1:2, 2:3: 1:3, and 1:4; Brannon et al., 2008). Moreover, when ratio was held constant and absolute values were made to vary, the ERP did not vary. That is, the "hallmark" scalar property is also obtained in the firing patterns of neurons coding for time (see also, Brannon et al., 2004b). Infants also revealed a slight right lateralization in the ERP for time magnitude estimation.

IN CHILDHOOD

Electrophysiological studies in children suggest that number processing in the inferior parietal cortex begins as a right-lateralized process and the left hemisphere gradually takes over, while right-lateralized activity does not show such age-related changes (e.g., Ansari and Dhital, 2006). More recently, Heine et al. (2011) studied elementary school children (around 7 years of age) on a non-symbolic number discrimination task using a range of numerical magnitudes, both within and beyond the subitizing range. They report late parietal ERP's that were proportionally affected by the relative distance between the magnitudes, and which were more right- than left-lateralized, including those in the subitizing range. Temple and Posner (1998) have shown that the brain activity associated with symbolic number discrimination shows little change between the age of 5-years and adulthood. They report that while the reaction times for numerical comparisons of Arabic numerals and dot arrays dropped threefold between 5 years and adulthood, the numerical distance ERP effects and the loci of activity remained constant between children and adults. The consistency in patterns of brain activity is impressive given that dramatic changes in numerical language and skill occur between 5 and 20 years of age.

It has been revealed through functional neuroimaging (fMRI) that young children can discriminate between numerical values across different notation systems, both symbolic and non-symbolic, and recruit the same parts of the brain as adults when doing so (occipitio-temporal and parietal cortex), plus a few regions more (inferior frontal; e.g., Cantlon et al., 2009). For instance, Cantlon et al. (2006) tested non-symbolic and area discrimination in 4-year olds, and revealed similar IPS activation to number as in adults.

This approach also reveals age-related fronto-parietal shifts in number processing, of basic and advanced numerical tasks (Ansari and Dhital, 2006; Ansari, 2008; Holloway and Ansari, 2010). The decreasing involvement of prefrontal cortex is assumed to reflect a developmental disengagement of domain-general processes related to executive control and working memory (Ansari et al., 2005; Rivera et al., 2005). These findings can be taken as support for the idea that a core neural system integrates notation-independent numerical representations, and that mental arithmetic may have functional specialization on the left inferior parietal cortex.

Kaufmann et al. (2006, 2008) have reported neural overlap between non-symbolic numerical and spatial processing in children around 8 years old (using hand and finger stimuli). In contrast to adults, children reveal increased activity in bilateral supramarginal gyrus, post-and-precentral gyrus, and anterior-lateral portions of the IPS. Cantlon et al. (2011) attempted to measure activity to symbols (numbers and letters, and a variety of other comparison stimuli), and compared to adults, children reveal comparable left-lateralized mid-fusiform/inferior temporal gyrus activity for both letters and numbers.

As pertains to developmental disabilities, individuals with developmental dyscalculia also present with presumed neuropsychological damage to the IPS, thus providing additional support for this neurological locus in numerical processing and abstract number. It has been thought this disorder may characterize a deficit with the "mental number line" (Bachot et al., 2005) or in the linking between non-symbolic magnitude and symbolic notation (Rubinsten and Henik, 2005; Rousselle and Noël, 2007). Kaufmann et al. (2009) reveal that during non-symbolic number processing, children with dyscalculia reveal stronger activations in the left inferior parietal cortex and reduced deactivations in the right inferior parietal cortex, perhaps suggestive of an impaired number sense and compensatory neural activity. However, Mussolin et al. (2009) required affected children aged 9–11 years old to identify the *larger* numeral in a pair (with a variety of numerical distances; i.e., 2 vs. 4; 2 vs. 8) and report that affected children show absence of typical numerical distance effect modulations of the IPS (as typical children do). They also observed other differences between typical and dyscalculic children: typically there is stronger right intraparietal sulcus (IPS; and right middle frontal gyrus) activation for small than large numerical distances, while children with dyscalculia show left supramarginal gyrus and middle frontal gyrus activation; affected children also revealed postcentral gyrus activation for number in contrast to color comparison.

It has been revealed that older children (10–15 years) with ADHD show decreased activation on a time discrimination task contrasted by a temporal order task in right dorsolateral and inferior frontal cortex, and right anterior cingulate into SMA (Smith et al., 2008). There is unpublished fMRI data to suggest that children with autism spectrum disorder reveal differences in activity in cortico-cerebellar and cortico-striatal circuits when timing relatively short (2-s) and longer (8-s) durations: children with autism may recruit a "longer" timing system for shorter durations (Allman et al., in preparation).

IN ADULTS

Electrophysiological recordings in adults have revealed the magnitude of an ERP is proportional to the ratio of the difference between temporal and numerical magnitudes (scalar property). As it relates to time estimation, there has been much speculation as to whether brain rhythms may serve as the "tick" of a clock (Treisman, 1984). This includes alpha and theta rhythms, and event-related de-synchronizations. Perhaps the most oft cited is the slow negative wave called the contingent negative variation (CNV; for a discussion, see Pouthas, 2003). However it has recently been suggested that rather than being directly implicated in the accumulation process, the CNV likely represents time-based decision and response processes (van Rijn et al., 2011).

Szucs and Soltesz (2007) were able to dissociate ERP's associated with both facilitation and interference on the (number-size) numerical Stroop paradigm (i.e., judge number magnitude with physically smaller and bigger Arabic digits). "In a nutshell, in the numerical task we found an ERP facilitation effect related to perceptual processing" (Szucs and Soltesz, 2007:3196). They also report that number had a slower processing speed than size, and an ERP numerical distance effect which was stronger over right (than left) parietal regions. The timing of the ERP was also associated with distance effects, and occurred at the same time as the Stroop facilitation effect, "suggesting the facilitation effect appeared when numerical information was just being evaluated or was already available. . .Most probably, the faster processed irrelevant size information could prime and accelerate the processing of the slower processed numerical information in the common magnitude representation" system (Szucs and Soltesz, 2007:3197).

As it relates to numerical processing, Libertus et al. (2007) employed non-symbolic (dots) and symbolic (Arabic digits; 1–10) numbers and required adults to judge whether the presented number was less/more than five. For symbolic numbers, they report distance-related ERP modulation across parietal and temporal-occipital regions, and greater right-lateralized posterior positive ERP's for symbolic digits closer to the comparison (5; than those further apart, e.g., 9), however this was not found small non-symbolic number distances; and ERP's increased as numerosity increased (size effect). With a greater range of values (8–30) they did obtain similar ERP distance effects as symbolic digits (indicative of input-notation independence).

As it relates to the question of the "magic number four," there is evidence that small and large number processing can be dissociated in adults at the electrophysiological level with respect to both pattern and time: small cardinal numbers (within the 'subitizing' range) invoke an early visuo-spatial attentional component, and the ERP is largest for three objects, then two, then one; while

larger numbers modulate a mid-latency component in the right intraparietal region that is sensitive to ratios. In the same study, Hyde and Spelke (2012) also report lateralization effects, and identified several distinct loci, for small and large non-symbolic numbers. The authors surmised a single system represents all numerosities, but is constrained by cognitive processes related to the limits of an early attentional selection processes; small numbers (e.g., four objects) might be selected (by attentional processing) as a group, but larger numbers likely require (more demanding) parallel processing.

In a procedure combining electrophysiological and fMRI, it has been shown that patterns of cortical activity are attributable to the input of symbolic notation (verbal or Arabic). For instance, bilateral extrastriate cortices and a left-lateralized precentral region are more activated during verbal (than Arabic) numbers, while activity in right fusiform gyrus (the "expert" area), bilateral inferior parietal and frontal regions is greater for Arabic (than verbal) notation. Bilateral activation along the interparietal sulcus and precuneus that corresponds to numerical distance was also noted (Pinel et al., 2001). This is consistent with a basic notation-independent system of magnitude (see also, Piazza et al., 2007). Piazza et al. (2004) report the percent signal change of IPS response to deviant numerosities increased with the disparity between the habituated and deviant numerosities. The general conclusion of this study was that the IPS responds to changes in the numerical quantity of a stimulus even when explicit comparison of stimuli is not required and regardless of whether the stimuli involve Arabic numerals or dot arrays (but see, Shuman and Kanwisher, 2004).

Using fMRI, Pinel et al. (2004) examined adults' magnitude estimation for size, luminance and number; and revealed at both the behavioral and neural level, number interfered with size, but not with luminance. It has also been suggested that number-space interactions (i.e., "mental number line") might be mediated by shared parietal circuits for external attention to space and internal representations of number (Hubbard et al., 2005). For instance, it has been reported that there is left-lateralized parietal activation when participants' attention is directed to time, right-lateralized parietal activation when attending to space, and bilateral activation when processing both dimensions simultaneously (Coull and Nobre, 1998), and patients with spatial neglect (i.e., damage to right parietal cortex produces failure to attend or response to left space) reveal a variety of timing deficits (e.g., see Danckert et al., 2007; Hoeckner et al., 2008; Calabria et al., 2011). For example, Vuilleumier et al. (2004) report patients with neglect are slower to classify numbers (Arabic) if they are smaller (than larger) than a target number, which they attributed to difficulties spatially representing numbers in the left side of the mental number line.

In adults, symbolic number processing (and complex math ability) is usually characterized by bilateral, and in some instances, left-lateralized IPS activity (for details, see Dehaene et al., 2003; Santens et al., 2010). For instance, Piazza et al. (2002) report the IPS is active when participants estimate numerosity across non-symbolic numerical stimuli such as sets of visual objects or auditory events, and Kadosh et al. (2005) report notation-independent activity in IPS between symbolic (digits, number words) and non-symbolic number (dots; see also, Naccache and Dehaene, 2001; Eger et al., 2003). Further, right-lateralized IPS activation is greater when participants compare the values of Arabic numerals (or numerosity, ANS) than when they compare stimuli of other such semantic categories as animals, body parts, or abstract symbols along continuous dimensions like ferocity, relative position, and orientation (Le Clec'h et al., 2000). Bilateral IPS is selectively activated when participants perform approximate arithmetic calculations on symbolic numerical stimuli such as Arabic numerals and number words (Pesenti et al., 2000; Simon et al., 2004; for reviews see, Dehaene, 2003; Dehaene et al., 2004). This activation is not related to factual knowledge of arithmetic outcomes because greater IPS activation is also found when participants roughly estimate the answers to arithmetic problems. The activation can be dissociated from the patterns of IPS activation associated with the calculation of precise arithmetic outcomes (Dehaene et al., 1999). For example, when participants are presented with the problem "$4 + 5$," the IPS is activated when they choose the closest answer from the options "8 or 3" but the IPS is not activated when they identify the answer precisely from the choices "7 or 9." IPS activation is found when participants are asked to compute the outcomes of various addition and subtraction computations but not when they are simply asked to read number words (e.g., Chochon et al., 1999). The bilateral posterior superior parietal lobe is believed to correspond to spatial attention along the "mental number line," while the left angular gyrus supports verbally learned facts (e.g., $2 + 2 = 4$).

Pinel and Dehaene (2010) investigated whether individual differences in functional asymmetry (left-lateralization) in areas involved in sentence listening and reading are mirrored in the asymmetry of areas involved in mental arithmetic, and found this to be the case. They report arithmetic processing recruits frontal, parietal and subcortical regions. "Specifically, the profile of asymmetry in the posterior superior temporal sulcus during sentence processing co-varied with the asymmetry of calculation-induced activation in the IPS" (Pinel and Dehaene, 2010:48).

As it relates to time estimation, similar patterns of activation are observed during supra-second perception or production timing tasks and all timing tasks (i.e., even those involving "thinking" about time) typically activate motor regions such as the basal ganglia, supplemental motor area (SMA) and pre-SMA (for a review, see Macar et al., 2002; Kotz and Schwartze, 2011; van Rijn et al., 2011). It is widely held that relatively small (less than a second) and longer duration magnitudes (in the seconds to minutes range) may be represented by different timing systems (e.g., see Buhusi and Meck, 2005; Jahanshahi et al., 2006; Buhusi and Cordes, 2011). Sub-second timing may be more cerebellar-dependent due to this region's role in motor coordination, and timing in the supra-seconds range may depend more upon the basal ganglia and prefrontal regions, as this type of temporal processing recruits more attentional (switch and accumulator) and working memory processes (see **Figure 1**; see also Hinton and Meck, 1997), however they are not mutually exclusive as cerebellar activation is also found in adult fMRI studies using supra-second durations (and basal ganglia for millisecond durations). Similarly, different molecular and neurophysiological systems underlie interval and circadian (i.e., 24-h) timing (see Agostino et al., 2011). Given the wealth of such findings (as it

relates to humans and adults), a complete account of neurophysiological findings of timing and time perception in adults is beyond the scope of this review (e.g., but see, Harrington and Haaland, 1999; Matell and Meck, 2000; Meck and Benson, 2002; Meck, 2003, 2005; Nenadic et al., 2003; Hinton and Meck, 2004; Meck and Malapani, 2004; Pastor et al., 2004; Buhusi and Meck, 2005; Coull et al., 2011; Allman and Meck, 2012). However, a common feature of many adult neuroimaging studies is the explicit attempt to dissect the contribution of different timing components (e.g., clock, memory, and decision stages) as it relates to a neurobiological instantiation of scalar expectancy theory (Gibbon et al., 1984).

For example using fMRI, Harrington et al. (2010); see also, Harrington et al. (2004) examined patterns of neural activity during the perceptual (encoding), memory and decision stages of a duration (and pitch) ordinality task. Encoding of time selectively activated the striatum; the striatum was equally active for time (as for pitch) during the maintenance stage, and striatal activation was greatest for time during the decision stage. As acknowledged by the authors, these findings are consistent with the SBF model of interval timing (Matell and Meck, 2004). fMRI studies have revealed the preSMA and basal ganglia likely serve a function in the "accumulation processes" as there is increased activation in these regions to longer durations (e.g., see Coull et al., 2004; Pouthas et al., 2005); memory processes are likely served by lateral premotor and right inferior frontal corticies (see Rao et al., 2001; Pouthas et al., 2005) and decision processes by the anterior cingulate (see also Rao et al., 2001).

In their study, Coull et al. (2004) made use of dynamically changing visual stimulus attributes (e.g., color and duration), requiring selective attention (on the part of the participants) to either dimension. Increasing attentional allocation to time selectively increased activity in a cortico-striatal network that included the pre-supplementary motor area, the right frontal operculum, and the right putamen.

Harrington et al. (2011) scanned adults while studying the "sounds are judged longer than lights" effect. Subjective perceptions of time slowing or quickening were associated with different patterns of superior temporal, posterior insula, and middle occipital activity, which reveal stronger effective connectivity when time was dilated. The within-trial evolution of interval timing has also been examined (Rao et al., 2001), and it was found that activation in the basal ganglia (right putamen and caudate) occurred early and continued into the trial and was uniquely associated with encoding time intervals, whereas cerebellar activation unfolded later, suggesting an involvement of processes other than explicit timing. Early activation in right inferior parietal cortex (and bilateral premotor) was associated with encoding, implicating these systems in attention and temporary maintenance of intervals. Later activation in the right dorsolateral prefrontal cortex emerged during comparison of time intervals.

SUMMARY AND CONCLUSIONS

Evidence from infants, children and adults, and non-human animals, suggests numerical and temporal processes are remarkably accurate, and conform to qualities of sensory perception (i.e., scalar property), across a variety of different methods: behavioral looking patterns of infants, social timing, behavioral responses in children as young as 3-years old, and in the electrophysiological potentials of neurons.

The studies cited in this review tend to support the notion that typical infants possess a "built in" time and number sense (e.g., Brannon and Roitman, 2003). Performance on time and number tasks is modulated by ratio-dependence in children and adults, and this is found with non-symbolic and symbolic stimuli (e.g., Arabic numerals and words). Typically developing 6-month-old infants reveal sensitivity to numerosity in temporal sequences and spatial arrays, and sensitivity to time with respect to deviant durations, area, speed and distance, but only when constrained by the 1:2 ratio requirement, although this quite quickly develops (over a few months) to encompass "more difficult" 2:3 ratio sensitivities. This review has attempted to reconcile such findings within a "mode-control" model perspective (Meck and Church, 1983; Church and Meck, 1984). In this model, temporal and numerical quantity is measured by the accumulation of pulses (in the run/stop and event modes, respectively).

As studies examining the relative extent of conformities between magnitude estimation for different dimensions continue, so too does support for the idea that there is a general principle (of the type described by the mode-control model) operating on a multitude of dimensions (of the type described by ATOM) upon which we rely to make sense of events in our world (time, area, number, size, distance, speed). However there is (as yet) no model that is able to provide a complete account of multi-dimensional magnitude estimation (accumulation) processes. Both types of account predict cross-dimension interaction effects (between time and number; across different quantities). Of course, given the co-linearity between time and numerosity in the mode-control model, and in ATOM (Walsh, 2003), it becomes difficult to dissociate between these two types of accounts given the aforementioned developmental similarities between magnitude estimates of time and number.

Infants are able to perform numerical addition and subtraction, and more advanced temporal and numerical abilities also require similar forms of arithmetic operations of magnitudes, such as calculating speed (space divided by time) or rate of return (number divided by time), and number sense appears to be associated with math ability. The fact that infants resources are being directed toward improving sensitivity to different quantities at such a critical period in brain development, speaks to the importance of this as a "foundational" ability for other cognitive and behavioral functions. Of course during infancy, a wide variety of abilities are starting to take shape (e.g., walking, inhibiting actions) and it comes as no surprise that the time from birth to 2 years and middle to late childhood is particularly important for the development of NEUTIN. It will be useful for future research to identify the precise developmental sequences of sensitivities to different quantities, and how they relate to other forms of cognitive development (e.g., attention, memory), and to adapt the mode-control to accommodate findings for different dimensions (see also, Lustig, 2011).

Given the literature, it seems likely that a (right-lateralized) non-symbolic number system provides the foundation for the (left-lateralized) symbolic number system over the course of

development (see Cantlon et al., 2009). Across childhood, it appears the discrimination of analogue magnitudes improves with age, which is perhaps inextricably linked with the development of attentional capacities or the ability to maintain information in working memory. There is debate about whether smaller magnitude estimates (i.e., numerosities) are processed differently than larger ones. The question of how the brain develops a sense of number and time raises serious computational issues for cognitive neuroscience. As adults, we have the ability to make decisions based on abstract mental representations of magnitudes of time (e.g., "do I have enough time to get to the shop") and complex number abstractions (e.g., calculating change left over from a purchase at the shop), and of course our attention is distributed in time and space, and our subjective experience of time is modulated by attention (see Coull et al., 2004).

It will be important for future research to identify the neural correlates of time and number representation in children, and corresponding changes in brain function that underlie normative developments in these domains (i.e., brain maturation and the relationship to timing and counting). This is relevant to children with developmental disabilities, particularly those with apparent difficulty with time and number (e.g., math disability, autism spectrum disorder, Williams syndrome), as it offers a "bench-to-bedside" approach with therapeutic potential. For example, there is evidence that external temporal supports (e.g., picture schedules, timers) are extremely effective in the training and treatment of individuals with autism, and other neurological populations who experience problems with cognitive adaptation (for details, see Allman and Meck, 2012).

A developmental perspective to time and number can also help unravel interactions among seemingly disparate levels of organization, such as the molecular biology of gene expression and the development of cognitive abilities. For example, assuming a basic deficit in time sense in those with autism spectrum disorder, it should follow that aspects of the behavioral phenotype are related to subtle and early neuropathology that ultimately affects multiple neural systems involved in number and time representation, directly and through compensatory experience-dependent reorganization. This is still yet to be determined, but this idea is congruous with current theories of autism spectrum disorder that emphasize differences in "neural signatures" (Kaiser et al., 2010), or the adaptive functioning of long-range (multiple neural systems) in neurocognitive function (Allman, 2011; Barttfield et al., 2011). Potentially at least, this type of neural-systems approach to the development of NEUTIN may provide a neural signature or "endophenotype" that corresponds to impairments in autism spectrum disorder (and potentially, to co-morbid disorders). The goal for the quest for the "endophenotype" is to identify pathophysiological mechanisms that "cause" the disorder (Kaiser et al., 2010).

On a final note, it is parsimonious (from an ontogenic developmental perspective) to surmise that our "built in" quantity sense and "integration" mechanism is likely at the root of our cognitive ability to think about metaphysical aspects of time and space, such as pondering how big or old the milky way is, and what the word "vast" means to our subjective estimations of magnitude.

ACKNOWLEDGMENTS

This work was supported in part by a Pathway to Independence award to Melissa J. Allman from the Eunice Kennedy Shriver National Institute of Child Health and Human Development (K99 HD058698). The authors are grateful to the reviewers for their comments.

REFERENCES

Agostino, P. V., Golombek, D. A., and Meck, W. H. (2011). Unwinding the molecular basis of interval and circadian timing. *Front. Integr. Neurosci.* 5:64. doi: 10.3389/fnint.2011.00064

Allan, L. G., and Gibbon, J. (1991). Human bisection at the geometric mean. *Learn. Motiv.* 22, 39–58.

Allman, M. J. (2011). Deficits in temporal processing associated with autistic disorder. *Front. Integr. Neurosci.* 5:2. doi: 10.3389/fnint.2011.00002

Allman, M. J., and DeLeon, I. G. (2009). "No time like the present: time perception in autism," in *Causes and Risks for Autism*, eds A. C. Giordano and V. A. Lombardi (New York, NY: Nova Science Publishers), 65–76.

Allman, M. J., DeLeon, I. G., and Wearden, J. H. (2011). A psychophysical assessment of timing in individuals with autism. *Am. J. Intellect. Dev. Disabil.* 116, 165–178.

Allman, M. J., and Meck, W. H. (2012). Pathophysiological distortions in time perception and timed performance. *Brain* 135, 656–677.

Ansari, D. (2008). Effects of development and enculturation on number representation in the brain. *Nat. Rev. Neurosci.* 9, 278–291.

Ansari, D., and Dhital, B. (2006). Age-related changes in the activation of the intraparietal sulcus during nonsymbolic magnitude processing: an event-related functional magnetic resonance imaging study. *J. Cogn. Neurosci.* 18, 1820–1828.

Ansari, D., Garcia, N., Lucas, E., Hamon, K., and Dhital, B. (2005). Neural correlates of symbolic number processing in children and adults. *Neuroreport* 16, 1769–1773.

Ansari, D., Donlan, C., Thomas, M. S. C., Ewing, S. A., Peen, T., and Karmiloff-Smith, A. (2003). What makes counting count? Verbal and visuo-spatial contributions to typical and atypical number development. *J. Exp. Child Psychol.* 85, 50–62.

Antell, S. E., and Keating, D. P. (1983). Perception of numerical invariance in neonates. *Child Dev.* 54, 695–701.

Ashkenazi, S., and Henik, A. (2010). Attentional networks in developmental dyscalculia. *Behav. Brain Funct.* 6, 2.

Ashkenazi, S., Mark-Zigdon, N., and Henik, A. (2009). Numerical distance effect in developmental dyscalculia. *Cogn. Dev.* 24, 387–400.

Bachot, J., Gevers, W., Fias, W., and Roeyers, H. (2005). Number sense in children with visuospatial disabilities: orientation of the mental number line. *Psychol. Sci.* 47, 172–183.

Barkley, R. A., Koplowitz, S., Anderson, T., and McMurray, M. B. (1997). Sense of time in children with ADHD: effects of duration, distraction and stimulant medication. *J. Int. Neuropsychol. Soc.* 3, 359–369.

Barth, H., La Mont, K., Lipton, J., and Spelke, E. S. (2005). Abstract number and arithmetic in young children. *Proc. Natl. Acad. Sci. U.S.A.* 39, 14117–14121.

Barttfield, P., Wicker, B., Cukier, S., Navarta, S., Lew, S., and Sigman, M. (2011). A big-world network in ASD: dynamical connectivity analysis reflects a deficit in long-range connections and an excess of short-range connections. *Neuropsychologia* 49, 254–263.

Block, R. A., Zakay, D., and Hancock, P. A. (1999). Developmental changes in human duration judgments: a meta-analytic review. *Dev. Rev.* 19, 183–211.

Bijeljac-Babic, R., Bertoncini, J., and Mehler, J. (1993). How to 4-day old infants categorize multisyllabic utterances? *Dev. Psychol.* 29, 711–721.

Bobin-Bègue, A., Provasi, J., Marks, A., and Pouthas, V. (2006). Influence of auditory tempo on the endogenous rhythm of non-nutritive sucking. *Eur. Rev. Appl. Psychol.* 56, 239–245.

Booth, J. L., and Siegler, R. S. (2006). Developmental and individual differences in pure numerical estimation. *Dev. Psychol.* 42, 189–201.

Booth, J. L., and Siegler, R. S. (2008). Numerical magnitude representations influence arithmetic learning. *Child Dev.* 79, 1016–1031.

Boucher, J. (2001). "Lost in a sea of time: Time-parsing and autism," in *Time and Memory*, eds C. Hoerl and T. McCormack (Oxford, UK: Oxford University Press), 111–135.

Boucher, J., Pons, F., Lind, S., and Williams, D. (2007). Temporal cognition in children with autistic spectrum disorder: tests of diachronic thinking. *J. Autism Dev. Disord.* 37, 1413–29.

Brannon, E. M. (2002). The development of ordinal numerical knowledge in infancy. *Cognition* 83, 223–240.

Brannon, E. M., Abbott, S., and Lutz, D. J. (2004a). Number bias for the discrimination of large visual sets in infancy. *Cognition* 93, B59–B68.

Brannon, E. M., Roussel, L. W., Meck, W. H., and Woldorff, M. (2004b). Timing in the baby brain. *Cogn. Brain Res.* 21, 227–233.

Brannon, E. M., Libertus, M. E., Meck, W. H., and Woldorff, M. G. (2008). Electrophysiological measures of time processing in infant and adult brains: Weber's law holds. *J. Cogn. Neurosci.* 20, 193–203.

Brannon, E. M., Lutz, D., and Cordes, S. (2006). The development of area discrimination and its implications for number representation in infancy. *Dev Sci.* 9, F59–64.

Brannon, E. M., and Roitman, J. D. (2003). "Nonverbal representations of time and number in animals and human infants," in *Functional and Neural Mechanisms of Interval Timing*, ed W. H. Meck (Boca Raton, FL: CRC Press), 143–182.

Brannon, E. M., Suanda, S., and Libertus, K. (2007). Temporal discrimination increases in precision over development and parallels the development of numerosity discrimination. *Dev. Sci.* 10, 770–777.

Brannon, E. M., and Terrace, H. S. (1998). Ordering of the numerosities 1 to 9 by monkeys. *Science* 282, 746–749.

Brannon, E. M., and Terrace, H. S. (2000). Representation of the numerosities 1–9 by rhesus macaques (Macaca mulatta). *J. Exp. Psychol. Anim. Behav. Process.* 26, 31–49.

Brannon, E. M., and Van de Walle, G. A. (2001). The development of ordinal numerical competence in young children. *Cogn. Psychol.* 43, 53–81.

Brannon, E. M., Wusthoff, C. J., Gallistel, C. R., and Gibbon, J. (2001). The subjective scaling of number representation. *Psychol. Sci.* 12, 238–243.

Breukelaar, J. W. C., and Dalrymple-Alford, J. C. (1998). Timing ability and numerical competence in rats. *J. Exp. Psychol. Anim. Behav. Process.* 24, 84–97.

Breukelaar, J. W. C., and Dalrymple-Alford, J. C. (1999). Effects of lesions to the cerebellar vermis and hemispheres on timing and counting in rats. *Behav. Neurosci.* 113, 78–90.

Broadbent, H. A., Rakitin, B. C., Church, R. M., and Meck, W. H. (1993). "Quantitative relationships between timing and counting," in *The Development of Numerical Competence: Animal and Human Models*, eds S. Boysen and E. J. Capaldi (Hillsdale, NJ: Erlbaum), 171–187.

Brown, S. W. (1997). Attentional resources in timing: interference effects in concurrent temporal and non-temporal working memory tasks. *Percept. Psychophys.* 5, 1118–1140.

Buckley, P. B., and Gilman, C. B. (1974). Comparison of digits and dot patterns. *J. Exp. Psychol.* 103, 1131–1136.

Bueti, D., and Walsh, V. (2009). The parietal cortex and the representation of time, space, number and other magnitudes. *Philos. Trans. R. Soc. Lond. B Bio. Sci.* 364, 1831–1840.

Buhusi, C. V., and Cordes, S. (2011). Time and number: the privileged status of small values in the brain. *Front. Integr. Neurosci.* 5:67. doi: 10.3389/fnint.2011.00067

Buhusi, C. V., and Meck, W. H. (2005). What makes us tick? Functional and neural mechanisms of interval timing. *Nat. Rev. Neurosci.* 6, 755–765.

Buhusi, C. V., and Meck, W. H. (2009a). Relative time sharing: new findings and an extension of the resource allocation model of temporal processing. *Phil. Trans. R. Soc. Lond. B Biol. Sci.* 364, 1875–1885.

Buhusi, C. V., and Meck, W. H. (2009b). Relativity theory and time perception: single or multiple clocks? *PLoS One* 4:e6268. doi:10.1371/journal.pone.0006268

Butterworth, B. (2010). Foundational numerical capacities and the origins of dyscalculia. *Trends Cogn. Sci.* 14, 534–541.

Calabria, M., Jacquin-Courtois, S., Miozzo, A., Rossetti, Y., Padovani, A., Cotelli, M., and Miniussi, C. (2011). Time perception in spatial neglect: a distorted representation. *Neuropsychology* 25, 193–200.

Camos, V. (2009). Numerosity discrimination in children with Down syndrome. *Dev. Neuropsychol.* 34, 435–447.

Cantlon, J. F., Brannon, E. M., Carter, E. J., and Pelphrey, K. A. (2006). Functional imaging of numerical processing in adults and four-year-old children. *PLoS Biol.* 4:0844–0854. doi: 10.1371/journal.pbio.0040125

Cantlon, J. F., Libertus, M. E., Pinel, P., Dehaene, S., Brannon, E. M., and Pelphrey, K. A. (2009). The neural development of an abstract concept of number. *J. Cogn. Neurosci.* 21, 2217–2229.

Cantlon, J. F., Pinel, P., Dehaene, S., and Pelphrey, K. A. (2011). Cortical representations of symbols, objects, and faces are pruned back during early childhood. *Cereb. Cortex* 21, 191–199.

Cantlon, J. F., Safford, K. E., and Brannon, E. M. (2010). Spontaneous analog number representations in 3-year-old children. *Dev. Sci.* 13, 289–297.

Cappelletti, M., Freeman, E. D., and Cipolotti, L. (2009). Dissociations and interactions between time, numerosity and space processing. *Neuropsychologia* 47, 2732–2748.

Cappelletti, M., Freeman, E. D., and Cipolotti, L. (2011). Numbers and time doubly dissociate. *Neuropsychologia* 49, 3078–3092.

Carey, S. (1998). Knowledge of number: its evolution and ontogenesis. *Science* 242, 641–642.

Carey, S. (2001). "On the very possibility of discontinuties in conceptual development," in *Language, Brain, and Cognitive Development: Essays in Honor of Jacques Mehler*, ed E. Dupoux (Cambridge, MA: MIT Press), 303–324.

Carey, S. (2004). Bootstrapping and the origin of concepts. *Daedalus* 133, 59–68.

Casini, L., and Ivry, R. B. (1999). Effects of divided attention on temporal processing in patients with lesions of the cerebellum or frontal lobe. *Neuropsychology* 13, 10–21.

Casasanto, D., and Boroditsky, L. (2008). Time in the mind: using space to think about time. *Cognition* 106, 579–593.

Casarotti, M., Michielin, M., Zorzi, M., and Umiltà, C. (2007). Temporal order judgment reveals how number magnitude affects visuospatial attention. *Cognition* 102, 101–117.

Chen, K.-M., and Yeh, S.-L. (2009). Asymmetric cross-modal effects in time perception. *Acta Psychol.* 130, 225–234.

Cheng, R. K., MacDonald, C. J., and Meck, W. H. (2006). Differential effects of cocaine and ketamine on time estimation: implications for neurobiological models of interval timing. *Pharmacol. Biochem. Behav.* 85, 114–122.

Cheng, R. K., MacDonald, C. J., Williams, C. L., and Meck, W. H. (2008). Prenatal choline supplementation alters the timing, emotion, and memory performance (TEMP) of adult male and female rats as indexed by differential reinforcement of low-rate schedule behavior. *Learn. Mem.* 15, 153–162.

Chiang, H. M., and Lin, Y. H. (2007). Mathematical ability of students with Asperger syndrome and high-functioning autism: a review of the literature. *Autism* 11, 547–556.

Chiang, W. C., and Wynn, K. (2000). Infants' tracking of objects and collections. *Cognition* 77, 169–195.

Chochon, F., Cohen, L., van de Moortele, P. F., and Dehaene, S. (1999). Differential contributions of the left and right inferior parietal lobules to number processing. *J. Cogn. Neurosci.* 11, 617–630.

Church, R. M., and Broadbent, H. A. (1990). Alternative representations of time, number and rate. *Cognition* 37, 55–81.

Church, R. M., and Deluty, M. Z. (1977). Bisection of temporal intervals. *J. Exp. Psychol. Anim. Behav. Process.* 3, 216–228.

Church, R. M., and Gibbon, J. (1982). Temporal generalization. *J. Exp. Psychol. Anim. Behav. Process.* 8, 165–186.

Church, R. M., and Meck, W. H. (1984). "The numerical attribute of stimuli," in *Animal Cognition*, eds H. L. Roitblat, T. G. Bever, and H. S. Terrace (Hillsdale, NJ: Erlbaum), 445–464.

Clearfield, M. W., and Mix, K. S. (1999). Number versus contour length in infants' discrimination of small visual sets. *Psychol. Sci.* 10, 408–411.

Clément, A., and Droit-Volet, S. (2006). Counting in a time discrimination task in children and adults. *Behav. Process.* 71, 164–171.

Clifton, R. K. (1974). Heart rate conditioning in the newborn infant. *J. Exp. Child Psychol.* 18, 9–21.

Cohen, L., and Dehaene, S. (1996). Cerebral networks for number processing: evidence from a case of posterior callosal lesion. *Neurocase* 155–174.

Cordes, S., and Brannon, E. M. (2009). Crossing the divide: infants discriminate small from large numerosities. *Dev. Psychol.* 45, 1583–1594.

Cordes, S., Gelman, R., Gallistel, C. R., and Whalen, J. (2001). Variability signatures distinguish verbal from nonverbal counting for both large and small numbers. *Psychon. Bull. Rev.* 8, 698–707.

Cordes, S., Williams, C. L., and Meck, W. H. (2007). Common representations of abstract quantities. *Curr. Dir. Psychol. Sci.* 16, 156–161.

Coull, J. T., Cheng, R. K., and Meck, W. H. (2011). Neuroanatomical and neurochemical substrates of timing. *Neuropsychopharmacology* 36, 3–25.

Coull, J. T., and Nobre, A. C. (1998). Where and when to pay attention: the neural systems for directing attention to spatial locations and to time intervals as revealed by both PET and fMRI. *J. Neurosci.* 18, 7426–7435.

Coull, J. T., Vidal, F., Nazarian, B., and Macar, F. (2004). Functional anatomy of the attentional modulation of time estimation. *Science* 303, 1506–1508.

Danckert, J., Ferber, S., Pun, C., Broderick, C., Striemer, C., Rock, S., and Stewart, D. (2007). Neglected time: impaired temporal perception of multisecond intervals in unilateral neglect. *J. Cogn. Neurosci.* 19, 1706–1720.

Dehaene, S. (1997). *The Number Sense: How the Mind Creates Mathematics*. New York, NY: Oxford University Press.

Dehaene, S. (2003). The neural basis of the Weber-Fechner law: a logarithmic mental number line. *Trends Cogn. Sci.* 7, 145–147.

Dehaene, S., Bossini, S., and Giraux, P. (1993). The mental representation of parity and number magnitude. *J. Exp. Psychol. Gen.* 122, 371–396.

Dehaene, S., and Brannon, E. M. (2010). Space, time, and number: a Kantian research program. *Trends Cogn. Sci.* 14, 517–519.

Dehaene, S., and Changeux, J. (1993). Development of elementary numerical abilities: a neuronal model. *J. Cogn. Neurosci.* 5, 390–407.

Dehaene, S., Molko, N., Cohen, L., and Wilson, A. J. (2004). Arithmetic and the brain. *Curr. Opin. Neurobiol.* 14, 218–224.

Dehaene, S., Piazza, M., Pinel, P., and Cohen, L. (2003). Three parietal circuits for number processing. *Cogn. Neuropsychol.* 20, 487–506.

Dehaene, S., Spelke, E., Pinel, P., Stanescu, R., and Tsivkin, S. (1999). Sources of mathematical thinking: behavioral and brain-imaging evidence. *Science* 284, 970–974.

DeLong, A. J. (1981). Phenomenological space-time: toward an experiential relativity. *Science* 213, 681–683.

de Hevia, M. D., Girelli, L., Bricolo, E., and Vallar, G. (2008). The representational space of numerical magnitude: illusions of length. *Q. J. Exp. Psychol.* 61, 1496–1514.

De Smedt, B., Verschaffel, L., and Ghesqiere, P. (2009). The predictive value of numerical magnitude comparison for individual differences in mathematics achievement. *J. Exp. Child Psychol.* 103, 469–479.

Dormal, V., and Pesenti, M. (2007). Numerosity-length interference: a Stroop Experiment. *Exp. Psychol.* 54, 289–297.

Dormal, V., Seron, X., and Pesenti, M. (2006). Numerosity-duration interference: a Stroop experiment. *Acta Psychol. (Amst)* 121, 109–124.

Droit, S. (1994). Temporal regulation of behavior with an external clock in 3-year-old children: differences between waiting and response duration tasks. *J. Exp. Child Psychol.* 58, 332–345.

Droit, S. (1995). Learning by doing in 3- and 4-year-old children: adapting to time. *Eur. Bull. Cogn. Psychol.* 14, 283–299.

Droit, S., Pouthas, V., and Jacquet, A. Y. (1990). Temporal learning in 4 12- and 6-year-old children: role of instructions and prior knowledge. *J. Exp. Child Psychol.* 50, 305–321.

Droit-Volet, S. (1998). Time estimation in young children: an initial force rule governing time production. *J. Exp. Child Psychol.* 68, 236–249.

Droit-Volet, S. (2002). Scalar timing in temporal generalization in children with short and long durations. *Q. J. Exp. Psychol. A* 55, 1193–1209.

Droit-Volet, S. (2003a). "Temporal experience and timing in children," in *Functional and Neural Mechanisms of Interval Timing*, ed W. H. Meck (Boca Raton, FL: CRC Press LLC), 183–208.

Droit-Volet, S. (2003b). Alerting attention and time perception in children. *J. Exp. Child Psychol.* 85, 372–384.

Droit-Volet, S., Cleìment, A., and Fayol, M. (2003). Time and number discrimination in a bisection task with a sequence of stimuli: a developmental approach. *J. Exp. Child Psychol.* 84, 63–76.

Droit-Volet, S., Cleìment, A., and Fayol, M. (2008). Time, number and length: similarities and differences in discrimination in adults and children. *Q. J. Exp. Psychol.* 61, 1827–1846.

Droit-Volet, S., Clément, A., and Wearden, J. H. (2001). Temporal generalization in 3- to 8-year-old children. *J. Exp. Child Psychol.* 80, 271–288.

Droit-Volet, S., and Meck, W. H. (2007). How emotions colour our perception of time. *Trends Cogn. Sci.* 11, 504–513.

Droit-Volet, S., Meck, W. H., and Penney, T. B. (2007). Sensory modality and time perception in children and adults. *Behav. Processes* 74, 244–250.

Droit-Volet, S., and Rattat, A-C. (1999). Are time and action dissociated in young children's time estimation? *Cogn. Dev.* 14, 573–595.

Droit-Volet, S., Tourret, S., and Wearden, J. (2004). Perception of the duration of auditory and visual stimuli in children and adults. *Q. J. Exp. Psychol. A* 57, 797–818.

Droit-Volet, S., and Wearden, J. H. (2001). Temporal bisection in children. *J. Exp. Child Psychol.* 80, 142–159.

Eger, E., Sterzer, P., Russ, M. O., Giraud, A. L., and Kleinschmidt, A. (2003). A supramodal number representation in human intraparietal cortex. *Neuron* 37, 719–725.

Eimas, P. D., and Miller, J. L. (1980). Contextual effects in infant speech perception. *Science* 209, 1140–1141.

Emmerton, J. (1998). Numerosity differences and effects of stimulus density on pigeons' discrimination performance. *Anim. Learn. Behav.* 26, 243–256.

Falter, C. M., and Noreika, V. (2011). Interval timing deficits and abnormal cognitive development. *Front. Integr. Neurosci.* 5:26. doi: 10.3389/fnint.2011.00026

Feigenson, L. (2005). A double-dissociation in infants' representations of object arrays. *Cognition* 95, B37–48.

Feigenson, L. (2007). The equality of quantity. *Trends Cogn. Sci.* 11, 185–187.

Feigenson, L., Carey, S., and Hauser, M. D. (2002). Infant's spontaneous judgements of ordinality. *Psychol. Sci.* 13, 150–156.

Feigenson, L., Carey, S., and Spelke, E. (2002). Infants' discrimination of number vs. continuous extent. *Cogn. Psychol.* 44, 33–66.

Feigenson, L., Dehaene, S., and Spelke, E. (2004). Core systems of number. *Trends Cogn. Sci.* 8, 307–314.

Feron, J., Gentaz, E., and Streri, A. (2006). Evidence of amodal representation of small numbers across visuo-tactile modalities in 5-month-old infants. *Cogn. Dev.* 21, 81–92.

Fetterman, J. G. (1993). Numerosity discrimination: both time and number matter. *J. Exp. Psychol. Anim. Behav. Process.* 19, 149–164.

Fetterman, J. G., and MacEwen, D. (1989). Short-term memory for responses: the "choose-small" effect. *J. Exp. Anal. Behav.* 52, 311–324.

Fias, W., Lammertyn, J., Reynvoet, B., Dupont, P., and Orban, G. A. (2003). Parietal representation of symbolic and nonsymbolic magnitude. *J. Cogn. Neurosci.* 15, 47–56.

Fraisse, P. (1967). *Psychology of Time*. Paris: PUF.

Frassinetti, F., Magnani, B., and Oliveri, M. (2009). Prismatic lenses shift time perception. *Psychol. Sci.* 20, 949–954.

Fuson, K. (1992). "Relationships between counting and cardinality from age 2 to age 8," in *Pathways to Number: Children's Developing Numerical Abilities*, eds J. Bideaud, C. Meljac, and J. P. Fischer (Hillsdale, NJ: Lawrence Erlbaum Associates), 349–361.

Gallistel, C. R. (1989). Animal cognition: the representation of space, time and number. *Ann. Rev. Psychol.* 40, 155–189.

Gallistel, C. R. (1990). *The Organization of Learning*. Cambridge, MA: MIT Press.

Gallistel, C. R., and Gelman, R. (1992). Preverbal and verbal counting and computation. *Cognition* 44, 43–74.

Gallistel, C. R., and Gelman, R. (2000). Non-verbal numerical cognition: from reals to integers. *Trends Cogn. Sci.* 4, 59–65.

Gautier, T., and Droit-Volet, S. (2001). Attention and time estimation in 5- and 8-year-old children: a dual-task procedure. *Behav. Processes.* 28, 57–66.

Geary, D. C., Hoard, M. K., Byrd-Craven, J., Nugent, L., and Numtee, C. (2007). Cognitive mechanisms underlying achievement deficits in children with mathematical learning disability. *Child Dev.* 78, 1343–1359.

Gelman, R., and Cohen, M. (1988). "Qualitative differences in the way Down syndrome and normal children solve a novel counting problem," in *The Psychobiology of Down's Syndrome*, ed L. Nadel (Cambridge, MA: MIT Press), 51–99.

Gelman, R., and Cordes, S. (2001). "Counting in animals and humans," in *Language, Brain, and Cognitive Development: Essays in Honor of Jacques Mehler*, ed E. Dupoux (Cambridge, MA: MIT Press), 279–301.

Gelman, R., and Gallistel, C. R. (1978). *The Child's Understanding of Number*. Cambridge, MA: Harvard University Press.

Gelman, R., and Gallistel, C. R. (2004). Language and the origin of numerical concepts. *Science* 306, 441–443.

Gibbon, J. (1977). Scalar expectancy theory and Weber's Law in

animal timing. *Psychol. Rev.* 84, 279–325.
Gibbon, J., and Church, R. M. (1981). Time left: linear versus logarithmic subjective time. *J. Exp. Psychol. Anim. Behav. Process.* 7, 87–107.
Gibbon, J., Church, R. M., and Meck, W. H. (1984). Scalar timing in memory. *Ann. N.Y. Acad. Sci.* 423, 52–77.
Gibbon, J., Malapani, C., Dale, C. L., and Gallistel, C. (1997). Toward a neurobiology of temporal cognition: advances and challenges. *Curr. Opin. Neurobiol.* 7, 170–184.
Grondin, S., Meilleur-Wells, G., and Lachance, R. (1999). When to start explicit counting in a time-intervals discrimination task: a critical point in the timing process of humans. *J. Exp. Psychol. Hum. Percept. Perform.* 25, 993–1004.
González-Garrido, A. A., Ruiz-Sandoval, J. L., Gomez-Velazquez, F. R., de Alba, J. L., and Villasenor-Cabrera, T. (2002). Hypercalculia in savant syndrome: central executive failure. *Arch. Med. Res.* 33, 586–589.
Gooch, D., Snowling, M., and Hulme, C. (2011). Time perception, phonological skills and executive function in children with dyslexia and/or ADHD symptoms. *J. Child Psychol. Psychiatry* 52, 195–203.
Gu, B. M., and Meck, W. H. (2011). New perspectives on Vierordt's law: memory-mixing in ordinal temporal comparison tasks. *Lect. Notes Comp. Sci.* 6789 LNAI, 67–78.
Halberda, J., and Feigenson, L. (2008). Developmental change in the acuity of the "Number Sense": the approximate number system in 3-, 4-, 5-, and 6- year olds and adults. *Dev. Psychol.* 44, 1457–1465.
Harrington, D. L., Boyd, L. A., Mayer, A. R., Sheltraw, D. M., Lee, R. R., Huang, M., and Rao, S. M. (2004). Neural representation of interval encoding and decision making. *Cogn. Brain Res.* 21, 193–205.
Harrington, D. L., Castillo, G. N., Fong, C. H., and Reed, J. D. (2011). Neural underpinnings of distortions in the experience of time across senses. *Front. Integr. Neurosci.* 5:32. doi: 10.3389/fnint.2011.00032
Harrington, D. L., and Haaland, K. Y. (1999). Neural underpinnings of temporal processing: a review of focal lesion, pharmacological, and functional imaging research. *Rev. Neurosci.* 10, 91–116.
Harrington, D. L., Zimbelman, J. L., Hinton, S. C., and Rao, S. M. (2010). Neural modulation of temporal encoding, maintenance, and decision processes. *Cereb Cortex.* 20, 1274–1285.
Henik, A., Rubinsten, O., and Ashkenazi, S. (2011). The "where" and "what" in developmental dyscalculia. *Clin. Neuropsychol.* 25, 989–1008.
Heine, A., Tamm, S., Wissmann, J., and Jacobs, A. M. (2011). Electrophysiological correlates of non-symbolic numerical magnitude processing in children: joining the dots. *Neuropsychologia* 49, 3238–3246.
Hinton, S. C., Harrington, D. L., Binder, J. R., Durgerian, S., and Rao, S. M. (2004). Neural systems supporting timing and chronometric counting: an FMRI study. *Cogn. Brain Res.* 21, 183–192.
Hinton, S. C., and Meck, W. H. (1997). The 'internal clocks' of circadian and interval timing. *Endeavour* 21, 82–87.
Hinton, S. C., and Meck, W. H. (2004). Frontal-striatal circuitry activated by human peak-interval timing in the supra-seconds range. *Cogn. Brain Res.* 21, 171–182.
Hinton, S. C., and Rao, S. M. (2004). "One-thousand one . . . one-thousand two . . .": chronometric counting violates the scalar property in interval timing. *Psychon. Bull. Rev.* 11, 24–30.
Hoeckner, S. H., Moeller, K., Zauner, H., Wood, G., Haider, C., Gassner, A., and Nuerk, H. C. (2008). Impairments of the mental number line for two-digit numbers in neglect. *Cortex* 44, 429–438.
Holloway, I. D., and Ansari, D. (2010). Developmental specialization in the right intraparietal sulcus for the abstract representation of numerical magnitude. *J. Cogn. Neurosci.* 22, 2627–2637.
Holmes, K. J., and Lourenco, S. F. (2009). "Spatial organization of magnitude in the representation of number and emotion," in *Proceedings of the 31th Annual Conference of the Cognitive Science Society*, eds N. A. Taatgen and H. van Rijn (Austin, TX: Cognitive Science Society), 2402–2407.
Hubbard, E. M., Piazza, M., Pinel, P., and Dehaene, S. (2005). Interactions between number and space in parietal cortex. *Nat. Rev. Neurosci.* 6, 435–448.
Huntley-Fenner, G. (2001). Children's understanding of number is similar to adults' and rats': numerical estimation by 5–7-year-olds. *Cognition* 78, B27–40.
Huntley-Fenner, G., and Cannon, E. (2000). Preschoolers' magnitude comparisons are mediated by a preverbal analog mechanism. *Psychol. Sci.* 11, 147–152.
Huttenlocher, J., Jordan, N. C., and Levine, S. C. (1994). A mental model for early arithmetic. *J. Exp. Psychol. Gen.* 123, 284–296.
Hyde, D. C. (2011). Two systems of non-symbolic numerical cognition. *Front. Hum. Neurosci.* 5:150. doi: 10.3389/fnhum.2011.00150
Hyde, D. S., Boas, D. A., Blair, C., and Carey, S. (2010). Near-infrared spectroscopy shows right parietal specialization for number in pre-verbal infants. *Neuroimage* 53, 647–652.
Hyde, D. C., and Spelke, E. S. (2011). Neural signatures of number processing in human infants: evidence for two core systems underlying numerical cognition. *Dev. Sci.* 360–371.
Hyde, D. C., and Spelke, E. S. (2012). Spatiotemporal dynamics of processing nonsymbolic number: an event-related potential source localization study. *Hum. Brain Mapp.* (in press).
Izard, V., Dehaene-Lambertz, G., and Dehaene, S. (2008). Distinct cerebral pathways for object identity and number in human infants. *PLoS Biol.* 6:e11. doi: 10.1371/journal.pbio.0060011
Izard, V., Sann, C., Spelke, E. S., and Streri, A. (2009). Newborn infants perceive abstract numbers. *Proc. Natl. Acad. Sci. U.S.A.* 106, 10382–10385.
Jaffe, J., Beebe, B., Feldstein, S., Crown, C., and Jasnow, M. (2001). Rhythms of dialogue in infancy. *Monogr. Soc. Res. Child Dev.* 66 (2 Serial No. 265).
Jahanshahi, M., Jones, C. R., Dirnberger, G., and Frith, C. D. (2006). The substantia nigra pars compacta and temporal processing. *J. Neurosci.* 22, 12266–12273.
Jevons, W. S. (1871). The power of numerical discrimination. *Nature* 363–372.
Jones, C. R., Happé, F., Baird, G., Simonoff, E., Marsden, A. J., Tregay, J., Phillips, R. J., Goswami, U., Thomson, J. M., and Thompson, J. M. (2009a). Auditory discrimination and auditory sensory behaviors in autism spectrum disorders. *Neuropsychologia* 47, 2850–2858.
Jones, C. R., Happé, F., Golden, H., Marsden, A. J., Tregay, J., Simonoff, E., Pickles, A., Baird, G., and Charman, T. (2009b). Reading and arithmetic in adolescents with autism spectrum disorders: peak and dips in attainment. *Neuropsychology* 23, 718–728.
Jordan, K. E., and Brannon, E. M. (2006). The multisensory representation of number in infancy. *Proc. Natl. Acad. Sci. U.S.A.* 103, 3486–3489.
Jordan, N. C., Kaplan, D., Olah, L. N., and Locuniak, M. N. (2006). Number sense growth in kindergarten: a longitudinal investigation of children at risk for mathematics difficulties. *Child Dev.* 77, 153–175.
Jordan, N. C., Kaplan, D., Locuniak, M. N., and Ramineni, C. (2007). Predicting first-grade math achievement from developmental number sense trajectories. *Learn. Disabil. Res. Pract.* 22, 36–46.
Jordan, K. E., Suanda, S. H., and Brannon, E. M. (2008). Intersensory redundancy accelerates preverbal numerical competence. *Cognition* 108, 210–212.
Jordan, N. C., Kaplan, D., Ramineni, C., and Locuniak, M. N. (2009). Early math matters: kindergarten number competence and later mathematics outcomes. *Dev. Psychol.* 45, 850–867.
Jusczyk, P. W., Pisoni, D. B., Reed, M. A., Fernald, A., and Myers, M. (1983). Infants' discrimination of the duration of a rapid spectrum change in nonspeech signals. *Science* 222, 175–177.
Kadosh, R. C., Kadosh, K. C., Linden, D. E. J., Gevers, W., Berger, A., and Henik, A. (2005). The brain locus of interaction between number and size: a combined functional magnetic resonance imaging and event-related potential study. *J. Cogn. Neurosci.* 19, 957–970.
Kahneman, D., Treisman, A., and Gibbs, B. J. (1992). The reviewing of object files: object-specific integration of information. *Cogn. Psychol.* 24, 175–219.
Kaiser, M. D., Hudac, C. M., Shultz, S., Lee, S. M., Cheung, C., Berken, A. M., Deen, B., Pitskel, N. B., Sugrue, D. R., Voos, A. C., Saulnier, C. A., Ventola, P., Wolf, J. M., Klin, A., Vander Wyk, B. C., and Pelphrey, K. A. (2010). Neural signatures of autism. *Proc. Natl. Acad. Sci. U.S.A.* 107, 21223–21228.
Kaufmann, L., Koppelstaetter, F., Siedentopf, C., Haala, I., Haberlandt, E., Zimmerhackl, L-B., Felber, S., and Ischebeck, A. (2006). Neural correlates of a number–size interference task in children. *Neuroreport* 17, 587–591.
Kaufmann, L., and Nuerk, H. C. (2006). Interference effects in a numerical Stroop paradigm in 9- to 12-year-old children with ADHD-C. *Child Neuropsychol.* 12, 223–243.
Kaufmann L., and Neurk, H. C. (2008). Basic number processing deficits in ADHD: a broad examination of elementary and complex number

processing skills in 9- to 12-year-old children with ADHD-C. *Dev. Sci.* 11, 692–699.

Kaufmann, L., Vogel, S. E., Starke, M., Kremser, C., Schocke, M., and Wood, G. (2009). Developmental dyscalculia: compensatory mechanisms in left intraparietal regions in response to nonsymbolic magnitudes. *Behav. Brain Funct.* 5, 35.

Kaufmann, L., Vogel, S. E., Wood, G., Kremser, C., Schocke, M., Zimmerhacki, L. B., and Koten, J. W. (2008). A developmental fMRI study of nonsymbolic numerical and spatial processing. *Cortex* 44, 376–385.

Killeen, P. R., and Fetterman, J. G. (1988). A behavioral theory of timing. *Psychol. Rev.* 95, 274–295.

Kobayashi, T., Hiraki, K., Mugitani, R., and Hasegawa, T. (2004). Baby arithmetic: one object plus one tone. *Cognition* 91, B23–B34.

Kopec, C. D., and Brody, C. D. (2010). Human pereformance on the temporal bisection task. *Brain Cogn.* 74, 262–272.

Kotz, S. A. E., and Schwartze, M. (2011). Differential input of the supplementary motor area to a dedicated temporal processing network: functional and clinical implications. *Front. Integr. Neurosci.* 5:86. doi: 10.3389/fnint.2011.00086

Krajcsi, A., Lukacs, A., Igacs, J., Racsmany, M., and Pleh, C. (2009). Numerical abilities in Williams syndrome: dissociating the analogue magnitude system and verbal retrieval. *J. Clin. Exp. Neuropsychol.* 31, 439–446.

Kramer, P., Bressan, P., and Grassi, M. (2011). Time estimation predicts mathematical intelligence. *PLoS One* 6:e28621. doi: 10.1371/journal.pone.0028621

Kwakye, L. D., Foss-Feig, J. H., Cascio, C. J., Stone, W. L., and Wallace, M. T. (2011). Altered auditory and multisensory temporal processing in autism spectrum disorders. *Front. Integr. Neurosci.* 4:129. doi: 10.3389/fnint.2010.00129

Lalli, J. S., Casey, S., Goh, H., and Merlino, J. (1994). Treatment of escape-maintained aberrant behavior with escape extinction and predictable routines. *J. Appl. Behav. Anal.* 27, 705–714.

Landerl, K., Bevan, A., and Butterworth, B. (2004). Developmental dyscalculia and basic numerical capacities: a case study of 8–9-year-old students. *Cognition* 93, 99–125.

Le Clec'h, H. G., Dehaene, S., Cohen, L., Mehler, J., Dupoux, E., Poline, J. B., Lehéricy, S., van de Moortele, P. F., and Le Bihan, D. (2000). Distinct cortical areas for names of numbers and body parts independent of language and input modality. *Neuroimage* 12, 381–391.

Le Corre, M., and Carey, S. (2007). One, two, three, four, nothing more: an investigation of the conceptual sources of the verbal counting principles. *Cognition* 105, 395–438.

Le Corre, M., and Carey, S. (2008). Why the verbal counting principles are constructed out of representations of small sets of individuals: a reply to Gallistel. *Cognition* 107, 650–662.

Leon, M. I., and Shadlen, M. N. (2003). Representation of time by neurons in the posterior parietal cortex of the macaque. *Neuron* 38, 317–327.

Levin, I. (1977). The development of time concepts in young children: reasoning about duration. *Child Dev.* 48, 435–444.

Levin, I. (1979). Interference of time related and unrelated cues with duration comparisons of young children: analysis of Piaget's formulation of the relation of time and speed. *Child Dev.* 50, 469–477.

Levin, I. (1982). "The nature and development of time concepts in children. The effects of interfering cues," in *The Developmental Psychology of Time*, ed W. J. Friedman (New York, NY: Academic Press), 47–85.

Libertus, M. E., and Brannon, E. M. (2010). Stable individual differences in number discrimination in infancy. *Dev. Sci.* 13, 900–906.

Libertus, M. E., Feigenson, L., and Halberda, J. (2011a). Preschool acuity of the approximate number system correlates with school math ability. *Dev. Sci.* 14, 1292–1300.

Libertus, M. E., Brannon, E. M., and Woldorff, M. G. (2011b). Parallels in stimulus-driven oscillatory brain responses to numerosity changes in adults and seven-month-old infants. *Dev. Neuropsychol.* 36, 651–667.

Libertus, M. E., Pruitt, L. B., Woldorff, M. G., and Brannon, E. M. (2009). Induced alpha-band oscillations reflect ratio-dependent number discrimination in the infant brain. *J. Cogn. Neurosci.* 21, 2398–2406.

Libertus, M. E., Woldorff, M. G., and Brannon, E. M. (2007). Electrophysiological evidence for notation independence in numerical processing. *Behav. Brain Funct.* 3, 1.

Lipton, J. S., and Spelke, E. S. (2003). Origins of number sense. Large-number discrimination in human infants. *Psychol. Sci.* 14, 396–401.

Lipton, J. S., and Spelke, E. S. (2005). Preschool children's mapping of number words to nonsymbolic numerosities. *Child Dev.* 76, 978–988.

Loetscher, T., Schwarz, U., Schubiger, M., and Brugger, P. (2008). Head turns bias the brain's internal random generator. *Curr. Biol.* 18, R60–R62.

Longo, M. R., and Lourenco, S. F. (2010). Bisecting the mental number line in near and far space. *Brain Cogn.* 72, 362–367.

Lourenco, S. F., and Longo, M. R. (2010). General magnitude representation in human infants. *Psychol. Sci.* 21, 873–881.

Lustig, C. (2011). The neuroscience of time and number: untying the Gordian knot. *Front. Integr. Neurosci.* 5:47. doi: 10.3389/fnint.2011.00047

Lustig, C., Matell, M. S., and Meck, W. H. (2005). Not "just" a coincidence: frontal-striatal synchronization in working memory and interval timing. *Memory* 13, 441–448.

Lustig, C., and Meck, W. H. (2001). Paying attention to time as one gets older. *Psychol. Sci.* 12, 478–484.

Lustig, C., and Meck, W. H. (2005). Chronic treatment with haloperidol induces working memory deficits in feedback effects of interval timing. *Brain Cogn.* 58, 9–16.

Lustig, C., and Meck, W. H. (2011). Modality differences in timing and temporal memory throughout the lifespan. *Brain Cogn.* 77, 298–303.

Macar, F., Lejeune, H., Bonnet, M., Ferrara, A., Pouthas, V., Vidal, F., and Maquet, P. (2002). Activation of the supplementary motor area and of attentional networks during temporal processing. *Exp. Brain Res.* 142, 475–485.

Martin, J. S., Poirier, M., and Bowler, D. M. (2009). Brief report: impaired temporal reproduction performance in adults with autism spectrum disorder. *J. Austim Dev. Disord.* 40, 640–646.

Matell, M. S., Bateson, M., and Meck, W. H. (2006). Single-trials analyses demonstrate that increases in clock speed contribute to the methamphetamine-induced horizontal shifts in peak-inetrval timing functions. *Psychopharmacology* 188, 201–212.

Matell, M. S., King, G. R., and Meck, W. H. (2004). Differential adjustment of interval timing by the chronic administation of intermittent or continuous cocaine. *Behav. Neurosci.* 118, 150–156.

Matell, M. S., and Meck, W. H. (2000). Neuropsychological mechanisms of interval timing behavior. *Bioessays* 22, 94–103.

Matell, M. S., and Meck, W. H. (2004). Cortico-striatal circuits and interval timing: coincidence-detection of oscillatory processes. *Cogn. Brain Res.* 21, 139–170.

Matell, M. S., Meck, W. H., and Nicolelis, M. A. L. (2003). Interval timing and the encoding of signal duration by ensembles of cortical and striatal neurons. *Behav. Neurosci.* 117, 760–773.

Matell, M. S., Shea-Brown, E., Gooch, C., Wilson, A. G., and Rinzel, J. (2011). A heterogeneous population code for elapsed time in rat medial agranular cortex. *Behav. Neurosci.* 125, 54–73.

Matsuzawa, T. (1985). Use of numbers by a chimpanzee. *Nature* 315, 57–59.

Maquet, P., Lejeune, H., Pouthas, V., Bonnet, M., Casini, L., Macar, F., Timsit-Berthier, M., Vidal, F., Ferrara, A., Degueldre, C., Quaglia, L., Delfiore, G., Luxen, A., Woods, R., Mazziotta, J. C., and Comar, D. (1996). Brain activation induced by estimation of duration: a PET study. *Neuroimage* 3, 119–126.

McCormack, T., Brown, G. D. A., Maylor, E. A., Darby, R. J., and Green, D. (1999). Developmental changes in time estimation: comparing childhood and old age. *Dev. Psychol.* 35, 1143–1155.

McCormack, T., Brown, G. D., Smith, M. C., and Brock, J. (2004). A timing-specific memory disortion effects in young children. *J. Exp. Child Psychol.* 87, 33–56.

McCrink, K., and Wynn, K. (2004). Large-number addition and subtraction by 9-month-old infants. *Psychol. Sci.* 15, 776–781.

Meck, W. H. (1983). Selective adjustment of the speed of internal clock and memory processes. *J. Exp. Psychol. Anim. Behav. Process.* 9, 171–201.

Meck, W. H. (1984). Attentional bias between modalities: effect on the internal clock, memory, and decision stages used in animal time discrimination. *Ann. N.Y. Acad. Sci.* 423, 528–541.

Meck, W. H. (1996). Neuropharmacology of timing and time perception. *Cogn. Brain Res.* 3, 227–242.

Meck, W. H. (1997). "Application of a mode-control model of temporal integration to counting and timing behaviour," in *Time and Behaviour: Psychological and Neurobiological Analyses*, eds. C. M. Bradshaw and E. Szabadi (New York, NY: Elsevier), 133–184.

Meck, W. H. (2003). *Functional and Neural Mechanisms of Interval Timing.* Boca Raton, FL: CRC Press LLC.

Meck, W. H. (2005). Neuropsychology of timing and time perception. *Brain Cogn.* 58, 1–8.

Meck, W. H. (2006a). Frontal cortex lesions eliminate the clock speed effect of dopaminergic drugs on interval timing. *Brain Res.* 1108, 157–167.

Meck, W. H. (2006b). Neuroanatomical localization of an internal clock: a functional link between mesolimbic, nigrostriatal, and mesocortical dopaminergic systems. *Brain Res.* 1109, 93–107.

Meck, W. H., and Benson, A. M. (2002). Dissecting the brain's internal clock: how frontal-stratial circuitry keeps time and shifts attention. *Brain Cogn.* 48, 195–211.

Meck, W. H., and Church, R. M. (1983). A mode-control model of counting and timing processes. *J. Exp. Psychol. Anim. Behav. Process.* 9, 320–334.

Meck, W. H., and Church, R. M. (1987). Cholinergic modulation of the content of temporal memory. *Behav. Neurosci.* 101, 457–464.

Meck, W. H., Church, R. M., and Gibbon, J. (1985). Temporal integration in duration and number discrimination. *J. Exp. Psychol. Anim. Behav. Process.* 11, 591–597.

Meck, W. H., and Malapani, C. (2004). Neuroimaging of interval timing. *Cogn. Brain Res.* 21, 133–137.

Meck, W. H., Penney, T. B., and Pouthas, V. (2008). Cortico-striatal representation of time in animals and humans. *Curr. Opin. Neurobiol.* 18, 145–152.

Meck, W. H., and Williams, C. L. (1997). Characterization of the facilitative effects of perinatal choline supplementation on timing and temporal memory. *Neuroreport* 8, 2831–2835.

Melgire, M., Ragot, R., Samson, S., Penney, T. B., Meck, W. H., and Pouthas, V. (2005). Auditory/visual duration bisection in patients with left or right medial-temporal lobe resection. *Brain Cogn.* 58, 119–124.

Mix, K. S. (1999). Preschoolers' recognition of numerical equivalence: sequential sets. *J. Exp. Child Psychol.* 74, 309–332.

Mix, K. S., Huttenlocher, J., and Levine, S. C. (1996). Do preschool children recognize auditory-visual numerical correspondences? *Child Dev.* 67, 1592–1608.

Mix, K. S., Huttenlocher, J., and Levine, S. C. (2002). Multiple cues for quantification in infancy: is number one of them? *Psychol. Bull.* 128, 278–294.

Mix, K. S., Moore, J. A., and Holcomb, E. (2011). One-to-one correspondence promotes numerical equivalence concepts. *J. Cogn. Dev.* 12, 463–480.

Möhring, W., Libertus, M. E., and Bertin, E. (2012). Speed discrimination in 6- and 10-month-old infants follows Weber's law. *J. Exp. Child Psychol.* 111, 405–418.

Moyer, R. S., and Landauer, T. K. (1967). Time required for judgments of numerical inequality. *Nature* 215, 1519–1520.

Mussolin, C., De Volder, A., Grandin, C., Schlogel, X., Nassogne, M-C., and Noel, M-P. (2009). Neural correlates of symbolic number comparison in developmental dyscalculia. *J. Cogn. Neurosci.* 22, 860–874.

Myers, G. E. (1971). Williams James on time perception. *Philos. Sci.* 38, 353–360.

Naccache, L., and Dehaene, S. (2001). The priming method: imaging unconscious repetition priming reveals an abstract representation of number in the parietal lobes. *Cereb. Cortex* 11, 966–974.

Navon, D. (1978). On a conceptual hierarchy of time, space, and other dimensions. *Cognition* 6, 223–228.

Nenadic, I., Gaser, C., Volz, H. P., Rammsayer, T., Hager, F., and Sauer, H. (2003). Processing of temporal information and the basal ganglia: new evidence from fMRI. *Exp. Brain Res.* 148, 238–246.

Newcombe, N. S. (2002). The nativist-empiricist controversy in the context of recent research on spatial and quantitative development. *Psychol. Sci.* 13, 395–401.

Nicholls, M. E., Forte, J. D., Loetscher, T., Orr, C. A., Yates, M. J., and Bradshaw, J. L. (2011a). Near, yet so far: the effect of pictorial cues on spatial attention. *Brain Cogn.* 76, 349–352.

Nicholls, M. E., Lew, M., Loetscher, T., and Yates, M. J. (2011b). The importance of response type to the relationship between temporal order and numerical magnitude. *Atten. Percept. Psychophys.* 73, 1604–1613.

Nicholls, M. E. R., Loftus, A., and Gevers, W. (2008). Look, no hands: a perceptual task shows that number magnitude induces shifts of attention. *Psychon. Bull. Rev.* 15, 413–418.

Nieder, A. (2004). The number domain- can we count on parietal cortex? *Neuron* 44, 407–409.

Nieder, A., Freedman, D. J., and Miller, E. K. (2002). Representation of the quantity of visual items in the primate prefrontal cortex. *Science* 297, 1708–1711.

Nieder, A., and Miller, E. K. (2003). Coding of cognitive magnitude: compressed scaling of numerical information in the primate prefrontal cortex. *Neuron* 37, 149–157.

Nieder, A., and Miller, E. K. (2004a). Analog numerical representations in Rhesus monkeys: evidence for parallel processing. *J. Cogn. Neurosci.* 16, 889–901.

Nieder, A., and Miller, E. K. (2004b). A parieto-frontal network for visual numerical information in the monkey. *Proc. Natl. Acad. Sci. U.S.A.* 101, 7457–7462.

Nye, J., Fluck, M., and Buckley, S. (2001). Counting and cardinal understanding in children with Down syndrome and typically developing children. *Down Syndr. Res. Pract.* 7, 68–78.

O'Hearn, K., Hoffman, J. E., and Landau, B. (2011). Small subitizing range in people with Williams syndrome. *Vis. Cogn.* 19, 289–312.

O'Hearn, K., and Luna, B. (2009). Mathematical skills in Williams syndrome: Insight into the importance of underlying representations. *Dev. Disabil. Res. Rev.* 15, 11–20.

O'Hearn, K., and Landau, B. (2007). Mathematical skill in individuals with Williams syndrome: evidence from a standardized mathematics battery. *Brain Cogn.* 64, 238–246.

Oliveri, M., Vicario, C. M., Salerno, S., Koch, G., Turriziani, P., Mangano, R., Chillemi, G., and Caltagirone, C. (2008). Perceiving numbers alters time perception. *Neurosci. Lett.* 438, 308–311.

Ornstein, R. (1969). *On the Experience of Time.* Harmondsworth, UK: Penguin.

Pastor, M. A., Day, B. L., Macaluso, E., Friston, K. J., and Frackowiak, R. S. (2004). The functional neuroanatomy of temporal discrimination. *J. Neurosci.* 24, 2585–2591.

Paterson, S. J., Girelli, L., Butterworth, B., and Karmiloff-Smith, A. (2006). Are numerical impairments syndrome specific? Evidence from Williams syndrome and Down's syndrome. *J. Child Psychol. Psychiatry* 47, 190–204.

Penney, T. B., Gibbon, J., and Meck, W. H. (2000). Differential effects of auditory and visual signals on clock speed and temporal memory. *J. Exp. Psychol. Hum. Percept. Perform.* 26, 1770–1787.

Penney, T. B., Gibbon, J., and Meck, W. H. (2008). Categorical scaling of duration bisection in pigeons (Columba livia), mice (Mus musculus), and humans (homo sapiens). *Psychol. Sci.*19, 1103–1109.

Pepperberg, I. M. (2006). Ordinality and inferential abilities of a Grey Parrot (Psittacus erithacus). *J. Comp. Psychol.* 120, 205–216.

Pesenti, M., Thioux, M., Seron, X., and De Volder, A. (2000). Neuroanatomical substrates of Arabic number processing, numerical comparison, and simple addition: a PET study. *J. Cogn. Neurosci.* 12, 461–479.

Pessoa, L., and Desimone, R. (2003). From humble neural beginnings comes knowledge of numbers. *Neuron* 37, 4–6.

Pezzulo, G., and Rigoli, F. (2011). The value of foresight: how prospection affects decision-making, *Front. Neurosci.* 5:79. doi: 10.3389/fnins.2011.00079

Piaget, J. (1946). *The Development of the Notion of Time in Children.* Paris: PUF.

Piaget, J. (1952). *The Child's Conception of Number.* New York, NY: Norton.

Piazza, M., Izard, V., Pinel, P., Le Bihan, D., and Dehaene, S. (2004). Tuning curves for approximate numerosity in the human intraparietal sulcus. *Neuron* 44, 547–555.

Piazza, M., Mechelli, A., Butterworth, B., and Price, C. J. (2002). Are subitizing and counting implemented as separate or functionally overlapping processes? *Neuroimage* 15, 435–446.

Piazza, M., Pinel, P., Le Bihan, D., and Dehaene, S. (2007). A magnitude code common to numerosities and number symbols in human intraparietal cortex. *Neuron* 53, 293–305.

Pinel, P., and Dehaene, S. (2010). Beyond hemispheric dominance: brain regions underlying the joint lateralization of language and arithmetic to the left hemisphere. *J. Cogn. Neurosci.* 22, 48–66.

Pinel, P., Dehaene, S., Rivière, D., and LeBihan, D. (2001). Modulation of parietal activation by semantic distance in a number comparison task. *Neuroimage* 14, 1013–1026.

Pinel, P., Piazza, M., Le Bihan, D., and Dehaene, S. (2004). Distributed and overlapping cerebral representations of number, size, and luminance during comparative judgments. *Neuron* 41, 983–993.

Porter, J. (1999). Learning to count: a difficult task? *Down Syndr. Res. Pract.* 6, 85–94.

Pouthas, V. (2003). "Electrophysiological evidence for specific processing of temporal information in humans," in *Functional and Neural Mechanisms of Interval*

Timing, ed W. H. Meck (Boca Raton, FL: CRC Press LLC), 439–456.

Pouthas, V., Droit, S., Jacquet, A. Y., and Wearden, J. (1990). Temporal differentiation of response duration in children of different ages: developmental changes in relations between verbal and nonverbal behavior. *J. Exp. Anal. Behav.* 53, 21–31.

Pouthas, V., George, N., Poline, J. B., Pfeuty, M., Vandemoorteele, P. F., Hugueville, L., Ferrandez, A. M., Lehéricy, S., Lebihan, D., and Renault, B. (2005). Neural network involved in time perception: an fMRI study comparing long and short interval estimation. *Hum. Brain Mapp.* 25, 433–441.

Provasi, J., Rattat, A. C., and Droit-Volet, S. (2011). Temporal bisection in 4-month olds. *J. Exp. Psychol. Anim. Behav. Process.* 37, 108–113.

Rao, S. M., Mayer, A. R., and Harrington, D. L. (2001). The evolution of brain activation during temporal processing. *Nat. Neurosci.* 4, 317–323.

Rattat, A. C., and Droit-Volet, S. (2005). The long-term retention of time: a developmental study. *Q. J. Exp. Psychol. B* 58, 163–176.

Revkin, S. K., Piazza, M., Izard, V., Cohen, L., and Dehaene, S. (2008). Does subitizing reflect numerical estimation? *Psychol. Sci.* 19, 607–614.

Rivera, S. M., Reiss, A. L., Eckert, M. A., and Menon, V. (2005). Developmental changes in mental arithmetic: evidence for increased functional specialization in the left inferior parietal cortex. *Cereb. Cortex* 15, 1779–1790.

Roberts, W. A. (1995). Simultaneous numerical and temporal processing in the pigeon. *Curr. Dir. Psychol. Sci.* 4, 47–51.

Roberts, W. A. (2002). Are animals stuck in time? *Psychol. Bull.* 128, 473–489.

Roberts, W. A., and Boisvert, M. J. (1998). Using the peak procedure to measure timing and counting processes in pigeons. *J. Exp. Psychol. Anim. Behav. Process.* 24, 416–430.

Roberts, W. A., Coughlin, R., and Roberts, S. (2000). Pigeons flexibly time or count on cue. *Psychol. Sci.* 11, 218–222.

Roberts, W. A., Macuda, T., and Brodbeck, D. R. (1995). Memory for number of light flashes in the pigeon. *Anim. Learn. Behav.* 23, 182–188.

Roberts, W. A., and Mitchell, S. (1994). Can a pigeon simultaneously process temporal and numerical information? *J. Exp. Psychol. Anim. Behav. Process.* 20, 66–78.

Roitman, J. D., Brannon, E. M., Andrews, J. R., and Platt, M. L. (2007). Nonverbal representation of time and number in adults. *Acta Psychol.* 124, 296–318.

Rousselle, L., and Noël, M. P. (2007). Basic numerical skills in children with mathematics learning disabilities: a comparison of symbolic vs. non-symbolic number magnitude processing. *Cognition* 102, 361–395.

Rousselle, L., Palmers, E., and Noel, M. P. (2004). Magnitude comparison in preschoolers: what counts? Influence of perceptual variables. *J. Exp. Child Psychol.* 87, 57–84.

Rubinsten, O., and Henik, A. (2005). Automatic activation of internal magnitudes: a study of developmental dyscalculia. *Neuropsychology* 5, 641–648.

Rumbaugh, D. M., Savage-Rumbaugh, S., and Hegel, M. T. (1987). Summation in the chimpanzee (Pan troglodytes). *J. Exp. Psychol. Anim. Behav. Process.* 13, 107–115.

Sandhofer, C. M., and Smith, L. B. (1999). Learning color words involves learning a system of mappings. *Dev. Psychol.* 35, 668–679.

Santens, S., Roggeman, C., Fias, W., and Verguts, T. (2010). Number processing pathways in human parietal cortex. *Cereb. Cortex* 20, 77–88.

Sarrazin, J. C., Giraudo, M. D., Pailhous, J., and Bootsma, R. J. (2004). Dynamics of balancing space and time in memory: tau and kappa effects revisited. *J. Exp. Psychol. Hum. Percept. Perform.* 30, 411–430.

Schubotz, R. I., Friederici, A. D., and von Cramon, D. Y. (2000). Time perception and motor timing: a common cortical and subcortical basis revealed by fMRI. *Neuroimage* 11, 1–12.

Schubotz, R. I., and von Cramon, D. Y. (2001). Interval and ordinal properties of sequences are associated with distinct premotor areas. *Cereb. Cortex* 11, 210–222.

Sereno, M. I., Pitzalis, S., and Martinez, A. (2001). Mapping of contralateral space in retinotopic coordinates by a parietal cortical area in humans. *Science* 294, 1350–1354.

Shuman, M., and Kanwisher, N. (2004). Numerical magnitude in the human parietal lobe; tests of representational generality and domain specificity. *Neuron* 44, 557–569.

Siegel, L. S. (1974). Heterogeneity and spatial factors as determinants of numeration ability. *Child Dev.* 45, 532–534.

Siegler, R. S., and Booth, J. L. (2004). Development of numerical estimation in young children. *Child Dev.* 75, 428–444.

Siegler, R. S., and Ramani, G. B. (2009). Playing linear number board games-but not circular ones-improves low-income preschoolers' numerical understanding. *J. Educ. Psychol.* 101, 545–560.

Simen, P., Balci, F., deSouza, J., Cohen, J. D., and Holmes, P. (2011). Interval timing by long-range temporal integration. *Front. Integr. Neurosci.* 5:28. doi: 10.3389/fnint.2011.00028

Simon, O., Kherif, F., Flandin, G., Poline, J. B., Riviere, D., Mangin, J. F., LeBihan, D., and Dehane, S. (2004). Automatized clustering and functional geometry of human parietofrontal networks for language, space and number. *Neuroimage* 23, 1192–1202.

Skinner, B. F. (1938). *The Behavior of Organisms.* New York, NY: Appleton-Century.

Skinner, B. F. (1948). "Superstition" in the pigeon. *J. Exp. Psychol.* 38, 168–172.

Smith, L. B., and Sera, M. D. (1992). A developmental analysis of the polar structure of dimensions. *Cogn. Psychol.* 24, 99–142.

Smith, A. B., Taylor, E., Brammer, M., Halari, R., and Rubia, K. (2008). Reduced activation in right lateral prefrontal cortex and anterior cingulated gyrus in medication-naïve adolescents with attention deficit hyperactivity disorder during time discrimination. *J. Child Psychol. Psychiatry* 49, 977–985.

Spaepen, E., Coppola, M., Spelke, E. S., Carey, S. E., and Goldin-Meadow, S. (2011). Number without a language model. *Proc. Natl. Acad. Sci. U.S.A.* 108, 3163–3168.

Spelke, E. (2000). Core knowledge. *Am. Psychol.* 55, 1233–1243.

Spelke, E. (2011). Quinian bootstrapping or Fodorian combination? Core and constructed knowledge of number. *Behav. Brain Sci.* 34, 149–150.

Starkey, P. (1992). The early development of numerical reasoning. *Cognition* 43, 93–126.

Starkey, P., and Cooper, R. G. Jr. (1980). Perception of numbers by human infants. *Science* 210, 1033–1035.

Starkey, P., Spelke, E. S., and Gelman, R. (1983). Detection of intermodal numerical correspondences by human infants. *Science* 222, 179–181.

Starkey, P., Spelke, E. S., and Gelman, R. (1990). Numerical abstraction by human infants. *Cognition* 36, 97–127.

Strauss, M. S., and Curtis, L. E. (1981). Infant perception of numerosity. *Child Dev.* 52, 1146–1152.

Stern, D., and Gibbon, J. (1978). "Temporal expectancies of social behaviors in mother-infant play," in *Origins of the Infant's Social Responsiveness*, ed. E. Thoman (New York, NY: Wiley), 409–429.

Szelag, E., Kowalska, J., Galkowski, T., and Poppel, E. (2004). Temporal processing deficits in high-functioning children with autism. *Br. J. Psychol.* 95, 269–282.

Szucs, D., and Soltesz, F. (2007). Event-related potentials dissociate facilitation and interference effects in the numerical Stroop paradigm. *Neuropsychology* 45, 3190–3202.

Temple, C. M. (1992). "Developmental dyscalculia," in *Handbook of Neuropsychology: Vol. 7, Child Neuropsychology*, eds S. J. Segalowitz and I. Rapin (New York, NY: Elsevier), 211–222.

Temple, E., and Posner, M. I. (1998). Brain mechanisms of quantity are similar in 5-year-old children and adults. *Proc. Natl. Acad. Sci. U.S.A.* 95, 7836–7841.

Thioux, M., Stark, D. E., Klaiman, C., and Schulz, R. T. (2006). The day of the week when you were born in 700 ms: calendar computation in an Autistic savant. *J. Exp. Psychol. Hum. Percept. Perform.* 32, 1155–1168.

Trehub, S. E., and Thorpe, L. A. (1989). Infants' perception of rhythm: categorization of auditory sequences by temporal structure. *Can. J. Psychol.* 43, 217–229.

Treisman, M. (1984). Temporal rhythms and cerebral rhythms. *Ann. N.Y. Acad. Sci.* 423, 542–565.

Trick, L. M., and Pylyshyn, Z. W. (1994). Why are small and large numbers enumerated differently? A limited-capacity preattentive stage in vision. *Psychol. Rev.* 101, 80–102.

Valko, L., Schneider, G., Doehnert, M., Müller, U., Brandeis, D., Steinhausen, H-C., and Drechsler, R. (2010). Time processing in children and adults with ADHD. *J. Neural. Transm.* 117, 1213–1228.

Van Herwegen, J., Ansari, D., Xu, F., and Karmiloff-Smith, A. (2008). Small and large number processing in infants and toddlers with Williams syndrome. *Dev. Sci.* 11, 637–643.

van Loosbroek, E., and Smitsman, A. D. (1990). Visual perception of numerosity in infancy. *Dev. Psychol.* 26, 916–922.

van Marle, K., and Wynn, K. (2006). Six-month old infants use analog

magnitudes to represent duration. *Dev. Sci.* 9, F41–49.
van Rijn, H., Kononowicz, T. W., Meck, W. H., Ng, K. K., and Penney, T. B. (2011). Contingent negative variation and its relation to time estimation: a theoretical evaluation. *Front. Integr. Neurosci.* 5:91. doi: 10.3389/fnint.2011.00091
Vicario, C. M. (2011). Perceiving numbers affects the subjective temporal midpoint. *Perception* 40, 23–29.
Vicario, C. M., Caltagirone, C., and Oliveri, M. (2007). Optokinetic stimulation affects temporal estimation in healthy humans, *Brain Cogn.* 64, 68–73.
Von Gast, H. (1957). Der Umgang mit Zahlen und Zahlge- bilden in der frühen Kindheit. *Zeitschrift für Psychologie* 161, 1–90.
Vuilleumier, P., Ortigue, S., and Brugger, P. (2004). The number space and neglect. *Cortex* 40, 399–410.
Wackermann, J. (2008). Measure of time: a meeting point of psychophyscis and fundamental physics. *Mind Matter* 6, 9–50.
Wallace, G. L., and Happé, F. (2008). Time perception in autism spectrum disorders. *Res. Autism Spectr. Disord.* 2, 447–455.
Walsh, V. (2003). A theory of magnitude: common cortical metrics of time, space and quantity. *Trends Cogn. Sci.* 7, 483–488.
Washburn, D. A. (1994). Stroop-like effects for monkeys and humans: processing speed or strength of association? *Psychol. Sci.* 5, 375–379.
Washburn, D. A., and Rumbaugh, D. M. (1991). Ordinal judgments of numerical symbols by macaques (Macaca Mulatto).*Psychol. Sci.* 2, 190–193.
Wearden, J. H. (1991). Do humans possess an internal clock with scalar timing properties? *Learn. Motiv.* 22, 59–83.
Wearden, J. H. (2005). "The wrong tree: time perception and time experience in the elderly," in *Measuring the Mind: Speed, Age and Control*, eds. J. Duncan, L. Philips, and P. McLeod (Oxford: Oxford University Press), 137–158.
Wearden, J. H., Edwards, H., Fakhri, M., and Percival, A. (1998). Why "sounds are judged longer than lights": application of a model of the internal clock in humans. *Q. J. Exp. Psychol.* 51B, 97–120.
Wearden, J. H., and Ferrara, A. (1995). Stimulus spacing effects in temporal bisection by humans. *Q. J. Exp. Psychol.* 48B, 289–310.
Wearden, J. H., and Ferrara, A. (1996). Stimulus range effects in temporal bisection by humans. *Q. J. Exp. Psychol.* 49B, 24–44.
Whalen, J., Gallistel, C. R., and Gelman, R. (1999). Non-verbal counting in humans: the psychophysics of number representation. *Psychol. Sci.* 10, 130–137.
Wilkening, F., Levin, I., and Druyan, S. (1987). Children's counting strategies for time quantification and integration. *Dev. Psychol.* 23, 822–883.
Williams, C. L. (2011). Sex differences in counting and timing. *Front. Integr. Neurosci.* 5:88. doi: 10.3389/fnint.2011.00088
Wimpory, D. (2002). Social timing, clock genes and autism: a new hypothesis. *J. Intellect. Disabil. Res.* 46, 352–358.
Wood, J. N., and Spelke, E. (2005). Infants' enumeration of actions: numerical discrimination and its signature limits. *Dev. Sci.* 8, 173–181.
Wynn, K. (1990). Children's understanding of counting. *Cognition* 36, 155–193.
Wynn, K. (1992). Addition and subtraction by human infants. *Nature* 358, 749–750.
Wynn, K. (1995). Infants possess a system of numerical knowledge. *Curr. Dir. Psychol. Sci.* 4, 172–177.
Wynn, K. (1996). Infants' individuation and enumeration of actions. *Psychol. Sci.* 7, 164–169.
Wynn, K. (1998). Psychological foundations of number: numerical competence in human infants. *Trends Cogn. Sci.* 2, 296–303.
Wynn, K., Bloom, P., and Chiang, W-C. (2002). Enumeration of collective entities by 5-month-old infants. *Cognition* 83, B55–B62.
Wynn, K., and Chiang, W-C. (1998). Limits to infants' knowledge of objects: the case of magical appearance. *Psychol. Sci.* 9, 448–455.
Xu, F. (2003). Numerosity discrimination in infants: evidence for two systems of representations. *Cognition* 89, B15–B25.
Xu, F., and Spelke, E. (2000). Large number discrimination in 6-month-old infants. *Cognition* 74, B1–B11.
Xu, F., Spelke, E. S., and Goddard, S. (2005). Number sense in human infants. *Dev. Sci.* 8, 88–101.
Xuan, B., Zhang, D., He, S., and Chen, X. C. (2007). Larger stimuli are judged to last longer. *J. Vis.* 7, 1–5.
Zélanti, P. S., and Droit-Volet, S. (2011). Cognitive abilities explaining age-related changes in time perception of short and long durations. *J. Exp. Child Psychol.* 109, 143–157.
Zentall, S. S., Smith, Y. N., Lee, Y. B., and Wieczorek, C. (1994). Mathematical outcomes of attention-deficit hyperactivity disorder. *J. Learn. Disabil.* 27, 510–519.
Zur, O., and Gelman, R. (2004). Young children can add and subtract by predicting and checking. *Early Child. Res. Q.* 19, 121–137.

Conflict of Interest Statement: The authors declare that the research was conducted in the absence of any commercial or financial relationships that could be construed as a potential conflict of interest.

Received: 01 August 2011; paper pending published: 14 October 2011; accepted: 10 February 2012; published online: 06 March 2012.
*Citation: Allman MJ, Pelphrey KA and Meck WH (2012) Developmental neuroscience of time and number: implications for autism and other neurodevelopmental disabilities. Front. Integr. Neurosci. **6**:7. doi: 10.3389/fnint.2012.00007*

frontiers in
INTEGRATIVE NEUROSCIENCE

GENERAL COMMENTARY
published: 16 March 2012
doi: 10.3389/fnint.2012.00012

Time and number sense develop in tandem?

Mark J. Yates*

Department of Psychology, University of Melbourne, Parkville, VIC, Australia
**Correspondence: mjyates@unimelb.edu.au*

A commentary on

Developmental neuroscience of time and number: implications for autism and other neurodevelopmental disabilities
by Allman, M. J., Pelphrey, K. A., and Meck, W. H. (2012). Front. Integr. Neurosci. 6:7 doi: 10.3389/fnint.2012.00007

The last two decades have seen a marked rise in interest in what might be termed "time sense" and "number sense" and the potential relationship between them (for reviews see Buhusi and Meck, 2005; Bueti and Walsh, 2009; Nieder and Dehaene, 2009). "Time sense" refers to the ability that allows human adults (as well as infants and animals) to discriminate which of two sequentially presented stimuli is greater in duration. "Number sense" refers to the ability to determine – in the absence of explicit counting – which of two stimuli (each comprising of a number of separate elements) contains the greater number of elements. The "elements" in question might be presented simultaneously (e.g., visual dots in an array) or sequentially (e.g., a series of taps to the arm).

A major new review appearing within this issue (Allman et al., 2012) provides an update on research into both time and number sense. Unique to this review is its focus on the developmental trajectory of time and number sense. This is paired with an overview of developmental disorders in which basic time and/or number sense appears to be impaired, and coverage of findings concerning the neural correlates of time and number representation.

Charting the developmental trajectory of time and number sense potentially provides insights beyond those that can be gleaned from a "snapshot" of the same abilities in their mature form in adulthood. One obvious advantage is that characterizing time and number sense at certain critical moments of development (e.g., at birth) can differentiate, for instance, between innate versus experience-dependent aspects of time and number abilities, or between aspects of time and number sense that are present prior to exposure with cultural number symbol systems versus those that emerge after such exposure.

A second advantage is the opportunity it provides to shed light on the question of whether a single "magnitude accumulation" system underlies both time and number perception (and possibly other dimensions as well), as proposed by two theoretical models discussed in the review (Meck and Church, 1983; Walsh, 2003). Over the course of normal development, performance on both numerosity and duration discrimination tasks improves with signature trajectories. In theory, if these changes in acuity occur in lockstep across the two different dimensions, this would lend at least *prima facie* support for the existence of a common magnitude processing mechanism that is recruited during both types of discrimination task. Such evidence would be more convincing than mere similarities in performance for time and number discrimination tasks at any given snapshot of time. In practice, the picture is more complex. Various lines of evidence indicate that time sense and number sense do in fact appear to develop at least roughly in tandem, but there are many caveats: discrimination performance sometimes improves for a selected segment of the range of possible durations/numerosities rather than uniformly across the entire range, numerosity discrimination for sequences of elements differs from that for simultaneously presented elements, improvements in discrimination performance over development are not unique to time and number sense but rather reflect a general feature of perceptual abilities, and so on. Furthermore, even if it could be shown that the developmental trajectories of time and number sense are perfectly synchronized, this could not be counted as definitive support for shared time and number magnitude processing given that simultaneous improvements in discrimination performance across the two dimensions might also be explained by the development/improvement of a third factor (such as attention or working memory) which contributes to both types of discrimination task. Nevertheless, despite the complexities, a systematic investigation of how time and number sense become refined over the course of development may yet prove to be very informative for the shared magnitude representation hypothesis, currently an especially active area of interest within cognitive neuroscience.

Finally, a sharper picture of the trajectory of time and number sense during typical development provides an important baseline against which atypical development of these abilities can be better delineated and understood. In the latter part of the review, the focus turns to developmental disorders which possibly stem from, or are at least in some way associated with, impairments in basic time and number sense. The most obvious example is developmental dyscalculia, a disorder marked by selective impairment of numerical/mathematical ability against a background of otherwise normal academic achievement. While there is still considerable debate about the nature of the underlying deficit in this disorder, there is evidence that it involves an impairment of basic number sense (i.e., non-symbolic numerical processing; e.g., Price et al., 2007) though an alternative account is that the deficit is in linking number symbols with non-symbolic numerical magnitudes (i.e., attaching meaning to numerical symbols; e.g., Rousselle and Noël, 2007). Interestingly, the study of developmental dyscalculia can also assist in clarifying the relationship between time and number sense. If basic number sense is impaired in dyscalculia, and if time and number sense are subserved by a fully shared magnitude system, then time sense should also be impaired in this disorder. Cappelletti et al. (2011) recently tested this prediction, and found that basic time sense is not impaired in

developmental dyscalculia (at least not in the sub-second duration range). However, they found that numbers did interfere with temporal processing, both in those with dyscalculia and controls, though in different ways. They concluded that their data supported the existence of a partially shared magnitude system for number and time, as this is the only possibility that can account for both dissociations as well as interactions between number and time sense, as were observed.

There is now also increasing interest in the possibility that ADHD and autism spectrum disorder involve an impairment of basic time sense and/or number sense (e.g., Boucher, 2001; Allman, 2011; Gooch et al., 2011). An intriguing hypothesis put forward by the review authors is that the striking preoccupation with symbolic numbers commonly observed in autism spectrum disorder – along with unusual levels of interest in timetables, calendars, and routines (these latter three can be conceived as "external" temporal supports – Lalli et al., 1994) – may, in fact, reflect an adaptive strategy to compensate for a deficit in basic time sense. Such speculations are to be encouraged. Arguably somewhat belatedly, time and number sense are now recognized as fundamental mental abilities integral to perception and behavior. An increased focus on the possible clinical manifestations of disordered time and number sense can only be welcomed.

REFERENCES

Allman, M. J. (2011). Deficits in temporal processing associated with autistic disorder. *Front. Integr. Neurosci.* 5:2. doi: 10.3389/fnint.2011.00002

Allman, M. J., Pelphrey, K. A., and Meck, W. H. (2012). Developmental neuroscience of time and number: implications for autism and other neurodevelopmental disabilities. *Front. Integr. Neurosci.* 6:7. doi: 10.3389/fnint.2012.00007

Boucher, J. (2001). "Lost in a sea of time: time-parsing and autism," in *Time and Memory*, eds C. Hoerl and T. McCormack (Oxford: Oxford University Press), 111–135.

Bueti, D., and Walsh, V. (2009). The parietal cortex and the representation of time, space, number and other magnitudes. *Philos. Trans. R. Soc. Lond. B Biol. Sci.* 364, 1831–1840.

Buhusi, C. V., and Meck, W. H. (2005). What makes us tick? Functional and neural mechanisms of interval timing. *Nat. Rev. Neurosci.* 6, 755–765.

Cappelletti, M., Freeman, E. D., and Butterworth, B. L. (2011). Time processing in dyscalculia. *Front. Psychol.* 2:364. doi: 10.3389/fpsyg.2011.00364

Gooch, D., Snowling, M., and Hulme, C. (2011). Time perception, phonological skills and executive function in children with dyslexia and/or ADHD symptoms. *J. Child Psychol. Psychiatry* 52, 195–203.

Lalli, J. S., Casey, S., Goh, H., and Merlino, J. (1994). Treatment of escape-maintained aberrant behaviour with escape extinction and predictable routines. *J. Appl. Behav. Anal.* 27, 705–714.

Meck, W. H., and Church, R. M. (1983). A mode control model of counting and timing processes. *J. Exp. Psychol. Anim. Behav. Process.* 9, 320–334.

Nieder, A., and Dehaene, S. (2009). Representation of number in the brain. *Annu. Rev. Neurosci.* 32, 185–208.

Price, G. R., Holloway, I., Räsänen, P., Vesterinen, M., and Ansari, D. (2007). Impaired parietal magnitude processing in developmental dyscalculia. *Curr. Biol.* 17, R1042–R1043.

Rousselle, L., and Noël, M. P. (2007). Basic numerical skills in children with mathematics learning disabilities: a comparison of symbolic vs. non-symbolic number magnitude processing. *Cognition* 102, 361–395.

Walsh, V. (2003). A theory of magnitude: common cortical metrics of time, space and quantity. *Trends Cogn. Sci. (Regul. Ed.)* 7, 483–488.

Received: 23 February 2012; accepted: 29 February 2012; published online: 16 March 2012.

*Citation: Yates MJ (2012) Time and number sense develop in tandem? Front. Integr. Neurosci. **6**:12. doi: 10.3389/fnint.2012.00012*

frontiers in
INTEGRATIVE NEUROSCIENCE

OPINION ARTICLE
published: 25 March 2011
doi: 10.3389/fnint.2011.00002

Deficits in temporal processing associated with autistic disorder

Melissa J. Allman*

Kennedy Krieger Institute, Johns Hopkins University School of Medicine, Baltimore, MD, USA
**Correspondence: allman@kennedykrieger.org*

Currently idiopathic autism is typically diagnosed according to an observational assessment of certain behavioral, social, and cognitive tendencies across dimensions of language, social interaction, imaginative play, and restricted or repetitive cognitions and behavior. Parent interview is required to confirm presence of specific tendencies within the first 3 years of life. There is, as yet, no bio-medical test or marker for autism, although certain neurological, genetic, and physiological differences are known. There are often common co-morbid disorders, such as problems with sleep, motor function and attention-hyperactivity. An individual is diagnosed along spectrum of impairment (autistic disorder or autism spectrum disorder). Thus any psychological theory of autism is required to describe differences, and similarities, across a range of behavioral, social and cognitive abilities, within and between affected individuals. Arguably the three most dominant theories of autistic disorder relate to weak central coherence (or information processing), executive functioning, and theory of mind. There may be another hitherto, rather unacknowledged possibility: a deficit in temporal processing.

An adaptive sensitivity to the duration of events, and time between them, is critical to adaptive cognitive, behavioral, and social function. There are anecdotal and clinical reports of problems with time in autistic disorder, and successful applied behavioral educational and therapeutic supports with this population often include external signals to indicate the passage of time, temporal structure, and upcoming events. Currently, the empirical literature on temporal processing in autistic disorder is relatively scant, and encompasses findings spanning a range of psychology; neurological, genetic, behavioral, and cognitive, observational, and computational assessments. These include reports that children with autism experience difficulties imaging past and future changes of a current situation and understanding that successive events are part of a unitary process; differences in temporal reproduction and duration perception (in the interval range); and electrophysiological reports of disordered temporal binding of stimulus input, apparently over extended periods (than is typical). These findings are usually complementary, although vary greatly in the nature of the methods and analysis used (for a review, see Allman and Meck, 2011). There is preliminary evidence from data modeling to suggest that aspects of the perception of duration might be "developmentally delayed" in this population (see Allman et al., 2011).

Consistent among these aforementioned findings is the interpretation of results within the context of a deficit in (some aspect of) temporal processing in autistic disorder (e.g., Boucher et al., 2007). These range from suppositions that affected individuals experience problems thinking about time and higher temporal cognition, to notions that there are fundamental differences in the quality of the "subjective present" as it relates to the temporal processing of sensory information. Clock gene anomalies have been related to sleep, memory, and timing problems in autistic disorder. There have been several attempts to assert a hypothesis of temporal processing disturbance in autistic disorder, both within the discussion of published reports, or in more speculative accounts which go so far as to describe diagnostic features of autistic disorder as manifestations of atypical aspects of temporal processing (for details, see Allman and DeLeon, 2009). However, there is as yet, no well-defined profile of temporal processing abilities in these individuals, and no sufficiently specified theory.

Perhaps the appeal of a temporal deficit hypothesis of autism might be its ability to assimilate the traditional, and well supported accounts of autism into one, encompassing and testable hypothesis. It might also be possible to account for diagnostic features of the disorder. For instance, atypical social synchrony and temporal patterning may reduce the quality of social bonding, joint attention, and the to- and fro of social reciprocity, and communication (the latter are heavily implicated in autism). Differences in the ability to integrate sensory inputs and events over time may create problems with perception, learning and memory, and create problems of weak central coherence. Deficits in temporal processing might influence and be related to known differences in patterns of local and global information processing (couched within information-processing traditions), and executive functions (e.g., episodic memory, planning). Pathological restricted and repetitive behaviors and interests, rituals and routines, might otherwise have adaptive significance, such that they serve to parse or regulate temporal processing and compensate for a failure to predict events, and reduce posited disorientation in time. The relative length and complexity of rituals or routines has previously been posited to correspond to the extent (boundary) of temporal thought in affected individuals. Assuming that sensitivity to duration is related to our subjective sense of time, then autistic problems with imaginative play, empathizing, and theory of mind might be otherwise considered related to deficits in aspects of temporal processing – being able to export oneself into the mind of another person likely requires some form of "mental time travel."

It is important to stress that to-date the study of temporal processing in autism is in its infancy, however a temporal deficit hypothesis of autistic disorder does not appear premature given the relevant literature. At a more general level, there is little doubt that increased knowledge of temporal processing in autism is both necessary and likely fruitful both for the scientist, and the affected individual who has the potential to

benefit from improved social and non-social temporal supports. Collectively, there are reasonable, and promising grounds to support a hypothesis of autism based on deficits in temporal processing.

ACKNOWLEDGMENT

The author is supported by a Pathway to Independence award (K99 HD058698) from the Eunice Kennedy Shriver National Institute of Child Health and Human Development.

REFERENCES

Allman, M. J., and DeLeon, I. G. (2009). "No time like the present: time perception in autism," in *Causes and Risks for Autism*, eds A. C. Giordano and V. A. Lombardi (New York: Nova Science Publishers), 65–76.

Allman, M. J., and Meck, W. H. (2011). Pathological distortions in time perception and timed performance. *Brain* (in press).

Allman, M. J., DeLeon, I. G., and Wearden, J. H. (2011). A psychophysical assessment of timing in individuals with autism. *Am. J. Intellect. Dev. Disabil.* 116, 165–178.

Boucher, J., Lind, S., and Williams, D. (2007). Temporal cognition in children with autistic spectrum disorder: tests of diachronic thinking. *J. Autism Dev. Disord.* 37, 1413–1429.

Received: 28 February 2011; accepted: 16 March 2011; published online: 25 March 2011.

Citation: Allman MJ (2011) Deficits in temporal processing associated with autistic disorder. Front. Integr. Neurosci. ***5****:2. doi: 10.3389/fnint.2011.00002*

frontiers in
INTEGRATIVE NEUROSCIENCE

OPINION ARTICLE
published: 13 June 2011
doi: 10.3389/fnint.2011.00026

Interval timing deficits and abnormal cognitive development

Christine M. Falter[1]* and Valdas Noreika[1,2]

[1] *Department of Psychiatry, University of Oxford, Oxford, UK*
[2] *Department of Psychology, Centre for Cognitive Neuroscience, University of Turku, Turku, Finland*
**Correspondence: christine.falter@psych.ox.ac.uk*

Time perception deficits represent an aspect of cognitive malfunctioning shared by developmental disorders, which otherwise seem distinct with respect to their individual primary symptom clusters, such as autism spectrum disorders (ASD) and attention-deficit/hyperactivity disorder (ADHD). Multiple impairments of social interaction, communication, and restricted interests constitute the diagnostic criteria for ASD, whereas behavioral symptoms of ADHD comprise inattention, hyperactivity, and impulsivity (DSM-IV-TR; American Psychiatric Association, 2000). Both ASD and ADHD are additionally associated with non-diagnostic secondary symptoms in perception and cognition. A secondary symptom observed in both ASD and ADHD is abnormal interval timing, i.e., processing of stimulus duration (for a review see Falter and Noreika, accepted). For instance, it has been reported that reproduction of auditory and visual intervals of 1–5.5 s was impaired in individuals with ASD (Szelag et al., 2004). Similarly, Barkley et al. (2001) found that individuals with ADHD were impaired in reproducing intervals of 2–60 s.

It is difficult to assess whether secondary symptoms in general and interval timing abnormalities in particular play a causal role in developmental disorders. There are several possible relationships. First, a direct causal relationship would characterize a case in which impairment of an interval timing system could directly disrupt (otherwise possibly unimpaired) cognitive functions relying on accurate timing information, resulting in the known primary symptoms. Although such a direct causal relationship might be found in adult neuropsychology, it is not applicable to the study of developmental disorders, which are characterized by atypical neurogenetic pathways of cognitive development. Rather, as a second option, an ontogenetic causal relationship is conceivable in which an impaired interval timing system could affect the development of all processes downstream, which rely on accurate timing information. Finally, a third option would be that abnormal interval timing could be an epiphenomenon of developmental disorders without bearing a causal relationship to other symptoms.

The idea of an ontogenetic causal relationship raises the question of why the phenomenological outcomes of the disorders differ so strongly. The apparent lack of specificity of interval timing deficits to ASD and ADHD raises the question of their explanatory relevance for the ontogenesis of a particular developmental disorder. A further challenge for the causality assumption is the lack of universality of interval timing abnormalities. A few studies report null findings (Wallace and Happe, 2008; Jones et al., 2009), and in studies showing group differences not all individuals with ASD or ADHD perform atypically. Indeed, the range of reproduced time intervals can be quite variable and the variability is often increased in ASD and ADHD compared to typically developing controls (Toplak et al., 2003; Martin et al., 2010). At the current stage of knowledge, therefore, it seems premature to suggest that interval timing abnormalities can be the sole ontogenetic cause of ASD or ADHD.

Nevertheless, before we discard any causal account in favor of the alternative view of interval timing as a mere epiphenomenon of atypical cognitive development, we suggest that a more associative view of the role of interval timing in cognitive development be adopted. Indeed, there is strong evidence for the association between temporal processing and other typical cognitive functions such as social cognition (Trevarthen and Daniel, 2005; Striano et al., 2006), language processing (Tallal et al., 1993), and understanding of causality (Freeman, 2008). Therefore, it is difficult to conceive how an impairment of interval timing would have no relevance for developmental disorders, which show deficits in cognitive functions relying on accurate timing. Furthermore, the incidence of interval timing abnormalities is increased in developmental disorders, as shown by group differences in performance even for relatively small sample sizes (Szelag et al., 2004). Thus, in spite of the lack of universality of interval timing deficits, the increased incidence rate needs to be explained. Moreover, it has been suggested that ADHD and ASD share some susceptibility genes (Castellanos and Tannock, 2002), which makes it likely that some dysfunctions are shared between them or their subtypes. We propose that the focus of research needs to be on the association of interval timing abnormalities and other functional deficits. For instance, although a Theory of Mind deficit can hamper the understanding of social situations in its own right, an additional interval timing deficit could result in a lack of precise perception of temporal cues of eye gaze, and thereby increase misinterpretations of social situations. It has been proposed that different symptoms can be independent dimensions of impairment, which nevertheless interact with and modulate one another, leading to the characteristic phenomenology of an individual with a developmental disorder (Happe et al., 2006). In this line of thought, interval timing abnormalities might interact with primary dysfunctions.

In fact, several ADHD studies confirmed significant associations between duration perception and other cognitive functions. Toplak and Tannock (2005) reported significant correlations between time discrimination thresholds and working memory measures in participants with ADHD, but not in healthy individuals. Rubia and colleagues argued persuasively that the primary ADHD symptom of impulsiveness is based on poor inhibition and attention functions, as well as on poor interval timing (Rubia, 2002; Rubia et al., 2009). Even though interaction between interval timing and other cognitive functions is much less investigated in ASD than in ADHD, preliminary findings show significant correlation between timing measures in a temporal bisection task and primary ASD symptoms in the language and communication domain (Allman et al., 2011).

Taken together, these reports demonstrate complex associations between abnormally developing cognitive functions, and suggest that interval timing might play an important yet under-investigated role in developmental disorders by interacting with and modulating primary symptoms.

ACKNOWLEDGMENTS

Christine M. Falter is supported by the German Research Council and the Baily Thomas Charitable Fund. Valdas Noreika is supported by the Academy of Finland, the Signe and Ane Gyllenberg Foundation, and the National Graduate School of Psychology in Finland. The collaboration between Christine M. Falter and Valdas Noreika is supported by a European Cooperation in Science and Technology (COST) action on Time in Mental Activity (TIMELY; TD0904).

REFERENCES

Allman, M., DeLeon, I. G., and Wearden, J. H. (2011). A psychophysical assessment of timing in individuals with autism. *Am. J. Intellect. Dev. Disabil.* 116, 165–178.

American Psychiatric Association. (2000). *Diagnostic and Statistical Manual of Mental Disorders*, 4th Edn. – Test Revision (DSM-IV-TR). Washington, DC: American Psychiatric Association.

Barkley, R. A., Murphy, K. R., and Bush, T. (2001). Time processing and reproduction in young adults with attention deficit hyperactivity disorder. *Neuropsychology* 15, 351–360.

Castellanos, F. X., and Tannock, R. (2002). Neuroscience of attention-deficit/hyperactivity disorder: the search for endophenotypes. *Nat. Rev. Neurosci.* 3, 617–628.

Freeman, W. J. (2008). Perception of time and causation through the kinesthesia of intentional action. *Integr. Psychol. Behav. Sci.* 42, 137–143.

Happe, F., Ronald, A., and Plomin, R. (2006). Time to give up on a single explanation for autism. *Nat. Neurosci.* 9, 1218–1220.

Jones, C. R. G., Happé, F., Baird, G., Simonoff, E., Marsden, A. J. S., Tregay, J., Phillips, R. J., Goswami, U., Thomson, J. M., and Charman, T. (2009). Auditory discrimination and auditory sensory behaviours in autism spectrum disorders. *Neuropsychologia* 47, 2850–2858.

Martin, J. S., Poirier, M., and Bowler, D. M. (2010). Brief report: impaired temporal reproduction performance in adults with autism spectrum disorder. *J. Autism Dev. Disord.* 40, 640–646.

Rubia, K. (2002). The dynamic approach to neurodevelopmental psychiatric disorders: Use of fMRI combined with neuropsychology to elucidate the dynamics of psychiatric disorders, exemplified in ADHD and schizophrenia. *Behav. Brain Res.* 130, 47–56.

Rubia, K., Halari, R., Christakou, A., and Taylor, E. (2009). Impulsiveness as a timing disturbance: neurocognitive abnormalities in attention-deficit hyperactivity disorder during temporal processes and normalization with methylphenidate. *Philos. Trans. R. Soc. Lond. B Biol. Sci.* 364, 1919–1931.

Striano, T., Henning, A., and Stahl, D. (2006). Sensitivity to interpersonal timing at 3 and 6 months of age. *Interact. Stud.* 7, 251–271.

Szelag, E., Kowalska, J., Galkowski, T., and Pöppel, E. (2004). Temporal processing deficits in high-functioning children with autism. *Br. J. Psychol.* 95, 269–282.

Tallal, P., Miller, S., and Fitch, R. H. (1993). Neurobiological basis of speech: a case for the preeminence of temporal processing. *Ann. N. Y. Acad. Sci.* 14, 27–47.

Toplak, M. E., Rucklidge, J. J., Hetherington, R., John, S. C. F., and Tannock, R. (2003). Time perception deficits in attention-deficit/hyperactivity disorder and comorbid reading difficulties in child and adolescent samples. *J. Child Psychol. Psychiatry* 44, 888–903.

Toplak, M. E., and Tannock, R. (2005). Time perception: modality and duration effects in attention-deficit/hyperactivity disorder (ADHD). *J. Abnorm. Child. Psychol.* 33, 639–654.

Trevarthen, C., and Daniel, S. (2005). Disorganized rhythm and synchrony: early signs of autism and Rett syndrome. *Brain Dev.* 27(Suppl. 1), 25–34.

Wallace, G. L., and Happe, F. (2008). Time perception in autism spectrum disorders. *Res. Autism Spectr. Disord.* 2, 447–455.

Received: 31 May 2011; accepted: 03 June 2011; published online: 13 June 2011.

*Citation: Falter CM and Noreika V (2011) Interval timing deficits and abnormal cognitive development. Front. Integr. Neurosci. **5**:26. doi: 10.3389/fnint.2011.00026*

frontiers in
INTEGRATIVE NEUROSCIENCE

OPINION ARTICLE
published: 31 October 2011
doi: 10.3389/fnint.2011.00067

Time and number: the privileged status of small values in the brain

Catalin V. Buhusi[1]* and Sara Cordes[2]

[1] *Department of Neurosciences, Medical University of South Carolina, Charleston, SC, USA*
[2] *Department of Psychology, Boston College, Boston, MA, USA*
**Correspondence: buhusi@musc.edu*

When dancing, one follows the rhythm without much conscious control, while also singing, entertaining a conversation, planning intricate sequences of steps, or estimating the time until the end of the song. Processing of rapid beats, in the sub-second range seems to be done automatically and doesn't appear to interfere with timekeeping in the range of seconds or minutes, required for planning the steps, or estimating the duration left until the end of the song. This may be because the processing of rapid beats and slow sequences is split between different timing mechanisms and/or the left and the right hemispheres of our brain (Hancock, 2011).

Relatively distinct brain circuits process time in the millisecond, seconds-to-minutes, or circadian range (Buhusi and Meck, 2005), but the distinction blurs around 1-s intervals. Circadian timing, which operates over roughly 24 h, and controls functions such as the sleep–wake cycle and the metabolic processes, is based on a molecular clock in the suprachiasmatic nucleus (Gallego and Virshup, 2007; Allman and Meck, 2011). Millisecond timing engages a variety of specialized local circuits in the cerebellum (De Zeeuw et al., 2011), for fast and fine movement control, or in the auditory cortex, for speech processing (Nourski and Brugge, 2011). Finally, planning and motor control in the seconds range engages the cortico-striatal circuits, motor, parietal, and prefrontal cortices, both in animals (Meck et al., 2008; Buhusi and Meck, 2009) and humans (Coull et al., 2004, 2011; Stevens et al., 2007). The relative separation of these circuits explains why one can deal with different attributes simultaneously, but also raises the possibility of conflicts or cooperation between these circuits for time intervals around 1 s.

The question of whether sub- and supra-second timing engages distinct brain circuits was recently investigated in patients with unilateral hemispheric lesions (Gooch et al., 2011). Rather than selecting patients by lesion, the study used voxel-based lesion-symptom mapping (Bates et al., 2003) in patients with various lesions, and evaluated the contribution of each voxel for the overall performance in all patients, thus tapping into the circuits critical for timing without using *a priori* assumptions regarding the location of interest.

Three findings bear noting. First, patients with lesions in the frontal or parietal cortices were less accurate than controls, thus supporting neurobiological models of timing suggesting that cortico-striatal circuits (Matell and Meck, 2004; Buhusi and Meck, 2005; Oprisan and Buhusi, 2011) and parietal circuits (Leon and Shadlen, 2003) develop neural representations of time. Second, the right hemisphere was involved in timing both sub- and supra-second timing, consistent with previous studies implicating right cortical regions in interval timing (Schubotz et al., 2000; Rubia et al., 2003; Smith et al., 2003; Coull et al., 2004; Meck and Malapani, 2004; Lewis and Miall, 2006; Bueti et al., 2008), and supporting the hypothesis that right dorsolateral prefrontal cortex is crucial for timekeeping (Lewis and Miall, 2006; Meck et al., 2008). Instead, the left temporal lobe was involved in timing sub-second durations only, consistent with its implication in processing fast, auditory information. Thus, whereas all durations required the same circuitry in the right hemisphere, only the shortest intervals (<1 s) involved additional left-hemisphere structures, suggesting millisecond timing may have a special status in the brain.

This distinction between short (sub-second) and longer intervals (supra-second) is not unique to time. Remarkable parallels exist between counting and timing, such that it has long been thought that counting may tap into similar cognitive and neural mechanisms as that of time (Meck and Church, 1983; Walsh, 2003; Feigenson, 2007; Cantlon et al., 2009). Timing and counting abilities are found in a diverse range of non-human animal species, from honeybees and rats to dolphins and monkeys (Meck and Church, 1983; Cantlon and Brannon, 2007; Cordes et al., 2007; Dacke and Srinivasan, 2008), and they share striking similarities, including Weber's law: The ease with which two durations or numbers are discriminated is based upon their ratio, not their absolute difference (Meck and Church, 1983; Cantlon and Brannon, 2007). All species share a system for representing time and number that must have arisen early in evolutionary history and is present early in development (Xu and Spelke, 2000; vanMarle and Wynn, 2006; Brannon et al., 2007, 2008 – see Gallistel, 1990). In fact, time and number may even be represented using a common metric, in which the representation of one count is equivalent to 200 ms of time (Meck and Church, 1983; but see Balci and Gallistel, 2006). Support for the claim that representations of time and number are derived from the same mechanism is also provided by neurobiological studies of numerical processing, which like those of temporal processing, implicate parietal areas and, at least early in development, this activation is unique to the right hemisphere (Rivera et al., 2005; Cantlon et al., 2006) as in the case of time.

Furthermore, whereas both behavioral and neural evidence suggests a distinction between sub-second and supra-second timing, a similar distinction exists between representations of small (<4 or 5) sets and larger sets. Behavioral data from adults, infants, non-human primates, and even mosquitofish reveal that small sets are treated differently than large sets (e.g., Trick and Pylyshyn, 1994; Hauser and Carey, 2003; Agrillo et al., 2008; Cordes and Brannon, 2009a,b). For example, when asked to rapidly identify the number of items in a set, adults reveal little to

no reaction time cost for each additional item in a small set (termed "subitizing"), but once set sizes exceed 4 or 5 items, the slope of the reaction time function markedly increases. More strikingly, despite strict adherence to Weber's law for large set discriminations, infants and non-human animals reveal sharper discrimination abilities when sets are exclusively small (e.g., discriminating 2 from 3 but not 4 from 6, despite similar ratios; Feigenson et al., 2002) yet consistently fail to discriminate small from large sets despite a favorable ratio (e.g., failing to discriminate 2 from 4 or 3 from 6, despite successfully detecting twofold changes in number for larger sets, e.g., 4 vs 8 or 8 vs 16; Xu, 2003; Cordes and Brannon, 2009b). Lastly, infants with Williams syndrome discriminate small sets (2 from 3) but fail in large set discrimination (4 vs 8), suggesting these distinct numerical systems can be selectively affected (Van Herwegen et al., 2008). Whereas, unlike in the case of time where sub-second and supra-second durations are presumably both represented via a common currency of continuous mental magnitudes, evidence suggests that small numerical values may be represented in a distinctly different fashion from large ones (discrete object files for small sets and noisy analog magnitudes for large). Regardless, striking similarities in discontinuities are observed across both systems suggesting there may be something special about these small quantities.

Neural activation patterns for small numbers also selectively involve secondary brain areas distinct from those for large sets. Like time, small and large numerosities alike activate similar neural circuitry, however, again as in the case of time, additional activation is found in distinct structures (the right temporo-parietal junction) when small sets are encountered (Ansari et al., 2006). Interestingly, activation in this additional small-number structure is negatively correlated with reaction times during large number judgments suggesting that it is through the inhibition of this small-number system that large sets are processed. Therefore, much like the case of sub-second timing, additional neural circuitry appears to be dedicated to small numerosities, indicating the ability to process small values may have been favored throughout evolution.

Why is this the case? Processing short durations and small sets are critical to survival. In the case of time, a number of important skills, including speech production and comprehension, motor planning and even musical performance, are dependent upon sub-second timing (e.g., Shannon et al., 1995; Merchant and Georgopoulos, 2006; Tallal and Gaab, 2006). Differences in the order of tens of milliseconds can lead to dramatic differences in phonological processing (in the case of language), motor coordination, and even rhythm perception. In fact, millisecond timing is so crucial for speech that basic training in rhythm and intonation has been found to help patients with non-fluent aphasia regain their speech through singing words they cannot speak (Melodic Intonation Therapy: Naeser and Helm-Estabrooks, 1985; Popovici, 1995; Norton et al., 2009). Similarly, the ability to track small sets of objects can also make the difference between life and death when those objects are predators, prey, or even offspring. Presumably, attending to more than one item at a time should also subserve proper functioning in more complex situations such as social interactions and multi-tasking.

Although much has been learned regarding the behavioral and neural signatures across the time and number spectrums, many questions remain unanswered. How does the brain negotiate timing and counting conflicts at these small/large boundaries? Since evidence suggests large numbers are efficiently processed through the inhibition of the small-number brain area, does a similar inhibitory mechanism underlie the processing of durations longer than 1 s? Despite distinct localizations and functions of small set processing and sub-second timing, are there common features to their behavioral or neural make-up? Understanding the competition and cooperation between brain regions involved in interval timing and counting (Lewis and Meck, 2011) may lead to a better understanding of the mechanisms disregulated in disorders such as schizophrenia, dyslexia, Parkinson's disease, Williams syndrome, and dyscalculia – all characterized by timing and/or counting deficits – and the development and refinement of behavioral therapies to alleviate them (e.g., Sparks et al., 1974; Overy, 2003; Wilson et al., 2006; Breier et al., 2010; Wan et al., 2010; Vines et al., 2011).

ACKNOWLEDGMENTS

This work was supported by the National Institutes of Health grants MH65561 and MH73057 to Catalin V. Buhusi, and an Alfred P. Sloan Research Fellowship to Sara Cordes. We would like to thank Warren H. Meck for insightful comments on an earlier version of this manuscript.

REFERENCES

Agrillo, C., Dadda, M., Serena, G., and Bisazza, A. (2008). Do fish count? Spontaneous discrimination of quantity in female mosquitofish. *Anim. Cogn.* 11, 495–503.

Allman, M. J., and Meck, W. H. (2011). Pathophysiological distortions in time perception and timed performance. *Brain.* doi: 10.1093/brain/awr210

Ansari, D., Lyons, I. M., van Eimeren, L., and Xu, F. (2006). Linking visual attention and number processing in the brain: the role of the temporo-parietal junction in small and large symbolic and nonsymbolic number comparison. *J. Cogn. Neurosci.* 19, 1845–1853.

Balci, F., and Gallistel, C. R. (2006). Cross-domain transfer of quantitative discriminations: is it all a matter of proportion? *Psychon. Bull. Rev.* 13, 636–642.

Bates, E., Wilson, S. M., Saygin, A. P., Dick, F., Sereno, M. I., Knight, R. T., and Dronkers, N. F. (2003). Voxel-based lesion-symptom mapping. *Nat. Neurosci.* 6, 448–450.

Brannon, E. M., Libertus, M. E., Meck, W. H., and Woldorff, M. G. (2008). Electrophysiological measures of time processing in infant and adult brains: Weber's law holds. *J. Cogn. Neurosci.* 20, 193–203.

Brannon, E. M., Suanda, S., and Libertus, K. (2007). Temporal discrimination increases in precision over development and parallels the development of numerosity discrimination. *Dev. Sci.* 10, 770–777.

Breier, J. I., Randle, S., Maher, L. M., and Papanicolaou, A. C. (2010). Changes in maps of language activity activation following melodic intonation therapy using magnetoencephalography: two case studies. *J. Clin. Exp. Neuropsychol.* 32, 309–314.

Bueti, D., Walsh, V., Frith, C., and Rees, G. (2008). Different brain circuits underlie motor and perceptual representations of temporal intervals. *J. Cogn. Neurosci.* 20, 204–214.

Buhusi, C. V., and Meck, W. H. (2005). What makes us tick? Functional and neural mechanisms of interval timing. *Nat. Rev. Neurosci.* 6, 755–765.

Buhusi, C. V., and Meck, W. H. (2009). Relative time sharing: new findings and an extension of the resource allocation model of temporal processing. *Philos. Trans. R. Soc. Lond. B Biol. Sci.* 364, 1875–1885.

Cantlon, J. F., and Brannon, E. M. (2007). Basic math in monkeys and college students. *PLoS Biol.* 5, e328. doi: 10.1371/journal.pbio.0050328

Cantlon, J. F., Brannon, E. M., Carter, E. J., and Pelphrey, K. A. (2006). Functional imaging of numerical processing in adults and 4-y-Old Children. *PLoS Biol.* 4, e125. doi: 10.1371/journal.pbio.0040125

Cantlon, J. F., Platt, M. L., and Brannon, E. M. (2009). Beyond the number domain. *Trends Cogn. Sci. (Regul. Ed.)* 13, 83–91.

Cordes, S., and Brannon, E. M. (2009a). The relative salience of discrete and continuous quantities in infants. *Dev. Sci.* 12, 453–463.

Cordes, S., and Brannon, E. M(2009b). Crossing the divide: infants discriminate small from large numerosities. *Dev. Psychol.* 45, 1583–1594.

Cordes, S., King, A. P., and Gallistel, C. R. (2007). Time left in the mouse. *Behav. Processes* 74, 142–151.

Coull, J. T., Cheng, R. K., and Meck, W. H. (2011). Neuroanatomical and neurochemical substrates of timing. *Neuropsychopharmacology* 36, 3–25.

Coull, J. T., Vidal, F., Nazarian, B., and Macar, F. (2004). Functional anatomy of the attentional modulation of time estimation. *Science* 303, 1506–1508.

Dacke, M., and Srinivasan, M. V. (2008). Evidence for counting in insects. *Anim. Cogn.* 11, 683–689.

De Zeeuw, C. I., Hoebeek, F. E., Bosman, L. W., Schonewille, M., Witter, L., and Koekkoek, S. K. (2011). Spatiotemporal firing patterns in the cerebellum. *Nat. Rev. Neurosci.* 12, 327–344.

Feigenson, L. (2007). The equality of quantity. *Trends Cogn. Sci. (Regul. Ed.)* 11, 185–187.

Feigenson, L., Carey, S., and Hauser, M. (2002). The representations underlying infants' choice of more: object files versus analog magnitudes. *Psychol. Sci.* 13, 150–156.

Gallego, M., and Virshup, D. M. (2007). Post-translational modifications regulate the ticking of the circadian clock. *Nat. Rev. Mol. Cell Biol.* 8, 139–148.

Gallistel, C. R. (1990). *The Organization of Behavior*. Cambridge, MA: MIT Press.

Gooch, C. M., Wiener, M., Hamilton, A., and Coslett, H. B. (2011). Temporal discrimination of sub- and supra-second time intervals: a voxel-based lesion mapping analysis. *Front. Integr. Neurosci.* 5:59. doi: 10.3389/fnint.2011.00059

Hancock, P. A. (2011). On the left hand of time. *Am. J. Psychol.* 124, 177–188.

Hauser, M., and Carey, S. (2003). Spontaneous representations of small numbers of objects by rhesus macaques: examinations of content and format. *Cogn. Psychol.* 47, 367–401.

Leon, M. I., and Shadlen, M. N. (2003). Representation of time by neurons in the posterior parietal cortex of the macaque. *Neuron* 38, 317–327.

Lewis, P. A., and Meck, W. H. (2011). Does sleep contribute to degeneracy in neural timing? *The Psychologist* (in press).

Lewis, P. A., and Miall, R. C. (2006). A right hemispheric prefrontal system for cognitive time measurement. *Behav. Processes* 71, 226–234.

Matell, M. S., and Meck, W. H. (2004). Cortico-striatal circuits and interval timing: coincidence detection of oscillatory processes. *Brain Res. Cogn. Brain Res.* 21, 139–170.

Meck, W. H., and Church, R. M. (1983). A mode control model of counting and timing processes. *J. Exp. Psychol. Anim. Behav. Process.* 9, 320–334.

Meck, W. H., and Malapani, C. (2004). Neuroimaging of interval timing. *Brain Res. Cogn. Brain Res.* 21, 133–137.

Meck, W. H., Penney, T. B., and Pouthas, V. (2008). Cortico-striatal representation of time in animals and humans. *Curr. Opin. Neurobiol.* 18, 145–152.

Merchant, H., and Georgopoulos, A. P. (2006). Neurophysiology of perceptual and motor aspects of interception. *J. Neurophysiol.* 95, 1–13.

Naeser, M. A., and Helm-Estabrooks, N. (1985). CT scan lesion localization and response to melodic intonation therapy with nonfluent aphasia cases. *Cortex* 21, 203–223.

Norton, A., Zipse, L., Marchina, S., and Schlaug, G. (2009). Melodic intonation therapy: shared insights on how it is done and why it might help. *Ann. N. Y. Acad. Sci.* 1169, 431–436.

Nourski, K. V., and Brugge, J. F. (2011). Representation of temporal sound features in the human auditory cortex. *Nat. Rev. Neurosci.* 22, 187–203.

Oprisan, S. A., and Buhusi, C. V. (2011). Modeling pharmacological clock and memory patterns of interval timing in a striatal beat-frequency model with realistic, noisy neurons. *Front. Integr. Neurosci.* 5:52. doi: 10.3389/fnint.2011.00052

Overy, K. (2003). Dyslexia and music. From timing deficits to musical intervention. *Ann. N. Y. Acad. Sci.* 999, 497–505.

Popovici, M. (1995). Melodic intonation therapy in the verbal decoding of aphasics. *Rom. J. Neurol. Psychiatry* 33, 57–97.

Rivera, S. M., Reiss, A. L., Eckert, M. A., and Menon, V. (2005). Developmental changes in mental arithmetic: evidence for increased functional specialization of the left inferior parietal cortex. *Cereb. Cortex* 15, 1779–1790.

Rubia, K., Smith, A. B., Brammer, M. J., and Taylor, E. (2003). Right inferior prefrontal cortex mediates response inhibition while mesial prefrontal cortex is responsible for error detection. *Neuroimage* 20, 351–358.

Schubotz, R. I., Friederici, A. D., and Von Cramon, D. Y. (2000). Time perception and motor timing: a common cortical and subcortical basis revealed by fMRI. *Neuroimage* 11, 1–12.

Shannon, R. V., Zeng, F. G., Kamath, V., Wygonski, J., and Ekelid, M. (1995). Speech recognition with primarily temporal cues. *Science* 270, 303–304.

Smith, A., Taylor, E., Lidzba, K., and Rubia, K. (2003). A right hemispheric frontocerebellar network for time discrimination of several hundreds of milliseconds. *Neuroimage* 20, 344–350.

Sparks, R., Helm, N., and Albert, M. (1974). Aphasia rehabilitation resulting from melodic intonation therapy. *Cortex* 10, 303–316.

Stevens, M. C., Kiehl, K. A., Pearlson, G., and Calhoun, V. D. (2007). Functional neural circuits for mental timekeeping. *Hum. Brain Mapp.* 28, 394–408.

Tallal, P., and Gaab, N. (2006). Dynamic auditory processing, musical experience, and language development. *Trends Neurosci.* 29, 382–390.

Trick, L., and Pylyshyn, Z. (1994). Why are small and large numbers enumerated differently? A limited capacity preattentive stage in vision. *Psychol. Rev.* 101, 80–102.

Van Herwegen, J., Ansari, D., Xu, F., and Karmiloff-Smith, A. (2008). Small and large number processing in infants and toddlers with Williams syndrome. *Dev. Sci.* 11, 637–643.

vanMarle, K., and Wynn, K. (2006). Six-month-old infants use analog magnitudes to represent duration. *Dev. Sci.* 9, F41–F49.

Vines, B. W., Norton, A. C., and Schlaug, G. (2011). Non-invasive brain stimulation enhances the effects of melodic intonation therapy *Front. Psychol.* 2:230. doi: 10.3389/fpsyg.2011.00230

Walsh, V. (2003). A theory of magnitude: common cortical metrics of time, space, and quantity. *Trends Cogn. Sci. (Regul. Ed.)* 7, 483–488.

Wan, C. Y., Uber, T. R., Hohmann, A., and Schlaug, G. (2010). The therapeutic effects of singing in neurological disorders. *Music Percept.* 27, 287–295.

Wilson, A. J., Dehaene, S., Pinel, P., Revkin, S. K., Cohen, L., and Cohen, D. (2006). Principles underlying the design of "The Number Race," an adaptive computer game for remediation of dyscalculia. *Behav. Brain Funct.* 2, 1–14.

Xu, F. (2003). Numerosity discrimination in infants: evidence for two systems of representations. *Cognition* 89, B15–B25.

Xu, F., and Spelke, E. S. (2000). Large number discrimination in 6-month-old infants. *Cognition* 74, B1–B11.

Received: 06 October 2011; accepted: 06 October 2011; published online: 31 October 2011.

*Citation: Buhusi CV and Cordes S (2011) Time and number: the privileged status of small values in the brain. Front. Integr. Neurosci. **5**:67. doi: 10.3389/fnint.2011.00067*

frontiers in
INTEGRATIVE NEUROSCIENCE

OPINION ARTICLE
published: 05 January 2012
doi: 10.3389/fnint.2011.00088

Sex differences in counting and timing

Christina L. Williams

Department of Psychology and Neuroscience, Duke University, Durham, NC, USA
**Correspondence: williams@psych.duke.edu*

It is generally agreed that there are significant and reliable sex differences in human cognition that can be revealed using laboratory based tasks (reviewed by Kimura, 1996; Loring-Meier and Halpern, 1999; Weiss et al., 2003). Animal models have shown that for at least one type of cognitive process, visual–spatial navigation, these sex differences are organized by exposure to gonadal steroids early in life (Williams et al., 1990; Williams and Meck, 1991, 1993) and are modulated by exposure to activational estrogens after puberty (Rapp et al., 2003; Sandstrom and Williams, 2004) as well as androgens (Bimonte-Nelson et al., 2003). Moreover, hormonally induced alterations in the hippocampus, and in the basal forebrain cholinergic projections to the hippocampus (Gould et al., 1991; Ragbetli et al., 2002; Berger-Sweeney, 2003; Veng et al., 2003; Gibbs, 2010) appear to be the neural mechanisms underlying these sex differences in spatial cognition.

Interestingly, there are a number of studies that suggest that men outperform women on tests of temporal discrimination and reproduction when the interval being timed is short, in the milliseconds to seconds range (Roeckelein, 1972; Strang et al., 1973; Rammsayer and Lustnauer, 1989; Wittmann and Szelag, 2003). It is less clear whether there are sex differences in the perception or production of longer intervals (seconds to minutes – see Friedman, 1977, but also see Block et al., 2000). These data suggest that there may be hormonally organized or activated differences in interval timing, a fundamental property of brain that is important for many behaviors (e.g., motor control, optimal foraging, spatial navigation, and higher-level cognition). To date, relatively little work has been done to examine possible underlying neuroendocrine development and modulation of interval timing. An examination of the neural and neuroendocrine underpinning of timing and time perception is particularly important because there are well known sex differences in the expression of developmental disabilities in learning and cognition (e.g., autism), as well as psychiatric illness (e.g., depression and schizophrenia) and neurodegenerative disease (e.g., Alzheimer's and Parkinson's disease).

Meck and colleagues (Meck and Church, 1983; Meck et al., 1985) developed a mode-control model of temporal integration in which the same analog magnitude estimation system is used in different modes of pulse accumulation for both timing (run mode) and counting (event mode). In such a system, a count is equivalent to the amount of time that the accumulation process is active during the enumeration of the event. As a result, the final accumulation of counts in the event mode is functionally equivalent to the final accumulation of pulses during the run mode used for the timing of signal durations. Consequently, if counting and timing are considered basic building blocks for symbolic cognition (Cordes and Gelman, 2005; Cordes et al., 2007; Lustig, 2011), and if the temporal integration processes common to both abilities would be affected by neuroendocrine mechanisms, then one might be able to use deficits in temporal integration as early predictors of these disorders (see Allman, 2011; Allman and Meck, 2011; Allman et al., 2011; Falter and Noreika, 2011).

These findings raise several interesting questions. First, what is the extent of sex differences in temporal integration as related to timing and counting? Are sex differences in temporal integration seen only at short (small), millisecond intervals (counts) or across all temporal intervals (counts) as discussed by Buhusi and Cordes (2011)? Is the smallest unit of temporal integration (e.g., quantal unit) similar in male and female rats? While the behavioral data from male rats using signal durations over 2 s suggest that time and number are represented in the same fashion (Meck, 1997), similar procedures suggest differences between counting and timing in male rats when using intervals in the milliseconds range (Clarke et al., 1996) as well as differences between counting and timing in female rats (Breukelaar and Dalrymple-Alford, 1998).

A second issue is whether sex differences in timing and counting are modulated by organizational and activational effects of gonadal steroids? To date only a few studies have evaluated the effect of estradiol on timing and counting in adult female rats. Ross and Santi (2000) found that systemic administration of estradiol for 2 weeks impaired the ability of ovarectomized rats to use both time and number as discriminative stimuli. Two more recent studies have reported an increase in clock speed following the administration of estradiol to ovariectomized females (Sandstrom, 2007), but not to castrated males (Pleil et al., 2011), suggesting a sex difference in responsiveness to estradiol replacement. There is also some evidence that organizational actions of gonadal hormones may modify clock speed of adult rats (Pleil et al., 2011). A third unresolved issue is the determination of the neural representation of time and number in males and females. Current data indicate that cortico-striatal circuits, as well as dopaminergic afferents from the substantia nigra pars compacta, play a central role in interval timing (Harrington et al., 1998; Harrington and Haaland, 1999; Matell and Meck, 2000, 2004; Matell et al., 2003; Coull et al., 2011) and these circuits and their response to estrogen and dopaminergic agonists are sexually dimorphic (e.g., Becker, 1990, 1999; Bazzett and Becker, 1994; Xiao and Becker, 1994). In fact, the striatum is sexually dimorphic even during embryonic development, when the striata of females are more densely packed with dopamine axons and the GABAergic neurons that form striatal synapses than those of males (Ovtscharoff et al., 1992). To date most studies of the neural representation of time and number have used male subjects. Male rats with lesions of the dorsal striatum or substantia nigra pars compacta behave as though they have a severely impaired perception of time (Meck, 2006a,b). Dopaminergic drug administration either systemically (Meck, 1996, 2007; Cheng et al., 2007a,b,c) or intrastriatally (Neil and Herndon, 1978) alters the speed of interval timing processes. Moreover, male

Parkinson's disease patients show deficits in reproducing durations when they are off of their dopaminergic medications (Malapani et al., 1998, 2002; Jahanshahi et al., 2010; Jones and Jahanshahi, 2011; Jones et al., 2011). Brain imaging studies in humans show the cortex and striatum are activated during timing tasks (Rao et al., 1997, 2001; Harrington et al., 1998; Hinton and Meck, 2004; Meck and Malapani, 2004; Meck et al., 2008; Allman and Meck, 2011; Coull et al., 2011). To date, no studies have compared neural activations during timing and counting tasks in males versus females.

Male–female differences have also been reported in the likelihood temporal information versus number information are used to solve discriminations. For example, when durations are larger than 2 s male rats readily and equally use both time and number to solve discrimination tasks (Meck and Church, 1983) while females preferentially use temporal cues over counting (Breukelaar and Dalrymple-Alford, 1998). Possible sex differences between temporal integration and numerical ability using durations in the order of hundreds of milliseconds remain to be investigated. The procedure that has been used to collect these data is the bisection procedure (Church and Deluty, 1977; Meck, 1983) and the specific variant of this procedure used to study counting and timing was developed by Meck and Church (1983) and has several features that make it ideally suited for these sex differences studies. The bisection procedures can be used to study counting and timing simultaneously (Breukelaar and Dalrymple-Alford, 1998; Paule et al., 1999), in a variety of species (rat: Meck and Church, 1983; Pleil et al., 2011; mouse: Penney et al., 2008; monkey: Merritt et al., 2010; human: Allan and Gibbon, 1991; Roitman et al., 2007) and across developmental stages (children: Droit-Volet and Meck, 2007; Droit-Volet et al., 2007; Lustig and Meck, 2011; aged adult: Lustig and Meck, 2001, 2011). As well, these procedures have the advantage of being able to dissociate timing at the short (millisecond to second) and long (seconds to minutes) durations as demonstrated by Breukelaar and Dalrymple-Alford (1998) and Melgire et al. (2005). Briefly, male and female rats can be trained to discriminate between four standard stimuli (sequences of on/off auditory events) which are either "time-relevant" or "number-relevant"; the "number-relevant" standard stimuli have a total duration of 4.0 s with either two or eight sound-on events, whereas the "time-relevant" standard stimuli have a total duration of 2.0 or 8.0 s with the total number of events held constant at four. After the discrimination is acquired, the four periodic standards are pseudorandomly mixed with probe (test) signals with variable duration (3.0, 4.0, 5.0, and 6.0 s) but constant number of events, four, and probe signals of constant duration (4.0 s) consisting of either 3, 4, 5, and 6 events (see Cordes et al., 2007). By using continuous or segmented stimuli in this procedure it is also possible to compute the equivalent time interval corresponding to one increment in counting, also known as "quantal unit" (Meck et al., 1985). The quantal unit has been show to be about 200 ms in male rats (Meck and Church, 1983) and humans (Whalen et al., 1999). As yet, separate quantal units for males and females tested in the same procedures remain to be determined.

SEXUAL DIFFERENTIATION OF TIMING AND COUNTING

As has been suggested recently (McCarthy and Arnold, 2011), there are a number of ways that sex differences in timing and counting might develop. The classic model (Phoenix et al., 1959) is that adult brain and behavior become sexually differentiated or organized during early development by gonadal hormones, which are released at high levels by male but not female fetuses. Thus, as a first step in exploring the underlying neuroendocrine basis of sex differences in timing and counting the early hormone environment of males and female can be manipulated and their adult behavior examine. This comparison allows for the determination of whether gonadal steroid exposure soon after birth hormonally organizes sex differences in timing/counting. To date, no study has manipulated hormones early in development and examined the consequences for both adult counting and timing, although as mentioned previously, clock speed appears to be organized by early gonadal hormones (Pleil et al., 2011).

It is also possible that sex differences in counting and timing might emerge because of sex differences in the effects of circulating estrogens in the adult female versus testosterone in the male. While this potential sex difference has never been explored, one study has evaluated the effect of estradiol on timing and counting in females (Ross and Santi, 2000) and revealed that low dose exposure to estradiol in females decreases both timing (in the 2–8 s range) and counting accuracy, but does not dissociate performance on timing and counting tasks. However, this study did not study male rats, and did not examine timing in the millisecond range. Future work should manipulate hormone exposure both developmentally and in adulthood in both males, and females across several cycles and compare the accuracy and precision of their timing and counting performance (see Pleil et al., 2011).

Recent evidence suggests that some sexually dimorphic pathways and behavior emerge because of direct genetic sex differences, rather than a cascade of hormonal events that stem from male–female genetic differences. For example, only males express the *Sry* gene, which is known to cause the differentiation of the male testes. Interestingly, Sry is also expressed in dopaminergic neurons in the substantia nigra that project to the striatum and have direct male-specific effects (Dewing et al., 2006). When Sry expression is reduced in adult rats, the expression of tyrosine hydroxylase in the substantia nigra and striatum are reduced and motor performance declines. Thus it is possible that direct, sex-specific effects of a sex chromosome gene may cause sex differences in the neural pathways underlying counting and timing. This possibility also remains unexplored.

THE NEURAL REPRESENTATION OF TIME AND NUMBER

Future studies should explore the representation of time and number by a network of neural substrates (including the basal ganglia, frontal cortex, and parietal cortex) in males and females using ensemble recordings at multiple sites (Vodolazhskaya and Beier, 2002; Varga et al., 2010; Coull et al., 2011). We hypothesize that the same neural substrates are involved in processing both temporal and numerical information, but that sexual dimorphisms in the neural substrates in temporal processing underlie differences in temporal integration and synchronization of the timing pattern as well as learning and memory for time in males and females (see Cheng et al., 2008).

REFERENCES

Allan, L. G., and Gibbon, J. (1991). Human bisection at the geometric mean. *Learn. Motiv.* 22, 39–58.

Allman, M. J. (2011). Deficits in temporal processing associated with autistic disorder. *Front. Integr. Neurosci.* 5:2. doi: 10.3389/fnint.2011.00002

Allman, M. J., and Meck, W. H. (2011). Pathophysiological distortions in time perception and timed performance. *Brain* (in press). doi: 10.1093/brain/awr21

Allman, M. J., Pelphrey, K. A., and Meck, W. H. (2011). Developmental neuroscience of time and number: implications for autism and other neurodevelopmental disabilities. *Front. Integr. Neurosci.* (in press).

Bazzett, T. J., and Becker, J. B. (1994). Sex differences in the rapid and acute effects of estrogen on striatal D2 dopamine receptorbinding. *Brain Res.* 637, 163–172.

Becker, J. B. (1990). Direct effect of 17 β-estradiol on striatum: sex differences in dopamine release. *Synapse* 5, 157–164.

Becker, J. B. (1999). Gender differences in dopaminergicf unction in striatum and nucleus accumbens. *Pharmacol. Biochem. Behav.* 64, 803–812.

Berger-Sweeney, J. (2003). The cholinergic basal forebrain system during development and its influence on cognitive processes: important questions and potential answers. *Neurosci. Biobehav. Rev.* 27, 401–411.

Bimonte-Nelson, H. A., Singleton, R. S., Nelson, M. E., Eckman, C. B., Barber, J., Scott, T. Y., and Granholm, A.-C. E. (2003). Testosterone, but not nonaromatizable dihydrotestosterone, improves working memory and alters nerve growth factor levels in aged male rats. *Exp. Neurol.* 181, 301–312.

Block, R. A., Hancock, P. A., and Zakay, D. (2000). Sex differences in duration judgments: a meta-analytic review. *Mem. Cognit.* 28, 1333–1346.

Breukelaar, J. W. C., and Dalrymple-Alford, J. C. (1998). Timing ability and numerical competence in rats. *J. Exp. Psychol. Anim. Behav. Process.* 24, 84–97.

Buhusi, C. V., and Cordes, S. (2011). Time and number: the privileged status of small values in the brain. *Front. Integr. Neurosci.* 5:67. doi: 10.3389/fnint.2011.00067

Buhusi, C. V., and Meck, W. H. (2005). What makes us tick? Functional and neural mechanisms of interval timing. *Nat. Rev. Neurosci.* 6, 755–765.

Cheng, R. K., Ali, Y. M., and Meck, W. H. (2007a). Ketamine "unlocks" the reduced clock-speed effect of cocaine following extended training: evidence for dopamine-glutamate interactions in timing and time perception. *Neurobiol. Learn. Mem.* 88, 149–159.

Cheng, R. K., Etchegaray, M., and Meck, W. H. (2007b). Impairments in timing, temporal memory, and reversal learning linked to neurotoxic regimens of methamphetamine intoxication. *Brain Res.* 1186, 255–266.

Cheng, R. K., Hakak, O. L., and Meck, W. H. (2007c). Habit formation and the loss of control of an internal clock: inverse relationship between the level of baseline training and the clock-speed enhancing effects of methamphetamine. *Psychopharmacology (Berl.)* 193, 351–362.

Cheng, R. K., MacDonald, C. J., Williams, C. L., and Meck, W. H. (2008). Prenatal choline supplementation alters the timing, emotion, and memory performance (TEMP) of adult male and female rats as indexed by differential reinforcement of low-rate schedule behavior. *Learn. Mem.* 15, 153–162.

Church, R. M., and Deluty, M. Z. (1977). Bisection of temporal intervals. *J. Exp. Psychol. Anim. Behav. Process.* 3, 216–228.

Clarke, S., Ivry, R., Grinband, J., Roberts, S., and Shimizu, N. (1996). "Exploring the domain of cerebellar timing," in *Time, Internal Clocks and Movement*, eds M. A. Pastor and J. Artieda (Amsterdam: Elsevier), 257–280.

Cordes, S., and Gelman, R. (2005). "The young numerical mind: when does it count?" in *Handbook of Mathematical Cognition*, ed. J. Campbell (New York: Psychology Press), 127–142.

Cordes, S., Williams, C. L., and Meck, W. H. (2007). Common representations of abstract quantities. *Curr. Dir. Psychol. Sci.*16, 156–161.

Coull, J. T., Cheng, R. K., and Meck, W. H. (2011). Neuroanatomical and neurochemical substrates of timing. *Neuropsychopharmacology* 36, 3–25.

Dewing, P., Chiang, C. W., Sinchak, K., Sim, H., Fernagut, P. O., Kelly, S., Chesselet, M. F., Micevych, P. E., Albrecht, K. H., Harley, V. R., and Vilain, E. (2006). Direct regulation of adult brain function by the male-specific factor SRY. *Curr. Biol.* 16, 415–420.

Droit-Volet, S., and Meck, W. H. (2007). How emotions colour our perception of time. *Trends Cogn. Sci. (Regul. Ed.)* 11, 504–513.

Droit-Volet, S., Meck, W. H., and Penney, T. B. (2007). Sensory modality and time perception in children and adults. *Behav. Processes* 74, 244–250.

Falter, C. M., and Noreika, V. (2011). Interval timing deficits and abnormal cognitive development. *Front. Integr. Neurosci.* 5:26. doi: 10.3389/fnint.2011.00026

Friedman, E. R. (1977). Judgments of time intervals by young children. *Percept. Mot. Skills* 45, 715–720.

Gibbs, R. B. (2010). Estrogen therapy and cognition: a review of the cholinergic hypothesis. *Endocr. Rev.* 31, 224–253.

Gould, E., Woolley, C. S., and McEwen, B. S. (1991). The hippocampal formation: morphological changes induced by thyroid, gonadal and adrenal hormones. *Psychoneuroendocrinology* 116, 67–84.

Harrington, D. L., and Haaland, K. Y. (1999). Neural underpinnings of temporal processing: a review of focal lesion, pharmacological, and functional imaging research. *Rev. Neurosci.* 10, 91–116.

Harrington, D. L., Haaland, K. Y., and Hermanowicz, N. (1998). Temporal processing in the basal ganglia. *Neuropsychology* 12, 3–12.

Hinton, S. C., and Meck, W. H. (2004). Frontal-striatal circuitry activated by human peak-interval timing in the supra-seconds range. *Cogn. Brain Res.* 21, 171–182.

Jahanshahi, M., Jones, C. R., Zijlmans, J., Katzenschlager, R., Lee, L., Quinn, N., Frith, C. D., and Lees, A. J. (2010). Dopaminergic modulation of striato-frontal connectivity during motor timing in Parkinson's disease. *Brain* 133, 727–745.

Jones, C. R., Claassen, D., Yu, M., Spies, J. R., Malone, T., Dirnberger, G., Jahanshahi, M., and Kubovy, M. (2011). Modelling accuracy and variability of motor timing in treated and untreated Parkinson's disease and healthy controls. *Front. Integr. Neurosci.* 5:81. doi: 10.3389/fnint.2011.00081

Jones, C. R. G., and Jahanshahi, M. (2011). Dopamine modulates striato-frontal functioning during temporal processing. *Front. Integr. Neurosci.* 5:70. doi: 10.3389/fnint.2011.00070

Kimura, D. (1996). Sex, sexual orientation and sex hormones influence human cognitive function. *Curr. Opin. Neurobiol.* 6, 259–263.

Loring-Meier, S., and Halpern, D. F. (1999). Sex differences in visuospatial working memory: components of cognitive processing. *Psychon. Bull. Rev.* 6, 464–471.

Lustig, C. (2011). The neuroscience of time and number: untying the Gordian knot. *Front. Integr. Neurosci.* 5:47. doi: 10.3389/fnint.2011.00047

Lustig, C., and Meck, W. H. (2001). Paying attention to time as one gets older. *Psychol. Sci.* 12, 478–484.

Lustig, C., and Meck, W. H. (2011). Modality differences in timing and temporal memory throughout the lifespan. *Brain Cogn.* 77, 298–303.

Malapani, C., Deweer, B., and Gibbon, J. (2002). Separating storage from retrieval dysfunction of temporal memory in Parkinson's disease. *J. Cogn. Neurosci.* 14, 311–322.

Malapani, C., Rakitin, B., Levy, R., Meck, W. H., Deweer, B., Dubois, B., and Gibbon, J. (1998). Coupled temporal memories in Parkinson's disease: a dopamine-related dysfunction. *J. Cogn. Neurosci.* 10, 316–331.

Matell, M. S., and Meck, W. H. (2000). Neuropsychological mechanisms of interval timing behaviour. *Bioessays* 22, 94–103.

Matell, M. S., and Meck, W. H. (2004). Cortico-striatal circuits and interval timing: coincidence-detection of oscillatory processes. *Cogn. Brain Res.* 21, 139–170.

Matell, M. S., Meck, W. H., and Nicolelis, M. A. L. (2003). Interval timing and the encoding of signal duration by ensembles of cortical and striatal neurons. *Behav. Neurosci.*117, 760–773.

McCarthy, M. M., and Arnold, A. P. (2011). Reframing sexual differentiation of the brain. *Nat. Neurosci.* 14, 677–683.

Meck, W. H. (1983). Selective adjustment of the speed of internal clock and memory processes. *J. Exp. Psychol. Anim. Behav. Process.* 9, 171–201.

Meck, W. H. (1996). Neuropharmacology of timing and time perception. *Cogn. Brain Res.* 3, 227–242.

Meck, W. H. (1997). "Application of a mode-control model of temporal integration to counting and timing behaviour," in *Time and behaviour: Psychological and neurobiological analyses*, eds C. M. Bradshaw and E. Szabadi (New York: Elsevier), 133–184.

Meck, W. H. (2006a). Frontal cortex lesions eliminate the clock speed effect of dopaminergic drugs on interval timing. *Brain Res.* 1108, 157–167.

Meck, W. H. (2006b). Neuroanatomical localization of an internal clock: a functional link between mesolimbic, nigrostriatal, and mesocortical dopaminergic systems. *Brain Res.* 1109, 93–107.

Meck, W. H. (2007). Acute ethanol potentiates the clock-speed enhancing effects of nicotine on timing and temporal memory. *Alcohol. Clin. Exp. Res.* 31, 2106–2113.

Meck, W. H., and Church, R. M. (1983). A mode control model of counting and timing processes. *J. Exp. Psychol. Anim. Behav. Process.* 9, 320–334.

Meck, W. H., Church, R. M., and Gibbon, J. (1985). Temporal integration in duration and number discrimination. *J. Exp. Psychol. Anim. Behav. Process.* 11, 591–597.

Meck, W. H., and Malapani, C. (2004). Neuroimaging of interval timing. *Cogn. Brain Res.* 21, 133–137.

Meck, W. H., Penney, T. B., and Pouthas, V. (2008). Cortico-striatal representation of time in animals and humans. *Curr. Opin. Neurobiol.* 18, 145–152.

Melgire, M., Ragot, R., Samson, S., Penney, T. B., Meck, W. H., and Pouthas, V. (2005). Auditory/visual duration bisection in patients with left or right medial temporal lobe resection. *Brain Cogn.* 58, 119–124.

Merritt, D. J., Casasanto, D., and Brannon, E. M. (2010). Do monkeys think in metaphors? Representations of space and time in monkeys and humans. *Cognition* 117, 191–202.

Neil, D. B., and Herndon, J. G. Jr. (1978). Anatomical specificity within rat striatum for the dopaminergic modulation of DRL responding and activity. *Brain Res.* 153, 529–538.

Ovtscharoff, W., Eusterschulte, B., Zie-necker, R., Reisert, I., and Pilgrim, C. (1992). Sex differences indensities of dopaminergic fibers and GABAergic neurons in the prenatal rat striatum. *J. Comp. Neurol.* 323, 299–304.

Paule, M. G., Meck, W. H., McMillan, D. E., McClure, G. Y. H., Bateson, M., Popke, E. J., Chelonis, J. J., and Hinton, S. C. (1999). The use of timing behaviors in animals and humans to detect drug and/or toxicant effect. *Neurotoxicol. Teratol.* 21, 491–502.

Penney, T. B., Gibbon, J., and Meck, W. H. (2008). Categorical scaling of duration bisection in pigeons (*Columba livia*), mice (*Mus musculus*), and humans (*Homo sapiens*). *Psychol. Sci.* 19, 1103–1109.

Phoenix, C. H., Goy, R. W., Gerall, A. A., and Young, W. C. (1959). Organizing action of prenatally administered testosterone propionate on the tissues mediating mating behavior in the female guinea pig. *Endocrinology* 65, 369–382.

Pleil, K. E., Cordes, S., Meck, W. H., and Williams, C. L. (2011). Rapid and acute effects of estrogen on time perception in male and female rats. *Front. Integr. Neurosci.* 5:63. doi: 10.3389/fnint.2011.00063

Ragbetli, M. C., Aydinlioglu, A., and Kaplan, S. (2002). Sex differences and right-left asymmetries in rat hippocampal components. *Int. J. Neurosci.* 112, 81–95.

Rammsayer, T., and Lustnauer, S. (1989). Sex differences in time perception. *Percept. Mot. Skills* 68, 195–198.

Rao, S. M., Harrington, D. L., Haaland, K. Y., Bobholz, J. A., Cox, R. W., and Binder, J. R. (1997). Distributed neural systems underlying the timing of movements. *J. Neurosci.* 17, 5528–5535.

Rao, S. M., Mayer, A. R., and Harrington, D. L. (2001). The evolution of brain activation during temporal processing. *Nat. Neurosci.* 4, 317–323.

Repp, P. R., Morrison, J. H., and Roberts, J. A. (2003). Cyclic estrogen replacement improves cognitive function in aged ovariectomized rhesus monkeys. *J. Neurosci.* 23, 5708–5714.

Roeckelein, J. E. (1972). Sex differences in time estimation. *Percept. Mot. Skills* 35, 859–862.

Roitman, J. D., Brannon, E. M., Andrews, J. R., and Platt, M. L. (2007). Nonverbal representation of time and number in adults. *Acta Psychol. (Amst.)* 124, 296–318.

Ross, L., and Santi, A. (2000). The effects of estrogen on temporal and numerical processing in ovariectomized female rats. *Psychobiology* 28, 394–405.

Sandstrom, N. J. (2007). Estradiol modulation of the speed of an internal clock. *Behav. Neurosci.* 121, 422–432.

Sandstrom, N. J., and Williams, C. L. (2004). Spatial memory retention is enhanced by acute and continuous estradiol replacement. *Horm. Behav.* 45, 128–135.

Strang, H. R., Rust, J. O., and Garrison, S. G. (1973). Sex differences in short-term time estimation. *Percept. Mot. Skills* 36, 1109–1110.

Varga, M. E., Pavlova, O. G., and Nosova, S. V. (2010). The counting function and its representation in the parietal cortex in humans and animals. *Neurosci. Behav. Physiol.* 40, 185–196.

Veng, L. M., Granholm, A.-C., and Rose, G. M. (2003). Age-related sex differences in spatial learning and basal forebrain cholinergic neurons in F344 rats. *Physiol. Behav.* 80, 27–36.

Vodolazhskaya, M. G., and Beier, E. V. (2002). Assessment of disturbances in internal time counting and emotional behavior in rats with lesions to the striatum and hippocampus. *Neurosci. Behav. Physiol.* 32, 485–493.

Weiss, E. M., Kemmler, G., Deisenhammer, E. A., Fleischhacker, W. W., and Delazer, M. (2003). Sex differences in cognitive functions. *Pers. Indiv. Differ.* 35, 863–875.

Whalen, J., Gallistel, C. R., and Gelman, R. (1999). Nonverbal counting in humans: the psychophysics of number representation. *Psychol. Sci.* 10, 130–137.

Williams, C. L., Barnett, A. M., and Meck, W. H. (1990). Organizational effects of early gonadal secretions on sexual differentiation in spatial memory. *Behav. Neurosci.* 104, 84–97.

Williams, C. L., and Meck, W. H. (1991). Organizational effects of gonadal steroids on sexually dimorphic spatial ability. *Psychoneuroendocrinology* 16, 157–177.

Williams, C. L., and Meck, W. H. (1993). "Organizational effects of gonadal hormones induce qualitative differences in visuospatial navigation," in *The Development of Sex Differences and Similarities in Behavior*, eds M. Haug, R. E. Whalen, C. Aron, K. L. Olsen (Amsterdam: Kluwer Academic Publishers), 175–189.

Wittmann, M., and Szelag, E. (2003). Sex differences in perception of temporal order. *Percept. Mot. Skills* 96, 105–112.

Xiao, L., and Becker, J. B. (1994). Quantitative microdialysis determination of extracellular striatal dopamine concentration in male and female rats: effects of estrous cycle and gonadectomy. *Neurosci. Lett.* 180, 155–158.

Received: 02 December 2011; accepted: 02 December 2011; published online: 05 January 2012.

*Citation: Williams CL (2012) Sex differences in counting and timing. Front. Integr. Neurosci. **5**:88. doi: 10.3389/fnint.2011.00088*

frontiers in
INTEGRATIVE NEUROSCIENCE

OPINION ARTICLE
published: 09 September 2011
doi: 10.3389/fnint.2011.00047

The neuroscience of time and number: untying the Gordian knot

Cindy Lustig*

Department of Psychology, University of Michigan, Ann Arbor, MI, USA
**Correspondence: clustig@umich.edu*

Many aspects of the neuroscience of time and number (NEUTIN), as well as its associated psychophysics, have objective, absolute qualities reminiscent of Newtonian physics. For example, both time and number representations have been hypothesized to be based on the absolute value of a pulse-accumulation process generated by a neural pacemaker whose temporal integration is linear with the duration and/or number of events (Gibbon et al., 1984; Buhusi and Meck, 2005; Allman et al., 2011). Moreover, it has been shown that a single "count" within such a pacemaker/accumulator equals a fixed amount of time (e.g., 200 ms). This finding suggests that "pulses" have a uniform size and serve as a common currency for both time and number as long as the pulse-accumulation process can be operated simultaneously in "event" (count) or "run" (time) modes (Meck and Church, 1983; Meck et al., 1985; Meck, 1997; Breukelaar and Dalrymple-Alford, 1998; Roberts et al., 2000; Brannon and Roitman, 2003; Cordes et al., 2007; Roitman et al., 2007). On the other hand, our experience of time and number evokes another well-known characteristic of physics, relativity theory. This aspect is captured by the scalar property: Temporal and numerical judgments are based on the proportional relationships among the durations being timed and/or the objects or events being counted (Gibbon, 1977; Gibbon et al., 1984; Brannon et al., 2001, 2008; Cheng and Meck, 2007; Buhusi and Meck, 2009a,b).

Information processing models of time and number magnitude describe the scalar property as deriving from cognitive processes such as attention, short-term memory, and reference memory (e.g., the mode-control model of counting and timing; Meck and Church, 1983; Meck et al., 1985). Distortions in numerical and temporal cognition occur in neurological and psychiatric conditions that disrupt these processes (e.g., attention deficit hyperactivity disorder, autism, dyscalculia, Parkinson's disease, and schizophrenia) – see Allman and Meck (2011). However, our understanding of the mechanisms underlying NEUTIN and their specific relations to the brain mechanisms underlying other aspects of cognitive processing remains in its infancy.

One barrier to understanding the intricate, intertwined nature of the relations among temporal, numerical, and other aspects of cognitive processing is that researchers have often adopted an Alexandrian solution – that is, divided these aspects into different fields of study. This has led to a lack of consistent agreement on terminology, creating further obstacles to a unified understanding (Paule et al., 1999; Meck and Benson, 2002; Buhusi and Meck, 2005; Meck, 2005; Meck et al., 2008; Coull et al., 2011). There is also a need for technological advances to improve the spatial and, especially critical in this context, temporal resolution of current neuroimaging methods. However, if these efforts are undertaken, the exploration of how the brain performs temporal integration across multiple time scales is expected to be among the premier topics to unite systems, cellular, computational, and cognitive neuroscience over the next decade (Buonomano, 2007).

Questions concerning the impact of development, sensory modality, sleep-dependent memory consolidation, stimulus field/whole-body motion, and genetic predispositions toward increased/decreased neurotransmitter activities of dopamine, glutamate, and serotonin systems in cortico-striatal circuits will be important components in future studies of numerical and temporal cognition (Libertus and Brannon, 2009; Dehaene and Brannon, 2010; Sysoeva et al., 2010; Agostino et al., 2011; Wiener et al., 2011). Meanwhile several theoretical and empirical developments promise a more integrated view. In particular, we have suggested that the identity properties of an item (color, shape, size, location, etc.) may be coded by which cortical neurons are firing while temporal properties are coded by the oscillatory properties of that firing (Lustig et al., 2005). Attention serves to modulate and maintain the integrity of this representation, and striatal neurons act as "coincidence detectors" first encoding and then responding to behaviorally relevant patterns of identity and oscillatory inputs. This approach brings together feature-based views of representations in short- and long-term memory (e.g., Oberauer and Kliegl, 2006; see Jonides et al., 2008; Lustig et al., 2009 for discussion) with views that emphasize oscillatory processes and the detection of specific oscillatory patterns for working memory and timing (e.g., Matell and Meck, 2004; Hazy et al., 2006).

Recent findings from Harrington et al. (2010) are interesting from this perspective. Cortico-striatal activation patterns differed at encoding depending on whether participants attended to the pitch or the duration of a tone; in particular, the striatum was especially active during duration encoding, possibly reflecting its role in integrating oscillations across cycles to represent the passage of time (Matell and Meck, 2004; Meck et al., 2008; Allman and Meck, 2011; Harrington et al., 2011a,b; Portugal et al., 2011). However, during retention, striatal activation was equivalent for the two stimulus classes (and greater than a control task), consistent with a striatal role in modulating thalamocortical structures to recurrently maintain the activation patterns associated with relevant stimuli. Another study (Manning et al., 2011) found direct evidence for the role of oscillations in encoding temporal-order information using intercranial recording methods. When patients recalled items they had previously studied, not only were oscillatory patterns present at encoding recapitulated, but the similarity between the oscillatory patterns associated with different items at retrieval varied linearly with the distance between those items at encoding. In addition, those patients that had stronger reinstatement patterns in neural oscillations

were also more likely to show temporal clustering in their behavioral recall. Interest in fMRI and EEG measures of oscillatory activity in both resting-state and task-oriented neural networks is also rising (e.g., Laufs et al., 2003; Achard et al., 2006) and presents an exciting opportunity for integration with NEUTIN.

The translational impetus to further integrate NEUTIN with other aspects of basic and cognitive neuroscience is compelling. First, accurate estimation of time and number is an essential component of organized behavior (Gallistel and Gibbon, 2000). Disruptions in NEUTIN-related processes are characteristic of and may even be causal in the symptoms of disrupted organization or synchronization present in several neuropsychiatric disorders including dyslexia, aphasia, Parkinson's, and schizophrenia (Eagleman et al., 2005; Wojtecki et al., 2011). Second, timing and counting involve several fundamental cognitive processes (e.g., attention, working memory, long-term memory) for which a long tradition of research has identified dissociable behavioral signatures and neural substrates. These tasks may thus provide, within a single testing session, well-validated measures of multiple cognitive constructs important for diagnosis and treatment. Third, many timing and counting tasks can be administered similarly across species, increasing confidence when extrapolating from animal models to human neurophysiological and cognitive function in the testing and development of drugs for the treatment of schizophrenia, Alzheimer's disease, and other forms of dementia (Meck and Church, 1983; Church et al., 1994; Rakitin et al., 1998; Roitman et al., 2007; Penney et al., 2008; Gu et al., 2011; Meck et al., 2011; Ward et al., 2011). Targeting NEUTIN tasks that have demonstrated cross-species behavioral validity (e.g., Penney et al., 2008) for further development in psychometrics, genetic and pharmacologic manipulations, exploration of neural substrates, and sensitivity to disease models will be an important step in bringing this potential to fruition (for a related example of task development in the control of attention, see Demeter et al., 2008, 2011; Nuechterlein et al., 2009; Luck et al., 2011).

Finally, the ability to use temporal and numerical processing tasks both across species (e.g., Penney et al., 2008) and across the lifespan (Lustig and Meck, 2001, 2011) makes them attractive tools for helping to elucidate the evolutionary and ontogenetic development of cognitive processes. As noted above, basic temporal and numerical processing abilities appear to be present even in relatively simple organisms and in very young children, but NEUTIN-related tasks also seem quite sensitive to irregularities in the functioning of attention and memory. They may therefore be useful in screening children at a very young age to identify those at-risk for difficulties in important educational activities (especially mathematics; Libertus et al., 2011) and even provide a basis for training and intervention (Shaffer et al., 2001; Cosper et al., 2009).

To summarize, temporal and numerical processing is both fundamental and complex. These two domains have often been studied separately from each other, and from other cognitive domains such as attention, memory, and emotion. However, recent developments including a new appreciation of the importance of oscillatory processes in neural function and of the translational value of temporal/numerical processing tasks hold great promise for a better understanding of both NEUTIN *per se* and how the brain produces organized behavior more generally.

REFERENCES

Achard, S., Salvador, R., Whitcher, B., Suckling, J., and Bullmore, E. (2006). A resilient, low-frequency, small-world human brain functional network with highly connected association cortical hubs. *J. Neurosci.* 26, 63–72.

Agostino, P. V., Golombek, D. A., and Meck, W. H. (2011). Unwinding the molecular basis of interval and circadian timing. *Front. Integr. Neurosci.* (in press).

Allman, M. J., and Meck, W. H. (2011). Pathophysiological distortions in time perception and timed performance. *Brain* (in press).

Allman, M. J., Pelphrey, K. A., and Meck, W. H. (2011). Developmental neuroscience of time and number: implications for autism and other neurodevelopmental disabilities. *Front. Integr. Neurosci.* (in press).

Brannon, E. M., Libertus, M. E., Meck, W. H., and Woldorff, M. G. (2008). Electrophysiological measures of time processing in infant and adult brains: Weber's law holds. *J. Cogn. Neurosci.* 20, 193–203.

Brannon, E. M., and Roitman, J. D. (2003). "Nonverbal representation of time and number in animals and human infants," in *Functional and Neural Mechanisms of Interval Timing*, ed. W. H. Meck (Boca Raton: CRC Press), 143–182.

Brannon, E. M., Wusthoff, C. J., Gallistel, C. R., and Gibbon, J. (2001). Subtraction in the pigeon: evidence for a linear subjective number scale. *Psychol. Sci.* 1, 238–243.

Breukelaar, J. W. C., and Dalrymple-Alford, J. C. (1998). Timing ability and numerical competence in rats. *J. Exp. Psychol. Anim. Behav. Process.* 24, 84–97.

Buhusi, C. V., and Meck, W. H. (2005). What makes us tick? Functional and neural mechanisms of interval timing. *Nat. Rev. Neurosci.* 6, 755–765.

Buhusi, C. V., and Meck, W. H. (2009a). Relative time sharing: new findings and an extension of the resource allocation model of temporal processing. *Philos. Trans. R. Soc. Lond. B Biol. Sci.* 364, 1875–1885.

Buhusi, C. V., and Meck, W. H. (2009b). Relativity theory and time perception: single or multiple clocks? *PLoS ONE* 4, e6268. doi: 10.1371/journal.pone.0006268

Buonomano, D. V. (2007). The biology of time across different scales. *Nat. Chem. Biol.* 3, 594–597.

Cheng, R. K., and Meck, W. H. (2007). Prenatal choline supplementation increases sensitivity to time by reducing non-scalar sources of variance in adult temporal processing. *Brain Res.* 1186, 242–254.

Church, R. M., Meck, W. H., and Gibbon, J. (1994). Application of scalar timing theory to individual trials. *J. Exp. Psychol. Anim. Behav. Process.* 20, 135–155.

Cordes, S., Williams, C. L., and Meck, W. H. (2007). Common representations of abstract quantities. *Curr. Dir. Psychol. Sci.* 16, 156–161.

Cosper, S. M., Lee, G. P., Peters, S. B., and Bishop, E. (2009). Interactive metronome training in children with attention deficit and developmental coordination disorders. *Int. J. Rehabil. Res.* 32, 331–336.

Coull, J. T., Cheng, R. K., and Meck, W. H. (2011). Neuroanatomical and neurochemical substrates of timing. *Neuropsychopharmacology* 36, 3–25.

Dehaene, S., and Brannon, E. M. (2010). Space, time, and number: a Kantian research program. *Trends Cogn. Sci. (Regul. Ed.)* 14, 517–519.

Demeter, E., Hernandez-Garcia, L., Sarter, M., and Lustig, C. (2011). Challenges to attention: a continuous arterial spin labeling (ASL) study of the effects of distraction on sustained attention. *Neuroimage* 54, 1518–1529.

Demeter, E., Sarter, M., and Lustig, C. (2008). Rats and humans paying attention: cross-species task development for translational research. *Neuropsychology* 22, 787–799.

Eagleman, D. M., Tse, P. U., Buonomano, D., Janssen, P., Nobre, A. C., and Holcombe, A. O. (2005). Time and the brain: how subjective time relates to neural time. *J. Neurosci.* 25, 10369–10371.

Gallistel, C. R., and Gibbon, J. (2000). Time, rate, and conditioning. *Psychol. Rev.* 107, 289–344.

Gibbon, J. (1977). Scalar expectancy and Weber's law in animal timing. *Psychol. Rev.* 84, 279–325.

Gibbon, J., Church, R. M., and Meck, W. H. (1984). Scalar timing in memory. *Ann. N. Y. Acad. Sci.* 423, 52–77.

Gu, B. M., Yin, B., Cheng, R. K., and Meck, W. H. (2011). Quinpirole-induced sensitization to noisy/sparse periodic input: temporal synchronization as a component of obsessive-compulsive disorder. *Neuroscience* 179, 143–150.

Harrington, D. L., Castillo, G. N., Fong, C. H., and Reed, J. D. (2011a). Neural underpinnings of distortions in the experience of time across senses. *Front. Integr. Neurosci.* 5:32. doi: 10.3389/fnint.2011.00032

Harrington, D. L., Castillo, G. N., Greenberg, P. A., Song, D. D., Lessig, S., Lee, R. R., and Rao, S. M. (2011b). Neurobehavioral mechanisms of temporal processing deficits in Parkinson's disease. *PLoS ONE* 6, e17461. doi: 10.1371/journal.pone.0017461

Harrington, D. L., Zimbelmann, J. L., Hinton, S. C., and Rao, S. M. (2010). Neural modulation of temporal encoding, maintenance, and decision processes. *Cereb. Cortex* 20, 1274–1285.

Hazy, T. E., Frank, M. J., and O'Reilly, R. C. (2006). Banishing the homunculus: making working memory work. *Neuroscience* 139, 105–118.

Jonides, J., Lewis, R. L., Nee, D. E., Lustig, C., Berman, M. G., and Moore, K. S. (2008). The mind and brain of short-term memory. *Annu. Rev. Psychol.* 59, 193–224.

Laufs, H., Krakow, K., Sterzer, P., Eger, E., Beyerle, A., Salek-Haddadi, A., and Kleinschmidt, A. (2003). Electroencephalographic signatures of attentional and cognitive default modes in spontaneous brain activity fluctuations at rest. *Proc. Natl. Acad. Sci. U.S.A.* 100, 11053–11058.

Libertus, M. E., and Brannon, E. M. (2009). Behavioral and neural basis of number sense in infancy. *Curr. Dir. Psychol. Sci.* 18, 346–351.

Libertus, M. E., Feigenson, L., and Halberda, J. (2011). Preschool acuity of the approximate number system correlates with school math ability. *Dev. Sci.* doi: 10.1111/j.1467-7687.2011.01080.x

Luck, S. J., Ford, J. M., Sarter, M., and Lustig, C. (2011). CNTRICS final biomarker selection: control of attention. *Schizophr. Bull.* doi: 10.1093/schbul/sbr065

Lustig, C., Berman, M., Nee, D. E., Lewis, R. L., Moore, K. S., and Jonides, J. (2009). "Psychological and neural mechanisms of short-term memory," in *Handbook of Neuroscience for the Behavioral Sciences*, eds G. G. Bernston and J. T. Cacciopo (Hoboken, NJ: John Wiley & Sons), 567–585.

Lustig, C., Matell, M. S., and Meck, W. H. (2005). Not "just" a coincidence: frontal-striatal synchronization in working memory and interval timing. *Memory* 13, 441–448.

Lustig, C., and Meck, W. H. (2001). Paying attention to time as one gets older. *Psychol. Sci.* 12, 478–484.

Lustig, C., and Meck, W. H. (2011). Modality differences in timing and temporal memory throughout the lifespan. *Brain Cogn.* (in press).

Manning, J. R., Polyn, S. M., Baltuch, G. H., Litt, B., and Kahana, M. J. (2011). Oscillatory patterns in temporal lobe reveal context reinstatement during memory search. *Proc. Natl. Acad. Sci. U.S.A.* 108, 12893–12897.

Matell, M. S., and Meck, W. H. (2004). Cortico-striatal circuits and interval timing: coincidence detection of oscillatory processes. *Brain Res. Cogn. Brain Res.* 21, 139–170.

Meck, W. H. (1997). "Application of a mode-control model of temporal integration to counting and timing behaviour," in *Time and Behaviour: Psychological and Neurobiological Analyses*, eds C. M. Bradshaw and E. Szabadi (New York: Elsevier), 133–184.

Meck, W. H. (2005). Neuropsychology of timing and time perception. *Brain Cogn.* 58, 1–8.

Meck, W. H., and Benson, A. M. (2002). Dissecting the brain's internal clock: how frontal-stratial circuitry keeps time and shifts attention. *Brain Cogn.* 48, 195–211.

Meck, W. H., Cheng, R. K., MacDonald, C. J., Gainetdinov, R. R., Caron, M. G., and Çevik, M. Ö. (2011). Gene-dose dependent effects of methamphetamine on interval timing in dopamine-transporter knockout mice. *Neuropharmacology.* doi: 10.1016/j.neuropharm.2011.01.042. [Epub ahead of print].

Meck, W. H., and Church, R. M. (1983). A mode-control model of counting and timing processes. *J. Exp. Psychol. Anim. Behav. Process.* 9, 320–334.

Meck, W. H., Church, R. M., and Gibbon, J. (1985). Temporal integration in duration and number discrimination. *J. Exp. Psychol. Anim. Behav. Process.* 11, 591–597.

Meck, W. H., Penney, T. B., and Pouthas, V. (2008). Cortico-striatal representation of time in animals and humans. *Curr. Opin. Neurobiol.* 18, 145–152.

Nuechterlein, K. H., Luck, S. J., Lustig, C., and Sarter, M. (2009). CNTRICS final task selection: control of attention. *Schizophr. Bull.* 35, 182–196.

Oberauer, K., and Kliegl, R. (2006). A formal model of capacity limits in working memory. *J. Mem. Lang.* 55, 601–626.

Paule, M. G., Meck, W. H., McMillan, D. E., McClure, G. Y. H., Bateson, M., Popke, E. J., Chelonis, J. J., and Hinton, S. C. (1999). The use of timing behaviors in animals and humans to detect drug and/or toxicant effects. *Neurotoxicol. Teratol.* 21, 491–502.

Penney, T. B., Gibbon, J., and Meck, W. H. (2008). Categorical scaling of duration bisection in pigeons (*Columba livia*), mice (*Mus musculus*), and humans (*Homo sapiens*). *Psychol. Sci.* 19, 1103–1109.

Portugal, G. S., Wilson, A. G., and Matell, M. S. (2011). Behavioral sensitivity of temporally modulated striatal neurons. *Front. Integr. Neurosci.* 5:30. doi: 10.3389/fnint.2011.00030

Rakitin, B. C., Gibbon, J., Penney, T. B., Malapani, C., Hinton, S. C., and Meck, W. H. (1998). Scalar expectancy theory and peak-interval timing in humans. *J. Exp. Psychol. Anim. Behav. Process.* 24, 15–33.

Roberts, W. A., Coughlin, R., and Roberts, S. (2000). Pigeons flexibly time or count on cue. *Psychol. Sci.* 11, 218–222.

Roitman, J. D., Brannon, E. M., Andrews, J. R., and Platt, M. L. (2007). Nonverbal representation of time and number in adults. *Acta Psychol. (Amst.)* 124, 296–318.

Shaffer, R. J., Jacokes, L. E., Cssily, J. F., Greenspan, S. I., Tuchman, R. F., and Stemmer, P. J. Jr. (2001). Effect of interactive metronome training on children with ADHD. *Am. J. Occup. Ther.* 55, 155–162.

Sysoeva, O. V., Tonevitsky, A. G., and Wackermann, J. (2010). Genetic determinants of time perception mediated by the serotonergic system. *PLoS ONE* 5, e12650. doi: 10.1371/journal.pone.0012650

Ward, R. D., Kellendonk, C., Kandel, E. R., and Balsam, P. D. (2011). Timing as a window on cognition in schizophrenia. *Neuropharmacology.* doi: 10.1016/j.neuropharm.2011.04.014. [Epub ahead of print].

Wiener, M., Lohoff, F. W., and Coslett, H. B. (2011). Double dissociation of dopamine genes and timing in humans. *J. Cogn. Neurosci.* 23, 2811–2821.

Wojtecki, L., Elben, S., Timmermann, L., Reck, C., Maarouf, M., Jörgens, S., Ploner, M., Südmeyer, M., Groiss, S., Sturm, V., Niedeggen, M., and Schnitzler, A. (2011). Modulation of human time processing by subthalamic deep brain stimulation. *PLoS ONE* (in press).

Received: 16 August 2011; accepted: 16 August 2011; published online: 09 September 2011.

*Citation: Lustig C (2011) The neuroscience of time and number: untying the Gordian knot. Front. Integr. Neurosci. **5**:47. doi: 10.3389/fnint.2011.00047*

frontiers in
INTEGRATIVE NEUROSCIENCE

ORIGINAL RESEARCH ARTICLE
published: 28 July 2011
doi: 10.3389/fnint.2011.00032

Neural underpinnings of distortions in the experience of time across senses

Deborah L. Harrington[1,2]*, Gabriel N. Castillo[1,2], Christopher H. Fong[2] and Jason D. Reed[1,2]

[1] *Research Service, Veterans Affairs San Diego Healthcare System, San Diego, CA, USA*
[2] *Department of Radiology, University of California San Diego, San Diego, CA, USA*

Edited by:
Warren H. Meck, Duke University, USA

Reviewed by:
Hugo Merchant, Universidad Nacional Autónoma de México, Mexico
John F. Araujo, Federal University of Rio Grande do Norte, Brazil
Marc Wittmann, Institute for Frontier Areas of Psychology and Mental Health, Germany

***Correspondence:**
Deborah L. Harrington, Research Service, Veterans Affairs San Diego Healthcare System, 116A-13, San Diego, CA 92161, USA.
e-mail: dharrington@ucsd.edu

Auditory signals (A) are perceived as lasting longer than visual signals (V) of the same physical duration when they are compared together. Despite considerable debate about how this illusion arises psychologically, the neural underpinnings have not been studied. We used functional magnetic resonance imaging (fMRI) to investigate the neural bases of audiovisual temporal distortions and more generally, intersensory timing. Adults underwent fMRI while judging the relative duration of successively presented standard interval–comparison interval (CI) pairs, which were unimodal (A–A, V–V) or crossmodal (V–A, A–V). Mechanisms of time dilation and compression were identified by comparing the two crossmodal pairs. Mechanisms of intersensory timing were identified by comparing the unimodal and crossmodal conditions. The behavioral results showed that auditory CIs were perceived as lasting longer than visual CIs. There were three novel fMRI results. First, time dilation and compression were distinguished by differential activation of higher-sensory areas (superior temporal, posterior insula, middle occipital), which typically showed stronger effective connectivity when time was dilated (V–A). Second, when time was compressed (A–V) activation was greater in frontal cognitive-control centers, which guide decision making. These areas did not exhibit effective connectivity. Third, intrasensory timing was distinguished from intersensory timing partly by decreased striatal and increased superior parietal activation. These regions showed stronger connectivity with visual, memory, and cognitive-control centers during intersensory timing. Altogether, the results indicate that time dilation and compression arise from the connectivity strength of higher-sensory systems with other areas. Conversely, more extensive network interactions are needed with core timing (striatum) and attention (superior parietal) centers to integrate time codes for intersensory signals.

Keywords: temporal processing, audiovisual temporal distortions, crossmodal timing, fMRI, striatum, sensory integration, attention

INTRODUCTION

Humans possess a remarkable ability to estimate the passage of time, which is vital for behavior. Yet the experience of time is not isomorphic to physical time and depends on many factors including properties of stimuli, past experiences, and behavioral contexts. For example, emotionally charged, larger magnitude, and more intense stimuli are known to expand estimates of time whereas events that are repeated, higher probability, and non-salient tend to compress perceived duration (Tse et al., 2004; Droit-Volet and Meck, 2007; van Wassenhove et al., 2008; Eagleman and Pariyadath, 2009; Matthews et al., 2011). Decades of psychophysical studies have debated the mechanisms of temporal distortions. By pacemaker-counter models (Penney et al., 2000; Ulrich et al., 2006), attention is a central factor that causes time to speed up or slow down by closing or opening a switch, which allows pulses generated from a clock during event timing to be accumulated and counted. Arousal is another factor that ostensibly increases the speed of the pacemaker. Indeed, the level of attention devoted to timing influences perceived duration (Casini and Macar, 1997; Coull et al., 2004) as does heightened physiological arousal induced by emotionally negative sounds (Mella et al., 2011). However, a more complete understanding of how temporal distortions arise has been hampered by scant investigations into the underlying neural mechanisms.

The present study used functional magnetic resonance imaging (fMRI) to investigate the neural underpinnings of the illusion that auditory (A) signals are perceived as lasting longer than visual (V) signals of the same physical duration when they are compared together (Wearden et al., 1998; Gamache and Grondin, 2010). This temporal distortion is of considerable interest because an understanding of its mechanisms may help elucidate how synchrony is maintained across senses to form coherent representations of multisensory events. The modality effect on perceived duration is often attributed to a pacemaker–accumulator "clock" system that runs faster for auditory than visual stimuli, possibly due to an attentional switch that allows pulses to accumulate faster for auditory information (Penney et al., 2000; Wearden et al., 2006). Audiovisual distortions are classically studied using the temporal bisection procedure. However, the present study employed a comparison procedure wherein a standard interval (SI) and a

comparison interval (CI) were successively presented, and participants judged whether the CI was longer or shorter in duration than the SI (Ulrich et al., 2006). SI–CI pairs were either unimodal (A–A, V–V) or crossmodal (V–A, A–V). Using this method, V–A pairs are perceived as lasting longer than A–V pairs, which is due to the longer interpulse time for visual than auditory CIs (Ulrich et al., 2006).

Our primary aim was to identify neural systems underlying time dilation and compression by comparing activation patterns in the crossmodal conditions (V–A versus A–V) where the amount of visual and auditory stimulation was the same. Our hypotheses were motivated by the striatal beat frequency (SBF) model (Matell and Meck, 2004), which suggests that audiovisual differences in timing could arise from cortical oscillatory patterns in the cortex or from the striatum. Specifically, the time code for signal duration is thought to arise from the firing of cortical neurons that have different oscillation rates, which should produce distinct temporal and spatial signatures for auditory and visual signals. On the other hand, the striatum serves as a core timer by detecting and integrating cortical oscillatory states over time. Thus, activation in auditory and visual centers should differ between the crossmodal conditions if modality effects are related to different temporal signatures in sensory and association regions of the cortex. Alternatively, striatal activation should differ between the crossmodal conditions if modality effects are related to differences in the rate of detecting and integrating auditory and visual oscillatory states. We also were interested in whether interactions of the brain with key regions that modulated modality effects were stronger for the time dilation than the compression condition (i.e., effective connectivity). If time dilation is due to an attentional mechanism that favors auditory signals (Penney et al., 2000; Wearden et al., 2006), connectivity might be stronger for V–A than A–V comparisons.

A secondary aim was to investigate neural mechanisms that distinguish intrasensory from intersensory timing by comparing the unimodal and crossmodal conditions in regions that did not exhibit time dilation or compression effects. Current knowledge of the neural underpinnings of temporal processing comes solely from studies of intrasensory timing. Intersensory timing presumably differs in that attention must be switched between senses and time codes must be integrated across senses. Although not explicitly addressed by the SBF model, the detection and integration of oscillatory states by the striatum might be enhanced when timing signals within the same modality because they share similar spatial signatures, which facilitates temporal integration, thereby producing a more robust neuronal response relative to crossmodal timing. If the striatum differentially modulates intra- and intersensory timing, we also speculated that the strength of striatal interactions with the cortex would differ for unimodal and crossmodal timing.

MATERIALS AND METHODS

PARTICIPANTS

Twenty healthy adults participated in the study (8 female and 12 male; mean age = 24.4 years, range: 19–35 years, SD = 4.5; mean education = 15.5 years, range: 13–20 years, SD = 1.6). Participants were excluded if they had a history of neurologic disturbance (e.g., seizures, head injury), learning disability, major psychiatric disturbance, or substance abuse. All participants gave their written informed consent according to guidelines of the Human Research Protections Program at the University of California San Diego (UCSD).

FMRI TASK

Participants performed a time perception task while undergoing fMRI scanning. The task involved presentation of filled-auditory (1000 Hz pure tones) and visual (blue ellipse) stimuli. Tone stimuli were delivered binaurally through a headphone that together with earplugs attenuated background scanner noise by about 40 db. Visual stimuli were viewed through a NordicNeuroLab goggle system. Participants made a two-choice key-press response on a button box using the index or middle finger of their right hand.

Figure 1A shows the experimental design and trial events. Pairs of auditory (A) and/or visual (V) stimuli were successively presented. In two unimodal conditions, the SI and the CI were of the same modality (A–A, V–V) and in two crossmodal conditions they were different (A–V, V–A). Throughout the experiment, the subject maintained fixation on a white cross at the center of the display. Prior to trial onset, a warning signal (i.e., flashing yellow cross and mixed 700-Hz tone) appeared for 350 ms followed by a 500-ms delay. A trial began with the presentation of the SI, followed by a 1.5-s delay, and then the CI. The participant indicated if the CI was shorter or longer than the SI by pressing a key with the right index or middle finger, respectively. Four SIs (1467, 1540, 1620, and 1710 ms) were used to increase the demands of encoding an interval on each trial (**Figure 1B**). For each SI, there were three shorter and three longer CIs that differed from the SI by successive increments of ±7%. Accuracy and reaction time (RT; measured from CI offset to the key press) were recorded.

There were 24 trials per condition (i.e., A–A, V–V, A–V, V–A). Within each of the conditions there were four trials per CI (i.e., 7, 14, and 21% shorter or longer than the SI). These trials were equally divided among the four different SI–CI combinations (**Figure 1B**). The order of the conditions was randomized across four runs, each of which contained 24 trials. At the end of the CI, there was a 3-s "filler" epoch (i.e., fixation) wherein subjects made their response. At the end of this response window, the inter-trial interval was jittered between 3 and 7 s to allow for the best sampling of the hemodynamic response and establishment of a baseline resting state in the model (i.e., fixation plus ambient scanner noise). Six additional filler images were added to the beginning and the end of each run to respectively allow for T1 equilibration and the delayed hemodynamic response of the final trial. Each run consisted of 180 images acquired over 6 min.

MRI METHODS

Image acquisition

Event-related fMRI was conducted at the UCSD Center for FMRI using a GE 3-T Excite MRI system equipped with an 8-channel head coil. Foam padding was used to limit head motion within the coil. Prior to functional imaging, high-resolution T1-weighted anatomic images were collected for anatomic localization and co-registration (TE 3.0 ms, TR 7.8 ms, 12° flip angle, NEX 1, 1-mm axial slice thickness, FOV 25 cm, 256 × 256 matrix). Echo-planar images were acquired using a single-shot, blipped, gradient-echo,

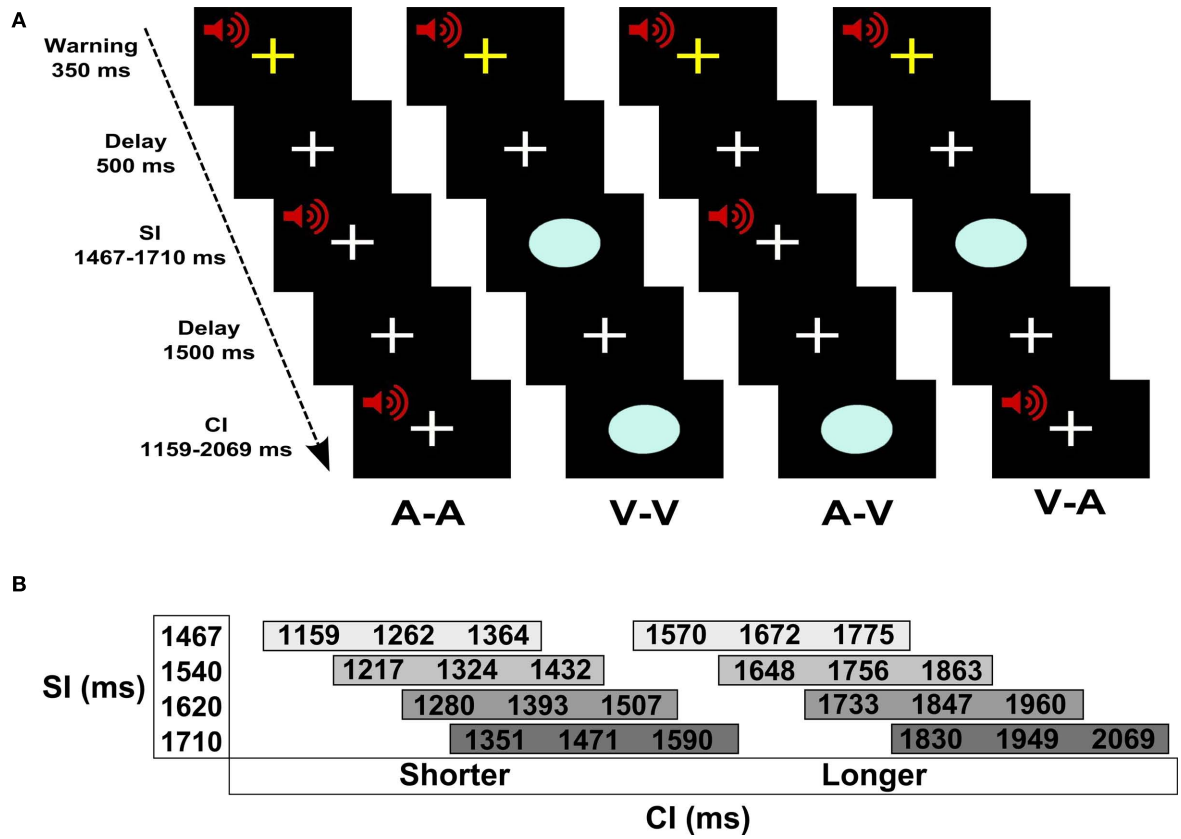

FIGURE 1 | Time perception task. (A) Trial of events for each of the four conditions. Pairs of auditory (A) and/or visual (V) stimuli were successively presented. The standard (SI) and the comparison (CI) intervals were of the same modality in the unimodal conditions (A–A, V–V) and were different modalities in the crossmodal conditions (A–V, V–A). Prior to trial onset, a warning signal (flashing yellow cross and mixed 700-Hz tone) appeared for 350 ms followed by a 500-ms delay. A trial began with the presentation of the SI, followed by a 1.5-s delay, and then the CI. The participant indicated if the CI was shorter or longer than the SI by pressing a key with the right index or middle finger, respectively. **(B)** SI and CI durations. There were four different SIs. Each SI was paired with three shorter and three longer CIs that differed from the SI by successive increments of ±7%.

echo-planar pulse sequence (TE 30 ms, TR 2.0 s, 90° flip angle, FOV 24 cm, 64 × 64 matrix, NEX 1, interleaved slice acquisition). Each functional imaging volume included 37 contiguous, axial 4-mm slices (3.75-mm × 3.75-mm × 4-mm voxel size) to provide coverage of the entire brain.

Image analysis

Functional images were generated using Analysis of Functional NeuroImages (AFNI) software. Time series images were spatially registered in three-dimensional space and corrected for time-slice acquisition differences. The time series for each participant was deconvolved using trial onset (i.e., presentation of the SI) separately for each of the four conditions (A–A, V–V, A–V, V–A). This analysis produces hemodynamic response functions (HRFs) of the fMRI signal on a voxel-wise basis. The HRFs are estimates of the hemodynamic response for each condition relative to the baseline state (i.e., filler images), and are generated without making *a priori* assumptions about the shape, delay, or magnitude of the HRF. The deconvolution was modeled for 8 time points (i.e., 16 s). Six head-motion parameters were included as covariates of no interest. Area under the curve (AUC) was calculated using the volumes that captured peak activation during the SI (volumes 2 and 3 beginning at 4.0 and 6.0 s post-trial onset) and the CI and response (volumes 4 and 5 beginning at 8.0 and 10.0 s post-trial onset). AUC maps were then interpolated to volumes with 1-mm^3 voxels, co-registered, converted to Talairach coordinate-space, and blurred using a 6-mm Gaussian full-width half maximum filter.

Repeated-measures analyses of variance (ANOVAs) were performed on a voxel-wise basis to generate statistical parametric maps that identified voxels that showed main effects of timing condition (unimodal, crossmodal), CI modality (auditory, visual), and the interaction. Voxel-wise thresholds were derived from 3000 Monte Carlo simulations (AFNI AlphaSim), which computed the voxel-probability and minimum cluster-size threshold needed to obtain a 0.05 familywise alpha. Because spatial thresholds are biased against smaller activation clusters of *a priori* interest (i.e., basal ganglia), statistical thresholds were derived separately for basal ganglia and cortical volumes (Worsley et al., 1996). This was accomplished by creating a basal ganglia mask (i.e., putamen, globus pallidus, caudate) using the Talairach Daemon dataset; the mask was then expanded to include any voxels within a 2-mm radius. The cortical mask included all other regions of the brain. Each mask was used in the Monte Carlo simulations to determine the appropriate combination of individual voxel-probability and

minimum cluster-size threshold. For the basal ganglia volume, we used a voxel-wise threshold of $p < 0.006$ and a minimum cluster size of 0.338 ml. For the cortical volume, we used a voxel-wise threshold of $p < 0.004$ and a minimum cluster size of 0.675 ml.

The objectives of our study were to investigate regional differences associated with (1) signal modality (A–A versus V–V), (2) timing condition (unimodal versus crossmodal), and (3) the interaction of modality × timing condition. Planned comparisons of significant interactions focused on the contrast between the two crossmodal pairs (A–V versus V–A) since this directly tests for regional activation associated with the time dilation effect while controlling for sensory processing demands. To accomplish these objectives, a functional region of interest (fROI) analysis was conducted to directly evaluate regional differences associated with each of these effects. The fROI map was generated by conjoining activated regions associated with the main effect and interaction tests that were identified in the above voxel-wise analyses. As some fROI were quite large, we separated them into smaller regions along minimum contour lines of the voxel-wise map using a watershed algorithm. This algorithm first uses AFNI 3dExtrema to find a set of local maxima separated by at least 20 mm and then creates boundaries for clusters containing these maxima along the minimum value contour lines (Cox, 1996). The watershed algorithm was applied to the conjoined fROI map using the normalized maximum intensity value from each voxel. The results from *F* tests conducted on the fROI were the focus of the study.

Effective connectivity analyses

We also asked if connectivity of key regions with the entire brain were modulated by the timing condition (unimodal versus crossmodal) or by dilation/compression effects on perceived duration (V–A versus A–V). This was achieved by conducting voxel-based tests of psychophysiological interactions (PPI; Friston et al., 1997) for key regions, which were identified by the above fROI analyses. For PPI analyses pertaining to timing condition, key regions were selected that (1) exhibited differences between the unimodal and crossmodal conditions, (2) did not show a timing condition × CI modality interaction, and (3) have been implicated in temporal processing. For PPI analyses pertaining to time dilation/compression, key regions were selected that exhibited a timing condition × CI modality interaction that was related to differences in activation between the two crossmodal pairs (V–A versus A–V). Voxels in these key regions were the seed ROI and were selected for each subject based on the conjunctive maps generated for the fROI analyses. Seeds were constructed by drawing a 5-mm radius sphere that was centered close to the peak activation within a fROI. In one PPI analysis, the experimental variable was the timing condition (unimodal versus crossmodal). In the other PPI analysis, the experimental variable was the time dilation/compression effect (V–A versus A–V). Multiplication of the deconvolved time series for the seed areas with each experimental variable formed the interaction term (i.e., PPI regressor), which tested whether connectivity of a key region with the whole brain was modulated by the experimental variable. A $p < 0.006$ voxel-wise threshold and a 0.338-ml minimum cluster size was the criterion for significance.

RESULTS

BEHAVIORAL RESULTS

The analyses collapsed across SI duration. Hence, CIs that were ±7, 14, and 21% increments of the SI duration were also averaged. The main dependent measure was accuracy, which was converted to the percent longer responses for each CI. A repeated-measures ANOVA tested the main effect of CI modality (auditory, visual), timing condition (unimodal, crossmodal), CI duration (±7, 14, 21%), and the interactions. The Huynh–Feldt correction was applied to multiple DOF effects to adjust for violations of sphericity. The main results are graphed in **Figure 2**.

All first-order interactions were significant [CI modality × timing condition: $F(1,19) = 96.3$, $p < 0.0001$, $\eta^2 = 0.84$; timing condition × CI duration: $F(4.4, 83) = 8.3$, $p < 0.0001$, $\eta^2 = 0.30$; CI modality × CI duration: $F(5,95) = 2.8$, $p < 0.025$, $\eta^2 = 0.13$]. Planned comparisons of the CI modality × timing

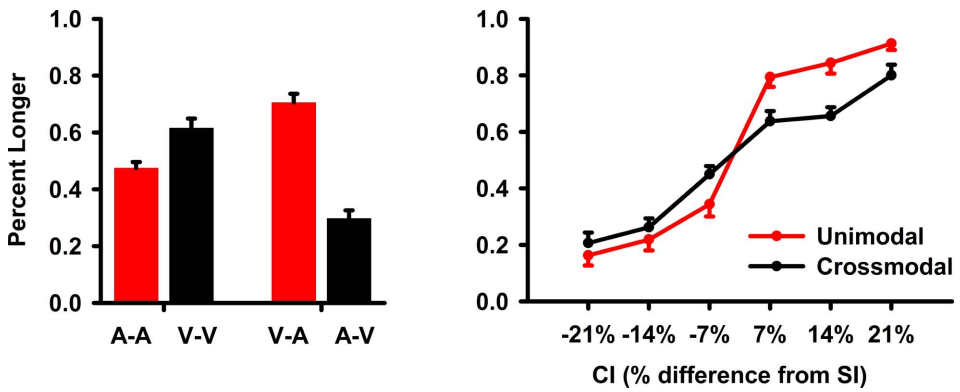

FIGURE 2 | Task performance during fMRI scanning. Accuracy data were converted to the mean (standard error bars) percent longer and then averaged across the standard interval (SI) conditions and their respective comparison intervals (CIs). The left graph shows the mean percent longer responses for each unimodal (A–A, V–V) and crossmodal (V–A, A–V) condition. The right graph plots the mean percent longer responses for the unimodal and crossmodal conditions as a function of the CI duration. On the *x* axis, ±7, 14, and 21 designate CIs that were 7, 14, and 21% shorter (negative values) or longer (positive values) than the SI.

condition interaction (**Figure 2**, left graph) showed that in the unimodal condition, visual CIs were perceived as lasting longer than auditory CIs [V–V > A–A; $F(1,19) = 21.0$, $p < 0.0001$, $\eta^2 = 0.53$]. Though no differences were expected between A–A and V–V pairs, this was found previously (Ulrich et al., 2006) and relates to the greater variability in timing visual signals (Merchant et al., 2008; Grondin and McAuley, 2009). In contrast, auditory CIs were perceived as lasting longer than visual CIs in the crossmodal conditions [V–A > A–V; $F(1,19) = 70.6$, $p < 0.0001$, $\eta^2 = 0.79$]. Pairwise comparisons between the unimodal and crossmodal conditions indicated that perceived duration was dilated for intersensory timing of auditory CIs [A–A < V–A; $F(1,19) = 47.8$, $p < 0.0001$, $\eta^2 = 0.72$; V–V < V–A; $F(1,19) = 6.7$, $p < 0.02$, $\eta^2 = 0.26$] and was compressed for intersensory timing of visual CIs [A–A > A–V; $F(1,19) = 22.9$, $p < 0.0001$, $\eta^2 = 0.55$; V–V > A–V; $F(1,19) = 79.9$, $p < 0.0001$, $\eta^2 = 0.81$]. The timing condition × CI duration interaction showed that differences between the two timing conditions grew as CI duration increased (**Figure 2**, right graph). The CI modality × CI duration interaction showed that CI modality differences also grew as CI duration increased. The second-order interaction was not significant [$F(3.9,75) = 1.8$, $p = 0.14$].

Secondary analyses of the RT data showed a trend for a CI modality × timing condition interaction [$F(1,19) = 3.8$, $p = 0.067$, $\eta^2 = 0.17$]. Planned comparisons showed the interaction was due to faster RTs for V–A (mean = 776.3 ms, SE = 50.5) than A–V pairs (mean = 899.9 ms, SE = 51.0) [$t(1,19) = 3.1$, $p < 0.01$], but not for A–A (mean = 861.7 ms, SE = 50.2) than V–V pairs (mean = 874.1 ms; SE = 52.1).

MRI RESULTS

Functional ROI results

The conjoined fMRI activation masks in **Figures 3** and **4** display 25 regions that exhibited effects of CI modality, timing condition, and/or an interaction. **Table 1** provides the details of these activation foci. For each fROI, the table also summarizes the results from statistical analyses that tested for the effects of signal modality (A–A versus V–V), timing condition (unimodal versus crossmodal), and the interaction of modality × timing condition.

Audition versus vision. **Table 1** and **Figure 3** (left column; red) show that the modality of unimodal pairs affected activation largely in posterior cortical areas including in the parietal (superior parietal cortex and precuneus), temporal (posterior portions of superior temporal cortex and insula, middle temporal cortex, parahippocampus, hippocampus), and occipital cortices (middle-occipital cortex and cuneus). An exception was the modality effect on activation of the medial frontal/anterior cingulate areas. In most regions activation was greater for visual than auditory unimodal pairs, except for the medial frontal/anterior cingulate and superior temporal/insular cortices wherein activation was greater for auditory than visual pairs.

Intrasensory versus intersensory timing. **Table 1**, **Figure 3** (middle column; yellow), and **Figure 4** show that the timing condition also affected activation of the frontal [SMA, precentral, paracentral, middle frontal gyrus (MFG)/ inferior frontal gyrus (IFG)], superior parietal, temporal [middle temporal gyrus (MTG), parahippocampus, hippocampus], and middle-occipital cortices, the thalamus (pulvinar nucleus, lateral geniculate body)

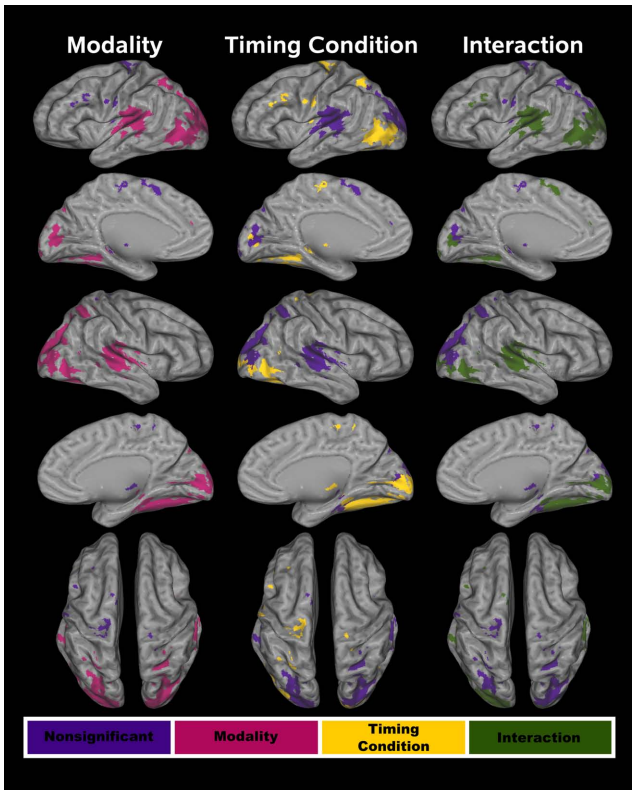

FIGURE 3 | Cortical functional ROI (fROI). Twenty-one cortical fROI were identified by conjoining activation maps from the voxel-wise analyses. Tests of modality, timing condition, and the interaction were conducted on these fROI. The fROI are color coded according to whether activation was affected by each of these factors. In all three columns, purple denotes no effect of a particular factor on activation. For the test of modality (left column), red designates a significant difference between the A–A and V–V conditions. For the test of timing condition (middle column), yellow signifies a significant difference between the unimodal and the crossmodal conditions. In the right column, green signifies a significant CI modality × timing condition interaction.

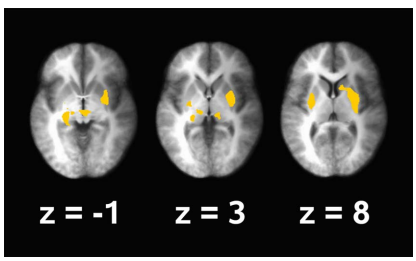

FIGURE 4 | Subcortical functional ROI (fROI). Four subcortical fROI were identified by conjoining the activation maps from the voxel-wise analyses. In all of the fROI, activation was greater in the unimodal than the crossmodal timing condition. No other effects were significant. *z* coordinates are the superior (+)/inferior (−) distance in millimeter from the anterior commissure.

Table 1 | Regions showing significant effects of modality, timing condition, and the interaction.

Region	BA	*x*	*y*	*z*	ml	Modality[1]	Timing condition[2]	Interaction[3]
FRONTAL								
L preSMA	6	−7	6	56	1.2	–	–	0.0001
L SMA, precentral	6	−16	−21	56	2.6	–	0.0001	–
R SMA, paracentral	6	14	−31	55	1.5	–	0.0001[b]	–
L precentral	4,6	−57	−6	31	1.0	–	0.0001	–
L medial frontal, anterior cingulate	9,32	−21	34	14	1.1	0.005[a]	–	0.0001
L MFG/IFG	9	−37	16	30	1.2	–	0.0001[b]	0.017
PARIETAL								
L superior parietal	7	−30	−54	47	1.8	0.0001	0.03[b]	–
L precuneus, cuneus	7,19	−25	−71	29	4.4	0.0001	–	–
R precuneus, superior parietal	7	26	−52	46	3.5	0.0001	–	–
TEMPORAL–OCCIPITAL								
L superior temporal, posterior insula	13,22	−47	−27	11	19.7	0.0001[a]	–	0.0001
R superior temporal, posterior insula	13,22	48	−20	10	19.5	0.0001[a]	–	0.0001
L parahippocampal gyrus	37	−22	−47	13	2.3	–	0.0001[b]	–
L parahippocampus, hippocampus	37	−31	−38	−2	0.9	–	0.0001[b]	–
R parahippocampal gyrus	35,36	27	−27	−12	1.1	0.008	–	–
R middle temporal	22	32	−54	16	1.0	–	0.0001	–
L middle occipital, parahippocampus	18,19,36,37	−35	−62	−4	18.7	0.0001	0.007	0.015
R middle occipital, cuneus, parahippocampus	17,18,36,37	28	−63	−4	24.6	0.0001	0.01	0.036
L middle occipital, cuneus	17,18	−17	−89	10	12.8	0.0001	–	0.013
R middle occipital, cuneus	18,19	28	−78	19	12.0	0.0001	–	–
B cuneus	18	−4	−77	13	3.1	0.0001	–	–
SUBCORTICAL								
L thalamus (pulvinar, LGB)		−21	−25	−1	0.7	–	0.034	–
B thalamus (pulvinar, red nucleus)		1.4	−20	2	0.7	–	0.0001	–
L claustrum		−25	−15	18	0.9	–	0.0001	–
L putamen		−26	−8	10	1.7	–	0.0001	–
R putamen, caudate body		25	−3	8	4.4	–	0.0001	–

Brodmann areas (BA) were defined by the Talairach and Tournoux atlas. Coordinates represent distance in millimeter from anterior commissure: x, right (+)/left (−); y, anterior (+)/posterior (−); z, superior (+)/inferior (−). Regional volumes are expressed in milliliter. B, bilateral hemispheres; L, left hemisphere; R, right hemisphere; SMA, supplementary motor area; MFG, middle frontal gyrus; IFG, inferior frontal gyrus; LBG, lateral geniculate body.

[1] Regions showing a significant (p value) difference between A–A and V–V pairs.

[2] Regions showing a significant (p value) difference between the unimodal (A–A, V–V) and crossmodal (A–V, V–A) conditions.

[3] Regions showing a significant (p value) CI modality × timing condition interaction.

[a] These regions showed greater activation for A–A than V–V pairs. All other areas showed greater activation for V–V than A–A pairs.

[b] These regions showed greater activation for crossmodal than unimodal pairs. All other areas showed greater activation for unimodal than crossmodal pairs.

and the basal ganglia (putamen, caudate body). **Figure 5** displays graphs of signal change for the unimodal and crossmodal conditions in representative regions. For most regions, activation was greater for unimodal than crossmodal pairs. Exceptions included the MFG/IFG and superior parietal cortex, wherein activation was greater for crossmodal than unimodal pairs. Activation was also greater for the crossmodal than the unimodal condition, but negative, in the right SMA/paracentral lobule and the left parahippocampus/hippocampus (**Table 1**, clusters 14 and 15).

Time dilation and compression. **Table 1** and **Figure 3** (right column; green) display regions wherein CI modality interacted with the timing condition. All posterior, but not anterior, regions that showed an interaction also showed modality effects (A–A versus V–V; **Figure 3**, left column; red). However, we were principally interested in whether activation differed between the two crossmodal pairs (V–A versus A–V) since this contrast directly tests for regional activation associated with time dilation and compression, while controlling for the amount of auditory and visual stimulation. There were three patterns of interactions. First, for the left medial frontal/anterior cingulate, the interaction was due to greater activation in the auditory than the visual unimodal condition (**Table 1**), yet no difference between A–V and V–A pairs ($p > 0.10$). Second, **Figure 6** shows that for the left preSMA and MFG/IFG, the interaction was due to greater activation for the A–V than the V–A pairs ($p < 0.0001$ and $p < 0.02$, respectively); auditory and visual unimodal conditions did not differ. For the third interaction pattern, **Table 1** and **Figure 6** show that large regional biases for timing unimodal auditory (right and left superior temporal/insula cortex) or visual pairs (right and left middle-occipital

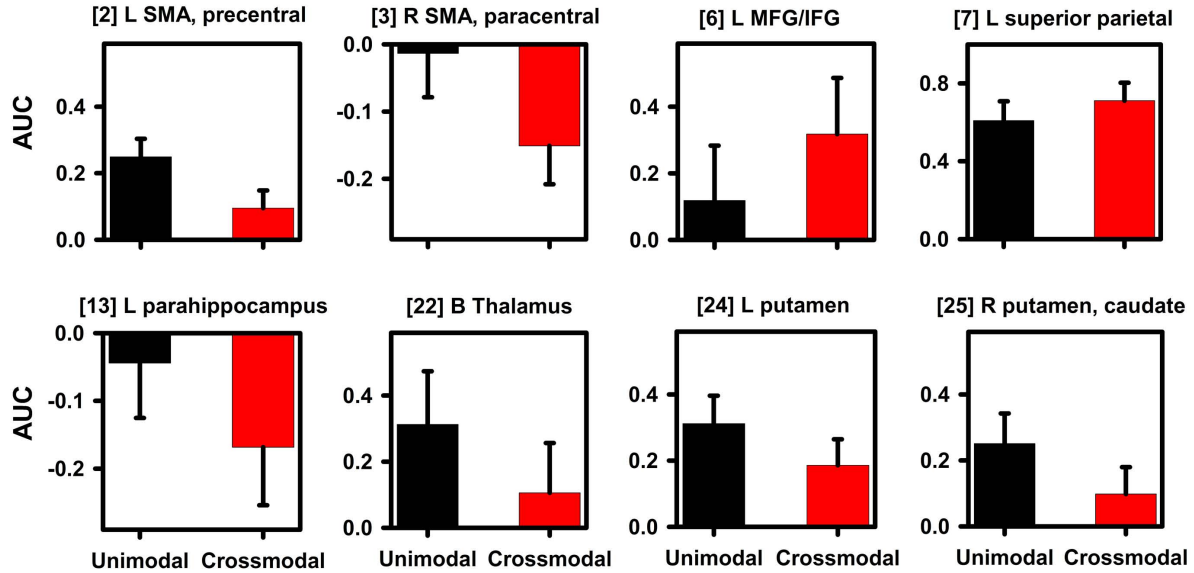

FIGURE 5 | Signal change in regions showing an effect of timing condition. Graphs display representative regions showing differences in activation between the unimodal (A–A, V–V) and crossmodal (V–A, A–V) conditions. Mean (standard error bars) area under the curve (AUC) is plotted for each condition. Bracketed numbers reference regions detailed in **Table 1**. L, left hemisphere; R, right hemisphere; B, bilateral hemispheres; SMA, supplementary motor area; MFG, middle frontal gyrus; IFG, inferior frontal gyrus.

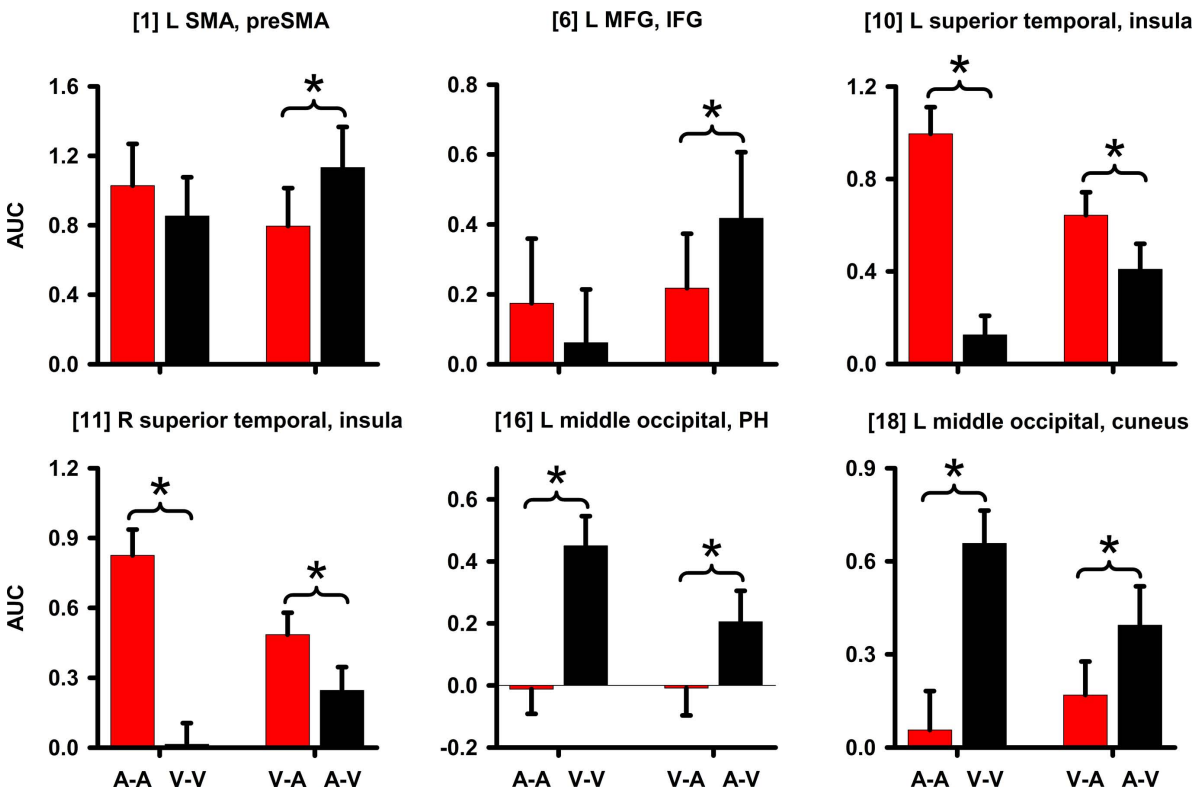

FIGURE 6 | Signal change in regions showing an interaction. Graphs display regions showing a CI modality × timing condition interaction. Mean (standard error bars) area under the curve (AUC) is plotted for each condition. An asterisk designates the significance of key follow-up planned comparisons between the unimodal (A–A versus V–V) and crossmodal (V–A versus A–V) conditions. Bracketed numbers reference regions detailed in **Table 1**. L, left hemisphere; R, right hemisphere; SMA, supplementary motor area; MFG, middle frontal gyrus; IFG, inferior frontal gyrus; PH, parahippocampus.

cortex) translated into smaller, but significant differences between the two crossmodal conditions. Specifically, activation was greater for V–A pairs in the right and left superior temporal/insula cortex ($p < 0.006$ and $p < 0.02$, respectively) and greater for A–V pairs in the right and left middle-occipital cortex (**Table 1**, clusters 16, 17, 19; $p < 0.002$, $p < 0.007$, and $p < 0.01$, respectively). Finally, for all other regions listed in **Table 1**, *post hoc* comparisons between A–V and V–A pairs were non-significant.

Effective connectivity results

Intrasensory versus intersensory timing. For the connectivity analyses that used timing condition as an experimental variable, six seed ROI were selected including the left and right putamen (−26, −8, 11; 23, 0, 8), right caudate body (10, 10, 8), left and right SMA (−11, −16, 66; 5, −26, 55), and left superior parietal cortex (−34, −55, 50). The left putamen failed to show significant connectivity with other regions. **Figure 7** displays spatial maps of regions exhibiting significant effective connectivity with each seed that was modulated by the timing condition. **Table 2** describes the details of these interacting regions. For all seeds, effective connectivity was stronger in the crossmodal than the unimodal condition. The striatum and most cortical ROI showed connectivity with encoding/retrieval hubs (posterior cingulate, precuneus). The right caudate also showed connectivity with cognitive control [rostral medial frontal (BA 10), higher association (inferior parietal), and visual centers (MTG, lingual gyrus, vermis; **Figure 7A**)]. Connectivity of the left and/or right SMA was found with cognitive control [e.g., preSMA, precentral gyrus, MFG/superior frontal gyrus (SFG; BA 10, 47), IFG (BA 45, 47), memory (parahippocampus), and visual centers (fusiform and lingual gyrus), and with the ventral putamen and cerebellum (declive/culmen; **Figure 7B**)]. Left superior parietal cortex showed connectivity with cognitive control [preSMA/SMA, MFG (6), IFG (BA 9)] and visual centers (MTG), and with the thalamus (**Figure 7C**).

Time dilation and compression. For the connectivity analyses that used the two crossmodal conditions as an experimental variable, nine seed ROI were selected including the left preSMA (−4, 11, 50), left MFG (−45, 14, 32), left and right superior temporal cortex (−55, −22, 10; 57, −21, 10), left and right posterior insula (−42, −13, 3; 43, −14, 5), and two left and one right middle-occipital areas (−5, −95, 4; −37, −77, −9; 30, −80, 1). Of these seeds, effective connectivity was not found for the left preSMA, left MFG, and two occipital seeds (**Table 1**, clusters 1, 6, 16, and 17). **Figure 8** displays spatial maps of regions showing significant effective connectivity with each seed that was modulated by the time dilation and compression conditions. **Table 3** describes the details of these interacting regions. Two patterns of effective connectivity were found. First, the predominant pattern was characterized by stronger connectivity in the V–A "time dilation" condition. For this pattern, the right and/or left superior temporal cortex showed connectivity with cognitive control [MFG (BA 6, 9, 10), IFG (6), SMA, preSMA], attention/association (superior/inferior parietal), sensory integration (anterior insula, claustrum), and visual centers, and with the caudate body and culmen (**Figure 8A**). Similarly, the left and/or right insula showed connectivity with cognitive control (SMA, preSMA), higher association (inferior parietal), and sensory integration areas (anterior insula), and with the putamen (**Figure 8B**). By comparison, the left middle-occipital seed showed more limited connectivity with sensory integration (anterior insula) and visual centers (cuneus; **Figure 8C**). Second, a less common pattern was characterized by stronger connectivity of some seeds with medial cortical areas in the A–V "time compression" condition (**Figures 8A,B**, sagittal views). Specifically, the left superior temporal cortex and the left and right insula showed stronger connectivity with rostral medial frontal cortex (9, 10) for A–V pairs. The right superior temporal cortex also showed stronger connectivity with the cingulate (BA 30, 31).

DISCUSSION

Our behavioral findings confirmed that auditory CIs were perceived as lasting longer than visual CIs in the crossmodal condition (Ulrich et al., 2006). Moreover, pairwise comparisons of each crossmodal and unimodal condition demonstrated that perceived duration was dilated when the CI was auditory (V–A) and compressed when it was visual (A–V). Additionally, crossmodal RTs were faster when perceived duration was dilated, possibly because auditory signals are more salient in the context of temporal processing, wherein audition dominates vision (Repp and Penel, 2002; Recanzone, 2003; Mayer et al., 2009). We also found that differences between the unimodal and crossmodal conditions in judgments of time grew with CI duration, irrespective of CI modality. By pacemaker-accumulator models, this result suggests that intersensory timing affects the flow of pulses from the pacemaker rather than a delay in the start of the clock, which would have a constant effect across CI durations (Wearden et al., 1998, 2010; Penney et al., 2000).

The neural underpinnings of these behavioral findings were elucidated for the first time by the present study, which uncovered four main findings. First, we showed that time dilation and compression were distinguished by differential activation of higher-sensory areas (superior temporal/insula, middle occipital) associated with the modality of the CI. Effective connectivity of these areas with middle frontal and parietal cortices, anterior insula, and the striatum was typically stronger when perceived duration was dilated (V–A). We suspect that this result is due to the engagement of distributed neural networks when timing more salient auditory signals. Second, time compression (A–V) was characterized by greater activation of cognitive-control centers (preSMA, MFG/IFG), although these centers did not exhibit effective connectivity with other regions. This finding suggests that A–V comparisons required more cognitive effort, consistent with the longer RTs when perceived duration was compressed. Third, audiovisual distortions in subjective duration were not mediated by the striatum, suggesting that the rate of detection or integration of cortical oscillatory states is not faster for auditory than visual signals. Fourth, intersensory timing was distinguished from intrasensory timing by decreased activation of the striatum and SMA, but increased activation of an attention center (superior parietal cortex). These regions showed stronger connectivity with frontal, parietal, and visual areas during crossmodal than unimodal timing, which may signify the greater demands on core timing and attention systems in integrating audiovisual

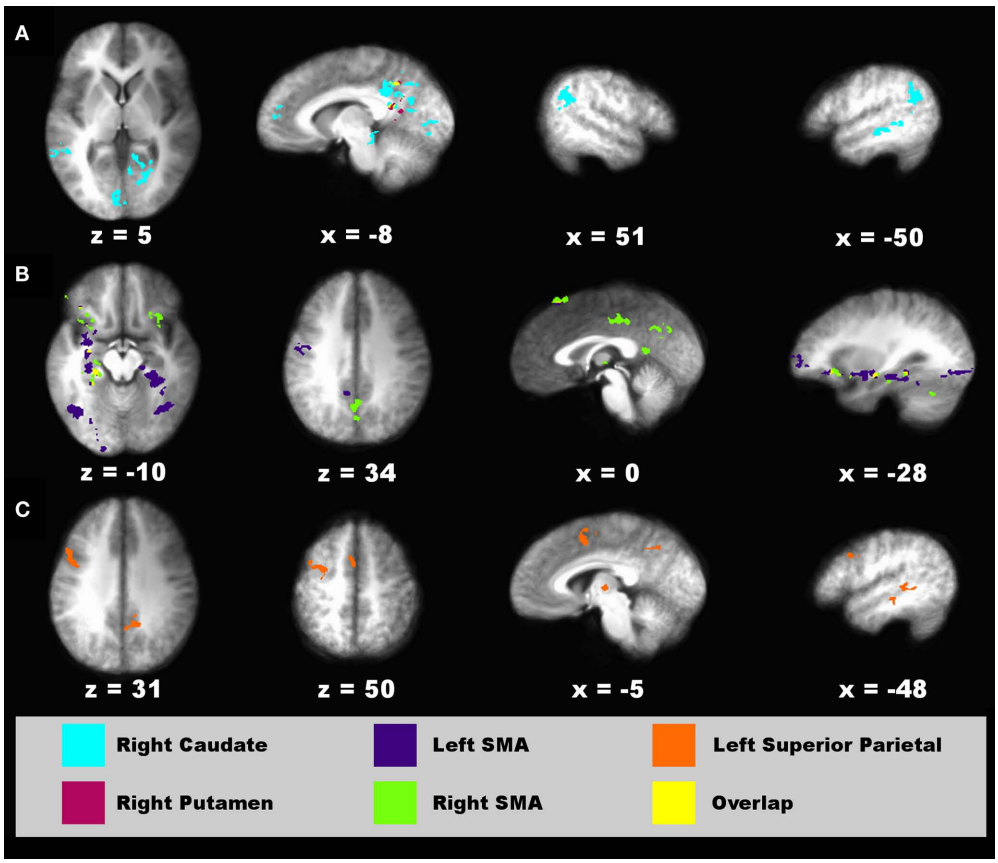

FIGURE 7 | Regions showing connectivity with the striatum, SMA, and parietal cortex that was modulated by timing condition. Spatial locations of regions showing interactions with a seed fROI are displayed on sagittal and axial sections (neurological view). **(A)** Right caudate (turquoise) and right putamen (red) seeds. **(B)** Left (blue) and right (green) supplementary motor area (SMA) seeds. **(C)** Left superior parietal cortex seed (orange). The spatial overlap between two seeds in their interacting regions **(A,B)** is shown in yellow. Coordinates beneath sagittal and axial sections represent the distance in millimeter from the anterior commissure: *x*, right (+)/left (−); superior (+)/inferior (−). See **Table 2** for details about individual activation foci.

time codes. We now turn to a more complete discussion of these findings.

TIME DILATION AND COMPRESSION

Audiovisual distortions in perceived duration were largely distinguished by activity in higher-sensory areas, wherein the magnitude of activation and the strength of effective connectivity both depended on the time dilation/compression conditions. Despite equivalent stimulation of the two senses, activation was greater in bilateral superior temporal and posterior insular cortex when perceived duration was dilated (V–A) and greater in bilateral middle-occipital cortex when it was compressed (A–V). These results indicated that the modality of the CI drove differential activation in these areas, consistent with their respective bias for timing unimodal auditory or visual signals. At the same time, secondary auditory and visual centers are multisensory (Ghazanfar and Schroeder, 2006) and are thought to support audiovisual integration (Calvert, 2001; Klemen and Chambers, 2011). This prospect was suggested by our effective connectivity results wherein higher-sensory areas typically showed stronger connectivity when time was dilated rather than compressed.

Common to all of these higher-sensory areas was stronger connectivity with the anterior insula. The insula integrates processing from disparate domains (e.g., interoception, working memory, emotion) including time (Nenadic et al., 2003; Harrington et al., 2010; Kosillo and Smith, 2010; Wittmann et al., 2010a). It has also been linked to the dilation of perceived duration by salient features of visual signals (Wittmann et al., 2010b). Importantly, the insula mediates the perception of audiovisual asynchrony (Bushara et al., 2001; Calvert et al., 2001), implicating it in the synthesis of crossmodal signals based on their temporal correspondence. The anterior insula is also thought to be an attentional hub that assists central executive networks in generating accurate responses to salient or task-relevant events (Menon and Uddin, 2010). Auditory signals are more salient than visual signals in the context of temporal processing (Repp and Penel, 2002; Recanzone, 2003; Mayer et al., 2009). This is likely due to past experiences in timing principally via audition (e.g., music, speech), which over time may build up the connectivity strength of networks that mediate temporal processing of auditory signals. Thus, enhanced sensitivity in the anterior insula to auditory oscillatory patterns may contribute to time dilation. Time dilation was also related

Table 2 | Regions showing effective connectivity with the striatum and cortical ROI that was modulated by the timing condition (unimodal versus crossmodal).

Seed region – interacting regions	BA	*x*	*y*	*z*	ml
R PUTAMEN					
B posterior cingulate, precuneus	7,31	−4	−53	24	3.0
R CAUDATE					
L rostral medial frontal	10	−12	52	15	0.4
B precuneus, posterior cingulate	7,31	−7	−59	29	13.3
R inferior parietal	39,40	45	−53	27	2.1
L inferior parietal	39,40	−47	−52	22	2.0
L MTG	22	−53	−42	4	0.6
L MTG (21)	21	−50	−26	−5	0.4
B lingual gyrus	18	1	−80	−1	1.7
R lingual gyrus	18	18	−59	4	0.7
B vermis		0	−32	−9	0.5
L SUPPLEMENTARY MOTOR AREA (BA 6)					
B preSMA	6	8	22	54	1.1
L precentral	6	−47	−10	33	0.4
L MFG/SFG	10	−26	54	4	0.6
L IFG	45	−46	24	14	1.0
L IFG	47	−34	31	−7	0.6
R postcentral	3,4	46	−17	46	0.4
L precuneus	7	−9	−47	35	0.4
L parahippocampus	36	−30	−33	−12	1.0
R parahippocampus	36	28	−33	−11	0.8
L fusiform gyrus	37	−41	−60	−9	0.6
R fusiform gyrus	37	33	−58	−10	0.4
L lingual gyrus	18	−22	−84	−4	1.3
L ventral putamen		−30	−2	−8	1.3
R SUPPLEMENTARY MOTOR AREA (BA 6)					
B preSMA	6	0	27	57	0.5
L MFG/IFG	47	−28	25	−6	1.4
R IFG	47	29	21	−9	0.5
B precuneus	7	−3	−61	30	0.6
B cingulate	29,30	0	−49	14	0.4
B cingulate	31	−2	−28	40	0.8
L parahippocampus	35	−23	−21	−8	1.1
L declive/culmen		−33	−64	−23	0.4
L SUPERIOR PARIETAL (BA 7)					
L preSMA/SMA	6	−4	2	49	0.4
L MFG	6	−30	−3	52	0.5
L IFG	6	−45	7	31	0.3
R posterior cingulate	31	9	−53	31	0.7
L precuneus	7	−7	−53	39	0.4
L MTG	21	−53	−23	−5	0.5
L MTG	21	−50	−35	3	0.4
B thalamus (medial dorsal nucleus)		−2	−14	4	0.5

Regions showing effective connectivity with each seed region (bold font) are displayed in ***Figure 7.***

For all seed-interacting regions, connectivity was stronger for the crossmodal than the unimodal condition. Brodmann areas (BA) were defined by the Talairach and Tournoux atlas. Cerebellar lobules were defined by the Schmahmann atlas (Schmahmann et al., 2000). Coordinates represent distance in millimeter from anterior commissure: x, right (+)/left (−); y, anterior (+)/posterior (−); z, superior (+)/inferior (−). Regional volumes are expressed in milliliter. B, bilateral hemispheres; L, left hemisphere; R, right hemisphere; SMA, supplementary motor area; MFG, middle frontal gyrus; IFG, inferior frontal gyrus; SFG, superior frontal gyrus.

Table 3 | Regions showing effective connectivity with cortical ROI that was modulated by the effects of time dilation and compression on perceived duration (V–A versus A–V).

Seed region – interacting regions	BA	*x*	*y*	*z*	ml
L SUPERIOR TEMPORAL (BA 22)					
B rostral medial frontal*	9,10	−1	53	14	0.4
B SMA, preSMA, cingulate	6,32	2	14	41	5.1
L MFG	6	−25	−5	60	0.6
R MFG	6	20	3	58	0.5
R MFG	9	39	24	29	2.1
L IFG, MFG, insula, caudate body	6,9,13	−39	13	19	7.8
R anterior insula	13	36	17	9	2.9
L superior and inferior parietal, precuneus	7,40	−32	−53	41	2.0
R superior parietal, precuneus	7	28	−60	46	0.6
L cuneus	18	−13	−75	31	0.4
R culmen		29	−51	−28	0.3
R SUPERIOR TEMPORAL (BA 22)					
R MFG	46	40	29	27	0.7
B SMA	6	0	10	44	0.7
R claustrum, anterior insula	13	28	21	10	1.3
L POSTERIOR INSULA (BA 13)					
L rostral medial frontal*	10	−3	54	15	0.4
B SMA, preSMA	32	0	5	48	0.9
L inferior parietal	40	−40	−49	49	0.6
L anterior insula, putamen	13	−36	7	8	3.4
R POSTERIOR INSULA (BA 13)					
L rostral medial frontal*	10	−4	53	9	1.4
B cingulate*	31	−2	−43	34	2.0
L posterior cingulate*	30	−6	−49	15	0.6
L anterior insula, putamen	13	−39	7	9	4.2
R anterior insula, precentral, putamen	13,44	42	13	9	1.1
L MIDDLE OCCIPITAL (BA 18)					
L anterior insula	13	−40	6	2	0.4
R anterior insula	13	36	4	6	0.4
R cuneus	19	11	−83	35	1.4

*Regions showing effective connectivity with each seed region (bold font) are displayed in **Figure 8**.*

Brodmann areas (BA) were defined by the Talairach and Tournoux atlas. Cerebellar lobules were defined by the Schmahmann atlas (Schmahmann et al., 2000). Coordinates represent distance in millimeter from anterior commissure: x, right (+)/left (−); y, anterior (+)/posterior (−); z, superior (+)/inferior (−). Regional volumes are expressed in milliliter. B, bilateral hemispheres; L, left hemisphere; R, right hemisphere; SMA, supplementary motor area; MFG, middle frontal gyrus; IFG, inferior frontal gyrus; SFG, superior frontal gyrus.

**Connectivity was typically stronger for the V–A than the A–V condition. Exceptions are regions marked by an asterisk wherein connectivity was stronger for the A–V than the V–A condition.*

to stronger connectivity of superior temporal and insular cortices with the striatum (caudate and putamen), an alleged core-timing system (Matell and Meck, 2004), and with higher association areas (parietal cortex), sensorimotor areas (cerebellum), and cognitive-control centers (preSMA, MFG, IFG), which are also involved in audiovisual integration (Lewis et al., 2000; Bushara et al., 2001; Calvert et al., 2001). By comparison, only one of three middle-occipital fROI showed effective connectivity, which was inter-regionally restricted to the anterior insula. Taken together, these results indicate that a mechanism underlying audiovisual temporal distortions is the strength of superior temporal/posterior insular cortex connectivity with distributed networks that mediate multisensory integration, cognitive control, and timekeeping.

A less common finding was stronger connectivity in the time compression condition of the left superior temporal and bilateral insular cortices with medial cortical regions involved in more abstract decision making (rostral medial frontal; BA 9, 10) and executive control (posterior cingulate). This circumscribed connectivity pattern may reflect the greater difficulty of A–V than V–A judgments, consistent with their longer RTs. This prospect was also supported by our fROI analyses, wherein activation was greater in classic working memory and attention regions (preSMA, MFG, IFG) when time was compressed than when it was dilated. These regions, however, did not exhibit significant effective connectivity. This leads us to conclude that the preSMA and MFG/IFG are supramodal centers that direct attention and working memory

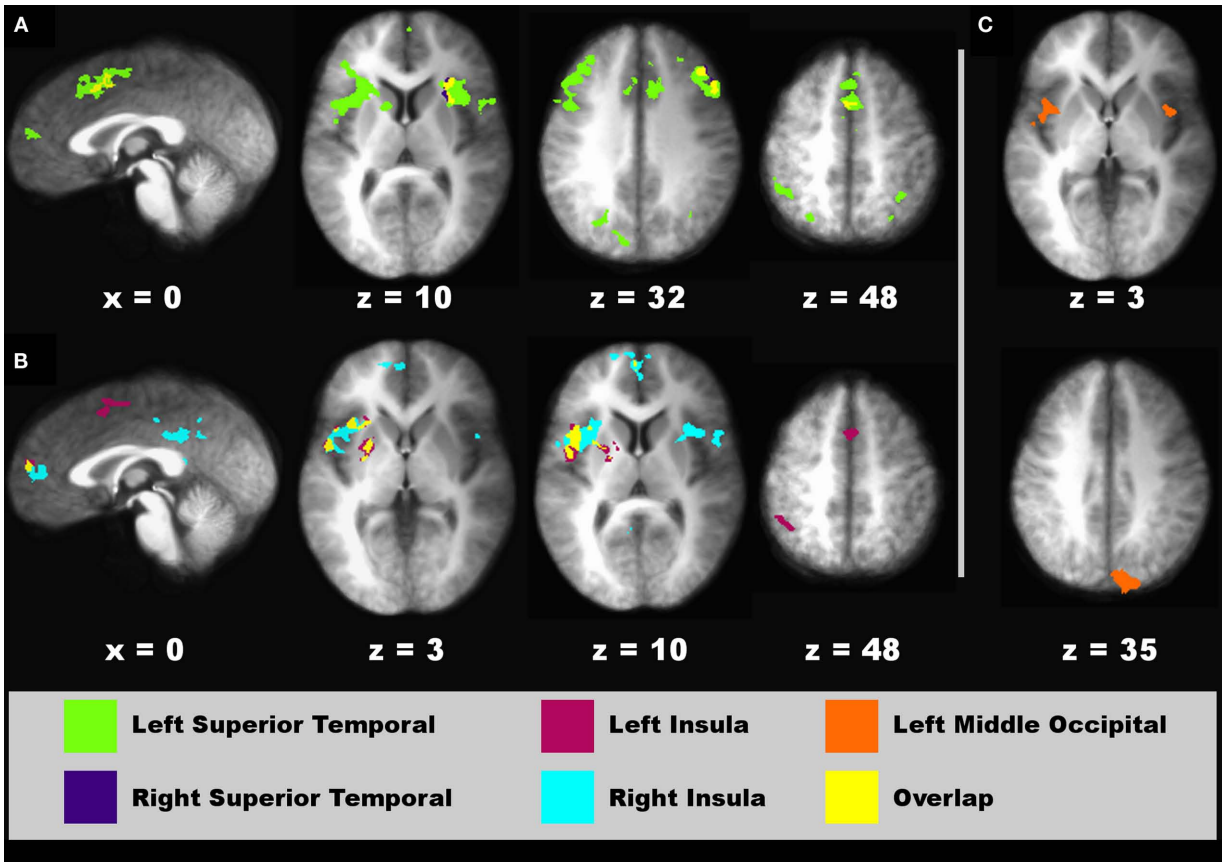

FIGURE 8 | Regions showing connectivity with higher-sensory areas that was modulated by the time dilation and compression conditions. Spatial locations of regions showing interactions with a seed fROI are displayed on sagittal and axial sections (neurological view). **(A)** Left (green areas) and right superior temporal (blue areas) seeds. **(B)** Left (red) and right (turquoise) posterior insula seeds. **(C)** Left middle-occipital seed (orange). The spatial overlap between two seeds in their interacting regions **(A,B)** is shown in yellow. Coordinates beneath sagittal and axial sections represent the distance in millimeter from the anterior commissure: *x*, right (+)/left (−); superior (+)/inferior (−). See **Table 3** for details about individual activation foci.

resources during intersensory timing, but do not give rise to audiovisual effects on perceived duration *per se*.

INTERSENSORY AND INTRASENSORY TIMING

Our fROI results did not suggest that audiovisual distortions in subjective duration were mediated by the striatum. Rather, we found that putamen and caudate activation was greater when timing unimodal than crossmodal signals, irrespective of the CI modality. This result was not consistent with classic attentional switching accounts of striatal function (van Schouwenburg et al., 2010), wherein greater activation would be expected in the crossmodal than the unimodal condition. Attentional switching should also produce a constant effect on perceived duration across CI durations for the crossmodal condition, which was not found.

The mechanisms by which time is synthesized across the senses are not understood. Crossmodal stimulation often enhances neuronal responses in multisensory integration centers (e.g., superior colliculus, association areas; Calvert et al., 2001), including the striatum (Nagy et al., 2006), but depression of neuronal responses is also found, especially when intersensory signals are spatially incongruent or asynchronous as in our study (Calvert et al., 2001). Increased striatal activation during unimodal timing may relate to the role of the striatum in detecting and integrating cortical oscillatory states, which provide the temporal code for signal duration (Matell and Meck, 2004). Stronger striatal responses might arise when timing unimodal signals because they share similar spatial signatures. Detection and temporal integration of oscillatory states might therefore speed up because evidence for the time code accumulates faster when the CI duration can be mapped onto the neural time-code of the SI modality, which is active in memory. Conversely, different spatial signatures for crossmodal signals may render temporal integration noisy, resulting in a diminished striatal response. Though speculative, this account may also relate to the increased activation and reduced suppression in the left and right SMA for unimodal than crossmodal timing. The SMA is sensitive to elapsed time (Pouthas et al., 2005; Mita et al., 2009; Wencil et al., 2010), but unlike the striatum, it mediates maintenance of temporal and non-temporal information (Harrington et al., 2010). The SMA may therefore maintain temporal representations online for other networks to make use of to affect behavior. Stronger SMA activation when timing unimodal than crossmodal signals may signify a stronger neural representation of the time code.

Despite the increased activation of the striatum and SMA during intrasensory timing, connectivity of these areas with the brain was stronger during crossmodal timing. For example, these regions showed stronger connectivity with a core memory hub (precuneus, posterior cingulate, parahippocampus), possibly signifying the greater dependence of striatum and SMA on output from encoding and retrieval systems during intersensory timing. The caudate and SMA also showed stronger connectivity with visual (fusiform and lingual gyrus, MTG), but not auditory centers, and frontal cognitive-control centers (medial frontal, MFG, SFG, IFG). These findings may relate in part to the more deliberate timing of visual signals (Repp and Penel, 2002; Mayer et al., 2009), which renders synthesis of audiovisual temporal codes more difficult.

Intersensory timing was also associated with increased activation of a frontal–parietal attention network. Though increased MFG/IFG activation was largely related to the more difficult A–V judgments, our results suggest that the synthesis of audiovisual temporal codes increases attentional processing in the superior parietal cortex, irrespective of the CI modality. This was consistent with the stronger connectivity of the superior parietal cortex with frontal control-systems (MFG, IFG) during crossmodal timing, but also with higher visual areas (MTG) and a memory encoding hub (precuneus, posterior cingulate). Altogether, these effective connectivity patterns suggest that more extensive network interactions with the striatum, SMA, and superior parietal cortex are needed to time intersensory than intrasensory signals.

CONCLUSION

Our results indicate that audiovisual effects on the experience of time emanate from higher-sensory areas, in which connectivity is stronger and far more inter-regionally distributed when timing auditory than visual signals. Though we found greater activation in cognitive-control centers for the more difficult (time compression) than easy (time dilation) crossmodal comparisons, effective connectivity of these regions was not modulated by the modality effect. This may suggest that cognitive-control centers play a supramodal role in directing attention or allocating working memory resources during decision making. We also found that audiovisual distortions in perceived duration were not driven by the striatum, suggesting that the presumed core-timing system (Matell and Meck, 2004) operates at the same rate for visual and auditory signals. Rather, during crossmodal timing, striatal activation was decreased and connectivity was stronger with visual, memory encoding and cognitive-control centers. These findings were attributed to the greater demands on striatal integration of crossmodal time codes. The present findings have implications for understanding neural mechanisms of temporal processing distortions in maturation and disease. For example, enhanced modality effects in children (Droit-Volet et al., 2007) and in individuals at risk for schizophrenia (Penney et al., 2005) are due to impaired timing of visual signals. Our results suggest that this might arise from developmental differences and preclinical changes in frontal cognitive-control centers, but also the connectivity of higher-sensory association areas with executive control centers (medial cortex). Conversely, audiovisual distortions in perceived duration are diminished in diagnosed schizophrenics, largely due to inaccurate timing of auditory signals (Carroll et al., 2008). This is consistent with changes in temporal cortex in schizophrenia, which may well alter inter-regional connectivity. Altogether, the present study demonstrates that intersensory synthesis of temporal information and time dilation and compression effects are mediated by different patterns of regional activation and inter-regional connectivity. Future studies are needed that further elucidate interactions among multiple brain regions, which are fundamental to temporal processing and likely breakdown in certain neurological and psychiatric disorders.

ACKNOWLEDGMENTS

This research was supported by grants from the Department of Veterans Affairs (#1IO1CX000146-01 and #B501R), NIH/NINDS #NS040068, an ONR DURIP award (#N000140811114), and the McDonnell Foundation (#220020185).

REFERENCES

Bushara, K. O., Grafman, J., and Hallett, M. (2001). Neural correlates of auditory-visual stimulus onset asynchrony detection. *J. Neurosci.* 21, 300–304.

Calvert, G. A. (2001). Crossmodal processing in the human brain: insights from functional neuroimaging studies. *Cereb. Cortex* 11, 1110–1123.

Calvert, G. A., Hansen, P. C., Iversen, S. D., and Brammer, M. J. (2001). Detection of audio-visual integration sites in humans by application of electrophysiological criteria to the BOLD effect. *Neuroimage* 14, 427–438.

Carroll, C. A., Boggs, J., O'Donnell, B. F., Shekhar, A., and Hetrick, W. P. (2008). Temporal processing dysfunction in schizophrenia. *Brain Cogn.* 67, 150–161.

Casini, L., and Macar, F. (1997). Effects of attention manipulation on judgments of duration and of intensity in the visual modality. *Mem. Cognit.* 25, 812–818.

Coull, J. T., Vidal, F., Nazarian, B., and Macar, F. (2004). Functional anatomy of the attentional modulation of time estimation. *Science* 303, 1506–1508.

Cox, R. W. (1996). AFNI: software for analysis and visualization of functional magnetic resonance neuroimages. *Comput. Biomed. Res.* 29, 162–173.

Droit-Volet, S., and Meck, W. H. (2007). How emotions colour our perception of time. *Trends Cogn. Sci. (Regul. Ed.)* 11, 504–513.

Droit-Volet, S., Meck, W. H., and Penney, T. B. (2007). Sensory modality and time perception in children and adults. *Behav. Processes* 74, 244–250.

Eagleman, D. M., and Pariyadath, V. (2009). Is subjective duration a signature of coding efficiency? *Philos. Trans. R. Soc. Lond B Biol. Sci.* 364, 1841–1851.

Friston, K. J., Buechel, C., Fink, G. R., Morris, J., Rolls, E., and Dolan, R. J. (1997). Psychophysiological and modulatory interactions in neuroimaging. *Neuroimage* 6, 218–229.

Gamache, P. L., and Grondin, S. (2010). The lifespan of time intervals in reference memory. *Perception* 39, 1431–1451.

Ghazanfar, A. A., and Schroeder, C. E. (2006). Is neocortex essentially multisensory? *Trends Cogn. Sci. (Regul. Ed.)* 10, 278–285.

Grondin, S., and McAuley, D. (2009). Duration discrimination in crossmodal sequences. *Perception* 38, 1542–1559.

Harrington, D. L., Zimbelman, J. L., Hinton, S. C., and Rao, S. M. (2010). Neural modulation of temporal encoding, maintenance, and decision processes. *Cereb. Cortex* 20, 1274–1285.

Klemen, J., and Chambers, C. D. (2011). Current perspectives and methods in studying neural mechanisms of multisensory interactions. *Neurosci. Biobehav. Rev.* doi: 10.1016/j.neubiorev.2011.04.015. [Epub ahead of print].

Kosillo, P., and Smith, A. T. (2010). The role of the human anterior insular cortex in time processing. *Brain Struct. Funct.* 214, 623–628.

Lewis, J. W., Beauchamp, M. S., and DeYoe, E. A. (2000). A comparison of visual and auditory motion processing in human cerebral cortex. *Cereb. Cortex* 10, 873–888.

Matell, M. S., and Meck, W. H. (2004). Cortico-striatal circuits and interval timing: coincidence detection of oscillatory processes. *Cogn. Brain Res.* 21, 139–170.

Matthews, W. J., Stewart, N., and Wearden, J. H. (2011). Stimulus intensity and the perception of duration. *J. Exp. Psychol. Hum. Percept. Perform.* 37, 303–313.

Mayer, A. R., Franco, A. R., Canive, J., and Harrington, D. L. (2009). The effects of stimulus modality and frequency of stimulus presentation on cross-modal distraction. *Cereb. Cortex* 19, 993–1007.

Mella, N., Conty, L., and Pouthas, V. (2011). The role of physiological arousal in time perception: psychophysiological evidence from an emotion regulation paradigm. *Brain Cogn.* 75, 182–187.

Menon, V., and Uddin, L. Q. (2010). Saliency, switching, attention and control: a network model of insula function. *Brain Struct. Funct.* 214, 655–667.

Merchant, H., Zarco, W., and Prado, L. (2008). Do we have a common mechanism for measuring time in the hundreds of millisecond range? Evidence from multiple-interval timing tasks. *J. Neurophysiol.* 99, 939–949.

Mita, A., Mushiake, H., Shima, K., Matsuzaka, Y., and Tanji, J. (2009). Interval time coding by neurons in the presupplementary and supplementary motor areas. *Nat. Neurosci.* 12, 502–507.

Nagy, A., Eordegh, G., Paroczy, Z., Markus, Z., and Benedek, G. (2006). Multisensory integration in the basal ganglia. *Eur. J. Neurosci.* 24, 917–924.

Nenadic, I., Gaser, C., Volz, H. P., Rammsayer, T., Hager, F., and Sauer, H. (2003). Processing of temporal information and the basal ganglia: new evidence from fMRI. *Exp. Brain Res.* 148, 238–246.

Penney, T. B., Gibbon, J., and Meck, W. H. (2000). Differential effects of auditory and visual signals on clock speed and temporal memory. *J. Exp. Psychol. Hum. Percept. Perform.* 26, 1770–1787.

Penney, T. B., Meck, W. H., Roberts, S. A., Gibbon, J., and Erlenmeyer-Kimling, L. (2005). Interval-timing deficits in individuals at high risk for schizophrenia. *Brain Cogn.* 58, 109–118.

Pouthas, V., George, N., Poline, J. B., Pfeuty, M., Vandemoorteele, P. F., Hugueville, L., Ferrandez, A.-M., Lehéricy, S., Lebihan, D., and Renault, B. (2005). Neural network involved in time perception: an fMRI study comparing long and short interval estimation. *Hum. Brain Mapp.* 25, 433–441.

Recanzone, G. H. (2003). Auditory influences on visual temporal rate perception. *J. Neurophysiol.* 89, 1078–1093.

Repp, B. H., and Penel, A. (2002). Auditory dominance in temporal processing: new evidence from synchronization with simultaneous visual and auditory sequences. *J. Exp. Psychol. Hum. Percept. Perform.* 28, 1085–1099.

Schmahmann, J., Doyon, J., Toga, A., Petrides, M., and Evans, A. (2000). *MRI Atlas of the Human Cerebellum.* San Diego: Academic Press.

Tse, P. U., Intriligator, J., Rivest, J., and Cavanagh, P. (2004). Attention and the subjective expansion of time. *Percept. Psychophys.* 66, 1171–1189.

Ulrich, R., Nitschke, J., and Rammsayer, T. (2006). Crossmodal temporal discrimination: assessing the predictions of a general pacemaker-counter model. *Percept. Psychophys.* 68, 1140–1152.

van Schouwenburg, M. R., den Ouden, H. E., and Cools, R. (2010). The human basal ganglia modulate frontal-posterior connectivity during attention shifting. *J. Neurosci.* 30, 9910–9918.

van Wassenhove, V., Buonomano, D. V., Shimojo, S., and Shams, L. (2008). Distortions of subjective time perception within and across senses. *PLoS ONE* 3, e1437. doi: 10.1371/journal.pone.0001437

Wearden, J. H., Edwards, H., Fakhri, M., and Percival, A. (1998). Why "sounds are judged longer than lights": application of a model of the internal clock in humans. *Q. J. Exp. Psychol. B* 51, 97–120.

Wearden, J. H., O'Rourke, S. C., Matchwick, C., Min, Z., and Maeers, S. (2010). Task switching and subjective duration. *Q. J. Exp. Psychol. (Colchester)* 63, 531–543.

Wearden, J. H., Todd, N. P., and Jones, L. A. (2006). When do auditory/visual differences in duration judgements occur? *Q. J. Exp. Psychol. (Colchester)* 59, 1709–1724.

Wencil, E. B., Coslett, H. B., Aguirre, G. K., and Chatterjee, A. (2010). Carving the clock at its component joints: neural bases for interval timing. *J. Neurophysiol.* 104, 160–168.

Wittmann, M., Simmons, A. N., Aron, J. L., and Paulus, M. P. (2010a). Accumulation of neural activity in the posterior insula encodes the passage of time. *Neuropsychologia* 48, 3110–3120.

Wittmann, M., van Wassenhove, V., Craig, A. D., and Paulus, M. P. (2010b). The neural substrates of subjective time dilation. *Front. Hum. Neurosci.* 4:2. doi: 10.3389/neuro.09.002.2010

Worsley, K. J., Marrett, S., Neelin, P., Vandal, A. C., Friston, K. J., and Evans, A. C. (1996). A unified statistical approach for determining significant signals in images of cerebral activation. *Hum. Brain Mapp.* 4, 58–73.

Conflict of Interest Statement: The authors declare that the research was conducted in the absence of any commercial or financial relationships that could be construed as a potential conflict of interest.

Received: 01 June 2011; paper pending published: 28 June 2011; accepted: 13 July 2011; published online: 28 July 2011.

Citation: Harrington DL, Castillo GN, Fong CH and Reed JD (2011) Neural underpinnings of distortions in the experience of time across senses. Front. Integr. Neurosci. ***5****:32. doi: 10.3389/fnint.2011.00032*

frontiers in
INTEGRATIVE NEUROSCIENCE

ORIGINAL RESEARCH ARTICLE
published: 23 December 2011
doi: 10.3389/fnint.2011.00081

Modeling accuracy and variability of motor timing in treated and untreated Parkinson's disease and healthy controls

Catherine R. G. Jones[1]*, Daniel O. Claassen[2], Minhong Yu[3], Jeffrey R. Spies[3], Tim Malone[4], Georg Dirnberger[5], Marjan Jahanshahi[5] and Michael Kubovy[3]*

[1] *Department of Psychology, University of Essex, Essex, UK*
[2] *Department of Neurology, Vanderbilt University, Nashville, TN, USA*
[3] *Department of Psychology, University of Virginia, Charlottesville, VA, USA*
[4] *Royal Devon & Exeter Hospital, Devon, UK*
[5] *Sobell Department of Motor Neuroscience and Movement Disorders, University College London Institute of Neurology, London, UK*

Edited by:
Warren H. Meck, Duke University, USA

Reviewed by:
Regina H. Silva, Federal University of Rio Grande do Norte, Brazil
John F. Araujo, Federal University of Rio Grande do Norte, Brazil

****Correspondence:***
Catherine R. G. Jones, Department of Psychology, University of Essex, Colchester, Essex, CO4 3SQ, UK.
email: crgjones@essex.ac.uk;
Michael Kubovy, Department of Psychology, University of Virginia, P. O. Box 400400, Charlottesville, VA 22904-4400, USA.
e-mail: kubovy@virginia.edu

Parkinson's disease (PD) is characterized by difficulty with the timing of movements. Data collected using the synchronization–continuation paradigm, an established motor timing paradigm, have produced varying results but with most studies finding impairment. Some of this inconsistency comes from variation in the medication state tested, in the inter-stimulus intervals (ISI) selected, and in changeable focus on either the synchronization (tapping in time with a tone) or continuation (maintaining the rhythm in the absence of the tone) phase. We sought to re-visit the paradigm by testing across four groups of participants: healthy controls, medication naïve *de novo* PD patients, and treated PD patients both "on" and "off" dopaminergic medication. Four finger tapping intervals (ISI) were used: 250, 500, 1000, and 2000 ms. Categorical predictors (group, ISI, and phase) were used to predict accuracy and variability using a linear mixed model. Accuracy was defined as the relative error of a tap, and variability as the deviation of the participant's tap from group predicted relative error. Our primary finding is that the treated PD group (PD patients "on" and "off" dopaminergic therapy) showed a significantly different pattern of accuracy compared to the *de novo* group and the healthy controls at the 250-ms interval. At this interval, the treated PD patients performed "ahead" of the beat whilst the other groups performed "behind" the beat. We speculate that this "hastening" relates to the clinical phenomenon of motor festination. Across all groups, variability was smallest for both phases at the 500-ms interval, suggesting an innate preference for finger tapping within this range. Tapping variability for the two phases became increasingly divergent at the longer intervals, with worse performance in the continuation phase. The data suggest that patients with PD can be best discriminated from healthy controls on measures of motor timing accuracy, rather than variability.

Keywords: motor timing, Parkinson's disease, temporal processing, synchronization, continuation, dopamine, linear mixed model

INTRODUCTION

The ability to accurately time movements is a critical component of motor function and the study of motor timing has provided insight into the functions of a hypothetical "internal clock" (see Jones and Jahanshahi, 2009 for a review). Motor timing has been most commonly measured using an elegant and influential paradigm known as the synchronization–continuation task (e.g., Wing and Kristofferson, 1973a,b). The task has proved a useful paradigm for studying both normal and pathological patterns of motor timing. The participant first synchronizes their tapping rate (usually the index finger of their dominant hand) with an externally provided cue (typically an auditory tone). The pacing stimulus is presented at a regular interval that generally falls within the period of several hundred milliseconds (ms) to a couple of seconds. After a criterion number of taps the pacing stimulus is stopped and the participant has to maintain the rhythm unaided; this is the continuation phase. Thus, the task measures the ability to entrain a motor response to a timed cue and to then maintain the learnt rhythm unaided.

Analysis of the task has focused on the quantification of the accuracy and variability of tapping. Both measure important characteristics of performance, with accuracy reflecting the closeness of a response to its target and variability reflecting how spread repeated responses are from the target. Investigation of accuracy has been typically explored using mean effects, either using the mean inter-response interval or mean absolute error (e.g., O'Boyle et al., 1996; Pope et al., 2006; Merchant et al., 2008a). Variability has been assessed using common statistical constructs such as the SD (e.g., Merchant et al., 2008a) or coefficient of variation (e.g., Pope et al., 2006). However, the exploration of variability has

been dominated by an influential model (Wing and Kristofferson, 1973a,b) that seeks to decompose the variability on the continuation phase of the task into that attributable to "clock" processes or alternatively to motor execution. However, the Wing and Kristofferson model is not without caveats. First, the model assumes that the hypothetical clock and motor processes are independent of one another. Second, it does not allow for the drift in the length of the produced taps, a phenomenon that is commonly observed in human tapping data (e.g., Collier and Ogden, 2001; Madison, 2001). Additionally, the Wing and Kristofferson model is focused on variability during the continuation phase. This ignores the useful information that can be gained from exploring performance on the paced section of the paradigm. For example, impaired performance on the continuation phase could be due to an inability to reproduce a learnt rhythm, or it could be a reflection of the inability to master the rhythm during the synchronization phase.

The task has been readily adopted to assess motor timing in Parkinson's disease (PD). PD is a complex neurodegenerative disorder characterized by impairments of motor function resulting in the clinical symptoms of bradykinesia, rigidity, tremor, and postural instability. The cardinal motor symptoms emerge following dopaminergic cell loss in the substantia nigra pars compacta. As such, research establishing that people with PD are impaired at the synchronization–continuation task has been pivotal to the hypothesis that the basal ganglia are essential to temporal processing (e.g., Pastor et al., 1992; Freeman et al., 1993; Harrington et al., 1998; although see Ivry and Keele, 1989; Yahalom et al., 2004; Spencer and Ivry, 2005). Our recent work has shown that the neural correlates of motor tapping show a distinct pattern for individuals with PD (Jahanshahi et al., 2010). Specifically, patients with PD do not show the typical pattern of activation of striato-frontal sites seen in healthy controls and instead show greater activation of the cerebellum.

Although the majority of studies report atypical performance on this task in PD, the pattern of dysfunction varies across studies. Analysis of accuracy has suggested faster (O'Boyle et al., 1996), slower (Pastor et al., 1992), and unimpaired (Yahalom et al., 2004; Spencer and Ivry, 2005) tapping in PD. Variability data are more consistent, with studies tending to find it elevated (e.g., Pastor et al., 1992; O'Boyle et al., 1996; Harrington et al., 1998; Merchant et al., 2008b), although some null results also exist (e.g., Ivry and Keele, 1989; Spencer and Ivry, 2005). The variation in the results could be attributable to many factors. As mentioned previously, most studies have not looked at variability performance on the synchronization section of the task. Further, not all studies assessed participants both "on" and "off" dopaminergic replacement therapy. Finally, many studies tested only one or two tapping rates. There is substantial evidence to suggest that performance might differ at different interval ranges, particularly in the "short" milliseconds vs. "long" seconds range (e.g., Nakamura et al., 1978; Peters, 1989).

The aim of this paper was to take a fresh and comprehensive look at motor timing in PD using the synchronization–continuation paradigm. We were interested in modeling both accuracy and variability performance on the task, across both the synchronization and continuation sections of the paradigm. The aims for the study were: (1) to develop a novel way for describing and modeling finger tapping data, (2) to look for group differences between participants with and without PD (3) to examine if acute manipulation ("on" vs. "off") or chronic (treated PD vs. *de novo* PD) medication state influenced performance. To predict the pattern of the data, we fitted a linear mixed model according to three different predictors of performance: (1) groups of participants (treated PD patients both "on" and "off" medication, PD patients yet to start medication treatment, and healthy controls), (2) tapping rate (250, 500, 1000, 2000 ms), and (3) the two types of tapping (synchronization and continuation).

MATERIALS AND METHODS

PARTICIPANTS

The study included three groups: (a) 14 patients with PD-treated with dopaminergic medication (PD-treated group), (b) eight PD patients yet to start dopaminergic therapy (PD-*de novo* group), and (c) 20 healthy participants (control group). Criteria for a diagnosis of PD was based on the UK Parkinson Disease Society Brain Bank criteria (Hughes et al., 1992), established by a physician experienced in PD diagnosis and management.

Participants in the PD-treated group were tested both "on" and "off" medication (PD-treated-on and PD-treated-off) where the "off" state was conducted after overnight withdrawal of medication (mean time since last medication = 14.43 h, SD = 3.48). Two patients were tested in the "off" condition only, while the remaining 12 were tested in both conditions, in a counterbalanced order. Details of the patients, including medication, can be seen in **Table 1**.

Participant groups were matched for age [PD-treated group: mean age = 64.07 years, SD = 7.45 years; PD-*de novo* group: 62.62 (10.27); Control group: 67.65 (8.87)]. None of the participants had a history of psychiatric or other neurological disease, head injury or alcohol/drug abuse. Participants were screened for cognitive impairment using the mini-mental state examination (MMSE: Folstein et al., 1975), with all scoring above the required cut-off of 27. Scores on the beck depression inventory (BDI: Beck et al., 1961) indicated that one participant in the control group had a score of 22 and one participant in the PD-treated group had a score of 20, both above the cut-off for moderate self-reported depression (range 19–29). All other participants were in the minimal or mild range. The three groups did not differ in terms of age, estimated premorbid verbal IQ (using the national adult reading test, NART: Nelson, 1982), or ability to maintain focused attention (paced auditory serial addition task, PASAT: Gronwall and Wrightson, 1981; Mann Whitney U, all p-values > 0.1). A summary of these measures can be found in **Table 2**.

The study had the approval of the Joint Medical Ethics Committee of the National Hospital for Neurology and Neurosurgery and the UCL Institute of Neurology and the North and East Devon Local Research Ethics Committee. Written, informed consent was obtained from all participants prior to the experiment.

TASKS

Clinical and behavioral measures of motor performance

Stage and severity of PD was assessed with the Hoehn and Yahr rating scale (Hoehn and Yahr, 1967) and Part III (Motor) score of the Unified PD Rating Scale (UPDRS: Fahn et al., 1987). In

Table 1 | Dopaminergic medication for the PD-treated group (for Sinemet, amount of levodopa in brackets).

Patient number	Duration of illness (years)	Dose of medication
1	9	Sinemet 550 mg (500 mg) Ropinirole 6 mg
2	10	Sinemet Plus 250 mg (200 mg) Sinemet CR 375 mg (300 mg) Amantadine 100 mg
3	10	Pramipexole 2.16 mg
4	10	Ropinirole 12 mg
5	13	Sinemet 375 mg (300 mg) Selegiline 10 mg
6	7	Sinemet CR 625 mg (500 mg) Pergolide 3 mg
7	3	Ropinirole 24 mg
8	4	Pergolide 4.5 mg
9	11	Sinemet CR 250 mg (200 mg) Sinemet 715 mg (650 mg) Cabergoline 4 mg
10	10	Sinemet Plus 750 mg (600 mg) Sinemet CR 250 mg (200 mg) Pramipexole 3.18 mg Amantadine 200 mg
11	10	Sinemet Plus 750 mg (600 mg) Sinemet CR 250 mg (200 mg) Ropinirole 24 mg
12	4	Sinemet Plus 375 mg (300 mg) Cabergoline 3 mg
13	5	Sinemet CR 250 mg (200 mg)
14	17	Sinemet CR 375 mg (300 mg)

addition, motor speed and finger dexterity was measured with the Purdue Pegboard (Tiffin and Asher, 1948). The test comprises of a set of metal pegs and a pegboard. Participants pick up the pegs one at a time and place them one by one in one in the pegboard as quickly as possible. This was done three times: with the right hand, with the left hand and bimanually. The number of pegs placed in the holes in 30 s was recorded on each occasion.

Repetitive tapping task

The participant sat at a table in a quiet room. The task was programmed in Quick Basic and run on a Dell laptop. A response box (15 cm × 8 cm × 5 cm) with two identical circular response buttons (diameter 2.5 cm) was used to record responses. All the participants were instructed to use the same button and to ignore the second button. The travel of the button, which had a flat plastic surface and made a "click" sound when pressed, was 2.5 mm and the operating force was 0.8 N. All responses were made with the dominant or choice index finger of the participant (**Table 2**). Response times were recorded to the nearest millisecond. Participants were instructed to tap in synchrony with a tone (1000 Hz, duration 50 ms) presented with a constant inter-stimulus interval (ISI) of either 250, 500, 1000, or 2000 ms (synchronization phase). After 31 taps (30 intervals) the tone stopped and participants continued to tap and maintain the rhythm for a further 30 intervals (continuation phase). A loud tone indicated the end of the trial.

Participants performed the task over two blocks. Each block consisted of the presentation of four runs of trials (one of each interval type, i.e., 250, 500, 1000, and 2000 ms), with a counterbalanced order used. Erroneous responses were considered to be those where the inter-tap interval (ITI) was 50% longer or shorter than the target ISI. These responses were considered outliers and were excluded from the analysis, although the remainder of the run was kept. Relating to a concern over collecting enough valid data, for some participants a particular ISI was administered more than twice. This resulted in seven controls and three PD-*de novo* with additional runs of trials. For the PD-treated group, only four runs of trials were collected for three of the participants when "off" medication, and only four runs of trials from one participant and only seven runs of trials from two participants when "on" medication. An illustration of the task is provided in **Figure 1**.

ANALYSIS

Descriptive data

Analysis of descriptive data used independent or paired *t*-tests, and Mann Whitney *U* and Wilcoxon signed ranks tests, depending on whether the data were normally distributed.

Repetitive tapping analysis

We used linear mixed models (LMM; also known as multilevel analyses or hierarchical linear models) with categorical predictors to explore the accuracy and variability of the responses of the participants. The focus of the analysis was to find the best-fitting model for the data and to explore the effects of these predictors and their interactions. Our conclusions are based on LMMs computed using the function lmer (Bates et al., 2011) running on R 2.13.0. (R Development Core Team, 2011). Mixed-effects analyses (see Kreft and De Leeuw, 1998; Snijders and Bosker, 1999; Raudenbush and Bryk, 2002; Baayen, 2008) have considerable advantages over traditional repeated measures analyses, which are based on quasi-*F* tests, by-subjects analyses, combined by-subjects and by-items analyses, and random regression (Maxwell and Delaney, 2004; Baayen et al., 2008). In predicting the outcome variable – be it accuracy or variability – LMM allows us to assess how a participant's clinical and experimental classification predicts performance.

We measured accuracy by calculating a relative error value for each tap: (ITI−ISI)/ISI. This value is comparable across ISIs and provides a quantitative assessment of the directionality of each tap: if the relative error is negative then the participant is ahead of the beat, or "leading," and if the relative error is positive then the participant is behind the beat, or "lagging." For the LMM of accuracy (the relative error), three categorical variables served as fixed effects in the model: group (Group: PD-treated-on, PD-treated-off, PD-*de novo* and control), ISI (ISI: 250, 500, 1000, and 2000 ms), and task phase (Task phase: synchronization or continuation). The participant served as the random effect.

We measured variability of performance by calculating the participants' deviation from the predicted group relative error in the LMM of accuracy for each tap (i.e., participant observed relative error minus group predicted relative error). This approach allows

Table 2 | Descriptive data for the three participating groups.

	PD-treated				PD-*de novo*		Control	
	OFF		ON					
N	14[a]				8[b]		20	
Sex (M:F)	8:6				5:3		13:7	
Handedness (R:L)	14:0				8:0		18:2	
Hand used (R:L)	13:1				7:3		18:2	
	M	**SD**	***M***	**SD**	***M***	**SD**	***M***	**SD**
Age (years)	64.07	7.45			62.62	10.27	67.65	8.87
Duration of PD (years)	8.79	3.87			3.38	1.85		
MMSE	29.29	0.73			28.88	0.99	28.45	0.95
NART IQ	122.64	3.25			120.50	4.44	120.05	6.49
PASAT-errors	5.42	5.23			4.86	4.63	5.60	5.81
BDI	10.14	4.83			5.63	3.74	7.2	5.68
Pegboard-L	9.57	1.65	10.17	1.90	10.43	2.23	13.53	2.76
Pegboard-R	10.14	1.88	12.50	2.47	8.71	1.98	13.53	2.91
Pegboard-B	6.86	2.18	8.58	1.56	6.86	1.46	9.90	1.29
Hoehn and Yahr	2.50	0.44	1.68	0.54	1.63	0.58		
UPDRS III	34.50	10.28	17.07	8.93	25.62	7.96		

MMSE, mini-mental state examination; NART IQ, national adult reading test IQ; PASAT, paced auditory serial addition test-mean number of errors; BDI, beck depression inventory; Pegboard-L/R/B, Purdue Pegboard with left hand/right hand/bilaterally; UPDRS III, unified Parkinson's disease rating scale – part III motor score.

[a] *N = 12 for PASAT and Pegboard.*

[b] *N = 7 for PASAT and Pegboard.*

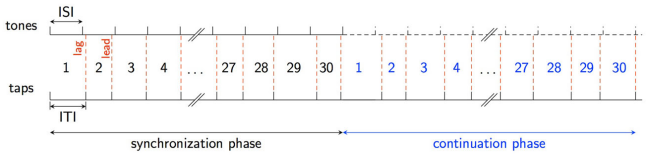

FIGURE 1 | The repetitive tapping task. The red dotted lines indicate a participant's response, which can either lag or lead the target ISI. The tones cease in the continuation phase, as indicated by the black dotted line. ISI, inter-stimulus interval; ITI, inter-tap interval.

for an assessment of individual performance based on group-specific estimates of accuracy, thus accounting for group patterns of performance. This method also has the benefit of modeling variability as it occurs on each trial, rather than calculating it as mean performance across an entire run of trials (i.e., instead of one variability score for a run of trials, we have 30 variability scores per phase). In essence, our variability measurement quantifies the deviation of each observed tap from the accuracy model for a given group. Since random noise in the data results in outliers that skew its distribution, this "residual" error does not conform to a normal distribution. Therefore, we transformed it by calculating the square root of the absolute value to create an adjusted measure of variability. A highly variable participant would produce a wide range of $\sqrt{\text{abs}}$(residuals), while constant performance would produce a narrow range. The LMM of variability was identical in structure to the model for accuracy, with three categorical variables as fixed effects and participant as random effect.

The significance of the fixed effects (predictors) was determined through interpretation of the 95% confidence intervals; if the lower and upper confidence intervals did not cross zero then the effect and corresponding estimated coefficient was considered significant at $p < 0.05$.

RESULTS

CLINICAL AND BEHAVIORAL MEASURES OF MOTOR PERFORMANCE

As expected, for the Hoehn and Yahr scale and the UPDRS Part III Motor score, the PD-treated group were significantly worse in the "off" than "on" medication state [Hoehn and Yahr: Wilcoxon signed ranks, $Z = -3.11$, $p = 0.002$; UPDRS: $t(13) = -7.50$, $p < 0.001$]. The PD-treated group tested "off" medication were significantly worse compared to the PD-*de novo* group [Hoehn and Yahr: $t(20) = -4.00$, $p = 0.001$; UPDRS: $t(20) = -2.10$, $p = 0.05$], reflecting more advanced stage of illness in the former group. However, the severity of motor symptoms of the PD-treated group were not significantly worse when they were compared in the "on" medication state to the *de novo* group, although there was a trend toward poorer performance for the UPDRS (UPDRS: $p = 0.07$; Hoehn and Yahr: $p > 0.9$).

For the Purdue pegboard, statistical analysis was confined to the right hand data to reduce the number of statistical tests; the right hand data were selected as they produced the most divergent results. Performance indicated that the PD-treated group when "off" medication and the PD-*de novo* group performed

significantly more poorly than the control group. (Mann Whitney U for control vs. PD-treated-off: $U = 38.50$, $p < 0.001$. For control vs. PD-*de novo*: $U = 8.50$, $p < 0.001$; Bilateral $U = 6.5$, $p < 0.001$). However, when the treated PD group was "on" medication they did not differ from controls ($p > 0.4$). Not surprisingly, therefore, pegboard performance was better "on" than "off" medication for the PD-treated group [$t(11) = 4.60$, $p = 0.001$]. The PD-*de novo* group were equivalent to the PD-treated group when the treated patients were "off" medication ($p < 0.1$), but were worse than the treated group when they were "on" medication [$t(16) = -2.95$, $p = 0.005$]. See **Table 2** for a summary of these results.

ACCURACY

We used three predictors (Group, ISI, and Task Phase) as fixed effects to model relative error. The model also included three random-effects: a subject-by-subject variation in intercept, in the effect of ISI, and in the effect of Task Phase. The best-fitting LMM (Akaike information criterion, AIC was used for model comparison) included the triple interaction, all three two-way interactions and all main effects as fixed effects (see **Table A1** in Appendix for the model coefficients and confidence intervals). **Figure 2** shows the relative error predicted by this model for of all the conditions; the error bars represent 1 SE from the predicted value. To aid understanding of the complex data, we have presented it in two ways: **Figure 2A**: with the groups on the x axis to enable direct comparison of the groups at each ISI; **Figure 2B**: with the ISI on the x axis to enable the individual pattern for each group to be more easily ascertained. The model was complex in that it included the significant three-way interaction and all significant two-way interactions. Thus, we cannot explain the effect of one predictor without considering the variation of the other predictors. Reflecting this, we focused on patterns of interest with a second, refined model fitted to aid interpretation of these patterns.

Results are best interpreted by first focusing on the longer intervals (500, 1000, and 2000 ms) and then the shortest interval (250 ms). For the longer intervals, all groups of participants tapped with a negative relative error, i.e., responses were ahead of the beat. Further, all groups had smaller (i.e., closer to 0) predicted relative error during the synchronization phase (see **Figure 2A**). At 500 ms, the PD-*de novo* group had a greater negative error than the control group, and this pattern persisted at 1000 ms. Aside from this exception, performance across the groups was not distinguishable.

At the 250-ms ISI the pattern was more complex and was where meaningful group differences were observed. During the synchronization phase at 250 ms the control participants tapped with a positive relative error, i.e., they tapped "behind the beat." This is in contrast to the PD-treated group (both "on" and "off" medication), who showed a negative or "ahead of the beat" performance at 250 ms. The PD-*de novo* group was more similar to the control group than the PD-treated group at 250 ms and showed a positive mean relative error score (but note that the SE bar included 0).

During the continuation phase at 250 ms, the pattern of effects was similar but the differences between control and PD-treated patients were more striking. Again, the control participants tapped with a positive relative error (behind the bead) and the PD-treated group (both "on" and "off" medication) showed a negative relative error (ahead of the beat). As with the synchronization phase, the PD-*de novo* group was more similar to the control group than the PD-treated group.

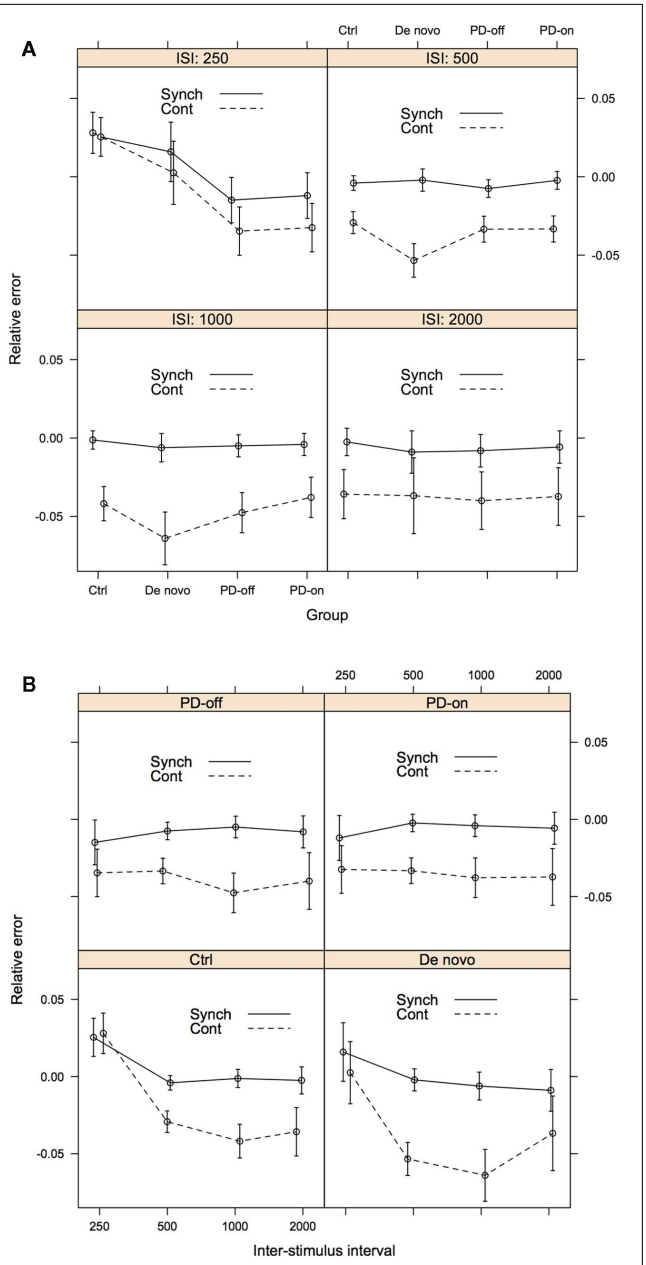

FIGURE 2 | Accuracy as assessed by predicted relative error, for illustrative purposes presented both by ISI (A) and Group (B). The error bars represent 1 SE from the predicted relative error. For **(A)**, lines connecting the data points do not imply that intermediate levels exist between the treatments. Rather they serve to facilitate the understanding of the data. Group: Ctrl, control; *De novo*, PD-*de novo*; PD-off, PD-treated-off; PD-on, PD-treated-on; Task Phase: Synch, synchronization; Cont, continuation; ISI, inter-stimulus interval.

We developed a second model to assess our interpretation of the pattern of data in a manner analogous to *post hoc* testing. We used three newly coded predictors as fixed effects to model relative error: Treatment [treated (PD-on and PD-off) vs.

untreated (PD-*de Novo* and Control)], ISI [short (250 ms) vs. long (500, 1000, and 2000 ms)], and Task Phase (synchronization vs. continuation). The model included the same random-effects as in the previous model: a subject-by-subject variation in intercept, in the effect of ISI, and in the effect of Task Phase. The three predictors appeared as a significant triple interaction in the new model. The estimated values of the model coefficients and associated confidence intervals can be seen in **Table 3**, whilst **Figure 3** shows the relative error predicted by this model for of all the conditions. This analysis more clearly illustrated the pattern evident in the first model. First, the treated and untreated groups were indistinguishable at the long ISI (500, 1000, 2000 ms), with both groups showing greater relative error in the continuation phase. Second, the groups diverged at the short ISI (250 ms), with the treated group showing hastening (negative relative error) compared to the untreated group. Further, the hastening was more pronounced for the continuation phase, whereas the untreated group showed no differentiation between phases at the short ISI (see **Figure A1** in Appendix for supporting evidence in two *post hoc* models for the short and long intervals). In sum, participants with a diagnosis of PD who have been treated with dopaminergic medication (whether "off" or "on" at the time of testing) are differentiated from control and *de novo* PD patients at the short ISI of 250 ms, but not at longer intervals.

Table 3 | Estimated values of the model coefficients for the second model of accuracy (relative error).

Effect	Estimate	Lower CI	Upper CI
Intercept (short, untreated, synch)	0.020	0.014	0.026
ISI	−0.024	−0.030	−0.018
Task phase	0.003	−0.003	0.008
Treatment	−0.034	−0.046	−0.021
ISI × task phase	−0.039	−0.045	−0.032
ISI × treatment	0.031	0.021	0.042
Task phase × treatment	−0.022	−0.031	0.014
Task phase × treatment × ISI	0.028	0.018	0.038

CI, confidence intervals.

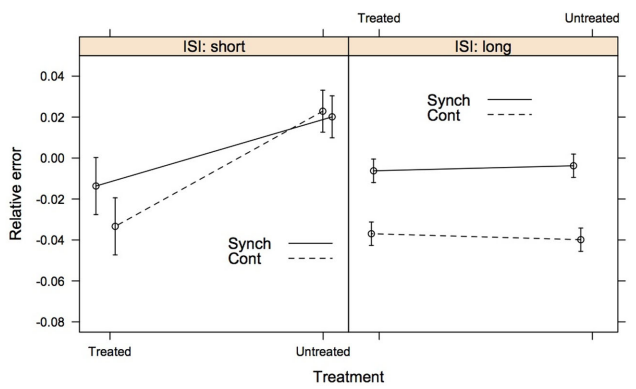

FIGURE 3 | The second model of accuracy comparing the PD patients receiving dopaminergic medication (treated group) to PD patients who were dopamine naïve and healthy controls (untreated group). ISI tapping rates are collapsed into short (250 ms) and long (500, 1000, and 2000 ms). The error bars represent 1 SE from the predicted relative error. Lines connecting the data are placed to illustrate group differences. Synch, synchronization phase; Cont, continuation phase.

VARIABILITY

Our approach to modelling variability was identical to our LMM model for accuracy. We used the same three predictors as fixed effects: Group, ISI, and Task Phase. The model also included the same three random-effects: a subject-by-subject variation in intercept, in the effect of ISI, and in the effect of Task Phase. The best-fitting LMM included the triple interaction, all three two-way interactions and all main effects as fixed effects, see **Table A2** in Appendix for the model coefficients and confidence intervals. **Figure 4** shows the variability predicted by this model for of all the conditions; the error bars represent 1 SE from the predicted value. As with the accuracy model, to aid understanding of the data we have presented it in two formats: **Figure 4A**: with the groups on the x axis to enable direct comparison of the groups at each ISI; **Figure 4B**: with the ISI on the x axis to enable the individual pattern for each group to be more easily ascertained. Again, as the three-way interaction was significant we focused on complex patterns of interest.

When comparing the two task phases, we found that the predicted variability of the synchronization phase was lower than that of the continuation phase. Across all groups, variability was lowest at the 500-ms condition and increased across the 1000- and 2000-ms ISIs, particularly during the continuation phase. **Figure 4B** clearly illustrates that the difference between the synchronization and continuation phases increased with the ISI for the intervals 500-2000 ms. It is noteworthy that the variability between groups and task phases at the 250-ms ISI was overlapping and highly similar. Compared to the accuracy models, group differences were less striking. However, there was some suggestion of differentiation of the patient groups from the control group at the higher ISIs (see **Figure 4A**). First, the PD-treated group showed reduced variability at the 1000 ISI compared to the other groups during the continuation phase, this was more evident when they were "off" medication. This pattern was less distinct at 2000 ms and with evidence more compelling for the synchronization phase. Second, the PD-*de novo* group showed increased variability compared to the other groups at the 2000 ISI, with the effect being more distinct for the continuation phase.

DISCUSSION

This study applied a linear mixed model approach to explore the relative patterns of accuracy and variability on the synchronization–continuation task for treated and *de novo* patients with PD and healthy controls. In one of the most comprehensive assessments to date, our primary finding is that the treated PD group are distinguishable from the PD-*de novo* and control groups when tapping at the 250-ms rate. The treated PD patients tap "ahead" of the beat, whilst the other groups tap "behind" the beat. We liken this anticipatory motor response to the clinical phenomenon of motor "hastening" or festination. Regarding variability, motor timing at an ISI of 500 ms reduced the variability

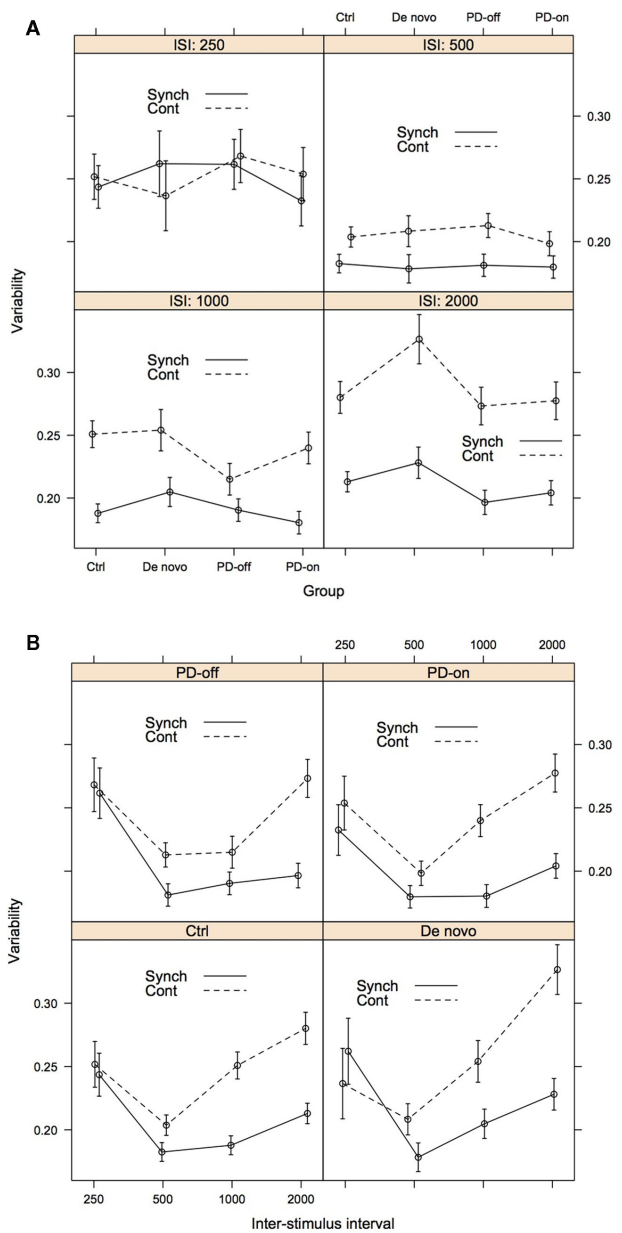

FIGURE 4 | Variability as assessed by participant deviation from predicted relative error, for illustrative purposes presented both by ISI (A) and Group (B). The error bars represent 1 SE from the predicted relative error. For **(A)**, lines connecting the data are placed to illustrate group differences. Group: Ctrl, control; *De novo*, PD-*de novo*; PD-off, PD-treated-off; PD-on, PD-treated-on; Task Phase: Synch, synchronization; Cont, continuation; ISI, inter-stimulus interval.

for all participants, which we speculate is indicative of a preferred finger tapping rate. For the longer (>250 ms) intervals, accuracy, and variability were compromised during the self-paced continuation phase compared to the synchronization phase. Related to this, the continuation phase was a better discriminator of performance, with the participants with PD showing more atypical motor timing behavior during continuation tapping.

Dopaminergic medication, although improving the UPDRS Part III motor score, did not have a substantive effect on motor timing performance in the PD-treated group. There are several possible explanations for this finding. The overnight medication withdrawal may be too short, or the individual pharmacokinetic or pharmacodynamic properties of different dopaminergic therapies may need to be taken into account. An alternative interpretation is that dopaminergic intervention does not produce robust changes in repetitive finger tapping or that the use of compensatory motor circuits when "off" medication can enable performance (see Jahanshahi et al., 2010). Previous research on repetitive tapping in PD has tested participants either exclusively "on" or "off" medication (e.g., Pastor et al., 1992; Freeman et al., 1993; Harrington et al., 1998; Yahalom et al., 2004), thus surprisingly little data on the effect of dopaminergic therapy on motor timing exists. The data that do exist are distinctly mixed in their findings. Pastor et al. (1992) assessed nine of their 42 PD patients "off" medication and after administration of 250 mg of levodopa. Dopaminergic therapy improved accuracy, as measured by the mean ITI, for the shorter intervals (400, 500, and 666 ms) but did not affect longer intervals (1000 and 2000 ms). O'Boyle et al. (1996) found that variability was worse "off" than "on" medication, although accuracy was not significantly different. Contradicting this, another study suggests no differences in variability between PD whether "on" or "off" medication (Merchant et al., 2008a).

To assess if treated PD patients performed differently to the other two groups, we compared the accuracy data collected both "off" and "on" medication (treated group) to healthy controls and *de novo* PD patients (untreated group). We found significant differences in the direction of the predicted relative error between the two groups for "short" (250 ms) compared to "long" (500, 1000, and 2000 ms) ISIs. This suggests that either long-term medication use influences performance, or that progression of PD results in more notable alterations to timing accuracy, especially during short intervals. A longitudinal study with a focus on modeling therapeutic dose and disease severity could help disambiguate these alternative hypotheses.

For all participants, performance on the synchronization phase was better than on the continuation phase for both accuracy and variability during the longer (500, 1000, 2000 ms) intervals. Previously, papers investigating motor timing in PD have tended not to explore the synchronization phase. One previous study found that performance for the PD group deteriorated in the continuation phase but that control group performance was maintained (Freeman et al., 1993). Our data are clear in showing that *all* groups found maintaining the rhythm more difficult in the continuation phase for intervals $\geq$ 500 ms. For these longer intervals, the difference in variability becomes greater as the target ISI increases, whereas accuracy is more stable. We have previously demonstrated that synchronization phase and continuation phase tapping activate distinct regions, which demonstrate the differential behavioral demands (Jahanshahi et al., 2010). Particularly, the continuation phase is unique in activating the dorsolateral prefrontal cortex (Jahanshahi et al., 2010), which is known to play a role in "willed" or "internally generated" actions (Jahanshahi et al., 1995). It has been shown that people with PD show greater differences from healthy controls in neural activation for internally generated than

externally triggered movements (Jahanshahi et al., 1995). This would predict a polarized performance between the continuation and synchronization phases for the PD patients. Indeed, the data indicate that the PD group show greater relative impairment on the continuation phase than the synchronization phase.

ACCURACY OF MOTOR TIMING

For the accuracy model, the key finding is that participants in the PD-treated group showed a hastening of their tapping (i.e., were "ahead of the beat") at 250 ms, whereas the PD-*de novo* and control groups were behind the beat. This effect was more striking in the continuation phase. Indeed, for the continuation phase the estimated means and SEs of the two groups were distinctly either side of zero relative error, suggesting potential in the future for this task to be used in discriminating treated PD from other populations. A second model that dichotomized the intervals into "short" (250 ms) and "long" (500, 1000, 2000 ms) confirmed that the 250-ms interval can successfully discriminate the PD-treated group from the other participants in the study, whereas the groups were equivalent at the longer durations. The PD-*de novo* and control groups were able to maintain their level of accuracy at 250 ms during the more challenging continuation phase, whereas the performance of the PD-treated group became more extreme. For the longer durations, all groups showed deterioration in accuracy from the synchronization phase to the continuation phases. Indeed, the groups were close to zero relative error during the synchronization phase but behind the beat in the continuation phase.

If the control group is taken as the model for "typical" performance, the pattern of data suggest that the PD-treated group show an atypical hastening in their tapping at very short (250 ms) intervals. This finding is similar to the clinical phenomenon of festinating movements. Festination is the tendency to speed up when performing a repetitive movement and, for experimental studies, is typically identified when movement rate exceeds that of the healthy control group by a specified margin (e.g., Logigian et al., 1991; Moreau et al., 2007). Previously, oral festination has been measured by asking participants to repeat a syllable at different frequencies, synchronized to an auditory pacing tone (Logigian et al., 1991; Moreau et al., 2007). Consistent with our findings, festination (measured as either 2 or 3 SDs from control performance) was apparent for ISIs between 200 and 333 ms in the study by Moreau et al. (2007) and for ISIs below 400 ms in the study by Logigian et al. (1991) and was not observed for longer intervals. Speeded movements during finger and wrist versions of the synchronization (Nakamura et al., 1978; Logigian et al., 1991; Freeman et al., 1993; Stegemöller et al., 2009) and continuation tasks (Freeman et al., 1993) have also been observed. Nakamura et al. (1978) and Stegemöller et al. (2009) reported the phenomenon around an ISI of 400 ms, whereas Freeman et al. (1993) showed hastening compared to the control group in some participants at intervals between 250 and 500 ms. Logigian et al. (1991) required participants to perform isometric contractions of the index finger at different frequencies. In line with our findings, performance was comparable to controls at ISIs of 833 and 476 ms, but speeded between 185 and 385 ms, with the effects most obvious at 286 ms. There is a paucity of studies exploring the neurobiological correlates of motor festination in PD. Previous studies have speculated that aberrant oscillatory brain activity (Nakamura et al., 1978; Stegemöller et al., 2009) or motor activity influenced by tremor rate (Logigian et al., 1991) may explain the phenomenon. Stegemöller et al. (2009) found that increases in movement frequency were accompanied by a decrease in movement amplitude in participants with PD. Future research could benefit from integrated physiological exploration.

In interpreting the patient group data it is important to comment of the performance of our control group in comparison to previously reported healthy populations. It has been established that synchronization with a pacing stimulus produces a negative relative error in healthy individuals, i.e., tapping ahead of the beat (e.g., see Aschersleben, 2002). As with previous research (e.g., Flach, 2005), we find that the negative relative error is maintained in the continuation phase and is exaggerated. Flach's (2005) explanation for this phenomenon is that the internal timing mechanism is systematically underestimating the ISI and this is being maintained in the self-paced condition. All our groups showed a negative relative error at ISIs of 500, 1000, and 2000 ms, but the control group showed a clear positive relative error, or tapping behind the beat, at 250 ms. A similar pattern of findings was found in a much earlier study by Peters (1989). Here, participants tapped in synchrony at ISIs ranging from 180 to 1000 ms. Healthy participants tapped behind the beat at 180 and 210 ms and ahead of the beat at intervals of 240 ms and greater. These findings speak to hypotheses that seek to establish a qualitative difference between different timing intervals and it has been speculated that different mechanisms might be in operation for the timing of very short intervals. One proposal is that when tapping speed is sufficiently fast the participant no longer experiences the taps as individual events and performance is in "automatic" rather than "controlled" mode (Peters, 1989). Within our own dataset, further evidence for a dissociation comes from the observation that the accuracy of performance was maintained in the switch to continuation tapping in the control group at 250 ms, whereas performance deteriorated for the longer intervals.

The difference between the PD-treated group and the other two groups at 250 ms was the most compelling evidence of differential accuracy performance in PD for motor timing. However, aside from the PD-*de novo* group showing greater negative error at 500 ms, and to a lesser extent at 1000 ms, there was no other evidence that the PD groups (PD-treated or PD-*de novo*) performed differently compared to the control group. Reflecting the current study, previous research has reported unimpaired repetitive timed movements in PD at durations of and above 476 ms (Logigian et al., 1991), 666 ms (Pastor et al., 1992) and 1000 ms (Jahanshahi et al., 2010). O'Boyle et al. (1996), Harrington et al. (1998), and Ivry and Keele (1989) have all found that a group with PD tapped at a significantly faster rate than a control group when "on" medication at intervals between 300 and 600 ms. In contrast, Pastor et al. (1992) reported that a group with PD were significantly slower at tapping with an ISI of 400 and 500 ms. In summary, despite the commonly asserted proposition that motor timing accuracy is impaired in PD, patients often perform well at longer intervals. The interval between 400 and 600 ms is subject to the most contrary findings, indicating that this is the key transition period for discriminating between groups. In light of this, future

studies should place emphasis on the tapping intervals ≤ 600 ms when exploring accuracy in PD.

VARIABILITY OF MOTOR TIMING

Our variability measure was specifically calculated to take account of how much the error for each tap deviated from the predicted error for the group. Thus, we were quantifying how typical a participant's performance was of their particular group.

Despite the significant three-way interaction, group differences were less striking for variability than for accuracy. The most distinct patterns were that the *de novo* PD group showed greater variability at the 2000-ms interval compared to all groups and particularly the treated PD group. One possibility is that this greater motor timing variability in the PD-*de novo* reflects the greater heterogeneity of this group. Alternatively, it is possible that the long-term use of dopamine has enduring effects on motor performance that persevere to an extent even in the "off" state. These effects could operate to reduce variability in motor timing in the treated PD group. Similar to previous work on cognition (e.g., Kulisevsky et al., 2000), future investigation of the chronic effect of dopaminergic therapy on motor timing in patients with or without motor fluctuations would be informative. There was some, albeit not consistent, suggestion of the PD-treated group showing reduced variability compared to the other groups at the higher intervals, most compellingly for the continuation phase at 1000 ms. This is difficult to interpret although this is not the first study to report reduced variance in PD (e.g., Jones et al., 2008).

Previous research has almost exclusively focused on variability during the continuation task. Two studies using a target interval of 550 ms have found no evidence of impaired variability in patients with PD, at least at the group level (Ivry and Keele, 1989; Spencer and Ivry, 2005), although O'Boyle et al. (1996) reported impairment using an identical duration. However, Merchant et al. (2008a) reported a deficit in PD for intervals between 350 and 1000 ms, albeit using a much shorter number of taps, and Harrington et al. (1998) reported impairment in PD for intervals of 300 and 600 ms. Pastor et al. (1992) also found increased variability for repetitive wrist movements at ISIs ranging from 400 to 2000 ms ISI. Variability in the synchronization task does not appear to be impaired in PD in previous studies, at least at the whole group level (e.g., Yahalom et al., 2004). However, the approach taken in our study is somewhat different to previous work. In including each tap in the model we improve the fidelity of our analysis. Further, we compare taps to the predicted group relative error, rather than a person's own mean. What is clear in the current data set is that all groups showed the same pattern of increasing variability between 500 and 2000 ms, with the variability produced by the continuation phase becoming increasingly divergent from the better synchronization phase performance.

It is notable that variability was lowest in all groups for the 500-ms interval. Yahalom et al. (2004) asked participants with and without PD to tap at their most comfortable pace. For the control group this was around 580 ms and for the PD group around 685 ms. Thus, 500 ms is an interval that approximately aligns with the rhythm that participants are likely to find most "natural" and as a result show less variability in their performance. Given that our accuracy data, combined with a review of previous literature, suggests that the point at which the accuracy of repetitive tapping is compromised in PD is somewhere between 250 and 500 ms, this further supports the idea that this very short interval range is of particular significance in understanding motor timing behavior. It can be hypothesized that participants will not show atypical accuracy and variability at their preferred tapping rate, so perhaps the mixed results across studies reflect that some groups with PD have a higher natural rhythm preference. Reflecting on both the work of Yahalom et al. (2004) and Logigian et al. (1991), further work could seek to combine data on motor timing using the synchronization–continuation task, natural or preferred tapping rate preference, and inherent tremor oscillation rate. The interplay between these three factors may prove illuminating.

CONCLUSION

Our data find a striking phenomenon of tapping ahead of the beat for treated patients with PD at intervals of 250 ms. The data add to a sparse but generally consistent literature that festination occurs in PD for fast (ISI < 500 ms) repetitive movements. Whereas patients with PD diverge from control performance at short intervals for measures of accuracy, they are more distinct at longer intervals (ISI of 1000 and 2000 ms) for variability. Whilst dopaminergic medication state at the time of testing ("on" vs. "off" medication) did not affect performance across any of the conditions, there is suggestion of differences between the treated and *de novo* patients for both accuracy and variability. This highlights the need to look at chronic medication effects in PD. The performance of the PD patients and the control group were more similar for the synchronization phase than the continuation phase. This likely reflects the difficulties that individuals with PD have with internally generated movements (e.g., Jahanshahi et al., 1995). Future research would benefit from exploring heterogeneity within the population with PD as well as correlating clinical phenotypes, such as festinating gait, to motor timing.

ACKNOWLEDGMENTS

The collection of these data was supported by a grant from the Brain Research Trust, UCL Institute of Neurology and a Medical Research Council Ph.D. studentship. Analysis was supported by a Collaborative Development Award from the British Council.

REFERENCES

Aschersleben, G. (2002). Temporal control of movements in sensorimotor synchronization. *Brain Cogn.* 48, 66–79.

Baayen, R. H. (2008). *Analyzing Linguistic Data. A Practical Introduction to Statistics Using R.* Cambridge: Cambridge University Press.

Baayen, R. H., Davidson, D. J., and Bates, D. M. (2008). Mixed-effects modeling with crossed random effects for subjects and items. *J. Mem. Lang.* 59, 390–412.

Bates, D., Maechler, M., and Bolker, B. (2011). lme4: Linear mixed-effects models using S4 classes. R package version 0.999375-42. Available at: http://CRAN.R-project.org/package=lme4

Beck, A. T., Ward, C. H., Mendelson, M., Mock, J., and Erbaugh, J. (1961). An inventory for measuring depression. *Arch. Gen. Psychiatry* 4, 561–571.

Collier, G. L., and Ogden, R. T. (2001). Variance decomposition of tempo drift in isochronous rhythmic tapping. *Ann. N. Y. Acad. Sci.* 930, 405–408.

Fahn, S., Elton, R. L., and Committee, M. O. T. U. D. (1987). "Unified Parkinson's disease rating scale," in *Recent Developments in Parkinson's Disease*, eds S. Fahn, C. D. Marsden, D. B. Calne, and M. Goldstein (Florham Park, NJ: Macmillan Healthcare Information), 153–164.

Flach, R. (2005). The transition from synchronization to continuation tapping. *Hum. Mov. Sci.* 24, 465–483.

Folstein, M. F., Folstein, S. E., and Mchugh, P. R. (1975). "Mini-mental state": a practical method for grading the cognitive state of patients for the clinician. *J. Psychiatr. Res.* 12, 189–198.

Freeman, J. S., Cody, F. W., and Schady, W. (1993). The influence of external timing cues upon the rhythm of voluntary movements in Parkinson's disease. *J. Neurol. Neurosurg. Psychiatr.* 56, 1078–1084.

Gronwall, D., and Wrightson, P. (1981). Memory and information processing capacity after closed head injury. *J. Neurol. Neurosurg. Psychiatr.* 44, 889–895.

Harrington, D. L., Haaland, K. Y., and Hermanowicz, N. (1998). Temporal processing in the basal ganglia. *Neuropsychology* 12, 3–12.

Hoehn, M. M., and Yahr, M. D. (1967). Parkinsonism: onset, progression and mortality. *Neurology* 17, 427–442.

Hughes, A. J., Daniel, S. E., Kilford, L., and Lees, A. J. (1992). Accuracy of clinical diagnosis of idiopathic Parkinson's disease: a clinico-pathological study of 100 cases. *J. Neurol. Neurosurg. Psychiatr.* 55, 181–184.

Ivry, R. B., and Keele, S. W. (1989). Timing functions of the cerebellum. *J. Cogn. Neurosci.* 1, 136–152.

Jahanshahi, M., Jenkins, I. H., Brown, R. G., Marsden, C. D., Passingham, R. E., and Brooks, D. J. (1995). Self-initiated versus externally triggered movements. I. An investigation using measurement of regional cerebral blood flow with PET and movement-related potentials in normal and Parkinson's disease subjects. *Brain* 118(Pt 4), 913–933.

Jahanshahi, M., Jones, C. R. G, Zijlmans, J., Katzenschlager, R., Lee, L., Quinn, N., Frith, C. D., and Lees, A. J. (2010). Dopaminergic modulation of striato-frontal connectivity during motor timing in Parkinson's disease. *Brain* 133, 727–745.

Jones, C. R. G., Malone, T. J., Dirnberger, G., Edwards, M., and Jahanshahi, M. (2008). Basal ganglia, dopamine and temporal processing: performance on three timing tasks on and off medication in Parkinson's disease. *Brain Cogn.* 68, 30–41.

Jones, C. R. G., and Jahanshahi, M. (2009). The substantia nigra, the basal ganglia, dopamine and temporal processing. *J. Neural Transm. Suppl.* 73, 161–171.

Kreft, I., and De Leeuw, J. (1998). *Introducing Multilevel Modeling*. Thousand Oaks, CA: Sage.

Kulisevsky, J., García-Sánchez, C., Berthier, M. L., Barbanoj, M., Pascual-Sedano, B., Gironell, A., and Estévez-González, A. (2000). Chronic effects of dopaminergic replacement on cognitive function in Parkinson's disease: a two-year follow-up study of previously untreated patients. *Mov. Disord.* 15, 613–626.

Logigian, E., Hefter, H., Reiners, K., and Freund, H. J. (1991). Does tremor pace repetitive voluntary motor behavior in Parkinson's disease? *Ann. Neurol.* 30, 172–179.

Madison, G. (2001). Variability in isochronous tapping: higher order dependencies as a function of intertap interval. *J. Exp. Psychol. Hum. Percept. Perform.* 27, 411–422.

Maxwell, S. E., and Delaney, H. D. (2004). *Designing Experiments and Analyzing Data: A Model Comparison Perspective*. Mahwah, NJ: Lawrence Erlbaum Associates.

Merchant, H., Luciana, M., Hooper, C., Majestic, S., and Tuite, P. (2008a). Interval timing and Parkinson's disease: heterogeneity in temporal performance. *Exp. Brain Res.* 184, 233–248.

Merchant, H., Zarco, W., and Prado, L. (2008b). Do we have a common mechanism for measuring time in the hundreds of millisecond range? Evidence from multiple-interval timing tasks. *J. Neurophysiol.* 99, 939–949.

Moreau, C., Ozsancak, C., Blatt, J. L., Derambure, P., Destee, A., and Defebvre, L. (2007). Oral festination in Parkinson's disease: biomechanical analysis and correlation with festination and freezing of gait. *Mov. Disord.* 22, 1503–1506.

Nakamura, R., Nagasaki, H., and Narabayashi, H. (1978). Disturbances of rhythm formation in patients with Parkinson's disease: part I. Characteristics of tapping response to the periodic signals. *Percept. Mot. Skills* 46, 63–75.

Nelson, H. C. (1982). *National Adult Reading Test (NART): Test Manual*. Windsor: NFER-Nelson.

O'Boyle, D. J., Freeman, J. S., and Cody, F. W. (1996). The accuracy and precision of timing of self-paced, repetitive movements in subjects with Parkinson's disease. *Brain* 119(Pt 1), 51–70.

Pastor, M. A., Jahanshahi, M., Artieda, J., and Obeso, J. A. (1992). Performance of repetitive wrist movements in Parkinson's disease. *Brain* 115(Pt 3), 875–891.

Peters, M. (1989). The relationship between variability of intertap intervals and interval duration. *Psychol. Res.* 51, 38–42.

Pope, P. A., Praamstra, P., and Wing, A. M. (2006). Force and time control in the production of rhythmic movement sequences in Parkinson's disease. *Eur. J. Neurosci.* 23, 1643–1650.

Raudenbush, S. W., and Bryk, A. S. (2002). *Hierarchical Linear Models: Applications and Data Analysis Methods*. Newbury Park, CA: Sage.

R Development Core Team (2011). R: a language and environment for statistical computing. R Foundation for Statistical Computing, Vienna, Austria. Available at: http://www.R-project.org/.

Snijders, T., and Bosker, R. (1999). *Multilevel Analysis: An Introduction to Basic and Applied Multilevel Analysis*. London: Sage.

Spencer, R. M., and Ivry, R. B. (2005). Comparison of patients with Parkinson's disease or cerebellar lesions in the production of periodic movements involving event-based or emergent timing. *Brain Cogn.* 58, 84–93.

Stegemöller, E. L., Simuni, T., and MacKinnon, C. (2009). Effec of movement frequency on repetitive finger movements in patients with Parkinson's disease. *Mov. Disord.* 24, 1162–1169.

Tiffin, J., and Asher, E. J. (1948). The Purdue pegboard; norms and studies of reliability and validity. *J. Appl. Psychol.* 32, 234–247.

Wing, A. M., and Kristofferson, A. B. (1973a). Response delays and timing of discrete motor responses. *Percept. Psychophys.* 14, 5–12.

Wing, A. M., and Kristofferson, A. B. (1973b). Timing of interresponse intervals. *Percept. Psychophys.* 13, 455–460.

Yahalom, G., Simon, E. S., Thorne, R., Peretz, C., and Giladi, N. (2004). Hand rhythmic tapping and timing in Parkinson's disease. *Parkinsonism Relat. Disord.* 10, 143–148.

Conflict of Interest Statement: The authors declare that the research was conducted in the absence of any commercial or financial relationships that could be construed as a potential conflict of interest.

Received: 01 August 2011; paper pending published: 14 September 2011; accepted: 26 November 2011; published online: 23 December 2011.

Citation: Jones CRG, Claassen DO, Yu M, Spies JR, Malone T, Dirnberger G, Jahanshahi M and Kubovy M (2011) Modeling accuracy and variability of motor timing in treated and untreated Parkinson's disease and healthy controls. Front. Integr. Neurosci. ***5****:81. doi: 10.3389/fnint.2011.00081*

APPENDIX

Table A1 | Estimated values of the model coefficients for the model of accuracy (relative error).

Effect	Estimate	Lower CI	Upper CI
Intercept (250 ms, cont, control)	0.02796	0.02252	0.03362
ISI (500 ms)	−0.05731	−0.06485	−0.04961
ISI (1000 ms)	−0.06992	−0.07774	−0.06219
ISI (2000 ms)	−0.06377	−0.07123	−0.05622
Type (synch)	−0.00261	−0.00959	0.00426
Group (*de novo*)	−0.02546	−0.03532	−0.01552
Group (PD-off)	−0.06268	−0.07202	−0.05343
Group (PD-on)	−0.06038	−0.07014	−0.05071
ISI (500 ms) × type (synch)	0.02792	0.01841	0.03712
ISI (1000 ms) × type (synch)	0.04325	0.0338	0.05253
ISI (2000 ms) × type (synch)	0.03589	0.02674	0.045
ISI (500 ms) × group (*de novo*)	0.0014	−0.01229	0.01545
ISI (1000 ms) × group (*de novo*)	0.00348	−0.01261	0.0198
ISI (2000 ms) × group (*de novo*)	0.02452	0.00988	0.03915
ISI (500 ms) × group (PD-off)	0.05864	0.04627	0.07094
ISI (1000 ms) × group (PD-off)	0.05693	0.04411	0.06997
ISI (2000 ms) × group (PD-off)	0.05855	0.04586	0.07125
ISI (500 ms) × group (PD-on)	0.05645	0.04377	0.06948
ISI (1000 ms) × group (PD-on)	0.06452	0.0517	0.07731
ISI (2000 ms) × group (PD-on)	0.05882	0.04617	0.07153
Group (*de novo*) × type (synch)	0.01603	0.00337	0.02903
Group (PD-off) × type (synch)	0.02245	0.01055	0.03399
Group (PD-on) × type (synch)	0.02302	0.01014	0.03564
ISI (500 ms) × type (synch) × group (*de novo*)	0.00995	−0.00669	0.02709
ISI (1000 ms) × type (synch) × group (*de novo*)	0.00118	−0.01615	0.01778
ISI (2000 ms) × type (synch) × group (*de novo*)	−0.02156	−0.03839	−0.00498
ISI (500 ms) × type (synch) × group (PD-off)	−0.02182	−0.0374	−0.0062
ISI (1000 ms) × type (synch) × group (PD-off)	−0.02043	−0.03595	−0.00501
ISI (2000 ms) × type (synch) × group (PD-off)	−0.02391	−0.03921	−0.0081
ISI (500 ms) × type (synch) × group (PD-on)	−0.01727	−0.0334	−0.00134
ISI (1000 ms) × type (synch) × group (PD-on)	−0.02983	−0.0461	−0.01406
ISI (2000 ms) × type (synch) × group (PD-on)	−0.02465	−0.04108	−0.00863

CI, confidence interval.

Table A2 | Estimated values of the model coefficients for the model of variability.

Effect	Estimate	Lower CI	Upper CI
Intercept (250 ms, cont, control)	0.2517	0.243096	0.260687
ISI (500 ms)	−0.048018	−0.058764	−0.037401
ISI (1000 ms)	−0.000902	−0.01147	0.009778
ISI (2000 ms)	0.028457	0.018295	0.03854
Type (synch)	−0.008171	−0.018128	0.001891
Group (*de novo*)	−0.015247	−0.03115	0.000501
Group (PD-off)	0.016445	0.002237	0.030399
Group (PD-on)	0.002018	−0.012465	0.016332
ISI (500 ms) × type (synch)	−0.013017	−0.024462	−0.001402
ISI (1000 ms) × type (synch)	−0.054922	−0.066291	−0.043449
ISI (2000 ms) × type (synch)	−0.058917	−0.070028	−0.048043
ISI (500 ms) × group (*de novo*)	0.019669	0.000739	0.039167
ISI (1000 ms) × group (*de novo*)	0.018481	−0.003951	0.040627
ISI (2000 ms) × group (*de novo*)	0.06166	0.04277	0.081444
ISI (500 ms) × group (PD-off)	−0.007414	−0.024044	0.009641
ISI (1000 ms) × group (PD-off)	−0.05216	−0.070004	−0.034681
ISI (2000 ms) × group (PD-off)	−0.023282	−0.04043	−0.006039
ISI (500 ms) × group (PD-on)	−0.007361	−0.02444	0.010221
ISI (1000 ms) × group (PD-on)	−0.013041	−0.029997	0.004508
ISI (2000 ms) × group (PD-on)	−0.004706	−0.021931	0.012593
Group (*de novo*) × type (synch)	0.033879	0.014932	0.05142
Group (PD-off) × type (synch)	0.001712	−0.014814	0.018176
Group (PD-on) × type (synch)	−0.013099	−0.030587	0.004073
ISI (500 ms) × type (synch) × group (*de novo*)	−0.042551	−0.062729	−0.021934
ISI (1000 ms) × type (synch) × group (*de novo*)	−0.019894	−0.040783	0.000742
ISI (2000 ms) × type (synch) × group (*de novo*)	−0.064971	−0.085184	−0.044943
ISI (500 ms) × type (synch) × group (PD-off)	−0.012014	−0.031389	0.007652
ISI (1000 ms) × type (synch) × group (PD-off)	0.036763	0.017727	0.055633
ISI (2000 ms) × type (synch) × group (PD-off)	−0.011303	−0.030111	0.007829
ISI (500 ms) × type (synch) × group (PD-on)	0.01592	−0.00381	0.035583
ISI (1000 ms) × type (synch) × group (PD-on)	0.016524	−0.00282	0.036193
ISI (2000 ms) × type (synch) × group (PD-on)	0.007052	−0.012213	0.026366

CI, confidence interval.

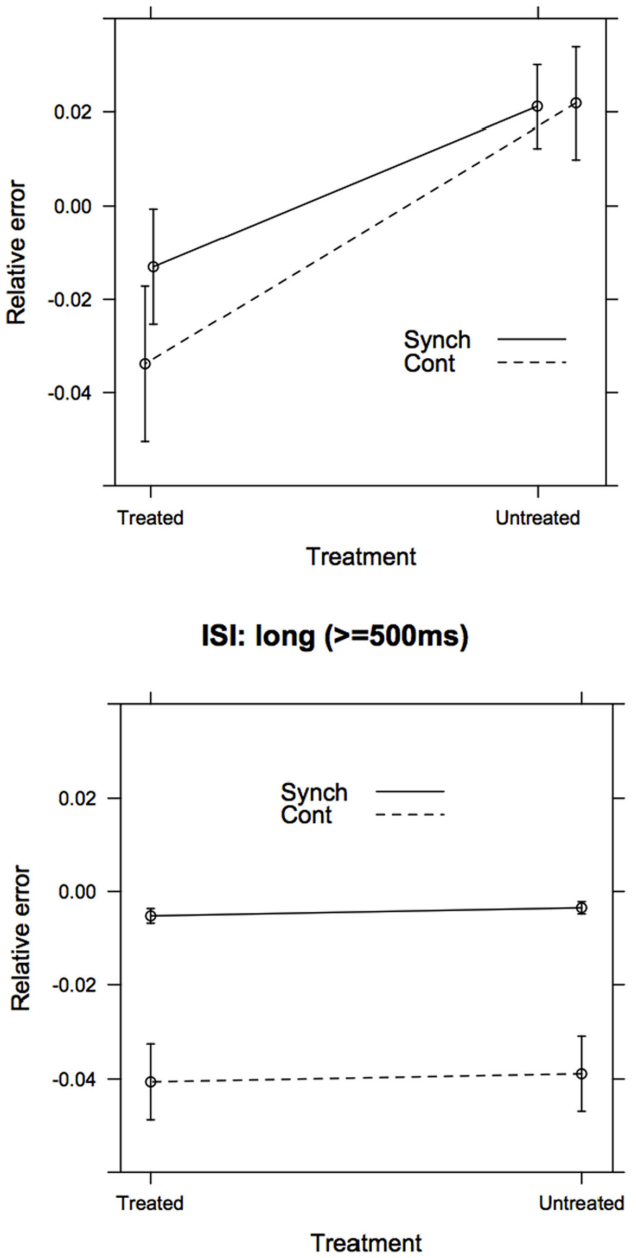

FIGURE A1 | Separate *post hoc* models for the accuracy (relative error) of short (ISI = 250 ms) and long (ISI ≥ 500 ms) intervals. As predicted, the Group (treated vs. untreated) × Task Phase (Synchronization vs. Continuation) interaction was significant in the Short ISI model, but not in the Long ISI model.

frontiers in
INTEGRATIVE NEUROSCIENCE

ORIGINAL RESEARCH ARTICLE
published: 21 November 2011
doi: 10.3389/fnint.2011.00076

Anatomy of human sensory cortices reflects inter-individual variability in time estimation

***Sharon Gilaie-Dotan*[1,2]*, *Ryota Kanai*[1] *and Geraint Rees*[1,2]**

[1] *Institute of Cognitive Neuroscience, University College London, London, UK*
[2] *Wellcome Trust Centre for Neuroimaging, University College London, London, UK*

Edited by:
Warren H. Meck, Duke University, USA

Reviewed by:
Xu Cui, Stanford University, USA
Melissa J. Allman, Kennedy Krieger Institute, USA

***Correspondence:**
Sharon Gilaie-Dotan, Institute of Cognitive Neuroscience and Wellcome Trust Centre for Neuroimaging, Alexandra House, 17 Queen Square, London WC1N 3AR, UK.
e-mail: shagido@gmail.com; s.gilaie-dotan@ucl.ac.uk

The ability to estimate duration is essential to human behavior, yet people vary greatly in their ability to estimate time and the brain structures mediating this inter-individual variability remain poorly understood. Here, we showed that inter-individual variability in duration estimation was highly correlated across visual and auditory modalities but depended on the scale of temporal duration. We further examined whether this inter-individual variability in estimating durations of different supra-second time scales (2 or 12 s) was reflected in variability in human brain anatomy. We found that the gray matter volume in both the right posterior lateral sulcus encompassing primary auditory and secondary somatosensory cortex, plus parahippocampal gyrus strongly predicted an individual's ability to discriminate longer durations of 12 s (but not shorter ones of 2 s) regardless of whether they were presented in auditory or visual modalities. Our findings suggest that these brain areas may play a common role in modality-independent time discrimination. We propose that an individual's ability to discriminate longer durations is linked to self-initiated rhythm maintenance mechanisms relying on the neural structure of these modality-specific sensory and parahippocampal cortices.

Keywords: individual differences, modality-independent, neural structure, supra-seconds time perception, VBM

INTRODUCTION

The ability to estimate time is fundamental to human behavior. Over a few seconds, judging how long an event lasts appears effortless and easy, whether the duration is just a few seconds or longer and regardless of sensory modality. However, people do vary considerably in their abilities to estimate the duration of an event, and the neural mechanisms underlying such variability in time estimation remain poorly understood. It is unclear whether such individual abilities rely on a single modality-independent mechanism or different modality-specific mechanisms (Treisman et al., 1990; Lewis and Miall, 2003; Mauk and Buonomano, 2004; Ivry and Schlerf, 2008). Moreover, it is also unclear whether judging durations of just a few seconds and judging longer durations are supported by the same neural mechanisms (Poppel, 1997; Morillon et al., 2009).

Most approaches investigating the neural mechanisms underlying time estimation have related perception to neural activity averaged across small groups of individuals (Rao et al., 2001; Coull et al., 2004; Bueti et al., 2008; Cui et al., 2009). This approach necessarily ignores any variability in time perception across individuals, averaging across the data. To examine whether time perception across different durations or sensory modalities is supported by common or distinct mechanisms, we explicitly examined such variability in time estimation. We adopted an experimental design previously used in a study by Brown et al. (1995) who specifically investigated individual differences in time estimation for supra-second durations of 2 and 12 s. Although the original study examined time estimation in the visual modality, alone we now extended the paradigm to the auditory modality to allow comparisons of individual differences across modalities. Systematic individual differences in time estimation correlated across different modalities or for different durations would support the existence of common underlying neural mechanisms across durations or for different modalities (Vogel and Awh, 2008).

To probe the neural structures underlying individual differences in auditory and visual time estimation, we further tested whether these behavioral measures were associated with variability in the anatomical microstructure of the brain measured using structural magnetic resonance imaging (MRI). Because brain structure is relatively invariant to the context in which it is measured, this provided a way to relate multiple different behavioral measures of time estimation to a single neural measure (Kanai and Rees, 2011). Brain structure is reliably associated with individual differences in motor performance or training on tasks such as juggling (May and Gaser, 2006; Ilg et al., 2008) and keyboard playing (Gaser and Schlaug, 2003), and can reflect differences in visual perception (Fleming et al., 2010; Kanai et al., 2010; Schwarzkopf et al., 2011). Here, we hypothesized that variability across participants in time estimation would be reflected in the anatomical neural structure of the human brain.

MATERIALS AND METHODS

PARTICIPANTS

A group of 31 naive participants [12 males and 19 females, aged 25.2 ± 4.9 (SD)] took part in the main behavioral experiments and structural MRI scans. All had normal or corrected-to-normal vision, and normal hearing. Thirteen healthy participants [seven females, aged 23.8 ± 4.25 (SD), normal or corrected-to-normal

vision] participated in the three control experiments. All participants gave written informed consent to participate in the study before participating in the study that had been approved by the local ethics committee.

MAIN EXPERIMENTS

Stimuli

Visual. Visual stimuli were presented centrally on an SVGA 19″ monitor set at 1024 × 768 resolution and a refresh rate of 75 Hz, and were viewed from 58 cm distance. Following the design of a previous study of individual differences in time perception (Brown et al., 1995), the visual target (see **Figure 1**) consisted of a blue central rectangle with a purple inner border and a lavender outer border (Brown et al., 1995) subtending a visual angle of 14.14° × 6.61° (width × height). The fixation cross subtended a visual angle of 0.017° × 0.017°.

Auditory. The auditory stimulus was a sine wave at a frequency of 600 Hz and was conveyed via headphones. At the beginning of each experimental session (see below) the loudness level was subjectively adjusted for each participant to ensure that the participant heard the stimulus and the sound level was comfortable (not too loud).

Experimental setup

Participants were given detailed instructions before the beginning of the first experimental session. Each participant undertook short training of 4–5 trials before the experiment began. Participants were instructed to keep their eyes still on the fixation cross that appeared on the screen throughout all the experimental trials (visual and auditory). Headphones were worn throughout all the experiment in all blocks and trials (visual and auditory). The monitor and a chin rest were mounted on a height-adjustable table, so that the distance between the head and the monitor was constant for all participants. The head position was fixed using the chin rest at a comfortable height for each participant, to minimize head and body motion. The experiment took place in a darkened testing room.

Duration discrimination

Our behavioral experimental paradigm followed closely Brown's study (Brown et al., 1995) that examined individual differences in time perception for durations of 2 and 12 s in the visual modality, which we here also extended to audition. The experiment comprised four conditions in a factorial design: Vis2 (visual target of 2 s, non-target 2.2 s), Aud2 (auditory target of 2 s, non-target 2.2 s), Vis12 (visual target of 12 s, non-target 13.2 s), and Aud12 (auditory target of 12 s, non-target 13.2 s). The experiment was run in 12 blocks: 3 blocks for each of the 4 conditions (Vis2, Aud2, Vis12, and Aud12). In order to complete all the blocks participants attended three sessions (one session for the 2 s blocks and two sessions for the 12 s blocks), typically on two different days within the same week. Each session lasted 1–1.5 h.

Participants started either with the '2 s' or with the '12 s' blocks and completed all the 6 blocks of that specific duration before starting with the blocks of the other duration. Half of the participants started with the '2 s' blocks and half with the '12 s' blocks.

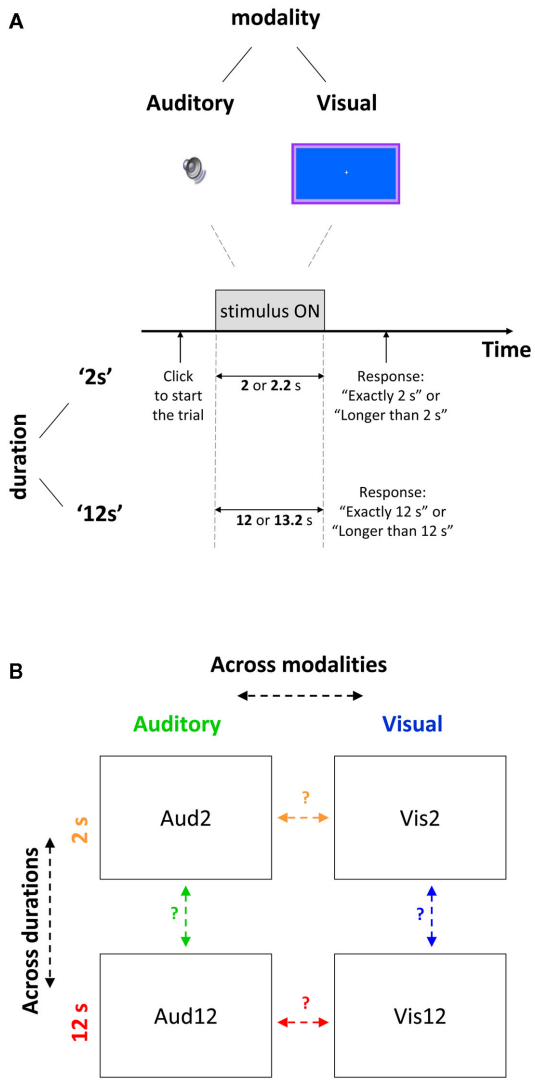

FIGURE 1 | Experimental design (A) Depiction of a duration discrimination trial, presented either visually or aurally for shorter (2 s) or longer (12 s) durations. Trials were blocked by condition and lasted for target duration (2 or 12 s respectively) or 10% longer. To begin each trial participants had to press a key. After stimulus offset participants had to indicate via button press whether target or non-target duration was presented in a 2AFC manner. **(B)** Predictions for common neural mechanisms across different modalities (orange arrow for shorter duration, red for longer duration) or for different durations (green for auditory, blue for visual) based on correlation strengths of the variability in time estimation.

Within a specific duration half of the participants started either with an auditory block and half with a visual block. Visual and auditory blocks of the same duration were interleaved and their order was controlled for within each participant (to control for potential learning effects) and between participants. A participant that started the '2 s' condition with a visual block started the '12 s' condition with an auditory block and vice versa.

Each block included 70 trials of the same modality and the same duration discrimination (either 2 s discrimination or 12 s

discrimination), so that for each condition there were 210 trials (in the 3 blocks). Participants were notified before each block which modality they would be tested on next.

The 70 grouped trials in each block included 35 target trials (2 or 12 s depending on the block) and 35 longer-than-target trials (2.2 or 13.2 s accordingly, 10% longer-than-target). The order of trials within a block was random, and the participants were notified about this before the experiment began.

Participants were prompted by an instruction on the screen to press a key in order to start each trial (see **Figure 1**). Two-hundred milliseconds after they pressed a key, the stimulus appeared for target or non-target duration.

Participants were instructed to estimate covertly the duration of the stimulus and to respond promptly after stimulus offset whether the stimulus was present for "*exactly a certain duration*" (e.g., "exactly 2 s") or for "*more than a certain duration*" (e.g., "more than 2 s") in a two-alternative forced choice manner (see **Figure 1**) via key presses. No feedback was given. An inter-trial interval of 1500 ms displaying the fixation cross followed the participant response before the prompt for the next trial appeared. Participants were allowed to take breaks between trials within a block, although this rarely happened.

Behavioral analysis

Participant responses to each block were classified as hits, misses, correct rejections, or false alarms with the 12 s trials being targets for this signal detection based analysis. For each participant response accuracy of each block was determined as (hits + correct rejections)/(all responses). Individual's accuracies on each of the three blocks of each condition (Vis2, Aud2, Vis12, Aud12) were averaged to yield four individual condition-based performance measures. D prime (d') was calculated as the discrimination sensitivity for each condition [i.e., the distance between the distributions of the targets (12 s) and the non-targets (13.2 s)] according to the formula $d' = Z(\text{hit rate}) - Z(\text{false alarm rate})$, where $Z(p)$ is the inverse of the cumulative Gaussian distribution for p [0,1]. Since sensitivity measures (d') were highly consistent with accuracy performance [accuracy to d' correlations were $R^2 \geq 0.9$, $t_{(29)} \geq 17$, $p < 10^{-15}$, for all the conditions] we report here the accuracy results.

Individual accuracy performances on each of the three blocks were taken as independent measures for the test–retest analysis. Test–retest results presented include correlation between the first and second blocks, or between the first and third blocks (to avoid dependent measures).

Correlation analyses between conditions (across durations or across modalities, see **Figure 2A**) were performed by correlating accuracy (or d') measures of all participants (participant order fixed) between two conditions and assessing these for statistical significance in a conventional fashion.

CONTROL EXPERIMENT 1

Estimating individual temporal discrimination ability for 12 s with original task and with finer adaptive method

We conducted an additional experiment to yield a finer psychometric measure of individuals' ability to discriminate intervals around 12 s. This was done by applying a Bayesian paradigm that efficiently estimates perceptual thresholds (QUEST; Watson and Pelli, 1983) to long duration discrimination sensitivity. We varied the duration increment applied to a 12 s pedestal and estimated the minimum increment that could be successfully discriminated at a level of 75% accuracy. In each trial, an interval of either 12 s or longer was presented. In trials of duration longer than 12 s, the duration increment (from the 12 s pedestal) was adaptively estimated by QUEST based on the participant's previous responses until that trial. Participants were informed that they had to judge whether a trial [consisting of the appearance of a rectangle (Brown et al., 1995), as in the main experiment; see Materials and Methods] lasted for 12 s or longer, and that trials longer than 12 s could vary in duration. Trials of 12 s (6) were interspersed randomly among longer duration (14) trials. The temporal perceptual threshold was defined as the estimated duration increment that allowed each participant to discriminate 12 s and 12+ increment seconds at the predetermined accuracy level, as described above. All other procedures were as in the original main experiments 12 s discrimination task. Temporal discrimination ability according to the original task (discriminating 12 from 13.2 s) was also estimated. Each participant performed 10 trials of 12 or 13.2 s randomly ordered, following the original task experimental procedures.

CONTROL EXPERIMENT 2

Estimating individual temporal discrimination ability for 2 s with finer adaptive method

The ability of temporal discrimination for 2 s intervals was also estimated using the finer adaptive QUEST procedure described above (Watson and Pelli, 1983). The procedure was as described above for 12 s durations, but now for shorter 2 s durations.

CONTROL EXPERIMENT 3

Possible non-specific confounds

To examine whether the time discrimination ability measured for longer durations (12 s) was time-specific or reflected potentially confounding processes such as sustained attention or motivational factors we constructed a paradigm inspired by Coull et al. (2004). In this new experimental paradigm, our participants performed either a temporal discrimination task (discriminating between 12 and 13.2 s durations) or a color discrimination task. In both tasks, the physical stimuli and presentation paradigm were identical and only the task that participants performed varied. The temporal discrimination task was identical to our main experimental task, to discriminate between 12 and 13.2 s durations while ignoring the colored flashing circles that appeared. In the color discrimination task participants had to attend the color of the circles that appeared and judge whether the color of the last appearing circle in a trial was identical to or different than the color of the preceding circle.

Stimuli

Visual stimuli were presented centrally on a black background. A small white fixation empty circle (visual angle of 0.286°) appeared in the beginning of the trial at the center of the screen to indicate that the trial has started and remained present until the trial ended. During the trial a number of flickering colored circles appeared at the center of the screen. Each circle was presented for 250 ms, and had a diameter of 7.44° of visual angle when viewed from a

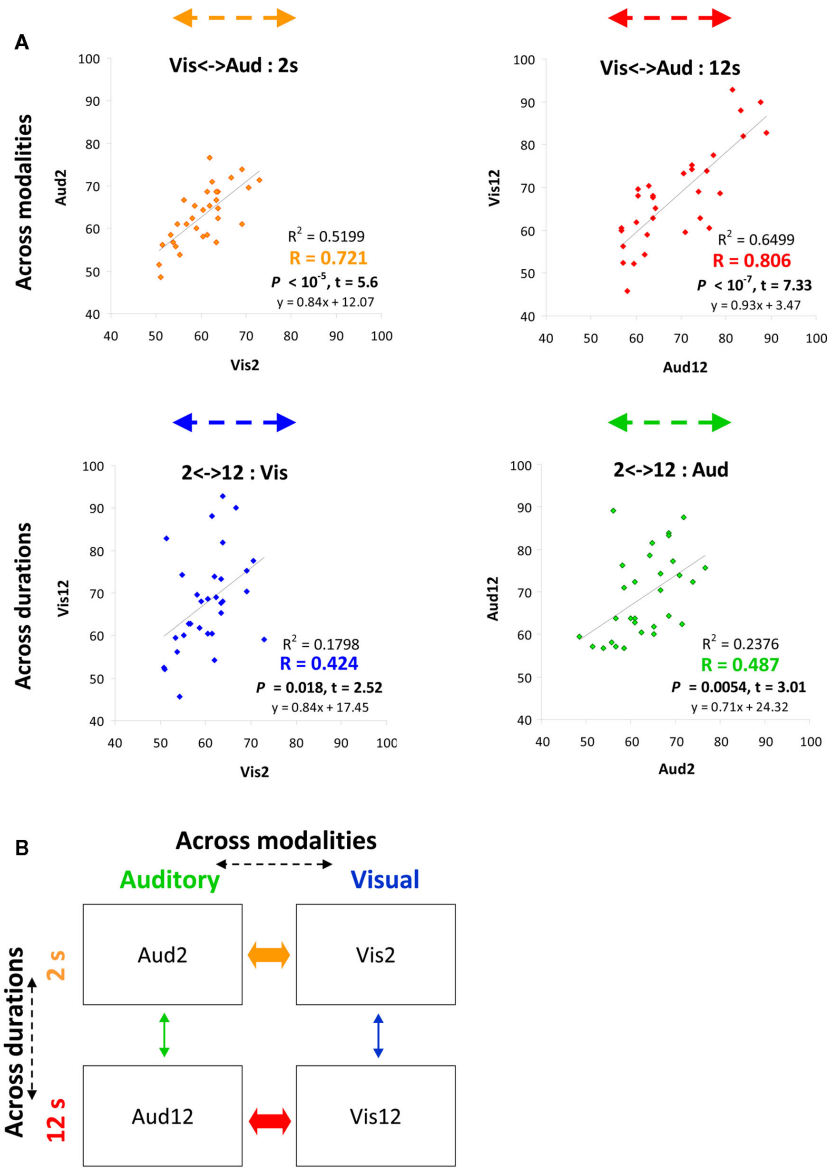

FIGURE 2 | Behavioral performance strongly correlated across different modalities of temporal judgments. (A) Plots convey temporal estimation correlations between conditions either across modalities (top) or across durations (bottom). Colored arrows at the top of each plot correspond to the correlation arrows in **Figure 1A**. *x* and *y* axes indicate accuracy level (% correct) of specific conditions (condition name indicated on axis title). Each point depicts data from one participant ($n = 31$). Correlation strength and significance are indicated at the bottom right of each plot. See also **Figures 6A–C**. **(B)** Inter-individual variability in time estimation is strongly correlated across modalities **(A)** as depicted by thick arrows (orange for shorter durations, red for longer), indicating common neural mechanisms for time estimation across different modalities. Thin arrows (across durations) indicate weaker correlations.

distance of 50 cm. The circle colors were similar to the color shades reported by (Coull et al., 2004) and were reddish [$(R, G, B) = (139, 0, 65)$], pinkish (139, 7, 108), purple (116, 0, 213), another shade of purple (100, 19, 111), and blue (60, 20,168). The number of flickering circles in a trial varied across trials (between three and nine circles per trial, average of 6.25). The color order and the number of colors used varied across trials. The flickering circles appeared in an asynchronous manner within each trial (SOA between 400 and 7300 ms, mean 1831 ms), and the onsets of circle appearances varied across trials. The stimuli were presented at 1024 × 768 resolution and a refresh rate of 60 Hz via Cogent MATLAB toolbox (http://www.vislab.ucl.ac.uk/cogent_2000.php).

Procedure

Prior to each condition (temporal or color discrimination) participants were instructed about the task and then underwent a four trial practice to check that they understood the instructions (see task descriptions above). Each participant then performed 36 main trials of that condition that were administered in 3 blocks (12 trials in each block). All 13 participants performed 36 trials

of the time discrimination condition. Ten participants performed 36 trials of the color condition, and three participants performed only 24 trials of the color condition due to time constraints. In order to reduce expectancy of the upcoming stimuli, we created two ordering versions that differed only in the color flashing order and in the trial order within a block. The order of 12 and 13.2 s trials was counterbalanced within and across versions. Trials ending in different colored circles (expected response "different" in the color task) were also counter balanced, and we also ensured that half of the "different" colored trials were 12 s long and half were 13.2 s long, and the same for "same" colored circles. Factors such as number of circle appearances in a trial and distribution of the SOA between trials were also controlled for in the design of the experiment. Responses were provided via key presses.

Analysis

Participant responses to each block were classified as correct or incorrect. Individual accuracy measures for the time task or the color task were averaged over all responses from the three blocks of that condition.

MRI DATA ACQUISITION

MR images were acquired on a 1.5-T Siemens Sonata MRI scanner (Siemens Medical, Erlangen, Germany) at The Wellcome Trust Centre for Neuroimaging, UCL. High-resolution anatomical images were acquired using a T1-weighted 3-D modified driven equilibrium Fourier transform (MDEFT) sequence (TR = 12.24 ms; TE = 3.56 ms; field of view = 256 mm × 256 mm; voxel size = 1 mm × 1 mm × 1 mm). During scanning, head motion was restrained by padding inserted between the participant's head and the head RF coil.

STRUCTURAL MRI VOXEL-BASED MORPHOMETRY ANALYSES

For each participant the T1-weighted MR images were first segmented to gray matter (GM) and white matter (WM) using the segmentation tools in SPM8 (http://www.fil.ion.ucl.ac.uk/spm). Subsequently, we performed diffeomorphic anatomical registration through exponentiated lie algebra (DARTEL; Ashburner, 2007) in SPM8 for inter-participant registration of the GM images. The registered images were smoothed with a Gaussian kernel (FWHM = 8 mm) and were then transformed to MNI stereotactic space using affine and non-linear spatial normalization implemented in SPM8 for multiple regression analysis. The gender and age of the participants were included in the design matrix as covariates of no interest, and were thus regressed out. Multiple regression analysis was performed separately for each of the four conditions of the main experiment (Vis2, Aud2, Vis12, Aud12), each time with gender and age as the covariates of no interest. The global GM volume was also entered into the regression as an additional covariate following ANCOVA normalization. All analyses were applied with $p < 0.001$ uncorrected as the criterion to detect voxels with a significant correlation with individual's temporal discrimination for each duration and modality. Following this we applied non-stationary whole-brain cluster-level correction to correct for non-uniform smoothness in the VBM data-set that affects cluster size inference (http://fmri.wfubmc.edu/cms/NS-General) (Worsley et al., 1999; Hayasaka et al., 2004) using SPM5. We report here only results that survived non-stationary correction for multiple comparisons across the whole-brain at a threshold of $p < 0.05$ (see **Figure 3**).

OVERLAYING VBM RESULTS ON PROBABILISTIC ATLAS

To localize more precisely the specific brain structures revealed in the different conditions with respect to the auditory and secondary somatosensory cortices' cyto-anatomical parcellations, we overlaid our statistical VBM maps on probabilistic histological-based atlases (Morosan et al., 2001; Rademacher et al., 2001; Eickhoff et al., 2006a,b; see **Figure 4**). These probabilistic atlases are based on cytoarchitectural postmortem analyses of human brains and provide a veridical estimate for the likelihood that a specific location within MNI stereotactic space (as used here) is within a specific brain structure. The regions delineated here were the A1/PAC structures (TE1.0, TE1.1, and TE1.2) and SII structures (OP1–OP4). For each of these brain structures the borders in **Figure 4** indicate a probability >0.4 to be in that structure (i.e., each brain voxel with $p > 0.4$ to be in that region is within the delineated borders).

Figures 5A–C provides further quantitative statistical estimates to the data presented in **Figure 4** (average statistics of longer duration discrimination structural correlates for each of the sensory structures).

RESULTS

TEMPORAL DISCRIMINATION PERFORMANCE

A group of 31 healthy adult human participants made two alternative forced choice temporal increment discriminations on either shorter (∼2 s) or longer (∼12 s) supra-second duration stimuli presented in either visual or auditory modalities (see Materials and Methods for full details and **Figure 1**). The experimental design thus represented a 2 × 2 factorial design where input modality and overall duration of the discriminated stimuli varied independently. This gave rise to four conditions, which we will refer to as Vis2, Aud2, Vis12, and Aud12.

We found large inter-individual variability in temporal discrimination ability in all four conditions [**Figure 2**, Vis2: 50.7–72.9%, mean 60.4 ± 5.8% (SD); Aud2: 48.8–76.7%, mean 63.1 ± 6.8%; Vis12: 45.7–92.9%, mean 67.9 ± 11.4%; Aud12: 56.7–89%, mean 68.9 ± 9.9%].

Across individuals, variability in behavior was strongly and significantly correlated across sensory modalities, both for the longer duration discriminations [Vis12 to Aud12: $R^2 = 0.6499$, $p < 10^{-7}$, $t(29) = 7.33$, see **Figure 2A** in red] and for the shorter durations [Vis2 to Aud2: $R^2 = 0.5199$, $p < 10^{-5}$, $t(29) = 5.6$, see **Figure 2A** in orange).

Inter-individual correlations in temporal discrimination ability *within* a particular modality for different durations were considerably weaker than those between modalities described above, although reaching significance [Aud2 to Aud12: $R^2 = 0.2376$, $p = 0.0054$, $t(29) = 3.01$, see **Figure 2A** in green; Vis2 to Vis12: $R^2 = 0.1798$, $p = 0.018$, $t(29) = 2.52$, **Figure 2A** in blue]. We further confirmed this in our control experiments (see below).

We further verified the reliability of our behavioral temporal measures in additional experiments. Those included verifying that the temporal discrimination ability we measured for the longer

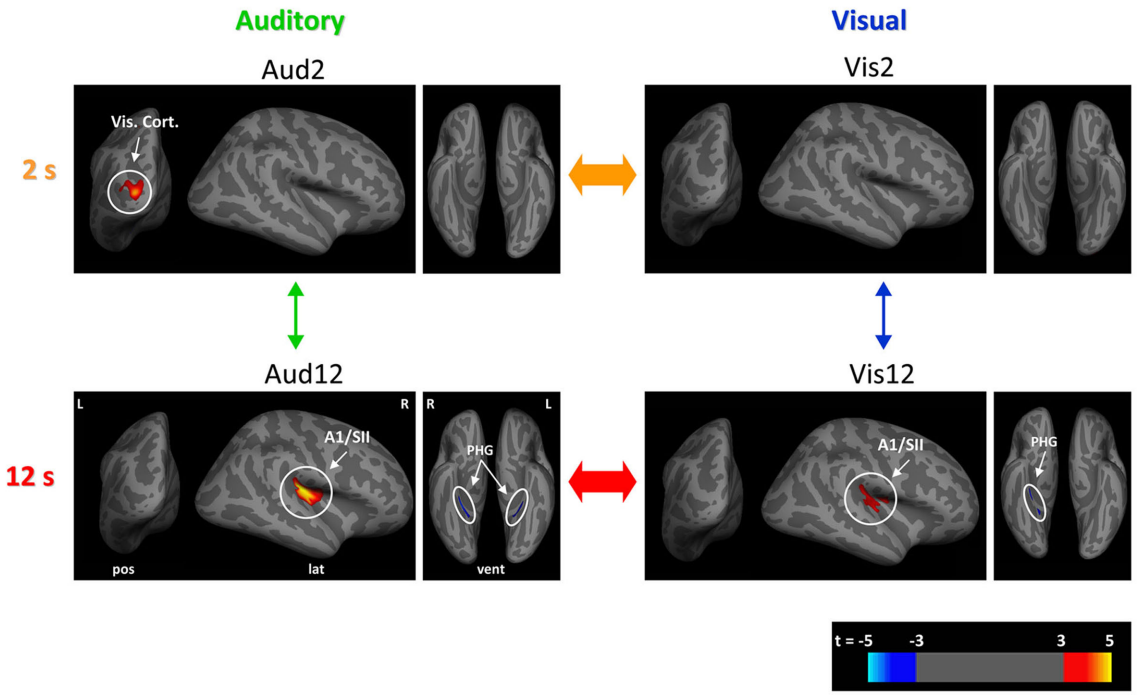

FIGURE 3 | Neural structural correlates of duration discrimination. For each of the experimental conditions, shown in red to yellow (blue) are those cortical loci where our analyses of cortical thickness revealed a significant positive (negative) correlation between cortical thickness and duration discrimination ($p < 0.05$, corrected) across the group of participants ($n = 31$). Aud2 (top left), Vis2 (top right), Aud12 (bottom left), Vis12 (bottom right). Data are shown overlaid onto an inflated template brain in a standard stereotactic space where sulci are represented in dark gray and gyri in light gray. Significant clusters are shown at *t*-values according to scale bar (bottom right) for visualization purposes (see **Table 1** for further details). Note the common structural correlates for estimation of longer durations in right A1/PAC (primary auditory) and SII (secondary somatosensory) cortices for both longer visual and longer auditory durations. R, right; L, left; PHG, parahippocampal gyrus; Vis. Cort, visual cortex; lat, lateral; pos, posterior; vent, ventral.

durations was an accurate and valid way to characterize individual differences in temporal judgments, that the temporal discrimination measure was not too crude a measure for longer duration discrimination ability, that individual temporal ability was not influenced by non-temporal factors such as attention and motivational factors, and that inter-individual correlations in temporal discrimination ability for short and long durations were weak (see details below and **Figure 6**).

STRUCTURAL CORRELATES OF TEMPORAL DISCRIMINATION PERFORMANCE

We next examined whether the differences in temporal discrimination ability across individuals were reflected in the GM volume of any cortical regions. To address this question we used voxel-based morphometry analyses (Ashburner and Friston, 2000) of structural MRI images using individual performance on each of the four temporal discrimination conditions as regressors (see Materials and Methods for full details). We then used statistical contrasts (see Materials and Methods) to determine for each condition whether individual differences in behavior correlated with GM volume throughout the brain. Due to the exploratory nature of the analyses, we used a conservative statistical threshold corrected for multiple comparisons throughout the whole-brain.

Longer auditory duration discrimination (Aud12)

We found one large cluster (7118 mm^3) in the posterior part of lateral sulcus where GM volume exhibited significant correlation [$t(26) = 5.52$, $p(\text{corr.}) < 0.001$, $R = 0.74$) with inter-individual variability in temporal discrimination performance (see **Figure 3** bottom left, **Table 1** for full loci details). Anatomically, this cluster stretched from the posterior segment of the lateral sulcus on its most medial (inner) aspect extending anteriorly onto both the inferior and superior banks of the lateral sulcus, into the circular insular sulcus on the inferior and superior segments. On the inferior bank of the lateral sulcus this cluster extended to and included the short insular gyrus and Heschl's (transverse temporal) gyri, and on the superior bank it extended to and included the parietal and central/rolandic operculum (see **Figure 4A**). This cluster comprised primary auditory cortex (PAC/A1) structure TE1.1 (Morosan et al., 2001; Rademacher et al., 2001), and secondary somatosensory structures OP2–OP3 (Eickhoff et al., 2006a,b; see **Figures 4A** and **5A–C** for more details). In addition the GM volumes of bilateral parahippocampal gyri were significantly negatively correlated [$t(26) = 4.92$, $p(\text{corr.}) = 0.007$, $R = -0.70$, $t(26) = 4.63$, $p(\text{corr.}) = 0.048$, $R = -0.68$ for right and left respectively, see **Table 1** for full details] with individual differences in Aud12 performance. No other brain regions exhibited positive or negative correlation with inter-individual

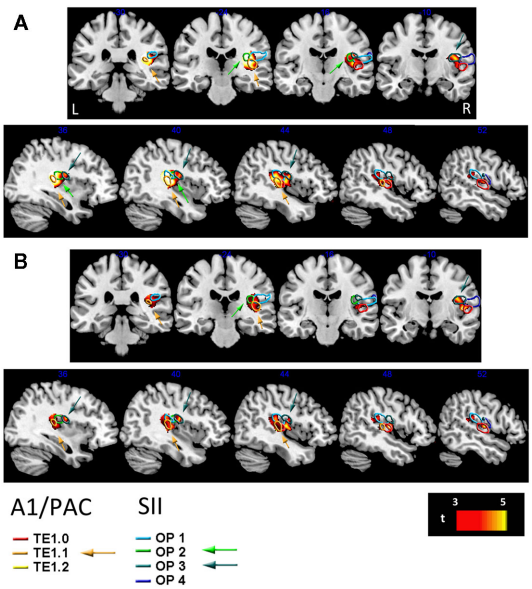

FIGURE 4 | Overlay of longer duration structural correlates on right A1/PAC (primary auditory) and SII (secondary somatosensory) cortices. Cortical loci where our analyses of cortical thickness revealed a significant positive correlation between cortical thickness and longer auditory [Aud12, **(A)**] or longer visual [Vis12, **(B)**] duration discrimination shown in red to bright yellow (*t*-values indicated on scale bar) superimposed on structures of A1/PAC and SII. A1/PAC and SII structures are denoted by colored contours according to the legend at the bottom (see Materials and Methods). Coronal (top) and sagittal (bottom) views. Arrows point to substantial portions of these structures that are correlated with longer duration discrimination ability, which are TE1.1 (PAC/A1, see orange arrows) and OP2–3 (SII, see blue and turquoise arrows). See also **Figures 5A–C**. R, right; L, left.

variability in performance in this condition ($p > 0.05$, whole-brain corrected).

Longer visual duration discrimination (Vis12)

We identified one large cluster (2467 mm^3) in the posterior part of lateral sulcus anatomically extending into the right auditory and somatosensory cortices where GM volume positively and significantly correlated [$t(26) = 4.71$, $p(\text{corr.}) = 0.008$, $R = 0.68$] with inter-individual variability in temporal discrimination performance in the Vis12 condition. This region exhibited extensive overlap with the areas that correlated with individuals' performance in the Aud12 condition [cf. **Figure 3** bottom right and left (Aud12), and **Figure 4B** with **Figure 4A** (Aud12), see also **Table 1**]. It stretched from the posterior segment of the lateral sulcus on its most medial (inner) aspect extending anterior wise on both the inferior and superior banks of the lateral sulcus, into the posterior aspects of the circular insular sulcus (inferior and superior segments). On the inferior bank of the lateral sulcus this cluster extended to and included the short insular gyrus and Heschl's (transverse temporal) gyri, and on the superior bank it included the parietal operculum, the posterior part of the circular insular sulcus, and then the anterior part of the circular insular sulcus without the middle part of it (see **Figure 4B**). This cluster comprised PAC/A1 structure TE1.1 (Morosan et al., 2001; Rademacher et al., 2001), and secondary somatosensory structures OP2–OP3 (Eickhoff et al., 2006a,b; see **Figures 5A–C** for more details), similar to the sensory structures revealed in Aud12 analysis. In addition, GM volume in the right parahippocampal region was significantly and negatively correlated [$t(26) = 5.34$, $p(\text{corr.}) = 0.029$, $R = -0.72$] with individuals' ability to discriminate visually presented longer durations. Again, this overlapped with the areas identified as showing similar negative correlations with the longer auditory duration discrimination (cf. **Figure 3** Vis12 and Aud12 ventral views, and see **Table 1**).

Shorter auditory duration discrimination (Aud2)

We found that only one region, in left extrastriate visual cortex (**Figure 3**; **Table 1**), where GM volume showed a significant positive correlation with individuals' performance in the shorter auditory duration discrimination task [$t(26) = 5.05$, $p(\text{corr.}) = 0.046$, $R = 0.71$]. No other regions showed a positive or negative correlation between GM volume and duration discrimination performance of shorter auditory durations at the whole-brain corrected level of statistical significance ($p < 0.05$ corrected). For completeness, we examined the data at a more lenient threshold ($p < 0.001$ uncorrected) but this did not reveal any significant correlation between auditory or somatosensory cortex GM volume and shorter duration auditory temporal discrimination performance.

Shorter visual duration discrimination (Vis2)

At our conservative whole-brain corrected threshold, we did not identify any brain region that showed a positive (or negative) correlation between GM volume and individuals' performance on shorter visual duration discriminations. For completeness, we also examined the data at a more lenient threshold ($p < 0.001$ uncorrected). This revealed a region in left extrastriate visual cortex (**Figure 3**; **Table 1**) where GM volume was positively correlated with performance [$t(26) = 4.63$, $p(\text{corr.}) = 0.189$, $R = 0.68$]. This area partially overlapped the left extrastriate locus whose GM volume correlated with shorter duration auditory discrimination performance (cf. **Figure 3** Vis2 and Aud2, and see **Table 1**).

RELIABILITY OF PERFORMANCE MEASUREMENTS

To verify that the temporal discrimination ability we measured for the longer durations (discriminating between two fixed durations of 12 and 13.2 s) was an accurate and valid way to characterize individual differences in temporal judgments, we assessed test–retest reliability for individual performance. Test–retest reliability on a block to block basis was highly significant [blocks 1–2 and 1–3 correlations: Vis12: $R^2 > 0.397$, $t_{(29)} > 4.37$, $p < 10^{-3}$; Aud12: $R^2 > 0.357$, $t_{(29)} > 4.01$, $p < 10^{-3}$; Vis2: $R^2 > 0.201$, $t_{(29)} > 2.7$, $p < 0.02$; Aud2: $R^2 > 0.239$, $t > 3$, $p < 0.01$].

In order to validate that the temporal discrimination measure was not too crude a measure for longer duration discrimination ability, we performed additional measurements to compare inter-individual variability in the original temporal discrimination estimates (12 vs. 13.2 s) to that for finer temporal estimates (see control experiments and **Figure 6**). Using an adaptive staircase method (QUEST, see Materials and Methods) we estimated the

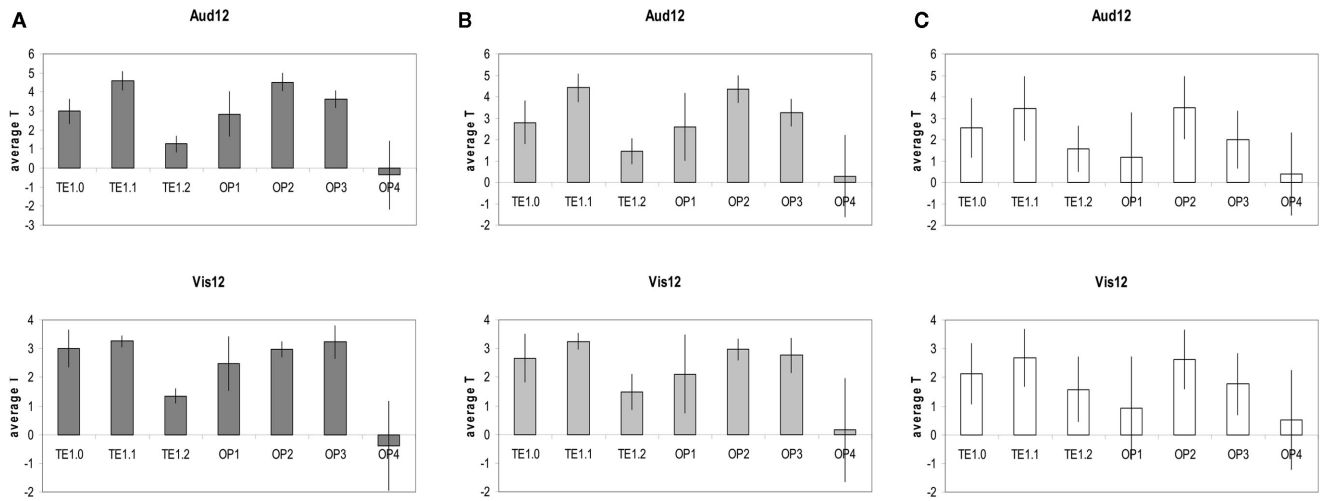

FIGURE 5 | (A) Top: average *T* statistics of the Aud12 structural correlates *t*-map (as seen in **Figure 3** bottom left and in **Figure 4A**). For each structure of A1/PAC (i.e., TE1.0, TE1.1, TE1.2) and for each structure of SII (i.e., OP1–OP4) the average is done over all the MNI coordinates that are highly likely (probability of 60–100%) to be in that structure according to the Juelich atlas (http://www.fz-juelich.de/inm/and SPM toolbox http://www.fz-juelich.de/ime/spm_anatomy_toolbox). Bottom: same analysis for the Vis12 structural correlates. The data show that the structural correlates of Aud12 and Vis12 are robust within TE1.1, OP2, and OP3 and are highly consistent and stable within these regions. Error bars, SD. **(B)** Same as **(A)** but over all the MNI coordinates that have a medium likelihood (probability of 40–60%) to be in the structures of A1/PAC and SII according to the Juelich atlas (see above). **(C)** Same as **(A)** but over all the MNI coordinates that have some likelihood (probability of 10–40%) of being in the structures of A1/PAC and SII according to the Juelich atlas (see above).

minimum duration difference enabling an individual to discriminate a 12 s stimulus presentation. We found that inter-individual variability in accuracy levels on the 12 vs. 13.2 s discrimination task (our original measurement) were significantly correlated with this duration difference measure [$R^2 = 0.2951$, $p = 0.028$, $t_{(11)} = -2.15$, see **Figure 6A** and Materials and Methods]. Thus, accuracy levels in our original task reliably predicted individual time increment discrimination ability for 12 s intervals.

To control for non-temporal factors that could underlie longer duration discrimination performance such as sustained attention ability or motivational factors, we further measured in a third behavioral experiment whether temporal estimation ability correlated with non-temporal color discrimination ability for the same physical stimuli while systematically manipulating task requirements (paradigm inspired by Coull et al., 2004; see **Figure 6B** and Materials and Methods for details). We deliberately ensured both temporal and non-temporal (color) tasks were of comparable difficulty and both required sustained attention during task performance. Consequently lack of association between individuals' performance on temporal and color discrimination tasks would indicate that an individual's longer duration discrimination performance was related to temporal estimation ability and not to other non-temporal factors. Consistent with this hypothesis, we found that there was no significant correlation between longer duration discrimination and color discrimination [$R^2 = 0.0028$, $p > 0.86$, $t_{(11)} = -0.174$, see **Figure 6B** and Materials and Methods). Thus, our behavioral results (**Figure 2B**, red and orange connections) suggest a common neural mechanism across sensory modalities underlying variability in temporal discrimination ability that does not reflect sustained attention or other non-temporal factors.

We further assessed whether the weaker correlations between the longer and shorter duration discrimination performance might have originated from factors such as the poorer performance or smaller variability in performance on shorter durations, from task differences, or since shorter and longer duration discriminations were not necessarily measured on the same session. To do this, we used the same adaptive staircase method (QUEST, see Materials and Methods) to estimate temporal difference discrimination for shorter intervals (2 s). Since the method was adaptive, it estimated an individual's sensitivity for shorter (or longer, see above) durations without imposing fixed durations (as in our original task) that might have led to floor performance or enhanced task difficulty in the shorter duration conditions. We then examined the relationship between these finer estimations of individual sensitivities for longer and shorter durations. Consistent with our original analyses, individual sensitivities for longer and shorter durations were not significantly correlated [$R^2 = 0.021$, $p = 0.318$, $t(11) = -0.485$, see **Figure 6C** and Materials and Methods]. Thus, it seems that individual temporal estimation ability is consistent across modalities, yet estimation of shorter durations of 2 s and longer durations of 12 s may rely on different underlying mechanisms (Fortin and Couture, 2002; Ulbrich et al., 2007).

DISCUSSION

We examined whether the ability to estimate time for different supra-second durations or in different sensory modalities was associated with common mechanisms (Treisman, 1963; Treisman et al., 1990; Buonomano and Merzenich, 1995; Poppel, 1997; Rammsayer, 1999; Lewis and Miall, 2003; Mauk and Buonomano, 2004; Buhusi and Meck, 2005; Karmarkar and Buonomano, 2007;

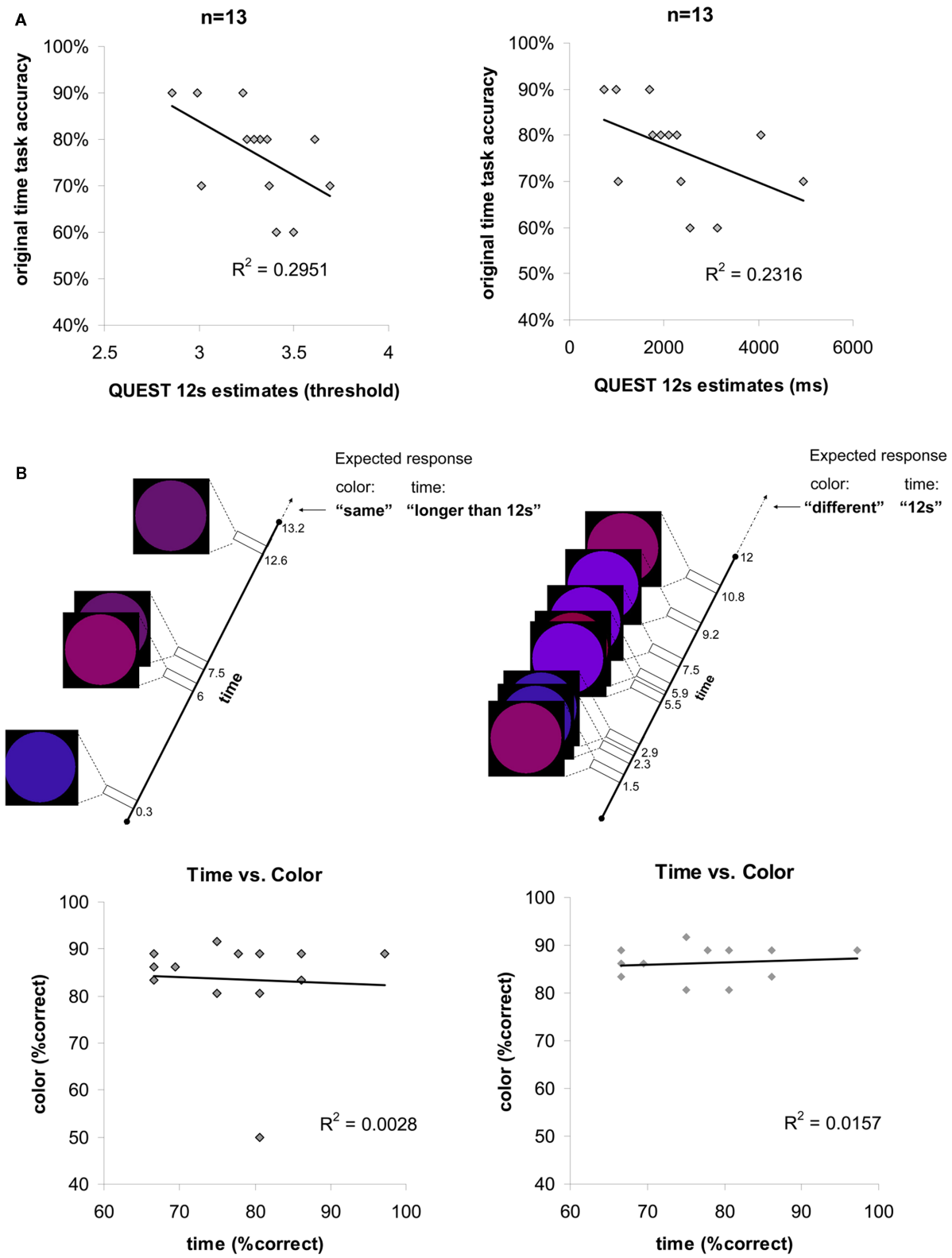

FIGURE 6 | Continued

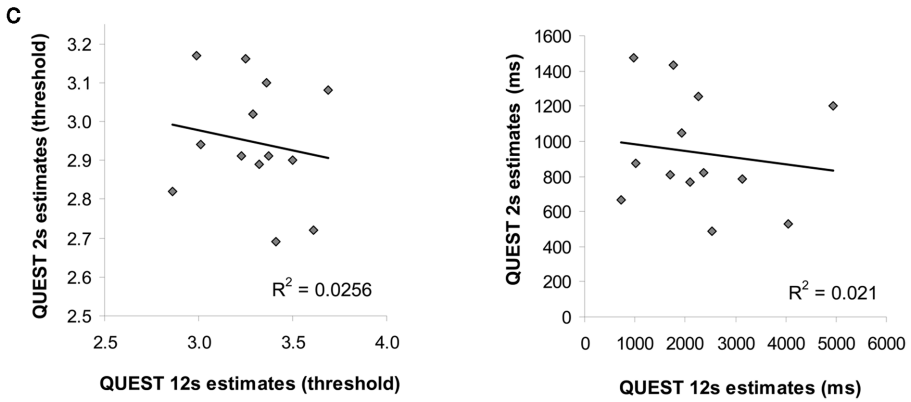

FIGURE 6 | (A) Individual temporal discrimination ability for 12 s durations, as estimated by the original main experimental task and by a finer adaptive method (QUEST, see Materials and Methods). Each point in the scatter plots (left plot in threshold values, right plot same data in ms units) represents data from one participant ($n = 13$). The number of ms (right plot x axis) represents the duration difference needed for that individual to discriminate longer 12 s durations at a fixed accuracy level of 75%. Discrimination accuracy when the duration difference is fixed (discrimination of 12 from 13.2 s) is indicated on the y axis. The significant correlations found between these two measurements indicate on the reliability of the original main experimental task for estimating individual longer temporal discriminations ability. **(B)** Time discrimination performance vs. color discrimination performance: experimental design and results. Top: timeline and stimuli from two experimental trials in the experiment. Same paradigm was used for time discrimination task or color discrimination task (see Materials and Methods). The temporal task required discriminating between 12 and 13.2 s durations while ignoring the colored circles, the color task required discriminating between the colors of the last circle in the trial with the one preceding it ("same" or "different"). Expected responses according to the task are indicated on the top right corner. Both color and time task required attention and motivation throughout the task since the number of flashing circles and their appearances were unexpected [number of circles per trial varied across trials and stimulus appearances were asynchronous (different SOA)]. Bottom: correlation between individuals' longer temporal duration discrimination performance and color discrimination performance is not significant. Each point in the scatter plots (left plot $n = 13$, right plot $n = 12$ without the outlier) represents one individual. **(C)** Correlation between shorter duration and longer duration discrimination abilities across all participants based on a finer adaptive QUEST procedure (see Materials and Methods). Each point in the scatter plots (left plot in threshold values, right plot same data in ms units) represents data from one participant. For shorter 2 s on y axis, and for longer 12 s on x axis, the number of ms (right plot) represents the duration difference needed for that individual to discriminate durations of that length at a fixed accuracy level of 75%. Thus, the duration difference for shorter durations does not correlate with the duration difference for longer durations, consistent with the results presented in **Figure 2A** bottom panels.

Bueti et al., 2008; Ivry and Schlerf, 2008; Vogel and Awh, 2008; Cui et al., 2009). Rather than discarding the differences that exist among individuals in their ability to estimate time, we used these individual differences to probe the underlying brain structure, reasoning that variability in time estimation would exhibit correlations with the GM volume of structures involved in such a process.

We found that the ability to estimate temporal durations was significantly correlated across input modalities (for either longer or shorter durations) suggesting a common neural mechanism associated with variability in time estimation across sensory modalities. For longer durations of 12 s we found that the structure (GM volume) of right auditory and somatosensory cortices, as well as parahippocampal gyri, predicted an individual's ability to discriminate longer durations in both auditory and visual modalities.

For shorter duration discriminations, results were less consistent. The GM volume in left extrastriate cortex predicted inter-individual variability in the shorter auditory duration discriminations. As with longer duration discriminations, there was overlap of cortical structures showing an association with inter-individual variation in temporal discrimination in different modalities. However, the GM volume of extrastriate cortex was only associated with shorter duration visual discriminations at a lower (uncorrected) statistical threshold and did not reach our stringent (whole-brain corrected) levels of significance set for our exploratory study. This shortcoming could be due to lower performance levels in the shorter duration conditions and the smaller variability in performance compared to the longer duration conditions. Thus, we cannot conclude at this point whether inter-individual variability in short duration estimation is reflected in extrastriate cortex structure in a modality-specific manner or not. Further research should therefore seek to replicate these findings before advancing particular theoretical interpretations.

Our principal findings that the GM density of primary auditory and secondary somatosensory cortices reflected both auditory and visual longer duration discrimination performance are interesting because neither of these cortices typically responds to visual stimulation *per se*. This suggests that these regions are involved in timing-related functions independent of sensory modality beyond unimodal sensory processing. Such a notion is consistent with a growing body of evidence that early sensory areas, which are previously thought to be purely unimodal, play roles in multimodal sensory processing. For example, although there is an evident tonotopic organization in PAC/A1, many multisensory factors influence processing in PAC/A1 (Ghazanfar and Schroeder, 2006). Moreover, in addition to a coarse somatotopic organization of secondary somatosensory cortex evident in OP1 and OP4 structures and to a minor extent in OP3 (Disbrow et al., 2000; Eickhoff et al., 2007), association and multi-modal integration

Table 1 | Anatomical and statistical details of the brain regions where gray matter volume correlated significantly with inter-individual variability in duration discrimination ability.

Condition	Corr. sign	Region	MNI coordinates			VBM results details		
			X	*Y*	*Z*	Cluster size (mm^3)	*p*(corr.)	*T*(26)
Aud12	pos	Right auditory and somatosensory cortex	35	−28	24	7118	0.001	5.52
			39	−25	16			5.40
			39	−21	10			5.38
			41	−27	4			5.37
			41	−12	10			4.48
			42	−9	16			4.33
			36	−9	22			4.20
			50	−34	18			3.52
	neg	R-PHG	21	−36	−14	901	0.007	4.92
			24	−28	−18			4.71
		L-PHG	−23	−40	−17	533	0.048	4.63
			−17	−43	−9			3.90
Vis12	pos	Right auditory and somatosensory cortex	47	−10	7	2467	0.008	4.71
			42	−25	3			4.70
			36	−9	22			4.13
			38	−27	25			3.93
			42	−27	19			3.92
			39	−21	9			3.88
			51	−27	21			3.68
	neg	R-PHG	15	−45	−8	500	0.029	5.34
Aud2	pos	L-visual	−21	−93	6	1316	0.046	5.05
			−35	−93	12			4.27
	neg	L-SMA	−6	11	67	810	0.07	5.18
		R-LO	51	−43	−12	783	0.069	4.85
Vis2	pos	L-visual	−23	−97	−3	1033	0.189	4.63
	neg	L-SMA	−2	0	64	905	0.053	5.26

For each cluster, the set of MNI coordinates indicate local maxima more than 4 mm apart within that cluster. Whole-brain corrected significant correlations ($p < 0.05$) are emphasized in bold. R, right; L, left; PHG, parahippocampal gyrus; SMA, supplementary motor area; LO, lateral occipital.

functions have been proposed for human secondary somatosensory cortex (Robinson and Burton, 1980; Eickhoff et al., 2006a). The OP2 structure may participate in the vestibular cortical network (Eickhoff et al., 2006c), and a recent study shows that the accuracy of temporal perception over seconds correlates with the ability to estimate bodily interoceptive (heartbeat) perception. Interoceptive perception is associated with activity in lateral sulcus/insular cortex (Meissner and Wittmann, 2011). Here, we showed that temporal ability for longer durations was related to the GM volume of different sensory cortices, conceivably to provide a more precise sense of time from multiple sources. The modality-independent roles of these structures in temporal processing shed a new light on the functionality of these regions and support the idea that these cortices are not as modality-specific as previously considered.

Our finding that GM structure of parahippocampal gyrus was negatively correlated with temporal discrimination ability for longer durations is intriguing. Several studies show that hippocampal regions are associated with temporal processing. For example, lesions to hippocampal regions in rats lead to underestimation of time intervals, while lesions to frontal regions produce opposite effects (Meck, 1996). Lesions to rat hippocampus (but not frontal cortex), produces "temporal amnesia" to the working memory of a prolonged interval (Meck et al., 1984, 1987; Olton et al., 1987). A recent study shows that rat hippocampal firing patterns can predict elapsed time in the order of seconds with very high precision (Itskov et al., 2011). In humans, several lesion studies point to the involvement of temporal and middle temporal lesions in timing of supra-second durations (Vidalaki et al., 1999; Melgire et al., 2005). This suggests that hippocampal regions may be a source of activity that supports estimations of longer durations – a process that might conceivably be contributing to successful performance in our study in the longer duration discrimination tasks. Yet the negative correlations we find suggest that smaller GM volume in the parahippocampal gyri was associated with improved temporal ability for longer durations. Several studies suggest that the process of pruning (Goldin et al., 2001; Kantor and Kolodkin, 2003; Watts et al., 2003; Low and Cheng, 2006), where excessive neural connections are "diluted" in a regulated manner to achieve more efficient neural networks, occurs in the hippocampus (Gao et al., 1999; Bagri et al., 2003; Gogtay et al., 2004, 2006; Faulkner et al., 2007). These effects are attributed to

the plasticity of the hippocampus following dynamic functions it serves such as memory and navigation. Thus, pruning processes to hippocampal structures that are related to temporal processing (Itskov et al., 2011) may underlie enhanced abilities for longer duration estimation.

Our findings also demonstrate that estimation of time is associated with local changes in brain structure. Several studies suggest that neural activity in the regions where we observed a correlation between brain structure and ability to discriminate time is related to time processing. fMRI signals in adjacent regions of cortex at coordinates overlapping with the areas of somatosensory and auditory cortices where we observed correlations between brain structure and discrimination ability selectively increase during the encoding of long duration intervals (∼9–18 s), but not during either short interval encoding or reproduction of time intervals (Wittmann et al., 2010). Moreover, MEG signals in right auditory cortex and also in parahippocampal regions very similar to the regions where we found an association between structure and temporal discrimination performance, are associated with the encoding of temporal intervals. The activity of these regions is modulated according to the temporal metrics of the sequence (Fujioka et al., 2010). Furthermore, auditory cortex plays a causal role in time related processing as transcranial magnetic stimulation (TMS) applied to right auditory cortex impairs time related processing (Bueti et al., 2008; Bolognini et al., 2010) independent of input modality (Kanai et al., 2011). Taken together, our anatomical study goes beyond these purely functional studies to provide converging evidence for the involvement of primary auditory, secondary somatosensory and parahippocampal cortices in temporal aspects of sensory discrimination. It remains an open question whether the structural variability we found across participants is also associated with variability in activation of these regions.

Could these local changes in brain structure associated with individual time estimation ability for longer durations be attributed to a genetic origin? Recent studies show that individual's veridical supra-second duration representation is influenced by genetic factors such as serotonin-related genes (Wackermann and Ehm, 2006; Sysoeva et al., 2010). Other studies provide evidence for genetic influence on brain structure (Baare et al., 2001; Thompson et al., 2001; Wright et al., 2002). Hence individual's time estimation ability for supra-second duration could be driven by genetic factors, however this has to be tested directly in future studies.

One possible cognitive mechanism to account for our findings is that individual ability to successfully discriminate longer durations relies on one's ability to maintain a consistent and stable rhythm over time, whether through counting, rehearsing a musical piece, or some other mental process. The right auditory and secondary somatosensory cortices and perhaps adjacent amodal association cortices as well as the parahippocampal regions could be orchestrating such rhythmic activity at various time scales (Ahissar and Vaadia, 1990; E. Ahissar, personal communication). Thus, we speculate the differences in the structure of the right auditory and secondary somatosensory cortices that exist between individuals may result in differences in the ability to maintain such internal rhythms.

CONCLUSION

Our study revealed a significant variability in individuals' ability to discriminate supra-second durations, whether shorter or longer durations, and through different modalities. This variability was very consistent across modalities, suggesting a common neural mechanism for temporal discrimination across modalities. The neural structure of right sensory cortices including A1 and SII substructures was significantly and positively correlated with individual ability to discriminate longer durations regardless of whether provided through vision or audition. Our findings show that the amodal sense of time is reflected in brain structure, and interestingly in the brain structure of sensory cortices, suggesting that the roles of these sensory cortices extend beyond modality-specific processing into the temporal perception domain.

ACKNOWLEDGMENTS

We thank Bahador Bahrami and Marieke Scholvinck for their comments. This work was supported by the Wellcome Trust (Geraint Rees), by a European Commission Marie-Curie fellowship FP7-236021 (Sharon Gilaie-Dotan), and the JSPS (Ryota Kanai). The Wellcome Trust Centre for Neuroimaging is supported by core funding from the Wellcome Trust 091593/Z/10/Z.

REFERENCES

Ahissar, E., and Vaadia, E. (1990). Oscillatory activity of single units in a somatosensory cortex of an awake monkey and their possible role in texture analysis. *Proc. Natl. Acad. Sci. U.S.A.* 87, 8935–8939.

Ashburner, J. (2007). A fast diffeomorphic image registration algorithm. *Neuroimage* 38, 95–113.

Ashburner, J., and Friston, K. J. (2000). Voxel-based morphometry – the methods. *Neuroimage* 11, 805–821.

Baare, W. F., Hulshoff Pol, H. E., Boomsma, D. I., Posthuma, D., de Geus, E. J., Schnack, H. G., van Haren, N. E., van Oel, C. J., and Kahn, R. S. (2001). Quantitative genetic modeling of variation in human brain morphology. *Cereb. Cortex* 11, 816–824.

Bagri, A., Cheng, H. J., Yaron, A., Pleasure, S. J., and Tessier-Lavigne, M. (2003). Stereotyped pruning of long hippocampal axon branches triggered by retraction inducers of the semaphorin family. *Cell* 113, 285–299.

Bolognini, N., Papagno, C., Moroni, D., and Maravita, A. (2010). Tactile temporal processing in the auditory cortex. *J. Cogn. Neurosci.* 22, 1201–1211.

Brown, S. W., Newcomb, D. C., and Kahrl, K. G. (1995). Temporal-signal detection and individual differences in timing. *Perception* 24, 525–538.

Bueti, D., van Dongen, E. V., and Walsh, V. (2008). The role of superior temporal cortex in auditory timing. *PLoS ONE* 3, e2481. doi:10.1371/journal.pone.0002481

Buhusi, C. V., and Meck, W. H. (2005). What makes us tick? Functional and neural mechanisms of interval timing. *Nat. Rev. Neurosci.* 6, 755–765.

Buonomano, D. V., and Merzenich, M. M. (1995). Temporal information transformed into a spatial code by a neural network with realistic properties. *Science* 267, 1028–1030.

Coull, J. T., Vidal, F., Nazarian, B., and Macar, F. (2004). Functional anatomy of the attentional modulation of time estimation. *Science* 303, 1506–1508.

Cui, X., Stetson, C., Montague, P. R., and Eagleman, D. M. (2009). Ready. . .go: amplitude of the FMRI signal encodes expectation of cue arrival time. *PLoS Biol.* 7, e1000167. doi:10.1371/journal.pbio.1000167

Disbrow, E., Roberts, T., and Krubitzer, L. (2000). Somatotopic organization of cortical fields in the lateral sulcus of *Homo sapiens*: evidence for SII and PV. *J. Comp. Neurol.* 418, 1–21.

Eickhoff, S. B., Amunts, K., Mohlberg, H., and Zilles, K. (2006a). The human parietal operculum. II. Stereotaxic maps and correlation with functional imaging results. *Cereb. Cortex* 16, 268–279.

Eickhoff, S. B., Schleicher, A., Zilles, K., and Amunts, K. (2006b). The human parietal operculum. I. Cytoarchitectonic mapping of subdivisions. *Cereb. Cortex* 16, 254–267.

Eickhoff, S. B., Weiss, P. H., Amunts, K., Fink, G. R., and Zilles, K. (2006c). Identifying human parieto-insular vestibular cortex using fMRI and cytoarchitectonic mapping. *Hum. Brain Mapp.* 27, 611–621.

Eickhoff, S. B., Grefkes, C., Zilles, K., and Fink, G. R. (2007). The somatotopic organization of cytoarchitectonic areas on the human parietal operculum. *Cereb. Cortex* 17, 1800–1811.

Faulkner, R. L., Low, L. K., and Cheng, H. J. (2007). Axon pruning in the developing vertebrate hippocampus. *Dev. Neurosci.* 29, 6–13.

Fleming, S. M., Weil, R. S., Nagy, Z., Dolan, R. J., and Rees, G. (2010). Relating introspective accuracy to individual differences in brain structure. *Science* 329, 1541–1543.

Fortin, C., and Couture, E. (2002). Short-term memory and time estimation: beyond the 2-second "critical" value. *Can. J. Exp. Psychol.* 56, 120–127.

Fujioka, T., Zendel, B. R., and Ross, B. (2010). Endogenous neuromagnetic activity for mental hierarchy of timing. *J. Neurosci.* 30, 3458–3466.

Gao, P. P., Yue, Y., Cerretti, D. P., Dreyfus, C., and Zhou, R. (1999). Ephrin-dependent growth and pruning of hippocampal axons. *Proc. Natl. Acad. Sci. U.S.A.* 96, 4073–4077.

Gaser, C., and Schlaug, G. (2003). Brain structures differ between musicians and non-musicians. *J. Neurosci.* 23, 9240–9245.

Ghazanfar, A. A., and Schroeder, C. E. (2006). Is neocortex essentially multisensory? *Trends Cogn. Sci. (Regul. Ed.)* 10, 278–285.

Gogtay, N., Giedd, J. N., Lusk, L., Hayashi, K. M., Greenstein, D., Vaituzis, A. C., Nugent, T. F. III, Herman, D. H., Clasen, L. S., Toga, A. W., Rapoport, J. L., and Thompson, P. M. (2004). Dynamic mapping of human cortical development during childhood through early adulthood. *Proc. Natl. Acad. Sci. U.S.A.* 101, 8174–8179.

Gogtay, N., Nugent, T. F. III, Herman, D. H., Ordonez, A., Greenstein, D., Hayashi, K. M., Clasen, L., Toga, A. W., Giedd, J. N., Rapoport, J. L., and Thompson, P. M. (2006). Dynamic mapping of normal human hippocampal development. *Hippocampus* 16, 664–672.

Goldin, M., Segal, M., and Avignone, E. (2001). Functional plasticity triggers formation and pruning of dendritic spines in cultured hippocampal networks. *J. Neurosci.* 21, 186–193.

Hayasaka, S., Phan, K. L., Liberzon, I., Worsley, K. J., and Nichols, T. E. (2004). Nonstationary cluster-size inference with random field and permutation methods. *Neuroimage* 22, 676–687.

Ilg, R., Wohlschlager, A. M., Gaser, C., Liebau, Y., Dauner, R., Woller, A., Zimmer, C., Zihl, J., and Muhlau, M. (2008). Gray matter increase induced by practice correlates with task-specific activation: a combined functional and morphometric magnetic resonance imaging study. *J. Neurosci.* 28, 4210–4215.

Itskov, V., Curto, C., Pastalkova, E., and Buzsaki, G. (2011). Cell assembly sequences arising from spike threshold adaptation keep track of time in the hippocampus. *J. Neurosci.* 31, 2828–2834.

Ivry, R. B., and Schlerf, J. E. (2008). Dedicated and intrinsic models of time perception. *Trends Cogn. Sci. (Regul. Ed.)* 12, 273–280.

Kanai, R., Bahrami, B., and Rees, G. (2010). Human parietal cortex structure predicts individual differences in perceptual rivalry. *Curr. Biol.* 20, 1626–1630.

Kanai, R., Lloyd, H., Bueti, D., and Walsh, V. (2011). Modality-independent role of the primary auditory cortex in time estimation. *Exp. Brain Res.* 209, 465–471.

Kanai, R., and Rees, G. (2011). The structural basis of inter-individual differences in human behaviour and cognition. *Nat. Rev. Neurosci.* 12, 231–242.

Kantor, D. B., and Kolodkin, A. L. (2003). Curbing the excesses of youth: molecular insights into axonal pruning. *Neuron* 38, 849–852.

Karmarkar, U. R., and Buonomano, D. V. (2007). Timing in the absence of clocks: encoding time in neural network states. *Neuron* 53, 427–438.

Lewis, P. A., and Miall, R. C. (2003). Distinct systems for automatic and cognitively controlled time measurement: evidence from neuroimaging. *Curr. Opin. Neurobiol.* 13, 250–255.

Low, L. K., and Cheng, H. J. (2006). Axon pruning: an essential step underlying the developmental plasticity of neuronal connections. *Philos. Trans. R. Soc. Lond. B Biol. Sci.* 361, 1531–1544.

Mauk, M. D., and Buonomano, D. V. (2004). The neural basis of temporal processing. *Annu. Rev. Neurosci.* 27, 307–340.

May, A., and Gaser, C. (2006). Magnetic resonance-based morphometry: a window into structural plasticity of the brain. *Curr. Opin. Neurol.* 19, 407–411.

Meck, W. H. (1996). Neuropharmacology of timing and time perception. *Brain Res. Cogn. Brain Res.* 3, 227–242.

Meck, W. H., Church, R. M., and Olton, D. S. (1984). Hippocampus, time, and memory. *Behav. Neurosci.* 98, 3–22.

Meck, W. H., Church, R. M., Wenk, G. L., and Olton, D. S. (1987). Nucleus basalis magnocellularis and medial septal area lesions differentially impair temporal memory. *J. Neurosci.* 7, 3505–3511.

Meissner, K., and Wittmann, M. (2011). Body signals, cardiac awareness, and the perception of time. *Biol. Psychol.* 86, 289–297.

Melgire, M., Ragot, R., Samson, S., Penney, T. B., Meck, W. H., and Pouthas, V. (2005). Auditory/visual duration bisection in patients with left or right medial-temporal lobe resection. *Brain Cogn.* 58, 119–124.

Morillon, B., Kell, C. A., and Giraud, A. L. (2009). Three stages and four neural systems in time estimation. *J. Neurosci.* 29, 14803–14811.

Morosan, P., Rademacher, J., Schleicher, A., Amunts, K., Schormann, T., and Zilles, K. (2001). Human primary auditory cortex: cytoarchitectonic subdivisions and mapping into a spatial reference system. *Neuroimage* 13, 684–701.

Olton, D. S., Meck, W. H., and Church, R. M. (1987). Separation of hippocampal and amygdaloid involvement in temporal memory dysfunctions. *Brain Res.* 404, 180–188.

Poppel, E. (1997). A hierarchical model of temporal perception. *Trends Cogn. Sci. (Regul. Ed.)* 1, 56–61.

Rademacher, J., Morosan, P., Schormann, T., Schleicher, A., Werner, C., Freund, H., and Zilles, K. (2001). Probabilistic mapping and volume measurement of human primary auditory cortex. *Neuroimage* 13, 669–683.

Rammsayer, T. H. (1999). Neuropharmacological evidence for different timing mechanisms in humans. *Q. J. Exp. Psychol. B* 52, 273–286.

Rao, S. M., Mayer, A. R., and Harrington, D. L. (2001). The evolution of brain activation during temporal processing. *Nat. Neurosci.* 4, 317–323.

Robinson, C. J., and Burton, H. (1980). Somatic submodality distribution within the second somatosensory (SII), 7b, retroinsular, postauditory, and granular insular cortical areas of *M. fascicularis*. *J. Comp. Neurol.* 192, 93–108.

Schwarzkopf, D. S., Song, C., and Rees, G. (2011). The surface area of human V1 predicts the subjective experience of object size. *Nat. Neurosci.* 14, 28–30.

Sysoeva, O. V., Tonevitsky, A. G., and Wackermann, J. (2010). Genetic determinants of time perception mediated by the serotonergic system. *PLoS ONE* 5, e12650. doi:10.1371/journal.pone.0012650

Thompson, P. M., Cannon, T. D., Narr, K. L., van Erp, T., Poutanen, V. P., Huttunen, M., Lonnqvist, J., Standertskjold-Nordenstam, C. G., Kaprio, J., Khaledy, M., Dail, R., Zoumalan, C. I., and Toga, A. W. (2001). Genetic influences on brain structure. *Nat. Neurosci.* 4, 1253–1258.

Treisman, M. (1963). Temporal discrimination and the indifference interval. Implications for a model of the "internal clock." *Psychol. Monogr.* 77, 1–31.

Treisman, M., Faulkner, A., Naish, P. L., and Brogan, D. (1990). The internal clock: evidence for a temporal oscillator underlying time perception with some estimates of its characteristic frequency. *Perception* 19, 705–743.

Ulbrich, P., Churan, J., Fink, M., and Wittmann, M. (2007). Temporal reproduction further evidence for two processes. *Acta Psychol.* 125, 51–65.

Vidalaki, V. N., Ho, M. Y., Bradshaw, C. M., and Szabadi, E. (1999). Interval timing performance in temporal lobe epilepsy: differences between patients with left and right hemisphere foci. *Neuropsychologia* 37, 1061–1070.

Vogel, E. K., and Awh, E. (2008). How to exploit diversity for scientific gain: using individual differences to constrain cognitive theory. *Curr. Dir. Psychol. Sci.* 17, 171–176.

Wackermann, J., and Ehm, W. (2006). The dual klepsydra model of internal time representation and time reproduction. *J. Theor. Biol.* 239, 482–493.

Watson, A. B., and Pelli, D. G. (1983). QUEST: a Bayesian adaptive psychometric method. *Percept. Psychophys.* 33, 113–120.

Watts, R. J., Hoopfer, E. D., and Luo, L. (2003). Axon pruning during *Drosophila* metamorphosis: evidence for local degeneration and requirement of the ubiquitin-proteasome system. *Neuron* 38, 871–885.

Wittmann, M., Simmons, A. N., Aron, J. L., and Paulus, M. P. (2010). Accumulation of neural activity in the posterior insula encodes the passage of time. *Neuropsychologia* 48, 3110–3120.

Worsley, K. J., Andermann, M., Koulis, T., MacDonald, D., and Evans, A. C. (1999). Detecting changes in nonisotropic images. *Hum. Brain Mapp.* 8, 98–101.

Wright, I. C., Sham, P., Murray, R. M., Weinberger, D. R., and Bullmore, E. T. (2002). Genetic contributions to regional variability in human brain structure: methods and preliminary results. *Neuroimage* 17, 256–271.

Conflict of Interest Statement: The authors declare that the research was conducted in the absence of any commercial or financial relationships that could be construed as a potential conflict of interest.

Received: 23 October 2011; accepted: 02 November 2011; published online: 21 November 2011.

Citation: Gilaie-Dotan S, Kanai R and Rees G (2011) Anatomy of human sensory cortices reflects inter-individual variability in time estimation. Front. Integr. Neurosci. ***5****:76. doi: 10.3389/fnint.2011.00076*

frontiers in
INTEGRATIVE NEUROSCIENCE

ORIGINAL RESEARCH ARTICLE
published: 04 October 2011
doi: 10.3389/fnint.2011.00059

Temporal discrimination of sub- and suprasecond time intervals: a voxel-based lesion mapping analysis

Cynthia M. Gooch[1]*, Martin Wiener[1], A. Cris Hamilton[2] and H. Branch Coslett[1]

[1] *University of Pennsylvania Medical Center, Philadelphia, PA, USA*
[2] *Rice University, Houston, TX, USA*

Edited by:
Warren H. Meck, Duke University, USA

Reviewed by:
Catalin V. Buhusi, Medical University of South Carolina, USA
Sara Cordes, Boston College, USA

****Correspondence:***
Cynthia M. Gooch, Department of Neuroscience, Temple University, Room 818 Weiss Hall, 1701 N. 13th Street, Philadelphia, PA 19122-6085, USA.
e-mail: cgooch@temple.edu

We used voxel-based lesion-symptom mapping (VLSM) to determine which brain areas are necessary for discriminating time intervals above and below 1 s. VLSM compares behavioral scores of patients that have damage to a given voxel to those that do not on a voxel-by-voxel basis to determine which voxels are critical for the given behavior. Forty-seven subjects with unilateral hemispheric lesions performed a temporal discrimination task in which a standard stimulus was compared on each trial to a test stimulus. In different blocks of trials, standard stimuli were either 600 or 2000 ms. Behavioral measures included the point of subjective equality, a measure of accuracy, and the coefficient of variation, a measure of variability. Lesions of the right middle and inferior frontal gyri were associated with decrements in performance on both durations. In addition, lesions of the left temporal lobe and right precentral gyrus were associated exclusively with impaired performance for subsecond stimuli. In line with results from other studies, these data suggest that different circuits are necessary for timing intervals in these ranges, and that right frontal areas are particularly important to timing.

Keywords: time perception, lesion, temporal discrimination, VLSM

INTRODUCTION

There has been a surge of interest in the cognitive neuroscience of time perception over the past decade. Whereas potential contributions of the basal ganglia and cerebellum to the perception of short time intervals have been explored by a number of investigators, the cortical basis of interval processing has more recently come to the forefront. For example, models of timing such as striatal beat frequency (SBF; Matell and Meck, 2004) suggest that cortex may be crucial to interval timing. On this account, input from cortical neurons is integrated by spiny neurons in the striatum to encode a remembered duration. Additionally, electrophysiologic investigations of cortical neurons have demonstrated that cells in parietal (Leon and Shadlen, 2003) and frontal (Niki and Watanabe, 1979; Genovesio et al., 2006) cortex, including supplementary motor area (SMA; Macar et al., 2004; Mita et al., 2009) exhibit ramping and other behaviors that are consistent with the hypothesis that these cells mark the passage of time.

Many (Gibbon et al., 1997; Rammsayer, 1999, 2001; Lewis and Miall, 2003) investigators have argued for a fundamental distinction between timing of short (usually less than 1 s) and long (usually more than 1 s) intervals. Although different structures (Lewis and Miall, 2003; Wiener et al., 2010b) and neurotransmitters (Rammsayer, 1999, 2001; Wiener et al., 2011) have been proposed to support these two functions, the degree to which routines involved in sub- and suprasecond timing are distinct remains unclear (e.g., Macar et al., 2002). One reason for the persistent controversy is that few studies of timing have assessed both sub- and suprasecond intervals (e.g., Harrington et al., 1998; Hinton and Meck, 2004; Shih et al., 2009).

There have been exceptions to this generalization, however. For example Lewis and Miall (2003) reported an imaging study in which a temporal discrimination task at 600 and 3000 ms was employed. They found bilateral DLPFC, and right inferior parietal cortex (angular gyrus), among other areas, to be commonly activated during timing of both intervals. Subsecond intervals also activated the cerebellum, right superior temporal gyrus, and prefrontal operculum, among other areas, while suprasecond intervals additionally activated left inferior parietal cortex and the posterior cingulate. More recently, we (Wiener et al., 2010b) performed a meta-analysis using the activation likelihood estimation (ALE) technique in which both sub- and suprasecond timing were included. This analysis showed two brain regions common to timing sub- and suprasecond durations: SMA and right inferior frontal gyrus (IFG). Additionally, when studies were sorted according to stimulus duration, we found that timing of subsecond durations were more likely to activate the cerebellum and basal ganglia, while suprasecond durations were more likely to activate cortical structures.

Transcranial magnetic stimulation (TMS), a technique for producing temporary, virtual lesions in a circumscribed cortical region, has also produced data comparing cortical contributions to timing of durations above and below 1 s. Jones et al. (2004) showed that TMS over right DLPFC disrupts temporal reproduction in the seconds range, but not in the subsecond range. An additional study by Koch et al. (2007) replicated the exclusive effect of right DLPFC stimulation on suprasecond timing and extended the results by demonstrating that stimulation of the cerebellum disrupted performance for subsecond stimuli only.

There have been two studies involving subjects with focal brain lesions in which both sub- and suprasecond intervals have been tested (Nichelli et al., 1995; Mangels et al., 1998). Both studies suggested that lesions of the prefrontal cortex disrupt discrimination of both sub- and suprasecond intervals. Another study examined frontal lesion patients' performance on a tapping task with a response period of 1.5 s (Picton et al., 2006). They found that participants with damage to right lateral BA 45 had the most difficulty with this task. Patients with damage to right lateral BA 6 also showed a trend toward disruption in performance.

Another cortical lesion study of timing behavior bears noting. Harrington et al. (1998) administered a temporal discrimination task using subsecond stimuli (300 and 600 ms standards) in 37 subjects with cortical lesions. Grouping subjects on the basis of involvement in specified brain regions, they found both frontal and parietal areas in the right hemisphere to be important to timing these intervals. Finally, Coslett et al. (2009) reported data from 31 subjects with focal cortical lesions on temporal production, estimation, and reproduction tasks using stimuli from 2 to 12 s; they found that these patients underproduced and overestimated all but the shortest interval.

We report an additional study of the hemispheric basis of temporal processing. Our study differs from previous investigations in several important respects. First, subjects were not selected on the basis of lesion locus. Using a convenience sample rather than subjects selected on the basis of lesion locus permits us to investigate a wider range of brain structures; whereas selecting subjects on the basis of frontal lobe damage, for example, will permit one to draw conclusions about the role of frontal regions in timing, such an approach offers no information regarding the role of other brain regions. Second, with 47 subjects with focal lesions, our study is the largest to date to explore the hemispheric basis of temporal processing. Third, rather than just group subjects on the basis of a common region of interest (e.g., "predominantly frontal"), we also employ voxel-based lesion-symptom mapping, or VLSM (Bates et al., 2003), a technique derived from work in functional imaging. In this technique, at each voxel the performance of subjects with a lesion at that voxel is compared to the performance of subjects without a lesion at that voxel using a *t*-test. Voxels at which lesioned subjects perform significantly less well than subjects without lesions are assumed to be important for the behavioral measure. VLSM has a number of advantages over traditional methods of studying behavioral deficits in brain-lesioned patients. It allows us to examine all areas of the brain without *a priori* assumptions, thereby offering the possibility of finding areas not previously known to be involved in the behavior studied. It also gives a more precise picture of which areas are important to the given behavior than traditional region of interest or overlap studies of brain-lesioned patients.

MATERIALS AND METHODS

SUBJECTS

Forty-seven subjects (22 female) with a single hemispheric vascular lesion documented by brain imaging participated in this study. Patients were recruited through the University of Pennsylvania Center for Cognitive Neuroscience patient database (Fellows et al., 2008). Sixteen healthy control subjects also participated. The mean age of the patients was 59 ± 11 years, and the mean age of controls was 57 ± 9 years. Patients had suffered their stroke an average of 6.3 ± 5.3 years previously. No subject had a history of substance abuse or psychiatric illness. See **Table 1** for details on each patient. The research was approved the Institutional Review Board of the University of Pennsylvania.

BEHAVIORAL TASK

Subjects were asked to indicate if a test interval was longer or shorter than the standard interval. At the onset of each trial, a central fixation point was presented for 1 s and immediately succeeded by a red square that persisted for either 600 or, in a different block of trials, 2000 ms (standard duration). After a blank screen lasting 1 s, a second red square was presented for a variable duration (comparison duration) as determined by a maximum-likelihood procedure, the Parameter Estimation by Sequential Testing (PEST) algorithm (Pentland, 1980). The current upper or lower threshold value is presented as the comparison duration for each trial. Furthermore, the range and frequency of comparison stimuli is different for each subject, allowing task difficulty to be scaled to individual performance. We set the initial lower and upper thresholds to equal 50 and 150% of the standard interval duration, respectively. The initial stepsize for adjustments in the comparison duration was set to 15% of the standard duration for the first 20 trials, then to 5% for the remaining 40 trials. If the comparison stimulus was judged to be longer, subjects depressed the "L" key whereas if the comparison stimulus was judged to be shorter, subjects depressed the "S" key. Subjects were not told the range of stimulus durations and were not given feedback regarding accuracy. Each interval (600, 2000 ms) was assessed in a separate block of 60 trials. The order of blocks was counterbalanced across subjects.

DATA ANALYSIS

Curve fitting

The probability of the subject making a "longer" response choice was plotted as a function of the comparison interval. These data were then fit with a sigmoidal, psychometric curve using the psignifit version 2.5.6 software package (see bootstrap-software.org/psignifit/) for Matlab, which implements the maximum-likelihood method described by Wichmann and Hill (2001a). Upper and lower thresholds, the approximate points at which the subject is 25 and 75% likely to judge the comparison stimulus as longer, were calculated using the bias-corrected bootstrap method implemented by psignifit based on 4999 simulations (Wichmann and Hill, 2001b). For each block of trials for each subject two measures of performance were calculated. First, the point of subjective equality (PSE), or the duration at which participants responded "longer" 50% of the time was determined; this is considered a measure of accuracy. Second, the difference limen (DL), or the interval between the durations at which participants responded "longer" 25 and 75% of the time, was calculated; for example, if subjects indicated that the test interval of 450 ms was longer on 25% of trials and a test interval of 800 ms was longer on 75% of trials, the DL would be 350 ms.

In order to facilitate comparison of performance across different intervals, PSE was transformed into an absolute proportional

Table 1 | Patient demographic information.

Participant	Gender	Age (years)	Education (years)	Years post-stroke	Lesion hemisphere	Lesion area
1	F	61	15	12	L	Frontal
2	M	57	14	7	L	Frontal
3	M	68	16	4	L	Frontal
4	M	64	14	3	L	Frontal
5	F	61	12	3	L	Frontal
6	M	44	20	5	L	Frontal
7	F	32	14	1	L	Frontal
8	F	61	14	2	L	Frontal
9	M	74	15	1	L	Frontal
10	M	64	12	8	L	Frontal, parietal, temporal
11	M	60	18	6	L	Frontal, parietal, temporal
12	M	45	12	9	L	Frontal, temporal
13	M	50	12	7	L	Frontal, temporal
14	M	62	18	15	L	Frontal, temporal, parietal
15	F	53	12	6	L	Occipital
16	M	77	21	1	L	Parietal
17	F	57	12	7	L	Striatum (caudate/putamen)
18	M	53	12	5	L	Temporal
19	M	47	12	5	L	Temporal
20	M	70	12	5	L	Temporal
21	M	75	12	6	L	Temporal
22	F	34	9	2	L	Temporal, occipital
23	F	65	16	8	R	Frontal
24	F	43	12	9	R	Frontal
25	F	78	18	7	R	Frontal
26	F	57	16	8	R	Frontal
27	M	64	12	4	R	Frontal
28	M	67	12	4	R	Frontal
29	M	51	10	4	R	Frontal, parietal, temporal
30	M	64	11	3	R	Frontal, parietal, temporal
31	F	47	12	2	R	Frontal, parietal, temporal
32	M	62	18	1	R	Frontal, parietal, temporal
33	F	66	18	1	R	Frontal, parietal, temporal, occipital
34	F	55	18	33	R	Frontal, temporal
35	F	58	16	14	R	Frontal, temporal
36	F	70	18	4	R	Frontal, temporal
37	F	43	16	1	R	Occipital
38	M	56	14	6	R	Occipital
39	M	62	12	5	R	Parietal
40	F	75	12	4	R	Parietal, occipital
41	M	54	12	1	R	Parietal, occipital
42	M	73	18	1	R	Parietal, temporal
43	M	53	12	11	R	Temporal
44	F	50	12	7	R	Temporal
45	F	73	12	7	R	Temporal, occipital
46	F	62	21	6	R	Temporal, occipital
47	F	69	12	9	R	Thalamus

error (|[PSE–standard]/standard|) value; similarly, the DL was divided by the PSE to generate the coefficient of variation (CV); CV, therefore, is a measure of variability that is independent of stimulus duration.

In order to minimize erroneous results driven by extremely poor participants, the data were winsorized, so that values that were greater than 3 SD from the mean were recoded to be the value at 3 SD from the mean. Although they understood the task

and performed adequately in other domains, six subjects performed extremely poorly with the result that a psychometric curve could not be generated; for these individuals, absolute PSE proportional error and CV were coded to be 3 SD from the mean of the patient data on these measures. These patients were not excluded from analysis based on their poor performance because to do so would eliminate those patients whose performance was most aberrant and therefore potentially most informative regarding temporal processing. Absolute proportional error was used as we were unable to determine if the poor performance of the six subjects reflected under- or over-estimation of the intervals. Further, we had no *a priori* assumptions regarding whether lesions to certain cortical areas would result in an increase or decrease perceived duration, and, it is possible that two patients with a similar lesion could display inaccuracies in time perception in opposite directions. For this reason, using an absolute error measure makes the VLSM process more sensitive to perturbations in time perception that may occur in either direction (speeding up or slowing down), as any disturbance in timing accuracy will contribute to a significant result. It is understood that this gain in sensitivity comes at the cost of making claims regarding lengthening or shortening effects of brain lesions.

Imaging methods

Structural images were acquired using MRI ($n = 14$) or CT ($n = 33$). All scans were obtained at least 2 months after the infarct and were judged to be of good quality by an experienced neurologist.

VLSM methods

For patients with high-resolution MRI scans ($n = 14$), lesions were identified in native space (that is, on the subject's MRI scan) manually by a neurologist (HBC) who was naïve with respect to the behavioral data. The marked structural scans were then registered to a common template using a symmetric diffeomorphic registration algorithm (Avants et al., 2006; see also http://www.picsl.upenn.edu/ANTS/). This same mapping was then applied to the lesion maps. To optimize the automated registration, volumes were first registered to an intermediate template constructed from images acquired on the same scanner. A single mapping from this intermediate template to the Montreal Neurological Institute (MNI) space "Colin27" volume (Holmes et al., 1998) was used to complete the mapping from subject space to MNI space. For patients with CT scans the lesions were rendered on the Colin27 template using MRICro by the same neurologist. Resolution for the Colin27 template was 1 voxel = 1 mm^3.

Behavioral analysis

Separate mixed-model ANOVAs were performed for absolute PSE proportional error and CV. Duration (600 or 2000 ms) was a within-subjects factor and group (patient or control) was a between-subjects factor. In subsequent analyses exploring the hemispheric basis of temporal processing deficits, separate ANOVAs were performed for patients with left and right hemisphere lesions, comparing each to controls.

Although VLSM was the primary technique by which issues of the anatomic bases of performance was analyzed, in an effort to address previously reported findings (e.g., Harrington et al., 1998), we also divided subjects on the basis of the lesion locus as defined by involvement of specific brain regions. In the current study patients were subdivided into those with and without lesions that were predominantly frontal (at least 10% damage to BAs 5, 6, 8, 9, 10, 11, 44, 45, 46, and 47; 13 patients). Also, patients with and without predominantly posterior parietal lesions (at least 10% damage to BAs 39, 40, 5, and 7; seven patients) were compared to controls. In keeping with previous studies, those patients whose lesions involved both frontal and parietal structures were assigned to the frontal or parietal groups on the basis of the relative size of the frontal or parietal involvement. Four patients with very extensive involvement in both regions were omitted from these analyses. For both analyses, percent damage was determined using the Brodmann area map in MRICron. *Post hoc* t-tests were administered where appropriate. Correlations were also performed between size of lesion (in cc) and performance on the timing tasks, as measured by CV or absolute proportional error of PSE at each interval.

VLSM analysis

Voxels in which fewer than two patients were lesioned were excluded from the VLSM analyses. At each voxel, a t-test comparing the scores between patients with and without lesions was performed with the MRICron (http://www.sph.sc.edu/comd/rorden/mricron/) brain imaging package. The resulting t-map was thresholded to control the false discovery rate (FDR; Genovese et al., 2002) at $q = 0.05$, where q is the expected proportion of false positives among supra-threshold voxels.

RESULTS

BEHAVIORAL ANALYSIS

Patients versus controls

Data for the CV and absolute proportional error for both controls and patients is presented in **Table 2**. ANOVA for the CV data demonstrated a main effect of group [$F(1,61) = 5.3$, $p < 0.05$], but no significant effect for duration [$F(1,61) = 0.1$, ns] and no interaction between duration and group [$F(1,61) = 1.0$, ns]. ANOVA for absolute proportional error demonstrated a significant effect of group [$F(1,61) = 11.2$, $p < 0.05$] and there was no main effect of duration [$F(1,61) = 0.2$, ns]. There was no group by duration interaction [$F(1,61) = 2.4$, ns].

VLSM ANALYSIS

600 ms interval

In the analysis for the CV measure significant voxels were found in the right precentral gyrus (lateral BA 6, 3231 voxels) and IFG (BA 44, 925 voxels). On the left side, significant areas were the basal ganglia (caudate, putamen, and pallidum, 8802 voxels), the

Table 2 | Patient versus control performance.

	CV 600 ms	CV 2000 ms	Abs. prop. error PSE 600 ms	Abs. prop. error PSE 2000 ms
Control	0.20 ± 0.02	0.17 ± 0.02	0.07 ± 0.02	0.12 ± 0.02
Patient	0.37 ± 0.05	0.45 ± 0.08	0.32 ± 0.05	0.25 ± 0.03

superior and middle temporal lobe (35523 voxels), and hippocampus (2303 voxels, see **Figure 1**). No significant voxels were found in the absolute PSE proportional error analysis.

2000 ms interval

The CV measure analysis yielded significant voxels in the right hemisphere in the same areas as the 600 ms interval: lateral BA 6 (3444 voxels) and BA 44 (1571 voxels), and also in the right middle frontal gyrus (MFG; BA 9, 73 voxels). No significant voxels were found on the left side for this measure, or for the PSE measure (see **Figure 2**). No significant voxels were found in the absolute PSE proportional error analysis.

Power

In VLSM analyses, power to detect behavioral differences is due in part to differences in the number of patients with lesions at each voxel. **Figure 3** shows a color map of the number of patients with lesions in each voxel and thus provides a measure of the relative (not absolute) power to observe an effect at each voxel, as power is maximized where voxels are lesioned in about half the population for 0/1 lesion scores (Kimberg et al., 2007) As is typical in studies involving VLSM (e.g., Schwartz et al., 2009), the relative power is greatest in the peri-sylvian regions irrigated by the Middle Cerebral Artery.

FURTHER BREAKDOWN OF BEHAVIORAL ANALYSIS

Hemispheric differences

Table 3 compares control data to patients with left hemisphere and right hemisphere lesions. ANOVA on CV between patients with right hemisphere lesions and controls showed a significant effect of group [$F(1,39) = 5.1$, $p < 0.05$], but no effect of duration

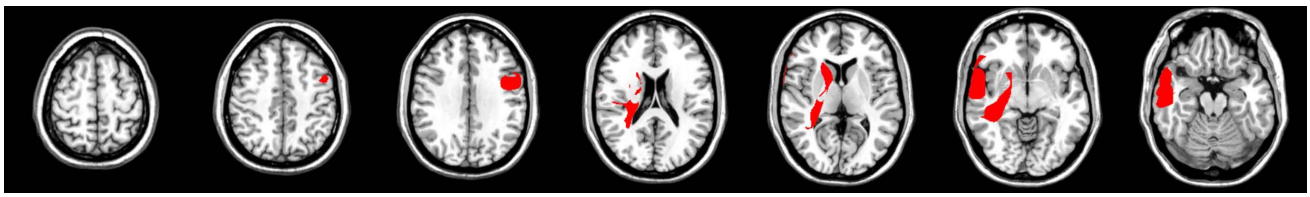

FIGURE 1 | Results for the CV measure, 600 ms. Separate analyses were performed for left and right hemisphere-lesioned patients. All FDR cutoff values are $q = 0.05$. All images are in neurological convention.

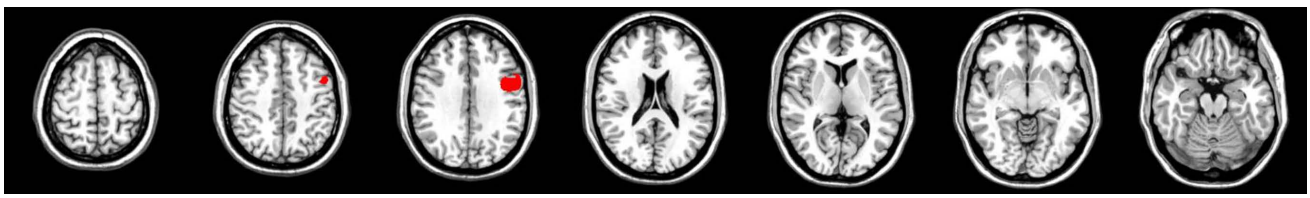

FIGURE 2 | Results for the CV measure, 2000 ms.

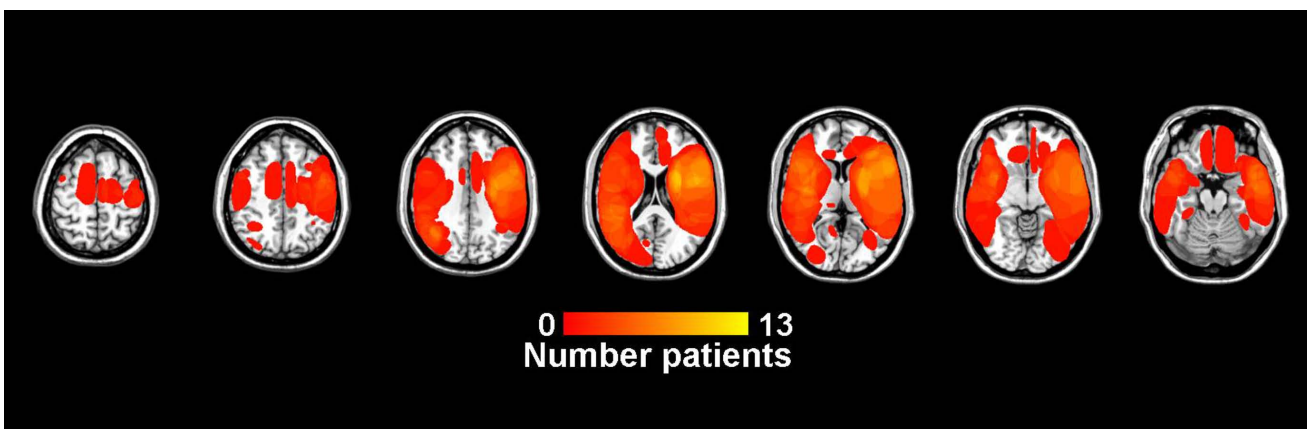

FIGURE 3 | Lesion overlap showing the number of patients with lesions at each voxel. In VLSM analyses, power to detect behavioral differences is due in part to differences in the number of patients with lesions at each voxel. The scale runs from dark red to bright yellow, with brighter yellow indicating a greater number of patients with a lesion at that voxel. Lower right is a legend with number of lesions at each voxel.

or the interaction between duration and group. Left-hemisphere patients differed from controls overall [$F(1,36) = 5.5$, $p < 0.05$], but no significant effects of duration or the interaction of duration and group were found.

When comparing patients with right-sided lesions to controls, ANOVA on absolute proportional error demonstrated a main effect of group [$F(1,39) = 13.7$, ns] but there was no significant main effect of duration [$F(1,39) = 0.3$, ns] or duration by group interaction [$F(1,39) = 2.3$, ns]. Left-sided lesion patients were significantly different from controls also [$F(1,36) = 9.6$, $p < 0.05$], but no effect of duration or the interaction between duration and group was found.

No significant differences were found between left- and right-sided lesion patients for either the CV measure, or the absolute error of PSE measure.

Frontal damage

Table 4 compares control data to patients with lesions that are predominantly frontal and those with lesions that are primarily posterior parietal. Overlap images of patient lesions contributing to the predominantly frontal group are presented in **Figure 4**. The overall ANOVA for the CV measure showed a significant difference between controls and patients with predominantly frontal damage [$F(1,29) = 7.0$, $p < 0.05$]. The duration factor, and the interaction between group and duration were not significant in this analysis.

For the absolute proportional error of PSE measure, the main effect of group was significant between controls and patients who had frontal damage [$F(1,29) = 10.4$, $p < 0.05$]. No effect of duration or the interaction between duration and group was found.

Table 3 | Performance of controls versus left- and right-sided lesion patients.

	CV 600 ms	CV 2000 ms	Abs. prop. error PSE 600 ms	Abs. prop. error PSE 2000 ms
Control	0.20 ± 0.02	0.17 ± 0.02	0.07 ± 0.02	0.12 ± 0.02
Left-side lesion	0.38 ± 0.08	0.52 ± 0.13	0.33 ± 0.07	0.27 ± 0.05
Right-side lesion	0.37 ± 0.04	0.38 ± 0.09	0.32 ± 0.06	0.22 ± 0.04

Table 4 | Performance of controls versus patients with predominantly frontal lesions and those with predominantly posterior parietal lesions.

	CV 600 ms	CV 2000 ms	PSE 600 ms	PSE 2000 ms
Control	0.20 ± 0.02	0.17 ± 0.02	0.07 ± 0.02	0.12 ± 0.02
Predom. Frontal	0.39 ± 0.11	0.46 ± 0.16	0.36 ± 0.10	0.25 ± 0.06
Predom. PPC	0.34 ± 0.10	0.40 ± 0.22	0.12 ± 0.02	0.26 ± 0.05

Posterior parietal damage

Figure 5 depicts an overlap image of lesions in patients comprising the posterior parietal damage group. The overall ANOVA for the CV measure showed no significant difference between controls and patients who had damage predominantly to posterior parietal regions [$F(1,21) = 4.0$, ns], The interaction between group and duration was not significant in this analysis.

For absolute proportional error, a significant main effect of group emerged between patients with significant posterior parietal damage and controls [$F(1,21) = 15.1$, $p < 0.05$].

Predominantly frontal versus predominantly posterior parietal damage

There were no significant differences found between patients who had damage that was primarily frontal and those that had damage that was primarily posterior parietal in nature for either the CV or absolute error of PSE measure.

CORRELATIONS

Size of lesion correlated with CV at both the 600 ms (Pearson's $r = 0.34$, $p < 0.05$) and the 2000 ms (Pearson's $r = 0.32$, $p < 0.05$) intervals. Size of lesion did not correlate with absolute proportional error of PSE at either interval. Partial correlations with inferior frontal volume as a controlling factor removed the significant correlations of volume with CV at 600 ms ($r = 0.26$, ns) and 2000 ms ($r = 0.15$, ns). In contrast, partial correlations

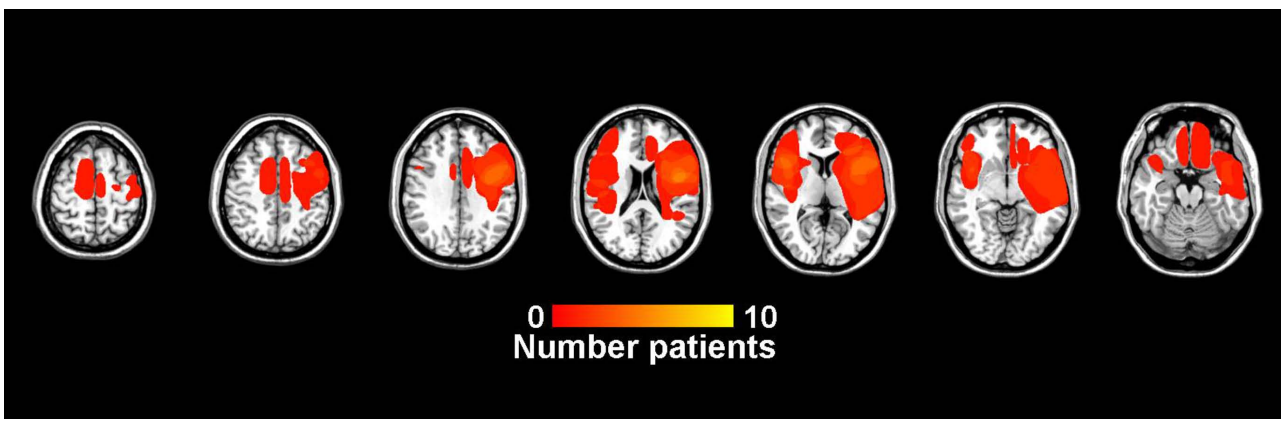

FIGURE 4 | Lesion overlap for patients in the predominantly frontal lesion group.

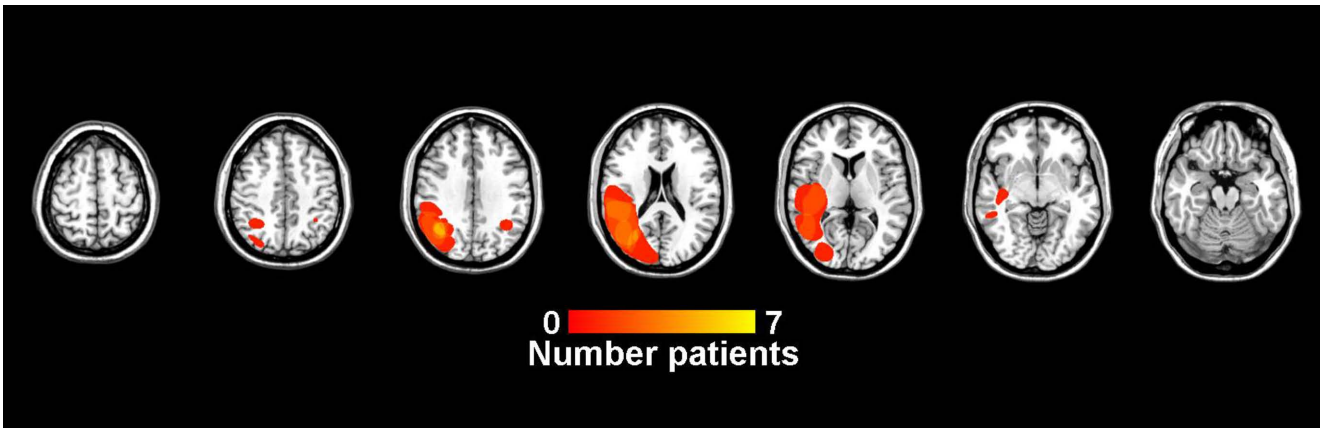

FIGURE 5 | Lesion overlap for patients in the predominantly posterior parietal lesion group.

between CV and lesion volume with posterior parietal volume as a controlling factor did not remove the significant correlations (600 ms: $r = 0.38$, $p < 0.05$; 2000 ms: $r = 0.33$, $p < 0.05$). This suggests that, while IFG volume is a significant factor influencing the CV measures, PPC is not.

DISCUSSION

Comparisons of all patients with brain lesions and controls demonstrated significant differences in performance for sub- and suprasecond intervals. Subsequent analyses in which subjects were partitioned on the basis of lesion location further demonstrated significant behavioral differences. Patients with significant frontal damage were less accurate and more variable than controls. Patients with damage to posterior parietal regions were less accurate than controls. These data are in line with previous suggestions that there may be specific cortical regions that are influential in the computation of time. To further examine this possibility, we turned to VLSM as a method to localize lesioned areas important to timing making no *a priori* assumptions regarding location of interest.

Voxel-based lesion-symptom mapping analysis revealed several areas important to perceptual timing for both 600 and 2000 ms intervals. These were the right precentral gyrus (lateral BA 6), the right MFG (BA 9), and the right IFG (BA 44).

These data are consistent with a number of other demonstrations from functional imaging and brain lesion subjects implicating regions of the right frontal lobe in timing. The IFG, for example, has been found to be active in numerous functional imaging studies of timing. Coull et al. (2004) reported activation of the IFG when subjects directed attention to time. The IFG has also been found to be active during a rhythm monitoring task (Schubotz et al., 2000), a task using tapping procedures in temporal reproduction (Bueti et al., 2008), and many others (e.g., Smith et al., 2003; Lewis and Miall, 2006).

A variety of different roles have been assigned to the IFG in timing. One hypothesis emphasized by Lewis and Miall (2006) is that the IFG and other regions of the DLPFC underlie working memory for time. Several lines of evidence are consistent with this. First, neurons in this region exhibit patterns of discharge that suggest that they monitor interval duration. Pouthas et al. (2005), for example, demonstrated in an fMRI investigation that activation in this area correlates with the length of the duration to be timed. Additionally, it is noteworthy that regions of the IFG, including those implicated in our study, are commonly activated in working memory tasks (Rissman et al., 2008; Lemus et al., 2009). For example, BA 6 has been shown to be related to working memory load (Cohen et al., 1997) and right premotor cortex is involved in spatial working memory storage (Smith and Jonides, 1999).

Other accounts of the role of the frontal lobe have also been proposed. Penhune et al. (1998) suggested that the IFG is responsible for short-term memory retrieval of standard time intervals. Rao et al. (1997) suggest that right IFG is involved, along with STG, in retrieval and rehearsal of representations of time intervals. Still other evidence suggests the IFG is active during recovery from attention lapses (Weissman et al., 2006). Further, right IFG was implicated in temporal decision-making processes by an fMRI study that measured decision-making activity as that activity that correlated with task difficulty (Wencil et al., 2010).

Our data implicate right but not left frontal regions in temporal processing. This finding is consistent with some (e.g., Rao et al., 1997; Brunia et al., 2000) but not all functional imaging studies (Schubotz et al., 2000; Shih et al., 2009). We note, however, that our recent voxel-wise meta-analysis of the functional imaging literature also demonstrated a substantial asymmetry in frontal activation; we found that the right but not left IFG was implicated in both sub- and suprasecond timing (Wiener et al., 2010b). Taken together, the data reported here from brain lesion subjects as well as the functional imaging meta-analysis strongly suggest that the right frontal lobe is a core element of the neural circuitry involved in temporal processing.

ADDITIONAL SUBSECOND FINDINGS

We also found that the basal ganglia, hippocampus, and left temporal lobe are important to discriminating time intervals of around

600 ms. The basal ganglia have long been implicated in timing behavior (for review, see Meck et al., 2008). Although we find a significant effect of basal ganglia damage for the subsecond duration only, the thrust of the literature depicts these structures as necessary for timing longer time intervals as well (e.g., Malapani et al., 1998; Matell et al., 2003). We note, however, that the association of lesions of the left basal ganglia with deficits in timing at 600 ms is inconsistent with a recent report from our lab that two subjects with extensive bilateral striatal lesions performed well on a variety of tasks, including the temporal discrimination task with 600 ms stimuli employed here, assessing timing of both sub- and suprasecond intervals (Coslett et al., 2010). One possible account for this discrepancy is that subjects with damaged voxels in the basal ganglia also had damage in other neural regions; as such, it is possible that damage to the basal ganglia only provided a timing impairment in the context of disruptions in other regions. Currently, VLSM does not allow one to distinguish between these alternatives. However, in light of our earlier findings, we suggest that the basal ganglia, when lesioned in isolation, are not necessary for many timing procedures in which they are nevertheless activated.

The left temporal lobe has been implicated in temporal discrimination by numerous imaging studies (Rao et al., 1997). Left temporal activation has been demonstrated not only in temporal discrimination with auditory stimuli (Rao et al., 2001) but also with visual stimuli as well (Coull et al., 2004, 2008). These findings support the auditory dominance hypothesis, which posits that auditory cortex, by virtue of the temporal acuity developed for language processing, is better tuned for temporal processing and thus is called upon to process time, regardless of the modality presented. Further evidence for this hypothesis comes from a study demonstrating that TMS to auditory cortex during somatosensory timing interferes with precision in a temporal discrimination task (Bolognini et al., 2009). Additionally, a recent study by Kanai et al. (2011) demonstrated that TMS to the auditory cortex disrupted performance on visual and auditory temporal discrimination tasks to the same degree, whereas visual cortex stimulation only disrupted performance for visually timed intervals.

Hippocampal involvement in memory for time has been shown in lesion work in rats (Olton et al., 1987) and humans (Noulhiane et al., 2007), although in humans medial temporal lesions only affected estimations of time intervals of greater than 3 min. The current results suggest a broader contribution of the hippocampus to timing.

Our VLSM analyses yielded no significant effects of parietal lesions on temporal discrimination, failing to replicate the results of numerous imaging (Coull et al., 2004; Shih et al., 2009), as well as TMS (Wiener et al., 2010a) studies. Perhaps of even greater relevance, our findings are inconsistent with several previous studies demonstrating abnormalities in temporal processing in subjects with parietal lesions (Harrington et al., 1998; Oliveri et al., 2009). One possible explanation for this discrepancy appeals to differences between VLSM and alternative methods for grouping subjects according to lesion location that are used to identify the site of pathology associated with a behavioral deficit. As previously described, the level of analysis in VLSM is the single voxel; traditional methods have employed analyses at a much coarser anatomic level (e.g., lobe or hemisphere). One consequence of the fact that the analysis is performed over single voxels is that VLSM is well suited to interrogate cognitive operations that are tightly linked to a specific brain structure. Techniques in which subjects are grouped on the basis of "frontal" or "parietal" involvement, in contrast, may be useful in the identification of brain–behavior relationships that have a more variable brain basis or which depend on neural systems distributed across larger brain regions. For example, if timing is disrupted by lesions anywhere in the posterior parietal cortex, subjects with lesions involving the supramarginal or angular gyri would be expected to exhibit deficits in temporal processing. Such lesions may not involve overlapping voxels, however, and therefore would not be identified with VLSM.

If multiple regions or large areas of abnormality in the posterior parietal lobe are necessary to generate abnormalities in timing, then, one might expect subjects grouped on the basis of damage in the posterior parietal cortex to be impaired on timing tasks in the absence of a discrete locus of abnormality on a VLSM analysis. Consistent with this speculation, we, like Harrington et al. (1998) observe deficits in subjects with lesions involving the posterior parietal cortex. Thus, although our VLSM analysis does not identify specific voxels in the parietal lobe that are associated with impaired performance on our timing task, these data do not permit one to infer that the parietal lobe is not relevant to timing.

Finally, we note that the failure to identify voxels in the parietal lobe that are associated with poor performance on the timing tasks is unlikely to be attributable solely to a lack of power. As demonstrated in the overlap map (**Figure 4**), there were as many subjects with lesions in this region as in the frontal regions in which significant effects were observed.

Several weaknesses of the study should be acknowledged. First, although we report the largest series of brain lesion subjects tested on a timing task to date, we are unable to offer any information about a number of brain regions that may be relevant to temporal processing. As we only included patients with hemispheric lesions, we are unable to assess the potential contributions of the cerebellum to timing. Furthermore, because most vascular lesions involve the peri-sylvian regions irrigated by the Middle Cerebral Artery, we lack power to detect effects of lesions involving the SMA, a structure that has been implicated in timing in a number of studies (Macar et al., 1999, 2004; Ferrandez et al., 2003; Wiener et al., 2010b).

Second, the temporal discrimination task utilized in the current study requires participants to compare two time intervals presented in close succession. Because the same "clock" is used to measure both intervals, this task is unlikely to be sensitive to differences in clock speed (cf, Wiener and Coslett, 2008).

In summary, VLSM analysis showed regions in the right frontal lobe to be common to timing intervals above and below 1 s. Lesions involving the left superior temporal cortex, hippocampus, and basal ganglia were found to be correlated with the ability to time the 600 ms interval only. The demonstration that subjects with posterior parietal lesions do not exhibit an abnormality on the VLSM analysis but perform abnormally relative to controls is consistent with the hypothesis that the posterior parietal lobe is important for interval timing but that the procedure(s) supported by the parietal lobe are not tightly localized.

REFERENCES

Avants, B., Schoenemann, P. T., and Gee, J. C. (2006). Lagrangian frame diffeomorphic image registration: morphometric comparison of human and chimpanzee cortex. *Med. Image Anal.* 10, 397–412.

Bates, E., Wilson, S. M., Saygin, A. P., Dick, F., Sereno, M. I., Knight, R. T., and Dronkers, N. F. (2003). Voxel-based lesion-symptom mapping. *Nat. Neurosci.* 6, 448–450.

Bolognini, N., Papagno, C., Moroni, D., and Maravita, A. (2009). Tactile temporal processing in the auditory cortex. *J. Cog. Neurosci.* 22, 1201–1211.

Brunia, C. H., de Jong, B. M., van den Berg-Lenssen, M. M., and Paans, A. M. (2000). Visual feedback about time estimation is related to a right hemisphere activation measured by pet. *Exp. Brain Res.* 130, 328–337.

Bueti, D., Walsh, V., Frith, C., and Rees, G. (2008). Different brain circuits underlie motor and perceptual representations of temporal intervals. *J. Cog. Neurosci.* 20, 204–214.

Cohen, J. D., Perlstein, W. M., Braver, T. S., Nystrom, L. E., Noll, D. C., Jonides, J., and Smith, E. E. (1997).Temporal dynamics of brain activation during a working memory task. *Nature* 386, 604–608.

Coslett, H. B., Shenton, J., Dyer, T., and Wiener, M. (2009). Cognitive timing: neuropsychology and anatomic basis. *Brain Res.* 1254, 38–48.

Coslett, H. B., Wiener, M., and Chatterjee, A. (2010). Dissociable neural systems for timing: evidence from subjects with basal ganglia lesions. *PLoS ONE* 5, e10324. doi:10.1371/journal.pone.0010324

Coull, J. T., Nazarian, B., and Vidal, F. (2008). Timing, storage, and comparison of stimulus duration engage discrete anatomical components of a perceptual timing network. *J. Cogn. Neurosci.* 20, 1–12.

Coull, J. T., Vidal, F., Nazarian, B., and Macar, F. (2004). Functional anatomy of the attentional modulation of time estimation. *Science* 303, 1506–1508.

Fellows, L. K., Stark, M., Berg, A., and Chatterjee, A. (2008). Patient registries in cognitive neuroscience research: advantages, challenges, and practical advice. *J. Cogn. Neurosci.* 20, 1107–1113.

Ferrandez, A. M., Hugueville, L., Lehericy, S., Poline, J. B., Marsault, C., and Pouthas, V. (2003). Basal ganglia and supplementary motor area subtend duration perception: an FMRI study. *Neuroimage* 19, 1532–1544.

Genovese, C. R., Lazar, N. A., and Nichols, T. (2002). Thresholding of statistical maps in functional neuroimaging using the false discovery rate. *Neuroimage* 15, 870–878.

Genovesio, A., Tsujimoto, S., and Wise, S. P. (2006). Neuronal activity related to elapsed time in prefrontal cortex. *J. Neurophysiol.* 95, 3281–3285.

Gibbon, J., Malapani, C., Dale, C. L., and Gallistel, C. (1997). Toward a neurobiology of temporal cognition: advances and challenges. *Curr. Opin. Neurobiol.* 7, 170–184.

Harrington, D. L., Haaland, K. Y., and Knight, R. T. (1998). Cortical networks underlying mechanisms of time perception. *J. Neurosci.* 18, 1085–1095.

Hinton, S. C., and Meck, W. H. (2004). Frontal-striatal circuitry activated by human peak-interval timing in the supra-seconds range. *Brain Res. Cogn. Brain Res.* 21, 171–182.

Holmes, C. J., Hoge, R., Collins, L., Woods, R., Toga, A. W., Evans, A. C. (1998). Enhancement of MR images using registration for signal averaging. *J. Comput. Assist. Tomogr.* 22, 324–333.

Jones, C. R. G., Rosenkranz, K., Rothwell, J. C., and Jahanshahi, M. (2004). The right dorsolateral prefrontal cortex is essential in time reproduction: an investigation with repetitive transcranial magnetic stimulation. *Exp. Brain Res.* 158, 366–372.

Kanai, R., Lloyd, H., Bueti, D., and Walsh, V. (2011). Modality-independent role of the primary auditory cortex in time estimation. *Exp. Brain Res.* 209, 465–471.

Kimberg, D. Y., Coslett, H. B., and Schwartz, M. F. (2007). Power in voxel-based lesion-symptom mapping. *J. Cogn. Neurosci.* 19, 1067–1080.

Koch, G., Oliveri, M., Torriero, S., Salerno, S., Lo Gerfo, E., and Caltagirone, C. (2007). Repetitive TMS of cerebellum interferes with millisecond time processing. *Exp. Brain Res.* 179, 291–299.

Lemus, L., Hernandez, A., and Romo, R. (2009). Neural encoding of auditory discrimination in ventral premotor cortex. *Proc. Natl. Acad. Sci. U.S.A.* 106, 14640–14645.

Leon, M. I., and Shadlen, M. N. (2003). Representation of time by neurons in the posterior parietal cortex of the macaque. *Neuron* 38, 317–327.

Lewis, P. A., and Miall, R. C. (2003). Distinct systems for automatic and cognitively controlled time measurement: evidence from neuroimaging. *Curr. Opin. Neurobiol.* 13, 250–255.

Lewis, P. A., and Miall, R. C. (2006). A right hemispheric prefrontal system for cognitive time measurement. *Behav. Processes* 71, 226–234.

Macar, F., Anton, J.-L., Bonnet, M., and Vidal, F. (2004). Timing functions of the supplementary motor area: an event-related fmri study. *Brain Res. Cogn. Brain Res.* 21, 206–215.

Macar, F., Lejeune, H., Bonnet, M., Ferrara, A., Pouthas, V., Vidal, F., and Maquet, P. (2002). Activation of the supplementary motor area and of attentional networks during temporal processing. *Exp. Brain Res.* 142, 475–485.

Macar, F., Vidal, F., and Casini, L. (1999). The supplementary motor area in motor and sensory timing: evidence from slow brain potential changes. *Exp. Brain Res.* 125, 271–280.

Malapani, C., Rakitin, B., Levy, R., Meck, W. H., Deweer, B., Dubois, B., and Gibbon, J. (1998). Coupled temporal memories in parkinson's disease: a dopamine-related dysfunction. *J. Cogn. Neurosci.* 10, 316–331.

Mangels, J. A., Ivry, R. B., and Shimizu, N. (1998). Dissociable contributions of the prefrontal and neocerebellar cortex to time perception. *Brain Res. Cogn. Brain Res.* 7, 15–39.

Matell, M. S., and Meck, W. H. (2004). Cortico-striatal circuits and interval timing: coincidence detection of oscillatory processes. *Brain Res. Cogn. Brain Res.* 21, 139–170.

Matell, M. S., Meck, W. H., and Nicolelis, M. A. (2003). Interval timing and the encoding of signal duration by ensembles of cortical and striatal neurons. *Behav. Neurosci.* 117, 760–773.

Meck, W. H., Penney, T. B., and Pouthas, V. (2008). Cortico-striatal representation of time in animals and humans. *Curr. Opin. Neurobiol.* 18, 145–152.

Mita, A., Mushiake, H., Shima, K., Mitsuzaka, Y., and Tanji, J. (2009). Interval time coding by neurons in the presupplementary and supplementary motor areas. *Nat. Neurosci.* 12, 502–507.

Nichelli, P., Clark, K., Hollnagel, C., and Grafman, J. (1995). Duration processing after frontal lobe lesions. *Ann. N. Y. Acad. Sci.* 769, 183–190.

Niki, H., and Watanabe, M. (1979). Prefrontal and cingulate unit activity during timing behavior in the monkey. *Brain Res.* 171, 213–224.

Noulhiane, M., Pouthas, V., Hasboun, D., Baulac, M., and Samson, S. (2007). Role of the medial temporal lobe in time estimation in the range of minutes. *Neuroreport* 18, 1035–1038.

Oliveri, M., Koch, G., Salerno, S., Torriero, S., Lo Gerfo, E., and Caltagirone, C. (2009). Representation of time intervals in the right posterior parietal cortex: implications for a mental time line. *Neuroimage* 46, 1173–1179.

Olton, D. S., Meck, W. H., and Church, R. M. (1987). Separation of hippocampal and amygdaloid involvement in temporal memory dysfunctions. *Brain Res.* 404, 180–188.

Penhune, V. B., Zatorre, R. J., and Evans, A. C. (1998). Cerebellar contributions to motor timing: a pet study of auditory and visual rhythm reproduction. *J. Cogn. Neurosci.* 10, 752–765.

Pentland, A. (1980). Maximum likelihood estimation: the best PEST. *Percept. Psychophys.* 28, 377–379.

Picton, T. W., Stuss, D. T., Shallice, T., Alexander, M. P., and Gillingham, S. (2006). Keeping time: effects of focal frontal lesions. *Neuropsychologia* 44, 1195–1209.

Pouthas, V., George, N., Poline, J.-B., Pfeuty, M., VandeMoorteele, P.-F., Hugueville, L., Ferrandez, A.-M., Lehericy, S., LeBihan, D., and Renault, B. (2005). Neural network involved in time perception: an fMRI study comparing long and short interval estimation. *Hum. Brain Map.* 25, 433–441.

Rammsayer, T. H. (1999). Neuropharmacological evidence for different timing mechanisms in humans. *Q. J. Exp. Psych. B* 52, 273–286.

Rammsayer, T. H. (2001). Effects of pharmacologically induced changes in NMDA-receptor activity on long-term memory in humans. *Learn. Mem.* 8, 20–25.

Rao, S. M., Harrington, D. L., Haaland, K. Y., Bobholz, J. A., Cox, R. W., and Binder, J. R. (1997). Distributed neural systems underlying the timing of movements. *J. Neurosci.* 17, 5528–5535.

Rao, S. M., Mayer, A. R., and Harrington, D. L. (2001). The evolution of brain activation during temporal processing. *Nat. Neurosci.* 4, 317–323.

Rissman, J., Gazzaley, A., and D'Esposito, M. (2008). Dynamic adjustments in prefrontal, hippocampal, and inferior temporal interactions with increasing visual working memory load. *Cereb. Cortex* 18, 1618–1629.

Schubotz, R. I., Friederici, A. D., and Yves von Cramon, D. (2000). Time perception and motor timing: a common cortical and subcortical basis revealed by FMRI. *Neuroimage* 11, 1–12.

Schwartz, M. F., Kimberg, D. Y., Walker, G. M., Faseyitan, O., Brecher, A., Dell, G. S., and Coslett, H. B. (2009). Anterior temporal involvement in semantic word retrieval: voxel-based lesion-symptom mapping evidence from aphasia. *Brain* 132, 3411–3427.

Shih, L. Y. L., Kuo, W.-J., Yeh, T.-C., Tzeng, O. J. L., and Hsieh, J.-C. (2009). Common neural mechanisms for explicit timing in the sub-second range. *Neuroreport* 20, 897–901.

Smith, A., Taylor, E., Lidzba, K., and Rubia, K. (2003). A right hemispheric frontocerebellar network for time discrimination of several hundreds of milliseconds. *Neuroimage* 20, 344–350.

Smith, E. E., and Jonides, J. (1999). Storage and executive processes in the frontal lobes. *Science* 283, 1657–1661.

Weissman, D. H., Roberts, K. C., Visscher, K. M., and Woldorff, M. G. (2006). The neural basis of momentary lapses in attention. *Nat. Neurosci.* 9, 971–978.

Wencil, E. B., Coslett, H. B., Aguirre, G. K., and Chatterjee, A. (2010). Carving the clock at its component joints: neural bases for interval timing. *J. Neurophysiol.* 104, 160–168.

Wichmann, F. A., and Hill, N. J. (2001a). The psychometric function: I. Fitting, sampling, and goodness of fit. *Percept. Psychophys.* 63, 1293–1313.

Wichmann, F. A., and Hill, N. J. (2001b). The psychometric function: II. Bootstrap-based confidence intervals and sampling. *Percept. Psychophys.* 63, 1314–1329.

Wiener, M., and Coslett, H. B. (2008). Disruption of temporal processing in a subject with probable frontotemporal dementia. *Neuropsychologia* 46, 1927–1939.

Wiener, M., Hamilton, R., Turkeltaub, P., Matell, M. S., and Coslett, H. B. (2010a). Fast forward: supramarginal gyrus stimulation alters time measurement. *J. Cogn. Neurosci.* 22, 23–31.

Wiener, M., Turkeltaub, P., and Coslett, H. B. (2010b). The image of time: a voxel-wise meta-analysis. *Neuroimage* 49, 1728–1740.

Wiener, M., Lohoff, F. W., and Coslett, H. B. (2011). Double dissociation of dopamine genes and timing in humans. *J. Cogn. Neurosci* 23, 2811–2821.

Conflict of Interest Statement: The authors declare that the research was conducted in the absence of any commercial or financial relationships that could be construed as a potential conflict of interest.

Received: 30 June 2011; paper pending published: 21 July 2011; accepted: 14 September 2011; published online: 04 October 2011.

Citation: Gooch CM, Wiener M, Hamilton AC and Coslett HB (2011) Temporal discrimination of sub- and suprasecond time intervals: a voxel-based lesion mapping analysis. Front. Integr. Neurosci. ***5****:59. doi: 10.3389/fnint.2011.00059*

frontiers in
INTEGRATIVE NEUROSCIENCE

OPINION ARTICLE
published: 18 August 2011
doi: 10.3389/fnint.2011.00038

Obsessive–compulsive disorder and memory-mixing in temporal comparison: is implicit learning the missing link?

Bon-Mi Gu[1]* and Keshav Kukreja[2]

[1] *Department of Psychology and Neuroscience, Duke University, Durham, NC, USA*
[2] *Department of Neuroscience, Rhodes College, Memphis, TN, USA*
**Correspondence: bg43@duke.edu*

Humans cope with uncertainty in their daily lives in a variety of ways. At one end of the spectrum would be individuals diagnosed with obsessive–compulsive disorder (OCD). OCD patients have difficulty tolerating even the slightest amount of uncertainty if it is related to their symptoms (see Gentes and Ruscio, 2011 for review). For example, a patient may wash his hands continuously for an hour to avoid germs, check the door repeatedly to ensure that it is locked safely, or hoard everything for the slight chance that they might need it later. In contrast, healthy individuals are able to ignore these uncertainties because they exploit their prior experiences, providing themselves with a sense of security. Acknowledging the reasons for their anxiety as trivial does not necessarily attenuate obsessive thoughts, and deficits in implicit processes dealing with uncertainty could be a potential reason for their sustained obsession. Dysfunctions in implicit learning have been reported in patients with OCD (Deckersbach et al., 2002; Kathmann et al., 2005), suggesting a possible role of implicit contextual knowledge in reducing the anxiety underlying obsessive behaviors.

The application of implicit knowledge could be useful in terms of optimizing behavioral performance in many cases, but it can also bias our behavior in unfavorable ways. For example, if a seasoned squash player were learning to play tennis for the first time, he would perform better than a novice due to the level of similarity between these two sports with regard to fine hand and wrist coordination. However, because he is accustomed to the shorter squash racquet, it would be difficult for him to adjust to the noticeably longer tennis racquet. Therefore, although this implicit knowledge would most likely increase the player's precision in performance by reducing the variability of hand movements, it would sacrifice accuracy due to the inherent differences between the racquet sizes and the required motor actions of grip balance and strength.

It was recently demonstrated that a Bayesian model, which optimizes reasoning through the trade-off between accuracy and precision, could simulate the biased performance of participants in situations where they are instructed to reproduce specific stimulus durations (Jazayeri and Shadlen, 2010; Mamassian and Landy, 2010). Participants tend to bias their reproductions toward the mean of the distribution; specifically, they overestimate "short" durations and underestimate "long" durations. This phenomenon was first referred to as Vierordt's law (Woodrow, 1951; Lejeune and Wearden, 2009; Mamassian and Landy, 2010) and, more recently, has been described as a form of "memory-mixing," which represents the distortions in temporal memory caused by the encoding of multiple signal durations into a single memory distribution (Penney et al., 1998, 2000; Klapproth, 2009; Grondin, 2010; Gu and Meck, 2011).

The reasons for the existence of "memory-mixing" remain largely unknown, although instructional ambiguity has been proposed as a possible explanation (Klapproth, 2009) and factors dealing with the scalar property of temporal memory may also be involved (Gibbon et al., 1984). Another plausible explanation is that the implicit knowledge of the underlying stimulus distribution generates behaviors that are less variable, but still biased. Devoting less attention to the encoding of the immediate stimulus could result in the reliance on prior context through automatic processing, thus generating a form of "memory-mixing." If "memory-mixing" is in fact generated by implicit knowledge of prior contexts and reliance on automatic processing, we could then hypothesize that patients with OCD, who are known to have deficits in implicit learning (Deckersbach et al., 2002; Kathmann et al., 2005), will display a lesser degree of "memory-mixing" on a temporal reproduction/comparison task in comparison to healthy participants.

Furthermore, there is evidence showing that patients with OCD could compensate for their deficiency in implicit learning with hippocampal-dependent explicit knowledge (Rauch et al., 2007). A combination of normal explicit learning and a deficit in implicit learning would suggest that an OCD patient's perception of the current trial's signal duration would be less influenced by the context of prior signal durations. Therefore, it is highly probable that they compensate for their inability to exploit implicit knowledge of the context (e.g., trial sequence and mixture of different signal durations) with increased vigilance to the present signal duration that they are asked to encode. This will eventually reduce the degree of uncertainty as well as the effect of "memory-mixing."

Nevertheless, we cannot discount the possibility that the "memory-mixing" could be caused by other factors. Instead of the implicit knowledge of the entire distribution of prior signal durations, the residual of the immediately preceding duration could be the main source of "memory-mixing." The effects of the most recent trial have been shown to significantly influence the subsequent trial (Gu and Meck, 2011), implicating a process whereby temporally close events have a greater effect on the current trial. If this is the case, then the strength of the residual components of the previous trial will determine the resulting degree of "memory-mixing."

Cognitive inflexibility in OCD patients has been observed through deficits in task-switching and reversal learning (Chamberlain et al., 2008; Gu et al., 2008). These effects imply that the mental rigidity of OCD patients causes them to maintain their previous memory sets, which creates difficulty in rapidly updating memory with new information. Therefore, patients

with OCD will display stronger residuals from previous trials during their performance on the subsequent trial, resulting in an increase of "memory-mixing." Furthermore, it is expected that the attention of OCD patients would be especially captured by information encoded during the previous trial if it is related to feedback and/or has an emotional valence (see Droit-Volet and Meck, 2007; Gu et al., 2011). For example, if a neutral and OC-related emotional stimulus are presented in combination with 1.0 and 0.6 s durations, respectively, it is likely that the reproduction of the durations associated with the neutral stimulus preceded by the shorter emotional stimulus would be underestimated.

In conclusion: We have hypothesized two scenarios whereby "memory-mixing" would be expected to occur within a temporal reproduction/comparison task for patients with OCD who are thought to have altered dopaminergic activity in the cortico-striatal circuits involved in timing and time perception (Buhusi and Meck, 2005; Meck et al., 2008; Allman and Meck, 2011; Gu et al., 2011). It is possible that OCD patients would exhibit more "memory-mixing" than control participants due to the strong residuals from the previous trial. However, it would be more plausible that they exhibit a lesser degree of "memory-mixing" due to their inability to exploit implicit knowledge while simultaneously displaying increased vigilance toward the signal presented on the current trial. This would be especially likely if a sufficiently long inter-trial interval is presented without the intervention of any emotional stimuli. The potential significance of this hypothesis lies within its ability to aid in our understanding of how normal individuals and OCD patients deal with uncertainty in their environment. We necessarily choose a balance between utilizing our accumulated implicit knowledge and increasing our vigilance to systematic changes in the environment (Buhusi and Meck, 2009; Gu et al., 2011).

REFERENCES

Allman, M. J., and Meck, W. H. (2011). Pathophysiological distortions in time perception and timed performance. *Brain* (in press).

Buhusi, C. V., and Meck, W. H. (2005). What makes us tick? Functional and neural mechanisms of interval timing. *Nat. Rev. Neurosci.* 6, 755–765.

Buhusi, C. V., and Meck, W. H. (2009). Relative time sharing: new findings and an extension of the resource allocation model of temporal processing. *Philos. Trans. R. Soc. Lond. B. Biol. Sci.* 364, 1875–1885.

Chamberlain, S. R., Menzies, L., Hampshire, A., Suckling, J., Fineberg, N. A., del Campo, N., Aitken, M., Craig, K., Owen, A. M., Bullmore, E. T., Robbins, T. W., and Sahakian, B. J. (2008). Orbitofrontal dysfunction in patients with obsessive-compulsive disorder and their unaffected relatives. *Science* 321, 421–422.

Deckersbach, T., Savage, C. R., Curran, T., Bohne, A., Wilhelm, S., Baer, L., Jenike, M. A., and Rauch, S. L. (2002). A study of parallel implicit and explicit information processing in patients with obsessive-compulsive disorder. *Am. J. Psychiatry* 159, 1780–1782.

Droit-Volet, S., and Meck, W. H. (2007). How emotions colour our perception of time. *Trends Cogn. Sci. (Regul. Ed.)* 11, 504–513.

Gentes, E. L., and Ruscio, A. M. (2011). A meta-analysis of the relation of intolerance of uncertainty to symptoms of generalized anxiety disorder, major depressive disorder, and obsessive-compulsive disorder. *Clin. Psychol. Rev.* 31, 923–933.

Gibbon, J., Church, R. M., and Meck, W. H. (1984). Scalar timing in memory. *Ann. N. Y. Acad. Sci.* 423, 52–77.

Grondin, S. (2010). Timing and time perception: a review of recent behavioral and neuroscience findings and theoretical directions. *Atten. Percept. Psychophys* 72, 561–582.

Gu, B. M., and Meck, W. H. (2011). "New perspectives on Vierordt's law: memory-mixing in ordinal temporal comparison tasks," in *Time and Time Perception 2010, LNAI 6789*, eds A. Vatakis, A. Esposito, F. Cummins, G. Papadelis, and M. Giagkou (Berlin: Springer-Verlag), 67–78.

Gu, B. M., Park, J. Y., Kang, D. H., Lee, S. J., Yoo, S. Y., Jo, H. J., Choi, C. H., Lee, J. M., and Kwon, J. S. (2008). Neural correlates of cognitive inflexibility during task-switching in obsessive-compulsive disorder. *Brain* 131, 155–164.

Gu, B. M., Cheng, R. K., Yin, B., and Meck, W. H. (2011). Quinpirole-induced sensitization to noisy/sparse periodic input: temporal synchronization as a component of obsessive-compulsive disorder. *Neuroscience* 179, 143–150.

Jazayeri, M., and Shadlen, M. N. (2010). Temporal context calibrates interval timing. *Nat. Neurosci.* 13, 1020–1026.

Kathmann, N., Rupertseder, C., Hauke, W., and Zaudig, M. (2005). Implicit sequence learning in obsessive-compulsive disorder: further support for the fronto-striatal dysfunction model. *Biol. Psychiatry* 58, 239–244.

Klapproth, F. (2009). Single-modality memory mixing in temporal generalization: an effect due to instructional ambiguity. *Neuroquantology* 7, 85–94.

Lejeune, H., and Wearden, J. H. (2009). Vierordt's "the experimental study of the time sense" (1868) and its legacy. *Eur. J. Cogn. Psychol.* 21, 941–960.

Mamassian, P., and Landy, M. S. (2010). It's that time again. *Nat. Neurosci.* 13, 914–916.

Meck, W. H., Penney, T. B., and Pouthas, V. (2008). Cortico-striatal representation of time in animals and humans. *Curr. Opin. Neurobiol.* 18, 145–152.

Penney, T. B., Allan, L. G., Meck, W. H., and Gibbon, J. (1998). "Memory mixing in duration bisection," in *Timing of Behavior: Neural, Psychological and Computational Perspectives*, eds D. A. Rosenbaum and C. E. Collyer (Cambridge, MA: MIT Press), 165–193.

Penney, T. B., Gibbon, J., and Meck, W. H. (2000). Differential effects of auditory and visual signals on clock speed and temporal memory. *J. Exp. Psychol. Hum. Percept. Perform.* 26, 1770–1787.

Rauch, S. L., Wedig, M. M., Wright, C. I., Martis, B., McMullin, K. G., Shin, L. M., Cannistraro, P. A., and Wilhelm, S. (2007). Functional magnetic resonance imaging study of regional brain activation during implicit sequence learning in obsessive-compulsive disorder. *Biol. Psychiatry* 61, 330–336.

Woodrow, H. (1951). "Time perception," in *Handbook of Experimental Psychology*, ed. S. S. Stevens (New York, NY: Wiley), 1224–1236.

Received: 26 July 2011; accepted: 30 July 2011; published online: 18 August 2011.

Citation: Gu B-M and Kukreja K (2011) Obsessive–compulsive disorder and memory-mixing in temporal comparison: is implicit learning the missing link? Front. Integr. Neurosci. ***5****:38. doi: 10.3389/fnint.2011.00038*

frontiers in
INTEGRATIVE NEUROSCIENCE

ORIGINAL RESEARCH ARTICLE
published: 19 October 2011
doi: 10.3389/fnint.2011.00060

Slow modulation of ongoing discharge in the auditory cortex during an interval-discrimination task

Juan M. Abolafia[1], Marina Martinez-Garcia[2], Gustavo Deco[2,3] and Maria V. Sanchez-Vives[1,3]*

[1] *Institut d'Investigacions Biomèdiques August Pi i Sunyer, Barcelona, Spain*
[2] *Computational Neuroscience Group, Department of Information and Communication Technologies, Universitat Pompeu Fabra, Barcelona, Spain*
[3] *Institució Catalana de Recerca i Estudis Avançats, Barcelona, Spain*

Edited by:
Agnes Gruart, University Pablo de Olavide, Spain

Reviewed by:
Israel Nelken, Hebrew University, Israel
Manuel S. Malmierca, University of Salamanca, Spain

****Correspondence:***
Maria V. Sanchez-Vives, Institut d'Investigacions Biomèdiques August Pi i Sunyer, Roselló 149-153, 08036 Barcelona, Spain.
e-mail: msanche3@clinic.ub.es; sanchez.vives@gmail.com

In this study, we recorded single unit activity from rat auditory cortex while the animals performed an interval-discrimination task. The animals had to decide whether two auditory stimuli were separated by either 150 or 300 ms, and go to the left or right nose poke accordingly. Spontaneous firing in between auditory responses was compared in the attentive versus non-attentive brain states. We describe the firing rate modulation detected during intervals while there was no auditory stimulation. Nearly 18% of neurons ($n = 14$) showed a prominent neuronal discharge during the interstimulus interval, in the form of an upward or downward ramp towards the second auditory stimulus. These patterns of spontaneous activity were often modulated in the attentive versus passive trials. Modulation of the spontaneous firing rate during the task was observed not only between auditory stimuli, but also in the interval preceding the stimulus. These slow modulatory components could be locally generated or the result of a top-down influence originated in higher associative association areas. Such a neuronal discharge may be related to the computation of the interval time and contribute to the perception of the auditory stimulus.

Keywords: auditory, decision-making, spontaneous, awake, rat

INTRODUCTION

Sensory areas such as primary auditory cortex are primarily associated with stimulus encoding and there are different aspects of neuronal responses relevant to this function. Spike count (Polley et al., 2004; Weinberger, 2004; Fritz et al., 2005, 2007; Nelken et al., 2005), spike timing (Kayser et al., 2010), a combination of both spike count and spike timing (Lu and Wang, 2004; Imaizumi et al., 2010), or neuronal firing pattern (Kayser et al., 2009) have all been associated to cortical auditory encoding. However there is increasing evidence that early cortices, and in particular auditory cortex, are not only feature detectors. Multimodal responses (Kayser et al., 2008; Lemus et al., 2010), attentional modulation (Hubel et al., 1959; Gottlieb et al., 1989; Otazu et al., 2009), expectation (Jaramillo and Zador, 2011), or reward-modulation (Shuler and Bear, 2006) illustrate additional contextual aspects that modulate responses even in early sensory cortices. While fast responses to auditory stimuli have been characterized in detail in auditory cortex, the slow modulation of neuronal firing to evoked and spontaneous activity has barely been studied. Slow modulation of sustained responses has been found to predict the behavioral decisions during auditory categorization tasks in monkeys, including errors (Selezneva et al., 2006). Sensory or behavioral events contingent on reinforcement can also result on slow modulation of firing rate or sustained firing as a consequence of a learning process (Brosch et al., 2011b). Therefore, slow modulation of firing could constitute an anticipatory mechanism that associates events (stimulus–behavior–reinforcer) that are relevant or adaptive to the environment. These cognitive components associated to stimulus discrimination tasks have been more commonly associated to higher areas such as frontal areas (Romanski and Goldman-Rakic, 2002; Lemus et al., 2009).

In the present study we recorded the activity of 86 neurons from the auditory cortex of the behaving rat. We aimed at exploring the slow modulation of neuronal firing in the intervals between stimuli while the rat was performing an interval-based decision-making task.

MATERIALS AND METHODS

Single unit recordings from two Lister Hooded rats were obtained by means of chronically implanted tetrodes in the primary auditory cortex (Doron et al., 2002). Surgical protocol and recordings were the same as the ones described in (Abolafia et al., 2011). Rats were cared for and treated in accordance with the Spanish regulatory laws (BOE 256; 25 October 1990) which comply with the EU guidelines on protection of vertebrates used for experimentation (Strasbourg 18 March 1986).

EXPERIMENTAL SET UP

The recordings were performed inside a box built in black acrylic with a surface of 22 cm (L) × 25.5 cm (W) × 35 cm (H). The box in which the recordings were performed was placed inside two wooden boxes placed inside the other. Between each box, two isolating foam rubbers (4 and 2 cm thick) were placed to soundproof for low and high frequencies. A wooden lid and equal soundproof foams closed the whole recording chamber. A hole permitted the entry of a recording wire (2 mm thick) connected to a preamplifier. Water-valves were placed outside the wooden boxes. Animals poked their nose into three different sockets, each one 2 cm wide

and separated by 3 cm. The top part of the socket did not have a lid to avoid being hit with the microdrive. During the recordings, the rat could move freely within the limited space of the chamber. Recordings were obtained in the dark, and the experiment was filmed with an infrared camera placed above the recording chamber.

BEHAVIORAL PROTOCOL

The experimental procedure consisted of a sequence of different recording stages, including passive and attentive stages and with a total duration of *ca.* 3 h. Animals only went through the whole session once a day.

A tuning curve (*ca.* 24 min) and a passive listening recording stage (*ca.* 17 min) were performed before and after the attentive stage (*ca.* 40 min). The final stage comprised a passive recording with a reward (*ca.* 40 min) delivery after each pair of stimuli was presented. The aim was to compare the neuronal responses while the idle animal listened to stimuli presentation with respect to the attentive brain state during task performance. In the attentive task, the animal was trained to poke its nose into the center socket which immediately triggered the onset of two identical stimuli (80 dB, 5.3 kHz, 50 ms duration). The animal had to remain in the center socket until the end of the stimuli presentation. The animals had to discriminate whether the two stimuli were separated (from the end of stimulus 1 to beginning of stimulus 2) by 150 or 300 ms. This required a left or a right nose poke in order to get a water reward. In the attentive task, false alarms (poking in the opposite side) or early withdrawals (withdrawal before stimuli termination) were punished with a 3-s timeout and a white noise (WAV-file, 0.5 s, 80 dB SPL). Passive stages had the same amount of trials (180 trials each side), stimuli (50 ms; 80 dB; 5.3 kHz), interstimulus interval (150 and 300 ms), and intertrial interval (2–3 s) as for the attentive task.

Animals were implanted and recorded whenever they reached 75% correct trials.

PRESENTATION OF SOUND STIMULI

Protocols of stimulation were controlled through Matlab®, a National Instrument card (BNC-2110), and a breakout box (FS 300 kHz). Sound triggers had microseconds precision. Sound stimuli were delivered through earphones (ER.6i Isolator, Etymotic Research Inc.) screwed in each recording session to earphone holders chronically attached to the animal skull with dental cement. The earphones were adjusted inside the ear with a silicone tip which allowed the isolation from any sound unrelated to the protocol. Sound calibration was performed with a microphone (MM1, Beyerdynamic) placed 1 mm away from the earphone, and a preamplifier (USB Dual Pre, Applied Research and Technology). The sound stimuli during the passive and attentive recording stages had a 50-ms duration, an intensity of 80 dBs SPL, and pure tones of 5322 Hz with a 6-ms rise/fall cosine ramps. It was therefore identical for both the first and second stimulus. Interstimulus intervals were 150 or 300 ms, and both had the same amount of trials (180). Similarly, the total number of correct trials in the attentive stage was the same as in the passive one (180). The intertrial interval also had a similar duration in the attentive and passive stages (2–3 s).

DATA ANALYSIS

Cluster cutting and peri-stimulus time histograms (PSTH) were performed according to the methods described in (Abolafia et al., 2011). Cluster cutting (isolating single units from the multiunit recorded data) was performed using an Off-Line Spike Sorter (OFSS, Plexon). Waveforms were first sorted into units by using the valley-seeking algorithm (Koontz and Fukunaga, 1972). Waveforms were considered to have been generated by a single neuron when they occurred simultaneously in the four electrodes that defined a discrete cluster in 3D principal component (or peak-to-peak) space distinct from clusters for other units using a MANOVA test ($p < 0.05$). Single units exhibited a recognizable refractory period (>1 ms) in their InterSpikeInterval histograms and had a characteristic and distinct waveform shape and peak-to-peak amplitude when compared to other spikes. Additional criteria were used in order to isolate single units such as the difference between InterSpikeInterval histograms or the crosscorrelograms among the recorded neurons.

RESULTS

Eighty-six single units from the rat auditory cortex were isolated and classified (Recanzone, 2000; Hromadka et al., 2008) according to their phasic auditory responses as: *onset* (26%), *onset* + *offset* (13%), *offset* (2%), *non-responsive* (43%), *suppressive* (13%), and *"other"* (3%). The percentage of non-responsive neurons was similar to the one reported by means of cell-attached recordings in the head-fixed awake animal (Hromadka et al., 2008).

We designed an interval-discrimination task where the rat had to go to the left or to the right depending on the duration of the interval between stimuli (150 or 300 ms; **Figure 1**). The interval between stimuli was thus behaviorally relevant in this task. In this study we describe different patterns of neuronal discharges

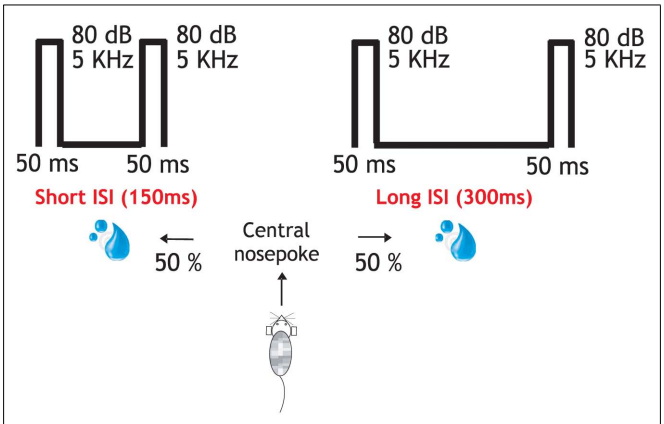

FIGURE 1 | Behavioral protocol and performance. In the attentive task the rat entered in the central socket and two identical stimuli (50 ms; 80 dB; 5322 Hz) were presented through earphones. About 150 or 300 ms interstimulus interval indicated left or right reward delivery, respectively. These same stimuli (interstimulus interval (150 and 300 ms), intertrial interval (2–3 s), and trial repetitions (180) were delivered under different stages: "Initial passive," attentive, "passive post" identical to the "initial passive" one and another passive recording but now followed by a reward after each pair of stimuli presentation. The total duration of the recording protocol was 3 h.

occurring during the intervals in between stimuli and thus in the absence of auditory stimulation. We show that the neuronal firing occurring between auditory stimuli in the auditory cortex can be quite prominent and that is often modulated by attention. Finally, the possible functional role of this slow modulation of neuronal discharge is discussed.

We found that 17.4% ($n = 14$) of the recorded neurons showed a prominent neuronal discharge during the interstimulus interval, in the form of either an upward or downward ramp towards the second auditory stimulus. While in some of the neurons the activity during the interval ramped up toward the second stimuli ($n = 6$; **Figures 2A,B**, and **3A,B,C**), in others the activity ramped down following a sort of post-discharge ($n = 6$; **Figures 3D,E** and **4A,B**). In the two remaining neurons the activity during the interval remained rather in a plateau (**Figure 3F**). The neurons shown here further illustrate the large heterogeneity of neuronal responses that have been described in auditory cortex.

Figure 2 illustrates the PSTHs from two different neurons while the rat was performing the task. During the passive sound stimulation, the neuron in **Figure 2A** had a weak offset response to the first auditory stimulus and a subsequent decrease in the firing during the interval, that progressively increased towards the second stimulus. During attention these responses became more prominent (**Figure 2A**; top PSTHs). The offset response was increased, and neuronal activity ramped up toward the second stimulus well above the spontaneous activity preceding the first stimulus. Interestingly, the response to the second stimulus was not an offset response but a sustained one. This is the case for both the short and the long interval trials, which were randomly given. The neuron illustrated in **Figure 2B** is of a different type, a "suppressive" response (Hromadka et al., 2008), since its discharge was silenced by auditory stimulation. This is well appreciated in the raster plots that correspond to the attentional trials (**Figure 2B**, top PSTHs). Still, even when the neuron was silenced by the auditory stimulation, its activity ramped up toward the second stimulus, more prominently in the attentional trials than in the passive ones. The second auditory stimulus again decreased its firing rate, which remained decreased for 200 ms following stimulation.

Out of the six neurons with increasing activity toward the second stimulus, all of them had an up-regulation of this activity during attentive trials. When the average firing rate during the first half of the interval was compared against that during the second, the activity increased in a 17% in passive trials and 246% in attentive ones for the short (150 ms) intervals. For the long (300 ms) intervals these values were 58 and 192% respectively.

In some cases, the activity occurring in between auditory stimuli was not ramping-up toward the second stimulus, as the one illustrated above, but rather appeared as a prominent post-discharge following the auditory stimulation (**Figures 3D,E** and **4A**.) In the neuron illustrated in **Figure 4A**, each auditory response was followed by a post-discharge lasting around 200 ms. In this neuron, not only the auditory responses but also the auditory post-discharge was significantly increased by attention. A total of five neurons showed a similar modulation by attention, the post-discharge increasing an average of 45% (short ISIs) and 53% (long ISIs) in attentive versus passive trials. In one neuron, the post-discharge was decreased in a 40% by attention. In the case

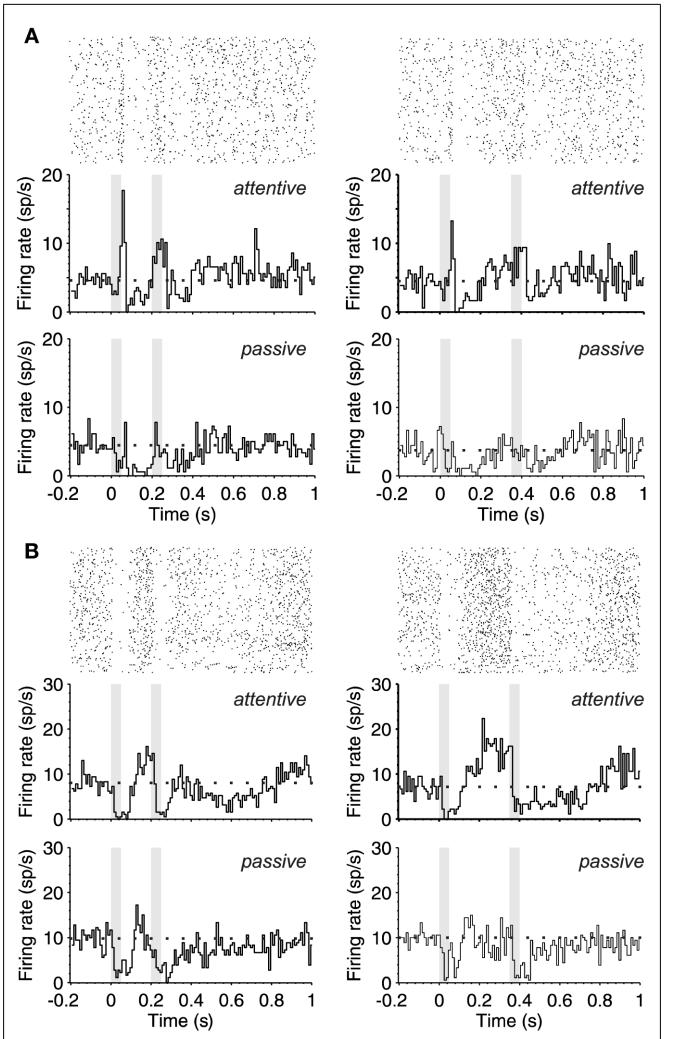

FIGURE 2 | Ramping-up activity during the interstimulus interval. (A) Upper part. PSTH (180 trials) of the response (bottom) and raster plot (top) of a single neuron during the attentive task shows the response pattern to two identical stimuli (50 ms; 80 dB; 5322 Hz) separated by 150 ms (left) and 300 ms (right). The gray boxes correspond to the periods of auditory stimulation. The PSTH shows an offset response to stimulus 1 and onset response during stimulus 2 while in the passive brain state (lower part) there is an overall decrease of excitability and no monotonic increase of spontaneous activity toward S2 presentation. **(B)** Same as in **(A)**, but this other neuron is silenced by the auditory stimulation followed by an increase of firing until S2 occurrence (upper part), while in the passive brain state (lower part) the neuronal firing is markedly reduced. In **(A,B)** the mean spontaneous activity is represented with a dotted line.

of the neuron illustrated in **Figure 4A**, the firing rate during the 200-ms preceding the first auditory stimulus was also significantly increased by attention. This is the period of time that takes place when the animal is heading to the central nose poke that triggers stimulus presentation.

The firing rate during the period preceding auditory stimulation was also significantly increased during attentive trials in the neuron displayed in **Figure 4B**, which on the other hand had a rather different auditory response. This neuron had a weak

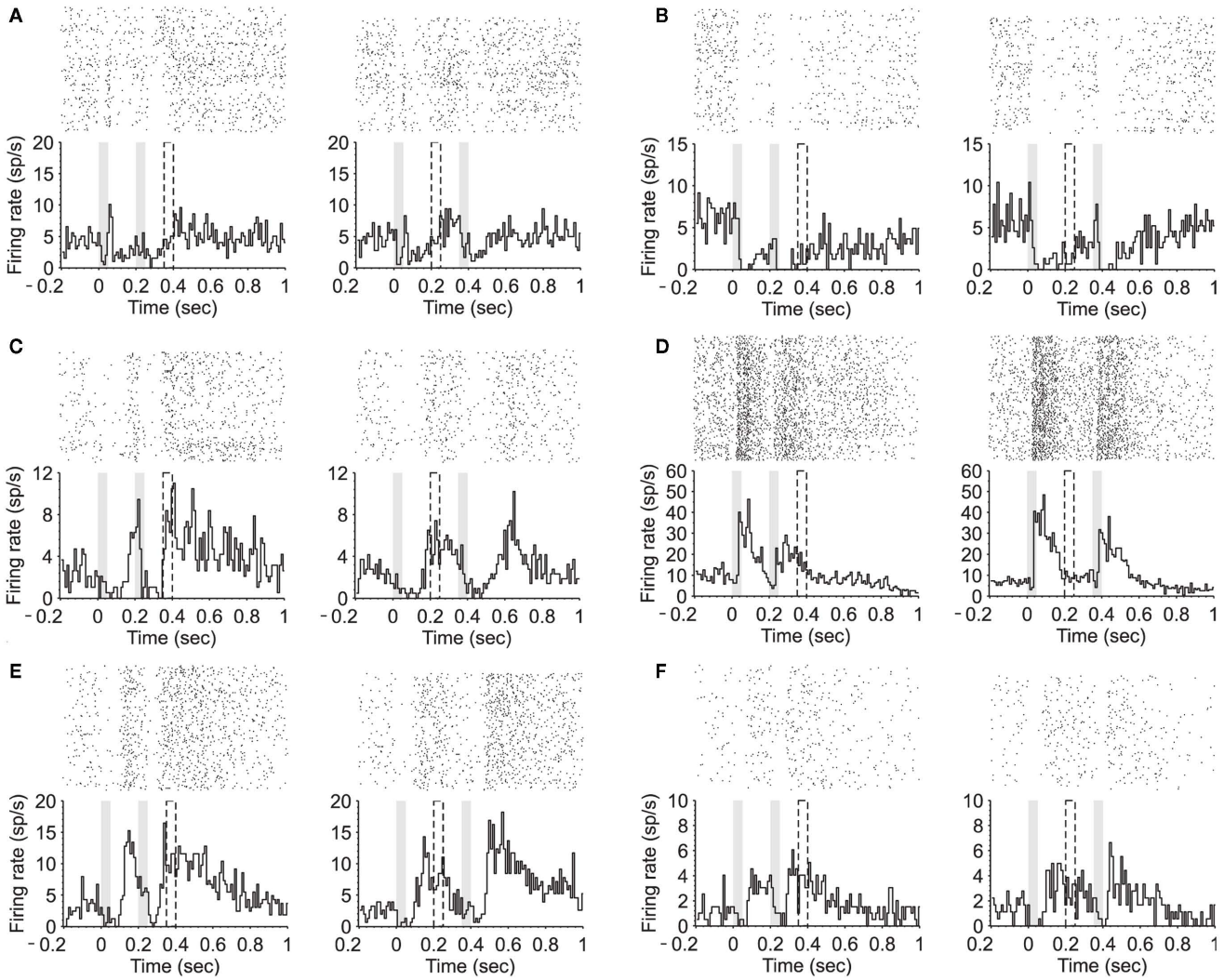

FIGURE 3 | Modulation of neuronal firing between stimuli presentation. (A–C) PSTH (180 trials) of two equal stimuli (50 ms; 80 dB; 5322 Hz) separated by either 150 ms (left) or 300 ms (right). Three example neurons during the attentive task show suppressive activity during stimuli presentation followed by an increased firing until S2 is presented. **(D,E)** PSTHs of two different neurons showing firing activity during the interval that decreases toward the second stimulus. **(F)** PSTH of an example neuron showing a late onset response accompanied by a sustained activity after stimuli termination.

spontaneous discharge preceding the auditory stimulation, and no response to the auditory stimulus. However, a very large post-discharge followed each auditory stimulus. This unusual pattern of response took place during non-attentional trials. During attentional trials, those prominent post-discharges disappeared, and instead, the discharge preceding the first stimulus was increased, as did the example in **Figure 4A**. An enhanced firing rate preceding the occurrence of the first stimulus could be related to stimulus expectancy (Jaramillo and Zador, 2011) or to prediction of reward (Shuler and Bear, 2006), both described in early sensory cortices.

DISCUSSION

We recorded from neurons from the rat primary auditory cortex while the animal was performing an interval-discrimination task. Here we report about 14 particular neurons that showed prominent responses during the intervals between stimuli, with firing rates that either increased or decreased toward the second stimulus. These neuronal discharges could be refered to as spontaneous activity, since they occurred while there was no auditory stimulation. However the term "spontaneous activity" has been avoided since these neuronal discharges were often associated to the preceding auditory responses, even if with a slow time course of over 150 ms. The neuronal discharges occurring in the absence of auditory stimulation were enhanced by attention in 12 (out of 14) cases, while they were decreased in the remaining two.

Most of the studies of the effects of attention on auditory responses have focused on how phasic responses modulate their

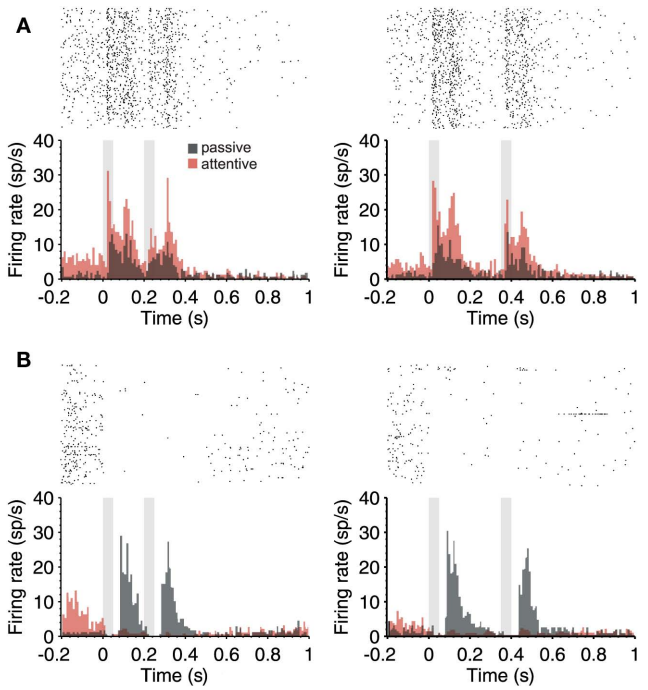

FIGURE 4 | Attention-modulated firing rate in the periods in between auditory stimuli. (A) PSTH (180 trials) of a single neuron during the passive (gray) and attentive (red) task where two identical stimuli (50 ms; 80 dB; 5322 Hz) separated by 150 ms (left) and 300 ms (right) were delivered. Notice that not only the response but also prominent responses in the absence of stimuli (preceding and between stimuli) are up regulated by attention. **(B)** Example neuron that had no auditory response, but a prominent and slow response after the termination of auditory stimuli during passive trials. This response was silenced during the attentive trials. However, notice that the activity preceding the first auditory stimulus was increased during attention (in red). In both cases **(A,B)**, the raster plots correspond to the attentive trials. In all cases, 150 and 300 ms intervals were given randomly during the same sessions.

response properties according to the brain state (Hocherman et al., 1976; Pfingst et al., 1977; Benson and Hienz, 1978; Fritz et al., 2003; Schnupp et al., 2006; Yin et al., 2008; Otazu et al., 2009; Liu et al., 2010). Slow modulation of firing rate in the auditory cortex of the behaving monkey has been previously found to be related to the processing of stimuli, motor decision, or even reward (Selezneva et al., 2006; Yin et al., 2008; Brosch et al., 2011b), as it has been in primary visual cortex (Shuler and Bear, 2006). During behavioral experiments, this slow or sustained (up to several seconds) part of the response is related to event sequences during a task and provides a neuronal mechanism for anticipation and association of events related to hearing and relevant to behavior (Brosch et al., 2011b). Altogether, slow modulation of firing could complement the representation of the timing of auditory stimuli as well as the codification of stimuli by means of phasic responses. A similar pattern was reported by (Gottlieb et al., 1989; Durif et al., 2003; Yin et al., 2008).

Some studies have found no changes in spontaneous activity under attentional demands (Pfingst et al., 1977; Benson and Hienz, 1978; Otazu et al., 2009). On the other hand, an increase in spontaneous firing rate at the end of the trial under attention with respect to the passive state has been reported, enhancement that could be reflecting motor-related aspects (Scott et al., 2007). Single units from auditory cortex have also been shown to have enhanced sustained responses preceding a target stimulus (Sakurai, 1990). Here we have shown that the spontaneous discharge is increased by attention in the period preceding the first stimulus in two neurons (**Figures 4A,B**).

The mechanisms for these slow modulations of firing rate are not known. One possibility would be that they reflect top-down modulation. Not only cortical, but also subcortical areas present modulation of spontaneous activity within tasks. Late trial neuronal activity in the monkey inferior colliculus has been described to be modulated by context, like a "reward expectation" signal (Metzger et al., 2006). Reward-modulation of the late activity after the end of the auditory stimulus has also been described in the rat auditory thalamus (Komura et al., 2005). A difference of these ramping activities with respect to the ones we have illustrated (**Figure 2**) is that the ramping-up here was preceding the second stimulus, and not the reward (Yin et al., 2008; Brosch et al., 2011a). The reward in our protocols occurred after the second stimulus, whenever the animal poked his nose in the correct side and thus triggered its delivery. It did not occur at a fixed time (usually after 1 s in the illustrated PSTHs). The ramping activity illustrated in **Figure 2B** between 0.6 and 1 s could be interpreted as such or associated to motor activity. We can speculate that the ramping-up activity in between stimuli (**Figures 2A,B**) could be rather associated to stimulus expectation or to interval-computation. In this respect, a recent study (Jaramillo and Zador, 2011) showed that neurons from the primary auditory cortex increased their firing rate as the target approached. This firing rate modulation reflected a temporal expectation which improved sound processing, therefore increasing the probability of obtaining a reward.

In all, neuronal firing in early auditory cortex in the absence of auditory stimulation could provide a neuronal mechanism for anticipation and memory, reflecting a learning process where consecutive sensory and behavioral events are associated with reinforcement. The slow modulation of ongoing firing during the interval between stimuli and the post-stimulus period could act as a mechanism to track and integrate time between stimuli presentations and be part of the neuronal basis of interval-categorization by means of tonic firing, particularly in attentive stages.

ACKNOWLEDGMENTS

We thank A. Zador, S. Jaramillo, G. Otazu for their help, and suggestions about the behavioral paradigm, to S. Aliagas for the animal training. We also thank L. Alonso, L. Pérez-Méndez, and D. Perez-Marcos for their programming work. Supported by a grant from the Ministerio de Ciencia e Innovación (BFU2008-01371/BFI) to MVS–V. MM–G and GD were supported by the European Union grant BRAINSCALES, by the Spanish Research Project SAF2010-16085 and by the CONSOLIDER-INGENIO 2010 Programme CSD2007-00012, and EU FP7/2007-2013 under grant agreement 214728-2.

REFERENCES

Abolafia, J. M., Vergara, R., Arnold, M. M., Reig, R., and Sanchez-Vives, M. V. (2011). Cortical auditory adaptation in the awake rat and the role of potassium currents. *Cereb. Cortex* 21, 977–990.

Benson, D. A., and Hienz, R. D. (1978). Single-unit activity in the auditory cortex of monkeys selectively attending left vs. right ear stimuli. *Brain Res.* 159, 307–320.

Brosch, M., Selezneva, E., and Scheich, H. (2011a). Representation of reward feedback in primate auditory cortex. *Front. Syst. Neurosci.* 5:5. doi:10.3389/fnsys.2011.00005

Brosch, M., Selezneva, E., and Scheich, H. (2011b). Formation of associations in auditory cortex by slow changes of tonic firing. *Hear. Res.* 271, 66–73.

Doron, N. N., Ledoux, J. E., and Semple, M. N. (2002). Redefining the tonotopic core of rat auditory cortex: physiological evidence for a posterior field. *J. Comp. Neurol.* 453, 345–360.

Durif, C., Jouffrais, C., and Rouiller, E. M. (2003). Single-unit responses in the auditory cortex of monkeys performing a conditional acousticomotor task. *Exp. Brain Res.* 153, 614–627.

Fritz, J., Elhilali, M., and Shamma, S. (2005). Active listening: task-dependent plasticity of spectrotemporal receptive fields in primary auditory cortex. *Hear. Res.* 206, 159–176.

Fritz, J., Shamma, S., Elhilali, M., and Klein, D. (2003). Rapid task-related plasticity of spectrotemporal receptive fields in primary auditory cortex. *Nat. Neurosci.* 6, 1216–1223.

Fritz, J. B., Elhilali, M., David, S. V., and Shamma, S. A. (2007). Does attention play a role in dynamic receptive field adaptation to changing acoustic salience in A1? *Hear. Res.* 229, 186–203.

Gottlieb, Y., Vaadia, E., and Abeles, M. (1989). Single unit activity in the auditory cortex of a monkey performing a short term memory task. *Exp. Brain Res.* 74, 139–148.

Hocherman, S., Benson, D. A., Goldstein, M. H. Jr., Heffner, H. E., and Hienz, R. D. (1976). Evoked unit activity in auditory cortex of monkeys performing a selective attention task. *Brain Res.* 117, 51–68.

Hromadka, T., Deweese, M. R., and Zador, A. M. (2008). Sparse representation of sounds in the unanesthetized auditory cortex. *PLoS Biol.* 6, e16. doi:10.1371/journal.pbio.0060016

Hubel, D. H., Henson, C. O., Rupert, A., and Galambos, R. (1959). Attention units in the auditory cortex. *Science* 129, 1279–1280.

Imaizumi, K., Priebe, N. J., Sharpee, T. O., Cheung, S. W., and Schreiner, C. E. (2010). Encoding of temporal information by timing, rate, and place in cat auditory cortex. *PLoS ONE* 5, e11531. doi:10.1371/journal.pone.0011531

Jaramillo, S., and Zador, A. M. (2011). The auditory cortex mediates the perceptual effects of acoustic temporal expectation. *Nat. Neurosci.* 14, 246–251.

Kayser, C., Logothetis, N. K., and Panzeri, S. (2010). Millisecond encoding precision of auditory cortex neurons. *Proc. Natl. Acad. Sci. U.S.A.* 107, 16976–16981.

Kayser, C., Montemurro, M. A., Logothetis, N. K., and Panzeri, S. (2009). Spike-phase coding boosts and stabilizes information carried by spatial and temporal spike patterns. *Neuron* 61, 597–608.

Kayser, C., Petkov, C. I., and Logothetis, N. K. (2008). Visual modulation of neurons in auditory cortex. *Cereb. Cortex* 18, 1560–1574.

Komura, Y., Tamura, R., Uwano, T., Nishijo, H., and Ono, T. (2005). Auditory thalamus integrates visual inputs into behavioral gains. *Nat. Neurosci.* 8, 1203–1209.

Koontz, W. L. G., and Fukunaga, K. (1972). Asymptotic analysis of a nonparametric clustering technique. *IEEE Trans. Comput.* 21, 967–974.

Lemus, L., Hernandez, A., Luna, R., Zainos, A., and Romo, R. (2010). Do sensory cortices process more than one sensory modality during perceptual judgments? *Neuron* 67, 335–348.

Lemus, L., Hernandez, A., and Romo, R. (2009). Neural encoding of auditory discrimination in ventral premotor cortex. *Proc. Natl. Acad. Sci. U.S.A.* 106, 14640–14645.

Liu, Y., Qin, L., Zhang, X., Dong, C., and Sato, Y. (2010). Neural correlates of auditory temporal-interval discrimination in cats. *Behav. Brain Res.* 215, 28–38.

Lu, T., and Wang, X. (2004). Information content of auditory cortical responses to time-varying acoustic stimuli. *J. Neurophysiol.* 91, 301–313.

Metzger, R. R., Greene, N. T., Porter, K. K., and Groh, J. M. (2006). Effects of reward and behavioral context on neural activity in the primate inferior colliculus. *J. Neurosci.* 26, 7468–7476.

Nelken, I., Chechik, G., Mrsic-Flogel, T. D., King, A. J., and Schnupp, J. W. (2005). Encoding stimulus information by spike numbers and mean response time in primary auditory cortex. *J. Comput. Neurosci.* 19, 199–221.

Otazu, G. H., Tai, L. H., Yang, Y., and Zador, A. M. (2009). Engaging in an auditory task suppresses responses in auditory cortex. *Nat. Neurosci.* 12, 646–654.

Pfingst, B. E., O'Connor, T. A., and Miller, J. M. (1977). Response plasticity of neurons in auditory cortex of the rhesus monkey. *Exp. Brain Res.* 29, 393–404.

Polley, D. B., Heiser, M. A., Blake, D. T., Schreiner, C. E., and Merzenich, M. M. (2004). Associative learning shapes the neural code for stimulus magnitude in primary auditory cortex. *Proc. Natl. Acad. Sci. U.S.A.* 101, 16351–16356.

Recanzone, G. H. (2000). Response profiles of auditory cortical neurons to tones and noise in behaving macaque monkeys. *Hear. Res.* 150, 104–118.

Romanski, L. M., and Goldman-Rakic, P. S. (2002). An auditory domain in primate prefrontal cortex. *Nat. Neurosci.* 5, 15–16.

Sakurai, Y. (1990). Cells in the rat auditory system have sensory-delay correlates during the performance of an auditory working memory task. *Behav. Neurosci.* 104, 856–868.

Schnupp, J. W., Hall, T. M., Kokelaar, R. F., and Ahmed, B. (2006). Plasticity of temporal pattern codes for vocalization stimuli in primary auditory cortex. *J. Neurosci.* 26, 4785–4795.

Scott, B. H., Malone, B. J., and Semple, M. N. (2007). Effect of behavioral context on representation of a spatial cue in core auditory cortex of awake macaques. *J. Neurosci.* 27, 6489–6499.

Selezneva, E., Scheich, H., and Brosch, M. (2006). Dual time scales for categorical decision making in auditory cortex. *Curr. Biol.* 16, 2428–2433.

Shuler, M. G., and Bear, M. F. (2006). Reward timing in the primary visual cortex. *Science* 311, 1606–1609.

Weinberger, N. M. (2004). Specific long-term memory traces in primary auditory cortex. *Nat. Rev. Neurosci.* 5, 279–290.

Yin, P., Mishkin, M., Sutter, M., and Fritz, J. B. (2008). Early stages of melody processing: stimulus-sequence and task-dependent neuronal activity in monkey auditory cortical fields A1 and R. *J. Neurophysiol.* 100, 3009–3029.

Conflict of Interest Statement: The authors declare that the research was conducted in the absence of any commercial or financial relationships that could be construed as a potential conflict of interest.

Received: 07 July 2011; accepted: 18 September 2011; published online: 19 October 2011.

Citation: Abolafia JM, Martinez-Garcia M, Deco G and Sanchez-Vives MV (2011) Slow modulation of ongoing discharge in the auditory cortex during an interval-discrimination task. Front. Integr. Neurosci. ***5****:60. doi: 10.3389/fnint.2011.00060*

frontiers in
INTEGRATIVE NEUROSCIENCE

ORIGINAL RESEARCH ARTICLE
published: 30 August 2011
doi: 10.3389/fnint.2011.00039

Timing and causality in the generation of learned eyelid responses

Raudel Sánchez-Campusano*, Agnès Gruart, and José M. Delgado-García

División de Neurociencias, Universidad Pablo de Olavide, Seville, Spain

Edited by:
Warren H. Meck, Duke University, USA

Reviewed by:
Carlos Acuña, University of Santiago de Compostela, Spain
Chris I. De Zeeuw, Erasmus University Rotterdam, Netherlands

****Correspondence:***
Raudel Sánchez-Campusano, División de Neurociencias, Universidad Pablo de Olavide, Ctra. de Utrera, Km 1, 41013 Sevilla, Spain.
e-mail: rsancam@upo.es

The cerebellum-red nucleus-facial motoneuron (Mn) pathway has been reported as being involved in the proper timing of classically conditioned eyelid responses. This special type of associative learning serves as a model of event timing for studying the role of the cerebellum in dynamic motor control. Here, we have re-analyzed the firing activities of cerebellar posterior interpositus (IP) neurons and orbicularis oculi (OO) Mns in alert behaving cats during classical eyeblink conditioning, using a delay paradigm. The aim was to revisit the hypothesis that the IP neurons (IPns) can be considered a neuronal phase-modulating device supporting OO Mns firing with an emergent timing mechanism and an explicit correlation code during learned eyelid movements. Optimized experimental and computational tools allowed us to determine the different causal relationships (temporal order and correlation code) during and between trials. These intra- and inter-trial timing strategies expanding from sub-second range (millisecond timing) to longer-lasting ranges (interval timing) expanded the functional domain of cerebellar timing beyond motor control. Interestingly, the results supported the above-mentioned hypothesis. The causal inferences were influenced by the precise motor and pre-motor spike timing in the cause-effect interval, and, in addition, the timing of the learned responses depended on cerebellar–Mn network causality. Furthermore, the timing of CRs depended upon the probability of simulated causal conditions in the cause-effect interval and not the mere duration of the inter-stimulus interval. In this work, the close relation between timing and causality was verified. It could thus be concluded that the firing activities of IPns may be related more to the proper performance of ongoing CRs (i.e., the proper timing as a consequence of the pertinent causality) than to their generation and/or initiation.

Keywords: timing, causality, correlation code, dynamic motor control, motor learning, interpositus nucleus, cerebellum, cats

INTRODUCTION

Interval timing is usually defined as the ability to modify a behavioral response as a function of the arbitrary duration (seconds to hours) of a given time interval (Staddon and Higa, 1999; Gallistel and Gibbon, 2000; Lewis and Miall, 2003; Lewis et al., 2003; Staddon and Cerutti, 2003; Buhusi and Meck, 2005). Thus, interval timing could be distinguished from other types of timed behavior (Clarke et al., 1996; Buonomano and Karmarkar, 2002; Mauk and Buonomano, 2004; Medina et al., 2005; Buonomano and Laje, 2010; Svensson et al., 2010). In experimental studies of interval timing, subjects are presented with time intervals of different durations, with the main aim being to determine how the temporal distribution of responses changes as a function of interval duration. Results obtained in these types of study indicate that, in many occasions, they are time-scale invariant (Gibbon, 1977; Lejeune and Wearden, 2006; Wearden and Lejeune, 2008) and that the temporal distributions of responses for two different interval durations are the same if the time-axis is divided by the duration of the interval (Almeida and Ledberg, 2010).

Although data collected from different types of experiments indicate that wide brain areas – including cerebral and cerebellar cortices, as well as basal ganglia – are involved in different aspects of interval timing (Schöner and Kelso, 1988; Ivry, 1996; Meck, 1996; Schöner, 2002; Spencer et al., 2003; Ivry and Spencer, 2004; Mauk and Buonomano, 2004; Buhusi and Meck, 2005), the information on the actual neural mechanisms supporting those timed behaviors is rather scarce (Matell and Meck, 2004; Meck et al., 2008). Available data reveal a wide range of interval durations over which time-scale invariance has been demonstrated. Indeed, in some tasks this range covers two orders of magnitude (Gibbon, 1977; Gibbon and Church, 1990; Gibbon et al., 1997). This flexibility in timing temporal durations makes it implausible that the neuronal mechanisms involved are dependent on fixed time constants as, for example, has been proposed in models of timing behavior in the context of classical conditioning (Grossberg and Schmajuk, 1989; Fiala et al., 1996). In this sense, some authors have developed a model of an interval timing device of bistable units with random state that is consistent with time-scale invariant behavior over a substantial time-range (Miall, 1992, 1993; Okamoto and Fukai, 2001; Okamoto et al., 2007; Almeida and Ledberg, 2010).

In the same way, the generation of eyelid CRs is a slow process requiring a large number of paired conditioned stimulus (CS)/unconditioned stimulus (US) presentations, as we have already described for mice, rats, rabbits, and cats (Gruart et al., 1995, 2000a,b, 2006; Trigo et al., 1999; Domínguez-del-Toro et al., 2004; Sánchez-Campusano et al., 2007; Valenzuela-Harrington et al., 2007; Porras-García et al., 2010). This associative learning process

involves different temporal domains of measurement (Buhusi and Meck, 2005) for multiple parameters, including milliseconds timing (intra-trial events), the temporal range of definition of interval timing (seconds-to-minutes-to-hours, inter-trail and inter-block interactions), and the temporal evolution across a proper sequence of training days or successive conditioning sessions (inter-session interactions). The idea of working with different durations of the inter-stimulus interval (ISI) and to study the different temporal distributions of the response is essential in studying timing behaviors. However, in a first approach it is possible to explore the spatiotemporal or time–intensity dispersion patterns of the different data distributions for the same duration of ISI, and to simulate the dispersion patterns when the duration of different intervals is adjusted to angular distribution on a circle.

In previous studies (Sánchez-Campusano et al., 2007, 2009, 2010; Porras-García et al., 2010), during the kinetic and kinematic characterization of the conditioning process, each parameter was treated as an independent magnitude, without going deeper into the parametric time–intensity association that logically each one of them established. In this paper, we show the necessity of including the temporal evolution (dynamics) of each magnitude in a coherent association with their variations in intensity, using circular statistics for the time–intensity data distributions in the CS–US interval. This idea is in accord with a specific spatiotemporal firing pattern including spike-rate and spike-timing codes (De Zeeuw et al., 2011) and a correlation code (Sánchez-Campusano et al., 2009; Porras-García et al., 2010) between the neuronal recordings in the neural pathway of CR generation. Here, we present some evidence that such spatiotemporal coding and the parametric timing–intensity and time delay–strength dispersion patterns determine a functional neuronal state (Sánchez-Campusano et al., 2010) evoked by the learning process.

In accordance with the above points, we decided to investigate the functional interdependencies between timing of motor learned responses and the cerebellar–Mns network causality, using a coherent mixture of simple circular statistics (timing–intensity and time delay–strength dispersion patterns), directional analysis (time delays and correlation code, including asymmetric information), and causality (time-dependent causal inferences) for the data acquired (timing, kinetic and kinematic parameters, electrophysiological recordings, and other physiological signals and time series) during the conditioning process.

MATERIALS AND METHODS

ANIMALS

Experiments were carried out with eight female adult cats (weighing 2.3–3.2 kg) obtained from an authorized supplier (Iffa-Credo, Arbresle, France). Experiments were carried out in accordance with the guidelines of the European Union (86/609/EU, 2003/65/EU) and Spanish regulations (BOE 252/34367-91, 2005) for the use of laboratory animals in chronic studies. Selected data collected from these animals have been published elsewhere (Trigo et al., 1999; Sánchez-Campusano et al., 2007, 2010). Here we will concentrate on the analysis of the temporal organization of neuronal firing of identified IP neurons (IPns) and facial Mns during the acquisition of classically conditioned eyeblink responses.

SURGERY

Animals were anesthetized with sodium pentobarbital (35 mg/kg, i.p.) following a protective injection of atropine sulfate (0.5 mg/kg, i.m.) to prevent unwanted vagal responses. A search coil (5 turns, 3 mm in diameter) was implanted into the center of the left upper eyelid at ≈2 mm from the lid margin (**Figure 1A**). The coil was made from Teflon-coated multi-stranded stainless steel wire (50 μm external diameter). Coils weighed ≈1.5% of the cat's upper lid weight and did not impair eyelid responses. Animals were also implanted in the ipsilateral orbicularis oculi (OO) muscle with bipolar hook electrodes aimed for electromyographic (EMG) recordings. These electrodes were made from the same wire as the coils, and bared 1 mm at their tips.

Four of the animals were prepared for the chronic recording of antidromically identified facial Mns projecting to the OO muscle. For this, two stainless steel hook electrodes were implanted on the zygomatic subdivision of the left facial nerve, 1–2 mm posterior to the external canthus. The other four animals were prepared for the chronic recording of antidromically identified left posterior IPns. In this case, a bipolar stimulating electrode, made of 200 μm enamel-coated silver wire, was implanted in the magnocellular division of the right (contralateral) red nucleus following stereotaxic coordinates (Berman, 1968). A recording window (5 mm × 5 mm) was opened in the occipital bone of all of the animals to allow access to the facial or the IP nuclei. The dura mater was removed, and an acrylic chamber was constructed around the window. The cerebellar surface was protected with a piece of silicone sheet and sterile gauze, and hermetically closed using a plastic cap. Finally, animals were provided with a head-holding system for stability and proper references of coil and recording systems. All the implanted electrodes were soldered to a socket fixed to the holding system. A detailed description of this chronic preparation can be found elsewhere (Trigo et al., 1999; Gruart et al., 2000a; Jiménez-Díaz et al., 2004; Sánchez-Campusano et al., 2007).

RECORDING AND STIMULATION PROCEDURES

Eyelid movements were recorded with the magnetic field search-coil technique (Gruart et al., 1995). The gain of the recording system was set at 1 V = 10°. The EMG activity of the OO muscle was recorded with differential amplifiers at a bandwidth of 0.1 Hz to 10 kHz. Action potentials were recorded in facial and IP nuclei with glass micropipettes filled with 2 M NaCl (3–5 MΩ resistance) using a NEX-1 preamplifier (Biomedical Engineering Co., Thornwood, NY, USA). For the antidromic activation of recorded neurons, we used single or double (interval of 1–2 ms) cathodal square pulses (50 μs in duration) with current intensities <300 μA. Only antidromically identified OO Mns and IPns were stored and analyzed in this study (**Figure 1D**). Site location and identification procedures have been described in detail for facial Mns (Trigo et al., 1999) and posterior IPns (Gruart et al., 2000a; Jiménez-Díaz et al., 2004; Sánchez-Campusano et al., 2007).

CLASSICAL EYEBLINK CONDITIONING

Classical eyeblink conditioning was achieved by the use of a delay conditioning paradigm (**Figure 1B**). A tone (370 ms, 600 Hz, 90 dB) was used as CS. The tone was followed 270 ms from its onset by an air puff (100 ms, 3 kg/cm^2) directed at the left cornea as a US.

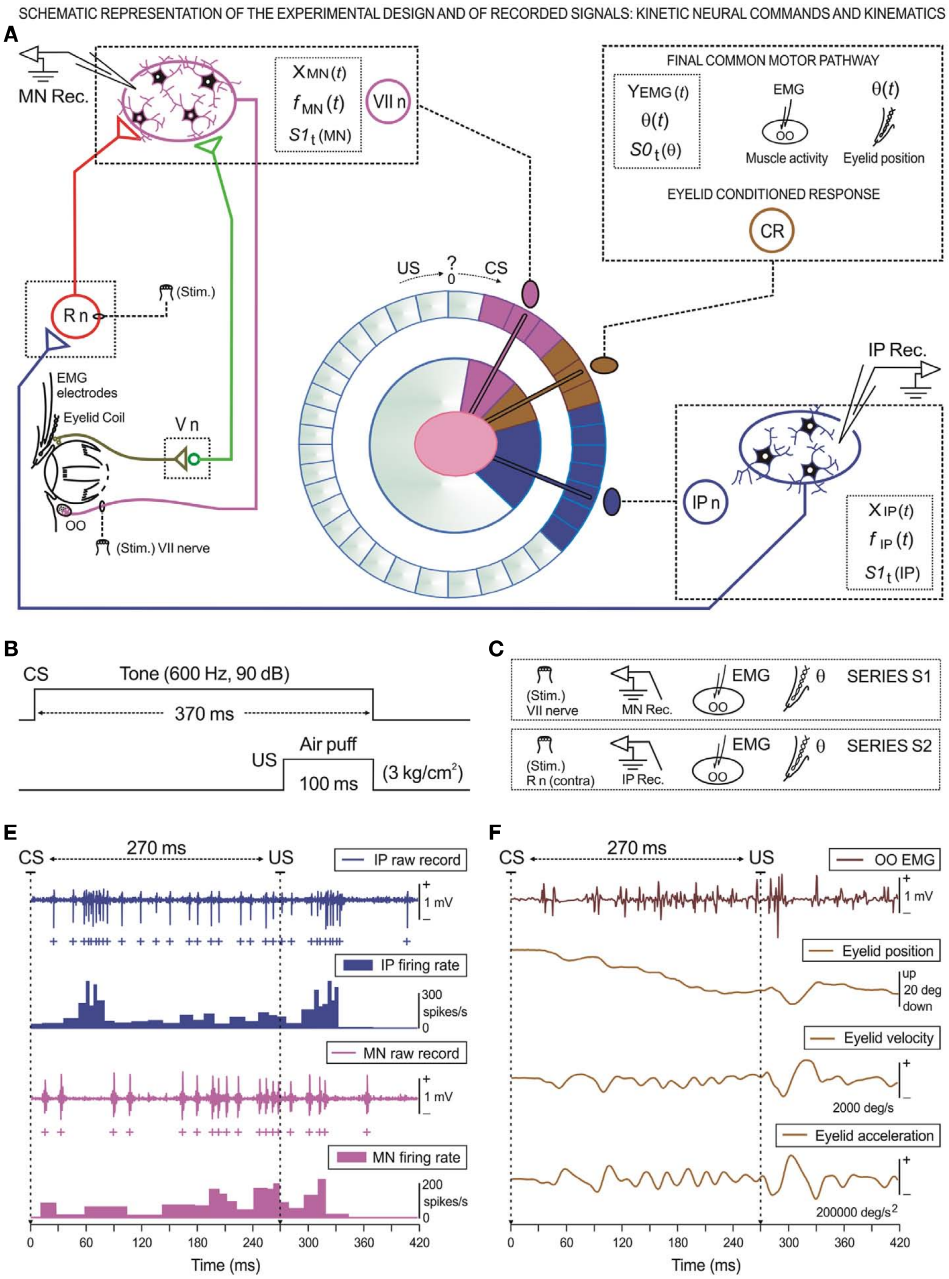

FIGURE 1 | Schematic representation of the experimental design and of the recorded physiological signals, including the kinetic neural commands and kinematics of eyelid response. (A) Diagram illustrating the stimulating (Stim.) and recording (Rec.) sites, as well as the eyelid coil and electromyographic (EMG) electrodes implanted in the upper eyelid. Kinetic neuronal commands were computed from the firing activities of antidromically identified OO Mns located in the facial nucleus (VII n) and from neurons located in the ipsilateral cerebellar posterior IP nucleus (IP n). Abbreviations: R n, red nucleus; V n, trigeminal nucleus; CR, conditioned response; CS, conditioned stimulus; US, unconditioned stimulus. Here, the circle of colors is a diagram illustrating the idea of the conversion of a conventional data distribution to an angular distribution in order to study the corresponding time-dispersion patterns. **(B)** For classical conditioning of eyelid responses we used a delay paradigm consisting of a tone as a conditioned stimulus (CS). The CS started before, but co-terminated with, an air puff used as an unconditioned stimulus (US). Here the CS–US interval was 270 ms. **(C)** Diagrammatic representation of the experimental series, S1 for Mn and S2 for IP neuron recordings, both obtained in simultaneity with the EMG activities of the OO muscle and eyelid position recordings during classical eyeblink conditioning. **(D,E)** A set of recordings collected from the 10th conditioning session from two representative animals. Here are represented the kinetic [neural commands, in **(D)**] and the performance [kinematics, in **(E)**] of eyelid CR. **(D)** The action potentials (IP spikes) marked with blue plus signs correspond to the direct representation of the neuronal activity in the IP n (IP raw recordings) and its respective instantaneous frequency (IP firing rate). Action potentials (Mn spikes recorded from an OO Mn) are indicated with magenta plus signs. The direct representation of the neuronal activity in the facial nucleus (Mn raw recordings) and its corresponding instantaneous frequency (Mn firing rate) are shown. **(E)** These traces illustrate the EMG activity of the OO muscle (OO EMG), the direct recording of the eyelid position by the magnetic field search-coil technique, and the estimated eyelid velocity and acceleration curves. For each of the physiological signals represented, the magnitude and the respective unit of measurement are indicated.

Thus, the tone and the air puff terminated simultaneously. Tones were applied from a loudspeaker located 80 cm below the animal's head. Air puffs were applied through the opening of a plastic pipette (3 mm in diameter) located 1 cm away from the left cornea.

Each animal followed a sequence of two habituation, 10 conditioning, and three extinction sessions. A conditioning session consisted of 12 blocks separated by a variable (5 ± 1 min) interval. Each block consisted of 10 trials separated by intervals of 30 ± 10 s. Within each block, the CS was presented alone during the first trial – i.e., it was not followed by the US. A complete conditioning session lasted for ≈2 h. The CS was presented alone during habituation and extinction sessions for the same number of blocks per session and trials per block and with similar random inter-block and inter-trial distributions (Gruart et al., 1995).

HISTOLOGY

At the end of the recording sessions, animals were deeply re-anesthetized (50 mg/kg sodium pentobarbital, i.p.). Electrolytic marks were placed in selected recording sites with a tungsten electrode (1 mA for 30 s). Animals were perfused transcardially with saline and phosphate-buffered formalin. Serial sections (50 μm) including the cerebellum and the brainstem were mounted on glass slides and stained with toluidine blue or cresyl violet, for confirmation of the recording sites (Gruart et al., 2000a; Jiménez-Díaz et al., 2004).

DATA COLLECTION AND MULTI-PARAMETRIC STATISTICAL ANALYSIS

The neuronal activity recorded in facial and cerebellar-IP nuclei, the EMG of the OO muscle, the eyelid position, and rectangular pulses corresponding to CS and US presentations, were stored digitally on a computer, using an analog–digital converter (CED 1401 Plus; Ceta Electronic Design, Cambridge, UK). Commercial computer programs (Spike 2 and SIGAVG; Ceta Electronic Design) were employed for acquisition and on-line conventional analyses. The multivariate off-line analyses of electrophysiological signals (including the analysis for the linear and non-linear correlation coefficients, the time delays, and the causality indices), the analytical procedures (including spike detection, multi-parametric cluster technique, circular time-dispersion method, and the fast Fourier transform), and the quantification and representation programs used for data illustrated in the main text, were developed by one of us (Raudel Sánchez-Campusano) with the help of MATLAB routines (The MathWorks, Natick, MA, USA). Only data from successful animals (i.e., those that allowed a complete study with an appropriate functioning of both recording and stimulating systems) were computed and analyzed.

The raw activities recorded from OO Mns and IPns were computed and quantified. The quantification algorithm also took into account the identification of the activity's standard waveform and the classification of probability patterns of spikes in time and frequency domains (Jarvis and Mitra, 2001; Brown et al., 2004; Sánchez-Campusano et al., 2007), and in the phase space (Aksenova et al., 2003). Since raw neuronal recordings usually contain overlapping spikes, we selected the following analytical procedure. Using a spike-sorting method, overlapping spikes within an interval of 1 ms were regarded as a single spike (according to the absolute refractory period) and overlapping spikes within an interval of 1–3 ms were regarded as spikes of different classes due to the interspike interval (i.e., the relative refractory period of the neuron) criterion in spike detection. The cluster tools enabled us to determine the numbers of cells, classes, and spikes and their centers by measuring the distances between their trajectories in phase space (Porras-García et al., 2010). Spike phase space reconstruction was implemented using the time delay technique (Chan et al., 2008), and the reconstructed spike waveform (an ideal and undisturbed spike that can be used as a template for the sorting method) preserves essential characteristics and the major phase space trajectory of the original spike. Finally, the instantaneous firing rate was calculated as the inverse of the interspike intervals. Velocity and acceleration profiles were computed digitally as the first and second derivatives of eyelid position records after low-pass filtering of the data (−3 dB cutoff at 50 Hz and zero gain at ≈100 Hz; Domingo et al., 1997; Sánchez-Campusano et al., 2007).

Maximum eyelid displacements during CRs were determined in the CS–US interval, and the function corresponding to the collected data (frequency sample at 1000 Hz) in the CS–US interval was adjusted by a simple regression method. This method enabled fixing the trend for the points near the zero level of eyelid position and establishing a standardized algorithm for all the responses across all the blocks of trials. In this way, the typical randomness in the determination of CR onset was avoided. The onset of a CR was determined as the latency from CS presentation to the interception of the regression function with the maximum amplitude level (see **Figure 2A**). This method was applied across the successive conditioning sessions, always showing the appropriate precision and robustness.

Computed results were processed for statistical analysis using the Statistics MATLAB Toolbox. As statistical inference procedures, both ANOVA (estimate of variance both within-groups and between-groups, on the basis of one dependent measure) and multivariate ANOVA (MANOVA, estimate of variance in multiple dependent parameters across groups) were used to assess the statistical significance of differences between groups. The corresponding statistical significance test (that is, the $F_{[(m-1),(m-1)\times(n-1),(l-m)]}$ statistics and the resulting probability at the predetermined significance level $P < 0.05$) was performed, with sessions as repeated measures, coupled with contrast analysis when appropriate (Hair et al., 1998; Grafen and Hails, 2002). The orders m (number of groups), n (number of animals), and l (number of multivariate observations) were reported accompanying the F statistic values (Sánchez-Campusano et al., 2007, 2009). Wilk's lambda criterion and its transformation to the χ^2-distribution used in MATLAB were used to extract significant differences from MANOVA results (cluster analysis for cells-classes-spikes classification during the spike-sorting problem in the phase space, and hierarchical cluster free reconstruction during both actual and simulated causality conditions). The corresponding statistical significance tests (i.e., Student's t-test and F statistic) were performed for the parameters of non-linear correlation analysis and causal inference method (see Linear and Non-linear Multivariate Analyses of Physiological Signals). Here, the hypothesis test is done by using the modified Fisher's z-transformation (w) to associate each measured non-linear association index (η) with a corresponding w-transformation (see Non-linear Dynamic Associations Between Electrophysiological Recordings). For the

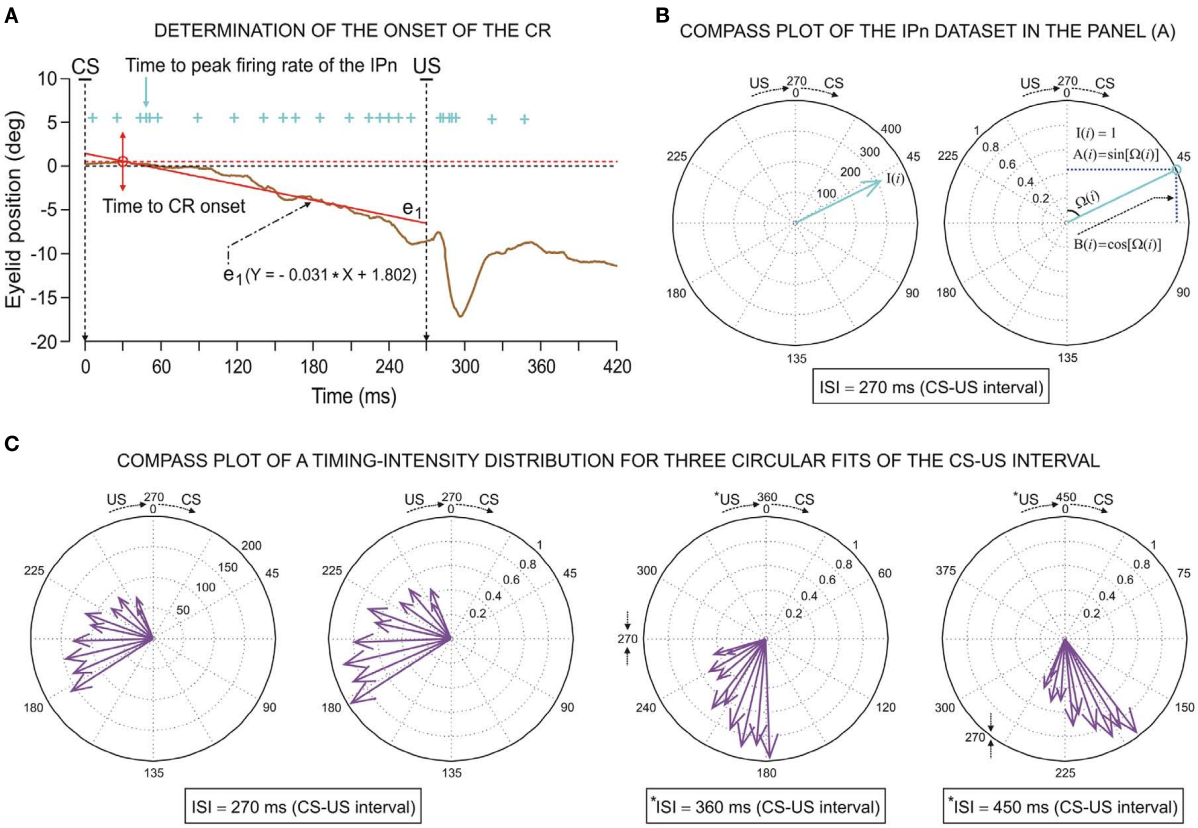

FIGURE 2 | Determination of the onset of the eyelid conditioned response (CR) and some examples of the circular representation of the dataset distributions. **(A)** Illustration of an eyelid CR (eyelid position, in degrees) collected from a single trial during the 10th conditioning session. The onset of the CR (red arrow, from direct eyelid position recording using the magnetic search-coil technique) was determined as the latency (with respect to the conditioning stimulus (CS) presentation) corresponding to the interception (the red circle) of the regression function (see the red strength line and the equation e_1) with the maximum amplitude level (red dashed line). In this example, the time to CR onset is 30.0 ms. The action potentials (IPn spikes), marked with cyan plus signs, correspond to the direct representation of the firing activity in the IP neuron (311.1 spikes/s) collected during the same trial. The cyan arrow indicates the time to peak firing rate of the IPn (48.1 ms). **(B)** The circular representation of both parametric timing–intensity vector [48.1 ms, 311.1 spikes/s] and parametric timing unitary vectors [48.1 ms, 1 unit] of the IPn dataset represented as cyan plus signs in the **(A)**. The blue dashed lines in **(B)** (see the second circle) serve to illustrate the sine and cosine components of the above angular data point. **(C)** The compass plots of parametric timing–intensity distribution of the Mn activity across the 10 conditioning sessions. Here, the dataset distribution is [time to peak firing rate of the OO Mns, Mn peak firing rate] (see the arrows for the actual values of the intensity components (in spike/s, see the first circle) and the normalized values of these (see the other three circle in this row) with respect to the maximum of the peak firing rates across conditioning sessions). The circles represent the three conversions of the CS–US interval to the angular plot (inter-stimulus interval, ISI = 270 ms; *ISI = 360 ms; *ISI = 450 ms) where *ISI denotes the simulated time conditions for studying the simulated dispersion patterns of the same dataset distribution.

circular statistics (Fisher, 1993; Jammalamadaka and SenGupta, 2001; Berens, 2009), we used both the Rayleigh and the Watson hypothesis tests to the *von Mises distribution* (Ψ, the circular analog of the normal distribution; see Circular Statistics to Analyze Time-Dispersion Patterns During Motor Learning for more details).

LINEAR AND NON-LINEAR MULTIVARIATE ANALYSES OF PHYSIOLOGICAL SIGNALS

Multivariate analysis is extensively used with the aim of studying the relationship between simultaneously recorded signals or their equivalent time series. Multivariate time series tools [*Non-linear dynamic association* (see Non-linear Dynamic Associations Between Electrophysiological Recordings) and *Time-dependent causality analysis* (see Time-Dependent Causality Analysis Between Neuronal Firing Command and Learned Motor Response)] enabled us to determine the functional relatedness, asymmetry, time delay, direction in coupling, and causal inferences between physiological time series [i.e., neuronal activities generated in facial and cerebellar-IP nuclei (VII n or IP n, in **Figures 1A,D**), and learned motor responses (OO EMG activity or conditioned eyelid responses, in **Figures 1A,E**)] collected during classical conditioning sessions. In practice, we illustrated the use of multivariate analyses for the assessment of the strength (strong, moderate, or weak), type (linear or non-linear), directionality (unidirectional or bidirectional) and functional nature (feedforward or feedback relationships) of interdependencies between these physiological time series.

Non-linear dynamic associations between electrophysiological recordings

We used non-linear correlation analysis to investigate the following dynamic associations:

(1) $Y_{EMG}(t)$ vs. $X_{MN}(t)$; between the EMG activity of the OO muscle and the neuronal activity of facial nucleus (the OO Mns).
(2) $Y_{EMG}(t)$ vs. $X_{IP}(t)$; between the EMG activity of the OO muscle and the neuronal activity of IPns.
(3) $Y_{MN}(t)$ vs. $X_{IP}(t)$; between Mn and IPn activities.

The non-linear association index ($\eta^2_{\langle Y|X\rangle}$) between the electrophysiological time series $X(t)$ and $Y(t)$ was computed as,

$$\eta^2_{\langle Y|X\rangle} = 1 - \frac{\sum_{j=1}^{Nb}\sum_{k\in B_j}\left[Y_k - \Im(X_j)\right]^2}{\sum_{k=1}^{Ns}(Y_k - \bar{Y})^2}, \quad (1)$$

with Ns being the number of samples of the signals, $\bar{Y}$ being the average of all amplitudes Y_k, and $\Im(X_j)$ being the piecewise approximation of the non-linear regression curve. In the above mathematical expression, Nb is the number of bins and B_j (with $j = 1,\ldots,Nb$) are the different bins in the corresponding scatter representations. The measure of association in the opposite direction $\eta^2_{\langle Y|X\rangle}$ can be calculated analogously. In this formulation, the subscript $_{\langle Y|X\rangle}$ denotes the coupling from signal $X(t)$ to the signal $Y(t)$, $_{\langle X|Y\rangle}$ indicates the coupling in the opposite direction – that is, from signal $Y(t)$ to the signal $X(t)$, and $_{\langle -|-\rangle}$ denotes either of the two directions of coupling.

To assess the direction of coupling between the electrophysiological signals $X(t)$ and $Y(t)$, we used the following direction index (Wendling et al., 2001),

$$D = \frac{1}{2}[\mathrm{sgn}(\Delta\eta^2) + \mathrm{sgn}(\Delta\tau)], \quad (2)$$

where $\Delta\eta^2 = \eta^2_{\langle Y|X\rangle} - \eta^2_{\langle X|Y\rangle}$ and $\Delta\tau = \tau_{\langle Y|X\rangle} - \tau_{\langle X|Y\rangle}$, with $\tau_{\langle Y|X\rangle}$ (corresponding to $\eta_{\langle Y|X\rangle}$ and $\eta^2_{\langle Y|X\rangle}$) and $\tau_{\langle X|Y\rangle}$ (corresponding to $\eta_{\langle X|Y\rangle}$ and $\eta^2_{\langle X|Y\rangle}$) being the time delays (i.e., the time shift $\tau_{\langle -|-\rangle}$ for which $\eta^2_{\langle -|-\rangle}(\tau)$ is maximum) between signals.

Indeed, if $X(t)$ causes $Y(t)$, $\tau_{\langle Y|X\rangle}$ will be positive and $\tau_{\langle X|Y\rangle}$ will be negative, so that the difference $\Delta\tau$ will also be positive. In this case, the degree of asymmetry of the non-linear coupling $\Delta\eta^2$ will also be positive and therefore the direction index $D = +1$. These five previous conditions ($\tau_{\langle Y|X\rangle} > 0$; $\tau_{\langle X|Y\rangle} < 0$; $\Delta\tau > 0$; $\Delta\eta^2 > 0$ and $D = +1$) should be satisfied simultaneously, to conclude that the relationship is of the type $X(t) \xrightarrow{\text{YES}} Y(t)$ – that is, a unidirectional coupling between signals. In all the other combinations of conditions, the relationship will be false [i.e., a spurious unidirectional coupling, $X(t) \xrightarrow{(?)} Y(t)$].

If $Y(t)$ causes $X(t)$, $\tau_{\langle Y|X\rangle}$ will be negative and $\tau_{\langle X|Y\rangle}$ will be positive, so that the difference $\Delta\tau$ will also be negative. In this case, the degree of asymmetry of the non-linear coupling $\Delta\eta^2$ will also be negative, and as a consequence $D = -1$. These five previous conditions ($\tau_{\langle Y|X\rangle} < 0$; $\tau_{\langle X|Y\rangle} > 0$; $\Delta\tau < 0$; $\Delta\eta^2 < 0$ and $D = -1$) should be satisfied simultaneously, to conclude that the relationship is of the type $Y(t) \xrightarrow{\text{YES}} X(t)$ – that is, a unidirectional coupling between signals. In all the other combinations of conditions, the relationship will be false [i.e., a spurious unidirectional coupling, $Y(t) \xrightarrow{(?)} X(t)$].

If a feedback relationship between the signals $X(t)$ and $Y(t)$ is verified, then the time delays $\tau_{\langle Y|X\rangle}$ and $\tau_{\langle X|Y\rangle}$ will be positive, so that $\mathrm{sgn}(\Delta\tau) \neq \mathrm{sgn}(\Delta\eta^2)$ and therefore the direction index $D = 0$. The five previous conditions [($\tau_{\langle Y|X\rangle} > 0$; $\tau_{\langle X|Y\rangle} > 0$; $\Delta\tau < 0$; $\Delta\eta^2 > 0$ and $D = 0$) or ($\tau_{\langle Y|X\rangle} > 0$; $\tau_{\langle X|Y\rangle} > 0$; $\Delta\tau > 0$; $\Delta\eta^2 < 0$ and $D = 0$)] should be satisfied simultaneously, to conclude that the relationship is of the type $X(t) \xrightleftarrows{\text{YES}} Y(t)$ – that is, a bidirectional coupling or a feedback relationship between signals. If the signal $Y(t)$ can be explained by the preceding signal $X(t)$ better than vice versa, then $X(t) \xrightleftarrows{\text{YES}} Y(t)$, in the contrary case $X(t) \xleftrightarrows{\text{YES}} Y(t)$. In all the other combinations of conditions, the relationship will be false [i.e., a spurious bidirectional coupling, $X(t) \xrightleftarrows{(?)} Y(t)$].

The statistical significance tests (i.e., Student's *t*-test and *F* statistic) were performed for the parameters of non-linear correlation analysis (association indices and time delays). The hypothesis test was done by using the modified Fisher's *w*-transformation ($w_{\langle -|-\rangle}$) to associate each measured non-linear association index ($\eta_{\langle -|-\rangle}$) with a corresponding $w_{\langle -|-\rangle}$ function,

$$w_{\langle -|-\rangle} = \frac{1}{2}\ln\left(\frac{\eta^2_{\langle -|-\rangle}}{1 - \eta^2_{\langle -|-\rangle}}\right), \text{ with } \eta\text{- square dependence} \quad (3)$$

For more details about linear and non-linear piecewise approximations of the regression curves, and statistical "multiple comparison" analyses, the reader may refer to Sánchez-Campusano et al. (2009, 2010) and Porras-García et al. (2010).

Time-dependent causality analysis between neuronal firing command and learned motor response

We investigated the dynamic regression models and causal inferences between neuronal firing function [SI_t; $S1_t$ (MN), with $f_{MN}(t)$ for facial Mn or $S2_t$ (IP) with $f_{IP}(t)$ for IPn instantaneous firing frequencies] and learned motor response [$S0_t$ (θ), with θ(*t*) for eyelid positions during conditioned eyeblink responses] using the time-dependent causality analysis as a particular case of the transfer function models (TFM), a model frequently used to measure the functional interdependence between time series (Box and Jenkins, 1976; Granger, 1980; Nolte et al., 2008).

Relationships between Ns physiological time series [corresponding to instantaneous frequencies $f_{MN}(t)$ and $f_{IP}(t)$, and conditioned eyelid responses θ(*t*)] can be represented by transfer function models of the form

$$S0_{ht} = \sum_{i\in Ns(h)} \nu_{hi}(B)\mathrm{SI}_{it} + U_{ht} \quad (4)$$

in which

$$\nu_{hi}(B) = \frac{\omega_{m_{hi}}(B)}{\delta_{a_{hi}}(B)}B^{b}hi \quad (5)$$

are the impulsive responses or transfer functions of the models. *B* is the back-shift operator such that $BSI_t = SI_{t-1}$, and $h = 1, 2, \ldots, Ns$. The moving average $\omega_{m_{hi}}(B)$ and autoregressive $\delta_{a_{hi}}(B)$ operators are also polynomials in *B* with orders *m* and *a*, respectively. The parameters b_{hi} are non-negative integers representing certain periods of delay in the transmission of the effects between the input SI_{it} and output $S0_{ht}$ time series. The structure of the processes of

inertia or uncertainties $U_{ht} = [\phi_{q_h}(B)/\varphi_{p_h}(B)]n_{ht}$ can be represented by the univariate operators (with orders p and q) in the stochastic difference equations of the form $\varphi_{p_h}(B)\mathrm{SI}_{it} = \phi_{q_h}(B)n_{ht}$, where n_{ht} are Ns independent Gaussian white-noise processes with variances ρ_h and zero means (Tiao and Box, 1981).

Transfer function models of this form assume that the time series, when suitably arranged, possess a triangular relationship (Geweke, 1982; Harvey, 1994), implying for example that $S2_t$ depends only on its own past (i.e., the Granger causality indices are such that $G_{0\to 2} \approx 0$ and $G_{1\to 2} \approx 0$); $S1_t$ depends on its own past and on the present and past of $S2_t$ (i.e., $G_{1\to 2} = 0$ and $G_{2\to 1} > 0$, for unidirectional coupling); $S0_t$ depends on its own past and on the present and past of $S1_t$ and $S2_t$ (i.e., $G_{0\to 1} = 0$, $G_{1\to 0} > 0$, and $G_{0\to 2} = 0$, $G_{2\to 0} > 0$, respectively); and so on. If $S1_t$ depends on its own past and on the present and past of $S2_t$, and $S2_t$ depends on its own past and on the present and past of $S1_t$, then we must have a model that allows for this feedback (i.e., high and significant values of the causality indices in both senses $G_{2\to 1} > 0$ and $G_{1\to 2} > 0$, indicating bidirectional coupling). The normal ($G_{1\to 0}$) and normalized ($R^2_{I\to 0}$) Granger and Granger–Sargent ($\mathrm{GS}^2_{I\to 0}$) causality indices were calculated as

$$\begin{cases} G_{I\to 0} = \ln\left(\dfrac{V_0}{V_{I0}}\right) \\ R^2_{I\to 0} = 1 - e^{-G_{I\to 0}} \\ \mathrm{GS}^2_{I\to 0} = \dfrac{\varepsilon_0^2 - \varepsilon_{I0}^2}{\varepsilon_{I0}^2} \end{cases} \tag{6}$$

where V_0 and V_{10} are the variances of the prediction errors and ε_0^2 and ε_{I0}^2 the mean squared errors for both univariate and bivariate models (Kaminski and Liang, 2005). For more details about the theoretical formulation of these transfer function models and the above time-dependent Granger causality indices (Eq. 6), the reader may refer to Sánchez-Campusano et al. (2009).

CIRCULAR STATISTICS TO ANALYZE TIME-DISPERSION PATTERNS DURING MOTOR LEARNING

This section provides a brief introduction to circular statistics (for more details see Batschelet, 1981; Fisher, 1993; Jammalamadaka and SenGupta, 2001; Berens, 2009). The term "circular statistics" describes a set of techniques used to analyze and to model distributions of random variables that are cyclic in nature (Mardia, 1975; Mardia and Jupp, 1999). For example, angles or directions differing by an integer multiple of 360° or 2π radians are considered to be equivalent. These techniques have enjoyed popularity in a number of areas where exploration, modeling, and testing hypotheses of directional information have played a role. Surprisingly, most work involving circular statistics has concentrated on directional data as described above, although the timing dataset such as the time of day, phase of the moon, or day of the year are also cyclic in nature. Circadian rhythms (or circadian timing) are most recognizable in nature but interval (in a wide seconds-to-minutes-to-hours range) and millisecond timing (sub-second range) also guide fundamental animal behaviors (Buhusi and Meck, 2005) that exhibit different periodicity and precision in various timing tasks. Therefore, timing across different timescales (sub-second range, seconds-to-minutes-to-hours range, and days-to-weeks range) may be also fitted to an angular scale.

In practical terms, circular quantification and compass representation do not require a cyclic or periodic condition (Batschelet, 1981). A compass plot is a two-dimensional polar plot with position vectors from the origin. While a compass plot can be drawn for arbitrary values it is useful to associate the plot with a polar trajectory definition. In fact, an appropriate time–angular correspondence was sufficient. The circular technique displays a compass plot having d arrows, where d is the number of elements in each one of the mean data $T(i)$ (parametric timing or time delay) or $I(i)$ (intensity or strength). The location of the base of each arrow is the origin. The location of the tip of each arrow is a point relative to the base and determined by the ith-observation $[T(i), I(i)]$ where $i = 1,\ldots, d$. In our application of circular distribution, the index d is the number of days (sessions) along the conditioning, or the number of blocks of the same session, or the total number of trials for all of the blocks of the same session, or the number of trials of the same block.

To convert parametric timing/time delay data $T(i)$ in milliseconds to angles in degrees we assumed a direct interdependence determined by Eq. 7 at the intra-trail domain. Thus, the time dataset can be converted to a common angular scale in radians by the following equation:

$$\Omega(i) = 2\pi\frac{\Theta(i)}{k_\Theta} = 2\pi\frac{T(i)}{k_T} \tag{7}$$

where $\Theta(i)$ and $T(i)$ are the representations of the data in degrees and timescale, respectively, and $\Omega(i)$ is its angular representation in radians. k_Θ and k_T are the total numbers of steps on the scales used to measure $\Theta(i)$ and $T(i)$. For example, if we have $T(i)$ representing milliseconds from 0 ms (i.e., the CS onset instant) to 360 ms (i.e., 10 ms prior to the end of the US), then k_T = 360 steps of 1 ms – i.e., the simplest correspondence between time (in milliseconds) and angle (in degrees). However, we are interested in fitting the duration of the ISI to the circle according to our delay paradigm (see **Figure 2B**), where the actual duration of the ISI was 270 ms. Therefore, the total number of steps is k_T = 270 (i.e., 270 steps of 1.3333 ms, approximately). Note that this simple fitting to the circle is always possible for the different durations of the *ISI (the simulated time conditions for the different durations of the CS–US interval). In the array Eq. 8, we summarized the values for two simple conversions to the circle (see **Figure 2C**): (1) for ISI = 270 ms (i.e., less of a conventional cycle, 270 steps of 1.3333 ms), and (2) for *ISI = 450 ms (i.e., for more of a conventional cycle, 450 steps of 0.8 ms) in relation to the values of the conventional circle.

$$\begin{cases} \mathrm{ISI} = 270\ \mathrm{ms} \rightarrow & 0 & 45 & 90 & 135 & 180 & 225 & 270 & dt = 1.3333\ \mathrm{ms} \\ {}^*\mathrm{ISI} = 360\ \mathrm{ms} \rightarrow & 0 & 60 & 120 & 180 & 240 & 300 & 360 & dt = 1.0\ \mathrm{ms} \\ {}^*\mathrm{ISI} = 450\ \mathrm{ms} \rightarrow & 0 & 75 & 150 & 225 & 300 & 375 & 450 & dt = 0.8\ \mathrm{ms} \end{cases} \tag{8}$$

This strategy of transformation of the CS–US interval to the circle is easy to apply for *ISI ranging from sub-second range (millisecond timing) to seconds-to-minutes-to-hours range (interval timing); for example: *ISI of 1 s and 80 ms (1080 ms, i.e., 1080 steps of 0.3333 ms); *ISI of 1 min-4 s and 800 ms ($1080 \times 60 = 64800$ ms, i.e., 1080×60 steps of 0.3333/60 ms); and *ISI of 1 h-4 min and 48 s ($1080 \times 60^2 = 3888000$ ms, i.e., 1080×60^2 steps of $0.3333/60^2$ ms), according to the following array:

$$\begin{cases} {}^*\mathrm{ISI} = 1080\ \mathrm{ms} & 0 \quad 180 \quad 360 \quad 540 \quad 720 \quad 900 \quad 1080 & dt = 0.3333\ \mathrm{ms} \\ {}^*\mathrm{ISI} = 1080 \times 60\ \mathrm{ms} & (0 \quad 180 \quad 360 \quad 540 \quad 720 \quad 900 \quad 1080) \times 60 & dt = 0.3333/60\ \mathrm{ms} \\ {}^*\mathrm{ISI} = 1080 \times 60^2\ \mathrm{ms} & (0 \quad 180 \quad 360 \quad 540 \quad 720 \quad 900 \quad 1080) \times 60^2 & dt = 0.3333/60^2\ \mathrm{ms} \end{cases} \tag{9}$$

Note that the relationship between the number of steps (i.e., the duration of the CS–US interval) and the time of sampling (dt) could be adapted in function of the temporal resolution of the data distribution. For example, if we have $T(i)$ ranging from seconds to 1 min, then $k_T = 60$ steps of 1 s, and the time window (e.g., of the ISI) of 1 min is fitted to the circle according to the Eq. 7; for $T(i)$ ranging from minutes to 1 h, $k_T = 60$ steps of 1 min, and the time window of 1 h is fitted to the circle; for $T(i)$ ranging from hours to 1 day, $k_T = 24$ steps of 1 h, and the time window of 1 day is fitted to the circle; and finally, for $T(i)$ ranging from days to 1 week, $k_T = 7$ steps of 1 day, and the time window of 1 week is fitted to the angular distribution also according to the Eq. 7.

The parametric timing–intensity (or time delay–strength) distributions $[T(i), I(i)]$ with $i = 1,\ldots, d$, were represented as points on the circumference of a unitary circle – i.e., $I(i) = 1$ for all of the intensity/strength values, in the two-dimensional space. This is illustrated in **Figure 2B**, where a data point marked by a cyan circle lies on the unitary circumference. As indicated for the blue point in **Figure 2B**, the A(i)-coordinate of a point corresponds to the sine of the angle $\Omega(i)$ and the B(i)-coordinate to the cosine,

$$\begin{cases} \mathrm{A}(i) = \mathrm{I}(i)\sin[\Omega(i)] \\ \mathrm{B}(i) = \mathrm{I}(i)\cos[\Omega(i)] \end{cases} \tag{10}$$

and the components of vectors $[\mathrm{A}(i), \mathrm{B}(i)]$ were averaged as

$$\begin{cases} \overline{\mathrm{A}} = \frac{1}{d}\sum_{i}^{d} \mathrm{A}(i) \\ \overline{\mathrm{B}} = \frac{1}{d}\sum_{i}^{d} \mathrm{B}(i) \end{cases} \tag{11}$$

Thus, a more appropriate circular mean (in the circular statistics sense), denoted by $\overline{\Omega}$ in radians, was defined as

$$\overline{\Omega} = \begin{cases} \arctan\left(\overline{\mathrm{A}}/\overline{\mathrm{B}}\right) & \text{if } \overline{\mathrm{B}} \geq 0 \\ \arctan\left(\overline{\mathrm{A}}/\overline{\mathrm{B}}\right) + \pi & \text{if } \overline{\mathrm{B}} < 0 \end{cases} \tag{12}$$

and the circular mean of the temporal distributions of the responses $\overline{\mathrm{T}}$ was

$$\overline{\mathrm{T}} = \left(k_T/2\pi\right)\overline{\Omega} \tag{13}$$

If all the angular measurements are represented as points on a circle, then a relatively simple geometrical interpretation of the circular mean may be shown, where the coordinates $\left[\overline{\mathrm{A}}, \overline{\mathrm{B}}\right]$ determine the centroid – i.e., the geometric center of the represented points. Thus, data sets (in radians or degrees) with a greater degree of circular spread (or dispersion index) have centroids closer to the center of the circle. Finally, the dispersion index σs was calculated as

$$\begin{cases} \sigma\mathrm{s} = \dfrac{1-\rho}{2\overline{\mathrm{C}}^2} \\ \overline{\mathrm{C}} = \dfrac{1}{d}\sqrt{\overline{\mathrm{A}}^2 + \overline{\mathrm{B}}^2} \\ \rho = \dfrac{1}{d}\sum_{i}^{d}\cos\left(2\left[\Omega(i) - \overline{\Omega}\right]\right) \end{cases} \tag{14}$$

Note that $\overline{\mathrm{C}}$ is the radius of the circumference that describes the centroid with respect to the origin, and that higher values of $\overline{\mathrm{C}}$ are associated with less spread in the data. However, the dispersion index σs is in some respects more akin to the non-circular measurement of SD, as it has no upper bound, and larger values of ρs correspond to greater degrees of spread. In Eq. 14, ρ is a measurement of circular kurtosis, and a value close to one is indicative of a strongly peaked distribution (Berens, 2009). The circular variance V_C and standard angular deviation S_C are closely related to the mean resultant radius $\overline{\mathrm{C}}$. These circular measurements are defined as $V_C = 1 - \overline{\mathrm{C}}$ and $S_C = \sqrt{2(1-\overline{\mathrm{C}})}$. The circular variance is bounded in the interval $[0,1]$ and the standard angular deviation lies in the interval $[0, \sqrt{2}]$ (Berens, 2009). Furthermore, notice that the variable ρ is an implicit function of k_T [i.e., the total number of steps on the timescale used to measure $T(i)$]:

$$\rho\left(k_T\right) = \frac{1}{d}\sum_{i}^{d}\cos\left(2\left[\left(2\pi/k_T\right)\left(T(i) - \overline{\mathrm{T}}\right)\right]\right) \tag{15}$$

The mathematical expression (15) indicates that the time-dispersion index (σ) and time–intensity dispersion index (σs) are functions of the total number of steps (k_T) on the timescale, and therefore of the ISI (or CS–US interval), at least in this circular statistical sense.

The same applies to the *von Mises distribution* (Ψ, the circular analog of the normal distribution) where the probability densities of $\overline{\mathrm{T}}$ are given by

$$\Psi\left[T(i), \mu_T, \lambda k_T\right] = \frac{k_T}{(2\pi)^2 J_0(\lambda)}\exp\left[\lambda\cos\left(\left[\left(2\pi/k_T\right)\left(T(i) - \mu_T\right)\right]\right)\right] \tag{16}$$

where μ_T is the mean value of $T(i)$ (i.e., the maximum likelihood estimator of μ_T is $\overline{T}$), λ is the concentration parameter related to the circular spread, and $J_0(\lambda)$ is a normalization constant to ensure that the probability density integrates to one. In addition to this, it is also possible to carry out two hypothesis tests (Jammalamadaka and SenGupta, 2001):

(1) Rayleigh hypothesis test: explores whether $T(i)$ has a uniform distribution – i.e., the concentration parameter related to the circular spread $\lambda = 0$;
(2) Watson hypothesis test: explores whether $T(i)$ has the same mean for p distributions – i.e., $\mu 1_T = \mu 2_T = \ldots = \mu\, p_T$.

Finally, we assumed two circumstances for the dispersion analyses:

(1) Inter-stimulus interval of fixed duration (e.g., 270 ms) and different parametric timing–intensity (or time delay–strength) data distributions of the type $[T(i), I(i)]$. For example: (the time to IPn peak firing rate, the amplitude of this peak), or (the time to CR onset, the percentage of the CR), or other time delay–strength distributions. In this circumstance, we determined the dispersion patterns for the different time–intensity distributions of the datasets [i.e., (timing parameters, kinetic neural commands, and kinematic parameters), and (time delays, correlation code parameters)].
(2) Inter-stimulus interval of different durations as the simulated time conditions (e.g., 360 ms; 450 ms; 1080 ms, 1080 ms × 60 ms, 1080 ms × 60^2 ms; see the Eqs. 8 and 9) for the same time–intensity (or time delay–strength) data distribution $[T(i), I(i)]$. This circumstance is not interval timing (seconds-to-minutes-to-hours range), but it allowed us to show how the timing tasks can be treated mathematically using the circular distribution, an approach that we are already exploring in the different temporal domains (the inter-trials dispersion of the same block, the inter-blocks dispersion of the same session, and the inter-sessions dispersion along the process). Thus, we calculated the dispersion patterns of the same dataset distribution as a function of the ISI duration.

Consequently, for two time–intensity distributions $[T1(i), I1(i)]$ and $[T2(i), I2(i)]$ in a fixed CS–US interval (circumstance 1) or for two different ISI (ISI1 and ISI2) of the same time–intensity distribution (circumstance 2), it is always possible to calculate the time–intensity dispersion indices $\sigma s1$ and $\sigma s2$, respectively, and therefore, the fraction of dispersion indices is defined as

$$\frac{\sigma s1}{\sigma s2} = \left(\frac{1-\rho 1}{1-\rho 2}\right)\left(\frac{\overline{C2}}{\overline{C1}}\right)^2 \tag{17}$$

Notice in (17) the following relationships between the indices $\overline{C}$, ρ, and σs,

If $\overline{C2} > \overline{C1}$ (the radii that describe the centroids with respect to the origin), then $\rho 2 > \rho 1$, and therefore $\sigma s2 < \sigma s1$.

If $\overline{C1} > \overline{C2}$ (the radii that describe the centroids with respect to the origin), then $\rho 1 > \rho 2$, and therefore $\sigma s1 < \sigma s2$.

In this paper, we calculated the following dispersion indices in the different temporal domains (the inter-trials dispersion of the same block, the inter-blocks dispersion of the same session, and the inter-sessions dispersion along the process).

(a) σ_{MN} and σs_{MN}, for the timing and timing–intensity distributions from the firing activity of the Mns (e.g., see **Figure 2C**).
(b) σ_{CR} and σs_{CR}, for the timing and timing–intensity distributions from the eyelid CRs.
(c) σ_{IP} and σs_{IP}, for the timing and timing–intensity distributions from the firing activity of the IPn.
(d) $\sigma 0$ and $\sigma s0$, for the time delay and time delay–strength distributions from $\tau 0_{\langle f\,IP\,|\,\theta\rangle}$ and $r_{\max\langle f\,IP\,|\,\theta\rangle}$
(e) $\sigma 1$ and $\sigma s1$, for the time delay and time delay–strength distributions from $\tau 1_{\langle EMG\,|\,MN\rangle}$ and $\eta 1_{\max\langle EMG\,|\,MN\rangle}$
(f) $\sigma 2$ and $\sigma s2$, for the time delay and time delay–strength distributions from $\tau 2_{\langle MN\,|\,EMG\rangle}$ and $\eta 2_{\max\langle MN\,|\,EMG\rangle}$
(g) $\sigma 3$ and $\sigma s3$, for the time delay and time delay–strength distributions from $\tau 3_{\langle EMG\,|\,IP\rangle}$ and $\eta 3_{\max\langle EMG\,|\,IP\rangle}$
(h) $\sigma 4$ and $\sigma s4$, for the time delay and time delay–strength distributions from $\tau 4_{\langle IP\,|\,EMG\rangle}$ and $\eta 4_{\max\langle IP\,|\,EMG\rangle}$
(i) $\sigma 5$ and $\sigma s5$, for the time delay and time delay–strength distributions from $\tau 5_{\langle MN\,|\,IP\rangle}$ and $\eta 5_{\max\langle MN\,|\,IP\rangle}$
(j) $\sigma 6$ and $\sigma s6$, for the time delay and time delay–strength distributions from $\tau 6_{\langle IP\,|\,MN\rangle}$ and $\eta 6_{\max\langle IP\,|\,MN\rangle}$

RESULTS

We recorded a total of 105 posterior IPns, classified as type A (**Figures 1A,D**). Type A neurons increase their firing in the time interval between conditioned (CS) and unconditioned (US) stimulus presentations across successive conditioning sessions (Gruart et al., 2000a; Sánchez-Campusano et al., 2007). In addition, we recorded 102 antidromically identified OO MNs (**Figures 1A,D**). Characteristically, OO Mns encode eyelid position during CRs (Trigo et al., 1999; Sánchez-Campusano et al., 2009). The two pools of neurons were recorded in separate experiments during classical eyelid conditioning (**Figures 1A,C**) using a delay paradigm (**Figures 1A,B**, see Materials and Methods). The present study was centered on the analysis of data collected in CS–US intervals across the successive sessions during the motor learning process. A more detailed description of OO Mn and IPn firing peculiarities during classical eyeblink conditioning can be found elsewhere (Trigo et al., 1999; Gruart et al., 2000a; Sánchez-Campusano et al., 2007, 2009, 2010).

MULTIPLE PARAMETRIC EVOLUTIONS OF THE TIMING, KINETIC NEURAL COMMANDS, AND KINEMATIC PARAMETERS DURING CLASSICAL CONDITIONING OF EYELID RESPONSES

A representation of the different parameters collected across conditioning sessions is illustrated in **Figure 3**. In **Figure 3A**, we show the timing parameters and in **Figure 3B** the kinetic (neural commands) and kinematic (performance of learned motor response) parameters computed here, presenting a coherent timing–intensity association between them (e.g., parameters 1 and 6; 2 and 7; 3 and 8; 4 and 9; 5 and either 10 or 11). In **Figure 3A**, the mean values of the relative refractory period of OO Mns (parameter 1) in the CS–US interval decreases across conditioning sessions [one-way

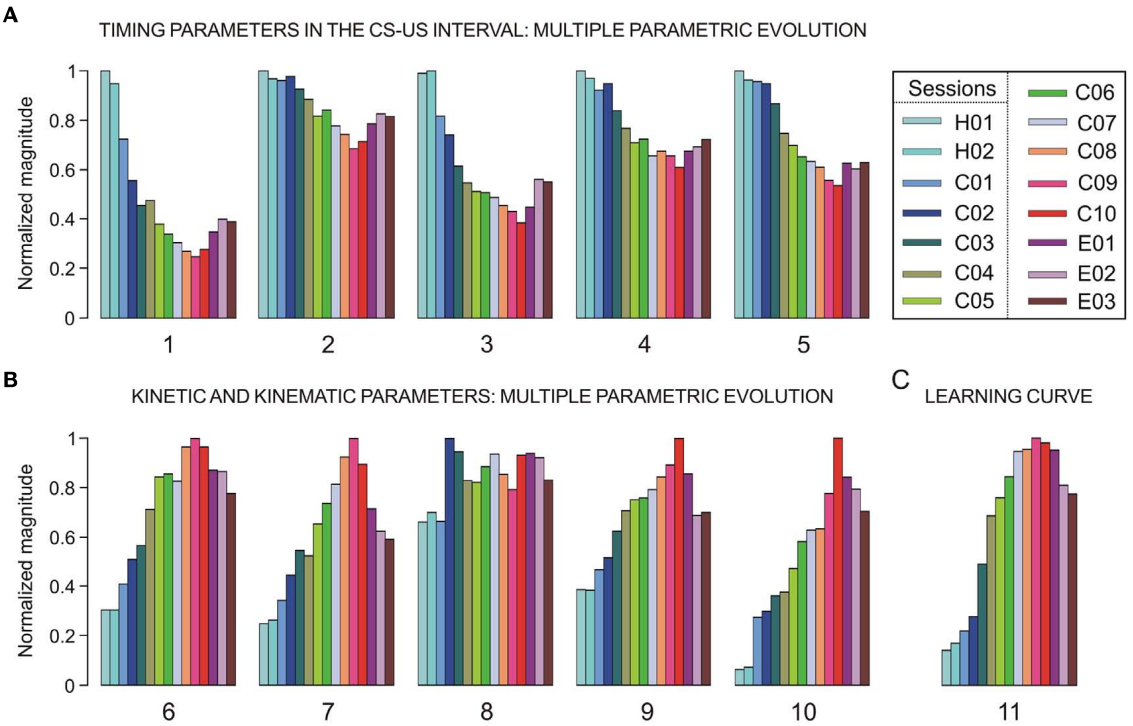

FIGURE 3 | A representation of multi-parametric evolution of timing, kinetic and kinematic parameters collected across habituation, conditioning, and extinction sessions. The color code indicates the corresponding conditioning session (from C01 to C10), each set of colored bars corresponds to the evolution of a given parameter (numbered from 1 to 11), and each colored bar indicates the mean parametric value resulting from averaging the trials of the same session, a procedure applied for each of the sessions. **(A)** The multiple parametric evolution of the timing parameters in the CS–US interval: parameters 1 and 3 (relative refractory period – i.e., the minimum interspike interval, in s), 2 and 4 (latency of the mean value of maximum instantaneous frequency with respect to CS presentation, in ms), and 5 (latency between the CS and the onset of the CR, in ms). **(B)** The multiple parametric evolution of the kinetic and kinematic parameters across sessions: parameters 6 and 8 (total number of spikes in the CS–US interval), 7 and 9 (mean peak firing rate, in spikes/s), and 10 (eyelid position amplitude at US presentation compared with the amplitude at the start of the CR, in degrees). The timing (parameters 1–4) and kinetic (parameters 6–9) parameters were calculated for both OO Mns (Mn, parameters 1, 2, 6, and 7) and IP neurons (parameters 3, 4, 8, and 9). The parameters 5, 10, and 11 characterize the proper timing and performance (kinematics) of learned eyelid responses. **(C)** The typical learning curve (evolution of the parameter 11) using this classical conditioning paradigm. For this timing–kinetic–kinematic multi-parametric representation, each parameter has been normalized in accordance with its maximum value across conditioning.

ANOVA F-test, $F_{(14,70,132)} = 206.20, P < 0.01$], and the latency of their maximum instantaneous frequency with respect to CS presentation [parameter 2, $F_{(14,70,132)} = 53.19, P < 0.01$] also decreases. The similar inverted evolution (from long to short periods or latencies) was obtained for the mean values of the relative refractory period of the IPns [parameter 3, $F_{(14,70,132)} = 126.44, P < 0.01$] and for the latency (with respect to CS onset) of their maximum instantaneous frequency in the CS–US interval [parameter 4, $F_{(14,70,132)} = 93.87$, $P < 0.01$] across conditioning sessions. Finally, the parameter 5 (mean values of the latency between the CS onset and the start of the CR, see **Figure 2A**) also decreases with significant statistical differences [$F_{(14,70,132)} = 123.50, P < 0.01$] along the conditioning process.

As illustrated in **Figure 3B**, the kinetic neural commands and kinematic parameters presented in general an opposite evolution (from low to high values) across conditioning sessions with respect to the evolution of the timing parameters shown in **Figure 3A**. For example, the total number of spikes generated by OO Mns (parameter 6) during the CS–US interval increases across conditioning sessions [one-way ANOVA F-test, $F_{(14,70,132)} = 187.12, P < 0.01$] and their mean peak firing rate (parameter 7) also increases [$F_{(14,70,132)} = 207.31, P < 0.01$], indicating that this dorsolateral portion of the facial nucleus (the site where OO Mns are located) was involved as the neural element driving (kinetic neural command) the eyelid CRs. Interestingly, the mean number of spikes (parameter 8) generated by IPns in the CS–US interval did not change significantly [$F_{(14,70,132)} = 1.63, P > 0.05$] across conditioning. In contrast, the mean peak firing rate of IPns [parameter 9, $F_{(14,70,132)} = 143.86, P < 0.01$] increased across conditioning sessions and decreased progressively during the three extinction sessions. These contrasting evolutions suggest that the increase in IP neuronal firing rate after CS presentation represented a reorganization (rather than a net increase) of their mean spontaneous firing. Finally, parameter 10 in **Figure 3B** corresponds to the peak amplitude of the evoked CR. Note that this parameter also increased steadily across conditioning sessions and decreased progressively during the three extinction sessions [$F_{(14,70,132)} = 251.27, P < 0.01$].

The evolution of these intensity/amplitude parameters (6, 7, 9, and 10 in **Figure 3B**) across conditioning was analogous to that verified for the parameter 11 [$F_{(14,70,132)} = 129.40, P < 0.01$] – i.e., the percentage of CRs across conditioning (**Figure 3C**) – and to the one observed previously in typical learning curves using the same

classical conditioning paradigm (Domínguez-del-Toro et al., 2004; Gruart, et al., 1995; Sánchez-Campusano et al., 2007, 2009, 2010; Porras-García et al., 2010). Finally, note that in **Figure 3**, the parameters were normalized in accordance with their maximum values across conditioning. Thus, the maximum values of the mean latencies of the maximum instantaneous frequencies were 259.14 ms (parameter 2, session H01) and 93.06 ms (parameter 4, session H01) for Mns and IPns, respectively; the maximum values of mean number of spikes generated in the CS–US interval (parameters 6 and 8) were 9.83 spikes (in session C09) and 15.38 spikes (in session C02) for Mns and IPns, respectively; and the maximum values of mean peak of the firing rate were 158.27 spikes/s (parameter 7, session C09) and 322.60 spike/s (parameter 9, session C10) for both Mns and IPns, respectively.

THE EVOLUTION OF THE CORRELATION CODE PARAMETERS AND FALLING CORRELATION PROPERTY OF THE INTERPOSITUS NUCLEUS NEURONS

In the previous sections, we have presented results relating to the acquisition and representation of the physiological multiparametric data (**Figure 3**) collected across conditioning sessions and the level of expression of eyelid CRs. These results (quantitative multi-parametric analyses and the learning curve) were necessary but insufficient for a precise dynamic description of the conditioning process. In this section, we use an analytical approach (the non-linear multivariate analysis of electrophysiological recordings) to understand the functional correlation code and the directional coupling mechanisms (see Non-linear Dynamic Associations Between Electrophysiological Recordings) between the EMG activity of the OO muscle and crude recordings of both facial and IP nuclei, and between the two neuronal recordings (Mn and IPn activities) during the classical conditioning of eyelid responses.

In a previous study from our group (Sánchez-Campusano et al., 2009) we showed the non-linear association analyses at the asymptotic level of acquisition (i.e., the 10th conditioning session) of this associative learning test (details regarding the theoretical formulation of this dynamic association method for the electrophysiological recordings can be found in Sánchez-Campusano et al., 2009, 2010 and in Porras-García et al., 2010). In the present paper, we carry out the exhaustive analyses of dynamic associations between the recordings during all the conditioning sessions (see **Figure 4A**). The degree of association between the EMG activity of the OO muscle $[Y_{EMG}(t)]$ and crude recordings of neuronal

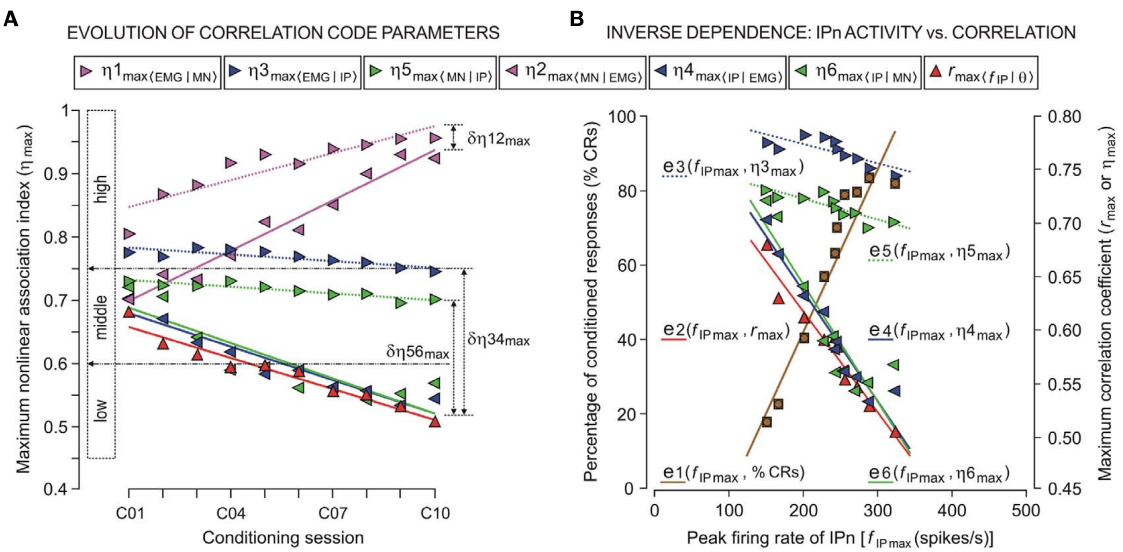

FIGURE 4 | The trend in the evolution of the correlation code parameters (linear and non-linear correlation coefficients and the asymmetry information) and the inverse dependence of this on the evolution of the peak firing rate of IP neurons across conditioning sessions (from C01 to C10). **(A)** The color code indicates the four dynamic associations [magenta, for Mn raw activity vs. OO EMG recording (OO EMG); blue, for IP neuron raw activity vs. OO EMG; green, for IPn vs. Mn raw recordings; and red, for IP neuron instantaneous frequency $f_{IP}(t)$ vs. the eyelid position $\theta(t)$ response] for this analysis. Each colored triangle pointing toward the right corresponds to the mean value of maximum non-linear association index in the preferential direction of coupling [$\eta 1_{max\langle EMG \mid MN\rangle}$, $\eta 3_{max\langle EMG \mid IP\rangle}$, and $\eta 5_{max\langle MN \mid IP\rangle}$] and each colored triangle pointing toward the left indicates the mean values of maximum non-linear association index in the opposite direction [$\eta 2_{max\langle MN \mid EMG\rangle}$, $\eta 4_{max\langle IP \mid EMG\rangle}$, and $\eta 6_{max\langle IP \mid MN\rangle}$, see the legend]. Each red triangle pointing up corresponds to the mean value of maximum linear correlation coefficient [$r_{max\langle fIP \mid \theta\rangle}$] calculated during a conditioning session. The colored lines represent the linear regression models for each set of maximum association indices across conditioning sessions. The three ranges of correlation coefficient values (high, middle, and low) are indicated. The magnitudes $\delta\eta 12_{max}$, $\delta\eta 34_{max}$ and $\delta\eta 56_{max}$ indicate the difference (asymmetry information) between the pairs of maximum association indices at the asymptotic level (the 10th session) of acquisition of this associative learning test. **(B)** The abscissa and the left ordinate illustrate the relationship between the peak firing rate of IP neurons ($f_{IP\,max}$) and the percentage of CRs (%CRs; brown squares; e1 regression line). The abscissa and the right ordinate illustrate the relationship between $f_{IP\,max}$ and the correlation code (red triangles, $r_{max\langle fIP \mid \theta\rangle}$ linear correlation coefficients, e2 regression line; blue and green triangles, $\eta 3_{max\langle EMG \mid IP\rangle}$, …, $\eta 6_{max\langle IP \mid MN\rangle}$ non-linear association indices, e3, …, e6 regression lines). Note that both the level of expression of CRs (i.e., %CRs) and the evolution of $f_{IP\,max}$ depend inversely on the evolution of strength (from strong to moderate, or from moderate to weak) of the dynamic associations (i.e., the linear and non-linear correlation coefficients) between the IP neuron (IPn) activity and either the Mn kinetic neural command or kinematic variable (eyelid position or OO EMG). In **Table 1** are summarized the regression parameters for this figure.

responses $[X_{NR}(t)]$ collected from facial $[X_{MN}(t)]$ and IP $[X_{IP}(t)]$ neurons was obtained by computing the non-linear association index $\eta_{\langle -|- \rangle}$ as a function of a time shift $\tau_{\langle -|- \rangle}$ between these muscular and neuronal electrophysiological recordings. The association between the two neuronal activities was also analyzed [$Y_{MN}(t)$ vs. $X_{IP}(t)$ and vice versa].

The non-linear association functions corresponding to the trials taken from the same session were averaged, session by session and for each experimental subject. The present study was centered on the analysis of the data (correlation codes and time delays) collected at CS–US intervals across the 10 conditioning sessions (C01–C10). In **Figure 4A**, we represent the maximum values of non-linear association indices (η_{max}) and their evolution across training. The maximum indices between Mns activity and OO EMG recording remained high ($\eta_{max} \geq 0.75$) across conditioning sessions. The magenta regression lines [for the evolution of the indices $\eta 1_{max\,\langle EMG\,|\,MN\rangle}$ and $\eta 2_{max\,\langle MN\,|\,EMG\rangle}$] showed a strongly increasing trend (see the parameters of this trend analysis – i.e., the magnitudes and signs of the correlation coefficients *R*, the significances *P*, and the equations (slope and intercept) of the regression lines, in **Table 1**). Thus, motoneuronal activities correlate significantly [one-way ANOVA *F*-tests, $F_{(9,\,27,\,98)} = 3.06$, $P < 0.01$ for $\eta 1_{max\,\langle EMG\,|\,MN\rangle}$; and $F_{(9,\,27,\,98)} = 2.51$, $P < 0.01$ for $\eta 2_{max\,\langle MN\,|\,EMG\rangle}$] with the EMG activity of the OO muscle during the performance of conditioned eyelid responses in all the conditioning sessions. However, the increase in the mean peak firing rate of IPns (parameter 9 in **Figure 3B**), together with the decrease in its time of occurrence (parameter 4 in **Figure 3A**), always lagged the start of the CR (see **Figure 2A**) and caused a decrease in the non-linear association indices between IPn activity and eyelid CRs (determined by OO EMG activity) across conditioning (see **Figure 4A**). A standard analysis of the trends using linear regression models enabled us to determine the evolution of the η_{max} across training (in all of the regressions see the signs of *R* and the slope in **Table 1**). For example, the blue and green regression lines [for the evolution of the indices $\eta 3_{max\,\langle EMG\,|\,IP\rangle}$, $\eta 4_{max\,\langle IP\,|\,EMG\rangle}$, $\eta 5_{max\,\langle MN\,|\,IP\rangle}$, and $\eta 6_{max\,\langle IP\,|\,MN\rangle}$] showed clear negative slopes (see **Table 1**), and therefore a decrease (the negative signs of *R*) of correlation levels in accord with non-linear correlation analyses. In turn, the values of the maximum non-linear association indices were statistically significant across conditioning sessions [one-way ANOVA *F*-tests, $F_{(9,\,27,\,98)} = 7.26$, $P < 0.01$, for $\eta 3_{max\,\langle EMG\,|\,IP\rangle}$; $F_{(9,\,27,\,98)} = 11.02$, $P < 0.01$, for $\eta 4_{max\,\langle IP\,|\,EMG\rangle}$; $F_{(9,\,27,\,98)} = 9.45$, $P < 0.01$, for $\eta 5_{max\,\langle MN\,|\,IP\rangle}$; $F_{(9,\,27,\,98)} = 12.33$, $P < 0.01$, for $\eta 6_{max\,\langle IP\,|\,MN\rangle}$], although their values showed only a slight coupling ($0.5 \leq \eta_{max} < 0.8$, i.e., the two signals were moderately related) between the neuronal activity recorded at the IP nucleus $[X_{IP}(t)]$ and either the EMG activity of the OO muscle $[Y_{EMG}(t)]$ or Mn neuronal recording $[X_{MN}(t)]$ during the performance of the conditioned eyelid responses. In this particular case, the maximum values of mean association indices always lagged the zero reference point (i.e., the moment at which the conditioned eyelid response started, see red arrow in **Figure 2A**) in all the successive conditioning sessions.

Table 1 | The parameters of the linear regression analyses [the correlation coefficient (R), the significance level (*P*), and the linear equation parameters (slopes and intercepts)] for the Figures 4A,B.

	The parameters of the linear regression		
	Correlation coefficient (*R*)	**Significance (*P*)**	**Linear equation (slope and intercept)**
FIGURE 4A			
Maximum association index evolution			
$\eta 1_{max\,\langle EMG\,|\,MN\rangle}$ vs. sessions	0.9029	0.0003	$Y = 0.0143\,X + 0.8332$
$\eta 2_{max\,\langle MN\,|\,EMG\rangle}$ vs. sessions	0.9817	0.0000	$Y = 0.0268\,X + 0.6710$
$\eta 3_{max\,\langle EMG\,|\,IP\rangle}$ vs. sessions	–0.8439	0.0021	$Y = -0.0035\,X + 0.7860$
$\eta 4_{max\,\langle IP\,|\,EMG\rangle}$ vs. sessions	–0.9595	0.0000	$Y = -0.0179\,X + 0.6969$
$\eta 5_{max\,\langle MN\,|\,IP\rangle}$ vs. sessions	–0.9280	0.0001	$Y = -0.0037\,X + 0.7355$
$\eta 6_{max\,\langle IP\,|\,MN\rangle}$ vs. sessions	–0.8766	0.0009	$Y = -0.0187\,X + 0.7059$
$r_{max\,\langle f_{IP\,|\,\theta}\rangle}$ vs. sessions	–0.9734	0.0000	$Y = -0.0165\,X + 0.6736$
FIGURE 4B			
Peak firing rate of IPn dependence			
e1 ($f_{IP\,max}$, %CRs)	0.9523	0.0000	$Y = 0.4400\,X - 44.6746$
e2 ($f_{IP\,max}$, r_{max})	–0.9744	0.0000	$Y = -0.0009\,X + 0.8076$
e3 ($f_{IP\,max}$, $\eta 3_{max}$)	–0.7618	0.0104	$Y = -0.0002\,X + 0.8095$
e4 ($f_{IP\,max}$, $\eta 4_{max}$)	–0.9619	0.0000	$Y = -0.0010\,X + 0.8421$
e5 ($f_{IP\,max}$, $\eta 5_{max}$)	–0.8578	0.0015	$Y = -0.0002\,X + 0.7614$
e6 ($f_{IP\,max}$, $\eta 6_{max}$)	–0.8971	0.0004	$Y = -0.0011\,X + 0.8633$

Here, R is the well-known Pearson's product moment correlation coefficient – i.e., the conventional index frequently used to measure the linear correlation between two variables. For ***Figure 4A*** *are summarized the regression parameters for the evolution of maximum values of each non-conventional dynamic correlation coefficient [*$\eta 1_{max\,\langle EMG\,|\,MN\rangle}, \ldots, \eta 6_{max\,\langle IP\,|\,MN\rangle}$, *or* $r_{max\,\langle f\,IP\,|\,\theta\rangle}$*] across the conditioning sessions (trend analysis from C01 to C10). For* ***Figure 4B*** *are listed the regression parameters corresponding to the linear equations e1,…, e6. The signs of the slopes of these equations and the signs of R indicate that both the level of expression of CRs (i.e., %CRs) and the evolution of peak firing rate ($f_{IP\,max}$) of IPns (see equation e1) depend inversely on the evolution of the strength of the dynamic associations across learning (see equations e2,…, e6).*

Interestingly, for all the dynamic association analyses, the degree of asymmetry of the non-linear coupling between the pairs of electrophysiological recordings (IPn activity vs. either Mn or OO EMG recordings) was positive during all the conditioning sessions. Here we summarize the results for the information of asymmetry in the 10th conditioning session [$\Delta(\eta 12)^2_{max} = \eta 1^2_{max} - \eta 2^2_{max} \approx 0.0602$, with $\delta\eta 12_{max} = \eta 1_{max} - \eta 2_{max} \approx 0.0320$; $\Delta(\eta 34)^2_{max} = \eta 3^2_{max} - \eta 4^2_{max} \approx 0.2587$, with $\delta\eta 34_{max} = \eta 3_{max} - \eta 4_{max} \approx 0.2010$; $\Delta(\eta 56)^2_{max} = \eta 5^2_{max} - \eta 6^2_{max} \approx 0.1698$, with $\delta\eta 56_{max} = \eta 5_{max} - \eta 6_{max} \approx 0.1340$] (see **Figure 4A** in this paper, and Sánchez-Campusano et al., 2009 for details of the non-linear association curves and their maximum correlation values). Note that, for the coupling between Mns [$X_{MN}(t)$] and OO EMG [$Y_{EMG}(t)$] recordings, the values $\Delta(\eta 12)^2_{max}$ and $\delta\eta 12_{max}$ [for the indices $\eta 1_{max\langle EMG \mid MN\rangle}$ and $\eta 2_{max\langle MN \mid EMG\rangle}$] across conditioning sessions indicate a decrease in the degree of asymmetry in coupling [e.g., a variation of 7.21% for $\delta\eta 12_{max}$, which diminishes from 0.1041 (in session C01) to 0.0320 (in session C10)]. In geometrical terms, the progressive convergence of the red regression lines (i.e., a progressive loss in the degree of asymmetry) and the proper gain in the strength (the non-linear association indices, see **Figure 4A**) of coupling along conditioning allowed us to conclude that at the asymptotic level of acquisition of this associative learning test (session C10), the recording $Y_{EMG}(t)$ can be explained as a quasi-linear transformation of the Mns activity $X_{MN}(t)$.

However, the degree of asymmetry increased across conditioning sessions for the other two dynamic associations [$Y_{EMG}(t)$ vs. $X_{IP}(t)$, a variation of 12.9% for $\delta\eta 34_{max}$, which increased from 0.0720 (in session C01) to 0.2010 (in session C10); and $Y_{MN}(t)$ vs. $X_{IP}(t)$, a variation of 12.45% for $\delta\eta 56_{max}$, which increased from 0.0095 (in session C01) to 0.1340 (in session C10)]. Thus, one signal [i.e., $Y_{EMG}(t)$ or $Y_{MN}(t)$] can be explained as a transformation, possibly non-linear, of the other [i.e., $X_{IP}(t)$]. This gain in the degree of asymmetry (see in **Figure 4A** the increasing divergence between the blue (or green) pair of regression lines) and the verified loss in the strength of coupling (negative trends in the evolutions of the non-linear association indices) along conditioning demonstrated that a quasi-linear and unidirectional coupling between the recordings [$X_{IP}(t)$ vs. $Y_{MN}(t)$ or $X_{IP}(t)$ vs. $Y_{EMG}(t)$] was very unlikely, at least in the statistical sense. Finally, we could verify the falling correlation property of the IP nucleus across the successive training sessions, using the linear correlation coefficient $r_{max\langle fIP \mid \theta\rangle}$ [one-way ANOVA F-tests, $F_{(9, 27, 98)} = 161.54$, $P < 0.01$] between the firing rate of IPns $f_{IP}(t)$ and the eyelid position response $\theta(t)$ (see the red triangles and red regression lines in **Figure 4A**).

INVERSE DEPENDENCE BETWEEN THE STRENGTH OF DYNAMIC ASSOCIATIONS AND THE FIRING RATE OF INTERPOSITUS NUCLEUS NEURONS

In Section "Multiple Parametric Evolutions of the Timing, Kinetic Neural Commands, and Kinematic Parameters During Classical Conditioning of Eyelid Responses" and "The Evolution of the Correlation Code Parameters and Falling Correlation Property of the Interpositus Nucleus Neurons" we analyzed the multiple parametric evolutions of the kinetic neural commands (parameters 6, 7, 8, and 9 in **Figure 3B**) and kinematic parameters (parameters 10 and 11), as well as the trends in the evolution of the correlation code parameters [the linear and non-linear correlation coefficients in **Figure 4B**, $r_{max\langle fIP \mid \theta\rangle}$; $\eta 1_{max\langle EMG \mid MN\rangle}$ and $\eta 2_{max\langle MN \mid EMG\rangle}$; $\eta 3_{max\langle EMG \mid IP\rangle}$ and $\eta 4_{max\langle IP \mid EMG\rangle}$; $\eta 5_{max\langle MN \mid IP\rangle}$ and $\eta 6_{max\langle IP \mid MN\rangle}$, respectively] across conditioning. In this section, we summarize the dependence between the strength of the dynamic associations (correlation coefficient values in **Figure 4A**) and both the evolution of the peak firing rate of the IPns (i.e., the maximum amplitude of the instantaneous frequency $f_{IP\,max}$ in the CS–US interval, parameter 10 in **Figure 3B**) and the level of expression of conditioned eyeblink responses (i.e., the percentage of CRs, parameter 11 in **Figure 3B**) across this associative learning process.

In **Figure 4B**, note that the increase in the peak firing rate of IPns $f_{IP\,max}$ (e1 regression line) together with the decrease in its time of occurrence (it always lagged the start of CRs), caused a decrease in the linear correlation coefficient (e2 regression line for $r_{max\langle fIP \mid \theta\rangle}$) across conditioning sessions. In turn, a similar decrease was observed for the maximum values of the non-linear association indices [see the regression lines, e3 for $\eta 3_{max\langle EMG \mid IP\rangle}$; e4 for $\eta 4_{max\langle IP \mid EMG\rangle}$; e5 for $\eta 5_{max\langle MN \mid IP\rangle}$; and e6 for $\eta 6_{max\langle IP \mid MN\rangle}$]. Thus, the evolution of the strength (strong, moderate, or weak) of the linear and non-linear dynamic associations (i.e., the coefficients r_{max} and $\eta 3_{max}$, …, $\eta 6_{max}$) depends inversely on the level of expression of conditioned eyeblink responses (i.e.,%CR) and of the evolution of $f_{IP\,max}$ across learning. There is a significant increase (see $R > 0$, $P < 0.01$, and the positive sign of the slope of the regression line e1 in **Figure 4B** and **Table 1**) in the amplitude–intensity mutual evolution ($f_{IP\,max}$ as a kinetic neural command and %CR as a measure of the performance of learned motor responses) and a significant decrease (see $R < 0$, $P < 0.01$, and the negative signs of the slopes of the regression lines e2, e3, e4, e5, and e6 in **Figure 4B** and **Table 1**) in the amplitude–strength mutual evolution ($f_{IP\,max}$ and r_{max}, $\eta 3_{max}$, $\eta 4_{max}$, $\eta 5_{max}$, and $\eta 6_{max}$) across conditioning sessions.

INTERACTIONS BETWEEN THE PARAMETRIC TIMING INFORMATION AND THE TIME DELAYS IN COUPLING BETWEEN THE ELECTROPHYSIOLOGICAL RECORDINGS

In previous sections, we showed the evolution of the parametric timing information (see the timing parameters in **Figure 3A**) collected across conditioning. Additionally, we used the so-called "time delay information" to express the temporal order in the cerebellar–Mns network. According to the dynamic association method (see non-linear dynamic associations between electrophysiological recordings), the shift for which the maximum of the non-linear association index $\eta_{\langle - \mid - \rangle}$ was reached provided an estimate of the time delay $\tau_{\langle - \mid - \rangle}$ in coupling between the electrophysiological time series during this associative learning process. Thus, we were able to determine whether the maximum correlation (strong, moderate, or weak) between the recordings was before or after the zero reference point (i.e., the moment at which the CR started, **Figure 2A**).

At the same time, a set of techniques referred to as circular statistics has been developed for the analysis of directional and orientational data. The unit of measurement for such data is angular (usually in either degrees or radians) and the circular distributions underlying the techniques are characterized by the proper time–degree correspondence. In this paper, we assert that such approaches can be easily adapted to analyze

the different events in the 0- to 270-ms interval (the duration of ISI, i.e., the CS–US interval) during the performance of the CR – for example, the angle of 0 degrees is deemed as corresponding to a time of 0 ms – that is, the CS onset instant; and the angle of 270° is deemed as corresponding to the time of US presentation – that is, 270 ms after CS onset, according to our delay paradigm (see **Figure 1B**). In **Figures 5A and 6A** we show the circular distributions of both parametric timing–intensity

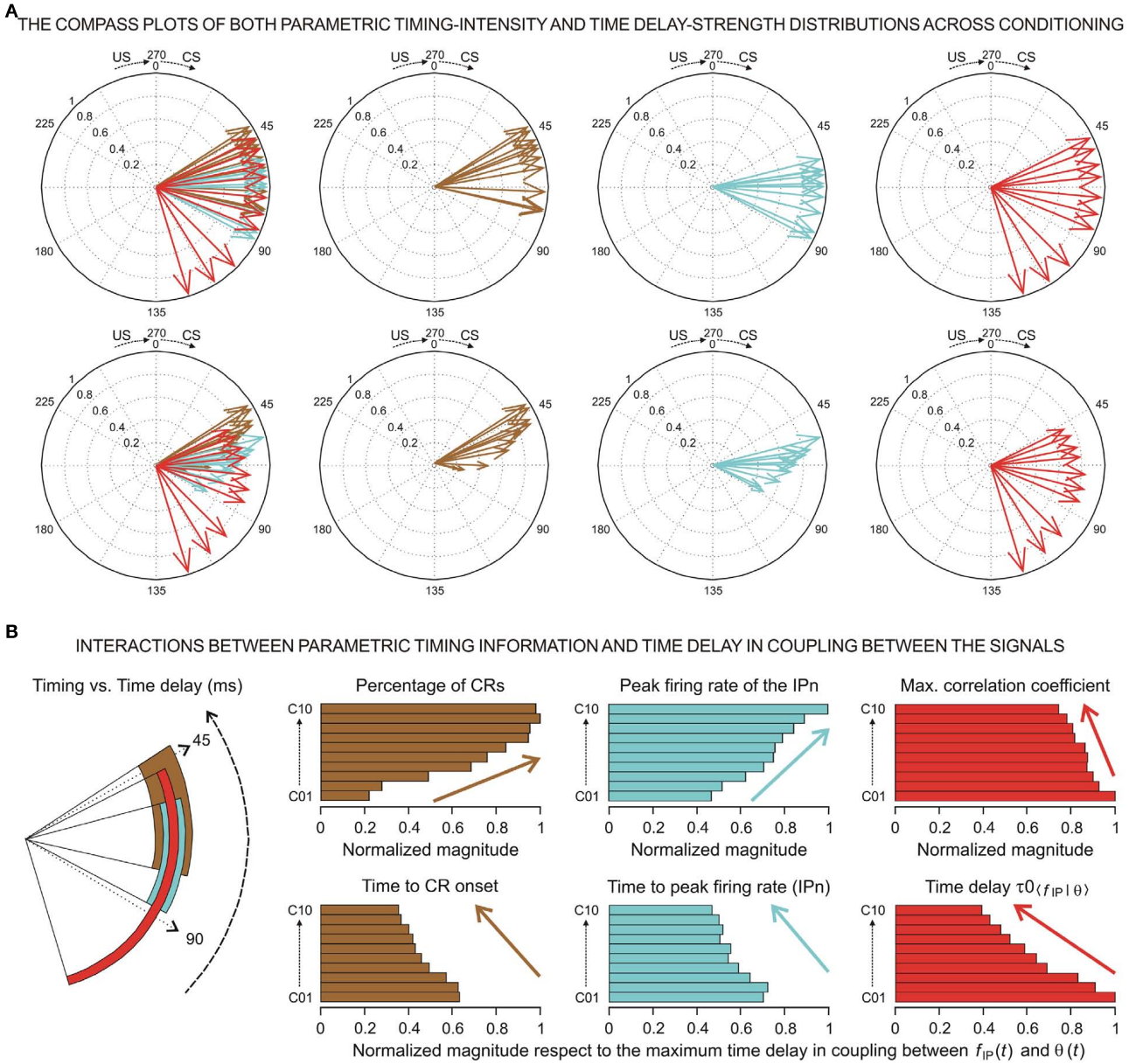

FIGURE 5 | (A) The compass plots of both parametric timing–intensity and time delay–strength distributions across the 10 conditioning sessions. In this representation, the timing–intensity distributions (1) [time to CR onset, and percentage of CR], see brown arrows, and (2) [time to peak firing rate of IP neurons (IPn) peak firing rate], see cyan arrows, and the time delay–strength distributions (3) [time delay in coupling $\tau 0_{\langle f_{IP}|\theta\rangle}$, maximum linear correlation coefficient $r_{max(f_{IP}|\theta)}$], see red arrows, were plotted using the circular approach for the inter-stimulus interval of 270 ms (CS–US interval). The 10 colored arrows (10 conditioning sessions, C01–C10) in each circle illustrate the circular dispersion of the angular datasets represented. The first row of circles corresponds to the representation of the time (timing and time delay) distributions on the unitary circle to explore the time-dispersion patterns of datasets (see the dispersion parameters in **Table 2**), and the second row of circles shows the time–intensity distributions in accordance with the actual intensity/strength components to investigate the time–intensity dispersion patterns across conditioning (see the dispersion parameters in **Table 3**). **(B)** Interactions between parametric timing information and time delay in coupling between the firing rate of the IPn neurons $f_{IP}(t)$ and the eyelid position $\theta(t)$ response. The colored circular sectors illustrate the time-dispersion range of the data distributions represented in **(A)** (see **Table 2**). The colored histograms show the normalized mean values of intensity/strength components of the distributions and the normalized mean values of timing/time delay components with respect to the maximum time delay in coupling between $f_{IP}(t)$ and $\theta(t)$ [i.e., the maximum values of $\tau 0_{\langle f_{IP}|\theta\rangle}$ across conditioning sessions].

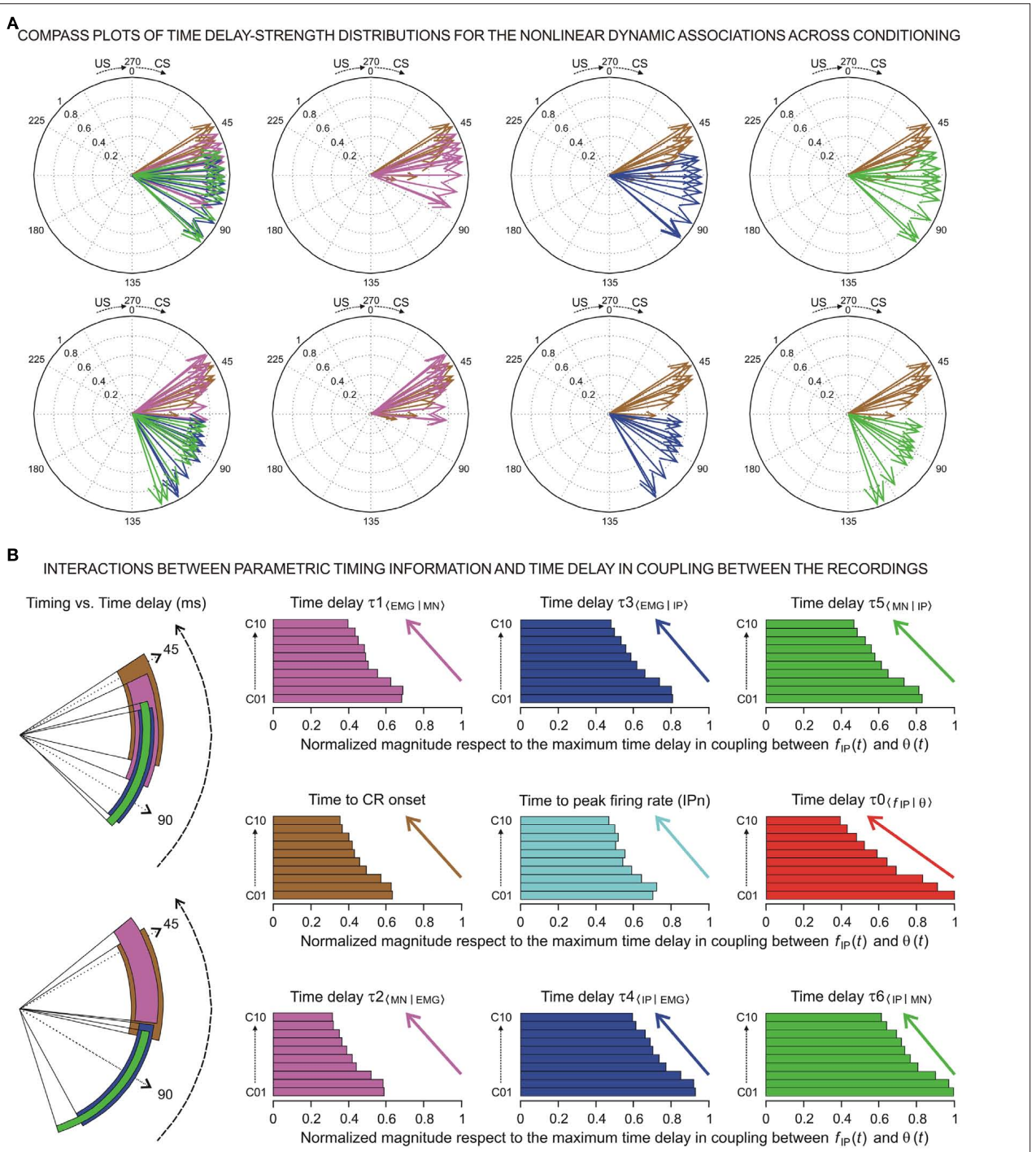

FIGURE 6 | (A) The compass plots of time delay–strength distributions for the non-linear dynamic associations across the 10 conditioning sessions. In this representation, the time delay–strength distributions (1) [$\tau 1_{\langle EMG \mid MN \rangle}$, $\eta 1_{max\,\langle EMG \mid MN \rangle}$] and (2) [$\tau 2_{\langle MN \mid EMG \rangle}$, $\eta 2_{max\,\langle MN \mid EMG \rangle}$], see magenta arrows, (3) [$\tau 3_{\langle EMG \mid IP \rangle}$, $\eta 3_{max\,\langle EMG \mid IP \rangle}$] and (4) [$\tau 4_{\langle IP \mid EMG \rangle}$, $\eta 4_{max\,\langle IP \mid EMG \rangle}$], see blue arrows, and (5) [$\tau 5_{\langle MN \mid IP \rangle}$, $\eta 5_{max\,\langle MN \mid IP \rangle}$] and (6) [$\tau 6_{\langle IP \mid MN \rangle}$, $\eta 6_{max\,\langle IP \mid MN \rangle}$], see green arrows, were plotted using the circular statistics method for the inter-stimulus interval of 270 ms (CS–US interval). The 10 colored arrows (10 conditioning sessions, C01–C10) in each circle illustrate the circular dispersion of the angular datasets represented. The two rows of circles show the time delay–strength distributions to explore the time–strength dispersion patterns across conditioning (see the dispersion parameters in **Table 3**). **(B)** Interactions between parametric timing information and time delays in coupling between the recordings. The colored circular sectors illustrate the time-dispersion range of the data distributions represented in **(A)** (see the dispersion parameters **Table 2**). The colored histograms show the normalized mean values of timing/time delay components of the distributions with respect to the maximum time delay in coupling between $f_{IP}(t)$ and $\theta(t)$ [i.e., the maximum values of $\tau 0_{\langle f\,IP \mid \theta \rangle}$ across conditioning sessions].

and time delay–strength distributions across conditioning sessions, using a compass plot to analyze time–intensity dispersion patterns in this learning process.

In **Figure 5**, we selected as the timing components of the distributions the time to CR onset (see brown arrows) and the time to peak firing rate of the IPn (see cyan arrows), and the corresponding intensity components of the represented distributions were the percentage of CRs and the peak firing rate of the IPn, respectively (see **Figures 5A,B**). In many situations, the interpretation of the evolution of a physical magnitude lacks a proper complementation between the evolution of its intensities/amplitudes and the temporal dynamics of its variations. Thus, these timing–intensity associations enabled us to illustrate the simultaneous evolution of the timing and intensity components of these data distributions across conditioning sessions (see **Figure 2C** and the second row in **Figure 5A**). Notice the inverse interrelations between the percentage of CRs and the time to CR onset (arrows and histogram in brown), and between the peak firing rate of the IPn and their corresponding time of occurrence (arrows and histogram in cyan) across this associative learning test (**Figures 5A,B**). However, the time to peak firing rate of the IPn always lagged the beginning of the CR (see the cyan and brown circular sectors and histograms in **Figure 5B**).

In this paper, the circular statistics enabled us to determinate the index of dispersion, which measures the degree of spread for these physiological circular data (see Circular Statistics to Analyze Time-Dispersion Patterns During Motor Learning). Thus, the dispersion patterns could provide an appropriate means of estimating the contribution (time-intensity) of the different centers (in the cerebellar-IP/red-nucleus-Mns pathway) participating in the conditioning process. The left-hand circumferences in **Figures 5A and 6A** and the left-hand circular sectors in **Figures 5B and 6B** show the circular dispersions of the timing and time delay parameters. For example, in **Figure 5A** the mean values of the time to peak firing rate of the IPn across the conditioning sessions (cyan arrows) were less spread out than the mean values of either time to CR onset (brown arrows) or time delay $\tau 0_{\langle f\,\mathrm{IP}\,|\,\theta\rangle}$ in coupling between IPn instantaneous frequency and eyelid position response (red arrows). Interestingly, the time-dispersion range for the time delay $\tau 0_{\langle f\,\mathrm{IP}\,|\,\theta\rangle}$ showed a significant [one-way ANOVA *F*-tests, $F_{(9,27,98)} = 223.54$, $P < 0.01$] transition from larger to smaller values, than the time to peak firing rate of IPn across the sessions. Thus, to the beginning of the learning process the IPns encoded (from moderate to weak correlation) eyelid position response after reaching their maximum firing rate, but at the end of the process (i.e., at the asymptotic level of acquisition of this associative learning test) the IPns encoded (with barely significant correlation) eyelid kinematics before their peak firing rate (but always after the beginning of the CR).

In geometric terms, the centroid (in a two-dimensional space with a fixed intensity component and variable timing component) of the cyan circular sector (corresponding to the time to peak firing rate of the IPn in **Figure 5B**) was much further away from the center of the circumference than the centroid of the red circular sector [corresponding to $\tau 0_{\langle f\,\mathrm{IP}\,|\,\theta\rangle}$] was from the center of the same circumference – that is, the index of circular spread of the cyan circular sector (σ_{IP}, for IPn timing component, see **Table 2**) was smaller than the time-dispersion index of the red circular sector [$\sigma 0$, for time delay component $\tau 0_{\langle f\,\mathrm{IP}\,|\,\theta\rangle}$]. This is generally the case – data sets with a greater degree of dispersion have centroids closer to the center of the circumference.

In **Figure 6**, the time delay–strength distributions were conformed using the time delays in coupling between the physiological signals [$\tau 0_{\langle f\,\mathrm{IP}\,|\,\theta\rangle}$, see red arrows; $\tau 1_{\langle \mathrm{EMG}\,|\,\mathrm{MN}\rangle}$ and $\tau 2_{\langle \mathrm{MN}\,|\,\mathrm{EMG}\rangle}$, see magenta arrows; $\tau 3_{\langle \mathrm{EMG}\,|\,\mathrm{IP}\rangle}$ and $\tau 4_{\langle \mathrm{IP}\,|\,\mathrm{EMG}\rangle}$, see blue arrows; $\tau 5_{\langle \mathrm{MN}\,|\,\mathrm{IP}\rangle}$ and $\tau 6_{\langle \mathrm{IP}\,|\,\mathrm{MN}\rangle}$, see green arrows] and their corresponding correlation code parameters [$r_{\max\langle f\,\mathrm{IP}\,|\,\theta\rangle}$; $\eta 1_{\max\langle \mathrm{EMG}\,|\,\mathrm{MN}\rangle}$ and $\eta 2_{\max\langle \mathrm{MN}\,|\,\mathrm{EMG}\rangle}$; $\eta 3_{\max\langle \mathrm{EMG}\,|\,\mathrm{IP}\rangle}$ and $\eta 4_{\max\langle \mathrm{IP}\,|\,\mathrm{EMG}\rangle}$; $\eta 5_{\max\langle \mathrm{MN}\,|\,\mathrm{IP}\rangle}$ and $\eta 6_{\max\langle \mathrm{IP}\,|\,\mathrm{MN}\rangle}$]. For the dynamic associations between IPns and either OO Mns or OO EMG recordings the relationships between the time delay ($\tau 3,\ldots,\tau 6$) and strength ($\eta 3_{\max},\ldots,\eta 6_{\max}$) components of the distributions were direct but diminishing across the conditioning sessions (see the blue and green arrows in **Figure 6A** and the blue and green histograms in **Figure 6B**). In contrast, for the coupling between Mns and OO EMG recordings, the relationships between time delay and strength components were inverse – that is, while the non-linear association indices [$\eta 1_{\max\langle \mathrm{EMG}\,|\,\mathrm{MN}\rangle}$ and $\eta 2_{\max\langle \mathrm{MN}\,|\,\mathrm{EMG}\rangle}$] were increasing, their corresponding time delays [$\tau 1_{\langle \mathrm{EMG}\,|\,\mathrm{MN}\rangle}$, $F_{(9,27,98)} = 66.29$, $P < 0.01$; and $\tau 2_{\langle \mathrm{MN}\,|\,\mathrm{EMG}\rangle}$, $F_{(9,27,98)} = 49.16$, $P < 0.01$] were decreasing across conditioning sessions in the opposed sense to the hands of the clock (i.e., from US to CS, see the black circular arrows in the left-hand circular sectors in **Figures 5B and 6B**).

According to the circular representations in **Figure 6B**, the time-dispersion indices of the green circular sectors [$\sigma 5$ and $\sigma 6$, for time delay components corresponding with $\tau 5_{\langle \mathrm{MN}\,|\,\mathrm{IP}\rangle}$, $F_{(9,27,98)} = 121.78$, $P < 0.01$; and $\tau 6_{\langle \mathrm{IP}\,|\,\mathrm{MN}\rangle}$, $F_{(9,27,98)} = 188.40$, $P < 0.01$, respectively] were larger than the indices of circular spread of the blue circular sectors [$\sigma 3$ and $\sigma 4$, for time delay components corresponding with $\tau 3_{\langle \mathrm{EMG}\,|\,\mathrm{IP}\rangle}$, $F_{(9,27,98)} = 119.36$, $P < 0.01$; and $\tau 4_{\langle \mathrm{IP}\,|\,\mathrm{EMG}\rangle}$, $F_{(9,27,98)} = 171.05$, $P < 0.01$, respectively]. Furthermore, the time delays between the cerebellar-IPn raw recording and the OO EMG activity in the two directions of coupling (see the blue histograms for $\tau 3_{\langle \mathrm{EMG}\,|\,\mathrm{IP}\rangle}$ and $\tau 4_{\langle \mathrm{IP}\,|\,\mathrm{EMG}\rangle}$ in **Figure 6B**) always lagged the start of the CR (see the brown histogram and the brown circular sector corresponding to the time-dispersion index σ_{CR}).

Here we also summarize the results of the relative time delays in coupling, with respect to the start of the CR, in the 10th conditioning session ($\Delta\tau 12 = \tau 1 - \tau 2 \approx 10.03$ ms, $\Delta\tau 34 = \tau 3 - \tau 4 \approx -13.69$ ms, and $\Delta\tau 56 = \tau 5 - \tau 6 \approx -18.08$ ms; see **Figure 6A** in this study, and Sánchez-Campusano et al., 2009 for details of the non-linear association curves and their time delays). Note that whereas the relative time delay in coupling $\Delta\tau 12$ between Mns $X_{\mathrm{MN}}(t)$ and muscle $Y_{\mathrm{EMG}}(t)$ recordings was positive [in geometric terms, the positive difference (session by session) between the magenta circular sectors in **Figure 6B**], the relative time delays in coupling between IPns $X_{\mathrm{IP}}(t)$ and either Mns $Y_{\mathrm{MN}}(t)$ or electromyography $Y_{\mathrm{EMG}}(t)$ recordings – i.e., $\Delta\tau 34$ and $\Delta\tau 56$ – were always negative across conditioning sessions [in geometric terms, the negative difference (session by session) between the blue (or green) circular sectors in **Figure 6B**]. The foregoing was due to the following specific mathematical relationships between the time delays in the two directions of coupling across conditioning sessions: $\tau 1 > 0$ and $\tau 2 < 0$; $\tau 3 > 0$ and $\tau 4 > 0$, but $\tau 4 > \tau 3$; $\tau 5 > 0$ and $\tau 6 > 0$, but $\tau 6 > \tau 5$.

Table 2 | The parametric timing and time delay dispersion indices (σ) corresponding to the circular distributions of the datasets across conditioning sessions, and for three different durations of the inter-stimulus interval (ISI).

Mean angle (in radians)		Mean timing (in milliseconds)		Mean radius of the centroid		Circular kurtosis index		Time-dispersion index	
ISI = 270 ms (CS–US INTERVAL, IN THE SUB-SECONDS RANGE)									
$\overline{\Omega}_{MN}$	5.0202	$\overline{T}_{MN}$	215.7259	$\overline{C}_{MN}$	0.0832	ρ_{MN}	0.4199	σ_{MN}	41.9183
$\overline{\Omega}_{CR}$	1.3434	$\overline{T}_{CR}$	57.7294	$\overline{C}_{CR}$	0.0962	ρ_{CR}	0.8539	σ_{CR}	7.8896
$\overline{\Omega}_{IP}$	1.6228	$\overline{T}_{IP}$	69.7354	$\overline{C}_{IP}$	0.0972	ρ_{IP}	0.8910	σ_{IP}	5.7710
$\overline{\Omega}0$	1.8227	$\overline{T}0$	78.3229	$\overline{C}0$	0.0850	$\rho0$	0.4864	$\sigma0$	35.5164
$\overline{\Omega}1$	1.4978	$\overline{T}1$	64.3623	$\overline{C}1$	0.0962	$\rho1$	0.8536	$\sigma1$	7.9113
$\overline{\Omega}2$	1.2120	$\overline{T}2$	52.0832	$\overline{C}2$	0.0962	$\rho2$	0.8551	$\sigma2$	7.8237
$\overline{\Omega}3$	1.7772	$\overline{T}3$	76.3711	$\overline{C}3$	0.0948	$\rho3$	0.8017	$\sigma3$	11.0338
$\overline{\Omega}4$	2.1122	$\overline{T}4$	90.7634	$\overline{C}4$	0.0949	$\rho4$	0.8049	$\sigma4$	10.8351
$\overline{\Omega}5$	1.7645	$\overline{T}5$	75.8225	$\overline{C}5$	0.0941	$\rho5$	0.7775	$\sigma5$	12.5633
$\overline{\Omega}6$	2.2227	$\overline{T}6$	95.5117	$\overline{C}6$	0.0937	$\rho6$	0.7628	$\sigma6$	13.5142
***ISI = 360 ms (CS–US INTERVAL, IN THE SUB-SECONDS RANGE)**									
$\overline{\Omega}_{MN}$	3.7658	$\overline{T}_{MN}$	215.7643	$\overline{C}_{MN}$	0.0903	ρ_{MN}	0.6441	σ_{MN}	21.8045
$\overline{\Omega}_{CR}$	1.0081	$\overline{T}_{CR}$	57.7627	$\overline{C}_{CR}$	0.0979	ρ_{CR}	0.9161	σ_{CR}	4.3784
$\overline{\Omega}_{IP}$	1.2176	$\overline{T}_{IP}$	69.7624	$\overline{C}_{IP}$	0.0984	ρ_{IP}	0.9376	σ_{IP}	3.2203
$\overline{\Omega}0$	1.3720	$\overline{T}0$	78.6083	$\overline{C}0$	0.0914	$\rho0$	0.6838	$\sigma0$	18.9297
$\overline{\Omega}1$	1.1239	$\overline{T}1$	64.3936	$\overline{C}1$	0.0979	$\rho1$	0.9159	$\sigma1$	4.3923
$\overline{\Omega}2$	0.9096	$\overline{T}2$	52.1186	$\overline{C}2$	0.0979	$\rho2$	0.9168	$\sigma2$	4.3442
$\overline{\Omega}3$	1.3337	$\overline{T}3$	76.4144	$\overline{C}3$	0.0971	$\rho3$	0.8853	$\sigma3$	6.0854
$\overline{\Omega}4$	1.5849	$\overline{T}4$	90.8055	$\overline{C}4$	0.0971	$\rho4$	0.8871	$\sigma4$	5.9854
$\overline{\Omega}5$	1.3244	$\overline{T}5$	75.8846	$\overline{C}5$	0.0967	$\rho5$	0.8705	$\sigma5$	6.9279
$\overline{\Omega}6$	1.6681	$\overline{T}6$	95.5762	$\overline{C}6$	0.0964	$\rho6$	0.8616	$\sigma6$	7.4427
***ISI = 450 ms (CS–US INTERVAL, IN THE SUB-SECONDS RANGE)**									
$\overline{\Omega}_{MN}$	3.0129	$\overline{T}_{MN}$	215.7805	$\overline{C}_{MN}$	0.0938	ρ_{MN}	0.7630	σ_{MN}	13.4836
$\overline{\Omega}_{CR}$	0.8067	$\overline{T}_{CR}$	57.7778	$\overline{C}_{CR}$	0.0986	ρ_{CR}	0.9458	σ_{CR}	2.7848
$\overline{\Omega}_{IP}$	0.9742	$\overline{T}_{IP}$	69.7748	$\overline{C}_{IP}$	0.0990	ρ_{IP}	0.9598	σ_{IP}	2.0534
$\overline{\Omega}0$	1.0993	$\overline{T}0$	78.7320	$\overline{C}0$	0.0944	$\rho0$	0.7891	$\sigma0$	11.8251
$\overline{\Omega}1$	0.8993	$\overline{T}1$	64.4079	$\overline{C}1$	0.0986	$\rho1$	0.9456	$\sigma1$	2.7942
$\overline{\Omega}2$	0.7279	$\overline{T}2$	52.1347	$\overline{C}2$	0.0986	$\rho2$	0.9462	$\sigma2$	2.7637
$\overline{\Omega}3$	1.0672	$\overline{T}3$	76.4339	$\overline{C}3$	0.0981	$\rho3$	0.9257	$\sigma3$	3.8596
$\overline{\Omega}4$	1.2681	$\overline{T}4$	90.8245	$\overline{C}4$	0.0981	$\rho4$	0.9268	$\sigma4$	3.7990
$\overline{\Omega}5$	1.0599	$\overline{T}5$	75.9126	$\overline{C}5$	0.0979	$\rho5$	0.9159	$\sigma5$	4.3936
$\overline{\Omega}6$	1.3349	$\overline{T}6$	95.6053	$\overline{C}6$	0.0977	$\rho6$	0.9099	$\sigma6$	4.7174

*These results are in correspondence with the two circumstances described in Section "Circular Statistics to Analyze Time-Dispersion Patterns During Motor Learning," with the first row of circles in **Figure 5A**, and with the circular sectors in **Figures 5B–7B**. The ISI = 270 ms is the actual CS–US interval and both *ISI = 360 ms and *ISI = 450 ms are the simulated time conditions for studying the simulated dispersion patterns of the same dataset distribution. Here, the matrix of intensity/strength components has been substituted by a matrix of those to fit their values to the unitary circle. Note that for all the distributions the time-dispersion indices satisfy the mathematical relationship σ (270 ms) > σ (360 ms) > σ (450 ms).*

Using the circular distributions, we also calculated the timing–intensity (σs_{IP} and σs_{CR}) and the time delay–strength (σs0; σs1 and σs2; σs3 and σs4; σs5 and σs6) dispersion indices in a two-dimensional space where both the timing/time-delay or intensity/strength components were changing simultaneously (see the magnitude and the temporal dynamics of the arrows in **Figures 5A and 6A**). This approach of dynamic analysis (i.e., the temporal evolution, including parametric timing and time delay information) of the kinetic neural commands, kinematic parameters, and correlation code indices was applied successfully for all the trials taken from all the blocks of the same session, and finally for all the successive sessions across conditioning (see the circular representation in **Figures 5 and 6**).

Moreover, we extended the circular approach of our data distributions to different durations of the inter-stimulus interval (*ISI – i.e., the simulated time conditions for studying the simulated dispersion patterns of the same dataset distribution). This strategy of transformation of the CS–US interval to the circle was easy to apply for *ISI extending from sub-second range [millisecond timing, e.g., *ISI = 360 ms; *ISI = 450 ms, see **Figures 2C and 7**, **Tables 2 and 3**, and expression (8)] to seconds-to-minutes-to-hours range [interval timing, e.g., *ISI of 1 s and 80 ms; *ISI of 1 min-4 s and 800 ms; *ISI of 1 h-4 min and 48 s, see **Table 4** and expression (9)]. In **Tables 2–4** we summarize the results including the statistical parameters that enabled us to describe the different patterns of

dispersions for our dataset distributions. Notice the difference in the values of the dispersion indices between the time distributions (**Table 2**) and time-intensity distributions (**Table 3**) of the datasets. For the reports in **Tables 3 and 4**, the intensity/strength components for all the data distributions have been normalized previously in accord with their maximum value across conditioning. Note that for all the distributions the time–intensity dispersion indices (σs, see the fifth column) satisfy the relationships: (1) σs(270 ms) > σs(360 ms) > σs(450 ms), see **Figures 2C, 5–7**, and **Tables 2 and 3**; (2) σs(1080 ms) > σs(1080 ms × 60 ms) > σs(1080 ms × 60^2 ms), see **Table 4**. Thus, while the radius of the centroid ($\overline{C}$, see the third column in **Tables 2–4**) and the circular kurtosis index (ρ, see the fourth column) increase with the ISI duration, the mean values of both parametric timing and time delay ($\overline{T}$, see the second column) remain practically invariable, for all the ISI durations. This was expected, because we used the same dataset distribution, and datasets with a greater degree of kurtosis have centroids much further from the center of the circumference. Note that in **Table 4**, the values of the parametric timing–intensity (and time delay–strength) dispersion indices (σs) for *ISI of 1 h-4 min and 48 s reach the minimum values (values of zero) at the same time as the kurtosis indices (ρ) reach the maximum values (values of one), for all the

Table 3 | The parametric timing–intensity and time delay–strength dispersion indices (σs) corresponding to the circular distributions of the datasets across conditioning sessions, and for three different durations of the inter-stimulus interval (ISI).

Mean angle (in radians)		Mean timing (in milliseconds)		Mean radius of the centroid		Circular kurtosis index		Time–intensity dispersion index	
ISI = 270 ms (CS–US INTERVAL, IN THE SUB-SECONDS RANGE)									
$\overline{\Omega}_{MN}$	4.8316	$\overline{T}_{MN}$	207.6207	$\overline{C}_{MN}$	0.0584	ρ_{MN}	0.3939	σs_{MN}	88.9450
$\overline{\Omega}_{CR}$	1.2371	$\overline{T}_{CR}$	53.1593	$\overline{C}_{CR}$	0.0698	ρ_{CR}	0.8368	σs_{CR}	16.7375
$\overline{\Omega}_{IP}$	1.5741	$\overline{T}_{IP}$	67.6409	$\overline{C}_{IP}$	0.0717	ρ_{IP}	0.8875	σs_{IP}	10.9241
$\overline{\Omega}0$	1.8710	$\overline{T}0$	80.3985	$\overline{C}0$	0.0725	ρ0	0.4777	σs0	49.6615
$\overline{\Omega}1$	1.4849	$\overline{T}1$	63.8078	$\overline{C}1$	0.0918	ρ1	0.8535	σs1	8.6952
$\overline{\Omega}2$	1.1867	$\overline{T}2$	50.9959	$\overline{C}2$	0.0847	ρ2	0.8545	σs2	10.1295
$\overline{\Omega}3$	1.7811	$\overline{T}3$	76.5368	$\overline{C}3$	0.0930	ρ3	0.8015	σs3	11.4755
$\overline{\Omega}4$	2.1409	$\overline{T}4$	91.9969	$\overline{C}4$	0.0807	ρ4	0.8029	σs4	15.1480
$\overline{\Omega}5$	1.7693	$\overline{T}5$	76.0321	$\overline{C}5$	0.0922	ρ5	0.7773	σs5	13.1097
$\overline{\Omega}6$	2.2578	$\overline{T}6$	97.0221	$\overline{C}6$	0.0781	ρ6	0.7596	σs6	19.7203
***ISI = 360 ms (CS–US INTERVAL, IN THE SUB-SECONDS RANGE)**									
$\overline{\Omega}_{MN}$	3.6289	$\overline{T}_{MN}$	207.9192	$\overline{C}_{MN}$	0.0628	ρ_{MN}	0.6212	σs_{MN}	48.0369
$\overline{\Omega}_{CR}$	0.9285	$\overline{T}_{CR}$	53.1975	$\overline{C}_{CR}$	0.0706	ρ_{CR}	0.9052	σs_{CR}	9.5164
$\overline{\Omega}_{IP}$	1.1811	$\overline{T}_{IP}$	67.6730	$\overline{C}_{IP}$	0.0725	ρ_{IP}	0.9354	σs_{IP}	6.1448
$\overline{\Omega}0$	1.4073	$\overline{T}0$	80.6312	$\overline{C}0$	0.0781	ρ0	0.6800	σs0	26.2217
$\overline{\Omega}1$	1.1143	$\overline{T}1$	63.8423	$\overline{C}1$	0.0933	ρ1	0.9158	σs1	4.8364
$\overline{\Omega}2$	0.8908	$\overline{T}2$	51.0383	$\overline{C}2$	0.0861	ρ2	0.9163	σs2	5.6426
$\overline{\Omega}3$	1.3365	$\overline{T}3$	76.5780	$\overline{C}3$	0.0952	ρ3	0.8853	σs3	6.3286
$\overline{\Omega}4$	1.6062	$\overline{T}4$	92.0272	$\overline{C}4$	0.0826	ρ4	0.8861	σs4	8.3440
$\overline{\Omega}5$	1.3281	$\overline{T}5$	76.0918	$\overline{C}5$	0.0947	ρ5	0.8705	σs5	7.2261
$\overline{\Omega}6$	1.6942	$\overline{T}6$	97.0690	$\overline{C}6$	0.0805	ρ6	0.8600	σs6	10.8009
***ISI = 450 ms (CS–US INTERVAL, IN THE SUB-SECONDS RANGE)**									
$\overline{\Omega}_{MN}$	2.9049	$\overline{T}_{MN}$	208.0490	$\overline{C}_{MN}$	0.0649	ρ_{MN}	0.7457	σs_{MN}	30.1811
$\overline{\Omega}_{CR}$	0.7430	$\overline{T}_{CR}$	53.2150	$\overline{C}_{CR}$	0.0709	ρ_{CR}	0.9384	σs_{CR}	6.1201
$\overline{\Omega}_{IP}$	0.9451	$\overline{T}_{IP}$	67.6878	$\overline{C}_{IP}$	0.0729	ρ_{IP}	0.9582	σs_{IP}	3.9325
$\overline{\Omega}0$	1.1272	$\overline{T}0$	80.7316	$\overline{C}0$	0.0808	ρ0	0.7870	σs0	16.3157
$\overline{\Omega}1$	0.8916	$\overline{T}1$	63.8580	$\overline{C}1$	0.0940	ρ1	0.9456	σs1	3.0792
$\overline{\Omega}2$	0.7129	$\overline{T}2$	51.0577	$\overline{C}2$	0.0868	ρ2	0.9459	σs2	3.5949
$\overline{\Omega}3$	1.0695	$\overline{T}3$	76.5967	$\overline{C}3$	0.0962	ρ3	0.9257	σs3	4.0138
$\overline{\Omega}4$	1.2851	$\overline{T}4$	92.0409	$\overline{C}4$	0.0835	ρ4	0.9262	σs4	5.2893
$\overline{\Omega}5$	1.0628	$\overline{T}5$	76.1187	$\overline{C}5$	0.0958	ρ5	0.9158	σs5	4.5819
$\overline{\Omega}6$	1.3556	$\overline{T}6$	97.0900	$\overline{C}6$	0.0816	ρ6	0.9090	σs6	6.8292

*These results are in correspondence with the two circumstances described in Section "Circular Statistics to Analyze Time-Dispersion Patterns During Motor Learning," with the second row of circles in **Figure 5A**, and with the circles in **Figures 2C, 6A and 7A**. The ISI = 270 ms is the actual CS–US interval, and both *ISI = 360 ms and *ISI = 450 ms are the simulated time conditions for studying the simulated dispersion patterns of the same dataset distribution. Here, the intensity/strength components have been normalized in accordance with their maximum value across conditioning. Note that for all the distributions the time–intensity dispersion indices (σs, see the fifth column) satisfy the relationship σs (270 ms) > σs (360 ms) > σs (450 ms).*

Table 4 | The parametric timing–intensity and time delay–strength dispersion indices (σs) corresponding to the circular distributions of the datasets across conditioning sessions, and for three different durations of the inter-stimulus interval (ISI).

Mean angle (in radians)		Mean timing (in milliseconds)		Mean radius of the centroid		Circular kurtosis index		Time–intensity dispersion index	
***ISI = 1080 ms (CS–US INTERVAL, IN THE SECONDS RANGE)**									
$\overline{\Omega}_{MN}$	1.2114	$\overline{T}_{MN}$	208.2310	$\overline{C}_{MN}$	0.0681	ρ_{MN}	0.9527	σs_{MN}	5.1017
$\overline{\Omega}_{CR}$	0.3097	$\overline{T}_{CR}$	53.2407	$\overline{C}_{CR}$	0.0714	ρ_{CR}	0.9891	σs_{CR}	1.0700
$\overline{\Omega}_{IP}$	0.3939	$\overline{T}_{IP}$	67.7093	$\overline{C}_{IP}$	0.0734	ρ_{IP}	0.9926	σs_{IP}	0.6826
$\overline{\Omega}0$	0.4705	$\overline{T}0$	80.8715	$\overline{C}0$	0.0848	$\rho 0$	0.9608	$\sigma s0$	2.7211
$\overline{\Omega}1$	0.3716	$\overline{T}1$	63.8808	$\overline{C}1$	0.0951	$\rho 1$	0.9904	$\sigma s1$	0.5305
$\overline{\Omega}2$	0.2972	$\overline{T}2$	51.0858	$\overline{C}2$	0.0877	$\rho 2$	0.9905	$\sigma s2$	0.6200
$\overline{\Omega}3$	0.4458	$\overline{T}3$	76.6236	$\overline{C}3$	0.0977	$\rho 3$	0.9869	$\sigma s3$	0.6877
$\overline{\Omega}4$	0.5356	$\overline{T}4$	92.0607	$\overline{C}4$	0.0849	$\rho 4$	0.9870	$\sigma s4$	0.9056
$\overline{\Omega}5$	0.4431	$\overline{T}5$	76.1575	$\overline{C}5$	0.0976	$\rho 5$	0.9851	$\sigma s5$	0.7848
$\overline{\Omega}6$	0.5650	$\overline{T}6$	97.1202	$\overline{C}6$	0.0833	$\rho 6$	0.9838	$\sigma s6$	1.1649
***ISI = 1080 × 60 ms (CS–US INTERVAL, IN THE MINUTES RANGE)**									
$\overline{\Omega}_{MN}$	0.0202	$\overline{T}_{MN}$	208.2680	$\overline{C}_{MN}$	0.0688	ρ_{MN}	1.0000	σs_{MN}	0.0014
$\overline{\Omega}_{CR}$	0.0052	$\overline{T}_{CR}$	53.2461	$\overline{C}_{CR}$	0.0715	ρ_{CR}	1.0000	σs_{CR}	0.0003
$\overline{\Omega}_{IP}$	0.0066	$\overline{T}_{IP}$	67.7138	$\overline{C}_{IP}$	0.0735	ρ_{IP}	1.0000	σs_{IP}	0.0002
$\overline{\Omega}0$	0.0078	$\overline{T}0$	80.8998	$\overline{C}0$	0.0857	$\rho 0$	1.0000	$\sigma s0$	0.0007
$\overline{\Omega}1$	0.0062	$\overline{T}1$	63.8856	$\overline{C}1$	0.0953	$\rho 1$	1.0000	$\sigma s1$	0.0001
$\overline{\Omega}2$	0.0050	$\overline{T}2$	51.0916	$\overline{C}2$	0.0879	$\rho 2$	1.0000	$\sigma s2$	0.0002
$\overline{\Omega}3$	0.0074	$\overline{T}3$	76.6292	$\overline{C}3$	0.0981	$\rho 3$	1.0000	$\sigma s3$	0.0002
$\overline{\Omega}4$	0.0089	$\overline{T}4$	92.0648	$\overline{C}4$	0.0852	$\rho 4$	1.0000	$\sigma s4$	0.0003
$\overline{\Omega}5$	0.0074	$\overline{T}5$	76.1655	$\overline{C}5$	0.0979	$\rho 5$	1.0000	$\sigma s5$	0.0002
$\overline{\Omega}6$	0.0094	$\overline{T}6$	97.1264	$\overline{C}6$	0.0837	$\rho 6$	1.0000	$\sigma s6$	0.0003
***ISI = 1080 × 60² ms (CS–US INTERVAL, IN THE HOURS RANGE)**									
$\overline{\Omega}_{MN}$	0.0003	$\overline{T}_{MN}$	208.2680	$\overline{C}_{MN}$	0.0688	ρ_{MN}	1.0000	σs_{MN}	0.0000
$\overline{\Omega}_{CR}$	0.0000	$\overline{T}_{CR}$	53.2461	$\overline{C}_{RP}$	0.0715	ρ_{CR}	1.0000	σs_{CR}	0.0000
$\overline{\Omega}_{IP}$	0.0000	$\overline{T}_{IP}$	67.7138	$\overline{C}_{IP}$	0.0735	ρ_{IP}	1.0000	σs_{IP}	0.0000
$\overline{\Omega}0$	0.0000	$\overline{T}0$	80.8998	$\overline{C}0$	0.0857	$\rho 0$	1.0000	$\sigma s0$	0.0000
$\overline{\Omega}1$	0.0000	$\overline{T}1$	63.8856	$\overline{C}1$	0.0953	$\rho 1$	1.0000	$\sigma s1$	0.0000
$\overline{\Omega}2$	0.0000	$\overline{T}2$	51.0916	$\overline{C}2$	0.0879	$\rho 2$	1.0000	$\sigma s2$	0.0000
$\overline{\Omega}3$	0.0000	$\overline{T}3$	76.6292	$\overline{C}3$	0.0981	$\rho 3$	1.0000	$\sigma s3$	0.0000
$\overline{\Omega}4$	0.0000	$\overline{T}4$	92.0648	$\overline{C}4$	0.0852	$\rho 4$	1.0000	$\sigma s4$	0.0000
$\overline{\Omega}5$	0.0000	$\overline{T}5$	76.1655	$\overline{C}5$	0.0979	$\rho 5$	1.0000	$\sigma s5$	0.0000
$\overline{\Omega}6$	0.0002	$\overline{T}6$	97.1264	$\overline{C}6$	0.0837	$\rho 6$	1.0000	$\sigma s6$	0.0000

*These results are in correspondence with the two circumstances described in Section "Circular Statistics to Analyze Time-Dispersion Patterns During Motor Learning." Here, *ISI = 1080 ms (in the seconds range), *ISI = 1080 × 60 ms (in the minutes range), and *ISI = 1080 × 60² ms (in the hours range) are the simulated time conditions for studying the simulated dispersion patterns of the same dataset distribution. Here, the intensity/strength components have been normalized in accordance with their maximum value across conditioning. Note that for all the distributions the time–intensity dispersion indices satisfy the mathematical relationship σs (1080 ms) > σs (1080 ms × 60 ms) > σs (1080 ms × 60² ms). For *ISI of 1 h-4 min and 48 s (1080 × 60² ms), the dispersion indices (σs) reach values of zero and the circular kurtosis indices (ρ) reach values of one, for all the distributions.*

dataset distributions. The foregoing means that the threshold values of the dispersion patterns of a data distribution can be obtained by the simulated time conditions – that is, with a strategy that uses different durations of the CS–US interval.

These intra- and inter-trial timing strategies extending from sub-second range (millisecond timing, for the intra-trial domain) to seconds-to-minutes-to-hours range (interval timing, for the inter-trial and inter-block domains) expanded the functional domain of cerebellar timing beyond motor control. In fact, we calculated the different dispersion indices (σs) to reveal the true parametric timing–intensity (and time delay–strength) dispersion patterns between the IPn activity and either Mn or OO EMG recordings in the different temporal domains (inter-trials dispersion of the same block, inter-blocks dispersion of the same session, and inter-sessions dispersion along the process) – i.e., the time–intensity contributions (at least in the circular statistical sense) of the different neuronal centers (cerebellar interpositus and facial nuclei) participating in this associative learning process. It could thus be concluded that the firing activities of IPns and their temporal dynamics may be related more with the proper performance of ongoing CRs (including the proper parametric timing–intensity and time delay–strength dispersion patterns) than with their generation and/or initiation.

RELATIONSHIPS BETWEEN PHASE SYNCHRONIZATION AND BOTH TIMING AND CAUSALITY IN THE CEREBELLAR–MOTONEURON NETWORK

A question of great interest is whether there is a "causal" relationship between two simultaneous recordings collected during associative motor learning without any specific information on the direction of the coupling or on the time-dispersion pattern of the physiological data. The linear cross-correlation function, the non-linear association method, and the circular dispersion approach are, in principle, able to indicate the time delays in coupling and their circular distributions, but inferring causality from the mere directionality or the time-dispersion pattern is not always straightforward (Granger, 1980; Lopes da Silva et al., 1989; Pereda et al., 2005). Therefore, we decided to investigate the putative functional interdependencies between neuronal activity [firing rates of OO Mns, $f_{MN}(t)$, or IPns, $f_{IP}(t)$] and learned motor responses [i.e., conditioned eyelid responses, $\theta(t)$], using time-dependent causality analysis (see Time-Dependent Causality Analysis Between Neuronal Firing Command and Learned Motor Response, and Sánchez-Campusano et al., 2009 for details).

The physiological time series $f_{MN}(t)$, $f_{IP}(t)$, and $\theta(t)$ exhibit non-stationary behaviors. The stationary time series $S1_t$ (MN), $S2_t$ (IP), $S3_t$ (SUM), and $S0_t$ (θ) were determined here by successive regular differentiation of averaged relative variation functions and afterward by high-pass filtering of integrated neuronal firing activities [resulting from $f_{MN}(t)$ for Mns, and from $f_{IP}(t)$ for IPns] and of learned motor responses [resulting from eyelid position $\theta(t)$ during conditioned eyelid responses, CRs; see Sánchez-Campusano et al., 2007 for details]. From here on, the significant values of the transfer function (or sample impulse response) are those that are outside the confidence bounds (horizontal red dashed lines, approximately 95% confidence interval), indicating the number of SD of the sample impulse response estimation error to compute, assuming that the input and output physiological time series are uncorrelated. The causal inferences between the kinetic neuronal commands [$S1_t$ (MN), for the activity of OO Mns; and $S2_t$ (IP), for the activity of IPns] and the kinematics [$S0_t$ (θ), for CRs] were determined using the normal and normalized Granger causality indices. Readers may refer to the above-mentioned reports for a detailed and practical description of this technique.

In **Figures 7 and 8** are represented transfer function models (TFM) for the physiological time series corresponding to data collected from the 10th conditioning session, in particular, the activities of three representative IPns and a representative Mn were selected for each experimental subject (n = 8; Series S1: C10, 4 cats, 4 Mns; Series S2: C10, 4 cats, 12 IPns). For the curves shown in **Figure 8A**, the significant values of the transfer function presented a bimodal distribution for both positive ($\nu_{k+} \neq 0$) and negative ($\nu_{k-} \neq 0$) lags, indicating that $S0_t$ (θ) depends on its own past and on the past of $S2_t$ (IP), whilst $S2_t$ (IP) depends on its own past and on the past of $S0_t$ (θ). That is, significant values of the causality indices in both senses ($G_{2\to0} > 0$ and $G_{0\to2} > 0$) indicate a bidirectional coupling or feedback relationship between these time series. At the same time, and as illustrated in **Figure 8B**, the functional coupling (or feedback relationship, the same as in **Figure 6A**) between $S1_t$ (MN) and $S2_t$ (IP), was bidirectional in the sense of Granger causality ($G_{2\to1} > 0$, $G_{1\to2} > 0$, $\nu_{k+} \neq 0$ and $\nu_{k-} \neq 0$), and these causal inferences signify that the neuronal activity in the posterior IP nucleus causes both the activity present in the final common pathway (i.e., that of the Mns participating in the generation of the selected motor responses) and the CRs of the eyelid motor system, and vice versa [$S1_t$ (MN) depends on its own past and on the past of $S2_t$ (IP), and $S2_t$ (IP) depends on its own past and on the past of $S1_t$ (MN)].

The transfer function models shown in **Figures 8F,G** assume that the stationary time series [$S2_\tau$ (IP) and $S2_\tau$ (θ), as shown in **Figure 8F**, or $S2_\tau$ (IP) and $S1_\tau$ (MN), as indicated in **Figure 8G**], possess a unidirectional interdependence after phase synchronization as a simulated causal condition. Thus, the relationships between phase synchronization and both timing and causality in the cerebellar–Mn network were explored at the millisecond scale – i.e., taking into account the Mn and IPn spike timing. The phase corresponding to $S2_\tau$ (IP) in the instant $\tau = t - t1 - t2$ was equivalent to the phases corresponding to $S0_\tau$ (θ) and $S1_\tau$ (IP) in the instants $\tau = t - t1$ and $\tau = t$, respectively, as illustrated in **Figures 8C,D**. The actual values for $t1$ (time elapsed from activation of Mn firing to the zero reference point – i.e., the start of the CR, see **Figure 2A**) and $t2$ (time elapsed from the zero reference point to the activation of IPn firing) were 5.98 ± 0.26 (mean ± SEM, range, 3.41–8.56) ms and 23.5 ± 0.31 (mean ± SEM, range, 20.41–26.59) ms, respectively. With these simulated causal conditions of phase synchronization, the Granger causality indices are such that $G_{2\to0} > 0$ and $G_{0\to2} =$, $\nu_{k+} \neq 0$ and $\nu_{k-} = 0$ (see **Figure 8F**), implying that $S0_\tau$ (θ) depends on its own past and on the past of $S2_\tau$ (IP); and $G_{2\to1} > 0$, $G_{1\to2} = 0$, $\nu_{k+} \neq 0$, and $\nu_{k-} = 0$ (see **Figure 8G**), which signifies that $S1_\tau$ (MN) depends on its own past and on the past of $S2_\tau$ (IP). This phase analysis demonstrates that causal inferences are dependent on the phase information status, as indicated in **Figures 8F,G**.

As illustrated in **Figure 9A**, the functional interdependence between $S0_t$ (θ) and $S1_t$ (MN) was unidirectional (significant values of the transfer function alone for lags >0, $\nu_{k+} \neq 0$ and $\nu_{k-} = 0$) – i.e., the Granger causality indices are such that $G_{2\to0} > 0$ and $G_{0\to1} = 0$, which signifies that $S0_\tau$ (θ) depends on its own past and on the past of $S1_t$ (MN) and, as a result, OO Mns consistently lead the OO muscle during conditioned eyelid responses. In contrast, the relationship between $S0_\tau$ (θ) and $S3_\tau$ (SUM) was unidirectional ($G_{3\to0} > 0$, $G_{0\to3} = 0$, $\nu_{k+} \neq 0$ and $\nu_{k-} \neq 0$), which indicates that this causal inference is dependent on the phase information, as shown in **Figure 9D**.

Finally, the maximum amplitude of the Mn relative variation function was significant [$F_{(9, 27, 98)} = 170.26$, $P < 0.01$] both in the CS–US interval and after the US presentation. Furthermore, the oscillation amplitude of the IPn relative variation function increased progressively across the learning process, reaching significant values [$F_{(9, 27, 98)} = 59.51$, $P < 0.01$] during the 10th conditioning session (**Figures 8C–E**). Furthermore, the illustrated spectra (**Figures 9B,C**) presented a significant predominance of spectral components at ≈ 20 Hz, and significant differences between their spectral power [$F_{(3, 9, 236)} = 25.81$, $P < 0.01$] at the asymptotic level of acquisition of this associative learning test (session C10). In addition, we found significant differences in the power spectra for both Mns $S1_t$ (MN) [$F_{(9, 27, 98)} = 225.48$, $P < 0.01$] and IPns $S2_\tau$ (IP) [$F_{(9, 27, 98)} = 216.28$, $P < 0.01$] physiological time series across conditioning sessions.

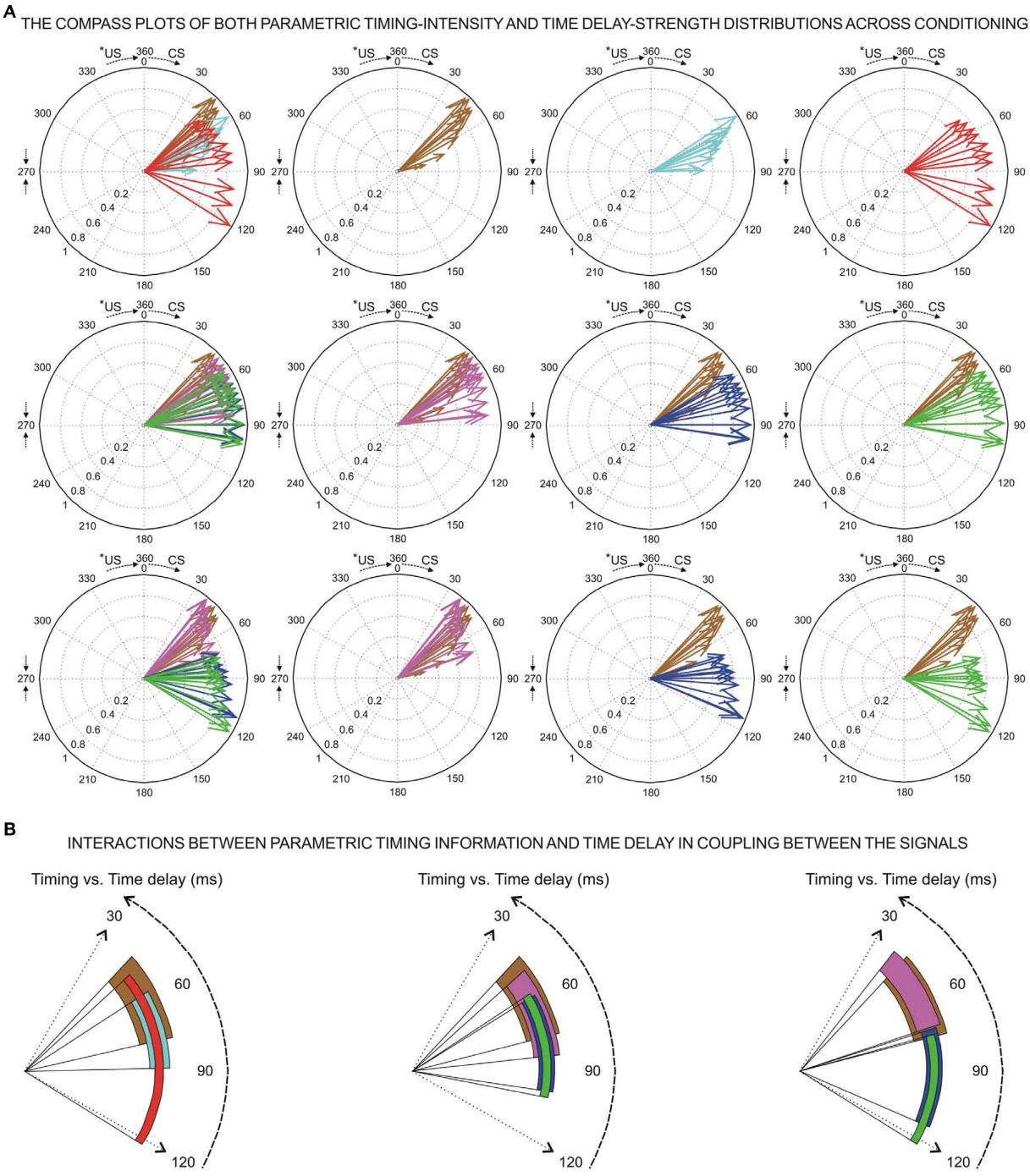

FIGURE 7 | (A) The compass plots of both parametric timing–intensity and time delay–strength distributions across the 10 conditioning sessions, and for the simulated time condition *ISI = 360 ms. In this representation, the timing–intensity distributions (1) [time to CR onset, percentage of CR], see brown arrows, and (2) [time to peak firing rate of the IP neurons, IPn peak firing rate], see cyan arrows, and the time delay–strength distributions (3) [time delay in coupling $\tau 0_{\langle f|IP|\theta\rangle}$, maximum linear correlation coefficient $r_{\max\langle f|IP|\theta\rangle}$], see red arrows, (4) [$\tau 1_{\langle EMG|MN\rangle}$, $\eta 1_{\max\langle EMG|MN\rangle}$] and (5) [$\tau 2_{\langle MN|EMG\rangle}$, $\eta 2_{\max\langle MN|EMG\rangle}$], see magenta arrows, (6) [$\tau 3_{\langle EMG|IP\rangle}$, $\eta 3_{\max\langle EMG|IP\rangle}$] and (7) [$\tau 4_{\langle IP|EMG\rangle}$, $\eta 4_{\max\langle IP|EMG\rangle}$], see blue arrows, and (8) [$\tau 5_{\langle MN|IP\rangle}$, $\eta 5_{\max\langle MN|IP\rangle}$] and (9) [$\tau 6_{\langle IP|MN\rangle}$, $\eta 6_{\max\langle IP|MN\rangle}$], see green arrows, were plotted using the circular statistics. The 10 colored arrows (10 conditioning sessions, C01–C10) in each circle illustrate the circular dispersion of the angular datasets represented. The first row of circles shows the parametric timing–intensity dispersion patterns, and the second and third rows of circles show the time delay–strength circular distributions across conditioning sessions (see the dispersion parameters in **Table 3**). **(B)** Interactions between parametric timing information and time delays in coupling between the physiological signals. The colored circular sectors illustrate the time-dispersion range of the data distributions represented in **(A)** (see the dispersion parameters in **Table 2**).

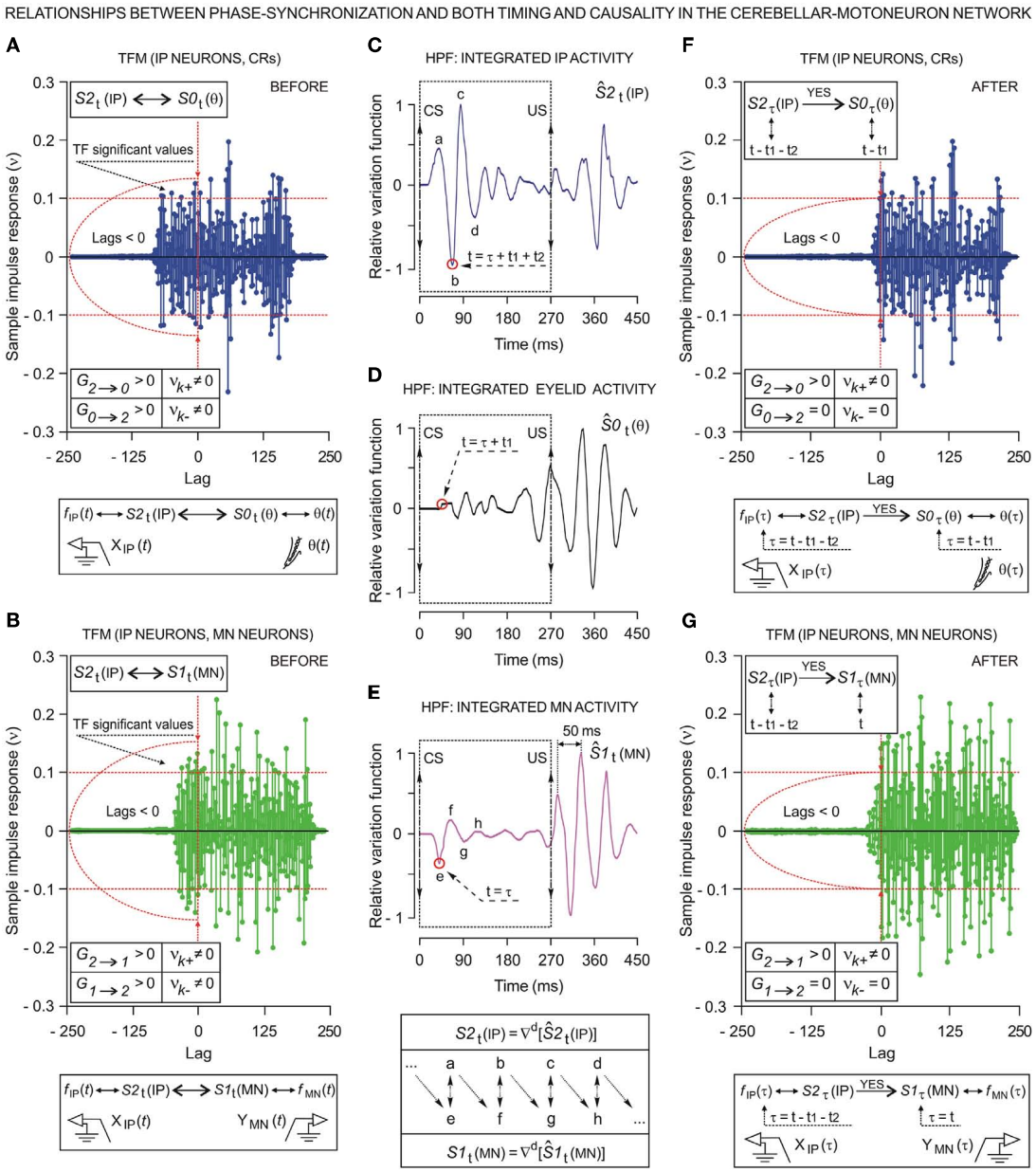

FIGURE 8 | Relationships between phase synchronization and both timing and causality in the cerebellar–Mn network using transfer function models (TFM) between kinetic neuronal commands of the IP neurons (IPn) and motor activities [activity of OO Mns (Mn) and eyelid CRs], before [see (A,B)] and after [see (F,G)] the phase synchronization as a simulated causal condition [see (C–E)]. (A,B) Before the phase synchronization, the transfer function models assume that the stationary time series $S1_t$(MN), $S2_t$(IP) and $S0_t(\theta)$ have a functional and dynamic relationship. In **(A)**, the causality indices are such that $G_{2\to 0} > 0$ and $G_{0\to 2} > 0$, $\nu_{k+} \neq 0$ and $\nu_{k-} \neq 0$ – i.e., $S0_t(\theta)$ depends on its own past and on the past of $S2_t$(IP), and $S2_t$(IP) depends on its own past and on the past of $S0_t(\theta)$. In **(B)**, $S1_t$(MN) depends on its own past and on the past of $S2_t$(IP), and $S2_t$(IP) depends on its own past and on the past of $S1_t$(MN) – i.e., significant values of the causality indices in both senses: $G_{2\to 1} > 0$, $G_{1\to 2} > 0$, $\nu_{k+} \neq 0$ and $\nu_{k-} \neq 0$. The transfer function models in **(A,B)** indicate the feedback relationships between IPn time series $S2_t$(IP) and either $S0_t(\theta)$ or $S1_t$(MN), at least in the statistical sense of causality. **(C–E)** Oscillatory curves (relative variation functions) resulting from high-pass filtering (HPF, –3 dB cutoff at 5 Hz and zero gain at 15 Hz) of integrated neuronal firing activities (IPn and Mn) and of eyelid position corresponding to the same set of records. The operator ∇^d enabled the stationary time series $S1_t$(MN), $S2_t$(IP), and $S0_t(\theta)$ to be obtained after making $n = d$ regular differentiations to the non-stationary time series [i.e., the relative variation curves, as shown in **(C–E)**]. Note that in the oscillating curves shown here, components a–d are totally out-of-phase with components e–h. The transfer function models **(F,G)** assume that the stationary time series possess a direct interdependence after phase synchronization as a simulated causal condition [i.e., the phases corresponding to $\tau = t - t1 - t2$, for $S2_\tau$(IP), $\tau = t - t1$, for $S0_\tau(\theta)$, and $\tau = t$, for $S1_\tau$(MN)], implying that $S0_\tau(\theta)$ depends on its own past and on the past of $S2_\tau$(IP) (i.e., the indices are such that $G_{2\to 0} > 0$ and $G_{0\to 2} = 0$, $\nu_{k+} \neq 0$ and $\nu_{k-} = 0$, see *F* for a unidirectional coupling); and that $S1_\tau$(MN) depends on its own past and on the past of $S2_\tau$(IP) (i.e., $G_{2\to 1} > 0$, $G_{1\to 2} = 0$, $\nu_{k+} \neq 0$, and $\nu_{k-} = 0$, see the panel G for another unidirectional coupling). Red horizontal dashed lines in **(A,B)** and **(F,G)** indicate the approximate upper and lower confidence bounds (approximately 95% confidence interval), assuming the input and output physiological time series are completely uncorrelated.

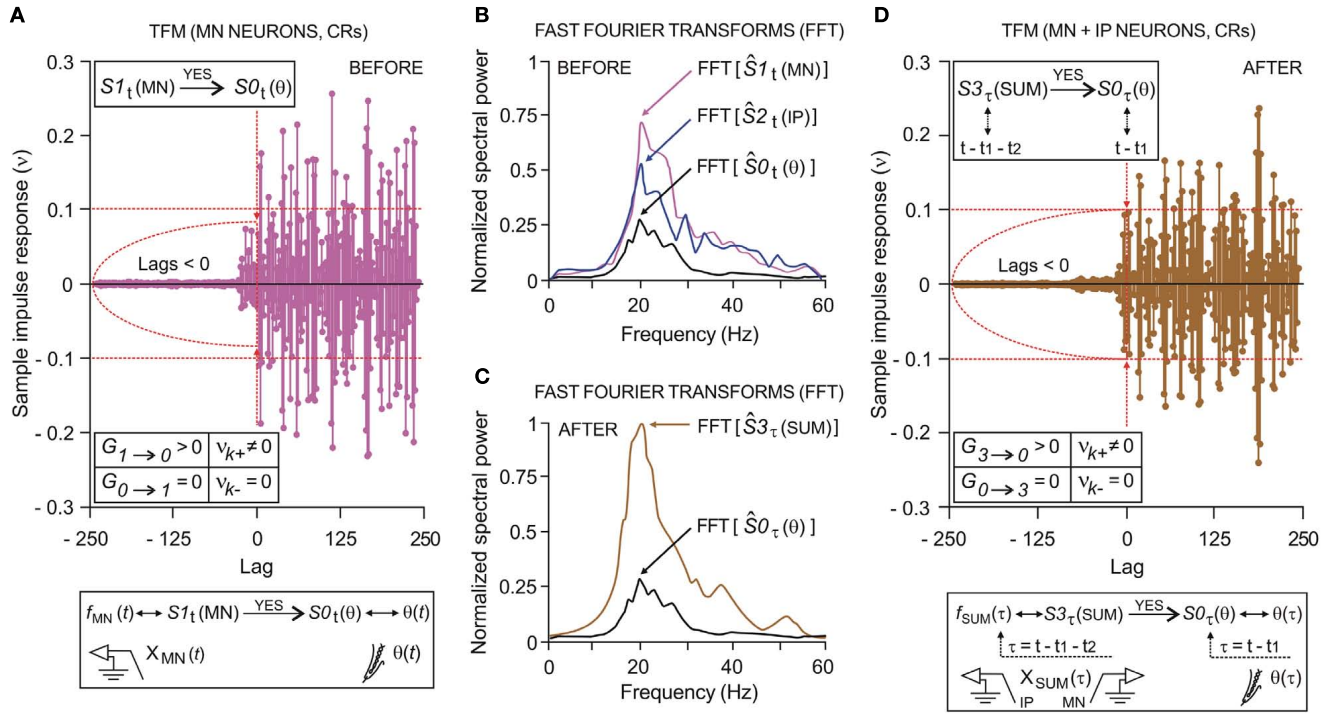

FIGURE 9 | Transfer function models (TFM) between Mns kinetic neuronal commands and conditioned eyelid responses, before [see (A)] and after [see (D)] the phase synchronization as a simulated causal condition. In **(A)**, the transfer function model establishes that the stationary time series $S0_t$ (θ) depends on its own past and on the past of $S1_t$ (MN) – i.e., the causality indices are such that $G_{1\rightarrow 0} > 0$ and $G_{0\rightarrow 1} = 0$, $\nu_{k+} \neq 0$ and $\nu_{k-} = 0$, indicating a unidirectional coupling in the final motor pathway of eyelid motor response. **(B,C)** Fast Fourier Transforms (FFT) for the oscillating curves shown in **Figures 8C–E**, before [see **(B)**] and after [see **(C)**] the phase synchronization (the sum of the contributions is possible only assuming both the frequency and phase synchronizations). Note that the illustrated spectra presented a significant predominance of spectral components at ≈ 20 Hz, and significant differences between their power spectra [$F_{(3, 9, 236)} = 25.81$, $P < 0.01$]. In **(D)**, the causality indices are such that $G_{3\rightarrow 0} > 0$, $G_{0\rightarrow 3} = 0$, $\nu_{k+} \neq 0$ and $\nu_{k-} = 0$, also indicating a unidirectional coupling. Note that $S3_\tau$ (SUM) depends only on its own past (i.e., $G_{0\rightarrow 3} = 0$), and that the unidirectional relationship in the opposite direction [as shown in **(D)**] was possible because $S1_t$ (MN) and $S2_t$ (IP) were induced toward a phase synchronization as a simulated causal condition (i.e., the relative phase difference will be close to zero for the $S1_\tau$ (MN) and $S2_\tau$ (IP) signals). Red horizontal dashed lines in A and D indicate the approximate upper and lower confidence bounds (approximately 95% confidence interval), assuming the input and output physiological time series are completely uncorrelated.

DISCUSSION

DESIGN OF OPTIMIZED EXPERIMENTAL AND ANALYTICAL TOOLS TO ANALYZE TIMING, TIME DELAYS, AND CAUSALITY DURING MOTOR LEARNING

The multivariate analyses of physiological signals (non-linear dynamic associations and time-dependent Granger causality), the circular statistics of the dataset distributions, and the hierarchical cluster technique are optimal analytical tools for studying the interactions among timing parameters (i.e., the latencies and relative refractory periods, **Figure 3A**), kinetic neural commands (i.e., motor and pre-motor neuronal activities, **Figure 3B**), kinematic variables (i.e., motor activities computed from actual eyelid movement and their quantitative evolution, **Figures 3B,C**), correlation codes (i.e., the type and strength in coupling, **Figures 4A,B**), time delay information (i.e., the temporal order, **Figures 6B and 7B**), dispersion patterns (i.e., time–intensity circular distributions, **Figures 5A–7A**), and finally, the directionality/causality indices (**Figures 8 and 9**) conforming the 40-dimension vectors of learning states (**Figure 10A**) during motor learning. The results used here enable us to determine the intrinsic coherence (**Figure 10B**) of collected data and the relationship between timing and causality in the cerebellar–Mns network in different temporal domains (in the range of milliseconds for intra-trials interactions; in the range of seconds, minutes, and hours for both inter-trials and inter-blocks interactions; and in the range of days for the inter-sessions interactions along the process). For this, we have developed the necessary computer programs and algorithmic procedures to deal with such a huge amount of data (40 parameters quantified across 180 averaged blocks and 15 experimental sessions collected from 8 experimental animals). The computer program arranged the data in a total of 180 blocks (15 conditioning sessions × 12 blocks) according to their significant homogeneity: namely, blocks within clusters were displayed close together when plotted geometrically according to linkage distances, whereas different clusters were displayed far apart.

The main result according to the actual causality inferences (see the left-hand hierarchical cluster trees in **Figure 10B**) indicated that up to 147 blocks could be correctly assigned to the corresponding experimental (habituation, conditioning, or extinction) session, and only data collected from 33 blocks were discarded because of their low homogeneity with the corresponding session. Here, the

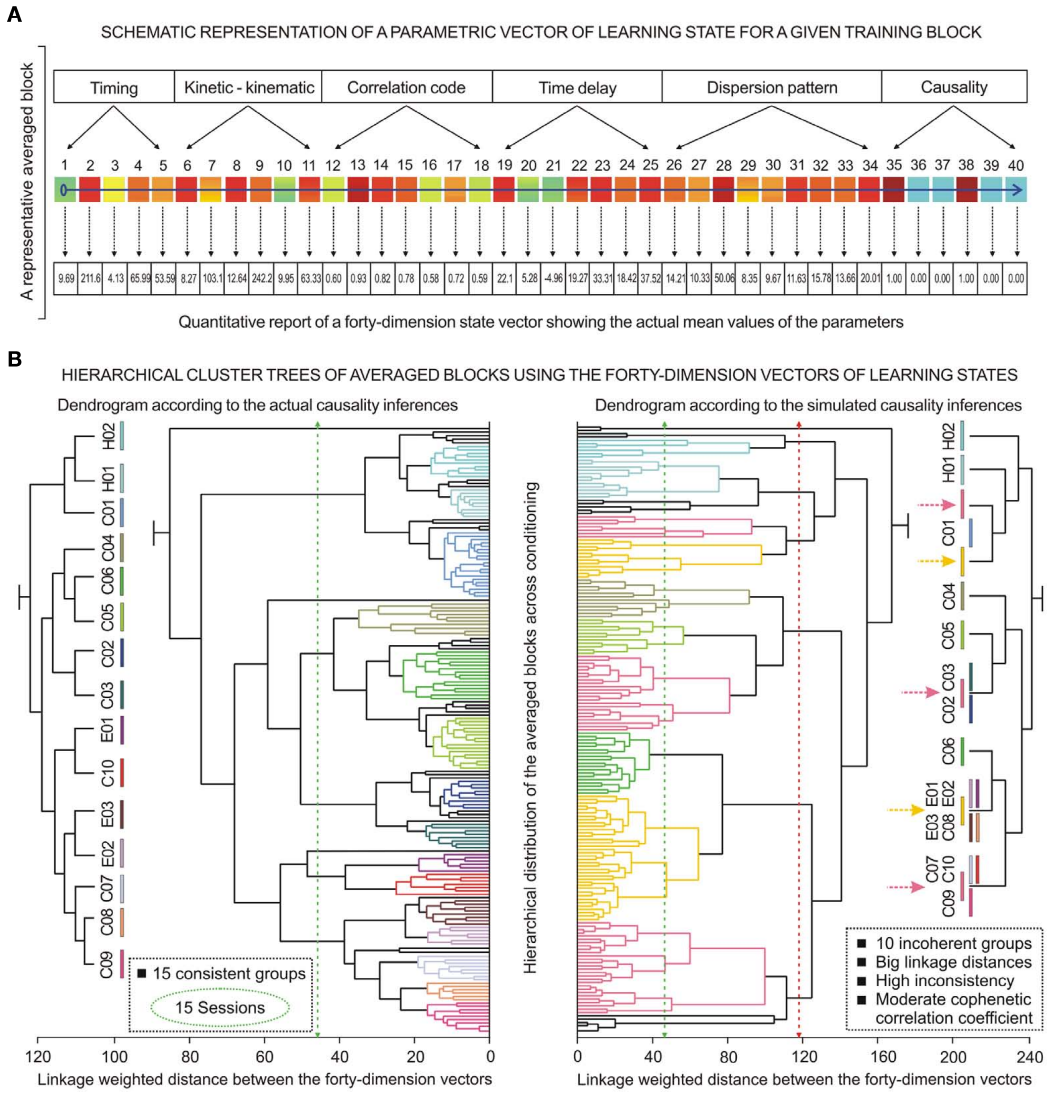

FIGURE 10 | (A) Schematic representation of a parametric vector corresponding to the learning state for a given training block. The diagram illustrates the qualitative definition of a 40-dimension state vector formed by 5 timing parameters (from 1 to 5, see **Figure 3A**), 4 kinetic neural commands (from 6 to 9, see **Figure 3B**), 2 kinematic variables (10 and 11, **Figure 3B**), 7 correlation code parameters (from 12 to 18, see **Figure 4A**), 7 time delays (from 19 to 25, **Figure 6B**), 9 dispersion patterns (from 26 to 34, **Figures 5A and 6A**, and **Table 3**), and finally 6 directional and causality indices (from 35 to 40, **Figures 8 and 9**). A color map representation of the parametric vector (the horizontal blue arrow) is also illustrated. Note the alternation of ranges of colors describing in qualitative and quantitative terms a functional state of the cerebellar–Mn pathway during motor learning. **(B)** Hierarchical cluster trees of averaged blocks using the 40-dimension vectors of learning states collected across habituation (H01–H02), conditioning (C01–C10), and extinction (E01–E03) sessions. The dendrograms illustrate the hierarchical distributions of the averaged blocks of trials across the classical conditioning and in accordance with both actual (the left-hand dendrogram, D1) and simulated (the right-hand dendrogram, D2) causality inferences. Each bar at the bottom of the dendrograms represents an averaged conditioning block. The linkage-weighted distances between the vectors are represented on the *x*-axes in arbitrary units. The comparison depth was of 16 levels to both sides of the objective level, and the clusters were formed without specifying the maximum number of clusters. The *y*-axes represent, as colored (not black) lines, the statistically significant clusters [D1, 15 significant clusters, 147 averaged blocks, $F_{(14,\ 70,\ 132)} = 36.1213$, $P < 0.01$, Wilk's lambda = 0.09, with Nr = 5; D2, 10 significant clusters, 166 averaged blocks, $F_{(9,\ 45,\ 156)} = 2.4290$, $P < 0.05$, Wilk's lambda = 0.26, with Nr = 5]. The black lines represent the averaged blocks (33, in D1; 14 in D2) that fall into the remaining statistically non-significant clusters (16 in D1; 4 in D2). According to the left-hand dendrogram D1 (for the actual causality inferences), the 15 significant clusters corresponded to 147 averaged blocks distributed in the 15 experimental sessions during the delay conditioning paradigm (H01–H02 = 19, C01–C10 = 108, and E01–E03 = 20 blocks). Here, notice a coherent nodal distribution (see the vertical colored bars in the left-hand panel) in correspondence with a proper trend in the evolution of the conditioning process. However, for the right-hand dendrogram D2 (simulated causality inferences), the total number of significant clusters was of 10 groups – i.e., an insufficient number of groups to match with the 15 conditioning sessions. Note that in D2 the clusters were obtained with evident linkage alterations that affect the typical and sequential temporal distribution of training blocks (see the yellow and pink horizontal bars) and sessions (see the vertical colored bars in the right nodal distribution) along the conditioning process. The green and red vertical dashed lines indicate the threshold linkage distances (46.57 and 117.94 units for D1 and D2, respectively) for these hierarchical cluster distributions.

threshold linkage distance was of only 46.57 units (see the vertical green dashed line) and the hierarchical cluster trees were significantly consistent (high cophenetic correlation coefficient, 0.9802; the closer this value is to 1, the better the clustering) with the actual conditioning sessions. For example, and given the similarity of the data collected in the corresponding trials and blocks, the two habituation sessions (H01, H02) were clustered close to the 1st conditioning session (C01). In addition, the 1st extinction session (E01) was clustered close to the 10th conditioning session (C10), while the following extinction sessions (E02, E03) were clustered close to the C07–C09 conditioning sessions. Finally, the middle experimental sessions (C02–C06) formed a distinct set of clusters. Importantly, these positive results indicated that neural firing properties recorded from different animals during the same conditioning paradigm can be correctly assigned to the corresponding experimental session (i.e., in agreement with the actual CR evoked during the CS–US interval).

However, for the simulated causality conditions (see the right-hand hierarchical cluster trees in **Figure 10B**), where only the directionality and causality indices that involved the IPn interdependencies were modified randomly (sequence of 0 or 1 for the parameters 36, 37, 39 and 40 of each averaged block, in **Figure 10A**) prior to application of the clustering algorithm, the clusters were obtained with evident linkage alterations and inconsistency (moderate cophenetic correlation coefficient, 0.6836) affecting the typical and sequential temporal distribution of training blocks (see the yellow and pink horizontal bars) and experimental sessions (see the vertical colored bars in the right nodal distribution) along the conditioning process. For example, (1) the formation of two independent groups (see the first pink and yellow arrows and the indicated bars) for the same conditioning session C01; (2) the high similarity between two different experimental sessions (C02 and C03, see the second pink arrow and the indicated bar), and the significant similarity of them with the session C05; (3) the high similarity between the conditioning session C06 and the extinction sessions E01–E03 (see the second yellow arrow and the indicated bar); and finally, the high homogeneity of linkage for three experimental conditioning sessions (C07, C09, and C10, see the third pink arrow and the indicated bar) which showed significant differences for the actual causality inferences. Furthermore, note that in the right-hand dendrogram D2 for averaged blocks and in the right nodal distribution for sessions, the total number of significant clusters was of 10 groups – i.e., an insufficient number of clusters to match with 15 experimental conditioning sessions. Moreover, the threshold linkage distance was 117.94 units (see the vertical red dashed line) – i.e., a linkage distance that does not allow a valid rejection of the non-significant data corresponding to averaged blocks.

This strategy of the simulated causality conditions by a controlled random modification of the directionality and causality inferences (the parameters 36, 37, 39, and 40, which involved IPn interdependencies, **Figure 10A**) in the temporal domains of the inter-trials and inter-sessions interactions strongly suggests that the proper timing of CRs is plausibly a consequence of the pertinent cerebellar–Mn network causality (**Figures 8–10**) – i.e., the simulated causal conditions affect the typical temporal distribution of training blocks and experimental sessions along the conditioning process, and therefore the temporal evolution of the level of expression of eyelid CRs. In the temporal range of interval timing (seconds-to-minutes-to-hours) these dynamic changes were determined by the emergence of spurious causality interdependencies from inter-blocks data interactions to inter-sessions data interactions. At the milliseconds scale the spikes timing (the dynamic firing properties of the Mns and IPns) was also modified by an induced sequence of phase synchronization (i.e., the relative phase difference will be close to zero). Indeed, as shown in a previous study from our group (Sánchez-Campusano et al., 2007, 2009), the reinforcing-modulating role of cerebellar circuits of ongoing conditioned eyelid responses is highly dependent on its adequate phase-modulation with respect to intrinsic facial Mn oscillatory properties. To be efficient, IPn activities need to go through a learning process to become 180° out-of-phase OO Mns firing (Sánchez-Campusano et al., 2007). Thus, IPn activities (following a relay in the red nucleus) reach OO Mns right at the moment of maximum motoneuronal hyperpolarization (Trigo et al., 1999), and IPns facilitate a quick repolarization of OO Mns, reinforcing their tonic firing during the performance of eyelid CRs (Sánchez-Campusano et al., 2009).

An additional advantage of this approach is that for the actual causality conditions, once collected data were properly arranged according to the hierarchical cluster tree (and that non-significant data were rejected), it was possible to determine analytically the multiple and coherent evolution of timing parameters (**Figure 3A**), kinetic and kinematic variables (**Figures 3B,C**), the dynamic non-linear association functions relating Mn and IPn activities to EMG responses (**Figure 4**), the time–intensity dispersion patterns (**Figures 5–7**) of the dataset distributions in the CS–US interval using circular statistics, and – finally – the relationship between the causal inferences and phase-inversion properties (**Figures 8 and 9**) of OO Mns and IPns with regard to acquired CRs. This phase-synchronization analysis demonstrates that causal inferences are dependent on the phase information status and that the timing of learned eyelid responses depends on the causal relationships present in the cerebellar–Mn network. Finally, these novel (experimental and analytical) approaches to the study of actual neuronal mechanisms underlying the acquisition of new motor abilities will certainly contribute to the better understanding of brain functioning in alert behaving animals.

A MORE PRECISE PICTURE OF THE FUNCTIONAL STATES INVOLVED IN THE ACTUAL ACQUISITION OF NEW MOTOR AND COGNITIVE ABILITIES

Our intention here was to deal with the putative cerebellar nuclear mechanisms involved in the acquisition and performance of conditioned eyeblinks, compared with the role play by facial motoneurons. In this regard, and according to a long series of studies carried out by some of us in alert behaving cats, posterior interpositus neurons fire in response to every type of eyelid displacement: spontaneous, reflex, or classically conditioned with either delay or trace paradigms. In contrast such an activity was not detected in other interpositus areas (Gruart and Delgado-García, 1994; Gruart et al., 2000a; Delgado-García and Gruart, 2002). Previous electrophysiological recordings of putative cerebellar nuclei units carried out in rabbits reported that eyeblink-related neurons are located in the rostral part of the interpositus nucleus (McCormick

and Thompson, 1984; Berthier and Moore, 1990). However, and in agreement with recordings carried out in behaving monkeys (Van Kan, et al., 1993), a detailed mapping of the three cerebellar nuclei in alert behaving cats indicates that neurons related to eyelid movements are mostly located in the rostro-dorso-lateral aspect of the posterior interpositus nucleus (Gruart and Delgado-García, 1994; Gruart et al., 2000). Moreover, data collected from mice (Porras-García et al., 2010) and rats (Morcuende et al., 2002; Chen and Evinger, 2006) also located eyeblink-related neurons in the dorsolateral hump and in the posterior interpositus nucleus, but not in the anterior subdivision of the nucleus. Until now, there is no better explanation for these disparities in the location of eyeblink-related neurons that the possible neural differences within different species. On the other hand, we have analyzed here just the firing activities of interpositus type A neurons (Gruart et al., 2000). In a forthcoming study, we will analyze in detail the firing properties of interpositus type B neurons (i.e., neurons that pause during the CS–US interval; Gruart et al., 2000), as well as the discharge rates of overlying type A and B Purkinje cells (in preparation).

In a recent work from our group (Sánchez-Campusano et al., 2010) we presented a quantitative statistical analysis of several separate but similar experiments in order to test the pooled data for statistical significance revealing how IPns can change their activity during delayed eyeblink conditioning. That previous meta-analysis enabled a comparison for learning and performance in different species. The present experimental design in alert behaving cats (for a single animal species) enables the incorporation of further parameters (timing information, time delays, time–intensity dispersion patterns, directionality in coupling, and causality indices) with the sole condition that the same experimental conditioning situation is reproduced (i.e., the same delay conditioning paradigm). Although we have checked here the firing characteristics of only OO Mns and IPns, the intrinsic coherence demonstrated among timing information, kinetic and kinematic parameters, time delays and correlation code properties, time–intensity dispersion patterns, directional outcomes, and causality inferences conforming the 40-dimension vectors of learning states (**Figure 10A**) strongly suggests the presence of a functional neuronal state involving many different cerebral centers evoked by the learning process (Delgado-García and Gruart, 2002; Sánchez-Campusano et al., 2007, 2009, 2010).

The recent demonstration of the existence of the "brain states" (Petersen, 2007; Poulet and Petersen, 2008; Crochet et al., 2011) determined by oscillation of the membrane potential in synchronized pyramidal cells may be compared with our experimental data showing similar oscillations in the OO Mns (Trigo et al., 1999). Thus, in the cerebellar–Mns network the oscillations of IPns (modulating signal) modulates and/or reinforces eyelid motor responses inversely (by progressively inverting phase information) to the initial contribution of OO Mns (modulated signals). In previous reports (Gruart and Delgado-García, 1994; Gruart et al., 2000a; Sánchez-Campusano et al., 2007, 2009), we demonstrated by different means that neuronal activity in the IP nucleus does not lead the performance of learned motor responses, but follows neural motor commands originated in different neuronal sources. Although it is highly speculative at the moment, we can suggest that a driving common source in motor cortex and/or in related cortical areas could act as both a trigger and a distributor of significant functional information in relation with the timing and performance of conditioned eyelid responses. As a whole, IPns could be considered to behave as a neuronal phase-modulating device supporting OO Mns firing during learned eyelid movements.

Furthermore, according to the recently reviewed general principles of the brain network (De Zeeuw et al., 2011), the spatiotemporal coding, in addition to firing rate coding, might support cerebellar processing. These spatiotemporal patterns (firing rate, and spike timing) may be compared with our results showing parametric timing–intensity and time delay–strength dispersion patterns of the neurons at different timescales – i.e., the spike-rate code, the spike-timing code, and correlation code (the strength and type of interdependence between signals, including the asymmetry information) – all together as a central spatiotemporal pattern. In the milliseconds range (intra-trial interaction), the firing properties of the IPns (i.e., the peak firing rate and the total number of spikes in the CS–US interval), the parametric timing (i.e., the time to peak firing and relative refractory periods), the time delay in coupling (i.e., the time to maximum correlation code between the neuronal recordings), the time–intensity dispersion patterns, and – finally – the causality inferences (correlation code and temporal order) were conforming a more exhaustive spatiotemporal pattern or a more precise picture of the functional states involved in the actual acquisition of new motor and cognitive abilities. In this paper, the results of the causal analyses for the time-dependent relative variation functions of the IPns and OO Mns firing rates (**Figures 8 and 9**) enabled investigation of the relationship between the relevance of spike timing and the novel spatiotemporal pattering (as a neuronal state vector at the milliseconds timescale) characterizing the firing properties and their dynamic patterns (time-dispersion and temporal evolution), as well as the strength of the interdependencies between neuronal activities and the performance (kinematics) of eyelid conditioned responses. This idea was extended to inter-trials, inter-blocks (**Figure 10A**), and inter-sessions (**Figure 10B**) interactions of the datasets using the corresponding averaged firing rates of IPns and OO Mns and their causality interdependencies (all as a more exhaustive averaged spatiotemporal pattern) to study the timing of averaged eyelid CRs, the sequential temporal distribution of averaged datasets corresponding to averaged blocks and experimental sessions along the conditioning process.

Finally, the same experimental protocols and analytical procedures (including as an essential method the circular distribution of the experimental data) could also be applied to different durations of CS–US interval as an alternative approach to provide interval-based representations in order to understand better the interval timing mechanisms. In the first instance, the simulated time conditions where the data distribution is fitted to the circle may be extended to the standard interval timing strategy with the aim of exploring the quantifiable changes in the time–intensity dispersion patterns of data distributions depending on the duration of the CS–US interval. In the second instance, these experimental and analytical approaches could also be applied to many pharmacological manipulations that modify the spatiotemporal firing pattern (spike rate, spike timing, and correlation codes) within the cerebellar-IP nucleus-red-nucleus-Mns network. These modifications in the spatiotemporal patterns lead to a dynamic

change in the functional neuronal state (timing and their corresponding kinetic neural commands and dispersion patterns) evoked by the learning process, and consequently to some change in the timing and performance of the learned motor responses – i.e., in the motor behavior.

ACKNOWLEDGMENTS

Work supported by grants MICINN-BFU2008-0899, P07-CVI-2487 and JA-BIO-122 to José M. Delgado-García, and MICINN-BFU2008-03390 and P07-CVI-02686 to Agnès Gruart. We thank Roger Churchill for his editorial help.

REFERENCES

Aksenova, T. I., Chibirova, O. K., Dryga, O. A., Tetko, I. V., Benabid, A. L., and Villa, A. E. P. (2003). An unsupervised automatic method for sorting neuronal spike waveforms in awake and freely moving animals. *Methods* 30, 178–187.

Almeida, R., and Ledberg, A. (2010). A biologically plausible model of time-scale invariant interval timing. *J. Comput. Neurosci.* 28, 155–175.

Batschelet, E. (1981). *Circular Statistics in Biology*. New York: Academic Press.

Berens, P. (2009). CircStat: a MATLAB toolbox for circular statistics. *J. Stat. Softw.* 31, 1–21.

Berman, A. L. (1968). *The Brain Stem of the Cat: A Cytoarchitectonic Atlas with Stereotaxic Coordinates*. Madison, WI: University of Wisconsin Press.

Berthier, N. E., and Moore, J. W. (1990). Activity of deep cerebellar nuclear cells during classical conditioning of nictitating membrane extension in rabbits. *Exp. Brain Res.* 83, 44–54.

Box, G. E. P., and Jenkins, G. M. (1976). *Time Series Analysis: Forecasting and Control*. San Francisco: Holden-Day.

Brown, E. N., Kass, R. E., and Mitra, P. P. (2004). Multiple neural spike train data analysis: state-of-the-art and future challenges. *Nat. Neurosci.* 7, 456–461.

Buhusi, C. V., and Meck, W. H. (2005). What makes us tick? Functional and neural mechanisms of interval timing. *Nat. Rev. Neurosci.* 6, 755–765.

Buonomano, D. V., and Karmarkar, U. R. (2002). How do we tell time? *Neuroscientist* 8, 42–51.

Buonomano, D. V., and Laje, R. (2010). Population clocks: motor timing with neural dynamics. *Trends Cogn. Sci. (Regul. Ed.)* 14, 520–527.

Chan, H. L., Wu, T., Lee, S. T., Fang, S. C., Chao, P. K., and Lin, M. A. (2008). Classification of neuronal spikes over the reconstructed phase space. *J. Neurosci. Methods* 168, 203–211.

Chen, F. P., and Evinger, C. (2006). Cerebellar modulation of trigeminal reflex blinks: interpositus neurons. *J. Neurosci.* 26, 10569–10576.

Clarke, S., Ivry, R., Grinband, J., Roberts, S., and Shimizu, N. (1996). "Exploring the domain of the cerebellar timing system," in *Time, Internal Clocks, and Movement*, eds M. A. Pastor and J. Artieda (New York: Elsevier), 257–280.

Crochet, S., Poulet, J. F., Kremer, Y., and Petersen, C. C. (2011). Synaptic mechanisms underlying sparse coding of active touch. *Neuron* 69, 1160–1175.

De Zeeuw, C. I., Hoebeek, F. E., Bosman, L. W., Schonewille, M., Witter, L., and Koekkoek, S. K. (2011). Spatiotemporal firing patterns in the cerebellum. *Nat. Rev. Neurosci.* 12, 327–344.

Delgado-García, J. M., and Gruart, A. (2002). The role of interpositus nucleus in eyelid conditioned responses. *Cerebellum* 1, 289–308.

Domingo, J. A., Gruart, A., and Delgado-García, J. M. (1997). Quantal organization of reflex and conditioned eyelid responses. *J. Neurophysiol.* 78, 2518–2530.

Domínguez-del-Toro, E., Rodríguez-Moreno, A., Porras-García, E., Sánchez-Campusano, R., Blanchard, V., Lavilla, M., Böhme, G. A., Benavides, J., and Delgado-García, J. M. (2004). An in vitro and in vivo study of early deficits in associative learning in transgenic mice that over-express a mutant form of human APP associated with Alzheimer's disease. *Eur. J. Neurosci.* 20, 1945–1952.

Fiala, J. C., Grossberg, S., and Bullock, D. (1996). Metabotropic glutamate receptor activation in cerebellar Purkinje cells as substrate for adaptive timing of the classically conditioned eye-blink response. *J. Neurosci.* 16, 3760–3774.

Fisher, N. I. (1993). *Statistical Analysis of Circular Data*. New York: Cambridge University Press.

Gallistel, C. R., and Gibbon, J. (2000). Time, rate, and conditioning. *Psychol. Rev.* 107, 289–344.

Geweke, J. (1982). Measurement of linear dependence and feedback between multiple time series. *J. Am. Stat. Assoc.* 77, 304–313.

Gibbon, J. (1977). Scalar expectancy-theory and Weber's law in animal timing. *Psychol. Rev.* 84, 279–325.

Gibbon, J., and Church, R. M:(1990). Representation of time. *Cognition* 37, 23–54.

Gibbon, J., Malapani, C., Dale, C. L., and Gallistel, C. R. (1997). Toward a neurobiology of temporal cognition: advances and challenges. *Curr. Opin. Neurobiol.* 7, 170–184.

Grafen, A., and Hails, R. (2002). *Modern Statistics for the Life Sciences*. New York: Oxford University Press Inc.

Granger, C. W. J. (1980). Testing for causality: a personal viewpoint. *J. Econ. Dyn. Control* 2, 329–352.

Grossberg, S., and Schmajuk, N. A. (1989). Neural dynamics of adaptive timing and temporal discrimination during associative learning. *Neural Netw.* 2, 79–102.

Gruart, A., Blázquez, P., and Delgado-García, J. M. (1995). Kinematics of unconditioned and conditioned eyelid movements in the alert cat. *J. Neurophysiol.* 74, 226–248.

Gruart, A., and Delgado-García, J. M. (1994). Discharge of identified deep cerebellar nuclei neurons related to eye blinks in the alert cat. *Neuroscience* 61, 665–681.

Gruart, A., Guillazo-Blanch, G., Fernández-Mas, R., Jiménez-Díaz, L., and Delgado-García, J. M. (2000a). Cerebellar posterior interpositus nucleus as an enhancer of classically conditioned eyelid responses in alert cats. *J. Neurophysiol.* 84, 2680–2690.

Gruart, A., Schreurs, B. G., Domínguez-del-Toro, E., and Delgado-García, J. M. (2000b). Kinetic and frequency-domain properties of reflex and conditioned eyelid responses in the rabbit. *J. Neurophysiol.* 83, 836–852.

Gruart, A., Muñoz, M. D., and Delgado-García, J. M. (2006). Involvement of the CA3-CA1 synapse in the acquisition of associative learning in behaving mice. *J. Neurosci.* 26, 1077–1087.

Hair, J. F., Anderson, R. E., Tatham, R. L., and Black, W. C. (1998). *Multivariate Data Analysis*. New Jersey: Prince–Hall, Inc.

Harvey, A. (1994). *Time Series I–II*. Cambridge: Cambridge University Press.

Ivry, R. B. (1996). The representation of temporal information in perception and motor control. *Curr. Opin. Neurobiol.* 6, 851–857.

Ivry, R. B., and Spencer, R. M. C. (2004). The neural representation of time. *Curr. Opin. Neurobiol.* 14, 225–223.

Jammalamadaka, S. R., and SenGupta, A. (2001). *Topics in Circular Statistics*. Singapore: World Scientific Press.

Jarvis, M. R., and Mitra, P. P. (2001). Sampling properties of the spectrum and coherency in sequences of action potentials. *Neural. Comput.* 13, 717–749.

Jiménez-Díaz, L., Navarro-López, J. de D., Gruart, A., and Delgado-García, J. M. (2004). Role of cerebellar interpositus nucleus in the genesis and control of reflex and conditioned eyelid responses. *J. Neurosci.* 24, 9138–9145.

Kaminski, M., and Liang, H. (2005). Causal influence: advances in neurosignal analysis. *Crit. Rev. Biomed. Eng.* 33, 347–430.

Lejeune, H., and Wearden, J. H. (2006). Scalar properties in animal timing: conformity and violations. *Q. J. Exp. Psychol.* 59, 1875–1908.

Lewis, P. A., and Miall, R. C. (2003). "Overview: an image of human neural timing," in *Functional and Neural Mechanisms of Interval Timing*, ed. W. H. Meck (Boca Raton, FL: CRC), 515–532.

Lewis, P. A., Miall, R. C., Daan, S., and Kacelnik, A. (2003). Interval timing in mice does not rely upon the circadian pacemaker. *Neurosci. Lett.* 348, 131–134.

Lopes da Silva, F. H., Pijn, J. P., and Boeijinga, P. (1989). Interdependence of EEG signals: linear vs. nonlinear associations and the significance of time delays and phase shifts. *Brain Topogr.* 2, 9–18.

Mardia, K. V. (1975). Statistics of directional data (with discussion). *J. R. Stat. Soc. Series B Stat. Methodol.* 37, 349–393.

Mardia, K. V., and Jupp, P. E. (1999). *Directional Statistics*. Chichester: Wiley.

Matell, M. S., and Meck, W. H. (2004). Cortico-striatal circuits and interval timing: coincidence detection of oscillatory processes. *Brain Res. Cogn. Brain Res.* 21, 139–170.

Mauk, M. D., and Buonomano, D. V. (2004). The neural basis of temporal processing. *Annu. Rev. Neurosci.* 27, 307–340.

McCormick, D. A., and Thompson, R. F. (1984). Neuronal responses of the rabbit cerebellum during acquisition and performance of a classically conditioned nictitating membrane-eyelid response. *J. Neurosci.* 4, 2811–2822.

Meck, W. H. (1996). Neuropharmacology of timing and time perception. *Brain Res. Cogn. Brain Res.* 3, 227–242.

Meck, W. H., Penney, T. B., and Pouthas, V. (2008). Corticostriatal representation of time in animals and humans. *Curr. Opin. Neurobiol.* 18, 145–152.

Medina, J. F., Carey, M. R., and Lisberger, S. G. (2005). The representation of time for motor learning. *Neuron* 45, 157–167.

Miall, R. C. (1992). "Oscillators, predictions and time," in *Time, Action and Cognition: Bridging the Gap*, NATO ASI Series D, Vol. 66, eds F. Macar, V. Pouthas, and W. Friedman (Dordrecht: Kluwer Academic Publishers), 215–227.

Miall, R. C. (1993). Neural networks and the representation of time. *Psychol. Belg.* 33, 255–269.

Morcuende, S., Delgado-García, J. M., and Ugolini, G. (2002). Neuronal premotor networks involved in eyelid responses: retrograde transneuronal tracing with rabies virus from the orbicularis oculi muscle in the rat. *J. Neurosci.* 22, 8808–8818.

Nolte, G., Ziehe, A., Nikulin, V. V., Schlögl, A., Krämer, N., Brismar, T., and Müller, K. R. (2008). Robustly estimating the flow direction of information in complex physical systems. *Phys. Rev. Lett.* 100, 1–4.

Okamoto, H., and Fukai, T. (2001). Neural mechanism for a cognitive timer. *Phys. Rev. Lett.* 86, 3919–3922.

Okamoto, H., Isomura, Y., Takada, M., and Fukai, T. (2007). Temporal integration by stochastic recurrent network dynamics with bimodal neurons. *J. Neurophysiol.* 97, 3859–3867.

Pereda, E., Quian-Quiroga, R., and Bhattacharya, J. (2005). Nonlinear multivariate analysis of neurophysiological signals. *Prog. Neurobiol.* 77, 1–37.

Petersen, C. C. H. (2007). The functional organization of the barrel cortex. *Neuron* 56, 339–355.

Porras-García, E., Sánchez-Campusano, R., Martínez-Vargas, D., Domínguez-del-Toro, E., Cendelín, J., Vožeh, F., and Delgado-García, J. M. (2010). Behavioral characteristics, associative learning capabilities, and dynamic association mapping in an animal model of cerebellar degeneration. *J. Neurophysiol.* 104, 346–365.

Poulet, J. F. A., and Petersen, C. C. H. (2008). Internal brain state regulates membrane potential synchrony in barrel cortex of behaving mice. *Nature* 454, 881–885.

Sánchez-Campusano, R., Gruart, A., and Delgado-García, J. M. (2007). The cerebellar interpositus nucleus and the dynamic control of learned motor responses. *J. Neurosci.* 27, 6620–6632.

Sánchez-Campusano, R., Gruart, A., and Delgado-García, J. M. (2009). Dynamic associations in the cerebellar-motoneuron network during motor learning. *J. Neurosci.* 29, 10750–10763.

Sánchez-Campusano, R., Gruart, A., and Delgado-García, J. M. (2010). Dynamic changes in the cerebellar-interpositus/red-nucleus-motoneuron pathway during motor learning. *Cerebellum*. doi: 10.1007/s12311-010-0242-1. [Epub ahead of print].

Schöner, G. (2002). Timing, clocks, and dynamical systems. *Brain Cogn.* 48, 31–51.

Schöner, G., and Kelso, J. A. S. (1988). Dynamic pattern generation in behavioral and neural systems. *Science* 239, 1513–1520.

Spencer, R. M. C., Zelaznik, H. N., Diedrichsen, J., and Ivry, R. B. (2003). Disrupted timing of discontinuous but not continuous movements by cerebellar lesions. *Science* 300, 1437–1439.

Staddon, J. E. R., and Cerutti, D. T. (2003). Operant conditioning. *Annu. Rev. Psychol.* 54, 115–144.

Staddon, J. E. R., and Higa, J. J. (1999). Time and memory: towards a pacemaker-free theory of interval timing. *J. Exp. Anal. Behav.* 71, 215–251.

Svensson, P., Jirenhed, D. A., Bengtsson, F., and Hesslow, G. (2010). Effect of conditioned stimulus parameters on timing of conditioned Purkinje cell responses. *J. Neurophysiol.* 103, 1329–1336.

Tiao, G. C., and Box, G. E. P. (1981). Modeling Multiple Time Series with Applications. *J. Am. Stat. Assoc.* 26, 71–130.

Trigo, J. A., Gruart, A., and Delgado-García, J. M. (1999). Discharge profiles of abducens, accessory abducens, and orbicularis oculi motoneurons during reflex and conditioned blinks in alert cats. *J. Neurophysiol.* 81, 1666–1684.

Valenzuela-Harrington, M., Gruart, A., and Delgado-García, J. M. (2007). Contribution of NMDA receptor NR2B subunit to synaptic plasticity during associative learning in behaving rats. *Eur. J. Neurosci.* 25, 830–836.

Van Kan, P. L. E., Houk, J. C., and Gibson, A. R. (1993). Output organization of intermediate cerebellum of the monkey. *J. Neurophysiol.* 69, 57–73.

Wearden, J. H., and Lejeune, H. (2008). Scalar properties in human timing: conformity and violations. *Q. J. Exp. Psychol.* 61, 569–587.

Wendling, F., Bartolomei, F., Bellanger, J. J., and Chauvel, P. (2001). Interpretation of interdependencies in epileptic signals using a macroscopic physiological model of the EEG. *Clin. Neurophysiol.* 112, 1201–1218.

Conflict of Interest Statement: The authors declare that the research was conducted in the absence of any commercial or financial relationships that could be construed as a potential conflict of interest.

Received: 30 June 2011; paper pending published: 16 July 2011; accepted: 01 August 2011; published online: 30 August 2011.

*Citation: Sánchez-Campusano R, Gruart A and Delgado-García JM (2011) Timing and causality in the generation of learned eyelid responses. Front. Integr. Neurosci. **5**:39. doi: 10.3389/fnint.2011.00039*

frontiers in
INTEGRATIVE NEUROSCIENCE

ORIGINAL RESEARCH ARTICLE
published: 30 November 2011
doi: 10.3389/fnint.2011.00072

Adaptive timing of motor output in the mouse: the role of movement oscillations in eyelid conditioning

Selmaan N. Chettih, Samuel D. McDougle, Luis I. Ruffolo and Javier F. Medina*

Department of Psychology, University of Pennsylvania, Philadelphia, PA, USA

Edited by:
Agnes Gruart, University Pablo de Olavide, Spain

Reviewed by:
S. K. E. Koekkoek, Erasmus MC, Netherlands
Raudel Sánchez-Campusano, Universidad Pablo de Olavide, Spain

****Correspondence:***
Javier F. Medina, Department of Psychology, University of Pennsylvania, Solomon Labs Building, 3720 Walnut Street, Philadelphia, PA 19104, USA.
e-mail: jmed@psych.upenn.edu

To survive, animals must learn to control their movements with millisecond-level precision, and adjust the kinematics if conditions, or task requirements, change. Here, we examine adaptive timing of motor output in mice, using a simple eyelid conditioning task. Mice were trained to blink in response to a light stimulus that was always followed by a corneal air-puff at a constant time interval. Different mice were trained with different intervals of time separating the onset of the light and the air-puff. As in previous work in other animal species, mice learned to control the speed of the blink, such that the time of maximum eyelid closure matched the interval used during training. However, we found that the time of maximum eyelid speed was always in the first 100 ms after movement onset and did not scale with the training interval, indicating that adaptive timing is not accomplished by slowing down (or speeding up) the eyelid movement uniformly throughout the duration of the blink. A new analysis, specifically designed to examine the kinematics of blinks in single trials, revealed that the underlying control signal responsible for the eyelid movement is made up of oscillatory bursts that are time-locked to the light stimulus at the beginning of the blink, becoming desynchronized later on. Furthermore, mice learn to blink at different speeds and time the movement appropriately by adjusting the amplitude, but not the frequency of the bursts in the eyelid oscillation.

Keywords: eyeblink, cerebellum, interstimulus interval, invariance, learning

INTRODUCTION

Timing is everything. The meaning of this expression is perhaps most obvious in motor control, where a delay of just few milliseconds can make the difference between hitting a home-run or striking out (Williams and Underwood, 1986; Gray, 2002). To achieve such remarkable precision, we must learn to estimate temporal contingencies accurately despite living in an ever-changing world, and adjust the timing of our movements accordingly. For example, good hitters are capable of adapting their swing depending on pitch type, often taking into account external factors that affect the speed of the baseball, like wind, humidity, temperature, or altitude (Williams and Underwood, 1986; Gray, 2002; Fortenbaugh, 2011).

In the laboratory, adaptive timing has been studied extensively using the eyelid conditioning task (Gormezano et al., 1983). Subjects learn to blink in response to a conditioned stimulus (CS), like a light, that precedes and is repeatedly paired with an air-puff directed at the eye. Previous work in a variety of animal species has demonstrated that the timing of the conditioned eyelid response is adjusted to match the interstimulus interval (ISI): maximum eyelid closure in "test-trials" without an air-puff occurs at the time when the air-puff is normally delivered, regardless of the particular ISI used during training (Boneau, 1958; Mauk and Ruiz, 1992; Domingo et al., 1997; Freeman et al., 2003; Koekkoek et al., 2003). Measuring the latency to maximum eyelid closure, however, does not provide information about the particular trajectory that the eyelid takes from open to closed.

To really understand the control signals used to achieve timing, it is necessary to characterize the kinematics of the movement and examine how it unfolds in time. Most experimental work supports the notion that the timing of the conditioned eyelid response is achieved by adjusting the speed, and to a lesser extent the onset, of the movement (Boneau, 1958; Levey and Martin, 1968; Mauk and Ruiz, 1992; Domingo et al., 1997; Freeman et al., 2003; Koekkoek et al., 2003). Although a full description of blink kinematics at different ISIs is still lacking, this type of trajectory has been modeled as being timescale-invariant (Grossberg and Schmajuk, 1989; Lepora et al., 2007): the timing of movement is adaptively adjusted by slowing down (or speeding up) the entire movement trajectory, from beginning to end, by a constant factor. For many movements, the underlying rules of adaptive timing are known, and appear to be compatible with the timescale invariance hypothesis (Schmidt and Lee, 2005), but see (Gentner, 1987). In contrast, and despite the existing wealth of data about adaptive timing in the eyelid conditioning task, the rules for adjusting the conditioned eyelid trajectory remain poorly understood.

One source of complication is that most studies have examined the timing of the conditioned eyelid movement by averaging trajectories over many trials (Levey and Martin, 1968; Mauk and Ruiz, 1992; Domingo et al., 1997; Freeman et al., 2003; Koekkoek et al., 2003), masking the fact that individual blinks are not smooth. As documented by work in a variety of animal species, including human (Marquis and Porter, 1939), rabbit (Gruart et al., 2000), cat (Domingo et al., 1997), ferret (Ivarsson and Svensson, 2000),

guinea pig (Gruart et al., 2000), rat (Gruart et al., 2000), and mouse (Koekkoek et al., 2002), conditioned eyelid movements display prominent oscillations, accelerating and decelerating in brief bursts which can be detected in the electromyographic (EMG) activity of the orbicularis oculi muscle (Gruart et al., 1995, 2000; Trigo et al., 1999; Ivarsson and Svensson, 2000). In theory, adaptive timing could be achieved by modulating the amplitude, rate, and/or number of these bursts, in ways that could make the movement timescale-invariant or not. Which control strategy is actually implemented by the brain is not known.

In this study we characterize the kinematics of the conditioned eyelid response in mice trained to different ISIs. Our results demonstrate that the conditioned eyelid movement consists of two phases: an initial acceleration phase from movement onset to maximum eyelid speed that is highly stereotyped and has the same duration regardless of ISI, and a subsequent deceleration phase from maximum eyelid speed to the moment of maximum eyelid closure, whose duration is adjusted and is proportional to the ISI. The resulting conditioned eyelid trajectory is not timescale-invariant, but nonetheless it achieves maximum eyelid closure around the time of the particular interval used during training. Single-trial analyses reveal that these adjustments to the timing of the conditioned eyelid response are made by neural mechanisms that modulate the amplitude of the underlying bursts of movement, but not the frequency at which they occur.

RESULTS

Although there have been sporadic accounts of adaptive timing during eyelid conditioning in mice (Koekkoek et al., 2003; Van Der Giessen et al., 2008; Boele et al., 2010), no systematic study of the eyelid trajectories has been carried out. Thus, we begin by characterizing in full detail the kinematic properties of the conditioned eyelid response in mice trained at different ISIs. Light was used as the CS because it did not cause startle-responses, unlike the more commonly used auditory tone CS (Boele et al., 2010). In all our experiments the light stimulus was visible by the two eyes, the puff was delivered to the left eye, and conditioned responses were measured exclusively by examining the left eye. To allow for unbiased comparisons across different ISI conditions, analysis was performed on test sessions that began after asymptotic performance had been achieved, and by examining conditioned eyelid responses only on CS-alone trials in which no air-puff is delivered (see Materials and Methods). As shown in **Table 1**, mice trained with 175 or 250 ms intervals showed high-levels of conditioning and generated conditioned eyelid responses reliably, while performance for mice trained with 325 or 400 ms intervals exhibited greater variance.

GENERAL KINEMATIC PROPERTIES OF THE CONDITIONED EYELID MOVEMENT

Conditioned eyelid responses were adaptively timed. As ISI increased from 175 to 400 ms, the learned blinks became smaller in amplitude, and latency to maximum eyelid closure increased adaptively to match the ISI used during training (**Table 1**; **Figure 1A**; $p < 0.001$ confirmed with sequential t-tests between the different ISI conditions). Responses appeared to become broader as the ISI was lengthened, rather than simply translated later in time. In other words, over the range of ISIs in **Figure 1**, mice appear to achieve precise timing by regulating the velocity, but not the onset latency of the eyelid movement (**Figures 1B,C**). As shown in **Figure 1C**, maximum velocity and maximum eyelid closure were strongly correlated in individual trials (R-values ranged from 0.62 to 0.72 for the different conditions), and the average of both kinematic parameters decreased with ISI ($p < 0.001$ confirmed with sequential t-tests). The regression lines overlapped for ISIs in the range 250–400 ms, suggesting that the same relationship between maximum velocity and maximum eyelid closure is applicable across these different conditions. The relationship was still present in mice trained with the 175-ms ISI (red regression line), but in this group, conditioned eyelid responses of comparable maximum closure reached higher speeds than in mice trained with the other ISIs.

Table 1 | Kinematic properties of the average conditioned eyelid response for each of the mice in this study.

ISI (ms)	% CR	Max closure (FEC)	Time max closure (ms)	Max vel (FEC/s)
175	81 ± 4	0.49 ± 0.17	237 ± 74	16 ± 7.0
	87 ± 5	0.59 ± 0.18	235 ± 76	18 ± 6.5
	93 ± 4	0.60 ± 0.16	237 ± 53	15 ± 4.7
250	83 ± 6	0.37 ± 0.13	275 ± 71	9.2 ± 3.9
	92 ± 7	0.42 ± 0.17	274 ± 65	9.1 ± 3.7
	90 ± 4	0.72 ± 0.20	365 ± 114	15 ± 6.1
	85 ± 5	0.44 ± 0.13	284 ± 79	10 ± 4.0
325	79 ± 7	0.43 ± 0.14	397 ± 122	11 ± 4.8
	72 ± 6	0.43 ± 0.16	368 ± 90	9.0 ± 4.8
	56 ± 14	0.37 ± 0.16	367 ± 141	8.5 ± 5.1
	95 ± 4	0.44 ± 0.14	386 ± 161	9.1 ± 4.3
400	52 ± 10	0.35 ± 0.17	436 ± 144	6.7 ± 3.7
	67 ± 9	0.34 ± 0.18	390 ± 144	9.2 ± 5.9
	88 ± 9	0.45 ± 0.16	411 ± 114	9.0 ± 4.7

Error ranges for "% CR" are SD over individual sessions; all other error ranges are SD over all trials. CR, conditioned response; FEC, fraction eyelid closure.

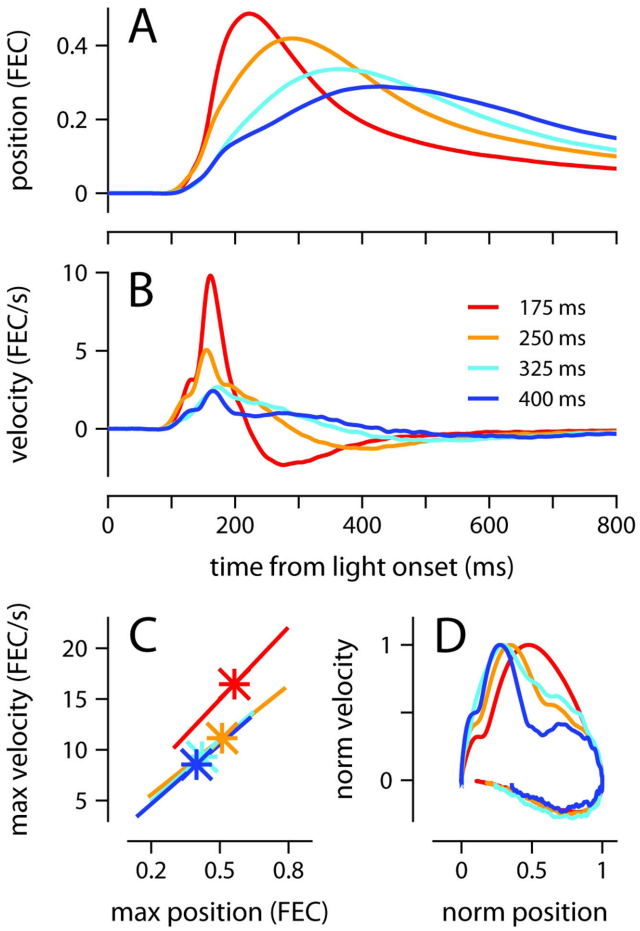

FIGURE 1 | Kinematic properties of the conditioned eyelid movement. **(A)** Average eyelid position, and **(B)** average eyelid velocity for mice trained with four different ISIs. **(C)** Asterisks indicate the average maximum position and maximum velocity for each ISI. X-range of the linear regression lines is mean of position maxima ± std across all trials for a particular ISI. **(D)** Normalized phase plots for the data shown in **(A,B)**. Color code for all plots indicates trained ISI and is shown in **(B)**. FEC, fraction eyelid closure.

The broadening of the conditioned response as the ISI was lengthened was not a simple timescale-invariant stretching of the movement. This can be appreciated visually by comparing the peaks of the traces in **Figures 1A,B**. The time of maximum eyelid closure scales proportionally with the ISI whereas the time of maximum eyelid velocity remains relatively constant. Indeed, the normalized phase plots in **Figure 1D** do not overlap each other, and clearly show that for example, maximum velocity was attained when the eyelid had closed 50% of the size of the full conditioned response in the 175-ms group (red line), but only 25% in the 400-ms group (blue line). The same asymmetric pattern in the temporal scaling of eyelid position vs. velocity was clearly visible when the kinematic data from individual mice was analyzed separately and normalized to emphasize temporal structure over differences in amplitude (**Figures 2A,B**). As shown in the probability density plots of **Figures 2C,D**, this effect was not an artifact of averaging many conditioned eyelid responses: the time of maximum eyelid closure in individual trials became more variable with longer ISIs, but was also clearly shifted later in time (**Figure 2C**). In stark contrast, most eyelid movements reached maximum velocity between 150 and 180 ms after light onset for all mice, regardless of the ISI used during training, although the range of peak-times did appear to extend later in time as ISI increased (**Figure 2D**).

Because **Figures 1** and **2** clearly demonstrate that conditioned eyelid responses are not timescale-invariant, understanding the rules of response timing necessitates moving beyond traditional latency-to-peak analyses to a richer understanding of the temporal evolution of the movement kinematics. This is the focus of the next sections.

CONDITIONED EYELID MOVEMENTS BEGIN WITH TWO TIME-LOCKED BURSTS OF ACCELERATION

The mean velocity of the eyelid movement exhibited a stereotyped profile in the first 200 ms after the presentation of the light regardless of ISI (**Figures 2B** and **3**), with onset occurring around 100 ms, a small bump or local peak prior to 150 ms, and a second peak between 150 and 180 ms, which was always the velocity maximum. The velocity then ramped down with a somewhat idiosyncratic trajectory, remaining positive (eyelid closing) for a duration that was inversely related to ISI. This stereotyped profile was strikingly similar for all trained ISIs, and was not an artifact of averaging over multiple recording sessions because the same pattern was clearly observed in individual sessions (**Figures 3A,B**).

To investigate the underlying cause of this stereotyped profile, which represents the average over many conditioned eyelid movements, we examined eyelid velocity on individual trials. **Figures 3C,D** show eyelid velocity and position traces from three example trials taken from the mouse in **Figure 3B**. The velocity profile in the first 200 ms of individual trials exhibited an underlying oscillation, with multiple peaks (**Figure 3E**) separated by a mean interpeak-interval of ∼30 ms (**Figure 3F**), with many separated by exactly 29 ms. We found many trials in which the oscillation began at the same time and remained synchronized and in phase for the first 200 ms (**Figure 3C**), accounting for the two peaks in the velocity profile that appear at the same location on mean behavior (**Figure 3B**). Though the oscillation in eyelid velocity remains for the entire duration of the movement, it appears to become desynchronized across trials after 200 ms from the time of light onset (**Figure 3C**).

This effect, which suggests that the eyelid accelerates and decelerates in discrete bursts which are precisely time-locked early in the movement, and less so later on, was further examined as follows (see Materials and Methods for details): local peaks and troughs in the oscillatory eyelid velocity were detected in individual trials, and this information was used to compute the difference between the probability of finding a peak and the probability of finding a trough as a function of time, for each mouse separately (**Figure 3G**), and also averaged across individuals trained with the same ISI (**Figure 3H**). There were slight differences between mice, but there is a clear tendency for peaks of eyelid velocity to cluster at two separate times in the first 200 ms after light onset. The location of the two clusters did not appear related to the trained ISI (**Figures 3G,H**). Although the number of peaks and troughs

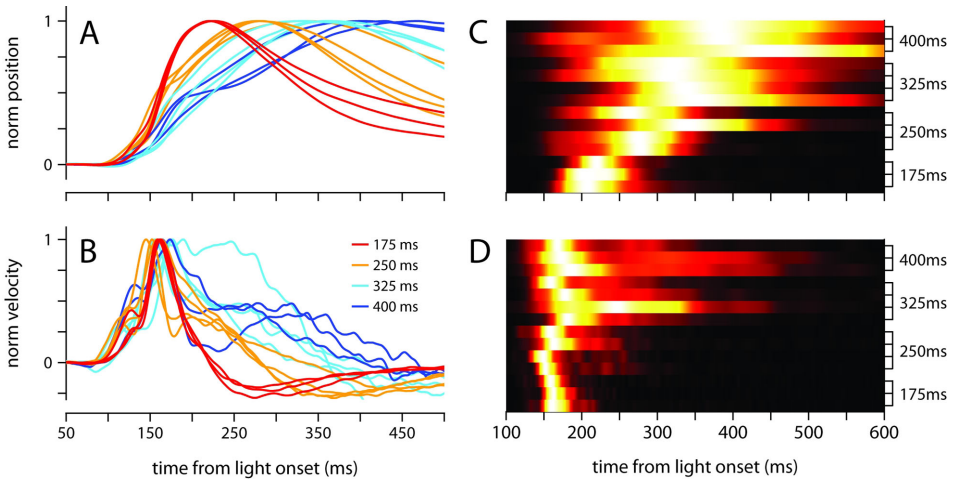

FIGURE 2 | Temporal profile of the conditioned eyelid movement in individual mice. (A) Normalized average position, and **(B)** normalized average velocity, of each mouse's conditioned eyelid responses. Color code indicates trained ISI and is shown in **(B)**. **(C)** Probability density functions for latency to maximum eyelid closure, and **(D)** latency to maximum velocity. Each row of the heat map contains the probability density function for an individual mouse, with trained ISI indicated on the *y*-axis. For display purposes, each row is normalized to have the same maximum (white).

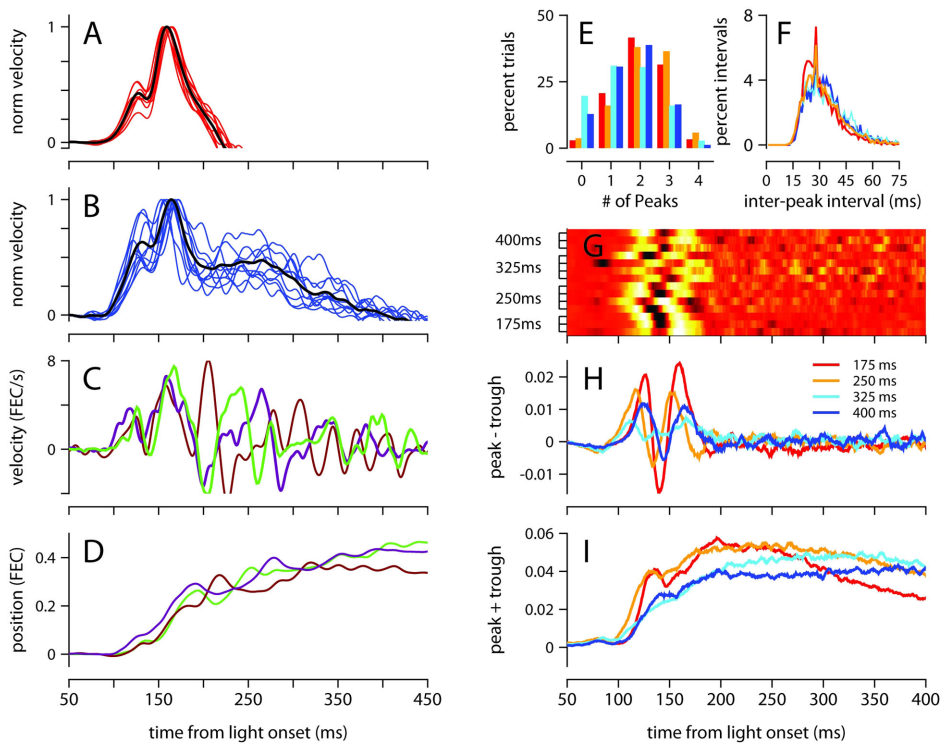

FIGURE 3 | Analysis of velocity peaks. (A) Normalized eyelid velocity averaged over all trials (black), and averaged separately for individual sessions (red) for a mouse trained with a 175-ms, and **(B)** for a mouse trained with a 400-ms ISI (individual sessions shown in blue). **(C)** Eyelid velocity, and **(D)** eyelid position for three trials taken from the subject in **(B)**. **(E)** Number of velocity peaks found in single trials between 100 and 200 ms from light onset, and **(F)** the interval of time between consecutive velocity peaks. Histograms were computed separately for each mouse and averaged over ISI condition. **(G)** Difference between the probability of finding a peak and a trough at each ms from light onset. Each row of the heat map contains the difference in peak and trough probability functions for an individual mouse, with trained ISI indicated on the *y*-axis. For display purposes, each row is converted to a *z*-score. **(H)** Difference, and **(I)** sum of probability functions for peaks and troughs, averaged over ISI condition. Color code for **(E)**, **(F)**, **(H)**, and **(I)** indicates trained ISI and is shown in **(H)**. FEC, fraction eyelid closure.

remained high after the first 200 ms (**Figures 3C,I**), the clustering disappeared (**Figures 3G,H**), indicating that the location of peaks and troughs is not time-locked and varies from trial to trial during the later part of the eyelid movement.

OSCILLATORY PROPERTIES OF CONDITIONED EYELID MOVEMENTS AT DIFFERENT ISIs

We now characterize in detail the oscillatory properties of conditioned eyelid movements in single trials, and determine if these properties are differentially modulated as a function of ISI. **Figure 3F** already hints at an underlying oscillation of 33 Hz (30 ms interpeak-interval) in the first 200 ms after light onset, but peak detection is not the optimal way to measure the oscillatory properties of eyelid movements because it depends on an arbitrary cutoff threshold, and cannot distinguish between the strength of oscillations at different frequencies (see Materials and Methods). Thus, we follow the example of previous authors (Domingo et al., 1997; Koekkoek et al., 2002), and focus instead on the frequency-domain characteristics revealed by the spectrogram of the eyelid acceleration signal (**Figure 4**).

The mean power spectrum of acceleration showed a broad peak centered around 30 Hz for all ISIs (clearly visible in **Figure 4**, which shows the spectrogram for one of the mice trained with an ISI of 175 ms), both during the early part of the eyelid movement (**Figure 5A**) and also later on (**Figure 5B**). This is consistent with the idea that regardless of ISI, the eyelid has a tendency to accelerate and decelerate in bursts, oscillating in the 30-Hz frequency range for the entire duration of the movement (**Figures 3C** and **4**). There was a clear modulation of total power according to the trained ISI in the early response period (**Figure 5A**), which suggests that acceleration bursts during this period are larger for the fast eyelid movements generated at short ISIs, and smaller for the slower eyelid movements at longer ISIs (**Figure 1B**). However, this straightforward relationship between total power and ISI appeared to dissipate with time and could no longer be detected in the later parts of the eyelid movement (**Figure 5B**).

Thus, to further evaluate how the frequency and power of oscillations evolve over time, we computed the spectrogram of the acceleration signal throughout the extent of the eyelid movement (**Figure 4**). For each time point, we determined the frequency at which power was maximal (**Figure 5D**), and the power at this frequency (**Figure 5C**). Power in the interval 150–250 ms after light onset decreased as the ISI was lengthened (**Figure 5C**; all pairwise comparisons $p = 0.001$). As shown in **Figure 5D**, there was

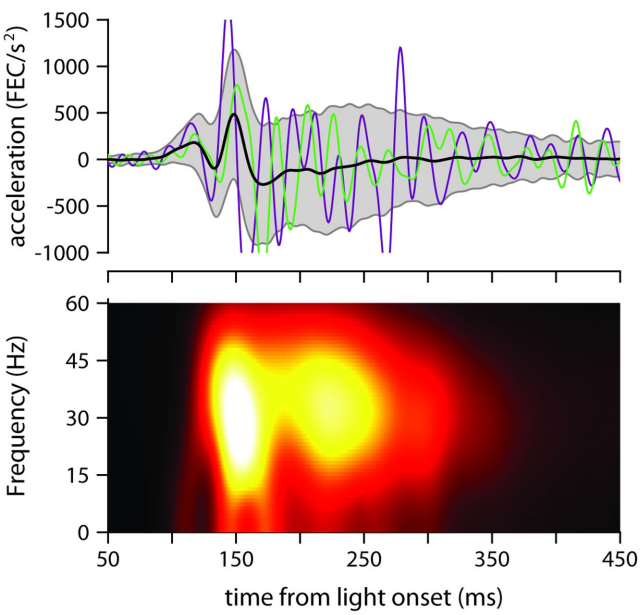

FIGURE 4 | Eyelid acceleration. *Top*: mean eyelid acceleration (black) ±1 SD (gray shaded region), and example acceleration records from two randomly selected trials (green and purple), for one of the mice trained with a 175-ms ISI (same mouse as in **Figure 3A**). *Bottom*: mean of all single-trial spectrograms of the eyelid acceleration signal for the same mouse (see Materials and Methods for details about spectrogram generation).

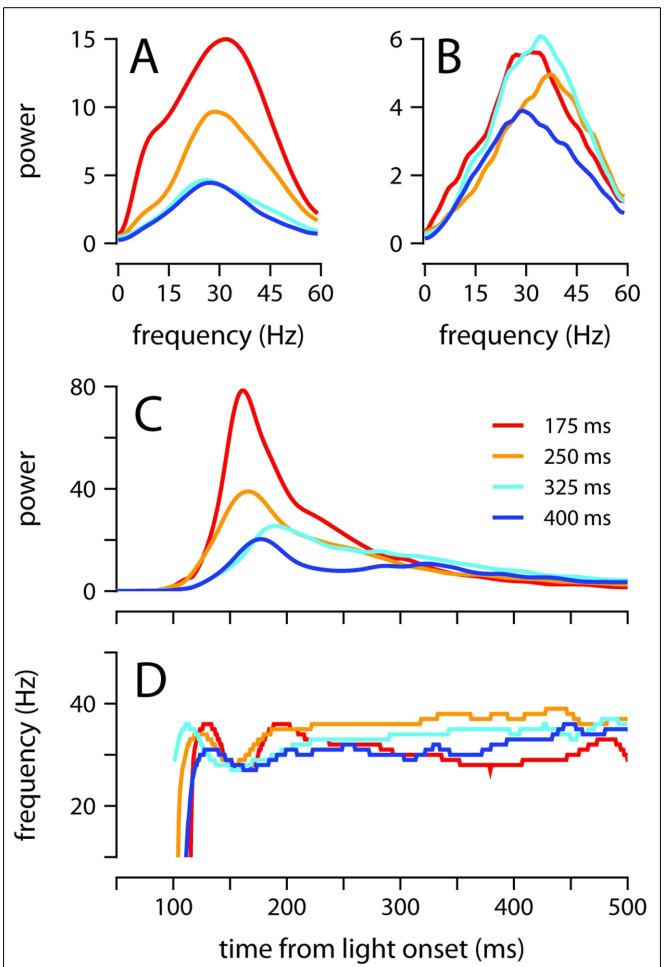

FIGURE 5 | Oscillatory properties of the conditioned eyelid response. **(A)** Average power spectrum of eyelid acceleration during the first 200 ms, and **(B)** from 200 to 500 ms after light onset. Spectra are plotted for each ISI separately. **(C)** Maximum power, and **(D)** dominant frequency of oscillation, in the eyelid acceleration signal. The value plotted at each moment in time in **(C,D)** is computed over a ~50 ms spectrogram window centered at that moment (see Materials and Methods). Each ISI plotted separately. For all plots, power is in units of (fraction eyelid closure/s²)² $Hz^{-1} \times 10^4$, and color code indicates trained ISI as shown in **(C)**.

a small dip in the dominant frequency of the eyelid oscillation at the time of maximum power, but it is clear that for the majority of the eyelid movement the dominant frequency remained within 30–40 Hz with no apparent dependence on ISI (**Figure 5D**). These results indicate that mice adjust the speed of the conditioned eyelid movement by modulating the amplitude of acceleration bursts, but not the rate at which individual bursts occur.

CONDITIONED EYELID MOVEMENTS ARE NEITHER STARTLE- NOR FIXED SHORT-LATENCY RESPONSES

Because the onset latency of the conditioned eyelid movement appears relatively fixed and unaffected by ISIs in the range 175–400 (**Figures 2A,B**), it is reminiscent of startle-reflex and short-latency blinks previously observed during eyelid conditioning in mice trained with an auditory stimulus (Boele et al., 2010). However, the data in **Figure 6** demonstrate that under certain circumstances, our mice were able to adjust the onset of the movement, which is inconsistent with the known properties of startle and short-latency responses. We trained two mice with an ISI of 100 ms, an interval that is shorter than the latency of the first velocity peak in our experiments (**Figure 2B**). Both mice showed adaptive timing, achieving maximum eyelid closure ∼75 ms earlier than the mice trained with the 175-ms interval (**Figure 6A**). Timing was achieved by shifting movement onset and increasing the magnitude of the first velocity peak relative to the second (**Figure 6B**). The early period with the two time-locked velocity peaks resembled early periods for other ISIs, but appeared shifted slightly earlier in time (**Figure 6C**). This adaptive shift in onset latency and the profile of response contrasts with the fixed onset latency and inflexible trajectory of startle and short-latency responses in previous studies that have used an auditory stimulus instead of a light (Boele et al., 2010).

Startle, short-latency and conditioned eyelid responses can also be distinguished with regards to their development during training (Boele et al., 2010). Startle-responses are small non-associative blinks that can be detected from the very first presentation of the CS before any air-puffs have been given, and short-latency responses are learned very quickly, typically within the first session of conditioning (<100 trials). In contrast, **Figure 7** shows that conditioned eyelid movements in our mice developed very gradually and took many sessions to appear. Furthermore, when conditioned eyelid movements were first observed, mean behavior did not immediately exhibit the characteristic "two-peak" velocity profile found at the completion of training (compare yellow and brown traces in **Figure 7**). Instead, the conditioned eyelid movements acquired their characteristic shape over weeks of conditioning, unlike startle- and short-latency blinks, whose kinematic profiles and onset latencies remain constant from the beginning (Boele et al., 2010).

COMPARISON BETWEEN MDMT AND HIGH-SPEED VIDEO RECORDING

To rule out the possibility that our results are an artifact of the MDMT technology that we have used to monitor eyelid position (Koekkoek et al., 2002), we developed a high-speed video capture system and recorded conditioned eyelid movements in one of the 250-ms mice with both systems simultaneously. There were some minor differences between the two methods, particularly

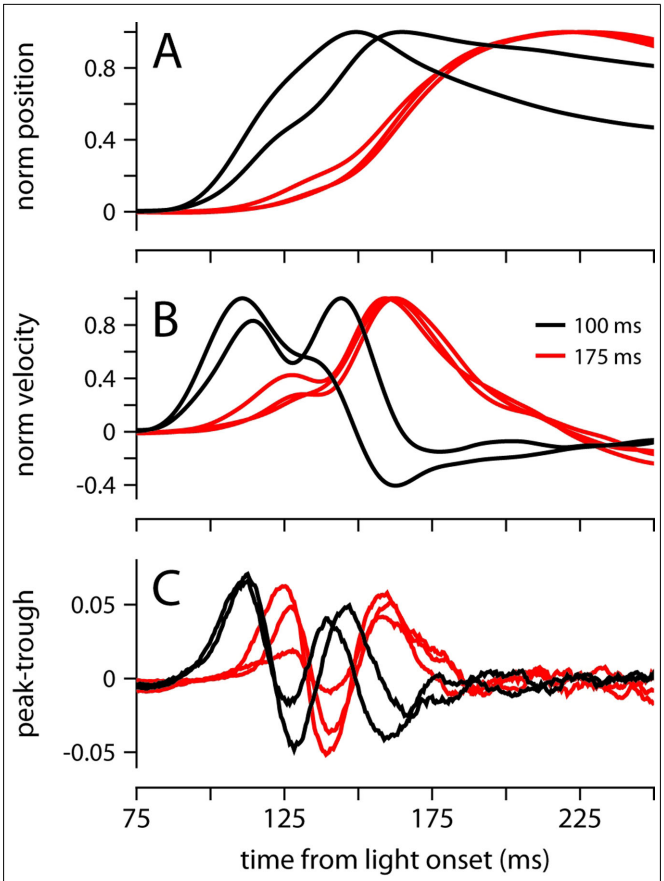

FIGURE 6 | Conditioned eyelid movements with a 100-ms ISI. (A) Normalized average eyelid position, and **(B)** normalized average velocity for mice trained with a 100-ms (black) or 175 ms ISI (red). **(C)** Difference between the probability of finding a peak and a trough at each ms from light onset. Color code for all plots indicates ISI and is shown in **(B)**.

with regards to the precise eyelid position around the time of maximum eyelid closure (see Materials and Methods); however, all major findings from the preceding analysis were verified by the video data: maximum eyelid closure occurred at the same time (**Figure 8A**, MDMT: 268 ± 75 ms, Video: 279 ± 78 ms), the characteristic two-peaked velocity profile was observed (**Figures 8B,C**), and acceleration power spectrums largely overlapped with a peak around 30 Hz (**Figure 8D**). Finally, we also used video to record eyelid movements in a session without the magnet glued on the eyelid (no MDMT signal) and found that the general properties of the data were unchanged (data not shown).

DISCUSSION

We have shown that mice trained with different ISIs can learn to time eyelid movements appropriately. Our data indicate that for ISIs in the 175–400-ms range, mice achieve precise timing by modulating the velocity of the blink but not its onset, in a manner that is incompatible with the timescale-invariant hypothesis. Analysis of movement kinematics in individual trials reveals the details of how this high-level control strategy is implemented by the brain: (1) conditioned eyelid movements are composed of discrete bursts

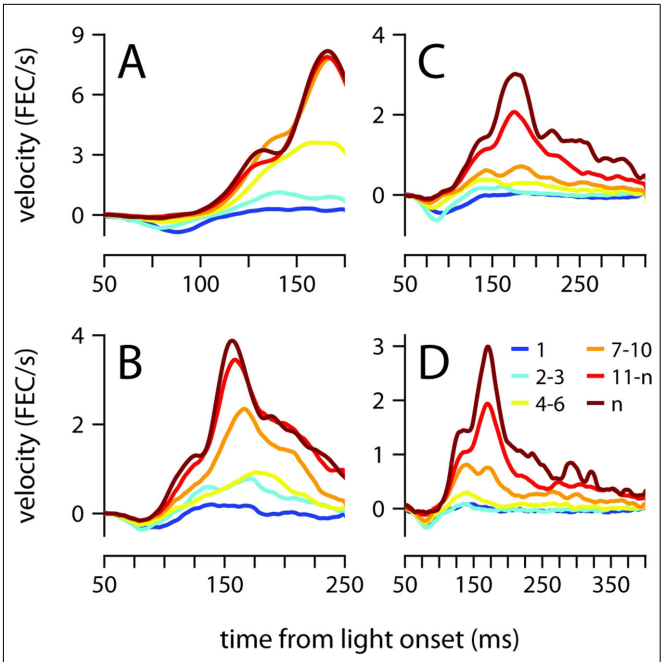

FIGURE 7 | Acquisition of the conditioned eyelid response. (A) Eyelid velocity averaged across different sessions during the training phase, for mice trained with ISIs of 175 ms, **(B)** 250 ms, **(C)** 325 ms, and **(D)** 400 ms. The sessions that were used to compute each average are indicated by the color code shown in **(D)**, where n represents number of the last training session for each mouse. FEC, fraction eyelid closure.

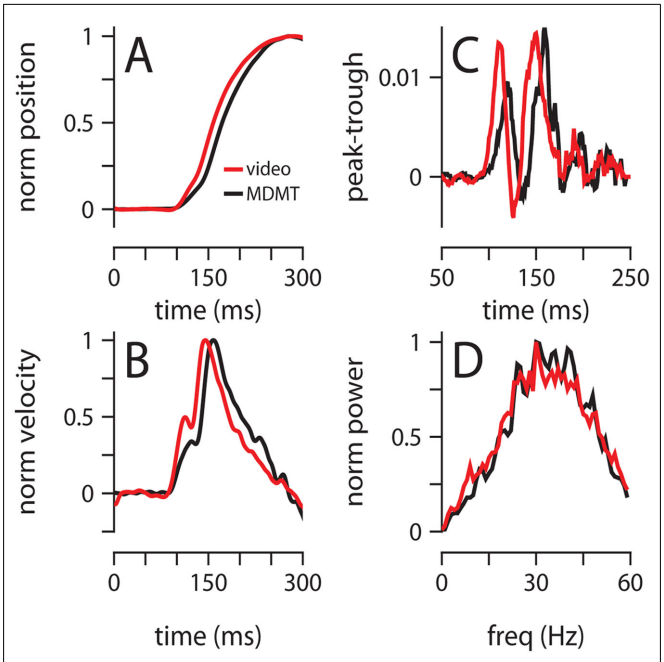

FIGURE 8 | Comparison of video and MDMT. (A) Normalized average position, and **(B)** normalized average velocity. **(C)** Difference between the probability of finding a peak and a trough at each millisecond from light onset. **(D)** Normalized average power spectrum of eyelid acceleration. Color code for all plots indicates the type of recording system and is shown in **(A)**. All data is from two 300-trial sessions with a mouse trained with a 250-ms ISI.

that occur at a dominant frequency of ∼30 Hz, (2) the first two bursts of movement are time-locked to the light onset, whereas the precise timing of subsequent bursts is less consistent from trial to trial, (3) maximum eyelid velocity is inversely related to the ISI, and is usually reached during the second burst of the movement, (4) eyelid velocity is controlled by adjusting the amplitude of bursts, but not the frequency at which they are generated.

We decided to do this study in mice because we wanted to open up the door for future investigations using genetic tools not available in other species. But mouse behavior is notorious for being finicky and unstable during eyelid conditioning (Vogel et al., 2002; Boele et al., 2010), and for this reason it may seem surprising that we were able to detect changes in the eyelid movement that were often on the order of just a few tens of milliseconds. Before we discuss the implications of our findings for the neural control of movement, we summarize some of the key methodological advances that have made our work possible.

A NEW EXPERIMENTAL APPROACH TO STUDY ADAPTIVE TIMING IN MICE

We have introduced a number of technical and procedural modifications to improve performance and to help isolate the adaptively timed component of the conditioned eyelid movement: (1) we have used low-intensity light as the CS because previous work has shown that in mice, the eyelid response to the more traditional tone stimulus includes a non-associative auditory startle-reflex that complicates the analysis of onset latency and may interfere with the production of the conditioned eyelid movement (Vogel et al., 2002; Boele et al., 2010). (2) We have used a very mild air-puff because it has been suggested recently that the much stronger periorbital stimulation typically employed for eyeblink conditioning in mice leads to a fear-related blink with a relatively fixed short-latency (Boele et al., 2010), and there is indirect evidence that in some cases this short-latency response can interfere with the adaptively timed component of the conditioned eyelid response (Aiba et al., 1994; Sakamoto and Endo, 2011). (3) We have developed a system that allows mice to be conditioned while they are actively engaged in one of their favorite activities: treadmill walking. Maintaining activity levels high helps minimize the otherwise frequent periods of "quiet wakefulness" that are partly responsible for the low levels of conditioning observed in previous studies (Boele et al., 2010). Indeed, all our mice performed at a very high level throughout the testing phase (**Table 1**), which included many sessions, and many trials in each session. This excellent performance, together with the lack of startle or fear-related short-latency eyelid responses, and the advantages of a head-fixed preparation, make our cylindrical treadmill system ideally suited for future studies aimed at investigating the neural mechanisms underlying the adaptive timing of movement.

MOTONEURON CONTROL OF MOVEMENT SPEED: A HYPOTHESIS

Electromyographic recordings from blink-related muscles like the orbicularis oculi can help us understand how the brain controls eyelid movement. As already noted, blinks are made by accelerating and decelerating the eyelid in brief bursts that can be identified in individual trials as velocity peaks in the eyelid movement. Previous

work has established that these peaks of velocity are correlated with peaks in the orbicularis oculi EMG signal (Trigo et al., 1999; Gruart et al., 2000; Ivarsson and Svensson, 2000), a finding that is consistent with earlier work demonstrating that there is a tight relationship between the maximum velocity of the eyelid during reflex blinks and the peak of the EMG response (Evinger et al., 1991; Gruart et al., 1995). Because EMG signals sum the action potentials that occur in a large population of motoneurons, the amplitude of a velocity peak is thought to reflect the number of motoneurons that are synchronously activated at that time (Evinger et al., 1991).

Given these considerations, our behavioral findings suggest a particular mechanism by which motoneuron firing could control the velocity of the conditioned eyelid response, and thus help adjust the time of maximum eyelid closure: when the ISI is short, velocity peaks are large and movement is fast because there is a large number of motoneurons that have been recruited and fire synchronously at the dominant frequency of ∼30 Hz. When the ISI is longer, less motoneurons are active, but those recruited still fire at ∼30 Hz, which helps explain why the interval between velocity peaks remains the same regardless of ISI. Since a smaller fraction of the motor pool is active, velocity peaks are smaller and the resulting movement is slower.

Similar versions of this recruitment strategy have been proposed for linearizing the plant during blink-related movements of the nictitating membrane in rabbits (Lepora et al., 2007, 2009; Mavritsaki et al., 2007), raising the possibility that recruitment could play a similar role in the eyelid system. We note that in other animal species, the frequency at which the eyelid oscillates is different from ∼30 Hz, and it appears to be related to body weight (Gruart et al., 2000). However, there is no reason why the mechanisms we have suggested here for mice could not be applied to motor control in other animals as well. The key feature of the "recruitment-only" strategy proposed above is that adaptive timing is achieved by dynamically regulating the number of motor units that contribute to the movement rather than their individual firing rates.

ORIGIN OF THE OSCILLATORY CONTROL SIGNAL

It is known that the periodic peaks of velocity in the conditioned eyelid response are caused by oscillatory bursts of EMG activity in the orbicularis oculi (Gruart et al., 1995, 2000; Trigo et al., 1999; Ivarsson and Svensson, 2000); what is yet to be determined are the neural mechanisms that give rise to the oscillation in the EMG signal in the first place. Some authors have suggested that intrinsic properties of facial motoneurons may be responsible for generating oscillatory bursts in the orbicularis oculi muscle (Trigo et al., 1999). The general idea behind this proposal is that because blink-related motoneurons have conductances that cause spike after-hyperpolarizations with a duration that matches the period of the EMG oscillation (Baker et al., 1980; Fanardjian et al., 1983), they may be able to generate rhythmic output at approximately the right frequency. However, it is worth noting that the interval between velocity peaks remained the same for all conditions, and across the entire duration of movement, even though the velocity of the movements varied greatly. It seems unlikely that intrinsic membrane conductances could continue to generate an output signal at the same frequency despite receiving input signals varying in strength over several orders of magnitude. Furthermore, even if intrinsic properties allow individual motoneurons to fire rhythmically, these properties alone cannot explain why the activity of the population is synchronized at a particular frequency during movement.

Our finding that the first two velocity peaks of the conditioned eyelid response are time-locked indicates that orbicularis oculi motoneurons become synchronized with remarkable temporal precision at the beginning of the movement, suggesting that they may receive common rhythmic drive from upstream areas. The cerebellar interpositus nucleus (CIN) is particularly well-suited for providing this drive during the generation of the conditioned eyelid response because: (1) it projects to orbicularis oculi motoneurons, both monosynaptically and via the red nucleus (Fanardjian and Manvelyan, 1984; Morcuende et al., 2002), (2) it is necessary for generating the conditioned eyelid response (McCormick and Thompson, 1984; Chen et al., 1996), (3) if stimulated artificially, it generates eyelid movements with velocity peaks occurring at the frequency of stimulation (Jimenez-Diaz et al., 2004), and (4) it contains neurons whose firing oscillates and tracks the rhythmic bursts in the EMG of the orbicularis oculi and the velocity peaks of the conditioned eyelid response (Sanchez-Campusano et al., 2007). The specific role of the CIN remains an open question, however, and it has been suggested that its activity may be used to modulate rather than drive the eyelid movements (Delgado-Garcia and Gruart, 2002; Sanchez-Campusano et al., 2009). Future studies will aim to define the function of the CIN and understand the role that it plays in the different aspects of the control strategy for adaptive timing that we have uncovered here.

The same strategy may be used in other movements whose timing is under cerebellar control. For example, much like eyeblink conditioning (Medina et al., 2000), the execution and adaptation of saccades requires the cerebellum (Hopp and Fuchs, 2004; Catz and Thier, 2007). It is intriguing that saccade velocity trajectories are strikingly similar to the eyelid trajectories analyzed here, revealing a fixed-duration acceleration phase followed by a deceleration phase which is lengthened or shortened for longer or shorter saccade durations (Van Opstal and Van Gisbergen, 1987). Understanding why such a peculiar control strategy is utilized may provide some clues about the rules and goals governing information processing in the cerebellum.

MATERIALS AND METHODS

ANIMALS

Sixteen C57BL/6J mice (*Mus musculus*), acquired from The Jackson Laboratory, were used as subjects. Animals were kept on a 12:12-h light/dark cycle, set for 7 a.m.–7 p.m. darkness so that all experiments took place during the dark period. Mice were between the ages of 10 and 13.5 weeks before surgery and had not been used in any prior experiments. To prepare the animals to be head-fixed, mice were anesthetized with isoflurane and placed in a stereotaxic apparatus. Two screws were inserted into the surface of the skull, and a custom-cut rectangular metal head plate was cemented to the screws and skull using C&B-Metabond®. After allowing 3 + days for recovery from surgery, mice were then habituated to being placed in the experimental apparatus for 3–5 days before

training began. All procedures had been approved in advance by the *Institutional Animal Care and Use Committee* at The University of Pennsylvania and were in accordance with the *NIH Guide for the Care and Use of Laboratory Animals*.

EXPERIMENTAL APPARATUS, STIMULUS CONTROL AND DATA ACQUISITION

All our experiments were done in head-fixed mice that were placed on top of a "cylindrical treadmill" and allowed to walk on top of it. An Exervo TeraNova™EVA foam roller with a diameter of 15.24 cm (6″) was cut into approximately 12.7 cm (5″) wide slices, and a hole was drilled through the axis of the resulting cylinder, in order to mount the cylinder on a horizontal pole outfitted with ball bearings. This freely rotating cylinder was then positioned below a custom-built head-fixing device onto which the mouse's head plate could be mounted. The entire experimental apparatus was placed within a soundproof box (Med Associates, Inc.), and kept in the dark.

TDT System 3 processors were used to control the timing of stimuli, and to acquire the eyelid signal at a sampling rate of 2034.5 Hz. The unconditioned stimulus was a nitrogen air-puff (80 psi, 20 ms duration) controlled by an API MPPI-3 pressure injector, and delivered via a 27.5 gauge needle positioned ∼1 cm from the subject's left cornea. Because inherent delays in the electronics, and the time it takes for the air to travel from the pressure injector to the mouth of the needle, the air-puff hits the cornea 12–15 ms after the stimulus is triggered. All our mice were successfully conditioned even though the air-puff stimulation was relatively mild and its perceived intensity may have been reduced even further during a conditioned response, when the eyelid is partially closed and protecting the cornea. In this regard, as with all previous studies using air-puff stimulation, the learned eyelid response is likely to be the result of both classical and instrumental/operant conditioning processes. The CS was a blue LED, positioned 2–3 cm directly in front of the subject. Because the experimental box was kept dark, the blue light is a salient stimulus easily detectable by both eyes. During a conditioned response, however, the eyelids are partially closed, and in theory this could interfere with the detection and processing of the light stimulus. No attempt was made to examine this potential interference, or to investigate how the properties of the conditioned eyelid movement differ when the light is presented exclusively to the left or right eye. Nevertheless, the very high-levels of performance in all the mice (**Table 1**) indicate that if present, interference due to partially closed eyelids is minimal. Furthermore, our results examining the kinematic properties of the eyelid movement at different ISIs clearly demonstrate that light stimuli in our eyeblink conditioning task are well-suited for investigating adaptive timing of motor behavior in mice.

We used the MDMT method commercially available from www.neurasmus.com to measure movement of the left eyelid (ipsilateral to the air-puff stimulation; Koekkoek et al., 2002): before each conditioning session, mice were briefly anesthetized with isoflurane and a small neodymium magnet was attached to the left lower eyelid with cyanoacrylate ("Super Glue™"). An NVE GMR magnetometer positioned above the upper left eyelid was used to detect the movement of the magnet and obtain an electrical signal proportional to lower eyelid position. In a few experiments, we also performed high-speed video recording of eyelid movements, using an AVT GE680 monochromatic camera to monitor a 256 × 256 pixel region (approximately the smallest rectangle which completely enclosed the eye) at 350 fps. Lighting was provided by an infrared illuminator. Video capture was controlled via custom-written code in Matlab (The Mathworks, Natick, MA, USA). Small differences between video and MDMT signals were the result of a non-linearity in the NVE chip that generates exponentially bigger signals for any given eyelid displacement as the small neodymium magnet gets closer to the magnetometer.

DESIGN

Each mouse was assigned an ISI prior to training. Experiments consisted of three phases: 3 days of habituation, followed by 14–15 daily training sessions, and 7–10 daily test sessions. For each habituation session, mice were placed on top of the cylindrical treadmill with the head-fixed for 30–40 min, but no stimuli were presented. Daily conditioning sessions during the training phase consisted of 100 paired presentations of CS and US, separated by the assigned ISI. Learning proceeded gradually, and performance (as measured by percent of trials with a conditioned eyelid response) typically stabilized after 10 days of training. Training in the two mice with the lowest performance in the 400-ms ISI group was extended to 22 sessions, but no improvements were observed. During the testing phase, sessions began with 5–7 US-alone trials, used to calibrate our measurements. This was followed by 200–300 trials, half paired presentations at the same ISI used during training, and half CS-alone trials, presented in alternating order (except two mice, with 175 ms ISI, for whom this order was randomized). The inter-trial interval was set according to the following constraints: at least 10 s had to elapse, the eyelid had to be open below a predetermined threshold, and eyelid position had to be stable for at least 1 s for a trial to begin. Threshold and stability parameters were adjusted for each session by the experimenter. Experiments were performed at approximately the same time of day for each mouse.

ANALYSIS

Eyelid data was imported into Matlab and filtered in the forward and reverse direction with a fifth-order low-pass Butterworth filter and a cutoff frequency at 60 Hz. We verified that similar velocity peaks were found on the mean of the filtered and un-filtered signal, and that changing the order or cutoff frequency of our filter did not drastically alter acceleration power spectra. The signal was calibrated for each session so that the size of a full blink was 1, and eyelid position in the 100-ms preceding each trial was subtracted from that trial, resulting in all trials beginning from a position of 0. For video recording data, the area of eye exposed was calculated in each frame by thresholding the gray scale image and summing the number of pixels in the low-intensity "eye-region" of the resulting image. This signal was calibrated in the same manner as the MDMT data.

All data analysis was done on trials with a conditioned eyelid response. An eyelid movement was counted as a conditioned response if the eyelid displacement in a CS-alone trial exceeded 10% of full closure within 500 ms of light onset. Probability density functions of position and velocity maxima (**Figures 2C,D**) were generated by smoothing raw data

with a gaussian kernel, using the Matlab function *ksdensity*. Local peak detection was performed using the freely available program *peakdet* (http://billauer.co.il/peakdet.html). Peak and trough probability were computed for each sample by dividing the number of peaks or troughs found over all response trials at each sample by the total number of trials. Differences or sums of peak and trough probabilities were then smoothed with a 10-ms-wide running average. For display purposes in **Figure 3G**, the peak-trough probability difference for each mouse was standardized to a *z*-score. Spectrograms were computed using the Matlab function *spectrogram*: the acceleration signal was divided into overlapping 49.15 ms sections, with 0.98 ms increments between windows, and each section was smoothed with a hamming window. The power spectrum of each segment was then computed as the square of the absolute value of the short-time Fourier transform of each segment. For all power spectral analyses, spectra were first computed for individual trials, averaged over all trials within a mouse, then averaged across mice within condition.

ACKNOWLEDGMENTS

We are grateful to M. Moser for technical assistance, and to R. Lee, S. Martin, and J. Andrews-Labenski for help with machining and electrical design. C. De Zeeuw, H. J. Boele, and S. Koekkoek were instrumental in helping us set up the MDMT system, and S. Wang, I. Ozden, A. Giovannucci, and F. Najafi helped develop the original "floating ball" apparatus for eyeblink conditioning on which our "rotating treadmill" is based. Work supported with funds from a Searle Scholars Foundation grant to Javier F. Medina.

REFERENCES

Aiba, A., Kano, M., Chen, C., Stanton, M. E., Fox, G. D., Herrup, K., Zwingman, T. A., and Tonegawa, S. (1994). Deficient cerebellar long-term depression and impaired motor learning in mGluR1 mutant mice. *Cell* 79, 377–388.

Baker, R., McCrea, R. A., and Spencer, R. F. (1980). Synaptic organization of cat accessory abducens nucleus. *J. Neurophysiol.* 43, 771–791.

Boele, H. J., Koekkoek, S. K., and De Zeeuw, C. I. (2010). Cerebellar and extracerebellar involvement in mouse eyeblink conditioning: the ACDC model. *Front. Cell. Neurosci.* 3:19. doi:10.3389/neuro.03.019.2009

Boneau, C. A. (1958). The interstimulus interval and the latency of the conditioned eyelid response. *J. Exp. Psychol.* 56, 464–471.

Catz, N., and Thier, P. (2007). Neural control of saccadic eye movements. *Dev. Ophthalmol.* 40, 52–75.

Chen, L., Bao, S., Lockard, J. M., Kim, J. K., and Thompson, R. F. (1996). Impaired classical eyeblink conditioning in cerebellar-lesioned and Purkinje cell degeneration (pcd) mutant mice. *J. Neurosci.* 16, 2829–2838.

Delgado-Garcia, J. M., and Gruart, A. (2002). The role of interpositus nucleus in eyelid conditioned responses. *Cerebellum* 1, 289–308.

Domingo, J. A., Gruart, A., and Delgado-Garcia, J. M. (1997). Quantal organization of reflex and conditioned eyelid responses. *J. Neurophysiol.* 78, 2518–2530.

Evinger, C., Manning, K. A., and Sibony, P. A. (1991). Eyelid movements. Mechanisms and normal data. *Invest. Ophthalmol. Vis. Sci.* 32, 387–400.

Fanardjian, V. V., and Manvelyan, L. R. (1984). Peculiarities of cerebellar excitation of facial nucleus motoneurons. *Neurosci. Lett.* 49, 265–270.

Fanardjian, V. V., Manvelyan, L. R., and Kasabyan, S. A. (1983). Mechanisms regulating the activity of facial nucleus motoneurones – 1. Antidromic activation. *Neuroscience* 9, 815–822.

Fortenbaugh, D. M. (2011). The biomechanics of the baseball swing. *Open Access Dissertations* 540, 1–235.

Freeman, J. H. Jr., Nicholson, D. A., Muckler, A. S., Rabinak, C. A., and DiPietro, N. T. (2003). Ontogeny of eyeblink conditioned response timing in rats. *Behav. Neurosci.* 117, 283–291.

Gentner, D. R. (1987). Timing of skilled motor performance: tests of the proportional duration model. *Psychol. Rev.* 94, 255.

Gormezano, I., Kehoe, E. J., and Marshall, B. S. (1983). Twenty years of classical conditioning research with the rabbit. *Prog. Psychobiol. Physiol. Psychol.* 10, 197–275.

Gray, R. (2002). Behavior of college baseball players in a virtual batting task. *J. Exp. Psychol. Hum. Percept. Perform.* 28, 1131.

Grossberg, S., and Schmajuk, N. A. (1989). Neural dynamics of adaptive timing and temporal discrimination during associative learning. *Neural Netw.* 2, 79–102.

Gruart, A., Blazquez, P., and Delgado-Garcia, J. M. (1995). Kinematics of spontaneous, reflex, and conditioned eyelid movements in the alert cat. *J. Neurophysiol.* 74, 226–248.

Gruart, A., Schreurs, B. G., del Toro, E. D., and Delgado-Garcia, J. M. (2000). Kinetic and frequency-domain properties of reflex and conditioned eyelid responses in the rabbit. *J. Neurophysiol.* 83, 836–852.

Hopp, J. J., and Fuchs, A. F. (2004). The characteristics and neuronal substrate of saccadic eye movement plasticity. *Prog. Neurobiol.* 72, 27–53.

Ivarsson, M., and Svensson, P. (2000). Conditioned eyeblink response consists of two distinct components. *J. Neurophysiol.* 83, 796–807.

Jimenez-Diaz, L., Navarro-Lopez Jde, D., Gruart, A., and Delgado-Garcia, J. M. (2004). Role of cerebellar interpositus nucleus in the genesis and control of reflex and conditioned eyelid responses. *J. Neurosci.* 24, 9138–9145.

Koekkoek, S. K., Den Ouden, W. L., Perry, G., Highstein, S. M., and De Zeeuw, C. I. (2002). Monitoring kinetic and frequency-domain properties of eyelid responses in mice with magnetic distance measurement technique. *J. Neurophysiol.* 88, 2124–2133.

Koekkoek, S. K., Hulscher, H. C., Dortland, B. R., Hensbroek, R. A., Elgersma, Y., Ruigrok, T. J., and De Zeeuw, C. I. (2003). Cerebellar LTD and learning-dependent timing of conditioned eyelid responses. *Science* 301, 1736–1739.

Lepora, N. F., Mavritsaki, E., Porrill, J., Yeo, C. H., Evinger, C., and Dean, P. (2007). Evidence from retractor bulbi EMG for linearized motor control of conditioned nictitating membrane responses. *J. Neurophysiol.* 98, 2074–2088.

Lepora, N. F., Porrill, J., Yeo, C. H., Evinger, C., and Dean, P. (2009). Recruitment in retractor bulbi muscle during eyeblink conditioning: EMG analysis and common-drive model. *J. Neurophysiol.* 102, 2498–2513.

Levey, A. B., and Martin, I. (1968). Shape of the conditioned eyelid response. *Psychol. Rev.* 75, 398–408.

Marquis, D., and Porter, Jr. J. (1939). Differential characteristics of conditioned eyelid responses established in reflex and voluntary reinforcement. *J. Exp. Psychol.* 24, 347–365.

Mauk, M. D., and Ruiz, B. P. (1992). Learning-dependent timing of Pavlovian eyelid responses: differential conditioning using multiple interstimulus intervals. *Behav. Neurosci.* 106, 666–681.

Mavritsaki, E., Lepora, N., Porrill, J., Yeo, C. H., and Dean, P. (2007). Response linearity determined by recruitment strategy in detailed model of nictitating membrane control. *Biol. Cybern.* 96, 39–57.

McCormick, D. A., and Thompson, R. F. (1984). Cerebellum: essential involvement in the classically conditioned eyelid response. *Science* 223, 296–299.

Medina, J. F., Nores, W. L., Ohyama, T., and Mauk, M. D. (2000). Mechanisms of cerebellar learning suggested by eyelid conditioning. *Curr. Opin. Neurobiol.* 10, 717–724.

Morcuende, S., Delgado-Garcia, J. M., and Ugolini, G. (2002). Neuronal premotor networks involved in eyelid responses: retrograde transneuronal tracing with rabies virus from the orbicularis oculi muscle in the rat. *J. Neurosci.* 22, 8808–8818.

Sakamoto, T., and Endo, S. (2011). Amygdala, deep cerebellar nuclei and red nucleus contribute to delay eyeblink conditioning in C57BL/6 mice. *Eur. J. Neurosci.* 32, 1537–1551.

Sanchez-Campusano, R., Gruart, A., and Delgado-Garcia, J. M. (2007). The cerebellar interpositus nucleus and the dynamic control of learned motor responses. *J. Neurosci.* 27, 6620–6632.

Sanchez-Campusano, R., Gruart, A., and Delgado-Garcia, J. M. (2009). Dynamic associations in the cerebellar-motoneuron network during motor learning. *J. Neurosci.* 29, 10750–10763.

Schmidt, R. A., and Lee, T. D. (2005). *Motor Control and Learning: A Behavioral Emphasis.* Champaign, IL: Human Kinetics.

Trigo, J. A., Gruart, A., and Delgado-Garcia, J. M. (1999). Discharge profiles of abducens, accessory abducens, and orbicularis oculi motoneurons during reflex and conditioned blinks in alert cats. *J. Neurophysiol.* 81, 1666–1684.

Van Der Giessen, R. S., Koekkoek, S. K., van Dorp, S., De Gruijl, J. R., Cupido, A., Khosrovani, S., Dortland, B., Wellershaus, K., Degen, J., Deuchars, J., Fuchs, E. C., Monyer, H., Willecke, K., De Jeu, M. T., and De Zeeuw, C. I. (2008). Role of olivary electrical coupling in cerebellar motor learning. *Neuron* 58, 599–612.

Van Opstal, A. J., and Van Gisbergen, J. A. (1987). Skewness of saccadic velocity profiles: a unifying parameter for normal and slow saccades. *Vision Res.* 27, 731–745.

Vogel, R. W., Ewers, M., Ross, C., Gould, T. J., and Woodruff-Pak, D. S. (2002). Age-related impairment in the 250-millisecond delay eyeblink classical conditioning procedure in C57BL/6 mice. *Learn. Mem.* 9, 321–336.

Williams, T., and Underwood, J. (1986). *The Science of Hitting.* New York: Simon and Schuster.

Conflict of Interest Statement: The authors declare that the research was conducted in the absence of any commercial or financial relationships that could be construed as a potential conflict of interest.

Received: 13 July 2011; accepted: 11 October 2011; published online: 30 November 2011.

Citation: Chettih SN, McDougle SD, Ruffolo LI and Medina JF (2011) Adaptive timing of motor output in the mouse: the role of movement oscillations in eyelid conditioning. Front. Integr. Neurosci. 5:72. doi: 10.3389/fnint.2011.00072

frontiers in
INTEGRATIVE NEUROSCIENCE

REVIEW ARTICLE
published: 03 October 2011
doi: 10.3389/fnint.2011.00053

Anatomical pathways involved in generating and sensing rhythmic whisker movements

Laurens W. J. Bosman[1,2], Arthur R. Houweling[1], Cullen B. Owens[1], Nouk Tanke[1], Olesya T. Shevchouk[1], Negah Rahmati[1], Wouter H. T. Teunissen[1], Chiheng Ju[1], Wei Gong[1], Sebastiaan K. E. Koekkoek[1] and Chris I. De Zeeuw[1,2]*

[1] Department of Neuroscience, Erasmus MC, Rotterdam, Netherlands
[2] Netherlands Institute for Neuroscience, Royal Academy of Arts and Sciences, Amsterdam, Netherlands

Edited by:
Agnes Gruart, University Pablo de Olavide Seville, Spain

Reviewed by:
Michael Brecht, Humboldt University Berlin, Germany
Josè M. Delgado-García, University Pablo de Olavide Seville, Spain

***Correspondence:**
Chris I. De Zeeuw, Department of Neuroscience, Erasmus MC, PO Box 2040, 3000 CA Rotterdam, Netherlands.
e-mail: c.dezeeuw@erasmusmc.nl

The rodent whisker system is widely used as a model system for investigating sensorimotor integration, neural mechanisms of complex cognitive tasks, neural development, and robotics. The whisker pathways to the barrel cortex have received considerable attention. However, many subcortical structures are paramount to the whisker system. They contribute to important processes, like filtering out salient features, integration with other senses, and adaptation of the whisker system to the general behavioral state of the animal. We present here an overview of the brain regions and their connections involved in the whisker system. We do not only describe the anatomy and functional roles of the cerebral cortex, but also those of subcortical structures like the striatum, superior colliculus, cerebellum, pontomedullary reticular formation, zona incerta, and anterior pretectal nucleus as well as those of level setting systems like the cholinergic, histaminergic, serotonergic, and noradrenergic pathways. We conclude by discussing how these brain regions may affect each other and how they together may control the precise timing of whisker movements and coordinate whisker perception.

Keywords: vibrissa, follicle–sinus complex, barrel cortex, basal ganglia, cerebellum, sensorimotor integration, rhythmic movements, anatomy

INTRODUCTION

Rodents have highly mobile whiskers, with which they can rapidly locate and discriminate objects in their environment. The rodent whisker system has become a popular model system for brain development, experience-dependent plasticity, perceptual learning, repetitive, timed motor responses, sensorimotor integration, and robotics. Of the many brain regions involved in the whisker system, the trigeminal brainstem, thalamus and primary somatosensory cortex (S1), and to a lesser extent the whisker motor cortex (wM1), have attracted most attention (for reviews see Kleinfeld et al., 1999; Deschênes et al., 2005; Brecht, 2007; Petersen, 2007; Alloway, 2008; Diamond et al., 2008). Other brain regions and the structures of the whisker pad itself have received less attention. Here we aim to integrate the current knowledge on subcortical structures into the well-known whisker pathways, thus presenting an overview of the most important structures of the whisker system and their interconnections as a whole. In addition, we discuss how these structures may cooperate to generate and sense whisker movements.

Tactile hairs are specialized hairs that, due to the presence of sensitive mechanoreceptors at their follicles, provide accurate somatosensory input. Tactile hairs which grow from a follicle–sinus complex (FSC) are called "vibrissae" or "whiskers." Almost all mammals, except humans and egg-laying mammals (monotremes), have vibrissae (Chernova, 2006; Muchlinski, 2010). Vibrissae can grow from all body parts, but are mainly located on the face (Sarko et al., 2011). Most likely, all vibrissae can be moved, but there is a large variability in movement mechanics. Some vibrissae, like the genal vibrissae in the hamster, lack musculature and are moved solely by vascular and connective tissue dynamics (Wineski, 1985). Other vibrissae can be moved by muscles involved in the erection of hairs (m. arrector pili; Hyvärinen et al., 2009), while mystacial vibrissae can be moved by a group of specialized muscles (Brecht et al., 1997; Haidarliu et al., 2010; Sarko et al., 2011). In some species, including shrews (Munz et al., 2010) and rodents such as rats, mice, gerbils, hamsters, chinchillas, and porcupines (Woolsey et al., 1975), the mystacial vibrissae can move fast and rhythmically (**Figure 1A**). This behavior is called "whisking," and in accordance we reserve the term "whiskers" here for those vibrissae that can be whisked. Whisking behavior is absent in most species, including well-studied species like rabbits, cats, and seals (Woolsey et al., 1975; Dehnhardt and Kaminski, 1995). The main function of vibrissae is to complement or replace near-vision (Welker, 1964; Gogan et al., 1981; Ahl, 1986). In addition, marine mammals use their vibrissae for long-distance sensing. For instance, a seal may "feel" prey fish at more than 180 m distance (Dehnhardt et al., 2001). Vibrissae also help to locate, identify, and capture prey (Anjum et al., 2006; Munz et al., 2010; Favaro et al., 2011). In addition, vibrissae inform about body posture, especially in water (Ahl, 1982), and play a central role in social behavior (Miller, 1975; Blanchard et al., 1977).

Well-timed, rhythmic whisker movements are instrumental in exploring the environment (Carvell and Simons, 1990; Grant et al., 2009; Hartmann, 2011). When doing so, rats make large whisker

movements at a relatively low frequency (5–15 Hz). Once their interest has been caught, they can thrust their whiskers forward and make smaller movements at higher frequencies (15–25 Hz) to identify objects and textures (Carvell and Simons, 1995; Harvey et al., 2001; Berg and Kleinfeld, 2003a). Small variations in surface texture may halt the whisker tip for a short while, after which it slips past the fine obstruction (**Figure 1B**; Neimark et al., 2003; Ritt et al., 2008; Wolfe et al., 2008). Such "slip-stick" movements can trigger stereotypical neuronal responses allowing the animal to sense subtle features of surfaces (**Figure 1C**; Jadhav et al., 2009). The combination of rhythmic movements and precisely timed sensory input thus greatly increases the acuity of whisker input.

WHISKERS

THE WHISKER PAD

The organization of the whiskers on the mystacial pad varies greatly between different species, but is relatively similar between rats and mice (Woolsey et al., 1975; Brecht et al., 1997). Rats and mice have five rows of whiskers. The upper two rows (A–B) have four whiskers each, while the lower three rows (C–E) each contain about seven whiskers. In addition, there are four particularly large whiskers ("straddlers"), labeled α–δ, at the caudal edge of the mystacial pad (**Figure 2A**). The muscles of the mystacial pad are divided into extrinsic and intrinsic muscles, all of which are innervated by specific branches of the facial nerve (**Figure 2A**; Dörfl, 1985). The intrinsic muscles are completely situated within the mystacial pad, while the extrinsic muscles have their origins outside the mystacial region (Dörfl, 1982; Jin et al., 2004; Haidarliu et al., 2010). During a normal, exploratory whisking cycle, the whiskers first protract and then retract. Whisker protraction is initiated by contraction of the medial inferior and medial superior parts of the extrinsic muscle m. nasolabialis profundus and completed by contraction of the intrinsic capsular muscles. Subsequent whisker retraction is under control of two extrinsic muscles, the m. nasolabialis and the m. maxillolabialis (**Figures 2A,B**; Berg and Kleinfeld, 2003a; Hill et al., 2008; Simony et al., 2010). Whisker retraction during foveal whisking is a relatively passive process, involving virtually no muscle activity; during foveal whisking the vibrissae are thrust forward and palpate objects with low-amplitude movements at high frequency (Berg and Kleinfeld, 2003a). Rodents can also move the whole mystacial pad. Pad movements may contribute to the normal whisking cycle (Bermejo et al., 2005), but can also involve rotation or resizing of the whisker pad to optimize object contact (Haidarliu et al., 2010; Towal et al., 2011). For instance, contraction of m. nasolabialis superficialis moves the A and B rows dorsally, and contraction of m. buccinatorius pars orbicularis oris moves the C–E rows ventrally, thereby adjusting the mystacial field size (Haidarliu et al., 2010). Although the general structure of the mystacial pad is similar in mice (Dörfl, 1982), hamsters (Wineski, 1985), and rats (Haidarliu et al., 2010), minor differences between species do occur, mainly in the organization of the m. nasolabialis profundus (cf Haidarliu et al., 2010).

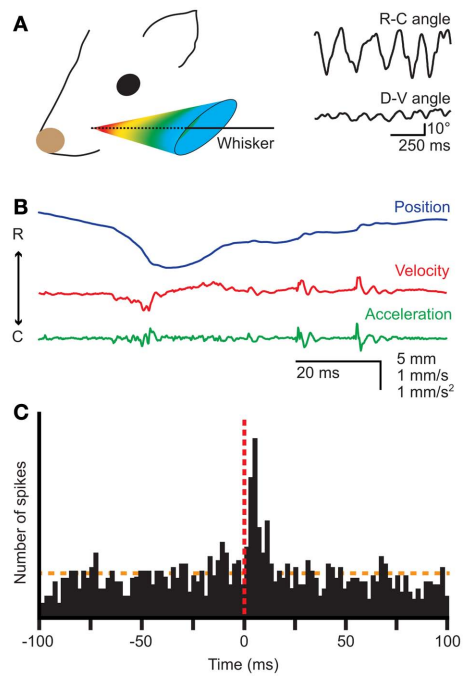

FIGURE 1 | Whisker movements. (A) Whiskers move rhythmically back-and-forth during exploratory whisking in the rat. The deflection along the rostro-caudal axis is much larger than that on the dorso-ventral axis. The left panel is a schematic drawing of the space in which a whisker can be moved, based on Bermejo et al. (2002). The right panels are reproduced with permission from Hill et al. (2008). **(B)** Position, velocity, and acceleration of a rat D3 whisker during one whisking cycle on P150 sandpaper. Irregularities in the sandpaper surface cause "slip-stick" movements. Reproduced with permission from Wolfe et al. (2008). **(C)** Slips can trigger neuronal responses in rat wS1, as shown by a peri-stimulus time histogram of the spike times of a single neuron aligned on the first slips of whisker movements. Reproduced with permission from Jadhav et al. (2009).

FOLLICLE–SINUS COMPLEXES

Vibrissae differ from other (pelagic) hairs in that each of their (epidermal) follicles is surrounded by a (dermal) blood sinus, which in most species is composed of a distal ring sinus and a proximal cavernous sinus (**Figures 2B,C**; Szymonowicz, 1895; Ebara et al., 2002; Kim et al., 2011). It has been suggested that animals can modulate the dynamic range of the vibrissal mechanoreceptors by changing the blood pressure in the blood sinus (Vincent, 1913; Nilsson, 1969; Gottschaldt et al., 1973). In addition, the size of the FSC seems to be adapted for the behavior and environment of the animals. In general, the largest FSCs are found in marine mammals, intermediate FSCs in semi-aquatic species, like otters and water rats, and the smallest FSCs in purely terrestrial mammals (Dehnhardt et al., 1999; Hyvärinen et al., 2009). Larger FSCs make the vibrissal movements more resistant to water, which has a much higher density than air, and allows better thermal insulation of mechanoreceptors to cold or warm water (Dehnhardt et al., 1998, 1999). The larger size of the FSCs of marine mammals is due to the presence of a second, external cavernous sinus (**Figure 2C**; Sarko et al., 2007; Hyvärinen et al., 2009). In species where the vibrissal system is relatively unimportant, such as marsupials and primates, the FSCs lack a ring sinus (Van Horn, 1970; Hollis and Lyne, 1974; Marotte et al., 1992). Thus, the adaptations in the FSC-anatomy are in line with specific behavioral requirements.

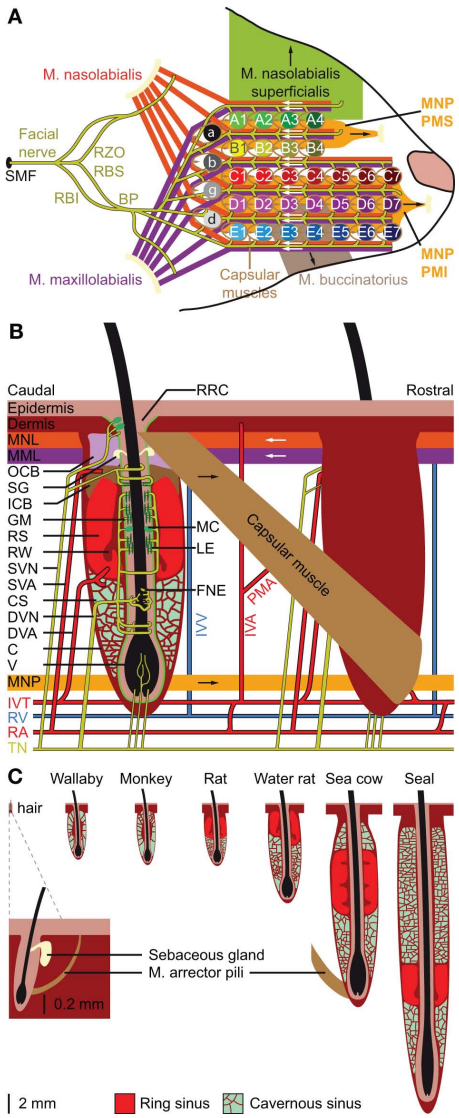

FIGURE 2 | Location and structure of the whiskers. (A) The whiskers are organized in rows on the mystacial pad. Mice and rats have five rows of whiskers, as well as four "straddlers" caudal to these rows. Each whisker is associated with an intrinsic capsular muscle [see also **(B)**]. Extrinsic muscles connect to multiple whiskers. The m. nasolabialis profundis (MNP) consists of two parts, the mediosuperior (PMS) and the medioinferior (PMI) parts, both of which are involved in whisker protraction. The m. nasolabialis and m. maxillolabialis are involved in whisker retraction. The other extrinsic whiskers, including the m. nasolabialis superficialis and the m. buccinatorius, are involved in resizing the entire mystacial pad. The mystacial muscles are almost exclusively innervated by the facial nerve, which leaves the skull via the stylomastoid foramen (SMF). After leaving the SMF, the facial nerve splits up in two streams. The lower stream consists of the rami buccolabialis superior (RBS) and inferior (RBI), which anastomose in the buccal plexus (BP). From the BP all extrinsic and intrinsic whisker muscles are innervated, with the exception of m. nasolabialis, which is innervated by the upper stream, which includes the ramus zygomatico-orbitalis (RZO). **(B)** Schematic drawing of the follicle–sinus complex (FSC) of the rat. The vibrissa (V) lies within a follicle that is derived from the epidermis and that is surrounded by the glassy membrane (GM). Around the follicle is a blood sinus derived from the dermis, and which is composed of two sinuses: the cavernous sinus (CS), which has numerous collagenous trabeculae, and the ring sinus (RS), which is an open structure. At the bottom of the ring sinus, there is an asymmetric structure of connective tissue: the ringwulst (RW). At the distal end of the ring sinus, the inner conical body (ICB) links the follicle strongly to the capsule (C). Distal to the ICB is the outer conical body (OCB) that contains the sebaceous gland (SG). Intrinsic capsular muscles connect pairs of FSCs. Extrinsic muscles are located just below the skin (m. nasolabialis, MNL and m. maxillolabialis, MML), or at the lower end of the FSC (m. nasolabialis profundus, MNP). The arrows indicate whether contraction of the muscle causes pro- or retraction of the vibrissae. The vibrissae are surrounded by three different types of mechanoreceptors: Merkel cells (MC), lanceolate endings (LE), and free nerve endings (FNE). Mechanoreceptors in the upper part of the FSC are innervated by superficial vibrissal nerves (SVN) and those in the lower part by the deep vibrissal nerve (DVN). In addition, there are some small-caliber fibers at the bottom. The sensory fibers come together with fibers from other parts of the face to form the infraorbital branch of the trigeminal nerve (TN). Blood supply to the FSCs is organized via row arteries (RA) located between the whisker rows, with superficial vibrissal arteries (SVA) supplying the upper parts and deep vibrissal arteries (DVA) the lower parts of the FSCs. The DVA does not directly branch from a RA, but from the anastomozing intervibrissal trunks (IVT). In between the FSCs are intervibrissal arteries (IVA) that supply the skin and hair follicles. The capsular muscles receive their blood from arterioles (PMA) branching from the IVA and directly from the IVT. Venal drainage is organized by intervibrissal veins (IVV) that empty in row veins (RV). **(C)** Schematic drawings of the follicle of a typical mammalian body hair (left) and of the structure of the blood sinuses of FSCs in different species. A hair follicle lacks a blood sinus and can be moved by contraction of the m. arrector pili. In marsupials and primates, the blood sinus is composed of a single compartment (the cavernous sinus), as illustrated for the tammar wallaby (*Macropus eugenii*; Marotte et al., 1992) and the rhesus monkey (Van Horn, 1970). Most species, however, have two sinuses: the ring sinus and the cavernous sinus, as illustrated for the rat (*Rattus sp.*; Ebara et al., 2002) and the Australian water rat (*Hydromys chrysogaster*; Dehnhardt et al., 1999). Pinnipeds have tricompartite blood sinuses, including an outer cavernous sinus, as illustrated for a sea cow, the Florida manatee (*Trichechus manatus latirostris*; Reep et al., 2001), and the ringed seal (*Phoca hispida*; Hyvärinen et al., 2009). Non-whisking species can generally move their vibrissae using m. arrector pili muscles, as indicated for the FSC of the sea cow.

Cavernous sinuses contain trabeculae of connective tissue, with the spaces in between filled with blood and nerve fibers (Rice, 1993; Hyvärinen et al., 2009; Kim et al., 2011). The ring sinus is an open structure, lacking trabeculae. At the bottom of the ring sinus, most species have an asymmetric, collagenous appendix: the ringwulst. Most likely, the rigid ringwulst transmits vibrations to the soft ring sinus with which it is associated (Stephens et al., 1973), while the ring sinus probably acts to dampen these vibrations (Yohro, 1977). This would imply that the anatomy of the blood sinus, including that of the ringwulst, determines the sensitivity range, which can be fine-tuned by modulating the pressure of the blood sinus. In conclusion, specific adaptations to environmental conditions and behavioral requirements, may have led to variations in the anatomy of the FSC. Such diversity can also be observed between FSCs at various body regions of a single animal. In the Florida manatee, for instance, the facial FSCs are substantially larger and more complex than those at other body regions (Sarko et al., 2007), consistent with the prominent role of facial vibrissae during feeding (Reep et al., 2001).

TRANSDUCTION OF SENSORY INPUT

TRIGEMINAL NERVE

Mechanoreceptors

Vibrissal vibrations are detected by several types of mechanoreceptors with different functional properties. Each FSC is innervated by several small superficial vibrissal nerves (SVN), a single, large deep vibrissal nerve (DVN) containing 100–200 fibers (Rice et al., 1986), as well as a number of unmyelinated fibers at the base of the FSC (**Figure 2B**). The SVN and the DVN contain mainly Aβ and Aδ fibers. Thickly myelinated Aβ fibers have Merkel cell endings, which are slowly adapting (SA) mechanoreceptors, or lanceolate endings, which are rapidly adapting (RA). Hence, Merkel cell endings will primarily signal ongoing movements, while lanceolate endings will predominantly detect unexpected movements (Gottschaldt et al., 1973; Halata et al., 2010; Lumpkin et al., 2010). Merkel cells are located within the epidermis at two regions: at the rete ridge collar and at the level of the ring sinus (Ebara et al., 2002). Remarkably, in the mystacial FSCs of rats, the Merkel cells at the rete ridge collar are almost exclusively found at the caudal site of the FSC, implying that they predominantly transmit backward deflections (Fundin et al., 1994; Ebara et al., 2002). Circumferentially oriented lanceolate endings are mainly located at the level of the inner conical body, while longitudinally oriented lanceolate endings are mostly restricted to the level of the ring sinus (Ebara et al., 2002). The thinly myelinated Aδ fibers supply a highly heterogeneous group of other endings, including spindle-like, club-like, reticular, spiny, and encapsulated endings. These endings are dispersed through the epidermal sheet of the FSC, but enriched at the level of the cavernous sinus (Ebara et al., 2002; Sarko et al., 2007). The specific functions of these mechanoreceptors are presently unclear. At the base of the FSC are unmyelinated C fibers (Ebara et al., 2002). Since C fibers predominantly conduct nociceptive stimuli, they could signal pulling of the vibrissae.

Trigeminal ganglion

The cell bodies of the trigeminal nerve fibers are located either in the trigeminal ganglion or in the mesencephalic nucleus (see Trigeminal Mesencephalic Nucleus). As a rule, each neuron in the trigeminal ganglion receives input only from a single vibrissa (Kerr and Lysak, 1964; Zucker and Welker, 1969; Lichtenstein et al., 1990). However, neurons receiving input from very small vibrissae may be connected to two or three individual vibrissae (Kerr and Lysak, 1964). In addition, very large deflections of a single vibrissa can cause deformation of the skin, and in that way also activate mechanoreceptors of adjacent FSCs (Simons, 1985). The receptive fields of the trigeminal ganglion are loosely arranged in a somatotopic fashion, with the caudal part of the face projecting to the dorsal part of the ganglion, and the rostral part of the face to the ventral part of the ganglion. The whisker projections follow this general pattern (Erzurumlu and Killackey, 1983; Leiser and Moxon, 2006). Originally, it was reported that dorsal vibrissae are represented medially and ventral vibrissae laterally within the trigeminal ganglion (Zucker and Welker, 1969), but Leiser and Moxon (2006) could not reproduce this medio-lateral patterning.

During rest, when the vibrissae are neither moving nor being touched, the neurons of the trigeminal ganglion are silent (Gibson and Welker, 1983; Lichtenstein et al., 1990; Leiser and Moxon, 2007). Based on their response pattern to vibrissal movement, the majority of trigeminal ganglion neurons are classified as SA, while the others are RA (Fitzgerald, 1940; Kerr and Lysak, 1964; Lichtenstein et al., 1990; Leiser and Moxon, 2007). During whisking in air, SA neurons fire about three times as often as RA neurons (Leiser and Moxon, 2007). Upon touching an object, both SA and RA neurons increase their firing rate. Both types of neurons reach similar firing rates upon whisker touching (Jones et al., 2004; Leiser and Moxon, 2007). Overall, trigeminal ganglion neurons have a broad range of activation thresholds that vary mainly in amplitude and speed, but also in direction of whisker movement (Arabzadeh et al., 2005; Leiser and Moxon, 2007; Khatri et al., 2009; Gerdjikov et al., 2010). Most trigeminal ganglion neurons receive whisker sensory input via the DVN rather than the SVN, but the information content of both types of fibers seems to be very similar (Waite and Jacquin, 1992).

Trigeminal mesencephalic nucleus

A subset of trigeminal nerve fibers does not have their somata in the trigeminal ganglion, but in the trigeminal mesencephalic nucleus (MeV). Thus, MeV houses primary sensory neurons within the CNS, which makes it a unique structure. MeV neurons mainly innervate muscle spindles in the masticatory and extraocular muscles and are thus involved in proprioception. In addition, several other types of receptors in the dental, oral, and peri-oral domain are innervated by MeV neurons (Lazarov, 2002). Although whisker muscles lack spindles, MeV contains neurons that innervate the mystacial pad and that respond to spontaneous whisker movements (Mameli et al., 2010). MeV projects to, among others, the dorsomedial part of the principal trigeminal nucleus, the pontomedullary reticular formation (RF), and the superior colliculus (SC; Matesz, 1981; Ndiaye et al., 2000).

SENSORY TRIGEMINAL NUCLEI

The sensory trigeminal nuclei form the main entrance to the brain for whisker input. The principal trigeminal nucleus (PrV) lies anterior to the spinal trigeminal nucleus (SpV), which consists of an oral (SpVo), an interpolar (SpVi), and a caudal part (SpVc; **Figure 3A**). Afferent fibers of the trigeminal root bifurcate to form a rostral branch ascending to PrV and a caudal branch descending to SpV (Hayashi, 1980). Of the individual fibers, some target only PrV or SpV, while others bifurcate and innervate both. Afferents to SpV can terminate in all three subregions (Hayashi, 1980). All compartments, except SpVo and the rostral part of SpVi, have barrelettes, discrete groups of neurons that receive input from the same vibrissa and that can be visualized by cytochrome oxidase staining (**Figure 3B**; Belford and Killackey, 1979; Ma, 1991; Li et al., 1994; Erzurumlu et al., 2010). Neurons in the barrelettes are relatively small and their dendritic trees are confined within the borders of the barrelette (Veinante and Deschênes, 1999). Roughly one-third of the neurons dedicated to whisker input are located between the barrelettes. These interbarrelette cells have widespread dendritic trees and receive input from multiple vibrissae, mainly located within a single row on the mystacial pad (Veinante and Deschênes, 1999). The barrelettes are organized according to an inverted somatotopy, with dorsal whiskers having a ventral representation and rostral whiskers a medial one (Ma, 1991; Erzurumlu

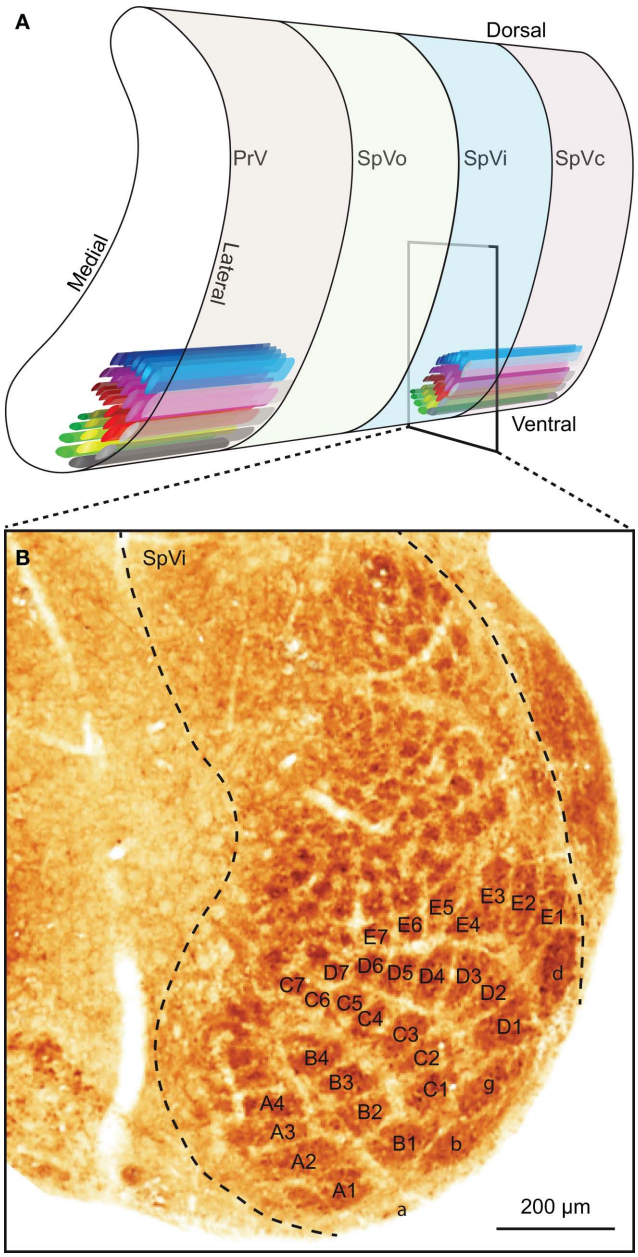

FIGURE 3 | The trigeminal nuclei. (A) The sensory trigeminal nuclei consist of two nuclei, oriented along the antero-posterior axis. The principal nucleus (PrV) is located at the anterior end and the spinal nucleus (SpV) at the posterior site. The SpV can be subdivided into an oral (SpVo), interpolar (SpVi), and caudal part (SpVc). The facial vibrissae project to the ventral part of the trigeminal nuclei. In PrV, SpVc, and the caudal part of SpVi, each vibrissa has its own projection field: a barrelette. The orientation of the barrelettes of the facial macro-vibrissae is indicated schematically. **(B)** Coronal section of a neonatal mouse brain, showing the location of the barrelettes of the facial macro-vibrissae in the ventral part of SpVi. Following cytochrome oxidase staining, barrelettes appear as dark patches. Note the inverted somatotopy: dorsal vibrissae project to ventral barrelettes. The smaller patches dorsal to the barrelettes of the E-row are the receptive fields of the facial micro-vibrissae. The photomicrograph was kindly provided by Dr. R. S. Erzurumlu.

et al., 2010). In addition to the large barrelettes representing the whiskers, smaller barrelettes can be seen that mainly represent the facial micro-vibrissae (**Figure 3B**). We will restrict ourselves to the description of the neuronal circuitry of the whiskers, rather than that of the other vibrissae.

In PrV, output neurons can be found both within and between barrelettes (Veinante and Deschênes, 1999). In SpVi, however, single-whisker neurons project mainly within the trigeminal nuclei, while multi-whisker neurons project to other brain regions (Woolston et al., 1983; Jacquin et al., 1989a,b). The small single-whisker neurons of SpVi are part of an extensive, inter-trigeminal network. GABAergic and glycinergic neurons of SpVc project to SpVi, and GABAergic and glycinergic neurons of SpVi project to PrV (Furuta et al., 2008). In addition, glutamatergic interneurons of SpVc project to both SpVi and PrV (Furuta et al., 2008). In this way, SpV can modulate the sensitivity of PrV to whisker inputs (Timofeeva et al., 2005; Furuta et al., 2008; Lee et al., 2008a). This SpV-mediated modulation of PrV in turn is subject to modulation by the somatosensory cortex (Furuta et al., 2010). This allows for central control of the whisker sensitivity. Most likely, this pathway is being used during active whisking, when the whisker-induced output of PrV is suppressed (Lee et al., 2008a). Since there is no strong, direct pathway from wM1 to SpV, this effect is most likely mediated by the whisker area of S1 (wS1). Thus, activity in wM1 activates wS1, which in turn activates the inhibitory projection from SpVi to PrV, reducing the output of PrV (Lee et al., 2008a). This could help the trigeminal nuclei to filter out irrelevant inputs, which may be particularly prominent during movement. Another way to reduce irrelevant input is selective adaptation. PrV responses triggered by weak sensory inputs rapidly desensitize, but are relatively unaffected by repeated strong inputs (Ganmor et al., 2010). Finally, the activity of the sensory trigeminal nuclei can be modulated by several inputs that mainly reflect the general state of alertness, including a cholinergic projection from the pedunculopontine tegmental nuclei (PPTg; Timofeeva et al., 2005; Beak et al., 2010), a serotonergic projection from the raphe nuclei (Lee et al., 2008c) and a noradrenergic projection from the locus coeruleus (Moore and Bloom, 1979). Taken together, the level of detail of the sensory information forwarded to the rest of the brain by the trigeminal nuclei depends on the behavioral state of the animal.

Apart from the contralateral projections to the thalamus described in detail below, there are also contralateral projections from the trigeminal nuclei to the pontine nuclei (see The Pontine Nucleus and the Nucleus Reticularis Tegmenti Pontis), the inferior olive (IO; see Cerebellum and Inferior Olive), the SC (see Superior Colliculus), and the zona incerta (ZI; see Zona Incerta). In addition, there are predominantly ipsilateral connections to the cerebellum (see Cerebellum and Inferior Olive), the pontomedullary RF (see Pontomedullary Reticular Formation), and the lateral facial nucleus. The trigemino-facial connections originate from all four subnuclei, but mainly from SpVc (Erzurumlu and Killackey, 1979; Pinganaud et al., 1999; Hattox et al., 2002). Since the lateral facial nucleus houses whisker motor neurons (Klein and Rhoades, 1985; Herfst and Brecht, 2008), this connection forms a direct feedback loop (Nguyen and Kleinfeld, 2005). It has been suggested that SpV also receives motor input from wS1,

the information of which might be forwarded to the lateral facial nucleus via the direct connection (Matyas et al., 2010).

THALAMUS AND TRIGEMINO-THALAMO-CORTICAL PATHWAYS

The thalamus is the main gateway to the cerebral cortex. It is composed of several nuclei, two of which are critically involved in the transmission of whisker stimuli to wS1: the ventral posterior medial nucleus (VPM) and the medial posterior nucleus (Pom). There are at least six pathways conveying whisker input from the trigeminal nuclei to the cerebral cortex (**Figure 4E**). To some extent, these pathways convey different aspects of whisker sensation (Yu et al., 2006). The pathways that make synapses in VPM convey whisker input with short latencies, while those via Pom have considerably longer latencies. VPM receives both single- and multiple-whisker input, Pom only multi-whisker input. An anatomical difference between VPM and Pom is that VPM, in contrast to Pom, contains barreloids, analogous to the barrelettes in the trigeminal nuclei, and the barrels in wS1. The barreloids are prominent in the dorsomedial part of VPM (VPMdm), but fade away toward the ventrolateral part (VPMvl; Van der Loos, 1976; Land et al., 1995; Haidarliu and Ahissar, 2001). As a consequence, VPMdm processes mainly single-whisker input and

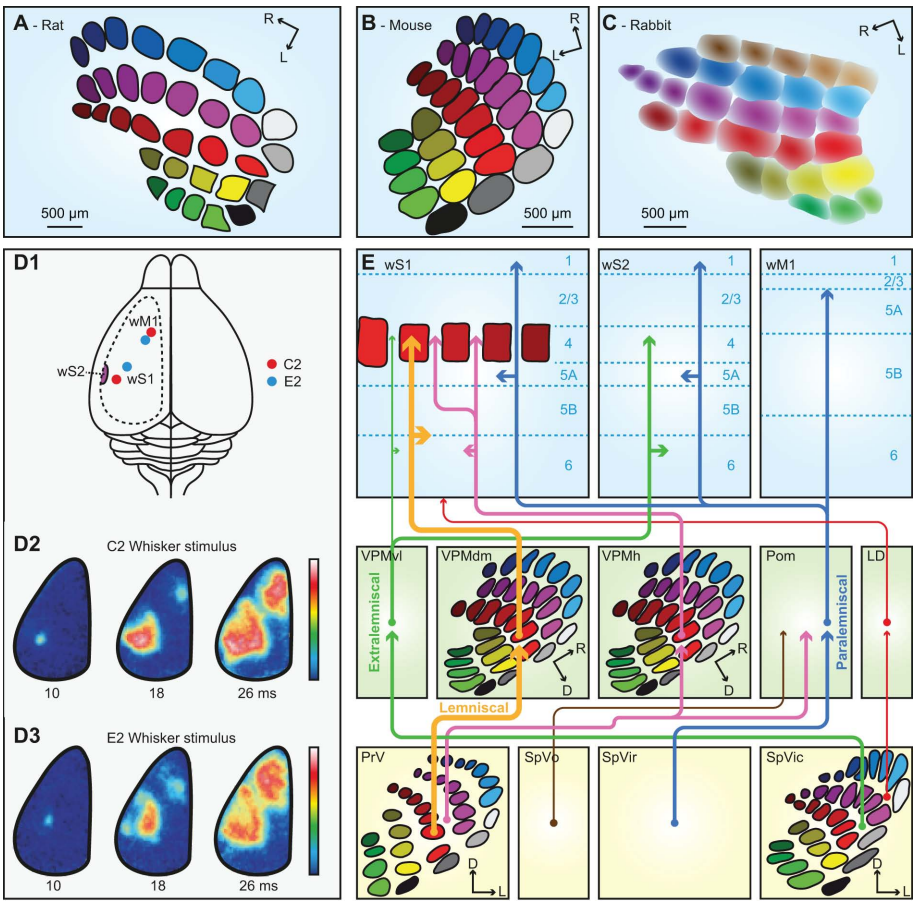

FIGURE 4 | The trigemino-thalamo-cortical pathways. Schematic drawing of the organization of the barrels in layer 4 of a tangential slice of an adult rat **(A)**, mouse **(B)**, and rabbit **(C)**. Note that the septa are prominent in rats but very small in mice. In adult rabbits, barrels are absent. Instead, the somatotopic representation of the vibrissae is more gradual. **(D1)** Schematic drawing of a rat brain. The dotted line indicates the recording area for the panels **(D2,D3)**. The red dots indicate the representations of the C2 whisker, and the blue dots those of the E2 whisker in wS1 and wM1. wS2 is partially visible on the extreme left of the recording area. **(D2)** Voltage-sensitive dye images in urethane-anesthetized mice showing that stimulation of the contralateral C2 whisker initially evokes a very local signal in the C2 barrel of wS1. Consecutively, the signal spreads over the rest of wS1, and also to wM1, and to a lesser extent also to wS2. The time points indicate the time since the onset of whisker deflection, the scale bar the fluorescent signal (blue = weak, white = high). **(D3)** Idem, but for the E2 whisker. Note that the early responses to the C2 and E2 whiskers are at different locations, but this difference is less obvious during later phases of the response. Panel D is reproduced with permission from Aronoff et al. (2010). **(E)** Schematic representation of the trigemino-thalamo-cortical pathways discussed in the main text. The arrowheads indicate the termination areas of the axons. Note that (in the cerebral cortex) the postsynaptic cells may have their somata in other layers. The line thickness indicates the relative importance of the pathways. The barreloids in VPM are indicated in an oblique coronal slice, the barrelettes of the trigeminal nuclei in coronal slices. D = dorsal; L, lateral; LD, laterodorsal nucleus of the thalamus; Pom, medial posterior nucleus of the thalamus; PrV, primary trigeminal nucleus; R, rostral; SpVic, caudal part of spinal trigeminal nucleus pars interpolaris; SpVio, oral part of SpVi; SpVo, spinal trigeminal nucleus pars oralis; VPMdm, dorsomedial part of the ventroposterior medial nucleus of the thalamus; VPMh, "head" area of VPM; VPMvl, ventrolateral part of VPM; wM1, whisker motor cortex; wS1, whisker part of primary sensorimotor cortex; wS2, whisker part of secondary sensorimotor cortex.

VPMvl multi-whisker input. Within a barreloid, the neurons are ordered according to their angular preference (Timofeeva et al., 2003).

Of all trigemino-thalamo-cortical pathways, the lemniscal pathway is the only one that predominantly conveys single-whisker input. This disynaptic pathway links the barrelettes of PrV to the barrels of wS1 via the barreloids of VPMdm (Erzurumlu et al., 1980; Williams et al., 1994; Veinante and Deschênes, 1999). The main targets are the barrels of layer 4 in wS1, but there are also terminals in layers 5/6 of wS1 (Killackey, 1973; Koralek et al., 1988; Chmielowska et al., 1989; Lu and Lin, 1993; Bureau et al., 2006; Petreanu et al., 2009; Meyer et al., 2010a). The thalamic relay cells in the barreloids of VPMdm respond with precisely timed single action potentials to deflections of a single principle whisker at short latencies (4–8 ms; Ito, 1988; Simons and Carvell, 1989; Armstrong-James and Callahan, 1991; Diamond et al., 1992b; Brecht and Sakmann, 2002b).

A second pathway synapsing in VPM is the extralemniscal pathway. In contrast to the lemniscal pathway, the extralemniscal pathway passes through VPMvl, where the barreloids are not as distinct as in VPMdm. The input of the extralemniscal pathway originates from the multi-whisker, interbarrelette cells of the caudal part of SpVi, and the output is targeted to layers 4 and 6 of wS2, as well as the septal columns of wS1 (Pierret et al., 2000).

The third pathway, the paralemniscal pathway, arises from the multi-whisker cells in the rostral part of SpVi (Erzurumlu and Killackey, 1980; Peschanski, 1984; Williams et al., 1994; Veinante et al., 2000a), contacts relay cells in Pom and targets wS1, wS2, and wM1. Pom axons terminate mainly throughout layers 5a and 1 of wS1 as well as in layer 4 of the septa (Koralek et al., 1988; Chmielowska et al., 1989; Lu and Lin, 1993; Bureau et al., 2006; Petreanu et al., 2009; Wimmer et al., 2010), where they also provide synaptic input to pyramidal neurons in layers 3 and 5a (Bureau et al., 2006; Petreanu et al., 2009; Meyer et al., 2010a). In addition, Pom terminals are found in wS2 and wM1 (Carvell and Simons, 1987). From Pom, there are also projections to the striatum (Alloway et al., 2006), the perirhinal cortex and the insular cortex (Deschênes et al., 1998). Responses of relay cells in Pom to single-whisker deflections differ from those in VPM: in Pom, the receptive fields are larger, the latencies longer and more variable and the activity is under control of a strong cortical feedback (Diamond et al., 1992b; Ahissar et al., 2000). The variable and relatively long response latencies (19–27 ms) of Pom cells are likely caused by inhibitory inputs from ZI gating peripheral inputs to Pom (Trageser and Keller, 2004).

In addition, there are at least three other trigemino-thalamo-cortical pathways. All of these convey multi-whisker information. The first arises from the interbarrelette cells of PrV, projects to Pom and to multi-whisker relay cells in the "heads" of the barreloids at the dorsomedial margin of VPM (VPMh; Veinante and Deschênes, 1999; Urbain and Deschênes, 2007b). The head barreloid cells send axons to the septal columns of wS1 (Furuta et al., 2009). A second multi-whisker pathway involves projections from SpVi to the thalamic laterodorsal nucleus (LD), which projects mainly to the cingulate and retrosplenial cortex, and only sparsely to wS1 (Bezdudnaya and Keller, 2008). And finally, there is a relatively sparse and poorly characterized pathway originating from multi-whisker neurons in SpVo and projecting to caudal thalamic regions including the most posterior parts of VPM and Pom (Jacquin and Rhoades, 1990; Veinante et al., 2000a). These thalamic regions receive inputs from different sensory modalities and project to the perirhinal cortex, striatum, and amygdala (Groenewegen and Witter, 2004).

Apart from being the relay station between the trigeminal nuclei and the cerebral cortex, the thalamus also contains intra-thalamic projections. As such the reticular nucleus (RT) is involved in several negative feedback loops that modulate the flow of information through trigemino-thalamo-cortical pathways discussed above. RT forms a sheet of GABAergic neurons surrounding the thalamus and it contains a somatotopic body map with a large representation of the whiskers (Shosaku et al., 1984; Guillery and Harting, 2003; Pinault, 2004). Axons of VPM and Pom cells give off collaterals in RT (Crabtree et al., 1998; Lam and Sherman, 2011), while RT in turn provides strong inhibitory input to VPM and Pom (Pinault et al., 1995; Cox et al., 1997; Brecht and Sakmann, 2002b). The VPM-projections from RT cells are whisker-specific: they target the barreloid of their own principle whisker (Desilets-Roy et al., 2002). Since RT neurons adapt stronger to repeated, high-frequency stimulation than VPM neurons, strong whisker stimulation can lead to disinhibition of VPM neurons (Hartings et al., 2003; Ganmor et al., 2010). Furthermore, VPM cells can influence activity in Pom through intra-thalamic pathways involving RT (Crabtree et al., 1998). Additional indirect inhibitory feedback loops to Pom involve ZI (see Other Structures Projecting to the Facial Nucleus), which receives both peripheral and cortico-thalamic input and provides a significant portion of GABAergic synaptic terminals in Pom (Barthó et al., 2002; Bokor et al., 2005).

PRIMARY SOMATOSENSORY CORTEX (S1)

The whisker part of S1 (wS1) is of crucial importance for perception and processing of whisker input. For instance, wS1 is required for whisker-based object localization (O'Connor et al., 2010a), gap-crossing (Hutson and Masterton, 1986), and aperture width discrimination (Krupa et al., 2001). Direct stimulation of wS1 in rabbits can substitute for peripheral vibrissa stimulation (Leal-Campanario et al., 2006). This suggests that wS1 can form sensory percepts, but does not differentiate between peripheral and central stimulation (see also Huber et al., 2008). Recent evidence indicates that wS1 also has a previously unanticipated role in motor control of whisker retraction (Matyas et al., 2010).

As all cortical areas, wS1 is composed of layers. Layer 4 is the main input layer, and in mice it is organized in patches ("barrels") of neurons primarily receiving input from a single whisker (**Figure 4B**; Woolsey and Van der Loos, 1970). Within a mouse barrel, most neurons are found at the borders, leaving the barrel center relatively empty. In rats, a similar organization is found (**Figure 4A**), but the barrel diameters are larger (∼400 μm) than in mice (∼280 μm), and the cells are equally distributed within the barrels (Welker and Woolsey, 1974). In mice, a single barrel column contains, distributed over all layers, ∼6,500 neurons (C2 barrel; Lefort et al., 2009), while the rat C2 barrel contains ∼19,000 neurons (Meyer et al., 2010b). The barrels are strictly organized in a somatotopic pattern (Welker, 1971). In between the barrels are the septa, which mainly receive multi-whisker input (Brumberg

et al., 1999; Furuta et al., 2009). The septa are larger in rats than in mice (Welker, 1971; Woolsey et al., 1975). Within the class of mammals, rats and mice are quite exceptional in having barrels in wS1. Barrels are only present in some rodents, as well as a few other species (Woolsey et al., 1975; Rice, 1985). In adult rabbits, for instance, barrels cannot be identified. Yet, also rabbits probably have a somatotopic representation of their vibrissae in S1, but the borders between the whisker receptive fields are fuzzier than in animals with barrels (**Figure 4C**; Woolsey et al., 1975; McMullen et al., 1994).

Throughout wS1, sensory-evoked responses are sparse and near-simultaneous, but the response probabilities are layer- and cell type-specific (Brecht and Sakmann, 2002a; Brecht et al., 2003; Manns et al., 2004; De Kock et al., 2007). In the barrel columns, spiking responses in excitatory neurons across all layers are largely restricted to deflections of the principle whisker, except for thick-tufted layer 5 pyramidal neurons (Welker, 1971; Simons, 1978; Manns et al., 2004; De Kock et al., 2007). Subthreshold synaptic responses, however, can also be triggered by the movement of several whiskers surrounding the principle whisker (Brecht and Sakmann, 2002a). Sensory-evoked responses in layer 4 cells are brief due to the recruitment of powerful thalamo-cortical feed-forward inhibition (Swadlow, 2002; Gabernet et al., 2005; Sun et al., 2006; Cruikshank et al., 2007). Angular tuning domains have been observed within layers 4 (Bruno et al., 2003) and 2/3 in adult rats (Andermann and Moore, 2006; Kremer et al., 2011). During free whisking, neurons across all layers respond to active touch (Curtis and Kleinfeld, 2009; O'Connor et al., 2010b; Crochet et al., 2011) and to slip-stick motion events (**Figure 1C**; Jadhav et al., 2009). Sensory-evoked activity patterns in wS1 correlate well with psychophysical performance in whisker-dependent tactile discrimination tasks (Krupa et al., 2004; von Heimendahl et al., 2007; Stüttgen and Schwarz, 2008; O'Connor et al., 2010b). The activity of wS1 neurons encodes the spatial location of the whiskers over time (Fee et al., 1997; Crochet and Petersen, 2006; De Kock and Sakmann, 2009). This is also true for GABAergic interneurons (Gentet et al., 2010). Such a reference signal is required for decoding horizontal object position (Diamond et al., 2008), for example by neurons in wS1 for which phase in the whisk cycle gates the response to touch (Curtis and Kleinfeld, 2009).

In comparison to responses in the barrel columns, those in the septal columns are less whisker-specific. The barrel and septal columns have been proposed to represent two partially segregated circuits that process different aspects of whisker movements (Kim and Ebner, 1999; Shepherd and Svoboda, 2005; Alloway, 2008). However, the segregation between barrels and septa, while prominent in rats, is not so clear in other species, like mice which have only very thin septa (cf Bureau et al., 2006).

The microcircuit of wS1 has been extensively characterized, yielding increasingly detailed connectivity schemes (Lübke and Feldmeyer, 2007; Schubert et al., 2007; Lefort et al., 2009; Petreanu et al., 2009). Layer 4 barrel neurons, which are the main recipients of the lemniscal pathway, project to all layers within their own barrel column, but most prominently to other layer 4 cells as well as layer 2/3 pyramidal cells (Kim and Ebner, 1999; Lübke et al., 2000; Petersen and Sakmann, 2000; Schubert et al., 2001; Feldmeyer et al., 2002, 2005; Shepherd and Svoboda, 2005; Lefort et al., 2009). Layer 2/3 pyramidal cells project both within their own barrel column as well as over long distances across barrel columns (Lübke and Feldmeyer, 2007). They contact cells within all layers except layer 4, with a particularly strong connection to other layer 2/3 pyramidal neurons and to thick-tufted layer 5b pyramidal cells (Reyes and Sakmann, 1999; Schubert et al., 2001; Lefort et al., 2009; Petreanu et al., 2009). Layer 5a neurons, which are the main recipients of the paralemniscal pathway, project strongly within their own barrel column to other pyramidal cells across layer 5 (Lefort et al., 2009), and to layer 2 cells distributed across multiple columns and preferentially located above the septa (in rats, but not in mice; Shepherd and Svoboda, 2005; Bureau et al., 2006). Layer 2 neurons receive additional inputs from layer 3 neurons located above barrels (Bureau et al., 2006), providing one of several possible points of convergence for the lemniscal and paralemniscal pathways (Lübke and Feldmeyer, 2007). Inhibitory input to excitatory neurons is derived from cells within the same cortical layer as well as from cells from other cortical layers (Helmstaedter et al., 2009; Kätzel et al., 2011). In addition to the aforementioned intracolumnar connections within wS1, intracortical projections extend throughout much of wS1 and its dysgranular zone (Chapin et al., 1987; Hoeflinger et al., 1995; Kim and Ebner, 1999; Aronoff et al., 2010).

The whisker area of S1 forms reciprocal connections with several other cortical areas, including the whisker part of the secondary somatosensory cortex (wS2), wM1, insular cortex, and perirhinal cortex (White and DeAmicis, 1977; Welker et al., 1988; Fabri and Burton, 1991; Cauller et al., 1998; Aronoff et al., 2010). The contralateral wS1 is targeted via callosal projections (Larsen et al., 2007; Petreanu et al., 2007). Axonal projections to wS2 originate from the infragranular and supragranular layers of wS1 and arborize across all layers in wS2 (Welker et al., 1988; Fabri and Burton, 1991; Cauller et al., 1998; Chakrabarti and Alloway, 2006; Aronoff et al., 2010). The wS1 to wM1 projection is somatotopically arranged such that a column in wS1 connects to a column of the same whisker in wM1 (Izraeli and Porter, 1995; Hoffer et al., 2003; Ferezou et al., 2007). Layer 2/3 pyramidal cells of wS1 densely innervate layers 5/6 of wM1, while those of layers 5/6 preferentially innervate layers 1 and 2/3 in wM1 (Porter and White, 1983; Miyashita et al., 1994; Aronoff et al., 2010). The majority of connections to wM1 arises from neurons located in septal columns (Crandall et al., 1986; Alloway et al., 2004; Chakrabarti et al., 2008). The reciprocal projection, from wM1 to wS1, innervates mainly layers 5/6 and 1 (Cauller et al., 1998; Veinante and Deschênes, 2003; Matyas et al., 2010).

Cortico-thalamic projections originate in layer 5/6 and target relay cells in VPM and Pom, as well as GABAergic neurons in RT (Hoogland et al., 1987; Welker et al., 1988; Chmielowska et al., 1989; Bourassa et al., 1995; Deschênes et al., 1998; Veinante et al., 2000b; Killackey and Sherman, 2003). The projections to VPM originate from layer 6a pyramidal neurons (located below both the barrels and the septa) and target the barreloid of the corresponding principal whisker as well as those of several whiskers located within the same arc (Hoogland et al., 1987; Bourassa et al., 1995). VPMvl, which is the thalamic relay station for the extralemniscal pathway, receives cortical input from layer 6 pyramidal cells, both from wS1 and from wS2 (Bokor et al., 2008). The heads of

the barreloids in VPM, which participate in a multi-whisker lemniscal pathway, receive collaterals from layer 6b pyramidal cells projecting to Pom (Bourassa et al., 1995; Deschênes et al., 1998). The relay cells of Pom also receive input from layer 6a pyramidal cells (located below the septa) and layer 5b tall-tufted pyramidal cells (located below both the barrels and the septa), whose axons form large and powerful synapses that can drive Pom neurons (Hoogland et al., 1991; Killackey and Sherman, 2003; Larsen et al., 2007; Groh et al., 2008). These relay cells project to wS2, forming a cortico-thalamo-cortical pathway (Theyel et al., 2010). Layer 5b neurons also project to ZI (Bourassa et al., 1995; Mitrofanis and Mikuletic, 1999; Veinante et al., 2000b; Barthó et al., 2007), which is involved in state-dependent suppression of whisker sensory responses in Pom (see Zona Incerta). RT cells are innervated by collaterals of cortico-thalamic axons from layer 6 cells, but not layer 5 cells (Bourassa et al., 1995), which strongly activate RT cells and evoke disynaptic inhibition in thalamo-cortical relay cells (Cruikshank et al., 2010; Lam and Sherman, 2010). Other projections of wS1 include projections from layer 5a pyramidal cells to the striatum (see Basal Ganglia) and from layer 5b pyramidal cells to the anterior pretectal (APT) nucleus (Aronoff et al., 2010), SC (see Superior Colliculus), the red nucleus (see Anterior Pretectal Nucleus), the pontine nuclei (see The Pontine Nucleus and the Nucleus Reticularis Tegmenti Pontis), and the sensory trigeminal nuclei (see Sensory Trigeminal Nuclei).

SECONDARY SOMATOSENSORY CORTEX (S2)

S2 contains a highly organized somatotopic representation of the whiskers (wS2) that occupies around 14% of the total area of S2 and that is located in the parietal cortex, lateral to wS1 (Carvell and Simons, 1986; Koralek et al., 1990; Fabri and Burton, 1991; Hoffer et al., 2003; Benison et al., 2007). The whisker receptive fields in wS2 are larger than in wS1; wS2 neurons generally respond equally well to several adjacent whiskers (Welker and Sinha, 1972; Carvell and Simons, 1986; Kwegyir-Afful and Keller, 2004). Responses in wS2 to single-whisker deflections are weaker than those in wS1, but they display stronger direction selectivity, while the onset latencies are comparable (Kwegyir-Afful and Keller, 2004). The local connections within wS2 are similar to those within wS1. However, in contrast to wS1, the projections from layer 2/3 to layer 5 are stronger than those from layer 4 to layer 3 (Hooks et al., 2011). Furthermore, the reciprocal connections between layers 5 and 6, which are weak in wS1, are more pronounced in wS2 (Hooks et al., 2011). Whisker input reaches wS2 via the extralemniscal pathway through VPMvl (Pierret et al., 2000; Bokor et al., 2008), but also via Pom (Carvell and Simons, 1987; Spreafico et al., 1987; Alloway et al., 2000; Theyel et al., 2010) and from both the barrel and septal columns of wS1 (Kim and Ebner, 1999; Chakrabarti and Alloway, 2006). The connections between wS1 and wS2 are reciprocal (Carvell and Simons, 1987; Aronoff et al., 2010). In addition, there are reciprocal connections between wS2 and wM1 (Porter and White, 1983; Miyashita et al., 1994). There are also projections to the striatum (see Basal Ganglia), the pontine nuclei (see The Pontine Nucleus and the Nucleus Reticularis Tegmenti Pontis), and to several thalamic nuclei, including VPM, Pom, and RT (Liao et al., 2010). wS2 also receives cholinergic input from the nucleus basalis magnocellularis (Deurveilher and Semba, 2011).

WHISKER MOTOR CONTROL

Rhythmic whisker movements increase the acuity of the whisker system (Szwed et al., 2003; Knutsen et al., 2006). Whisker movements are generated in the facial nucleus, whose activity is affected by a large number of brain regions. It has been proposed that higher-order areas can initiate movement, but that the rhythmicity of the whiskers is caused by a brainstem central pattern generator (CPG; see Serotonin).

FACIAL NUCLEUS

The motor neurons of both the intrinsic and the extrinsic muscles of the whisker pad are located in the lateral facial nucleus (Ashwell, 1982; Klein and Rhoades, 1985; Herfst and Brecht, 2008). Of the lateral facial nucleus neurons that evoke whisker movements, about 80% induce the protraction of a single whisker and about 20% the retraction of multiple whiskers (Herfst and Brecht, 2008). Each intrinsic capsular muscle has about 25–50 motoneurons in the lateral facial nucleus (Klein and Rhoades, 1985). The motor commands are forwarded to the whisker muscles via the facial nerve (**Figure 2A**; Dörfl, 1985; Haidarliu et al., 2010). In addition, there is sparse innervation of the extrinsic muscles by the hypoglossal nucleus via the infraorbital branch of the trigeminal nerve (Mameli et al., 2008).

Single motor neurons in the lateral facial nucleus evoke fast, short, and stereotypic whisker movements, whereas single neurons in wM1 evoke slow, small, and long-lasting rhythmic movements (Brecht et al., 2004b; Herfst and Brecht, 2008). This discrepancy makes it unlikely that wM1 directly commands activity of the lateral facial nucleus, despite the possible existence of a sparse monosynaptic projection from wM1 to the contralateral lateral facial nucleus (Grinevich et al., 2005). Instead, wM1 may induce rhythmic whisker movements via oligosynaptic pathways to the lateral facial nucleus. Remarkably, rhythmic whisker movements persist in the absence of wM1 (Welker, 1964; Semba and Komisaruk, 1984; Gao et al., 2003). Hence, it has been proposed that wM1 projects to a CPG in the brainstem, possibly the dorsal raphe nucleus, that in turn activates the lateral facial nucleus (Hattox et al., 2003; see Serotonin). In addition, the lateral facial nucleus receives input from several other subcortical structures, all of which are directly or indirectly innervated by wM1. These afferent regions include the ipsilateral sensory trigeminal nuclei (Nguyen and Kleinfeld, 2005), the ipsilateral pontomedullary RF (Zerari-Mailly et al., 2001), and the contralateral SC (Miyashita and Mori, 1995; Hattox et al., 2002). In addition, the lateral facial nucleus is targeted by cholinergic, histaminergic, and noradrenergic connections, which may set the overall activity level of the whisker movements (see Arousal, Alertness, and Attention). Altogether, there is a strong convergence of inputs at the level of the lateral facial nucleus, allowing the integration of whisker movements and other forms of behavior.

CEREBRAL CORTEX

Primary motor cortex (M1)

The primary motor cortex (M1) is a large area in the frontal cortex involved in movement. M1 has an agranular appearance, low stimulation thresholds for evoking movements, and a topographic and complete representation of the body muscles

(Gioanni and Lamarche, 1985; Brecht et al., 2004a). M1 can be divided into the agranular medial field (AGm), the agranular lateral field (AGl), and the cingulate area (Cg1). The topographic representation of whiskers is almost exclusively located in AGm (Brecht et al., 2004a). Sensory input from the whiskers to whisker M1 (wM1) comes predominantly via wS1 (Armstrong-James and Fox, 1987), but also directly from Pom (Deschênes et al., 1998). The latencies to whisker stimulation are 10–20 ms longer in wM1 than in wS1 (**Figure 4D**; Ferezou et al., 2007). Microstimulation of wM1 can generate whisker motion that strongly resembles natural exploratory whisking (Berg and Kleinfeld, 2003b; Brecht et al., 2004b; Haiss and Schwarz, 2005; Matyas et al., 2010). During a training paradigm, mice can learn to protract their whiskers following an auditory conditioned stimulus (CS; Troncoso et al., 2004). Such associative learning probably involves synaptic plasticity of layer 5 pyramidal cells in wM1 (Troncoso et al., 2007). This suggests that whisker movements are subject to change following long-term synaptic plasticity in wM1. Although complete ablation of wM1 does not abolish whisking, it does disrupt whisking kinematics, coordination, and temporal organization such as whisking synchrony (Gao et al., 2003). There are several indirect routes from wM1 to the lateral facial nucleus, for example via SC (see Superior Colliculus) or the pontomedullary RF (see Pontomedullary Reticular Formation) and wS1 (see Somatosensory Cortex as a Premotor Area). In addition, wM1 is involved in several feedback loops, including reciprocal connections with wS1 (Aronoff et al., 2010), thalamus (Cicirata et al., 1986; Colechio and Alloway, 2009), and loops involving the basal ganglia (see Basal Ganglia), the cerebellum (see The Cerebellar System), and the claustrum (see Bilateral Coordination of Whisker Movements). Finally, wM1 projects to the deep mesencephalic nucleus, the periaqueductal gray, and the red nucleus (Alloway et al., 2010). This network of inputs and outputs enables wM1 to adjust whisker movements both to sensory input and to the general behavior.

The output of wM1 is not uniform. Layer 5 pyramidal cells project to cells around the facial nucleus while those of layer 6 project to the thalamus. Evidence for strong myelinization and an expanded layer 5 in AGm points to the possible contribution to high speed whisking (Brecht et al., 2004b). Layer 5 output may correspond with timing of individual whisking movements and may be able to reset these rhythms, while layer 6 output may correspond with grouping of multiple whisking movement bursts where action potential frequency determines movement direction and amplitude (Brecht et al., 2004b).

Somatosensory cortex as a premotor area

Microstimulation of wM1 can induce both whisker protraction and retraction depending on the location of stimulation in wM1 (Gioanni and Lamarche, 1985; Haiss and Schwarz, 2005; Matyas et al., 2010). A recent study found that stimulation of wS1 induces whisker retraction at shorter latencies than wM1 stimulation. In fact, the wM1-induced whisker retraction can be mediated by synaptic activation in wS1 (Matyas et al., 2010). Contrary to stimulation of wM1, stimulation of wS1 does not evoke whisker protraction (Matyas et al., 2010). In the same study, the authors suggest that wS1 exerts its effect on whisker movement by a disynaptic pathway via SpV to the facial nucleus. Thus, wM1 and wS1 could together form an additional source of rhythmic whisker movements, alongside the putative brainstem pattern generators (see Serotonin). Such an organization is in line with the idea that wM1 specifies motor programs rather than simple muscle activity (Brecht et al., 2004b).

BASAL GANGLIA

The first somatosensory feedback system to be discussed involves the basal ganglia, which are important for a wide variety of (sensori-)motor functions. In the oculomotor system, the basal ganglia have been associated with orienting saccadic eye movements based on reward expectancy (Hikosaka et al., 2006). A similar function for the whisker system could very well be possible. The basal ganglia are a heterogeneous group of brain regions, whose main components are the striatum, the globus pallidus (GP), the substantia nigra (SN), and the subthalamic nucleus (STN). The GP consists of two parts: an external (GPe) and an internal part (GPi). In rodents, GPi is commonly referred to as the entopeduncular nucleus (EPN; Nambu, 2007). SN is composed of a pars compacta (SNc) and a pars reticulata (SNr). In general, the information from the cerebral cortex enters the striatum, is forwarded to other parts of the basal ganglia and the output to the thalamus and SC is eventually generated by EPN and SNr (**Figure 5A**).

The striatum, or "neostriatum," is a single area in rodents, but in higher mammals it is composed of two nuclei: the caudate and the putamen (Tepper et al., 2007). Based on function and connectivity, the striatum can be divided into a dorsolateral and a ventromedial part (Voorn et al., 2004). The striatum is involved in the acquisition of habits, goal-directed behaviors and in the motivation to perform. The whisker receptive fields of the dorsolateral striatum are organized in a loosely somatotopic manner: dorsal whiskers project laterally and caudal whiskers project dorsally (**Figure 5B**; Alloway et al., 1999; Wright et al., 1999). There is much overlap between the projection areas of whiskers from a single row, but hardly any from whiskers in different rows. There is also a weaker whisker representation in the ventromedial striatum (Alloway et al., 1999; Wright et al., 1999). The cortico-striatal projections are predominantly ipsilateral and originate from layer 5 pyramidal cells in both barrels and septa (Alloway et al., 2006). Thus, cortico-striatal projections serve to integrate rather than segregate input from different whiskers. In addition, the striatum receives input from wS2, wM1, and other cortical areas, including motor, cognitive, and other sensory areas (Wright et al., 2001; Alloway et al., 2006; Tepper et al., 2007). Hence, the striatum can integrate the whiskers and general behavior.

Apart from the extensive input from the cerebral cortex, the striatum also receives direct input from the thalamus. The thalamo-striatal connections originate mainly in the intralaminar nuclei of the thalamus (Smith et al., 2004; Tepper et al., 2007) and in Pom (Alloway et al., 2006). During whisker stimulation at low frequencies, the responses of the medium-spiny neurons in the dorsolateral striatum are approximately 5 ms later than in wS1 (Mowery et al., 2011; Pidoux et al., 2011; Syed et al., 2011). However, during repeated whisker stimulation at 5–8 Hz, striatal responses actually preceded those in wS1 (Mowery et al., 2011). In addition, the striatal responses showed less adaptation to repeated

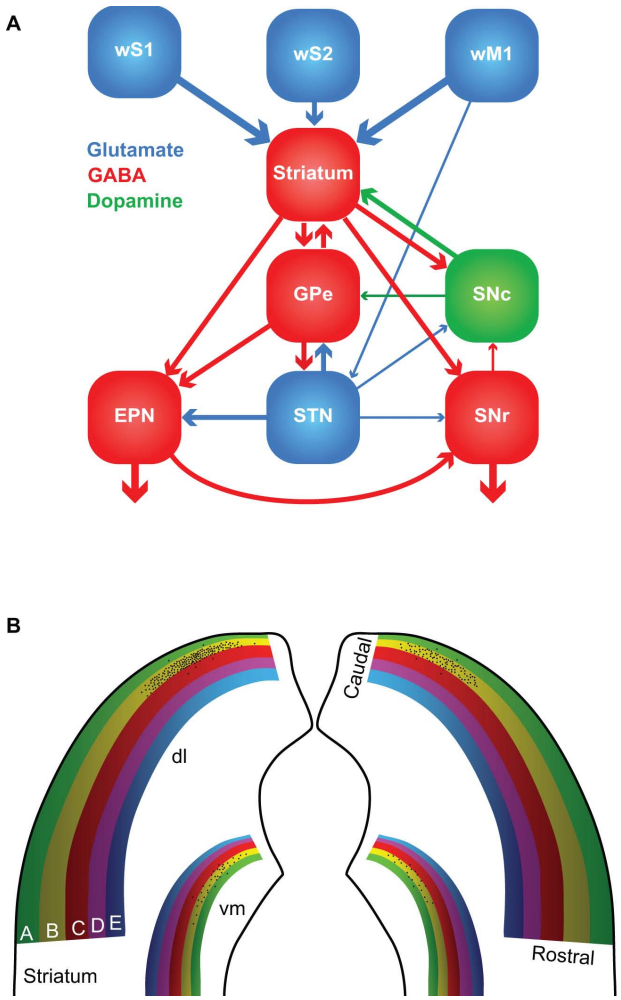

FIGURE 5 | The basal ganglia. (A) The major connections between the components of the basal ganglia. Most of the input comes from the cerebral cortex (in this case: wS1, wS2, and wM1), and is directed to the striatum. GABAergic medium-spiny neurons of the striatum project to the external part of the globus pallidus (GPe), the entopeduncular nucleus (EPN), and the reticular (SNr) and compact (SNc) parts of the substantia nigra. SNc provides dopaminergic input to the striatum, and the subthalamic nucleus (STN) glutamatergic input to GPe, EPN, and SNr. The main output of the basal ganglia is directed to the thalamus, via GPe and SNr, and the superior colliculus, via SNr. The line thickness indicates the relative importance for the whisker system. **(B)** Whisker responses in the dorsolateral (dl) striatum follow a loose somatotopy, which is mainly organized according to whisker rows. The black dots indicate schematically the projections of the layer 5 pyramidal cells in the B2 barrel of left wS1. The projection is mainly, but not exclusively, ipsilateral, and largely within the "B row" area in the striatum. There is considerable overlap, however, with the projection areas of other B row whiskers. "Rostral" and "caudal" refer to the positions of the whiskers on the mystacial pad. A smaller and less characterized projection area is also present in the ventromedial (vm) striatum.

whisker stimulation as responses in wS1 (Mowery et al., 2011). The latter findings support an important role for the direct thalamo-striatal pathway, in addition to the well-established thalamo-cortico-striatal route. The thalamo-striatal pathway conveying whisker information originates mainly in Pom (Alloway et al., 2006). Relay cells in Pom are inhibited during rest and become disinhibited during periods of activity (see Zona Incerta and Anterior Pretectal Nucleus). Although the disinhibition of Pom has been predominantly linked to active whisking (Bokor et al., 2005; Lavallée et al., 2005; Urbain and Deschênes, 2007a), it might also be evoked by repeated, passive whisker input. Other inputs to the striatum come from the amygdala (Kelley et al., 1982; Popescu et al., 2009), the dorsal raphe nuclei (Di Matteo et al., 2008), GP and SN (Tepper et al., 2007). The main output of the striatum is composed of GABAergic projections to GP and SN.

The GABAergic output of the striatum is the dominant input to SNc, but SNc also receives GABAergic input from SNr and glutamatergic input from the amygdala, and to a lesser extent also from STN (Kita and Kitai, 1987; Gonzales and Chesselet, 1990; Misgeld, 2004). SNc also receives histaminergic input from the tuberomammillary nuclei (Lee et al., 2008b). SNc forms dopaminergic connections to the striatum and is implicated in the reward system (Hikosaka et al., 2006; Redgrave et al., 2008). Its degeneration is an important cause of the motor problems associated with Parkinson's disease (Gibb and Lees, 1988; Esposito et al., 2007). SNr receives GABAergic input from the striatum and, to a lesser extent also glutamatergic input from STN and the cerebral cortex (Kita and Kitai, 1987; Naito and Kita, 1994; Tepper et al., 2007). SNr sends GABAergic projections to the ventromedial thalamus and the SC (Beckstead et al., 1979; Di Chiara et al., 1979; Grofova et al., 1982). Activation of the nociceptin/orphanin FQ (N/OFQ) receptors in SNr modulates whisker motor output (Marti et al., 2009).

The external globus pallidus receives GABAergic input from the striatum and glutamatergic input from STN. Sparse innervation comes from the cerebral cortex, the intralaminar nuclei of the thalamus, SNc, the dorsal raphe nuclei, and PPTg (Kita, 2007). The main output areas of GPe are EPN, STN, and the striatum (Kita, 2007). EPN receives GABAergic input from GPe and the striatum, and glutamatergic input from STN (Nambu, 2007). In turn, EPN projects to the ventrolateral thalamic nucleus (VL; Nambu, 2007). To our knowledge, no systematic study of the role of GP in the rodent whisker system has been undertaken. However, GP neurons in cats show responses to vibrissal stimulation, whereby the response depends on the direction of vibrissal movement (Schneider et al., 1982).

The lateral half of STN shows responses to contralateral whisker stimulation. Interestingly, each neuron that responds to contralateral whisker stimulation, also responds to somatosensory stimulation of another area, e.g., forepaw or ipsilateral whisker stimulation (Hammond et al., 1978). This is in line with the putative role of the basal ganglia in bringing different behavioral aspects together. STN receives input from the cerebral cortex, predominantly wM1, and GPe, and projects to GPe, EPN, and SNr (Kita and Kitai, 1987; Joel and Weiner, 1997).

SUPERIOR COLLICULUS

The second sensorimotor feedback system involves SC, which is also known as the "tectum." The upper layers of SC process sensory information, the intermediate layers sensorimotor information, and the lower layers motor information. SC receives sensory input

via direct connections from all four parts of the sensory trigeminal nuclei (Steindler, 1985; Cohen et al., 2008), and provides a direct output to the facial nucleus. However, the SC neurons that receive trigeminal input are not the same as those that innervate the facial nucleus (Hemelt and Keller, 2008). Hence, SC does not function as a simple, "reflexive" relay station between the trigeminal nuclei and the facial nucleus. Similarly, the input to SC from wM1 is also not directly relayed to the facial nucleus, since microstimulation of wM1 and SC show qualitatively and quantitatively different whisker responses (Hemelt and Keller, 2008). Instead, the main function of SC for the whisker system may be closely related to its best known function, which is to control saccadic eye movements and direct the gaze direction toward an interesting visual cue (Boehnke and Munoz, 2008; Gandhi and Katnani, 2011). SC can direct all mobile senses toward an object of interest. Microstimulation at a single spot in the intermediate or deep layers of SC can induce coherent movements of the eyes, the auricles, and the whiskers together (McHaffie and Stein, 1982). While microstimulation within wM1 induces rhythmic whisker movements (Brecht et al., 2004b; Matyas et al., 2010), microstimulation in SC causes sustained whisker protraction (Hemelt and Keller, 2008), which is in accordance with its putative function in the direction of the whiskers. In addition, SC also responds to whisker input. Passive touch (air puff) as well as whisking in air and active touch (surface contact during whisking) evoked SC neuronal responses which were subject to strong adaptation. Passive and active touch evoked stronger responses than whisking in air. As a consequence, whisking in air at 10 Hz hardly evokes any response in SC, but active touch does (Bezdudnaya and Castro-Alamancos, 2011). SC responses can have different latencies. Fast responses (<10 ms) are probably due to the direct trigemino-tectal input and slow responses are likely mediated by wS1 (Bezdudnaya and Castro-Alamancos, 2011).

The superior colliculus receives strong input from ipsilateral wM1 (Miyashita et al., 1994; Alloway et al., 2010), wS1 (Wise and Jones, 1977; Cohen et al., 2008; Aronoff et al., 2010) and the cerebellar nuclei, mainly the dentate and interpositus nucleus, and to a lesser extent also from the fastigial nucleus (May, 2006). Other inputs come, as mentioned before, from the trigeminal nuclei (Steindler, 1985; Cohen et al., 2008), and also from ZI, which supplies both glutamatergic and GABAergic efferents (Beitz, 1989; Kim et al., 1992), from SNr (Beckstead et al., 1979; Kaneda et al., 2008) as well as from the visual cortex (Boehnke and Munoz, 2008). There is also input from the thalamus, but this seems to relate more to the visual than to the whisker system (Cosenza and Moore, 1984; Taylor and Lieberman, 1987). SC projects to the lateral facial nucleus. This connection is mainly ipsilateral, but there are distinct patches of neurons within SC that project to the contralateral lateral facial nucleus (Hemelt and Keller, 2008). SC also projects to the contralateral nucleus reticularis tegmenti pontis (NRTP; Westby et al., 1993; May, 2006), which provides mossy fiber input to the cerebellar cortex and cerebellar nuclei (Mihailoff, 1993). There is also a projection from SC to the contralateral medial accessory olive (MAO; Huerta et al., 1983; May, 2006), which is a source of climbing fibers to the cerebellar cortex. Thus, there are two disynaptic pathways from SC to the cerebellar cortex, which projects back to SC via the cerebellar nuclei.

THE CEREBELLAR SYSTEM

The third somatosensory feedback system is that of the cerebellum, which receives most of its mossy fiber afferents from the pons and all its climbing fiber afferents from IO (**Figure 6**).

The pontine nucleus and the nucleus reticularis tegmenti pontis

The pontine nucleus (or "basal pons") forms the main gateway to the cerebellum for efferents from the cerebral cortex. The main input to the pontine nucleus comes from layer 5 neurons

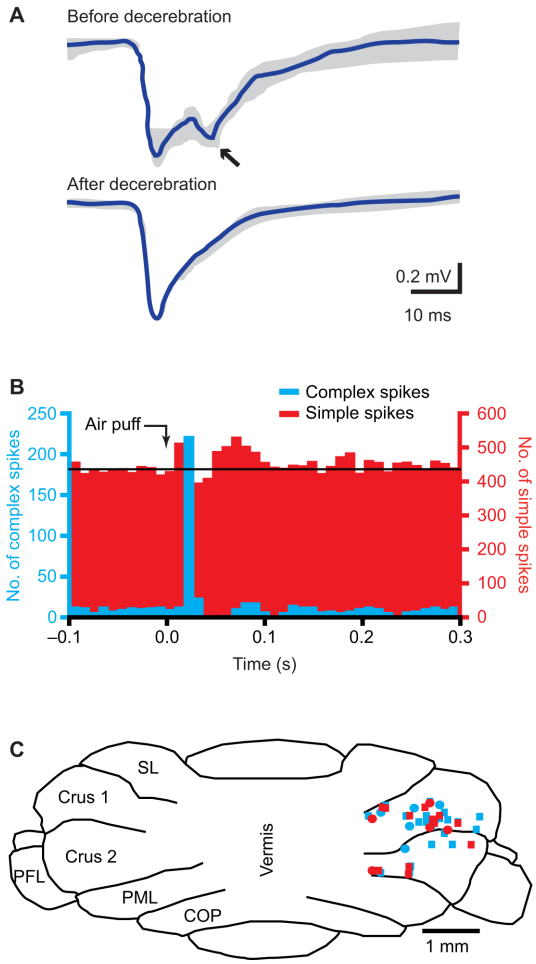

FIGURE 6 | The cerebellum. (A) Tactile stimulation of the upper lip evokes a bi-phasic response in the cerebellar cortex, as measured with field potential recordings in the granule cell layer in crus 2 of adult rats. Complete midcollicular decerebration abolished the late phase response, indicating that the late phase response (arrow) is induced by the cerebral cortex, while the early phase is not. Schematic drawing based on Morisette and Bower (1996). **(B)** Peri-stimulus time histograms of complex spike (blue) and simple spike (red) responses to ipsilateral air puff stimulation of the whiskers in a Purkinje cell in crus 1 of an awake mouse. The complex spike response is uni-phasic, while clear early and late phase simple spike responses can be observed. Reproduced with permission from Bosman et al. (2010). **(C)** Cross section of the cerebellar cortex, showing the locations where Purkinje cell responses to ipsilateral stimulation of whisker from the C row were observed in crus 1 and crus 2. COP, copula pyramidis; PFL, paraflocculus; PML, paramedian lobule; SL, simple lobule. Modified with permission from Bosman et al. (2010).

throughout the entire ipsilateral cerebral cortex, and the efferents all go to the cerebellum (Legg et al., 1989; Brodal and Bjaalie, 1992). Cerebral cortical inputs are mapped multiply and in different combinations to the pontine nucleus (Schwarz and Möck, 2001; Leergaard et al., 2004, 2006). In general, cortico-pontine projections from different cortical regions do not overlap. This seems to hold true also for the barrels of wS1, implying that the pontine nucleus may receive single-whisker input (Schwarz and Möck, 2001). Nevertheless, the whisker-related parts of wS1, wS2, and wM1, sometimes project to adjacent, or even partially overlapping regions (Leergaard et al., 2004). Thus, the somatotopy in the pontine nucleus is somewhat intermediate between the continuous somatotopy of the cerebral cortex and the fractured somatotopy of the cerebellum.

The pontine nucleus sends bilateral (but mainly contralateral) mossy fiber connections to the cerebellar cortex, which give off collaterals to the cerebellar nuclei (Eller and Chan-Palay, 1976; Parenti et al., 2002; Leergaard et al., 2006). The cerebellar cortex also projects to the cerebellar nuclei. This feedback loop is completed by afferents from the cerebellar nuclei back to the pontine nucleus (De Zeeuw et al., 2011; Ruigrok, 2011). In addition to the input from the cerebral cortex, which is the dominant input, and of the cerebellar nuclei, the pontine nucleus also receives inputs from dozens of other brain regions (Mihailoff et al., 1989). The functional relevance of these other inputs is not very clear, and their specific functions for the whisker system are currently unknown. The inputs that could be of importance for the whisker system include projections from the sensory trigeminal nuclei (mainly SpVi; Swenson et al., 1984; Mihailoff et al., 1989), SC (Burne et al., 1981; Mihailoff et al., 1989), ZI (Ricardo, 1981; Mihailoff, 1995), the dorsal raphe nuclei (Mihailoff et al., 1989), PPTg (Mihailoff et al., 1989), and the tuberomammillary nuclei (Pillot et al., 2002). Recently, a direct connection from STN to the pontine nuclei has been described in cebus monkeys (Bostan et al., 2010). This could underlie a direct coupling between the basal ganglia and the cerebellar system.

Immediately dorsal of the pontine nucleus is the NRTP. The main input to NRTP comes from the cerebellar nuclei (Torigoe et al., 1986b; Brodal and Bjaalie, 1992). Other inputs come from SC and the pontomedullary RF (Torigoe et al., 1986b). NRTP also receives input from layer 5 pyramidal cells of the cerebral cortex, mainly bilaterally from the cingulate cortex and to a lesser extent also ipsilaterally from motor areas (Brodal, 1980; Torigoe et al., 1986a). NRTP projects, amongst others, ipsilaterally to the cerebellar cortex and the cerebellar nuclei (Mihailoff, 1993; Parenti et al., 2002) and bilaterally to the lateral facial nucleus (Isokawa-Akesson and Komisaruk, 1987; Hattox et al., 2002). Hence, NRTP may be a relay station between the cerebellar nuclei and the lateral facial nucleus, but whether it has a role in the whisker system is not clear yet.

Cerebellum and inferior olive

The cerebellum has a central role in sensorimotor integration and motor learning (Ito, 2000; De Zeeuw and Yeo, 2005; Krakauer and Shadmehr, 2006). It receives sensory input from the whiskers (**Figure 6B**; Axelrad and Crepel, 1977; Brown and Bower, 2001; Loewenstein et al., 2005; Bosman et al., 2010; Chu et al., 2011) and its activity can affect whisker movements (Esakov and Pronichev, 2001; Lang et al., 2006). The cerebellar cortex has two afferent pathways, the climbing fiber and mossy fiber/parallel fiber pathway, that converge on the cerebellar Purkinje cells, which form the sole efferent projection to the cerebellar and vestibular nuclei (De Zeeuw et al., 2011).

Each adult Purkinje cell is innervated by a single climbing fiber only, with the climbing fiber-to-Purkinje cell synapse being extraordinarily strong (Eccles et al., 1964; Bosman et al., 2008; Davie et al., 2008). Thus, climbing fiber activity reliably evokes postsynaptic spikes, which are, due to their complex waveforms, called "complex spikes" (Davie et al., 2008; De Zeeuw et al., 2011). Climbing fibers originate exclusively from the contralateral IO. IO comprises three main nuclei, all of which receive input from SpV, but not from PrV (Molinari et al., 1996; Yatim et al., 1996). Trigemino-olivary connections originate from all three compartments of SpV and target mainly the contralateral rostromedial part of the dorsal accessory olive (DAO) and the adjacent dorsal leaf of the principal olive (PO), and to a lesser extent the ventral leaf of the PO and the caudal part of the MAO (Huerta et al., 1983; Molinari et al., 1996; Yatim et al., 1996). Ipsilateral trigemino-olivary projections mirror the contralateral ones, but are relatively sparse (Molinari et al., 1996; Yatim et al., 1996). Altogether, most IO neurons react to somatosensory input (Gellman et al., 1985; Gibson et al., 2004). IO also receives input from many other regions. These include direct and indirect spinal projections (Miskolczy, 1931; Swenson and Castro, 1983), as well as projections from SC (Akaike, 1992), ZI (Brown et al., 1977), the raphe nuclei (Brown et al., 1977), and the ipsilateral cerebral cortex, both from somatosensory and motor areas (Swenson et al., 1989). As a consequence, Purkinje cells fire complex spikes in response to stimulation of wM1 (Lang, 2002; Lang et al., 2006).

The subnuclei of IO project to specific parasagittal zones of the cerebellar cortex (Voogd and Glickstein, 1998; Apps and Hawkes, 2009). The IO area with the strongest trigeminal input, the rostromedial DAO and dorsal PO, projects to the C3 and D zones, while the other areas project mainly to the A zones (Yatim et al., 1996; Apps and Hawkes, 2009). Indeed, most Purkinje cells showing complex spike responses to whisker stimulation were found in the C3 and D zones in lobule crus 1, and to a lesser extent also in crus 2 (**Figure 6C**; Bosman et al., 2010). Climbing fiber responses have also been found in the A zones of lobule VII (Thomson et al., 1989). In lobule IX, mossy fiber whisker responses have been reported, but climbing fiber responses were not evaluated (Joseph et al., 1978).

Climbing fiber input to the cerebellar cortex does not follow a somatotopic organization on single-whisker level. For most Purkinje cells, the receptive field of the climbing fiber input is restricted to a single whisker, where nearby Purkinje cells may receive inputs from totally unrelated whiskers (Axelrad and Crepel, 1977; Bosman et al., 2010). In the rare cases where a Purkinje cell received input from multiple whiskers, these whiskers were located within the same row (Bosman et al., 2010). Complex spike responses to whisker stimulation are relatively sparse, encoding typically about 10% of the stimuli in responsive Purkinje cells, show a large jitter in the latencies and depend on the direction of whisker movement (Thomson et al., 1989; Bosman et al., 2010).

Mossy fibers terminate at the cerebellar granule cells, whose axons form the parallel fibers, that run transversely over a long distance, innervating numerous Purkinje cells on their way, but with each parallel fiber-to-Purkinje cell synapse being only very weak (De Zeeuw et al., 2011). There are two main mossy fiber routes via which whisker sensory information reaches the cerebellar cortex. First, there is a direct mossy fiber projection from the trigeminal nuclei to the cerebellar cortex. The trigemino-cerebellar mossy fibers originate from ipsilateral PrV, SpVo, and SpVi, and to a lesser extent from SpVc (Yatim et al., 1996). This direct pathway can evoke Purkinje cell simple spike responses with a short latency. The second main mossy fiber input originates in the pontine nucleus, which in turn is activated by wS1. This cerebro-cerebellar pathway evokes Purkinje cell simple spike responses with a long latency. Lesioning of the cerebral cortex abolishes the long-latency response, while leaving the short-latency responses in tact (**Figure 6A**; Kennedy et al., 1966; Morisette and Bower, 1996). There is also a direct, trigemino-pontine connection from SpVi, but its relevance for the whisker system is not clear (Swenson et al., 1984; Mihailoff et al., 1989).

Whisker input can also inhibit Purkinje cell simple spike firing, with the inhibitory response having a longer latency than the excitatory response (**Figure 6B**; Bosman et al., 2010; Chu et al., 2011). This reflects most likely the feedforward inhibition by molecular layer interneurons within the cerebellar cortex (Chu et al., 2011; De Zeeuw et al., 2011). The complex spike and simple spike responses of an individual Purkinje cell are largely uncorrelated, both at the level of the receptive field and on the level of individual trials (Bosman et al., 2010). Simple spikes receptive fields usually involve multiple whiskers, without any obvious somatotopic ordering. And, also in contrast to complex spike responses, simple spike responses are not affected by the direction of whisker stimulation (Bosman et al., 2010). Mossy fiber-mediated whisker input seems to be strongest in crus 1, strong in crus 2 and lobules VII and IX in the vermis, and sparse in the simplex and paramedian lobules (Joseph et al., 1978; Shambes et al., 1978; Thomson et al., 1989; Bosman et al., 2010).

Thus, large parts of the cerebellar cortex receive whisker input. The output of the GABAergic Purkinje cells in the whisker-sensitive regions is fully directed to the cerebellar nuclei. From there, the cerebellar output to the whisker system mainly follows three pathways: (i) to IO, where it closes the olivo-cortico-nuclear feedback loop (Voogd and Glickstein, 1998; De Zeeuw et al., 2011); (ii) to the VL nucleus of the thalamus (Aumann et al., 1994) to provide feedback to the cerebral cortex (Aumann et al., 1994), and possibly also to the basal ganglia (Hoshi et al., 2005); and (iii) to regions that directly project to the lateral facial nucleus, such as SC (Westby et al., 1993) and NRTP (Torigoe et al., 1986b). So these latter routes may allow the cerebellum to directly affect motor output.

Both the striatum and the pontine nuclei receive input from the cerebral cortex. Interestingly, the cortico-pontine pathway has a stronger convergence of inputs from related regions in wS1 and wS2 than the cortico-striatal pathway (Leergaard et al., 2004). This could imply that the cerebellar system is especially suited for the processing of sensory data. Recent findings in primates link the cerebellar system and the basal ganglia via reciprocal disynaptic pathways. The dentate nucleus projects via the thalamus to the striatum (Hoshi et al., 2005) and STN projects via the pontine nuclei to the cerebellar cortex (Bostan et al., 2010).

VENTROLATERAL NUCLEUS OF THE THALAMUS

Both the basal ganglia and the cerebellum have an ascending projection to wM1 via the ventrolateral nucleus (VL) of the thalamus. VL incorporates input from EPN (Nambu, 2007), the cerebellar nuclei (Aumann et al., 1994), and wM1 (Miyashita et al., 1994; Alloway et al., 2008). VL itself has a somatotopic representation, including a separate area related to the whiskers (Tlamsa and Brumberg, 2010). Thus, VL is a crucial part of the central motor control system.

OTHER STRUCTURES PROJECTING TO THE FACIAL NUCLEUS

Pontomedullary reticular formation

The pontomedullary RF is a premotor area, whose activation can cause widespread movements (Quessy and Freedman, 2004; Stapley and Drew, 2009). Within RF, several distinct regions can be discriminated. Of these, the dorsal medullary reticular field and the parvocellular reticular nucleus receive strong input from SpVi and SpVc, while the gigantocellular reticular nucleus receives moderate input from SpVo (Zerari-Mailly et al., 2001). Relatively weak inputs from SpV to the other parts of RF can also be found, as well as a few connections between PrV and RF (Zerari-Mailly et al., 2001). The dorsal reticular nucleus (DRN) is probably a pain modulating area (Villanueva et al., 1988; Bouhassira et al., 1992). DRN forms, as other parts of RF, strong bilateral connections to the facial nucleus (Hattox et al., 2002; Leite-Almeida et al., 2006). Indeed, mice move their whiskers, as well as other parts of the face, in response to pain (Langford et al., 2010). In addition, DRN projects to dozens of other brain structures, including other parts of RF, the ipsilateral amygdala, periaqueductal gray, red nucleus, and SpV, as well as the contralateral IO, SC, ZI, and several nuclei of the thalamus, including Pom and to a lesser extent VPM (Leite-Almeida et al., 2006). Apart from a role in pain transmission, RF is also involved in "normal" whisker movements. RF neurons receiving trigeminal input project to the lateral facial and hypoglossal nuclei (Dauvergne et al., 2001). In addition, RF receives direct input from wM1, and RF stimulation causes whisker retraction (Matyas et al., 2010). RF also receives cholinergic input from the pedunculopontine tegmental nuclei (Jones, 1990) and noradrenergic input from the locus coeruleus (Jones, 1991), indicating that RF activity is strongly modulated by the general state of alertness.

Zona incerta

The zona incerta can be functionally divided into rostral (ZIr), dorsal (ZId), ventral (ZIv), and caudal (ZIc) sectors (Kim et al., 1992; Ma et al., 1992; Nicolelis et al., 1992, 1995b) and contributes to the whisker paralemniscal somatosensory pathway (Urbain and Deschênes, 2007a). It has been said to have connections with almost every center in the neuraxis (Mitrofanis, 2005). Multiple whisker receptive fields have been found in both ZId and ZIv. A somatotopic map was found to be partial in ZId and complete in ZIv. The ZId somatotopic map was characterized by large facial receptive fields including the whiskers (Nicolelis et al., 1992; Simpson et al., 2008). Direct whisker input reaches ZI mainly from both

PrV and SpVi (Lin et al., 1990; Kolmac et al., 1998; Lavallée et al., 2005), but also via wS1 (Lin et al., 1990; Aronoff et al., 2010). Most likely, the main impact of ZI on the whisker system is by its GABAergic output to Pom. The thalamus can be divided into first order and higher-order nuclei where the latter can be defined by different coding strategies, receptive field properties and cortical layer 5 input (Diamond et al., 1992a; Ojima, 1994; Ahissar et al., 2000). ZI forms GABAergic projections that terminate on such higher-order thalamic nuclei (Barthó et al., 2002). During rest, ZIv inhibits whisker sensory transmission via Pom (Lavallée et al., 2005). However, wM1 input to the motor subsector of ZI can induce GABAergic interneurons that inhibit the whisker sensory subsector of ZI, which in turn disinhibits the relay cells of Pom, providing a mechanism of lateral inhibition in ZI (Urbain and Deschênes, 2007b). Thus, during active whisker movements, wM1 activity releases the inhibition on sensory gating in Pom. This implies that Pom transmits more details on whisker input during active movement than during periods of rest. Apart from wM1, also cholinergic input from PPTg and the laterodorsal tegmental nucleus (LDTg) can reduce the inhibitory output of ZIv to Pom (Trageser et al., 2006). Since the cholinergic input to ZI is highest during active states (Trageser et al., 2006), this is a possible second form of gating of the whisker input to wS1 under control of ZI. ZI forms also GABAergic projections to the intermediate and deep layers of SC, that in turn project back to ZI (Roger and Cadusseau, 1985; May, 2006). In addition, ZId has glutamatergic projections to the basal ganglia (Heise and Mitrofanis, 2004).

Anterior pretectal nucleus

Like ZI, the APT nucleus provides strong GABAergic inhibition in Pom. The morphology of the projections to Pom from ZI and APT are similar, forming multiple synapses on the thick dendrites of relay cells, and different from RT projections that form single synapses on the thin, distal dendrites of relay cells (Bokor et al., 2005; Wanaverbecq et al., 2008). Input from APT strongly suppresses whisker responses in Pom (Murray et al., 2010). In view of the heterogeneity in firing patterns of APT neurons observed *in vivo*, it has been suggested that APT, like ZI, controls the thalamo-cortical output in a state-dependent manner (Bokor et al., 2005). ZI and APT are reciprocally connected. There is a strong projection of both GABAergic and non-GABAergic APT neurons to ZIv, from where the thalamic projections originate (May et al., 1997). The reciprocal connection from ZIv to APT is relatively sparse (May et al., 1997; Giber et al., 2008). Thus, ZI and APT may cooperate in controlling the flow of information from Pom to the cerebral cortex in a state-dependent manner.

Apart from ZI and Pom, APT also targets a large number of brain regions. The functional relevance of these other outputs for the whisker system is still unclear, but potentially relevant target areas are SC, the pontomedullary RF, the pontine nucleus, red nucleus, and (dorsal) IO (Cadusseau and Roger, 1991; Terenzi et al., 1995; Zagon et al., 1995). In turn, APT receives strong input from amongst others wS1, SC, the deep mesencephalic nucleus, and PPTg, as well as sparse input from the locus coeruleus and the periaqueductal gray (Foster et al., 1989; Cadusseau and Roger, 1991).

Red nucleus

The red nucleus is closely associated with limb movements (Massion, 1988; Muir and Whishaw, 2000) and is composed of two parts. The magnocellular part receives input from the cerebral cortex, including wS1 and wM1 (Alloway et al., 2010), as well as from the cerebellar interposed nucleus (Teune et al., 2000), and sends its output to the contralateral limbs via the rubrospinal tract (ten Donkelaar, 1988; Paul and Gould, 2010). The parvocellular part receives its input from the cerebellar dentate nucleus (Teune et al., 2000) and sends its output to the contralateral facial nucleus (Hattox et al., 2002). Thus, from an anatomical point of view, the red nucleus is strongly implicated in the whisker system. However, electrical stimulation of the red nucleus did not evoke whisker movements in a consistent way (Isokawa-Akesson and Komisaruk, 1987).

Pontine respiratory group

The parabrachial complex and the Kölliker-Fuse nucleus, both part of the pontine respiratory group, provide strong, ipsilateral projections to the lateral facial nucleus (Isokawa-Akesson and Komisaruk, 1987; Hattox et al., 2002). The pontine respiratory group projects to several areas of the medullar respiratory group, and may therefore affect the respiratory rhythm (Smith et al., 2009). Thus, the connection between the pontine respiratory group and the lateral facial nucleus may facilitate the synchronization of sniffing and whisking. Such coupling is prominent during exploratory whisking (Welker, 1964).

Ambiguus nucleus

The ambiguus nucleus has a dense projection to the ipsilateral lateral facial nucleus (Isokawa-Akesson and Komisaruk, 1987; Hattox et al., 2002). Electrical stimulation of the ambiguus nucleus could evoke ipsilateral, rhythmic whisker movements with a remarkably low stimulation threshold (Isokawa-Akesson and Komisaruk, 1987). Since the ambiguus nucleus is mainly involved in respiration (Delgado-García et al., 1983) and swallowing (Broussard and Altschuler, 2000), it could serve to synchronize whisker movements to respiration and swallowing.

Other brain regions

This list of brain regions is incomplete since we lack sufficient knowledge of other brain regions which might be involved in the whisker system. Potentially important areas include the deep mesencephalic nucleus and the periaqueductal gray. The deep mesencephalic nucleus receives a strong, ipsilateral input from wM1, and forms dense projections to the lateral facial nucleus (Hattox et al., 2002; Alloway et al., 2010). Yet, its function for the whisker system is not clear. The periaqueductal gray is, amongst others, important for pain transmission and integrating defensive behavior (Behbehani, 1995; Graeff, 2004). Stimulating the periaqueductal gray results in whisker twitches (Verberne and Struyker Boudier, 1991). The periaqueductal gray receives serotonergic input from the dorsal raphe nucleus (Graeff, 2004), strong input from ipsilateral wM1 (Alloway et al., 2010), and forms relatively sparse, bilateral connections to the lateral facial nucleus (Hattox et al., 2002). For further connections of the periaqueductal gray, see Vianna and Brandão (2003).

BILATERAL COORDINATION OF WHISKER MOVEMENTS

In the absence of object contact and head movements, whisker movements on both sides of the head tend to be symmetric. However, during active exploration, in particular involving head movements, whisker movements are often asymmetric (Towal and Hartmann, 2006, 2008; Mitchinson et al., 2007). This implies that both hemispheres are interconnected, but can be decoupled if the actual behavior requires to do so. In line with this, many, if not most, of the connections discussed in this review are actually bilateral, although the strengths of the ipsi- and contralateral projections are often quite different (see also Alloway et al., 2010). Putative candidates for the modification of interhemispheric connections, especially involving wM1, are the feedback loops with the thalamus, the basal ganglia, and the claustrum (Alloway et al., 2008, 2009, 2010). Particularly the claustrum has been proposed to facilitate interhemispheric communication of wM1 (Alloway et al., 2009; Smith and Alloway, 2010). wM1 targets the claustrum mainly contralaterally, and the claustrum projects mainly ipsilaterally to wM1. These projections are highly specific: the cortico-claustro-cortical projections connect the same whisker fields in wM1 of both hemispheres (Smith and Alloway, 2010).

AROUSAL, ALERTNESS, AND ATTENTION

Whisker movements and the processing of whisker input depend on the general state of alertness. For instance, stimulation of wM1 leads to larger whisker movements in aroused rather than in awake, but sessile rats (Berg et al., 2005). Furthermore, whisker stimuli evoke smaller responses in wS1 showing less spreading during whisking than during rest (Ferezou et al., 2007). The neural systems that control the general state of alertness affect many brain regions and are not specific for the whisker system. We discuss here those systems of which clear effects on the whisker system have been documented or can be expected based on anatomical connections.

ACETYLCHOLINE

Central cholinergic projections, mainly originating from the basal forebrain and the tegmentum, affect the whisker system at different levels (Woolf, 1991; Dani and Bertrand, 2007). Roughly, the basal forebrain targets wS1 and wM1, while the tegmentum targets several subcortical areas. The basal forebrain is composed of several areas that provide cholinergic output, including the nucleus basalis magnocellularis (NBM; known as the Meynert nucleus in primates) of the substantia innominata. NBM is active during waking and REM sleep, but not during slow-wave sleep (Lee et al., 2005). The main projection areas of the cholinergic neurons of NBM are the entire cerebral cortex and the amygdala (Wenk, 1997; Deurveilher and Semba, 2011). Electrical stimulation of the cholinergic neurons of the NBM leads to an increased effect of wM1 stimulation on whisker movements. This effect of NBM stimulation is only observed in sessile, but less so in aroused rats (Berg et al., 2005). This could indicate that NBM is already endogenously active in aroused rats.

In addition to enhancing motor performance, cholinergic afferents also increase the sensitivity to sensory stimuli. The response to whisker stimulation in wS1 is increased due to acetylcholine (ACh; Oldford and Castro-Alamancos, 2003; Constantinople and Bruno, 2011). This effect is partly due to stimulation of the basal forebrain, which enhances especially the responses to non-dominant whiskers (Kuo et al., 2009). In addition, cholinergic projections from PPTg and LDTg, increase the responses to whisker stimulation in VPM, and consequently also in wS1 (Hirata and Castro-Alamancos, 2010, 2011). Furthermore, the responsiveness to whisker input of Pom is increased by cholinergic input from PPTg as well as from LDTg, due to both direct connections to Pom, where the cholinergic fibers suppress the release of GABA from projections originating in ZI (Masri et al., 2006), as well as indirectly by decreasing the neuronal activity of GABAergic projection neurons in ZI (Trageser et al., 2006). In SpVi, a similar phenomenon occurs as in wS1: activity of the cholinergic input from PPTg increases the responsivity of sensory neurons to inputs from adjacent whiskers (Timofeeva et al., 2005). Finally, there are also cholinergic projections from PPTg and LDTg to SC, PrV, and the lateral facial nucleus (Satoh and Fibiger, 1986; Beak et al., 2010), but their specific functions for the whisker system are currently unknown.

The nucleus basalis magnocellularis receives strong input from the amygdala, the hypothalamus, and the thalamus, as well as from specific areas of the cerebral cortex, probably including the prefrontal and motor cortex (Haring and Wang, 1986; Irle and Markowitsch, 1986). In addition, there are weaker inputs from many other (subcortical) regions (Haring and Wang, 1986; Irle and Markowitsch, 1986). Inputs to PPTg and LDTg come from a wide range of brain regions, including the medial prefrontal and cingulate cortex (but not wS1, wS2, and wM1), the thalamus, the hypothalamus, ZI, the periaqueductal gray, SC, the pontomedullary RF, the dorsal raphe nuclei as well as from many other regions not directly involved in the whisker system (Semba and Fibiger, 1992). The input from the trigeminal and cerebellar nuclei is relatively weak (Semba and Fibiger, 1992).

In conclusion, when the cholinergic system is quiet, as during slow-wave sleep (Lee et al., 2005), whisker sensitivity is reduced, and primarily focused on the dominant whiskers. During more attentive states, input from non-dominant whiskers is processed, yielding a more detailed impression of the environment. At the same time, the cholinergic system facilitates whisker movements during arousal, which increases the sensitivity of the whisker system even further.

NORADRENALINE

Noradrenergic projections have similar effects on the sensitivity to whisker stimulation as cholinergic projections. The origin of noradrenaline is the locus coeruleus and adjacent brainstem regions (Aston-Jones and Cohen, 2005). Noradrenaline suppresses spontaneous activity of VPM via RT. As a consequence, sensory input is passed on to wS1 with a higher signal-to-noise ratio (Hirata et al., 2006; Hirata and Castro-Alamancos, 2011). In addition, the locus coeruleus can directly modulate the network dynamics of wS1 (Constantinople and Bruno, 2011). Activity of the locus coeruleus is closely related to awakeness and alertness (Aston-Jones and Cohen, 2005). Indeed, a novel environment can stimulate activity of the locus coeruleus and the anterior cingulate cortex, and thus keep the animal fully awake (Gompf et al., 2010). The main inputs to the locus coeruleus come from RF and the hypoglossal nucleus

(Jones, 1991). Other relevant outputs are directed to RF, the facial nucleus, ZI, and NBM (Jones, 1991). Thus, although noradrenaline works via different mechanisms than ACh, both increase the level of arousal as well as the sensitivity toward whisker input.

HISTAMINE

Histamine is also only released during wakefulness (Takahashi et al., 2006). It promotes, amongst others, vigilance (Anaclet et al., 2009; Thakkar, 2011) and the coordination of goal-directed behaviors (Valdés et al., 2010). The sole source of histamine in the brain is the hypothalamus, most notably the tuberomammillary nuclei and perhaps also the surrounding tissue (Wouterlood et al., 1986; Passani and Blandina, 2011). The tuberomammillary nuclei project to almost all brain regions, including cerebral cortex, thalamus, brainstem, and cerebellum (Pillot et al., 2002). Histaminergic connections of particular importance for the whisker system include ipsilateral projections from the ventrolateral tuberomammillary nucleus to wS1 and wM1 (Hong et al., 2010). The dorsomedial tuberomammillary nucleus projects bilaterally to PrV and the lateral facial nucleus (Hong et al., 2010). In addition, all layers of SC, but mainly the superficial ones, receive histaminergic input (Manning et al., 1996). Thus, there are histaminergic connections to many of the important whisker regions, and although the specific functions of these connections are currently unknown, it seems likely that histamine has a general, stimulating effect on the whisker system, comparable to that of acetylcholine and noradrenaline.

SEROTONIN

The activity of most serotonergic neurons of the dorsal raphe nucleus is strongly affected by the sleep/wake rhythm. In the awake state, they fire at very regular intervals (McGinty and Harper, 1976; Kocsis et al., 2006; Urbain et al., 2006). The dorsal raphe nucleus projects to the lateral facial nucleus (Hattox et al., 2003; Cramer and Keller, 2006; Lee et al., 2008c), where serotonin facilitates a persistent inward current (PIC) in the whisker motor neurons. This lowers their activation thresholds (Cramer et al., 2007). Indeed, spontaneous as well as wM1-induced whisker movements are largely abolished following block of serotonin receptors (**Figure 7B**; Hattox et al., 2003; Cramer and Keller, 2006). Thus, serotonin is both required and sufficient to generate a rhythmic whisker movement pattern, and it also modulates inputs from wM1. That makes the serotonergic system a fourth system that modulates the whisker system according to the state of alertness of the animal, together with the cholinergic, noradrenergic, and histaminergic systems.

The dorsal raphe nucleus receives inputs from wM1, but also from a wide range of cortical and subcortical areas. Particularly strong inputs come from regions with an emotional and/or cognitive function, such as the medial prefrontal cortex and the amygdala (Lee et al., 2003; Hale and Lowry, 2011). The regular spiking patterns of the dorsal raphe nucleus are in line with its putative function as CPG for rhythmic whisker movements (Hattox et al., 2003). The spiking pattern of the dorsal raphe nucleus can be perturbed by, amongst others, whisker touch and, to a lesser extent, free whisking in air (Waterhouse et al., 2004). The dorsal raphe nucleus projects to the prefrontal cortex and many regions directly involved in the whisker system. The midline region projects to ipsilateral wS1 and wM1, and the lateral wing division to ipsilateral VPMvl, PrV, and facial nucleus (**Figure 7A**; Kirifides et al., 2001; Sheibani and Farazifard, 2006; Lee et al., 2008c). Thus, next to being a CPG for rhythmic whisker movements via its direct connection to the lateral facial nucleus, the dorsal raphe nucleus affects several other regions of the whisker system.

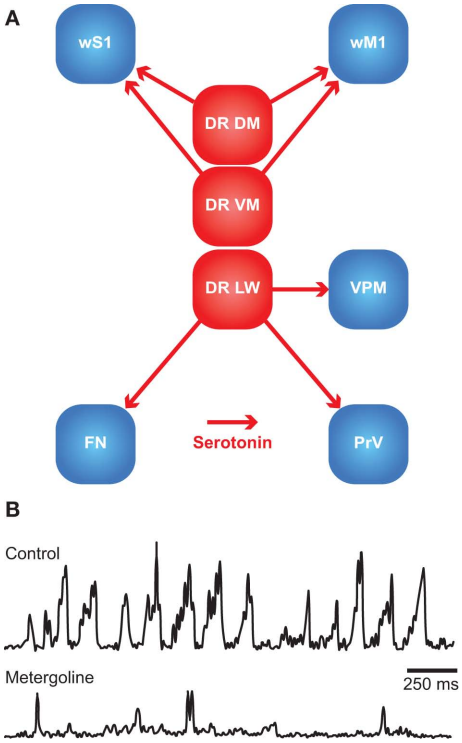

FIGURE 7 | The dorsal raphe nuclei as central pattern generator. (A) Schematic overview of the main serotonergic connections from the dorsal raphe nuclei to the brain regions of the whisker system. DR DM, dorsomedial dorsal raphe nucleus; DR LW, lateral wing division of the dorsal raphe nucleus; DR VM, ventromedial dorsal raphe nucleus; FN, facial nucleus; PrV, principal trigeminal nucleus; VPM, medial ventroposterior nucleus; wM1, whisker motor cortex; wS1, barrel cortex. **(B)** During exploratory whisking, rhythmic whisker movements occur, as shown here by EMG recordings of rat whisker muscles. Application of metergoline, an antagonist for the serotonin receptors 5-HT_1 and 5-HT_2, in the facial nucleus abolishes the rhythmicity of whisker movements unilaterally at the side of injection. Most likely, the dorsal raphe nuclei are the source of serotonin. This indicates that the dorsal raphe nuclei may act as central pattern generator for whisker movements. Reproduced with permission from Hattox et al. (2003).

TIMING IN THE WHISKER SYSTEM

Timing is essential for the whisker system. During active touch, rats move their whiskers rhythmically over an object. Irregularities in the surface texture cause small disruptions in the whisker movements, which evoke neuronal responses (**Figures 1B,C**; Szwed et al., 2003; Hartmann, 2009; Jadhav and Feldman, 2010). Active touch can be instrumental for several forms of behavior. For instance, Etruscan shrews use their whiskers to locate prey. On

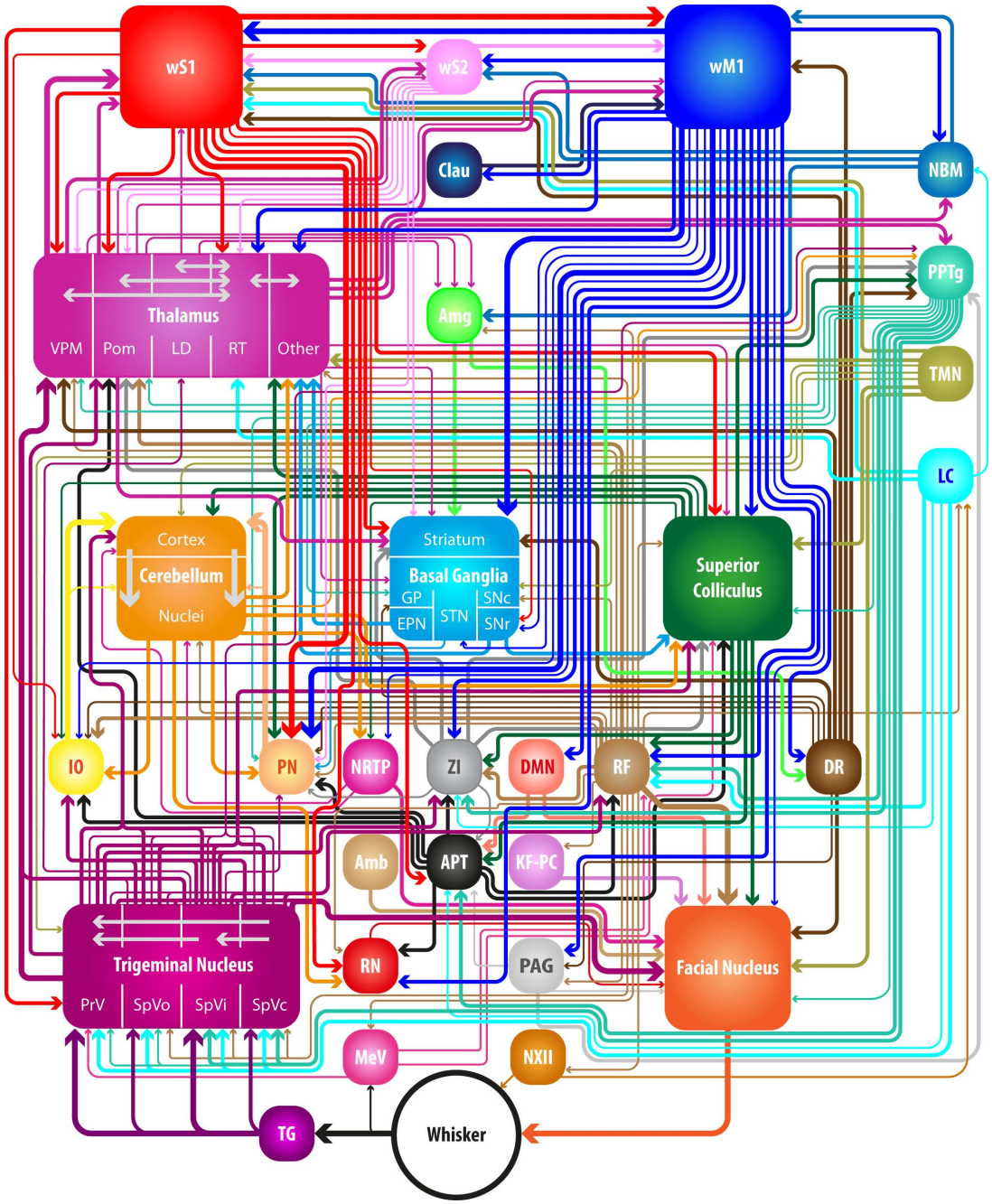

FIGURE 8 | Neuronal connections in the whisker system. Many brain regions are involved in controlling the whiskers. Schematic representation of the connections discussed in the main text. Thickness of the arrows corresponds to the robustness of the connection involved (divided among three different levels). Some local connections are indicated, but for the connections between the nuclei of the basal ganglia, see **Figure 5A**. Amb, ambiguus nucleus; Amg, amygdala; APT, anterior pretectal nucleus; Clau, claustrum; DMN, deep mesencephalic nucleus; DR, dorsal raphe nucleus; EPN, entopeduncular nucleus; GP, globus pallidus; IO, inferior olive; KF–PC, Kölliker-Fuse nucleus and parabrachial complex; LC, locus coeruleus; LD, laterodorsal nucleus; MeV, mesencephalic trigeminal nucleus; NBM, nucleus basalis magnocellularis; NRTP, nucleus reticularis tegmenti pontis; NXII, hypoglossal nucleus; PAG, periaqueductal gray; PN, pontine nucleus; Pom, medial posterior nucleus; PPTg, pedunculopontine tegmental nucleus and the laterodorsal tegmental nucleus; PrV, principal trigeminal nucleus; RF, pontomedullar reticular formation; RN, red nucleus; RT, reticular nucleus; SNc, substantia nigra pars compacta; SNr, substantia nigra pars reticulata; SpVc, spinal trigeminal nucleus pars caudalis; SpVi, spinal trigeminal nucleus pars interpolaris; SpVo, spinal trigeminal nucleus pars oralis; STN, subthalamic nucleus; TG, trigeminal ganglion; TMN, tuberomammillary nucleus; VPM, medial ventroposterior nucleus; wM1, whisker motor cortex; wS1, barrel cortex; wS2, whisker part of the secondary somatosensory cortex; ZI, zona incerta.

average, they initiate an attack on average 179 ms after the first whisker contact, but this interval can be as short as 53 ms (Munz et al., 2010). Indeed, the vibrissae can be used experimentally to explore interval timing. Stimulation of the vibrissae can act as a CS in eyeblink conditioning (Das et al., 2001; Leal-Campanario et al., 2006; Galvez et al., 2009). The reverse is also possible: to evoke vibrissal movements as an unconditioned response (UR; Troncoso et al., 2004).

Whisker responses are rapidly distributed over the brain. Many brain regions receive direct input from the trigeminal nuclei, often in addition to input from wS1 (**Figure 8**). As a consequence, the whisker responses in the cerebellum (Bosman et al., 2010) and SC (Bezdudnaya and Castro-Alamancos, 2011) are bi-phasic. Fast, direct whisker responses are followed by wS1-mediated responses with longer latencies. This allows for fast, multi-center processing of whisker data.

Although wM1 is able to evoke, on a cycle-by-cycle base, rhythmic whisker movements under experimental conditions involving artificial disinhibition (Castro-Alamancos, 2006), under more physiological conditions, the frequency of microstimulation in wM1 does not necessarily correspond to the frequency of the evoked whisker movements (Berg and Kleinfeld, 2003b; Haiss and Schwarz, 2005). However, widespread rhythmic activity (at 7–12 Hz) involving cerebral cortex, thalamus, and brainstem often precedes the onset of rhythmic whisker movements, which is then phase-locked to the brain oscillations (Nicolelis et al., 1995a). Nevertheless, it is likely that subcortical structures critically participate in the generation of rhythmicity of the whisker movements. The serotonergic projection from the dorsal raphe nuclei to the facial nucleus has especially been found to be effective in generating rhythmic whisker movements (Hattox et al., 2003). However also the cerebellum and IO may be involved. After blocking IO pharmacologically, as well as following cerebellectomy, the frequency-dependence of whisker movements following wM1 stimulation was altered (Lang et al., 2006). In contrast, SC does not seem to be involved in the generation of rhythmic movements, as its activity causes prolonged whisker protractions (Hemelt and Keller, 2008).

CONCLUSION

Whiskers play a central role in the lives and loves of rodents. Accordingly, many brain regions can affect whisker movements. Whisker movements depend on the general state of arousal, they are coupled to the movements of other mobile senses, like the eyes and the auricles, and integrated with other forms of behavior, like sniffing, swallowing, and locomotion. Animals orient their whiskers based on reward expectancy, for instance when searching for food. With respect to whisker input, the level of detail that is transmitted to higher brain areas depends on the general state of arousal as well as on the activity of the whisker motor cortex, and the context of the animal's environment. The sensory and motor systems of the whiskers are coupled by a number of sensorimotor feedback loops, allowing the animals to adjust whisker movements to sensory input. Unfortunately, many of the brain regions involved in these feedback loops have received relatively little attention with respect to the whisker system. Hence, our knowledge on the relative importance of these areas and their connections is incomplete. Yet, based on the current data available to us, we present a scheme of the relevant anatomical connections in **Figure 8**. Although these brain structures have many more connections, we have attempted to highlight the most prominent ones. However, the complexity of the whisker system seems to depend on the behavioral state; the more active an animal is, the more complex its whisker movements are and therefore a greater level of detail results during sensory and motor information processing.

ACKNOWLEDGMENTS

The authors thank Drs. Frank Rice and Hans Dringenberg for their comments on a previous version of the manuscript and Dr. Reha Erzurumlu for contributing an unpublished photomicrograph. We kindly thank the Netherlands Organization for Scientific Research (NWO; AH), the Dutch Organization for Medical Sciences (ZonMw; CIDZ), Life Sciences (ALW; CIDZ), Senter (Neuro-Bsik; CIDZ), Prinses Beatrix Fonds (CIDZ), and the SENSOPAC, CEREBNET, and C7 programs of the European Community (CIDZ) for their financial support. We also thank our lab members for valuable discussions.

REFERENCES

Ahissar, E., Sosnik, R., and Haidarliu, S. (2000). Transformation from temporal to rate coding in a somatosensory thalamocortical pathway. *Nature* 406, 302–306.

Ahl, A. S. (1982). Evidence of use of vibrissae in swimming in *Sigmodon fulviventer*. *Anim. Behav.* 30, 1203–1206.

Ahl, A. S. (1986). The role of vibrissae in behavior: a status review. *Vet. Res. Commun.* 10, 245–268.

Akaike, T. (1992). The tectorecipient zone in the inferior olivary nucleus in the rat. *J. Comp. Neurol.* 320, 398–414.

Alloway, K. D. (2008). Information processing streams in rodent barrel cortex: the differential functions of barrel and septal circuits. *Cereb. Cortex* 18, 979–989.

Alloway, K. D., Crist, J., Mutic, J. J., and Roy, S. A. (1999). Corticostriatal projections from rat barrel cortex have an anisotropic organization that correlates with vibrissal whisking behavior. *J. Neurosci.* 19, 10908–10922.

Alloway, K. D., Lou, L., Nwabueze-Ogbo, F., and Chakrabarti, S. (2006). Topography of cortical projections to the dorsolateral neostriatum in rats: multiple overlapping sensorimotor pathways. *J. Comp. Neurol.* 499, 33–48.

Alloway, K. D., Mutic, J. J., Hoffer, Z. S., and Hoover, J. E. (2000). Overlapping corticostriatal projections from the rodent vibrissal representations in primary and secondary somatosensory cortex. *J. Comp. Neurol.* 428, 51–67.

Alloway, K. D., Olson, M. L., and Smith, J. B. (2008). Contralateral corticothalamic projections from MI whisker cortex: potential route for modulating hemispheric interactions. *J. Comp. Neurol.* 510, 100–116.

Alloway, K. D., Smith, J. B., and Beauchemin, K. J. (2010). Quantitative analysis of the bilateral brainstem projections from the whisker and forepaw regions in rat primary motor cortex. *J. Comp. Neurol.* 518, 4546–4566.

Alloway, K. D., Smith, J. B., Beauchemin, K. J., and Olson, M. L. (2009). Bilateral projections from rat MI whisker cortex to the neostriatum, thalamus, and claustrum: forebrain circuits for modulating whisking behavior. *J. Comp. Neurol.* 515, 548–564.

Alloway, K. D., Zhang, M., and Chakrabarti, S. (2004). Septal columns in rodent barrel cortex: functional circuits for modulating whisking behavior. *J. Comp. Neurol.* 480, 299–309.

Anaclet, C., Parmentier, R., Ouk, K., Guidon, G., Buda, C., Sastre, J. P., Akaoka, H., Sergeeva, O. A., Yanagisawa, M., Ohtsu, H., Franco, P., Haas, H. L., and Lin, J. S. (2009). Orexin/hypocretin and histamine: distinct roles in the control of wakefulness demonstrated using knockout mouse models. *J. Neurosci.* 29, 14423–14438.

Andermann, M. L., and Moore, C. I. (2006). A somatotopic map of vibrissa motion direction within a barrel column. *Nat. Neurosci.* 9, 543–551.

Anjum, F., Turni, H., Mulder, P. G. H., van der Burg, J., and Brecht, M. (2006). Tactile guidance of prey capture in Etruscan shrews. *Proc. Natl. Acad. Sci. U.S.A.* 103, 16544–16549.

Apps, R., and Hawkes, R. (2009). Cerebellar cortical organization: a one-map hypothesis. *Nat. Rev. Neurosci.* 10, 670–681.

Arabzadeh, E., Zorzin, E., and Diamond, M. E. (2005). Neuronal encoding of texture in the whisker sensory pathway. *PLoS Biol.* 3, e17. doi: 10.1371/journal.pbio.0030017

Armstrong-James, M., and Callahan, C. A. (1991). Thalamo-cortical processing of vibrissal information in the rat. II. Spatiotemporal convergence in the thalamic ventroposterior medial nucleus (VPm) and its relevance to generation of receptive fields of S1 cortical "barrel" neurones. *J. Comp. Neurol.* 303, 211–224.

Armstrong-James, M., and Fox, K. (1987). Spatiotemporal convergence and divergence in the rat S1 "barrel" cortex. *J. Comp. Neurol.* 263, 265–281.

Aronoff, R., Matyas, F., Mateo, C., Ciron, C., Schneider, B., and Petersen, C. C. H. (2010). Long-range connectivity of mouse primary somatosensory barrel cortex. *Eur. J. Neurosci.* 31, 2221–2233.

Ashwell, K. W. (1982). The adult mouse facial nerve nucleus: morphology and musculotopic organization. *J. Anat.* 135, 531–538.

Aston-Jones, G., and Cohen, J. D. (2005). An integrative theory of locus coeruleus-norepinephrine function: adaptive gain and optimal performance. *Annu. Rev. Neurosci.* 28, 403–450.

Aumann, T. D., Rawson, J. A., Finkelstein, D. I., and Horne, M. K. (1994). Projections from the lateral and interposed cerebellar nuclei to the thalamus of the rat: a light and electron microscopic study using single and double anterograde labelling. *J. Comp. Neurol.* 349, 165–181.

Axelrad, H., and Crepel, F. (1977). Représentation sélective des vibrisses mystaciales au niveau des cellules de Purkinje du cervelet par la voie des fibres grimpantes chez le rat. *C.R. Hebd. Seances Acad. Sci. Ser. D Sci. Nat.* 284, 1321–1324.

Barthó, P., Freund, T. F., and Acsády, L. (2002). Selective GABAergic innervation of thalamic nuclei from zona incerta. *Eur. J. Neurosci.* 16, 999–1014.

Barthó, P., Slézia, A., Varga, V., Bokor, H., Pinault, D., Buzsáki, G., and Acsády, L. (2007). Cortical control of zona incerta. *J. Neurosci.* 27, 1670–1681.

Beak, S. K., Hong, E. Y., and Lee, H. S. (2010). Collateral projection from the forebrain and mesopontine cholinergic neurons to whisker-related, sensory and motor regions of the rat. *Brain Res.* 1336, 30–45.

Beckstead, R. M., Domesick, V. B., and Nauta, W. J. H. (1979). Efferent connections of the substantia nigra and ventral tegmental area in the rat. *Brain Res.* 175, 191–217.

Behbehani, M. M. (1995). Functional characteristics of the midbrain periaqueductal gray. *Prog. Neurobiol.* 46, 575–605.

Beitz, A. J. (1989). Possible origin of glutamatergic projections to the midbrain periaqueductal gray and deep layer of the superior colliculus of the rat. *Brain Res. Bull.* 23, 25–35.

Belford, G. R., and Killackey, H. P. (1979). Vibrissae representation in subcortical trigeminal centers of the neonatal rat. *J. Comp. Neurol.* 183, 305–321.

Benison, A. M., Rector, D. M., and Barth, D. S. (2007). Hemispheric mapping of secondary somatosensory cortex in the rat. *J. Neurophysiol.* 97, 200–207.

Berg, R. W., Friedman, B., Schroeder, L. F., and Kleinfeld, D. (2005). Activation of nucleus basalis facilitates cortical control of a brain stem motor program. *J. Neurophysiol.* 94, 699–711.

Berg, R. W., and Kleinfeld, D. (2003a). Rhythmic whisking by rat: retraction as well as protraction of the vibrissae is under active muscular control. *J. Neurophysiol.* 89, 104–117.

Berg, R. W., and Kleinfeld, D. (2003b). Vibrissa movement elicited by rhythmic electrical microstimulation to motor cortex in the aroused rat mimics exploratory whisking. *J. Neurophysiol.* 90, 2950–2963.

Bermejo, R., Friedman, W., and Zeigler, H. P. (2005). Topography of whisking II: interaction of whisker and pad. *Somatosens. Mot. Res.* 22, 213–220.

Bermejo, R., Vyas, A., and Zeigler, H. P. (2002). Topography of rodent whisking I. Two-dimensional monitoring of whisker movements. *Somatosens. Mot. Res.* 19, 341–346.

Bezdudnaya, T., and Castro-Alamancos, M. A. (2011). Superior colliculus cells sensitive to active touch and texture during whisking. *J. Neurophysiol.* 106, 332–346.

Bezdudnaya, T., and Keller, A. (2008). Laterodorsal nucleus of the thalamus: a processor of somatosensory inputs. *J. Comp. Neurol.* 507, 1979–1989.

Blanchard, R. J., Takahashi, L. K., Fukunaga, K. K., and Blanchard, D. C. (1977). Functions of the vibrissae in the defensive and aggressive behavior of the rat. *Aggress. Behav.* 3, 231–240.

Boehnke, S. E., and Munoz, D. P. (2008). On the importance of the transient visual response in the superior colliculus. *Curr. Opin. Neurobiol.* 18, 544–551.

Bokor, H., Acsády, L., and Deschênes, M. (2008). Vibrissal responses of thalamic cells that project to the septal columns of the barrel cortex and to the second somatosensory area. *J. Neurosci.* 28, 5169–5177.

Bokor, H., Frère, S. G. A., Eyre, M. D., Slézia, A., Ulbert, I., Lüthi, A., and Acsády, L. (2005). Selective GABAergic control of higher-order thalamic relays. *Neuron* 45, 929–940.

Bosman, L. W. J., Koekkoek, S. K. E., Shapiro, J., Rijken, B. F. M., Zandstra, F., van der Ende, B., Owens, C. B., Potters, J. W., de Gruijl, J. R., Ruigrok, T. J. H., and De Zeeuw, C. I. (2010). Encoding of whisker input by cerebellar Purkinje cells. *J. Physiol. (Lond.)* 588, 3757–3783.

Bosman, L. W. J., Takechi, H., Hartmann, J., Eilers, J., and Konnerth, A. (2008). Homosynaptic LTP of the "winner" climbing fiber synapse in developing Purkinje cells. *J. Neurosci.* 28, 798–807.

Bostan, A. C., Dum, R. P., and Strick, P. L. (2010). The basal ganglia communicate with the cerebellum. *Proc. Natl. Acad. Sci. U.S.A.* 107, 8452–8456.

Bouhassira, D., Villanueva, L., Bing, Z., and le Bars, D. (1992). Involvement of the subnucleus reticularis dorsalis in diffuse noxious inhibitory controls in the rat. *Brain Res.* 595, 353–357.

Bourassa, J., Pinault, D., and Deschênes, M. (1995). Corticothalamic projections from the cortical barrel field to the somatosensory thalamus in rats: a single-fibre study using biocytin as an anterograde tracer. *Eur. J. Neurosci.* 7, 19–30.

Brecht, M. (2007). Barrel cortex and whisker-mediated behaviors. *Curr. Opin. Neurobiol.* 17, 408–416.

Brecht, M., Krauss, A., Muhammad, S., Sinai-Esfahani, L., Bellanca, S., and Margrie, T. W. (2004a). Organization of rat vibrissa motor cortex and adjacent areas according to cytoarchitectonics, microstimulation, and intracellular stimulation of identified cells. *J. Comp. Neurol.* 479, 360–373.

Brecht, M., Schneider, M., Sakmann, B., and Margrie, T. W. (2004b). Whisker movements evoked by stimulation of single pyramidal cells in rat motor cortex. *Nature* 427, 704–710.

Brecht, M., Preilowski, B., and Merzenich, M. M. (1997). Functional architecture of the mystacial vibrissae. *Behav. Brain Res.* 84, 81–97.

Brecht, M., Roth, A., and Sakmann, B. (2003). Dynamic receptive fields of reconstructed pyramidal cells in layers 3 and 2 of rat somatosensory barrel cortex. *J. Physiol. (Lond.)* 553, 243–265.

Brecht, M., and Sakmann, B. (2002a). Dynamic representation of whisker deflection by synaptic potentials in spiny stellate and pyramidal cells in the barrels and septa of layer 4 rat somatosensory cortex. *J. Physiol. (Lond.)* 543, 49–70.

Brecht, M., and Sakmann, B. (2002b). Whisker maps of neuronal subclasses of the rat ventral posterior medial thalamus, identified by whole-cell voltage recording and morphological reconstruction. *J. Physiol. (Lond.)* 538, 495–515.

Brodal, P. (1980). The cortical projection to the nucleus reticularis tegmenti pontis in the rhesus monkey. *Exp. Brain Res.* 38, 19–27.

Brodal, P., and Bjaalie, J. G. (1992). Organization of the pontine nuclei. *Neurosci. Res.* 13, 83–118.

Broussard, D. L., and Altschuler, S. M. (2000). Brainstem viscerotopic organization of afferents and efferents involved in the control of swallowing. *Am. J. Med.* 108(Suppl. 4a), 79S–86S.

Brown, I. E., and Bower, J. M. (2001). Congruence of mossy fiber and climbing fiber tactile projections in the lateral hemispheres of the rat cerebellum. *J. Comp. Neurol.* 429, 59–70.

Brown, J. T., Chan-Palay, V., and Palay, S. L. (1977). A study of afferent input to the inferior olivary complex in the rat by retrograde axonal transport of horseradish peroxidase. *J. Comp. Neurol.* 176, 1–22.

Brumberg, J. C., Pinto, D. J., and Simons, D. J. (1999). Cortical columnar processing in the rat whisker-to-barrel system. *J. Neurophysiol.* 82, 1808–1817.

Bruno, R. M., Khatri, V., Land, P. W., and Simons, D. J. (2003). Thalamocortical angular tuning domains within individual barrels of rat somatosensory cortex. *J. Neurosci.* 23, 9565–9574.

Bureau, I., von Saint Paul, F., and Svoboda, K. (2006). Interdigitated paralemniscal and lemniscal pathways in the mouse barrel cortex. *PLoS Biol.* 4, e382. doi: 10.1371/journal.pbio.0040382

Burne, R. A., Azizi, S. A., Mihailoff, G. A., and Woodward, D. J. (1981). The tectopontine projection the the rat with comments on visual pathways to the basilar pons. *J. Comp. Neurol.* 202, 287–307.

Cadusseau, J., and Roger, M. (1991). Cortical and subcortical connections of the pars compacta of the anterior pretectal nucleus in the rat. *Neurosci. Res.* 12, 83–100.

Carvell, G. E., and Simons, D. J. (1986). Somatotopic organization of the second somatosensory area (SII) in the cerebral cortex of the mouse. *Somatosens. Res.* 3, 213–237.

Carvell, G. E., and Simons, D. J. (1987). Thalamic and corticocortical connections of the second somatic sensory area of the mouse. *J. Comp. Neurol.* 265, 409–427.

Carvell, G. E., and Simons, D. J. (1990). Biometric analyses of vibrissal tactile discrimination in the rat. *J. Neurosci.* 10, 2638–2648.

Carvell, G. E., and Simons, D. J. (1995). Task- and subject-related differences in sensorimotor behavior during active touch. *Somatosens. Mot. Res.* 12, 1–9.

Castro-Alamancos, M. A. (2006). Vibrissa myoclonus (rhythmic retractions) driven by resonance of excitatory networks in motor cortex. *J. Neurophysiol.* 96, 1691–1698.

Cauller, L. J., Clancy, B., and Connors, B. W. (1998). Backward cortical projections to primary somatosensory cortex in rats extend long horizontal axons in layer I. *J. Comp. Neurol.* 390, 297–310.

Chakrabarti, S., and Alloway, K. D. (2006). Differential origin of projections from SI barrel cortex to the whisker representations in SII and MI. *J. Comp. Neurol.* 498, 624–636.

Chakrabarti, S., Zhang, M., and Alloway, K. D. (2008). MI neuronal responses to peripheral whisker stimulation: relationship to neuronal activity in si barrels and septa. *J. Neurophysiol.* 100, 50–63.

Chapin, J. K., Sadeq, M., and Guise, J. L. U. (1987). Corticocortical connections within the primary somatosensory cortex of the rat. *J. Comp. Neurol.* 263, 326–346.

Chernova, O. F. (2006). Evolutionary aspects of hair polymorphism. *Biol. Bull.* 33, 43–52.

Chmielowska, J., Carvell, G. E., and Simons, D. J. (1989). Spatial organization of thalamocortical and corticothalamic projection systems in the rat SmI barrel cortex. *J. Comp. Neurol.* 285, 325–338.

Chu, C. P., Bing, Y. H., and Qiu, D. L. (2011). Sensory stimulus evokes inhibition rather than excitation in cerebellar Purkinje cells in vivo in mice. *Neurosci. Lett.* 487, 182–186.

Cicirata, F., Angaut, P., Cioni, M., Serapide, M. F., and Papale, A. (1986). Functional organization of thalamic projections to the motor cortex. An anatomical and electrophysiological study in the rat. *Neuroscience* 19, 81–99.

Cohen, J. D., Hirata, A., and Castro-Alamancos, M. A. (2008). Vibrissa sensation in superior colliculus: wide-field sensitivity and state-dependent cortical feedback. *J. Neurosci.* 28, 11205–11220.

Colechio, E. M., and Alloway, K. D. (2009). Differential topography of the bilateral cortical projections to the whisker and forepaw regions in rat motor cortex. *Brain Struct. Funct.* 213, 423–439.

Constantinople, C. M., and Bruno, R. M. (2011). Effects and mechanisms of wakefulness on local cortical networks. *Neuron* 69, 1061–1068.

Cosenza, R. M., and Moore, R. Y. (1984). Afferent connections of the ventral lateral geniculate nucleus in the rat: an HRP study. *Brain Res.* 310, 367–370.

Cox, C. L., Huguenard, J. R., and Prince, D. A. (1997). Nucleus reticularis neurons mediate diverse inhibitory effects in thalamus. *Proc. Natl. Acad. Sci. U.S.A.* 94, 8854–8859.

Crabtree, J. W., Collingridge, G. L., and Isaac, J. T. R. (1998). A new intrathalamic pathway linking modality-related nuclei in the dorsal thalamus. *Nat. Neurosci.* 1, 389–394.

Cramer, N. P., and Keller, A. (2006). Cortical control of a whisking central pattern generator. *J. Neurophysiol.* 96, 209–217.

Cramer, N. P., Li, Y., and Keller, A. (2007). The whisking rhythm generator: a novel mammalian network for the generation of movement. *J. Neurophysiol.* 97, 2148–2158.

Crandall, J. E., Korde, M., and Caviness, V. S. Jr. (1986). Somata of layer V projection neurons in the mouse barrelfield cortex are in preferential register with the sides and septa of the barrels. *Neurosci. Lett.* 67, 19–24.

Crochet, S., and Petersen, C. C. H. (2006). Correlating whisker behavior with membrane potential in barrel cortex of awake mice. *Nat. Neurosci.* 9, 608–610.

Crochet, S., Poulet, J. F. A., Kremer, Y., and Petersen, C. C. H. (2011). Synaptic mechanisms underlying sparse coding of active touch. *Neuron* 69, 1160–1175.

Cruikshank, S. J., Lewis, T. J., and Connors, B. W. (2007). Synaptic basis for intense thalamocortical activation of feedforward inhibitory cells in neocortex. *Nat. Neurosci.* 10, 462–468.

Cruikshank, S. J., Urabe, H., Nurmikko, A. V., and Connors, B. W. (2010). Pathway-specific feedforward circuits between thalamus and neocortex revealed by selective optical stimulation of axons. *Neuron* 65, 230–245.

Curtis, J. C., and Kleinfeld, D. (2009). Phase-to-rate transformations encode touch in cortical neurons of a scanning sensorimotor system. *Nat. Neurosci.* 12, 492–501.

Dani, J. A., and Bertrand, D. (2007). Nicotinic acetylcholine receptors and nicotinic cholinergic mechanisms of the central nervous system. *Annu. Rev. Pharmacol. Toxicol.* 47, 699–729.

Das, S., Weiss, C., and Disterhoft, J. F. (2001). Eyeblink conditioning in the rabbit (*Oryctolagus cuniculus*) with stimulation of the mystacial vibrissae as a conditioned stimulus. *Behav. Neurosci.* 115, 731–736.

Dauvergne, C., Pinganaud, G., Buisseret, P., Buisseret-Delmas, C., and Zerari-Mailly, F. (2001). Reticular premotor neurons projecting to both facial and hypoglossal nuclei receive trigeminal afferents in rats. *Neurosci. Lett.* 311, 109–112.

Davie, J. T., Clark, B. A., and Häusser, M. (2008). The origin of the complex spike in cerebellar Purkinje cells. *J. Neurosci.* 28, 7599–7609.

De Kock, C. P. J., Bruno, R. M., Spors, H., and Sakmann, B. (2007). Layer and cell type specific suprathreshold stimulus representation in primary somatosensory cortex. *J. Physiol. (Lond.)* 581, 139.

De Kock, C. P. J., and Sakmann, B. (2009). Spiking in primary somatosensory cortex during natural whisking in awake head-restrained rats is cell-type specific. *Proc. Natl. Acad. Sci. U.S.A.* 106, 16446–16450.

De Zeeuw, C. I., Hoebeek, F. E., Bosman, L. W. J., Schonewille, M., Witter, L., and Koekkoek, S. K. (2011). Spatiotemporal firing patterns in the cerebellum. *Nat. Rev. Neurosci.* 12, 327–344.

De Zeeuw, C. I., and Yeo, C. H. (2005). Time and tide in cerebellar memory formation. *Curr. Opin. Neurobiol.* 15, 667–674.

Dehnhardt, G., Hyvärinen, H., Palviainen, A., and Klauer, G. (1999). Structure and innervation of the vibrissal follicle-sinus complex in the Australian water rat, *Hydromys chrysogaster*. *J. Comp. Neurol.* 411, 550–562.

Dehnhardt, G., and Kaminski, A. (1995). Sensitivity of the mystacial vibrissae of harbour seals (*Phoca vitulina*) for size differences of actively touched objects. *J. Exp. Biol.* 198, 2317–2323.

Dehnhardt, G., Mauck, B., Hanke, W., and Bleckmann, H. (2001). Hydrodynamic trail-following in harbor seals (*Phoca vitulina*). *Science* 293, 102–104.

Dehnhardt, G., Mauck, B., and Hyvärinen, H. (1998). Ambient temperature does not affect the tactile sensitivity of mystacial vibrissae in harbour seals. *J. Exp. Biol.* 201, 3023–3029.

Delgado-García, J. M., López-Barneo, J., Serra, R., and González-Barón, S. (1983). Electrophysiological and functional identification of different neuronal types within the nucleus ambiguus in the cat. *Brain Res.* 277, 231–240.

Deschênes, M., Timofeeva, E., Lavallée, P., and Dufresne, C. (2005). The vibrissal system as a model of thalamic operations. *Prog. Brain Res.* 149, 31–40.

Deschênes, M., Veinante, P., and Zhang, Z. W. (1998). The organization of corticothalamic projections: reciprocity versus parity. *Brain Res. Brain Res. Rev.* 28, 286–308.

Desilets-Roy, B., Varga, C., Lavallée, P., and Deschênes, M. (2002). Substrate for cross-talk inhibition between thalamic barreloids. *J. Neurosci.* 22, RC218.

Deurveilher, S., and Semba, K. (2011). Basal forebrain regulation of cortical activity and sleep-wake states: roles of cholinergic and non-cholinergic neurons. *Sleep Biol. Rhythms* 9, 65–70.

Di Chiara, G., Porceddu, M. L., Morelli, M., Mulas, M. L., and Gessa, G. L. (1979). Evidence for a GABAergic projection from the substantia nigra to the ventromedial thalamus and to the superior colliculus of the rat. *Brain Res.* 176, 273–284.

Di Matteo, V., Pierucci, M., Esposito, E., Crescimanno, G., Benigno, A., and Di Giovanni, G. (2008). Serotonin modulation of the basal ganglia circuitry: therapeutic implication for Parkinson's disease and other motor disorders. *Prog. Brain Res.* 172, 423–463.

Diamond, M. E., Armstrong-James, M., Budway, M. J., and Ebner, F. F. (1992a). Somatic sensory responses in the rostral sector of the posterior group (POm) and in the ventral posterior medial nucleus (VPM) of the rat thalamus: dependence on the barrel field cortex. *J. Comp. Neurol.* 319, 66–84.

Diamond, M. E., Armstrong-James, M., and Ebner, F. F. (1992b). Somatic sensory responses in the rostral sector of the posterior group (POm) and in the ventral posterior medial nucleus (VPM) of the rat thalamus. *J. Comp. Neurol.* 318, 462–476.

Diamond, M. E., von Heimendahl, M., Knutsen, P. M., Kleinfeld, D., and Ahissar, E. (2008). 'Where' and 'what' in the whisker sensorimotor system. *Nat. Rev. Neurosci.* 9, 601–612.

Dörfl, J. (1982). The musculature of the mystacial vibrissae of the white mouse. *J. Anat.* 135, 147–154.

Dörfl, J. (1985). The innervation of the mystacial region of the white mouse: a topographical study. *J. Anat.* 142, 173–184.

Ebara, S., Kumamoto, K., Matsuura, T., Mazurkiewicz, J. E., and Rice, F. L. (2002). Similarities and differences in the innervation of mystacial vibrissal follicle-sinus complexes in the rat and cat: a confocal microscopic study. *J. Comp. Neurol.* 449, 103–119.

Eccles, J., Llinás, R., and Sasaki, K. (1964). Excitation of cerebellar Purkinje cells by the climbing fibres. *Nature* 203, 245–246.

Eller, T., and Chan-Palay, V. (1976). Afferents to the cerebellar lateral nucleus. Evidence from retrograde transport of horseradish peroxidase after pressure injections through micropipettes. *J. Comp. Neurol.* 166, 285–301.

Erzurumlu, R. S., Bates, C. A., and Killackey, H. P. (1980). Differential organization of thalamic projection cells in the brain stem trigeminal complex of the rat. *Brain Res.* 198, 427–433.

Erzurumlu, R. S., and Killackey, H. P. (1979). Efferent connections of the brainstem trigeminal complex with the facial nucleus of the rat. *J. Comp. Neurol.* 188, 75–86.

Erzurumlu, R. S., and Killackey, H. P. (1980). Diencephalic projections of the subnucleus interpolaris of the brainstem trigeminal complex in the rat. *Neuroscience* 5, 1891–1901.

Erzurumlu, R. S., and Killackey, H. P. (1983). Development of order in the rat trigeminal system. *J. Comp. Neurol.* 213, 365–380.

Erzurumlu, R. S., Murakami, Y., and Rijli, F. M. (2010). Mapping the face in the somatosensory brainstem. *Nat. Rev. Neurosci.* 11, 252–263.

Esakov, S. A., and Pronichev, I. V. (2001). Movement representations of facial muscles and vibrissae in cerebellar cortex of the white mouse *Mus musculus*. *J. Evol. Biochem. Physiol.* 37, 642–647.

Esposito, E., Di Matteo, V., and Di Giovanni, G. (2007). Death in the substantia nigra: a motor tragedy. *Expert Rev. Neurother.* 7, 677–697.

Fabri, M., and Burton, H. (1991). Ipsilateral cortical connections of primary somatic sensory cortex in rats. *J. Comp. Neurol.* 311, 405–424.

Favaro, P. D. N., Gouvêa, T. S., de Oliveira, S. R., Vautrelle, N., Redgrave, P., and Comoli, E. (2011). The influence of vibrissal somatosensory processing in rat superior colliculus on prey capture. *Neuroscience* 176, 318–327.

Fee, M. S., Mitra, P. P., and Kleinfeld, D. (1997). Central versus peripheral determinants of patterned spike activity in rat vibrissa cortex during whisking. *J. Neurophysiol.* 78, 1144–1149.

Feldmeyer, D., Lübke, J., Silver, R. A., and Sakmann, B. (2002). Synaptic connections between layer 4 spiny neurone-layer 2/3 pyramidal cell pairs in juvenile rat barrel cortex: physiology and anatomy of interlaminar signalling within a cortical column. *J. Physiol. (Lond.)* 538, 803–822.

Feldmeyer, D., Roth, A., and Sakmann, B. (2005). Monosynaptic connections between pairs of spiny stellate cells in layer 4 and pyramidal cells in layer 5A indicate that lemniscal and paralemniscal afferent pathways converge in the infragranular somatosensory cortex. *J. Neurosci.* 25, 3423–3431.

Ferezou, I., Haiss, F., Gentet, L. J., Aronoff, R., Weber, B., and Petersen, C. C. H. (2007). Spatiotemporal dynamics of cortical sensorimotor integration in behaving mice. *Neuron* 56, 907–923.

Fitzgerald, O. (1940). Discharges from the sensory organs of the cat's vibrissae and the modification in their activity by ions. *J. Physiol. (Lond.)* 98, 163–178.

Foster, G. A., Sizer, A. R., Rees, H., and Roberts, M. H. T. (1989). Afferent projections to the rostral anterior pretectal nucleus of the rat: a possible role in the processing of noxious stimuli. *Neuroscience* 29, 685–694.

Fundin, B. T., Rice, F. L., Pfaller, K., and Arvidsson, J. (1994). The innervation of the mystacial pad in the adult rat studied by anterograde transport of HRP conjugates. *Exp. Brain Res.* 99, 233–246.

Furuta, T., Kaneko, T., and Deschênes, M. (2009). Septal neurons in barrel cortex derive their receptive field input from the lemniscal pathway. *J. Neurosci.* 29, 4089–4095.

Furuta, T., Timofeeva, E., Nakamura, K., Okamoto-Furuta, K., Togo, M., Kaneko, T., and Deschenes, M. (2008). Inhibitory gating of vibrissal inputs in the brainstem. *J. Neurosci.* 28, 1789–1797.

Furuta, T., Urbain, N., Kaneko, T., and Deschênes, M. (2010). Corticofugal control of vibrissa-sensitive neurons in the interpolaris nucleus of the trigeminal complex. *J. Neurosci.* 30, 1832–1838.

Gabernet, L., Jadhav, S. P., Feldman, D. E., Carandini, M., and Scanziani, M. (2005). Somatosensory integration controlled by dynamic thalamocortical feed-forward inhibition. *Neuron* 48, 315–327.

Galvez, R., Weiss, C., Cua, S., and Disterhoft, J. (2009). A novel method for precisely timed stimulation of mouse whiskers in a freely moving preparation: application for delivery of the conditioned stimulus in trace eyeblink conditioning. *J. Neurosci. Methods* 177, 434–439.

Gandhi, N. J., and Katnani, H. A. (2011). Motor functions of the superior colliculus. *Annu. Rev. Neurosci.* 34, 205–231.

Ganmor, E., Katz, Y., and Lampl, I. (2010). Intensity-dependent adaptation of cortical and thalamic neurons is controlled by brainstem circuits of the sensory pathway. *Neuron* 66, 273–286.

Gao, P., Hattox, A. M., Jones, L. M., Keller, A., and Zeigler, H. P. (2003). Whisker motor cortex ablation and whisker movement patterns. *Somatosens. Mot. Res.* 20, 191–198.

Gellman, R., Gibson, A. R., and Houk, J. C. (1985). Inferior olivary neurons in the awake cat: detection of contact and passive body displacement. *J. Neurophysiol.* 54, 40–60.

Gentet, L. J., Avermann, M., Matyas, F., Staiger, J. F., and Petersen, C. C. H. (2010). Membrane potential dynamics of GABAergic neurons in the barrel cortex of behaving mice. *Neuron* 65, 422–435.

Gerdjikov, T. V., Bergner, C. G., Stüttgen, M. C., Waiblinger, C., and Schwarz, C. (2010). Discrimination of vibrotactile stimuli in the rat whisker system: behavior and neurometrics. *Neuron* 65, 530–540.

Gibb, W. R. G., and Lees, A. J. (1988). The relevance of the Lewy body to the pathogenesis of idiopathic Parkinson's disease. *J. Neurol. Neurosurg. Psychiatr.* 51, 745–752.

Giber, K., Slézia, A., Bokor, H., Bodor, A. L., Ludányi, A., Katona, I., and Acsády, L. (2008). Heterogeneous output pathways link the anterior pretectal nucleus with the zona incerta and the thalamus in rat. *J. Comp. Neurol.* 506, 122–140.

Gibson, A. R., Horn, K. M., and Pong, M. (2004). Activation of climbing fibers. *Cerebellum* 3, 212–221.

Gibson, J. M., and Welker, W. I. (1983). Quantitative studies of stimulus coding in first-order vibrissa afferents of rats. 1. Receptive field properties and threshold distributions. *Somatosens. Mot. Res.* 1, 51–67.

Gioanni, Y., and Lamarche, M. (1985). A reappraisal of rat motor cortex organization by intracortical microstimulation. *Brain Res.* 344, 49–61.

Gogan, P., Guéritaud, J. P., Horcholle-Bossavit, G., and Tyc-Dumont, S. (1981). The vibrissal pad as a source of sensory information for the oculomotor system of the cat. *Exp. Brain Res.* 44, 409–418.

Gompf, H. S., Mathai, C., Fuller, P. M., Wood, D. A., Pedersen, N. P., Saper, C. B., and Lu, J. (2010). Locus ceruleus and anterior cingulate cortex sustain wakefulness in a novel environment. *J. Neurosci.* 30, 14543–14551.

Gonzales, C., and Chesselet, M. F. (1990). Amygdalonigral pathway: an anterograde study in the rat with *Phaseolus vulgaris leucoagglutinin* (PHA-L). *J. Comp. Neurol.* 297, 182–200.

Gottschaldt, K. M., Iggo, A., and Young, D. W. (1973). Functional characteristics of mechanoreceptors in sinus hair follicles of the cat. *J. Physiol. (Lond.)* 235, 287–315.

Graeff, F. G. (2004). Serotonin, the periaqueductal gray and panic. *Neurosci. Biobehav. Rev.* 28, 239–259.

Grant, R. A., Mitchinson, B., Fox, C. W., and Prescott, T. J. (2009). Active touch sensing in the rat: anticipatory and regulatory control of whisker movements during surface exploration. *J. Neurophysiol.* 101, 862–874.

Grinevich, V., Brecht, M., and Osten, P. (2005). Monosynaptic pathway from rat vibrissa motor cortex to facial motor neurons revealed by lentivirus-based axonal tracing. *J. Neurosci.* 25, 8250–8258.

Groenewegen, H. J., and Witter, M. P. (2004). "Thalamus," in *The Rat Nervous System*, ed. G. Paxinos, 3rd Edn (Sydney: Academic Press), 407–453.

Grofova, I., Deniau, J. M., and Kitai, S. T. (1982). Morphology of the substantia nigra pars reticulata projection neurons intracellularly labeled with HRP. *J. Comp. Neurol.* 208, 352–368.

Groh, A., de Kock, C. P. J., Wimmer, V. C., Sakmann, B., and Kuner, T. (2008). Driver or coincidence detector: modal switch of a corticothalamic giant synapse controlled by spontaneous activity and short-term depression. *J. Neurosci.* 28, 9652–9663.

Guillery, R. W., and Harting, J. K. (2003). Structure and connections of the thalamic reticular nucleus: advancing views over half a century. *J. Comp. Neurol.* 463, 360–371.

Haidarliu, S., and Ahissar, E. (2001). Size gradients of barreloids in the rat thalamus. *J. Comp. Neurol.* 429, 372–387.

Haidarliu, S., Simony, E., Golomb, D., and Ahissar, E. (2010). Muscle architecture in the mystacial pad of the rat. *Anat. Rec. (Hoboken)* 293, 1192–1206.

Haiss, F., and Schwarz, C. (2005). Spatial segregation of different modes of movement control in the whisker representation of rat primary motor cortex. *J. Neurosci.* 25, 1579–1587.

Halata, Z., Grim, M., and Baumann, K. I. (2010). Current understanding of Merkel cells, touch reception and the skin. *Expert Rev. Dermatol.* 5, 109–116.

Hale, M. W., and Lowry, C. A. (2011). Functional topography of midbrain and pontine serotonergic systems: implications for synaptic regulation of serotonergic circuits. *Psychopharmacology (Berl.)* 213, 243–264.

Hammond, C., Deniau, J. M., Rouzaire-Dubois, B., and Feger, J. (1978). Pepipheral input to the rat subthalamic nucleus, an electrophysiological study. *Neurosci. Lett.* 9, 171–176.

Haring, J. H., and Wang, R. Y. (1986). The identification of some sources of afferent input to the rat nucleus basalis magnocellularis by retrograde transport of horseradish peroxidase. *Brain Res.* 366, 152–158.

Hartings, J. A., Temereanca, S., and Simons, D. J. (2003). Processing of periodic whisker deflections by neurons in the ventroposterior medial and thalamic reticular nuclei. *J. Neurophysiol.* 90, 3087–3094.

Hartmann, M. J. Z. (2009). Active touch, exploratory movements, and sensory prediction. *Integr. Comp. Biol.* 49, 681–690.

Hartmann, M. J. Z. (2011). A night in the life of a rat: vibrissal mechanics and tactile exploration. *Ann. N. Y. Acad. Sci.* 1225, 110–118.

Harvey, M. A., Bermejo, R., and Zeigler, H. P. (2001). Discriminative whisking in the head-fixed rat: optoelectronic monitoring during tactile detection and discrimination tasks. *Somatosens. Mot. Res.* 18, 211–222.

Hattox, A., Li, Y., and Keller, A. (2003). Serotonin regulates rhythmic whisking. *Neuron* 39, 343–352.

Hattox, A. M., Priest, C. A., and Keller, A. (2002). Functional circuitry involved in the regulation of whisker movements. *J. Comp. Neurol.* 442, 266–276.

Hayashi, H. (1980). Distributions of vibrissae afferent fiber collaterals in the trigeminal nuclei as revealed by intra-axonal injection of horseradish peroxidase. *Brain Res.* 183, 442–446.

Heise, C. E., and Mitrofanis, J. (2004). Evidence for a glutamatergic projection from the zona incerta to the basal ganglia of rats. *J. Comp. Neurol.* 468, 482–495.

Helmstaedter, M., Sakmann, B., and Feldmeyer, D. (2009). Neuronal correlates of local, lateral, and translaminar inhibition with reference to cortical columns. *Cereb. Cortex* 19, 926–937.

Hemelt, M. E., and Keller, A. (2008). Superior colliculus control of vibrissa movements. *J. Neurophysiol.* 100, 1245–1254.

Herfst, L. J., and Brecht, M. (2008). Whisker movements evoked by stimulation of single motor neurons in the facial nucleus of the rat. *J. Neurophysiol.* 99, 2821–2832.

Hikosaka, O., Nakamura, K., and Nakahara, H. (2006). Basal ganglia orient eyes to reward. *J. Neurophysiol.* 95, 567–584.

Hill, D. N., Bermejo, R., Zeigler, H. P., and Kleinfeld, D. (2008). Biomechanics of the vibrissa motor plant in rat: rhythmic whisking consists of triphasic neuromuscular activity. *J. Neurosci.* 28, 3438–3455.

Hirata, A., Aguilar, J., and Castro-Alamancos, M. A. (2006). Noradrenergic activation amplifies bottom-up and top-down signal-to-noise ratios in sensory thalamus. *J. Neurosci.* 26, 4426–4436.

Hirata, A., and Castro-Alamancos, M. A. (2010). Neocortex network activation and deactivation states controlled by the thalamus. *J. Neurophysiol.* 103, 1147–1157.

Hirata, A., and Castro-Alamancos, M. A. (2011). Effects of cortical activation on sensory responses in barrel cortex. *J. Neurophysiol.* 105, 1495–1505.

Hoeflinger, B. F., Bennett-Clarke, C. A., Chiaia, N. L., Killackey, H. P., and Rhoades, R. W. (1995). Patterning of local intracortical projections within the vibrissae representation of rat primary somatosensory cortex. *J. Comp. Neurol.* 354, 551–563.

Hoffer, Z. S., Hoover, J. E., and Alloway, K. D. (2003). Sensorimotor corticocortical projections from rat barrel cortex have an anisotropic organization that facilitates integration of inputs from whiskers in the same row. *J. Comp. Neurol.* 466, 525–544.

Hollis, D. E., and Lyne, A. G. (1974). Innervation of vibrissa follicles in the marsupial *Trichosurus vulpecula*. *Aust. J. Zool.* 22, 263–276.

Hong, E. Y., Beak, S. K., and Lee, H. S. (2010). Dual projections of tuberomammillary neurons to whisker-related, sensory and motor regions of the rat. *Brain Res.* 1354, 64–73.

Hoogland, P. V., Welker, E., and Van der Loos, H. (1987). Organization of the projections from barrel cortex to thalamus in mice studied with *Phaseolus vulgaris*-leucoagglutinin and HRP. *Exp. Brain Res.* 68, 73–87.

Hoogland, P. V., Wouterlood, F. G., Welker, E., and Van der Loos, H. (1991). Ultrastructure of giant and small thalamic terminals of cortical origin: a study of the projections from the barrel cortex in mice using *Phaseolus vulgaris* leucoagglutinin (PHA-L). *Exp. Brain Res.* 87, 159–172.

Hooks, B. M., Hires, S. A., Zhang, Y. X., Huber, D., Petreanu, L., Svoboda, K., and Shepherd, G. M. G. (2011). Laminar analysis of excitatory local circuits in vibrissal motor and sensory cortical areas. *PLoS Biol.* 9, e1000572. doi: 10.1371/journal.pbio.1000572

Hoshi, E., Tremblay, L., Féger, J., Carras, P. L., and Strick, P. L. (2005). The cerebellum communicates with the basal ganglia. *Nat. Neurosci.* 8, 1491–1493.

Huber, D., Petreanu, L., Ghitani, N., Ranade, S., Hromádka, T., Mainen, Z., and Svoboda, K. (2008). Sparse optical microstimulation in barrel cortex drives learned behaviour in freely moving mice. *Nature* 451, 61–64.

Huerta, M. F., Frankfurter, A., and Harting, J. K. (1983). Studies of the principal sensory and spinal trigeminal nuclei of the rat: projections to the superior colliculus, inferior olive, and cerebellum. *J. Comp. Neurol.* 220, 147–167.

Hutson, K. A., and Masterton, R. B. (1986). The sensory contribution of a single vibrissa's cortical barrel. *J. Neurophysiol.* 56, 1196–1223.

Hyvärinen, H., Palviainen, A., Strandberg, U., and Holopainen, I. J. (2009). Aquatic environment and differentiation of vibrissae: comparison of sinus hair systems of ringed seal, otter and pole cat. *Brain Behav. Evol.* 74, 268–279.

Irle, E., and Markowitsch, H. J. (1986). Afferent connections of the substantia innominata/basal nucleus of Meynert in carnivores and primates. *J. Hirnforsch.* 27, 343–367.

Isokawa-Akesson, M., and Komisaruk, B. R. (1987). Difference in projections to the lateral and medial facial nucleus: anatomically separate pathways for rhythmical vibrissa movement in rats. *Exp. Brain Res.* 65, 385–398.

Ito, M. (1988). Response properties and topography of vibrissa-sensitive VPM neurons in the rat. *J. Neurophysiol.* 60, 1181–1197.

Ito, M. (2000). Mechanisms of motor learning in the cerebellum. *Brain Res.* 886, 237–245.

Izraeli, R., and Porter, L. L. (1995). Vibrissal motor cortex in the rat: connections with the barrel field. *Exp. Brain Res.* 104, 41–54.

Jacquin, M. F., Barcia, M., and Rhoades, R. W. (1989a). Structure-function relationships in rat brainstem subnucleus interpolaris: IV. Projection neurons. *J. Comp. Neurol.* 282, 45–62.

Jacquin, M. F., Golden, J., and Rhoades, R. W. (1989b). Structure-function relationships in rat brainstem subnucleus interpolaris: III. Local circuit neurons. *J. Comp. Neurol.* 282, 24–44.

Jacquin, M. F., and Rhoades, R. W. (1990). Cell structure and response properties in the trigeminal subnucleus oralis. *Somatosens. Mot. Res.* 7, 265–288.

Jadhav, S. P., and Feldman, D. E. (2010). Texture coding in the whisker system. *Curr. Opin. Neurobiol.* 20, 313–318.

Jadhav, S. P., Wolfe, J., and Feldman, D. E. (2009). Sparse temporal coding of elementary tactile features during active whisker sensation. *Nat. Neurosci.* 12, 792–800.

Jin, T. E., Witzemann, V., and Brecht, M. (2004). Fiber types of the intrinsic whisker muscle and whisking behavior. *J. Neurosci.* 24, 3386–3393.

Joel, D., and Weiner, I. (1997). The connections of the primate subthalamic nucleus: indirect pathways and the open-interconnected scheme of basal ganglia-thalamocortical circuitry. *Brain Res. Brain Res. Rev.* 23, 62–78.

Jones, B. E. (1990). Immunohistochemical study of choline acetyltransferase-immunoreactive processes and cells innervating the pontomedullary reticular formation in the rat. *J. Comp. Neurol.* 295, 485–514.

Jones, B. E. (1991). Noradrenergic locus coeruleus neurons: their distant connections and their relationship to neighboring (including cholinergic and GABAergic) neurons of the central gray and reticular formation. *Prog. Brain Res.* 88, 15–30.

Jones, L. M., Depireux, D. A., Simons, D. J., and Keller, A. (2004). Robust temporal coding in the trigeminal system. *Science* 304, 1986–1989.

Joseph, J. W., Shambes, G. M., Gibson, J. M., and Welker, W. (1978). Tactile projections to granule cells in caudal vermis of the rat's cerebellum. *Brain Behav. Evol.* 15, 141–149.

Kaneda, K., Isa, K., Yanagawa, Y., and Isa, T. (2008). Nigral inhibition of GABAergic neurons in mouse superior colliculus. *J. Neurosci.* 28, 11071–11078.

Kätzel, D., Zemelman, B. V., Buetfering, C., Wölfel, M., and Miesenböck, G. (2011). The columnar and laminar organization of inhibitory connections to neocortical excitatory cells. *Nat. Neurosci.* 14, 100–107.

Kelley, A. E., Domesick, V. B., and Nauta, W. J. H. (1982). The amygdalostriatal projection in the rat – an anatomical study by anterograde and retrograde tracing methods. *Neuroscience* 7, 615–630.

Kennedy, T. T., Grimm, R. J., and Towe, A. L. (1966). The role of cerebral cortex in evoked somatosensory activity in cat cerebellum. *Exp. Neurol.* 14, 13–32.

Kerr, F. W. L., and Lysak, W. R. (1964). Somatotopic organization of trigeminal-ganglion neurones. *Arch. Neurol.* 11, 593–602.

Khatri, V., Bermejo, R., Brumberg, J. C., Keller, A., and Zeigler, H. P. (2009). Whisking in air: encoding of kinematics by trigeminal ganglion neurons in awake rats. *J. Neurophysiol.* 101, 1836–1846.

Killackey, H. P. (1973). Anatomical evidence for cortical subdivisions based on vertically discrete thalamic projections from the ventral posterior nucleus to cortical barrels in the rat. *Brain Res.* 51, 326–331.

Killackey, H. P., and Sherman, S. M. (2003). Corticothalamic projections from the rat primary somatosensory cortex. *J. Neurosci.* 23, 7381–7384.

Kim, J. N., Koh, K. S., Lee, E., Park, S. C., and Song, W. C. (2011). The morphology of the rat vibrissal follicle-sinus complex revealed by three-dimensional computer-aided reconstruction. *Cells Tissues Organs* 193, 207–214.

Kim, U., and Ebner, F. F. (1999). Barrels and septa: separate circuits in rat barrels field cortex. *J. Comp. Neurol.* 408, 489–505.

Kim, U., Gregory, E., and Hall, W. C. (1992). Pathway from the zona incerta to the superior colliculus in the rat. *J. Comp. Neurol.* 321, 555–575.

Kirifides, M. L., Simpson, K. L., Lin, R. C. S., and Waterhouse, B. D. (2001). Topographic organization and neurochemical identity of dorsal raphe neurons that project to the trigeminal somatosensory pathway in the rat. *J. Comp. Neurol.* 435, 325–340.

Kita, H. (2007). Globus pallidus external segment. *Prog. Brain Res.* 160, 111–133.

Kita, H., and Kitai, S. T. (1987). Efferent projections of the subthalamic nucleus in the rat: light and electron microscopic analysis with the PHA-L method. *J. Comp. Neurol.* 260, 435–452.

Klein, B. G., and Rhoades, R. W. (1985). Representation of whisker follicle intrinsic musculature in the facial motor nucleus of the rat. *J. Comp. Neurol.* 232, 55–69.

Kleinfeld, D., Berg, R. W., and O'Connor, S. M. (1999). Anatomical loops and their electrical dynamics in relation to whisking by rat. *Somatosens. Mot. Res.* 16, 69–88.

Knutsen, P. M., Pietr, M., and Ahissar, E. (2006). Haptic object localization in the vibrissal system: behavior and performance. *J. Neurosci.* 26, 8451–8464.

Kocsis, B., Varga, V., Dahan, L., and Sik, A. (2006). Serotonergic neuron diversity: identification of raphe neurons with discharges time-locked to the hippocampal theta rhythm. *Proc. Natl. Acad. Sci. U.S.A.* 103, 1059–1064.

Kolmac, C. I., Power, B. D., and Mitrofanis, J. (1998). Patterns of connections between zona incerta and brainstem in rats. *J. Comp. Neurol.* 396, 544–555.

Koralek, K. A., Jensen, K. F., and Killackey, H. P. (1988). Evidence for two complementary patterns of thalamic input to the rat somatosensory cortex. *Brain Res.* 463, 346–351.

Koralek, K. A., Olavarria, J., and Killackey, H. P. (1990). Areal and laminar organization of corticocortical projections in the rat somatosensory cortex. *J. Comp. Neurol.* 299, 133–150.

Krakauer, J. W., and Shadmehr, R. (2006). Consolidation of motor memory. *Trends Neurosci.* 29, 58–64.

Kremer, Y., Léger, J. F., Goodman, D., Brette, R., and Bourdieu, L. (2011). Late emergence of the vibrissa direction selectivity map in the rat barrel cortex. *J. Neurosci.* 31, 10689–10700.

Krupa, D. J., Matell, M. S., Brisben, A. J., Oliveira, L. M., and Nicolelis, M. A. L. (2001). Behavioral properties of the trigeminal somatosensory system in rats performing whisker-dependent tactile discriminations. *J. Neurosci.* 21, 5752–5763.

Krupa, D. J., Wiest, M. C., Shuler, M. G., Laubach, M., and Nicolelis, M. A. L. (2004). Layer-specific somatosensory cortical activation during active tactile discrimination. *Science* 304, 1989–1992.

Kuo, M. C., Rasmusson, D. D., and Dringenberg, H. C. (2009). Input-selective potentiation and rebalancing of primary sensory cortex afferents by endogenous acetylcholine. *Neuroscience* 163, 430–441.

Kwegyir-Afful, E. E., and Keller, A. (2004). Response properties of whisker-related neurons in rat second somatosensory cortex. *J. Neurophysiol.* 92, 2083–2092.

Lam, Y. W., and Sherman, S. M. (2010). Functional organization of the somatosensory cortical layer 6 feedback to the thalamus. *Cereb. Cortex* 20, 13–24.

Lam, Y. W., and Sherman, S. M. (2011). Functional organization of the thalamic input to the thalamic reticular nucleus. *J. Neurosci.* 31, 6791–6799.

Land, P. W., Buffer, S. A. Jr., and Yaskosky, J. D. (1995). Barreloids in adult rat thalamus: three-dimensional architecture and relationship to somatosensory cortical barrels. *J. Comp. Neurol.* 355, 573–588.

Lang, E. J. (2002). GABAergic and glutamatergic modulation of spontaneous and motor-cortex-evoked complex spike activity. *J. Neurophysiol.* 87, 1993–2008.

Lang, E. J., Sugihara, I., and Llinás, R. (2006). Olivocerebellar modulation of motor cortex ability to generate vibrissal movements in rat. *J. Physiol. (Lond.)* 571, 101–120.

Langford, D. J., Bailey, A. L., Chanda, M. L., Clarke, S. E., Drummond, T. E., Echols, S., Glick, S., Ingrao, J., Klassen-Ross, T., Lacroix-Fralish, M. L., Matsumiya, L., Sorge, R. E., Sotocinal, S. G., Tabaka, J. M., Wong, D., van den Maagdenberg, A. M. J. M., Ferrari, M. D., Craig, K. D., and Mogil, J. S. (2010). Coding of facial expressions of pain in the laboratory mouse. *Nat. Methods* 7, 447–449.

Larsen, D. D., Wickersham, I. R., and Callaway, E. M. (2007). Retrograde tracing with recombinant rabies virus reveals correlations between projection targets and dendritic architecture in layer 5 of mouse barrel cortex. *Front. Neural Circuits* 1:5. doi: 10.3389/neuro.04.005.2007

Lavallée, P., Urbain, N., Dufresne, C., Bokor, H., Acsády, L., and Deschênes, M. (2005). Feedforward inhibitory control of sensory information in higher-order thalamic nuclei. *J. Neurosci.* 25, 7489–7498.

Lazarov, N. E. (2002). Comparative analysis of the chemical neuroanatomy of the mammalian trigeminal ganglion and mesencephalic trigeminal nucleus. *Prog. Neurobiol.* 66, 19–59.

Leal-Campanario, R., Delgado-García, J. M., and Gruart, A. (2006). Microstimulation of the somatosensory cortex can substitute for vibrissa stimulation during Pavlovian conditioning. *Proc. Natl. Acad. Sci. U.S.A.* 103, 10052–10057.

Lee, H. S., Kim, M. A., Valentino, R. J., and Waterhouse, B. D. (2003). Glutamatergic afferent projections to the dorsal raphe nucleus of the rat. *Brain Res.* 963, 57–71.

Lee, M. G., Hassani, O. K., Alonso, A., and Jones, B. E. (2005). Cholinergic basal forebrain neurons burst with theta during waking and paradoxical sleep. *J. Neurosci.* 25, 4365–4369.

Lee, S., Carvell, G. E., and Simons, D. J. (2008a). Motor modulation of afferent somatosensory circuits. *Nat. Neurosci.* 11, 1430–1438.

Lee, S. B., Chang, B. J., and Lee, H. S. (2008b). Organization of histamine-immunoreactive, tuberomammillary neurons projecting to the dorsal tier of the substantia nigra compacta in the rat. *Brain Res.* 1203, 79–88.

Lee, S. B., Lee, H. S., and Waterhouse, B. D. (2008c). The collateral projection from the dorsal raphe nucleus to whisker-related, trigeminal sensory and facial motor systems in the rat. *Brain Res.* 1214, 11–22.

Leergaard, T. B., Alloway, K. D., Pham, T. A. T., Bolstad, I., Hoffer, Z. S., Pettersen, C., and Bjaalie, J. G. (2004). Three-dimensional topography of corticopontine projections from rat sensorimotor cortex: comparisons with corticostriatal projections reveal diverse integrative organization. *J. Comp. Neurol.* 478, 306–322.

Leergaard, T. B., Lillehaug, S., De Schutter, E., Bower, J. M., and Bjaalie, J. G. (2006). Topographical organization of pathways from somatosensory cortex through the pontine nuclei to tactile regions of the rat cerebellar hemispheres. *Eur. J. Neurosci.* 24, 2801–2812.

Lefort, S., Tomm, C., Floyd Sarria, J. C., and Petersen, C. C. H. (2009). The excitatory neuronal network of the C2 barrel column in mouse primary somatosensory cortex. *Neuron* 61, 301–316.

Legg, C. R., Mercier, B., and Glickstein, M. (1989). Corticopontine projection in the rat: the distribution of labelled cortical cells after large injections of horseradish peroxidase in the pontine nuclei. *J. Comp. Neurol.* 286, 427–441.

Leiser, S. C., and Moxon, K. A. (2006). Relationship between physiological response type (RA and SA) and vibrissal receptive field of neurons within the rat trigeminal ganglion. *J. Neurophysiol.* 95, 3129–3145.

Leiser, S. C., and Moxon, K. A. (2007). Responses of trigeminal ganglion neurons during natural whisking behaviors in the awake rat. *Neuron* 53, 117–133.

Leite-Almeida, H., Valle-Fernandes, A., and Almeida, A. (2006). Brain projections from the medullary dorsal reticular nucleus: an anterograde and retrograde tracing study in the rat. *Neuroscience* 140, 577–595.

Li, Y., Erzurumlu, R. S., Chen, C., Jhaveri, S., and Tonegawa, S. (1994). Whisker-related neuronal patterns fail to develop in the trigeminal brainstem nuclei of NMDAR1 knockout mice. *Cell* 76, 427–437.

Liao, C. C., Chen, R. F., Lai, W. S., Lin, R. C. S., and Yen, C. T. (2010). Distribution of large terminal inputs from the primary and secondary somatosensory cortices to the dorsal thalamus in the rodent. *J. Comp. Neurol.* 518, 2592–2611.

Lichtenstein, S. H., Carvell, G. E., and Simons, D. J. (1990). Responses of rat trigeminal ganglion neurons to movements of vibrissae in different directions. *Somatosens. Mot. Res.* 7, 47–65.

Lin, C. S., Nicolelis, M. A. L., Schneider, J. S., and Chapin, J. K. (1990). A major direct GABAergic pathway from zona incerta to neocortex. *Science* 248, 1553–1556.

Loewenstein, Y., Mahon, S., Chadderton, P., Kitamura, K., Sompolinsky, H., Yarom, Y., and Häusser, M. (2005). Bistability of cerebellar Purkinje cells modulated by sensory stimulation. *Nat. Neurosci.* 8, 202–211.

Lu, S. M., and Lin, R. C. S. (1993). Thalamic afferents of the rat barrel cortex: a light- and electron-microscopic study using *Phaseolus vulgaris* leucoagglutinin as an anterograde tracer. *Somatosens. Mot. Res.* 10, 1–16.

Lübke, J., Egger, V., Sakmann, B., and Feldmeyer, D. (2000). Columnar organization of dendrites and axons of single and synaptically coupled excitatory spiny neurons in layer 4 of the rat barrel cortex. *J. Neurosci.* 20, 5300–5311.

Lübke, J., and Feldmeyer, D. (2007). Excitatory signal flow and connectivity in a cortical column: focus on barrel cortex. *Brain Struct. Funct.* 212, 3–17.

Lumpkin, E. A., Marshall, K. L., and Nelson, A. M. (2010). The cell biology of touch. *J. Cell Biol.* 191, 237–248.

Ma, P. M. (1991). The barrelettes – architectonic vibrissal representations in the brainstem trigeminal complex of the mouse. I. Normal structural organization. *J. Comp. Neurol.* 309, 161–199.

Ma, T. P., Hu, X. J., Anavi, Y., and Rafols, J. A. (1992). Organization of the zona incerta in the macaque: a Nissl and Golgi study. *J. Comp. Neurol.* 320, 273–290.

Mameli, O., Stanzani, S., Mulliri, G., Pellitteri, R., Caria, M. A., Russo, A., and De Riu, P. (2010). Role of the trigeminal mesencephalic nucleus in rat whisker pad proprioception. *Behav. Brain Funct.* 6, 69.

Mameli, O., Stanzani, S., Russo, A., Romeo, R., Pellitteri, R., Spatuzza, M., Caria, M. A., and De Riu, P. L. (2008). Hypoglossal nuclei participation in rat mystacial pad control. *Pflugers Arch.* 456, 1189–1198.

Manning, K. A., Wilson, J. R., and Uhlrich, D. J. (1996). Histamine-immunoreactive neurons and their innervation of visual regions in the cortex, tectum, and thalamus in the primate *Macaca mulatta*. *J. Comp. Neurol.* 373, 271–282.

Manns, I. D., Sakmann, B., and Brecht, M. (2004). Sub- and suprathreshold receptive field properties of pyramidal neurones in layers 5A and 5B of rat somatosensory barrel cortex. *J. Physiol. (Lond.)* 556, 601–622.

Marotte, L. R., Rice, F. L., and Waite, P. M. E. (1992). The morphology and innervation of facial vibrissae in the tammar wallaby, *Macropus eugenii*. *J. Anat.* 180, 401–417.

Marti, M., Viaro, R., Guerrini, R., Franchi, G., and Morari, M. (2009). Nociceptin/orphanin FQ modulates motor behavior and primary motor cortex output through receptors located in substantia nigra reticulata. *Neuropsychopharmacology* 34, 341–355.

Masri, R., Trageser, J. C., Bezdudnaya, T., Li, Y., and Keller, A. (2006). Cholinergic regulation of the posterior medial thalamic nucleus. *J. Neurophysiol.* 96, 2265–2273.

Massion, J. (1988). Red nucleus: past and future. *Behav. Brain Res.* 28, 1–8.

Matesz, C. (1981). Peripheral and central distribution of fibres of the mesencephalic trigeminal root in the rat. *Neurosci. Lett.* 27, 13–17.

Matyas, F., Sreenivasan, V., Marbach, F., Wacongne, C., Barsy, B., Mateo, C., Aronoff, R., and Petersen, C. C. H. (2010). Motor control by sensory cortex. *Science* 330, 1240–1243.

May, P. J. (2006). The mammalian superior colliculus: laminar structure and connections. *Prog. Brain Res.* 151, 321–378.

May, P. J., Sun, W., and Hall, W. C. (1997). Reciprocal connections between the zona incerta and the pretectum and superior colliculus of the cat. *Neuroscience* 77, 1091–1114.

McGinty, D. J., and Harper, R. M. (1976). Dorsal raphe neurons: depression of firing during sleep in cats. *Brain Res.* 101, 569–575.

McHaffie, J. G., and Stein, B. E. (1982). Eye movements evoked by electrical stimulation in the superior colliculus of rats and hamsters. *Brain Res.* 247, 243–253.

McMullen, N. T., Smelser, C. B., and Rice, F. L. (1994). Parvalbumin expression reveals a vibrissa-related pattern in rabbit SI cortex. *Brain Res.* 660, 225–231.

Meyer, H. S., Wimmer, V. C., Hemberger, M., Bruno, R. M., de Kock, C. P. J., Frick, A., Sakmann, B., and Helmstaedter, M. (2010a). Cell type-specific thalamic innervation in a column of rat vibrissal cortex. *Cereb. Cortex* 20, 2287–2303.

Meyer, H. S., Wimmer, V. C., Oberlaender, M., de Kock, C. P. J., Sakmann, B., and Helmstaedter, M. (2010b). Number and laminar distribution of neurons in a thalamocortical projection column of rat vibrissal cortex. *Cereb. Cortex* 20, 2277–2286.

Mihailoff, G. A. (1993). Cerebellar nuclear projections from the basilar pontine nuclei and nucleus reticularis tegmenti pontis as demonstrated with PHA-L tracing in the rat. *J. Comp. Neurol.* 330, 130–146.

Mihailoff, G. A. (1995). Orthograde axonal transport studies of projections from the zona incerta and pretectum to the basilar pontine nuclei in the rat. *J. Comp. Neurol.* 360, 301–318.

Mihailoff, G. A., Kosinski, R. J., Azizi, S. A., and Border, B. G. (1989). Survey of noncortical afferent projections to the basilar pontine nuclei: a retrograde tracing study in the rat. *J. Comp. Neurol.* 282, 617–643.

Miller, E. H. (1975). A comparative study of facial expressions of two species of pinnipeds. *Behaviour* 53, 268–284.

Misgeld, U. (2004). Innervation of the substantia nigra. *Cell Tissue Res.* 318, 107–114.

Miskolczy, D. (1931). Über die Endigungsweise der spino-cerebellaren Bahnen. *Z. Anat. Entwicklungsgesch.* 96, 537–542.

Mitchinson, B., Martin, C. J., Grant, R. A., and Prescott, T. J. (2007). Feedback control in active sensing: rat exploratory whisking is modulated by environmental contact. *Proc. Biol. Sci.* 274, 1035–1041.

Mitrofanis, J. (2005). Some certainty for the "zone of uncertainty"? Exploring the function of the zona incerta. *Neuroscience* 130, 1–15.

Mitrofanis, J., and Mikuletic, L. (1999). Organisation of the cortical projection to the zona incerta of the thalamus. *J. Comp. Neurol.* 412, 173–185.

Miyashita, E., Keller, A., and Asanuma, H. (1994). Input-output organization of the rat vibrissal motor cortex. *Exp. Brain Res.* 99, 223–232.

Miyashita, E., and Mori, S. (1995). The superior colliculus relays signals descending from the vibrissal motor cortex to the facial nerve nucleus in the rat. *Neurosci. Lett.* 195, 69–71.

Molinari, H. H., Schultze, K. E., and Strominger, N. L. (1996). Gracile, cuneate, and spinal trigeminal projections to inferior olive in rat and monkey. *J. Comp. Neurol.* 375, 467–480.

Moore, R. Y., and Bloom, F. E. (1979). Central catecholamine neuron systems: anatomy and physiology of the norepinephrine and epinephrine systems. *Annu. Rev. Neurosci.* 2, 113–168.

Morisette, J., and Bower, J. M. (1996). Contribution of somatosensory cortex to responses in the rat cerebellar granule cell layer following peripheral tactile stimulation. *Exp. Brain Res.* 109, 240–250.

Mowery, T. M., Harrold, J. B., and Alloway, K. D. (2011). Repeated whisker stimulation evokes invariant neuronal responses in the dorsolateral striatum of anesthetized rats: a potential correlate of sensorimotor habits. *J. Neurophysiol.* 105, 2225–2238.

Muchlinski, M. N. (2010). A comparative analysis of vibrissa count and infraorbital foramen area in primates and other mammals. *J. Hum. Evol.* 58, 447–473.

Muir, G. D., and Whishaw, I. Q. (2000). Red nucleus lesions impair overground locomotion in rats: a kinetic analysis. *Eur. J. Neurosci.* 12, 1113–1122.

Munz, M., Brecht, M., and Wolfe, J. (2010). Active touch during shrew prey capture. *Front. Behav. Neurosci.* 4:191. doi: 10.3389/fnbeh.2010.00191

Murray, P. D., Masri, R., and Keller, A. (2010). Abnormal anterior pretectal nucleus activity contributes to central pain syndrome. *J. Neurophysiol.* 103, 3044–3053.

Naito, A., and Kita, H. (1994). The cortico-nigral projection in the rat: an anterograde tracing study with biotinylated dextran amine. *Brain Res.* 637, 317–322.

Nambu, A. (2007). Globus pallidus internal segment. *Prog. Brain Res.* 160, 135–150.

Ndiaye, A., Pinganaud, G., VanderWerf, F., Buisseret-Delmas, C., and Buisseret, P. (2000). Connections between the trigeminal mesencephalic nucleus and the superior colliculus in the rat. *Neurosci. Lett.* 294, 17–20.

Neimark, M. A., Andermann, M. L., Hopfield, J. J., and Moore, C. I. (2003). Vibrissa resonance as a transduction mechanism for tactile encoding. *J. Neurosci.* 23, 6499–6509.

Nguyen, Q. T., and Kleinfeld, D. (2005). Positive feedback in a brainstem tactile sensorimotor loop. *Neuron* 45, 447–457.

Nicolelis, M. A. L., Baccala, L. A., Lin, R. C. S., and Chapin, J. K. (1995a). Sensorimotor encoding by synchronous neural ensemble activity at multiple levels of the somatosensory system. *Science* 268, 1353–1358.

Nicolelis, M. A. L., Chapin, J. K., and Lin, R. C. S. (1995b). Development of direct GABAergic projections from the zona incerta to the somatosensory cortex of the rat. *Neuroscience* 65, 609–631.

Nicolelis, M. A. L., Chapin, J. K., and Lin, R. C. S. (1992). Somatotopic maps within the zona incerta relay parallel GABAergic somatosensory pathways to the neocortex, superior colliculus, and brainstem. *Brain Res.* 577, 134–141.

Nilsson, B. Y. (1969). Structure and function of the tactile hair receptors on the cat's foreleg. *Acta Physiol. Scand.* 77, 396–416.

O'Connor, D. H., Clack, N. G., Huber, D., Komiyama, T., Myers, E. W., and Svoboda, K. (2010a). Vibrissa-based object localization in head-fixed mice. *J. Neurosci.* 30, 1947–1967.

O'Connor, D. H., Peron, S. P., Huber, D., and Svoboda, K. (2010b). Neural activity in barrel cortex underlying vibrissa-based object localization in mice. *Neuron* 67, 1048–1061.

Ojima, H. (1994). Terminal morphology and distribution of corticothalamic fibers originating from layers 5 and 6 of cat primary auditory cortex. *Cereb. Cortex* 4, 646–663.

Oldford, E., and Castro-Alamancos, M. A. (2003). Input-specific effects of acetylcholine on sensory and intracortical evoked responses in the "barrel cortex" in vivo. *Neuroscience* 117, 769–778.

Parenti, R., Zappalà, A., Serapide, M. F., Pantò, M. R., and Cicirata, F. (2002). Projections of the basilar pontine nuclei and nucleus reticularis tegmenti pontis to the cerebellar nuclei of the rat. *J. Comp. Neurol.* 452, 115–127.

Passani, M. B., and Blandina, P. (2011). Histamine receptors in the CNS as targets for therapeutic intervention. *Trends Pharmacol. Sci.* 32, 242–249.

Paul, G., and Gould, D. J. (2010). The red nucleus: past, present, and future. *Neuroanatomy* 9, 1–3.

Peschanski, M. (1984). Trigeminal afferents to the diencephalon in the rat. *Neuroscience* 12, 465–487.

Petersen, C. C. H. (2007). The functional organization of the barrel cortex. *Neuron* 56, 339–355.

Petersen, C. C. H., and Sakmann, B. (2000). The excitatory neuronal network of rat layer 4 barrel cortex. *J. Neurosci.* 20, 7579–7586.

Petreanu, L., Huber, D., Sobczyk, A., and Svoboda, K. (2007). Channelrhodopsin-2-assisted circuit mapping of long-range callosal projections. *Nat. Neurosci.* 10, 663–668.

Petreanu, L., Mao, T., Sternson, S. M., and Svoboda, K. (2009). The subcellular organization of neocortical excitatory connections. *Nature* 457, 1142–1145.

Pidoux, M., Mahon, S., Deniau, J. M., and Charpier, S. (2011). Integration and propagation of somatosensory responses in the corticostriatal pathway: an intracellular study in vivo. *J. Physiol. (Lond.)* 589, 263–281.

Pierret, T., Lavallée, P., and Deschênes, M. (2000). Parallel streams for the relay of vibrissal information through thalamic barreloids. *J. Neurosci.* 20, 7455–7462.

Pillot, C., Heron, A., Cochois, V., Tardivel-Lacombe, J., Ligneau, X., Schwartz, J. C., and Arrang, J. M. (2002). A detailed mapping of the histamine H(3) receptor and its gene transcripts in rat brain. *Neuroscience* 114, 173–193.

Pinault, D. (2004). The thalamic reticular nucleus: structure, function and concept. *Brain Res. Brain Res. Rev.* 46, 1–31.

Pinault, D., Bourassa, J., and Deschênes, M. (1995). The axonal arborization of single thalamic reticular neurons in the somatosensory thalamus of the rat. *Eur. J. Neurosci.* 7, 31–40.

Pinganaud, G., Bernat, I., Buisseret, P., and Buisseret-Delmas, C. (1999). Trigeminal projections to hypoglossal and facial motor nuclei in the rat. *J. Comp. Neurol.* 415, 91–104.

Popescu, A. T., Popa, D., and Paré, D. (2009). Coherent gamma oscillations couple the amygdala and striatum during learning. *Nat. Neurosci.* 12, 801–807.

Porter, L. L., and White, E. L. (1983). Afferent and efferent pathways of the vibrissal region of primary motor cortex in the mouse. *J. Comp. Neurol.* 214, 279–289.

Quessy, S., and Freedman, E. G. (2004). Electrical stimulation of rhesus monkey nucleus reticularis gigantocellularis. I. Characteristics of evoked head movements. *Exp. Brain Res.* 156, 342–356.

Redgrave, P., Gurney, K., and Reynolds, J. (2008). What is reinforced by phasic dopamine signals? *Brain Res. Rev.* 58, 322–339.

Reep, R. L., Stoll, M. L., Marshall, C. D., Homer, B. L., and Samuelson, D. A. (2001). Microanatomy of facial vibrissae in the Florida manatee: the basis for specialized sensory function and oripulation. *Brain Behav. Evol.* 58, 1–14.

Reyes, A., and Sakmann, B. (1999). Developmental switch in the short-term modification of unitary EPSPs evoked in layer 2/3 and layer 5 pyramidal neurons of rat neocortex. *J. Neurosci.* 19, 3827–3835.

Ricardo, J. A. (1981). Efferent connections of the subthalamic region in the rat. II. The zona incerta. *Brain Res.* 214, 43–60.

Rice, F. L. (1985). An attempt to find vibrissa-related barrels in the primary somatosensory cortex of the cat. *Neurosci. Lett.* 53, 169–172.

Rice, F. L. (1993). Structure, vascularization, and innervation of the mystacial pad of the rat as revealed by the lectin *Griffonia simplicifolia*. *J. Comp. Neurol.* 337, 386–399.

Rice, F. L., Mance, A., and Munger, B. L. (1986). A comparative light microscopic analysis of the sensory innervation of the mystacial pad. I. Innervation of vibrissal follicle-sinus complexes. *J. Comp. Neurol.* 252, 154–174.

Ritt, J. T., Andermann, M. L., and Moore, C. I. (2008). Embodied information processing: vibrissa mechanics and texture features shape micromotions in actively sensing rats. *Neuron* 57, 599–613.

Roger, M., and Cadusseau, J. (1985). Afferents to the zona incerta in the rat: a combined retrograde and anterograde study. *J. Comp. Neurol.* 241, 480–492.

Ruigrok, T. J. H. (2011). Ins and outs of cerebellar modules. *Cerebellum.* 10, 464–474

Sarko, D. K., Reep, R. L., Mazurkiewicz, J. E., and Rice, F. L. (2007). Adaptations in the structure and innervation of follicle-sinus complexes to an aquatic environment as seen in the Florida manatee (*Trichechus manatus latirostris*). *J. Comp. Neurol.* 504, 217–237.

Sarko, D. K., Rice, F. L., and Reep, R. L. (2011). Mammalian tactile hair: divergence from a limited distribution. *Ann. N. Y. Acad. Sci.* 1225, 90–100.

Satoh, K., and Fibiger, H. C. (1986). Cholinergic neurons of the laterodorsal tegmental nucleus: efferent and afferent connections. *J. Comp. Neurol.* 253, 277–302.

Schneider, J. S., Morse, J. R., and Lidsky, T. I. (1982). Somatosensory properties of globus pallidus neurons in awake cats. *Exp. Brain Res.* 46, 311–314.

Schubert, D., Kötter, R., and Staiger, J. F. (2007). Mapping functional connectivity in barrel-related columns reveals layer- and cell type-specific microcircuits. *Brain Struct. Funct.* 212, 107–119.

Schubert, D., Staiger, J. F., Cho, N., Kötter, R., Zilles, K., and Luhmann, H. J. (2001). Layer-specific intracolumnar and transcolumnar functional connectivity of layer V pyramidal cells in rat barrel cortex. *J. Neurosci.* 21, 3580–3592.

Schwarz, C., and Möck, M. (2001). Spatial arrangement of cerebro-pontine terminals. *J. Comp. Neurol.* 435, 418–432.

Semba, K., and Fibiger, H. C. (1992). Afferent connections of the laterodorsal and the pedunculopontine tegmental nuclei in the rat: a retro- and antero-grade transport and immunohistochemical study. *J. Comp. Neurol.* 323, 387–410.

Semba, K., and Komisaruk, B. R. (1984). Neural substrates of two different rhythmical vibrissal movements in the rat. *Neuroscience* 12, 761–774.

Shambes, G. M., Gibson, J. M., and Welker, W. (1978). Fractured somatotopy in granule cell tactile areas of rat cerebellar hemispheres revealed by micromapping. *Brain Behav. Evol.* 15, 94–140.

Sheibani, V., and Farazifard, R. (2006). Dorsal raphe nucleus stimulation modulates the response of layers IV and V barrel cortical neurons in rat. *Brain Res. Bull.* 68, 430–435.

Shepherd, G. M. G., and Svoboda, K. (2005). Laminar and columnar organization of ascending excitatory projections to layer 2/3 pyramidal neurons in rat barrel cortex. *J. Neurosci.* 25, 5670–5679.

Shosaku, A., Kayama, Y., and Sumitomo, I. (1984). Somatotopic organization in the rat thalamic reticular nucleus. *Brain Res.* 311, 57–63.

Simons, D. J. (1978). Response properties of vibrissa units in rat SI somatosensory neocortex. *J. Neurophysiol.* 41, 798–820.

Simons, D. J. (1985). Temporal and spatial integration in the rat SI vibrissa cortex. *J. Neurophysiol.* 54, 615–635.

Simons, D. J., and Carvell, G. E. (1989). Thalamocortical response transformation in the rat vibrissa/barrel system. *J. Neurophysiol.* 61, 311–330.

Simony, E., Bagdasarian, K., Herfst, L., Brecht, M., Ahissar, E., and Golomb, D. (2010). Temporal and spatial characteristics of vibrissa responses to motor commands. *J. Neurosci.* 30, 8935–8952.

Simpson, K., Wang, Y., and Lin, R. C. S. (2008). Patterns of convergence in rat zona incerta from the trigeminal nuclear complex: light and electron microscopic study. *J. Comp. Neurol.* 507, 1521–1541.

Smith, J. B., and Alloway, K. D. (2010). Functional specificity of claustrum connections in the rat: interhemispheric communication between specific parts of motor cortex. *J. Neurosci.* 30, 16832–16844.

Smith, J. C., Abdala, A. P. L., Rybak, I. A., and Paton, J. F. R. (2009). Structural and functional architecture of respiratory networks in the mammalian brainstem. *Philos. Trans. R. Soc. Lond. B Biol. Sci.* 364, 2577–2587.

Smith, Y., Raju, D. V., Pare, J. F., and Sidibe, M. (2004). The thalamostriatal system: a highly specific network of the basal ganglia circuitry. *Trends Neurosci.* 27, 520–527.

Spreafico, R., Barbaresi, P., Weinberg, R. J., and Rustioni, A. (1987). SII-projecting neurons in the rat thalamus: a single- and double-retrograde-tracing study. *Somatosens. Res.* 4, 359–375.

Stapley, P. J., and Drew, T. (2009). The pontomedullary reticular formation contributes to the compensatory postural responses observed following removal of the support surface in the standing cat. *J. Neurophysiol.* 101, 1334–1350.

Steindler, D. A. (1985). Trigeminocerebellar, trigeminotectal, and trigeminothalamic projections: a double retrograde axonal tracing study in the mouse. *J. Comp. Neurol.* 237, 155–175.

Stephens, R. J., Beebe, I. J., and Poulter, T. C. (1973). Innervation of the vibrissae of the California sea lion, *Zalophus californianus*. *Anat. Rec.* 176, 421–441.

Stüttgen, M. C., and Schwarz, C. (2008). Psychophysical and neurometric detection performance under stimulus uncertainty. *Nat. Neurosci.* 11, 1091–1099.

Sun, Q. Q., Huguenard, J. R., and Prince, D. A. (2006). Barrel cortex microcircuits: thalamocortical feedforward inhibition in spiny stellate cells is mediated by a small number of fast-spiking interneurons. *J. Neurosci.* 26, 1219–1230.

Swadlow, H. A. (2002). Thalamocortical control of feed-forward inhibition in awake somatosensory 'barrel' cortex. *Philos. Trans. R. Soc. Lond. B Biol. Sci.* 357, 1717–1727.

Swenson, R. S., and Castro, A. J. (1983). The afferent connections of the inferior olivary complex in rats. An anterograde study using autoradiographic and axonal degeneration techniques. *Neuroscience* 8, 259–275.

Swenson, R. S., Kosinski, R. J., and Castro, A. J. (1984). Topography of spinal, dorsal column nuclear, and spinal trigeminal projections to the pontine gray in rats. *J. Comp. Neurol.* 222, 301–311.

Swenson, R. S., Sievert, C. F., Terreberry, R. R., Neafsey, E. J., and Castro, A. J. (1989). Organization of cerebral cortico-olivary projections in the rat. *Neurosci. Res.* 7, 43–54.

Syed, E. C. J., Sharott, A., Moll, C. K. E., Engel, A. K., and Kral, A. (2011). Effect of sensory stimulation in rat barrel cortex, dorsolateral striatum and on corticostriatal functional connectivity. *Eur. J. Neurosci.* 33, 461–470.

Szwed, M., Bagdasarian, K., and Ahissar, E. (2003). Encoding of vibrissal active touch. *Neuron* 40, 621–630.

Szymonowicz, W. (1895). Beiträge zur Kenntniss der Nervenendigungen in Hautgebilden. *Arch. Mikrosk. Anat.* 45, 624–654.

Takahashi, K., Lin, J. S., and Sakai, K. (2006). Neuronal activity of histaminergic tuberomammillary neurons during wake-sleep states in the mouse. *J. Neurosci.* 26, 10292–10298.

Taylor, A. M., and Lieberman, A. R. (1987). Ultrastructural organisation of the projection from the superior colliculus to the ventral lateral geniculate nucleus of the rat. *J. Comp. Neurol.* 256, 454–462.

ten Donkelaar, H. J. (1988). Evolution of the red nucleus and rubrospinal tract. *Behav. Brain Res.* 28, 9–20.

Tepper, J. M., Abercrombie, E. D., and Bolam, J. P. (2007). Basal ganglia macrocircuits. *Prog. Brain Res.* 160, 3–7.

Terenzi, M. G., Zagon, A., and Roberts, M. H. T. (1995). Efferent connections from the anterior pretectal nucleus to the diencephalon and mesencephalon in the rat. *Brain Res.* 701, 183–191.

Teune, T. M., van der Burg, J., van der Moer, J., Voogd, J., and Ruigrok, T. J. (2000). Topography of cerebellar nuclear projections to the brain stem in the rat. *Prog. Brain Res.* 124, 141–172.

Thakkar, M. M. (2011). Histamine in the regulation of wakefulness. *Sleep Med. Rev.* 15, 65–74.

Theyel, B. B., Llano, D. A., and Sherman, S. M. (2010). The corticothalamocortical circuit drives higher-order cortex in the mouse. *Nat. Neurosci.* 13, 84–88.

Thomson, M. A., Piat, G., Cordonnier, V., Ellouze-Kallel, L., Delhaye-Bouchaud, N., and Mariani, J. (1989). Representation of vibrissae inputs through the climbing fiber pathway in lobule VII of the adult rat cerebellar vermis. *Brain Res.* 488, 241–252.

Timofeeva, E., Dufresne, C., Sik, A., Zhang, Z. W., and Deschênes, M. (2005). Cholinergic modulation of vibrissal receptive fields in trigeminal nuclei. *J. Neurosci.* 25, 9135–9143.

Timofeeva, E., Mérette, C., Émond, C., Lavallée, P., and Deschénes, M. (2003). A map of angular tuning preference in thalamic barreloids. *J. Neurosci.* 23, 10717–10723.

Tlamsa, A. P., and Brumberg, J. C. (2010). Organization and morphology of thalamocortical neurons of mouse ventral lateral thalamus. *Somatosens. Mot. Res.* 27, 34–43.

Torigoe, Y., Blanks, R. H., and Precht, W. (1986a). Anatomical studies on the nucleus reticularis tegmenti pontis in the pigmented rat. I. Cytoarchitecture, topography, and cerebral cortical afferents. *J. Comp. Neurol.* 243, 71–87.

Torigoe, Y., Blanks, R. H., and Precht, W. (1986b). Anatomical studies on the nucleus reticularis tegmenti pontis in the pigmented rat. II. Subcortical afferents demonstrated by the retrograde transport of horseradish peroxidase. *J. Comp. Neurol.* 243, 88–105.

Towal, R. B., and Hartmann, M. J. (2006). Right-left asymmetries in the whisking behavior of rats anticipate head movements. *J. Neurosci.* 26, 8838–8846.

Towal, R. B., and Hartmann, M. J. (2008). Variability in velocity profiles during free-air whisking behavior of unrestrained rats. *J. Neurophysiol.* 100, 740–752.

Towal, R. B., Quist, B. W., Gopal, V., Solomon, J. H., and Hartmann, M. J. Z. (2011). The morphology of the rat vibrissal array: a model for quantifying spatiotemporal patterns of whisker-object contact. *PLoS Comput. Biol.* 7, e1001120. doi: 10.1371/journal.pcbi.1001120

Trageser, J. C., Burke, K. A., Masri, R., Li, Y., Sellers, L., and Keller, A. (2006). State-dependent gating of sensory inputs by zona incerta. *J. Neurophysiol.* 96, 1456–1463.

Trageser, J. C., and Keller, A. (2004). Reducing the uncertainty: gating of peripheral inputs by zona incerta. *J. Neurosci.* 24, 8911–8915.

Troncoso, J., Múnera, A., and Delgado-García, J. M. (2004). Classical conditioning of eyelid and mystacial vibrissae responses in conscious mice. *Learn. Mem.* 11, 724–726.

Troncoso, J., Múnera, A., and Delgado-García, J. M. (2007). Learning-dependent potentiation in the vibrissal motor cortex is closely related to the acquisition of conditioned whisker responses in behaving mice. *Learn. Mem.* 14, 84–93.

Urbain, N., Creamer, K., and Debonnel, G. (2006). Electrophysiological diversity of the dorsal raphe cells across the sleep-wake cycle of the rat. *J. Physiol. (Lond.)* 573, 679–695.

Urbain, N., and Deschênes, M. (2007a). Motor cortex gates vibrissal responses in a thalamocortical projection pathway. *Neuron* 56, 714–725.

Urbain, N., and Deschênes, M. (2007b). A new thalamic pathway of vibrissal information modulated by the motor cortex. *J. Neurosci.* 27, 12407–12412.

Valdés, J. L., Sánchez, C., Riveros, M. E., Blandina, P., Contreras, M., Farías, P., and Torrealba, F. (2010). The histaminergic tuberomammillary nucleus is critical for motivated arousal. *Eur. J. Neurosci.* 31, 2073–2085.

Van der Loos, H. (1976). Barreloids in mouse somatosensory thalamus. *Neurosci. Lett.* 2, 1–6.

Van Horn, R. N. (1970). Vibrissae structure in the rhesus monkey. *Folia Primatol.* 13, 241–285.

Veinante, P., and Deschênes, M. (1999). Single- and multi-whisker channels in the ascending projections from the principal trigeminal nucleus in the rat. *J. Neurosci.* 19, 5085–5095.

Veinante, P., and Deschênes, M. (2003). Single-cell study of motor cortex projections to the barrel field in rats. *J. Comp. Neurol.* 464, 98–103.

Veinante, P., Jacquin, M. F., and Deschênes, M. (2000a). Thalamic projections from the whisker-sensitive regions of the spinal trigeminal complex in the rat. *J. Comp. Neurol.* 420, 233–243.

Veinante, P., Lavallée, P., and Deschênes, M. (2000b). Corticothalamic projections from layer 5 of the vibrissal barrel cortex in the rat. *J. Comp. Neurol.* 424, 197–204.

Verberne, A. J. M., and Struyker Boudier, H. A. J. (1991). Midbrain central grey: regional haemodynamic control and excitatory amino acidergic mechanisms. *Brain Res.* 550, 86–94.

Vianna, D. M. L., and Brandão, M. L. (2003). Anatomical connections of the periaqueductal gray: specific neural substrates for different kinds of fear. *Braz. J. Med. Biol. Res.* 36, 557–566.

Villanueva, L., Bouhassira, D., Bing, Z., and Le Bars, D. (1988). Convergence of heterotopic nociceptive information onto subnucleus reticularis dorsalis neurons in the rat medulla. *J. Neurophysiol.* 60, 980–1009.

Vincent, S. B. (1913). The tactile hair of the white rat. *J. Comp. Neurol.* 23, 1–36.

von Heimendahl, M., Itskov, P. M., Arabzadeh, E., and Diamond, M. E. (2007). Neuronal activity in rat barrel cortex underlying texture discrimination. *PLoS Biol.* 5, e305. doi: 10.1371/journal.pbio.0050305

Voogd, J., and Glickstein, M. (1998). The anatomy of the cerebellum. *Trends Neurosci.* 21, 370–375.

Voorn, P., Vanderschuren, L. J. M. J., Groenewegen, H. J., Robbins, T. W., and Pennartz, C. M. A. (2004). Putting a spin on the dorsal-ventral divide of the striatum. *Trends Neurosci.* 27, 468–474.

Waite, P. M. E., and Jacquin, M. F. (1992). Dual innervation of the rat vibrissa: responses of trigeminal ganglion cells projecting through deep or superficial nerves. *J. Comp. Neurol.* 322, 233–245.

Wanaverbecq, N., Bodor, A. L., Bokor, H., Slézia, A., Lüthi, A., and Acsády, L. (2008). Contrasting the functional properties of GABAergic axon terminals with single and multiple synapses in the thalamus. *J. Neurosci.* 28, 11848–11861.

Waterhouse, B. D., Devilbiss, D., Seiple, S., and Markowitz, R. (2004). Sensorimotor-related discharge of simultaneously recorded, single neurons in the dorsal raphe nucleus of the awake, unrestrained rat. *Brain Res.* 1000, 183–191.

Welker, C. (1971). Microelectrode delineation of fine grain somatotopic organization of (SmI) cerebral neocortex in albino rat. *Brain Res.* 26, 259–275.

Welker, C., and Sinha, M. M. (1972). Somatotopic organization of Smll cerebral neocortex in albino rat. *Brain Res.* 37, 132–136.

Welker, C., and Woolsey, T. A. (1974). Structure of layer IV in the somatosensory neocortex of the rat: description and comparison with the mouse. *J. Comp. Neurol.* 158, 437–453.

Welker, E., Hoogland, P. V., and Van der Loos, H. (1988). Organization of feedback and feedforward projections of the barrel cortex: a PHA-L study in the mouse. *Exp. Brain Res.* 73, 411–435.

Welker, W. I. (1964). Analysis of sniffing of the albino rat. *Behaviour* 22, 223–244.

Wenk, G. L. (1997). The nucleus basalis magnocellularis cholinergic system: one hundred years of progress. *Neurobiol. Learn. Mem.* 67, 85–95.

Westby, G. W. M., Collinson, C., and Dean, P. (1993). Excitatory drive from deep cerebellar neurons to the superior colliculus in the rat: an electrophysiological mapping study. *Eur. J. Neurosci.* 5, 1378–1388.

White, E. L., and DeAmicis, R. A. (1977). Afferent and efferent projections of the region in mouse SmL cortex which contains the posteromedial barrel subfield. *J. Comp. Neurol.* 175, 455–481.

Williams, M. N., Zahm, D. S., and Jacquin, M. F. (1994). Differential foci and synaptic organization of the principal and spinal trigeminal projections to the thalamus in the rat. *Eur. J. Neurosci.* 6, 429–453.

Wimmer, V. C., Bruno, R. M., de Kock, C. P. J., Kuner, T., and Sakmann, B. (2010). Dimensions of a projection column and architecture of VPM and POm axons in rat vibrissal cortex. *Cereb. Cortex* 20, 2265–2276.

Wineski, L. E. (1985). Facial morphology and vibrissal movement in the golden hamster. *J. Morphol.* 183, 199–217.

Wise, S. P., and Jones, E. G. (1977). Somatotopic and columnar organization in the corticotectal projection of the rat somatic sensory cortex. *Brain Res.* 133, 223–235.

Wolfe, J., Hill, D. N., Pahlavan, S., Drew, P. J., Kleinfeld, D., and Feldman, D. E. (2008). Texture coding in the rat whisker system: slip-stick versus differential resonance. *PLoS Biol.* 6, e215. doi: 10.1371/journal.pbio.0060215

Woolf, N. J. (1991). Cholinergic systems in mammalian brain and spinal cord. *Prog. Neurobiol.* 37, 475–524.

Woolsey, T. A., and Van der Loos, H. (1970). The structural organization of layer IV in the somatosensory region (SI) of mouse cerebral cortex. The description of a cortical field composed of discrete cytoarchitectonic units. *Brain Res.* 17, 205–242.

Woolsey, T. A., Welker, C., and Schwartz, R. H. (1975). Comparative anatomical studies of the SmI face cortex with special reference to the occurrence of "barrels" in layer IV. *J. Comp. Neurol.* 164, 79–94.

Woolston, D. C., La Londe, J. R., and Gibson, J. M. (1983). Corticofugal influences in the rat on responses of neurons in the trigeminal nucleus interpolaris to mechanical stimulation. *Neurosci. Lett.* 36, 43–48.

Wouterlood, F. G., Sauren, Y. M. H. F., and Steinbusch, H. W. M. (1986). Histaminergic neurons in the rat brain: correlative immunocytochemistry, Golgi impregnation, and electron microscopy. *J. Comp. Neurol.* 252, 227–244.

Wright, A. K., Norrie, L., Ingham, C. A., Hutton, E. A. M., and Arbuthnott, G. W. (1999). Double anterograde tracing of outputs from adjacent "barrel columns" of rat somatosensory cortex. Neostriatal projection patterns and terminal ultrastructure. *Neuroscience* 88, 119–133.

Wright, A. K., Ramanathan, S., and Arbuthnott, G. W. (2001). Identification of the source of the bilateral projection system from cortex to somatosensory neostriatum and an exploration of its physiological actions. *Neuroscience* 103, 87–96.

Yatim, N., Billig, I., Compoint, C., Buisseret, P., and Buisseret-Delmas, C. (1996). Trigeminocerebellar and trigemino-olivary projections in rats. *Neurosci. Res.* 25, 267–283.

Yohro, T. (1977). Structure of the sinus hair follicle in the big-clawed shrew, *Sorex unguiculatus. J. Morphol.* 153, 333–353.

Yu, C., Derdikman, D., Haidarliu, S., and Ahissar, E. (2006). Parallel thalamic pathways for whisking and touch signals in the rat. *PLoS Biol.* 4, e124. doi: 10.1371/journal.pbio.0040124

Zagon, A., Terenzi, M. G., and Roberts, M. H. T. (1995). Direct projections from the anterior pretectal nucleus to the ventral medulla oblongata in rats. *Neuroscience* 65, 253–272.

Zerari-Mailly, F., Pinganaud, G., Dauvergne, C., Buisseret, P., and Buisseret-Delmas, C. (2001). Trigemino-reticulo-facial and trigemino-reticulo-hypoglossal pathways in the rat. *J. Comp. Neurol.* 429, 80–93.

Zucker, E., and Welker, W. I. (1969). Coding of somatic sensory input by vibrissae neurons in the rat's trigeminal ganglion. *Brain Res.* 12, 138–156.

Conflict of Interest Statement: The authors declare that the research was conducted in the absence of any commercial or financial relationships that could be construed as a potential conflict of interest.

Received: 08 July 2011; accepted: 26 August 2011; published online: 03 October 2011.

Citation: Bosman LWJ, Houweling AR, Owens CB, Tanke N, Shevchouk OT, Rahmati N, Teunissen WHT, Ju C, Gong W, Koekkoek SKE and De Zeeuw CI (2011) Anatomical pathways involved in generating and sensing rhythmic whisker movements. Front. Integr. Neurosci. ***5****:53. doi: 10.3389/fnint.2011.00053*

frontiers in
INTEGRATIVE NEUROSCIENCE

OPINION ARTICLE
published:13 June 2011
doi: 10.3389/fnint.2011.00025

Possible functions of prefrontal cortical neurons in duration discrimination

Ken-ichi Oshio*

Department of Physiology, Kinki University Faculty of Medicine, Japan
**Correspondence: oshio@med.kindai.ac.jp*

The physical duration of a stimulus can be held invariant in different sensory modalities, such as vision and audition. The prefrontal cortex (PFC) is a region for convergence of inputs that originate in distinct sensory areas, and is considered an area of cross-modal association (Fuster et al., 2000). Assuming that the PFC participates in duration discrimination, such cross-modal integration appears crucial in support of an "amodal" clock used to time intervals in the seconds-to-minutes range (Meck and Church, 1982; Cordes et al., 2007). Indeed, brain-imaging studies have demonstrated that the PFC contributes to duration discrimination (for a review, see Meck et al., 2008). However, the actual roles of PFC neurons remain unclear. Although single-unit recording is effective in terms of elucidating the functional roles of each area, only a few investigations have been made of PFC neurons in interval-timing tasks in primates (for a rodent homolog of the role of PFC neurons in timing see Matell et al., 2003, 2011). Here, we review recent results of single-unit recording from monkey PFC neurons, discuss their possible functions, and then comment on future directions.

We recorded single-unit activity while monkeys were performing a duration discrimination task in a series of studies (Oshio et al., 2006, 2008). In the task, red and blue cues were presented consecutively on a computer monitor for different durations ranging from 0.2 to 2.0 s, and the monkeys were then required to choose which color cue had lasted longer. Each cue was followed by a delay period of 1.0 s. The first cue, first delay, second cue, and second delay are referred to as C1, D1, C2 and D2, respectively. First, we found that PFC neurons showed significantly different activity during either the D1 or D2 period when comparing activity in C1-longer (LS) and C2-longer (SL) trials (Oshio et al., 2006). As for the D1 activity, the result indicates that the PFC neurons responded as if they encoded the duration category (e.g., "long" or "short") of the C1 cue as early as the D1 period. Taken together with the correlated D2 activity, our findings suggest that PFC neurons not only encode duration category, but also implement strategic processes such as the representation of trial type (LS or SL) and the retention of cue information. Next, we analyzed neurons that were responsive during the C1 period, and found that phasic (transient) activity was the most common mode of activity (Oshio et al., 2008). Peak time of this phasic activity was broadly distributed with a delay of approximately 0.8 s after cue onset. Such phasic activity following a constant delay after cue onset might serve as a mechanism to filter or separate the current trial's cue duration from the peak time in activity. The most frequent peak time was close to the time separating cue durations into "long" and "short" categories. As a consequence, the activity of this peak time might have played a role in filtering or selecting the appropriate response for the duration discrimination. Outputs of this temporal filtering, as a function of the phasic activity, would have been represented as the categorical response in the D1 period. Recently, two other research groups have successfully recorded single-unit activity in the monkey PFC during an interval-timing task, and found neuronal activities with various temporal profiles, including phasic, tonic, ramping, and so on, during cue and/or delay periods. As a consequence, it was proposed that PFC neurons may play a variety of roles in temporal processing, including the monitoring of cue duration and memory encoding (Sakurai et al., 2004; Genovesio et al., 2009 – see also Matell et al., 2011).

There is considerable agreement among the above-mentioned studies that PFC neurons represent the absolute cue duration as well as other types of temporal information during ensuing delay periods. Scalar timing theory postulates three stages of temporal processes in duration discrimination: clock, memory, and comparison (Gibbon et al., 1984). The reported delay period activity suggests that PFC neurons contribute to the memory stage. This is reasonable, because PFC activity is well-known to support working memory function (e.g., Miller et al., 1996). Slight differences in PFC activity across various experiments have been attributed to differences in behavioral tasks, i.e., differences in the strategy that monkeys use to solve the task, etc. This also seems reasonable given that the PFC is considered to also serve strategic function. Moreover, subjects may actually adopt different strategies based on the nature of the timing task. The exact strategies taken by subjects can be inferred from behavioral data to some extent, but neuronal data may be more informative in this case and should be taken into consideration when analyzing the behavioral data.

There is controversy over whether the internal clock is modality-specific or modality-independent and centralized or distributed (see Buhusi and Meck, 2005; Bueti and Walsh, 2009). The PFC, an area of cross-modal association, is a candidate for a centralized, amodal timing mechanism. Experiments with timing tasks using unimodal and bimodal sensory stimuli, including vision and audition, should be carried out to clarify whether the PFC serves as a centralized clock or not. In addition, neuroimaging studies have revealed that other brain areas also participate in timing tasks, for example, the basal ganglia, the parietal cortex, the cerebellum, and the supplementary motor area (Buhusi and Meck, 2005). However, the contributions of these areas to duration discrimination are much less understood than the PFC. The PFC has anatomical connections with all of these areas, and is known to cooperate with those areas in cognitive and motor functions (Fuster, 2008). Therefore, further elucidation of the roles of the PFC would be helpful to uncover

their contributions to timing and time perception. In summary, the PFC is a key area to determine the functional and neural mechanisms of interval timing. More extensive research on the properties of PFC neurons is required in order to construct and test neurophysiological models of interval timing (see Matell and Meck, 2004; Lustig et al., 2005; Karmarkar and Buonomano, 2007).

ACKNOWLEDGMENT

The author is supported by grants from the Ministry of Education, Culture, Sports, Science and Technology of Japan (17021039, 18500314, 19500230, 21500264).

REFERENCES

Bueti, D., and Walsh, V. (2009). The parietal cortex and the representation of time, space, number and other magnitudes. *Philos. Trans. R. Soc. Biol. Sci.* 364, 1831–1840.

Buhusi, C. V., and Meck, W. H. (2005). What makes us tick? Functional and neural mechanisms of interval timing. *Nat. Rev. Neurosci.* 6, 755–765.

Cordes, S., Williams, C. L., and Meck, W. H. (2007). Common representations of abstract quantities. *Curr. Dir. Psychol. Sci.* 16, 156–161.

Fuster, J. M. (2008). *The Prefrontal Cortex*, 4th Edn. Boston: Academic Press.

Fuster, J. M., Bodner, M., and Kroger, J. K. (2000). Cross-modal and cross-temporal association in neurons of frontal cortex. *Nature* 405, 347–351.

Genovesio, A., Tsujimoto, S., and Wise, S. P. (2009). Feature- and order-based timing representations in the frontal cortex. *Neuron* 63, 254–266.

Gibbon, J., Church, R. M., and Meck, W. H. (1984). Scalar timing in memory. *Ann. N. Y. Acad. Sci.* 423, 52–77.

Karmarkar, U. R., and Buonomano, D. V. (2007). Timing in the absence of clocks: encoding time in neural network states. *Neuron* 53, 427–438.

Lustig, C., Matell, M. S., and Meck, W. H. (2005). Not "just" a coincidence: frontal-striatal interactions in working memory and interval timing. *Memory* 13, 441–448.

Matell, M. S., and Meck, W. H. (2004). Cortico-striatal circuits and interval timing: coincidence-detection of oscillatory processes. *Cogn. Brain Res.* 21, 139–170.

Matell, M. S., Meck, W. H., and Nicolelis, M. A. L. (2003). Interval timing and the encoding of signal duration by ensembles of cortical and striatal neurons. *Behav. Neurosci.* 117, 760–773.

Matell, M. S., Shea-Brown, E., Gooch, C., Wilson, A. G., and Rinzel, J. (2011). A heterogeneous population code for elapsed time in rat medial agranular cortex. *Behav. Neurosci.* 125, 54–73.

Meck, W. H., and Church, R. M. (1982). Abstraction of temporal attributes. *J. Exp. Psychol. Anim. Behav. Process.* 8, 226–243.

Meck, W. H., Penney, T. B., and Pouthas, V. (2008). Cortico-striatal representation of time in animals and humans. *Curr. Opin. Neurobiol.* 18, 145–152.

Miller, E. K., Erickson, C. A., and Desimone, R. (1996). Neural mechanisms of visual working memory in prefrontal cortex of the macaque. *J. Neurosci.* 16, 5154–5167.

Oshio, K., Chiba, A., and Inase, M. (2006). Delay period activity of monkey prefrontal neurons during duration-discrimination task. *Eur. J. Neurosci.* 23, 2779–2790.

Oshio, K., Chiba, A., and Inase, M. (2008). Temporal filtering by prefrontal neurons in duration discrimination. *Eur. J. Neurosci.* 28, 2333–2343.

Sakurai, Y., Takahashi, S., and Inoue, M. (2004). Stimulus duration in working memory is represented by neural activity in the monkey prefrontal cortex. *Eur. J. Neurosci.* 20, 1069–1080.

Received: 02 June 2011; accepted: 02 June 2011; published online: 13 June 2011.

*Citation: Oshio K (2011) Possible functions of prefrontal cortical neurons in duration discrimination. Front. Integr. Neurosci. **5**:25. doi: 10.3389/fnint.2011.00025*

frontiers in
INTEGRATIVE NEUROSCIENCE

ORIGINAL RESEARCH ARTICLE
published: 12 July 2011
doi: 10.3389/fnint.2011.00030

Behavioral sensitivity of temporally modulated striatal neurons

George S. Portugal[1], A. George Wilson[2] and Matthew S. Matell[3]*

[1] *Department of Anesthesiology, Columbia University Medical Center, New York, NY, USA*
[2] *Department of Psychology, Indiana University, Bloomington, IN, USA*
[3] *Department of Psychology, Villanova University, Villanova, PA, USA*

Edited by:
Warren H. Meck, Duke University, USA

Reviewed by:
Hugo Merchant, Universidad Nacional Autónoma de México, Mexico
Mark Laubach, The John B. Pierce Laboratory, USA

***Correspondence:**
Matthew S. Matell, Department of Psychology, Villanova University, 800 Lancaster Ave, Villanova, PA 19085, USA.
e-mail: matthew.matell@villanova.edu

Recent investigations into the neural mechanisms that underlie temporal perception have revealed that the striatum is an important contributor to interval timing processes, and electrophysiological recording studies have shown that the firing rates of striatal neurons are modulated by the time in a trial at which an operant response is made. However, it remains unclear whether striatal firing rate modulations are related to the passage of time alone (i.e., whether temporal information is represented in an "abstract" manner independent of other attributes of biological importance), or whether this temporal information is embedded within striatal activity related to co-occurring contextual information, such as motor behaviors. This study evaluated these two hypotheses by recording from striatal neurons while rats performed a temporal production task. Rats were trained to respond at different nosepoke apertures for food reward under two simultaneously active reinforcement schedules: a variable-interval (VI-15 s) schedule and a fixed-interval (FI-15 s) schedule of reinforcement. Responding during a trial occurred in a sequential manner composing three phases; VI responding, FI responding, VI responding. The vast majority of task-sensitive striatal neurons (95%) varied their firing rates associated with equivalent behaviors (e.g., periods in which their snout was held within the nosepoke) across these behavioral phases, and 96% of cells varied their firing rates for the same behavior within a phase, thereby demonstrating their sensitivity to time. However, in a direct test of the abstract timing hypothesis, 91% of temporally modulated "hold" cells were further modulated by the overt motor behaviors associated with transitioning between nosepokes. As such, these data are inconsistent with the striatum representing time in an "abstract' manner, but support the hypothesis that temporal information is embedded within contextual and motor functions of the striatum.

Keywords: interval timing, striatum, electrophysiology, time perception, rats

INTRODUCTION

The ability to adapt to the temporal structure of events in the seconds to minutes range, interval timing, is critical for behaving in an efficient manner with respect to an unstable, but predictable, environment (Gallistel, 1990; Brunner et al., 1996; Buhusi and Meck, 2005). Besides providing the important ability to predict when specific events should occur, interval timing may also be essential for the computational processes underlying associative learning (Gibbon and Balsam, 1981; Miller and Barnet, 1993; Gallistel and Gibbon, 2000; Balsam et al., 2006), adaptive foraging (Kacelnik and Bateson, 1996), and rate estimation (Brunner et al., 1992). In addition, disordered timing may contribute to behavioral deficits in addictive disorders (Bickel and Marsch, 2001; Perry and Carroll, 2008) as well as those seen in a variety of patient populations (Harrington et al., 1998; Malapani et al., 2002; Penney et al., 2005; Beste et al., 2007). However, despite the relevance of interval timing to adaptive behavior, the neural mechanisms underlying this capacity remain unclear. While recent electrophysiological results from rats have shown that primary visual cortex activity is modulated in timing tasks (Shuler and Bear, 2006), thereby opening the possibility that time is computed within single cortical structures (see also Karmarkar and Buonomano, 2007), behavioral work has shown that temporal memories can be transmitted or combined across modalities (Meck and Church, 1982; Roberts and Holder, 1984; Nagarajan et al., 1998; Swanton et al., 2009), thereby suggesting a centralized timing process that operates in an "abstract," or amodal, fashion (Walsh, 2003; van Wassenhove, 2009). Likewise, functional neuroimaging work in humans (Ferrandez et al., 2003; Nenadic et al., 2003; Coull, 2004; Harrington et al., 2004; Macar et al., 2004; Pouthas et al., 2005; Tregellas et al., 2006; Livesey et al., 2007; Stevens et al., 2007), lesion studies in rodents (Dietrich et al., 1997; Meck, 2006), and electrophysiological recordings from humans (Macar et al., 1999; Pfeuty et al., 2005), non-human primates (Brody et al., 2003; Leon and Shadlen, 2003; Sakurai et al., 2004; Janssen and Shadlen, 2005; Tsujimoto and Sawaguchi, 2005; Mita et al., 2009) and rodents (Matell et al., 2003, 2011), have implicated a broad network of non-sensory structures in interval timing, including parietal and frontal cortices, the basal

ganglia, and thalamus. Thus, the available evidence is consistent with the notion of an amodal temporal representation available for behavioral control.

In an attempt to integrate the wide array of neural structures involved in interval timing, Matell and Meck (2000, 2004) proposed the striatal beat frequency (SBF) model of interval timing. In SBF, cortical activity is hypothesized to evolve as a function of time since an event's occurrence, thereby functioning as a "clock" signal. The striatum is proposed to detect the state of the cortex and respond when the cortical pattern matches previously reinforced states, thereby serving as the memory and decision stages of an information processing model. Output from the striatum is then fed through basal ganglia output channels to the thalamus en route to the motor cortex, thereby engendering a behavioral response.

In order to examine the involvement of the cortex and striatum in interval timing, Matell et al. (2003) tested rats on a mixed 10-s, 40-s probabilistic fixed-interval schedule while recording single cell activity from both anterior cingulate cortex and dorsal anterior striatum. Due to a lower probability of reinforcement at the short duration compared to the long duration, average behavioral response rates ramped up to a maximum around 10 s, and if reinforcement was not delivered, responding ramped back down before ramping back up to an equivalent maximal rate at 40 s. Suggesting a direct relation to motor behavior, many neurons in both structures responded in a similar pattern (i.e., equivalent maximal activity at both 10 and 40 s). However, a subset of neurons showed differential firing rates at one of these times as compared to the other, demonstrating their sensitivity to time. The discrepancy in firing rate between 10 and 40 s was larger in the striatal neurons than the cortical neurons, thereby supporting SBF's contention that the striatum serves to "recognize" specific trained intervals.

Intriguingly, many of these temporally sensitive neurons showed maximal peak-shaped firing at 10 s, and a secondary, smaller increase in firing at 40 s (see **Figure 1A**). This activity pattern can be interpreted in two ways: temporally modulated motor coding (**Figure 1B**) versus "abstract" temporal coding (**Figure 1C**). In the temporally modulated motor coding scheme, the heightened activity at both 10 and 40 s critically depends upon the co-occurring motor activity of the rat which also peaked at 10 s and ramped to 40 s. In this scheme, the temporal specificity of the neurons is seen as a modulation in the strength of this motor-related firing at one time compared to another. For example, as shown in **Figure 1B**, a neuron that fires at a greater rate at 10 s than at 40 s could result from an increase in response related firing at 10 s as compared to response related firing at 40 s (the same result could also be due to a decrease in response related activity at 40 s). Support for this type of temporally modulated motor coding scheme comes from classic views of the basal ganglia as a set of motor structures (DeLong, 1983; Marsden, 1984; Schultz and Romo, 1988). In the latter, "abstract," coding scheme, temporally specific striatal activity would occur without modulation by the motor behaviors of the rat, and the elevated, but differential, firing rates at 10 and 40 s reflect a representation of both of these criterion durations. As shown in **Figure 1C**, the lower rate of activity at 40 s reflects the scalar variability that is characteristic of interval timing behavior (i.e., the decrease in precision and amplitude seen when subjects estimate longer durations (Gibbon, 1977). In this scheme, the motor activity is a "downstream" behavioral response to the temporal information reflected in the heighted firing rates of the striatal neurons. Support for a motor-independent "abstract" coding scheme comes from recording work in primates in which firing rates fluctuate in a duration-specific manner in the absence of observable behavior (Brody et al., 2003; Leon and Shadlen, 2003).

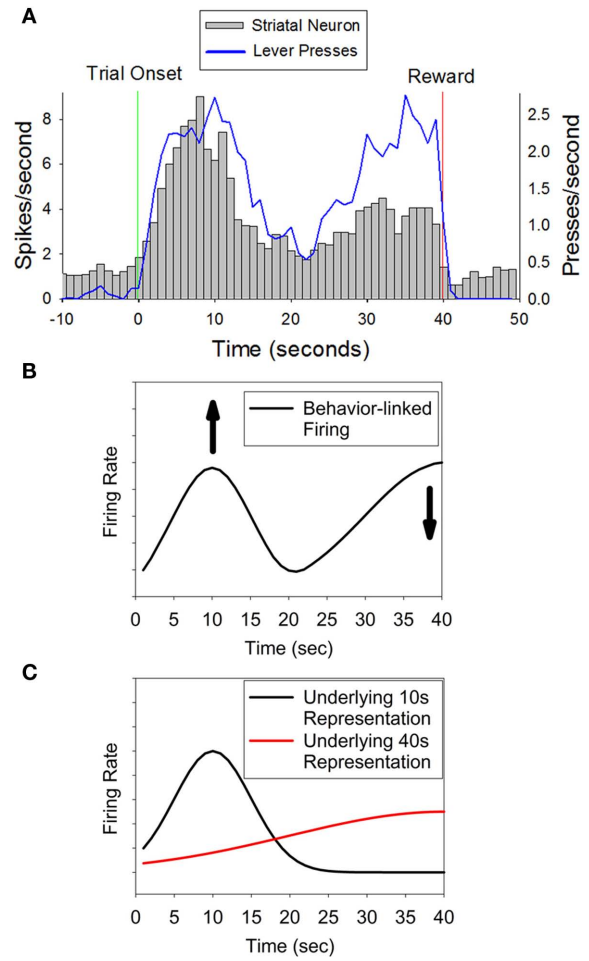

FIGURE 1 | Panel (A) (adapted from Matell et al., 2003) displays the activity pattern of a representative striatal neuron showing differential activity at two times associated with possible reinforcement (10 and 40 s), indicating sensitivity to specific temporal interval(s). Importantly, the behavioral response rate was equivalent at these two times, thereby ruling out a simple motor coding role of the striatum. The peak in firing at 10 s and the secondary increase in firing at 40 s could result from two processes. **(B)** Represents a temporally modulated motor coding scheme in which the neural activity is directly tied to the motor behavior of the rat, but firing is enhanced at 10 s, and/or diminished at 40 s, thereby demonstrating temporal expectation. **(C)** Represents an "abstract" temporal coding scheme, such that both 10 and 40 s are represented by the neuron, and the smaller magnitude at 40 s reflects scalar variability. In this latter coding scenario, the motor behavior of the rat is a "downstream" effect and does not contribute to striatal firing rates.

To further investigate the role of the striatum in the temporal control of behavior and the temporal expectation of reinforcement, and to assess the form of changes in firing rate that emerge across the trial, we recorded from striatal neurons in rats. Subjects were trained to nosepoke into different nosepoke apertures at different times within a trial, with different reinforcement schedules associated with each aperture. Specifically, rats were trained that nosepoking into a central nosepoke aperture would probabilistically deliver reinforcement after a fixed interval (FI) had elapsed, while poking into a peripheral nosepoke aperture would probabilistically deliver reinforcement at a variable time (VI) in the trial (Matell and Portugal, 2007). No information was provided to the rats to indicate the time or nosepoke aperture at which reinforcement, if any, could be earned on each trial. As such, their behavior during non-reinforced probe trials progressed in a sequential manner; it was directed toward the VI nosepoke aperture early in the trial, transitioned to the FI nosepoke aperture as time approached the criterion fixed-interval duration, and then transitioned back to the VI nosepoke aperture following the passage of the criterion time. Because reinforcement could be earned simply by the rat having its snout in the nosepoke, without making an active response, sustained nosepoke "holding" was generally continuous throughout the trial, except when the rats switched nosepokes, allowing us to address whether striatal neurons showed temporal modulation in their firing rates during matched behaviors by comparing activity across and within nosepoking phases. This design also allowed us to assess whether such temporal modulation was sensitive to the collateral motor behaviors made by the rat during the trial. Specifically, if striatal activity represents the time of predictable reinforcement irrespective of any collateral motor behaviors, neural activity during the behavioral transitions should fall within the range of firing rates occurring during the surrounding nosepoking phases. In contrast, if striatal neurons encode time within a behavioral context, the transition behaviors should produce abrupt changes in firing rate, such that the transition firing rates are outside the range of those associated with the surrounding nosepoke-related activity.

MATERIALS AND METHODS

SUBJECTS

Five male Sprague–Dawley rats (Harlan Labs, Indianapolis, IN, USA) that were approximately 60 days of age at the start of the experiment were used in this study. Rats were housed in pairs with a 12-h light–dark cycle, with lights on from 8 a.m. to 8 p.m. Animals were trained during the light phase of the cycle, and were given continuous access to water throughout the study. All rats were kept on a restricted feeding schedule and their body weights were maintained at 85–90% of their free-feeding weights, adjusted for growth. Following electrode implantation surgeries, rats were housed individually. All procedures were conducted in accordance with the Villanova University's Institutional Animal Care and Use Committee (IACUC).

APPARATUS

All behavioral data were obtained using standard operant-conditioning chambers (30.5 × 25.4 × 30.5 cm – Coulbourn Instruments). The sides of the chamber were ventilated Plexiglas, and the front wall, back wall and ceiling were aluminum. The floor was composed of stainless steel bars. A pellet dispenser attached to the back wall of the operant chamber delivered 45-mg sucrose pellets (Formula F; Noyes Precision, Lancaster, NH, USA) to a food cup. Three nosepoke response apertures with LED cue lights in their interior were placed on the front wall of the chamber. In order to ensure that responding on each nosepoke aperture was broadly similar in terms of body position, two aluminum "hallway" barriers (30.5 cm high × 8.2 cm length) were attached to the front wall so that a rat could not respond on the nosepokes unless its body was perpendicular to the front wall. These barriers also prevented the rat from rapidly switching between nosepokes. The operant chambers were also equipped with a houselight and a seven-tone audio generator. Behavioral data were transmitted to a computer program that recorded all events (Graphic State, Coulbourn Instruments, Whitehall, PA, USA). Following electrode implantation, all neural and behavioral data were recorded with a 40-kHz A-D data acquisition system (Recorder, Plexon Inc., Dallas, Texas).

BEHAVIOR

Magazine training (1 session)

In this procedure, a sucrose pellet was delivered once per min for 60 min.

Nosepoke autoshaping (2–3 sessions)

Following magazine training, rats were given sessions of nosepoke autoshaping. In this phase of training, reinforcement was delivered, independently of responding, once per min for the 60-min session. Prior to reinforcement, the center nosepoke cue light was turned on for 1 s. Responses made by the animal on the center nosepoke at any time during the session also resulted in reinforcement. Rats met the autoshaping criterion once they made 60 nosepokes within a session on two consecutive days.

Nosepoke discrimination training (1 session)

Rats were trained to respond on all three nosepokes for reinforcement. Trials began with the activation of a pulsing 1 kHz tone (pulse frequency = 12.5 Hz) and continuous onset of a randomly selected nosepoke light. Reinforcement was delivered for the first poke into the lit nosepoke aperture and the tone and nosepoke light were extinguished, ending the trial. Responses to unlit nosepokes had no consequence. Reinforcement was followed by a random 20–40 s inter-trial interval (ITI) on this and all subsequent procedures. Session duration was 60 min. All rats met the criterion of 20 responses on each active nosepoke during the first session.

Fixed-interval training (~15 sessions)

Rats were trained on a discrete trials 15 s fixed-interval schedule. Trials again commenced with a 12.5-Hz pulsing 1 kHz tone. In addition to the tone, the cue light of either the left or right nosepoke was activated, and a response made on the illuminated nosepoke initiated an FI trial. At the start of the FI trial, a continuous 4 kHz tone and the center nosepoke cue light were activated, and the side nosepoke light extinguished. Subjects were reinforced for the first response on the FI nosepoke after 15 s had elapsed.

Rats were also reinforced if their snout was inside the nosepoke when the criterion duration (15 s) was reached. The tone and cue light were terminated after reinforcement. Sessions lasted 120 min in this and all subsequent procedures. After several sessions, an examination of average response probability as a function of signal duration showed the classic scallop pattern of responding (Ferster and Skinner, 1957). Rats advanced to the next phase of training once the average response probability at the criterion duration (bin from 14–15 s) exceeded 80%.

Peak-interval training (∼10 sessions)

Peak-interval training was identical to fixed-interval training, except that a proportion of trials (50%) were non-reinforced probe trials. On probe trials, the 4-kHz tone and the cue light of the FI nosepoke remained on for 2.5–3.5 times the criterion duration (38–53 s), and all responses had no programmed consequence. No indication was given to the subject as to which trial type (FI or probe) had been selected. As with previous research (Roberts, 1981; Church et al., 1991), an examination of average response probability as a function of time since signal onset revealed a nearly symmetrical, Gaussian shaped function centered around 15 s. In order to quantify the accuracy and precision of temporal responding, this peak function was fit with a Gaussian curve, and the mean and standard deviation of this curve were used as a measure of the expected time of reinforcement (Peak Time), and the precision of this expectation (Peak Spread). The coefficient of variation (Peak Spread/Peak Time) was calculated, and rats were advanced to the next phase of training once this statistic was less than 0.5 for five non-consecutive sessions.

Variable-interval training (∼2–4 sessions)

In this procedure, rats were trained to respond on the left or right nosepoke, randomly selected on each trial, using a variable-interval (15 s) schedule of reinforcement. Trials began in the same manner as during fixed-interval and peak-interval training, with a poke into the illuminated left or right nosepoke. Once the rat self-initiated the trial, the continuous 4 kHz tone commenced and the same nosepoke light which had been flashing to indicate an opportunity to initiate the trial was illuminated continuously. While the rat's snout was inside of the active VI nosepoke, there was a 2% probability of reinforcement every 300 ms. This low probability of reinforcement resulted in a mean delay to reinforcement of 15 s if the rat occupied the nosepoke continuously. Responses made on the center FI nosepoke or the inactive VI nosepoke had no programmed consequence. Trials ended upon reinforcement. Rats were advanced to the next phase of training once the average response probability during each of the first 5 s of a trial was at least 50%. Following criterion performance, rats were given an additional session of peak-interval training before advancing to the final phase of training.

Peak procedure with variable-interval training/testing (∼ 15 sessions training)

In the final phase of training, rats were trained on a procedure that integrated the peak-interval and variable-interval phases of training, so that three possible trial types could be selected: 15 s FI trials, 38–53 s probe trials, and 15 s VI trials. On all trials, one of the VI nosepoke cue lights (left or right, randomly selected) and the center FI nosepoke cue light were illuminated. Each trial type had a 33% probability of being selected, and no external cues were provided to the animal to indicate which type of trial had been selected. Rats were trained on this procedure until their behavior on probe trials showed a sequential pattern of responding: initially poking on the active VI nosepoke aperture, switching to the FI nosepoke prior to the criterion duration of 15 s, and then returning to the active VI nosepoke after 15 s had passed. Once behavior stabilized, they were implanted with electrodes, given 1 week to recover, and re-trained on this procedure until performance returned to pre-surgical levels. Once criterion responding was restored, electrophysiological recording commenced.

SURGERY

Electrodes

Movable electrode ensembles were built using a design described in Bilkey and Muir (1999). Briefly, eight 25 μm HML-coated tungsten microwires were assembled into a bundle. The microwires were cannulated and held in place with epoxy. Through the use of a drive screw, the microdrive allowed implanted electrode bundles to move ventrally through the brain. The total dimension of the bundle of eight electrode tips was approximately 1 mm × 1 mm.

Procedure

Rats were anesthetized with an intramuscular injection of ketamine (100 mg/kg) and xylazine (10 mg/kg), and placed in a stereotaxic frame. The skin and muscle on the skull were retracted, and a small hole was drilled into the skull at the target coordinates (center at AP + 0.5, ML ± 3.0, DV − 3.0). The bundle was implanted into dorsal striatum, and recordings during implantation confirmed that electrodes were operating properly and had been placed in the target structure. In addition to the electrode, four skull screws were implanted to hold the electrode in place. A stainless steel wire was wound around the skull screws to serve as a ground for the electrode. A second electrode bundle was inserted into the frontal cortex (center at AP + 3.0, ML ± 1.5, DV − 0.5), but due to the electrode design, we failed to acquire acceptable recordings from these cortical electrodes. Once the bundles were in place, dental cement was used to secure the array to the skull. The wound was closed, and antibiotic ointment was applied. The animals were given 1 week to recover, during which time they had free access to food and water.

Recording procedure

Following recovery, electrophysiological recordings began once rats re-attained stable performance on the final version of the procedure. Before every session, the electrode assembly was lowered 79 μm (1/4 screw turn) ventrally into the striatum. Headstage cables were plugged into the implants, and the rat was placed in the operant chamber with the sound attenuating cabinet door open in order to differentiate the chamber context during spike thresholding. Subsequently, the door to the operant chamber was closed, and the behavioral session was started. The data acquisition system recorded all neural activity that surpassed a thresholded voltage on each mircowire, as well as all behavioral events.

Single unit discrimination

An off-line computer program (Offline Sorter, Plexon, Dallas, Texas) was used to discriminate and isolate action potentials ("spikes") from background noise, and from one another. This program allows the user to separate spikes by computing the principal components that maximally explain the variance in waveform shape. Single units were discriminated from noise by clustering in 3-D PCA space. Evaluation of the clustering of these principal components as a function of time in the session was performed to ensure stationarity of the signals. Once single units were discriminated, the timestamps of spikes and behavioral events were examined through a neural analysis program (NeuroExplorer, Nex Technologies, Littleton, MA, USA) and MatLab (The MathWorks, Natick, MA, USA).

ANALYSIS

The first 38 s of each probe trial and all VI trials with durations greater than 38 s were analyzed and are referred to throughout as probe trials. Our primary goal in this study was to assess whether striatal neurons that varied with time and/or temporal predictability of reward had additional sensitivity to the differential motor behaviors that occurred across the trial. Because nosepoking behavior in each phase was not limited to a single sustained nosepoke, but often consisted of several poke and hold behaviors (see **Figure 3B**), as well as occasional "checking" movements to the food magazine, we isolated nosepoking periods as the times in which the rats' snouts were within the nosepoke aperture. These periods were split into poke initiation, poke hold, and poke termination (see **Figure 2**). Specifically, the poke initiation period was composed of the first 200 ms following onset of a poke. The poke termination period was composed of the last 200 ms prior to termination of a poke. The poke hold period was defined as the remaining time window during which the snout was within the nosepoke aperture. We computed striatal firing rates during these nosepoking periods across the three nosepoking phases [the initial phase of VI nosepoking (VI1), the phase of FI nosepoking (FI), and the second phase of VI nosepoking (VI2)]. On trials with multiple pokes in each phase, the response rates/patterns were determined as the average response rates/patterns within a phase. We also assessed the firing rates during the transitions between nosepoke phases. Transitions were assessed over a 200-ms window immediately following the last nosepoke termination in each of the first two nosepoking phases (T1a and T2a following VI1 and FI withdrawal, respectively) and a 200-ms window immediately preceding the first nosepoke in the latter two nosepoking phases (T1b and T2b preceding FI and VI2 insertion, respectively). We then examined whether firing rates differed between and within behavioral phases to ascertain whether temporal aspects and/or motor behaviors modulated striatal activity. Each analysis is described below and significance was set at $p < 0.05$ for all analyses. Repeated measures ANOVAs were conducted by passing the data from MatLab to R, an open source statistical package implementing S, by utiziling the packages statconnDCOM (Baier and Neuwirth, 2007), and ezANOVA, using Type III sums of squares, and sum contrasts. Results were identical to those obtained from SPSS. **Figure 2** graphically shows these comparisons periods.

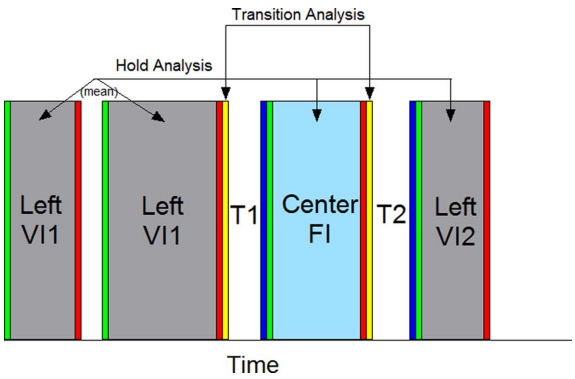

FIGURE 2 | A graphical representation of the behavioral windows used for analysis. The firing rates on each trial were segmented as depicted, splitting the trial into behaviors directed into the VI nosepoke and FI nosepoke. Periods of time in which the rat held its snout within the nosepoke aperture were analyzed, as were brief intervals just following or preceding these nosepoking windows. Responding on the VI nosepoke prior to responding on the FI nosepoke were classified as the VI1 period, and responding on the VI nosepoke following FI responding were classified as the VI2 period. The first 200 ms following the onset of each poke was deemed a poke initiation and is designated in green. The final 200 ms preceding the offset of each poke was deemed a poke termination and is designated in red. The time between poke initiation and poke termination was deemed a nosepoke hold and is colored grey for VI nosepoke holds and light blue for FI nosepoke holds. In order to switch from the VI nosepoke to the FI nosepoke, and vice-versa, the rat had to retreat down a hallway around current VI nosepoke and enter another hallway to advance toward the FI nosepoke. We classified the first and last 200 ms intervals of these switch periods as transitions. The retreat portion is designated yellow, and the procession portion is designated in dark blue. Some, but not all, response periods had multiple pokes/holds (e.g., VI1 here). Therefore, a mean firing rate for each response phase was computed. The response holds lasted varying durations, and the firing rate was simply reported as the total spike count/total duration of the hold. The remaining analytic windows (Poke Initiation, Poke Termination, Transition Retreat, and Transition advance) were of a fixed length, and were further split into ten 20 ms bins to evaluate changes in spike pattern (not shown). To identify whether a single neuron was modulated by the variables in question, repeated measure ANOVAs were conducted by comparing windows of equivalent color, representing equivalent behaviors, with each segment composing a within-subject phase. Individual trials served as "subjects." Trials were randomly chosen to have the active VI nosepoke on the left or right side of the operant chamber, and the spatial position of the active nosepoke served as a between-subjects factor.

Task-sensitivity

Firing rates during each task phase were computed and entered into a repeated measures ANOVA in which behavior (VI1 poke initiation, VI hold, VI1 poke termination, T1a, T1b, FI poke initiation, FI hold, FI poke termination, T2a, T2b, VI2 poke initiation, VI2 hold, VI2 poke termination) served as a within-subject factor, and VI spatial position (left or right VI trial) served as a between-subject factor.

Temporal/schedule modulation across nosepoking phases

Firing rates during the three nosepoking phases were compared with repeated measures ANOVAs examining VI1, FI, and VI2 (initiation, holds, or termination performed separately) as within-subject factors and spatial position of the active VI nosepoke for

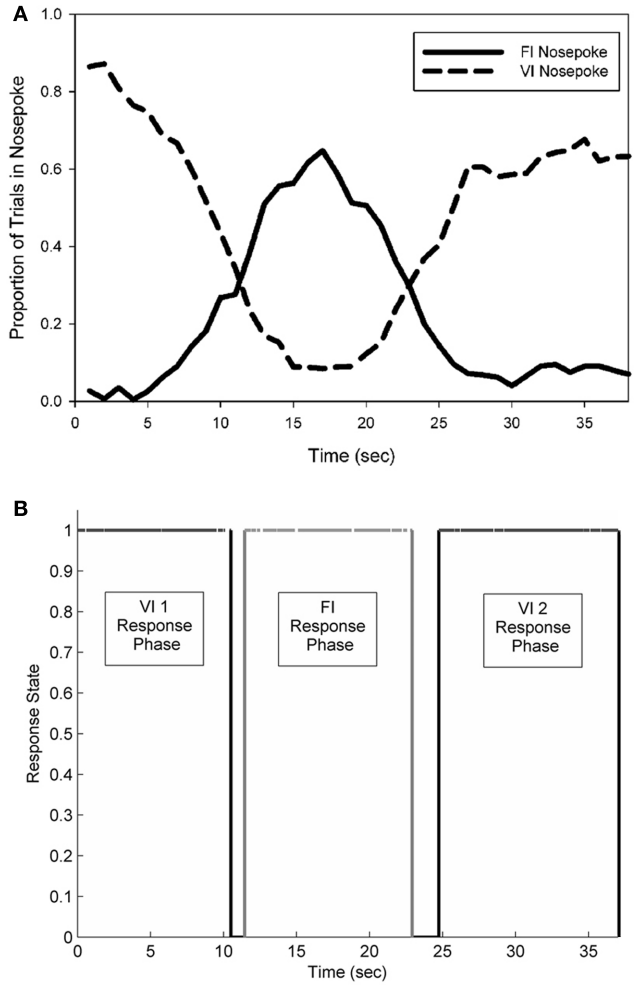

FIGURE 3 | A representative example of the average pattern of responding from a single rat observed during an electrophysiological recording session (A). FI nosepoke responses formed a near-symmetrical peak distribution, centered near 15 s, while two separate periods of responding occurred on the VI nosepoke. **(B)** Depicts the pattern of responding observed in an individual probe trial. Black lines indicate occupancy in the VI nosepoke, and grey lines indicate occupancy in the FI nosepoke.

each trial as a between-subject factor. With the nosepoke holds, because the hold duration varied across pokes and trials, we utilized the mean firing rate during all holds within a phase. For poke initiation and termination, we split the analysis window into ten 20 ms bins, and included time as a within-subject factor. In those neurons that had significant fluctuations in rate during hold behaviors across nosepoking phases, we broadly categorized their response pattern as ramping if firing rates grew in a monotonic manner, and peaking if firing rates were non-monotonic (i.e., low rate – high rate – low rate).

Temporal/schedule modulation across transition phases

Firing rates during the transition behaviors associated with switching nosepokes (200 ms windows as defined above) were compared with a repeated measures ANOVA with transition phase (e.g., T1a versus T2a) as a within-subject factor, and spatial position of the active VI nosepoke as a between-subject factor.

Sensitivity to overt motor behavior

As the majority of cells showed temporal sensitivity during the hold periods across nosepoking phases, we wished to examine whether these cells had firing rates that grew/decayed in a monotonic manner between phases, or whether their activity was influenced by the overt motor behaviors occurring during the transition between nosepokes. To this end, the expected firing rate was computed as a linear function from the mean rate during the last fifth of the preceding hold period to the mean rate during the first fifth of the forthcoming hold period. A repeated measures ANOVA was used to compare the actual firing rate during each transition period to this expected firing rate, with spatial location of the VI nosepoke serving as a between-subjects factor. For example, the firing rate during transition phase T1a was compared to the expected firing rate computed as a linear function from the firing rate during the last 1/5 of the preceding VI1 phase to the firing rate during the first 1/5 of the following FI phase.

Temporal modulation within a behavioral state

In many of the above analyses, the influence of phase/response schedule contingencies was confounded with the influence of elapsed time. Therefore, we analyzed the pattern of firing during nosepoke holding within a single trial. To this end, each phase of nosepoking was split into 5 equal duration sub-phases (Time), and spike rates during nosepoke holds in each of these sub-phases, on each trial, were entered into a repeated measures ANOVA with time as a within-subject factor and spatial position of the VI as a between-subject factor. Neurons with significant modulation within a phase were classified as ramping if the firing rates across their five sub-phases progressed in a monotonic manner, and as peaking if firing rate rose and fell (or vice-versa) in a bi-tonic manner with maximal (minimal) firing rate in the 3rd sub-phase. Because more than 75% of the duration of each phase was composed of nosepoke holding (rather than repeated poking throughout the phase), we performed a similar analysis on firing rates associated with poke initiation and termination, but we split each phase into halves rather than fifths to avoid missing values in the ANOVA.

Histological procedure

The final location of the electrodes was determined once data acquisition was completed. Rats were anesthetized, and a 100-μA current was passed through an electrode for 20 s, creating a small marking lesion. Subsequently, the rats were deeply anesthetized with pentobarbital and perfused intracardially with saline followed by 10% phosphate-buffered formalin. Brains were post-fixed for 1 week, immersed in 30% sucrose-formalin solution, frozen, and sectioned into 50 μm thick slices. Brain slices were stained with cresyl violet, and electrode tracks and placement were verified. Once the final location of each electrode bundle was determined histologically, the approximate location of the electrodes during recordings was computed based upon the number of ventral advancements made with the moveable electrode bundle.

RESULTS

A total of 160 single units were recorded from 5 rats. Electrophysiological recordings occurred over the course of 28 sessions per animal, with approximately 30–40 probe length trials per session. On average, 11 recording sessions (range 3 to 28 sessions) yielded isolatable units. The electrodes passed through the dorsal striatum at the average AP coordinates of +0.44 mm from bregma, and ML coordinates of ± 3.2 mm from bregma. Recordings occurred at DV coordinates that ranged from −2.81 to −6.12, with mean starting depth at −4.01 and mean termination depth at −5.22.

BEHAVIOR

Average behavioral response patterns

Subjects primarily engaged in three bouts of sequential responding: an early phase of holding their snouts in the VI nosepoke, a phase of FI nosepoke holding, and a 2nd phase of holding in the VI nosepoke. Responses made at the FI nosepoke formed a near-symmetrical peak distribution, with the mean of this distribution centered near the FI duration of 15 s. During electrophysiological recordings, the average peak time of FI responding was 16.6 (±1.1) s. The mean peak spread of this distribution was 4.9 (±0.5) s, which resulted in a coefficient of variation of 0.30 (±0.04). **Figure 3** (top panel) shows the average response pattern of a single representative rat on a single recording session.

Single trial behavioral responding

The nosepoke behavior on single probe trials was well characterized by the same sequential progression of responding as seen in the mean functions. The bottom panel of **Figure 3** shows a single trial from the session data shown in the top panel of **Figure 3**. Across all rats, nosepoking on the VI nosepoke came to an initial end at a mean time of 9.2 (±1.8) s, followed by initiation of poking on the FI nosepoke at a mean time of 11.3 (±1.8) s. The mean termination time of FI nosepoking occurred at 20.5 (±1.8) s, and the mean initiation time of the 2nd bout of VI nosepoking occurred at 24.0 (±2.0) s. These times led to a mean FI response period spread of 9.2 (±2.0) s, and a midpoint of FI responding at 15.9 (±1.5) s.

During these response phases, the rats were predominantly holding their snouts within the nosepoke aperture, but occasionally moved their snouts in and out of the aperture, or backed away from the nosepoke and engaged in other behaviors, such as checking the food cup. The percentage of time during these nosepoking phases in which the rats' snouts were held within the nosepoke aperture was 78% (±10). Mean poke duration was 1.13 (±0.9) s, with mean maximal poke duration (without snout removal) on each trial of 3.1 (±2.0) s. Our analyses were restricted to periods of time during which the rats snout was within the nosepoke aperture, or brief intervals (200 ms) immediately following or preceding phase transitions.

NEURAL ACTIVITY

Trial-wide striatal firing patterns

Individual striatal neurons showed a variety of activity patterns, including peak-shaped profiles (**Figure 4A**) and ramp-shaped profiles (**Figure 4B**), or more commonly, complex patterns of activity that showed peak activations around the transitions between nosepoke phases (**Figure 4C**) or contained both peak-like and ramp-like components (**Figure 4D**). While these trial wide patterns of neural activity may be meaningful, it is well known that the smooth peak functions obtained in temporal production procedures result from averaging step-like responding (as seen in **Figure 3B**) across trials (Gibbon and Church, 1990; Cheng and Westwood, 1993; Church et al., 1994; Gallistel et al., 2004; Matell et al., 2006a). In other words, the smooth curves are the direct result of considerable variability in the times of response initiation and termination. Due to this variability, the functions shown in **Figure 4** may mask abrupt firing rate changes associated with the behavioral transitions.

Task sensitivity

To quantitatively determine whether spike rates were reliably varying in a task-related manner, we computed the mean firing rates on each trial during the periods of time in which a subject initiated a poke (200 ms after poke onset), held its snout within the nosepoke aperture (excluding poke initiation and termination periods), and terminated a poke (200 ms prior to poke offset). In addition, firing rates associated with transitioning between nosepoke apertures were computed using 200 ms windows bordered by the termination or initiation of responding at each phase. Although we did not empirically monitor the rats' behaviors during these periods, anecdotal observation suggested that these brief 200 ms periods were wholly composed of locomotor behaviors in which the rats were either backing away (transition period A) or approaching (transition period B) the nosepoke. These behavioral periods compose the analytic windows on which all subsequent analyses are based (see **Figure 2**). Repeated measure ANOVAs with each behavioral period as a within subject factor, and spatial location of active VI nosepoke as a between-subject factor demonstrated that 137/160 (86%) of the neurons showed reliable firing rate fluctuations as a function of these behavioral periods. The remaining analyses were restricted to these task-sensitive neurons.

Temporal modulation across behavioral phases

To ascertain whether neuronal firing rates were modulated by temporal aspects of the task, repeated measures ANOVAs were performed as above, with matched behaviors comprising each phase (e.g., poke hold-related activity). In this way, differences in firing rate can be interpreted as being due to differences in time in the trial and/or the temporal predictability associated with the reinforcement schedule, rather than differences related to overt motor behavior.

First, we compared the mean firing rates that accrued during the periods of time in which the rat's snout was held within the VI and FI nosepokes (excluding the first and last 200 ms of each poke to minimize the contributions of overt motor behavior). Because these hold periods lasted for different durations of time for each poke, we analyzed the mean firing rate during these hold periods without including elapsed time of the hold as a factor. 64% (88/137) of task-sensitive neurons showed temporal sensitivity in their firing rates. 49/88 cells showed a main effect of Phase, with no effect of spatial position. An additional 39 cells showed an interaction between Phase and Space, indicating phase sensitivity for at least one trial type (i.e., left VI or right VI trials). Of the neurons showing only a main effect of phase, 78% (38) had a peak shape (22

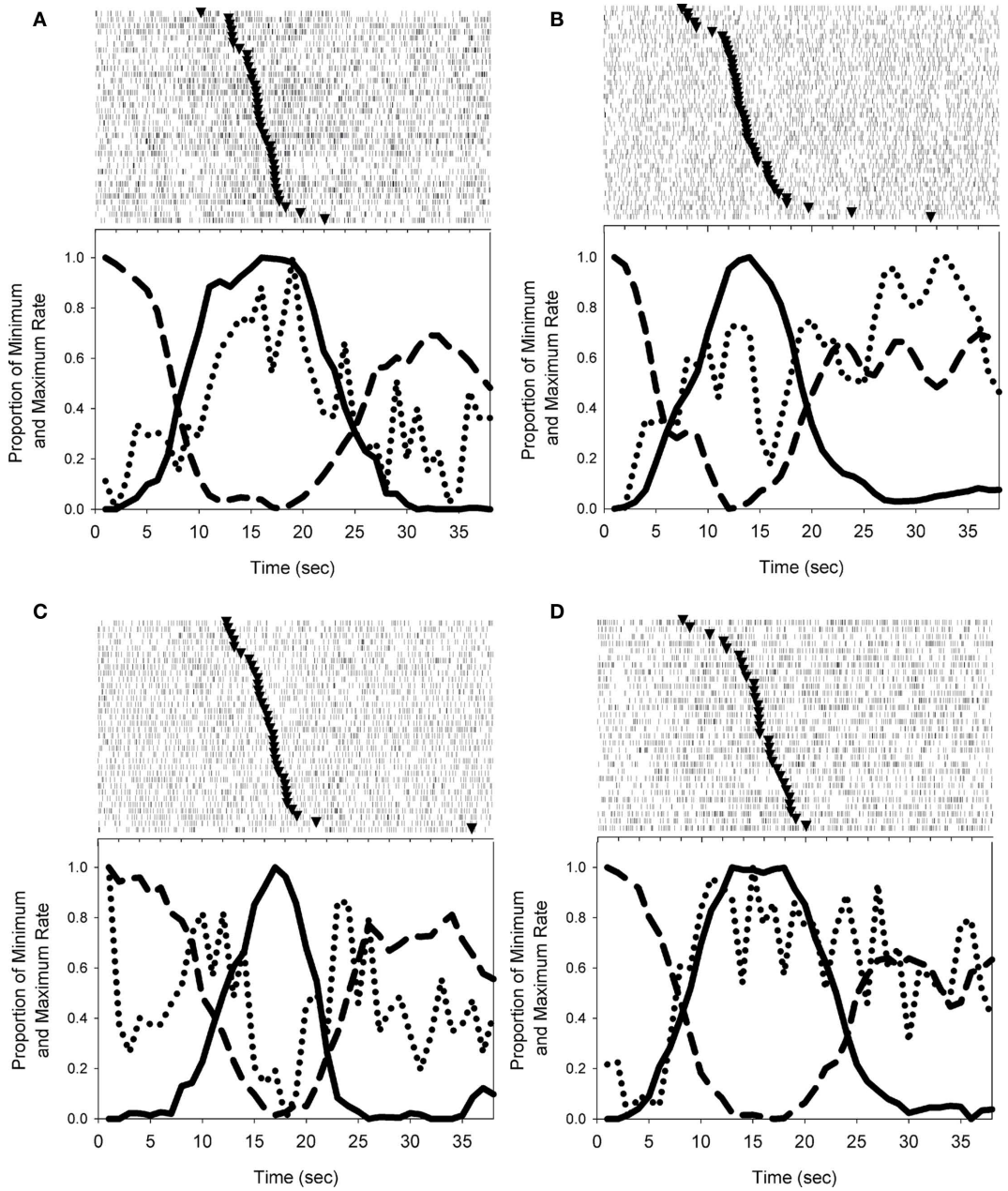

FIGURE 4 | Examples of the firing patterns observed during probe trials. Solid and dashed lines depict nosepoking, dotted lines depict striatal firing rates, and triangles in rasters indicate the midpoint of FI responding on each trial. **(A)** Depicts a striatal neuron with a peak-shaped activation profile across the trial. **(B)** Shows a roughly monotonic increase in spike rate as time elapses. In **(C)**, the activity of the cell differs across nosepoking phases (VI versus FI) in an inverted peak shape, but also shows abrupt excitations associated with the transition behaviors. **(D)** Displays a striatal neuron with both peak-like and ramp-like components. Trials displayed in peri-event rasters were ordered by the midpoint of FI responding.

positive, 16 negative), whereas 22% (11) had a monotonic ramping progression across the three phases (7 positive, 4 negative). Of the 39 cells showing an interaction of phase and side, 10 had the same pattern of activity across the two sides (7 peak, 3 ramp), with the interaction resulting from different magnitudes of changes. The remaining 29 cells had different patterns as a function of the spatial position of the active VI nosepoke.

In a similar analysis, we compared firing rates during a 200-ms window either immediately after initiating a nosepoke or immediately before terminating a nosepoke within a response phase. Because these windows were of fixed length, we also examined the pattern of activity by including Time (ten 20 ms bins) as an additional within-subject factor. For poke initiation, 59% of neurons showed phase sensitivity ($n = 81$), either as a main effect of

Phase alone ($n = 28$), and/or as an interaction of Phase with Side ($n = 30$), Time ($n = 21$), and/or the 3-way Phase × Time × Side interaction ($n = 9$). Similar results were found for poke termination, as 58% of neurons ($n = 80$) showed phase sensitivity. Of these neurons, 27 had a main effect of Phase alone, whereas the remaining neurons showed an interaction of Phase with Side ($n = 32$), Time ($n = 20$), and/or the 3-way interaction ($n = 18$). A total of 108 neurons showed sensitivity to phase for either poke initiation or poke termination, with 53 of these showing sensitivity to phase for both initiating and terminating a poke. Representative examples of poke-related activity that varied as a function of Phase are shown in **Figure 5**.

Finally, we compared firing rates during the 200 ms window around the transition period from VI poking to FI poking or vice-versa. Specifically, we compared firing rates while the subject was backing away from the VI nosepoke (at the end of VI1) with those obtained while the subject was backing away from the FI nosepoke. We also compared firing rates when the subject was approaching the FI nosepoke (and the end of VI1) with those from the period of time associated with approaching the VI nosepoke (to begin VI2). As with the poke-related activity, Time (ten 20 ms bins) was included as a factor in order to assess changes in firing pattern. Firing rates while backing away from the nosepoke differed as a function of Phase for 69 neurons (50%), with 19 showing only a main effect of Phase, and the other 50 showing an interaction with Space (33), Time (16) and/or both (16). Firing rates during nosepoke approach differed as a function of Phase in 61 neurons (45%), with 9 showing only a main effect of Phase, and the other 52 showing an interaction with Space (38), Time (15), and/or the 3-way interaction (12). Ninety-three of the neurons showed phase sensitivity to at least one of the transitions, with 37 of these neurons showing sensitivity for both backing away from and approaching the nosepoke. Representative examples of transition-related activity that varied as a function of Phase are shown in **Figure 6**.

Pooling over all of these comparisons between equivalent behaviors displayed at different phases within the task, 95% (131) of the task sensitive neurons showed sensitivity to phase for at least 1 behavior. Of these 131 neurons, 70 showed phase sensitivity to both holding and poking, 61 showed phase sensitivity to both holding and transitioning, and 77 showed phase sensitivity to poking and transitioning. Fifty neurons showed sensitivity to at least one of the poke responses (initiation or termination), one of the transition responses (backing away or approaching the nosepoke) and to holding, with 11 neurons showing sensitivity to phase for all five analyses (holding, poke in, poke out, transition-exiting, transition-entering).

Sensitivity to overt motor behavior

The primary question motivating this experiment was whether the hold-related firing of cells with temporal/phase modulation across the behavioral phases (i.e., holding during the VI and FI periods) had firing rates during one or more of the transition periods

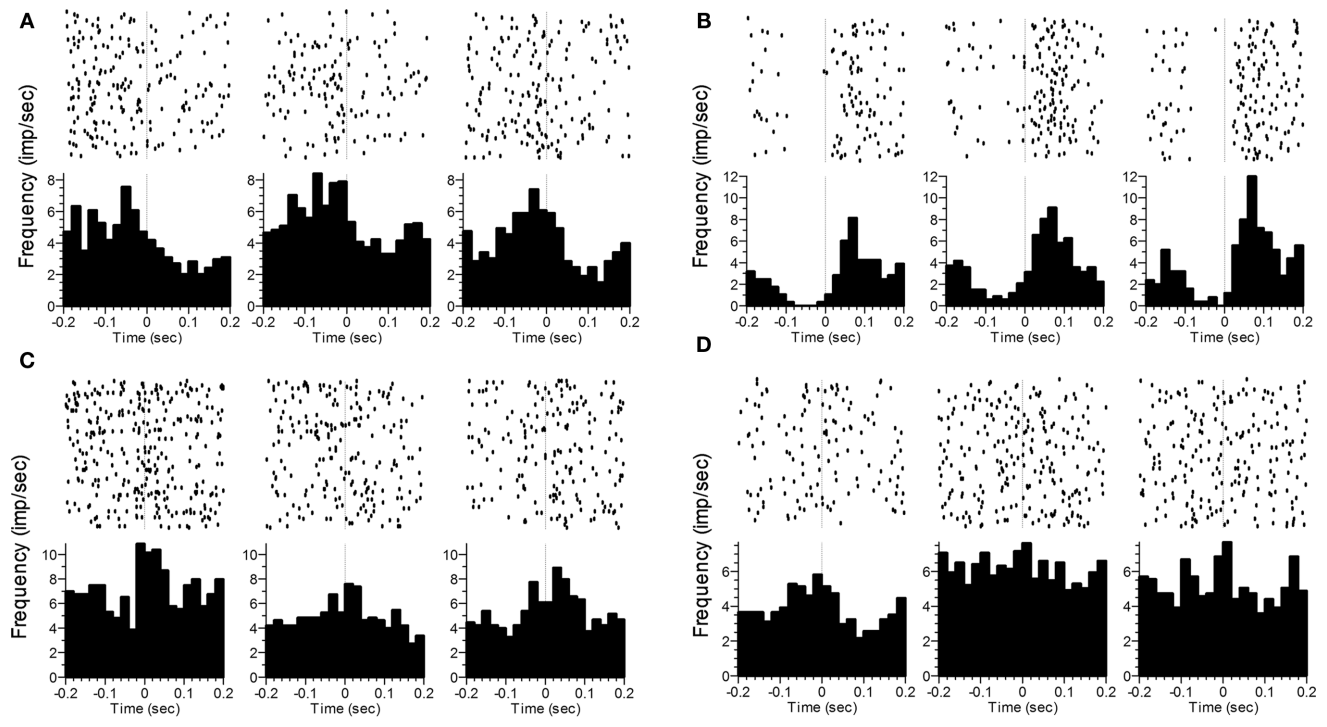

FIGURE 5 | Representative examples of changes in the rate and/or pattern of firing related to poke initiation (A–C) or poke termination (D). The time of photobeam switch breakage (initiation) or completion (termination) is indicated by the vertical dashed line at $t = 0$. The three columns represent the three phases (VI1 poking, FI poking, VI2 poking). Statistics analyses were performed on the time after poke onset in **(A–C)**, and prior to poke offset in **(D)**. In **(A)**, a significant difference as a function of Phase was seen. In **(B)**, significant effects were found for Phase and Time. In **(C)**, significant effects were seen for Phase, Time and the Phase × Time interaction. In **(D)**, only Phase was significant.

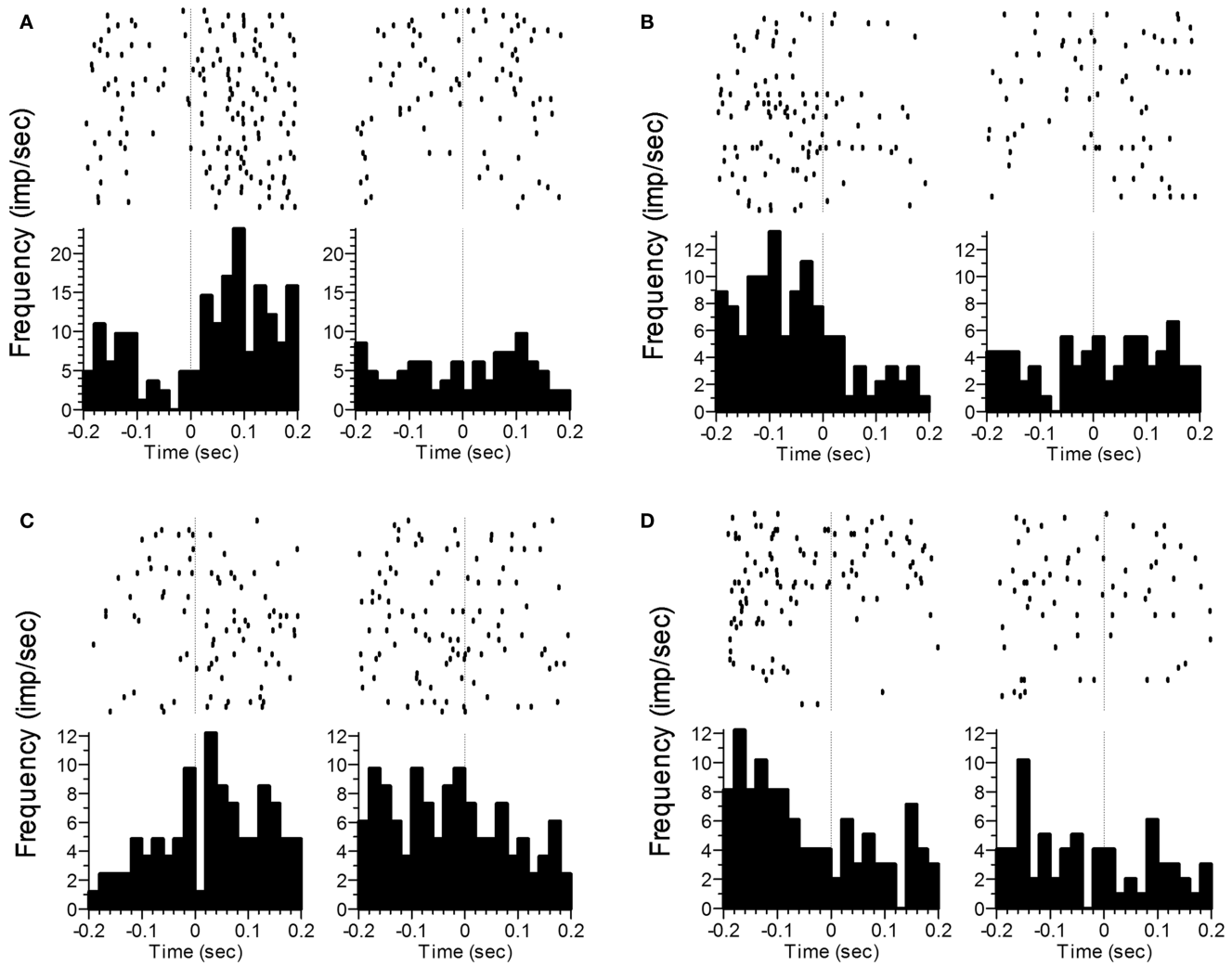

FIGURE 6 | Representative examples of changes in the rate and/or pattern of firing related to transition behaviors. Panels **(A)** and **(B)** correspond to the termination of poking and backing away from the nosepoke, whereas panels **(C)** and **(D)** correspond to nosepoke approach and initiation of poking. The vertical line at t = 0 indicates offset of the response phase **(A,B)** or onset of the response phase **(C,D)**. Statistics analyses were performed on the time after poke offset in panels **(A,B)**, and prior to poke onset in panels **(C,D)**. In panels **(A,C)**, a significant difference as a function of Phase was seen. In panels **(B,D)**, significant effects were found for Phase, Time, and the Phase × Time interaction.

that differed from that expected based upon monotonic growth or decay associated with the immediately surrounding response phases. Of the 88 cells showing temporal/phase sensitivity during nosepoke hold behaviors, 80 (91%) had firing rates during one or more of the transition phases that were significantly different from the firing rates expected from the surrounding hold periods. The non-monotonic nature of the transition-related firing is shown in **Figure 7**. Indeed, all 137 task sensitive cells showed mean activity rates during one or both transition periods that were outside the range of the surrounding nosepoke hold-related firing rates.

We also analyzed whether firing rates associated with nosepoke initiation or termination differed from that associated with holding the snout within the nosepoke. To this end, we ran a repeated measures ANVOA with phase (VI1, FI, VI2) and type (holding versus poking) as within subject factors, and spatial position of the active VI nosepoke as a between-subject factor. Of the 88 cells showing temporal/phase sensitivity during holding, 91% ($n = 80$) showed differential activity between holding and poking, with 64 neurons showing differences between holding and poke initiation, 56 neurons showing differences between holding and poke termination and 40 neurons showing differential activity for both initiation and termination. Together, 99% (87/88) of the neurons showing temporal sensitivity during nosepoke holds showed differential activity during overt motor behaviors (either poking or transitioning). 83% of these cells (73/88) showed differential activity between holding and both poking and transitioning. Such differential activity is incompatible with an abstract representation of time that evolves without sensitivity to the evolving behavior.

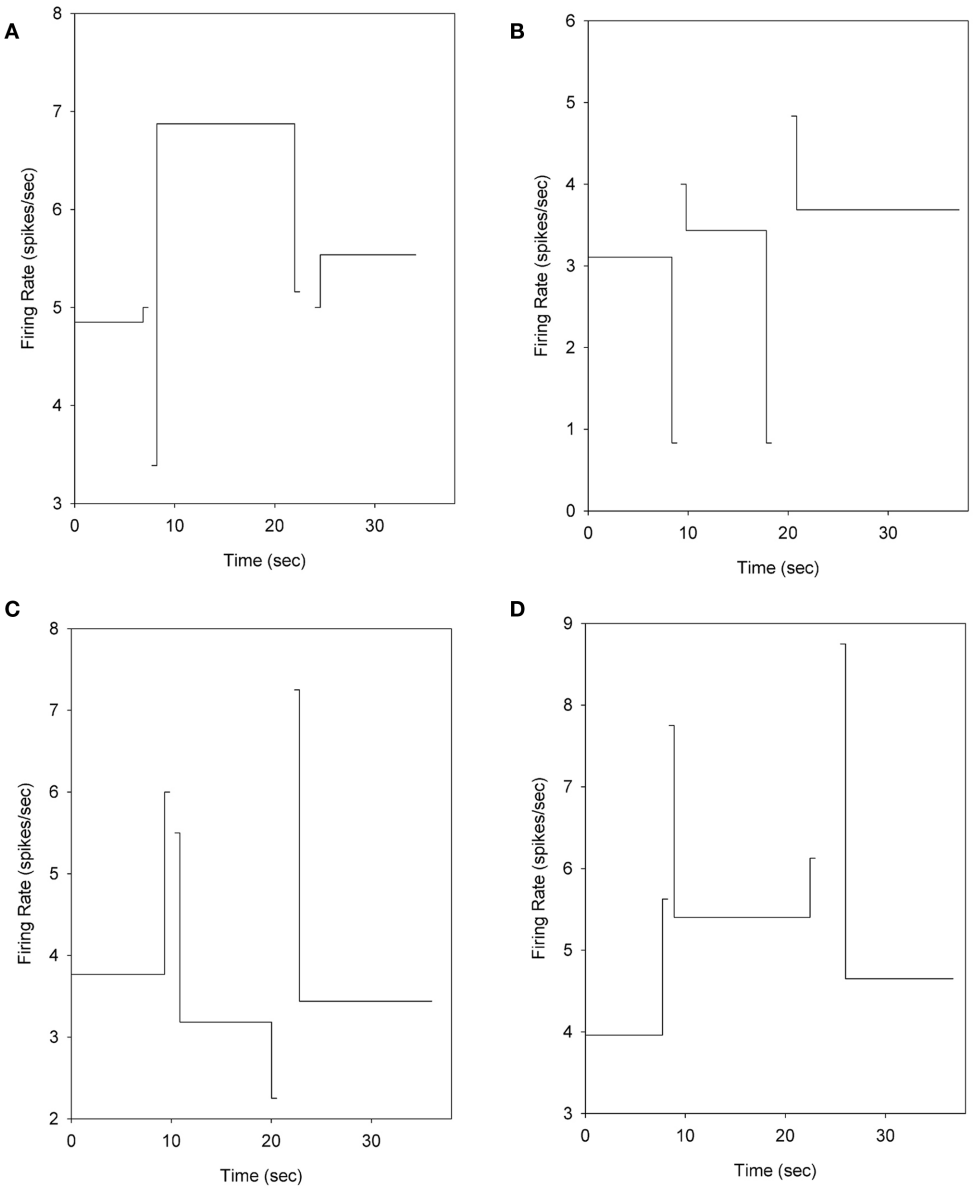

FIGURE 7 | Mean firing rates during the hold windows and transitioning phases. The firing rate of each phase is plotted at a point on the abscissa that corresponds to the mean time at which these phases began and ended. The firing rates are computed by "triggering" at the time of each phase's onset on a trial-by-trial basis to eliminate the temporal variability of each phase as it relates to trial onset. To facilitate display, the duration of the transition segments is shown over 500 ms, rather than the 200 ms used for analysis. The neurons in panels **(A–D)** are the same neurons shown in **Figures 4A–D**.

Modulation of activity within a response phase

As the above results suggested that striatal activity reflects temporal information as well as motor information, we sought to examine whether firing rates reliably varied as a function of time during nosepoke-holding behavior after controlling for the associated reinforcement schedule. To assess temporal sensitivity within a response phase, we divided the response phase on each trial into five equally spaced bins, and computed the firing rate during nosepoke holds during these bins. 67% (92) of the cells showed temporal sensitivity within at least one phase. Of the 49 cells showing only a main effect of phase in firing rate across the three response phases, without a spatial interaction (as described earlier), 34 (69%) showed significant variation in firing rate within one or more of these nosepoking phases, indicating that time in the trial influences the firing rate of these cells, in addition to any influence of reinforcement schedule. 20% of these cells (10/49) were modulated during the 1st VI phase, 41% of cells (20/49) had significant firing rate modulations during the FI phase, and 27% of these cells (13/49) were modulated during the 2nd VI phase. However, only 4 of these 49 cells showed a peak-shaped (3) or ramp pattern (1) during the FI period, with 7/49 cells showing ramp (3) or peak (4) patterns during one of

the VI periods. Thus, while a substantial number of cells had variations in firing rate across time while holding their snouts in the nosepoke under the contingencies of a particular reinforcement schedule, this variation was generally inconsistent with theoretical expectations (i.e., patterns were not peak or ramp shaped).

Similarly, we assessed whether the firing rate and/or pattern associated with nosepoke initiation or termination changed as a function of time within a phase. Due to relatively low rates of poking (as the majority of time within a phase was composed of hold responses), we assessed variation in firing pattern from the first half to second half of each phase. 95% of the cells (131/137) showed changes in their poke response as a function of time within a phase. Seventy-nine cells showed temporal sensitivity within the VI1 period, 95 showed sensitivity during the FI period, and 83 showed sensitivity during the VI2 period. Pooling across both types of behaviors, 133 cells (96%) showed within-phase modulation to either the poke or hold, with 78 cells (56%) showing within phase sensitivity to both poking and holding behaviors.

Maximal change in firing rate

Given the dynamics in firing both across and within phases of the task, we were interested in identifying the behavioral phase that was most effective in modulating the activity of these striatal cells. To this end, we examined whether the nosepoking, holding, transition phases were associated with the maximal change in firing rate compared to the average firing rate associated with these behaviors. Of the 137 task-modulated cells, 3 (2%) showed the maximal rate change during nosepoke holds, 14 (10%) showed the maximal rate during a poke (either initiation or termination), while 120 (88%) had a maximal rate change during one of the transition periods.

DISCUSSION

A number of recent studies have demonstrated that the striatum is a crucial component of the interval timing system (Rao et al., 2001; Malapani et al., 2002; Ferrandez et al., 2003; Matell et al., 2003; Coull, 2004; Harrington et al., 2004; Macdonald and Meck, 2005; Meck, 2006; Drew et al., 2007; Livesey et al., 2007; Stevens et al., 2007). The results of this study add further support to this idea by demonstrating that 95% of the behaviorally sensitive striatal neurons had different firing rates for equivalent behaviors as a function of the phase in the trial at which the behavior was emitted, indicating that either elapsed time and/or the temporal predictability of the reinforcement contingencies modulates firing rates. An equivalently high proportion of striatal cells (96%) showed variation in firing rate as a function of time within a single nosepoking period. As such, these data clearly indicate that the striatum is intimately involved in the temporal control of behavior. Nevertheless, the striatum is a functionally heterogeneous structure (Nisenbaum et al., 1988; Nakano et al., 2000; Chapman et al., 2003), and the large proportion of neurons showing temporal sensitivity should be interpreted with regard to the relatively small number ($n = 160$) of cells recorded. Still, our results are consistent with previous work showing that neural regions that innervate the striatum (cortex, thalamus, substantia nigra) have all been linked to interval timing (Lejeune et al., 1997; Harrington and Haaland, 1999; Macar et al., 1999, 2004; Komura et al., 2001; Rao et al., 2001; Brody et al., 2003; Ferrandez et al., 2003; Leon and Shadlen, 2003; Nenadic et al., 2003; Coull, 2004; Coull et al., 2004; Sakurai et al., 2004; Janssen and Shadlen, 2005; Tsujimoto and Sawaguchi, 2005; Jahanshahi et al., 2006; Matell et al., 2006a, 2011; Meck, 2006; Shuler and Bear, 2006; Mita et al., 2009). Such data led to the development of the SBF model of interval timing (Matell and Meck, 2000, 2000), which proposed that patterns of neural activity in the cortex evolve as a function of time, and that the striatum learns the cortical activity pattern occurring at the time of reinforcement via a dopaminergic reinforcement signal from the substantia nigra. In subsequent situations requiring the temporal control of behavior, striatal detection of a similar cortical activity pattern initiates responding. While the current data demonstrating striatal involvement in timing behavior provides support for this general interpretation, evaluation of the patterns of activity obtained in this study provide additional clarity regarding the possible roles played by this structure as well as providing some constraints for models of interval timing.

The present study was aimed at assessing whether striatal neurons might represent "abstract" temporal information (Walsh, 2003; van Wassenhove, 2009), divorced from the motor behaviors of the organism. Our results demonstrate that the vast majority of striatal cells cannot be viewed as reflecting the temporal predictability of reinforcement without also demonstrating sensitivity to the motor behaviors involved in obtaining this anticipated reward. In other words, the striatum does not appear to represent time in an "abstract" manner. Specifically, the results of the present study revealed that 99% of those cells showing modulation in hold-related activity as a function of phase had firing rates that were acutely and significantly modified by the overt motor behaviors of the animal in a manner that is inconsistent with a ramp or peak-shaped evolution of activity across the trial. Rather, the striatal activity recorded in the present study showed sensitivity to different behavioral phases and phase transitions, and also showed sensitivity to time within a behavioral phase, but such sensitivity was not reflected by a coherent trial-wide pattern. We note however, that due to trial-by-trial variation in behavioral patterning, neural activity was analyzed in relative rather than absolute time, and it is possible that this analytic approach may have limited our ability to detect coherent temporal patterns. Aside from this concern, given the lack of a coherent trial-wide activity pattern, the response rule(s) utilized for integrating the behavioral and temporal information remains unclear. One possibility is that temporal processing in the striatum is computed in a behavioral state dependent manner, such that the elapsed duration is assessed solely within a single behavioral state. Upon a state transition, the processing of time begins anew. In this scheme, the temporal organization of behavior across the entire trial might occur through striatal and cortical sensitivity to sequential or ordinal components, rather than time, *per se* (Cromwell and Berridge, 1996; Miyachi et al., 1997; Aldridge and Berridge, 1998; Suri and Schultz, 1998; Tanji, 2001). Indeed, given the interactions between time and sequence (Funahashi et al., 1993; Dominey, 1998; Matell et al., 2006b), studies that compare and contrast

these information sources will be necessary to understand their contributions.

Given the striatum's sensitivity to overt motor behavior, the current results are in conflict with the striatum playing a role as the accumulator in information processing models of interval timing, such as Scalar Timing Theory (SET – Gibbon, 1977) or the Multiple Time Scales model (MTS – Staddon and Higa, 1999). These models specify that the temporal control of the organism is based upon the accumulation or decay of a neural signal that is sequestered from the animal's behavior. Rather, the behavioral dependence seen here is, in some regards, closer in spirit to the Behavioral Theory of Timing (BET – Killeen and Fetterman, 1988) and a dynamic offshoot, Learning to Time Theory (LET – Machado, 1997), which specify that temporal control is predicated upon transitions in behavioral states. Further, while the present results showing behavioral sensitivity of the recorded neurons are roughly compatible with the proposal that the striatum serves as the decision stage of SET, MTS, and similar behaviorally sequestered models, these neurons cannot be functioning solely as decision stage processors for a single accumulation/decay signal. Rather, monitoring the passage of time appears to be but one of a host of internal and external signals that would be operated upon by the striatum. Similarly, while SBF is generally consistent with the present data in that the cortical activity patterns that are detected by the striatum can include motor cortical patterns that reflect current behavioral states, the finding that temporally modulated neurons are themselves behaviorally sensitive is difficult to reconcile with SBF's proposal that individual neurons learn a specific cortical activity pattern related to the time of reinforcement (Matell and Meck, 2000).

A related finding from the present work is that the transition periods were more effective at driving activity during the task compared to the nosepoke periods (88% of task-modulated cells had maximally modulated activity during one of the transition phases vs. 12% during either nosepoking or holding the snout within the nosepoke). These data suggest that the behavioral transitions, rather than the nosepoking behaviors which are the most proximately reinforced behaviors, are particularly relevant for driving striatal activity. This finding is at odds with most information-processing based timing models which view the interval between trial onset and the delivery of reinforcement to be the primary piece of temporal information learned by the organism (Gibbon, 1977; Gibbon and Church, 1984; Church and Broadbent, 1991; Staddon and Higa, 1999; Matell and Meck, 2000). As such, neural activity that represents biologically relevant times might be expected to peak at the criterion duration, much as the animal's responses do (see **Figure 3**), and several reports have identified maximal neural activity at this time point (Leon and Shadlen, 2003; Matell et al., 2003; Janssen and Shadlen, 2005; Shuler and Bear, 2006; Mita et al., 2009). In contrast, the present data suggest that the striatum may specifically encode the optimal time to begin and end responding, without representing a specific expectation of when reinforcement should arrive. Such transition related activity may be viewed as being consistent with the decision stage of interval timing models (i.e., detecting the times at which a currently elapsed interval is "similar enough" to previously reinforced times to generate responding (e.g., Ivry and Spencer, 2004; Lo and Wang, 2006). However, a simple instantiation of these models would predict that such decision stage activity would continue throughout the FI response phase, rather than being maximal at the onset or offset of this phase. Rather, the present results suggest that the striatum may serve to represent the appropriate time of action to effectively interface with the environment, rather than represent the time of external events which then demand action. These finding again are consistent with aspects of both BET and LET in that these models construe temporal control to result from a sequence of behavioral states, as the "action" in these models is the transition between behavioral states (Killeen and Fetterman, 1988).

While the current findings showed that the large majority of striatal cells had intra-state firing rate modulations, few of these firing patterns were of a theoretically predicted pattern (i.e., peaks or ramps) and none were consistent across all behavioral states (e.g., the few neurons that ramped during the 1st VI period did not continue to ramp or peak during the FI and 2nd VI periods). As with the sensitivity to the overt motor behavior associated with switching between nosepokes, this finding is difficult to reconcile with interval timing models that base temporal control on monotonic- or peak-shaped evolution of an internal clock signal that is sequestered from behavior. While previous investigators have noted ramp- and peak-shaped patterns of cortical activity in interval timing tasks (Kojima and Goldman-Rakic, 1982; Fuster, 1997; Brody et al., 2003; Leon and Shadlen, 2003; Sakurai et al., 2004; Janssen and Shadlen, 2005; Tsujimoto and Sawaguchi, 2005; Mita et al., 2009), these prior results have come from primates required to remain motionless across the entire period in which such activity patterns have been assessed. Thus, while typical interpretations of such data have been that these activity profiles are related to anticipated reinforcement, the current data suggest that they may be related to impending behavioral state changes. Indeed, recent work from our lab has shown a variety of peak and ramp patterns in a premotor cortical region during a steady state response period, but as in the present work, these patterns were not maintained throughout the entire trial (Matell et al., 2011). Conversely, while the behavioral timing models (BET and LET) do not view behavioral states as having meaningful temporal dynamics, which conflicts with the intra-state modulations seen in the present recordings, these models do not require that individual neural states directly map onto discrete behavioral states, but rather propose that some neural states and state transitions might be covert (Killeen and Fetterman, 1988). As such, the current data are consistent with these models. While not modeled as part of SBF, Matell and Meck (2000) suggested that, given the loop-circuitry of the cortico-striatal-thalamic network, it was likely that temporal information arises in a dynamic manner as activity propagates repeatedly through the circuit. In this manner, neural and behavioral state changes could be incorporated into the general framework of SBF.

ACKNOWLEDGMENTS

This work was supported by NIH grants R03DA18789 and R15DA029809 to Matthew S. Matell.

REFERENCES

Aldridge, J. W., and Berridge, K. C. (1998). Coding of serial order by neostriatal neurons: a "natural action" approach to movement sequence. *J. Neurosci.* 18, 2777–2787.

Baier, T., and Neuwirth, E. (2007). Excel :: COM :: R. *Comput. Stat.* 22, 91–108.

Balsam, P. D., Fairhurst, S., and Gallistel, C. R. (2006). Pavlovian contingencies and temporal information. *J. Exp. Psychol. Anim. Behav. Process.* 32, 284–294.

Beste, C., Saft, C., Andrich, J., Müller, T., Gold, R., and Falkenstein, M. (2007). Time processing in Huntington's disease: a group-control study. *PLoS ONE* 2, e1263. doi: 10.1371/journal.pone.0001263

Bickel, W. K., and Marsch, L. A. (2001). Toward a behavioral economic understanding of drug dependence: delay discounting processes. *Addiction* 96, 73–86.

Bilkey, D. K., and Muir, G. M. (1999). A low cost, high precision subminiature microdrive for extracellular unit recording in behaving animals. *J. Neurosci. Methods* 92, 87–90.

Brody, C. D., Hernandez, A., Zainos, A., and Romo, R. (2003). Timing and neural encoding of somatosensory parametric working memory in macaque prefrontal cortex. *Cereb. Cortex* 13, 1196–1207.

Brunner, D., Kacelnik, A., and Gibbon, J. (1992). Optimal foraging and timing processes in the starling Sturnus vulgaris: effect of intercapture interval. *Anim. Behav.* 44, 597–613.

Brunner, D., Kacelnik, A., and Gibbon, J. (1996). Memory for interreinforcement interval variability and patch departure decisions in the starling, Sturnis vulgaris. *Anim. Behav.* 51, 1025–1045.

Buhusi, C. V., and Meck, W. H. (2005). What makes us tick? Functional and neural mechanisms of interval timing. *Nat. Rev. Neurosci.* 6, 755–765.

Chapman, D. E., Keefe, K. A., and Wilcox, K. S. (2003). Evidence for functionally distinct synaptic NMDA receptors in ventromedial versus dorsolateral striatum. *J. Neurophysiol.* 89, 69–80.

Cheng, K., and Westwood, R. (1993). Analysis of single trials in pigeons timing performance. *J. Exp. Psychol. Anim. Behav. Process.* 19, 56–67.

Church, R. M., and Broadbent, H. A. (1991). "A connectionist model of timing," in *Neural Network Models of Conditioning and Action,* eds M. L. Commons, S. Grossberg, and J. E. R. Staddon (New Jersey, NJ: Lawrence Erlbaum Associates), 225–240.

Church, R. M., Meck, W. H., and Gibbon, J. (1994). Application of scalar timing theory to individual trials. *J. Exp. Psychol. Anim. Behav. Process.* 20, 135–155.

Church, R. M., Miller, K. D., Meck, W. H., and Gibbon, J. (1991). Symmetrical and asymmetrical sources of variance in temporal generalization. *Anim. Learn. Behav.* 19, 207–214.

Coull, J. T. (2004). fMRI studies of temporal attention: allocating attention within, or towards, time. *Cogn. Brain Res.* 21, 216–226.

Coull, J. T., Vidal, F., Nazarian, B., and Macar, F. (2004). Functional anatomy of the attentional modulation of time estimation. *Science* 303, 1506–1508.

Cromwell, H. C., and Berridge, K. C. (1996). Implementation of action sequences by a neostriatal site: a lesion mapping study of grooming syntax. *J. Neurosci.* 16, 3444–3458.

DeLong, M. R. (1983). The neurophysiologic basis of abnormal movements in basal ganglia disorders. *Neurobehav. Toxicol. Teratol.* 5, 611–616.

Dietrich, A., Frederick, D. L., and Alien, J. D. (1997). The effects of total and subtotal prefrontal cortex lesions on the timing ability of the rat. *Psychobiology* 25, 191–201.

Dominey, P. F. (1998). A shared system for learning serial and temporal structure of sensori-motor sequences? Evidence from simulation and human experiments. *Cogn. Brain Res.* 6, 163–172.

Drew, M. R., Simpson, E. H., Kellendonk, C., Herzberg, W. G., Lipatova, O., Fairhurst, S., Kandel, E. R., Malapani, C., and Balsam, P D. (2007). Transient overexpression of striatal D2 receptors impairs operant motivation and interval timing. *J. Neurosci.* 27, 7731–7739.

Ferrandez, A. M., Hugueville, L., Lehéricy, S., Poline, J. B., Marsault, C., and Pouthas, V. (2003). Basal ganglia and supplementary motor area subtend duration perception: an fMRI study. *Neuroimage* 19, 1532–1544.

Ferster, C. B., and Skinner, B. F. (1957). *Schedules of Reinforcement.* East Norwalk, CT: Appleton-Century-Crofts.

Funahashi, S., Inoue, M., and Kubota, K. (1993). Delay-related activity in the primate prefrontal cortex during sequential reaching tasks with delay. *Neurosci. Res.* 18, 171–175.

Fuster, J. M. (1997). *The Prefrontal Cortex: Anatomy, Physiology, and Neuropsychology of the Frontal Lobe.* Philadelphia: Lippincott-Raven.

Gallistel, C. R. (1990). *The Organization of Learning.* Cambridge, MA: MIT Press.

Gallistel, C. R., and Gibbon, J. (2000). Time, rate, and conditioning. *Psychol. Rev.* 107, 289–344.

Gallistel, C. R., King, A., and McDonald, R. (2004). Sources of variability and systematic error in mouse timing behavior. *J. Exp. Psychol. Anim. Behav. Process.* 30, 3–16.

Gibbon, J. (1977). Scalar expectancy theory and Weber's Law in animal timing. *Psychol. Rev.* 84, 279–325.

Gibbon, J., and Balsam, P. (1981). "Spreading associations in time," in *Autoshaping and Conditioning Theory,* eds C. M. Locurto, H. S. Terrace, and J. Gibbon (New York, NY: Academic Press), 219–253.

Gibbon, J., and Church, R. M. (1984). "Sources of variance in an information processing theory of timing," in *Animal Cognition,* eds H. L. Roitblat, T. G. Bever, and H. S. Terrace (Hillsdale, NJ: Erlbaum), 465–488.

Gibbon, J., and Church, R. M. (1990). Representation of time. *Cognition* 37, 23–54.

Harrington, D. L., Boyd, L. A., Mayer, A. R., Sheltraw, D. M., Lee, R. R., Huang, M., and Rao, S. M. (2004). Neural representation of interval encoding and decision making. *Cogn. Brain Res.* 21, 193–205.

Harrington, D. L., and Haaland, K. Y. (1999). Neural underpinnings of temporal processing: a review of focal lesion, pharmacological, and functional imaging research. *Rev. Neurosci.* 10, 91–116.

Harrington, D. L., Haaland, K. Y., and Hermanowicz, N. (1998). Temporal processing in the basal ganglia. *Neuropsychology* 12, 3–12.

Ivry, R. B., and Spencer, R. M. (2004). The neural representation of time. *Curr. Opin. Neurobiol.* 14, 225–232.

Jahanshahi, M., Jones, C. R., Dirnberger, G., and Frith, C. D. (2006). The substantia nigra pars compacta and temporal processing. *J. Neurosci.* 26, 12266–12273.

Janssen, P., and Shadlen, M. N. (2005). A representation of the hazard rate of elapsed time in macaque area LIP. *Nat. Neurosci.* 8, 234–241.

Kacelnik, A., and Bateson, M. (1996). Risky theories: the effects of variance on foraging decisions. *Am. Zool.* 36, 402–434.

Karmarkar, U. R., and Buonomano, D. V. (. (2007)). Timing in the absence of clocks: encoding time in neural network states. *Neuron* 53, 427–438.

Killeen, P. R., and Fetterman, J. G. (1988). A behavioral theory of timing. *Psychol. Rev.* 95, 274–295.

Kojima, S., and Goldman-Rakic, P. S. (1982). Delay-related activity of prefrontal neurons in rhesus monkeys performing delayed response. *Brain Res.* 248, 43–49.

Komura, Y., Tamura, R., Uwano, T., Nishijo, H., Kaga, K., and Ono, T. (2001). Retrospective and prospective coding for predicted reward in the sensory thalamus. *Nature* 412, 546–549.

Lejeune, H., Maquet, P., Bonnet, M., Casini, L., Ferrara, A., Macar, F., Pouthasd, V., Timsit-Berthier, M., and Vidal, F. (1997). The basic pattern of activation in motor and sensory temporal tasks: positronemission tomography data. *Neurosci. Lett.* 235, 21–24.

Leon, M. I., and Shadlen, M. N. (2003). Representation of time by neurons in the posterior parietal cortex of the macaque. *Neuron* 38, 317–327.

Livesey, A. C., Wall, M. B., and Smith, A. T. (2007). Time perception: manipulation of task difficulty dissociates clock functions from other cognitive demands. *Neuropsychologia* 45, 321–331.

Lo, C. C., and Wang, X. J. (2006). Cortico-basal ganglia circuit mechanism for a decision threshold in reaction time tasks. *Nat. Neurosci.* 9, 956–963.

Macar, F., Anton, J. L., Bonnet, M., and Vidal, F. (2004). Timing functions of the supplementary motor area: an event-related fMRI study. *Cogn. Brain Res.* 21, 206–215.

Macar, F., Vidal, F., and Casini, L. (1999). The supplementary motor area in motor and sensory timing: evidence from slow brain potential changes. *Exp. Brain Res.* 125, 271–280.

Macdonald, C. J., and Meck, W. H. (2005). Differential effects of clozapine and haloperidol on interval timing in the supraseconds range. *Psychopharmacology (Berl.)* 1–13.

Machado, A. (1997). Learning the temporal dynamics of behavior. *Psychol. Rev.* 104, 241–265.

Malapani, C., Deweer, B., and Gibbon, J. (2002). Separating storage from retrieval dysfunction of temporal memory in Parkinson's disease. *J. Cogn. Neurosci.* 14, 311–322.

Marsden, C. D. (1984). Motor disorders in basal ganglia disease. *Hum. Neurobiol.* 2, 245–250.

Matell, M., and Portugal, G. (2007). Impulsive responding on the peak-interval procedure. *Behav. Processes* 74, 198–208.

Matell, M. S., Bateson, M., and Meck, W. H. (2006a). Single-trials analyses demonstrate that increases in clock speed contribute to the methamphetamine-induced horizontal shifts in peak-interval timing functions. *Psychopharmacology (Berl.)* 188, 201–212.

Matell, M. S., Berridge, K. C., and Wayne Aldridge, J. (2006b). Dopamine D1 activation shortens the duration of phases in stereotyped grooming sequences. *Behav. Processes* 71, 241–249.

Matell, M. S., and Meck, W. H. (2000). Neuropsychological mechanisms of interval timing behavior. *Bioessays* 22, 94–103.

Matell, M. S., and Meck, W. H. (2004). Cortico-striatal circuits and interval timing: coincidence detection of oscillatory processes. *Cogn. Brain Res.* 21, 139–170.

Matell, M. S., Meck, W. H., and Nicolelis, M. A. (2003). Interval timing and the encoding of signal duration by ensembles of cortical and striatal neurons. *Behav. Neurosci.* 117, 760–773.

Matell, M. S., Shea-Brown, E., Gooch, C., Wilson, A. G., and Rinzel, J. (2011). A heterogeneous population code for elapsed time in rat medial agranular cortex. *Behav. Neurosci.* 125, 54–73.

Meck, W. H. (2006). Neuroanatomical localization of an internal clock: a functional link between mesolimbic, nigrostriatal, and mesocortical dopaminergic systems. *Brain Res.* 1109, 93–107.

Meck, W. H., and Church, R. M. (1982). Discrimination of intertrial intervals in cross-modal transfer of duration. *Bull. Psychon. Soc.* 19, 234–236.

Miller, R. R., and Barnet, R. C. (1993). The role of time in elementary associations. *Curr. Dir. Psychol. Sci.* 2, 106–111.

Mita, A., Mushiake, H., Shima, K., Matsuzaka, Y., and Tanji, J. (2009). Interval time coding by neurons in the presupplementary and supplementary motor areas. *Nat. Neurosci.* 12, 502–507.

Miyachi, S., Hikosaka, O., Miyashita, K., Kárádi, Z., and Rand, M. K. (1997). Differential roles of monkey striatum in learning of sequential hand movement. *Exp. Brain Res.* 115, 1–5.

Nagarajan, S. S., Blake, D. T., Wright, B. A., Nancy, B., and Merzenich, M. M. (1998). Practice-related improvements in somatosensory interval discrimination are temporally specific but generalize across skin location, hemisphere, and modality. *J. Neurosci.* 18, 1559–1570.

Nakano, K., Kayahara, T., Tsutsumi, T., and Ushiro, H. (2000). Neural circuits and functional organization of the striatum. *J. Neurol.* 247(Suppl. 5), V1–V15.

Nenadic, I., Gaser, C., Volz, H. P., Rammsayer, T., Häger, F., and Sauer, H. (2003). Processing of temporal information and the basal ganglia: new evidence from fMRI. *Exp. Brain Res.* 148, 238–246.

Nisenbaum, E. S., Orr, W. B., and Berger, T. W. (1988). Evidence for two functionally distinct subpopulations of neurons within the rat striatum. *J. Neurosci.* 8, 4138–4150.

Penney, T. B., Meck, W. H., Roberts, S. A., Gibbon, J., and Erlenmeyer-Kimling, L. (2005). Interval-timing deficits in individuals at high risk for schizophrenia. *Brain Cogn.* 58, 109–118.

Perry, J. L., and Carroll, M. E. (2008). The role of impulsive behavior in drug abuse. *Psychopharmacology (Berl.)* 200, 1–26.

Pfeuty, M., Ragot, R., and Pouthas, V. (2005). Relationship between CNV and timing of an upcoming event. *Neurosci. Lett.* 382, 106–111.

Pouthas, V., George, N., Poline, J. B., Pfeuty, M., Vandemoorteele, P. F., Hugueville, L., Ferrandez, A. M., Lehéricy, S., Lebihan, D., and Renault, B. (2005). Neural network involved in time perception: an fMRI study comparing long and short interval estimation. *Hum. Brain Mapp.* 25, 433–441.

Rao, S. M., Mayer, A. R., and Harrington, D. L. (2001). The evolution of brain activation during temporal processing. *Nat. Neurosci.* 4, 317–323.

Roberts, S. (1981). Isolation of an internal clock. *J. Exp. Psychol. Anim. Behav. Process.* 7, 242–268.

Roberts, S., and Holder, M. D. (1984). What starts an internal clock? *J. Exp. Psychol. Anim. Behav. Process.* 10, 273–296.

Sakurai, Y., Takahashi, S., and Inoue, M. (2004). Stimulus duration in working memory is represented by neuronal activity in the monkey prefrontal cortex. *Eur. J. Neurosci.* 20, 1069–1080.

Schultz, W., and Romo, R. (1988). Neuronal activity in the monkey striatum during the initiation of movements. *Exp. Brain Res.* 71, 431–436.

Shuler, M. G., and Bear, M. F. (2006). Reward timing in the primary visual cortex. *Science* 311, 1606–1609.

Staddon, J. E. R., and Higa, J. J. (1999). Time and memory: towards a pacemaker-free theory of interval timing. *J. Exp. Anal. Behav.* 71, 215–251.

Stevens, M. C., Kiehl, K. A., Pearlson, G., and Calhoun, V. D. (2007). Functional neural circuits for mental timekeeping. *Hum. Brain Mapp.* 28, 394–408.

Suri, R. E., and Schultz, W. (1998). Learning of sequential movements by neural network model with dopamine-like reinforcement signal. *Exp. Brain Res.* 121, 350–354.

Swanton, D. N., Gooch, C. M., and Matell, M. S. (2009). Averaging of temporal memories by rats. *J. Exp. Psychol. Anim. Behav. Process.* 35, 434–439.

Tanji, J. (2001). Sequential organization of multiple movements: involvement of cortical motor areas. *Annu. Rev. Neurosci.* 24, 631–651.

Tregellas, J. R., Davalos, D. B., and Rojas, D. C. (2006). Effect of task difficulty on the functional anatomy of temporal processing. *Neuroimage* 32, 307–315.

Tsujimoto, S., and Sawaguchi, T. (2005). Neuronal activity representing temporal prediction of reward in the primate prefrontal cortex. *J. Neurophysiol.* 93, 3687–3692.

van Wassenhove, V. (2009). Minding time in an amodal representational space. *Philos. Trans. R. Soc. Lond., B, Biol. Sci.* 364, 1815–1830.

Walsh, V. (2003). A theory of magnitude: common cortical metrics of time, space and quantity. *Trends Cogn. Sci.* 7, 483–488.

Conflict of Interest Statement: The authors declare that the research was conducted in the absence of any commercial or financial relationships that could be construed as a potential conflict of interest.

Received: 25 February 2011; paper pending published: 16 March 2011; accepted: 27 June 2011; published online: 12 July 2011.

Citation: Portugal GS, Wilson AG and Matell MS (2011) Behavioral sensitivity of temporally modulated striatal neurons. Front. Integr. Neurosci. ***5****:30. doi: 10.3389/fnint.2011.00030*

frontiers in
INTEGRATIVE NEUROSCIENCE

ORIGINAL RESEARCH ARTICLE
published: 06 December 2011
doi: 10.3389/fnint.2011.00074

Human processing of short temporal intervals as revealed by an ERP waveform analysis

Yoshitaka Nakajima*[1] *and Hiroshige Takeichi*[2]

[1] *Department of Human Science/Center for Applied Perceptual Research, Kyushu University, Fukuoka, Japan*
[2] *Laboratory for Mathematical Neuroscience, RIKEN Brain Science Institute, Wako, Japan*

Edited by:
Warren H. Meck, Duke University, USA

Reviewed by:
Hedderik Van Rijn, University of Groningen, Netherlands
Guido Marco Cicchini, Consiglio Nazionale delle Ricerche, Italy

***Correspondence:**
Hiroshige Takeichi, Laboratory for Mathematical Neuroscience, RIKEN Brain Science Institute, 2-1 Hirosawa, Wako, Saitama 351-0198, Japan.
e-mail: takeichi@riken.jp

To clarify the time course over which the human brain processes information about durations up to ∼300 ms, we reanalyzed the data that were previously reported by Mitsudo et al. (2009) using a multivariate analysis method. Event-related potentials were recorded from 19 scalp electrodes on 11 (nine original and two additional) participants while they judged whether two neighboring empty time intervals – called *t*1 and *t*2 and marked by three tone bursts – had equal durations. There was also a control condition in which the participants were presented the same temporal patterns but without a judgment task. In the present reanalysis, we sought to visualize how the temporal patterns were represented in the brain over time. A correlation matrix across channels was calculated for each temporal pattern. Geometric separations between the correlation matrices were calculated, and subjected to multidimensional scaling. We performed such analyses for a moving 100-ms time window after the *t*1 presentations. In the windows centered at <100 ms after the *t*2 presentation, the analyses revealed the local maxima of categorical separation between temporal patterns of perceptually equal durations versus perceptually unequal durations, both in the judgment condition and in the control condition. Such categorization of the temporal patterns was prominent only in narrow temporal regions. The analysis indicated that the participants determined whether the two neighboring time intervals were of equal duration mostly within 100 ms after the presentation of the temporal patterns. A very fast brain activity was related to the perception of elementary temporal patterns without explicit judgments. This is consistent with the findings of Mitsudo et al. and it is in line with the processing time hypothesis proposed by Nakajima et al. (2004). The validity of the correlation matrix analyses turned out to be an effective tool to grasp the overall responses of the brain to temporal patterns.

Keywords: temporal judgment, event-related potential, slow negative component, correlation matrix, multidimensional scaling, auditory temporal assimilation, processing time hypothesis, principal component analysis

INTRODUCTION

When people are presented a sound or a pair of sounds for a time interval shorter than one second and asked later to finger-tap for the same duration, they are typically able to replicate the duration precisely, with some occasional biases (Woodrow, 1951; see also Povel, 1981). Similarly, people are generally capable of discriminating the relative durations of two time intervals of less than a second, making Weber ratios below 10% (e.g., Getty, 1975). These simple observations indicate that the human brain is able to register, store, reproduce, retrieve, and compare short time intervals, which Buhusi and Meck (2005) called "millisecond timing." Indeed, processing time intervals below half a second is important in a number of situations for human beings, i.e., for motor control, speech generation and recognition, playing music, and dancing (Buhusi and Meck, 2005). There are a number of studies that have examined interval estimation within the millisecond range, including both psychophysical (e.g., Merchant et al., 2008; see Grondin, 2001 for a review) and neurophysiological studies (e.g., Gontier et al., 2007; Le Dantec et al., 2007; Gontier et al., 2009; Jin et al., 2009; Morillon et al., 2009; Harrington et al., 2010; see Gibbon et al., 1997; Macar and Vidal, 2004; Grondin, 2010 for reviews). They have addressed issues such as the laws and properties of time perception and timing processing, the cognitive modeling of such processing, and the underlying brain structures that mediate these processes. They have focused on veridical aspects of time perception and timing processing. However, the perceived or subjective durations can diverge from the actual duration in a consistent and systematic manner, as occurs when we are listening to musical rhythms. It is not clear how or when the representation of the actual duration is transformed in the brain into the representation of perceived duration.

In the present research, we focused on time perception of simple temporal patterns shorter than half a second. The participant was presented two neighboring empty time intervals marked by three successive tone bursts, and was asked to judge whether the two intervals had "equal" or "unequal" durations. An advantage of this paradigm is that we are able to dissociate physical equality and subjective equality of the two intervals exploiting an illusion called the

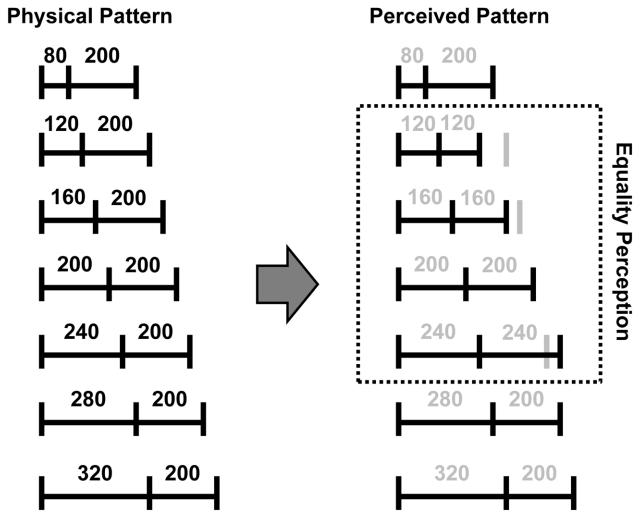

FIGURE 1 | A schematic description of the equality perceptions of the temporal patterns used in the present study. Horizontal lines represent empty time intervals. Vertical lines represent tone bursts. Numbers indicate durations in milliseconds.

"auditory temporal assimilation," which has been demonstrated by Nakajima et al. (1991) followed by Miyauchi and Nakajima (2005) and ten Hoopen et al. (2006; see also Sasaki et al., 1998; and Hasuo et al., 2011). In a typical situation, two adjacent empty time intervals are marked by three tone bursts that are very likely to be perceived as having the same duration if the first time interval ($t1$) and the second time interval ($t2$) satisfy the following relationship: $-80 \leq t1–t2 \leq 50$ (ms).Note that the range is asymmetric around zero. Specifically, when $t2$ is longer than $t1$ by up to 80 ms ($-80 \leq t1–t2 < 0$), $t2$ "shrinks" in its subjective duration as compared with its physical duration (see **Figure 1** for a schematic illustration of the phenomenon). Making use of this illusion, we were able to generate a set of different temporal patterns that induced equal duration perceptions and another set of temporal patterns that did not induce equal duration perceptions to probe how temporal equality and inequality were distinguished in the brain.

The auditory temporal assimilation may seem to be a specific instance of the time-order error (Fraisse, 1948; Allan, 1977; Hellström, 1985; Allan and Gibbon, 1994; see also Allan, 1979). However, as several investigators have argued (Sasaki et al., 2002; Nakajima et al., 2004), there are several differences between the extensively studied time-order error and the auditory temporal assimilation. First, the same patterns and magnitudes of the auditory temporal assimilation can be obtained robustly with a variety of psychophysical procedure, unlike the time-order error. Second, the magnitude of the perceptual change due to the auditory temporal assimilation can be as great as several tens of per cents. Third, the auditory temporal assimilation occurs only in a precisely restricted time range as described above.

Mitsudo et al. (2009) exploited this illusion and conducted event-related brain potential (ERP) experiments employing three-tone stimulus patterns. They measured EEGs while the participants were listening to a variety of temporal patterns. ERP waveforms were obtained by a conventional averaging method. In the *judgment* condition, the participants made judgments as to whether the two time intervals sounded equal in duration. In the *no-judgment* condition, they passively listened to the temporal patterns without judgments. For some temporal arrangements, the participants mostly perceived equality, either because the difference between them was below the limited accuracy of perceptual system, or because of the auditory temporal assimilation. In the other temporal arrangements, the participants mostly perceived inequality. Mitsudo et al. (2009) found a slow negative ERP component (SNCt) which was recorded from the right frontal recording sites immediately after the presentation of the whole temporal pattern in the judgment condition, but not in the no-judgment condition. Furthermore, they found that the SNCt was greater during the temporal patterns that were mostly perceived to have unequal durations.

The slow negative ERP component may be characterized in two ways. Because it is prominent in the comparison between the judgment and the no-judgment condition, it should be related to temporal judgment. In other words, it is a "time judgment" potential. In addition, because its amplitude is larger after perceptions of inequality than after perceptions of equality, it is also an "inequality detection" potential.

There was one unresolved issue in the study by Mitsudo et al. (2009). According to informal observations, the participants seem to have perceived equality or inequality even when it was not necessary to make related judgments. In the judgment condition, the SNCt was generated, and its amplitude allowed us to discriminate the participant's perception of temporal equality and inequality. In contrast, in the no-judgment condition, the SNCt was not observed. Accordingly, we have sought in the present study to develop a general scheme in which subjective equality or inequality can be extracted from brain-derived signals.

We reanalyzed the data reported by Mitsudo et al. (2009) to clarify the automatic processing of temporal patterns in the brain. We attempted to establish a method to probe the potential process that differentiates inequality from equality both in the judgment and in the no-judgment condition. One difficulty in observing the relationship between the brain responses to various temporal patterns was that the grand average waveforms are often unable to be compared directly in the time domain because different temporal patterns have different total durations. If we time-lock our analysis to the onset of the first tone so that we can investigate the brain responses during the presentation of the temporal pattern, then the ends of the presentation of the temporal patterns would be misaligned. If we time-lock our analysis to the onset of the third tone so that we can investigate the brain responses after the presentation of the temporal pattern, then the starts of the presentation of the temporal patterns would be misaligned. We thus propose a way to avoid this kind of problem: to calculate correlation matrices across recording sites for each temporal pattern in the judgment and in the no-judgment condition. Unlike the direct comparison, individual time points are independent in the calculation of the correlation matrix. Irrespective of to which time point we may time-lock the data, critical variations between the recording sites are represented in the correlation matrix. If the same

pattern of covariation appears at one interval in one time-series and at a different interval in another time-series, the covariation is reflected in the same manner in the resulting correlation matrices. We obtained and compared such correlation matrices.

MATERIALS AND METHODS

ERP RECORDING

The data reported by Mitsudo et al. (2009) were combined with additional data they obtained after publication. The combined data were reanalyzed under the approval of the ethical committee of the Faculty of Design, Kyushu University. Details of the experiment are briefly reviewed here. EEGs were recorded from 19 scalp electrodes on a total of 11 adult participants. EEGs were sampled at 683 Hz and bandpass-filtered for the components between 0.27 and 300 Hz. The stimuli consisted of two adjacent empty time intervals marked by three successive 1000-Hz tone bursts that lasted 20 ms. The duration of the first time interval ($t1$) varied from 80 to 320 ms in steps of 40 ms (80, 120, 160, 200, 240, 280, and 320 ms). The duration of the second time interval ($t2$) was fixed at 200 ms (see **Figure 1**). There were also "dummy" trials where the duration of $t2$ was not 200 ms, so that the participants should not assume $t2$ was fixed and base their judgment only on $t1$. EEGs were not recorded during the dummy trials. There were two conditions in this experiment. In the judgment condition, the participants made judgments as to whether or not $t1$ and $t2$ had the same duration subjectively. They responded by pressing one of two buttons after each stimulus presentation. In the no-judgment condition, they listened to the temporal patterns without making judgments. They pressed one of the two buttons after each presentation, as a control for the motor behavior that was exhibited in the judgment condition. The no-judgment condition was presented to each participant before the judgment condition. The grand average waveforms were calculated after a standard artifact rejection procedure.

CATEGORIZATION OF THE TEMPORAL PATTERNS

The participants consistently rated the intervals as equal when $t1 = 120$, 160, 200, or 240 ms while $t2 = 200$ ms, but not when $t1 = 80$, 280, or 320 ms. Thus, we categorized the stimulus temporal patterns based on $t1$ (as indicated in parentheses) into (1) temporal patterns that produced perceptions of equality between $t1$ and $t2$ in most trials (120, 160, 200, or 240 ms) and (2) temporal patterns that produced perceptions of inequality in most trials (80, 280, or 320 ms). These patterns will be referred to as the *equality patterns* and the *inequality patterns*. Note that an equality pattern does not imply $t1$ and $t2$ were physically equal.

MULTIDIMENSIONAL SCALING ANALYSIS

We used a time window that extended from the onset of the second tone burst up to 600 ms after the onset. We computed a correlation matrix of the grand average waveforms across the 19 recording sites in this time window for each temporal pattern for each condition as follows:

$$C_{i,j} = \frac{\sum_k \left(x_{i,k} - \bar{x}_i\right)\left(x_{j,k} - \bar{x}_j\right)}{\sqrt{\sum_k \left(x_{i,k} - \bar{x}_i\right)^2 \sum_k \left(x_{j,k} - \bar{x}_j\right)^2}} \quad (1)$$

where x is a 19 by 410 matrix representing the grand average waveform for each recording site, i and j denote the recording sites, and k denotes the time point. C is a 19 by 19 correlation matrix.

We then defined a *separation* between two matrices as the sum of squares of element-by-element differences between these correlation matrices.

$$\text{Separation}\,(X, Y) = \sum_{i,j} \left(X_{i,j} - Y_{i,j}\right)^2 \quad (2)$$

where X and Y are 19 by 19 correlation matrices, and i and j denote the row and column which correspond to the recording sites.

We thus calculated the separation between each pair of the temporal patterns. For example, we define a separation between the brain response to the $t1 = 80$ ms pattern and that to the $t1 = 120$ ms pattern as follows:

$$\text{Separation}\left(C^{t1\,=\,80\,\text{ms}}, C^{t1\,=\,120\,\text{ms}}\right) = \sum_{i,j} \left(C_{i,j}^{t1\,=\,80\,\text{ms}} - C_{i,j}^{t1\,=\,120\,\text{ms}}\right)^2 \quad (3)$$

where C^{t1} is the correlation matrix calculated from the selective grand average waveform for $t1$.

The obtained separations were considered to be dissimilarity measures and subjected to a metric multidimensional scaling (MDS) to visualize the represented relationships between the temporal patterns. The dissimilarity matrix was as follows:

$$\text{Dissimilarity}_{i,j} = \text{Separation}\left(C^{t1\,=\,s(i)}, C^{t1\,=\,s(j)}\right), \quad (4)$$

where $s(i)$ and $s(j)$ were either 80, 120, 160, 200, 240, 280, or 320 ms. The dissimilarity matrix was 7 by 7 if only one of the judgment and the no-judgment condition was considered, and it was 14 by 14 if both conditions were included.

In order to examine the robustness of the result of MDS, a bootstrap approach was undertaken. Namely, the data x was resampled and the whole procedure was repeated several times (10 times for the MDS analysis and 30 times for the time course analysis described later). An MDS result was discarded when the dissimilarity matrix was 7 by 7 and the stress was greater than 0.1 or when the dissimilarity matrix was 14 by 14 and the stress was greater than 0.2. Each trial in the bootstrapping procedure was represented by a plot in the MDS space. If a scatter of plots in an MDS configuration is dense, this indicates that the results are robust. The MDS was performed using MATLAB R2010b.

TIME COURSE ANALYSIS

Over the grand average ERP waveforms, we postulated fifty-one 100-ms time windows moving in 10-ms steps covering the 600-ms interval from the onset of the second tone burst to 400 ms after the onset of the third tone burst. For each time window, we computed the correlation matrix of the grand average waveforms across the 19 recording sites. Then, as described above, we calculated a separation that was defined as the sum of squares of element-by-element differences between the matrices for each pair of the temporal patterns. Finally, a relative categorical separation

(RCS) was calculated for each time window as the proportion of the sum of the separations between the equality–inequality pairs to the sum of the separations between all the pairs:

$$\mathrm{RCS}\left(\text{equal, unequal}\right) = \frac{\sum_{i \in \text{equal}, j \in \text{unequal}} \text{Separation}\left(C^i, C^j\right)}{\sum_{i,j} \text{Separation}\left(C^i, C^j\right)}, \quad (5)$$

where i and j denote the temporal patterns, and C^i and C^j denote the corresponding correlation matrices.

Utilizing correlation matrices to analyze EEG data is advantageous in several aspects. In the conventional ERP analyses, it is important to localize the component in space (in terms of the recording site) and in time (in terms of latency) precisely. In the analysis of correlation matrices, however, the focus is on more distributed properties of the response. The correlation matrix reflects covariations across different recording sites rather than variations at each individual site. The correlation matrix does not reflect timing or phase relationship of such covariations. In the analysis of distributed properties, a component is related to co-varying signals from multiple recording sites. Commonality between such components across responses to different temporal patterns must be reflected onto the correlation matrices. Distributed properties must be reflected in such comparisons. The present method is simple compared with conceptually similar measures such as coherence or phase locking (Lachaux et al., 1999). Despite its simplicity, the correlation matrix contains the most essential information as to which recording sites behave together. It is the basis for principal component analysis and other related multivariate analysis methods. An important advantage of utilizing correlation matrices is that a correlation matrix can be reduced to represent the most critical component(s) or factor(s).For example, it is useful to focus on specific principal components that are significant or to remove noise by eliminating insignificant components.

RESULTS

Figure 2A shows the two-dimensional MDS results. The points with shorter $t1$ are presented on the left side, while the points with longer $t1$ are presented on the right side in the judgment condition, except that the diamonds ($t1 = 320$ ms) is to the left of the squares ($t1 = 280$ ms) overlapping the leftward triangles ($t1 = 240$ ms). There was a separation between the points representing the judgment condition and those representing the no-judgment condition. The judgment condition data (open symbols) are presented in the upper part of the figure, while the no-judgment condition data (filled symbols) are presented in the lower part. Thus, the first dimension roughly corresponds to the stimulus in the judgment condition, while the second dimension to the task. In a vertically-magnified view in **Figure 2B**, there was also a separation, in the judgment condition, between the points that represent the equality patterns and those that represent the inequality patterns. The equality patterns (triangles) are presented in the relatively upper part in the judgment condition, while the inequality patterns (circles, squares, and diamonds) are presented in the relatively lower part, in the middle of the figure. The three-dimensional MDS data led us to the same conclusions as the two-dimensional MDS data.

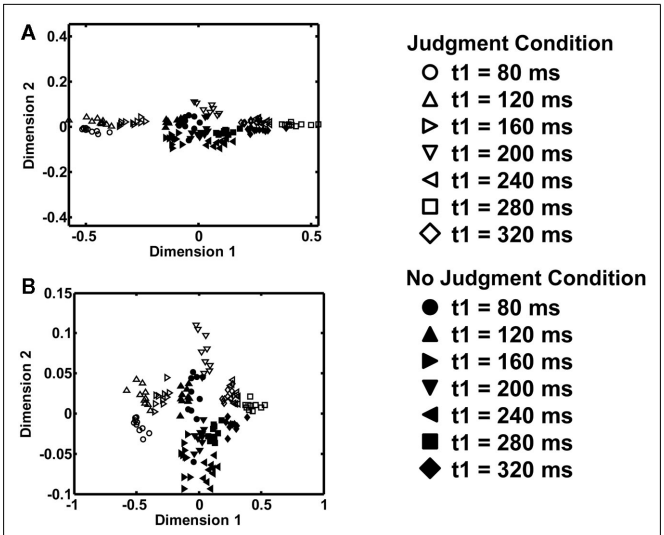

FIGURE 2 | Results of the multidimensional scaling (MDS) analyses. Points representing the activations by the temporal patterns are shown in a two-dimensional layout. Open symbols indicate the results for the judgment condition, and filled symbols the results for the no-judgment condition. Different types of symbols indicate different temporal patterns. The scatter of a symbol shows the variability across different resamplings in bootstrapping ($N = 10$). **(A)** The conventional representation. **(B)** A vertically elongated representation.

The results of the MDS analysis were consistent with the original ERP analysis as there were differences between the judgment and the no-judgment condition and differences between the equality patterns and the inequality patterns in the judgment condition. This implies that we can quantitatively compare and characterize the ERP waveforms by analyzing the obtained correlation matrices. Using this *correlation matrix method*, we further examined the changes in the representations over time, focusing on the separation between the representations of equality patterns and the representations of the inequality patterns.

Figure 3 shows the time course of the relative category separation as a function of the center of the time window for each condition. The "chance level" of the relative category separation is 0.57 assuming a homogeneous variance across the temporal patterns. Both in the judgment and in the no-judgment condition, separation peaks appeared after the second tone burst at −200 ms and after the third tone burst at 0 ms, i.e., after the first and after the second time interval.

The apparent categorical separation between the equality patterns and the inequality patterns after the first $t1$ interval is interpreted as reflecting responses to the first time $t1$ interval, which occurred immediately before the analysis window. We need to be careful in interpreting the "separation" in this case, because the discrimination of inequality from equality was not possible before $t2$ was presented. The implications of these early peaks will be discussed later. A more interesting finding was that we were able to find a local maximum of the RCS immediately after the second interval $t2$. This should not be a response to the third tone burst or the second time interval $t2$, which immediately preceded the time window, because all of the tone bursts were the same, and the

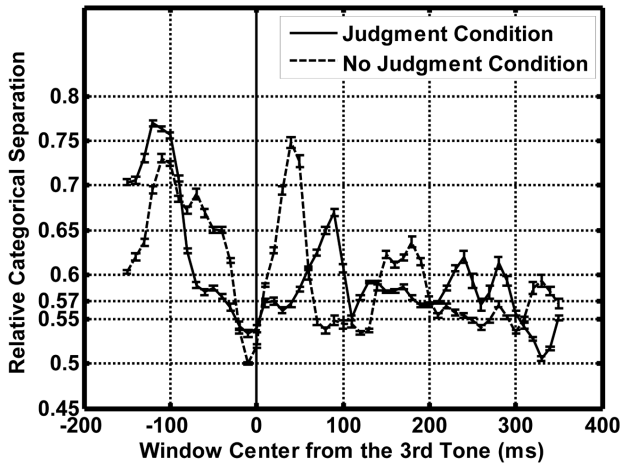

FIGURE 3 | The results of the time course analyses. Relative categorical separations are plotted as a function of the temporal position of the time-window center for each condition. Solid and dashed lines show the results for the judgment and the no-judgment condition, respectively. The "chance level" of the relative category separation is 0.57 assuming a homogeneous variance across the temporal patterns. Error bars represent SE estimated by the bootstrapping ($N = 30$).

duration of $t2$ was kept constant at 200 ms for the trials to be analyzed. This separation must reflect $t1$, and it is probably related to the comparison between $t1$ and $t2$. This plot can be related to the original finding of the SNCt in that a peak appears immediately after presentation of $t2$ in the judgment condition. In addition, there was a qualitative agreement in the waveforms between the judgment and the no-judgment condition although there was a difference in timing.

Figure 4 shows the two-dimensional MDS result in the judgment condition with the 100-ms window centered (i) at the −120-ms peak after the first interval in **Figure 4A**, (ii) at the 90-ms peak after the second interval in **Figure 4B**, or (iii) at the 110-ms valley after these peaks in **Figure 4C**. In **Figure 4B**, at the point where the relative categorical separation was large, while the inequality patterns (filled circles, squares, and diamonds) occupied the right upper corner of the panel, the equality patterns (open triangles) occupied the left lower corner of the panel. They can be linearly separated, which means that the MDS showed an axis of dimension along which inequality–equality contrast was represented. In **Figure 4C**, at the point where the relative categorical separation was small, the inequality patterns (filled circles, squares, and diamonds) and the equality patterns (open triangles) were not separated. While the equality–inequality separation ($t1 = 120$, 160, 200, or 240 versus 80, 280, or 320 ms) was found at the peak before the second interval in **Figure 4A** along the diagonal from upper-left to lower-right, a separation between the short-duration pattern and the long-duration pattern ($t1 = 80$, 120, or 160 versus 240, 280, or 320 ms) was also found along the other diagonal from lower-left to upper-right there. No such separation by duration was found in **Figure 4B**. One plausible description of the pattern in **Figure 4A**, but not in **Figure 4B**, may be that each temporal pattern was represented separately according to its actual duration.

Figure 5 shows the two-dimensional MDS results in the no-judgment condition with the 100-ms window centered (i) at the −110-ms peak after the first interval in **Figure 5A**, (ii) at the −70-ms peak after the first interval in **Figure 5B**, (iii) at the 40-ms peak after the second interval in **Figure 5C**, or (iv) at the 80-ms valley after the peaks in **Figure 5D**. In **Figure 5C**, at the point where the relative categorical separation was large, while the inequality patterns (filled circles, squares, and diamonds) occupied the right upper corner of the panel, the equality patterns (open triangles) occupied the left lower corner of the panel. They can be linearly separated, which means that the MDS showed an axis of dimension along which inequality–equality contrast was represented, similarly to the judgment condition. In **Figure 5D**, at the point where the relative categorical separation was small, the inequality patterns (filled circles, squares, and diamonds) and the equality patterns (open triangles) were not separated. At the peaks before the second interval in **Figures 5A,B**, we found the equality–inequality separation as well as the separation between the short-duration versus long-duration. The two-dimensional MDS described the categorical equality–inequality separation well, although the correlation matrices may have had three or more dimensions.

The peaks after the first interval may appear to represent an equality–inequality separation. One may argue that, after a couple of trials, the participants may have developed an implicit framework of $t2$, since, except for the dummy trials, the $t2$ interval in this experiment was fixed. If so, the participants may have started making comparisons before the second interval was presented.

This is unlikely, however, for two reasons. First, the asymmetry of the equality judgments observed in the judgment condition can be explained only by assuming that $t2$ was underestimated (Nakajima et al., 2004). Although the difference between $t1$ and $t2$ was 80 ms both when $t1 = 120$ ms and when $t1 = 280$ ms, equality was perceived only when $t1 = 120$ ms. According to Nakajima et al. (2004), $t2$ should be underestimated considerably in this particular condition, and this explains the asymmetry of equality judgment. This means that the participants judged equality/inequality after perceiving $t2$.

Second, the peaks after the first interval clearly represent the actual properties of the first interval. **Figures 6** and **7** show time course of MDS plots after the presentation of the first interval (from upper-left to lower-right). Note that both in the judgment (**Figure 6**) and in the no-judgment (**Figure 7**) condition, the representation changes from arrangements corresponding to the individual temporal patterns to arrangements corresponding to the equality–inequality segregation. At the peaks after the first interval, the MDS representations of the temporal patterns show separation and clustering of the individual patterns. They also show residual separation between the short-duration ($t1 = 80$, 120, or 160 ms) and the long-duration ($t1 = 240$, 280, or 320 ms) patterns. In contrast, at the peaks after the second interval, the MDS representations of the individual patterns are more obscure, and only a robust segregation between the equal ($t1 = 120$, 160, 200, or 240 ms) and unequal ($t1 = 80$, 280, or 320 ms) category patterns appeared. It is no longer possible to find a dimension

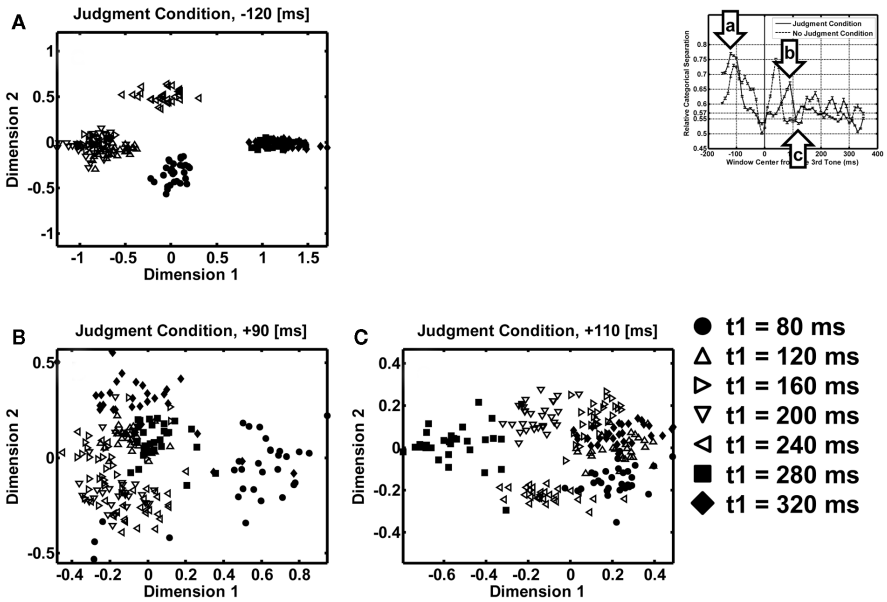

FIGURE 4 | Results of the multidimensional scaling (MDS) analyses at specific time points for the judgment condition. **(A)** MDS at 120 ms before the onset of the third tone. **(B)** MDS at 90 ms after the onset of the third tone – at the peak of relative categorical separation. **(C)** MDS at 110 ms after the onset of the third tone – at the valley of relative categorical separation. Different symbols represent different temporal patterns. Filled symbols represent perceptually unequal temporal patterns. Open symbols represent perceptually equal temporal patterns. The scatter of a symbol shows the variability across different resampling in bootstrapping ($N = 30$).

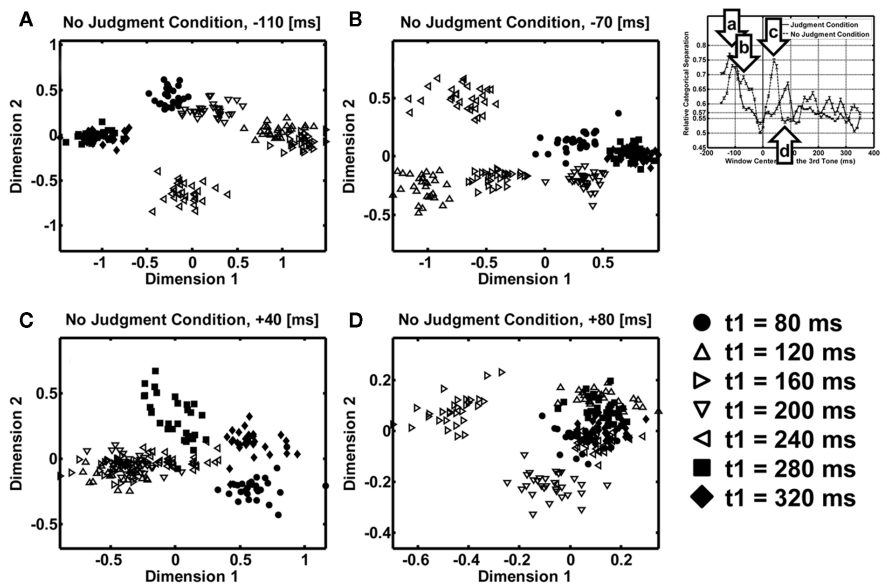

FIGURE 5 | Results of the multidimensional scaling (MDS) analyses at specific time points for the no-judgment condition. **(A)** MDS at 110 ms before the onset of the third tone. **(B)** MDS at 70 ms before the third tone. **(C)** MDS at 40 ms after the third tone – at the peak of the relative categorical separation. **(D)** MDS at 80 ms after the third tone – at the valley of the relative categorical separation. Filled symbols represent perceptually unequal temporal patterns. Open symbols represent perceptually equal temporal patterns. The scatter of a symbol shows the variability across different resampling in bootstrapping ($N = 30$).

along which the short-duration and the long-duration patterns are separated. In order to confirm the above observations, we calculated the RCS between the short-duration patterns ($t1 = 80$, 120, or 160 ms) and the long-duration patterns ($t1 = 240$, 280, or 320 ms) in the same way as we had calculated the RCS between the equality patterns and the inequality patterns, and we plotted them

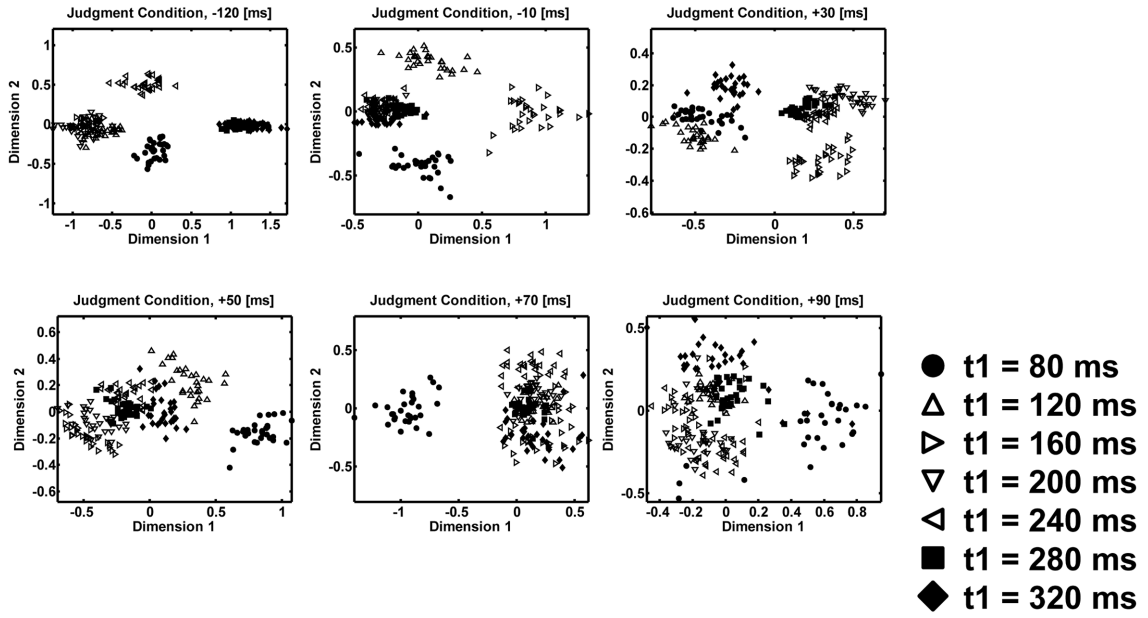

FIGURE 6 | Time course of the multidimensional scaling (MDS) analyses after the presentation of the whole temporal pattern for the judgment condition. Different symbols represent different temporal patterns. Filled symbols represent perceptually unequal temporal patterns. Open symbols represent perceptually equal temporal patterns. The scatter of a symbol shows the variability across different resampling in bootstrapping ($N = 30$).

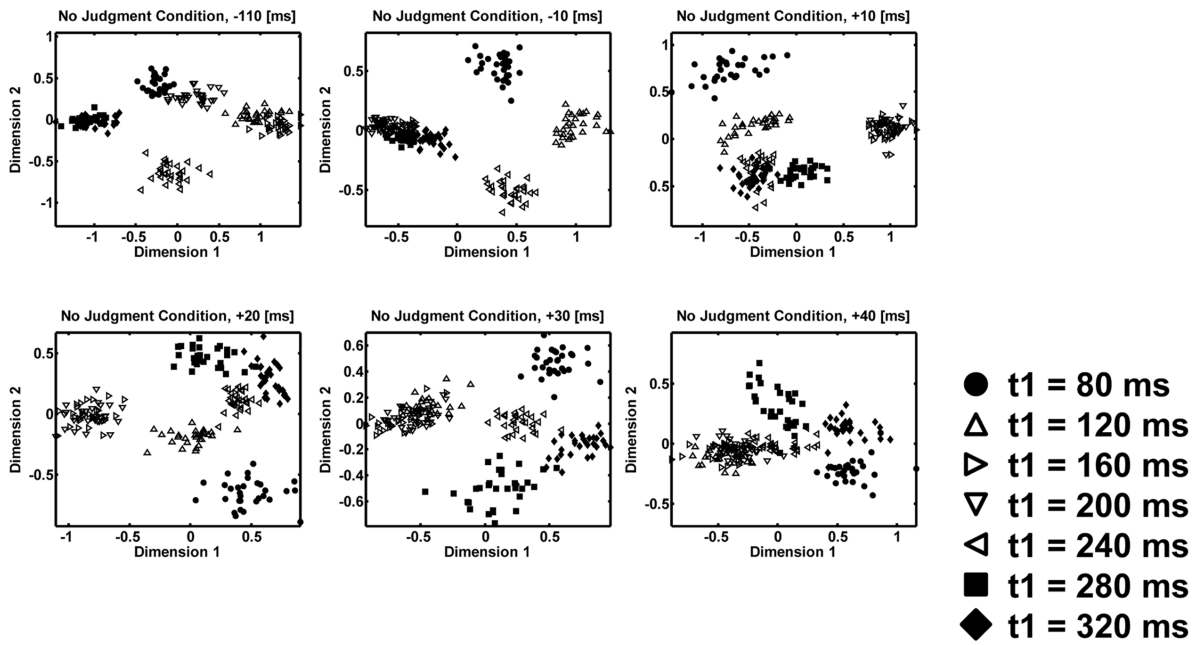

FIGURE 7 | Time course of the multidimensional scaling (MDS) analyses after the presentation of the whole temporal pattern for the no-judgment condition. Different symbols represent different temporal patterns. Filled symbols represent perceptually unequal temporal patterns. Open symbols represent perceptually equal temporal patterns. The scatter of a symbol shows the variability across different resampling in bootstrapping ($N = 30$).

in **Figure 8**. Whereas there were peaks after the first interval, no peak was found within 100 ms after the second interval. This plot corresponds to the above argument that the equality–inequality separations before and after the second interval have different implications. While the former is likely to be a by-product of the separate representations of individual time intervals, the latter seems to be related to the perception of the whole temporal patterns.

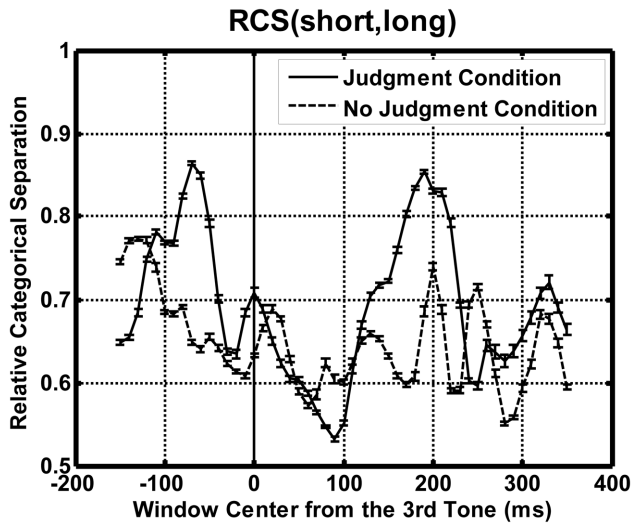

FIGURE 8 | The relative categorical separation (RCS) between short-duration ($t1 = 80$, 120, or 160 ms) and long-duration ($t1 = 240$, 280, or 320 ms) patterns is plotted as a function of the temporal position of the time-window center for each condition. Solid and dashed lines show the results for the judgment and the no-judgment condition, respectively. The "chance level" of the relative categorical separation is 0.6 assuming a homogeneous variance across the temporal patterns. Error bars represent the SE estimated by bootstrapping ($N = 30$).

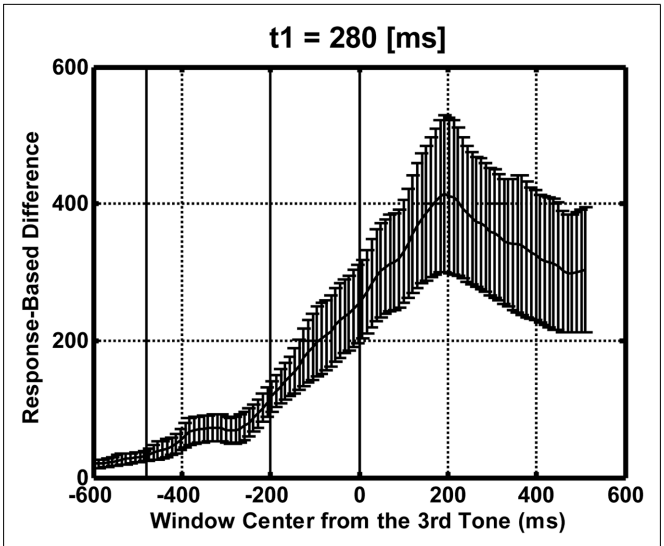

FIGURE 9 | Time course of the mean square of the difference waveforms between the selective averages for the equal and the unequal response trials, across recording sites for $t1 = 280$ ms. Moving average was calculated using a 100-ms square-shaped time window. Solid vertical lines indicate the timings of the three tones. Error bars represent the SE across the participants ($N = 11$).

Additionally, the waveforms after the second interval contain much more information related to the equality/inequality of the neighboring intervals than those before the second interval. To show this quantitatively, we calculated the selective average waveforms for the equal and unequal judgment trials, for $t1 = 280$ ms. We then calculated their difference waveform and the mean square difference at each temporal point across all the recording sites, as plotted in **Figure 9**. If the participants had already started making comparisons after the first interval, we would have observed comparable differences before and after the presentation of the second interval (the third tone). This was not the case. The difference was clearly much greater after the second interval was presented. This may also support the argument that the judgment was made after, and not before, the second interval was presented. Only the $t1 = 280$ ms case is shown here because either the number of equal responses or the number of unequal responses was too small to obtain the selective average waveforms reliably for the other durations of $t1$. In these cases, the responses were too highly biased toward equality (when $t1 = 120$, 160, 200, or 240 ms) or toward inequality (when $t1 = 80$ or 320 ms).

DISCUSSION

In both the judgment and no-judgment conditions, our analyses revealed a peak in categorical separation between the equality and inequality temporal patterns immediately after the second time interval was presented. It is likely that these processing phases are associated with equality/inequality judgments. The peaks in both conditions are likely to correspond to the perception of the equality/inequality of temporal patterns whether there is a judgment task or not. We may tend to perceive regularity/irregularity of temporal patterns even if we are passively listening to them, and our correlation matrix analyses seem to have captured a representation of rhythmic patterns in the brain.

In the general context of timing and time perception, the presence of a very short processing period in the brain after the presentation of a time interval is consistent with a dominant view in the field of time perception, i.e., the scalar expectancy theory (SET; Gibbon, 1977). Temporal judgments are assumed to be based on an internal clock that has been described as a pacemaker-counter device, and one possible cause of counting errors is the latency of accumulation in the pacemaker-counter device (Gibbon, 1991; Gibbon and Church, 1984; Grondin, 2010; see also Wearden and Lejeune, 2008). Specifically, the short processing time after the third tone that appeared in our study may be associated with the latency of this putative counter device (e.g., Taatgen et al., 2007; van Rijn and Taatgen, 2008; Taatgen and van Rijn, 2011). For instance, in the animal timing literature, it has been shown that the accumulation of pulses in the counter depends on a switch mode (Meck, 1984). Some latency in this switch process probably causes the processing time delay apparent in the brain activity. The magnitude of this delay (the switch effect) is likely associated with attentional processes (Grondin and Rammsayer, 2003; Meck, 1984).

In the specific context of auditory temporal assimilation, Nakajima et al. (2004) argued that a large part of the auditory temporal assimilation can be explained by their *processing time hypothesis* (Nakajima et al., 1988). The processing time hypothesis postulates that the perceived duration of a physical time interval t is in proportion to the actual duration of that interval t plus a positive constant α for additional processing of the interval, and the

total time perceived is in proportion to $t + \alpha$. This hypothesis is in line with our current findings in that the post-stimulus processing was critical for time perception. The additional processing time α in the processing time hypothesis was psychophysically estimated to be about 80 ms or shorter depending on the stimulus context. This agrees with the fact that the brain-derived signature of the equality/inequality perception was observed within 100 ms after the presentation of $t2$.

Explanations of the results by the SET models and the processing time hypothesis are not mutually exclusive. To examine the theoretical relationship between these two models can be an innovative attempt. In the current context, it is important to emphasize the consistency between the processing time hypothesis and the present analysis. The processing time hypothesis has been developed on the basis of, and used for the explanation of, various types of quantitative psychophysical results including those related to unilateral auditory temporal assimilation (e.g., Nakajima et al., 1988, 2004), and auditory temporal assimilation has been the paradigm of our current neurophysiological study.

Contingent negative variations (CNVs) have been associated with the perception of short time intervals (Pfeuty et al., 2003, 2008; Macar and Vidal, 2004; Gontier et al., 2007, 2009; Le Dantec et al., 2007). Mitsudo et al. (2009) found that CNVs after the presentation of $t1$ were quantitatively related to the duration of $t1$. It is possible that, while the CNV is used for processing one interval, the SNCt is used for processing the relationship between two intervals. Takeichi et al. (2011) showed in a classifier analysis that the SNCt, or the ERP waveform after $t2$, contained information about the participants' task and responses. In all the previous studies on time perception, the participants had been required to perform a perceptual task while their behavioral or neural responses had been recorded. One important characteristic of temporal processing, however, is that it can be automatic and can be performed irrespective of the task. Our current study captured such signals from the brain in relation to the perception of time intervals shorter than half a second. Linear separability was observed between the equality and the inequality patterns immediately after the presentation of $t2$, characterizing an equality/inequality dimension.

By calculating the separations between the correlation matrices, we determined categorical boundaries between equal and unequal cases in both the judgment and no-judgment conditions. We perceive rhythms in temporal patterns irrespective of whether we pay attention to those temporal patterns. It is well known that brain activity, such as mismatch negativity (Tervaniemi et al., 1994; Yabe et al., 1997) or gamma band activity (see Zanto et al., 2006), is observed in response to rhythmic irregularities without attention being paid to the stimulus. This current analysis is likely to be the first study in time perception research to relate observed brain activities to perceptions in the mind in a situation without explicit judgments, using brief, elementary temporal patterns. The fact that it is possible to observe related brain activities without explicit judgments within a period as short as 100 ms indicates that the current method should have a wide range of applications including clinical ones.

ACKNOWLEDGMENTS

The authors are grateful to Takako Mitsudo and Shozo Tobimatsu for allowing us to reanalyze their data. The authors are also grateful to Kazuo Ueda and Gerard B. Remijn for their useful comments on an earlier version of the manuscript. Simon Grondin also gave us valuable suggestions. The study was supported by Tateisi Science and Technology Foundation and Grants-in-aid for scientific research from the Ministry of Education, Culture, Sports, Science, and Technology, Japan (20653054, 23653227, and 19103003).

REFERENCES

Allan, L. G. (1977). The time-order error in judgments of duration. *Can. J. Psychol.* 31, 24–31.

Allan, L. G. (1979). The perception of time. *Percept. Psychophys.* 26, 340–354.

Allan, L. G., and Gibbon, J. (1994). A new temporal illusion or the TOE once again? *Percept. Psychophys.* 55, 227–229.

Buhusi, C. V., and Meck, W. H. (2005). What makes us tick? Functional and neural mechanisms of interval timing. *Nat. Rev. Neurosci.* 6, 755–765.

Fraisse, P. (1948). Les Erreursconstantesdans la reproduction de courts intervallestemporels. *Arch. Psychol.* 32, 161–176.

Getty, D. J. (1975). Discrimination of short temporal intervals: a comparison of two models. *Percept. Psychophys.* 18, 1–8.

Gibbon, J. (1977). Scalar expectancy theory and Weber's law in animal timing. *Psychol. Rev.* 84, 279–325.

Gibbon, J. (1991). Origins of scalar timing. *Learn. Motiv.* 22, 3–38.

Gibbon, J., and Church, R. M. (1984). "Sources of variance in an information processing theory of timing," in *Animal Cognition*, eds H. L. Roitblat, T. G. Bever, and H. S. Terrace (Hillsdale, NJ: Erlbaum), 465–488.

Gibbon, J., Malapani, C., Dale, C. L., and Gallistel, C. R. (1997). Toward a neurobiology of temporal cognition: advances and challenges. *Curr. Opin. Neurobiol.* 7, 170–184.

Gontier, E., Le Dantec, C., Leleu, A., Paul, I., Charvin, H., Bernard, C., and Lalonde, R. Rebaï, M. (2007). Frontal and parietal ERPs associated with duration discrimination with or without task interference. *Brain Res.* 1170, 79–89.

Gontier, E., Paul, I., Le Dantec, C., Pouthas, V., Jean-Marie, G., Bernard, C., Lalonde, R., and Rebaï, M. (2009). ERPs in anterior and posterior regions associated with duration and size discriminations. *Neuropsychology* 23, 668–678.

Grondin, S. (2001). From physical time to the first and second moments of psychological time. *Psychol. Bull.* 127, 22–44.

Grondin, S. (2010). Timing and time perception: a review of recent behavioral and neuroscience findings and theoretical directions. *Attent. Percept. Psychophys.* 72, 561–582.

Grondin, S., and Rammsayer, T. (2003). Variable foreperiods and duration discrimination. *Q. J. Exp. Psychol.* 56A, 731–765.

Harrington, D. L., Zimbelman, J. L., Hinton, S. C., and Rao, S. M. (2010). Neural modulation of temporal encoding, maintenance, and decision processes. *Cereb. Cortex* 20, 1274–1285.

Hasuo, E., Nakajima, Y., and Hirose, Y. (2011). Effects of sound marker durations on rhythm perception. *Perception* 40, 220–242.

Hellström, Å. (1985). The time-order error and its relatives: mirrors of cognitive processes in comparing. *Psychol. Bull.* 97, 35–61.

Jin, D. Z., Fujii, N., and Graybiel, A. M. (2009). Neural representation of time in cortico-basal ganglia circuits. *Proc. Natl. Acad. Sci. U.S.A.* 106, 19156–19161.

Lachaux, J. P., Rodriguez, E., Martinerie, J., and Varela, F. J. (1999). Measuring phase synchrony in brain signals. *Hum. Brain Mapp.* 8, 194–208.

Le Dantec, C., Gontier, E., Paul, I., Charvin, H., Bernard, C., Lalonde, R., and Rebaï, M. (2007). ERPs associated with visual duration discriminations in prefrontal and parietal cortex. *Acta Psychol.* 125, 85–98.

Macar, F., and Vidal, F. (2004). Event-related potentials as indices of time processing: a review. *J. Psychophysiol.* 18, 89–104.

Meck, W. H. (1984). "Attentional bias between modalities: effect on the internal clock, memory, and decision stages used in animal time discrimination," in *Annals of the New York Academy of Sciences : Vol. 423, Timing and Time Perception*, eds J. Gibbon and L. G. Allan (New York: New York Academy of Sciences), 528–541.

Merchant, H., Zarco, W., and Prado, L. (2008). Do we have a common mechanism for measuring time in the hundreds of millisecond range? Evidence from multiple-interval timing tasks. *J. Neurophysiol.* 99, 939–949.

Mitsudo, T., Nakajima, Y., Remijn, G. B., Takeichi, H., Goto, Y., and Tobimatsu, S. (2009). Electrophysiological evidence of auditory temporal perception related to the assimilation between two neighboring time intervals. *Neuroquantology* 7, 114–127.

Miyauchi, R., and Nakajima, Y. (2005). Bilateral assimilation of two neighboring empty time intervals. *Music Percept.* 22, 411–424.

Morillon, B., Kell, C. A., and Giraud, A.-L. (2009). Three stages and four neural systems in time estimation. *J. Neurosci.* 29, 14803–14811.

Nakajima, Y., Nishimura, S., and Teranishi, R. (1988). Ratio judgments of empty durations with numeric scales. *Perception* 17, 93–118.

Nakajima, Y., ten Hoopen, G., Sasaki, T., Yamamoto, K., Kadota, M., Simons, M., and Suetomi, D. (2004). Time-shrinking: the process of unilateral temporal assimilation. *Perception* 33, 1061–1079.

Nakajima, Y., ten Hoopen, G., and van der Wilk, R. (1991). A new illusion of time perception. *Music Percept.* 8, 431–448.

Pfeuty, M., Ragot, R., and Pouthas, V. (2003). When time is up: CNV time course differentiates the roles of the hemispheres in the discrimination of short tone durations. *Exp. Brain Res.* 151, 372–379.

Pfeuty, M., Ragot, R., and Pouthas, V. (2008). Brain activity during interval timing depends on sensory structure. *Brain Res.* 1204, 112–117.

Povel, D.-J. (1981). Internal representation of simple temporal patterns. *J. Exp. Psychol. Hum. Percept. Perform.* 7, 3–18.

Sasaki, T., Nakajima, Y., and ten Hoopen, G. (1998). Categorical rhythm perception as a result of unilateral assimilation in time-shrinking. *Music Percept.* 16, 201–222.

Sasaki, T., Suetomi, D., Nakajima, Y., and ten Hoopen, G. (2002). Time-shrinking, its propagation, and Gestalt principles. *Percept. Psychophys.* 64, 919–931.

Taatgen, N., and van Rijn, H. (2011). Traces of times past: representations of temporal intervals in memory. *Mem. Cogn.* 39, 1546–1560.

Taatgen, N., van Rijn, H., and Anderson, J. (2007). An integrated theory of prospective time interval estimation: the role of cognition, attention, and learning. *Psychol. Rev.* 114, 577–598.

Takeichi, H., Mitsudo, T., Nakajima, Y., Remijn, G. B., Goto, Y., and Tobimatsu, S. (2011). A neural decoding approach to auditory temporal assimilation. *Neural Comput. Appl.* 20, 965–973.

ten Hoopen, G., Sasaki, T., Nakajima, Y., Remijn, G., Massier, B., Rhebergen, K. S., and Holleman, W. (2006). Time-shrinking and categorical temporal ratio perception: evidence for a 1:1 temporal category. *Music Percept.* 24, 1–22.

Tervaniemi, M., Saarinen, J., Paavilainen, P., Danilova, N., and Näätänen, R. (1994). Temporal integration of auditory information in sensory memory as reflected by the mismatch negativity. *Biol. Psychol.* 38, 157–167.

van Rijn, H., and Taatgen, N. A. (2008). Timing of multiple overlapping intervals: how many clocks do we have? *Acta Psychol. (Amst.)* 129, 365–375.

Wearden, J. H., and Lejeune, H. (2008). Scalar properties in human timing: conformity and violations. *Q. J. Exp. Psychol.* 61, 569–587.

Woodrow, H. (1951). "Time perception," in *Handbook of Experimental Psychology*, ed. S. S. Stevens (New York: Wiley), 1224–1236.

Yabe, H., Tervaniemi, M., Reinikainen, K., and Näätänen, R. (1997). Temporal window of integration revealed by MMN to sound omission. *Neuroreport* 8, 1971–1974.

Zanto, T. P., Snyder, J. S., and Large, E. W. (2006). Neural correlates of rhythmic expectancy. *Adv. Cogn. Psychol.* 2, 221–231.

Conflict of Interest Statement: The authors declare that the research was conducted in the absence of any commercial or financial relationships that could be construed as a potential conflict of interest.

Received: 26 May 2011; paper pending published: 07 July 2011; accepted: 13 October 2011; published online: 06 December 2011.

*Citation: Nakajima Y and Takeichi H (2011) Human processing of short temporal intervals as revealed by an ERP waveform analysis. Front. Integr. Neurosci. **5**:74. doi: 10.3389/fnint.2011.00074*

frontiers in
INTEGRATIVE NEUROSCIENCE

ORIGINAL RESEARCH ARTICLE
published: 02 January 2012
doi: 10.3389/fnint.2011.00084

An electroencephalographic investigation of the filled-duration illusion

Takako Mitsudo[1], Caroline Gagnon[1], Hiroshige Takeichi[2] and Simon Grondin[1]*

[1] *École de Psychologie, Université Laval, Québec, QC, Canada*
[2] *Laboratory for Mathematical Neuroscience, Brain Science Institute, RIKEN, Wako, Japan*

Edited by:
Warren H. Meck, Duke University, USA

Reviewed by:
Matthew S. Matell, Villanova University, USA
Trevor B. Penney, National University of Singapore, Singapore

****Correspondence:***
Simon Grondin, École de psychologie, Université Laval, 2325 rue des Bibliothèques, Québec, QC, Canada G1V 0A6.
e-mail: simon.grondin@psy.ulaval.ca

The study investigated how the brain activity changed when participants were engaged in a temporal production task known as the "filled-duration illusion." Twelve right-handed participants were asked to memorize and reproduce the duration of time intervals (600 or 800 ms) bounded by two flashes. Random trials contained auditory stimuli in the form of three 20 ms sounds between the flashes. In one session, the participants were asked to ignore the presence of the sounds, and in the other, they were instructed to pay attention to sounds. The behavioral results showed that duration reproduction was clearly affected by the presence of the sounds and the duration of time intervals. The filled-duration illusion occurred when there were sounds; the participants overestimated the interval in the 600-ms interval condition with sounds. On the other hand, the participants underestimated the 800-ms interval condition without sounds. During the presentation of the interval to be encoded, the contingent negative variation (CNV) appeared around the prefrontal scalp site, and P300 appeared around the parieto-central scalp site. The CNV grew larger when the intervals contained the sounds, whereas the P300 grew larger when the intervals were 800 ms and did *not* contain the sounds. During the reproduction of the interval to be presented, the Bereitschaftspotential (BP) appeared over the fronto-central scalp site from 1000 ms before the participants' response. The BP could refer to the decision making process associated with the duration reproduction. The occurrence of three event-related potentials (ERPs), the P300, CNV, and BP, suggests that the fronto-parietal area, together with supplementary motor area (SMA), is associated with timing and time perception, and magnitude of these potentials is modulted by the "filled-duration illusion".

Keywords: EEG, filled-duration illusion, CNV, P300, BP, encoding, reproduction

INTRODUCTION

How does timing occur during an interval? How does the presence of additional sensory signals, during the process to be timed, interfere with this timing period? We use electroencephalographic (EEG) measures to determine how timing occurs in the context where additional signals are delivered.

The timing and time perception literature reveals that the occurrence of additional sensory information during an interval increases the perceived duration of this interval. This effect refers to the "filled-duration illusion." Technically, one may distinguish two branches of knowledge related to this effect. On the one hand, the effect may refer to the structure of a time interval, i.e., whether it is marked by two brief and distinct sensory signals (empty intervals) or by a continuous signal marking the onset and offset of the period to be timed (filled intervals; see Grondin, 1993; Grondin et al., 1998b). In this context, a relatively consistent finding is that filled intervals are perceived as being longer than empty ones (Wearden et al., 2007; ten Hoopen et al., 2008). This version of the filled-duration effect is not the one emphasized in the present article.

On the other hand, the "filled-duration illusion" (or the "filled-time illusion") refers to the fact that intervals marked by two brief signals, but filled with intermittent stimuli, are perceived as longer than empty intervals of equal physical duration (Hall and Jastrow, 1886; Thomas and Brown, 1974; Adams, 1977); this effect reminds one of the Oppel-Kundt illusion for space. Indeed, perceived duration increases when more sensory signals are presented during the interval (Grondin, 1992; Grondin et al., 1998a; Gamache et al., 2008).

Buffardi (1971) reported that the overestimation depends on the number of dividing sounds occurring during an interval. Filling an interval with additional signals provides an opportunity to segment the entire interval into a series of sub-intervals. One may capitalize on this opportunity for keeping track of time; these signals could be used to set some pace or can be substituted by numbers for inducing an implicit count of numbers (Grondin et al., 1999, 2004; Grondin, 2003). In addition to investigating the effects of sounds which subdivide the intervals, we tested the influence of orienting attention on the sounds marking sub-intervals. Previous studies which dealt with the relationship between attention and time perception revealed that perceived intervals were longer when observers paid attention to the intervals (Brown, 2008). The magnitude of the illusion should be larger when the participants were required to orient their attention to the stimuli

to keep track of time. In the present study, there were conditions where additional sensory signals for filling an interval either had to be ignored, or had to be used for counting numbers in the time estimation process.

Moreover, testing the relative effect on the "filled-duration illusion" of a passive attitude (ignore additional signals if they occur) vs. of an active use of the additional signals for explicit counting, the study aimed to provide an opportunity to search for cerebral indices related to the potential effect. Different cerebral imaging techniques contributed to develop hypotheses regarding the cerebral bases for processing temporal information (Grondin, 2010). The frontal cortex is most often reported as a key component involved in temporal tasks, with the role of accumulator being attributed to the supplementary motor area (SMA) and the storing and maintaining of temporal information being associated with the premotor cortex (Rubia and Smith, 2004). The parietal cortex, in particular the right inferior portion, would act as the moderator for directing attention to the stimulus marking time during the encoding of time intervals. The start and stop signals marking the period of accumulation of temporal information would be under the responsibility of the parietal cortex (Alexander et al., 2005; Bueti et al., 2008).

EEG has high temporal resolution, and is suitable to extract brain responses relevant to the perception from milliseconds to seconds intervals, from different brain areas at the same time. Previous studies with event-related potentials (ERPs) suggested that several ERP components corresponded to cognitive functions that are required to the perception of temporal intervals, such as working memory, attention, and decision making (Gibbon et al., 1997; Macar and Vidal, 2003, 2004). An ERP component often related to these functions is the contingent negative variation (CNV; Walter et al., 1964). The CNV has been observed in temporal perception and estimation tasks. It is related to the memorization of time intervals (Pouthas et al., 2000; Pfeuty et al., 2003a,b), duration reproduction (Macar et al., 1999), and accumulation processes (Pouthas et al., 2000; Montfort and Pouthas, 2003; Pfeuty et al., 2003b). The generator of the CNV in the task of duration discrimination is mostly considered to be the prefrontal cortex (Pouthas, 2003; Macar and Vidal, 2004). Another ERP component, the P300 (Picton, 1992), is also related to selective attention in temporal tasks (Macar and Vidal, 2003; Gontier et al., 2007, 2008, 2009; Le Dantec et al., 2007; Mitsudo et al., 2009). The parietal cortex is one of the critical sources of the P300 in the context of attention and working memory (Picton, 1992; Horn et al., 2003; Linden, 2005), and the relationships between the P300 and the parietal cortex were also discussed in the timing literature (Gontier et al., 2007, 2009; Mitsudo et al., 2009). Moreover, the slowly increasing negativity called the Bereitschaftspotential (BP), or the readiness potential (RP), is another measure of activity in the motor cortex of the brain caused by voluntary muscle movement; the SMA is argued to be the generator of this activity (Deecke and Kornhuber, 1978). Indeed, BP was reported as a signature for time reproduction (e.g., Macar et al., 1999).

There was one previous ERP study that examined the neural correlates of the "filled-duration illusion" (Pfeuty et al., 2008). The study adopted the filled (continuous tones) or empty (silent periods bounded by two brief tones) intervals and revealed that the CNV was closely related to the occurrence of the illusion. The CNV amplitude was larger for the filled than for the empty intervals, with a better discrimination performance with the empty than with the filled intervals during the recording. In contrast, the empty intervals in our study were segmented in four sub-intervals by additional auditory signals. Since each signal was expected to require orienting attention to keep track of time, our study was able to clarify the time course of the attention mechanisms relevant to temporal processing. Moreover, we intended to explore the EEG activity in the reproduction period, which enabled us to investigate the whole process required in time perception.

The goal of the present study is to investigate how the brain activity, as revealed by the EEG activity, changes when participants are engaged in a temporal reproduction task associated with the "filled-duration illusion." Participants were asked to memorize and reproduce the duration of a temporal interval (600 or 800 ms) bounded by two flashes. During this interval, three additional brief sounds were, or were not, presented, in a random order. In one session, participants were asked to ignore the presence of the sounds, and in the other one, they were instructed to use it for keeping track of time. We focused on two processes, encoding and reproduction. The brain signals of interest were related to attention and memory processes in the encoding period, and decision making processes in the reproduction period. Finally, as previous studies consistently reported the dominance of the right hemisphere when participants are engaged in memorizing or reproducing time intervals (Pouthas et al., 2000; Pfeuty et al., 2003b), it was planned to verify whether any hemispheric difference appeared during the task.

MATERIALS AND METHODS

PARTICIPANTS

Twelve volunteer right-handed participants aged 20–39 (five men, seven women) took part in this experiment. They received $24 CAN for their participation. All had normal or corrected-to-normal vision, and had no reported hearing deficits. The experimental procedures were approved by the Ethics Committee of Université Laval.

STIMULI

Each participant was seated in a dimly lit room in front of an LCD monitor connected to a computer at a viewing distance of approximately 60 cm. Two 20 ms flashes (red circles), which subtended a visual angle of 0.95° horizontally and 0.95° vertically, were used for marking the 600- or 800-ms temporal intervals by their onsets. Three additional brief sounds were 1 kHz sine waves presented binaurally at 77 dB (SPL) for a 20-ms duration via speakers placed on each side of the computer screen. Two-thousand milliseconds before the flashes, a white circle (visual angle of 0.95° horizontally and 0.95°vertically) was presented where the flashes would appear. After the second flash, the white circle remained presented for 950 ms until a visual instruction appeared.

PROCEDURE

Each trial consisted of two phases: *encoding* and *reproduction*. Participants were asked to memorize and reproduce the duration of one time interval (600 or 800 ms) bounded by two flashes (see **Figure 1**). In half of the trials in a random order, series of

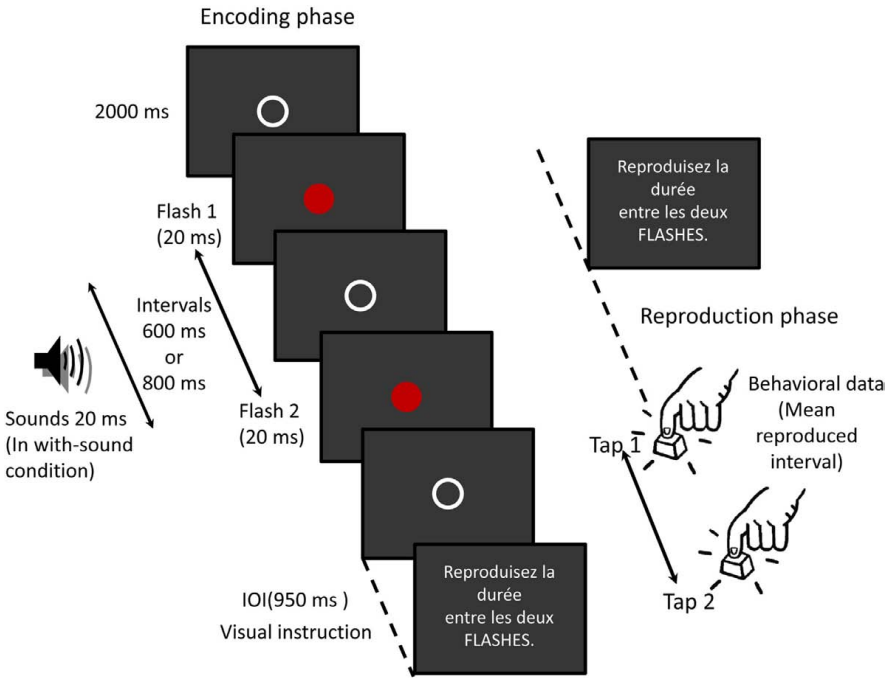

FIGURE 1 | Procedure of the experiment. In the encoding phase, the stimulus epoch begins 100 ms prior to the onset of the first flash and continues for 1200 ms. During half of the trials within a block, in a random order, series of three auditory stimuli (20 ms, 1 kHz) were presented. Before and after the flashes, a white circle was presented where the flash would appear. The sounds segmented the interval in four equal sub-intervals of 150 or 200 ms. The delay between the second flash and the first tap was determined by the timing when the participants decided to initiate the reproduction.

three auditory stimuli were presented during the interval. The sounds segmented the interval in four equal sub-intervals of 150 or 200 ms. Nine hundred fifty milliseconds after the interval presentation, a visual instruction was presented to let the participants reproduce the duration between the two flashes. The participants reproduced the duration by pressing a button on a keypad with their right index finger. The duration between the first tap and the second tap – the reproduced interval – was used for behavioral analyses. The delay between the second flash and the first tap was determined by the timing when the participants decided to initiate the reproduction.

There were two sessions. In one session, the participants had to pay attention to the sounds during their estimations and to use the sounds for segmenting the interval to be memorized into small sub-intervals (*Pay attention*). In the other session, they were asked to ignore the presence of any sound occurring during the interval to be memorized (*Ignore*). The order of the sessions was counterbalanced across participants. The participants performed the two sessions on different days. One session consisted of one practice block and five experimental blocks. The practice stimuli were presented 20 times before the beginning of the experimental blocks. Then each stimulus (600 ms without-sounds, 800 ms without-sounds, 600 ms with-sounds, or 800 ms with-sounds) was presented 25 times in a random order in each block, making a total of 100 trials per block. EEG activity was recorded from 32 scalp electrodes during the whole task (encoding and presentation + temporal reproduction phases).

EEG RECORDING

EEG was recorded continuously with a 32-channel Geodesic Sensor Net [Fp1, Fp2, Fpz, FT9, FT10, F7, F8, F3, F4, Fz, FCz, C5, C6, C3, C4, Cz, T3(T7), T4(T8), T5(P7), T6(P8), TP9, TP10, P3, P4, Pz, O1, O2, Oz, and four electrodes below each eye] using a NetAmps 300 (Electrical Geodesics Inc., Eugene, OR, USA). Cz was used as the reference. Electrooculogram (EOG) was monitored using electrodes placed below each eye. The electrode impedance was kept below 50 kΩ. This range was acceptable given the high input impedance of the amplifiers of this system. Off-line analyses of the data were performed using Net Station software (Electrical Geodesics, Inc., Eugene, OR, USA). The ERP and EOG data were sampled at a rate of 250 Hz. Trials were marked "bad" if the average amplitude exceeded 100 μV, if they contained more than 10 bad channels, or contained eye movement in excess of 55 μV. These automated criteria were supplemented by visual inspection. In the remaining trials, data for bad channels were replaced by interpolations from the remaining channels using Net Station software. A total of 54–87 responses were averaged, re-referenced at the mastoid, and baseline-corrected for each stimulus for each participant.

For the ERP analysis, each stimulus epoch began 100 ms prior to, and continued 1200 ms after the onset of the first flash in the encoding phase. In the temporal reproduction phase, for the Tap1 analysis, the stimulus epoch began 800 ms prior to this first tap with a baseline measured 100 ms before the first flash (backward analysis time-locked to Tap1). The baseline, which was 100 ms

before the first flash (at the beginning of each trial) was used because the period did not contain any artifact related to the task. For the Tap2 analysis, the stimulus epoch began 1500 ms prior to this tap, and continued 300 ms after, with a 100-ms baseline measured at the first flash (backward analysis time-locked to Tap2). Note that the EEG before tapping contained activities related to the encoding (see **Figure 1**). Each participant was instructed to keep their eyes open during stimulus presentation.

DATA ANALYSES

The effects of stimulus and attention

The dependent variable of interest was the mean reproduced interval. More specifically, in order to directly compare the 600 and the 800-ms intervals, we calculated the deviation from the standard interval – the constant error (CE) – as a variable of interest (CE = mean production – standard). A 2 (Sounds: with vs. without) × 2 (Attention: pay attention or ignore) × 2 (Duration: 600 vs. 800 ms) ANOVA with repeated measures was used to analyze the behavioral data.

The effect of session order

To explore whether there was an effect of order, e.g., participants really ignored the sounds in the second Ignore session when they used them in the first Pay attention session, we additionally checked the effect of session order. An ANOVA was used with Session order (first or second) as a between subject variable, and Attention (pay attention or ignore), Stimulus types (four levels: 600 ms with-sounds, 600 ms without-sounds, 800 ms with-sounds, and 800 ms without-sounds) as within-subject variables.

Event-related potentials

Encoding phase. We first checked whether CNV differed among conditions by analyzing a time course of the CNV in order to investigate the temporal development of the CNV during the encoding phase. Because of the difference of the stimulus duration, we analyzed the time course of 600 and 800 ms condition separately. For both 600 and 800 ms conditions, 100 ms temporal windows were applied. For 600 ms condition, each temporal window was set between 1 and 800 ms: tw1 = (1–100 ms), tw2 = (101–200 ms), tw3 = (201–300 ms), tw4 = (301–400 ms), tw5 = (401–500 ms), tw6 = (501–600 ms), tw7 = (601–700 ms), and tw8 = (701–800 ms). For 800 ms condition, each temporal window was set between 1 and 1000 ms: tw1 = (1–100 ms), tw2 = (101–200 ms), tw3 = (201–300 ms), tw4 = (301–400 ms), tw5 = (401–500 ms), tw6 = (501–600 ms), tw7 = (601–700 ms), tw8 = (701–800 ms), tw9 = (801–900 ms), and tw10 = (901–1000 ms). For each duration condition, a 2 (Sounds: with vs. without) × 2 (Attention: pay attention or ignore) × 8 or 10 (Temporal Window: tw1 to tw 8 for 600 ms, tw1 to tw10 for 800 ms) ANOVA was carried out on the mean CNV amplitude calculated over successive temporal windows on the averaged EEG activity of the six prefrontal electrodes (FP1, FP2, F3, F4, Fpz, and Fz). Subsequently, for P300, we measured maximal amplitude and the latency on the averaged EEG activity of the three parieto-central electrodes (Pz, Cz, and FCz). We measured first maximal positive peak between 150 and 350 ms after the offset of the second flash. In order to examine the characteristics of the P300, two 2 (Sounds: with vs. without) × 2 (Attention: pay attention or ignore) × 2 (Duration: 600 vs. 800 ms) ANOVAs with repeated measures were conducted on the amplitude and the latency of P300. Finally, a 2 (Sounds: with vs. without) × 2 (Attention: pay attention or ignore) × 2 (Duration: 600 vs. 800 ms) × 2 (Laterality: right or left) × 5 (Electrode sites: anterior to posterior) ANOVA was performed on the mean CNV amplitude calculated between 1 and 1000 ms over lateral electrodes (Fp1, F3, C3, P3, and O1 for the left hemisphere, Fp2, F4, C4, P4, and O2 for the right hemisphere) in order to test if there was any laterality effect.

Reproduction phase. EEG waveforms time-locked to Tap1 were averaged 500 ms preceding the first tap. Integrated amplitudes were then calculated with respect to a −500- to 0-ms temporal windows, respectively. Electrodes F3, Fz, F4, C3, Cz, C4, P3, Pz, and P4 were assigned to assess the differences in scalp distribution for each ERP component during the reproduction, according to the previous ERP studies where the CNV and the BP were used (e.g., Scheibe et al., 2009). A 2 (Sounds: with vs. without) × 2 (Attention: pay attention or ignore) × 2 (Duration: 600 vs. 800 ms) × 3 (Anterior to posterior distinctions: frontal, central, and parietal) × 3 (Laterality: medium-left, mid-sagittal, and medium-right) ANOVA was carried out for each temporal window. EEG waveforms time-locked to Tap2 were averaged in a temporal window extending from −360 to 0 ms for 600 ms, from −480 to 0 ms for 800 ms before the second tap. A 2 (Sounds: with vs. without) × 2 (Attention: pay attention or ignore) × 3 (Anterior to posterior distinctions: frontal, central, and parietal) × 3 (Laterality: medium-left, mid-sagittal, and medium-right) ANOVA was again carried out to confirm the location of the activation for each stimulus duration. These temporal windows were defined as the three-fifths of the total stimulus duration (see Macar et al., 1999).

In order to check the neural correlates of the illusion, it is important that the participants' behavior and EEG signal corresponded accurately. For the analysis reported for both encoding and reproduction phases, only trials corresponding to the artifact-free behavioral responses were included. We removed the five longest and five shortest reproduced intervals in each block in the behavioral data, and excluded the EEG data corresponding to these trials. Trial extraction corresponding to the behavioral data was processed using MATLAB R2007a (The MathWorks, Inc., Natick, MA, USA). Mean amplitude for each temporal window was calculated with R version 2.5.0. All statistical analyses were performed using SPSS 11.5J. Greenhouse-Geisser correction was included for >1 degrees of freedom. Bonferroni correction for multiple *post-hoc* comparisons were applied when required. For ANOVA, the η_p^2 were provided for the quantitative comparison of effect sizes. In multiple comparisons, the Cohen's *d* was provided for the effect sizes (the values were calculated by subtracting one mean from the other and dividing it by the pooled SD).

RESULTS

BEHAVIORAL DATA

The effects of stimulus and attention

Figure 2 shows the mean CE for each experimental condition. There was a significant main effect of Duration, F (1, 11) = 46.67, $p < 0.01$, $\eta_p^2 = 0.81$, and a marginally significant main effect of Sounds, F (1, 11) = 4.57, $p = 0.06$, $\eta_p^2 = 0.29$.

CE was more positive in the 600-ms than in the 800-ms condition, and tended to be more positive in the with-sounds than without-sounds condition. There was no main effect of Attention ($p < 0.50$). The Duration × Sounds interaction effect was significant, $F\ (1, 11) = 16.00$, $p < 0.01$, $\eta_p^2 = 0.59$, but the Attention × Sounds ($p = 0.21$) and Attention × Duration ($p = 0.55$) interaction effects were not. The CE difference between with- and without-sounds conditions was greater in the 800-ms condition ($p < 0.001$, $d = -0.62$) than in the 600-ms condition ($p = 0.20$, $d = -0.35$). The Duration × Sounds × Attention interaction was significant, $F\ (1, 11) = 6.39$, $p < 0.03$, $\eta_p^2 = 0.36$. For the 800-ms condition, the CE difference between with- and without-sounds conditions was greater in the Pay attention ($p < 0.02$, $d = -0.70$) than in the Ignore ($p < 0.01$, $d = -0.51$) condition.

The effect of session order

Table 1 shows the mean CE for each stimulus type and each session order and attention conditions. There was a significant main effect for Stimulus type, $F\ (3, 60) = 14.80$, $p < 0.001$, $\eta_p^2 = 0.43$, but there was no effect of Order ($p = 0.76$) or of Attention ($p = 0.73$). No significant interaction was found among stimulus type, attention or session order. The session order did not appear to have affected the behavioral results in the experiment.

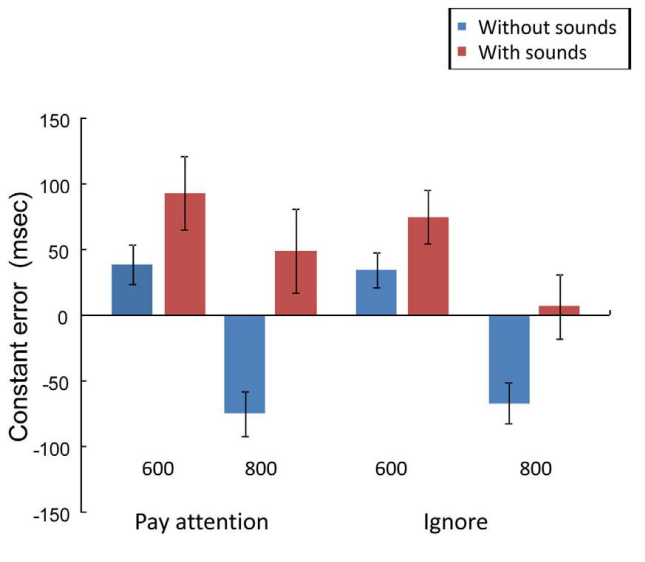

FIGURE 2 | Mean constant error (in ms) in the experimental conditions. Bars are SEs.

ERP DATA

Encoding phase

Time course analyses of CNV. As shown in **Figure 3**, CNV appeared at Fp1, Fp2, F3, F4, Fpz, and Fz electrodes in both the with- and without-sounds conditions. For both the 600- and 800-ms stimuli, the CNV resolved approximately 200 ms after the second flash, then a P300-like positive deflection followed around 200 ms after the second flash.

Figure 4 shows the mean CNV waveforms which were averaged over the six prefrontal electrodes. In the 600-ms condition, there were significant main effects of Sounds, $F\ (1, 11) = 37.13$, $p < 0.001$, $\eta_p^2 = 0.77$, and Temporal Window, $F\ (2.96, 32.5) = 7.74$, $p < 0.001$, $\eta_p^2 = 0.41$. The effect of Attention was not significant, $F\ (1, 11) = 2.20$, $p = 0.16$, $\eta_p^2 = 0.16$. The CNV was larger with- than without- sounds ($p < 0.001$, $d = 1.13$). **Figure 5A** shows the result of the multiple comparisons in the 600-ms condition among eight Temporal Windows on the mean CNV amplitude averaged between Pay attention and Ignore conditions. In the 600-ms duration condition, the CNV started to appear at tw3, became maximal at tw5, and resolved quickly after tw7. The Sounds × Temporal Window interaction was significant, $F\ (3.68, 40.45) = 22.6$, $p < 0.001$, $\eta_p^2 = 0.67$. The mean amplitude differences between with- and without-sounds significantly differed in tw3 ($p < 0.002$, $d = 1.31$), tw4 ($p < 0.004$, $d = 0.99$), tw5 ($p < 0.001$, $d = 1.34$), tw6 ($p < 0.001$, $d = 1.96$), tw7 ($p < 0.001$, $d = 1.49$), and tw8 ($p < 0.001$, $d = 1.15$).

In the 800-ms condition, there were significant main effects of Sounds, $F\ (1, 11) = 25.61$ $p < 0.001$, $\eta_p^2 = 0.69$, and Temporal Window, $F\ (3.02, 33.2) = 12.95$, $p < 0.001$, $\eta_p^2 = 0.54$; note the marginally significant effect of Attention $F\ (1, 11) = 3.21$, $p = 0.10$, $\eta_p^2 = 0.23$. The CNV was larger with-than without-sounds ($p < 0.001$, $d = 0.94$), and tended to be larger in the Pay attention than in the Ignore condition ($p = 0.10$, $d = -0.38$). **Figure 5B** shows the result of the multiple comparisons in the 800-ms condition among 10 Temporal Windows on the mean CNV amplitude averaged between Pay attention and Ignore conditions. In the 800-ms duration condition, the CNV started to appear at tw3 and continued until tw8. The Sounds × Temporal Window interaction was significant, $F\ (3.11, 34.21) = 15.30$, $p < 0.001$, $\eta_p^2 = 0.58$, and the Attention × Sounds × Temporal Window interaction was marginally significant, $F\ (2.77, 30.48) = 2.34$,

Table 1 | Mean CE (in ms with SE) in each experimental condition.

		600 ms without-sounds		600 ms with-sounds		800 ms without-sounds		800 ms with-sounds	
		First	Second	First	Second	First	Second	First	Second
Pay attention	Mean	75.2	1.1	114.2	72.4	−39.9	−112.1	81.81	15.2
	SE	6.7	0.2	9.5	4.9	−3.3	−16.1	5.8	1.0
Ignore	Mean	4.1	66.8	60.7	89.5	−80.2	−50.4	6.7	8.5
	SE	0.7	6.3	5.2	7.9	−9.8	−4.5	0.5	0.7

First and Second refer to session order.

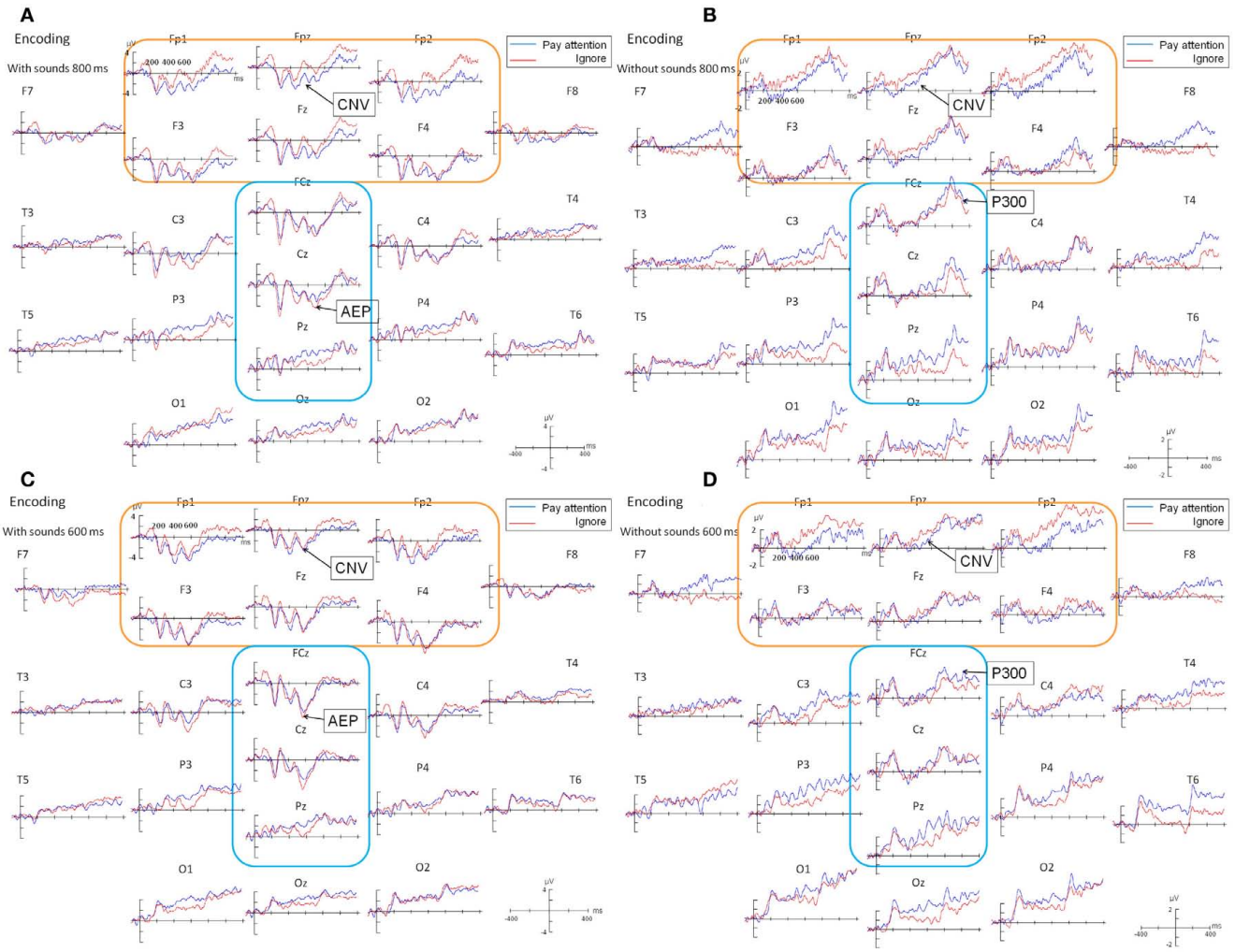

FIGURE 3 | Grand averaged ERP waveforms during the encoding phase of (A) 800 ms condition, with-sounds, (B) 800 ms condition, without-sounds, (C) 600 ms condition, with-sounds, and (D) 600 ms condition, without-sounds. There could be overlap of a few ERP components generated by the events that occurred at closer timing to the P300. For example, the visual P1 component may have appeared 100 ms after the second visual flash in the occipital site, while the CNV have resolved within 200 ms after the second flash around the prefrontal site. Because of these co-occurred components, the P300 may seem to develop on many electrodes.

$p < 0.09$, $\eta_p^2 = 0.17$. The Sounds × Temporal Window interaction indicated that in the tw3 ($p < 0.002$, $d = 1.12$), tw4 ($p < 0.003$, $d = 0.69$), tw5 ($p < 0.001$, $d = 1.15$), tw6 ($p < 0.001$, $d = 0.72$), tw7 ($p < 0.001$, $d = 1.24$), tw8 ($p < 0.001$, $d = 1.48$), tw9 ($p < 0.001$, $d = 1.14$), and the tw10 ($p < 0.001$, $d = 0.68$), the CNV was larger with-than without-sounds. The marginally significant effect of the Attention × Sounds × Temporal Window interaction revealed that when there were sounds, the amplitude differences between Pay attention condition and Ignore condition tended to be large at tw2 ($p < 0.01$, $d = -0.77$), tw6 ($p = 0.07$, $d = -0.70$), and tw10 ($p = 0.05$, $d = -0.65$).

P300 component. As for P300, activity was mainly observed at Pz, Cz, and FCz electrodes in the without-sounds condition (**Figures 3** and **6**). **Table 2** shows the mean P300 amplitudes and latencies which were averaged over the three parieto-central electrodes. For the P300 amplitude, there were significant main effects of Duration, F (1, 11) = 9.3, $p < 0.01$, $\eta_p^2 = 0.45$, and Sounds, F (1, 11) = 8.91, $p < 0.01$, $\eta_p^2 = 0.45$, but no effect of Attention ($p = 0.41$). The P300 was larger in the 800-ms than in the 600-ms condition ($p < 0.01$, $d = -0.53$), and larger without- than with-sounds condition ($p < 0.01$, $d = -0.40$). For the P300 latency, there was a significant main effect of Duration, F (1, 11) = 7.85, $p < 0.01$, $\eta_p^2 = 0.42$. The P300 latency was short in the 800-ms (maximally at 184 ms from the offset of the second flash) compared to the 600-ms (maximally at 214 ms from the offset of the second flash) condition ($p < 0.01$, $d = 0.46$). The effect of Attention was marginally significant, F (1, 11) = 4.31, $p < 0.06$, $\eta_p^2 = 0.28$. The P300 latency tended to be shorter in the Pay attention (186 ms) than in the Ignore (211 ms) condition ($p < 0.06$, $d = -0.37$). There was no main effect of Sounds ($p = 0.77$). No interaction effects were significant for either amplitude or latency.

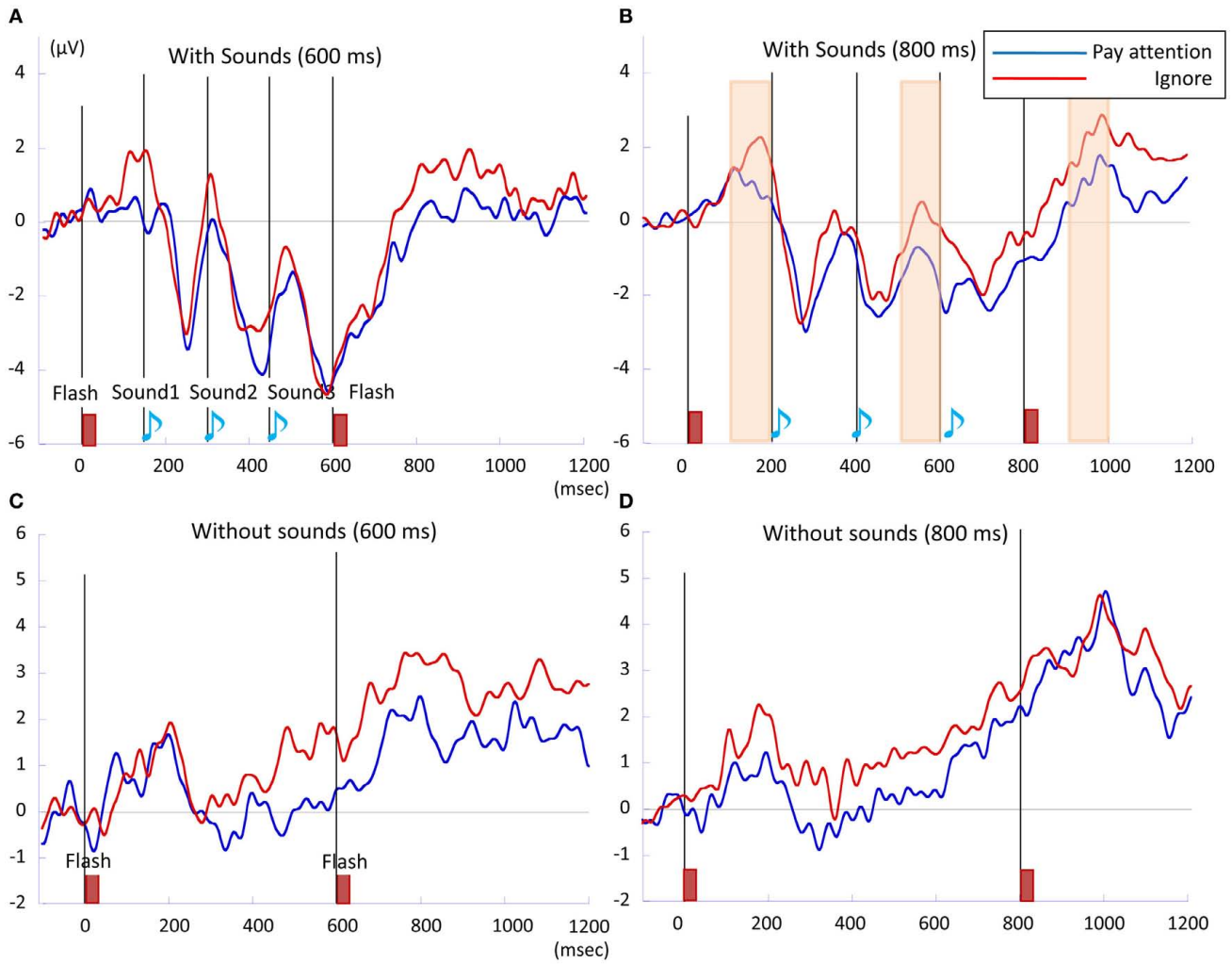

FIGURE 4 | The CNV waveforms of (A) 600 ms with-sounds, (B) 800 ms with-sounds, (C) 600 ms without-sounds, and (D) 800 ms without-sounds condition. The integrated CNV amplitude was calculated over successive temporal windows on the averaged activity of the six prefrontal electrodes (FP1, FP2, F3, F4, Fpz, and Fz). Pay attention condition is in blue, while Ignore condition is in red. Pale orange bars represent the temporal windows where the integrated amplitude in Pay attention condition is larger than in Ignore condition. Each is corresponding to the tw2, tw6, and tw10, respectively.

Laterality effect with the CNV. The ANOVA (2 Duration × 2 Sounds × 2 Attention × 2 Laterality × 5 Electrode) performed on the mean CNV amplitude calculated between 1 and 1000 ms over lateral electrodes revealed a significant effect of Sounds, $F\ (1,11) = 21.03$, $p < 0.01$, $\eta_p^2 = 0.65$, of Electrode, $F\ (2.36, 25.92) = 13.73$, $p < 0.01$, $\eta_p^2 = 0.56$, and an interaction between these factors, $F\ (2.0, 22.32) = 22.89$, $p < 0.01$, $\eta_p^2 = 0.67$. The CNV amplitude was larger with-sounds than without-sounds over centro-frontal electrodes. There was no sign of a laterality effect, $F\ (1, 11) < 0.001$, $p = 0.98$, $\eta_p^2 < 0.001$, and this factor was not involved in any interaction.

Reproduction phase

Tap 1. **Figure 7A** shows the grand averaged ERP waveforms time-locked to Tap1 in 800 ms condition with-sounds. As shown in the figure, transient positive potential (movement-related cortical potential, MRCP) triggered by the first tap appeared immediately after the button pressing in both Pay attention and Ignore conditions, and Bereitschaftspotential (BP), which was defined by the slow negative shift leading up to voluntary muscle movement, was observed at Cz and C3. A similar tendency was observed in the 800-ms without-sounds condition and in the 600-ms with- and without-sounds conditions. An ANOVA (2 Duration × 2 Sounds × 2 Attention × 3 Anterior to posterior × 3 Laterality) was carried out for −500 to 0 ms temporal windows. The result showed that the Anterior to posterior effect, $F\ (2, 22) = 8.85$, $p < 0.01$, $\eta_p^2 = 0.45$, was only significant (all others, $p > 0.30$). The central ($p < 0.001$, $d = 0.53$) was more negative, and the frontal ($p = 0.10$, $d = 0.40$) tended to be more negative than the parietal site.

Tap 2. **Figure 7B** shows the grand averaged ERP waveforms time-locked to Tap2 in 800 ms condition with-sounds. As shown in the figure, large BP was observed before Tap2 at Cz. The similar

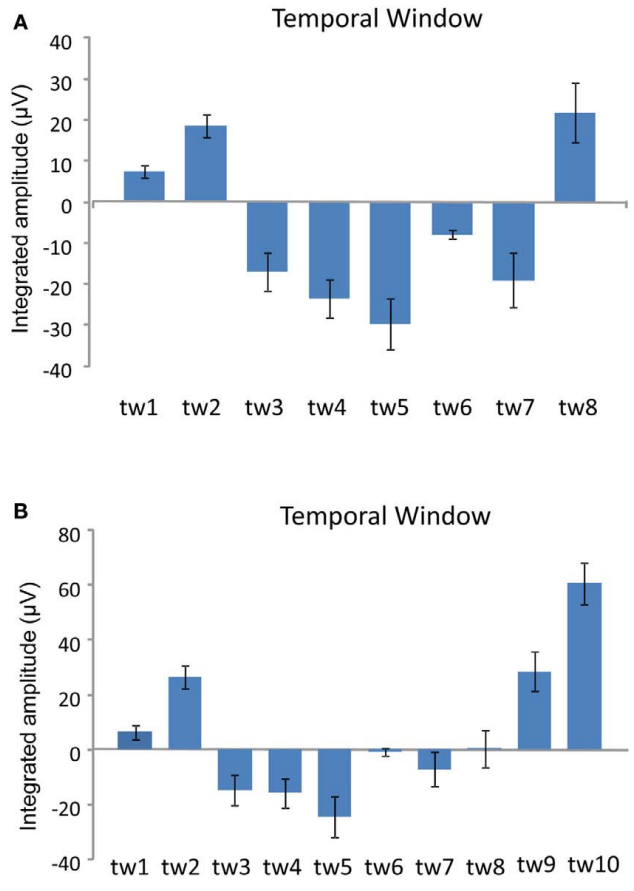

FIGURE 5 | The multiple comparisons among temporal windows on the mean CNV amplitude averaged between Pay attention and Ignore conditions calculated over successive temporal windows (tw) on the averaged activity of the six prefrontal electrodes (FP1, FP2, F3, F4, Fpz, and Fz). (A) 600 ms condition, and **(B)** 800 ms condition, respectively. The CNV appeared between tw3 and tw7, in the 600-ms condition, tw3 and tw8 in the 800-ms condition, which approximately corresponded to the interval between the first sound and the second flash.

tendency was observed in the 800-ms without-sounds condition and in the 600-ms with- and without-sounds conditions. An ANOVA (2 Sounds × 2 Attention × 3 Anterior to posterior × 3 Laterality) was carried out in a temporal window of −360 to 0 ms and −480 to 0 ms in each of 600 and 800 ms stimulus duration, respectively. For the 600-ms condition, the effects of Anterior to posterior, F (1.59, 17.44) = 7.622, $p < 0.006$, $\eta_p^2 = 0.41$, and Laterality, F (1.32, 14.49) = 7.32, $p < 0.01$, $\eta_p^2 = 0.40$, were significant (all the others, $p > 0.10$). The central was more negative than the frontal site ($p < 0.01$, $d = -0.44$). The activity at the mid-sagittal site was more positive than the one at medium-left ($p < 0.01$, $d = 0.38$). The Anterior to posterior × Laterality interactions were significant, F (4, 44) = 5.42, $p < 0.01$, $\eta_p^2 = 0.33$. At frontal site, the averaged amplitude was larger at mid-sagittal than at medium-right ($p < 0.01$, $d = -0.76$). Moreover, in the 600-ms condition at central site, the averaged amplitude at the mid-sagittal site was larger than the one at medium-left ($p < 0.003$, $d = 0.62$) and medium-right ($p < 0.001$, $d = 0.70$). For 800 ms condition, the effects of Anterior to posterior, F (1.98, 21.74) = 7.72, $p < 0.003$, $\eta_p^2 = 0.41$, and Laterality, F (1.49, 16.37) = 3.30, $p < 0.05$, $\eta_p^2 = 0.25$, were significant (all the others, $p > 0.10$). The central was more negative than the frontal site ($p < 0.005$, $d = 0.53$). The activity at the mid-sagittal site was more positive than the one at medium-left ($p < 0.008$, $d = 0.33$).

DISCUSSION

The present study investigated how the EEG activity changed when the participants were engaged in a temporal reproduction task associated with the "filled-duration illusion". As indicated by the behavioral data, the "filled-duration illusion" occurred in our study: Filled (with-sounds) intervals were perceived as longer than empty (without-sounds) intervals of equal physical duration (Grondin et al., 1998b). The illusion was affected by attention: The magnitude of the illusion was greater in the Pay attention condition of the 800-ms duration. In the encoding phase, the prefrontal CNV augmented during the stimulus presentation, corresponding to the perceived duration of the stimuli. The parietal P300 was maximal and its latency was shortened in the without-sounds condition especially in the 800-ms condition. Both the CNV and the P300 were modulated by attention, i.e., whether the participant ignored the sounds or used them for keeping track of time. The results suggested that the CNV is related to the perceived duration, while the P300 is related to orienting attention to the stimuli. Analyses of the reproduction phase revealed that the BPs were observed maximally at the central site when participants reproduced the memorized intervals by finger tapping. The BPs were associated with the voluntary movement and motor preparation.

TIMING PERFORMANCE WITH VS. WITHOUT ADDITIONAL SOUNDS

The presence of the sounds affected the reproduced intervals, which were longer with the sounds. The occurrence of additional sounds during an interval increased the perceived duration of that interval. Stimulus duration also affected the illusion. The magnitude of the "filled-duration illusion" was larger in the 800-ms condition. Finally, the effect of attention appeared in the 800-ms condition. The magnitude of the illusion was larger in the 800-ms Pay attention condition than in the 800-ms Ignore condition. The filled-duration effect was modulated by an active use of the additional auditory signals. In our experiment, at 600 ms in the with-sound conditions, the participants overestimated the interval between the two flashes, whereas at 800 ms without-sounds condition, participants underestimated the interval. This finding is consistent with the Vierordt's law which states that "short" time intervals tend to be overestimated, and "long" time intervals tend to be underestimated (Lejeune and Wearden, 2009).

ERPS DURING THE ENCODING PHASE

Contingent negative variation

The CNV, which was obtained from the prefrontal electrodes, became larger during stimulus presentation (**Figures 3** and **4**). The averaged CNV amplitude was larger in the with-sounds condition than in the without-sounds condition. The CNV time course suggested that the participants utilized the sound information to keep track of time. The effects of temporal window showed that

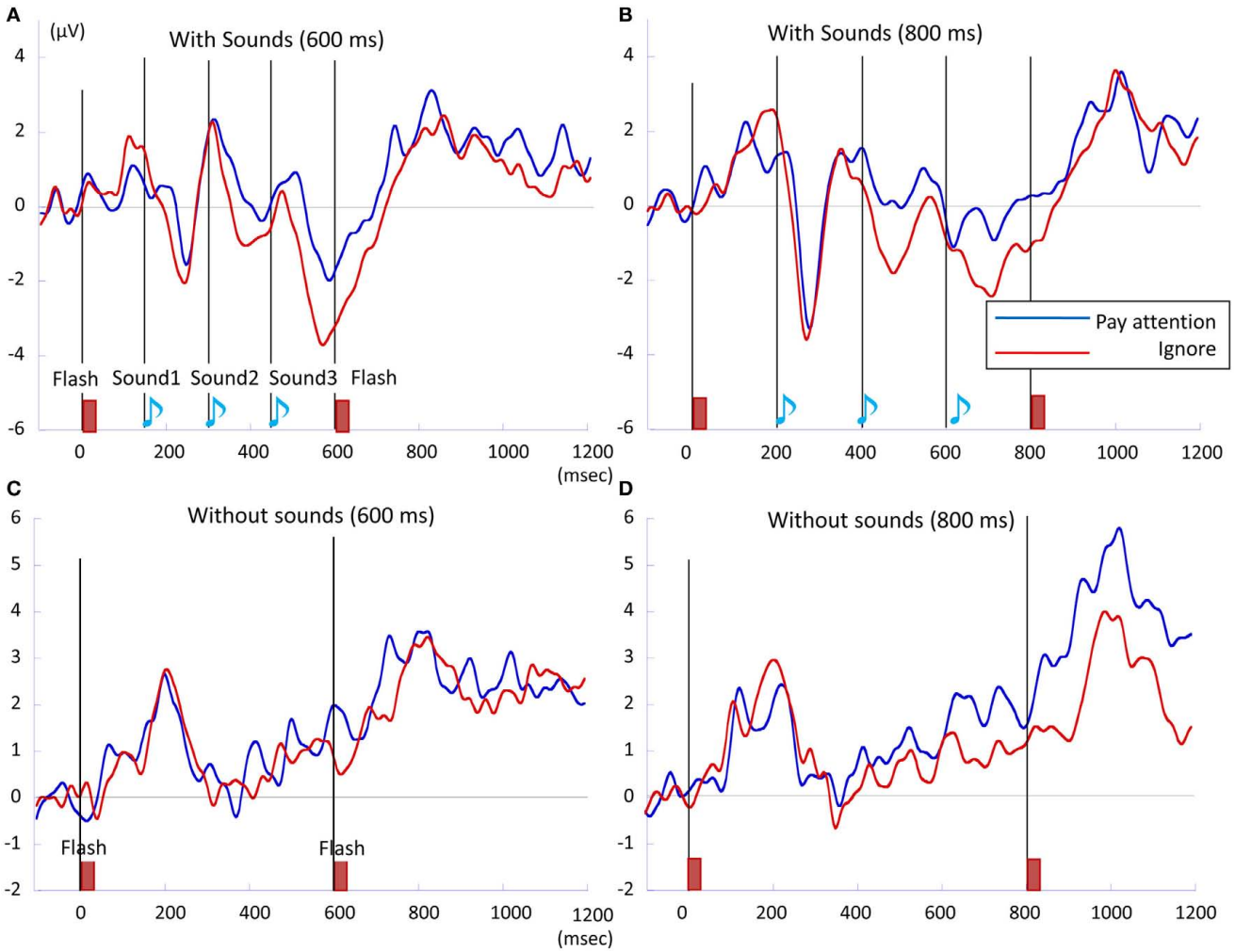

FIGURE 6 | The P300 waveforms of (A) 600 ms with-sounds, (B) 800 ms with-sounds, (C) 600 ms without-sounds, and (D) 800 ms without-sounds condition. The integrated P300 amplitude was calculated over successive temporal windows on the averaged activity of the three parieto-central electrodes (Fz, Cz, and Pz). Pay attention condition is in blue, while Ignore condition is in red. P300 was the largest in 800 ms Without-sounds condition.

Table 2 | Mean amplitudes (μv) and latencies (ms) of P300 in each condition ($N = 12$).

		600 ms without-sounds		600 ms with-sounds		800 ms without-sounds		800 ms with-sounds	
		Amplitude	**Latency**	**Amplitude**	**Latency**	**Amplitude**	**Latency**	**Amplitude**	**Latency**
Pay attention	Mean	4.6	194.3	3.1	212.7	5.7	182.0	4.2	158.7
	SE	2.0	7.2	2.3	5.2	2.0	4.7	2.2	4.9
Ignore	Mean	3.1	222.3	3.1	226.7	4.8	206.7	4.2	188.7
	SE	2.1	5.2	2.2	4.1	2.3	3.1	1.9	3.1

Amplitudes and latencies were measured from the offset of the second flash.

in the 600-ms condition, the CNV appeared between tw3 and tw7, while in the 800-ms condition, the CNV appeared between tw3 and tw8. These temporal windows corresponded to the interval between the first sound and 200 ms after the second flash (**Figure 5**). This result is consistent with previous studies where the CNV amplitude changed accordingly with the length of the memorized intervals (Macar et al., 1999; Pfeuty et al., 2003a,b). The Attention × Sounds × Temporal Window interaction in the 800-ms condition showed that the attention enhanced the CNV amplitude within temporal windows preceding the sounds by

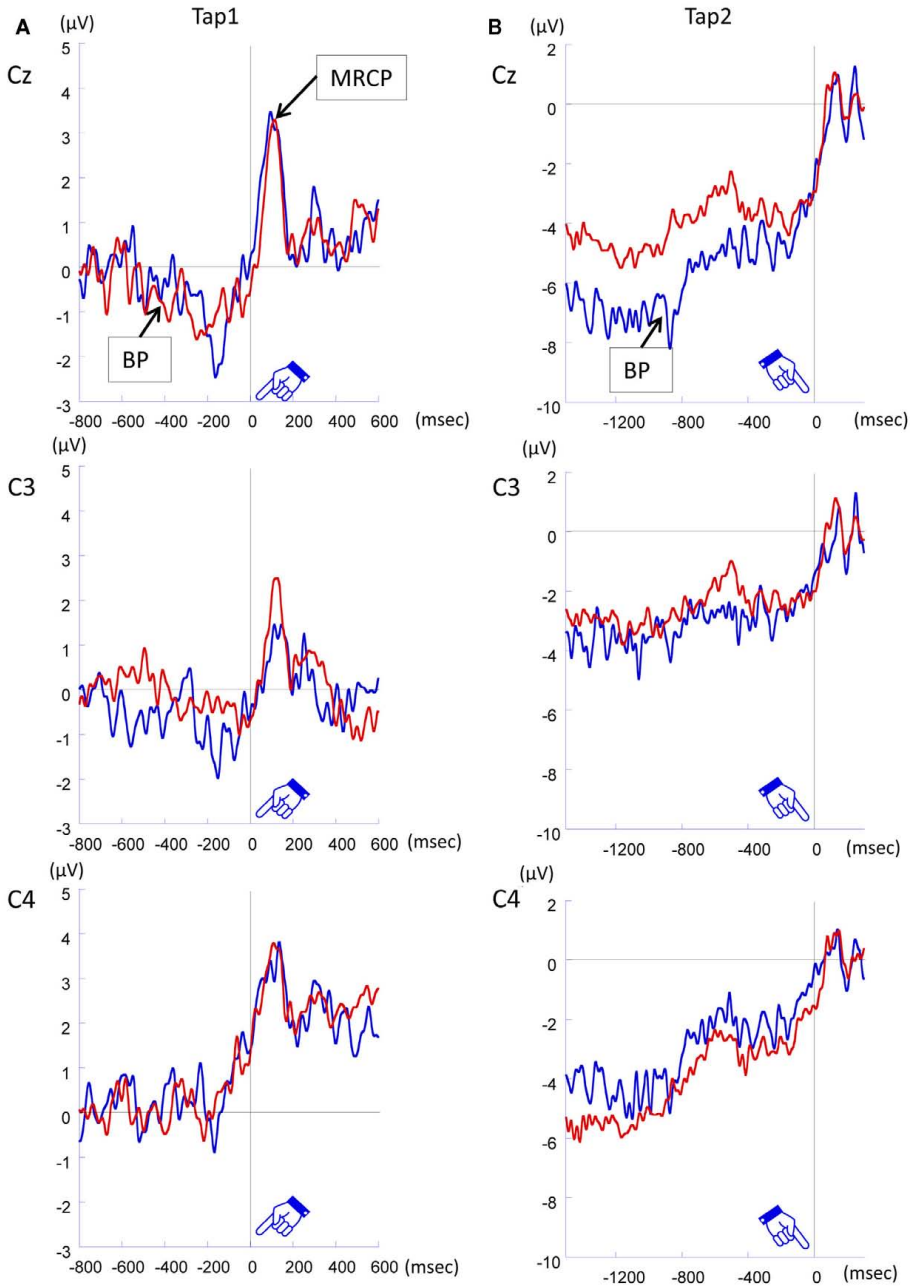

FIGURE 7 | Grand averaged ERP waveforms time-locked to Tap1 (800 ms condition with-sounds) (A), and (B) time-locked to Tap2 (800 ms condition with-sounds).

100 ms. When participants were instructed to attend to the sounds, they actively expected the timing of the occurrence of the sounds, which increased the CNV amplitude toward the first and the third sounds (in tw2 and tw6).

There was no effect of laterality on the CNV. The same tendency was observed in previous studies (Ruchkin et al., 1997; Pfeuty et al., 2003b, 2008). These studies showed that when participants had to retain a series of auditory stimuli in working memory, a bilateral frontal slow negativity developed during the task. They proposed that this bilateral frontal slow negativity reflects the automatic storage of the auditory information. In line with their proposal, the increase in the CNV amplitude may reflect the automatic storage of the successive sounds in working memory, which might be one possibility for the lack of laterality effect in the current study.

One may argue that there was a possible influence of auditory-evoked potentials (AEP) on the frontal CNV activity. Because AEP is a Cz-maximum response, it is natural that the activity was spread to the frontal site. The auditory signal might simply make the CNV apparently larger in the with-sounds condition than in the without-sounds condition. As Pfeuty et al. (2008) discussed,

the EEG activity observed in the filled (with-sounds) condition corresponds to the superimposition of timing-dependent activity and the sensory activity. Therefore, the auditory signal itself could contribute to the augmentation of the CNV. However, the CNV activity was also observed obviously in the empty (without-sounds) condition (see **Figures 3** and **4**). Even though there was an influence of the sounds on the development of the CNV, it is evident that the CNV develops depending on the memorization of the intervals. With regard to the mechanism of the occurrence of the filled-duration illusion, it is hypothesized that continuous or intermittent auditory input during an interval accelerates an internal pacemaker that emits pulses that are transmitted to an accumulator that measures interval duration in terms of pulse counts (Gibbon et al., 1984; Penney et al., 2000). We speculate that in the with-sounds condition, the brain processed the intermittent sound information in addition to the flash information, which resulted in the development of the greater CNV and in the longer reproduced intervals with-sounds than without-sounds.

P300 component

In the current study, we observed a slow positivity over parieto-central scalp sites that reached its maximum amplitude at approximately between 160 and 220 ms after the second flash (**Figure 6**; **Table 2**). We called this positivity P300. The maximum amplitude of the P300 was larger in the 800-ms condition than in the 600-ms condition. The P300 latency was shorter in the 800-ms than in the 600-ms condition. The sounds also affected the P300. The P300 was larger in the without-sounds condition than in the with-sounds condition. There was a marginal effect of attention. The P300 latency tended to be shorter in the attended than in the ignore condition. Overall, it was shown that the P300 was more prominent under the conditions in which the CE was more negative; the CE was more negative in the 800-ms than in the 600-ms condition, and tended to be more negative in the without-sounds than in the with-sounds condition. According to the literature, the P300 is evoked by infrequent, unpredictable stimulus shifts, regardless of whether the participants focused on the stimulus itself (Squires et al., 1975). Perhaps in those conditions, the participants anticipated durations longer than the physical durations, which caused the perception of the occurrence of the second flash at unexpectedly shorter timing, and resulted in prominent P300. It would be associated with the monitoring and accumulation of the temporal information, because during the encoding phase, the participants had to monitor the presentation of the second flash in order to memorize and reproduce the stimulus duration.

Since there were only two stimulus durations, the participants could recognize whether the stimulus duration was the longer or the shorter at the time point where the second flash would appear in the 600-ms condition. If the second flash appeared at 600 ms, the participants could notice that the stimulus was the shorter. If the second flash did not appear at that time point, they could notice that the stimulus presented in that trial would be the longer duration. In other words, the participants had to monitor the passage of time with full attention under uncertainty up to 600 ms after the first flash, while they could monitor the passage of time with less attention beyond 600 ms after the first flash. The accumulation beyond 600 ms after the first flash might have become careless and less accurate. Then, the encoded (memorized) time intervals might have been shortened, which may have caused the underestimation of the interval in the 800-ms condition.

ERP during the reproduction phase

When ERP was time-locked to Tap1, the BP was observed approximately 500 ms before the Tap1 in the central site. A previous report showed prominent BP activation in the central site when the ERP amplitudes were analyzed time-locked to the first trigger press (Macar et al., 1999). The similar tendency was observed in the current study. The BP before Tap1 appeared maximally at Cz electrodes. The location of its activation was in accord with the previous study reporting that the BP was often found maximal at the central, and also over the parietal areas (Deecke and Kornhuber, 1978). The left-dominant BPs suggest that the BPs triggered by Tap1 were related to motor preparation. The BP preceding the key pressing before Tap2 was also sensitive to the voluntary movement. In both 600 and 800 ms conditions, the BP was maximal at the mid-central site. Overall, the BP before Tap1 and Tap 2 did not have clear relationship with the memorized intervals; it is safe to conclude that the BPs in our study reflect motor preparation, rather than temporal processing in the SMA at present.

NEURAL CORRELATES FOR THE FILLED-DURATION ILLUSION

The present study revealed that several brain regions are conjointly associated with the occurrence of the "filled-duration illusion". We showed the EEG activity both in the encoding and in the reproduction period, which enabled us to investigate the whole process required in temporal processing. The P300 and the CNV appeared during the encoding period, while the BP appeared during the reproduction period. During the encoding phase, the CNV developed depending on the perceived duration. This is in accordance with previous ERP studies adopting temporal judgment tasks, where the CNV amplitudes were larger when time was subjectively estimated as longer (Pfeuty et al., 2003b; Gontier et al., 2007, 2009; Le Dantec et al., 2007). In addition, the CNV was modulated by attention. The effect of attention appeared especially when the participants expected the upcoming sounds. These results corresponded to the behavioral performance. The CNV may reflect the accumulation of the perceived duration. The frontal cortex, especially the dorsolateral prefrontal cortex, is considered to be a probable generator of the CNV (Rao et al., 2001; Pouthas, 2003; Macar and Vidal, 2004). The P300, a neural signature of directing attention, appeared at the parieto-central site. The amplitude of the P300 was enhanced and its latency was shortened depending on the occurrence of the second flash at an unexpected timing in the 800-ms condition. These results might be associated with the underestimation of the reproduced intervals. The source of the P300 is assumed to be the parietal cortex (Friedman et al., 2001; Horn et al., 2003). The occurrence and modulation of the P300 is in accord with the evidence that the parietal cortex was related to directing attention and accumulation of temporal information (Alexander et al., 2005; Bueti et al., 2008). In addition, the BP, which is reported to be derived from the SMA, was observed in relation to the participants' finger tapping. The location of the

BP activation suggested that the SMA activates in accord with the voluntary movement associated with experimental task.

We assumed that the CNV and the P300, together with BP, could be functionally connected with each other to process temporal information. However, it is also possible that there is an aspect of topographical overlap of the two components: the more negative the CNV, the further away the ERP is from zero, thus the less positive the P300. Both components have strong projections to the centro-parietal scalp, which may make the superficial covariation between the P300 and the CNV. We should take these facts into account for the interpretation of our results of these ERP components.

According to the information-processing version of the scalar expectancy theory of time perception, temporal judgments are based on the contribution of three distinct psychological processes: an internal clock accumulating units of time, a memory process, and a decision comparator (Gibbon et al., 1997, see Grondin, 2001, 2005). Our results could be explained in line with this theory. The encoding period contained attention and memory processes. The current results formed a simple representation of the "filled-duration illusion" in terms of these processing stages of time perception, as reflected in the reported EEG signatures.

CONCLUSION

We used EEG measures to determine how timing occurs in the context where additional signals are delivered. The CNV, which appeared as a signature of perceiving time, occurred during the encoding phase. The CNV is suggested to be generated from the prefrontal brain site. The presence of additional sensory signals interfered with the timing period. It corresponds to the superimposition of the timing-dependent activity (CNV) and the sensory activity (AEP). The P300, which was obtained from the parieto-central electrodes, correlated with the orienting of attention to the stimuli. Moreover, we observed the BP during the reproduction phase, the BP being actually related to the voluntary movement and motor preparation. The CNV and P300 reflect the cerebral bases for the filled-duration illusion electrophysiologically, which would represent the role of the accumulation and memory on temporal processing of sub-second intervals.

AUTHOR NOTE

This research was made possible by a research grant awarded to Simon Grondin by the Natural Sciences and Engineering Council of Canada (NSERC), and a Summer Scholarship from NSERC to Caroline Gagnon. The publication of this article also received support from Time In MEntaL activitY (TIMELY). We would like to express our gratitude to Nicolas Bisson, Félix Desautels, Mylène Ross-Plourde, Flore Morneau-Sévigny, Larissa Roy, Emi Hasuo, and to Pierre-Emmanuel Michon from the Consortium d'imagerie en neurosciences et santé mentale de Québec (CINQ), who provided precious help at various stages of the project. This study was presented at the 17th Annual Meeting of the Organization for Human Brain Mapping held in June in Québec City. Correspondence should be addressed to Simon Grondin, École de psychologie, 2325 rue des Bibliothèques, Université Laval, Québec, QC, Canada G1V 0A6. E-mail: simon.grondin@psy.ulaval.ca

REFERENCES

Adams, R. D. (1977). Intervening stimulus effects on category judgments of duration. *Percept. Psychophys.* 21, 527–534.

Alexander, I., Cowey, A., and Walsh, V. (2005). The right parietal cortex and time perception: back to Critchley and the Zeitraffer phenomenon. *Cogn. Neuropsychol.* 22, 306–315.

Brown, S. W. (2008). "Time and attention: review of the literature," in *Psychology of Time*, ed. S. Grondin (Bingley: Emerald Publisher), 111–138.

Bueti, D., Bahrami, B., and Walsh, V. (2008). Sensory and associative cortex in time perception. *J. Cogn. Neurosci.* 20, 1054–1062.

Buffardi, L. (1971). Factors affecting the filled-duration illusion in the auditory, tactual, and visual modalities. *Percept. Psychophys.* 10, 292–294.

Deecke, L., and Kornhuber, H. H. (1978). An electrical sign of participation of the mesial 'supplementary' motor cortex in human voluntary finger movement. *Brain Res.* 159, 473–476.

Friedman, D., Cycowicz, Y. M., and Gaeta, H. (2001). The novelty P3: an event-related brain potential (ERP) sign of the brain's evaluation of novelty. *Neurosci. Biobehav. Rev.* 25, 355–373.

Gamache, P.-L., Bisson, N., Hawke, L., Roussel, M.-È., and Grondin, S. (2008). "Exploration of the filled-time illusion with an interval production task," in *Fechner Day 2008: Proceedings of the 24th Annual Meeting of the International Society for Psychophysics*, eds B. Schneider, B. M. Ben-David, S. Parker, and W. Wong (Toronto: The ISP), 77–82.

Gibbon, J., Church, R. M., and Meck, W. (1984). Scalar timing in memory. *Ann. N. Y. Acad. Sci.* 423, 52–77.

Gibbon, J., Malapani, C., Dale, C. L., and Gallistel, C. (1997). Toward a neurobiology of temporal cognition: advances and challenges. *Curr. Opin. Neurobiol.* 7, 170–184.

Gontier, E., Le Dantec, C., Leleu, A., Paul, I., Charvin, H., Bernard, C., Lalonde, R., and Rebaï, M. (2007). Frontal and parietal ERPs associated with duration discriminations with or without task interference. *Brain Res.* 1170, 79–89.

Gontier, E., Le Dantec, C., Paul, I., Bernard, C., Lalonde, R., and Rebaï, M. (2008). A prefrontal ERP involved in decision making during visual duration and size discrimination tasks. *Int. J. Neurosci.* 118, 149–162.

Gontier, E., Paul, I., Le Dantec, C., Pouthas, V., Jean-Marie, G., Bernard, C., Lalonde, R., and Rebaï, M. (2009). ERPs in anterior and posterior regions associated with duration and size discriminations. *Neuropsychology* 23, 668–678.

Grondin, S. (1992). Production of time intervals from segmented and nonsegmented inputs. *Percept. Psychophys.* 52, 345–350.

Grondin, S. (1993). Duration discrimination of empty and filled intervals marked by auditory and visual signals. *Percept. Psychophys.* 54, 383–394.

Grondin, S. (2001). From physical time to the first and second moments of psychological time. *Psychol. Bull.* 127, 22–44.

Grondin, S. (2003). "Sensory modalities and temporal processing," in *Time and Mind II*, ed. H. Helfrich (Gottingen: Hogrefe and Huber), 75–92.

Grondin, S. (2005). Overloading temporal memory. *J. Exp. Psychol. Hum. Percept. Perform.* 31, 869–879.

Grondin, S. (2010). Unequal Weber fractions for the categorization of brief temporal intervals. *Atten. Percept. Psychophys.* 72, 1422–1430.

Grondin, S., Guay, I., Lapointe, M., and Poulin, J. (1998a). "The effect of segmented inputs on the production of short-time intervals," in *Fechner Day 98: Proceedings of the 14th Annual Meeting of the International Society for Psychophysics*, eds S. Grondin and Y. Lacouture (Québec: The ISP), 231–236.

Grondin, S., Meilleur-Wells, G., Ouellette, C., and Macar, F. (1998b). Sensory effects on judgments of short-time intervals. *Psychol. Res.* 61, 261–268.

Grondin, S., Meilleur-Wells, G., and Lachance, R. (1999). When to start explicit counting in a time-intervals discrimination task: a critical point in the timing process of humans. *J. Exp. Psychol. Hum. Percept. Perform.* 25, 993–1004.

Grondin, S., Ouellet, B., and Roussel, M.-E. (2004). Benefits and limits of explicit counting for discriminating temporal intervals. *Can. J. Exp. Psychol.* 58, 1–12.

Hall, G. S., and Jastrow, J. (1886). Studies of rhythm. *Mind* 11, 55–62.

Horn, H., Syed, N., Lanfermann, H., Maurer, K., and Dierks, T. (2003). Cerebral networks linked to the event-related potential P300. *Eur. Arch. Psychiatry Clin. Neurosci.* 253, 154–159.

Le Dantec, C., Gontier, E., Paul, I., Charvin, H., Bernard, C., Lalonde, R., and Rebaï, M. (2007). ERPs associated with visual duration discriminations in prefrontal and parietal cortex. *Acta Psychol. (Amst.)* 125, 85–98.

Lejeune, H., and Wearden, J. H. (2009). Vierordt's the experimental study of the time sense (1868) and its legacy. *Eur. J. Cogn. Psychol.* 21, 941–960.

Linden, D. E. (2005). The p300: where in the brain is it produced and what does it tell us? *Neuroscientist* 11, 563–576.

Macar, F., and Vidal, F. (2003). The CNV peak: an index of decision making and temporal memory. *Psychophysiology* 40, 950–954.

Macar, F., and Vidal, F. (2004). Event-related potentials as indices of time processing: a review. *J. Psychophysiol.* 18, 89–104.

Macar, F., Vidal, F., and Casini, L. (1999). The supplementary motor area in motor and sensory timing: evidence from slow brain potential changes. *Exp. Brain Res.* 125, 271–280.

Mitsudo, T., Nakajima, Y., Remijn, G. B., Takeichi, H., Goto, Y., and Tobimatsu, S. (2009). Electrophysiological evidence of auditory temporal perception related to the assimilation between neighboring two time intervals. *NeuroQuantology* 7, 114–127.

Montfort, V., and Pouthas, V. (2003). Effects of working memory demands on frontal slow waves in time-interval reproduction tasks in humans. *Neurosci. Lett.* 343, 195–199.

Penney, T. B., Gibbon, J., and Meck, W. H. (2000). Differential effects of auditory and visual signals on clock speed and temporal memory. *J. Exp. Psychol. Hum. Percept. Perform.* 26, 1770–1787.

Pfeuty, M., Ragot, R., and Pouthas, V. (2003a). Processes involved in tempo perception: a CNV analysis. *Psychophysiology* 40, 69–76.

Pfeuty, M., Ragot, R., and Pouthas, V. (2003b). When time is up: CNV time course differentiates the roles of the hemispheres in the discrimination of short tone durations. *Exp. Brain Res.* 151, 372–379.

Pfeuty, M., Ragot, R., and Pouthas, V. (2008). Brain activity during interval timing depends on sensory structure. *Brain Res.* 1024, 112–117.

Picton, T. W. (1992). The P300 wave of the human event-related potential. *J. Clin. Neurophysiol.* 9, 456–479.

Pouthas, V. (2003). "Electrophysiological evidence for specific processing of temporal information in humans," in *Functional and Neural Mechanisms of Interval Timing,* ed. W.H. Meck (Boca Raton, FL: CRC Press), 439–456.

Pouthas, V., Garnero, L, Ferrandez, A. M., and Renault, B. (2000). ERPs and PET analysis of time perception: spatial and temporal brain mapping during visual discrimination tasks. *Hum. Brain Mapp.* 10, 49–60.

Rao, S. M., Mayer, A. R., and Harrington, D. L. (2001). The evolution of brain activation during temporal processing. *Nat. Neurosci.* 4, 317–323.

Rubia, K., and Smith, A. (2004). The neural correlates of cognitive time management: a review. *Acta Neurobiol. Exp. (Wars)* 64, 329–340.

Ruchkin, D. S., Berndt, R. S., Johnson, R. Jr., Ritter, W., Grafman, J., and Canoune, H. L. (1997). Modality-specific processing streams in verbal working memory: evidence from spatio-temporal patterns of brain activity. *Brain Res. Cogn. Brain Res.* 6, 95–113.

Scheibe, C., Schubert, R., Sommer, W., and Heekeren, H. R. (2009). Electrophysiological evidence for the effect of prior probability on response preparation. *Psychophysiology* 46, 758–770.

Squires, N. K., Squires, C. S., and Hillyard, S. A. (1975). Two varieties of long-latency positive waves evoked by unpredictable auditory stimuli in man. *Electroencephalogr. Clin. Neurophysiol.* 38, 387–401.

ten Hoopen, G., Miyauchi, R., and Nakajima, Y. (2008). "Time-based illusions in the auditory mode," in *Psychology of Time*, ed. S. Grondin (Bingley: Emerald Publisher), 139–187.

Thomas, E. A. C., and Brown, I. (1974). Time perception and the filled duration illusion. *Percept. Psychophys.* 16, 449–458.

Walter, W. G., Cooper, R., Aldridge, V. J., McCallum, W. C., and Winter, A. L. (1964). Contingent negative variation: an electric sign of sensorimotor association and expectancy in the human brain. *Nature* 203, 380–384.

Wearden, J. H., Norton, R., Martin, S., and Montford-Bebb, O. (2007). Internal clock processes and the filled-duration illusion. *J. Exp. Psychol. Hum. Percept. Perform.* 33, 716–729.

Conflict of Interest Statement: The authors declare that the research was conducted in the absence of any commercial or financial relationships that could be construed as a potential conflict of interest.

Received: 27 May 2011; paper pending published: 26 June 2011; accepted: 30 November 2011; published online: 02 January 2012.

*Citation: Mitsudo T, Gagnon C, Takeichi H and Grondin S (2012) An electroencephalographic investigation of the filled-duration illusion. Front. Integr. Neurosci. **5**:84. doi: 10.3389/fnint.2011.00084*

frontiers in
INTEGRATIVE NEUROSCIENCE

ORIGINAL RESEARCH ARTICLE
published: 29 November 2011
doi: 10.3389/fnint.2011.00077

Temporal accumulation and decision processes in the duration bisection task revealed by contingent negative variation

Kwun Kei Ng[1], Simon Tobin[2] and Trevor B. Penney[1]*

[1] *Department of Psychology, National University of Singapore, Singapore*
[2] *École de Psychologie, Université Laval, Québec, QC, Canada*

Edited by:
Warren H. Meck, Duke University, USA

Reviewed by:
Niko Busch, Charité – Universitätsmedizin Berlin, Germany
Laurence Casini, Université de Provence, France

****Correspondence:***
Trevor B. Penney, Department of Psychology, National University of Singapore, 9 Arts Link, Singapore 117570.
e-mail: penney@nus.edu.sg

The duration bisection paradigm is a classic task used to examine how humans and other animals perceive time. Typically, participants first learn short and long anchor durations and are subsequently asked to classify probe durations as closer to the short or long anchor duration. However, the specific representations of time and the decision rules applied in this task remain the subject of debate. For example, researchers have questioned whether participants actually use representations of the short and long anchor durations in the decision process rather than merely a response threshold that is derived from those anchor durations. Electroencephalographic (EEG) measures, like the contingent negative variation (CNV), can provide information about the perceptual and cognitive processes that occur between the onset of the timing stimulus and the motor response. The CNV has been implicated as an electrophysiological marker of interval timing processes such as temporal accumulation, representation of the target duration, and the decision that the target duration has been attained. We used the CNV to investigate which durations are involved in the bisection categorization decision. The CNV increased in amplitude up to the value of the short anchor, remained at a constant level until about the geometric mean (GM) of the short and long anchors, and then began to resolve. These results suggest that the short anchor and the GM of the short and long anchors are critical target durations used in the bisection categorization decision process. In addition, larger mean N1P2 amplitude differences were associated with larger amplitude CNVs, which may reflect the participant's precision in initiating timing on each trial across a test session. Overall, the results demonstrate the value of using scalp-recorded EEG to address basic questions about interval timing.

Keywords: time perception, interval timing, duration bisection, EEG, slow potential, contingent negative variation, N1P2, temporal memory

INTRODUCTION

DURATION BISECTION

The duration bisection paradigm is a classic task used to examine how humans and other animals perceive time (e.g., Penney et al., 2008). In a typical duration bisection experiment with humans, participants are asked to classify probe durations as closer to either the short or the long anchor duration (e.g., 2 vs. 8 s) learned in training. The probe durations usually comprise either a geometric or an arithmetic series that includes the short and long anchors as well as intermediate durations. The point of subjective equality (PSE), the difference limen (DL), and the Weber fraction (WF) can be obtained from the participant's response function. The PSE is an index of perceived duration, while the DL and WF index temporal sensitivity (Grondin, 2010). These measures have been useful for the study of the perceptual and cognitive factors that can influence subjective perception of time (e.g., Penney et al., 2000; Vicario, 2011).

Although most information processing models of interval timing posit that timing decisions rely on comparisons of currently elapsing time with memory representations of previously experienced durations, the specific information that contributes to those representations and the decision rules applied remain the subject of debate (e.g., Allan, 2002; Wearden, 2004; Penney et al., 2008). For example, whether the short and long anchors are used during duration classification has been challenged by procedures in which the participant is not explicitly taught the anchor durations (Wearden and Ferrara, 1995) and by evidence that participants rely on a bisection criterion derived from the anchor durations rather than using the anchor durations themselves (Allan and Gerhardt, 2001). Similarly, whether the decision process relies on comparison of two time traces until a response threshold is reached (Wearden, 2004), a sequential application of decision rules (Penney et al., 2008), or some other mechanism is unclear. Our understanding of the memory representations and decision rules suffers from the fact that they are latent processes not easily determined by behavioral measures in a typical duration bisection task (e.g., the assumed relationship between the PSE and actual transition from a "short" to "long" decision, Balci et al., 2009).

Consequently, methods that provide information about the perceptual and cognitive processes that occur between the onset

of the timing stimulus and the motor response are desirable. Non-invasive electrophysiological measures such as electroencephalography (EEG) and event related potentials (ERPs) are complementary to behavioral measures because they can be used to reveal how distinct cognitive processes unfold at a higher temporal resolution than behavioral measures alone (Luck, 2005). One candidate EEG/ERP event that appears to be sensitive to sub and supra-second temporal information is the contingent negative variation (CNV).

THE CONTINGENT NEGATIVE VARIATION AND INTERVAL TIMING

Electroencephalography and ERP measures have been used extensively to reveal the brain's motor preparation processes (e.g., Brunia, 2004; van Boxtel and Böcker, 2004). One such measure is the CNV, which was termed the "expectancy wave" when first reported by Walter et al. (1964). Time is an essential dimension of preparation and anticipation (Buhusi and Meck, 2005; Coull and Nobre, 2008), so it is unsurprising that its role in CNV generation has also been examined (e.g., Birbaumer et al., 1990; Correa et al., 2006). Indeed, several research groups (Macar et al., 1999; Macar and Vidal, 2003, 2009; Pfeuty et al., 2003a,b, 2005, 2008; Praamstra et al., 2006) have reported relationships between CNV parameters (e.g., amplitude, peak latency, slope) and aspects of explicit and implicit interval timing (e.g., encoding, storage, and retrieval). The ramping negative potential of the CNV has been claimed to reflect an accumulation process resulting from spreading activation or signal integration of neurons in the medial frontal brain areas (König et al., 1996; Macar et al., 1999, 2006; Macar and Vidal, 2004; Pouthas et al., 2005; Meck et al., 2008; Simen et al., 2011).

For example, early work by Macar et al. (1999) showed a relationship between the amplitude of the CNV and the subjective duration of the interval in temporal reproduction. The authors categorized participant's responses into three groups according to accuracy, which indicated that the CNV amplitude decreased (i.e., became less negative) as the produced intervals decreased (2600 ∼ 2800; 2400 ∼ 2600; and 2200 ∼ 2400 ms) even though the participants were attempting to reproduce the same 2500 ms target duration in all cases.

Resolution of the CNV appears to bear a relationship to the memory representation of the target duration. Macar and Vidal (2003) used both visual and tactile temporal generalization tasks to show that the CNV peaked at the memorized target duration (2000 ms) rather than at the end of the probe duration (2500 or 3100 ms). Pfeuty et al. (2003b) obtained similar results with a S1–S2 duration comparison task. During S2, the CNV reached its negative peak at the S1 target duration (700 ms) at left hemisphere and medial frontal electrode locations, while at right hemisphere frontal electrode sites the CNV peaked at the end of S2. The authors suggested that the distinct CNV profiles at the right and left hemisphere electrodes reflected distinct memory representations for the S1 target duration and the elapsing S2 duration. In a subsequent S1–S2 experiment (Pfeuty et al., 2005), the authors showed that given the same S2 probe duration (794 ms), the peak latency of the CNV corresponded to the S1 target duration (600 vs. 794 ms), although they failed to obtain an effect of target duration on CNV amplitude. They, and others (Durstewitz, 2004), have suggested that the slope of the CNV reflects the rate of temporal accumulation within the information processing framework of the scalar expectancy theory (SET) of timing (Gibbon et al., 1984).

Finally, the relationship between the CNV and timing is not limited to explicit interval timing tasks. Praamstra et al. (2006) replicated the peak latency and slope effects (Macar and Vidal, 2003; Pfeuty et al., 2005) in an implicit motor timing task. In this task, participants pressed one of two keys depending on whether an arrow pointed to the left or the right. Each trial comprised a short sequence of cues, each presented isochronously (2000 ms) with the exception of the final cue. A CNV occurred between successive cues, but when the final cue was presented late (2500 ms), the CNV peaked at the expected inter-stimulus interval (2000 ms) and then began to resolve. In sum, the available evidence suggests a relatively robust relationship between interval timing and CNV peak latency and slope (e.g., Tarantino et al., 2010), while the relationship between CNV amplitude and timing stimulus duration is equivocal (e.g., Kononowicz and van Rijn, 2011).

Given the putative role of the CNV as a marker of interval timing, it should be possible to use it as a tool to examine information processing in the duration bisection task. Specifically, the research reviewed above suggests that the CNV at medial frontal electrode sites should reach its negative peak when elapsed time matches a remembered target duration, and begin to resolve (i.e., return to baseline) when the categorization decision is made, which in turn implies that the duration of the target criterion used for the decision has been reached. In the case of duration bisection, this means that if the critical information is whether the currently elapsing duration has exceeded the memory representation of the comparison memory duration, then the CNV should peak and resolve when the current duration exceeds the comparison duration. Therefore, if a bisection criterion (Allan and Gerhardt, 2001) is the target criterion, the CNV should peak and resolve before the end of probe durations that are longer than that criterion. If, however, the value of the entire probe duration is used in the decision process, then one might expect the CNV to peak and resolve at stimulus offset for the long duration probe trials. In other words, the electrophysiological response should identify the temporal information used during a bisection trial.

MATERIALS AND METHODS

PARTICIPANTS

Seventeen undergraduate students (nine female) at the National University of Singapore participated in return for payment ($9/h). All had normal or corrected to normal vision and 16 were right-handed. Data from five participants were omitted from the data analysis because of excessive eye or body movement artifact (see below).

STIMULI

Stimuli comprised seven 440 Hz tones, with 10 ms rise and fall times, played over stereo headphones at a comfortable level. The stimulus durations were geometrically spaced from 800 to 3200 ms (i.e., 800, 1008, 1270, 1600, 2016, 2540, and 3200 ms).

PROCEDURE

The duration bisection paradigm (Gibbon, 1981) was implemented in E-Prime (Psychology Software Tools, USA). At the

beginning of each block, the two anchor durations (800 and 3200 ms) were presented to the participants five times each. The presentation sequence of the 10 durations was randomized for each participant and feedback was provided on the computer screen after each presentation ("That was the Short/Long duration"). The subsequent test block comprised 196 trials with 28 trials at each of the 7 probe durations. The inter-trial interval (ITI) was a combination of participant's response time (RT) and a random duration between 1000 and 2000 ms. Trial order within a block was pseudo-randomized so that no consecutive probe trials were of the same duration. Each participant completed two test blocks.

Participants were seated in a dim, sound-attenuated room with their fingers resting on a computer keyboard. Participants were told that a series of tones would be presented and that they should press one of the two response keys (G or K) to indicate whether the tone duration was more similar to the "short" or "long" anchor when the tone terminated. Key to response assignment was counterbalanced across participants. The maximum RT allowed was 2000 ms following tone offset. Response ("short" or "long") and RT relative to signal offset were recorded.

EEG RECORDING

Electroencephalographic activity was recorded using a 64-channel Biosemi Active-Two system with sintered Ag/AgCl electrodes mounted in an elastic cap according to the extended 10–20 system. The electrooculogram (EOG) was recorded from electrodes positioned at the outer canthus of each eye and just above and below the left eye. The reference electrode was placed on the nose and the ground electrodes (CMS/DRL) were placed behind the vertex in the vincinity of POz. The EEG and EOG were recorded continuously from DC to 400 Hz at a sampling rate of 2048 Hz and subsequently downsampled offline to 256 Hz.

DATA ANALYSIS

Behavioral data

A behavioral response function was generated for each participant by determining the proportion of trials classified as "more similar to the long anchor" for each probe duration (i.e., n responses out of 56 for each of the 7 probe durations). The pseudologistic function from the Pseudo Logistic Model of Killeen et al. (1997) was fit to the classification data of each participant (Allan, 2002). The fitted function was used to obtain estimates of the PSE and the DL. The DL was calculated by subtracting the duration, derived from the fitted pseudologistic function at which the proportion of "long" responses equaled 0.25, from the duration, also derived from the fitted pseudologistic function, at which the proportion of "long" responses equaled 0.75, and dividing by 2.

EEG data

Electroencephalography data were processed using EEGLAB (Delorme and Makeig, 2004). The data were digitally filtered offline with a band-pass from 0.1 to 32 Hz. EEG epochs time-locked to the onset of the probe tone were computed at all recording sites for a time window from 200 ms before tone onset to 3500 ms thereafter for all probe durations. Independent component analysis (ICA; Stone, 2002) was used to isolate and remove eye blink, eye movement, and motor artifacts from the epoched data. The 200-ms immediately prior to the onset of the stimulus served as the baseline and was subtracted from each epoch after ICA. Data from five participants were excluded from further analyses because these artifacts could not be isolated. While data from FCz has typically been the focus of CNV analyses (e.g., Macar et al., 1999; Pfeuty et al., 2003a,b; Praamstra et al., 2006), here data from FCz and five adjacent electrodes (FC1, FC2, C1, C2, and Cz) were averaged to provide a better signal to noise ratio.

To further confirm the presence of the CNV component, current source density (CSD), was computed using the CSD toolbox (Kayser and Tenke, 2006; Kayser, 2009), based on the spherical spline algorithm derived by Perrin et al. (1989, 1990). CSD estimates the second spatial derivative of the scalp potentials, similar to what is done with the Surface Laplacian (Kayser and Tenke, 2006; Pizzagalli, 2007). For the CSD computed here, previously validated default values were used, i.e., the order of the Legendre polynomial (n) was 50, the flexibility of the spline (m) was set to 4, and the smoothing parameter (lambda) for the spline interpolation was 10^{-5} (Tenke et al., 1998). Each EEG epoch was first CSD transformed, baseline corrected, and then averaged.

To maximize the signal to noise ratio for examination of the ERP components up to the duration of the short anchor (i.e., 800 ms), the trials for the seven probe durations were averaged together to generate a single ERP waveform for each participant. We assumed that the EEG would be comparable for the first 800 ms of all probe duration presentations because 800 ms is the earliest time point at which a participant can learn the identity of the probe duration (i.e., at offset of the 800-ms probe). To determine whether the CNV peaked and began to resolve prior to the end of timing signal, however, the trials for the two longest probe durations (i.e., 2540 and 3200 ms) were averaged together to generate an ERP waveform for each participant.

Contingent negative variation slopes were obtained for several time windows to quantify (1) the ramping of the CNV (from the end of N1P2 to the end of the short anchor duration), (2) the development of the CNV between the "short" anchor duration (800 ms) and the geometric mean (GM; 1600 ms), (3) the development of the CNV between the GM and arithmetic mean (AM; 2000 ms), and (4) the development of the CNV between the AM and the duration of the second longest probe (2500 ms). For each participant, the average potential obtained by collapsing across the six frontal and central electrodes of interest (i.e., FCz, FC1, FC2, C1, C2, and Cz) in each of these four time windows was regressed against sample time (ordinary least squares) to obtain a linear slope of the change of potential amplitude across time (μV/ms). This procedure resulted in 12 slopes for each time window of interest, which were then statistically analyzed.

To identify the beginning of CNV ramping, global field power (GFP; Lehmann and Skrandies, 1980, 1984) was calculated at each time point as the SD of the electrical potential of the 64 scalp electrodes, resulting in a single value at each time sample. High GFP indicates stable scalp potential distribution and optimal signal to noise ratio, while low GFP indicates a change in distribution (Michel et al., 2009). As early ERP components are often associated with narrow time windows of high GFP and sharp transitions between components (Murray et al., 2008), using the distinct

transition of GFP from the transient P2 to the more diffuse CNV to define the slope onset should be better than an arbitrary zero-crossing point. The GFP indicated that a transition in the grand average of the data occurred at 246 ms, similar to that obtained in a previous study (240 ms, Pfeuty et al., 2005).

We also examined the relationship between the CNV and duration bisection performance. Epochs from a subset of the intermediate probe duration trials (1270, 1600, and 2016 ms) were allocated to either the "short" or "long" category based on the participant's response. This set of epochs allowed us to examine possible CNV differences between short and long judgments up to 1200 ms with better signal to noise ratio. The partial least squares (PLS) method (McIntosh and Lobaugh, 2004) was used (*cf.* Tarantino et al., 2010). PLS fits neuroimaging data using least squares and the solutions are "constrained to the part of the covariance structure that is attributable to experimental manipulations or that relates to behavior" (McIntosh and Lobaugh, 2004, S251). The salience and reliability of the ERP differences between conditions are verified using both bootstrapping and randomization tests, with statistical significance set at alpha = 0.05. For probe durations longer than 1200 ms, CNV resolution would be confounded by the different offset times of the three intermediate probes. Instead, we analyzed measures of event related synchronization and desynchronization (ERS/ERD, Pfurtscheller and Lopes da Silva, 1999), which preserve potentials not time-locked to the stimulus onset, and allow frequency-specific analysis of the EEG. We converted the "short" and "long" classification epochs into ERD/ERS time series (see Pfurtscheller and Lopes da Silva, 1999) using the 200-ms baseline as the reference power. We focused on the alpha band (~7–13 Hz) because a previous report implicated this band in temporal anticipation (Babiloni et al., 2004). ERS is indicated by a negative percentage, whereas ERD is indicated by a positive value.

Finally, we were also interested in the relationship between timing and early ERP components such as the N1P2 complex due to its reported association with subjective time perception (e.g., Bendixen et al., 2005; Xuan et al., 2009). The sensitivity of the N1P2 to attention and perceptual features of the probe onset marker (Näätänen and Picton, 1987) and its latency fit well with a role as a possible biomarker of timing initiation on each trial. To this end, the correlation between the magnitude of the N1P2 complex and the CNV amplitude was examined. The peak-to-peak amplitude of the N1P2 of each participant was taken as the difference between the maximum and minimum peak of the ERP of all seven probe durations in the time window from 50 to 280 ms following tone onset at the nine fronto-central electrodes (FC1, FC2, FCz, C1, C2, Cz, CP1, CP2, CPz) where the scalp projection of the N1P2 complex is the largest (Crowley and Colrain, 2004).

RESULTS

The bisection response function averaged across the 12 participants has the classic form of a smoothly increasing ogive (**Figure 1**). The group mean PSE was 1690 ms (SD = 280 ms), and the group mean DL was 260 ms (SD = 149 ms). **Figure 2** shows the grand average ERPs separately for each probe duration.

For each participant, the ERP elicited by the timing stimulus, independent of probe duration, was computed by averaging the trials from all the probe durations. The across participant grand

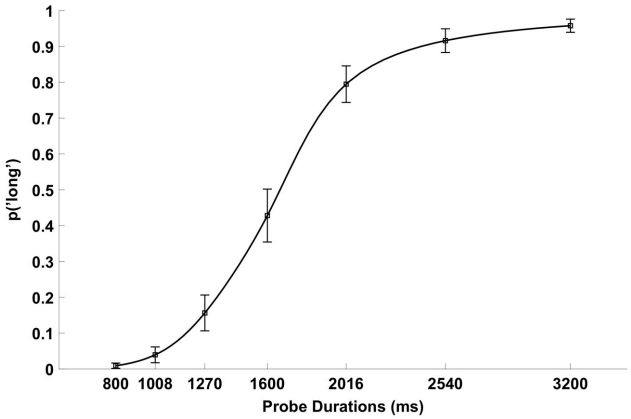

FIGURE 1 | Mean proportion of "long" responses as a function of probe duration averaged across the 12 participants. The error bars indicate 1 SEM. The smooth line illustrates the pseudologistic function (Killeen et al., 1997) fitted to these mean proportions.

average over the six frontal and central electrodes of interest is shown in **Figure 3**. Distinct N1 and P2 components are present, as is a steady increase in negative potential from about 250 ms to shortly before 1000 ms, after which the potential becomes less negative (i.e., CNV resolution). The CNV amplitude between 246 and 800 ms was examined by averaging the potential across the time window for each participant. The mean amplitude was −2.75 μV and a parametric, two-tailed, one-sample *t*-test against zero potential indicated the negativity was significantly greater than zero, 95% CI = [−4.04 to −1.46] μV, $t(11) = -4.70$, $p = 0.0006$, confirming the presence of a negative ERP component in the sample. The spatial topographic map of the CSD in the time window from 246 to 800 ms shows a bilateral distribution with a focus over frontal – central electrode sites (**Figure 4**).

As described in the Methods, examination of the GFP revealed that the transition from P2 to CNV occurred at approximately 246 ms, so a CNV slope was obtained for each participant in the time window from 246 to 800 ms. These 12 CNV slopes were tested against zero slope using a parametric, two-tailed, one-sample *t*-test. The mean slope was −0.0042 μV/ms, the 95% CI was [−0.0057 to −0.0014] μV/ms, $t(11) = -3.59$, $p = 0.0042$, indicating the negative slope was significantly different from zero over that time period. Furthermore, correlation analysis revealed that shallower CNV slopes were associated with longer PSEs, Pearson's $r = 0.67$, $p = 0.02$. However, mean CNV amplitude between 246 and 800 ms was not correlated with mean PSE, Pearson's $r = 0.42$, $p = 0.19$.

Note, however, that analysis of ERPs derived from all probe durations does not permit conclusions about when CNV resolution begins because stimulus offsets occur throughout the time period of interest. To determine when/whether CNV resolution began relative to the short anchor, as well as the GM and AM of the anchor durations, the ERP elicited by the timing stimulus was computed for each participant using trials at the two longest probe durations only (i.e., 2540 and 3200 ms). Slopes were obtained as described in Methods using time windows that framed the short

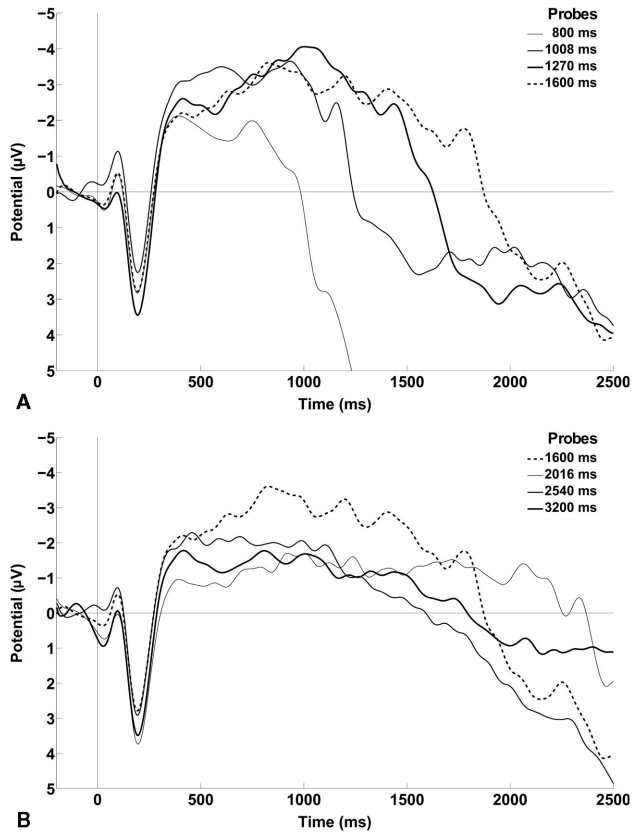

FIGURE 2 | Grand average of the ERP waveforms obtained by collapsing across the six frontal and central electrodes of interest (i.e., FCz, FC1, FC2, C1, C2, and Cz) time-locked to stimulus onset. (A) ERPs of the first four probe durations in the series: 800, 1008, 1270, and 1600 ms. **(B)** ERPs of the last four probe durations in the series: 1600, 2016, 2540, and 3200 ms. The ERP of 1600 ms is plotted in both panels for comparison. The data were smoothed with an eight-point Gaussian window for presentation only.

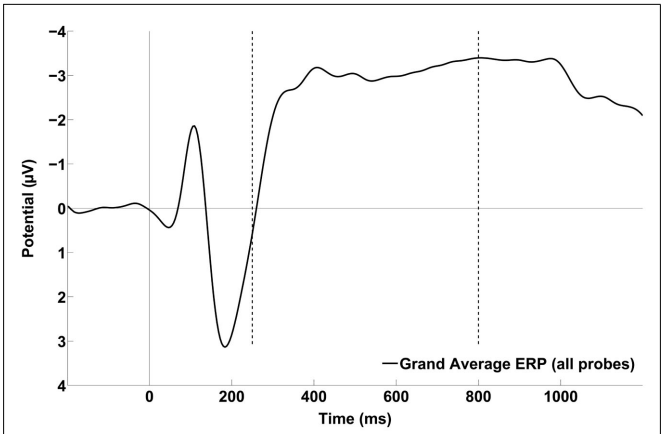

FIGURE 3 | Grand average of the ERP waveforms obtained by collapsing across the six frontal and central electrodes of interest (i.e., FCz, FC1, FC2, C1, C2, and Cz) time-locked to stimulus onset and including trials from all probe durations. Vertical dotted lines indicate the time window boundaries used to define the CNV slope. The data were smoothed with an eight-point Gaussian window for presentation only.

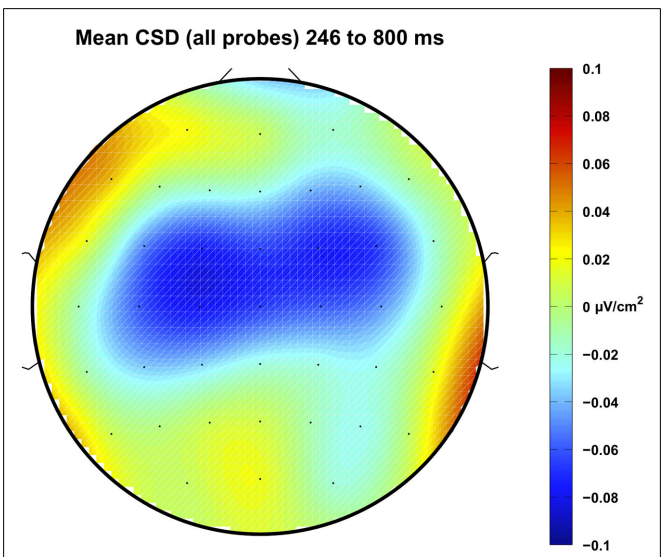

FIGURE 4 | The topographical distribution, viewed from above the head, of the mean current source density (CSD) between 246 and 800 ms computed using trials from all probe durations. Prominent bilateral negative sources can be seen in the fronto-central region, consistent with the polarity and topography of the CNV.

anchor to GM (800–1600 ms), the GM to the AM (1600–2000 ms), and the AM to shortly before offset of the second longest probe duration (2000–2500 ms).

The mean slope was 0.0007 μV/ms in the 800- to 1600-ms time window and −0.0009 μV/ms in the 2000- to 2500-ms time window, neither of which was significantly different from zero [$t(11) = 0.95$, $p = 0.36$ and $t(11) = -0.83$, $p = 0.42$, respectively]. However, the mean slope of 0.0030 μV/ms in the 1600- to 2000-ms was significantly different from zero, 95% CI = [0.0001 to 0.0059] μV/ms, [$t(11) = 2.27$, $p = 0.0045$], indicating a decline in negative potential (**Figure 5**).

The salience (i.e., the contrast between task conditions; McIntosh and Lobaugh, 2004) of the ERP differences between "long" and "short" response categories is shown in **Figure 6**. At the centro-frontal and centro-parietal sites, where the CNV was the most prominent, the salience of the difference was not statistically significant (PLS analyses) for most of the analysis time window, the only exception being the time window between 850 and 1100 ms. Moreover, the amplitude of the ERP corresponding to "long" responses was in fact less negative (indicated by positive salience in the plot) than that corresponding to "short" responses in this time window. Thus, we did not replicate the finding that larger CNV amplitude corresponds to larger perceived duration. Rather, when there was a difference, the effect was in the opposite direction.

Figure 7 shows the "short" and "long" response ERS time series averaged across the six frontal and central electrodes selected for the CNV ERP analyses. The ERS of the "long" responses between

246 and 800 ms in this fronto-central region was significantly stronger than that of the "short" responses (−16.9%) as confirmed by a parametric, two-tailed, paired sample t-test, $t(11) = 2.25$, $p = 0.046$, 95% CI = [−0.34 to −33.5%].

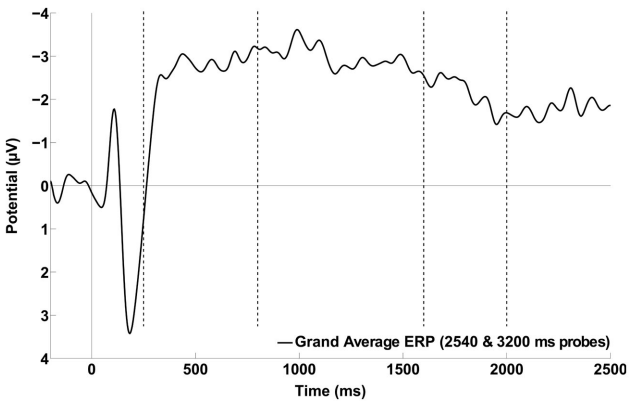

FIGURE 5 | Grand average of the ERP waveforms obtained by collapsing across the six frontal and central electrodes of interest (i.e., FCz, FC1, FC2, C1, C2, and Cz) time-locked to stimulus onset and including only the two longest probe durations. Time window boundaries used to define the various CNV slopes are indicated with vertical dotted lines. The data were smoothed with an eight-point Gaussian window for presentation only.

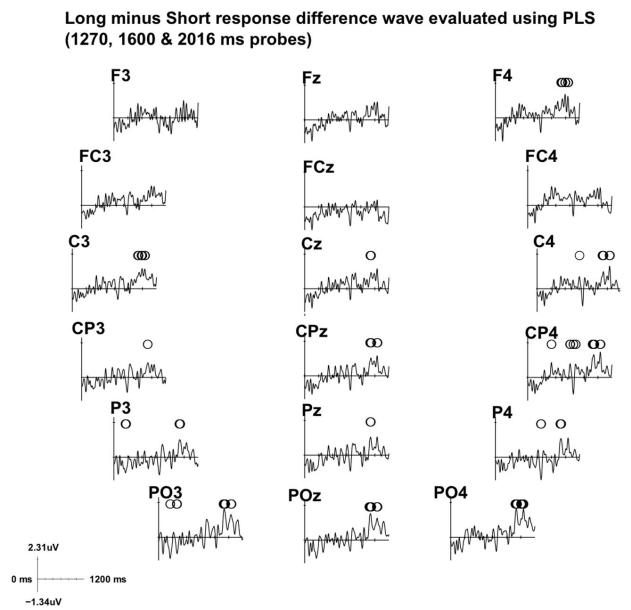

FIGURE 6 | Electrode salience of the ERP difference between "long" and "short" responses from a subset of data (intermediate probes 1270, 1600, and 2016 ms) is illustrated for the fronto-central and parieto-central electrodes. Statistical significance and stability of the differences between the two conditions at each time point was obtained by partial least square (PLS) analyses. Circles indicate statistical significance ($p < 0.05$). A positive salience difference indicates less negative amplitude in the ERP of the "long" responses. The time axis is segmented by 200 ms tick marks, and positive amplitude is plotted upward.

The mean CNV amplitude averaged across the six selected electrodes and the mean N1P2 peak-to-peak amplitude difference averaged across the nine selected electrodes were computed for the 246- to 800-ms time window for each participant by averaging trials across all probe durations. A Pearson's correlation revealed that the larger the mean N1P2 peak-to-peak amplitude difference of a participant, the larger the mean CNV amplitude of that participant, $r = -0.77$, $p = 0.003$ (**Figure 8**).

DISCUSSION

The group mean PSE was close to the GM of the long and short anchor durations, a result that is often obtained with the duration bisection procedure, particularly when the probe durations

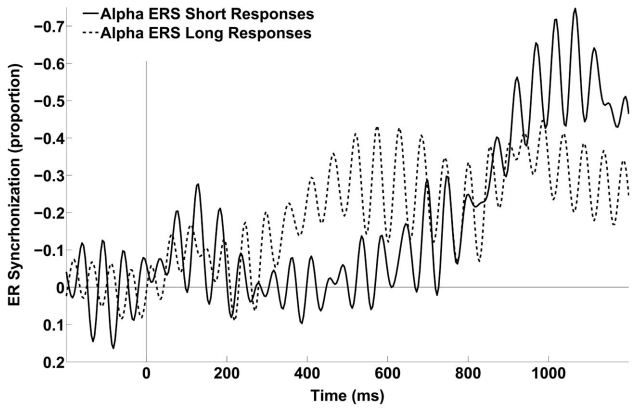

FIGURE 7 | Alpha (∼7–13 Hz) ERS time series averaged across the six frontal and central electrodes of interest (i.e., FCz, FC1, FC2, C1, C2, and Cz) for the two response categories, computed using epochs from the three intermediate probe durations. There was no statistically significant power difference in the baseline (−200 to 0 ms) or late (800–1200 ms) time windows, $t(11) = 0.1$ and −1.24 respectively.

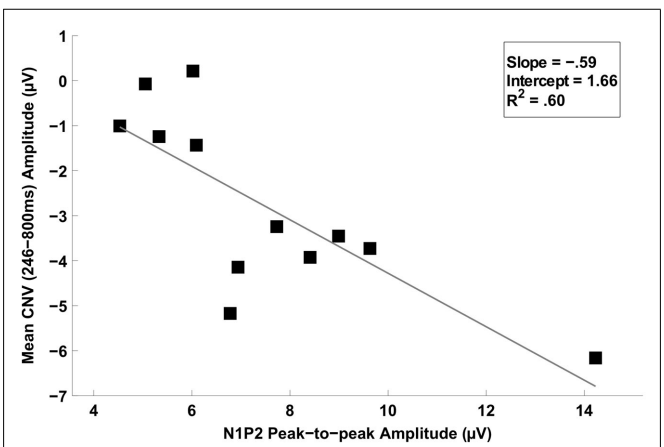

FIGURE 8 | Scatter plot depicting the linear relationship between the mean CNV potential (246–800 ms) and the N1P2 amplitude difference (peak-to-peak). Simple regression indicated that larger N1P2 amplitude differences were associated with larger amplitude CNVs. The Pearson correlation coefficient (r) was 0.77, and the percentage of variance explained by the regression (R^2) was 60%.

are spaced logarithmically (e.g., Penney et al., 2000). The mean DL was also comparable to those obtained in earlier studies using similar anchor durations and indicates that the participants performed the task with an acceptable level of temporal precision.

The critical question here, however, is whether or not scalp-recorded electrophysiological measures reveal information about the nature of the time keeping and decision processes in the duration bisection task. The timing stimuli used in the task elicited clear ERP components in the form of the N1, P2, and a sustained negativity. The slow negative ERP component, which had a diffuse central scalp distribution, dominated the time window between approximately 250 and 800 ms after tone onset. We interpret this component as a CNV due to the consistency of its topography with the CNV reported in previous studies. Specifically, the statistical analyses using six fronto-central electrodes as well as the topographical distribution of the CSD transformed EEG data showed that it was maximal at fronto-central electrode sites, which is the distribution reported in ERP (e.g., Pfeuty et al., 2003a,b), CSD (e.g., Gibbons and Rammsayer, 2004), and EEG/MEG source localization (N'Diaye et al., 2004) studies investigating temporal estimation. Moreover, although the increase in the CNV to its peak value was relatively rapid compared to studies that used longer target durations and response locked ERP derivations (e.g., 2500 ms; Macar et al., 1999), the waveform was similar to that obtained in studies that used stimulus locked ERP derivations and target durations comparable to the short anchor duration used here (e.g., 794 ms; Pfeuty et al., 2005).

As described in the "Introduction," the amplitude and the slope of the CNV have been interpreted as markers of temporal accumulation with longer subjective durations accompanied by larger amplitude CNVs (Macar et al., 1999; Macar and Vidal, 2004) and steep CNV slopes indicating faster temporal integration (Pfeuty et al., 2005). Moreover, the peak latency and resolution of the CNV have been interpreted as indicators of the memorized target duration (Macar and Vidal, 2003; Pfeuty et al., 2003b). We used these features of the CNV to examine the duration information participants use to solve the duration bisection task, and whether, on longer duration trials, participants categorize the timing stimulus before it offsets.

The data suggest that the short anchor duration is an important criterion that is used on a trial-to-trial basis in the standard duration bisection task. Specifically, the CNV slope was statistically different from zero between 246 and 800 ms (i.e., the short anchor duration). However, the CNV amplitude did not continue to increase even though the timing signal continued until either 2540 or 3200 ms in the trials that contributed to this analysis. Rather, the slope analysis indicated that approximately the same potential was maintained until about 1600 ms, at which point the potential declined until about 2000 ms. Pfeuty et al. (2003b, 2005) reported that the CNV peak occurred at the time of the target duration even when the timing signal was longer than the target duration. Therefore, we interpret the finding that CNV amplitude increased to a plateau at about 800 ms as indicating that the participants treated the short anchor duration as a target duration. In fact, up to this point in a duration bisection trial, stimulus presentation is quite similar to the S2 presentation in a typical S1–S2 trial: one pays attention from S2 onset, until either S2 is terminated or the remembered S1 duration has been reached, whichever is shorter.

Given Macar et al. (1999) have shown that the longer the timed signal the larger the accompanying CNV amplitude, it is curious that the CNV did not continue to increase beyond about 800 ms even though the timing stimulus remained on until either 2540 or 3200 ms for the trials that entered this analysis. Moreover, unlike the experiments of Pfeuty et al. (2003b, 2005) in which a decision about the probe duration could be made when the single target duration had been reached, in the duration bisection task used here the participant did not have enough information to make a long or short decision about a continuing stimulus based only on the knowledge that the short anchor target duration had elapsed.

However, there are other studies in which the CNV amplitude was not modulated by the duration being timed (Elbert et al., 1991; Gibbons and Rammsayer, 2004). Hence, it is possible that the CNV amplitude does not reflect accumulated duration in a linear fashion or that, if it does, the effect is detectable using scalp-recorded ERPs only for certain types of interval timing task. The putative presence of multiple target durations in the duration bisection task, such as the short and long anchors and/or a measure of central tendency, may make it difficult to detect robust EEG biomarkers for each of those critical durations. Nevertheless, the rise and fall of the CNV reported here is consistent with a time window during which participants have to sustain their attention in order to make a decision about the probe durations, as compared to some non-specific tonic attentional processes. Moreover, timing and non-timing decision making experiments have demonstrated plausible dissociations of memory and decision processes. For instance, using a psychological refractory period (PRP) paradigm, Rattat and Fortin (2011) found that a secondary digit recognition task interfered with interval timing only when the stimulus onset asynchrony (SOA) was reasonably long and led to an overlap of decision making and response selection. In a visual perceptual discrimination task, Ratcliff et al. (2009) found that a perceptual categorization ("face/car") decision could be separated into an evidence gathering phase and a decision making phase, each characterized by a unique single-trial EEG component. The implication is that gathering information about the short anchor as one of the target durations (CNV rise) is necessary, but not sufficient for a bisection decision. This dissociation between encoding and decision is not easily made in the S1–S2 paradigm, because there is presumably only one criterion that is critical for making a choice; decision follows upon expiration of the remembered S1 duration. From this perspective, the bisection paradigm may allow a more detailed examination of the CNV in time perception.

That the CNV began to resolve at approximately 1600 ms for the two longest probe durations, as indicated by the positive slope between 1600 and 2000 ms, implies that the GM of the long and short anchor durations (i.e., 1600 ms) served as a target duration or temporal criterion with the classification decision occurring at about the GM rather than at the time of stimulus offset (2540 or 3200 ms). Interestingly, the CNV amplitude was sustained from about the AM of the anchor durations (2000 ms) to 2500 ms, which suggests that the AM did not serve as a target duration or criterion. We did not analyze the change in potential at and

immediately following the offset of the long anchor duration (i.e., 3200 ms) because the EEG signal in that time range was contaminated by stimulus offset potentials and motor response related potentials (cf. Tarantino et al., 2010). Therefore, we do not have EEG data that addresses whether the long anchor was also treated as a target duration. Logically, however, if the GM of the short and long anchor durations is indeed used as a temporal criterion in the duration bisection decision process, then one might expect the brain to monitor the value of the longest probe duration so that adjustments to that criterion can be made if needed. This is in line with research suggesting that participants track temporal information on every trial in the duration bisection task (e.g., Brown et al., 2005; Penney et al., 2008).

Whereas the relationship between the CNV amplitude and the subjective perceived time was not as prominent as reported in previous experiments, a correlation analysis revealed that shallower CNV slopes were associated with longer PSEs. As noted in the "Introduction," several authors (Pfeuty et al., 2003b, 2005; Durstewitz, 2004) have suggested that the slope of the CNV reflects the rate of temporal accumulation. Hence, a shallower CNV slope means slower temporal accumulation, which results in a smaller perceived (i.e., subjective) duration for a given objective duration. An apparent difficulty with applying this interpretation to the duration bisection task, however, is that the slower accumulation would likely occur during both "short" and "long" anchor duration presentations also. If the probe duration, as well as the durations that are used, either directly or indirectly, in the "short"/"long" decision are all measured using the same accumulation rate by a given participant, it is not clear how a slow temporal accumulation would result in a longer PSE than a relatively faster PSE (although the response function may be sharper for the faster accumulation case). A 10 pulse probe accumulation holds the same relative position with respect to 5 and 15 pulse anchors as would be the case if the accumulation process were five times faster (i.e., 50 pulse probe, 25 and 75 pulse anchors). A possible solution to this explanatory difficulty is that the slow accumulation occurs on some trials only. Assuming the critical short and long anchor trials are not overrepresented among these trials, then the PSE could be longer due to the slower temporal accumulation because slow clock trials will be compared to anchor durations used in the decision process that were laid down with relatively faster temporal accumulation.

We also found an ERS difference between intermediate probe durations classified as short and long. Specifically, in the alpha band the ERS was stronger for "long" responses. In a foreperiod study, Babiloni et al. (2004) found that trials cued with a short foreperiod (600 ms) were associated with stronger alpha ERS (∼6–10 Hz) than were long foreperiod (1400 ms) trials. The authors postulated that stronger alpha ERS reflected stronger temporal expectation. Assuming stronger temporal expectation is a consequence of optimal allocation of temporal attention (e.g., Coull and Nobre, 2008), then the stronger ERS obtained here in "long" response trials may reflect "stronger and quicker" (Babiloni et al., 2004) initial allocation of attention. Within the SET framework, more efficient allocation of attention on a trial would mean loss of fewer pacemaker pulses as compared to a less attentive trial (Lejeune, 1998), and therefore a higher probability of a duration being classified as "long."

Finally, the finding that the larger the mean peak-to-peak amplitude of the N1P2 complex the more negative the subsequent mean CNV may be a consequence of the precision with which a participant is able to initiate timing on each trial across a test session. ERP components such as N1 and P2 are sensitive to physical features of the stimuli, and general state and attention of the individuals (e.g., Näätänen and Picton, 1987; Herrmann and Knight, 2001; Picton et al., 2002; Crowley and Colrain, 2004; Nagai et al., 2004). Hence, the N1P2 component may be a marker for the precision of the signal or "start-gun" that initiates timing when the bisection stimulus is presented. If timing is indeed achieved by groups of ramping neurons through spreading activation or signal integration (König et al., 1996; Simen et al., 2011), with the change in CNV amplitude reflecting that ramping process (Macar et al., 1999; Macar and Vidal, 2004), then a reduction in latency jitter of the component across trials would result in a larger average ERP component. For example, Trillenberg et al. (2000) found that the CNV amplitude was more negative when the SOA was the most probable one in the trial block in a Go/No-go task with variable SOAs. The RT was also fastest for the most probable SOA trials as compared to the other SOA trials. The authors argued that this was the moment when participants could most reliably orient attention. Co-variations in the N1P2 component and subjective perception of time have also been reported in a replication of Macar et al. (1999) that used sub-second auditory intervals (Bendixen et al., 2005) and in a number–time interaction study (Xuan et al., 2009). In both studies, larger N1P2 components were associated with longer perceived time, and accompanied by a more negative CNV component. We explored the possibility that the jittering in the N1P2 component may affect the CNV amplitude by calculating the inter-trial phase coherence (ITPC) at the time window of N1P2 (80–250 ms; Mørup et al., 2007). ITPC measures the synchronization between the time-locked event and the EEG across trials (Delorme and Makeig, 2004). It varies from 0 (no consistent synchronization) to 1 (perfect synchronization). Participants who initiate timing consistently (i.e., less jitter across trials) should show stronger synchronization between the time-locked event and the EEG signal. In our sample, ITPC in the theta range (∼4–7 Hz), whose event related power is dominant in this early time window (e.g., Yordanova et al., 2002), was significantly correlated with the N1P2 amplitude ($r = 0.64$, $p < 0.05$) and the CNV amplitude ($r = -0.63$, $p < 0.05$).

CONCLUSION

The relationship between temporal memory and the CNV has been based mainly on paradigms like temporal discrimination (e.g., Pfeuty et al., 2005), temporal generalization (e.g., Macar and Vidal, 2003), and reproduction (e.g., Elbert et al., 1991; Macar et al., 1999), in which the target or criterion duration is unambiguous. Here, we used the CNV as a tool in order to understand how the representations of the anchor durations in the bisection task are used to make categorical decisions. The ERP and CSD topographies of the negative slow potential (i.e., CNV) were consistent with those obtained in other timing tasks. It peaked at the time close to the short anchor duration (800 ms) and remained

stable until the GM (1600 ms) of the probe series, when it started to resolve. This pattern suggests that participants monitored the anchor durations and used the GM of the anchor durations as a bisection criterion (Kopec and Brody, 2010; *cf.* Wearden and Bray, 2001; Allan, 2002). In addition, while the association of the N1P2 component with interval timing has been relatively unexplored to date, we suggest that this component's relationship to CNV amplitude may indicate it is a marker of the initiation of timing. Indeed, the latency jitter of the timing "start-gun" may prove vital to understanding variability in timing performance and the manifestation of electrophysiological events during interval timing.

ACKNOWLEDGMENTS

Publication of this work has been partially supported by the European project COST ISCH Action TD0904 "Time In Mental activity: Theoretical, behavioral, bioimaging, and clinical perspectives" (TIMELY: www.timely-cost.eu). Simon Tobin was supported by the Natural Sciences and Engineering Research Council of Canada.

REFERENCES

Allan, L. G. (2002). The location and interpretation of the bisection point. *Q. J. Exp. Psychol. B* 55, 43–60.

Allan, L. G., and Gerhardt, K. (2001). Temporal bisection with trial referents. *Percept. Psychophys.* 63, 524–540.

Babiloni, C., Miniussi, C., Babiloni, F., Carducci, F., Cincotti, F., Del Percio, C., Sirello, G., Fracassi, C., Nobre, A. C., and Rossini, P. M. (2004). Sub-second "temporal attention" modulates alpha rhythms. A high-resolution EEG study. *Brain Res. Cogn. Brain Res.* 19, 259–268.

Balci, F., Freestone, D., and Gallistel, C. R. (2009). Risk assessment in man and mouse. *Proc. Natl. Acad. Sci. U.S.A.* 106, 2459–2463.

Bendixen, A., Grimm, S., and Schröger, E. (2005). Human auditory event-related potentials predict duration judgments. *Neurosci. Lett.* 383, 284–288.

Birbaumer, N., Elbert, T., Canavan, A. G., and Rockstroh, B. (1990). Slow potentials of the cerebral cortex and behavior. *Physiol. Rev.* 70, 1–41.

Brown, G. D. A., McCormack, T., Smith, M., and Stewart, N. (2005). Identification and bisection of temporal durations and tone frequencies: common models for temporal and nontemporal stimuli. *J. Exp. Psychol. Hum. Percept. Perform.* 31, 919–938.

Brunia, C. H. M. (2004). Slow potentials in anticipatory behavior. *J. Psychophysiol.* 18, 59–60.

Buhusi, C. V., and Meck, W. H. (2005). What makes us tick? Functional and neural mechanisms of interval timing. *Nat. Rev. Neurosci.* 6, 755–765.

Correa, A., Lupiáñez, J., Madrid, E., and Tudela, P. (2006). Temporal attention enhances early visual processing: a review and new evidence from event-related potentials. *Brain Res.* 1076, 116–128.

Coull, J., and Nobre, A. (2008). Dissociating explicit timing from temporal expectation with fMRI. *Curr. Opin. Neurobiol.* 18, 137–144.

Crowley, K. E., and Colrain, I. M. (2004). A review of the evidence for P2 being an independent component process: age, sleep and modality. *Clin. Neurophysiol.* 115, 732–744.

Delorme, A., and Makeig, S. (2004). EEGLAB: an open source toolbox for analysis of single-trial EEG dynamics including independent component analysis. *J. Neurosci. Methods* 134, 9–21.

Durstewitz, D. (2004). Neural representation of interval time. *Neuroreport* 15, 745–749.

Elbert, T., Ulrich, R., Rockstroh, B., and Lutzenberger, W. (1991). The processing of temporal intervals reflected by CNV-like brain potentials. *Psychophysiology* 28, 648–655.

Gibbon, J. (1981). On the form and location of the psychometric bisection function for time. *J. Math. Psychol.* 24, 58–87.

Gibbon, J., Church, R. M., and Meck, W. H. (1984). Scalar timing in temporal memory. *Ann. N. Y. Acad. Sci.* 423, 52–77.

Gibbons, H., and Rammsayer, T. H. (2004). Current-source density analysis of slow brain potentials during time estimation. *Psychophysiology* 41, 861–874.

Grondin, S. (2010). Timing and time perception: a review of recent behavioral and neuroscience findings and theoretical directions. *Atten. Percept. Psychophys.* 72, 561–582.

Herrmann, C. S., and Knight, R. T. (2001). Mechanisms of human attention: event-related potentials and oscillations. *Neurosci. Biobehav. Rev.* 25, 465–476.

Kayser, J. (2009). *Current Source Density (CSD) Interpolation Using Spherical Splines – CSD Toolbox (Version 1.1)*. New York: Division of Cognitive Neuroscience, New York State Psychiatric Institute.

Kayser, J., and Tenke, C. E. (2006). Principal components analysis of Laplacian waveforms as a generic method for identifying ERP generator patterns: I. Evaluation with auditory oddball tasks. *Clin. Neurophysiol.* 117, 348–368.

Killeen, P. R., Fetterman, J. G., and Bizo, L. A. (1997). "Time's causes," in *Time and Behaviour: Psychological and Neurological Analyses*, eds C. M. Bradshaw and E. Szabadi (Amsterdam: Elsevier Science), 79–131.

König, P., Engel, A. K., and Singer, W. (1996). Integrator or coincidence detector? The role of the cortical neuron revisited. *Trends Neurosci.* 19, 130–137.

Kononowicz, T. W., and van Rijn, H. (2011). Slow potentials in time estimation: the role of temporal accumulation and habituation. *Front. Integr. Neurosci.* 5:48. doi:10.3389/fnint.2011.00048

Kopec, C. D., and Brody, C. D. (2010). Human performance on the temporal bisection task. *Brain Cogn.* 74, 262–272.

Lehmann, D., and Skrandies, W. (1980). Reference-free identification of components of checkerboard-evoked multichannel potential fields. *Electroencephalogr. Clin. Neurophysiol.* 48, 609–621.

Lehmann, D., and Skrandies, W. (1984). Spatial analysis of evoked potentials in man – a review. *Prog. Neurobiol.* 23, 227–250.

Lejeune, H. (1998). Switching or gating? The attentional challenge in cognitive models of psychological time. *Behav. Process.* 44, 127–145.

Luck, S. J. (2005). *An Introduction to the Event-Related Potential Technique*. Cambridge, MA: MIT Press.

Macar, F., Coull, J., and Vidal, F. (2006). The supplementary motor area in motor and perceptual time processing: fMRI studies. *Cogn. Process.* 7, 89–94.

Macar, F., and Vidal, F. (2003). The CNV peak: an index of decision making and temporal memory. *Psychophysiology* 40, 950–954.

Macar, F., and Vidal, F. (2004). Event-related potentials as indices of time processing: a review. *J. Psychophysiol.* 18, 89–104.

Macar, F., and Vidal, F. (2009). Timing processes: an outline of behavioural and neural indices not systematically considered in timing models. *Can. J. Exp. Psychol.* 63, 227–239.

Macar, F., Vidal, F., and Casini, L. (1999). The supplementary motor area in motor and sensory timing: evidence from slow brain potential changes. *Exp. Brain Res.* 125, 271–280.

McIntosh, A. R., and Lobaugh, N. J. (2004). Partial least squares analysis of neuroimaging data: applications and advances. *Neuroimage* 23(Suppl. 1), S250–S263.

Meck, W. H., Penney, T. B., and Pouthas, V. (2008). Cortico-striatal representation of time in animals and humans. *Curr. Opin. Neurobiol.* 18, 145–152.

Michel, C. M., Koenig, T., Brandeis, D., Gianotti, L. R. R., and Wackermann, J. (eds). (2009). *Electrical Neuroimaging*. New York: Cambridge University Press.

Mørup, M., Hansen, L. K., and Arnfred, S. M. (2007). ERPWAVELAB a toolbox for multi-channel analysis of time-frequency transformed event related potentials. *J. Neurosci. Methods* 161, 361–368.

Murray, M. M., Brunet, D., and Michel, C. M. (2008). Topographic ERP analyses: a step-by-step tutorial review. *Brain Topogr.* 20, 249–264.

Näätänen, R., and Picton, T. (1987). The N1 wave of the human electric and magnetic response to sound: a review and an analysis of the component structure. *Psychophysiology* 24, 375–425.

Nagai, Y., Critchley, H. D., Featherstone, E., Fenwick, P. B. C., Trimble, M. R., and Dolan, R. J. (2004). Brain activity relating to the contingent negative variation: an fMRI investigation. *Neuroimage* 21, 1232–1241.

N'Diaye, K., Ragot, R., Garnero, L., and Pouthas, V. (2004). What is common to brain activity evoked by the perception of visual and auditory filled durations? A study with MEG and EEG co-recordings. *Brain Res. Cogn. Brain Res.* 21, 250–268.

Penney, T. B., Gibbon, J., and Meck, W. H. (2000). Differential effects of auditory and visual signals on clock speed and temporal memory. *J. Exp. Psychol. Hum. Percept. Perform.* 26, 1770–1787.

Penney, T. B., Gibbon, J., and Meck, W. H. (2008). Categorical scaling of duration bisection in pigeons (*Columba livia*), mice (*Mus musculus*), and humans (*Homo sapiens*). *Psychol. Sci.* 19, 1103–1109.

Perrin, F., Pernier, J., Bertrand, O., and Echallier, J. F. (1989). Spherical splines for scalp potential and current density mapping. *Electroencephalogr. Clin. Neurophysiol.* 72, 184–187.

Perrin, F., Pernier, J., Bertrand, O., and Echallier, J. F. (1990). Corrigenda EEG 02274. *Electroencephalogr. Clin. Neurophysiol.* 76, 565.

Pfeuty, M., Ragot, R., and Pouthas, V. (2003a). Processes involved in tempo perception: a CNV analysis. *Psychophysiology* 40, 69–76.

Pfeuty, M., Ragot, R., and Pouthas, V. (2003b). When time is up: CNV time course differentiates the roles of the hemispheres in the discrimination of short tone durations. *Exp. Brain Res.* 151, 372–379.

Pfeuty, M., Ragot, R., and Pouthas, V. (2005). Relationship between CNV and timing of an upcoming event. *Neurosci. Lett.* 382, 106–111.

Pfeuty, M., Ragot, R., and Pouthas, V. (2008). Brain activity during interval timing depends on sensory structure. *Brain Res.* 1204, 112–117.

Pfurtscheller, G., and Lopes da Silva, F. H. (1999). Event-related EEG/MEG synchronization and desynchronization: basic principles. *Clin. Neurophysiol.* 110, 1842–1857.

Picton, T. W., Alain, C., and McIntosh, A. R. (2002). "The theatre of the mind: physiological studies of the human frontal lobes," in *Principles of Frontal Lobe Function*, eds D. T. Stuss and R. T. Knight (New York: Oxford University Press), 109–127.

Pizzagalli, D. A. (2007). "Electroencephalography and high-density electrophysiological source localization," in *Handbook of Psychophysiology*, eds J. T. Cacioppo, L. G. Tassinaru, and G. G. Berntson (Cambridge: Cambridge University Press), 56–84.

Pouthas, V., George, N., Poline, J.-B., Pfeuty, M., Vandemoorteele, P.-F., Hugueville, L., Ferrandez, A.-M., Lehéricy, S., Lebihan, D., and Renault, B. (2005). Neural network involved in time perception: an fMRI study comparing long and short interval estimation. *Hum. Brain Mapp.* 25, 433–441.

Praamstra, P., Kourtis, D., Kwok, H. F., and Oostenveld, R. (2006). Neurophysiology of implicit timing in serial choice reaction-time performance. *J. Neurosci.* 26, 5448–5455.

Ratcliff, R., Philiastides, M. G., and Sajda, P. (2009). Quality of evidence for perceptual decision making is indexed by trial-to-trial variability of the EEG. *Proc. Natl. Acad. Sci. U.S.A.* 106, 6539–6544.

Rattat, A.-C., and Fortin, C. (2011). Modulating the interference effect in timing with varying stimulus onset asynchrony. *Can. J. Exp. Psychol.* 65, 151–162.

Simen, P., Balci, F., deSouza, L., Cohen, J. D., and Holmes, P. (2011). A model of interval timing by neural integration. *J. Neurosci.* 31, 9238–9253.

Stone, J. V. (2002). Independent component analysis: an introduction. *Trends Cogn. Sci. (Regul. Ed.)* 6, 59–64.

Tarantino, V., Ehlis, A.-C., Baehne, C., Boreatti-Huemmer, A., Jacob, C., Bisiacchi, P., and Fallgatter, A. J. (2010). The time course of temporal discrimination: an ERP study. *Clin. Neurophysiol.* 121, 43–52.

Tenke, C. E., Kayser, J., Fong, R., Leite, P., Towey, J. P., and Bruder, G. E. (1998). Response- and stimulus-related ERP asymmetries in a tonal oddball task: a Laplacian analysis. *Brain Topogr.* 10, 201–210.

Trillenberg, P., Verleger, R., Wascher, E., Wauschkuhn, B., and Wessel, K. (2000). CNV and temporal uncertainty with "ageing" and "non-ageing" S1-S2 intervals. *Clin. Neurophysiol.* 111, 1216–1226.

van Boxtel, G. J. M., and Böcker, K. B. E. (2004). Cortical measures of anticipation. *J. Psychophysiol.* 18, 61–76.

Vicario, C. M. (2011). Perceiving numbers affects the subjective temporal midpoint. *Perception* 40, 23–29.

Walter, W. G., Cooper, R., Aldridge, V. J., McCallum, W. C., and Winter, A. L. (1964). Contingent negative variation: an electric sign of sensorimotor association and expectancy in the human brain. *Nature* 203, 380–384.

Wearden, J. H. (2004). Decision processes in models of timing. *Acta Neurobiol. Exp. (Wars.)* 64, 303–317.

Wearden, J. H., and Bray, S. (2001). Scalar timing without reference memory? Episodic temporal generalization and bisection in humans. *Q. J. Exp. Psychol. B* 54, 289–309.

Wearden, J. H., and Ferrara, A. (1995). Stimulus spacing effects in temporal bisection by humans. *Q. J. Exp. Psychol. B* 48, 289–310.

Xuan, B., Chen, X. C., He, S., and Zhang, D.-R. (2009). Numerical magnitude modulates temporal comparison: an ERP study. *Brain Res.* 1269, 135–142.

Yordanova, J., Kolev, V., Rosso, O. A., Schürmann, M., Sakowitz, O. W., Özgören, M., and Basar, E. (2002). Wavelet entropy analysis of event-related potentials indicates modality-independent theta dominance. *J. Neurosci. Methods* 117, 99–109.

Conflict of Interest Statement: The authors declare that the research was conducted in the absence of any commercial or financial relationships that could be construed as a potential conflict of interest.

Received: 25 July 2011; paper pending published: 17 August 2011; accepted: 12 November 2011; published online: 29 November 2011.

Citation: Ng KK, Tobin S and Penney TB (2011) Temporal accumulation and decision processes in the duration bisection task revealed by contingent negative variation. Front. Integr. Neurosci. ***5****:77. doi: 10.3389/fnint.2011.00077*

frontiers in
INTEGRATIVE NEUROSCIENCE

ORIGINAL RESEARCH ARTICLE
published: 13 September 2011
doi: 10.3389/fnint.2011.00048

Slow potentials in time estimation: the role of temporal accumulation and habituation

Tadeusz W. Kononowicz and Hedderik van Rijn*

Experimental Psychology, University of Groningen, Groningen, Netherlands

Edited by:
Warren H. Meck, Duke University, USA

Reviewed by:
Xu Cui, Stanford University, USA
Franck Vidal, Université de Provence, France

****Correspondence:***
Hedderik van Rijn, Experimental Psychology, University of Groningen, Grote Kruistraat 2/1, 9712 TS Groningen, Netherlands.
e-mail: hedderik@van-rijn.org

Numerous studies have shown that contingent negative variation (CNV) measured at fronto-central and parietal–central areas is closely related to interval timing. However, the exact nature of the relation between CNV and the underlying timing mechanisms is still a topic of discussion. On the one hand, it has been proposed that the CNV measured at supplementary motor area (SMA) is a direct reflection of the unfolding of time since a perceived onset, whereas other work has suggested that the increased amplitude reflects decision processes involved in interval timing. Strong evidence for the first view has been reported by Macar et al. (1999), who showed that variations in temporal performance were reflected in the measured CNV amplitude. If the CNV measured at SMA is a direct function of the passing of time, habituation effects are not expected. Here we report two replication studies, which both failed to replicate the expected performance-dependent variations. Even more powerful linear-mixed effect analyses failed to find any performance related effects on the CNV amplitude, whereas habituation effects were found. These studies therefore suggest that the CNV amplitude does not directly reflect the unfolding of time.

Keywords: time production, interval timing, habituation, pulse accumulation, contingent negative variation, supplementary motor area, accumulator, performance-dependent variations

INTRODUCTION

Since the early days of EEG research have slow potentials, especially at midline locations, been linked to preparation processes and time estimation (e.g., Walter, 1964). Later research has suggested that the increase in contingent negative variation (CNV) amplitude is a reflection of the internal bookkeeping of the unfolding of time (e.g., Macar et al., 1999). Another phenomenon related to slow potentials in the context of time estimation is that the amplitude of the CNV decreases with increased accuracy or practice (e.g., McAdam, 1966). Although it has been argued that the time estimation-related amplitude effects in the CNV are not sensitive to habituation (Macar and Vidal, 2004), this assumption has not been empirically addressed.

The CNV is a slow negative electrophysiological shift, typically found at fronto-central, central, and parieto-central regions (Walter, 1964), which develops when a subject is expecting an event. The CNV has been associated with many psychological processes such as the preparation for a response and attention (for an early review, see Tecce, 1972), but also, already in some early CNV studies, with interval timing (e.g., Walter, 1964; McAdam, 1966; Weinberg et al., 1974; Ruchkin et al., 1977). Although in many studies the increase in CNV amplitude could also be related to the motor preparation that was required to signal the end of the interval, a series of elegant standard-comparison studies have provided strong evidence for a direct relation between CNV amplitude and cognitive timing (e.g., Pouthas et al., 2000; Macar and Vidal, 2003; Tarantino et al., 2010). In these studies, participants have to compare the duration of events to a previously learned standard duration. If the to-be-compared event takes longer than the standard duration, the CNV shows a positive deflection before the offset of the event, indicating that the CNV is related to the timing of the standard duration. Typically, the link between CNV amplitude and timing is explained within the framework of centralized internal clock theories.

According to the centralized internal clock theories (e.g., Creelman, 1962; Treisman, 1963), a pacemaker generates pulses at a given frequency, which are integrated in an accumulator module. When the duration of an event needs to be timed, the accumulator is set to zero at the onset of the event, and its value is read out at the offset of the event. The number of pulses accumulated can be used as an internal representation of the perceived duration. This internal representation is assumed to be stored in reference memory, and when the duration of the event needs to be reproduced, the system waits until the same amount of pulses have passed (a detailed model of this process is discussed in Taatgen and Van Rijn, 2011). This general outline has been very influential and multiple theories are essentially implementations of this basic idea (e.g., the scalar expectancy theory, SET; Gibbon, 1977; Gibbon and Allan, 1984; Wearden, 1991; the attentional-gate models, Zakay and Block, 1997; and the integrated time models, Taatgen et al., 2007; Van Rijn and Taatgen, 2008).

The pacemaker–accumulator models rely on the concept of accumulation as all decisions depend on the number of accumulated pulses. Given the similarities between the increasing negativity of the CNV and the increasing value of the accumulator over time, it has been suggested that the CNV reflects the accumulation process. This assumption also explains the coincidence between the CNV peak and the standard duration in temporal generalization or standard-comparison studies: The accumulator, reflected in the CNV, stops its activity when the currently unfolding

duration equals the memorized standard. Although the simplest assumption is that the observed CNV is a direct reflection of the value currently stored in the accumulator, an alternative explanation could be that the CNV reflects the unfolding of time in a more indirect way, for example by expressing the difference between the current time and the earlier perceived durations.

The most powerful empirical argument in favor of a more direct link between pulse accumulation and the CNV was provided by Macar et al. (1999). Given the assumption that trial-to-trial fluctuations in temporal performance are driven by differences in the current state of the accumulator, the observed fluctuations in behavioral responses should correlate with the measured CNV amplitude. Macar et al. (1999) tested this assumption of performance-dependent variations in the CNV amplitude by asking their participants to produce an earlier learned standard duration of 2.5 s by pressing a key twice. Trials were *post hoc* categorized into three groups: a group of "short" productions (2.2–2.4 s), of "correct" productions (2.4–2.6 s), and of "long" productions (2.6–2.8 s). The (Laplacian-based) CNV measured at the FCz electrode was compared for the three conditions. In line with their assumption that the buildup in the accumulator is reflected in the CNV, Macar et al. (1999) found a higher CNV amplitude in the long condition, an intermediate CNV amplitude in the correct condition, and a lower CNV amplitude in the short condition. The positive correlation between produced duration and CNV amplitude strongly suggests that the unfolding of time – and thus the value of the accumulator – is directly linked with the amplitude of the CNV. Of course, if one assumes a relative stable threshold in this well-trained interval production task, this interpretation hinges on the notion that participants failed to notice that the accumulator already reached the threshold in the long condition, and that participants responded before the accumulator reached the threshold in the short condition. This idea, and especially the assumption of a response well before the threshold is reached (see Figure 2 of Macar et al., 1999), is of course problematic from the perspective of the pacemaker–accumulator theories since these theories are based on the assumption that responses are triggered by the accumulator reaching the threshold. However, a similar finding was reported by Macar and Vidal (2002) in a study that focused on memory consolidation in time perception: Trials in which the interval was overestimated were associated with more negative CNV amplitudes.

Another phenomenon related to the amplitude of the CNV that has been known since the onset of EEG research is the habituation effect. McAdam (1966) demonstrated that the CNV amplitude changes over the course of an experimental session, with a lower amplitude during the later phases. McAdam (1966) related this habituation effect to higher accuracy, a finding that was supported by Ladanyi and Dubrovsky (1985) who reported lower CNV amplitudes for a group of accurate time estimators compared to a group of participants who over estimated the interval. Similar effects were reported by Macar and Vitton (1979) on the basis of a study in which cats were subjected to a schedule of temporal conditioning: with prolonged training, the observed negativity decreased. Taken together, these data has been interpreted that CNV habituation serves as an index of gradual automation of time processing (e.g., Pfeuty et al., 2003; Pouthas, 2003).

If, however, this habituation effect also played a role in the Macar et al. (1999) experiment, the observed effects might be partly due to a habituation-based decrease of amplitude. That is, if participants initially slightly overestimated the durations and improved during the experimental session, the initial trials will have a higher chance of being categorized as "long" than the later trials. Combined with a decrease in amplitude during the experiment due to habituation, this might have emphasized a correlation between estimated durations and CNV amplitude.

Given the importance of the Macar et al. (1999) results for the hypothesis that the CNV reflects the unfolding of time, we have conducted two replication experiments to assess the contributions of performance-dependent variations in, and the effect of habituation on the CNV amplitude.

MATERIALS AND METHODS

Both experiments reported here were run as the first part of two larger experiments on the effects of attention on time estimation. In this paper, we will only report on the first part of the experiments, which was set up as a replication of the study reported by Macar et al. (1999). Participants were, while performing the here reported study, not instructed on the later parts of the experiment.

We will discuss the materials and methods for both experiments before turning to the discussion of the results.

EXPERIMENT 1

Task

The participants were asked to produce a 2.5-s interval by pressing the spacebar twice. Feedback was presented after each trial indicating the deviation from the learned standard. During the entire interval a small circle (about 1 cm in diameter) served as a fixation point. Before the first key press, the circle was shown in light gray on a black background. The first key press changed the color of the circle to white, as a visual cue that the interval had started. The second key press removed the circle from the screen, and after 200 ms feedback was presented for a duration sampled from a uniform distribution between 1 and 1.5 s. The feedback was delivered as a row of five circles, immediately above the location of the fixation point. If the time production was "perfect" (between 2.4 and 2.6 s), the middle circle turned green. If time production was between 1.8 and 2.4 s or between 2.6 and 3.2 s, the circle just to the left or right of the middle circle turned green. If the time production was shorter than 1.8 or longer than 3.2 s, the left or right outer circle turned red. See **Figure 1** for a graphic depiction of the feedback screen. Participants were instructed that appearance of a red circle indicates a "too short" or "too long" time production, and that they should aim for as precise as possible temporal performance. Before each trial, a "Please blink" instruction was presented for 500 ms to reduce blinks during the time production trials.

Procedure

Experiment 1 consisted of a training and an experimental block. In the training block, participants were asked to learn the 2.5-s interval by adjusting their productions based on feedback. After producing three time productions between 2.4 and 2.6 s in succession, the training block was considered finished, and the experimental

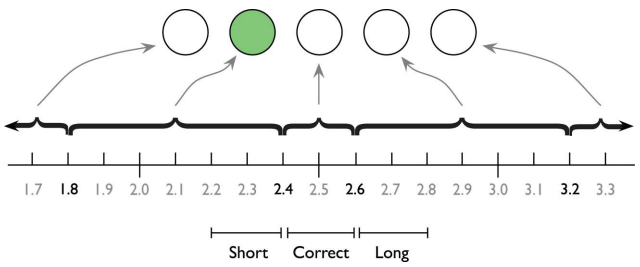

FIGURE 1 | The horizontal row of five circles depict an example feedback screen. The green circle indicates the participant that the produced interval was too short. The time line indicates the ranges associated with particular feedback circles. The three pseudo-experimental conditions as defined by Macar et al. (1999) on which the ANOVA analyses are based are illustrated below the timeline.

block started. The maximum length of the training block was set to 50 trials. The length of the experimental block was dynamically adjusted, as it lasted until 252 time productions between 1.8 and 3.2 s were obtained. Participants were instructed to use the feedback to estimate the interval as accurately as possible and to not use external timing strategies such as counting or foot tapping. Participants were allowed to take a break whenever necessary.

Participants

Twenty-two Psychology students participated in the experiment and received partial course credit. All participants had normal or corrected-to-normal visual acuity. Informed consent as approved by the Ethical Committee Psychology of the University of Groningen was obtained before testing. Nine subjects (mean age: 21.3, range: 20–25, 6 females) fulfilled the "3-in-a-row" criterion as set by Macar et al. (1999). Although this inclusion rate is rather low (approximately 40%), Macar et al. (1999) reported that they preselected their participants based on performance in other timing tasks. Here we did not apply any pre-selection criteria, which might explain the low inclusion criteria. Of the remaining participants, eight showed behavioral performance during the experimental phase that was similar to the "3-in-a-row" participants (i.e., needed less than 280 trials to achieve 252 time productions between 1.8 and 3.2 s). We will also report analyses on the extended dataset of 17 participants.

Electrophysiological recordings

Electrical brain activity was recorded from 30 scalp locations (AFz, F5, F3, F1, Fz, F2, F4, F6, FC5, FC3, FC1, FCz, FC2, FC4, FC6, C5, C3, C1, Cz, C2, C4, C6, CP3, CP1, CPz, CP2, CP4, P3, Pz, P4). Vertical and horizontal EOG activity and both mastoids were registered. For all channels Ag–AgCl electrodes were used and impedances were kept below 5 kΩ. Using the Refa system (TMS International B.V.), all channels were amplified and filtered with a digital FIR filter with a cutoff frequency of 135 Hz (low pass) and were recorded with a sampling rate of 500 Hz using Portilab (TMS International B.V.). Using BrainVision (Brain Products GmbH), the signals were referenced to the mastoids and a 50-Hz notch filter was applied to reduce line noise artifacts.

Data preprocessing and analysis

Parameters for data preprocessing were set to be as similar as possible to the settings reported by Macar et al. (1999). The average voltage over the first 100 ms preceding the first key press was used as baseline for second key press-locked plots and analyses, and the average voltage between 1 and 0.9 s preceding the first key press was used as baseline for first key press-locked plots and analyses. Trials in which the maximum absolute amplitude exceeded 100 μV or in which the amplitude range exceeded 150 μV were discarded. Eye blinks were corrected using the Gratton and Coles method (Gratton et al., 1983). Data were filtered offline with a bandpass of 0.01–100 Hz with 12 dB/Oct slope. Trials containing ocular artifacts, movement artifacts, or amplifier saturation were excluded from further processing by visual inspection. We will report on data from the FCz electrode both on monopolar electrophysiological activity and data obtained after Laplacian transformation (Hjorth, 1975). Note that Hjorth (1975) advocates the use of 5-point operator derivations (which, in our case, would involve AFz, CPz, FC3, and FC4), but to keep the reported analyses as similar as possible to the ones reported by Macar et al. (1999), we computed the Laplacians using the same triangular configuration (F3, F4, CPz) as presented by Macar et al., 1999; **Figure 1**) see Vidal et al. (2003), for more details on this method). However, informal comparisons between the triangular configuration and the 5-point operator derivations did not indicate that the interpretation of the data hinged on which method was chosen. As described in Vidal et al. (2011), we averaged the monopolar recordings that remained after artifact correction and rejection, and calculated the Laplacians on the basis of these monopolar averages [by using the formula $\{3xFCz - (F3 + F4 + CPz)\}/distance^2$, with distance equal to 7 cm]. Statistical tests on the average amplitude were computed for the interval that ranges from 1500 to 100 ms before the second key press that ended the time production. We will report Laplacian-based analyses for both the "3-in-a-row" and the extended group, and analyses on monopolar data for the extended group to provide additional insight.

EXPERIMENT 2

Task

In comparison to the procedure of Experiment 1, (1) the delay between the second response of the participant and the presentation of the feedback was increased from 200 to 500 ms, (2) the "please blink" instruction at the start of each trial was removed, and (3) the inter-trial delay was sampled from a uniform distribution with a range of 1500–3000 ms. These settings were chosen to better match the Macar et al. (1999) setup. All other details were left unchanged.

Procedure

In comparison to the procedure of Experiment 1, the maximum length of the training block was extended from 50 trials to 90 trials. All other details were left unchanged.

Participants

Twenty-four Psychology students participated in the experiment and received partial course credit. Eight participants (age: 22.9, range 19–31, 6 females) fulfilled the same "3-in-a-row" correct

criteria as used in the Macar et al. (1999) experiment. We again did not apply any pre-selection criteria. Another seven participants performed equally well during the experimental phase (less than 280 trials to achieve 252 time productions between 1.8 and 3.2 s) and were included in the analyses on the extended dataset.

Electrophysiological recordings

Data was recorded using the same setup as used for Experiment 1 from the following scalp locations: AF3, AFz, AF4, F3, Fz, F4, FC3, FC1, FCz, FC2, FC4, C3, C1, Cz, C2, C4, CP3, CPz, CP2, CP4, P3, P1, Pz, P2, P4, PO3, POz, PO4, O1, Oz, and O2.

Data preprocessing and analysis

Preprocessing and analysis procedures were identical to those reported for Experiment 1.

RESULTS

EXPERIMENT 1: ANOVA-BASED RESULTS

All analyses reported in this section are based on the pseudo-experimental categorization used by Macar et al. (1999), as depicted in **Figure 1**. Data were subjected to repeated measures analyses of variance (ANOVA).

The length of the training session depended on the subject's performance, and lasted between 10 and 49 trials for the "3-in-a-row" group. Macar et al. (1999) reported that the successful training criterion was reached after 16–55 trials in their experiment. Each averaged ERP waveform (i.e., per participant and per pseudo-experimental group) contained at least 30 and at most 115 trials, with an average of 55 trials. After preprocessing of electrophysiological data, the produced intervals were sorted into 0.2-s categories. Three categories, designated as "short" (2.2–2.4 s), "correct" (2.4–2.6 s), and "long" (2.6–2.8 s), served as pseudo-experimental conditions. Overall, 65% of the trials were included: 19% correct, 27% short, and 19% long. About 31% of all trials resulted in temporal productions outside the range of the pseudo-experimental groups, and 4% of all trials were rejected. On average, participants needed 267 trials to get at 252 correct trials. Performance for the eight participants who did not meet the "3-in-a-row" criterion was similar.

Performance-dependent variations

Figure 2 provides the Laplacian data during the 1-s period preceding a first button press. We did not find any differences during the 100-ms period prior to the first key press, nor for an extended period of 500 ms prior to the first key press (Fs < 1). **Figure 3** shows the second key press-locked averages for the three pseudo-experimental conditions. Analyses on the average Laplacian amplitudes (from 1.5 to 0.1 s before the second key press) showed no effect of pseudo-experimental groups for the FCz electrode for the "3-in-a-row" group ($F < 1$) nor for the extended group [$F(2,34) = 1.2$, $p = 0.32$]. The monopolar data for the extended group did not show any significant results either ($F < 1$).

Thus, neither the analysis based on monopolar nor on Laplacian-transformed data replicated the performance-dependent variations as reported by Macar et al. (1999).

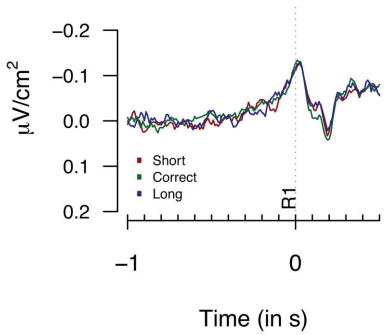

FIGURE 2 | Laplacians obtained at FCz during Experiment 1 as a function of participants' behavioral performance, plotted time-locked to the first key press (R1). Averages are based on nine participants who met the "3-in-a-row" criterion.

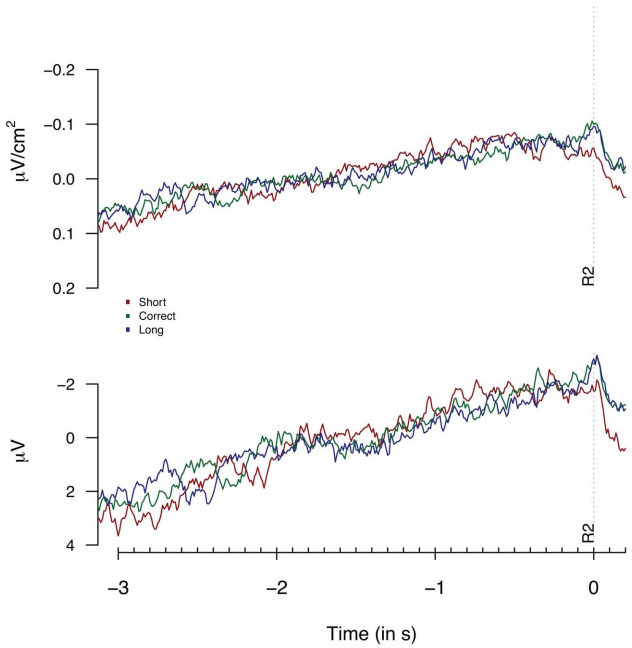

FIGURE 3 | Laplacians (top graph) and monopolar recordings (bottom graph) obtained at FCz during Experiment 1 as a function of participants' behavioral performance, plotted time-locked to the second key press (R2). Laplacians are based on 9 "3-in-a-row" participants, monopolar data are based on the extended dataset consisting of 17 participants.

Habituation effects

To check the presence of habituation effects in our data, the same trials as analyzed for the performance-dependent variations (i.e., time productions between 2200 and 2800 ms) were sorted into three equally sized groups based on the sequential order of trials during the experimental block. **Figure 4** shows the Laplacian and the monopolar traces for the three groups. The most elegant analysis would include factors for both habituation effects and performance-dependent variations, however, the number of

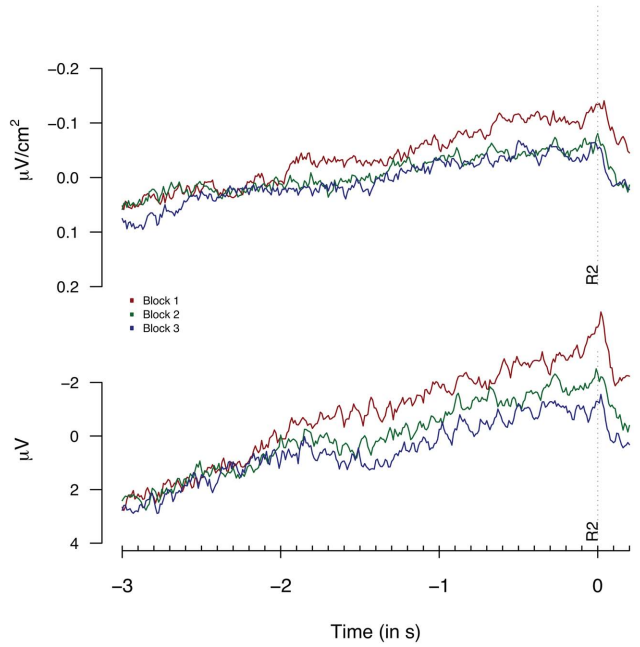

FIGURE 4 | Second response (R2) locked Laplacians (top graph, means based on 9 "3-in-a-row" participants) and monopolar recordings (bottom graph, means based on 17 participants) obtained at FCz during Experiment 1, plotted separately for the first, second, and third 33% of all trials.

observations per cell would differ too much in such a setup to allow for reliable tests based on cell means. Therefore, we will analyze habituation effects independently from performance-dependent variations. Note that we will discuss analyses on monopolar data in Section "Linear-Mixed Effect Model-Based Analysis of Experiment 1 and 2" that include both habituation and performance-dependent variations in a single analysis.

A repeated measures ANOVA on monopolar data for all participants (shown in **Figure 4**), showed significant effects, not only at FCz [$F(2,34) = 4.0$, $p = 0.02$] but at a broad range of fronto- and fronto-central electrodes: $F1$: $F = 5.8$; Fz: $F = 3.5$: $F2$: $F = 4.2$; FC1: $F = 3.1$; FC2: $F = 3.6$ and Cz = 3.9, all df(2,34); all $p < 0.05$. The analysis of Laplacian data failed to reach significance [$F < 1$ and $F(2,34) = 1.17$, $p = 0.3$ for the "3-in-a-row" and for all participants respectively]. However, visual inspection of **Figure 4** shows signatures of habituation effects for FCz in both monopolar and in Laplacian-transformed data, suggesting that the lack of effect in the Laplacian-transformed data might be related to the limited power of an analysis based on three categorial groups.

Given that these analyses are also based on differences in amplitude, it is even more surprising that we were unable to replicate the performance-dependent CNV amplitude effects. Because of some slight differences between the original study by Macar et al. (1999) and our Experiment 1, and to check the consistency of our results, we ran another replication study. The most important modification was the extension of the training block from 50 to 90 trials as in the Macar et al. (1999) experiment. Note that we originally set the training block to 50 trials as behavioral pilot studies showed that no extensive improvement in temporal accuracy was obtained after 50 trials.

EXPERIMENT 2: ANOVA-BASED RESULTS

The length of the training block depended on the subject's performance as the experimental block started as soon as a subject produced three trials in a row between 2.4 and 2.6 s. Participants who met this criterion needed between 30 and 58 trials, with only a single participant needing more than 50 trials. This level of performance is very similar to our Experiment 1 and to the Macar et al. (1999) study. Each averaged ERP waveform (i.e., per participant and per pseudo-experimental group) contained at least 30 and at most 92 trials, with an average of 54 trials. After preprocessing of electrophysiological data, 64% of all trials were included in the three specified pseudo-experimental groups: 22% in short, 26% in correct, and 16% in long. About 23% of all trials resulted in temporal productions outside the range of the pseudo-experimental groups, and 13% of all trials were rejected because of artifacts. On average 260 trials were needed to get at 252 correct trials.

Performance-dependent variations

Figure 5 provides the Laplacian data during the 1-s period preceding a first button press. We did not find any differences during the 100 or 500-ms period prior to the first key press [$F(2,14) = 1.82$, $p = 0.3$; $F(2,14) = 1.23$, $p = 0.19$ respectively]. The second key press-locked Laplacian data presented in **Figure 6** showed no effect for performance-dependent variations in CNV [$F(2,14) = 2.62$, $p = 0.108$; $F(2,28) = 2.68$, $p = 0.086$, for the "3-in-a-row" and for all participants respectively]. Note that the relatively big F values are driven by an opposite-to-expected order in CNV amplitudes, with short associated with the highest amplitude. The monopolar recordings did not reveal any significant effect ($F < 1$).

Habituation effects

As for Experiment 1, we tested for the presence of habituation effects. **Figure 7** shows the Laplacian-transformed and monopolar traces plotted separately for the first, second, and third 33% of all trials. No habituation effects for Laplacian and monopolar data reached significance (Fs < 1).

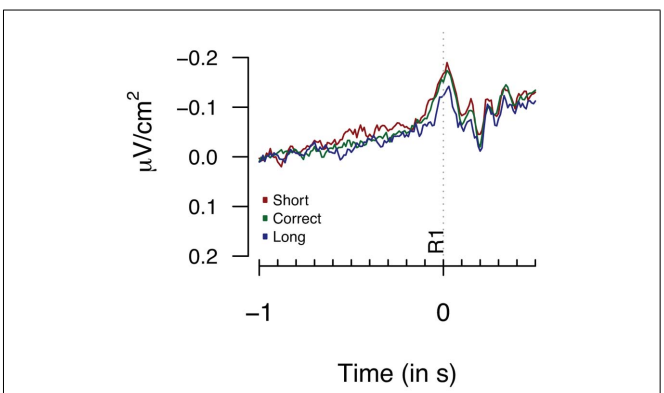

FIGURE 5 | Laplacians obtained at FCz during Experiment 1 as a function of participants' behavioral performance, plotted time-locked to the first key press (R1). Averages are based on eight participants.

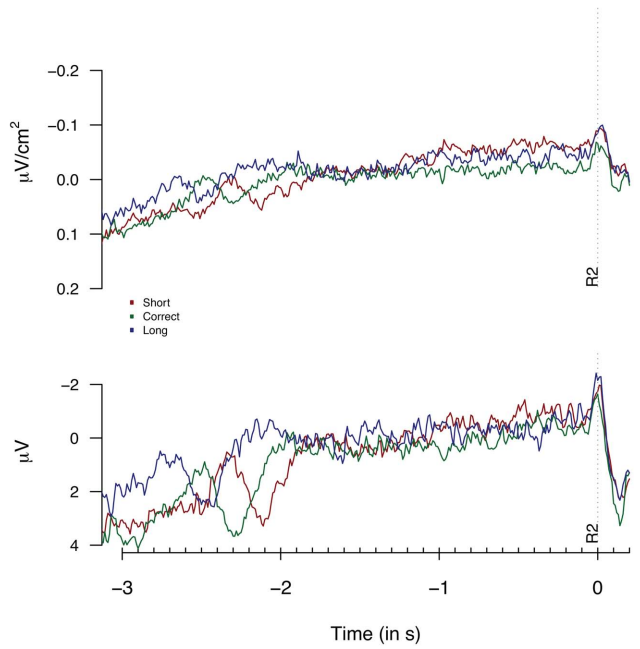

FIGURE 6 | Laplacians (top graph) and monopolar recordings (bottom graph) obtained at FCz during Experiment 2 as a function of participants' behavioral performance, plotted time-locked to the second key press (R2). Laplacians are based on 8 "3-in-a-row" participants, monopolar data are based on all 15 participants.

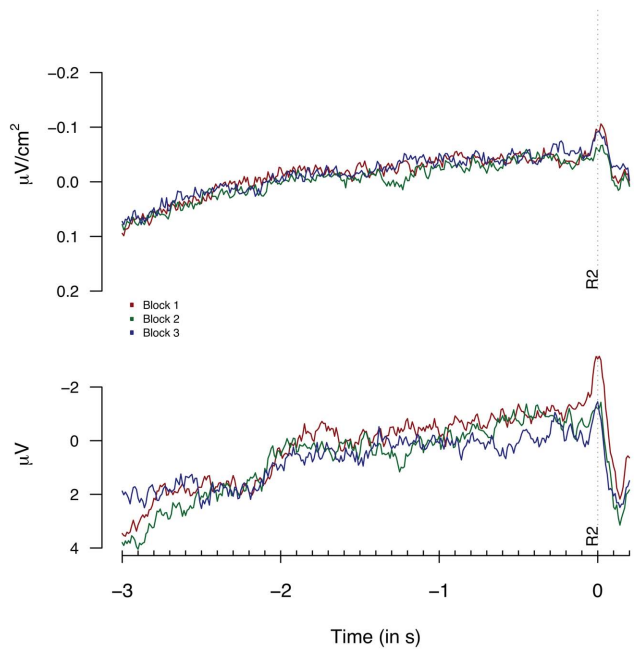

FIGURE 7 | Second response (R2) locked Laplacians (top graph, eight "3-in-a-row" participants) and monopolar recordings (bottom graph, all participants) obtained at FCz during Experiment 2 plotted separately for the first, second, and third 33% of all trials.

LINEAR-MIXED EFFECT MODEL-BASED ANALYSIS OF EXPERIMENT 1 AND 2

The analyses reported above are based on a *post hoc* categorization of the participants' responses. This categorization allows for comparing the amplitudes of short, correct, and long trials by means of traditional ANOVA. We have reported these as similar analyses are reported by Macar et al. (1999). However, the premise that variations in estimated durations correlate with the observed CNV amplitude at FCz should also hold if the actual durations are correlated with the amplitude, instead of comparing means based on aggregation in three bins. However, given the distribution of durations, increasing the number of bins and performing ANOVA-style analyses would likely violate the assumptions underlying an ANOVA. The same issue prevents doing analyses in which the effects of performance-based variations are tested simultaneously with habituation effects. As argued earlier, it might be that the habituation effects either artificially strengthen or conceal the effects of the performance-based variations, or vice versa.

An alternative type of analysis that allows for entering the raw durations of multiple factors instead of binned duration-categories are linear-mixed effects models (e.g., Pinheiro and Bates, 2000; Gelman and Hill, 2007; Baayen, 2008). These models allow for testing the effect of multiple continuous (pseudo-) experimental manipulations while taking the (repeated measures) structure of the design into account.

To improve on the power of the analyses, we will here report linear-mixed effect model-based analyses for just the monopolar data. As the reported Laplacians are based on averages (c.f., Macar et al., 1999), no trial-by-trial information is available. Therefore, we cannot report linear-mixed effect models on the Laplacian-transformed data but analyses based on spherical spline current source density (Perrin et al., 1989) transformations showed similar results to the monopolar data presented here. We will analyze both Experiment 1 and Experiment 2 separately, including just those participants who met the "3-in-a-row" criterion, but also perform a combined analysis in which we include participants from the extended groups of both Experiment 1 and 2.

Figure 8 shows the result of the linear-mixed effect model in which the monopolar average amplitude (calculated over 1.5–0.1 s before the second response, similar as for the ANOVA-based analyses) was entered as the dependent variable. All trials in which the absolute average amplitude exceeded 50 μV were removed. Both duration, a factor representing the effect of the performance-based variations, and habituation, a factor representing the overall time course of the experiment were entered as fixed factors. In addition to these fixed factors, we allowed for a random intercept per participant, and independent random effects for duration and habituation per participant. The factor duration was calculated by subtracting 2.5 s from the observed behavioral durations. The estimated effects for duration thus represent the change in microvolt per 1 s deviation from 2.5 s. Habituation is expressed as a function of trial number, with the first trial of each participant coded as 0, and the last trial as 1. Each of the dots represent the Markov Chain Monte Carlo-based estimated coefficient (Baayen, 2008) for the effect of that factor for each participant. The blue and red colored dots represent the participants who met the "3-in-a-row" criterion and who participated in Experiment 1 and Experiment

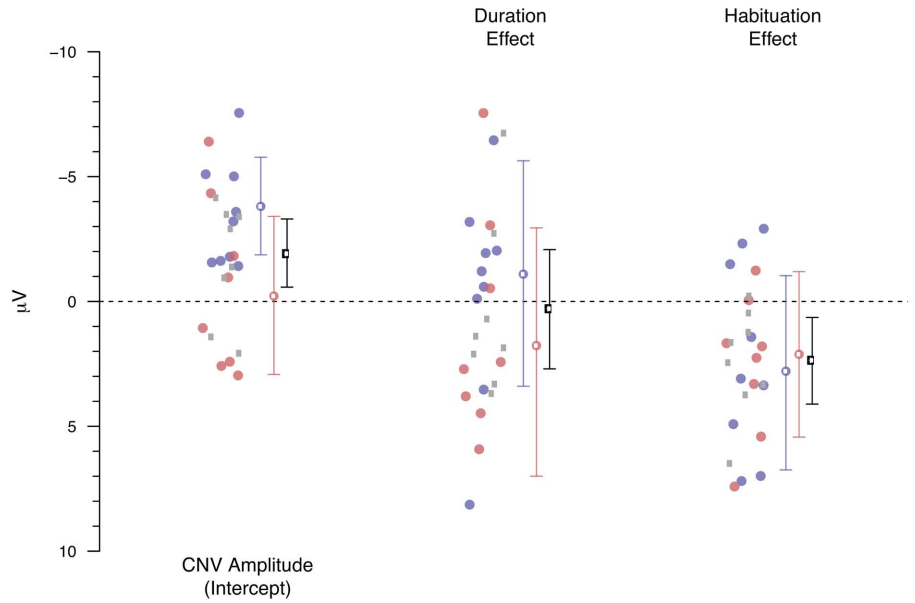

FIGURE 8 | Estimated monopolar-based effects for the CNV amplitude, the performance-based variations (Duration) and the habituation effect. Circles represent individual participants, mean and SE lines represented the estimated effect and HPD 95% confidence intervals. Blue represents Experiment 1, red Experiment 2, and the gray circles represent the participants who did not meet the "3-in-a-row" criterion. The black means and confidence intervals represent the overall analysis.

2 respectively. The gray dots represent the participants from both experiments who met the more relaxed criterion for inclusion in the extended dataset. As can be seen in **Figure 8**, the estimated effects of these extended group participants are similar to those of the "3-in-a-row" group. Therefore, we will focus the discussion on the overall analyses, represented by the black means and error bars (although the same information is available for the two subsets, color-coded in blue and red). The mean with the error bars denotes the overall effect of that factor and the 95% highest posterior density-based confidence intervals.

The monopolar-based linear-mixed effect model largely confirms the conclusions drawn from the ANOVA-based analyses. First, the overall model contains a negative intercept, reflecting the typical CNV effect ($\beta = -1.92$, $p < 0.001$). Second, we again found no indication of an effect of performance-based variations in CNV amplitude ($\beta = 0.32$, $p = 0.81$). Third, the overall habituation effect reaches significance ($\beta = 2.40$, $p = 0.008$), indicating that the negativity associated with the CNV is attenuated during the course of the experiment. Adding a Duration times Habituation interaction term does not improve the fit of the model to the data ($\chi^2 = 0.08$, df $= 1$, $p = 0.77$).

The habituation effect observed at FCz is not in line with Macar and Vidal (2004) suggestion that time estimation-related amplitude effects in the CNV are not sensitive to habituation. However, it might be that these effects are epiphenomena of an ongoing learning process that results in attenuation of the CNV over time. A signature of such a learning process would be an increased accuracy in temporal productions over the time course of the experiment. To test for learning, we assessed whether the absolute deviation of the standard decreased during the experiment. However, a linear-mixed effect model with absolute deviation from the standard as the dependent variable and trial number rescaled to a 0.1 range as fixed factor and subject as random factor did not show an effect of trial number ($\beta = -0.005$, HPD 95%: -0.021 0.011, $p = 0.519$, based on 10000 Markov chain Monte Carlo samples), which indicates that we failed to find any evidence in favor of participants still improving their estimations during the scope of the experiment.

To summarize, even the more powerful linear-mixed effect analysis did not provide any evidence in favor of the hypothesis that the duration of produced intervals correlate with the associated CNV amplitudes, while this analysis did find support for habituation effects.

DISCUSSION

It has been hypothesized that the CNV amplitude measured at the FCz electrode, which is assumed to measure supplementary motor area (SMA)-related activity, reflects an online temporal accumulation of the currently unfolding time interval (Macar et al., 1999; Macar and Vidal, 2002). Based on experimental data, Macar et al. (1999) concluded: "this region, which mainly includes the SMA, contains the temporal accumulator described in prominent models of time processing" or, "[a]lternatively, through thalamic relays, it may receive output from a temporal accumulator located in striatal structures" (p. 278). These conclusions, and especially the stronger conclusion that the activity in the SMA indicates to how much time has passed since the onset of an interval of course predicts a stable correlation between performance and observed CNV variations. However, early work on the brain correlates of time estimation showed that CNV decreased over the time course of

the experiment, often referred to as habituation (McAdam, 1966; Ladanyi and Dubrovsky, 1985). In two experiments, we have tested whether we could replicate these contradictory results.

However, neither in Experiment 1, nor in Experiment 2, nor in the combined analyses of all data did we find any systematic or consistent performance-based variations in the CNV amplitude. At the same time, we did find evidence in favor of the habituation effect in the linear-mixed effect analyses, indicating that the CNV amplitude decreases as a function of the time course of the experiment as was reported by earlier work (McAdam, 1966; Ladanyi and Dubrovsky, 1985; Pfeuty et al., 2003).

As we set out in the introduction, the performance-based variations might have been enhanced (or attenuated) by an interaction with the habituation effects if the behavioral data would have showed a progressive shortening of the estimated intervals over the time course of the experiment. Although we had to perform the ANOVA-based analyses separately for the habituation effect and for the performance-dependent variations, the linear-mixed effect model-based analyses contained both components in a single analysis which would have allowed for testing whether habituation effects might influence the performance-based variations. Since we did not find any performance-based amplitude effects, this hypothesis cannot be fully assessed.

Of course, as these results are in stark contrast to the results reported by Macar et al. (1999) the question arises what causes these differences. Given that we did find the expected CNV effect, effects of habituation, and typical ERPs, it is likely that we would have observed signatures of performance-dependent variations if at all present in this data. However, inspection of **Figure 8** shows large individual differences for the estimated effect of performance-dependent variations. This variability does suggest that if a small number of participants is tested, a Type I error might result. The probability of both Type I and Type II errors are also increased when discretized data is used in an analysis based on cell means, for example because the mean of a category can be strongly influenced by an extreme observation (see, for example, Royston et al., 2006; Wainer et al., 2006). Note that the ANOVA-based analyses reported by Macar et al. (1999) and replicated in this paper are based on discretized data and cell means, and as such might be biased, but that the linear-mixed effect analyses are not affected.

Another potential source of differences between our and Macar et al.'s (1999) work are the participant inclusion rates. Although the exact proportion of participants not meeting the "3-in-a-row" criterion is not reported in Macar et al. (1999), Vidal (personal communication, January 11, 2011) has indicated that their exclusion rate was quite a bit lower than the high exclusion rates observed for our two experiments. On the basis of this difference, one could argue that even the participants who met the "3-in-a-row" criterion in our experiments are in some aspects different from the participants tested by Macar et al. (1999) for example, because our participants might have been less motivated. However, this reasoning implies that the participants who met the "3-in-a-row" criterion are more similar to the participants tested by Macar et al. (1999) than the subset of participants who did not meet the "3-in-a-row" criterion. This hypothesis is not supported by the data, as visual inspection of **Figure 8** does not indicate any difference in the distributions of the blue/red colored circles versus the gray circles. We, therefore, consider it unlikely that the differences between Macar et al. (1999) and our experiments are purely due to differences in the participant groups.

To summarize, although we report on data of three times the number of participants as analyzed by Macar et al. (1999) and have analyzed the data with more powerful statistical techniques, we failed to replicate the performance-based variations. As discussed in the next paragraph, the literature provides more examples showing that the link between the SMA and the accumulator is not straightforward.

Besides the work presented by Macar et al. (Macar et al., 1999; Macar and Vidal, 2002) results obtained in monkeys during single-cell recording from the SMA and pre-SMA may be interpreted in favor of the performance-dependent variations hypothesis (Akkal et al., 2004; Mita et al., 2009). However, if one assumes that the slow cortical potentials measured at SMA/FCz reflect time accumulation processes, and one assumes that increased CNV amplitudes for longer intervals arises from increased activation of neural structures involved in timing (Macar et al., 1999; Macar and Vidal, 2004), then one should find similar effects in other paradigms where intervals of different durations are estimated. However, this is not regularly reported. For example, in an experiment in which subjects had to reproduce just perceived intervals selected from a 1 to 8-s range, no amplitude differences were observed (Elbert et al., 1991). A similar lack of results was reported for the amplitudes associated with estimations of intervals up to 6 s, even after CSD-based transformations (Gibbons and Rammsayer, 2004). Recently, an alternative explanation has been put forward that assumes that the accumulation in the CNV represents accumulation to a threshold, with the final value of the accumulator to be more or less constant over all trials (assuming a constant threshold). This idea, expressed in the work of Durstewitz (2003, 2004), does not predict amplitude differences for short and long productions, and has found support in timing paradigms (Pfeuty et al., 2005) and serial choice reaction time tasks (Praamstra et al., 2006). Moreover, Balci and Simon (submitted) have presented a drift–diffusion model that builds on the work of Simen et al. (2011) that explains temporal bisection variability in terms of accumulation to a fixed threshold. Since performance-dependent variations were not observed in our study, this data is more in line with the view that the SMA is related to the decision process instead of to the actual accumulation of temporal information.

Interestingly, recent work by Van Maanen and Forstmann (Forstmann et al., 2008; Van Maanen et al., submitted) might reconcile the paradox between the findings of Macar et al. (1999) and our experiments. Forstmann et al. (2008) has demonstrated the pre-SMA and striatum show increased levels of activation when decisions need to be made under time pressure in a speed–accuracy tradeoff experiment. Based on trail-by-trial analyses, Van Maanen et al. (submitted) have shown that this effect is driven by a positive correlation between fluctuations in response caution and the hemodynamic response in pre-SMA and dorsal anterior cingulate. However, this effect was only found when participants were instructed to value speed-over-accuracy. When participants were instructed to value accuracy over speed, Van Maanen et al. (submitted) found no such correlation. If participants respond later

if they are more cautious (as in non-temporal tasks), the paradox might be explained by assuming that the participants in the Macar et al. (1999) study performed as in the speed-over-accuracy condition of Van Maanen et al.'s (submitted) study, whereas the participants in our study might have performed as in the accuracy-over-speed condition. Of course, response speed and accuracy cannot be considered independently in an interval timing task where the response latency determines accuracy. However, in the studies by Forstmann et al. (2008) the speed–accuracy manipulations are considered to be a proxy of response caution, which might differ between individuals in an interval timing task. Moreover, Forstmann et al. (2008) showed that individual variation in the activation of striatum and pre-SMA is selectively associated with individual variation in behavior, supporting the notion that the paradox might be explained by different levels of response caution. However, this explanation is also based on the notion that the activity measured at (pre-)SMA is not a direct reflection of the unfolding of time, but a signature of the decision processes involved in interval timing.

Earlier work has identified a relation between levels of brain activity at prefrontal sites with temporal performance, with decreased activation associated with increased temporal performance (Casini et al., 1999), but this habituation effect was not observed at SMA. Based on this result it was hypothesized that "the activity from the SMA is resistant to the habituation because it indexes the increasing efficiency of temporal coding mechanisms with learning, which implies enhanced precision and stability, whereas the prefrontal activity anterior to the SMA rapidly diminishes due to the decreasing load of attentional effort and of possibly interfering mental strategies" (Macar and Vidal, 2004, p. 100). In contrast to the suggested habituation-resistant activity in the SMA, we found habituation effects in the monopolar data.

To conclude, this paper adds to the current discussion on the role of the SMA in time estimation, mainly focusing on the question whether the SMA incorporates or reflects the accumulator as expressed in information-processing models of time estimation, or whether its activity reflects a more indirect component of time estimation tasks such as comparisons to previous experiences or thresholds (see for a discussion, Coull et al., 2010). Where some EEG and fMRI studies link SMA activity to the accumulation of time units during the unfolding of time (e.g., Macar et al., 1999; Coull et al., 2004), other studies have linked similar activity to the indirect processes such as comparison to memorized time intervals (e.g., Pfeuty et al., 2003; Cui et al., 2009). If this latter view is correct, one might expect to see a decrease of CNV amplitude over the course of the experiment, since habituation has typically been related to increased neural proficiency (e.g., McAdam, 1966; Ladanyi and Dubrovsky, 1985; Pouthas, 2003). Given that our analyses did not result in any performance-dependent CNV amplitude variations but did show habituation effects, this data supports the view that the buildup of SMA activity during temporal processing reflects a more indirect process than the direct link between SMA activity and accumulation as proposed by Macar et al. (1999).

ACKNOWLEDGMENTS

The authors would like to thank Tobias Navarro Schröder for assisting with the data collection, Paolo Toffanin and Mark Span for assistance with setting up the experiment and analyzing the data, and the members of the cognitive modeling group for their useful comments. This work has been supported by the European project COST ISCH Action TD0904 "Time In MEntaL activitY: theoretical, behavioral, bioimaging, and clinical perspectives" (TIMELY; www.timely-cost.eu).

REFERENCES

Akkal, D., Escola, L., Bioulac, B., and Burbaud, P. (2004). Time predictability modulates pre-supplementary motor area neuronal activity. *Neuroreport* 15, 1283–1286.

Baayen, R H. (2008). *Analyzing Linguistic Data: A Practical Introduction to Statistics Using R*. Cambridge: Cambridge University Press.

Casini, L., Macar, F., and Giard, M. H. (1999). Relation between level of prefrontal activity and subject's performance. *J. Psychophysiol.* 13, 117–125.

Coull, J. T., Cheng, R. K., and Meck, W. H. (2010). Neuroanatomical and neurochemical substrates of timing. *Neuropsychopharmacology* 36, 3–25.

Coull, J. T., Vidal, F., Nazarian, B., and Macar, F. (2004). Functional anatomy of the attentional modulation of time estimation. *Science* 303, 1506–1508.

Creelman, C. D. (1962). Human discrimination of auditory duration. *J. Acoust. Soc. Am.* 34, 582–593.

Cui, X., Stetson, C., Montague, P. R., and Eagleman, D. M. (2009). Ready...go: amplitude of the FMRI signal encodes expectation of cue arrival time. *PLoS Biol.* 7, e1000167. doi: 10.1371/journal.pbio.1000167

Durstewitz, D. (2003). Self-organizing neural integrator predicts interval times through climbing activity. *J. Neurosci.* 23, 5342–5353.

Durstewitz, D. (2004). Neural representation of interval time. *Neuroreport* 15, 745–749.

Elbert, T., Ulrich, R., Rockstroh, B., and Lutzenberger, W. (1991). The processing of temporal intervals reflected by CNV-like brain potentials. *Psychophysiology* 28, 648–655.

Forstmann, B. U., Dutilh, G., Brown, S., Neumann, J., Von Cramon, D. Y., Ridderinkhof, K. R., and Wagenmaker, E. J. (2008). Striatum and pre-SMA facilitate decision-making under time pressure. *Proc. Natl. Acad. Sci. U.S.A.* 105, 17538–17542.

Gelman, A., and Hill, J. (2007). *Data Analysis Using Regression and Multilevel/Hierarchical Models*. New York: Cambridge University Press.

Gibbon, J. (1977). Scalar expectancy theory and Weber's law in animal timing. *Psychol. Rev.* 84, 279–325.

Gibbon, J., and Allan, L. (1984). *Timing and Time Perception*. New York: New York Academy of Sciences.

Gibbons, H., and Rammsayer, T. H. (2004). Current-source density analysis of slow brain potentials during time estimation. *Psychophysiology* 41, 861–874.

Gratton, G., Coles, M. G., and Donchin, E. (1983). A new method for off-line removal of ocular artifact. *Electroencephalogr. Clin. Neurophysiol.* 55, 468–484.

Hjorth, B. (1975). An on-line transformation of EEG scalp potentials into orthogonal source derivations. *Electroencephalogr. Clin. Neurophysiol.* 39, 526–530.

Ladanyi, M., and Dubrovsky, B. (1985). CNV and time-estimation. *Int. J. Neurosci.* 26, 253–257.

Macar, F., and Vidal, F. (2002). Time processing reflected by EEG surface Laplacians. *Exp. Brain Res.* 145, 403–406.

Macar, F., and Vidal, F. (2003). The CNV peak: an index of decision making and temporal memory. *Psychophysiology* 40, 950–954.

Macar, F., Vidal, F., and Casini, L. (1999). The supplementary motor area in motor and sensory timing: evidence from slow brain potential changes. *Exp. Brain Res.* 125, 271–280.

Macar, F., and Vitton, N. (1979). Contingent neagtive variation and accuracy of time estimation: a study on cats, Electroencephalogr. *Clin. Neurophysiol.* 47, 213–228.

Macar, F., and Vidal, F. (2004). Event-related potentials as indices of time processing: a review. *J. Psychophysiol.* 18, 89–104.

McAdam, D. W. (1966). Slow potential changes recorded from human brain during learning of a temporal interval. *Psychonomic Sci.* 6, 435–436.

Mita, A., Mushiake, H., Shima, K., Matsuzaka, Y., and Tanji, J. (2009). Interval time coding by neurons in the presupplementary and supplementary motor areas. *Nat. Neurosci.* 12, 502–507.

Perrin, F., Pernier, J., Bertrand, O., and Echallier, J. F. (1989). Spherical splines for scalp potential and current-density mapping. *Electroencephalogr. Clin. Neurophysiol.* 72, 184–187.

Pfeuty, M., Ragot, R., and Pouthas, V. (2003). When time is up: CNV time course differentiates the roles of the hemispheres in the discrimination of short tone durations. *Exp. Brain Res.* 151, 372–379.

Pfeuty, M., Ragot, R., and Pouthas, V. (2005). Relationship between CNV and timing of an upcoming event. *Neurosci. Lett.* 382, 106–111.

Pinheiro, J. C., and Bates, D. M. (2000). *Mixed-Effects Models in S and S-Plus.* New York: Springer.

Pouthas, V. (2003). "Electrophysiological evidence for specific processing of temporal information in humans," in *Functional and Neural Mechanisms of Interval Timing,* ed. W. H. Meck (Boca Raton: CRC Press), 439–456.

Pouthas, V., Garnero, L., Ferrandez, A. M., and Renault, B. (2000). ERPs and PET analysis of time perception: spatial and temporal brain mapping during visual discrimination tasks. *Hum. Brain Mapp.* 10, 49–60.

Praamstra, P., Kourtis, D., Kwok, H. F., and Oostenveld, R. (2006). Neurophysiology of implicit timing in serial choice reaction-time performance. *J. Neurosci.* 26, 5448–5455.

Royston, P., Altman, D. G., and Sauerbrei, W. (2006). Dichotomizing continuous predictors in multiple regression: a bad idea. *Stat. Med.* 25, 127–141.

Ruchkin, D. S., McCalley, M. G., and Glaser, E. M. (1977). Event related potentials and time estimation. *Psychophysiology* 14, 451–455.

Simen, P., Balci, F., deSouza, L., Cohen, J. D., and Holmes, P. (2011). Interval timing by long-range temporal integration. *Front. Integr. Neurosci.* 5:28. doi: 10.3389/fnint.2011.00028

Taatgen, N. A., and Van Rijn, H. (2011). Traces of times past: representations of temporal intervals in memory. *Mem. Cognit.* doi: 10.3758/s13421-011-0113-0. [Epub ahead of print].

Taatgen, N. A., Van Rijn, H., and Anderson, J. (2007). An integrated theory of prospective time interval estimation: the role of cognition, attention, and learning. *Psychol. Rev.* 114, 577–598.

Tarantino, V., Ehlis, A. C., Baehne, C., Boreatti-Huemmer, A., Jacob, C., Bisiacchi, P., and Fallgatter, A. J. (2010). The time course of temporal discrimination: an ERP study. *Clin. Neurophysiol.* 121, 43–52.

Tecce, J. J. (1972). Contingent negative variation (CNV) and psychological processes in man. *Psychol. Bull.* 77, 73–108.

Treisman, M. (1963). Temporal discrimination and the indifference interval. Implications for a model of the "internal clock." *Psychol. Monogr.* 77, 1–31.

Van Rijn, H., and Taatgen, N. A. (2008). Timing of multiple overlapping intervals: how many clocks do we have? *Acta Psychol.* 129, 365–375.

Vidal, F., Burle, B., Grapperon, J., and Hasbroucq, T. (2011). An ERP study of cognitive architecture and the insertion of mental processes: Donders revisited. *Psychophysiology* 48, 1242–1251.

Vidal, F., Grapperon, J., Bonnet, M., and Hasbroucq, T. (2003). The nature of unilateral motor commands in between-hand choice tasks as revealed by surface Laplacian estimation. *Psychophysiology* 40, 796–805.

Wainer, H., Gessaroli, M., and Verdi, M. (2006). Finding what is not there through the unfortunate binning of results: the mendel effect. *Chance* 19, 49–52.

Walter, W. G. (1964). Slow potential waves in the human brain associated with expectancy, attention and decision. *Arch. Psychiatr. Nervenkr.* 206, 309–322.

Wearden, J. H. (1991). Do humans possess an internal clock with scalar timing properties? *Learn. Motiv.* 22, 59–83.

Weinberg, H., Walter, W. G., Cooper, R., and Aldridge, V. J. (1974). Emitted cerebral events. *Electroencephalogr. Clin. Neurophysiol.* 36, 449–456.

Zakay, D., and Block, R. A. (1997). Temporal cognition. *Curr. Dir. Psychol. Sci.* 6, 12–16.

Conflict of Interest Statement: The authors declare that the research was conducted in the absence of any commercial or financial relationships that could be construed as a potential conflict of interest.

Received: 12 June 2011; paper pending published: 27 June 2011; accepted: 17 August 2011; published online: 13 September 2011.

Citation: Kononowicz TW and van Rijn H (2011) Slow potentials in time estimation: the role of temporal accumulation and habituation. Front. Integr. Neurosci. ***5****:48. doi: 10.3389/fnint.2011.00048*

frontiers in
INTEGRATIVE NEUROSCIENCE

PERSPECTIVE ARTICLE
published: 27 December 2011
doi: 10.3389/fnint.2011.00091

Contingent negative variation and its relation to time estimation: a theoretical evaluation

Hedderik van Rijn[1]*, Tadeusz W. Kononowicz[1], Warren H. Meck[2], Kwun Kei Ng[3] and Trevor B. Penney[3]

[1] Experimental Psychology, University of Groningen, Groningen, Netherlands
[2] Department of Psychology and Neuroscience, Duke University, Durham, NC, USA
[3] Department of Psychology, National University of Singapore, Singapore

Edited by:
Agnes Gruart, University Pablo de Olavide, Spain

Reviewed by:
Walter Ritter, The City College of New York, USA
Virginie van Wassenhove, Cognitive Neuroimaging Unit, France

***Correspondence:**
Hedderik van Rijn, Experimental Psychology, University of Groningen, Grote Kruistraat 2/1, 9712 TS Groningen, Netherlands.
e-mail: hedderik@van-rijn.org

The relation between the contingent negative variation (CNV) and time estimation is evaluated in terms of temporal accumulation and preparation processes. The conclusion is that the CNV as measured from the electroencephalogram (EEG) recorded at fronto-central and parietal-central areas is not a direct reflection of the underlying interval timing mechanism(s), but more likely represents a time-based response preparation/decision-making process.

Keywords: timing and time perception, temporal accumulation, response preparation, EEG/ERP, fronto-central and parietal-central areas

Half a century after the discovery of the contingent negative variation (CNV, Walter et al., 1964), it is still unclear what drives this slow negative wave in the electroencephalogram (EEG) when a participant is anticipating an event of interest. From the beginning, it has been suggested that the CNV, and more specifically its amplitude, reflects expectancy or motivation, all related to the intention to perform an act (e.g., McAdam et al., 1969; for a review, see Tecce, 1972). As the CNV only fully develops when a response is required at a predictable point in time, it depends on accurate temporal preparation, which requires the ability to estimate time. This ability has often been explained in terms of the influential pacemaker-accumulator models of interval timing (e.g., Treisman, 1963; Gibbon et al., 1984; Meck, 1996; Wearden, 1999; Meck and Benson, 2002; Taatgen et al., 2007). Given the similarity between the CNV and the hypothesized characteristics of the accumulation process in these models, it has been proposed that the CNV is the signature of a neural substrate of the temporal accumulator (see Macar and Vidal, 2009). According to the proponents of this view, a number of empirical studies support this hypothesis. Here we critically review these studies, focusing on two claims that are key to the idea that the CNV reflects the temporal accumulator.

PERFORMANCE-DEPENDENT VARIATIONS OF THE CNV

If the amplitude of the CNV is related to the value of the temporal accumulator, variations in the CNV should be reflected in timing performance. Macar et al. (1999, Experiment 1) observed a correlation between the reproduced duration and the CNV amplitude, a finding that has been interpreted as evidence in support of this hypothesis. In Macar et al.'s experiment, participants were asked to repeatedly reproduce an interval of 2.5 s. The average CNV amplitude was calculated separately for trials in which participants responded too early (2.2–2.4 s), correctly (2.4–2.6 s), or too long (2.6–2.8 s), and showed a positive correlation with reproduced duration (see Figure 1 in Casini and Vidal, 2011 for an illustration of these findings).

At first glance, this correlation between the CNV and the assumed state of the accumulator seems to be strong support in favor of the hypothesis that the CNV directly reflects the accumulation process. However, a careful analysis of the arguments in terms of the default pacemaker-accumulator model reveals a number of inconsistencies. For example, if the speed of the pacemaker is higher, pulses accumulate more quickly, and therefore, the threshold should be reached earlier. In other words, if larger CNV amplitudes reflect more accumulated pulses, then why don't participants respond before the target duration on high-amplitude CNV trials and after the target duration on low-amplitude CNV trials? Assuming continuous comparisons between the accumulator and threshold, the estimated duration should be "shorter" with higher pacemaker speeds since the threshold will be reached sooner and vice versa with lower pacemaker speeds.

Differences in amplitude can, in the context of a threshold-based pacemaker-accumulator account, only be explained when it is assumed that the comparisons between the accumulator and threshold are not continuously made. If comparisons are not made continuously, the number of pulses that reaches the accumulator between two comparisons is the maximum overshoot (plus one) that can be observed, yielding a correlation between the speed of the pacemaker and the value of the accumulator at the response. For example, if the threshold is known to be 100 pulses and five pulses reach the accumulator between subsequent threshold-accumulator comparisons, the maximum observed amplitude reflects $99 + 5 = 104$ pulses. However, if the speed of the pacemaker is doubled, the maximum amplitude is $99 + 10 = 109$ pulses. Although this might explain how an

increased pulse rate results in an increased CNV amplitude, the threshold will still be reached before (or at) the standard time. In other words, it is difficult to explain how a higher speed should result in increased CNV amplitudes *and* longer estimations if one assumes that the basic pacemaker-accumulator model is correct. An association between short estimations and lower CNV amplitudes is even more difficult to explain in the context of a threshold-driven pacemaker-accumulator model. If the CNV is still below the average value, it is unlikely that the accumulator already has reached the threshold.

An alternative explanation, favored by Macar et al. (1999), is that the trials resulting in "short," "correct," and "long" durations accumulate up to different thresholds. These investigators assume that the intrinsic properties of the neural system cause an increase in activation after the onset of an interval and that the response is given when the peak of activation is reached (Macar et al., 1999; Macar and Vidal, 2009). Thus, if an onset results in a higher boost of activation, the CNV will have a higher amplitude and a later deflection point, resulting in longer estimations. Although the idea of variations in threshold is often found in the literature (see, for example, computational models of the role of memory in interval timing, e.g., Jazayeri and Shadlen, 2010; Taatgen and van Rijn, 2011), this is not typically associated with performance-dependent variations in the CNV. This is not surprising because a link between different thresholds and CNV amplitudes would imply that different durations (e.g., durations of 1, 2, and 3 s) are associated with different amplitudes, whereas these correlations are not typically found (e.g., Elbert et al., 1991; Gibbons and Rammsayer, 2004; Praamstra et al., 2006, and see Praamstra, 2010 for a review of foreperiod effects).

In light of these theoretical issues, it is relevant to mention that Kononowicz and van Rijn (2011) recently failed to replicate the findings of Macar et al. (1999). In two experiments, which were close replicates of the original study, no performance-dependent variations in the CNV were found. In addition, Kononowicz and van Rijn (2011) found a habituation effect, which is not in line with the predicted role of the CNV, i.e., if the amplitude of the CNV has a one-to-one mapping to the state of the accumulator, it would be implausible for the CNV amplitude to diminish over the scope of the experiment while the time estimations stay constant. It should be noted that the Kononowicz and van Rijn (2011) study is not the only reported failure to replicate these results, as one condition of a study by Macar and Vidal (2002, labeled "Condition 1") was a close replication of the original experiment, but no performance-dependent variations in the CNV were observed. Moreover, although it may be that differences in CNV cannot be readily generalized to differences in blood oxygen level-dependent (BOLD) response, no performance-dependent variations in the pre-supplementary motor area (SMA, typically associated with the CNV) BOLD signal were found in a functional magnetic resonance imaging (fMRI) replication of the 1999 study (Macar et al., 2004). However, other studies have found differences in BOLD response during the reproduction and estimation of different intervals. For example, a stronger BOLD response was found in many brain areas, including the SMA, during the estimation and reproduction of a 1300 ms interval than during the estimation and reproduction of a 450 ms interval (Pouthas et al., 2005). Interestingly, when participants had to encode and reproduce durations of 9–18 s in a study by Wittmann et al. (2010), the activation of the posterior insula resembled an accumulation process, but the SMA activation followed an inverse U-shape pattern during encoding. Thus, although fMRI studies have been able to identify brain areas that are differentially active during the processing of different durations, it appears that the basic effects reported by Macar et al. (1999) are difficult to replicate in both EEG and fMRI studies.

A second experiment reported in Macar et al. (1999) has also been interpreted in favor of performance-dependent variations in the CNV. In this experiment, participants learned a standard duration and were later asked to categorize presented durations as either shorter, equal, or longer than the standard. The predicted pattern was found between CNV and duration estimation, with trials categorized as "long" being associated with a higher amplitude CNV than the trials categorized as "short." This finding was replicated in a study by Bendixen et al. (2005) in which participants had to indicate whether a 480 or 520 ms tone was longer or shorter than a previously learned standard of 500 ms.

However, these performance-dependent variations are difficult to reconcile with studies that show that the CNV deflects or resolves after a standard has been reached (e.g., Macar and Vidal, 2003, see also, Pfeuty et al., 2003, 2005; Ng et al., 2011). If the decision to categorize a particular trial as "long" is made on the basis of a comparison to the standard, then in these trials the accumulator should have already reached the value of the standard. This notion is supported by the duration bisection data presented in Ng et al. (2011). In this experiment, participants were presented a "long" and a "short" anchor of 800 and 3200 ms, and were asked to categorize seven intermediate durations as either more similar to the "long," or to the "short" anchor. When combining the three intermediate conditions (1270, 1600, and 2016 ms) in which neither answer category was dominant, a partial least squares analysis (McIntosh and Lobaugh, 2004) revealed that when a "long" categorization was given, the CNV was either similar to or had a lower amplitude than when a short categorization was provided. Moreover, although EEG differences have been observed in duration bisection for trials participants categorized as "short" or "long," this effect is related to the power of the alpha band in event-related synchronization rather than the amplitude of the CNV (Ng et al., 2011).

Thus, recent electrophysiological studies from a number of labs indicate that the presentation of a stimulus duration longer than the standard is associated with a deflection of the CNV at the time of the standard. As an "equal" response will be based on the accumulator reaching the threshold at the perceived time of stimulus offset, a "long" response assumes that the accumulator had reached the threshold some time before the offset of the stimulus. This in turn implies that the deflection should already have been observed and thus that the CNV amplitude for "long" estimations is lower than that for "short" or "correct" estimations. As higher CNV amplitudes were observed for the "long" estimations in Experiment 2 of Macar et al. (1999), these results are difficult to reconcile with a consistent application of the hypothesis that the CNV reflects function of the accumulator proposed

by pacemaker-accumulator models (Gibbon et al., 1984; Meck, 1996; Meck and Benson, 2002).

To summarize, although stable performance-dependent variations of the CNV would be evidence in favor of the CNV as the signature of a neural substrate of the temporal accumulator, none of the above-mentioned studies provides unequivocal evidence in favor of that view.

LOCALIZATION OF THE CNV

If the CNV reflects the neural substrate of the temporal accumulator, its location should be fairly stable. And indeed, both fMRI and EEG/Magnetoencephalography studies (see, for example, Pouthas, 2003; Meck et al., 2008; Coull et al., 2011; Schwartze et al., in press, for an overview) have shown that the SMA subserves a variety of timing tasks. However, arguing that this proves that the SMA serves as the common accumulator for temporal processing is an error of omission. That is, many EEG studies over the years have found CNV-like patterns at different locations. For example, Praamstra et al. (2006) have shown in a foreperiod study that the strongest signal was observed at the lateralized pre-motor cortices instead of at SMA, a finding that is in line with evidence from primate neurophysiology (Mauritz and Wise, 1986) and fMRI studies (e.g., Schubotz et al., 2000). Moreover, single-cell recording studies have shown ramping activation in neurons in the posterior parietal cortex (Leon and Shadlen, 2003), and the earlier mentioned fMRI study by Wittmann et al. (2010) has demonstrated accumulation patterns in the posterior insula.

As all of these locations show a ramping pattern of activation, all of these locations could, in principle, be a neural substrate of temporally mediated response preparation. These findings have, therefore, supported the view (e.g., Praamstra, 2010) that distinct neural substrates are implicated in temporal preparation in a task-dependent manner, probably depending on the type of temporal processing that is required for a particular behavior. In other words, although the activation measured at the SMAs does have a link with temporal performance, it is unlikely that the SMAs are the sole receiver of temporal information (see Buhusi and Meck, 2005 as well as Wiener et al., 2010, for a meta-analysis).

This idea is further supported by a recent fMRI study that examined which brain areas were uniquely involved in interval timing, and which brain areas were also influenced by non-temporal tasks (Livesey et al., 2007—see also Meck et al., 2008). Interestingly, the levels of activation measured in small portions of the inferior frontal gyrus, the anterior insulae and the left supramarginal gyrus, and the putamen were only influenced by time estimation, whereas the pre-SMA was also strongly influenced by the difficulty of the non-temporal task. This result led the authors to suggest that areas other than the pre-SMA are critically involved in temporal processing, and that activity in the pre-SMA is related to cognitive effort or task difficulty.

WHAT DOES THE CNV REPRESENT?

However, what does the buildup of negativity represent if the CNV is not the reflection of the accumulator of temporal information? Two proposals will be discussed here. The first proposes a direct link between oscillatory processes and the CNV and assumes that the CNV increases over time as larger groups of neurons fire simultaneously. The second proposal assumes that the CNV reflects a time-based preparation process.

Many of the CNV results could be viewed as being consistent with an "oscillator" process if one makes the following assumptions: (1) Scalp detected event-related potential (ERP) components, like the CNV, reflect postsynaptic potentials (PSPs) synchronized across many (i.e., thousands of) neurons. (2) The periodic cortical neurons that form a core component of oscillatory models (e.g., striatal beat-frequency model of Matell and Meck, 2000, 2004—see Oprisan and Buhusi, 2011) normally fire at random with respect to each other. Hence, summation of the PSPs that precede those action potentials is maintained at some baseline level. This is true both for neurons that have the same, as well as different periods. (3) According to the striatal beat-frequency model, a signal emitted from the substantia nigra at signal onset acts as a "start-gun" to reset the periodic cortical neurons such that neurons with the same periodicity are synchronized and those with different periodicities share the same initial start point. (4) As the timing signal elapses, the number of near simultaneous PSPs should increase and, therefore, the EEG mean voltage should move away from the baseline level present when the periodic neurons are active at random with respect to each other. Resolution of the CNV occurs when the periodicities return to a "random" relationship with each other, or when the oscillators are reset to start timing a new interval. Such a proposal has some obvious limitations, but it provides a reasonable account of some of the EEG/ERP effects that can be accounted for by oscillatory models and, equally important, it should be possible to design ways to test it (MacDonald and Meck, 2004, 2006; Brannon et al., 2008).

Another explanation of the CNV phenomena assumes that the CNV reflects readiness or preparation for the processing of an event instead of temporal accumulation (e.g., Elbert, 1993). According to this view, the increased negativity (which results in decreased information processing thresholds) reflects the anticipation of an upcoming and relevant event. Data that supports this view has both been provided using CNV-related research (for review see Elbert, 1993) and more recent fMRI research. For example, Forstmann and van Maanen (Forstmann et al., 2008; van Maanen et al., in press) have shown in a series of studies that the pre-SMA is more active in conditions in which a fast response is required than in conditions in which an accurate response is expected. Using similar arguments as Elbert (1993), Forstmann and van Maanen link the activity of the pre-SMA to a reduction of inhibition at the level of the basal ganglia. Combined, this work supports the idea that the buildup of negativity is not a source of temporal information, but a consequence of a temporal preparation for an upcoming event.

The "temporal preparation" hypothesis is supported by the Ng et al. (2011) duration-bisection study discussed above. An analysis of the EEG data showed a negative deflection, which started at the onset of the to-be bisected duration, and reached its maximum at 800 ms, the "short" anchor duration. Interestingly, the amplitude remained stable for about 800 ms, after which the CNV began to resolve. The deflection point at 1600 ms corresponds with the stimulus duration at which the participants switched from predominantly answering "short" to "long," and

is as such comparable to the effects found in the temporal generalization study of Macar and Vidal (2003). However, the stable CNV amplitude between 800 and 1600 ms (and similar stable patterns in Elbert et al., 1991 and Gibbons and Rammsayer, 2004) is difficult to reconcile with a direct link between the CNV and the temporal accumulator, as in this view a stable CNV amplitude indicates a constant subjective perceived duration. A constant subjective duration would have resulted in erratic performance, something that was not observed. In contrast, Ng et al. (2011) interpreted the boundaries of the plateau as two target durations, with the first target duration indicating that a relevant signal might appear from that point on, and the second target duration indicating that any upcoming signal would carry less relevance since the answer ("long") could already be deduced based on the passage of time. Consequently, these findings support the view that the CNV amplitude reflects the expectancy of a relevant event, something that is based on temporal information, but not the source of temporal information.

In conclusion, experiments that are often cited in favor of a direct link between the CNV and the temporal accumulator cannot be straightforwardly interpreted, and have shown to be difficult to replicate. It is, therefore, our view that proposals based on this direct link need to be re-evaluated in light of the inconsistencies in the supporting EEG data and lack of congruence with physiologically plausible models of interval timing (see Allman and Meck, in press; Coull et al., 2011; Matell et al., 2011; Oprisan and Buhusi, 2011; Portugal et al., 2011; Simen et al., 2011).

REFERENCES

Allman, M. J., and Meck, W. H. (in press). Pathophysiological distortions in time perception and timed performance. *Brain*.

Bendixen, A., Grimm, S., and Schröger, E. (2005). Human auditory event-related potentials predict duration judgments. *Neurosci. Lett.* 383, 284–288.

Brannon, E. M., Libertus, M. E., Meck, W. H., and Woldorff, M. G. (2008). Electrophysiological measures of time processing in infant and adult brains: Weber's law holds. *J. Cogn. Neurosci.* 20, 193–203.

Buhusi, C. V., and Meck, W. H. (2005). What makes us tick? Functional and neural mechanisms of interval timing. *Nat. Rev. Neurosci.* 6, 755–765.

Casini, L., and Vidal, F. (2011). The SMAs: neural substrate of the temporal accumulator. *Front. Integr. Neurosci.* 5, 35. doi: 10.3389/fnint.2011.00035

Coull, J. T., Cheng, R. K., and Meck, W. H. (2011). Neuroanatomical and neurochemical substrates of timing. *Neuropsychopharmacology* 36, 3–25.

Elbert, T. (1993). "Slow cortical potentials reflect the regulation of cortical excitability," in *Slow Potential Changes in the Human Brain (NATO Sciences Series: A)*, eds W. C. McCallum and S. H. Curry (New York: Plenum Press), 235–251.

Elbert, T., Ulrich, R., Rockstroh, B., and Lutzenberger, W. (1991). The processing of temporal intervals reflected by CNV-like brain potentials. *Psychophysiology* 28, 648–655.

Forstmann, B. U., Dutilh, G., Brown, S., Neumann, J., von Cramon, D. Y., Ridderinkhof, K. R., and Wagenmakers, E. J. (2008). Striatum and pre-SMA facilitate decision-making under time pressure. *Proc. Natl. Acad. Sci. U.S.A.* 105, 17538–17542.

Gibbon, J., Church, R. M., and Meck, W. H. (1984). Scalar timing in temporal memory. *Ann. N.Y. Acad. Sci.* 423, 52–77.

Gibbons, H., and Rammsayer, T. H. (2004). Current-Source density analysis of slow brain potentials during time estimation *Psychophysiology* 41, 861–874.

Jazayeri, M., and Shadlen, M. N. (2010). Temporal context calibrates interval timing. *Nat. Neurosci.* 13, 1020–1026.

Kononowicz, T. W., and van Rijn, H. (2011). Slow potentials in time estimation: the role of temporal accumulation and habituation. *Front. Integr. Neurosci.* 5, 48. doi: 10.3389/fnint.2011.00048

Leon, M. I., and Shadlen, M. N. (2003). Representation of time by neurons in the posterior parietal cortex of the macaque. *Neuron* 38, 317–327.

Livesey, A. C., Wall, M. B., and Smith, A. T. (2007). Time perception: manipulation of task difficulty dissociates clock functions from other cognitive demands. *Neuropsychologia* 45, 321–331.

Macar, F., Anton, J. L., Bonnet, M., and Vidal, F. (2004). Timing functions of the supplementary motor area: an event-related fMRI study. *Brain Res. Cogn. Brain Res.* 21, 206–215.

Macar, F., and Vidal, F. (2002). Time processing reflected by EEG surface Laplacians. *Exp. Brain Res.* 145, 403–406.

Macar, F., and Vidal, F. (2003). The CNV peak: an index of decision making and temporal memory. *Psychophysiology* 40, 950–954.

Macar, F., and Vidal, F. (2009). Timing processes: an outline of behavioural and neural indices not systematically considered in timing models. *Can. J. Exp. Psychol.* 63, 227–239.

Macar, F., Vidal, F., and Casini, L. (1999). The supplementary motor area in motor and sensory timing: evidence from slow brain potential changes. *Exp. Brain Res.* 125, 271–280.

MacDonald, C. J., and Meck, W. H. (2004). Systems-level integration of interval timing and reaction time. *Neurosci. Biobehav. Rev.* 28, 747–769.

MacDonald, C. J., and Meck, W. H. (2006). Interaction of raclopride and preparatory-interval effects on simple reaction-time performance. *Behav. Brain Res.* 175, 62–74.

Matell, M. S., and Meck, W. H. (2000). Neuropsychological mechanisms of interval timing behavior. *Bioessays* 22, 94–103.

Matell, M. S., and Meck, W. H. (2004). Cortico-striatal circuits and interval timing: coincidence detection of oscillatory processes. *Brain Res. Cogn. Brain Res.* 21, 139–170.

Matell, M. S., Shea-Brown, E., Gooch, C., Wilson, A. H., and Rinzel, J. (2011). A heterogeneous population code for elapsed time in rat medial agranular cortex. *Behav. Neurosci.* 125, 54–73.

Mauritz, K. H., and Wise, S. P. (1986). Premotor cortex of the rhesus monkey: neuronal activity in anticipation of predictable environmental events. *Exp. Brain Res.* 61, 229–244.

McAdam, D. W., Knott, J. R., and Rebert, C. S. (1969). Cortical slow potential changes in man related to interstimulus interval and to pre-trial prediction of interstimulus interval. *Psychophysiology* 5, 349–358.

McIntosh, A. R., and Lobaugh, N. J. (2004). Partial least squares analysis of neuroimaging data: applications and advances. *Neuroimage* 23, 250–263.

Meck, W. H. (1996). Neuropharmacology of timing and time perception. *Brain Res. Cogn. Brain Res.* 3, 227–242.

Meck, W. H., and Benson, A. M. (2002). Dissecting the brain's internal clock: how frontal-striatal circuitry keeps time and shifts attention. *Brain Cogn.* 48, 195–211.

Meck, W. H., Penney, T. B., and Pouthas, V. (2008). Cortico-striatal representation of time in animals and humans. *Curr. Opin. Neurobiol.* 18, 145–152.

Ng, K. K., Tobin, S., and Penney, T. B. (2011). Temporal accumulation and decision processes in the duration bisection task revealed by contingent negative variation. *Front. Integr. Neurosci.* 5, 77. doi: 10.3389/fnint.2011.00077

Oprisan, S. A., and Buhusi, C. V. (2011). Modeling pharmacological clock and memory patterns of interval timing in a striatal beat-frequency model with realistic, noisy neurons. *Front. Integr. Neurosci.* 5, 52. doi: 10.3389/fnint.2011.00052

Pfeuty, M., Ragot, R., and Pouthas, V. (2003). When time is up: CNV time course differentiates the roles of the hemispheres in the discrimination of short tone durations. *Exp. Brain Res.* 151, 372–379.

Pfeuty, M., Ragot, R., and Pouthas, V. (2005). Relationship between CNV and timing of an upcoming event. *Neurosci. Lett.* 382, 106–111.

Portugal, G. S., Wilson, A. G., and Matell, M. S. (2011). Behavioral sensitivity of temporally modulated striatal neurons. *Front. Integr. Neurosci.* 5, 30. doi: 10.3389/fnint.2011.00030

Pouthas, V. (2003). "Electrophysiological evidence for specific processing of temporal information in humans," in *Functional and Neural Mechanisms of Interval Timing*, ed W. H. Meck (Boca Raton, FL: CRC Press), 439–456.

Pouthas, V., George, N., Poline, J.-B., Pfeuty, M., VandeMoorteele, P.-F.,

Hugueville, L., Ferrandez, A.-M., Lehéricy, S., LeBihan, D., and Renault, B. (2005). Neural network involved in time perception: an fMRI study comparing long and short interval estimation. *Hum. Brain Mapp.* 25, 433–441.

Praamstra, P. (2010). "Electrophysiological markers of foreperiod effects," in *Attention and Time*, eds K. Nobre and J. T. Coull (New York, NY: Oxford University Press), 331–345.

Praamstra, P., Kourtis, D., Kwok, H. F., and Oostenveld, R. (2006). Neurophysiology of implicit timing in serial choice reaction-time performance. *J. Neurosci.* 26, 5448–5455.

Schubotz, R. I., Friederici, A. D., and von Cramon, D. Y. (2000). Time perception and motor timing: a common cortical and subcortical basis revealed by fMRI. *Neuroimage* 11, 1–12.

Schwartze, M., Rothermich, K., and Kotz, S. A. (in press). Functional dissociation of pre-SMA and SMA-proper in temporal processing. *Neuroimage*.

Simen, P., Balci, F., deSouza, L., Cohen, J. D., and Holmes, P. (2011). Interval timing by long-range temporal integration. *Front. Integr. Neurosci.* 5, 28. doi: 10.3389/fnint.2011.00028

Taatgen, N., and van Rijn, H. (2011). Traces of times past: representations of temporal intervals in memory. *Mem. Cognit.* 39, 1546–1560.

Taatgen, N. A., van Rijn, H., and Anderson, J. R. (2007). An integrated theory of prospective time interval estimation: the role of cognition, attention and learning. *Psychol. Rev.* 114, 577–598.

Tecce, J. J. (1972). Contingent negative variation (CNV) and psychological processes in man. *Psychol. Bull.* 77, 73–108.

Treisman, M. (1963). Temporal discrimination and the indifference interval: implications for a model of the "internal clock". *Psychol. Monogr.* 77, 1–31.

van Maanen, L., Brown, S. D., Eichele, T., Wagenmakers, E.-J., Ho, T., Serences, J., and Forstmann, B. U. (in press). Neural correlates of trial-to-trial fluctuations in response caution. *J. Neurosci.*

Walter, W. G., Cooper, R., Aldrigde, V. J., McCallum, W. C., and Winter, A. L. (1964). Contingent negative variation: an electric sign of sensori-motor association and expectancy in the human brain. *Nature* 203, 380–384.

Wearden, J. H. (1999). "Beyond the fields we know…": exploring and developing scalar timing theory. *Behav. Process.* 45, 3–21.

Wiener, M., Turkeltaub, P., and Coslett, H. B. (2010). The image of time: a voxel-wise meta-analysis. *Neuroimage* 49, 1728–1740.

Wittmann, M., Simmons, A. N., Aron, J. L., and Paulus, M. P. (2010). Accumulation of neural activity in the posterior insula encodes the passage of time. *Neuropsychologia* 48, 3110–3120.

Conflict of Interest Statement: The authors declare that the research was conducted in the absence of any commercial or financial relationships that could be construed as a potential conflict of interest.

Received: 30 October 2011; accepted: 13 December 2011; published online: 27 December 2011.

Citation: van Rijn H, Kononowicz TW, Meck WH, Ng KK and Penney TB (2011) Contingent negative variation and its relation to time estimation: a theoretical evaluation. Front. Integr. Neurosci. 5:91. doi: 10.3389/fnint.2011.00091

frontiers in
INTEGRATIVE NEUROSCIENCE

OPINION ARTICLE
published: 11 August 2011
doi: 10.3389/fnint.2011.00035

The SMAs: neural substrate of the temporal accumulator?

Laurence Casini and Franck Vidal*

Laboratoire de Neurobiologie de la Cognition, Aix-Marseille Université, CNRS, Marseille, France
**Correspondence: franck.vidall@univ-provence.fr*

One of the most widely cited models in time estimation is the "pacemaker-counter clock" which consists of a pacemaker generating pulses and an accumulator in which pulses are stored. The level reached in this accumulator at the end of an interval to be estimated sets the subjective elapsed time. Although this model is able to accurately describe temporal performance, it can nevertheless be considered no more than a good metaphor of actual temporal processing mechanisms. Finding specific brain areas behaving as a pacemaker and/or as an accumulator would provide additional support for this model. Evidence has now been amassed suggesting that the SMAs could be a neural substrate of the accumulator.

EEG EVIDENCE FOR A CUMULATIVE PROCESS IN THE SMA

In two different timing tasks (a production and a discrimination one) Macar et al. (1999) showed that the mesial frontal cortex, including the SMAs, behaves in an accumulator-like way. The authors recorded the contingent negative variation (CNV: Walter et al., 1964) an electrical activity of the brain which develops between two events of interest separated by a predictable time interval. In line with the results of Casini and Macar (1997), the authors hypothesized that spontaneous fluctuations of brain activation should influence the speed of the pacemaker, determining the number of accumulated pulses and, hence, subjective temporal estimation. Using the CNV as an index of the accumulation process, Macar et al. (1999) observed that the larger the estimated duration, the larger the CNV over the SMAs (**Figure 1**). These observations, suggesting that the SMAs act as an accumulator, have since been reproduced with identical intervals (Macar and Vidal, 2002) and with shorter intervals involving the auditory modality (Bendixen et al., 2005). Moreover, Noguchi and Kakigi (2006) recorded the magnetic counterpart of the CNV in a timing task and observed the same magnetic build-up of activity around the SMAs during the interval to be estimated. In addition, Noguchi and Kakigi found a positive correlation between the amplitude of the visual evoked magnetic field (VEF) and the size of the CNV-like field. If one hypothesizes that the amplitude of the VEF can be interpreted as an index of activation, a larger VEF is representative of a larger activation which, in agreement with the concept proposed by Macar et al. (1999) should be associated with more accumulated pulses and, hence, a larger magnetic CNV.

FMRI EVIDENCE FOR A CUMULATIVE PROCESS IN THE SMA

Functional magnetic resonance imaging data also point toward the SMAs playing a key role in time processing. According to Zakay (1989), the more attention is paid to time, the more pulses are accumulated, which accounts for the well known effects of attention on timing performance (e.g., Casini and Macar, 1996; for a review see Brown, 1997). Coull et al. (2004) showed that when the amount of attention is explicitly controlled SMA activity positively correlates with attention paid to timing. SMAs therefore behave as the accumulator postulated by the model. In addition, in reproduction tasks where time has to be successively coded and retrieved, the pacemaker-counter model postulates that the accumulator is necessarily switched on at the beginning of both stages (coding and retrieval). Several brain areas have now been shown to be active in a reproduction task. However, the SMAs were the only area to be engaged during both stages of the task (**Figure 2**; Coull et al., 2008). As such, the SMAs seem to be the only structure where the accumulation process can take place.

SINGLE CELL RECORDINGS EVIDENCE FOR A CUMULATIVE PROCESS IN THE SMA

Further evidence supporting the presence of a cumulative process in SMAs used for timing can be found in single unit recordings of awake monkeys, both in temporal production and estimation. In a production task, Mita et al. (2009) found neurons in the SMA and pre-SMA exhibiting decay

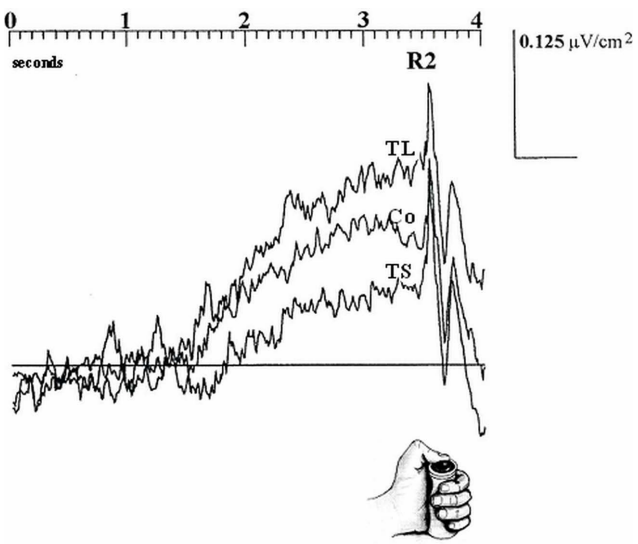

FIGURE 1 | Electrophysiological activity over the SMAs in 10 subjects during a time production task as a function of performance (TL, "too long"; Co, "correct";TS, "too short") time-locked to the end (button press) of the interval. Amplitude (negative up) on ordinates, time on abscissas. Adapted from Macar et al., 1999.

or build-up patterns evoking a cumulative process. In these so called "time graded" neurons the longer the interval to be produced, the higher the firing rate at the end of the interval (**Figure 3B**). In addition, Akkal et al. (2004) recorded neurons in the pre-SMA during a reaction time task using fixed or variable foreperiods. Only when the foreperiod was fixed, i.e., only when foreperiod duration could be accurately predicted, did pre-SMA neurons behave in an accumulator-like way: During the fixed foreperiod, neuronal activity exhibited a particular build-up pattern culminating at the end of the delay (**Figure 3A**). The authors concluded that the build-up pattern they observed could "… represent the neuronal substrate of the temporal accumulator property proposed by previous authors" (page, 1286). Indeed, the neuronal patterns observed in **Figure 3** are reminiscent of the time course of the CNV displayed in **Figure 1**.

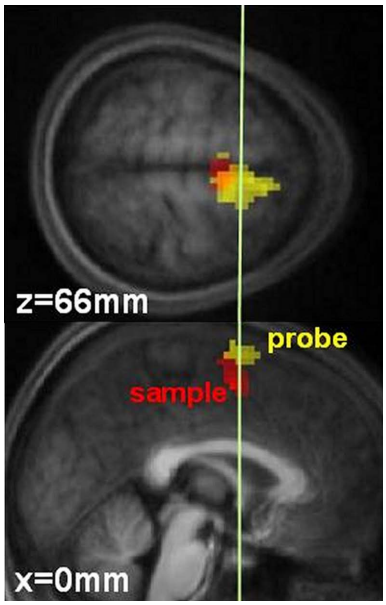

FIGURE 2 | Temporal processing by the SMAs in 14 subjects. Red represents activation obtained during sample stimuli presentation. Yellow represents activation obtained during probe stimuli presentation. The white line (y = 0 mm) denotes the border between the SMA proper and the pre-SMA. X and Z correspond to the coordinates of each slice. Adapted from Coull et al. (2008).

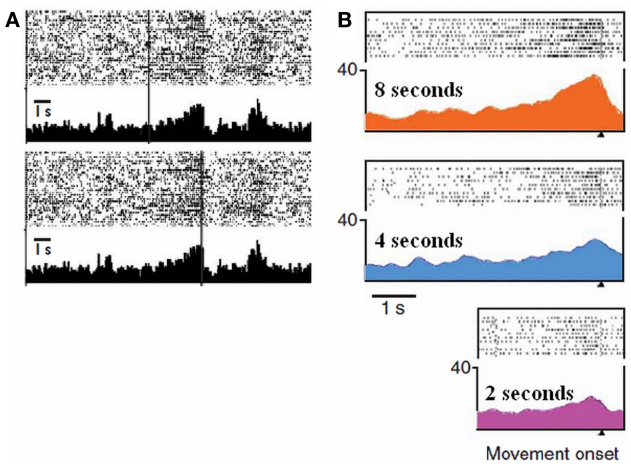

FIGURE 3 | Single unit activities as a function of elapsed time in a time estimation task (A) (adapted from Akkal et al., 2004) and in a production task (B) (adapted from Mita et al., 2009). (A) Raster displays and peri-event histograms: The figure represents an example of pre-SMA cells showing build-up neuronal activity as time elapses. The vertical bars indicate the onset (top) and the end (bottom) of the interval. Note that this pattern only occurs when the end of the interval can be predicted, that is when this interval is fixed. **(B)** Raster displays and spike-density functions: The figure represents an example of pre-SMA cells showing graded neuronal activity that depended on the time intervals to be produced: highest during a 8-s interval, moderate during a 4-s interval, and lowest during a 2-s interval. The displays are aligned according to the end of the produced interval.

OTHER TIMING PROCESSES OUTSIDE THE SMAS?

Where could pulses stored in the SMAs come from? Several arguments provided by animal as well as patient studies indicate that the basal ganglia could host the pacemaker system (for reviews see Buhusi and Meck, 2005; Coull et al., 2011). For example, dopaminergic drugs are known to selectively affect the speed of an internal clock in both animals and humans. Moreover, patients with Parkinson's disease show impaired temporal performance in both motor and sensory timing within both the second and sub-second time ranges. It should be noted that the SMAs are one of the main targets of the basal ganglia *via* the thalamus.

Finally, it is often assumed that to provide accurate timing, in addition to specific "clock" processes, distinct non-specific memory, and decisional components are also required. When subjects have to memorize a "target" duration and judge whether a probe interval is shorter, equal or longer, the CNV recorded during the probe ends at the moment when the target would end, even when the probe lasts longer (Macar and Vidal, 2003; Pfeuty et al., 2003). It is noteworthy that during these longer probes no external information indicates that the target duration is over. Therefore, this effect may only be explained by assuming subjects used internal information which can be viewed as temporal memory. However, Macar and Vidal (2003) showed that this temporal memory effect was not implemented by the SMAs but in other, not currently fully identified, structures. In sum, the functional role of the SMA in timing seems well confined to the cumulative process.

REFERENCES

Akkal, D., Escola, L., Bioulac, B., and Burbaud, P. (2004). Time predictability modulates pre-supplementary motor area neuronal activity. *Neuroreport* 15, 1283–1286.

Bendixen, A., Grimm, S., and Schroger, E. (2005). Human auditory event-related potentials predict duration judgments. *Neurosci. Lett.* 383, 284–288.

Brown, S. W. (1997). Attentional resources in timing: Interference effects in concurrent temporal and non-temporal working memory tasks. *Percept. Psychophys.* 59, 1118–1140.

Buhusi, C. V., and Meck, W. H. (2005). What makes us tick ? Functional and neural mechanisms of interval timing. *Nat. Rev. Neurosci.* 6, 755–765.

Casini, L., and Macar, F. (1996). Prefrontal slow potentials in temporal compared to nontemporal tasks. *J. Psychophysiol.* 10, 252–264.

Casini, L., and Macar, F. (1997). Effect of attention manipulation on judgments of duration and of intensity in the visual modality. *Mem. Cognit.* 25, 812–819.

Coull, J. T., Cheng, R., and Meck, W. H. (2011). Neuroanatomical and neurochemical substrates of timing. *Neuropsychopharmacol. Rev.* 36, 3–25.

Coull, J. T., Nazarian, B., and Vidal, F. (2008). Timing, storage and comparison of stimulus duration engage discrete anatomical components of a perceptual timing network. *J. Cogn. Neurosci.* 20, 2185–2197.

Coull, J. T., Vidal, F., Nazarian, B., and Macar, F. (2004). Functional anatomy of the attentional modulation of time estimation. *Science* 303, 1506–1508

Macar, F., and Vidal, F. (2002). Time processing reflected by EEG surface Laplacians. *Exp. Brain Res.* 145, 403–406.

Macar, F., and Vidal, F. (2003). The CNV peak: an index of decision making and temporal memory. *Psychophysiology* 40, 950–954.

Macar, F., Vidal, F., and Casini, L. (1999). Performance-dependent ERP changes in judgments of brief durations. *Exp. Brain Res.* 125, 271–280.

Mita, A., Mushiake, H., Shima, K., Matsuzaka, Y., and Tanji, J. (2009). Interval time coding by neurons in the presupplementary and supplementary motor areas. *Nat. Neurosci.* 12, 502–507.

Noguchi, Y., and Kakigi, R. (2006). Time representation can be made from nontemporal information in the brain: an MEG study. *Cereb. Cortex* 16, 1797–1808.

Pfeuty, M., Ragot, R., and Pouthas, V. (2003). When time is up: CNV time course differentiates the role of the hemispheres in the discrimination of short tone durations. *Exp. Brain Res.* 151, 372–379.

Walter, W. G., Cooper, R., Aldridge, V. J., McCallum, W. C., and Winter, A. L. (1964). Contingent negative variation: An electrical sign of sensorimotor association and expectancy in the human brain. *Nature* 203, 380–384.

Zakay, D. (1989). "Subjective and attentional resource allocation: an integrated model of time estimation" in *Time and Human Cognition*, ed. I. Levin and D. Zakay (North-Holland: Elsevier Science Publishers Eds.), 365–397.

Received: 26 July 2011; accepted: 26 July 2011; published online: 11 August 2011.

*Citation: Casini L and Vidal F (2011) The SMAs: neural substrate of the temporal accumulator? Front. Integr. Neurosci. **5**:35. doi: 10.3389/fnint.2011.00035*

frontiers in
INTEGRATIVE NEUROSCIENCE

OPINION ARTICLE
published: 22 December 2011
doi: 10.3389/fnint.2011.00086

Differential input of the supplementary motor area to a dedicated temporal processing network: functional and clinical implications

Sonja A. E. Kotz*† and Michael Schwartze†

Minerva Research Group "Neurocognition of Rhythm in Communication," Max Planck Institute for Human Cognitive and Brain Sciences, Leipzig, Germany
**Correspondence: kotz@cbs.mpg.de*
†Sonja A. E. Kotz and Michael Schwartze have contributed equally to this work.

The ability to track the temporal structure of events in a dynamic environment is crucial to cognition and action alike. In order to guide timely reactive and proactive behavior the individual has to draw upon some internal representation of temporal relations or temporal structure. Here an event may be defined as a perceived change in the formal structure of the environment, i.e., the identity ("what") or the position ("where") of an object. In turn, the temporal relation between events may be defined as the temporal structure ("when") of the environment.

Temporal structure develops on different timescales (Buonomano, 2007). For example, starting and stopping to walk from one position to another marks events with a certain temporal relation, typically in the seconds-to-minutes range. Yet, contact of a foot with the surface establishes another kind of event, with successive steps marking temporal structure in the milliseconds range. Such marking of the beginning and the end of an action sequence is represented in prefrontal and supplementary motor cortices (Fujii and Graybiel, 2003; Shima and Tanji, 2006). However, the question arises as to whether the perception and production of the corresponding temporal structure in the milliseconds-to-seconds range is intrinsic or whether it is based on an explicit representation generated by a dedicated temporal processing system (Karmarkar and Buonomano, 2007; Ivry and Schlerf, 2008; Spencer et al., 2009). Compelling evidence suggests that temporal processing, i.e., the neural mechanisms that engage in encoding, decoding, and evaluating of temporal structure, relies on brain regions involved in action control: the cerebellum, the basal ganglia, and the supplementary motor area (SMA; for a review see Coull et al., 2011).

However, a high-level function such as action control incorporates various lower-level processes. This becomes apparent if one considers the role of the SMA in action control. Located bilaterally in Brodmann area 6 of the medial frontal lobe, the SMA has traditionally been linked to the planning and the preparation of future, sequential, and rhythmic performance, as well as to the initiation, inhibition, preservation, and repetition of action (Brickner, 1939; Penfield, 1950; Goldberg, 1985; Tanji, 1996). Crucially, SMA lesions affect non-verbal and verbal behavior. They may result in the inability to speak, stuttering, hesitations, "slowliness," the prolonging of sounds, and persistent dysfluency, phenomena, which impact the continuous flow or pacing, i.e., the rate and rhythm of speech (Jonas, 1981; Ziegler et al., 1997). These phenomena corroborate a role of the SMA in controlling temporal relations in action, but leave open whether temporal processing is intrinsic or explicitly dedicated. However, evidence for a dedicated temporal processing system comes from studies, which confirm a role of the SMA not only in the production, but also in the perception of temporal structure (Macar et al., 2002; Ferrandez et al., 2003; Coull et al., 2004).

The SMA, or more specifically, the SMA and its striato-thalamic connections, is a candidate neural substrate for a "temporal accumulator" engaged in the encoding of temporal structure (Akkal et al., 2004; Pouthas et al., 2005; Macar et al., 2006; Casini and Vidal, 2011). Furthermore, considering a structural differentiation of the SMA into a rostral pre-SMA and a more caudal SMA-proper (Picard and Strick, 2001), it has been suggested that pre-SMA is essential for attention-dependent quantification (Coull et al., 2004; Macar et al., 2004) or "tagging" of temporal structure (Pastor et al., 2006). Such functional specification based on structural differentiation may reflect an interaction within a distributed temporal processing network, which is determined by unique connections from the pre-SMA and the SMA-proper to other cortical and subcortical regions (Johansen-Berg et al., 2004; Akkal et al., 2007).

Among others, connections from the pre-SMA target the prefrontal cortex, while connections from the SMA-proper target motor and pre-motor cortices (Johansen-Berg et al., 2004). However, the thalamus connects both pre-SMA and SMA-proper to essential nodes within a dedicated temporal processing network, namely the cerebellum and the basal ganglia. Connections from both SMA subareas to the basal ganglia maintain a rostro-caudal gradient in their structural and functional organization and establish a cortico-striato-thalamo-cortical looped system (Johansen-Berg et al., 2004; Draganski et al., 2008). Connections between the pre-SMA and the cerebellum originate in the non-motor part of the cerebellar dentate nucleus, whereas connections to the SMA-proper originate in its motor part (Dum and Strick, 2003; Akkal et al., 2007).

In general, the SMA receives more input from the basal ganglia than from the cerebellum (Akkal et al., 2007). Next to direct subcortico-subcortical connections (Hoshi et al., 2005; Bostan and Strick, 2010; Bostan et al., 2010), this structural embedding of the pre-SMA and the SMA-proper into subcortico-thalamo-cortical processing streams instantiates interaction between the cerebellum and the basal ganglia in temporal processing (Schwartze et al., in press). Note, that the role of the thalamus as a mere relay station is therefore simply underspecified (see Sherman, 2007). Rather, the thalamus should

be considered a key structure in modeling the neural basis of temporal processing. Thalamic neurons convey information to cortical targets in either a tonic or a burst firing mode (Sherman and Guillery, 2002). The tonic firing mode preserves input linearity, whereas the burst firing mode affords better input detectability. The burst firing mode is thus ideally suited to signal changes in the environment to cortical targets by means of stronger cortical excitation (Sherman, 2001). These firing mode characteristics not only support the linking of several nodes, but also allow speculating about their impact on functional interactions within such a dedicated temporal processing network (**Figure 1**).

In this network pre-SMA and SMA-proper engage in different but related aspects of temporal processing. On the one hand, in perception the pre-SMA plays a pivotal role in the allocation of attention in time and in the encoding of temporal relations conveyed in a sequence of events. On the other hand, in production, the SMA-proper engages in the corresponding implementation of sequential action. Crucially, the SMA-proper integrates information regarding the temporal relation between successive actions provided by the pre-SMA and the basal ganglia. In other words, the function of the pre-SMA relates to the explicit encoding of temporal structure in perception and production, while the SMA-proper uses this information to implement a sequential action. This account of pre-SMA function is compatible with, and extends the dual role of the pre-SMA in the planning and the acquisition of movement patterns (Tanji, 1996). If, for example, changes in the environment require the adaptation of an action sequence (i.e., walking on uneven ground) such adaptation necessitates proactive and reactive adjustments – processes, which in turn benefit from a precise representation of temporal structure. Consequently, imprecise temporal processing may affect both cognitive and motor behavior. Hence, the proposed network has major implications for the modeling of basal ganglia dysfunctions (i.e., motor and cognitive) as exemplified in Parkinson's disease (PD).

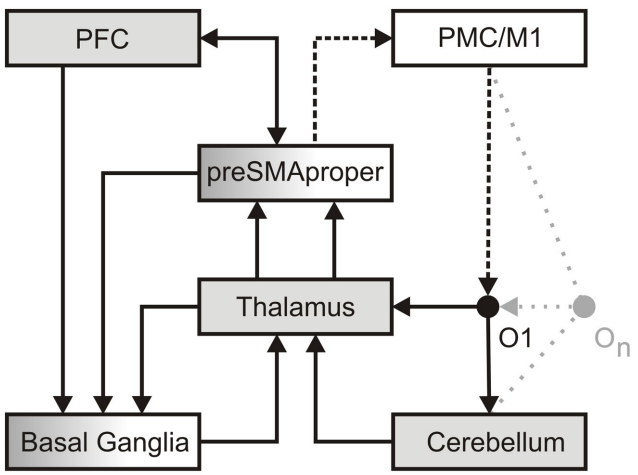

FIGURE 1 | A dedicated temporal processing network. In perception, detailed information regarding the formal structure of an object (O1) reaches the thalamus. This information is then transmitted in a linear, faithful fashion by means of thalamic tonic and burst firing (Sherman, 2001) to sensory cortices (not in view) in order to establish as well as to access a memory representation of an object. In parallel, less detailed information reaches the cerebellum. Here a salient change in the formal structure of an object is encoded as an event. A sequence of objects (O_n) may give rise to a precise event-based representation of temporal structure. Such event-based representation implicitly encodes the temporal relation between events. Potentially amplified via thalamic burst firing, events may provide attractors to adaptive cortical oscillations implicated in dynamic attending. Attention oscillations may generate an "expectancy scheme" via entrainment to different hierarchical levels of temporal structure (Large and Jones, 1999; Drake et al., 2000). Alternatively or additionally, events may activate ensembles of non-adaptive cortical oscillations, which, according to the influential striatal-beat-frequency model, provide a unique pattern of input to the basal ganglia (Matell and Meck, 2004). These oscillations serve interval-based temporal processing and, by additional recruitment of working memory, the subsequent evaluation of temporal structure. Both kinds of oscillations may reflect the combined effort of the pre-SMA and the prefrontal cortex (PFC), as well as the associated striato-thalamo-cortical loops to "tag" the temporal structure of the sequence. In production, the intention to act (PFC) draws upon the pre-SMA and its connections to the basal ganglia to initiate action and to define the temporal structure of a sequence of actions, i.e., the pre-SMA is recruited to temporally structure forthcoming motor behavior (Mita et al., 2009). The actual implementation of action (dotted line) recruits the SMA-proper and pre-motor/primary motor cortices (PMC/M1). Via its connections to the SMA-proper, the cerebellum may engage in the temporal fine-tuning of actions. In turn, each action constitutes an object in the environment. A sequence of actions (O_n) generates changes in the formal structure of the environment and establishes a sensorimotor processing cycle.

Parkinson's disease is but one of several pathologies associated with impaired temporal processing (for a review see Allman and Meck, 2011). Early on PD has been linked to temporal processing deficits both in production and perception (Pastor et al., 1992; O'Boyle et al., 1996; Harrington et al., 1998). More recent data suggest that such deficits are rather diverse and may be more pronounced in the suprasecond than the subsecond range (Smith et al., 2007; Koch et al., 2008, but see Jahanshahi et al., 2006), and probably reflect different PD subgroups (Merchant et al., 2008). These studies allow drawing conclusions about the involvement of the basal ganglia in temporal processing based on the known neuropathology of PD. However, it is evident that the basal ganglia are not the only brain region that engages in temporal processing and is affected by PD. Combined activation of the basal ganglia and the SMA is a common observation in temporal processing (e.g., Ferrandez et al., 2003; Pouthas et al., 2005; Jahanshahi et al., 2006; Stevens et al., 2007). This emphasizes that the basal ganglia and the SMA contribute to the pathogenesis of PD. Thus, if the basal ganglia and SMA are considered as nodes within a dedicated temporal processing network spanning both perception and production, the question arises as to whether connections originating in, and targeting the SMA are at the core of impaired temporal processing in PD. However, PD is a progressive disease and different stages of the disease may be reflected in dynamic changes in the network. For example, a selective loss of pyramidal neurons in the pre-SMA in PD may cause underactivity in this region (MacDonald and Halliday, 2002), which, in turn, may result in erratic temporal processing. In contrast, stronger activation of the pre-SMA in action

sequencing may reflect an early, preclinical compensation mechanism (Van Nuenen et al., 2009). Crucially, input from the cerebellum should influence this compensatory mechanism. Hyperactivation of cerebellar-pre-SMA connections as a consequence of internally cued actions during the early clinical stages of PD further supports this view (Wu and Hallett, 2005; Eckert et al., 2006; Lewis et al., 2007). However, hyperactivation is not necessarily limited to internally cued action. Rather, it may also reflect a stronger weighting toward cerebellar-SMA connections in externally cued action (i.e., finger-tapping: Sen et al., 2010). While this perspective is compatible with the proposed temporal processing network, i.e., a role of the cerebellum in transmitting the temporal structure of changes in the environment to the pre-SMA, such compensatory activity necessitates further differentiation of cerebellar function in the perception of temporal structure.

Functional connectivity indicates that during the perception of temporal structure the cerebellum projects to regions involved in perceptual orienting including the pre-SMA (Coull et al., 2004; O'Reilly et al., 2008). The functional interpretation of a larger network affected in PD is compatible with the notion of a dedicated and integrative temporal processing network (Kotz and Schwartze, 2010). Moreover, such a framework offers a suitable explanation for the effectiveness of intervention methods such as repetitive transcranial magnetic stimulation (rTMS) that allow targeting the respective functional contribution of network areas in PD. It has been shown that rTMS affects motor planning in PD patients and controls differently (Cunnington et al., 1996). Koch et al. (2004) showed that rTMS over the SMA improved time perception, while Hamada et al. (2008) reported improved motor behavior after similar rTMS treatment over the SMA. The fact that different rTMS protocols (Koch, 2010) and stimulation of target network nodes (i.e., bilateral cerebellum and SMA) lead to either improvement or slight functional loss (Koch et al., 2005) clearly suggest further intra- and inter-hemispheric structural and functional differentiation within relevant network nodes.

We conclude that the perception and production of temporal relations is not merely a by-product of cognition and action, but that temporal structure provides information that is central to efficient behavior. Moreover, high precision in temporal processing benefits behavior as it allows generating precise predictions about upcoming events, a phenomenon that appears to be affected in PD. The current opinion summarizes previous evidence and synthesizes as well as accentuates a novel perspective on the structural and functional differentiation of the "SMA" in temporal processing and its relevance in a broader and integrative subcortico-thalamo-cortical dedicated temporal processing network.

REFERENCES

Akkal, D., Dum, R. P., and Strick, P. L. (2007). Supplementary motor area and presupplementary motor area: targets of basal ganglia and cerebellar output. *J. Neurosci.* 27, 10659–10673.

Akkal, D., Escola, L., Bioulac, B., and Burbaud, P. (2004). Time predictability modulates pre-supplementary motor area neuronal activity. *Neuroreport* 15, 1283–1286.

Allman, M. J., and Meck, W. H. (2011). Pathophysiological distortions in time perception and timed performance. *Brain* doi: 10.1093/brain/awr210

Bostan, A. C., Dum, R. P., and Strick, P. L. (2010). The basal ganglia communicate with the cerebellum. *Proc. Natl. Acad. Sci. U.S.A.* 107, 8452–8456.

Bostan, A. C., and Strick, P. L. (2010). The cerebellum and basal ganglia are interconnected. *Neuropsychol. Rev.* 20, 261–270.

Brickner, R. M. (1939). A human cortical area producing repetitive phenomena when stimulated. *J Neurophysiol.* 3, 128–130.

Buonomano, D. V. (2007). The biology of time across different scales. *Nat. Chem. Biol.* 3, 594–597.

Casini, L., and Vidal, F. (2011). The SMAs: neural substrate of the temporal accumulator? *Front. Integr. Neurosci.* 5:35. doi: 10.3389/fnint.2011.00035

Coull, J. T., Cheng, R., and Meck, W. H. (2011). Neuroanatomical and neurochemical substrates of timing. *Neuropsychopharmacology* 36, 3–25.

Coull, J. T., Vidal, F., Nazarian, B., and Macar, F. (2004). Functional anatomy of the attentional modulation of time estimation. *Science* 303, 1506–1508.

Cunnington, R., Iansek, R., Thickbroom, G. W., Laing, B. A., Mastaglia, F. L., Bradshaw, J. L., and Phillips, J. G. (1996). Effects of magnetic stimulation over supplementary motor area on movement in Parkinson's disease. *Brain* 119, 815–822.

Draganski, B., Kherif, F., Klöppel, S., Cook, P. A., Alexander, D. C., Parker, G. J. M., Deichmann, R., Ashburner, J., and Frackowiak, R. S. J. (2008). Evidence for segregated and integrativeconnectivity patterns in the basal ganglia. *J. Neurosci.* 28, 7143–7152.

Drake, C., Jones, M. R., and Baruch, C. (2000). The development of rhythmic attending in auditory sequences: attunement, referent period, focal attending. *Cognition* 77, 251–288.

Dum, R. P., and Strick, P. L. (2003). An unfolded map of the cerebellar dentate nucleus and its projections to the cerebral cortex. *J. Neurophysiol.* 89, 634–639.

Eckert, T., Peschel, T., Heinze, H., and Rotte, M. (2006). Increased pre-SMA activation in early PD patients during simple self-initiated hand movements. *J. Neurol.* 253, 199–207.

Ferrandez, A. M., Hugueville, L., Lehéricy, S., Poline, J. B., Marsault, C., and Pouthas, V. (2003). Basal ganglia and supplementary motor area subtend duration perception: an fMRI study. *Neuroimage* 19, 1532–1544.

Fujii, N., and Graybiel, A. M. (2003). Representation of action sequence boundaries by macaque prefrontal cortical neurons. *Science* 301, 1246–1249.

Goldberg, G. (1985). Supplementary motor area structure and function: review and hypotheses. *Behav. Brain Sci.* 8, 567–616.

Hamada, M., Ugawa, Y., and Tsuji, S. (2008). High-frequency rTMS over the supplementary motor area for treatment of Parkinson's disease. *Mov. Disord.* 23, 1524–1531.

Harrington, D. L., Haaland, K. Y., and Hermanowicz, N. (1998). Temporal processing in the basal ganglia. *Neuropsychology* 12, 3–12.

Hoshi, E., Tremblay, L., Féger, J., Carras, P. L., and Strick, P. L. (2005). The cerebellum communicates with the basal ganglia. *Nat. Neurosci.* 8, 1491–1493.

Ivry, R. B., and Schlerf, J. E. (2008). Dedicated and intrinsic models of time perception. *Trends Cogn. Sci. (Regul. Ed.)* 12, 273–280.

Jahanshahi, M., Jones, C. R. G., Dirnberger, G., and Frith, C. D. (2006). The substantia nigra pars compacta and temporal processing. *J. Neurosci.* 26, 12266–12273.

Johansen-Berg, H., Behrens, T. E. J., Robson, M. D., Drobnjak, I., Rushworth, M. F. S., Brady, J. M., Smith, S. M., Higham, D. J., and Matthews, P. M. (2004). Changes in connectivity profiles define functionally distinct regions in human medial frontal cortex. *Proc. Natl. Acad. Sci. U.S.A.* 101, 13335–13340.

Jonas, S. (1981). The supplementary motor region and speech emission. *J. Commun. Disord.* 14, 349–373.

Karmarkar, U. R., and Buonomano, D. V. (2007). Timing in the absence of clocks: encoding time in neural network states. *Neuron* 53, 427–438.

Koch, G. (2010). rTMS effects on levodopa induced dyskinesias in Parkinson's disease patients: searching for effective cortical targets. *Restor. Neurol. Neurosci.* 28, 561–568.

Koch, G., Brusa, L., Caltagirone, C., Peppe, A., Oliveri, M., Stanzione, P., and Centonze, D. (2005). rTMS of supplementary motor area modulates therapy-induced dyskinesias in Parkinson disease. *Neurology* 65, 623–625.

Koch, G., Costa, A., Brusa, L., Peppe, A., Gatto, I., Torriero, S., Gerfo, E. L., Salerno, S., Oliveri, M., Carlesimo, G. A., and Caltagirone, C. (2008). Impaired reproduction of second but not millisecond time intervals in Parkinson's disease. *Neuropsychologia* 46, 1305–1313.

Koch, G., Oliveri, M., Brusa, L., Stanzione, P., Torriero, S., and Caltagirone, C. (2004). High-frequency rTMS improves time perception in Parkinson's disease. *Neurology* 63, 2405–2406.

Kotz, S. A., and Schwartze, M. (2010). Cortical speech processing unplugged: a timely subcortico-cortical framework. *Trends Cogn. Sci. (Regul. Ed.)* 14, 392–399.

Large, E. W., and Jones, M. R. (1999). The dynamics of attending: how we track time-varying events. *Psychol. Rev.* 106, 119–159.

Lewis, M. M., Slagle, C. G., Smith, A. B., Truong, Y., Bai, P., McKeown, M. J., Mailman, R. B., Belger, A., and Huang, X. (2007). Task specific influences of

Parkinson's disease on the striato-thalamo-cortical and cerebello-thalamo-cortical motor circuitries. *Neuroscience* 147, 224–235.

Macar, F., Anton, J., Bonnet, M., and Vidal, F. (2004). Timing functions of the supplementary motor area: an event-related fMRI study. *Brain Res. Cogn. Brain Res.* 21, 206–215.

Macar, F., Coull, J. T., and Vidal, F. (2006). The supplementary motor area in motor and perceptual time processing: fMRI studies. *Cogn. Process.* 7, 89–94.

Macar, F., Lejeune, H., Bonnet, M., Ferrara, A., Pouthas, V., Vidal, F., and Maquet, P. (2002). Activation of the supplementary motor area and of attentional networks during temporalprocessing. *Exp. Brain Res.* 142, 475–485.

MacDonald, V., and Halliday, G. M. (2002). Selective loss of pyramidal neurons in the pre-supplementary motor cortex in Parkinson's disease. *Mov. Disord.* 17, 1166–1173.

Matell, M. S., and Meck, W. H. (2004). Cortico-striatal circuits and interval timing: coincidence detection of oscillatory processes. *Brain Res. Cogn. Brain Res.* 21, 139–170.

Merchant, H., Luciana, M., Hooper, C., Majestic, S., and Tuite, P. (2008). Interval timing and Parkinson's disease: heterogeneity in temporal performance. *Exp. Brain Res.* 184, 233–248.

Mita, A., Mushiake, H., Shima, K., Matsuzaka, Y., and Tanji, J. (2009). Interval time coding by neurons in the presupplementary and supplementary motor areas. *Nat. Neurosci.* 12, 502–507.

O'Boyle, D. J., Freeman, J. S., and Cody, F. W. J. (1996). The accuracy and precision of timing of self-paced, repetitive movements in subjects with Parkinson's disease. *Brain* 119, 51–70.

O'Reilly, J. X., Mesulam, M. M., and Nobre, A. C. (2008). The cerebellum predicts the timing of perceptual events. *J. Neurosci.* 28, 2252–2260.

Pastor, M. A., Artieda, J., Jahanshahi, M., and Obeso, J. A. (1992). Time estimation and reproduction is abnormal in Parkinson's disease. *Brain* 115, 211–225.

Pastor, M. A., Macaluso, E., Day, B. L., and Frackowiak, R. S. J. (2006). The neural basis of temporal auditory discrimination. *Neuroimage* 30, 512–520.

Penfield, W. (1950). The supplementary motor area in the cerebral cortex of man. *Arch. Psychiatr. Nervenkr. Z. Gesamte Neurol. Psychiatr.* 185, 670–674.

Picard, N., and Strick, P. L. (2001). Imaging the premotor areas. *Curr. Opin. Neurobiol.* 11, 663–672.

Pouthas, V., George, N., Poline, J., Pfeuty, M., Van de Moorteele, P., Hugueville, L., Ferrandez, A., Lehéricy, S., LeBihan, D., and Renault, B. (2005). Neural network involved in time perception: an fMRI study comparing long and short interval estimation. *Hum. Brain Mapp.* 25, 433–441.

Schwartze, M., Rothermich, K., and Kotz, S. A. (in press). Functional dissociation of pre-SMA and SMA-proper in temporal processing. *Neuroimage.* doi: 10.1016/j.neuroimage.2011.11.089

Sen, S., Kawaguchi, A., Truong, Y., Lewis, M. M., and Huang, X. (2010). Dynamic changes in cerebello-thalamo-cortical motor circuitry during progression of Parkinson's disease. *Neuroscience* 166, 712–719.

Sherman, S. M. (2001). A wake-up call from the thalamus. *Nat. Neurosci.* 4, 344–346.

Sherman, S. M. (2007). The thalamus is more than just a relay. *Curr. Opin. Neurobiol.* 17, 417–422.

Sherman, S. M., and Guillery, R. W. (2002). The role of the thalamus in the flow of information to the cortex. *Philos. Trans. R. Soc. Lond. B Biol. Sci.* 357, 1695–1708.

Shima, K., and Tanji, J. (2006). Binary-coded monitoring of a behavioral sequence by cells in the pre-supplementary motor area. *J. Neurosci.* 26, 2579–2582.

Smith, J. G., Harper, D. N., Gittings, D., and Abernethy, D. (2007). The effect of Parkinson's disease on time estimation as a function of stimulus duration range and modality. *Brain Cogn.* 64, 130–143.

Spencer, R. M. C., Karmarkar, U., and Ivry, R. B. (2009). Evaluating dedicated and intrinsic models of temporal encoding by varyi ng context. *Philos. Trans. R. Soc. Lond. B Biol. Sci.* 364, 1853.1863.

Stevens, M. C., Kiehl, K. A., Pearlson, G., and Calhoun, V. D. (2007). Functional neural circuits for mental timekeeping. *Hum. Brain Mapp.* 28, 394–408.

Tanji, J. (1996). New concepts of the supplementary motor area. *Curr. Opin. Neurobiol.* 6, 782–787.

Van Nuenen, B. F. L., van Eimeren, T., van der Vegt, J. P. M., Buhmann, C., Klein, C., Bloem, B. R., and Siebner, H. R. (2009). Mapping preclinical compensation in Parkinson's disease: an imaging genomics approach. *Mov. Disord.* 24, S703–S710.

Wu, T., and Hallett, M. (2005). A functional MRI study of automatic movements in patients with Parkinson's disease. *Brain* 128, 2250–2259.

Ziegler, W., Kilian, B., and Deger, K. (1997). The role of the left mesial frontal cortex in fluent speech: evidence from a case of left supplementary motor area hemorrhage. *Neuropsychologia* 35, 1197–1208.

Received: 30 November 2011; accepted: 02 December 2011; published online: 22 December 2011.

Citation: Kotz SAE and Schwartze M (2011) Differential input of the supplementary motor area to a dedicated temporal processing network: functional and clinical implications. Front. Integr. Neurosci. ***5****:86. doi: 10.3389/fnint.2011.00086*

frontiers in
INTEGRATIVE NEUROSCIENCE

ORIGINAL RESEARCH ARTICLE
published: 14 March 2012
doi: 10.3389/fnint.2012.00010

Acquisition of "Start" and "Stop" response thresholds in peak-interval timing is differentially sensitive to protein synthesis inhibition in the dorsal and ventral striatum

Christopher J. MacDonald[1], Ruey-Kuang Cheng[2] and Warren H. Meck[3]*

[1] *Department of Psychology and Center for Memory and Brain, Boston University, Boston, MA, USA*
[2] *A*STAR/Duke-NUS Neuroscience Research Partnership, National University of Singapore, Singapore*
[3] *Department of Psychology and Neuroscience, Duke University, Durham, NC, USA*

Edited by:
Valerie Doyere, Centre National de la Recherche Scientifique, France

Reviewed by:
Joshua D. Berke, University of Michigan, USA
Michael Drew, University of Texas at Austin, USA

***Correspondence:**
Warren H. Meck, Department of Psychology and Neuroscience, Duke University, 572 Research Drive, Durham, NC 27708, USA.
e-mail: meck@psych.duke.edu

Time-based decision-making in peak-interval timing procedures involves the setting of response thresholds for the initiation ("Start") and termination ("Stop") of a response sequence that is centered on a target duration. Using intracerebral infusions of the protein synthesis inhibitor anisomycin, we report that the acquisition of the "Start" response depends on normal functioning (including protein synthesis) in the dorsal striatum (DS), but not the ventral striatum (VS). Conversely, disruption of the VS, but not the DS, impairs the acquisition of the "Stop" response. We hypothesize that the dorsal and ventral regions of the striatum function as a competitive neural network that encodes the temporal boundaries marking the beginning and end of a timed response sequence.

Keywords: timing and time perception, decision-making, reward prediction, cortico-striatal circuits, dopamine-glutamate interactions, memory consolidation, protein synthesis inhibitors

INTRODUCTION

Throughout their daily routines, humans and other animals perceive events as a function of the flow of time and make decisions based upon the relative durations of those events by means of a process known as scalar timing (Gibbon et al., 1984; Meck, 2003; Buhusi and Meck, 2005; Buhusi et al., 2009). Therefore, it is perhaps not surprising that timing and time perception within the seconds-to-minutes range—i.e., interval timing—plays a fundamental role in adaptive behavior, including optimal foraging, temporal discounting, and other aspects of intertemporal preferences and neuroeconomics (Brunner et al., 1992; Bateson, 2003; Zauberman et al., 2009; Cui, 2011; Ray and Bossaerts, 2011). Indeed, interval timing contributes importantly to decision-making as well as learning predictive relationships among stimuli in both appetitive and aversive contexts (Gibbon et al., 1997; Gallistel and Gibbon, 2000; Harrington et al., 2004; Tanaka et al., 2004; Maimon and Assad, 2006; Droit-Volet and Meck, 2007; Meck and MacDonald, 2007; Forstmann et al., 2008; Jones et al., 2011). In fact, temporal discounting and the anticipation of a future event's time of occurrence often emerge as critical variables that influence performance during tasks intended to characterize a variety of basic cognitive processes, including memory (Malapani et al., 1998; Lustig et al., 2005; Lustig and Meck, 2005, 2011), attention (Lustig and Meck, 2001; Buhusi and Meck, 2002, 2006, 2009a,b; Meck and Benson, 2002; Coull et al., 2004), choice (Fantino et al., 1979; McClure et al., 2004; Rudebeck et al., 2006), and reaction time (MacDonald and Meck, 2004, 2006).

Although dopamine-glutamate interactions within cortico-striatal circuits have been shown to support numerous aspects of interval timing (Meck, 1983, 1996, 2006a,b; Matell et al., 2004; Liao and Cheng, 2005; Cheng et al., 2006, 2007a,b,c; Drew et al., 2007; Pennartz et al., 2009; Meck et al., 2008, 2012; Williamson et al., 2008; Agostino et al., 2011; Coull et al., 2011; Gu et al., 2011; Hata, 2011; Höhn et al., 2011; Jones and Jahanshahi, 2011; Allman and Meck, 2012), it remains unclear what types of neural mechanisms are involved in the construction of decision thresholds for determining when to *start* and *stop* responding (see Meck, 2002, 2006c; Vink et al., 2005; Bromberg-Martin et al., 2010; van der Meer et al., 2010). In order to investigate this issue, we employed the peak-interval (PI) timing procedure which is a "classic" example of a duration reproduction task that has proven useful in the study of temporal cognition due to its applicability across a wide-variety of animal species—including fish, birds, rodents, and primates (Church et al., 1991, 1994; Rakitin et al., 1998; Paule et al., 1999; Buhusi and Meck, 2000; Buhusi et al., 2002, 2009; Gallistel et al., 2004; Hinton and Meck, 2004; Drew et al., 2005, 2007; Penney et al., 2008; Ward et al., 2009, 2012; Cheng et al., 2011) and stimulus modalities (Meck and Church, 1982; Meck, 1991; Penney et al., 2000; Bueti, 2011; Lustig and Meck, 2011; Allman and Meck, 2012). In the PI timing procedure, the subject is initially exposed exclusively to fixed-interval (FI) trials throughout a session, during which the onset of a signal (e.g., houselight) reliably predicts the time at which feedback/reward will be provided—thus establishing a temporal criterion. After sufficient training with FI trials, unreinforced probe trials are randomly intermixed within a session in order to characterize the accuracy and precision of temporal memory as illustrated in **Figure 1A**. During a probe trial, the signal stays on long past the temporal criterion and no feedback is provided. Following sufficient training with probe trials, the mean response rate for an individual subject averaged across all probe trials within a session resembles a Gaussian-shaped distribution—the *peak function*—whose mode is centered on the temporal criterion (Meck and Church, 1984; Church et al., 1994; Rakitin et al., 1998). In such

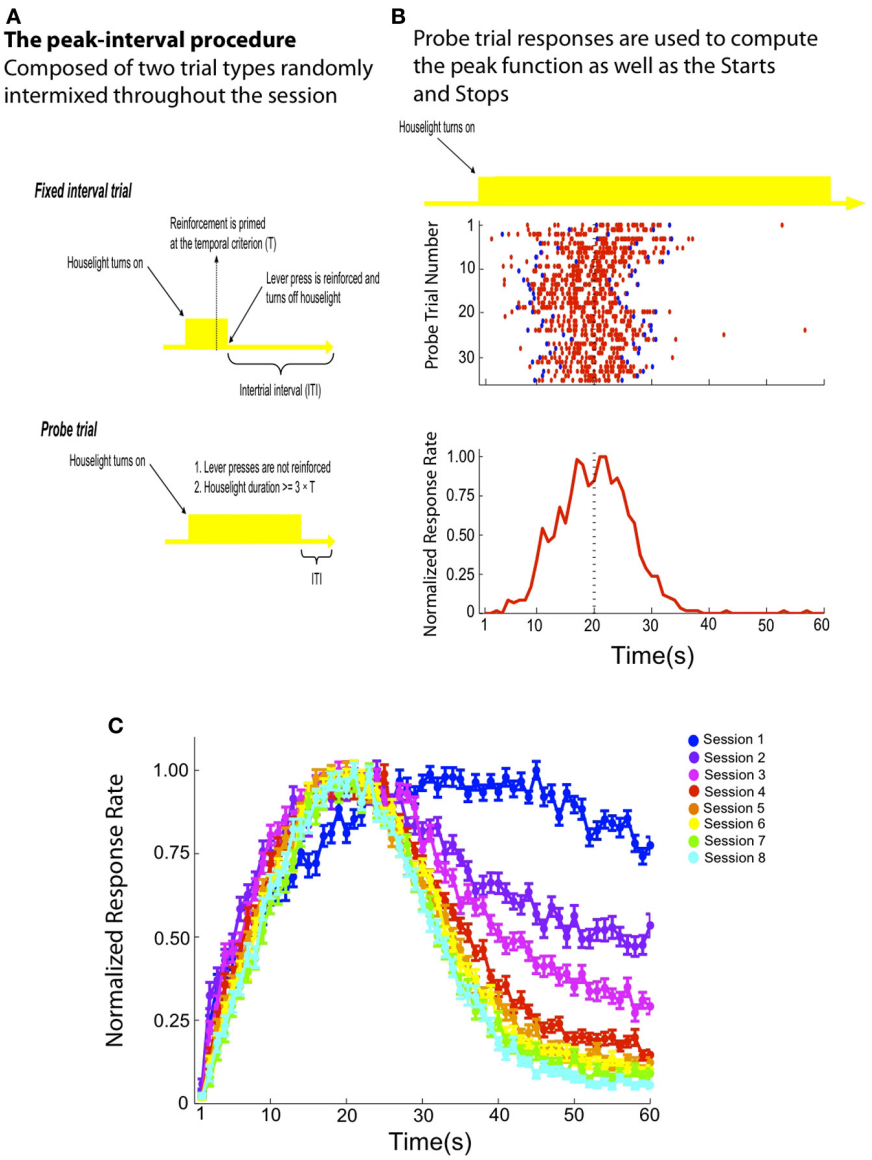

FIGURE 1 | (A) An illustration depicting the two trial types randomly intermixed throughout a standard peak-interval (PI) training session. The houselight serves as the signal being timed in this example. On FI trials, the houselight's onset predicts the availability of reinforcement at 20 s. Delivery of reward is contingent on a lever press made by the rat at or after this time, which also terminates the houselight and initiates an ITI. On probe trials, the houselight remains on for an extended period of time with a minimum of 60 s and reinforcement is never delivered. **(B)** A representative rat that is well-trained on the PI procedure. The raster plot (top) depicts each probe trial as a row and responses (red tics) are displayed across time during the probe trial. On each trial, a response sequence contains both a "Start" and "Stop" response (blue tics), which demarcates the beginning ("Start") and end ("Stop") of the "high state" (see Introduction and Methods). Probe trial responses are collapsed across trials within 1 s bins to create the peak function, which is normalized so that it expresses the percentage of maximum response rate as a function of signal duration (bottom). Because the signal extends well past the temporal criterion (e.g., 20 s), the accuracy and precision of the remembered time of reward is inferred by the rat's response rate before and after 20 s. **(C)** Before probe trials are randomly intermixed within a session, rats are exposed *only* to FI trials for multiple sessions (see Methods). This panel depicts a normalized peak function (± SEM) averaged across all rats during the first eight sessions in which probe trials are randomly intermixed with FI trials. Note that the degree of response inhibition after the remembered time of reward increases across sessions as the rats obtain more experience with partial extinction during unreinforced probe trials.

cases, a balance is often struck between starting the sequence of reinforced behavior in anticipation of the reward, but also giving up responding when the opportunity for reward is thought to have passed (Brunner et al., 1992, 1996, 1997; Bateson, 2003; Silva and Timberlake, 2005).

With rats and pigeons, for whom an appetitive reward can readily serve as a time marker (Freestone and Church, 2010), performance during a single probe trial can be described by an abrupt transition both into and out of a "high state" of responding, during which the subject responds at a relatively rapid,

constant rate as illustrated in **Figure 1B**. Remarkably, the variability in the onset ("Start") and offset ("Stop") of the "high state," as well as the duration of the "high state" itself, is proportional to the interval being timed (Church et al., 1994; Rakitin et al., 1998). This feature contributes to the *scalar property*, which describes the proportionality between the spread of the peak function and the value of the temporal criterion (i.e., Weber's law—Gibbon et al., 1984; Cheng and Meck, 2007). Importantly, the "Start" and "Stop" times are considered independent of one another because they are not well correlated on a trial-by-trial basis (Church et al., 1994; Gallistel et al., 2004; Matell et al., 2006; Buhusi and Meck, 2009b). In effect, these "Start" and "Stop" times are independent decision thresholds demarcating an *action sequence* that the subject "attempts" to center on the expected time of reward. Moreover, the presentation of unreinforced probe trials subsequently leads to the acquisition of the "Stop" response threshold (see Balci et al., 2009). At steady-state levels of performance this action sequence may be conceptualized as a distinct behavioral unit whose organization depends on the memory of the target duration (see Gibbon et al., 1984; Church et al., 1994).

However, despite the evidence supporting a clear dissociation between "Start" and "Stop" times, there has been no anatomical localization of these response thresholds for interval-timing tasks (see Mansfield et al., 2011). In addition, there is little understanding concerning (1) how the "Start" and "Stop" thresholds are acquired and (2) the underlying neural substrates for temporal conditioning (Gallistel and Gibbon, 2000). Regarding the first point, in the PI timing procedure the subject must learn to inhibit responding after the target duration during probe trials, which ultimately leads to the gradual acquisition of the "Stop" response as illustrated by the PI data from Experiment 1 plotted in **Figure 1C**. This occurs when partial extinction/unrewarded probe trials are first introduced, typically long after the emergence of the "Start" response which defines the beginning of the "high state" of responding acquired during initial FI training. Regarding the second point, there is reason to believe that the striatum is an important neural substrate for interval timing in a wide variety of timing procedures (Gibbon et al., 1997; Matell and Meck, 2000, 2004; Buhusi and Meck, 2005; Meck, 2006b; Harrington et al., 2011a,b; Kotz and Schwartze, 2011; Matell et al., 2011; Portugal et al., 2011; van Rijn et al., 2011). Indeed, the firing rate of neurons in the dorsal striatum (DS) is modulated with respect to the temporal criterion acquired in the PI timing procedure (Matell et al., 2003). Outside the context of interval timing, one proposed function of the DS is organizing the hierarchical structure of learned response sequences (Graybiel, 1998; Fujii and Graybiel, 2005; Jin et al., 2009; Jin and Costa, 2010), which is consistent with a direct relationship to interval timing. For example, single neurons within the rat's DS also encode the hierarchal context of a specific response within a systematic, natural response sequence like grooming (Aldridge and Berridge, 1998) and lesions of the DS can disrupt the expression of both natural and learned sequences (Cromwell and Berridge, 1996; Bailey and Mair, 2006). While the DS is believed to contribute to encoding of the temporal criterion, the ventral striatum (VS) is thought to play a modulatory role for interval timing, especially with respect to changes in the reward value associated with feedback at the temporal criterion (McClure et al., 2004; O'Doherty et al., 2004; MacDonald and Meck, 2005; Meck, 2006b). This connection is consistent with a broader framework for understanding VS function in which this region of the striatum appears to hold a closer relationship to affective processing than the DS and plays a role in "behavioral flexibility" by modulating ongoing natural and/or learned behaviors (Cardinal et al., 2002; Kelley, 2004; Pleil et al., 2011). For example, the VS contribute to inhibiting behavior that is made inappropriate so that novel behavioral strategies may be acquired (Tanaka et al., 2004, 2007; Floresco et al., 2006).

With these functional parallels in mind, we were interested in characterizing the role of the DS and VS in the PI timing procedure while rats acquired the "Start" and "Stop" responses. Learning entails enduring changes in the brain, which presumably requires a cascade of molecular events to take place beforehand (Abel and Lattal, 2001). Protein synthesis inhibitors, such as anisomycin (ANI), have proven to be useful tools for the characterization of this memory consolidation process in Pavlovian conditioning (Stafford and Lattal, 2009), spatial navigation (Morris et al., 2006), instrumental learning (Hernandez et al., 2002), and motor-skill acquisition (Wächter et al., 2010). In the following experiments, we used ANI microinjections administered prior to rats performing on variants of the PI timing procedure to conclude that the acquisition of the "Start" response depends on normal functioning (including protein synthesis) within the DS during training (see Castellucci et al., 1989; Okamoto et al., 2011). In contrast, disruption of normal functioning within the VS during training, but not the DS, impairs the acquisition of the "Stop" response.

MATERIALS AND METHODS

ANIMALS

Across both experiments, a total of 49 experimentally naïve Sprague–Dawley rats (Charles-River Laboratories, Raleigh, NC) weighing between 250–350 g at the start of the experiment were used. Rats were housed in pairs in a 12:12 light:dark cycle with lights on from 7:00 AM to 7:00 PM. Rats were given continuous access to water and maintained at 85% free-feeding weight with a daily ration of rat chow (Rodent Diet 5001, PMI Nutrition International, Inc., Brentwood, MO) given shortly after the test session. All procedures were conducted in accordance with the policies of the Duke University Institutional Animal Care and Use Committee.

APPARATUS

The apparatus consisted of 10 standard lever boxes (Model ENV-007, MED Associates, Inc., Albans, VT) housed in light and sound attenuating cubicles (Model ENV-019, MED Associates, Inc., Albans, VT). Each lever box had inside dimensions of approximately 24 cm × 31 cm × 31 cm. The top, side walls, and door were constructed of clear acrylic plastic. The front and back walls were constructed of stainless steel, and the floor was comprised of 19 parallel stainless steel bars. Each lever box was equipped with two retractable response levers (Model ENV-112, MED Associates, Inc., Albans, VT) situated on opposite sides of the front wall of the lever box. Precision food pellets (45 mg—Research Diets, Inc., New Brunswick, NJ) could be delivered by a pellet dispenser (Model ENV-203, MED Associates, Inc., Albans, VT) to a food

cup on the front wall, 1 cm above the floor, and in between the two levers. A 28 V, 100 mA, 2500 lx house light was mounted at the center-top of the front wall and could be used to illuminate the box. A white noise amplifier/speaker system (Model ENV-225, MED Associates, Inc., Albans, VT) was mounted on the opposite wall from the levers but was not used. A 66 dB sound produced by a ventilation fan was present throughout all procedures.

SURGERY

Rats were anesthetized with i.p. injections of both ketamine hydrochloride (100 mg/kg) and xylazine hydrochloride (20 mg/kg). Bilateral guide cannluae (Plastics One Inc., 26 gauge with stylets) were implanted into either the DS ($A = 1.2$ mm, $L = \pm 2.5$ mm, $V = 4.1$ mm) or VS ($A = 1.6$ mm, $L = \pm 1.9$ mm, $V = -6.3$ mm). The tips of the injector cannulae extended ∼1.5 mm from the base of the guide cannulae. The cannulae were fixed using dental cement and three small, skull screws. All rats were given at least five days of recovery.

HISTOLOGY

In order to confirm cannulae placement, following the experiment, all rats were perfused transcardially with 0.9% saline followed by 10% formalin. Brains were removed and stored in a 10% formalin solution before being transferred to a 10% formalin-sucrose solution before sectioning.

DRUGS AND INFUSIONS

ANI (Sigma-Aldrich, St Louis, MO) was dissolved in equimolar HCl and diluted with CSF (Harvard Apparatus, Holliston, ME—Experiment 1) or 0.9% saline (Sigma-Aldrich, St Louis, MO—Experiment 2), and adjusted to pH 7 with NaOH for a final concentration of 62.5 μg/0.5 μl. The ANI dose was selected based on preliminary data from our laboratory and a previous study that confirmed it as being an effective dose for behavioral tasks of this sort (Hernandez and Kelley, 2004). In memory consolidation experiments, protein synthesis is often inhibited after training is completed. Depending on the experimental question, this strategy can be especially effective when using tasks that require a limited numbers of trials (e.g., contextual fear conditioning) to meet some learning criteria. However, learning the "Stop" response requires multiple daily sessions that each include 60 or more total trials/session (**Figure 1C**). Because of this we couldn't be sure which specific trial or trials within the session constitute the "learning episode" as well as when the "Start" and "Stop" response thresholds are consolidated (or in fact whether these task components are reconsolidated at any point during the session). As a consequence, we chose to infuse ANI before the training session began in order to ensure that protein synthesis was maximally impaired throughout the session (see Wanisch and Wotjak, 2008 for data on the time course of protein synthesis inhibition).

All rats were given at least three days of mock infusions to habituate them to the injection procedure before testing. Bilateral infusions were given immediately before the sessions at a rate of 0.25 μl/min over the course of two minutes. Following the infusion, the injector cannulae were maintained in place for at least 1 min before being placed immediately in the lever box to begin the experiment.

EXPERIMENT 1: BEHAVIORAL TRAINING: EFFECTS OF ANISOMYCIN INFUSION ON "START" AND "STOP" RESPONSES DURING THE ACQUISITION OF A PEAK-INTERVAL (PI) 20 S RESPONSE SEQUENCE

Pre-training (Sessions 1–5)

All rats received six sessions of combined magazine and lever training. During these sessions, a food pellet was delivered once a min for 60 min, and was signaled at the 58 s mark by a 2 s lever retraction/extension sequence. Throughout the session, a lever press also resulted in the delivery of a food pellet.

Fixed-interval (FI) 20 s training (Sessions 6–55)

During FI 20 s training, trials were cued by the onset of a houselight and extension of the response lever for the duration of the trial. Any lever press before 20 s had no consequence. However, any lever press after 20 s resulted in (1) delivery of a food pellet, (2) offset of the houselight, (3) retraction of the lever, and (4) the beginning of an intertrial interval (ITI). An ITI was always 60 s plus a duration randomly selected from one of seven values (min = 1.1 s, max = 70.4 s) that were geometrically distributed. A new trial began at the end of an ITI and sessions lasted for approximately 2 h.

Post-surgical fixed-interval (FI) 20 s training (Sessions 56–65)

Following surgery, rats were given 10 additional sessions of FI training to ensure stable pre-treatment performance for the groups.

Peak-interval (PI) 20 s training (Sessions 66–80)

PI 20 s training consisted of 50% FI trials (see above) and 50% unreinforced probe trials. On any given trial, the chosen trial-type was random. Probe trials were like FI trials except that (1) lever presses after 20 s did not result in delivery of a food pellet and (2) the houselight remained on and the lever extended for 60 s plus a duration randomly selected from one of seven values (min = 1.1 s, max = 70.4 s) that were geometrically distributed. The end of a trial signaled the beginning of an ITI, whose parameters were the same as that described during FI training and sessions lasted approximately 2 h. Rats were microinjected with the appropriate solution (ANI or vehicle) 10 min prior to the beginning of the first 6 PI 20 s training sessions.

EXPERIMENT 2: EFFECTS OF ANISOMYCIN INFUSION ON "START" RESPONSES DURING THE TRANSITION FROM 20 S TO 50 S TEMPORAL CRITERION

Pre-training (Sessions 1–5)

All rats received six sessions of combined magazine and lever training. During these sessions, a food pellet was delivered once a min for 60 min, and was signaled at the 58 s mark by a 2 s lever retraction/extension sequence. Throughout the session, a lever press also resulted in the delivery of a food pellet.

Fixed-interval (FI) 20 s training (Sessions 6–20)

During FI training, trials were cued by the onset of a houselight and extension of the response lever. Any lever press before 20 s had no consequence. However, any lever press after 20 s resulted in (1) delivery of a food pellet, (2) offset of the houselight, (3) retraction of the lever, and (4) the beginning of an ITI. An ITI was always 60 s plus a duration randomly selected from one of seven values

(min = 1.1 s, max = 70.4 s) that were geometrically distributed. A new trial began at the end of an ITI and sessions lasted for approximately 2 h.

Peak-interval (PI) 20 s training (Sessions 21–35)

PI 20 s training consisted of 50% FI trials (see above) and 50% unreinforced probe trials. On any given trial, the chosen trial-type was random. Probe trials were similar to FI trials except that (1) lever presses after 20 s did not result in delivery of a food pellet and (2) the houselight remained on and the lever extended for 60 s plus a duration randomly selected from one of seven values (min = 1.1 s, max = 70.4 s) that were geometrically distributed. The end of a trial signaled the beginning of an ITI, whose parameters were the same as that described during FI training and sessions lasted approximately 2 h.

Post-surgical peak-interval (PI) 20 s training (Sessions 36–50)

Following surgery, rats were given 15 additional sessions of PI 20 s training to ensure stable pre-treatment performance for each of the groups.

Transition: peak-interval (PI) 50 s training (Sessions 51–90)

PI 50 s training was similar to PI 20 s sessions except that (1) the temporal criterion was extended to 50 s and (2) probe trials lasted 120 s plus a duration randomly selected from one of seven values (min = 1.1 s, max = 70.4 s) that were geometrically distributed. Rats were microinjected with the appropriate solution (ANI or vehicle) 10 min prior to the beginning of the first 10 PI 50 s training sessions (see Meck et al., 1984b for additional details concerning the transition from one temporal criterion to another).

DATA ANALYSIS

The time of each lever press was recorded to an accuracy of 10 ms and placed into 1 s time bins. Peak functions were generated by normalizing response rates to the time bin with the highest response rate. The single-trials analysis used has been described elsewhere (Church et al., 1994; Matell et al., 2006). Briefly, in a single trial, the "high state" is determined by fitting three contiguous, but non-overlapping horizontal lines to the response series over time during a single trial. Therefore, the slope of each line represents a response rate over an interval that is defined by the length of the line on the abscissa. The goal is to iteratively maximize the difference between the response rate defined by the middle horizontal line ("high state") and the response rate defined during the flanking horizontal lines. This calculation effectively fits a boxcar-like step function. The "Start" and "Stop" times of this response sequence are defined as the points in the fitted function at which the "high state" begins and ends, respectively.

RESULTS

Experiment 1: acquisition of the "Stop" response is impaired by anisomycin infusion in the ventral striatum, but not the dorsal striatum

Because the VS has been observed to contribute to learning and response inhibition within a variety of experimental contexts, the current study was designed to test whether the acquisition of a temporally controlled "Stop" response requires normal functioning (including protein synthesis) in the VS, but not the DS. Thirty rats were trained on a 20 s PI procedure. Depending on the group assignment, rats were microinjected with ANI (DS-ANI, $n = 7$; VS-ANI, $n = 7$) or vehicle solution (DS-CON, $n = 8$; DS-CON, $n = 8$) before the first six sessions during which probe trials were first introduced in a training session. We divided the data into two blocks and calculated the mean peak functions for treatment groups during these blocks.

Figure 2 illustrates the mean peak functions (left column) and results of the single-trials analysis (right column) for the CON treatment groups combined over the DS and VS conditions as well as the ANI treatment groups for the separate DS and VS conditions. In each case, the acquisition data are plotted in blocks of 3 sessions (rows), ANI Sessions 1–3 and ANI Sessions 4–6. The data from the CON rats for the DS and VS conditions were combined because there were no reliable differences between these two groups for the "Start" measures during sessions 1–3 ($t_{1,40} = 0.61, p > 0.05$) and sessions 4–6 ($t_{1,22} = 1.17, p > 0.05$), as well as for the "Stop" measures during sessions 1–3 ($t_{1,40} = 0.01, p > 0.05$) and sessions 4–6 ($t_{1,22} = 1.96, p > 0.05$). A One-Way ANOVA was conducted on the single-trial "Stop" times for ANI Sessions 1–3 and ANI Sessions 4–6. During ANI Sessions 1–3, there was no reliable effect of Treatment on the "Stop" times ($F_{2,87} = 0.76$, $p > 0.05$). However, during ANI Sessions 4–6, there was a significant effect of Treatment ($F_{2,69} = 11.32$, $p < 0.0001$). *Post-hoc* tests [Fischer's Least Significant Difference (LSD), $\alpha = 0.05$] confirmed that the VS-ANI group differed significantly from both the CON and DS-ANI groups in terms of the time of the "Stop" response. No other significant differences were confirmed, i.e., there were no significant differences between the CON-DS and ANI-DS groups or the CON-VS and ANI-VS groups, p's > 0.05.

During acquisition of the "Stop" response, anisomycin infusion in the dorsal striatum resulted in a more precise "Start" response

A similar One-Way ANOVA was used to determine the effect of Treatment on the single-trial "Start" response times. During ANI Sessions 1–3, there was no reliable effect of Treatment on the "Start" times ($F_{2,87} = 1.12$, $p > 0.05$), however, during ANI Sessions 4–6, a significant effect of Treatment on "Start" times was observed ($F_{2,69} = 5.13$, $p < 0.01$). *Post-hoc* tests (Fischer's LSD, $\alpha = 0.05$) confirmed that only the DS-ANI treatment group differed from both the CON and VS-ANI treatment groups. With respect to the expected time of reward, the DS-ANI treatment group withheld responding to a greater degree beginning from the onset of a probe trial. Therefore, rats in the DS-ANI treatment group entered the "high state" at a time that was significantly closer to the target duration, which suggests an increase in temporal precision (Church et al., 1991). The significant main effects observed during ANI Sessions 4–6 continued to be observed during post-ANI Sessions 1–3 during which no ANI treatments were given, $F_{2,69} = 10.29$, $p < 0.0001$ and $F_{2,69} = 10.52$, $p < 0.0001$ for "Start" and "Stop" response times, respectively.

The differential effects of ANI infusion on the acquisition of "Stop" response were essentially non-existent following extended training without ANI treatment as demonstrated by the lack of

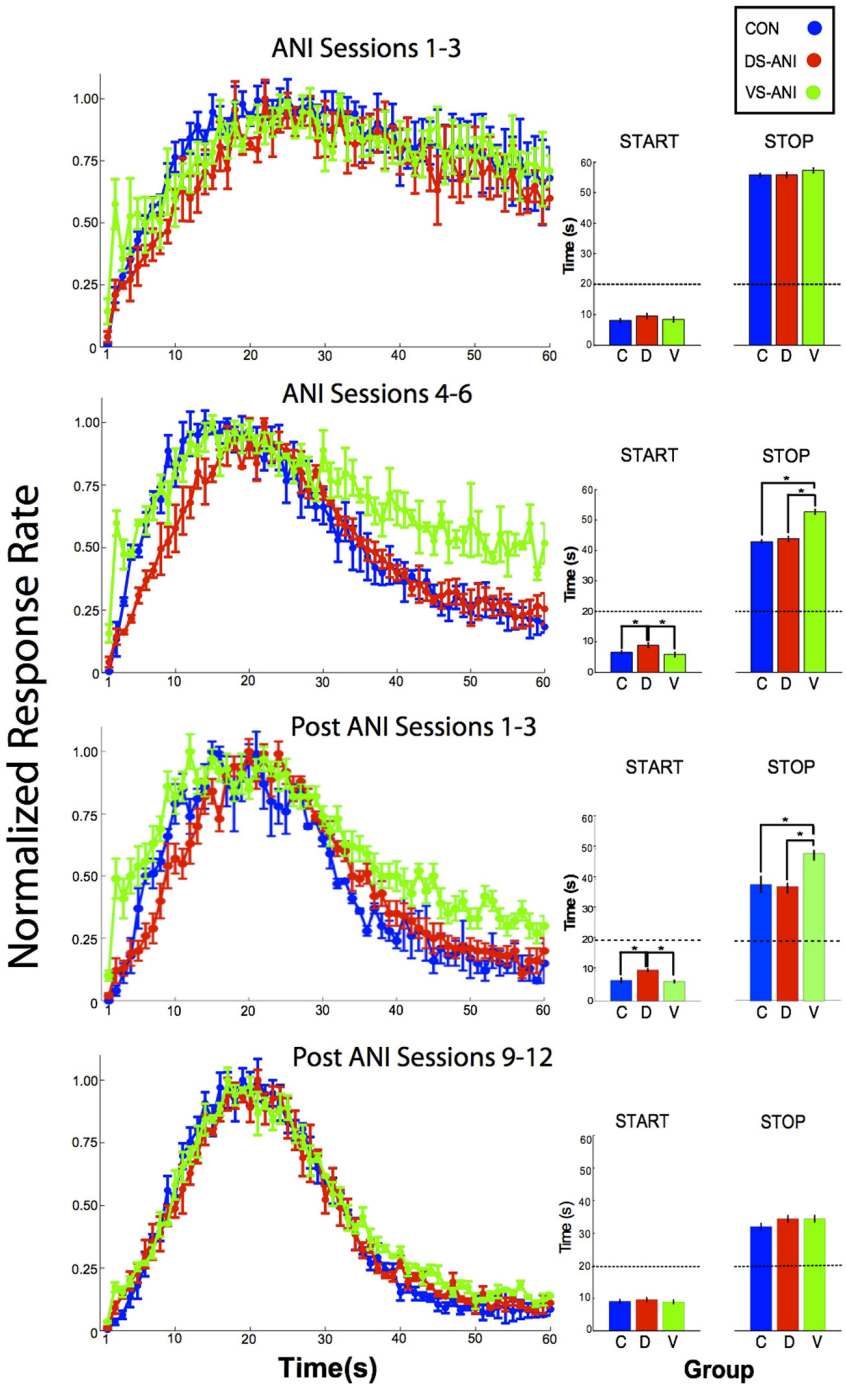

FIGURE 2 | Normalized mean (± SEM) peak functions (left column) for CON (blue), DS-ANI (red) and VS-ANI (green) treatment groups during four phases of the experiment: (A) ANI Sessions 1–3, (B) ANI Sessions 4–6, (C) post-ANI Sessions 1–3, and (D) post-ANI Sessions 12–14. Insets (right column) are included for each peak function to describe the "Start" and "Stop" times obtained from the signal-trials analysis conducted on the data obtained from that phase. Asterisks denote a significant difference between the treatment groups compared, which are bracketed by dark lines. ANI = anisomycin; CON = control; DS = dorsal striatum; VS = ventral striatum.

effect on the mean peak functions and the single-trials analysis of "Start" and "Stop" responses during post-ANI Sessions 12–14 (see bottom row of **Figure 2**). A One-Way ANOVA conducted on both the "Start" and "Stop" times during these post-ANI Sessions using Treatment condition as the main factor confirmed non-significant effects on both the "Start" and "Stop" measures, ($F_{2,69} = 0.37$, $p > 0.05$) and ($F_{2,69} = 1.87$, $p > 0.05$), respectively. These observations indicate that although the effects of

ANI lingered for a few sessions following its discontinuation (e.g., post-ANI Sessions 1–3), it did not damage the brain in a way that permanently disrupted the temporal control of behavior.

Anisomycin treatment lowered response rates to a comparable degree in both the dorsal striatum and ventral striatum treatment groups, but had no long-lasting effects on timing behavior

Mean (± SEM) response rate during probe trials for CON, DS-ANI, and VS-ANI treatment groups is plotted as a function of the six ANI microinjection sessions in **Figure 3**. A Two-Way ANOVA was conducted on the mean response rates during probe trials for each treatment group in order to verify the stability of the response rate across sessions. There was a significant effect of Treatment ($F_{2,142} = 10.89$, $p < 0.0001$), but non-significant effects of Session ($F_{5,142} = 0.99$, $p > 0.05$) and the Treatment × Session interaction ($F_{10,142} = 0.32$, $p >= 0.05$). *Post-hoc* tests (Fischer's LSD, $\alpha = 0.05$) confirmed that only the CON treatment group differed significantly from the DS-ANI ($F_{1,142} = 16.54$, $p < 0.0001$) and VS-ANI treatment groups ($F_{1,142} = 16.30$, $p < 0.0001$), whereas the DS-ANI and VS-ANI treatment groups did not differ reliably from one another ($F_{1,142} = 0.0001$, $p > 0.05$). Overall, the effect of ANI administration was to reduce responding to ∼60% of the levels observed in the CON treatment group ($S_{CON} = 0.26$, $S_{DS-A} = 0.15$, $S_{VS-A} = 0.15$)—although this effect did not change substantially across sessions. This finding further supports a reliable dissociation between the response rate index and measurements that characterize the precision of temporal memories (Roberts, 1993; Cheng and Meck, 2007). While the response rate in both ANI treatment groups decreased by the same degree relative to the CON treatment groups, the effects of ANI administration on the "Start" and "Stop" times for the DS-ANI and VS-ANI treatment groups were significantly different from each other as reported above.

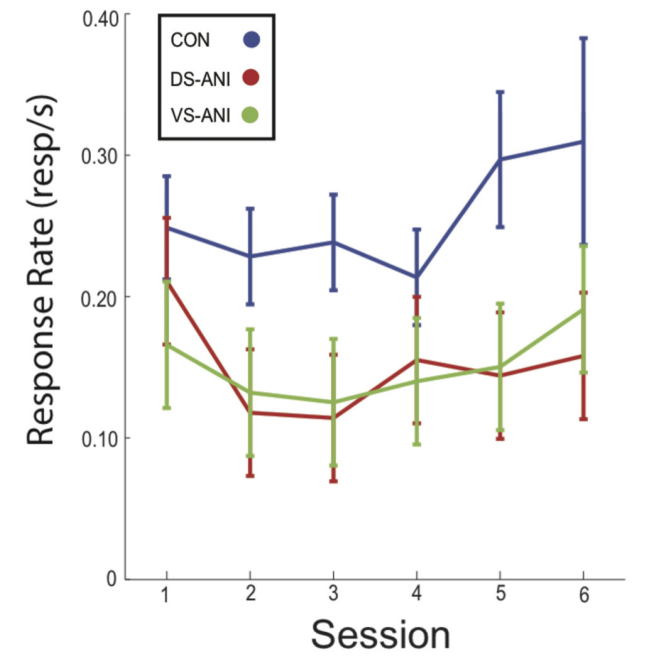

FIGURE 3 | Mean (± SEM) response rate (responses/s) during probe trials across each of the six ANI treatment sessions for CON (blue), DS-ANI (red), and VS-ANI (green) treatment groups in Experiment 1. ANI = anisomycin; CON = control; DS = dorsal striatum.

EXPERIMENT 2: ANISOMYCIN INFUSION INTO THE DORSAL STRIATUM IMPAIRS THE ACQUISITION OF THE "START" RESPONSE IN REFERENCE TO A SECOND TEMPORAL CRITERION

In the present experiment, normal functioning was disrupted by ANI infusion into the DS while a group of rats was transitioned from a previously acquired 20 s temporal criterion to a new 50 s criterion. The effect of ANI on the "Start" response was evaluated during the acquisition of a second temporal criterion rather than the initial temporal criterion in order to avoid non-specific disruption of behavior due to failure to consolidate the association of the lever press with food reinforcement as opposed to failure to establish a decision threshold associated with a specific temporal criterion. Investigation of the effects of striatal disruption (including inhibition of protein synthesis) on the acquisition of a second "Start" threshold provides the subject with the option of maintaining the original "Start" threshold in the absence of the ability to acquire a new "Start" threshold, thus providing a more specific test of decision thresholds as opposed to simple instrumental associations (see Meck et al., 1984b; Balci et al., 2009).

Nineteen rats were first trained on a 20 s PI procedure (see Methods) and were then divided into two groups, which differed with respect to whether ANI (DS-ANI, $n = 10$) or vehicle (DS-CON, $n = 9$) would be microinjected through bilateral cannulae placed into the DS. Within a session, 50% of the trials were FI trials. The remaining 50% of the trials were unreinforced probe trials during which the houselight stayed on for at least 60 s and no lever presses were reinforced (see **Figure 1A** and Methods section).

The baseline peak functions corresponding to probe trials obtained from the final two 20 s PI training sessions before ANI treatment are illustrated in **Figure 4A**. The peak functions are normalized with respect to the time-bin with the highest response rate (peak rate) in order to determine the shape of the temporal gradient and its centering around the target duration (peak time). Peak time and peak rate have been shown to be independent measures of performance with the former reflecting motivational factors and the later reflecting timing factors (Roberts, 1993; Cheng and Meck, 2007). "Start" times obtained from the single-trials analysis conducted across each of the PI 20 s baseline sessions are depicted in **Figure 4D** (left panel). A Two-Way ANOVA with Treatment and Session as factors indicated non-significant effects of Treatment ($F_{1,31} = 0.15$, $p > 0.05$) and Session ($F_{1,31} = 0.003$, $p > 0.05$), as well as a non-significant interaction between these two factors ($F_{1,31} = 0.02$, $p > 0.05$) during the initial training phase.

Each treatment group was then transitioned to a 50 s PI training protocol and rats were microinjected with ANI or CON prior to the first 10 test sessions. **Figure 4B** represents the mean peak functions obtained from Sessions 7–8 of ANI treatment while **Figure 4D** (center panel) illustrates the "Start" times obtained during each session of this transition phase as well as the PI 50 s baseline sessions (right panel). A Two-Way ANOVA conducted

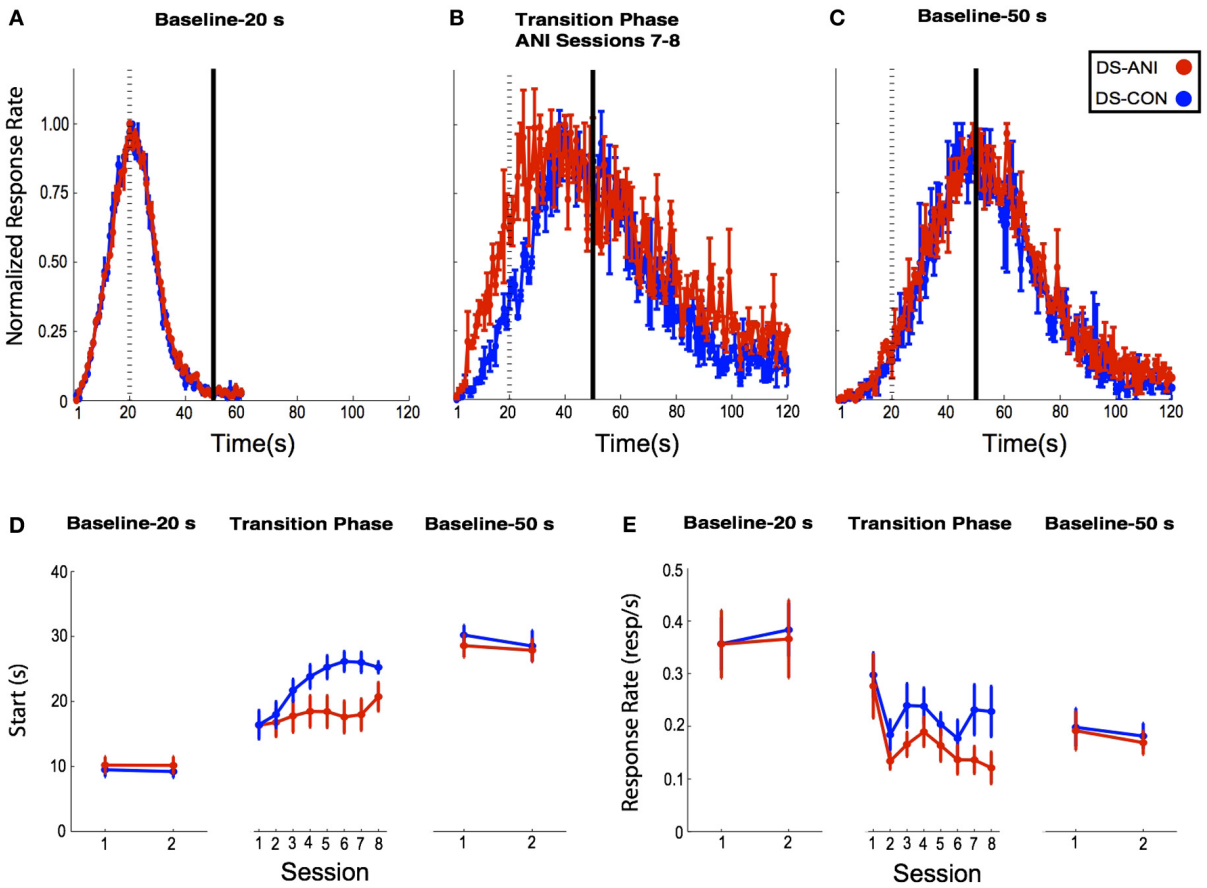

FIGURE 4 | (A) Baseline 20 s peak-interval (PI) functions for rats in the DS-CON (blue) and DS-ANI (red) treatment groups as a function of the last two sessions of 20 s PI training prior to the transition to 50 s PI training. **(B)** Peak functions for each treatment group during Sessions 7–8 following the transition from 20 s PI → 50 s PI training. **(C)** Baseline 50 s PI functions for both treatment groups averaged across two sessions three weeks after the ANI treatment ended. **(D)** "Start" times (s) for responding during the three specified phases of PI training for DS-CON and DS-ANI treatment groups. The Baseline 20 s PI and Baseline 50 s PI "Start" times during each session correspond to the peak functions displayed in **Figures 2A,C**. During the transition phase, individual data were smoothed across 10 sessions of microinjections using a running median with a 3-session window. **(E)** Mean (± SEM) response rate (responses/s) on probe trials during the three specified phases of the experiment for the DS-CON and DS-ANI groups. ANI = anisomycin; CON = control; DS = dorsal striatum.

on the 20 s → 50 s transition phase data revealed significant effects on "Start" times with respect to Treatment and Session, ($F_{1,17} = 4.47, p < 0.05$) and ($F_{7,119} = 7.14, p < 0.0001$), respectively. In addition, a significant Treatment × Session interaction was observed, ($F_{7,119} = 2.91, p < 0.01$). The mean response rates on probe trials during the three specified phases of the experiment for the DS-CON and DS-ANI treatment groups are illustrated in **Figure 4E**. A Two-Way ANOVA was conducted on each of these phases (Baseline-20 s, Transition Phase, and Baseline-50 s). During the Transition Phase, a significant effect of Session was observed ($F_{7,119} = 5.46$, $p < 0.0001$), but non-significant effects of Treatment ($F_{1,17} = 2.60$, $p > 0.05$) as well as the Session × Treatment interaction ($F_{7,119} = 0.69, p > 0.05$). In addition, there were no reliable effects of Session or Treatment on response rates during either of the 20 s or 50 s Baseline phases, p's > 0.05.

Following the completion of ANI or vehicle administration (CON), each treatment group continued to be trained on the 50 s PI procedure, but with microinjections discontinued. While ANI administration significantly impaired the acquisition of the "Start" response across the 10 treatment sessions, there did not appear to be any long-lasting functional damage to the DS with respect to the temporal control of behavior. **Figure 4C** shows the mean peak functions for each treatment group obtained approximately three weeks (post-ANI Sessions 21–22) following microinjections while **Figure 4D** (right panel) depicts the "Start" times during this Baseline-50 s phase. A Two-Way ANOVA with Treatment and Session as factors indicated non-significant effects of Treatment ($F_{1,32} = 0.71, p > 0.05$), Session ($F_{1,32} = 1.07, p > 0.05$), as well as the Treatment × Session interaction ($F_{1,32} = 0.11, p > 0.05$).

Histological examination for rats bearing bilateral, indwelling cannulae aimed at the DS and VS verified accurate placements for all rats in the ANI and CON treatment groups at both anatomical locations. A summary of these results for Experiment 1 and 2 is provided in **Figure 5** (panels A–C).

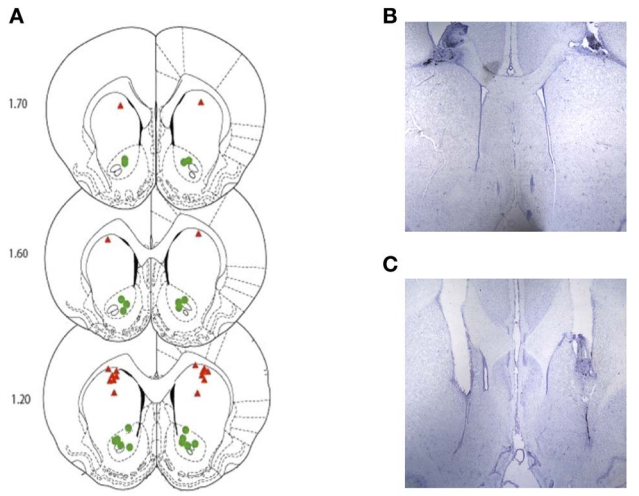

FIGURE 5 | (A) Depicts the approximate location of the injector tips for the DS-CON and DS-ANI treatment groups (red triangles) as well as the VS-CON and VS-ANI treatment groups (green circles) across both experiments. **(B** and **C)** Representative coronal brain sections depicting the injector tracts terminating in the DS and VS, respectively. ANI = anisomycin; CON = control; DS = dorsal striatum; VS = ventral striatum.

DISCUSSION

In this series of experiments we provide the first demonstrations that differential patterns of activity in the dorsal and VS are required for the types of decision-making used in the temporal control of response sequences. In particular, normal functioning of the DS is necessary for the acquisition of a timed "Start" response and similar activation in the VS, but not the DS, is required for the acquisition of a timed "Stop" response. Interestingly, during acquisition of the "Stop" response, the "Start" responses exhibited by the rats in the DS-ANI treatment group were sharper relative to the timing performance of the rats in the other treatment groups. This observation supports our finding in Experiment 2 that the DS is connected with the "Start" response. Therefore, ANI infusion into the DS maintained and/or increased the precision of the temporal estimate for the "Start" response while rats were acquiring the "Stop" response. The basis for this double dissociation might be grounded in the behavioral context that underlies PI training and the acquisition of a "Start" response. Indeed, this finding suggests that a decrease in the probability of reward relating to a predictive cue (i.e., houselight), which until this point in training had reliably signaled the expected time of reward delivery, brings about activational changes (possibly involving protein synthesis) in both the DS and VS.

In concert with mesolimbic dopaminergic input, the VS is believed to contribute to "behavioral switching," which reflects the reallocation of behavioral resources from current behavior(s) to subsequent one(s) in a flexible manner (Koob et al., 1978; Cools, 1980; Robbins and Brown, 1990; Redgrave et al., 1999). Indeed, the VS inhibit habitual responding in situations during which there is no reward or low stimulus control (Reading and Dunnett, 1991). Though interval timing is typically not studied within an associative framework (Kirkpatrick and Church, 1998), it is well-known that FI schedules can promote responding guided by "habitual" (S-R) associative content (Dickinson et al., 1983) and the transition to habitual responding can occasion changes within neurotransmitter systems that are directly related to interval timing (Choi et al., 2005; Faure et al., 2005; Yin and Knowlton, 2006; DeRusso et al., 2010). Moreover, it is often suggested that the VS contributes to goal-directed behavior by serving as an interface between limbic regions, which are thought to underlie affective (e.g., amygdalar) and contextual (e.g., hippocampal) processing, and provides a structural nexus whereby motivational information can gain access to predictive stimuli (Cardinal et al., 2002; Kelley, 2004; van der Meer et al., 2010). With this in mind, the VS might contribute to the acquisition of the "Stop" response by integrating updated, behavioraly-relevant information with output from a neural timing mechanism, which provides a signal for when the expected time of reward has passed. Downstream motor structures could then be triggered to coordinate the termination of an ongoing response sequence (see Roesch et al., 2009). In this sense, the "Stop" response in the PI timing procedure corresponds to the "giving-up time" in foraging situations where a subject has to decide when to leave a patch. "Giving-up times" have been shown to be more sensitive to the distribution of reinforcement times and magnitudes than the decision of when to enter a patch—which have been related to the differential control of "Start" and "Stop" responses in the PI timing procedure (Brunner et al., 1992, 1996, 1997; Taylor et al., 2007).

Conversely, activational changes (possibly involving protein synthesis) in the DS appear to contribute to the shaping of the "Start" response, which determines when the onset of the "high state" occurs. Some researchers have proposed that the DS plays an important role in the initiation of response sequences (Carli et al., 1985; Robbins and Brown, 1990; Graybiel, 1998; Bailey and Mair, 2006), but precise role(s) of the basal ganglia in kinematics and habits remain controversial (Graybiel, 2008; Desmurget and Turner, 2010; Turner and Desmurget, 2010). In Experiment 2, ANI infusion into the DS impaired the rightward transition in the "Start" response that normally takes place after switching from a 20 s to a 50 s temporal criterion. However, from our results, it is unclear how the acquisition of a "Start" response is mediated by activational changes in the DS. Indeed, in both Experiment 1 and 2, the differences observed with respect to the "Start" response in the DS-ANI group emerged (1) after an initial "Start" response was well-learned (i.e., following extensive training with one target duration) and (2) under conditions where uncertainty with regard to the expected time of reward delivery is present. This suggests that activational changes (including protein synthesis) in the DS can come on-line during transitional conditions in which the temporal contingencies that guided the "Start" response over an extended period need to be updated. Similarly, for example, the DS neuronal population changes on many dimensions as an animal learns to respond optimally on a T-maze. In this case, neurons gradually transition to preferably encode the beginning and end of the acquired response sequence in the T-maze. However, the specificity of the response profile for the beginning and end abruptly decreases during transitional conditions such as those reported in Barnes et al. (2005). In our experiment, ANI infusion

into the DS may resist a "reorganization" that takes place when unrewarded probe trials are first introduced, which is brought about by competing stimuli that change *when* a response sequence is initiated.

Unlike Experiment 1, the target duration was changed in the Experiment 2. Therefore, it is possible that striatal activation (possibly including protein synthesis) is required to encode a memory of the new target duration, making the effect on the "Start" response threshold ancillary. However, there is reason to suspect that this isn't the case. The change in the target duration was detected during the first session because the "Start" response from both DS and CON groups jumped to a later time even after ANI infusion. In fact, previous work has shown that memories for new target durations can be encoded after relatively few trials and response thresholds are shaped thereafter Meck et al., 1984b; Meck, 1988; Drew et al., 2004; Balsam and Gallistel, 2009. Given our findings from Experiment 1, it seems that activational changes in the DS are required to modulate the "Start" response. The target duration may be encoded either outside the DS or in a more specific DS sub-region than we targeted with the AIN infusions (Meck, 2006b; Yin and Knowlton, 2006). It's also worth considering that protein synthesis may not be required to encode the memory for a target duration, regardless of where it is stored (Routtenberg, 2008).

The dynamics of behavioral transitions in rodents, birds, and humans have demonstrated both abrupt and gradual transitions in the adjustment to changes in the time of reinforcement in the PI timing procedure (Meck et al., 1984a,b; Lejeune et al., 1997; Rodríguez-Gironés and Kacelnik, 1999; Simen et al., 2011). Whether or not these transitions initially involve an abrupt transition to an "intermediate" state appears to depend upon whether the adjustment is from a lower to a higher target duration or vice versa, the ratio of the times of reinforcement, the ratio of FI trials to unreinforced probe trials, and the subject's previous experience with such transitions (Meck et al., 1984a,b; Lejeune et al., 1997). Under the conditions used in the current experiment, it is expected that when rats are transitioned from a 20 s PI procedure to a 50 s PI procedure using a ratio of 50% FI trials to 50% unreinforced probe trials they will initially exhibit a relatively abrupt transition of their "Start" times from those appropriate to the 20 s target duration to an intermediate value near the geometric mean of the 20 s and 50 s target durations. This step is thought to result from the subject comparing the remembered rate of reinforcement under the 20 s condition to the experienced rate of reinforcement under the new 50 s condition and not necessarily the rapid acquisition of a new target duration—which would be expected to occur in a more gradual manner. Such continuous updating of the subjective probabilities of reinforcement operates in parallel to the adjustment of "Start" and "Stop" response thresholds centered around specific times of reinforcement—much like the processing of variable-interval vs. fixed-interval schedules of reinforcement (Hinton and Meck, 1997a,b; Rodríguez-Gironés and Kacelnik, 1999). Consequently, in the current experiment it might be expected that when rats are transitioned from a 20 s to a 50 s temporal criterion the initial adjustment of the "Start" response to an intermediate state would be unimpaired by ANI administration, whereas the second step involving the acquisition of a "Start" response appropriate to the 50 s target duration would be impaired as this requires the acquisition of a new temporal criterion and associated response thresholds as opposed to the monitoring of changes in the overall rates of reinforcement and the adjustment of previously acquired response thresholds (Lejeune et al., 1997). Moreover, the abrupt jump to an intermediate duration isn't influenced by hippocampal lesions and may be indicative of subjects using their old "Stop" threshold as a temporary "Start" threshold during this transition period (Meck et al., 1984a,b; Meck, 1988; MacDonald et al., 2007, 2009, 2011; Yin and Troger, 2011).

Our results also show that VS can contribute importantly to interval timing during learning. On the surface, it seems plausible that the "Stop" response ought to be mediated by behavioral and neural processes similar to those that operate during extinction (Myers and Davis, 2002; Lattal et al., 2006). Indeed, like extinction the acquisition of the "Stop" response appears to reflect new learning that is independent of the "Start" response. Moreover, several experiments have shown that VS lesions can lead to persistent responding during extinction of other operant tasks (Annett et al., 1989; Reading and Dunnett, 1991; Reading et al., 1991). However, in the case of the PI timing procedure, the extinction is partial. Reward is obtained on a random proportion (e.g., 50%) of FI trials and "extinction" of responding during the unreinforced probe trials exhibits a temporal gradient indicating that it is strongly guided by the memory of the target duration (see Kaiser, 2008).

Regardless of its relationship to extinction, the emergence of the "Stop" response might reflect learning that there is little value to sustaining a high response rate once the target duration has passed. In this regard, the VS may be involved in the "invigoration" of behavior (Cardinal et al., 2002; Robbins and Everitt, 2007), and may do so by dynamically tracking the value of the predictive signal O'Doherty et al., 2004; Atallah et al., 2007; Niv, 2007. Therefore, in order to terminate the ongoing response sequence, activational changes (possibly including protein synthesis) in the VS are required for the integration of time-related information with the "Stop" response. This allows the animal to reallocate its behavioral resources from current behavior(s) to subsequent one(s) in a flexible manner (Koob et al., 1978; Cools, 1980; Robbins and Brown, 1990).

The basal ganglia are known to receive rich and diffuse input from many brain regions, especially the midbrain dopaminergic area, which is sensitive to both the expected time of reward and changes in reward probability—two conditions that characterize each of our experimental contexts (Hollerman and Schultz, 1998; Fiorillo et al., 2003). Our results suggest a regional dissociation between how these different types of information might be integrated to influence behavior. Moreover, they are supported by a study that confirmed a double dissociation with respect to the role of the DS and VS on reconsolidation during the instrumental learning of a lever press (Hernandez et al., 2002). In this case, ANI impeded the acquisition of lever pressing following post-session administration into the accumbens core of the VS, the brain area primarily targeted in our experiments. In contrast, post-session ANI injections into the DS facilitated the acquisition of an instrumental response, which we speculate might arise from a decrease

in the effect of task-irrelevant stimuli impinging on the DS. An intriguing possibility is that these two striatal regions might function as a competitive network early in learning, which ultimately promotes optimal behavioral allocation (Hernandez et al., 2002; MacDonald and Meck, 2004, 2005; Kimchi and Laubach, 2009; Kimchi et al., 2009; Yin et al., 2009; Smith et al., 2010). In the present experiment, ANI was microinjected before the sessions began so we can't distinguish whether the effects we observed are targeting the memory consolidation, or a reconsolidation process. However, our experiments support and extend earlier findings by implicating a dissociable role for the DS and VS regarding *when* a response sequence should be initiated and terminated on the basis of a real-time temporal expectation.

The striatal beat-frequency (SBF) model of interval timing ascribes a mechanism for detecting event durations to medium spiny neurons within the DS (MacDonald and Meck, 2004; Matell and Meck, 2004; Buhusi and Meck, 2005; Lustig et al., 2005; Coull et al., 2011; Oprisan and Buhusi, 2011; Allman and Meck, 2012). These striatal neurons have a set of functional properties that place them in an ideal position to detect behaviorally relevant patterns of afferent cortical input (Beiser and Houk, 1998). Briefly, the SBF model posits that medium spiny neurons in the DS become entrained to fire in response to oscillating, coincident cortical inputs that become active at a particular duration. This timing model is particularly useful insofar as the striatal neurons modeled using the SBF framework behave as they do using multiunit electrical recordings during interval-timing procedures (Matell et al., 2003; Matell and Meck, 2004). However, in this model, there is relatively less focus on the role of the VS in interval timing primarily because timing behavior at steady state appears more influenced by manipulations targeting the DS rather than the VS (Gibbon et al., 1997; Meck, 2006b; Kurti and Matell, 2011). Moreover, our results suggest that the VS might contribute importantly to the acquisition of timing behavior. In this way, DS neurons would be responsible for encoding event durations, but feedback from the VS and other parts of the basal ganglia and/or limbic system are used to modulate the output of striatal spiny neurons in the DS (Berke et al., 2004; MacDonald and Meck, 2004, 2005; O'Doherty et al., 2004; Shea-Brown et al., 2006; Atallah et al., 2010; Gage et al., 2010; Coull et al., 2011).

SUMMARY

Despite numerous claims that the inhibition of protein synthesis following ANI administration directly interferes with memory formation (Abel and Lattal, 2001; Alberini, 2008; Kwapis et al., 2011; Okamoto et al., 2011), there are compelling reasons to be more cautious in this interpretation. Gold and colleagues, for example, have argued that ANI induces temporary amnesia rather than inhibition of memory formation *per se* (Canal and Gold, 2007; Canal et al., 2007; Gold, 2008; Qi and Gold, 2009; Sadowski et al., 2011). Such amnesia might result, in part, from the disruption of neurotransmitter systems, including the increased release of norepinephrine, dopamine, and serotonin (Canal et al., 2007). When these unintended "side effects" were blocked, leaving the inhibition of protein synthesis largely unchanged, no reliable memory impairment was observed (Canal et al., 2007; Qi and Gold, 2009; Sadowski et al., 2011). As a consequence, some investigators have been skeptical of the role of protein synthesis in memory formation (for review see Alberini, 2008; Gold, 2008; Rudy, 2008; Rudy and Sutherland, 2008). Moreover, even when ANI is administered post-session and, therefore, thought to only affect processes involved in memory consolidation and not behavioral performance during the task, there is the potential to impair instrumental learning by drug-induced devaluation of the reward (e.g., food or sucrose pellet) which can affect behavioral performance in subsequent sessions as demonstrated by Jonkman and Everitt (2009).

In the current study, ANI infusions were given prior to the start of a training session in order to maximize the chances of affecting learning and memory consolidation that would be expected to occur within the 2 h session. As a consequence, all of the concerns expressed above concerning performance variables are valid. The dissociation of timing performance for "Start" and "Stop" response thresholds as a function of ANI infusion into either the dorsal or VS suggests selective effects depending upon the type of response and brain region, as well as the degree of behavioral training and whether short-term or long-term memory processes are involved. In Experiment 2 for example, during the transition from a 20 s to a 50 s target duration, rats initially used a criterion that was intermediate between the two times of reinforcement. The determination of this intermediate target duration (which was never reinforced) presumably requires some sort of short-term memory process to be engaged. The observation that these early transitional processes were unaffected by ANI infusion, but that the more gradual acquisition of the "Start" response for the new 50 s target duration was selectively impaired by ANI infusion into the DS is consistent with a "protein synthesis" argument, i.e., that only those mechanisms responsible for the formation of long-term memories/response thresholds associated with the 50 s target duration were impacted by ANI infusion.

Taken together, our results point to a regional dissociation between how temporal information is used to guide separate components of a response sequence. Both the "Start" and "Stop" response thresholds serve as temporal boundaries that define transitions between two measurably different behavioral "states" occur. Clearly, there are many more questions as to why these transitions are different in the first place and require different brain structures. For example, it might be the case that the response topography of the state from which the transition leaves, or to which the transition leads represents an important factor. For some types of responses (e.g., discrete or sustained), response duration and the probability of response initiation can be differentiated by drugs that target D1 and D2 receptors, respectively (Gooch et al., 2007; Choi et al., 2005). Whatever the case, an intriguing possibility is that the dorsal and ventral striatal regions might function as a competitive network designed to respond to temporal information during the early stages of learning. The tracking of temporal regularities in the environment ultimately enhances adaptive behavior and may eventually lead to habit formation (Hernandez et al., 2002; MacDonald and Meck, 2004, 2005; Cheng et al., 2007a,c; Kimchi and Laubach, 2009; Kimchi et al., 2009; Yin et al., 2009; Smith et al., 2010). As such, most neurophysiological models of interval timing assume that target durations are encoded into a region's neuronal

network in part through the modification of synaptic weights (Coull et al., 2011; Oprisan and Buhusi, 2011; Allman and Meck, 2012). In this way, it is important to explicitly test how and where these long-term modifications might be carried out at the cellular level by making use of what we know in other learning settings. In this regard, while there remains much to explore, these experiments using ANI infusions are among the first to isolate the roles of the dorsal and VS in temporal processing (see Meck, 2006b).

ACKNOWLEDGMENTS

We would like to thank Elizabeth Clore, Erin Crawford, Antonia Laino, and Henry Yin for their assistance and support during the course of this project. This work was supported, in part, by an award from the James McKeen Cattell Fund (Warren H. Meck). Portion of this work have been previously reported at the annual meeting of the Society for Neuroscience (MacDonald et al., 2005, 2006).

REFERENCES

Abel, T., and Lattal, K. M. (2001). Molecular mechanisms of memory acquisition, consolidation and retrieval. *Curr. Opin. Neurobiol.* 11, 180–187.

Agostino, P. V., Golombek, D. A., and Meck, W. H. (2011). Unwinding the molecular basis of interval and circadian timing. *Front. Integr. Neurosci.* 5:64. doi: 10.3389/fnint.2011.00064

Alberini, C. M. (2008). The role of protein synthesis during the labile phases of memory: revisiting the skepticism. *Neurobiol. Learn. Mem.* 89, 234–246.

Aldridge, J. W., and Berridge, K. C. (1998). Coding of serial order by neostriatal neurons: a "natural action" approach to movement sequence. *J. Neurosci.* 18, 2777–2787.

Allman, M. J., and Meck, W. H. (2012). Pathophysiological distortions in time perception and timed performance. *Brain* 135, 656–677.

Annett, L. E., McGregor, A., and Robbins, T. W. (1989). The effects of ibotenic acid lesions of the nucleus accumbens on spatial learning and extinction in the rat. *Behav. Brain Res.* 31, 231–242.

Atallah, H. E., Lopez-Paniagua, D., Rudy, J. W., and O'Reilly, R. C. (2007). Separate neural substrates for skill learning and performance in the ventral and dorsal striatum. *Nat. Neurosci.* 10, 126–131.

Atallah, H. E., Lopez-Paniagua, D., Rudy, J. W., and O'Reilly, R. C. (2010). Separate neural substrates for skill learning and performance in the ventral and dorsal striatum. *Nat. Neurosci.* 10, 126–131.

Bailey, K. R., and Mair, R. G. (2006). The role of striatum in initiation and execution of learned action sequences in rats. *J. Neurosci.* 26, 1016–1025.

Balci, F., Gallistel, C. R., Allen, B. D., Frank, K. M., Gibson, J. M., and Brunner, D. (2009). Acquisition of peak responding: what is learned? *Behav. Process.* 80, 67–75.

Balsam, P. D., and Gallistel, C. R. (2009). Temporal maps and informativeness in associative learning. *Trends Neurosci.* 32, 73–78.

Barnes, T. D., Kubota, Y., Hu, D., Jin, D. Z., and Graybiel, A. M. (2005). Activity of striatal neurons reflects dynamic encoding and recoding of procedural memories. *Nature* 437, 1158–1161.

Bateson, M. (2003). "Interval timing and optimal foraging," in *Functional and Neural Mechanisms of Interval Timing*, ed W. H. Meck (Boca-Raton, FL: CRC Press), 113–141.

Beiser, D. G., and Houk, J. C. (1998). Model of cortical-basal ganglionic processing: encoding the serial order of sensory events. *J. Neurophysiol.* 79, 3168–3188.

Berke, J. D., Okatan, M., Skurski, J., and Eichenbaum, H. B. (2004). Oscillatory entrainment of striatal neurons in freely moving rats. *Neuron* 43, 883–896.

Bromberg-Martin, E. S., Matsumoto, M., and Hikosaka, O. (2010). Distinct tonic and phasic anticipatory activity in lateral habenula and dopamine neurons. *Neuron* 67, 144–155.

Brunner, D., Fairhurst, S., Stolovitzky, G., and Gibbon, J. (1997). Mnemonics for variability: remembering food delay. *J. Exp. Psychol. Anim. Behav. Process.* 23, 68–83.

Brunner, D., Kacelnik, A., and Gibbon, J. (1992). Optimal foraging and timing processes in the starling, Sturnus vulgaris: effect of intercapture interval. *Anim. Behav.* 44, 597–613.

Brunner, D., Kacelnik, A., and Gibbon, J. (1996). Memory for interreinforcement interval variability and patch departure decisions in the starling, *Sturnus vulgaris*. *Anim. Behav.* 51, 1025–1045.

Bueti, D. (2011). The sensory representation of time. *Front. Integr. Neurosci.* 5:34. doi: 10.3389/fnint.2011.00034

Buhusi, C. V., Aziz, D., Winslow, D., Carter, R. E., Swearington, J. E., and Buhusi, M. C. (2009). Interval timing accuracy and scalar timing in c57BL/6 mice. *Behav. Neurosci.* 123, 1102–1113.

Buhusi, C. V., and Meck, W. H. (2000). Timing for the absence of a stimulus: the gap paradigm reversed. *J. Exp. Psychol. Anim. Behav. Process.* 26, 305–322.

Buhusi, C. V., and Meck, W. H. (2002). Differential effects of methamphetamine and haloperidol on the control of an internal clock. *Behav. Neurosci.* 116, 291–297.

Buhusi, C. V., and Meck, W. H. (2005). What makes us tick? Functional and neural mechanisms of interval timing. *Nat. Rev. Neurosci.* 6, 755–765.

Buhusi, C. V., and Meck, W. H. (2006). Interval timing with gaps and distracters: evaluation of the ambiguity, switch, and time-sharing hypotheses. *J. Exp. Psychol. Anim. Behav. Process.* 32, 329–338.

Buhusi, C. V., and Meck, W. H. (2009a). Relative time sharing: new findings and an extension of the resource allocation model of temporal processing. *Philos. Trans. R. Soc. Lond. B Biol. Sci.* 364, 1875–1885.

Buhusi, C. V., and Meck, W. H. (2009b). Relativity theory and time perception: single or multiple clocks? *PLoS One* 4:e6268. doi: 10.1371/journal.pone.0006268

Buhusi, C. V., Sasaki, A., and Meck, W. H. (2002). Temporal integration as a function of signal/gap intensity in rats (*Rattus norvegicus*) and pigeons (*Columba livia*). *J. Comp. Psychol.* 116, 381–390.

Canal, C. E., Chang, Q., and Gold, P. E. (2007). Amnesia produced by altered release of neurotransmitters after intraamygdala injections of a protein synthesis inhibitor. *Proc. Natl. Acad. Sci. U.S.A.* 104, 12500–12505.

Canal, C. E., and Gold, P. E. (2007). Different temporal profiles of amnesia after intra-hippocampus and intra-amygdala infusions of anisomysin. *Behav. Neurosci.* 121, 732–741.

Cardinal, R. N., Parkinson, J. A., Hall, J., and Everitt, B. J. (2002). Emotion and motivation: the role of the amygdala, ventral striatum, and prefrontal cortex. *Neurosci. Biobehav. Rev.* 26, 321–352.

Carli, M., Evenden, J. L., and Robbins, T. W. (1985). Depletion of unilateral striatal dopamine impairs initiation of contralateral actions and not sensory attention. *Nature* 313, 679–682.

Castellucci, V. F., Blumenfeld, H., Goelet, P., and Kandel, E. R. (1989). Inhibitor of protein synthesis blocks longterm behavioral sensitization in the isolated gill-withdrawal reflex of Aplysia. *J. Neurobiol.* 20, 1–9.

Choi, W. Y., Balsam, P. D., and Horvitz, J. C. (2005). Extended habit training reduces dopamine mediation of appetitive response expression. *J. Neurosci.* 25, 6729–6733.

Cheng, R. K., Ali, Y. M., and Meck, W. H. (2007a). Ketamine "unlocks" the reduced clock-speed effect of cocaine following extended training: evidence for dopamine-glutamate interactions in timing and time perception. *Neurobiol. Learn. Mem.* 88, 149–159.

Cheng, R. K., Etchegaray, M., and Meck, W. H. (2007b). Impairments in timing, temporal memory, and reversal learning linked to neurotoxic regimens of methamphetamine intoxication. *Brain Res.* 1186, 255–266.

Cheng, R. K., Hakak, O. L., and Meck, W. H. (2007c). Habit formation and the loss of control of an internal clock: inverse relationship between the level of baseline training and the clock-speed enhancing effects of methamphetamine. *Psychopharmacology* 193, 351–362.

Cheng, R. K., Jesuthasan, S., and Penney, T. B. (2011). Time for zebrafish. *Front. Integr. Neurosci.* 5:40. doi: 10.3389/fnint.2011.00040

Cheng, R. K., MacDonald, C. J., and Meck, W. H. (2006). Differential effects of cocaine and ketamine on time estimation: implications for neurobiological models of interval timing. *Pharmacol. Biochem. Behav.* 85, 114–122.

Cheng, R. K., and Meck, W. H. (2007). Prenatal choline supplementation increases sensitivity to time by reducing non-scalar sources of variance in adult temporal processing. *Brain Res.* 1186, 242–254.

Church, R. M., Meck, W. H., and Gibbon, J. (1994). Application of scalar timing theory to individual trials. *J. Exp. Psychol. Anim. Behav. Process.* 20, 135–155.

Church, R. M., Miller, K. D., Meck, W. H., and Gibbon, J. (1991). Symmetrical and asymmetrical sources of variance in temporal generalization. *Anim. Learn. Behav.* 19, 207–214.

Cools, A. R. (1980). Role of the neostriatal dopaminergic activity in sequencing and selecting behavioural strategies: facilitation of processes involved in selecting the best strategy in a stressful situation. *Behav. Brain Res.* 1, 361–378.

Coull, J. T., Cheng, R. K., and Meck, W. H. (2011). Neuroanatomical and neurochemical substrates of timing. *Neuropsychopharmacology* 36, 3–25.

Coull, J. T., Vidal, F., Nazarian, B., and Macar, F. (2004). Functional anatomy of the attentional modulation of time estimation. *Science* 303, 1506–1508.

Cromwell, H. C., and Berridge, K. C. (1996). Implementation of action sequences by a neostriatal site: a lesion mapping study of grooming syntax. *J. Neurosci.* 16, 3444–3458.

Cui, X. (2011). Hyperbolic discounting emerges from the scalar property of interval timing. *Front. Integr. Neurosci.* 5:24. doi: 10.3389/fnint.2011.00024

DeRusso, A. L., Fan, D., Gupta, J., Shelest, O., Costa, R. M., and Yin, H. H. (2010). Instrumental uncertainty as a determinant of behavior under interval schedules of reinforcement. *Front. Integr. Neurosci.* 4:17. doi: 10.3389/fnint.2010.00017

Desmurget, M., and Turner, R. S. (2010). Motor sequences and the basal ganglia: kinematics, not habits. *J. Neurosci.* 30, 7685–7690.

Dickinson, A., Nicholas, D. J., and Adams, C. D. (1983). The effect of the instrumental training contingency on susceptibility to reinforcer devaluation. *Q. J. Exp. Psychol. B* 35, 35–51.

Drew, M. R., Simpson, E. H., Kellendonk, C., Herzberg, W. G., Lipatova, O., Fairhurst, S., Kandel, E. R., Malapani, C., and Balsam, P. D. (2007). Transient overexpression of striatal D2 receptors impairs operant motivation and interval timing. *J. Neurosci.* 27, 7731–7739.

Drew, M. R., Yang, C., Ohyama, T., and Balsam, P. D. (2004). Temporal specificity of extinction in autoshaping. *J. Exp. Psychol. Anim. Behav. Process.* 30, 163–176.

Drew, M. R., Zupan, B., Cooke, A., Couvillon, P. A., and Balsam, P. D. (2005). Temporal control of conditioned responding in goldfish. *J. Exp. Psychol. Anim. Behav. Process.* 31, 31–39.

Droit-Volet, S., and Meck, W. H. (2007). How emotions colour our perception of time. *Trends Cogn. Sci.* 11, 504–513.

Fantino, E., Dunn, R., and Meck, W. (1979). Percentage reinforcement and choice. *J. Exp. Anal. Behav.* 32, 335–340.

Faure, A., Haberland, U., Condé, F., and El Massioui, N. (2005). Lesion of the nigrostriatal dopamine system disrupts stimulus-response habit formation. *J. Neurosci.* 16, 2771–2780.

Fiorillo, C. D., Tobler, P. N., and Schultz, W. (2003). Discrete coding of reward probability and uncertainty by dopamine neurons. *Science* 299, 1898–1902.

Floresco, S. B., Ghods-Sharifi, S., Vexelman, C., and Magyar, O. (2006). Dissociable roles for the nucleus accumbens core and shell in regulating set shifting. *J. Neurosci.* 26, 2449–2457.

Forstmann, B. U., Dutilh, G., Brown, S., Neumann, J., von Cramon, D. Y., Ridderinkhof, K. R., and Wagenmakers, E. J. (2008). Striatum and pre-SMA facilitate decision-making under time pressure. *Proc. Natl. Acad. Sci. U.S.A.* 105, 17538–17542.

Freestone, D. M., and Church, R. M. (2010). The importance of the reinforcer as a time marker. *Behav. Process.* 84, 500–505.

Fujii, N., and Graybiel, A. M. (2005). Time-varying covariance of neural activities recorded in striatum and frontal cortex as monkeys perform sequential-saccade tasks. *Proc. Natl. Acad. Sci. U.S.A.* 102, 9032–9037.

Gage, G. J., Stoetzner, C. R., Wiltschko, A. B., and Berke, J. D. (2010). Selective activation of striatal fast-spiking interneurons during choice execution. *Neuron* 67, 466–479.

Gallistel, C. R., and Gibbon, J. (2000). Time, rate, and conditioning. *Psychol. Rev.* 107, 289–344.

Gallistel, C. R., King, A., and McDonald, R. (2004). Sources of variability and systematic error in mouse timing behavior. *J. Exp. Psychol. Anim. Behav. Process.* 30, 3–16.

Gibbon, J., Church, R. M., and Meck, W. H. (1984). Scalar timing in temporal memory. *Ann. N.Y. Acad. Sci.* 423, 52–77.

Gibbon, J., Malapani, C., Dale, C. L., and Gallistel, C. R. (1997). Toward a neurobiology of temporal cognition: advances and challenges. *Curr. Opin. Neurobiol.* 7, 170–184.

Gold, P. E. (2008). Protein synthesis inhibition and memory: formation vs amnesia. *Neurobiol. Learn. Mem.* 89, 201–211.

Gooch, C. M., Wiener, M., Portugal, G. S., and Matell, M. S. (2007). Evidence for separate neural mechanisms for the timing of discrete and sustained responses. *Brain Res.* 1156, 139–151.

Graybiel, A. M. (1998). The basal ganglia and chunking of action repertoires. *Neurobiol. Learn. Mem.* 70, 119–136.

Graybiel, A. (2008). Habits, rituals, and the evaluative brain. *Ann. Rev. Neurosci.* 31, 359–387.

Gu, B. M., Yin, B., Cheng, R. K., and Meck, W. H. (2011). Quinpirole-induced sensitization to noisy/sparse periodic input: temporal synchronization as a component of obsessive-compulsive disorder. *Neuroscience* 179, 143–150.

Harrington, D. L., Boyd, L. A., Mayer, A. R., Sheltraw, D. M., Lee, R. R., Huang, M., and Rao, S. M. (2004). Neural representation of interval encoding and decision making. *Cogn. Brain Res.* 21, 193–205.

Harrington, D. L., Castillo, G. N., Fong, C. H., and Reed, J. D. (2011a). Neural underpinnings of distortions in the experience of time across senses. *Front. Integr. Neurosci.* 5:32. doi: 10.3389/fnint.2011.00032

Harrington, D. L., Castillo, G. N., Greenberg, P. A., Song, D. D., Lessig, S., Lee, R. R., and Rao, S. M. (2011b). Neurobehavioral mechanisms of temporal processing deficits in Parkinson's disease. *PLoS One* 6:e17461. doi: 10.1371/journal.pone.0017461

Hata, T. (2011). Glutamate – a forgotten target for interval timing. *Front. Integr. Neurosci.* 5:27. doi: 10.3389/fnint.2011.00027

Hernandez, P. J., and Kelley, A. E. (2004). Long-term memory for instrumental response does not undergo protein synthesis-dependent reconsolidation upon retrieval. *Learn. Mem.* 11, 748–754.

Hernandez, P. J., Sadeghian, K., and Kelley, A. E. (2002). Early consolidation of instrumental learning requires protein synthesis in the nucleus accumbens. *Nat. Neurosci.* 5, 1327–1331.

Hinton, S. C., and Meck, W. H. (1997a). "How time flies: functional and neural mechanisms of interval timing," in *Time and Behaviour: Psychological and Neurobiological Analyses*, eds C. M. Bradshaw and E. Szabadi (New York, NY: Elsevier), 409–457.

Hinton, S. C., and Meck, W. H. (1997b). The "internal clocks" of circadian and interval timing. *Endeavour* 21, 82–87.

Hinton, S. C., and Meck, W. H. (2004). Frontal-striatal circuitry activated by human peak-interval timing in the supra-seconds range. *Cogn. Brain Res.* 21, 171–182.

Höhn, S., Dallérac, G., Faure, A., Urbach, Y., Nguyen, H. P., Riess, O., von Hörsten, S., Le Blanc, P., Desvignes, N., El Massioui, N., Brown, B. L., and Doyère, V. (2011). Behavioral and *in vivo* electrophysiological evidence for presymptomatic alteration of prefronto-striatal processing in the transgenic rat model for Huntington disease. *J. Neurosci.* 31, 8986–8997.

Hollerman, J. R., and Schultz, W. (1998). Dopamine neurons report an error in the temporal prediction of reward during learning. *Nat. Neurosci.* 1, 304–309.

Jin, D. Z., Fujii, N., and Graybiel, A. M. (2009). Neural representation of time in cortico-basal ganglia circuits. *Proc. Natl. Acad. Sci. U.S.A.* 106, 19156–19161.

Jin, X., and Costa, R. M. (2010). Striatal-specific deletion of NMDA receptors disrupts the development of start/top activity and impairs sequence learning. *Nature* 466, 457–462.

Jones, C. L., Minati, L., Harrison, N. A., Ward, J., and Critchley, H. D. (2011). Under pressure: response urgency modulates striatal and insula activity during decision-making under risk. *PLoS One* 6: e20942. doi: 10.1371/journal.pone.0020942

Jones, C. R. G., and Jahanshahi, M. (2011). Dopamine modulates striato-frontal functioning during temporal processing. *Front. Integr. Neurosci.* 5:70. doi: 10.3389/fnint.2011.00070

Jonkman, A., and Everitt, B. J. (2009). Post-learning infusion of anisomycin into the anterior cingulate cortex impairs instrumental acquisition through an effect on reinforcer valuation. *Learn. Mem.* 16, 706–713.

Kaiser, D. H. (2008). The proportion of fixed interval trials to probe trials affects acquisition of the peak procedure fixed interval timing task. *Behav. Process.* 77, 100–108.

Kelley, A. E. (2004). Ventral striatal control of appetitive motivation: role in ingestive behavior and reward-related learning. *Neurosci. Biobehav. Rev.* 27, 765–776.

Kimchi, E. Y., and Laubach, M. (2009). The dorsomedial striatum reflects response bias during learning. *J. Neurosci.* 29, 14891–14902.

Kimchi, E. Y., Torrefrossa, M. M., Taylor, J. R., and Laubach, M. (2009). Neuronal correlates of instrumental learning in the dorsal striatum. *J. Neurophysiol.* 102, 475–489.

Kirkpatrick, K., and Church, R. M. (1998). Are separate theories of conditioning and timing necessary? *Behav. Process.* 44, 163–182.

Koob, G. F., Riley, S. J., Smith, S. C., and Robbins, T. W. (1978). Effects of 6-hydroxydopamine lesions of the nucleus accumbens septi and olfactory tubercle on feeding, locomotor activity, and amphetamine anorexia in the rat. *J. Comp. Physiol. Psychol.* 92, 917–927.

Kotz, S. A. E., and Schwartze, M. (2011). Differential input of the supplementary motor area to a dedicated temporal processing network: functional and clinical implications. *Front. Integr. Neurosci.* 5:86. doi: 10.3389/fnint.2011.00086

Kurti, A. N., and Matell, M. S. (2011). Nucleus accumbens dopamine modulates response rate but not response timing in an interval timing task. *Behav. Neurosci.* 125, 215–225.

Kwapis, J. L., Jarome, T. J., Schiff, J. C., and Helmstetter, F. J. (2011). Memory consolidation in both trace and delay fear conditioning is disrupted by intra-amygdala infusion of the protein synthesis inhibitor anisomycin. *Learn. Mem.* 18, 728–732.

Lattal, K. M., Radulovic, J., and Lukowiak, K. (2006). Extinction: does it or doesn't it? The requirement of altered gene activity and new protein synthesis. *Biol. Psychiatry* 15, 344–351.

Lejeune, H., Ferrara, A., Simons, F., and Wearden, J. H. (1997). Adjusting to changes in the time of reinforcement: peak-interval transitions in rats. *J. Exp. Psychol. Anim. Behav. Process.* 23, 211–231.

Liao, R. M., and Cheng, R. K. (2005). Acute effects of d-amphetamine on the differential reinforcement of low-rate (DRL) schedule behavior in the rat: comparison with selective dopamine receptor antagonists. *Chin. J. Physiol.* 48, 41–50.

Lustig, C., Matell, M. S., and Meck, W. H. (2005). Not "just" a coincidence: frontal-striatal synchronization in working memory and interval timing. *Memory* 13, 441–448.

Lustig, C., and Meck, W. H. (2001). Paying attention to time as one gets older. *Psychol. Sci*.12, 478–484.

Lustig, C., and Meck, W. H. (2005). Chronic treatment with haloperidol induces working memory deficits in feedback effects of interval timing. *Brain Cogn.* 58, 9–16.

Lustig, C., and Meck, W. H. (2011). Modality differences in timing and temporal memory throughout the lifespan. *Brain Cogn.* 77, 298–303.

MacDonald, C. J., Cheng, R. K., Laino, A. M., and Meck, W. H. (2005). Protein synthesis and the "sculpting" of a temporal criterion: competitive interactions between dorsal and ventral striatum for learning when to start and stop responding. *Abstr. Soc. Neurosci.* 635.08.

MacDonald, C. J., Cheng, R. K., Clore, E. L., and Meck, W. H. (2006). Learning when to "start" and "stop" an action sequence: dissociable roles for *de novo* protein synthesis in the dorsal and ventral striatum. *Abstr. Soc. Neurosci.* 572.17.

MacDonald, C. J., Cheng, R. K., Williams, C. L., and Meck, W. H. (2007). Combined organizational and activational effects of short and long photoperiods on spatial and temporal memory in rats. *Behav. Process.* 74, 226–233.

MacDonald, C. J., LePage, K. Q., Eden, U. T., and Eichenbaum, H. (2011). Hippocampal "time cells" bridge the gap in memory for discontiguous events. *Neuron* 71, 737–749.

MacDonald, C. J., and Meck, W. H. (2004). Systems-level integration of interval timing and reaction time. *Neurosci. Biobehav. Rev.* 28, 747–769.

MacDonald, C. J., and Meck, W. H. (2005). Differential effects of clozapine and haloperidol on interval timing in the supraseconds range. *Psychopharmacology* 182, 232–244.

MacDonald, C. J., and Meck, W. H. (2006). Interaction of raclopride and preparatory-interval effects on simple reaction-time performance. *Behav. Brain Res.* 175, 62–74.

MacDonald, C. J., Meck, W. H., Simon, S. A., and Nicolelis, M. A. L. (2009). Taste-guided decision differentially engage neuronal ensembles across gustatory cortices. *J. Neurosci.* 29, 11271–11282.

Maimon, G., and Assad, J. A. (2006). A cognitive signal for the proactive timing of action in macaque LIP. *Nat. Neurosci.* 9, 948–955.

Malapani, C., Rakitin, B., Meck, W. H., Deweer, B., Dubois, B., and Gibbon, J. (1998). Coupled temporal memories in Parkinson's disease: a dopamine-related dysfunction. *J. Cogn. Neurosci.* 10, 316–331.

Mansfield, E. L., Karayanidis, F., Jamadar, S., Heathcote, A., and Forstmann, B. U. (2011). Adjustments of response threshold during task switching: a model-based functional magnetic resonance imaging study. *J. Neurosci.* 31, 14688–14692.

Matell, M. S., Bateson, M., and Meck, W. H. (2006). Single-trials analyses demonstrate that increases in clock speed contribute to the methamphetamine-induced horizontal shifts in peak-interval timing functions. *Psychopharmacology* 188, 201–212.

Matell, M. S., King, G. R., and Meck, W. H. (2004). Differential adjustment of interval timing by the chronic administation of intermittent or continuous cocaine. *Behav. Neurosci.* 118, 150–156.

Matell, M. S., and Meck, W. H. (2000). Neuropsychological mechanisms of interval timing behavior. *Bioessays* 22, 94–103.

Matell, M. S., and Meck, W. H. (2004). Cortico-striatal circuits and interval timing: coincidence-detection of oscillatory processes. *Cogn. Brain Res.* 21, 39–70.

Matell, M. S., Meck, W. H., and Nicolelis, M. A. L. (2003). Interval timing and the encoding of signal duration by ensembles of cortical and striatal neurons. *Behav. Neurosci.* 117, 760–773.

Matell, M. S., Shea-Brown, E., Gooch, C., Wilson, A. G., and Rinzel, J. (2011). A heterogeneous population code for elapsed time in rat medial agranular cortex. *Behav. Neurosci.* 125, 54–73.

Meck, W. H. (1983). Selective adjustment of the speed of internal clock and memory processes. *J. Exp. Psychol. Anim. Behav. Process.* 9, 171–201.

Meck, W. H. (1988). Hippocampal function is required for feedback control of an internal clock's criterion. *Behav. Neurosci.* 102, 54–60.

Meck, W. H. (1991). Modality-specific circadian rhythmicities influence mechanisms of attention and memory for interval timing. *Learn. Motiv.* 22, 153–179.

Meck, W. H. (1996). Neuropharmacology of timing and time perception. *Cogn. Brain Res.* 3, 227–242.

Meck, W. H. (2002). Choline uptake in the frontal cortex is proportional to the absolute error of a temporal memory translation constant in mature and aged rats. *Learn. Motiv.* 33, 88–104.

Meck, W. H. (2003). *Functional and Neural Mechanisms of Interval Timing*. Boca Raton, FL: CRC Press.

Meck, W. H. (2006a). Frontal cortex lesions eliminate the clock speed effect of dopaminergic drugs on interval timing. *Brain Res.* 1108, 157–167.

Meck, W. H. (2006b). Neuroanatomical localization of an internal clock: a functional link between mesolimbic, nigrostriatal, and mesocortical dopaminergic systems. *Brain Res.* 1109, 93–107.

Meck, W. H. (2006c). Temporal memory in mature and aged rats is sensitive to choline acetyltransferase inhibition. *Brain Res.* 1108, 168–175.

Meck, W. H., and Benson, A. M. (2002). Dissecting the brain's internal clock: how frontal-striatal circuitry keeps time and shifts attention. *Brain Cogn.* 48, 195–211.

Meck, W. H., Cheng, R. K., MacDonald, C. J., Gainetdinov, R. R., Caron, M. G., and Çevik, M. Ö. (2012). Gene-dose dependent effects of methamphetamine on interval timing in dopamine-transporter knockout mice. *Neuropharmacology* 62, 1221–1229.

Meck, W. H., and Church, R. M. (1982). Abstraction of temporal attributes. *J. Exp. Psychol. Anim. Behav. Process.* 8, 226–243.

Meck, W. H., and Church, R. M. (1984). Simultaneous temporal processing. *J. Exp. Psychol. Anim. Behav. Process.* 10, 1–29.

Meck, W. H., Church, R. M., and Olton, D. S. (1984a). Hippocampus, time, and memory. *Behav. Neurosci.* 98, 3–22.

Meck, W. H., Komeily-Zadeh, F. N., and Church, R. M. (1984b). Two-step acquisition: modification of an internal clock's criterion. *J. Exp. Psychol. Anim. Behav. Process.* 10, 297–306.

Meck, W. H., and MacDonald, C. J. (2007). Amygdala inactivation reverses fear's ability to impair divided attention and make time stand still. *Behav. Neurosci.* 121, 707–720.

Meck, W. H., Penney, T. B., and Pouthas, V. (2008) Cortico-striatal representation of time in animals and humans. *Curr. Opin. Neurobiol.* 18, 145–152.

McClure, S. M., Laibson, D. I., Lowenstein, G., and Cohen, J. D. (2004). Separate neural systems value immediate and delayed monetary rewards. *Science* 306, 503–507.

Morris, R. G. M., Inglis, J., Ainge, J. A., Olverman, H. J., Tulloch, J., Dudai, Y., and Kelly, P. A. T. (2006). Reconsolidation of spatial memory: differential sensitivity of distinct spatial memory tasks to local inhibition of protein-synthesis

in dorsal hippocampus following memory retrieval. *Neuron* 50, 479–489.

Myers, K. M., and Davis, M. (2002). Behavioral and neural analysis of extinction. *Neuron* 36, 567–584.

Niv, Y. (2007). Cost, benefit, tonic, phasic: what do response rates tell us about dopamine and motivation? *Ann. N.Y. Acad. Sci.* 1104, 357–376.

O'Doherty, J., Dayan, P., Schultz, J., Deichmann, R., Friston, K., and Dolan, R. J. (2004). Dissociable roles of ventral and dorsal striatum in instrumental conditioning. *Science* 304, 452–454.

Okamoto, T., Endo, S., Shirao, T., and Nago, S. (2011). Role of cerebellar cortical protein synthesis in transfer or memory trace of cerebellum-dependent motor learning. *J. Neurosci.* 31, 8958–8966.

Oprisan, S. A., and Buhusi, C. V. (2011). Modeling pharmacological clock and memory patterns of interval timing in a striatal beat-frequency model with realistic, noisy neurons. *Front. Integr. Neurosci.* 5:52. doi: 10.3389/fnint.2011.00052

Paule, M. G., Meck, W. H., McMillan, D. E., McClure, G. Y. H., Bateson, M., Popke, E. J., Chelonis, J. J., and Hinton, S. C. (1999). The use of timing behaviors in animals and humans to detect drug and/or toxicant effects. *Neurotoxicol. Teratol.* 21, 491–502.

Pennartz, C. M. A., Berke, J. D., Graybiel, A. M., Ito, R., Lansink, C. S., can der Meer, M., Redish, A. D., Smith, K. S., and Voorn, P. (2009). Corticostriatal interactions during learning, memory processing, and decision making. *J. Neurosci.* 29, 12831–12838.

Penney, T. B., Gibbon, J., and Meck, W. H. (2000). Differential effects of auditory and visual signals on clock speed and temporal memory. *J. Exp. Psychol. Hum. Percept. Perform.* 26, 1770–1787.

Penney, T. B., Gibbon, J., and Meck, W. H. (2008). Categorical scaling of duration bisection in pigeons (*Columba livia*), mice (*Mus musculus*), and humans (*Homo sapiens*). *Psychol. Sci.* 19, 1103–1109.

Pleil, K. E., Cordes, S., Meck, W. H., and Williams, C. L. (2011). Rapid and acute effects of estrogen on time perception in male and female rats. *Front. Integr. Neurosci.* 5:63. doi: 10.3389/fnint.2011.00063

Portugal, G., Wilson, A. G., and Matell, M. S. (2011). Behavioral sensitivity of temporally modulated striatal neurons. *Front. Integr. Neurosci.* 5:30. doi: 10.3389/fnint.2011.00030

Rakitin, B. C., Gibbon, J., Penney, T. B., Malapani, C., Hinton, S. C., and Meck, W. H. (1998). Scalar expectancy theory and peak-interval timing in humans. *J. Exp. Psychol. Anim. Behav. Process.* 24, 15–33.

Ray, D., and Bossaerts, P. (2011). Positive temporal dependence of the biological clock implies hyperbolic discounting. *Front. Neurosci.* 5:2. doi: 10.3389/fnins.2011.00002

Reading, P. J., and Dunnett, S. B. (1991). The effects of excitotoxic lesions of the nucleus accumbens on a matching to position task. *Behav. Brain Res.* 46, 17–29.

Reading, P. J., Dunnett, S. B., and Robbins, T. W. (1991). Dissociable roles of the ventral, medial and lateral striatum on the acquisition and performance of a complex visual stimulus-response habit. *Behav. Brain Res.* 45, 147–161.

Redgrave, P., Prescott, T. J., and Gurney, K. (1999). Is the short-latency dopamine response too short to signal reward error? *Trends Neurosci.* 22, 146–151.

Robbins, T. W., and Brown, V. J. (1990). The role of the striatum in the mental chronometry of action: a theoretical review. *Rev. Neurosci.* 2, 181–211.

Robbins, T. W., and Everitt, B. J. (2007). A role for mesencephalic dopamine in activation: commentary on Berridge (2006). *Psychopharmacology* 191, 433–437.

Roberts, S. (1993). "Use of independent and correlated measures to divide a time–discrimination mechanism into parts," in *Attention and Performance: XIV. Synergies in Experimental Psychology, Artificial Intelligence, and Cognitive Neuroscience*, eds D. E. Meyer and S. Kornblum (Cambridge, MA: MIT Press), 589–610.

Rodríguez-Gironés, M. A., and Kacelnik, A. (1999). Behavioral adjustment to modification in the temporal parameters of the environment. *Behav. Process.* 45, 173–191.

Roesch, M. R., Singh, T., Brown, P. L., Mullins, S. E., and Schoenbaum, G. (2009). Ventral striatal neurons encode the value of the chosen action in rats deciding between differently delayed or sized rewards. *J. Neurosci.* 29, 13365–13376.

Routtenberg, A. (2008). The substrate for long-lasting memory: if not protein synthesis, then what? *Neurobiol. Learn. Mem.* 89, 225–233.

Rudebeck, P. H., Walton, M. E., Smyth, A. N., Bannerman, D. M., and Rushworth, M. F. S. (2006). Separate neural pathways process different decision costs. *Nat. Neurosci.* 9, 1161–1168.

Rudy, J. W. (2008). Is there a baby in the bathwater? Maybe: some methodological issues for the de novo protein synthesis hypothesis. *Neurobiol. Learn. Mem.* 89, 219–224.

Rudy, J. W., and Sutherland, R. J. (2008). Is it systems or cellular consolidation? Time will tell. An alternative interpretation of the Morris group's recent science paper. *Neurobiol. Learn. Mem.* 89, 366–369.

Sadowski, R. N., Canal, C. E., and Gold, P. E. (2011). Lidocaine attenuates anisomycin-induced amnesia and release of norepinephrine in the amygdala. *Neurobiol. Learn. Mem.* 96, 136–142.

Shea-Brown, E., Rinzel, J., Rakitin, B. C., and Malapani, C. (2006). A firing rate model of Parkinsonian deficits in interval timing. *Brain Res.* 1070, 189–201.

Silva, K. M., and Timberlake, W. (2005). A behavior systems view of the organization of multiple responses during a partially or continuously reinforced inter-food clock. *Learn. Behav.* 33, 99–110.

Simen, P., Balci, F., deSouza, L., Cohen, J. D., and Holmes, P. (2011). A model of interval timing by neural integration. *J. Neurosci.* 31, 9238–9253.

Smith, N. J., Horst, N. K., Liu, B., Caetano, M. S., and Laubach, M. (2010). Reversible inactivation of rat premotor cortex impairs temporal preparation, but not inhibitory control, during simple reaction-time performance. *Front. Integr. Neurosci.* 4:124. doi: 10.3389/fnint.2010.00124

Stafford, J. M., and Lattal, K. M. (2009). Direct comparisons of the size and persistence of anisomycin-induced consolidation and reconsolidation deficits. *Learn. Mem.* 16, 494–503.

Tanaka, S. C., Doya, K., Okada, G., Ueda, K., Okamoto, Y., and Yamawaki, S. (2004). Prediction of immediate and future rewards differentially recruits cortico-basal ganglia loops. *Nat. Neurosci.* 7, 887–893.

Tanaka, S. C., Schweighofer, N., Asahi, S., Shishida, K., Okamoto, Y., Yamawaki, S., and Doya, K. (2007). Serotonin differentially regulates short- and long-term prediction of rewards in the ventral and dorsal striatum. *PLoS One* 2:e1333. doi: 10.1371/journal.pone.0001333

Taylor, K. M., Horvitz, J. C., and Balsam, P. D. (2007). Amphetamine affects the start of responding in the peak interval timing task. *Behav. Process.* 74, 168–175.

Turner, R. S., and Desmurget, M. (2010). Basal ganglia contributions to motor control: a vigorous tutor. *Curr. Opin. Neurobiol.* 20, 704–716.

Qi, Z., and Gold, P. E. (2009). Intrahippocampal infusions of anisomycin produce amnesia: contribution of increased release of norepinephrine, dopamine, and acetylcholine. *Learn. Mem.* 16, 308–314.

van der Meer, M. A., Johnson, A., Schmitzer-Torbert, N. C., and Redish, A. D. (2010). Triple dissociation of information processing in dorsal striatum, ventral striatum, and hippocampus on a learned spatial decision task. *Neuron* 67, 25–32.

van Rijn, H., Kononowicz, T. W., Meck, W. H., Ng, K. K., and Penney, T. B. (2011). Contingent negative variation and its relation to time estimation: a theoretical evaluation. *Front. Integr. Neurosci.* 5:91. doi: 10.3389/fnint.2011.00091

Vink, M., Kahn, R. S., Raemaekers, M., van den Heuvel, M., Boersma, M., and Ramsey, N. F. (2005). Function of striatum beyond inhibition and execution of motor responses. *Hum. Brain Mapp.* 25, 336–344.

Wächter, T., Röhrich, S., Frank, A., Molina-Luna, K., Pekanovic, A., Hartler, B., Schubring-Giese, M., and Luft, A. R. (2010). Motor skill learning depends on protein synthesis in the dorsal striatum after training. *Exp. Brain Res.* 200, 319–323.

Wanisch, K., and Wotjak, C. T. (2008). Time course and efficiency of protein synthesis inhibition following intracerebral and systemic anisomycin treatment. *Neurobiol. Learn. Mem.* 90, 485–494.

Ward, R. D., Kellendonk, C., Kandel, E. R., and Balsam, P. D. (2012). Timing as a window on cognition in schizophrenia. *Neuropharmacology* 62, 1175–1181.

Ward, R. D., Kellendonk, C., Simpson, E. H., Lipatova, O., Drew, M. R., Fairhurst, S., Kandel, E. R., and Balsam, P. D. (2009). Impaired timing precision produced by striatal D2 receptor overexpression is mediated by cognitive and motivational deficits. *Behav. Neurosci.* 123, 720–730.

Williamson, L. L., Cheng, R. K., Etchegaray, M., and Meck, W. H. (2008). "Speed" warps time:

methamphetamine's interactive roles in drug abuse, habit formation, and the biological clocks of circadian and interval timing. *Curr. Drug Abuse Rev.* 1, 203–212.

Yin, B., and Troger, A. B. (2011). Exploring the 4th dimension: hippocampus, time, and memory revisited. *Front. Integr. Neurosci.* 5:36. doi: 10.3389/fnint.2011.00036

Yin, H. H., and Knowlton, B. J. (2006). The role of the basal ganglia in habit formation. *Nat. Neurosci. Rev.* 7, 464–476.

Yin, H. H., Mulcare, S. P., Hilario, M. R., Clouse, E., Holloway, T., Davis, M. I., Hansson, A. C., Lovinger, D. M., and Costa, R. M. (2009). Dynamic reorganization of striatal circuits during the acquisition and consolidation of a skill. *Nat. Neurosci.* 12, 333–341.

Zauberman, G., Kim, B. K., Malkoc, S. A., and Bettman, J. R. (2009). Discounting time and time discounting: subjective time perception and intertemporal preferences. *J. Mark. Res.* XLVI, 543–556.

Conflict of Interest Statement: The authors declare that the research was conducted in the absence of any commercial or financial relationships that could be construed as a potential conflict of interest.

Received: 28 June 2011; paper pending published: 12 July 2011; accepted: 28 February 2012; published online: 14 March 2012.

Citation: MacDonald CJ, Cheng R-K and Meck WH (2012) Acquisition of "Start" and "Stop" response thresholds in peak-interval timing is differentially sensitive to protein synthesis inhibition in the dorsal and ventral striatum. Front. Integr. Neurosci. ***6****:10. doi: 10.3389/fnint.2012.00010*

frontiers in
INTEGRATIVE NEUROSCIENCE

ORIGINAL RESEARCH ARTICLE
published: 23 September 2011
doi: 10.3389/fnint.2011.00052

Modeling pharmacological clock and memory patterns of interval timing in a striatal beat-frequency model with realistic, noisy neurons

Sorinel A. Oprisan[1] and Catalin V. Buhusi[2]*

[1] *Department of Physics and Astronomy, College of Charleston, Charleston, SC, USA*
[2] *Department of Neurosciences, Medical University of South Carolina, Charleston, SC, USA*

Edited by:
Warren H. Meck, Duke University, USA

Reviewed by:
Adrian Rodriguez-Contreras, City College of New York, USA
Eric Shea-Brown, University of Washington, USA
Christopher MacDonald, Boston University, USA

***Correspondence:**
Catalin V. Buhusi, Department of Neurosciences, Medical University of South Carolina, 173 Ashley Avenue, 403 Basic Science Building, Charleston, SC 29425, USA.
e-mail: buhusi@musc.edu

In most species, the capability of perceiving and using the passage of time in the seconds-to-minutes range (interval timing) is not only accurate but also scalar: errors in time estimation are linearly related to the estimated duration. The ubiquity of scalar timing extends over behavioral, lesion, and pharmacological manipulations. For example, in mammals, dopaminergic drugs induce an immediate, scalar change in the perceived time (clock pattern), whereas cholinergic drugs induce a gradual, scalar change in perceived time (memory pattern). How do these properties emerge from unreliable, noisy neurons firing in the milliseconds range? Neurobiological information relative to the brain circuits involved in interval timing provide support for an striatal beat frequency (SBF) model, in which time is coded by the coincidental activation of striatal spiny neurons by cortical neural oscillators. While biologically plausible, the impracticality of perfect oscillators, or their lack thereof, questions this mechanism in a brain with noisy neurons. We explored the computational mechanisms required for the clock and memory patterns in an SBF model with biophysically realistic and noisy Morris–Lecar neurons (SBF–ML). Under the assumption that dopaminergic drugs modulate the firing frequency of cortical oscillators, and that cholinergic drugs modulate the memory representation of the criterion time, we show that our SBF–ML model can reproduce the pharmacological clock and memory patterns observed in the literature. Numerical results also indicate that parameter variability (noise) – which is ubiquitous in the form of small fluctuations in the intrinsic frequencies of neural oscillators within and between trials, and in the errors in recording/retrieving stored information related to criterion time – seems to be critical for the time-scale invariance of the clock and memory patterns.

Keywords: interval timing, striatal beat frequency, computer simulations, dopamine, acetylcholine, neural noise, noise

INTRODUCTION

The capability of perceiving and using the passage of time in the seconds-to-minutes range (interval timing) is essential for survival and adaptation, and its impairment leads to severe cognitive and motor dysfunctions (Gallistel, 1990; Buhusi and Meck, 2005; Meck et al., 2008). Considerable progress has been made in recent years toward elucidating the neural bases of time perception in the seconds-to-minutes range (Mauk and Buonomano, 2004; Buhusi and Meck, 2005, 2009; Meck et al., 2008). Recent studies point toward the cortico-striatal circuits as being critical for interval timing both, in animals (Matell and Meck, 2000; Matell et al., 2003; Meck, 2006) and humans (Coull et al., 2004, 2011; Stevens et al., 2007). Other experiments pointed toward an important role of the parietal lobe in timing behavior (Harrington et al., 1998; Schubotz et al., 2000; Onoe et al., 2001; Rao et al., 2001). In particular, Leon and Shadlen (2003) found evidences of a correlation between the judgment of time and cell-level neural activity in the lateral intraparietal area of the posterior parietal cortex of monkey (Leon and Shadlen, 2003). As Matell and Meck (2004); Leon and Shadlen (2003) and others highlighted, it is likely that the interval timing uses multiple mechanisms and time is represented in many structures in the brain. Moreover, severe deficiencies in reproducing temporal intervals were found in various neuropsychiatric disorders, such as Parkinson's (Harrington and Haaland, 1991; Malapani et al., 1998, 2002).

In most species interval timing is not only accurate but also *time-scale invariant*, or simply *scalar*, in that *the errors in time estimation are linearly related to the estimated duration* (Gibbon, 1977; Gibbon et al., 1984). In other words, interval timing is increasingly less precise as the interval being timed lengthens (**Figure 1A**). When timing a 30-s interval (left panel of **Figure 1A**), responses are distributed with a quasi–Gaussian distribution around the 30-s target duration. On the other hand, when timing a 90-s interval (right panel of **Figure 1A**), responses are distributed with a quasi–Gaussian distribution around the 90-s target duration. The scalar property is evident in that normalizing the response functions by the target duration and by the maximum response rate yields superimposition of response functions (middle panel of

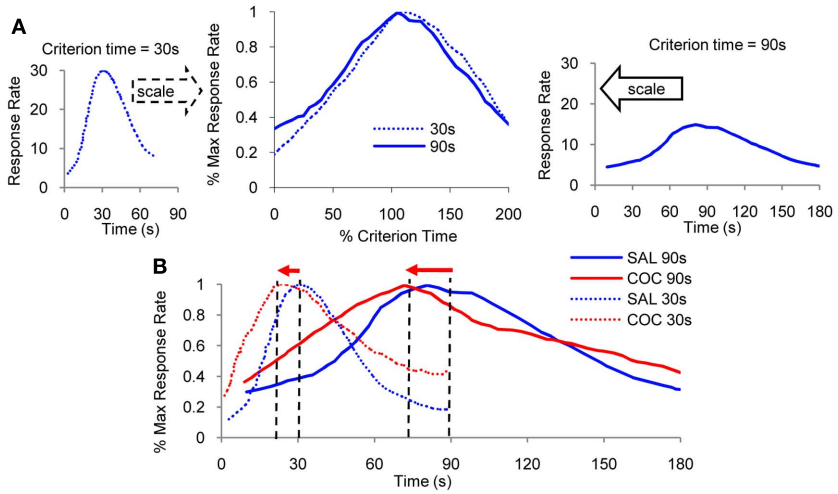

FIGURE 1 | Scalar property. (A) Mean lever-press response rate in peak-interval experiments with rats trained with a criterion time of 30 s (left panel), respectively, 90 s (right panel; re-drawn from Matell et al., 2004). When normalized by maximum response rate and by the criterion duration on the horizontal scale, response functions for the two criteria overlap (middle panel). **(B)** Administration of indirect dopamine agonist cocaine results in an immediate, scalar (proportional) leftward shift in response functions.

Figure 1A). The time-scalar invariance property of interval timing is ubiquitous in many species from invertebrates such as bees (Boisvert and Sherry, 2006), to many vertebrates, such as fish (Talton et al., 1999), birds (Cheng and Westwood, 1993), and mammals such as rats (Dews, 1962), mice (Buhusi et al., 2009) and humans (Rakitin et al., 1998). Scalar timing is particular to timing in the seconds-to-minutes range, but not to circadian timing, which is far more accurate than interval timing, but whose variance increases very little with the mean of the interval (Gibbon, 1977; Hinton and Meck, 1997).

The ubiquity of scalar timing extends over behavioral, lesion (Meck et al., 1987), and pharmacological manipulations of interval timing (Buhusi and Meck, 2010). For example, acute administration of cocaine results in a characteristic leftward shift of response functions (**Figure 1B**), consistent with the speeding up of an internal clock (Matell et al., 2004). Most interestingly, at the same dose, cocaine speeds up timing of a 90-s interval three times more than when timing a 30-s interval (**Figure 1B**), suggesting that the effect of the drug is proportional – *scalar* – to the timed interval. Moreover, when normalized in both amplitude and time as in **Figure 1A**, the response functions under cocaine (**Figure 1B**) superimpose, indicative of the scalar property.

In mammals, manipulations involving dopaminergic (DA) drugs such as cocaine induce a particular pattern of response – *clock pattern* – that is characterized by several features exemplified by the data presented in **Figure 2A** (Meck, 1996). **Figure 2A** shows the *clock pattern* obtained during seven sessions of administration of DA agonists (red dots) or antagonists (black squares), followed by seven sessions off-drug, in two groups of rats trained to time a criterion duration of either a 20-s (lower pattern), or 40s (upper pattern). *First*, DA drugs produce an immediate, scalar change in the perceived time when administered either systemically (Maricq et al., 1981; Maricq and Church, 1983; Meck, 1983, 1996; Matell and Meck, 1997; Matell et al., 2004), or directly into the anterior portion of the striatum (Neil and Herndon Jr., 1978); the pattern is often taken to be suggestive of a change in the speed of an internal clock, and thus is known as a "clock pattern" (Meck, 1996). For example, an immediate, scalar (proportional), leftward shift in perceived time (responding earlier in time than under control conditions) is evident following systemic DA agonist administration, e.g., methamphetamine or cocaine (black squares in **Figure 2A**, upper pattern for a 40-s criterion, lower pattern for a 20-s criterion). Similarly, an immediate, proportional, rightward shift in perceived time (responding later in time than under control conditions) occurs following systemic administration of DA antagonist, e.g., haloperidol (red circles in **Figure 2A**). *Second*, as shown in **Figure 1B**, the magnitude of the shift in the temporal response scales with the timed duration, and the response functions on- and off-drug overlap when normalized in amplitude and duration (**Figure 1B**). *Third*, upon chronic administration of DA drugs, the timing functions recalibrate, i.e., they shift back to the values prior to drug administration, an effect often interpreted as a relearning of the clock value associated with a particular duration (left side of the **Figure 2A**). *Fourth*, upon discontinuing the drug regimen, the timing functions rebound (in a scalar manner) in the *opposite direction* from the initial effects of the drug (Meck, 1983; right-side of **Figure 2A**). This rebound effect is a signature of the clock pattern. *Finally*, the magnitude of the shift in the temporal response scales roughly linearly with the dose (Meck, 1996; Matell and Meck, 1997; Meck et al., 2011), suggesting a tight relationship between synaptic dopamine levels and clock-speed.

On the other hand, pharmacological manipulations (Meck, 1983, 1996; Meck and Church, 1987a,b) and lesions (Meck et al., 1987) aimed at the cholinergic (ACh) systems produce gradual, scalar (proportional) effects on the memory storage, as shown in data from **Figure 3A**. **Figure 3A** shows the *memory pattern* obtained during seven sessions of administration of ACh agonists (red dots) or antagonists (black squares), followed by seven

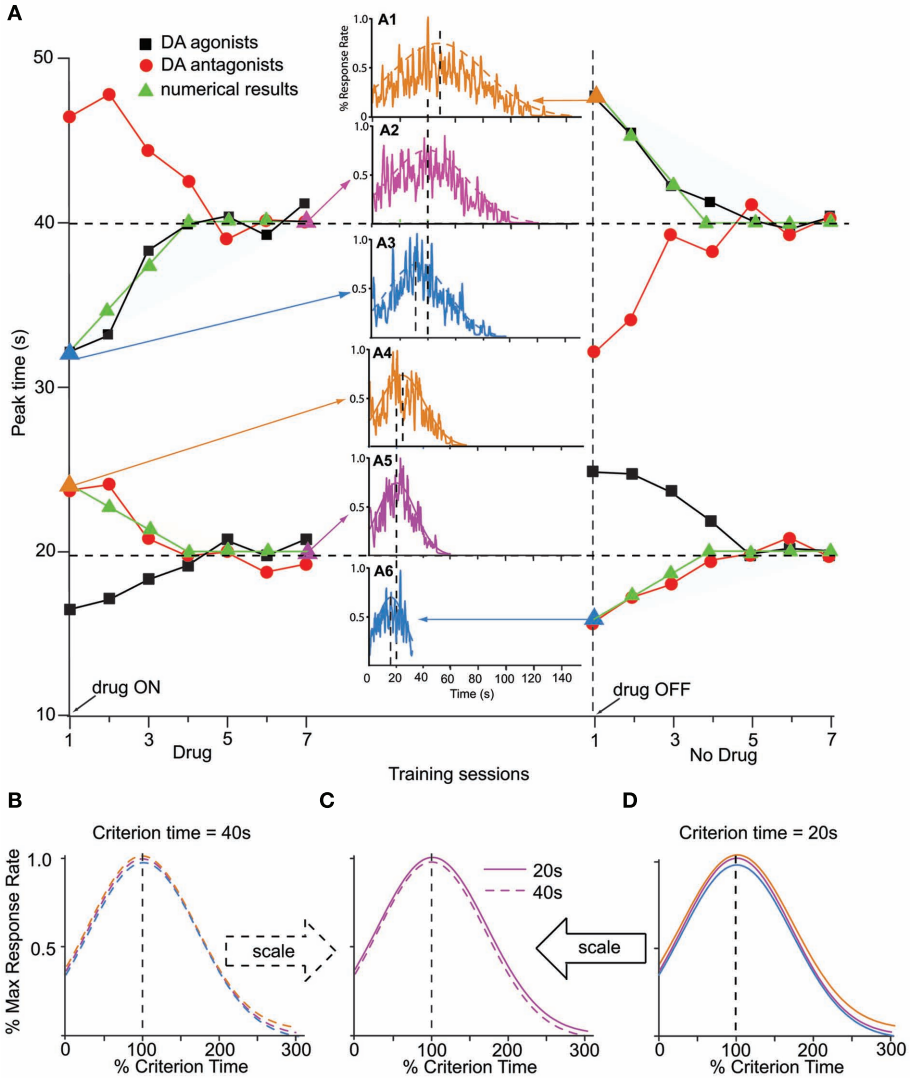

FIGURE 2 | Clock pattern. (A) The clock pattern of dopaminergic (DA) drugs (re-drawn from Meck, 1996): two groups of rats were trained off-drug to time a criterion time of either 40 s (upper pattern) or 20 s (lower pattern); they were then administered either DA agonists or antagonists for seven sessions, followed by seven session off-drug. The first administration of DA drugs results in an immediate, dose-dependent shift in timing, leftward (faster timing) for DA agonists (solid squares, methamphetamine), and rightward (slower timing) for DA antagonists (solid circles, haloperidol). Under continuous training with the pre-drug criterion time and despite continuing the drug administration, the timing functions recalibrate to the pre-drug criterion time. Upon discontinuing the drug, timing functions immediately rebound in the opposite direction, then gradually recalibrate to the pre-drug criterion time (Meck, 1996). Solid triangles indicate numerical simulations with the SBF–ML model. The insets indicate the response function generated by the SBF–ML model throughout the clock pattern (indicated by arrows, and by a triangle symbol of the color of the inset). Insets: A1: immediate rebound from $T = 40$ to $T^{**} = 48$ s upon discontinuing methamphetamine; A2: recalibration under methamphetamine; A3: immediate shift under methamphetamine from $T = 40$ to $T^{*} = 32$ s; A4: immediate shift under haloperidol from $T = 20$ to $T^{*} = 24$ s; A5: recalibration under haloperidol; A6: immediate rebound upon discontinuing haloperidol. The dashed **(A1–3)**, respectively, continuous **(A4–6)** smooth lines represent Gaussian fits. **(B)**. The Gaussian fits (dashed smooth lines) in **(A1–3)** are given by Gauss (48, 31 s), Gauss (40, 27 s), respectively, Gauss (32, 21 s). Timing functions at different points of the clock pattern for $T = 40$ s are time-scale invariant. **(C)**. Timing functions from the 20-s clock pattern and 40-s clock pattern are time-scale invariant. **(D)**. The Gaussian fits (continuous smooth lines) in **(A4–6)** are given by Gauss (24, 16 s), Gauss (20, 13 s), respectively, Gauss (16, 11 s). Timing functions at different points of the clock pattern for $T = 20$ s are time-scale invariant. Colors match the insets. All Gaussian fits of numerical simulations gave COD > 0.9 and $p < 0.0001$.

sessions off-drug, in two groups of rats trained to time a criterion duration of either a 20-s (lower pattern) or 40-s (upper pattern): *first*, administration of ACh drugs produced a gradual (rather than immediate), scalar temporal shift (Meck, 1996); ACh lesions produce permanent effects (Malapani and Fairhurst, 2002). *Second*, chronic administration amplifies (rather than recalibrates) the temporal shift (left side of **Figure 3A**). *Third*, upon discontinuing the drug administration, the timing functions gradually return to the original criterion time (**Figure 3A**, right-side). Finally, the magnitude of the shift in the temporal response scales with the

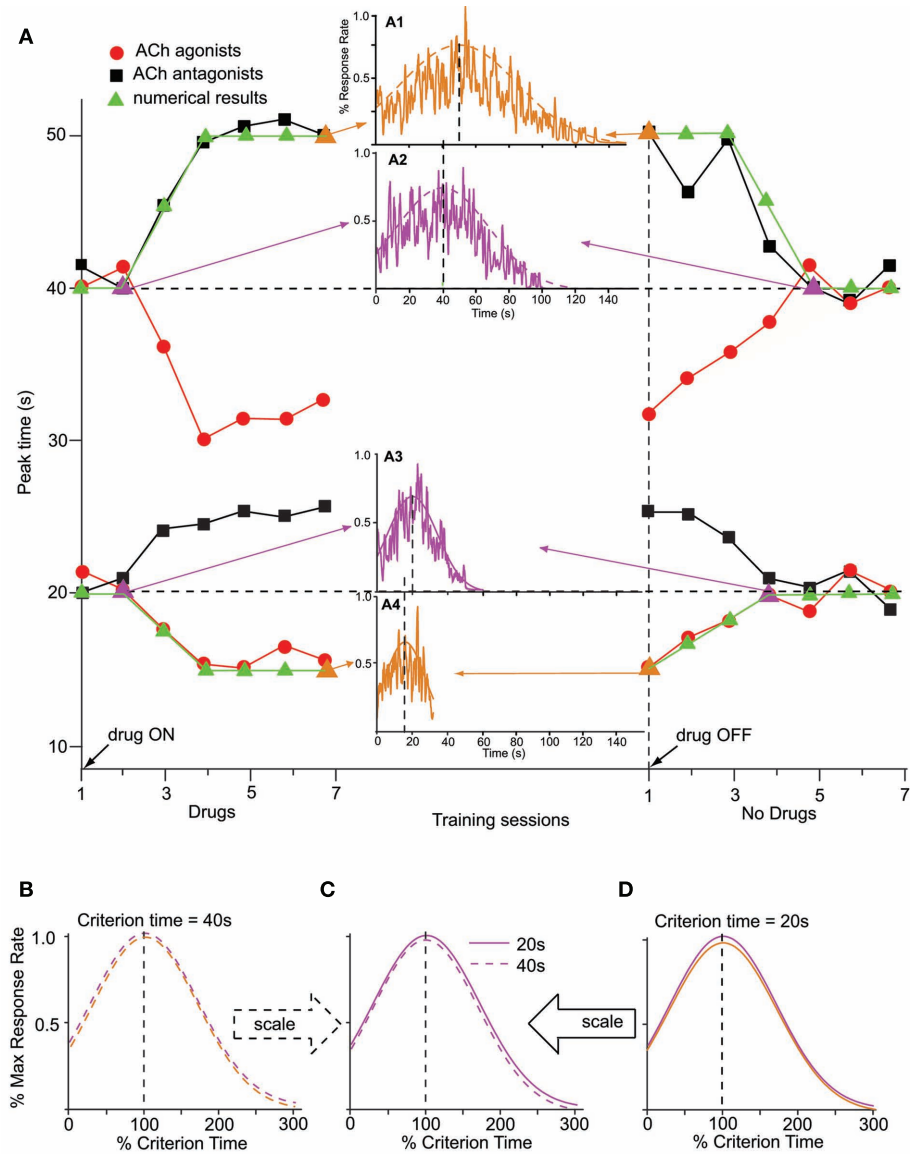

FIGURE 3 | Memory pattern. (A) The memory pattern of cholinergic (ACh) drugs (re-drawn from Meck, 1996): two groups of rats were trained off-drug to time a criterion time of either 40 s (upper pattern) or 20 s (lower pattern); they were then administered either ACh agonists or antagonists for seven sessions, followed by seven session off-drug. The first administration of ACh drugs results in a minimal effect; repeated ACh drug administration results in a gradual, dose-dependent shift in timing, leftward for ACh agonists (solid circles, physostigmine), and rightward for ACh antagonists (solid squares, atropine). Upon discontinuing the drug, timing functions gradually recalibrate to the initial criterion time (Meck, 1996). Solid triangles indicate numerical simulations obtained with the SBF–ML model. The insets indicate the output function generated by the SBF–ML model with biophysically realistic ML neurons throughout the memory pattern (indicated by arrows, and by a triangle symbol of the color of the inset). Insets: A1: gradual shift from $T = 40$ to $T^* = 50$ s under atropine; A2: gradual recalibration upon discontinuing atropine; A3: gradual recalibration upon discontinuing physostigmine; A4: gradual recalibration under physostigmine. The dashed **(A1,2)**, respectively, continuous **(A3,4)** smooth lines represent Gaussian fits. **(B)**. The Gaussian fits (dashed smooth lines) in **(A1,2)** are given by Gauss (50, 33 s), respectively, Gauss (40, 27 s). Timing functions at different points of the memory pattern for $T = 40$ s are time-scale invariant. **(C)**. Timing functions from the 20-s memory pattern and 40-s memory pattern are time-scale invariant. **(D)**. The Gaussian fits (continuous smooth lines) in **(A3,4)** are given by Gauss (20, 13 s), respectively, Gauss (15, 10 s). Timing functions at different points of the memory pattern for $T = 20$ s are time-scale invariant. Colors match the insets. All Gaussian fits of numerical simulations gave COD > 0.9 and $p < 0.0001$.

timed duration (Meck, 1996), twice as large for the 40-s group (upper pattern in **Figure 3A**) than for the 20-s group (lower pattern in **Figure 3A**). The memory pattern is consistent with alterations of the internal representation of the memorized criterion time (Meck, 1996).

How do the pharmacological properties of timing in the seconds-to-minutes range, including the scalar effect of dopaminergic (DA) and cholinergic (ACh) drugs, emerge from unreliable, noisy neurons firing in the milliseconds range? A response to these questions was recently proposed by a neurobiologically inspired

computational model of interval timing: the striatal beat frequency (SBF) model (Matell and Meck, 2000, 2004; Buhusi and Meck, 2005; **Figure 4**). The model is based on the idea that striatal spiny neurons integrate the activity of massive ensembles of cortical oscillators to produce coincidental beats that have periods spanning a much wider range of durations than the intrinsic periods of the cortical oscillators (Miall, 1989; Matell and Meck, 2004; Buhusi and Meck, 2005). Our implementation of the SBF–Morris–Lecar (ML) model closely follows Matell and Meck (2004) with three main changes: (1) we replaced the sine wave mathematical abstraction of oscillators with biophysically realistic and noisy ML (Morris and Lecar, 1981; Rinzel and Ermentrout, 1998) model neurons, and (2) we implemented neuromodulatory circuits that mimic the DA and ACh systems, and (3) we implemented the equivalent of trials and sessions, to address the effect of experimental DA, ACh, and lesion manipulations (**Figure 4**). Our SBF–ML implementation contains a time-base provided by a large number of neural oscillators presumably localized in the frontal cortex (FC; Matell et al., 2003). Following Matell and Meck (2004) review of the neuroanatomical foundations of the SBF model, among many other firing patterns observed in FC, the synchronized cortical oscillations in the 8- to 13-Hz range (alpha) could serve as pacemakers for temporal accumulation (Anliker, 1963). Furthermore, Rizzuto et al. (2003) have shown that alpha range oscillations in humans reset upon occurrence of to-be-remembered or probe stimuli, suggesting that the phase of these rhythms may be of importance in interval timing. The set of synaptic weights between neural oscillators in the FC and the spiny neurons in the striatum, which is the input to the basal ganglia (BG), represent a (long-term) memory buffer. Learning of the criteria times also depends on nucleus basalis magnocellularis (Meck et al., 1987), FC (Olton et al., 1988), and the hippocampus (Meck et al., 1987; Olton et al., 1988). A coincidence detector was implemented to mimic the spiny neurons in the striatum, which integrate a very large number of different inputs, and responds selectively to particular reinforced patterns (Houk, 1995; Houk et al., 1995; Beiser and Houk, 1998). As opposed to the existing implementations of the SBF model (Miall, 1989; Matell and Meck, 2004; Buhusi and Meck, 2005), a neuromodulatory circuit that mimics "a start gun" in regard to the effect of DA projections from substantia nigra pars compacta (SNc), a neuromodulatory circuit that models the DA projections from the ventral tegmental area (VTA) to the FC, and a cholinergic system which modulates the BG activity were also implemented in our SBF–ML model (**Figure 4**).

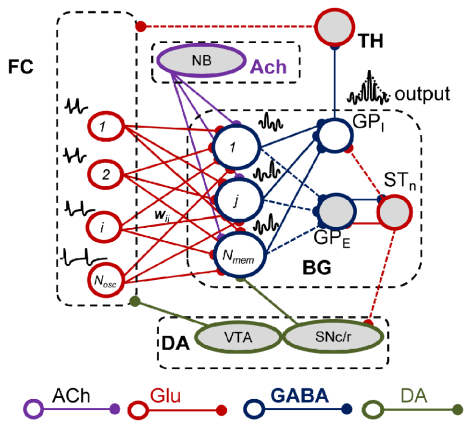

FIGURE 4 | The striatal beat frequency model. Schematic representation of the neurobiological structures involved in interval timing in the SBF model. Dashed lines signify couplings that are not implemented in our SBF version. Frontal oscillators are implemented as biophysically realistic ML neurons. ACh, acetylcholine; FC, frontal cortex; BG, basal ganglia; DA, dopamine; Glu, glutamate; GP_E, globus pallidus external; GP_I, globus pallidus internal; STn, subthalamic nucleus; SNc/r, substantia nigra pars compacta/reticulata; TH, thalamus; VTA, ventral tegmental area.

While "biologically plausible," the impracticality (or lack thereof) of perfect oscillators questions the robustness of an SBF model in a brain with real, noisy neurons, particularly after pharmacological manipulations. Here we explore the neural mechanisms required for clock (**Figure 2**), and memory (**Figure 3**) patterns in an SBF–ML model. *First*, we checked numerically that, in the limit of a very large number of neural oscillators and in the presence of noise, the output of an SBF–ML model is Gaussian-like (**Figure 5**). *Second*, under the assumption that DA drugs modulate the firing frequency of cortical oscillators, and that ACh drugs modulate the memory representation of the criterion time, we show that the SBF–ML model reproduces the pharmacological clock (**Figure 2**), and memory (**Figure 3**) patterns observed in the literature. *Third*, our numerical results support the conjecture (Matell and Meck, 2004) that parameter variability (noise) – which is ubiquitous in the form of small fluctuations in the intrinsic frequencies of the neural oscillators within and between trails, and in the errors in recording/retrieving stored information related to criterion time – is critical for the time-scale invariance of the clock and memory patterns of interval timing.

MATERIALS AND METHODS

NUMERICAL SIMULATIONS ASSUME BIOPHYSICALLY REALISTIC MORRIS–LECAR NEURONS.

Since action potential recordings from real neurons are never phase oscillators, i.e., sine waves, we departed from cortical phase oscillators (Matell and Meck, 2004) and we instead implemented biophysically realistic ML cortical neurons (Morris and Lecar, 1981; Rinzel and Ermentrout, 1998). The membrane potential of the ML model neuron is given by $C_m V' = I_{bias} - I_{Ca} - I_K - I_L$, where C_m is the membrane capacitance, prime denotes the derivative of the membrane potential V, I_{bias} is a constant bias current required to bring the model to the excitability threshold, $I_{Ca} = g_{Ca} m(V - E_{Ca})$ is the calcium current that involves the conductance g_{Ca}, the fraction m of calcium channels open at a given V, and the reversal potential E_{Ca} for calcium channels, $I_K = g_K n(V - E_K)$ is the potassium current that involves the conductance g_K, the fraction n of channels open at a given V, and the reversal potential E_K for potassium channels, $I_L = g_L(V - E_L)$ is a leak current that only involves a conductance g_L and a reversal potential E_L. (Morris and Lecar, 1981; Rinzel and Ermentrout, 1998).

THE SBF–ML MODEL

Briefly, a set of $N_{osc} = 600$ neural oscillators with uniformly distributed intrinsic frequencies f_i was assumed to activate through

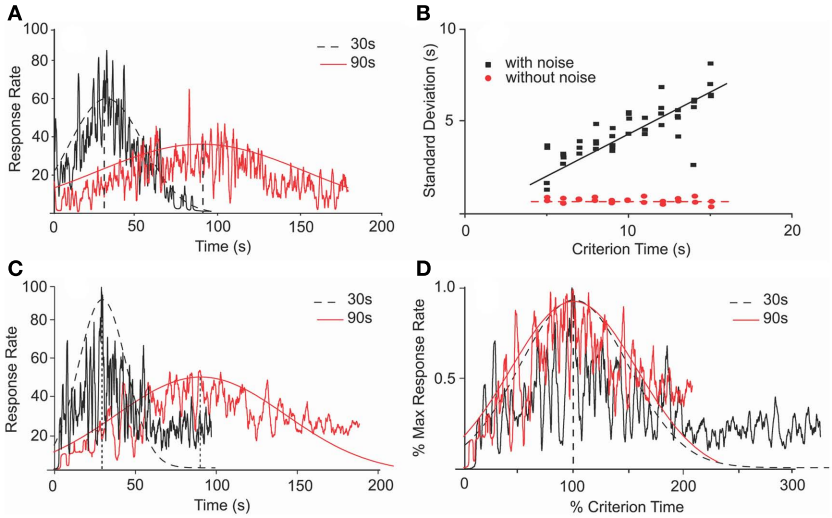

FIGURE 5 | Scalar property in an SBF–ML model is dependent on noise. **(A)** Numerical simulations of an SBF–ML model with Gaussian variability of the criterion time and between-trial variability in frequencies of cortical neurons generated response functions (jagged traces) with Gaussian-like envelopes (smooth curves). The dashed (continuous) envelope corresponds to 30 s (90 s) criterion time. **(B)** In the presence of noise, the variance of output function is proportional with the criterion time, thus indicating time-scale invariance (filled squares). The coefficient of correlation for the linear regression (continuous line) was $r = 0.9$ with a p-value less than 0.001. In the absence of the noise, the variance of the output function is constant (filled circles), thus violating the time-scale invariance. The coefficient of correlation for the linear regression (dashed line) was $r = 0.98$ with a p-value less than 0.0001. **(C)** Numerical simulations of an SBF–ML model with normally distributed variability for both the criterion time and both within- and between-trials variability in frequencies generate response functions (jagged traces) with Gaussian-like envelopes (smooth curves). The only noticeable difference when adding within-trial frequency variability is the occurrence of the skewness in the response rate at late times. A similar skewness was observed in the behavioral data (see **Figure 1**) **(D)** The Gaussian envelopes for the case of criterion time variability **(A)** are given by Gauss (30, 21 s), respectively, Gauss (90, 60 s). They overlap when normalized in amplitude and in time.

synaptic weights $w_{ij}(t)$ a set of $N_{mem} = 1000$ spiny neurons at time t (**Figure 4**; our choice of N_{osc} and N_{mem} was due to limitations on simulation duration, about 5 days on an HP Blade computer). The membrane potential of neural oscillators was normalized from $[-80, +40\,mV]$ to $[-1,1]$ by a linear transformation that preserves the shape of the action potential (Rinzel and Ermentrout, 1998). The modeled experimental setting included both reinforced and non-reinforced trials. At the onset of each trial, the oscillators were reset (0 phase), then neurons were set to fire with frequencies f_i, set during each trial, but variable from trial to trial. During reinforced trials, upon delivery of the reinforcement at criterion time T, a linear combination of oscillators' membrane potential in the current trial at the criterion time T was stored in long-term memory as criterion pattern $w_{ij}(T)$ (Matell and Meck, 2004). During non-reinforced (test) trials, spiny neurons were assumed to act as coincidence detectors by computing the projection (dot product) of the running weights $w_{ij}(t)$ stored in the working memory onto the retrieved reference weights $w_{ij}(T)$ stored in the long-term memory:

$$\text{output}(t) = \sum_{k=1}^{trials} \sum_{i=1}^{N_{osc}} \sum_{j=1}^{N_{mem}} w_{ij}(t) w_{ij}(T).$$

We assumed that both the storage and retrieval of the criterion time [stored as criterion pattern $w_{ij}(T)$] to and from long-term memory is affected by random biological noise, modeled as follows: criterion time variability was modeled by randomly distributing the criterion time T according to a normal density probability function pdf_T with $0.4T$ variance. This assumption accounts for the randomness in learned sample times (reinforced times) and in response time; e.g., in a peak-interval procedure (Gibbon et al., 1984) animals are reinforced for the first response after a criterion time, but since the animal's response is random, the reinforced time is random, though close in time to the criterion. Therefore, sample times stored in memory were assumed to be distributed around T. Additional randomness was included in our SBF–ML implementation by a Gaussian noise added to the intrinsic frequencies f_i of the neural oscillators within and between trails. The within-trial variability in frequencies f_i accounts for the randomness in response (e.g., for the first response reinforced), while the between-trial variability accounts for the observed differences in response between-trials (Church et al., 1994; Swearingen and Buhusi, 2010). Another reason to differentiate between within- and between-trial variability in frequencies f_i has to do with our focus on pharmacological manipulations, which experimentally are conducted in on- and off-drug sessions. Because we assumed that DA drugs change the frequencies f_i, this implies differences in coding and decoding of criterion time in on- and off-drug sessions (trials). This in turn implies variations in both the encoding and the recall of the criterion time due to the current (on- or off-drug) frequencies f_i.

THE CLOCK PATTERN OF DOPAMINERGIC DRUGS

We assumed that phasic release of dopamine from VTA to FC modulates the firing rate of FC neural oscillators, and that DA drugs affect the frequency of the cortical oscillators, $f_i^* = (1 + \alpha)f_i$, where α accounts for the action of the drug and its magnitude is dose-dependent, with $0 < \alpha < 1$ for dopamine agonists, such as methamphetamine or cocaine, and $-1 < \alpha < 0$ for dopamine antagonists, such as haloperidol. Simulations in **Figure 2** were carried out with an SBF–ML model using $N_{osc} = 600$ biophysically realistic ML cortical neurons firing in the range [8, 12] Hz, using $N_{mem} = 1000$ memory samples, with a drug dose effect $\alpha = \pm 0.25$.

RELEARNING OF THE CRITERION TIME ON-DRUG, AND OFF-DRUG

Meck (1996) suggested that the recalibration of the clock pattern may be due to relearning of the criterion time T under the drug. Numerically, we assumed that the criterion time is stored in long-term memory as a distribution of $N_{mem} = 1000$ samples, and that in each session, a fraction (25%) of the weights $w_{ij}(T)$ are updated, by storing the new pattern of the FC oscillators (off-drug or on-drug) upon delivery of reinforcement at criterion time T. We ran four sessions of 250 trials off-drug to acquire the distribution $w_{ij}(T)$ with the off-drug frequency set f_i which vary from trial to trial. For each trial, a sample $w_{ij}(T)$ was computed as a linear combination of the membrane potential at the criterion time T (Matell and Meck, 2004). During drug sessions, a fraction (25%) of the weights $w_{ij}(T)$ originally stored off-drug, are replaced with new running weights $w(T^*)$, stored on-drug, such that gradually the weights w stored in the reference (long-term) memory are characteristic of the on-drug state. Similarly, when discontinuing the drug, we assumed that the criterion time, stored in long-term memory as a distribution of $w(T^*)$ samples, stored on-drug, is replaced with a fraction (25%) during each off-drug session, such that with sufficient training, the weights w stored in the reference (long-term) memory will be characteristic of the off-drug state.

THE MEMORY PATTERN OF CHOLINERGIC DRUGS

Our numerical implementation assumes that administration of ACh drugs alters the re-coding of the criterion time in long-term memory (Meck, 1996; Matell and Meck, 2004). Briefly, we assumed that criterion time T is coded in long-term memory as a distribution of $N_{mem} = 1000$ samples $w(T)$, and that ACh drugs alter the process involved in memorizing this distribution, with about 25% samples learned in each session. The new samples are assumed to represent an altered, on-drug representation of the criterion time, $T^* = k^*T$, where the multiplicative coefficient k^* is both drug and dose-dependent (Gibbon et al., 1984; Meck, 1996). At the beginning of the drug administration, only a small subpopulation of the memory samples is affected; with continuing training on-drug, these altered samples make up the majority of the memory samples and lead to a progressive shift of the peak output to T^*. For simulations presented in **Figure 3** we assumed $k^* = 1.25$ for ACh antagonist atropine, and $k^* = 0.75$ for ACh agonist physostigmine.

STATISTICAL ANALYSES

Throughout this paper, the Origin package (OriginLab Co., Northampton, MA, USA) was used to perform data fits to smooth analytic curves, and to compare the degree of superposition between curves. The degree of superposition of curves was indexed by a coefficient of determination (COD) and the probability (p) to obtain a certain COD value by chance was estimated. Briefly, the COD measures the proportion of the total variation in the dependent variable that is explained by the regression equation (fit function), with $0 < \text{COD} < 1$ (Brockwell and Davis, 1991; Resnick, 2006). The correlation described by the COD is usually considered "good" if the COD > 0.7 (Nagelkerke, 1991; Cameron and Windmeijer, 1997; Anderson et al., 2009). If the regression curve is linear, then the COD reduces to the correlation coefficient (r).

RESULTS

THE SBF–ML EXHIBITS TIME-SCALE INVARIANCE

Previous studies indicated that in the absence of biological noise, an SBF model with cortical phase oscillators (sine waves) does not exhibit time-scale invariance (Matell and Meck, 2004). We found a similar behavior of our implementation of the SBF–ML model. In the presence of normally distributed variability in the criterion time, and between-trial variability in the frequencies of cortical neurons, the output functions were Gaussian-like (**Figure 5A**) and exhibited more variance when increasing the criterion duration T (filled squares in **Figure 5B**). On the other hand, in the absence of biological noise the SBF–ML model produces an output function whose envelope is *almost* Gaussian but *violates the scalar property* (filled circles in **Figure 5B**). Moreover, when adding normally distributed within-trial frequency variability on top of the existing between-trial frequency variability, and variability in criterion time, the output functions were still Gaussian-like with SD proportional to the criterion time (**Figure 5C**). Moreover, in the presence of these three sources of variability (**Figure 5C**) the output function has a long tail that does not decrease to zero as fast as the smooth Gaussian fit. Such a skewed and long-tailed Gaussian-like output function was observed in behavioral experiments (see **Figure 1**). When normalized in amplitude and over time, the envelopes of the response functions from **Figure 5C** overlap (**Figure 5D**). These findings support the conjecture made by Matell and Meck (2004) that in an SBF model at least one source of variability is required in order to observe time-scale invariance. Therefore, biological noise – which is ubiquitous in the form of small fluctuations of the intrinsic within- and between-trial frequencies of the neural oscillators, errors in recording/retrieving stored information related to criterion time – seems to be a rather critical component of this feature of the SBF–ML model. However, considering the focus of our paper on pharmacological manipulations, for numerical efficiency reasons and without reducing the generality of our results, in the following analyzes we only used two sources of variability (noise) when numerically integrating the equations of the SBF–ML model: normally distributed variability in the criterion time, and between-trial variability in the frequencies of cortical neurons.

THE CLOCK PATTERN OF DOPAMINERGIC DRUGS IN THE SBF–ML MODEL

Immediate shift upon changes in drug state

The clock effect of DA drugs can be easily understood as an interplay between the storage and retrieval of the criterion time representation $w_{ij}(T)$ on- and off-drug. A change in drug state

induced an immediate change in oscillator frequencies from the off-drug frequencies f to the on-drug frequencies f^*, respectively, from the on-drug frequencies f^* to the off-drug frequencies f. In our numerical implementation of the SBF–ML, the neural oscillators fire off-drug in the frequency range $[f_{\min}, f_{\max}]$ and that the criterion time T is represented off-drug as a set of synaptic weights $w_{ij}(T)$. The DA drugs alter the frequency of the cortical oscillators to $f_i^* = (1 + \alpha) f_i$ such that the on-drug frequency range changes to $[f_{\min}^*, f_{\max}^*]$. As a result, the projection (coincidence detection) of the vector of the current on-drug weights $w_{ij}^*(t)$ to the vector of reference off-drug weights $w_{ij}(T)$ peaks at a time T^* that differs from T.

Numerical simulations indicate that our implementation of the SBF–ML model shows the major features of the clock pattern effect: immediate, scalar shift in timing, and recalibration on-drug, followed by an immediate, scalar rebound, and recalibration off-drug (solid triangles in **Figure 2A**). Simulations carried with $\alpha > 0$ for dopamine agonists, indicate an immediate, leftward shift of the response function to $T^* < T$ (inset A3 in **Figure 2A**), in agreement with experimental data for DA agonists methamphetamine, and cocaine (Meck, 1996; Buhusi and Meck, 2002; Matell et al., 2004). On the other hand, for $\alpha < 0$ we replicated numerically an immediate rightward shift due to a slow down of cortical oscillators during retrieval $T^* > T$ (inset A4 in **Figure 2A**), in agreement with experimental observation of the effect of DA antagonist haloperidol (Meck, 1996; Buhusi and Meck, 2005).

Recalibration upon chronic drug administration

According to the clock pattern (Meck, 1996), chronic drug administration results in a gradual recalibration, such that the response time on-drug gradually approaches the response time off-drug drug, an effect which is not due to receptor desensitization, but rather attributed to relearning of the criterion time using the drug-altered cortical frequencies (Meck, 1996). In our implementation, the repeated drug administration results in the criterion time T – which is represented in memory by a distribution of learned patterns $w_{ij}(T)$ – to be gradually re-written with new samples of reinforced duration, samples which are computed using drug-altered oscillator frequencies. We found that our SBF–ML model exhibits recalibration of the criterion time T^* back to T under repeated methamphetamine administration ($\alpha > 0$, inset A2 of **Figure 2A**) as well as under repeated haloperidol administration ($\alpha < 0$, inset A5 of **Figure 2A**). A similar recalibration occurs after the drug is discontinued, when the model re-learns the weights $w_{ij}(T)$ for the criterion T off-drug (see right-side of **Figure 2A**). Interestingly, the rates of the two recalibration processes (**Figure 2A**) to the original criterion time T are not necessarily identical since the presence of the drugs may also significantly change the rate at which the memory is overwritten. In order to match pharmacological data from (Meck, 1996; Buhusi and Meck, 2002; Matell et al., 2004), we set the overwrite rate at 25% samples per session (**Figure 2A**).

Immediate rebound in the opposite direction, upon discontinuing the drug

In the SBF–ML model, discontinuing the drug results in a scalar rebound of the response in the opposite direction, due to the sudden change from on-drug cortical frequencies f^* to the off-drug cortical frequencies $f = (1 - \beta) f^*$. For example, an immediate leftward shift from $T = 40$ s (inset A2 in **Figure 2A**) to $T^* = 32$ s (inset A3 in **Figure 2A**) under methamphetamine is followed by relearning of the criterion on-drug; discontinuing the drug results in an immediate rightward displacement to $T^{**} = 48$ s (inset A1 in **Figure 2A**), followed again by a slow recalibration back to the original criterion time $T = 40$ s due to relearning of the criterion time with the new cortical frequencies.

Time-scale invariance of the clock-speed effect

For our implementation of the SBF–ML model, the preservation of time-scale invariance throughout the clock pattern is shown in the lower panels of **Figure 2**. For example, the amplitude of the immediate shift in response time at the transition between the off-drug to the on-drug state, and the amplitude of the immediate, opposite rebound at the transition between the on-drug to the off-drug state, are proportional to the criterion interval T (see **Figure 2B** for $T = 40$ s and **Figure 2D** for $T = 20$ s). Moreover, the variance in the response rate (width of response/output function), throughout the pharmacological manipulation remains proportional to the current response time, either off-drug T, or off-drug T^* (**Figures 2B** and **2D**). For the 40-s criterion, **Figure 2B** indicates that the envelopes of response functions in the insets A1, A2, and A3 of **Figure 2A** superimpose when renormalized in amplitude and time. Similarly, for the 20 s criterion time, **Figure 2D** indicates that the envelopes of response functions in the insets A4, A5, and A6 of **Figure 2A** superimpose when normalized in amplitude and time. Finally, the scalar property is preserved also between different criterion times: **Figure 2C** indicates that the envelopes of the response functions from inset A2 of **Figure 2A** ($T^{**} = 40$ s recalibrated under methamphetamine) and inset A5 of **Figure 2A** ($T^{**} = 20$ s recalibrated under haloperidol) superimposed when normalized in amplitude and in time.

THE MEMORY PATTERN OF CHOLINERGIC DRUGS IN THE SBF–ML MODEL

Previous research indicates that the administration of ACh agonist physostigmine results in a gradual, dose-dependent leftward shift of the response (solid circles in **Figure 3A**; Meck, 1996). Similarly, administration of ACh blocker atropine leads to a gradual and dose-dependent rightward shift of the psychophysical functions (solid squares in **Figure 3A**; Meck, 1996). Moreover, the magnitudes of the temporal shifts observed are dose-dependent and proportional to the intervals being timed (Meck, 1996). To address this issue, it was proposed that training under the influence of the ACh drug produces a gradually re-learning of an altered criterion time $T^* = k^*\mathrm{T}$ (Gibbon et al., 1984; Meck, 1996; Buhusi and Meck, 2010).

In the SBF–ML model, the dynamics of memory pattern (**Figure 3A**) is significantly different from that of the clock pattern (**Figure 2A**): while the clock pattern takes effect as soon as the frequencies of neural oscillators are changed by the drug, thus producing an immediate temporal shift because of the sudden mismatch in cortical frequencies during storage, and retrieval, *the memory pattern* is determined by a gradual alteration of representation of the criterion time in the long-term memory that affects a growing number of memorized sample weights. Relearning the

criterion under the ACh drug eventually overwrites the entire long-term memory with the altered representation k^*T of the criterion time T. This induces a gradual change in the content of the long-term memory that leads to an increasing mismatch between the contents of the working and the long-term memory (**Figure 3A**).

In our numerical implementation, for ACh agonist atropine, we assumed $k^* = 1.25$ in order to match the pharmacological data from Meck (1996). As shown in **Figure 3A** (solid triangles), the gradual change in memory samples under atropine gradually shifts the peak of the output function from the initial value, $T = 20$ s (inset A3 in **Figure 3A**), to the altered value $T^* = k^*\mathrm{T} = 15$ s (inset A4 in **Figure 3A**). A similar shift takes place for ACh antagonists, say from $T = 40$ s (inset A2 in **Figure 3A**) to $T^* = 50$ s (inset A1 in **Figure 3A**). Most importantly, both the amplitude of the gradual shift on-drug and the amplitude of the recalibration when the ACh drug is discontinued are proportional to the criterion interval T (**Figure 3A**). Moreover, the variance (width) of the response remains scalar, i.e., proportional to the current peak time, either off-drug, T, or on-drug, T^* (**Figure 3B** for $T = 40$ s and **Figure 3D** for $T = 20$ s). For the 40-s criterion time, **Figure 3B** indicates that the envelopes of response functions in the insets A1 and A2 of **Figure 3A** superimpose when normalized in amplitude and time. Similarly, for the 20-s criterion, **Figure 3D** indicates that the envelopes of response functions in the insets A3 and A4 of **Figure 3A** superimpose when normalized in amplitude and time. Finally, the scalar property is preserved also between different criterion times: **Figure 3C** indicates that the envelopes of the response functions from inset A2 of **Figure 3A** ($T = 40$ s, dashed line) and inset A3 of **Figure 3A** ($T = 20$ s, solid line) superimposed when normalized in amplitude and time.

DISCUSSION

In mammals, DA drugs induce an immediate, scalar change in the perceived time (clock pattern, **Figure 2**), whereas ACh drugs induce a gradual change in perceived time (memory pattern, **Figure 3**). To explain these patterns, we assumed that DA drugs induce a sudden change in the speed of an internal clock, while ACh drugs induce a gradual change in the memory of the criterion duration (Gibbon et al., 1984; Meck, 1996). Most importantly, both the clock and memory patterns are scalar, i.e., the drug effects are proportional to the criterion duration (Gibbon et al., 1984; Meck, 1996).

Current neurobiological data supports a SBF model, in which time is coded by the coincidental activation of striatal spiny neurons by cortical neural oscillators (Matell and Meck, 2000, 2004; Buhusi and Meck, 2005). While generally biologically plausible, the impracticality of perfect oscillators (or the lack thereof), questions the robustness of such a mechanisms in a brain with real, noisy neurons, particularly after pharmacological manipulations. Here we explored the neural mechanisms required for the time-scale invariance of the clock (**Figure 2**) and memory (**Figure 3**) patterns produced by the SBF–ML model (**Figure 4**). To our knowledge, this is the first time the SBF-type model was used to match pharmacological data, and the first time it is implemented using biophysically realistic neurons instead of simple sine waves. This combination of features opens the possibility of calibrating the timing network by adjusting conductances and half-activation voltages for specific ionic channels to mimic the effect of different drugs at channel-level.

Under the assumption that the biological noise is ubiquitous in the form of, e.g., variability of frequency within- and between-trails, variability in memory storage, and retrieval, etc., numerical simulations indicated that the SBF–ML model shows the scalar property, i.e., errors in time estimation are linearly related to the estimated duration (filled squares in **Figure 5B**). Interestingly, simply replacing crisp cortical phase oscillators with crisp cortical ML neurons did not produce scalar effects (filled circles in **Figure 5B**). It was only when at least one source of variability (noise) was introduced that the scalar property was evident. This result supports and extends the conjecture of Matell and Meck (2004) by which the SBF model requires at least one source of variance (noise) to address time-scale invariance.

Computational models of interval timing vary largely with respect to the hypothesized mechanisms by which temporal processing is explained, and by which time-scale invariance, or drug effects are explained. The putative mechanisms of timing rely on pacemaker/accumulator processes (Gibbon, 1977; Gibbon et al., 1984), sequences of behaviors (Killeen and Fetterman, 1988), pure sine oscillators (Church and Broadbent, 1990; Matell and Meck, 2000, 2004), memory traces (Grossberg and Schmajuk, 1989; Grossberg and Merrill, 1992; Machado, 1997; Buhusi and Schmajuk, 1999; Staddon and Higa, 1999), or cell and network-level models (Leon and Shadlen, 2003; Simen et al., 2011). For example, both neurometric functions from single neurons and ensemble of neurons successfully paralleled the psychometric functions for the to-be-timed intervals shorter than 1 s (Leon and Shadlen, 2003). Reutimann et al. (2004) also considered interacting populations that are subject to neuronal adaptation and synaptic plasticity based on the general principle of firing rate modulation in single-cell. Balancing LTP and LTD mechanisms are thought to modulate the firing rate of neural populations with the net effect that the adaptation leads to a linear decay of the firing rate in time. Therefore, the linear relationship between time and the number of clock ticks of the pacemaker–accumulator model in the scalar expectancy theory of interval timing (Gibbon, 1977) was successfully translated into a linearly decaying firing rate model that maps time and variable firing rate. As Matell and Meck (2004) stated, it may be that the brain uses both (relatively) stable neural oscillators in an SBF-based paradigm and a variable firing rate paradigm for interval timing.

Dopaminergic drugs modulation of the firing frequency of cortical oscillators led in our numerical simulations of the SBF–ML model to clock patterns (Meck, 1996): immediate change in timing (inset A3 of **Figure 2A**) and gradual re-calibration under the drug (inset A2 of **Figure 2A**), immediate re-bound in the opposite direction (inset A1 of **Figure 2A**) and gradual re-calibration upon discontinuing the drug, and scalar (proportional) effects (**Figures 2B–D**). ACh drugs modulation of the representation $w_{ij}(T)$ of the criterion time in the long-term memory led in our numerical simulations of the SBF–ML model to memory patterns (Meck, 1996): gradual change in timing on-drug (inset A1 of **Figure 3A**), gradual re-calibration upon discontinuing the drug (inset A3 of **Figure 3A**), and scalar (proportional) effects

(**Figures 3B–D**). Our interpretation of the clock and memory patterns within the SBF model is in accord with the interpretation of drug effect in the scalar expectancy theory (SET; Gibbon, 1977; Gibbon et al., 1984). As in SET, our numerical simulations assume that DA drugs alter the time-base of the model, and that ACh drugs alter memory processes. In recognition of this legacy, our description of the ACh memory effects continue to use the (rather famous) k^* factor (Gibbon et al., 1984; Meck, 1996).

In summary, numerical simulations with the SBF–ML model successfully reproduced the clock (**Figure 2**) and memory (**Figure 3**) effects reported in the literature (Meck, 1996), including their scalar effects (Gibbon, 1977; Gibbon et al., 1984; Meck, 1996), previously addressed only by a few established behavioral models in the field, such as SET (Gibbon, 1977; Gibbon et al., 1984), and STM (Grossberg and Schmajuk, 1989). Together with previous studies (Matell and Meck, 2000, 2004; Buhusi and Meck, 2005), the current results establish the SBF model as a neurobiologically realistic model of interval timing capable of explaining a large range of phenomena, from behavior, to lesions, and pharmacology, with the potential to provide insight into the neurobiological bases on interval timing.

ACKNOWLEDGMENTS

This research was supported the National Science Foundation CAREER award IOS 1054914 to Sorinel A. Oprisan. Catalin V. Buhusi was supported by the National Institutes of Health grants MH65561 and MH73057. We are also indebted to Warren H. Meck and Matthew S. Matell for helpful discussions about the SBF model, and to Joshua Swearingen for helpful comment on an early version of the manuscript.

REFERENCES

Anderson, D. R., Sweeney, D. J., and Williams, T. A. (2009). *Essentials of Statistics for Business and Economics.* Mason, OH: Thomson Higher Education.

Anliker, J. (1963). Variations in alpha voltage of the electroencephalogram and time perception. *Science* 140, 1307–1309.

Beiser, D. G., and Houk, J. C. (1998). Model of cortical-basal ganglionic processing: encoding the serial order of sensory events. *Clin. Neurophysiol.* 79, 3168–3188.

Boisvert, M. J. M. J., and Sherry, D. F. D. F. (2006). Interval timing by an invertebrate, the bumble bee Bombus impatiens. *Curr. biol.* 16, 1636–1640.

Brockwell, P. J., and Davis, R. A. (1991). *Time Series: Theory and Models*, 2nd Edn. New York: Springer.

Buhusi, C. V., Aziz, D., Winslow, D., Carter, R. E., Swearingen, J. E., and Buhusi, M. C. (2009). Interval timing accuracy and scalar timing in C57BL/6 mice. *Behav. Neurosci.* 123, 1102–1113.

Buhusi, C. V., and Meck, W. H. (2002). Differential effects of methamphetamine and haloperidol on the control of an internal clock. *Behav. Neurosci.* 116, 291–297.

Buhusi, C. V., and Meck, W. H. (2005). What makes us tick? Functional and neural mechanisms of interval timing. *Nat. Rev. Neurosci.* 6, 755–765.

Buhusi, C. V., and Meck, W. H. (2009). Relative time sharing: new findings and an extension of the resource allocation model of temporal processing. *Philos. Trans. R. Soc. Lond. B Biol. Sci.* 364, 1875–1885.

Buhusi, C. V., and Meck, W. H. (2010). "Timing behavior," in *Encyclopedia of Psychopharmacology*, ed. I. P. Stolerman (Berlin: Springer), 1319–1323.

Buhusi, C. V., and Schmajuk, N. A. (1999). Timing in simple conditioning and occasion setting: a neural network approach. *Behav. Process.* 45, 33–57.

Cameron, A. C., and Windmeijer, F. A. G. (1997). An R-squared measure of goodness of fit for some common nonlinear regression models. *J. Econom.* 77, 329–342.

Cheng, K., and Westwood, R. (1993). Analysis of single trials in pigeons' timing performance. *J. Exp. Psychol. Anim. Behav. Process.* 19, 56–67.

Church, R. M., and Broadbent, H. A. (1990). Alternative representations of time, number, and rate. *Cognition* 37, 55–81.

Church, R. M., Meck, W. H., and Gibbon, J. (1994). Application of scalar timing theory to individual trials. *J. Exp. Psychol. Anim. Behav. Process.* 20, 135–155.

Coull, J. T., Cheng, R. K., and Meck, W. H. (2011). Neuroanatomical and neurochemical substrates of timing. *Neuropsychopharmacology* 36, 3–25.

Coull, J. T., Vidal, F., Nazarian, B., and Macar, F. (2004). Functional anatomy of the attentional modulation of time estimation. *Science* 303, 1506–1508.

Dews, P. B. (1962). The effect of multiple S delta periods on responding on a fixed-interval schedule. *J. Exp. Anal. Behav.* 5, 369–374.

Gallistel, C. R. (1990). *The Organization of Behavior.* Cambridge, MA: MIT Press.

Gibbon, J. (1977). Scalar expectancy theory and Weber's law in animal timing. *Psychol. Rev.* 84, 279–325.

Gibbon, J., Church, R. M., and Meck, W. H. (1984). Scalar timing in memory. *Ann. N. Y. Acad. Sci.* 423, 52–77.

Grossberg, S., and Merrill, J. W. (1992). A neural network model of adaptively timed reinforcement learning and hippocampal dynamics. *Brain Res. Cogn. Brain Res.* 1, 3–38.

Grossberg, S., and Schmajuk, N. A. (1989). Neural dynamics of adaptive timing and temporal discrimination during associative learning. *Neural Netw.* 2, 79–102.

Harrington, D. L., and Haaland, K. Y. (1991). Sequencing in Parkinson's disease. Abnormalities in programming and controlling movement. *Brain Res.* 114, 99–115.

Harrington, D. L., Haaland, K. Y., and Knight, R. T. (1998). Cortical networks underlying mechanisms of time perception. *J. Neurosci.* 18, 1085–1095.

Hinton, S. C., and Meck, W. H. (1997). The 'internal clocks' of circadian and interval timing. *Endeavour* 21, 3–8.

Houk, J. C. (1995). "Information processing in modular circuits linking basal ganglia and cerebral cortex," in *Models of Information Processing in the Basal Ganglia*, eds J. C. Houk, J. L. Davis, and D. G. Beiser (Cambridge: MIT Press), 3–10.

Houk, J. C., Davis, J. L., and Beiser, D. G. (1995). *Computational Neuroscience, Models of Information Processing in the Basal Ganglia.* Cambridge: MIT Press.

Killeen, P. R., and Fetterman, J. G. (1988). A behavioral theory of timing. *Psychol. Rev.* 95, 274–295.

Leon, M. I., and Shadlen, M. N. (2003). Representation of time by neurons in the posterior parietal cortex of the macaque. *Neuron* 38, 317–327.

Machado, A. (1997). Learning the temporal dynamics of behavior. *Psychol. Rev.* 104, 241–265.

Malapani, C., Deweer, B., and Gibbon, J. (2002). Separating storage from retrieval dysfunction of temporal memory in Parkinson's disease. *J. Cogn. Neurosci.* 14, 311–322.

Malapani, C., and Fairhurst, S. (2002). Scalar timing in animals and humans. *Learn. Motiv.* 33, 156–176.

Malapani, C., Rakitin, B., Levy, R., Meck, W. H., Deweer, B., Dubois, B., and Gibbon, J. (1998). Coupled temporal memories in Parkinson's disease: a dopamine-related dysfunction. *J. Cogn. Neurosci.* 10, 316–331.

Maricq, A. V., and Church, R. M. (1983). The differential effects of haloperidol and methamphetamine on time estimation in the rat. *Psychopharmacology (Berl.)* 79, 10–15.

Maricq, A. V., Roberts, S., and Church, R. M. (1981). Methamphetamine and time estimation. *J. Exp. Psychol. Anim. Behav. Process.* 7, 18–30.

Matell, M. S., King, G. R., and Meck, W. H. (2004). Differential modulation of clock speed by the administration of intermittent versus continuous cocaine. *Behav. Neurosci.* 118, 150–156.

Matell, M. S., and Meck, W. H. (1997). A comparison of the tri-peak and peak-interval procedure in rats: equivalency of the clock speed enhancing effect of methamphetamine on interval timing. *Abst. Soc. Neurosci.* 23, 1315–1316.

Matell, M. S., and Meck, W. H. (2000). Neuropsychological mechanisms of interval timing behavior. *Bioessays* 22, 94–103.

Matell, M. S., and Meck, W. H. (2004). Cortico-striatal circuits and interval timing: coincidence detection of oscillatory processes. *Cogn. Brain Res.* 21, 139–170.

Matell, M. S., Meck, W. H., and Nicolelis, M. A. (2003). Interval timing and the encoding of signal duration by ensembles of cortical and striatal neurons. *Behav. Neurosci.* 117, 760–773.

Mauk, M. D., and Buonomano, D. V. (2004). The neural basis of temporal processing. *Annu. Rev. Neurosci.* 27, 307–340.

Meck, W. H. (1983). Selective adjustment of the speed of internal clock and memory processes. *J. Exp. Psychol. Anim. Behav. Process.* 171–201.

Meck, W. H. (1996). Neuropharmacology of timing and time perception. *Cogn. Brain Res.* 3, 227–242.

Meck, W. H. (2006). Neuroanatomical localization of an internal clock: a functional link between mesolimbic, nigrostriatal, and mesocortical dopaminergic systems. *Brain Res.* 1109, 93–107.

Meck, W. H., Cheng, R.-K., Macdonald, C. J., Gainetdinov, R. R., Caron, M. G., and Çevik, M. N. Ö. (2011). Gene-dose dependent effects of methamphetamine on interval timing in dopamine-transporter knockout mice. *Neuropharmacology* doi: 10.1016/j.neuropharm.2011.01.042. [Epub ahead of print].

Meck, W. H., and Church, R. M. (1987a). Cholinergic modulation of the content of temporal memory. *Behav. Neurosci.* 101, 457–464.

Meck, W. H., and Church, R. M. (1987b). Nutrients that modify the speed of internal clock and memory storage processes. *Behav. Neurosci.* 101, 465–475.

Meck, W. H., Church, R. M., Wenk, G. L., and Olton, D. S. (1987). Nucleus basalis magnocellularis and medial septal area lesions differentially impair temporal memory. *J. Neurosci.* 7, 3505–3511.

Meck, W. H., Penney, T. B., and Pouthas, V. (2008). Cortico-striatal representation of time in animals and humans. *Curr. Opin. Neurobiol.* 18, 145–152.

Miall, R. C. (1989). The storage of time intervals using oscillating neurons. *Neural Comput.* 1, 359–371.

Morris, C., and Lecar, H. (1981). Voltage oscillations in the barnacle giant muscle fiber. *Biophys. J.* 35, 193–213.

Nagelkerke, N. (1991). A note on a general definition of the coefficient of determination. *Biometrika* 78, 691–692.

Neil, D. B., and Herndon, J. D. Jr. (1978). Anatomical specificity within rat striatum for the dopaminergic modulation of DRL responding and activity. *Brain Res.* 153, 529–538.

Olton, D. S., Wenk, G. L., Church, R. M., and Meck, W. H. (1988). Attention and the frontal cortex as examined by simultaneous temporal processing. *Neuropsychologia* 26, 307–318.

Onoe, H., Komori, M., Onoe, K., Takechi, H., Tsukada, H., and Watanabe, Y. (2001). Cortical networks recruited for time perception: a monkey positron emission tomography (PET) study. *Neuroimage* 13, 37–45.

Rakitin, B. C., Gibbon, J., Penney, T. B., Malapani, C., Hinton, S. C., and Meck, W. H. (1998). Scalar expectancy theory and peak-interval timing in humans. *J. Exp. Psychol. Anim. Behav. Process.* 24, 15–33.

Rao, S. M., Mayer, A. R., and Harrington, D. L. (2001). The evolution of brain activation during temporal processing. *Nat. Neurosci.* 4, 317–323.

Resnick, S. I. (2006). *Heavy-Tail Phenomena: Probabilistic and Statistical Modeling.* New York: Springer.

Reutimann, J., Yakovlev, V., Fusi, S., and Senn, W. (2004). Climbing neuronal activity as an event-based cortical representation of time. *J. Neurosci.* 24, 3295–3303.

Rinzel, J., and Ermentrout, B. (1998). "Analysis of neural excitability and oscillations," in *Methods of Neuronal Modeling*, eds C. Koch and I. Segev (Cambridge, MA: MIT Press), 135–169.

Rizzuto, D. S., Madsen, J. R., Bromfield, E. B., Schulze-Bonhage, A., Seelig, D., Aschenbrenner-Scheibe, R., and Kahana, M. J. (2003). Reset of human neocortical oscillations during a working memory task. *Proc. Natl. Acad. Sci. U.S.A.* 100, 7931–7936.

Schubotz, R. I., Friederici, A. D., and Yves Von Cramon, D. (2000). Time perception and motor timing: a common cortical and subcortical basis revealed by fMRI. *Neuroimage* 11, 1–12.

Simen, P., Balci, F., Desouza, L., Cohen, J. D., and Holmes, P. (2011). A model of interval timing by neural integration. *J. Neurosci.* 31, 9238–9253.

Staddon, J. E., and Higa, J. J. (1999). Time and memory: towards a pacemaker-free theory of interval timing. *J. Exp. Anal. Behav.* 71, 215–251.

Stevens, M. C., Kiehl, K. A., Pearlson, G., and Calhoun, V. D. (2007). Functional neural circuits for mental timekeeping. *Hum. Brain Mapp.* 28, 394–408.

Swearingen, J. E., and Buhusi, C. V. (2010). The pattern of responding in the peak-interval procedure with gaps: an individual-trials analysis. *J. Exp. Psychol. Anim. Behav. Process.* 36, 443–455.

Talton, L. E., Higa, J. J., and Staddon, J. E. R. (1999). Interval schedule performance in the goldfish *Carassius auratus*. *Behav. Process.* 45, 193–206.

Conflict of Interest Statement: The authors declare that the research was conducted in the absence of any commercial or financial relationships that could be construed as a potential conflict of interest.

Received: 30 June 2011; paper pending published: 18 July 2011; accepted: 24 August 2011; published online: 23 September 2011.

Citation: Oprisan SA and Buhusi CV (2011) Modeling pharmacological clock and memory patterns of interval timing in a striatal beat-frequency model with realistic, noisy neurons. Front. Integr. Neurosci. ***5****:52. doi: 10.3389/fnint.2011.00052*

frontiers in
INTEGRATIVE NEUROSCIENCE

OPINION ARTICLE
published: 25 October 2011
doi: 10.3389/fnint.2011.00070

Dopamine modulates striato-frontal functioning during temporal processing

Catherine R. G. Jones[1]* and Marjan Jahanshahi[2]

[1] *Department of Psychology, University of Essex, Colchester, UK*
[2] *Sobell Department of Motor Neuroscience and Movement Disorders, UCL Institute of Neurology, London, UK*
**Correspondence: crgjones@essex.ac.uk*

With genesis in the ventral tegmental area and the substantia nigra pars compacta (SNc), the neurotransmitter dopamine influences brain function through three distinct pathways: the nigrostriatal, mesolimbic, and mesocortical. Dopamine plays a crucial role in a range of functions, for example: reward-related processing (Schultz et al., 1997) and reinforcement learning (Montague et al., 1996; Frank and Claus, 2006; Frank et al., 2007), working memory (Brozoski et al., 1979; Kimberg et al., 1997; Lustig et al., 2005; Cools et al., 2008), and motor function, including determining the vigor of actions (e.g., Niv et al., 2007; Smith and Villalba, 2008). Here our focus is on the role of dopamine in temporal processing, a less commonly recognized function (Meck, 1996; Buhusi and Meck, 2005; Meck et al., 2008; Jones and Jahanshahi, 2009; Allman and Meck, 2011; Coull et al., 2011 – but see Hata, 2011).

A growing body of research has sought to characterize the role of dopamine in interval timing, which can be broadly thought of as motor and perceptual timing in the milliseconds- and seconds-range. The influence of dopamine on interval timing has been demonstrated in pharmacological studies both with animals (Drew et al., 2003; Matell et al., 2006; Cheng et al., 2007; Meck et al., 2011) and humans (Rammsayer, 1993, 1997, for reviews see Meck et al., 2008; Jones and Jahanshahi, 2009; Coull et al., 2011). Using the peak-interval procedure, in which a learnt temporal interval is reproduced, animal research has established that dopamine agonists lead to the interval being underestimated, whereas dopamine antagonists lead to overestimation (e.g., Drew et al., 2003; Matell et al., 2004, 2006; MacDonald and Meck, 2005). These results have been interpreted as the effect of dopamine agonists and antagonists on speeding and slowing an "internal clock," respectively. Lesions to the SNc and the caudate–putamen (CPu) both impair temporal control on the task, while rats with lesions to the nucleus accumbens show no evidence of disrupted temporal performance (Meck, 2006a). This pattern implicates the nigrostriatal (substantia nigra–dorsal striatum) dopamine pathway in interval timing. Further, levodopa, a precursor to dopamine that is commonly used to treat Parkinson's disease (PD), restores timing performance in rats with lesions to the SNc but not in those with lesions to the CPu, which may reflect the distinct roles of these structures in temporal calculation (Meck, 2006a). Work on healthy humans has established that haloperidol, a non-specific D2 receptor antagonist, attenuates both milliseconds- and seconds-range perceptual timing (comparing the length of two stimuli), whereas remoxipride, which blocks D2 receptors in the mesolimbic and mesocortical tracts, only impairs seconds-range timing (Rammsayer, 1997). These results were considered to support the role of the nigrostriatal system in milliseconds-range timing. More recently, Wiener et al. (2011) were able to apply a more targeted investigation by studying the effect of different single-nucleotide genetic polymorphisms on perceptual timing. Participants with a polymorphism affecting the density of striatal D2 receptors showed increased variability for milliseconds- but not seconds-range perceptual timing. Conversely, participants with a polymorphism that affects an enzyme (COMT) influencing prefrontal dopamine showed greater variability only in the seconds-range. Thus, these data suggest a double dissociation, with the nigrostriatal pathway being important for milliseconds-range perceptual timing and the mesocortical pathway being important for seconds-range perceptual timing.

Parkinson's disease is a movement disorder associated with degeneration of dopaminergic neurons in the SNc. There is now a body of evidence that motor and perceptual timing within the milliseconds- and seconds-range are impaired in PD (see Jones and Jahanshahi, 2009; Allman and Meck, 2011; Coull et al., 2011). Dopaminergic medication often improves performance on perceptual (e.g., Pastor et al., 1992a; Malapani et al., 1998) and motor timing tasks (e.g., Pastor et al., 1992b; O'Boyle et al., 1996) in patients with PD; although the pattern of effects (e.g., whether accuracy or variability is affected) is variable and significant effects are not always found (e.g., Pastor et al., 1992b; O'Boyle et al., 1996; Jones et al., 2008; Harrington et al., 2011b). The variable findings might relate to the insufficiency of dopaminergic medication for fully restoring striato-frontal function (Harrington et al., 2011b), or to the inadequacy of medication withdrawal and the lingering effects of long-acting medication in patients tested "off" medication. Difficulties with interval timing have also been observed in other disorders that are associated with dopaminergic dysfunction, including schizophrenia and attention-deficit/hyperactivity disorder (ADHD; see Jones and Jahanshahi, 2009; Allman and Meck, 2011).

There is consensus from imaging studies that the basal ganglia, particularly the dorsal striatum, are engaged during interval timing (e.g., Rao et al., 2001; Harrington et al., 2004, 2010, 2011a,b; Jahanshahi et al., 2006, 2010; Coull et al., 2008, for reviews see Meck et al., 2008; Jones and Jahanshahi, 2009; Coull et al., 2011). The basal ganglia are closely connected to the cortex through a series of striato-cortical loops (Alexander et al., 1986). Recording from neural ensembles in animal studies supports the role of both striatal and cortical regions in encoding temporal intervals (e.g., Matell et al., 2003, 2011; Lebedev et al., 2008; Höhn et al., 2011), whilst cortical lesions in rats attenuate temporal performance (Meck, 2006b). Further, patients with cortical lesions and healthy individuals with short-lasting TMS-induced disruption to cortical function demonstrate difficulties on temporal

tasks (Jones et al., 2004; Coslett et al., 2009). Thus there has been increasing interest in explaining and exploring how interval timing might be distributed across key cortical and subcortical regions. The obvious mediator for this relationship is dopamine. To better examine the effects of dopamine on striato-frontal function in PD, we investigated the neural correlates of motor timing in a repetitive tapping task, in patients tested both "on" and "off" apomorphine, a non-selective dopamine receptor agonist (Jahanshahi et al., 2010). Using effective connectivity analysis, we established that task-related coupling between the left head of the caudate nucleus and the prefrontal cortex was increased when the patients were "on" medication compared to the "off" state. The data support the proposal that dopamine modulates the coupling between frontal and striatal regions during motor timing. Fronto-striatal connectivity in PD has also been investigated during a perceptual timing task where the durations of two stimuli were compared (Harrington et al., 2011b). Consistent with the previous study, greater activation of the putamen and superior frontal gyrus was observed "on" compared to "off" medication during the decision phase of the perceptual timing task. However, the dominant finding was that connectivity between the basal ganglia and cortex was greater "off" than "on" medication during this task.

A challenge for the field has been to develop a biologically plausible model of interval timing. The striatal beat frequency model (Matell and Meck, 2000, 2004) proposes that the striatum receives cortical and thalamic oscillatory activity that serves as a clock signal. Using a process of coincidence detection, striatal spiny neurons fire when a criterion number of neuronal inputs oscillate with the same beat frequency. It is suggested that nigrostriatal phasic dopamine signals the onset and offset of a timed interval, whereas tonic dopamine alters the frequencies of the cortical oscillations, thus directly modulating the speed of the "internal clock." According to this model, dopamine is a critical mediator of temporal calculations (see Allman and Meck, 2011; Oprisan and Buhusi, 2011).

Interval timing fits under the broad umbrella of temporal processing, which includes circadian rhythms through to the psychological relationship between time and memory. The different types of temporal experience are poorly defined and understood (Grondin, 2010), and the relationship between these various types of temporal processing has received little attention. A complete account of interval timing should seek to position this process within the wider context of temporal processing. Particularly, an unexplored question is whether the role of dopamine in interval timing can be integrated with ostensibly distinct areas of dopamine-focused research that have a temporal component. The temporal difference model of learning proposes that the phasic activity of midbrain dopamine neurons code the time discrepancy between the expected and actual delivery of reward, calculating a reward prediction error (e.g., Montague et al., 1996; Schultz et al., 1997; Hollerman and Schultz, 1998). Dopamine neurons in the substantia nigra have also been implicated in temporal discounting, which is the waning of reward value with increasing delay, and in the temporal uncertainty inherent in delayed rewards (Kobayashi and Schultz, 2008). Related to this, administration of dopamine antagonists to healthy participants increases the degree of temporal discounting, i.e., the relative value of delayed rewards decreases, leading to impulsive behavior (Pine et al., 2010). Other work proposes that tonic levels of dopamine in the nucleus accumbens play an important role in response vigor (i.e., the rate of responding) by calculating the average rate of reward (Niv et al., 2007), a process that has an intrinsic temporal component. Finally, mesocortical dopamine is critical for working memory (Brozoski et al., 1979; Kimberg et al., 1997; Cools et al., 2008), which is essentially the process of maintaining information "on line" over a time interval. To date, the investigation of the role of dopamine in reward prediction error, reinforcement learning, temporal discounting, working memory, response vigor, and interval timing have remained largely distinct fields. There may be a value in exploring whether the temporal components of these tangential fields can be integrated with research that seeks to formulate a role for dopamine in modulating interval timing.

REFERENCES

Alexander, G. E., Delong, M. R., and Strick, P. L. (1986). Parallel organization of functionally segregated circuits linking basal ganglia and cortex. *Annu. Rev. Neurosci.* 9, 357–381.

Allman, M. J., and Meck, W. H. (2011). Pathophysiological distortions in time perception and timed performance. *Brain*. doi: 10.1093/brain/awr210. [Epub ahead of print].

Brozoski, T. J., Brown, R. M., Rosvold, H. E., and Goldman, P. S. (1979). Cognitive deficit caused by regional depletion of dopamine in prefrontal cortex of rhesus monkey. *Science* 205, 929–932.

Buhusi, C. V., and Meck, W. H. (2005). What makes us tick? Functional and neural mechanisms of interval timing. *Nat. Rev. Neurosci.* 6, 755–765.

Cheng, R. K., Ali, Y. M., and Meck, W. H. (2007). Ketamine "unlocks" the reduced clock-speed effect of cocaine following extended training: evidence for dopamine-glutamate interactions in timing and time perception. *Neurobiol. Learn. Mem.* 88, 149–159.

Cools, R., Gibbs, S. E., Miyakawa, A., Jaqust, W., and D'Esposito, M. (2008). Working memory capacity predicts dopamine synthesis capacity in the human striatum. *J. Neurosci.* 28, 1208–1212.

Coslett, H. B., Shenton, J., Dyer, T., and Wiener, M. (2009). Cognitive timing: neuropsychology and anatomic basis. *Brain Res.* 1254, 38–48.

Coull, J. T., Cheng, R. K., and Meck, W. H. (2011). Neuroanatomical and neurochemical substrates of timing. *Neuropsychopharmacology* 36, 3–25.

Coull, J. T., Nazarian, B., and Vidal, F. (2008). Timing, storage, and comparison of stimulus duration engage discrete anatomical components of a perceptual timing network. *J. Cogn. Neurosci.* 12, 2185–2197.

Drew, M. R., Fairhurst, S., Malapani, C., Horvitz, J. C., and Balsam, P. D. (2003). Effects of dopamine antagonists on the timing of two intervals. *Pharmacol. Biochem. Behav.* 75, 9–15.

Frank, M. J., and Claus, E. D. (2006). Anatomy of a decision: striatal-orbitofrontal interactions in reinforcement learning, decision making, and reversal. *Psychol. Rev.* 113, 300–326.

Frank, M. J., Moustafa, A. A., Haughey, H. M., Curran, T., and Hutchinson, K. E. (2007). Genetic triple dissociation reveals multiple roles for dopamine in reinforcement learning. *Proc. Natl. Acad. Sci. U.S.A.* 9, 16311–16316.

Grondin, S. (2010). Timing and time perception: a review of recent behavioral and neuroscience findings and theoretical directions. *Atten. Percept. Psychophys.* 72, 561–582.

Harrington, D. L., Boyd, L. A., Mayer, A. R., Sheltraw, D. M., Lee, R. R., Huang, M., and Rao, S. M. (2004). Neural representation of interval encoding and decision making. *Brain Res. Cogn. Brain Res.* 21, 193–205.

Harrington, D. L., Castillo, G. N., Fong, C. H., and Reed, J. D. (2011a). Neural underpinnings of distortions in the experience of time across senses. *Front. Integr. Neurosci.* 5:32. doi: 10.3389/fnint.2011.00032

Harrington, D. L., Castillo, G. N., Greenberg, P. A., Song, D. D., Lessig, S., Lee, R. R., and Rao, S. M. (2011b). Neurobehavioral mechanisms of temporal processing deficits in Parkinson's disease. *PLoS ONE* 6, e17461. doi: 10.1371/journal.pone.0017461

Harrington, D. L., Zimbelman, J. L., Hinton, S. C., and Rao, S. M. (2010). Neural modulation of temporal encoding, maintenance, and decision processes. *Cereb. Cortex* 20, 1274–1285.

Hata, T. (2011). Glutamate – a forgotten target for interval timing. *Front. Integr. Neurosci.* 5:27. doi: 10.3389/fnint.2011.00027

Höhn, S., Dallérac, G., Faure, A., Urbach, Y., Nguyen, H. P., Riess, O., von Hörsten, S., Le Blanc, P., Desvignes, N., El Massioui, N., Brown, B. L., and Doyère, V. (2011).

Behavioral and in vivo electrophysiological evidence for presymptomatic alteration of prefronto-striatal processing in the transgenic rat model for Huntington disease. *J. Neurosci.* 31, 8986–8997.

Hollerman, J. R., and Schultz, W. (1998). Dopamine neurons report and error in the temporal prediction of reward during learning. *Nat. Neurosci.* 1, 304–309.

Jahanshahi, M., Jones, C. R., Dirnberger, G., and Frith, C. D. (2006). The substantia nigra pars compacta and temporal processing. *J. Neurosci.* 26, 12266–12273.

Jahanshahi, M., Jones, C. R., Zijlmans, J., Katzenschlager, R., Lee, L., Quinn, N., Frith, C. D., and Lees, A. J. (2010). Dopaminergic modulation of striato-frontal connectivity during motor timing in Parkinson's disease. *Brain* 133, 727–745.

Jones, C. R., and Jahanshahi, M. (2009). The substantia nigra, the basal ganglia, dopamine and temporal processing. *J. Neural Transm. Suppl.* 73, 161–171.

Jones, C. R., Rosenkranz, K., Rothwell, J. C., and Jahanshahi, M. (2004). The right dorsolateral prefrontal cortex is essential in time reproduction: an investigation with repetitive transcranial magnetic stimulation. *Exp. Brain Res.* 158, 66–372.

Jones, C. R. G., Malone, T. J., Dirnberger, G., Edwards, M., and Jahanshahi, M. (2008). Basal ganglia, dopamine and temporal processing: performance on three timing tasks on and off medication in Parkinson's disease. *Brain Cogn.* 68, 30–41.

Kimberg, D. Y., D'Esposito, M., and Farah, M. J. (1997). Effects of bromocriptine on human subjects depend on working memory capacity. *Neuroreport* 8, 3581–3585.

Kobayashi, S., and Schultz, W. (2008). Influence of reward delays on responses of dopamine neurons. *J. Neurosci.* 28, 7837–7846.

Lebedev, M. A., O'Doherty, J. E., and Nicolelis, M. A. (2008). Decoding of temporal intervals from cortical ensemble activity. *J. Neurophysiol.* 99, 166–186.

Lustig, C., Matell, M. S., and Meck, W. H. (2005). Not "just" a coincidence: frontal-striatal synchronization in working memory and interval timing. *Memory* 13, 441–448.

MacDonald, C. J., and Meck, W. H. (2005). Differential effects of clozapine and haloperidol on interval timing in the supraseconds range. *Psychopharmacology (Berl.)* 182, 232–244.

Malapani, C., Rakitin, B., Meck, W. H., Deweer, B., Dubois, B., and Gibbon, J. (1998). Coupled temporal memories in Parkinson's disease: a dopamine-related dysfunction. *J. Cogn. Neurosci.* 10, 316–331.

Matell, M. S., Bateson, M., and Meck, W. H. (2006). Single-trials analyses demonstrate that increases in clock speed contribute to the methamphetamine-induced horizontal shifts in peak-interval timing functions. *Psychopharmacology (Berl.)* 188, 201–212.

Matell, M. S., King, G. R., and Meck, W. H. (2004). Differential adjustment of interval timing by the chronic administation of intermittent or continuous cocaine. *Behav. Neurosci.* 118, 150–156.

Matell, M. S., and Meck, W. H. (2000). Neuropsychological mechanisms of interval timing behavior. *Bioessays* 22, 94–103.

Matell, M. S., and Meck, W. H. (2004). Cortico-striatal circuits and interval timing: coincidence detection of oscillatory processes. *Brain Res. Cogn. Brain Res.* 21, 139–170.

Matell, M. S., Meck, W. H., and Nicolelis, M. A. (2003). Interval timing and the encoding of signal duration by ensembles of cortical and striatal neurons. *Behav. Neurosci.* 117, 760–773.

Matell, M. S., Shea-Brown, E., Gooch, C., Wilson, A. G., and Rinzel, J. A. (2011). A heterogeneous population code for elapsed time in rat medial agranular cortex. *Behav. Neurosci.* 125, 54–73.

Meck, W. H. (1996). Neuropharmacology of timing and time perception. *Brain Res. Cogn. Brain Res.* 3, 227–242.

Meck, W. H. (2006a). Neuroanatomical localization of an internal clock: a functional link between mesolimbic, nigrostriatal, and mesocortical dopaminergic systems. *Brain Res.* 1109, 93–107.

Meck, W. H. (2006b). Frontal cortex lesions eliminate the clock speed effect of dopaminergic drugs on interval timing. *Brain Res.* 1108, 157–167.

Meck, W. H., Cheng, R. K., MacDonald, C. J., Gainetdinov, R. R., Caron, M. G., and Çevik, M. Ö. (2011). Gene-dose dependent effects of methamphetamine on interval timing in dopamine-transporter knockout mice. *Neuropharmacology*. doi: 10.1016.j.neuropharm.2011.01.042. [Epub ahead of print].

Meck, W. H., Penney, T. B., and Pouthas, V. (2008). Cortico-striatal representation of time in animals and humans. *Curr. Opin. Neurobiol.* 18, 145–152.

Montague, P. R., Dayan, P., and Sejnowski, T. J. (1996). A framework for mesenchephalic dopamine systems based on predictive Hebbian learning. *J. Neurosci.* 16, 1936–1947.

Niv, Y., Daw, N. D., Joel, D., and Dayan, P. (2007). Tonic dopamine: opportunity costs and the control of response vigor. *Psychopharmacology (Berl.)* 191, 507–520.

O'Boyle, D. J., Freeman, J. S., and Cody, F. W. (1996). The accuracy and precision of timing of self-paced, repetitive movements in subjects with Parkinson's disease. *Brain* 119, 51–70.

Oprisan, S. A., and Buhusi, C. V. (2011). Modeling pharmacological clock and memory patterns of interval timing in a striatal beat-frequency model with realistic, noisy neurons. *Front. Integr. Neurosci.* 5:52. doi: 10.3389/fnint.2011.00052

Pastor, M. A., Jahanshahi, M., Artieda, J., and Obeso, J. A. (1992a). Time estimation and reproduction is abnormal in Parkinson's disease. *Brain* 115, 875–891.

Pastor, M. A., Jahanshahi, M., Artieda, J., and Obeso, J. A. (1992b). Performance of repetitive wrist movements in Parkinson's disease. *Brain* 115, 211–225.

Pine, A., Shiner, T., Seymour, B., and Dolan, R. J. (2010). Dopamine, time, and impulsivity in humans. *J. Neurosci.* 30, 8888–8896.

Rammsayer, T. (1993). On dopaminergic modulation of temporal information processing. *Biol. Psychol.* 36, 209–222.

Rammsayer, T. H. (1997). Are there dissociable roles of the mesostriatal and mesolimbocortical dopamine systems on temporal information processing in humans? *Neuropsychobiology* 35, 36–45.

Rao, S. M., Mayer, A. R., and Harrington, D. L. (2001). The evolution of brain activation during temporal processing. *Nat. Neurosci.* 4, 317–323.

Schultz, W., Dayan, P., and Montague, P. R. (1997). A neural substrate of prediction and reward. *Science* 275, 1593–1599.

Smith, Y., and Villalba, R. (2008). Striatal and extrastriatal dopamine in the basal ganglia: an overview of its anatomical organization in normal and Parkinsonian brains. *Mov. Disord.* 23, 534–547.

Wiener, M., Lohoff, F. W., and Coslett, H. B. (2011). Double dissociation of dopamine genes and timing in humans. *J. Cogn. Neurosci.* 23, 2811–2821.

Received: 07 October 2011; accepted: 07 October 2011; published online: 25 October 2011.

*Citation: Jones CRG and Jahanshahi M (2011) Dopamine modulates striato-frontal functioning during temporal processing. Front. Integr. Neurosci. **5**:70. doi: 10.3389/fnint.2011.00070*

frontiers in
INTEGRATIVE NEUROSCIENCE

OPINION ARTICLE
published: 22 June 2011
doi: 10.3389/fnint.2011.00027

Glutamate – a forgotten target for interval timing

Toshimichi Hata*

Faculty of Psychology, Doshisha University, Kyoto, Japan
**Correspondence: thata@mail.doshisha.ac.jp*

Since the early 1980s, dopamine and acetylcholine have received much interest in research on the neural substrates of interval timing (e.g., Meck, 1983, 1996; Meck and Church, 1987; Cheng et al., 2007a,b). The information-processing component of scalar expectancy theory (SET) formed the theoretical basis for many of these pharmacological studies (Gibbon et al., 1984). Alternative theories, including the Behavioral Theory of timing (Killeen and Fetterman, 1988), the Learning-to-Time model (Machado, 1997), the Multiple-Time-Scale model (Staddon and Higa, 1999), and the Striatal Beat Frequency (SBF) model (Matell and Meck, 2004) have been proposed for overcoming some of the deficiencies of SET. Evaluation of the similarities and differences of these models has been undertaken elsewhere (Matell and Meck, 2000). From a neuroscientific perspective, however, the SBF model is the most appealing, because it is the only model that deals with the specific neural substrates of interval timing. The SBF model was developed to elucidate the role of glutamate (Glu), a forgotten target for the neural substrate of interval timing, emphasizing the role of cortico-striatal Glu on behavior. However, few studies have focused on the role of Glu in the temporal control of behavior in the seconds-to-minutes range (Cheng et al., 2006; Bhave et al., 2008). This article seeks to identify important points to consider when examining the role of Glu in interval timing guided by the SBF model.

In psychopharmacological studies, a direct injection of drugs such as Glu receptor antagonists into the dorsal striatum is preferable to systemic injection, because the model assumes that the cortical Glu input to the medium spiny neurons (MSNs) in the dorsal striatum, in which neural plasticity occurs, is important for "coincidence detection" underlying duration discrimination. Pioneering work by Miller et al. (2006) revealed that the NMDA receptor antagonist MK-801 increased the peak time and variance of the response rate function in the peak-interval procedure. Unfortunately, this study did not conclusively demonstrate the importance of the Glu in the dorsal striatum, because the drug was injected systemically.

In future studies, the role(s) of two distinct types of ion channel Glu receptors (AMPA and NMDA) should be examined in two distinct phases; acquisition (memory formation for specific target durations) and performance (accuracy and precision of timing behavior following acquisition). Glu synapses predominantly act through AMPA-type receptors to produce fast synaptic excitation (i.e., normal synaptic transmission). However, striatal long-term potentiation (LTP), a representative form of neural plasticity, requires activation of NMDA-type Glu receptors (Lovinger, 2010). Therefore, the role of AMPA and NMDA receptors may differ between the acquisition and performance phases of interval timing. Not only ion channel-type receptors, but also the role of metabotropic Glu receptors 1 and 5 should be clarified during the acquisition phase, because these receptors are thought to be important for neural plasticity among MSNs (Surmeier et al., 2007; López de Maturana and Sánchez-Pernaute, 2010).

In order to examine drug effects on memory formation for target durations, we propose the adoption of a "time-shift paradigm." In this paradigm, once the discrimination for the first required target duration (e.g., 20 s) is acquired in, for example, the peak-interval procedure, the required target duration is then changed (e.g., to 40 s), and behavioral training is continued (second phase). The drug effect is examined during the formation of memory for the target duration in the second phase. This "time-shift paradigm" can dissociate the effects of the drug on the formation of the memory for the target duration from the effect on other processes (e.g., learning task rules, which may be included in the first stage of learning). Recently, Höhn et al. (2010) adopted a version of the "time-shift paradigm" in delayed classical conditioning and immunohistochemical analysis against Arc protein was used to test whether a change in the CS–US interval (resulting in a new memory formation for duration) triggers plasticity in the dorsal striatum. In a similar fashion, the "time-shift paradigm" provides a powerful tool for isolating the role of Glu in the formation of memory for target durations.

Recently, we examined the effect of intraperitoneal injection of a non-competitive NMDA receptor antagonist, MK-801, on the formation of the memory for the target duration in a "time-shift paradigm" version of peak-interval procedure. Contrary to our expectations, the peak time in MK-801 group was immediately shifted in the earliest sessions of the second phase (unpublished observation). A previous study (Miller et al., 2006) reported that systemic injection of MK-801 immediately increased the peak time, which can mask the possible effects of MK-801 on memory formation in our study. The effect of intra-dorsal striatum injection of drugs should be examined in the "time-shift paradigm" in future studies. Taken together, the role of Glu in interval timing will be clarified more precisely by considering the above three points: injection routes, receptor subtypes, and learning phases.

ACKNOWLEDGMENT

This work was supported by Grants-in-Aid for Young Scientists (B) 23730712 from the Japan Society for the Promotion of Science.

REFERENCES

Bhave, S. R., Cheng, R. K., and Meck, W. H. (2008). "The metabotropic glutamate 2/3 receptor agonist LY379268 counteracts the clock-speed enhancing effects of cocaine," in *Poster Presentation Given at the 38th Annual Meeting of the Society for Neuroscience*, Washington, DC, 877.20.

Cheng, R. K., Ali, Y. M., and Meck, W. H. (2007a). Ketamine "unlocks" the reduced clock-speed effect of cocaine following extended training: evidence for dopamine-glutamate interactions in timing and time perception. *Neurobiol. Learn. Mem.* 88, 149–159.

Cheng, R. K., Hakak, O. L., and Meck, W. H. (2007b). Habit formation and the loss of control of an internal clock: inverse relationship between the level of baseline training and the clock-speed enhancing effects

of methamphetamine. *Psychopharmacology (Berl.)* 193, 351–362.
Cheng, R. K., MacDonald, C. J., and Meck, W. H. (2006). Differential effects of cocaine and ketamine on time estimation: implications for neurobiological models of interval timing. *Pharmacol. Biochem. Behav.* 85, 114–122.
Gibbon, J., Church, R. M., and Meck, W. H. (1984). Scalar timing in memory. *Ann. N. Y. Acad. Sci.* 423, 52–77.
Höhn, S., Schafe, G. E., and Doyere, V. (2010). "Is synaptic plasticity in the dorsal striatum involved in temporal memory?" in *Poster Presentation Given at the 40th Annual Meeting of the Society for Neuroscience*, San Diego, CA, 98.14.
Killeen, P. R., and Fetterman, J. G. (1988). A behavioral theory of timing. *Psychol. Rev.* 95, 274–295.
López de Maturana, R., and Sánchez-Pernaute, R. (2010). Regulation of corticostriatal synaptic plasticity by G protein-coupled receptors. *CNS Neurol. Disord. Drug Targets* 9, 601–615.
Lovinger, D. M. (2010). Neurotransmitter roles in synaptic modulation, plasticity and learning in the dorsal striatum. *Neuropharmacology* 58, 951–961.
Machado, A. (1997). Learning the temporal dynamics of behavior. *Psychol. Rev.* 104, 241–265.
Matell, M. S., and Meck, W. H. (2000). Neuropsychological mechanisms of interval timing behavior. *Bioessays* 22, 94–103.
Matell, M. S., and Meck, W. H. (2004). Cortico-striatal circuits and interval timing: coincidence detection of oscillatory processes. *Brain Res. Cogn. Brain Res.* 21, 139–170.
Meck, W. H. (1983). Selective adjustment of the speed of internal clock and memory processes. *J. Exp. Psychol. Anim. Behav. Process.* 9, 171–201.
Meck, W. H. (1996). Neuropharmacology of timing and time perception. *Brain Res. Cogn. Brain Res.* 3, 227–242.
Meck, W. H., and Church, R. M. (1987). Cholinergic modulation of the content of temporal memory. *Behav. Neurosci.* 101, 457–464.
Miller, J. P., McAuley, J. D., and Pang, K. C. (2006). Effects of the NMDA receptor antagonist MK-801 on short-interval timing in rats. *Behav. Neurosci.* 120,162–172.
Staddon, J. E. R., and Higa, J. J. (1999). Time and memory: towards a pacemaker-free theory of interval timing. *J. Exp. Anal. Behav.* 71, 215–251.
Surmeier, D. J., Ding, J., Day, M., Wang, Z., and Shen, W. (2007). D1 and D2 dopamine-receptor modulation of striatal glutamatergic signaling in striatal medium spiny neurons. *Trends Neurosci.* 30, 228–235.

Received: 25 May 2011; accepted: 13 June 2011; published online: 22 June 2011.
*Citation: Hata T (2011) Glutamate – a forgotten target for interval timing. Front. Integr. Neurosci. **5**:27. doi: 10.3389/fnint.2011.00027*

frontiers in
INTEGRATIVE NEUROSCIENCE

ORIGINAL RESEARCH ARTICLE
published: 14 October 2011
doi: 10.3389/fnint.2011.00063

Rapid and acute effects of estrogen on time perception in male and female rats

Kristen E. Pleil[1], Sara Cordes[2], Warren H. Meck[3] and Christina L. Williams[3]*

[1] *Bowles Center for Alcohol Studies, University of North Carolina, Chapel Hill, NC, USA*
[2] *Department of Psychology, Boston College, Chestnut Hill, MA, USA*
[3] *Department of Psychology and Neuroscience, Duke University, Durham, NC, USA*

Edited by:
Agnes Gruart, University Pablo de Olavide, Spain

Reviewed by:
Fuat Balci, Princeton University, USA
Angelo Santi, Wilfrid Laurier University, Canada

***Correspondence:**
Christina L. Williams, Department of Psychology and Neuroscience, Duke University, 572 Research Drive, Box 91050, GSRB-II, Room 3018, Durham, NC 27708, USA.
e-mail: williams@psych.duke.edu

Sex differences in the rapid and acute effects of estradiol on time perception were investigated in adult male and female Sprague-Dawley rats. Because estradiol has been shown to increase striatal dopamine release, it may be able to modify time perception and timed performance by increasing the speed of an internal clock in a manner similar to indirect dopamine agonists such as amphetamine and cocaine. Two groups of females (neonatally estradiol-treated/adult ovariectomized and neonatally oil-treated/adult ovariectomized) and two groups of males (neonatally castrated and adult castrated) were trained in a 2 vs. 8-s duration bisection procedure and tested using intermediate signal durations. After obtaining oil-injected baseline psychometric functions over several days, rats were administered 5 μg of estradiol for 4 days and behaviorally evaluated 30 min following each injection. This oil–estradiol administration cycle was subsequently repeated three times following the re-establishment of baseline training. Results revealed significant sex differences in the initial baseline functions that were not modifiable by organizational hormones, with males' duration bisection functions shifted horizontally to the left of females'. Upon the first administration of estradiol, females, but not males, showed a significant, transient leftward shift in their bisection functions, indicative of an increase in clock speed. After extensive retraining in the duration bisection procedure, rats that were exposed to gonadal hormones during the first week of life showed a significant rightward shift in their bisection functions on the fourth day of estradiol administration during each cycle, suggesting a decrease in clock speed. Taken together, our results support the view that there are multiple mechanisms of estrogens' action in the striatum that modulate dopaminergic activity and are differentially organized by gonadal steroids during early brain development.

Keywords: clock speed, interval timing, duration bisection, sex differences, striatum, dopamine

INTRODUCTION

Time and space are fundamental dimensions of behavior, and competencies in these perceptual domains are rooted in neural substrates shared by many species (Gallistel, 1990; MacDonald and Meck, 2004; Buhusi and Meck, 2005; MacDonald et al., 2007). Interval timing, defined as the processing of durations in the seconds-to-minutes range, is crucial to associative learning, optimal foraging, and working memory (Gibbon et al., 1997; Meck, 2003). While considerable attention has been given to elucidating the neuroendocrine basis and underlying brain mechanisms for the different modes of spatial processing in males and females (e.g., Williams and Meck, 1991; Maguire et al., 1999; Korol, 2004), there has been comparably little work done to describe and evaluate male–female differences in temporal processing or to examine the neural and neuroendocrine underpinnings of these differences.

This gap in our understanding of interval timing is especially surprising for several reasons. A number of developmental cognitive disorders (e.g., autism, attention deficit hyperactivity disorder – ADHD, and dyslexia), and neurodegenerative disorders (e.g., Parkinson's disease – PD) have associated difficulties with aspects of temporal processing and are also known to be sexually dimorphic in both their prevalence and presentation (Teicher et al., 2000; Allman and Meck, 2011). For example, ADHD is two to ninefold more prevalent in males (Anderson et al., 1987; Arnold, 1996); however, females may be far more severely affected (Zametkin and Ernst, 1999). And, ADHD patients show impairment in time perception (Smith et al., 2002; Meck, 2005; Allman and Meck, 2011). Similarly, most reports indicate that males have a higher prevalence of PD than females (e.g., Swerdlow et al., 2001) and neurocognitive testing reveals deficits in temporal processing in these patients (Malapani et al., 1998, 2002). In both these disorders, there are underlying disturbances in dopaminergic (DA) function and targets in the basal ganglia and frontal cortex. These circuits are critically involved in temporal processing, and are organized by gonadal steroids during early development and modulated by these hormones in the adult (e.g., Xiao and Becker, 1994; Jackson et al., 2006).

It has been proposed that the neural mechanisms of interval timing are modulated by thalamo-cortico-striatal circuits, requiring DA communication between the dorsal striatum and regions

of frontal cortex (Matell and Meck, 2000, 2004; Buhusi and Meck, 2002; MacDonald and Meck, 2004; Cheng et al., 2007b; Meck et al., 2008; Coull et al., 2011; Höhn et al., 2011). Electrophysiological studies in rats (e.g., Matell et al., 2003, 2011) and neuroimaging studies in humans (e.g., Rao et al., 2001; Hinton and Meck, 2004; Meck et al., 2008; Coull et al., 2011) have provided evidence that cortico-striatal circuits are crucially involved in the control of the internal clock. Interval timing is heavily reliant on its input from DA projections from the substantia nigra pars compacta (SNpc); lesions of the striatum (Glick and Cox, 1976; Meck, 2006b) and damaged DA projections from the SNpc to the striatum, as in PD, severely impair the ability to estimate both sub-second and supra-second durations (Malapani et al., 1998, 2002; Allman and Meck, 2011). Pharmacological manipulations of striatal DA, both systemically (Meck, 1983, 1986, 1996, 2006a; Matell et al., 2004, 2006) and intrastriatally (Neil and Herndon, 1978) alter time perception. For example, DA agonists increase the perceived amount of time that has passed, such that a given interval (e.g., 10 s) is judged as being proportionally longer (20% increase = 12 s), and DA antagonists decrease clock speed such that a given interval (e.g., 10 s) is judged as being proportionally shorter (e.g., 20% decrease = 8 s – see Meck, 1996; Buhusi and Meck, 2005; Coull et al., 2011).

Numerous studies have found sex differences in striatal DA function and its response to estrogen and DA agonists (e.g., Xiao and Becker, 1994; Xiao et al., 2003; Jackson et al., 2006; Quinlan et al., 2008). Interestingly, the structure of the striatum is sexually dimorphic even during embryonic development, when the striata of females are more densely packed with DA axons and the GABAergic neurons that form striatal synapses than those of males (Ovtscharoff et al., 1992). In adulthood, females have higher basal levels of striatal DA (e.g., Walker et al., 2006) and DA transporter (DAT) mRNA (Bossé et al., 1997) than males and are more sensitive to DA agonists (Robinson et al., 1980; Beatty et al., 1982; Walker et al., 2006), even when drug concentrations in the brain are comparable (Becker et al., 1982). Gonadectomized females have higher basal levels of extracellular DA in the striatum than gonadectomized males, but there is no difference in DA uptake, suggesting possible sex differences in DA properties such as production, release, and metabolism (Castner et al., 1993). Behaviors modulated by striatal DA, such as cocaine self-administration (Hu et al., 2004; Jackson et al., 2006) and behavioral sensitization to cocaine (Hu and Becker, 2003), are greater in females than in males rats.

The underlying causes of these sex differences in striatal function may be due to organizational actions of estrogens during brain development. In both sexes, aromatase mRNA expression and activity (Küppers and Beyer, 1998), as well as both estrogen receptors (ER) α and β (Küppers and Beyer, 1999) are present throughout the striatum prenatally, and these levels increase postnatally and remain throughout adulthood (but see Shughrue et al., 1997; Zhang et al., 2002). In addition, estrogen mRNA and receptor binding sites are co-localized in the female rat striatum at postnatal day 10–12 (Toran-Allerand et al., 1992). Estrogens not only increase the expression of DA receptors and their sensitivity in the striatum (Maus et al., 1990; Ferretti et al., 1992), but also influence the differentiation into (Agarti et al., 1997) and synaptogenesis of (Reisert et al., 1987; Beyer and Karolczak, 2000) dopaminergic neurons that project from the SNpc to the striatum, and the maturation of striatal GABAergic medium spiny neurons (MSNs; Stroppolo et al., 2004). Anti-estrogens administered to the neonatal male decrease adult striatal DA activity that is accompanied by decreased male sexual behavior (Gerardin et al., 2006). Taken together, these data suggest that like many other brain areas, estrogens may masculinize the striatum after its conversion from testosterone, causing the male striatum to function differently than that of the female.

In the adult, estrogens act as modulators of DA activity in the striatum through several mechanisms (Becker, 1999). Administration of estrogens directly into the striatum of adult ovariectomized rats facilitates paced mating behavior and other striatally mediated behaviors (e.g., Xiao and Becker, 1997). Ovariectomy decreases striatal DA release (Ohtani et al., 2001), D2 receptor binding (Levesque et al., 1992), and DAT activity (Le Saux and DiPaolo, 2006). While there is evidence that chronic replacement with estradiol via pulsatile or constant administration for two or more weeks restores these functions and associated behaviors, other research suggests that estrogens are only able to have these effects when administered in small, pulsatile doses over a period of several days (Becker, 1990a; Bazzett and Becker, 1994). A number of studies using DA agonists have shown that there is a rapid mechanism by which estrogens interact with striatal DA within 30 min of administration (Becker, 1990b; Xiao and Becker, 1994, 1998; Balthazart and Ball, 2006), and that this can be facilitated by priming with a longer-term physiological regimen of pulsatile estradiol (Becker and Rudick, 1999). For example, 30 min after a small dose of estradiol is given, the administration of amphetamine (AMPH) produces greater DA release in the striatum and rotational behavior than AMPH alone in OVX females but not castrated males (Castner et al., 1993); in addition, priming for 3 days with estradiol enhances this response to estradiol plus AMPH (Becker and Rudick, 1999). The immediate influence of estrogens on DA release are unlikely to be mediated by classical intracellular ER, but by membrane receptors that allow estrogens to rapidly alter membrane excitability. The enhanced rapid effect after several days of priming suggests that a classical estrogen receptor-mediated mechanism interacts with this rapid membrane mechanism to maximize the response to estrogen.

These data suggest that the organization and function of the striatal DA neurons that regulate interval timing may be influenced by estrogens through several different mechanisms. Therefore, adult males and females without circulating hormones may have a differentially structured and functioning striatal DA system, such that the perception of time is fundamentally different between the sexes. As a result of this sexually dimorphic organization, the clock speed of males and females may be differently altered by estradiol administration both rapidly and after priming.

Very little work has directly examined sex differences in time perception or timed performance (see MacDougall, 1904; Cheng et al., 2008a). The human literature suggests that overall, females overestimate time by approximately 10% while males do not, and females have greater variability in their time judgments (Yerkes and Urban, 1906; Eisler and Eisler, 1992; Hancock et al., 1994; Block et al., 2000; but also see Kellaris and Mantel, 1994). Sex

differences may only be found at very short durations (Szelag et al., 2004) and only males may be able to discriminate between durations of less than 1 s (Rammsayer and Lustnauer, 1989; Lotze et al., 1999). However, relatively little is known about timing in the supra-seconds range.

Two recent studies have examined the role of estrogen on time perception in females. Ovariectomized rats given chronic daily injections of estradiol benzoate for 2 weeks showed a decrease in discrimination accuracy on a previously acquired task in which they had to discriminate between 2 and 8 s (Ross and Santi, 2000). This effect was present throughout both weeks of estrogen treatment and the week following, but was greatest during the second week of estrogen exposure. However, following these 2 weeks, estrogen-treated and control rats did not differ in their judgments of time intervals. While this study did not find an alteration in time perception, it is possible that this was due to the estrogen regimen that was long-term and occurred prior to time perception testing.

In contrast, ovariectomized female rats trained to lever press for food reward at 7 and 21 s following the onset of the "to-be-timed" signal underestimated both intervals in a proportional manner after receiving a single injection of estradiol 30 min prior to testing (Sandstrom, 2007). This time production study suggests that estradiol increases clock speed, possibly via activation of the nigrostriatal DA system, and is evidence for a rapid estrogen mechanism in the striatum that acutely alters timed performance in a manner similar to AMPH and other DA agonists (Meck, 1996; Coull et al., 2011). To date, no study has examined sex differences in time perception or their possible neuroendocrine basis. And, there has been no attempt to examine the effects of estradiol administered acutely with and without several days of pulsatile priming.

The current study aims to determine whether or not there are sex differences in time perception without circulating hormones, and if so, whether these are caused by differential brain organization due to perinatal estrogen exposure, as are many other brain structures. We will also address both the rapid (estrogen injection given 30 min prior to testing) and priming (three consecutive days of estrogen plus an estrogen injection given 30 min prior to testing) activational effects of estrogen administration on time perception in male and female rats, as others have studied striatal DA and behaviors modulated by it (Becker and Rudick, 1999). These experiments will shed light on the extent of the effects of estrogen on temporal processing and determine possible sex differences in this response to estrogen.

Although a number of different procedures can be used to access time perception in rodents (Paule et al., 1999), there are several limiting factors that must be considered in the current experiment. Because this is the first study to directly compare time perception in male and female rats, it requires a procedure in which factors such as body size, motivation, and general motor activity do not greatly affect results. Consequently, a duration bisection procedure in which rats make a choice response following the presentation of the "to-be-timed" signal allows us to measure time perception in a way that is not influenced by other performance factors related to sex differences and hormonal status (Church and Deluty, 1977; Meck, 1983; Paule et al., 1999).

MATERIALS AND METHODS

ANIMALS

Subjects were 38 rats, the offspring of 14 timed-pregnant CD Sprague-Dawley rats purchased from Charles River Laboratories (Kingston, NY, USA). Pregnant dams arrived in our colony at Duke University on their ninth day of gestation and were singly housed in individually ventilated transparent shoebox cages with corn cob bedding and *ad libitum* access to water and a phytoestrogen-free diet (rodent diet AIN-76A with choline chloride substituted for choline bitartrate, purchased from Dyets, American Institute of Nutrition, ICN, Nutritional Biochemical, Cleveland, OH, USA). The temperature-controlled colony room was maintained on a 12:12-h light:dark cycle with lights on at 7 a.m. daily. Upon birth, pups from all 14 litters were sexed and randomly assigned to foster mothers, and litters were culled to approximately 10 pups (5 females, 5 males) per dam. Pups were assigned to hormone treatment conditions within 12 h of birth: (a) neonatally castrated males (NCM); (b) adult castrated males (ACM); (c) neonatally estrogen-treated females (NEF); and (d) adult ovariectomized females (AOF).

After weaning on postnatal day 25, rats were housed in like-treatment groups of 4–5 for approximately 1 week, and then in pairs for the remainder of the experiment, with the same food and living conditions described for dams above. At approximately 2 months of age (postnatal day 57–58), all gonadally intact subjects were gonadectomized (subjects in all groups except NCM). Rats were approximately 4 months of age at the beginning of training. Two weeks before magazine and lever training, rats were weighed and food restricted to 85–90% of their *ad libitum* weight and maintained at this weight throughout the experiment to ensure responding for the food rewards. All surgeries and experiments were conducted in accordance with standard procedures approved by the Institutional Animal Care and Use Committee of Duke University.

NEONATAL HORMONE MANIPULATIONS

All male rats were anesthetized approximately 12 h after birth by cryoanesthesia for 3–5 min. NCMs were castrated and ACMs received sham operations, which were identical to castration in every way except for surgical removal of the testicles. Wounds were sealed with surgical glue, and pups were cleaned with alcohol and warmed before being returned to their litters. All females received subcutaneous injections of either 10 μg estradiol benzoate (Steraloids, Inc., Newport, RI, USA) dissolved in 0.05 mL sesame oil (Sigma, St. Louis, MO, USA; NEF) or 0.05 mL of the oil vehicle alone (AOF) at the nape of the neck on postnatal days 0, 2, and 4. These neonatal hormone manipulations (male castration and administration of E to females) have previously been shown to sex-reverse brain regions such as the hippocampus (Williams et al., 1990) and sexually dimorphic nucleus of the hypothalamus (Döhler et al., 1984). Therefore, there were four treatment groups total: Males (1) and females (2) in which we did not disrupt their normal exposure to gonadal hormones developmentally and males (3) in which we prevented exposure to gonadal testosterone postnatally and females (4) in which we exposed them to high levels of gonadal hormones postnatally. These groups allowed us to determine the contributions of postnatal organizational hormones

and other factors (prenatal hormones and genetic factors) to be examined.

ADULT HORMONE MANIPULATIONS

At 2 months of age all rats were anesthetized for approximately 30 min with a cocktail of 80 mg/kg ketamine plus 10 mg/kg xylazine. ACMs underwent castrations via a medial incision in the scrotum, where testicles were exposed, tied off removed, and cauterized. The site of incision was sutured and antibiotic cream was applied. NCMs underwent sham surgeries identical to ACMs except that the testes were not tied off or removed. All females (AOF and NEF) were ovariectomized via bilateral dorsal incisions through the skin and muscle walls of the abdomen. The ovary and ovarian fat on each side of the body were exposed, tied off, and surgically removed with a scalpel. The site of removal was cauterized and carefully placed back into the abdominal cavity. The muscle wall was sutured, the skin was sutured, and antibiotic cream was applied to the wound site. These adult gonadectomies were performed in order to remove the influences of circulating gonadal hormones.

All rats received the same recovery procedures. Buprenorphine (0.5 mg/kg, i.p.) was administered at the end of all surgeries and again 12 h later as analgesic. Rats were kept warm on heating pads until they woke up and then returned to their home cage. Powdered food was offered in bowls on the cage floor for several days until rats were seen eating from the overhead food bin. Rats that recovered without complications from surgery were included in the subject pool for the experiment: NCM ($n = 8$); ACM ($n = 10$); NEF ($n = 10$); AOF ($n = 10$).

APPARATUS

All experimental data were collected in 10 standard Plexiglas and aluminum lever boxes designed for conditioning rats (Coulbourn Instruments, Allentown, PA, USA). A pellet dispenser delivered grain-based 45 mg food pellets (Research Diets, Inc., New Brunswick, NJ, USA) to a food cup located 10 cm above the floor on the front wall. Two stainless-steel retractable response levers (4 cm in width) located 2 cm from each sidewall were horizontally placed 2.5 cm above the grid floor. A 2.5-cm Sonalert calibrated to approximately 93 dB above background, was mounted above the food cup approximately 4 cm from the ceiling of the chamber was used to present auditory signals varying in duration. Each lever box was housed inside a sealed wooden sound- and light-attenuating chamber with an eyepiece viewer for observation, and was equipped with a 6-W white house light and a 10-cm ventilation fan. A Windows XP (Microsoft, Redmond, WA, USA) based computer system running MED-PC Version IV Research Control and Data Acquisition System software (Med Associates, St. Albans, VT, USA) attached to an electronic interface was used to control the experimental equipment and record the data.

BEHAVIORAL PROCEDURES

Magazine and lever training (10 sessions)

To prevent time of day or lever box related variation, each rat's daily experimental session occurred in the same lever box at approximately the same time each day, 7 days a week. In order to prevent distractions caused by odors from the opposite sex, especially during sessions following estradiol administration, lever boxes were assigned by genetic sex. Females (NEF and AOF) were randomly assigned to lever boxes 1–5, and males (ACM and NCM) to lever boxes 6–10. Each of four daily sessions contained 9–10 rats, beginning at approximately 09:00, 11:00, 13:00, and 15:00, with all treatment groups represented in each session.

To train the rats to press both levers, rats received 1-h sessions of combined magazine and lever training. During each 1-h session, one food pellet was dispensed automatically once each minute and in addition, every lever press produced a pellet. To signal the start of a session, the house light turned on and both levers were retracted. Then, one lever was extended into the chamber until 10 presses were made (producing 10 food pellets), at which time this lever retracted and the other lever was extended until 10 reinforced presses were made. The lever that was extended first (left or right) was counterbalanced within each treatment group. This alternation continued for the hour, at which time the house light turned off and both levers were extended, signifying the end of the session. When all rats lever pressed at least 100 times within the hour-long session, they were transitioned to duration-discrimination training.

Duration bisection procedure: two-signal training

Rats were trained in 1-h daily sessions of duration-discrimination training in which a tone was presented for a given duration (e.g., 2 or 8 s) followed by the extension of both levers. Half of the rats in each group were trained to press the left lever ("short" response) following a 2-s tone and the right lever ("long" response) following an 8-s tone. The remaining rats had this duration-lever association reversed. Each of the signal durations (2 and 8 s) was randomly presented with a probability of 0.5 on each trial. The tone was presented for the selected duration, and then the levers were extended into the lever box. A response on the correct lever caused the levers to retract and a food pellet to be delivered, and a press on the incorrect lever caused the levers to retract without reinforcement. If no response was made within 10 s, the levers retracted and the trial was considered a non-response. Each time the levers retracted, signifying the end of a trial, a new, randomly selected inter-trial interval (ITI) of 5 s plus an exponentially distributed duration with a mean of 35 s began.

At the end of the ITI, another signal duration was randomly selected for presentation on the next trial. A record was kept of the subject, signal duration (2 or 8 s), lever pressed (left or right), and the latency to respond for each trial. Training occurred for 14 days, by the end of which all rats maintained a high-level of discrimination between the two anchor durations (>85% correct responses) for two consecutive days.

Duration bisection procedure: six-signal training

Phase 1. The conditions of two-signal training were maintained except that each of the two anchor durations (2 and 8 s) were presented with a probability of 0.25 on each trial, and on the remaining trials, one of four probe signals of intermediate duration (3, 4, 5, and 6 s) was presented, each with equal probability. Responses on these probe trials always caused the levers to retract without reinforcement. Again, the subject, signal duration, lever pressed, and response latency were recorded for each trial.

The conditions of six-signal training were maintained except that rats received a subcutaneous injection of 0.1 mL sesame oil vehicle (Sigma, St. Louis, MO, USA) in the nape of the neck 30 min prior to being placed in the lever boxes for the start of the session each day for 2 days. Behavior of each rat on the second day was used as a baseline for comparison with task performance following estrogen administration.

Duration bisection: estrogen cycle 1

Baseline procedures continued, however rats received subcutaneous injections of 5 μg 17β-estradiol (Steraloids, Inc., Newport, RI, USA) dissolved in 0.1 mL sesame oil in the nape of the neck 30 min prior to being placed in the lever boxes to start the daily session for 4 days. This 4-day estradiol regimen has been shown to produce blood estradiol levels in the range of what is naturally produced during an estrus cycle and to increase DA activity in the striatum (Becker, 1999). Following these 4-days of estradiol administration, a 3-day "washout" period ensued, in which only the sesame oil vehicle was injected before behavioral testing.

Duration bisection: seven-signal training

Phase 2. Immediately following Phase 1, rats received vehicle injections and performed 14 daily sessions to gain experience with the duration bisection procedure. Beginning with these sessions, five intermediate signal durations were presented instead of four – 2.6, 3.2, 4, 5, and 6.4 s, which are spaced at equal logarithmic intervals between 2 and 8 s – so that a more accurate bisection function could be obtained in the manner of Maricq et al. (1981) and Meck (1983, 1991). Also, the probability of a training trial (reinforced 2 or 8 s tone) was reduced to 0.3 (0.15 probability of a 2-s trial, and 0.15 probability of an 8-s trial).

Duration bisection: estrogen cycles 2–4

After the 14 sessions of seven-signal training, three consecutive cycles of 1 day of vehicle administration followed by 4 days of estradiol administration and 9 days of vehicle washout on the seven-signal procedure ensued. For these three cycles, estrogen doses (5 μg E2/0.1 mL oil) were scaled to match relative average weights of each group: both genetic female groups (AOF and NEF) still received 1 mL of the cocktail, NCMs received 1.2 mL per dose, and ACMs received 1.4 mL per dose.

DATA ANALYSIS

The mean proportion "long" response for each signal duration was used to construct a psychometric function for each rat on each day of baseline and estrogen testing. All non-responses and responses with latencies over 4 s were excluded from these calculations because prior research has demonstrated that responses with long latencies are not well controlled by signal duration (e.g., Maricq et al., 1981; Maricq and Church, 1983). Days on which a rat performed poorer than 70% correct on both anchor durations were excluded and replaced with mean values of their respective groups for that session because their behavior was not reliable enough to be compared to their behavior on other sessions. This occurred on less than 10% of the sessions.

Each rat's data were fit to a three-parameter sigmoidal function in MATLAB (Mathworks – Natick, MA, USA) using a maximum likelihood method. The point of subjective equality (PSE), a measure of timing accuracy, was calculated for each subject by using this sigmoidal function to determine the signal duration that produced a "long" response 50% of the time. The difference limen (DL), a measure of variability, was calculated from the sigmoidal function by subtracting the signal duration at which 25% of responses were "long" responses from the signal duration at which 75% were "long" responses, and then dividing this value by 2. The Weber fraction (WF), a measure of relative variability in responding, was also obtained by dividing the DL by the PSE. ANOVAs and *t*-tests were used to determine significant differences in behavior between sessions using the PSE, DL, and WF of individual participants. The alpha level was set at $p < 0.05$ and all statistics were calculated using Statistica (StatSoft – Tulsa, OK, USA). In addition to the measures obtained from the sigmoidal functions, raw data points [% "long" responses at each intermediate signal duration – 3, 4, 5, 6, and 8 s (Phase 1) or 2.6, 3.2, 4, 5, and 6.4 s (Phase 2)] were compared statistically to confirm the fitted PSE results. All behavioral analyses for Phase 2 were conducted using sigmoidal fits obtained by combining each rat's raw data over cycles 2, 3, and 4 because there were no differences in experimental manipulation or timing behavior across these three cycles. Analyses for estrogen effects over 4 days always included the baseline (BL), the first day of estrogen (E1), and the fourth and final day of estrogen administration (E4) because rapid estrogen effects were hypothesized to occur on E1 and acute effects on E4 within the context of the current estrogen administration paradigm (Becker and Rudick, 1999).

RESULTS

PHASE 1: BASELINE DIFFERENCES

ANOVAs were conducted in order to evaluate the between-subjects factor of treatment group (AOF vs. NEF vs. ACM vs. NCM) on the baseline PSEs (day before estrogen administration). This test revealed a non-significant effect of treatment group, $F(3,34) = 2.57$, $p > 0.05$. In contrast, a (2×2) ANOVA evaluating the between-subjects factors of genetic sex and hormonal sex on the baseline PSEs revealed a main effect of genetic sex, $F(1,34) = 5.84$, $p < 0.05$, but no other reliable effects, $ps > 0.05$. A *post hoc* *t*-test showed a significant difference of baseline PSEs between genetic males and females, $t(36) = 2.32$, $p < 0.05$, revealing the mean PSE for genetic females (PSE $= 4.31 \pm 0.13$ s) was significantly greater than the PSE for genetic males (PSE $= 3.86 \pm 0.14$ s). Despite our hormonal manipulations, our results did not reveal any reliable PSE differences between hormonal males (NEF and ACM) and hormonal females (NCM and AOF) at baseline. The baseline duration bisection functions for all rats divided by (a) treatment group (acute estradiol vs. oil), (b) genetic sex (male vs. female), and (c) hormonal sex (exposure to gonadal hormones or estradiol perinatally vs. no exposure to postnatal gonadal hormones) are shown in **Figure 1**.

To follow up these analyses of the PSE's obtained from the sigmoidal fits of the individual psychometric functions; analyses were conducted on the raw data (probability of a rat pressing the "long" lever as a function of each intermediate signal duration). Using the raw data, a $(2 \times 2 \times 3 \times 4)$ repeated measures ANOVA testing the between-subjects factors of hormonal sex and genetic sex and the

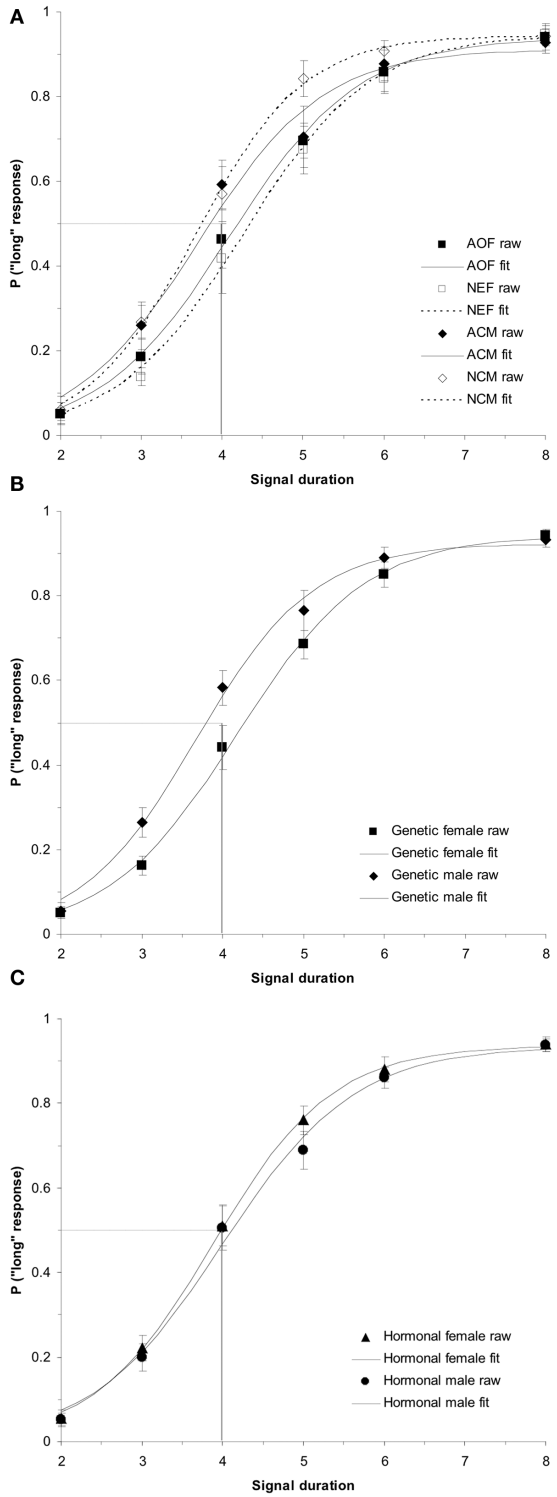

FIGURE 1 | Phase 1 duration baseline bisection function raw data and sigmoidal fits as a function of (A) treatment group (AOF, NEF, ACM, NCM); (B) genetic sex (female = AOF + NEF, male = ACM + NCM); and (C) hormonal sex (female = AOF + NCM, male = ACM + NEF), revealing a non-significant effect of treatment group ($p > 0.05$), a significant effect of genetic sex ($p < 0.05$), and a non-significant effect of hormonal sex ($p > 0.05$). Probability of a "long" response is plotted as a function of signal duration(s).

within-subjects factors of test day (BL, E1, E4) and intermediate signal duration (3, 4, 5, and 6 s) on the probability of pressing the "long" lever was conducted. It confirmed the main effect of genetic sex, $F(1,34) = 5.50$, $p < 0.05$, and no other significant effects ($ps > 0.05$). The main effect revealed that the females were less likely to press the "long" lever (genetic female $= 0.54 \pm 0.03$) than the males (genetic male $= 0.63 \pm 0.03$). Overall, these separate analyses show that genetic male PSEs and overall probability of pressing the "long" lever are significantly greater than those of genetic females, suggesting that the memory representations of the 2 and 8-s anchor duration for genetic males' are proportionally shorter than the memory representations of the same anchor durations for females' (Meck, 1983, 1991; Cheng et al., 2008b, 2011).

ACUTE ESTROGEN EFFECTS

A ($2 \times 2 \times 3$) repeated measures ANOVA testing the between-subjects variables of hormonal sex and genetic sex and the within-subjects variable test day (BL, E1, E4) on the PSEs showed a significant interaction between genetic sex and test day, $F(2,68) = 3.47$, $p < 0.05$, and no other significant main effects or interactions ($ps > 0.05$).

This significant interaction between genetic sex and test day was broken down into two one-way repeated measures ANOVAs for each genetic sex. First, the one-way ANOVA testing the within-subjects variable of test day (BL, E1, E4) on PSE for the genetic females revealed a significant effect of test day, $F(2,34) = 3.96$, $p < 0.05$ and no other significant main effects or interactions. Follow up t-tests for genetic females revealed significant differences between PSEs for BL (mean $= 4.31 \pm 0.13$) and E1 [mean $= 3.96 \pm 0.14$; $t(19) = 2.43$, $p < 0.05$], as well as E1 vs. E4 [mean $= 4.38 \pm 0.15$; $t(19) = 2.30$, $p < 0.05$], but not between BL and E4 [$t(19) = 0.45$, $p > 0.05$]. These results indicate that on the first day of estrogen administration, the genetic females revealed a leftward shift in the PSE (i.e., increase in clock speed), yet the PSE shifted back to baseline levels by the fourth day of estrogen administration. Secondly, the one-way ANOVA for genetic males between BL (mean $= 3.87 \pm 0.14$), E1 (mean $= 4.12 \pm 0.15$), and E4 (mean $= 4.09 \pm 0.15$) showed no reliable effect of day, $p > 0.05$, suggesting that performance did not vary significantly from day to day for these subjects. Bisection functions for the baseline and the first and fourth days of estrogen administration for (a) genetic females and (b) genetic males are shown in **Figure 2**. The mean PSEs as a function of genetic sex for the baseline day and each of the 4-days of estrogen administration are illustrated in **Figure 3A**.

When a similar analysis was performed on the raw data, a ($2 \times 2 \times 3 \times 4$) repeated measures ANOVA testing the between-subjects variables hormonal sex and genetic sex and the within-subjects factors of test day (BL, E1, E4) and intermediate signal duration (3, 4, 5, and 6 s) showed a significant day × genetic sex interaction, $F(2,68) = 3.00$, $p < 0.05$, but no other significant main effects or interactions, $ps > 0.05$.

In order to decompose this interaction, an ANOVA for genetic females testing the within-subjects factors of test day (BL, E1, E4) and intermediate signal duration (3, 4, 5, and 6 s) on the raw data (probability of a "long" response for each intermediate signal duration) showed a significant effect of day, $F(2,34) = 3.60$,

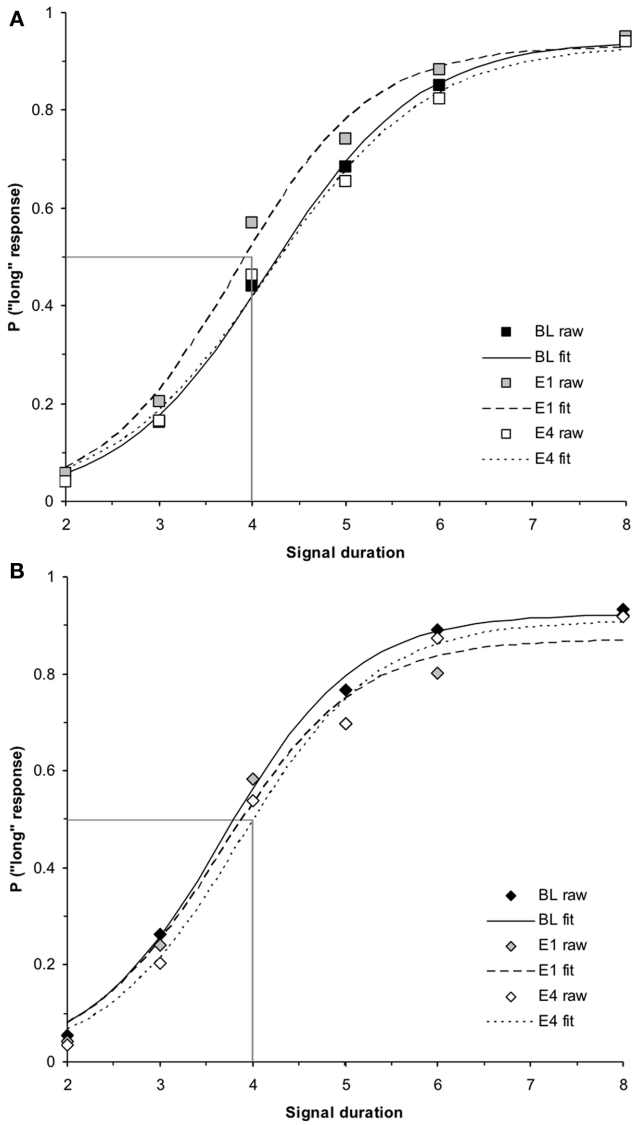

FIGURE 2 | Phase 1 duration bisection functions during baseline, E1, and E4 for (A) genetic females and (B) genetic males, revealing a significant transient leftward shift in females on E1 that returns to baseline by E4 ($p < 0.05$), and no effect in males. Probability of a "long" response is plotted as a function of signal duration(s).

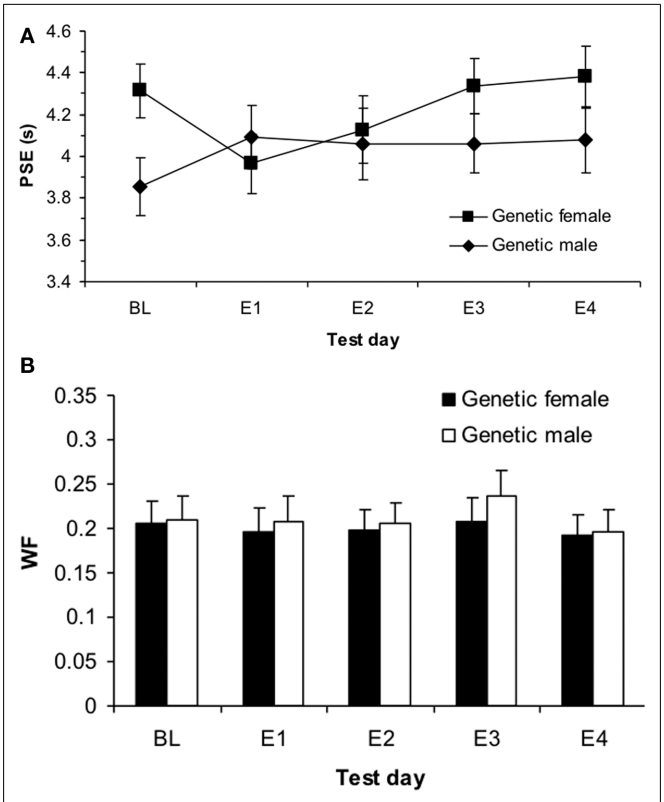

FIGURE 3 | Phase 1 sigmoidal function measures of (A) point of subjective equality (PSE) and (B) Weber fractions (WF) for genetic males and females showing a significant effect of estrogen on E1 for females in PSE ($p < 0.05$) and no effects in WF ($p > 0.05$).

$p < 0.05$ and no other significant main effects or interactions. Follow up t-tests showed significant differences between the overall proportion of "long" responses on BL (mean $= 0.54 \pm 0.03$) and E1 (mean $= 0.60 \pm 0.03$), $t(19) = 2.39$, $p < 0.05$, as well as E1 and E4 (mean $= 0.53 \pm 0.03$), $t(19) = 2.25$, $p < 0.05$, but not BL and E4, $t(19) = 0.30$, $p > 0.05$, reflecting the same pattern of results as found with the PSEs. A similar ANOVA for genetic males revealed no significant main effects or interactions, suggesting that performance on BL (mean $= 0.63 \pm 0.03$), E1 (mean $= 0.58 \pm 0.04$), and E4 (mean $= 0.58 \pm 0.03$), did not differ for the males $p > 0.05$. Taken together, these results show that genetic females were overall more likely to judge time intervals as "long" 30 min following a single injection of estradiol (increase in clock speed), and this effect returned to baseline by the fourth day of estrogen administration. Genetic males showed no changes in time perception at any time during their first 4-day exposure to estrogen. Interestingly, we again found no significant effects of hormonal sex, suggesting that genetic sex played the most important role in whether acute estrogen administration would affect time perception in Phase 1.

Difference limen and Weber fraction

In addition to analyses of the PSE, we were also interested in whether there were sex differences in variability in responding during baseline and after estradiol administration, as measured by the DL and WF. A (2×2) ANOVA testing the between-subjects variables of hormonal sex and genetic sex on the baseline DL revealed no significant effects or interactions, ps > 0.05. A similar ANOVA for the WF also found no significant differences, ps > 0.05.

A ($2 \times 2 \times 3$) repeated measures ANOVA with between-subjects variables of hormonal sex and genetic sex and the within-subjects variable test day (B, E1, E4) on the DL showed no significant effects, ps > 0.05, and a similar ANOVA for the WF also found no significant effects, ps > 0.05. These results suggest that there were no reliable differences in variability that could account for the initial baseline differences in time perception between genetic males and females, and also that estrogen administration did not cause any changes in variability. The mean WFs as a function of genetic sex for the baseline day and each of the 4-days of estrogen

Table 1 | Phase 1: duration bisection timing measures.

Genetic sex	Day	PSE	DL	WF	% "long"
Female	BL	4.31 ± 0.13	0.90 ± 0.11	0.21 ± 0.03	0.54 ± 0.03
	E1	3.96 ± 0.14	0.78 ± 0.11	0.20 ± 0.03	0.60 ± 0.03
	E2	4.13 ± 0.16	0.82 ± 0.11	0.20 ± 0.02	0.57 ± 0.04
	E3	4.34 ± 0.13	0.91 ± 0.13	0.21 ± 0.03	0.53 ± 0.02
	E4	4.38 ± 0.15	0.87 ± 0.11	0.19 ± 0.02	0.53 ± 0.03
Male	BL	3.86 ± 0.14	0.84 ± 0.12	0.21 ± 0.03	0.63 ± 0.03
	E1	4.10 ± 0.15	0.89 ± 0.12	0.21 ± 0.03	0.58 ± 0.03
	E2	4.06 ± 0.17	0.88 ± 0.11	0.21 ± 0.02	0.58 ± 0.04
	E3	4.06 ± 0.14	1.03 ± 0.14	0.24 ± 0.03	0.57 ± 0.03
	E4	4.08 ± 0.16	0.85 ± 0.12	0.20 ± 0.02	0.58 ± 0.03

PSE, point of subjective equality; DL, difference limen; WF, Weber fraction; BL, baseline day; E, estrogen day.

administration is shown in **Figure 3B**. **Table 1** displays each of the bisection measures (e.g., PSE, DL, and WF) as a function of genetic sex for Phase 1.

PHASE 2

Baseline effects

ANOVAs comparing group baseline PSEs during Phase 2 of the experiment found no significant treatment effects, ps > 0.05. In addition, we conducted a (2×2) ANOVA on baseline PSEs with between-subjects variables of hormonal sex and genetic sex, which indicated no significant main effects or interactions for PSE, ps > 0.05. This suggests that all rats had similar PSEs and therefore had similar baseline time judgment in this procedure during Phase 2 of training. The baseline duration bisection functions for all rats divided by (a) treatment group, (b) genetic sex, and (c) hormonal sex are shown in **Figure 4**.

Long-term estrogen effects

A $(2 \times 2 \times 3)$ repeated measures ANOVA with between-subjects variables of hormonal sex and genetic sex and the within-subjects variable of test day (BL, E1, E4) on the PSEs revealed a significant interaction between hormonal sex and test day, $F(2,68) = 3.312$, $p < 0.05$, but no other significant main effects or interactions, ps > 0.05. In order to evaluate this interaction, we conducted two follow up ANOVAs for each hormonal sex. An ANOVA on hormonal females testing the effect of test day (B, mean $= 4.19 \pm 0.12$; E1, mean $= 4.23 \pm 0.13$; E4, mean $= 4.17 \pm 0.13$) on the PSE showed a non-significant effect of test day, $p > 0.05$. In contrast, a similar ANOVA for hormonal males showed a significant effect of test day, $F(2,38) = 5.39$, $p < 0.01$. *Post hoc* t-tests on the hormonal males revealed significant differences in PSE between BL (mean $= 4.12 \pm 0.11$) and E4 (mean $= 4.45 \pm 0.15$), $t(19) = -2.59$, $p < 0.05$, as well as E1 (mean $= 4.23 \pm 0.13$) and E4, $t(19) = -3.21$, $p < 0.01$, but no significant difference between B and E1, $p > 0.05$. Interestingly, this acute estrogen effect was modifiable by organizational hormones, as hormonal sex determined whether the estradiol affected time perception.

A $(2 \times 2 \times 3 \times 5)$ repeated measures ANOVA with between-subjects variables of hormonal sex and genetic sex and the within-

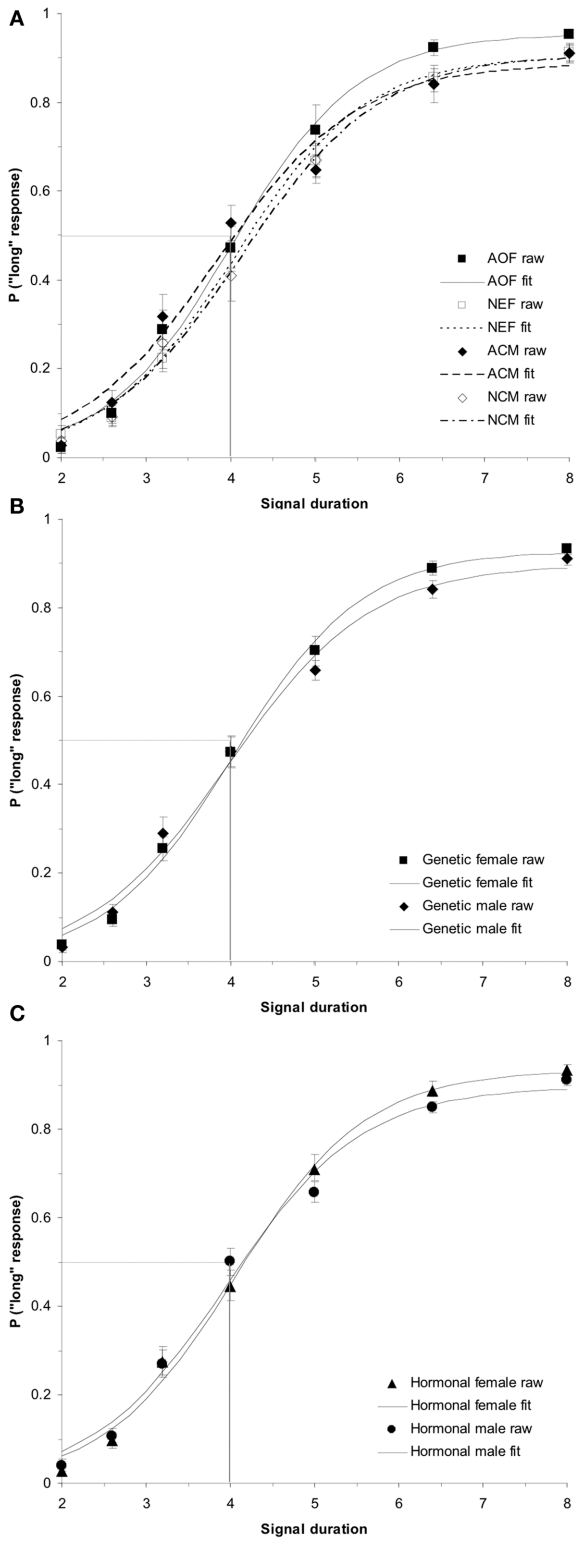

FIGURE 4 | Phase 2 baseline duration bisection functions. No significant effects were observed in the raw data or sigmoidal fits between **(A)** treatment groups ($p > 0.05$); **(B)** genetic sex ($p > 0.05$); or **(C)** hormonal sex ($p > 0.05$). Probability of a "long" response is plotted as a function of signal duration(s).

subjects variables test day (B, E1, E4) and intermediate signal duration (2.6, 3.2, 4, 5, and 6.4 s) on the raw data (probability of a "long" response) revealed a significant hormonal sex × test day interaction, $F(2,68) = 3.15$, $p < 0.05$, but no other reliable main effects or interactions, ps > 0.05.

The follow up ANOVA for hormonal females testing the within-subjects factors of test day (B, mean $= 0.48 \pm 0.02$; E1, mean $= 0.48 \pm 0.02$; E4, mean $= 0.49 \pm 0.02$) and intermediate signal duration (2.6, 3.2, 4, 5, and 6.4 s) showed no significant effects, $p > 0.05$. A similar ANOVA for hormonal males showed a significant main effect of day, $F(2,38) = 6.09$, $p < 0.01$, but no other reliable effects, ps > 0.05. *Post hoc* t-tests revealed significant differences in the probability of pressing the "long" lever between B (mean $= 0.48 \pm 0.02$) and E4 (mean $= 0.43 \pm 0.02$), $t(19) = 2.60$, $p < 0.05$, as well as E1 (mean $= 0.47 \pm 0.02$) and E4, $t(19) = 4.18$, $p < 0.01$, but not B and E1, $p > 0.05$. Taken together, these results reveal that after extensive experience with the seven-signal bisection procedure, hormonal males show a rightward shift in their bisection functions (increase in PSE, slowing down of the clock) by the fourth day of estrogen administration, while hormonal females show no changes in their time perception with this estrogen administration protocol.

Washout effect

While a $(2 \times 2 \times 2)$ repeated measures ANOVA for PSE using the between-subjects factors of hormonal sex and genetic sex and the within-subjects factors of day of testing (E4, WO) did not find a significant hormonal sex × test day interaction ($p > 0.05$), a $(2 \times 2 \times 2 \times 5)$ ANOVA conducted on the probability of pressing the "long" lever for the five intermediate signal durations revealed a significant hormonal sex × test day interaction, $F(1,34) = 5.19$, $p < 0.05$, but no other significant main effects or interactions, ps > 0.05. A *post hoc* t-test between the overall proportion of "long" responses for intermediate signal durations for hormonal males between E4 (mean $= 0.43 \pm 0.02$) and WO (mean $= 0.48 \pm 0.02$) was significant, $t(19) = -2.82$, $p < 0.05$. A similar t-test for hormonal females between E4 (mean $= 0.49 \pm 0.02$) and WO (mean $= 0.47 \pm 0.02$) showed no reliable effect, $p > 0.05$. These results show that the effect of 4 days of estrogen administration on hormonal males' time perception as revealed by a rightward shift in their bisection functions, is reversed once estrogen is no longer administered – duration bisection functions shift back to baseline; hormonal females maintain stable bisection functions throughout baseline, estrogen, and washout days. The duration bisection functions for BL, E1, E4, and WO for (a) hormonal females and (b) hormonal males are shown in **Figure 5**. The mean PSEs and WFs for hormonal females and males during baseline, 4 days of estrogen administration, and the washout day after estrogen administration are shown in **Figures 6A,B**, respectively.

Difference limen and Weber fraction

A (2×2) ANOVA for baseline DLs using the between-subjects factors of hormonal sex and genetic sex revealed no significant main effects or interactions, ps > 0.05; a similar ANOVA for baseline WFs also showed no significant main effects or interactions, ps > 0.05. A $(2 \times 2 \times 3)$ mixed-design ANOVA for the DL with the between-subjects factors of hormonal sex and genetic sex and within-subjects factor or test day (B, E1, E4) revealed a significant main effect of day, $F(3,102) = 5.07$, $p < 0.01$, but no other significant main effects or interactions, ps > 0.05. A similar ANOVA for the WF also found a significant effect of day, $F(3,102) = 4.03$, $p < 0.05$, but no other significant effects, ps > 0.05. *Post hoc* t-tests showed significant differences in the WF between B (mean $= 0.21 \pm 0.01$) and E4 (mean $= 0.24 \pm 0.01$), $t(37) = -2.32$, $p < 0.05$, as well as E1 (mean $= 0.22 \pm 0.01$) and E4, $t(37) = -2.182$, $p < 0.05$, but not B and E1, $p > 0.05$. A $(2 \times 2 \times 2)$ ANOVA for the DL using the between-subjects

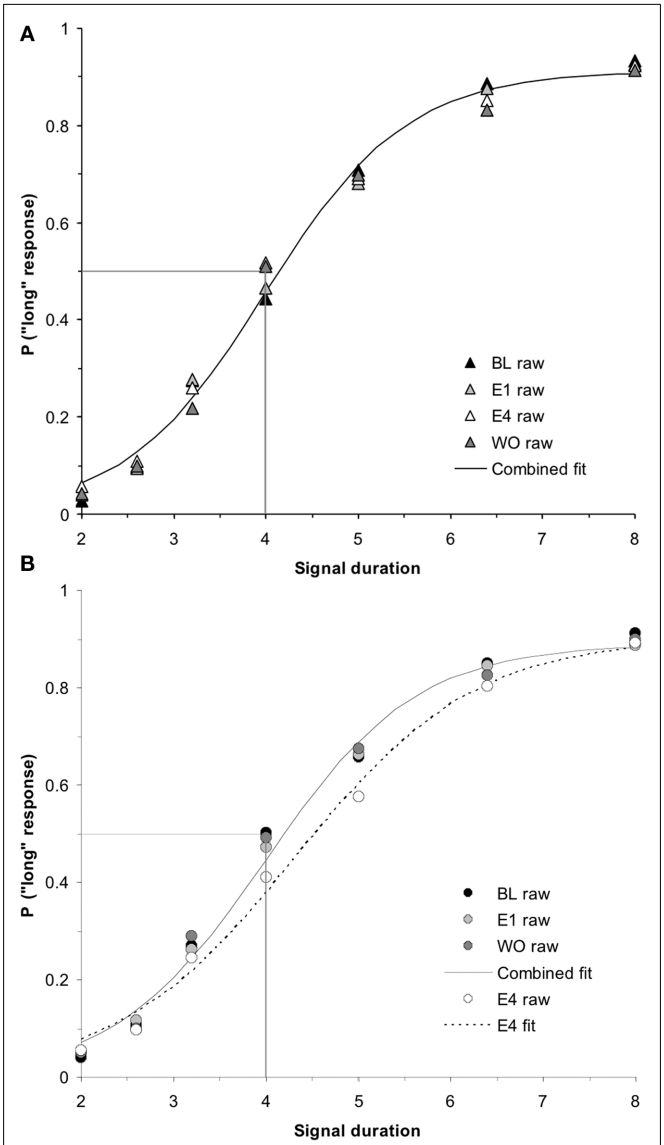

FIGURE 5 | Phase 2 duration bisection functions for (A) hormonal females and (B) hormonal males during baseline, E1, E4, and washout (WO), revealing no significant effects in females ($p > 0.05$), but a significant effect in males on E4 that returned to baseline the following day (WO; $p < 0.01$). Probability of a "long" response is plotted as a function of signal duration(s).

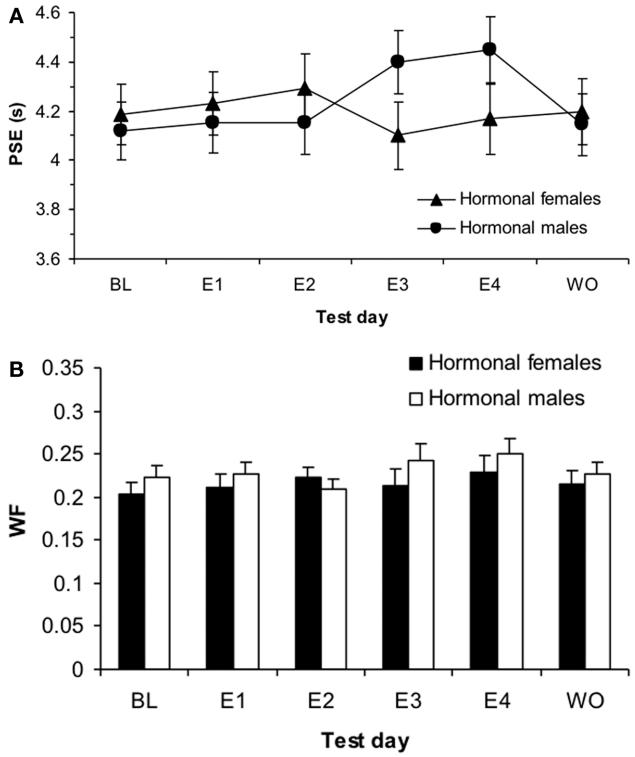

FIGURE 6 | Phase 2 sigmoidal function measures of (A) point of subjective equality (PSE) and (B) Weber fractions (WF) for hormonal males and females showing a significant effect of estrogen on E4 for males in PSE ($p < 0.01$) and a main effect of test day for WF ($p < 0.001$).

factors of hormonal sex and genetic sex and within-subjects factor test day (E4, mean = 1.05 ± 0.06; WO, mean = 0.93 ± 0.05) showed no effects, $p > 0.05$. A similar ANOVA for WF (E4, mean = 0.24 ± 0.01; WO, mean = 0.22 ± 0.01) also found no significant effects, $p > 0.05$. The mean duration bisection measures obtained for rats in each hormonal sex group are presented in **Table 2**. Taken together, these results suggest that there was overall more variability in timing behavior for all treatment groups on the fourth day of estrogen administration compared to baseline and the first day of estrogen.

DISCUSSION

Our duration bisection data suggest that there are fundamental sex differences in temporal processing that are sensitive to estrogen both during brain organization and in adulthood. Prior to exposure to adult circulating hormones, male and female rats showed significantly different judgments of auditory signal durations, with males' bisection functions shifted horizontally to the left of females'. This result suggests that during initial baseline training, the memory translation constant of genetic males was lower (e.g., <1.0) than that of genetic females. Such a result would occur if clock readings were "distorted" by a multiplicative translation constant (K*) during their transfer into reference memory (Gibbon et al., 1984). K* values less than 1.0 would produce remembered durations proportionally shorter than the physical durations and

Table 2 | Phase 2: duration bisection timing measures.

Hormonal sex	Day	PSE	DL	WF	% "long"
Female	BL	4.19 ± 0.12	0.86 ± 0.07	0.20 ± 0.01	0.48 ± 0.02
	E1	4.23 ± 0.13	0.91 ± 0. 07	0.21 ± 0.01	0.48 ± 0.02
	E2	4.29 ± 0.14	0.96 ± 0. 07	0.22 ± 0.01	0.47 ± 0.02
	E3	4.10 ± 0.14	0.90 ± 0.11	0.21 ± 0.02	0.49 ± 0.02
	E4	4.17 ± 0.15	0.98 ± 0.09	0.23 ± 0.02	0.49 ± 0.02
	WO	4.20 ± 0.13	0.91 ± 0.08	0.21 ± 0.02	0.47 ± 0.02
Male	BL	4.12 ± 0.12	0.92 ± 0. 07	0.22 ± 0.01	0.48 ± 0.02
	E1	4.15 ± 0.12	0.95 ± 0. 06	0.23 ± 0.01	0.47 ± 0.02
	E2	4.15 ± 0.13	0.88 ± 0. 07	0.21 ± 0.01	0.47 ± 0.02
	E3	4.40 ± 0.13	1.07 ± 0.10	0.24 ± 0.02	0.44 ± 0.02
	E4	4.45 ± 0.14	1.10 ± 0.09	0.25 ± 0.02	0.43 ± 0.02
	WO	4.15 ± 0.13	0.94 ± 0.07	0.23 ± 0.01	0.48 ± 0.02

PSE, point of subjective equality; DL, difference limen; WF, Weber fraction; BL, baseline; E, estrogen day; WO, washout.

K* values greater than 1.0 would produce remembered durations that are proportionally longer than the physical durations (Meck, 1983, 1991). These types of changes in K* are normally thought to involve alterations in cholinergic function in the cortex, but may also involve hippocampal and striatal circuits (Meck, 1996, 2002; Meck and Benson, 2002; Melgire et al., 2005; Balci et al., 2009). Moreover, estradiol administration and ovariectomy have been shown to have differential effects on cholinergic function, with estradiol administration counteracting the memory impairments produced by muscarinic receptor antagonism (Dohanich et al., 1994; Singh et al., 1994; Gibbs, 2000).

An additional finding was that following administration of a single low dose of estradiol, the clock speed of female, but not male, rats was increased such that the same signal durations were judged to be about 8% longer. These findings support and extend the observations of Sandstrom (2007), who reported that acute administration of 5 μg estradiol transiently increases clock speed in female rats performing in a temporal production task. The current findings replicate this effect in rats performing a perceptual timing task (e.g., duration bisection procedure) and extend the results by showing that this "clock speed" effect of activational estradiol does not occur in males. This "clock speed" interpretation of the horizontal shifts observed in the bisection functions following estradiol administration would be greatly strengthened by the utilization of multiple sets of anchor durations – thereby allowing for the determination of whether or not the horizontal shifts are proportional to the durations being timed (Maricq et al., 1981; Meck, 1996). Interestingly, this sex difference in the effects of acute estradiol administration on temporal processing in adult rats was not modifiable by our early postnatal hormone manipulations. Neonatal gonadectomy did not feminize males, causing them to be sensitive to adult estradiol administration and show "female" effects on temporal processing, nor did early postnatal estradiol administration masculinize females to make them less sensitive to estradiol in the duration bisection procedure.

We have also uncovered a second, distinctly different effect of estrogen on temporal processing. After extensive training in our

duration bisection procedure, chronic estrogen administration decreased clock speed of rats exposed to androgens or estrogen perinatally. Both male rats castrated as adults and females treated with estradiol postnatally judged durations as 8% shorter after 4 days of adult estradiol replacement, while this treatment had no effect on temporal processing in AOF or neonatally gonadectomized males. This effect appears to require estrogen priming for several days and concurrent estrogen activation, as duration bisection functions returned to baseline on the day following a 4-day cycle of estrogen treatment. This pattern of results reveals multiple actions of estrogen on temporal processing that are dependent, in part, on both the organizational and activational effects of estrogen.

SEX DIFFERENCES IN BASELINE DURATION BISECTION FUNCTIONS

Our data reveal that males and females have significantly different baseline functions when required to scale intermediate auditory signal durations in a duration bisection procedure. While there were no sex differences in the discrimination between the two anchor durations (2 vs. 8 s), males judged intermediate signal durations as significantly longer than females judged them. Interestingly, in our 2 vs. 8 s bisection procedure, the average PSE for males was to the left and the PSE for females to the right of 4.0 s, the geometric mean between 2.0 and 8.0 s, which has been observed as the bisection point in many previous studies using intact male rats (Church and Deluty, 1977; Meck, 1983; Cheng et al., 2007b) and pigeons (Stubbs, 1976). However, bisection functions obtained after extensive training with intermediate signal durations revealed no sex differences in timing behavior, as males gradually shifted to the right with further training such that their baseline functions were now virtually identical to those of females by the time the second baseline was established in the current experiment. These findings are novel, as no previous work has directly compared time perception in males and females. While it is not surprising that timing functions would become more stable and closer to the theoretically predicted PSE following sufficient experience with the procedure (see Gibbon, 1981; Meck, 1983; Allen and Gibbon, 1991), it is interesting that female rats appear to reach stability in baseline functions more quickly than male rats.

There are several potential reasons why we were not able to sex-reverse the brains of male and female rats with early postnatal hormone alteration. The most likely explanation is that our early postnatal manipulations missed the sensitive period for hormonal masculinization of the relevant striatal DA-modulated circuits. However, it is possible that gonadal hormones masculinize the striatum prenatally. For example, while many hippocampal-dependent behaviors, such as spatial ability, can be sex-reversed postnatally (e.g., Williams et al., 1990; Williams and Meck, 1991; Isgor and Sengelaub, 1998, 2003), the sexually dimorphic effects of stress on hippocampal-dependent trace eyeblink conditioning are organized prenatally – androgens must be removed from males early *in utero* in order for males to show female-typical learning effects in adulthood (Shors and Miesegaes, 2002). Moreover, both aromatase and ER α and β have been found in the striatum as early as ED 14 (Küppers and Beyer, 1999). Therefore, our data suggest that if organizational hormones masculinize the striatum, much of this masculinization is likely to be occurring prenatally. This would explain why we were unable to masculinize the striata of females with early postnatal estrogen administration and to demasculinize/feminize males' striata with early postnatal castration.

Another possible explanation is that this effect is dependent on genetic factors separate from effects of gonadal hormones on brain organization. Mechanisms underlying other adaptive behaviors, such as aggression, have been shown to be influenced by genes on the sex chromosome other than the Sry gene that codes for testes development and the resulting testosterone secretions (Gatewood et al., 2006). In addition, recent evidence shows that the Sry gene on the Y chromosome is only expressed in TH-containing neurons in the substantia nigra (SN) and can activate TH production in SN neurons that project to the striatum independently of gonadal hormones (Dewing et al., 2006). Inactivation of Sry drastically reduces the number of TH-containing neurons in the SN (38%) and STR (26%) without altering the total number of neurons in the SN. Our data provide functional/behavioral support for this mechanism of DA production by showing that at least one aspect of striatal function is not modifiable by postnatal hormone manipulation, suggesting that their may be a direct genetic contribution to sexually dimorphic striatal DA function.

RAPID ACTIVATIONAL EFFECT OF ESTRADIOL ON CLOCK SPEED

Our data demonstrate that a single injection of estradiol 30 min prior to performance in a duration bisection procedure significantly increases the clock speed of female rats, as illustrated by a leftward shift in the PSE, without a change in discrimination accuracy. This transient shift in the psychometric function immediately following estrogen administration supports the view that estrogen can mimic some of the properties of a DA agonist (Cheng et al., 2006) in order to produce an increase in clock speed. In addition, this clock speed effect diminishes after the first exposure to estrogen which is consistent with previous work showing that rats given repeated injections of DA agonists typically adjust to changes in clock speed by renormalizing their timing functions over sessions (Meck, 1983, 1996). In accordance with these findings, our data suggest that rats quickly adapt to a new clock speed by updating the anchor durations stored in memory in order to match this change in clock speed. This rescaling of duration results in a return to baseline performance within a few sessions even though the subject remains under the influence of estrogen and its putative impact on striatal DA activity and clock speed (Coull et al., 2011).

This is the first study to examine sex differences in the classification of supra-second durations using a duration bisection procedure. Our findings show that time perception of male rats is not altered by acute estradiol administration. These results are consistent with previous work showing that male rats, unlike females, do not respond to acute estradiol with increases in striatal DA release (Becker, 1990a,b, 1999; Castner et al., 1993), ACM are less sensitive to the behavioral effects of DA agonists, and male rats achieve less sensitization to DA agonists than ovariectomized females (e.g., Hu and Becker, 2003; Hu et al., 2004).

As indicated above, our data corroborate a previous report showing that a single injection of 5 μg of estradiol given to AOF 30 min before testing in a previously trained 7 and 21-s peak-interval procedure results in proportional leftward shifts in peak

time (i.e., an increase in clock speed of 4–5%) without a change in timing accuracy (Sandstrom, 2007). Interestingly, we found that with cyclic administration, this rapid effect on clock speed occurred only during the first estradiol cycle, while Sandstrom (2007) reported an acute effect on clock speed during several subsequent estradiol administration cycles. This may be due to our 4-day cyclic administration every 2 weeks as compared to Sandstrom's daily administration of estradiol, or it may be due to the extensive training we gave rats between the first and second estrogen cycles. Our rats may not have shown behavior reflective of an acute effect because they learned to adjust their timing behavior during the first 4-day cycle of estrogen administration or because of overtraining (see Cheng et al., 2007a,c).

Both the previous (Sandstrom, 2007) and the current study support the view that estrogens may cause the rapid release of DA and thus may act much like DA agonists, causing a perceptual shift such that intervals are perceived as being proportionally shorter (Meck, 1983, 1996). While our results are consistent with the findings of Sandstrom (2007), they do not support the discrimination accuracy or lack of clock speed effects previously reported for female rats treated with chronic estradiol (Ross and Santi, 2000). Unlike our methods, which focused primarily on the rapid and acute effects of estradiol administration during testing with intermediate signal durations, Ross and Santi (2000) administered estradiol during the baseline discrimination training that occurred prior to the inclusion of intermediate signal durations. Such training would be expected to lead to the rescaling of any estradiol-induced changes in clock speed prior to testing with the intermediate signal durations and hence reduce any observed effect on the horizontal placement of the psychometric functions (Meck, 1983).

Consistent with our baseline results, we were unable to alter responsivity to acute estradiol administration in adulthood with alterations of androgens or estrogens early in development. Neonatally and ACM rats were both unresponsive to estradiol in adulthood, while females that were neonatally exposed to estrogens were just as responsive to adult estrogens as females that were not exposed to neonatal estrogens. Little previous work has examined the possibility that neonatal hormone manipulations may be able to alter sensitivity to estrogen in adulthood (e.g., Anderson et al., 2005). Therefore, it is still unclear whether or not the striatal DA system's sensitivity to estrogens and psychostimulants are determined by organizational hormones. In addition to possible prenatal hormonal organization, the mechanism of Sry in DA production may be responsible for the apparent "genetic" sex difference found in the behavioral response to acute estrogen observed in the current experiment, as genetic males and females may have different mechanisms that respond differently to estrogen administration.

CHRONIC ESTRADIOL EFFECTS ON TEMPORAL PROCESSING

When estradiol was administered to rats daily after extensive training in our duration bisection procedure, a distinctly different effect on temporal processing was uncovered. By the fourth day of estradiol administration, rats exposed to estradiol or gonadal androgens during the first week of life underestimated signal durations, while there was no effect of estradiol on adult OVX females and NCM. When no estradiol was given on a fifth day, all rats showed accurate timing with no horizontal shifts in time perception – neonatally hormone-exposed rats returned to baseline performance. These data support previous research that suggests that rapid and acute effects of estrogens in the striatum may be modulated by separate mechanisms (e.g., Becker and Rudick, 1999). However, these mechanisms have previously been described as cooperative and have been hypothesized to consist of a classical estrogen receptor-mediated mechanism that enhances the rapid excitatory mechanism in females but not males. The results of the current study suggest that the striatal DA systems of males are affected by 4 days of estradiol administration, but that this effect is in the opposite direction than the rapid effect found in females, resulting in a decrease in clock speed. Interestingly, the acute 4-day mechanism was modifiable by postnatal gonadal hormones even though the rapid mechanism was not, further supporting the hypothesis that there are two distinct mechanisms of estrogen action in the striatum.

It is possible that females' internal clocks are less sensitive to fluctuations in circulating estrogen because it would not be adaptive for clock speed to change wildly in a cyclical manner along with estrogen levels. A time-dependent decrease of DAT density has been shown in the striatum and the nucleus accumbens following ovariectomy (Bossé et al., 1997). Moreover, this decrease in DAT density was not modified by estradiol administration and may have contributed to the insensitivity observed in the current study given that the DAT has been shown to be involved in the regulation of clock speed (Meck et al., 2011). In contrast, the striatal DA system of males may not be able to compensate for estradiol administration, so they may become sensitized as estrogens accumulate and down regulate DA receptors, leading to less synaptic DA activity in the striatum and a consequent decrease in clock speed. In addition, it is possible that these rats already had altered striatal DA function due to extensive training in this striatally mediated timing procedure (Cheng et al., 2007a,c).

While our results are not in complete agreement with previous interpretations of sex differences and/or estrogen effects on time perception and timed performance, they are consistent with most of the previous findings if certain procedural differences are taken into consideration (Ross and Santi, 2000; Sandstrom, 2007; Cheng et al., 2008a). Moreover, our data suggest that males may down regulate DA receptors under some conditions to compensate for stimulation of the striatal DA system by estrogen. Although this study was not designed to examine the mechanism(s) behind this acute effect in males, little previous research has examined the possible effects of estrogen on males. At this point, specific hypotheses about the mechanisms responsible for the rapid and acute effects of estrogen on clock speed remain speculative and are in need of further investigation.

ACKNOWLEDGMENTS

We would like to thank Lisa Myers and Donna Werlinig for assistance in behavioral testing and Ruey Chang and Chris MacDonald for technical guidance.

REFERENCES

Agarti, P., Ma, Z. Q., Patrone, C., Picotti, G. B., Pellicciari, C., Bondiolotti, G., Bottone, M. G., and Maggi, A. (1997). Dopaminergic phenotype induced by oestrogens in a human neuroblastoma cell line. *Eur. J. Neurosci.* 9, 1008–1016.

Allen, L. G., and Gibbon, J. (1991). Human bisection at the geometric mean. *Learn. Motiv.* 22, 39–58.

Allman, M. J., and Meck, W. H. (2011). Pathophysiological distortions in time perception and timed performance. *Brain.* doi: 10.1093/brain/awr210. [Epub ahead of print].

Anderson, J. C., Williams, S., McGee, R., and Silva, P. A. (1987). DSM-III disorders in preadolescent children: prevalence in a large sample from the general population. *Arch. Gen. Psychiatry* 44, 69–76.

Anderson, L. I., Leipheimer, R. E., and Dluzen, D. E. (2005). Effects of neonatal and prepubertal hormonal manipulations upon estrogen neuroprotection of the nigrostriatal dopaminergic system within female and male mice. *Neuroscience* 130, 369–382.

Arnold, L. E. (1996). Sex differences in ADHD: conference summary. *J. Abnorm. Child Psychol.* 24, 555–569.

Balci, F., Meck, W. H., Moore, H., and Brunner, D. (2009). "Timing deficits in aging and neuropathology," in *Animal Models of Human Cognitive Aging*, eds J. L. Bizon and A. Wood (Totowa, NJ: Humana Press), 161–201.

Balthazart, J., and Ball, G. F. (2006). Is brain estradiol a hormone or a neurotransmitter? *Trends Neurosci.* 29, 241–249.

Bazzett, T. J., and Becker, J. B. (1994). Sex differences in the rapid and acute effects of estrogen on striatal D2 dopamine receptor binding. *Brain Res.* 637, 163–172.

Beatty, W. W., Dodge, A. M., and Traylor, K. L. (1982). Stereotyped behavior elicited by amphetamine in the rat: influences of the testes. *Physiol. Behav.* 28, 649–652.

Becker, J. B. (1990a). Direct effect of 17(β-estradiol on striatum: sex differences in dopamine release. *Synapse* 5, 157–164.

Becker, J. B. (1990b). Estrogen rapidly potentiates amphetamine-induced striatal dopamine release and rotational behavior during microdialysis. *Neurosci. Lett.* 118, 169–171.

Becker, J. B. (1999). Gender differences in dopaminergic function in striatum and nucleus accumbens. *Pharmacol. Biochem. Behav.* 64, 803–812

Becker, J. B., Robinson, T. E., and Lorenz, K. A. (1982). Sex differences and estrous cycle variations in amphetamine-elicited rotational behavior. *Eur. J. Pharmacol.* 80, 65–72.

Becker, J. B., and Rudick, C. N. (1999). Rapid effects of estrogen or progesterone on the amphetamine-induced increase in striatal dopamine are enhanced by estrogen priming: a microdialysis study. *Pharmacol. Biochem. Behav.* 64, 53–57.

Beyer, C., and Karolczak, M. (2000). Estrogenic stimulation of neurite growth in midbrain dopaminergic neurons depends on cAMP/protein kinase A signalling. *J. Neurosci. Res.* 59, 107–116.

Block, R. A., Hancock, P. A., and Zakay, D. (2000). Sex differences in duration judgements: a meta-analytic review. *Mem. Cognit.* 28, 1333–1346.

Bossé, R., Rivest, R., and Di Paolo, T. (1997). Ovariectomy and estradiol treatment affect the dopamine transporter and its gene expression in the rat brain. *Brain Res. Mol. Brain Res.* 46, 343–346.

Buhusi, C. V., and Meck, W. H. (2002). Differential effects of methamphetamine and haloperidol on the control of an internal clock. *Behav. Neurosci.* 116, 291–297.

Buhusi, C. V., and Meck, W. H. (2005). What makes us tick? Functional and neural mechanisms of interval timing. *Nat. Rev. Neurosci.* 6, 755–765.

Castner, S. A., Xiao, L., and Becker, J. B. (1993). Sex differences in striatal dopamine: in vivo microdialysis and behavioral studies. *Brain Res.* 610, 127–134.

Cheng, R. K., Ali, Y. M., and Meck, W. H. (2007a). Ketamine "unlocks" the reduced clock-speed effect of cocaine following extended training: evidence for dopamine-glutamate interactions in timing and time perception. *Neurobiol. Learn. Mem.* 88, 149–159.

Cheng, R. K., Etchegaray, M., and Meck, W. H. (2007b). Impairments in timing, temporal memory, and reversal learning linked to neurotoxic regimens of methamphetamine intoxication. *Brain Res.* 1186, 255–266.

Cheng, R. K., Hakak, O. L., and Meck, W. H. (2007c). Habit formation and the loss of control of an internal clock: inverse relationship between the level of baseline training and the clock-speed enhancing effects of methamphetamine. *Psychopharmacology (Berl.)* 193, 351–362.

Cheng, R. K., Dyke, A. G., McConnell, M. W., and Meck, W. H. (2011). Categorical scaling of duration as a function of temporal context in aged rats. *Brain Res.* 1381, 175–186.

Cheng, R. K., MacDonald, C. J., and Meck, W. H. (2006). Differential effects of cocaine and ketamine on time estimation: implications for neurobiological models of interval timing. *Pharmacol. Biochem. Behav.* 85, 114–122.

Cheng, R. K., MacDonald, C. J., Williams, C. L., and Meck, W. H. (2008a). Prenatal choline supplementation alters the timing, emotion, and memory performance (TEMP) of adult male and female rats as indexed by differential reinforcement of low-rate schedule behavior. *Learn. Mem.* 15, 153–162.

Cheng, R. K., Scott, A. C., Penney, T. B., Williams, C. L., and Meck, W. H. (2008b). Prenatal choline availability differentially modulates timing of auditory and visual stimuli in aged rats. *Brain Res.* 1237, 167–175.

Church, R. M., and Deluty, M. Z. (1977). Bisection of temporal intervals. *J. Exp. Psychol. Anim. Behav. Process.* 3, 216–228.

Coull, J. T., Cheng, R. K., and Meck, W. H. (2011). Neuroanatomical and neurochemical substrates of timing. *Neuropsychopharmacology* 36, 3–25.

Dewing, P., Chiang, C. W., Sinchak, K., Sim, H., Fernagut, P. O., Kelly, S., Chesselet, M. F., Micevych, P. E., Albrecht, K. H., Harley, V. R., and Vilain, E. (2006). Direct regulation of adult brain function by the male-specific factor SRY. *Curr. Biol.* 16, 415–420.

Dohanich, G. P., Fader, A. J., and Javorsky, D. J. (1994). Estrogen and estrogen-progesterone treatments counteract the effect of scopolamine on reinforced T-maze alternation in female rats. *Behav. Neurosci.* 108, 988–992.

Döhler, K. D., Hancke, J. L., Srivastava, S. S., Hofmann, C., Shryne, J. E., and Gorski, R. A. (1984). Participation of estrogens in female sexual differentiation of the brain; neuroanatomical, neuroendocrine and behavioral evidence. *Prog. Brain Res.* 61, 99–117.

Eisler, H., and Eisler, A. D. (1992). Time perception: effects of sex and sound intensity on scales of subjective duration. *Scand. J. Psychol.* 33, 339–358.

Ferretti, C., Blengio, M., Vigna, I., Ghi, P., and Genazzani, E. (1992). Effects of estradiol on ontogenesis of striatal dopamine D1 and D2 receptor sites in male and female rats. *Brain Res.* 751, 212–217.

Gallistel, C. R. (1990). Representations in animal cognition: an introduction. *Cognition* 37, 1–22.

Gatewood, J. D., Wills, A., Shetty, S., Xu, J., Arnold, A. P., Burgoyne, P. S., and Rissman, E. F. (2006). Sex chromosome complement and gonadal sex influence aggressive and parental behaviors in mice. *J. Neurosci.* 26, 2335–2342.

Gerardin, D. C., Bernardi, M. M., Moreira, E. G., and Pereira, O. C. (2006). Neuroendocrine and reproductive aspects of adult male rats exposed neonatally to an antiestrogen. *Pharmacol. Biochem. Behav.* 83, 618–623.

Gibbon, J. (1981). On the form and location of the psychometric bisection function for time. *J. Math. Psychol.* 24, 58–87.

Gibbon, J., Church, R. M., and Meck, W. H. (1984). Scalar timing in memory. *Ann. N. Y. Acad. Sci.* 423, 52–77.

Gibbon, J., Malapani, C., Dale, C. L., and Gallistel, C. R. (1997). Toward a neurobiology of temporal cognition: advances and challenges. *Curr. Opin. Neurobiol.* 7, 170–184.

Gibbs, R. B. (2000). Effects of gonadal hormone replacement on measures of basal forebrain cholinergic function. *Neuroscience* 101, 931–938.

Glick, S. D., and Cox, R. D. (1976). Differential effects of unilateral and bilateral caudate lesions on side preferences and timing behavior in rats. *J. Comp. Physiol. Psychol.* 90, 528–535.

Hancock, P. A., Arthur, E. J., Chrysler, S. T., and Lee, J. (1994). The effects of sex, target duration, and illumination on the production of time intervals. *Acta Psychol. (Amst.)* 86, 57–67.

Hinton, S. C., and Meck, W. H. (2004). Frontal-striatal circuitry activated by human peak-interval timing in the supra-seconds range. *Brain Res. Cogn. Brain Res.* 21, 171–182.

Höhn, S., Dallérac, G., Faure, A., Urbach, Y., Nguyen, H. P., Riess, O., von Hörsten, S., Le Blanc, P., Desvignes, N., El Massioui, N., Brown, B. L., and Doyère, V. (2011). Behavioral and in vivo electrophysiological evidence for presymptomatic alteration of prefronto-striatal processing in the transgenic rat model for Huntington disease. *J. Neurosci.* 31, 8986–8997.

Hu, M., and Becker, J. B. (2003). Effects of sex and estrogen on behavioral sensitization to cocaine in rats. *J. Neurosci.* 23, 693–699.

Hu, M., Crombag, H. S., Robinson, T. E., and Becker, J. B. (2004). Biological basis of sex differences in the propensity to self-administer cocaine. *Neuropsychopharmacology* 29, 81–85.

Isgor, C., and Sengelaub, D. R. (1998). Prenatal gonadal steroids affect adult spatial behavior, CA1 and CA3

pyramidal cell morphology in rats. *Horm. Behav.* 34, 183–198.

Isgor, C., and Sengelaub, D. R. (2003). Effects of neonatal gonadal steroids on adult CA3 pyramidal neuron dendritic morphology and spatial memory in rats. *J. Neurobiol.* 55, 179–190.

Jackson, L. R., Robinson, T. E., and Becker, J. B. (2006). Sex differences and hormonal influences on acquisition of cocaine self-administration in rats. *Neuropsychopharmacology* 31, 129–138.

Kellaris, J. J., and Mantel, S. P. (1994). The influence of mood and gender on consumers' time perceptions. *Adv. Consum. Res.* 21, 514–518.

Korol, D. L. (2004). Role of estrogen in balancing contributions from multiple memory systems. *Neurobiol. Learn. Mem.* 82, 309–323.

Küppers, E., and Beyer, C. (1998). Expression of aromatase in the embryonic and postnatal mouse striatum. *Brain Res. Mol. Brain Res.* 63, 184–188.

Küppers, E., and Beyer, C. (1999). Expression of estrogen receptor-alpha and beta mRNA in the developing and adult mouse striatum. *Neurosci. Lett.* 276, 95–98.

Le Saux, M., and DiPaolo, T. (2006). Influence of oestrogenic compounds on monoamine transporters in rat striatum. *J. Neuroendocrinol.* 18, 25–32.

Levesque, D., Gagne, B., Barden, N., and DiPaolo, T. (1992). Chronic estradiol treatment increases anterior pituitary but not striatal D2 dopamine receptor mRNA levels in rats. *Neurosci. Lett.* 140, 5–8.

Lotze, M., Wittmann, M., von Steinbuchel, N., Poppel, E., and Roenneberg, T. (1999). Daily rhythm of temporal resolution in the auditory system. *Cortex* 35, 89–100.

MacDonald, C. J., Cheng, R. K., Williams, C. L., and Meck, W. H. (2007). Combined organizational and activational effects of short and long photoperiods on spatial and temporal memory in rats. *Behav. Processes* 74, 226–233.

MacDonald, C. J., and Meck, W. H. (2004). Systems-level integration of interval timing and reaction time. *Neurosci. Biobehav. Rev.* 28, 747–769.

MacDougall, R. (1904). Sex differences in the sense of time. *Science* 19, 707–708.

Maguire, E. A., Burgess, N., and O'Keefe, J. (1999). Human spatial navigation: cognitive maps, sexual dimorphism, and neural substrates. *Curr. Opin. Neurobiol.* 9, 171–177.

Malapani, C., Deweer, B., and Gibbon, J. (2002). Separating storage from retrieval dysfunction of temporal memory in Parkinson's disease. *J. Cogn. Neurosci.* 14, 311–322.

Malapani, C., Rakitin, B., Levy, R., Meck, W. H., Deweer, B., Dubois, B., and Gibbon, J. (1998). Coupled temporal memories in Parkinson's disease: a dopamine-related dysfunction. *J. Cogn. Neurosci.* 10, 316–331.

Maricq, A. V., and Church, R. M. (1983). The differential effects of haloperidol and methamphetamine on time estimation in the rat. *Psychopharmacology (Berl.)* 79, 10–15.

Maricq, A. V., Roberts, S., and Church, R. M. (1981). Methamphetamine and time estimation. *J. Exp. Psychol. Anim. Behav. Process.* 7, 18–30.

Matell, M. S., Bateson, M., and Meck, W. H. (2006). Single-trials analyses demonstrate that increases in clock speed contribute to the methamphetamine-induced horizontal shifts in peak-interval timing functions. *Psychopharmacology (Berl.)* 188, 201–212.

Matell, M. S., King, G. R., and Meck, W. H. (2004). Differential adjustment of interval timing by the chronic administation of intermittent or continuous cocaine. *Behav. Neurosci.* 118, 150–156.

Matell, M. S., and Meck, W. H. (2000). Neuropsychological mechanisms of interval timing behavior. *Bioessays* 22, 94–103.

Matell, M. S., and Meck, W. H. (2004). Cortico-striatal circuits and interval timing: coincidence-detection of oscillatory processes. *Brain Res. Cogn. Brain Res.* 21, 139–170.

Matell, M. S., Meck, W. H., and Nicolelis, M. A. (2003). Interval timing and the encoding of signal duration by ensembles of cortical and striatal neurons. *Behav. Neurosci.* 117, 760–773.

Matell, M. S., Shea-Brown, E., Gooch, C., Wilson, A. G., and Rinzel, J. (2011). A heterogeneous population code for elapsed time in rat medial agranular cortex. *Behav. Neurosci.* 125, 54–73.

Maus, M., Premont, J., and Glowinski, J. (1990). In vitro effects of 17 beta-oestradiol on the sensitivity of receptors coupled to adenylate cyclase on striatal neurons in primary culture. *Ciba Found. Symp.* 153, 145–153.

Meck, W. H. (1983). Selective adjustment of the speed of internal clock and memory processes. *J. Exp. Psychol. Anim. Behav. Process.* 9, 171–201.

Meck, W. H. (1986). Affinity for the dopamine D2 receptor predicts neuroleptic potency in decreasing the speed of an internal clock. *Pharmacol. Biochem. Behav.* 25, 1185–1189.

Meck, W. H. (1991). Modality-specific circadian rhythmicities influence mechanisms of attention and memory for interval timing. *Learn. Motiv.* 22, 153–179.

Meck, W. H. (1996). Neuropharmacology of timing and time perception. *Brain Res. Cogn. Brain Res.* 3, 227–242.

Meck, W. H. (2002). Choline uptake in the frontal cortex is proportional to the absolute error of a temporal memory translation constant in mature and aged rats. *Learn. Motiv.* 33, 88–104.

Meck, W. H. (2003). *Functional and Neural Mechanisms of Interval Timing.* Boca Raton, FL: CRC Press LLC.

Meck, W. H. (2005). Neuropsychology of timing and time perception. *Brain Cogn.* 58, 1–8.

Meck, W. H. (2006a). Frontal cortex lesions eliminate the clock speed effect of dopaminergic drugs on interval timing. *Brain Res.* 1108, 157–167.

Meck, W. H. (2006b). Neuroanatomical localization of an internal clock: a functional link between mesolimbic, nigrostriatal, and mesocortical dopaminergic systems. *Brain Res.* 1109, 93–107.

Meck, W. H., and Benson, A. M. (2002). Dissecting the brain's internal clock: how frontal-striatal circuitry keeps time and shifts attention. *Brain Cogn.* 48,195–211.

Meck, W. H., Cheng, R. K., MacDonald, C. J., Gainetdinov, R. R., Caron, M. G., and Çevik, M. Ö. (2011). Gene-dose dependent effects of methamphetamine on interval timing in dopamine-transporter knockout mice. *Neuropharmacology.* doi: 10.1016/j.neuropharm.2011.01.042. [Epub ahead of print].

Meck, W. H., Penney, T. B., and Pouthas, V. (2008). Cortico-striatal representation of time in animals and humans. *Curr. Opin. Neurobiol.* 18, 145–152.

Melgire, M., Ragot, R., Samson, S., Penney, T. B., Meck, W. H., and Pouthas, V. (2005). Auditory/visual duration bisection in patients with left or right medial-temporal lobe resection. *Brain Cogn.* 58, 119–124.

Neil, D. B., and Herndon, J. G. Jr. (1978). Anatomical specificity within rat striatum for the dopaminergic modulation of DRL responding and activity. *Brain Res.* 153, 529–538.

Ohtani, J., Nomoto, M., and Douchi, T. (2001). Chronic estrogen treatment replaces striatal dopaminergic function in ovariectomized rats. *Brain Res.* 900, 163–168.

Ovtscharoff, W., Eusterschulte, B., Zienecker, R., Reisert, I., and Pilgrim, C. (1992). Sex differences in densities of dopaminergic fibers and GABAergic neurons in the prenatal rat striatum. *J. Comp. Neurol.* 323, 299–304.

Paule, M. G., Meck, W. H., McMillan, D. E., Bateson, M., Popke, E. J., Chelonis, J. J., and Hinton, S. C. (1999). The use of timing behaviors in animals and humans to detect drug and/or toxicant effects. *Neurotoxicol. Teratol.* 21, 491–502.

Quinlan, M. G., Hussain, D., and Brake, W. G. (2008). Use of cognitive strategies: the role of estradiol and its interaction with dopamine. *Horm. Behav.* 53, 185–191.

Rammsayer, T., and Lustnauer, S. (1989). Sex differences in time perception. *Percept. Mot. Skills* 68, 195–198.

Rao, S. M., Mayer, A. R., and Harrington, D. L. (2001). The evolution of brain activation during temporal processing. *Nat. Neurosci.* 4, 317–323.

Reisert, I., Han, V., Lieth, E., Toran-Allerand, D., Pilgrim, C., and Lauder, J. (1987). Sex steroids promote neurite growth in mesencephalic tyrosine hydroxylase immunoreactive neurons in vitro. *Int. J. Dev. Neurosci.* 5, 91–98.

Robinson, T. E., Becker, J. B., and Ramirez, V. D. (1980). Sex differences in amphetamine-elicited rotational behavior and the lateralization of striatal dopamine in rats. *Brain Res. Bull.* 5, 539–545.

Ross, L., and Santi, A. (2000). The effects of estrogen on temporal and numerical processing in ovariectomized female rats. *Psychobiology (Austin, Tex.)* 28, 394–405.

Sandstrom, N. J. (2007). Estradiol modulation of the speed of an internal clock. *Behav. Neurosci.* 121, 422–432.

Shors, T. J., and Miesegaes, G. (2002). Testosterone in utero and at birth dictates how stressful experience will affect learning in adulthood. *Proc. Natl. Acad. Sci. U.S.A.* 99, 13955–13960.

Shughrue, P. J., Lane, M. V., and Merchenthaler, I. (1997). Comparative distribution of estrogen receptor-alpha and -beta mRNA in the rat central nervous system. *J. Comp. Neurol.* 388, 507–525.

Singh, M., Meyer, E. M., Millard, W. J., and Simpkins, J. W. (1994). Ovarian steroid deprivation results in a reversible learning impairment and compromised cholinergic function in female Sprague-Dawley rats. *Brain Res.* 644, 305–312.

Smith, A., Taylor, E., Rogers, J. W., Newman, S., and Rubia, K. (2002). Evidence for a pure time perception deficit in children with

ADHD. *J. Child Psychol. Psychiatry* 43, 529–542.

Stroppolo, A., Tian, C., Guinea, B., Olm, V., Sheffield, R., Sommer, J., and Ehrlich, M. E. (2004). 17(β-estradiol promotes striatal medium size spiny neuronal maturation in vitro. *Neuroendocrinology* 79, 259–267.

Stubbs, D. A. (1976). Scaling of stimulus duration by pigeons. *J. Exp. Anal. Behav.* 26, 15–25.

Swerdlow, R. H., Parker, W. D. Jr., Currie, L. J., Bennett, J. P. Jr., Harrison, M. B., Trugman, J. M., and Wooten, G. F. (2001). Gender ratio differences between Parkinson's disease patients and their affected relatives. *Parkinsonism Relat. Disord.* 7, 129–133.

Szelag, E., Kanabus, M., Kolodziejczyk, I., Kowalska, J., and Szuchnik, J. (2004). Individual differences in temporal information processing in humans. *Acta Neurobiol. Exp. (Wars.)* 64, 349–366.

Teicher, M. H., Anderson, C. M., Polcari, A., Glod, C. A., Maas, L. C., and Renshaw, P. F. (2000). Functional deficits in basal ganglia of children with attention-deficit/hyperactivity disorder shown with functional magnetic resonance imaging relaxometry. *Nat. Med.* 6, 470–473.

Toran-Allerand, C. D., Miranda, R. C., Hochberg, R. B., and MacLusky, N. J. (1992). Cellular variations in estrogen receptor mRNA translation in the developing brain: evidence from combined [125I] estrogen autoradiography and non-isotopic in situ hybridization histochemistry. *Brain Res.* 576, 25–41.

Walker, Q. D., Ray, R., and Kuhn, C. M. (2006). Sex differences in neurochemical effects of dopaminergic drugs in rat striatum. *Neuropsychopharmacology* 31, 1193–1202.

Williams, C. L., Barnett, A. M., and Meck, W. H. (1990). Organizational effects of early gonadal secretions on sexual differentiation in spatial memory. *Behav. Neurosci.* 104, 84–97.

Williams, C. L., and Meck, W. H. (1991). The organizational effects of gonadal steroids on sexually dimorphic spatial ability. *Psychoneuroendocrinology* 16, 155–176.

Xiao, L., and Becker, J. B. (1994). Quantitative microdialysis determination of extracellular striatal dopamine concentration in male and female rats: effects of estrous cycle and gonadectomy. *Neurosci. Lett.* 180, 155–158.

Xiao, L., and Becker, J. B. (1997). Hormonal activation of the striatum and the nucleus accumbens modulates paced mating behavior in the female rat. *Horm. Behav.* 32, 114–124.

Xiao, L., and Becker, J. B. (1998). Effects of estrogen agonists on amphetamine-stimulated striatal dopamine release. *Synapse* 29, 379–391.

Xiao, L., Jackson, L. R., and Becker, J. B. (2003). The effect of estradiol in the striatum is blocked by ICI 182,780 but not tamoxifen: pharmacological and behavioral evidence. *Neuroendocrinology* 77, 239–245.

Yerkes, R. M., and Urban, F. M. (1906). Time-estimation in its relations to sex, age, and physiological rhythms. *Harvard Psychol. Stud.* 2, 405–430.

Zametkin, A. J., and Ernst, M. (1999). Problems in the management of attention-deficit-hyperactivity disorder. *N. Engl. J. Med.* 340, 40–46.

Zhang, J.-Q., Cai, W.-Q., Zhou, D.-S., and Su, B.-Y. (2002). Distribution differences of estrogen receptor beta immunoreactivity in the brain of adult male and female rats. *Brain Res.* 935, 73–80.

Conflict of Interest Statement: The authors declare that the research was conducted in the absence of any commercial or financial relationships that could be construed as a potential conflict of interest.

Received: 29 June 2011; accepted: 28 September 2011; published online: 14 October 2011.

Citation: Pleil KE, Cordes S, Meck WH and Williams CL (2011) Rapid and acute effects of estrogen on time perception in male and female rats. Front. Integr. Neurosci. ***5****:63. doi: 10.3389/fnint.2011.00063*

frontiers in
INTEGRATIVE NEUROSCIENCE

REVIEW ARTICLE
published: 18 October 2011
doi: 10.3389/fnint.2011.00064

Unwinding the molecular basis of interval and circadian timing

Patricia V. Agostino*[1], *Diego A. Golombek*[1] *and Warren H. Meck*[2]

[1] *Laboratorio de Cronobiología, Departamento de Ciencia y Tecnología, Universidad Nacional de Quilmes, Buenos Aires, Argentina*
[2] *Department of Psychology and Neuroscience, Duke University, Durham, NC, USA*

Edited by:
Agnes Gruart, University Pablo de Olavide, Spain

Reviewed by:
John F. Araujo, Federal University of Rio Grande do Norte, Brazil
Olga V. Sysoeva, Washington University in St Louis School of Medicine, USA

***Correspondence:**
Warren H. Meck, Department of Psychology and Neuroscience, Duke University – Box 91050, 572 Research Drive, Durham, NC 27708-0086, USA.
e-mail: meck@psych.duke.edu

Neural timing mechanisms range from the millisecond to diurnal, and possibly annual, frequencies. Two of the main processes under study are the interval timer (seconds-to-minute range) and the circadian clock. The molecular basis of these two mechanisms is the subject of intense research, as well as their possible relationship. This article summarizes data from studies investigating a possible interaction between interval and circadian timing and reviews the molecular basis of both mechanisms, including the discussion of the contribution from studies of genetically modified animal models. While there is currently no common neurochemical substrate for timing mechanisms in the brain, circadian modulation of interval timing suggests an interaction of different frequencies in cerebral temporal processes.

Keywords: circadian system, interval timing, cortico-striatal circuits, suprachiasmatic nuclei, dopamine, glutamate, serotonin

INTRODUCTION

Timing is crucial to all aspects of our lives. Indeed, biological timing includes diverse time-related mechanisms that encompass several orders of magnitude (Hinton and Meck, 1997; Buhusi and Meck, 2005, 2009b; Buonomano and Laje, 2010). Besides interval timing (in the seconds-to-minutes range), most – if not all – organisms exhibit daily and circadian rhythms with periods of ca. 24 h, which also serve as the basis for seasonal-encoding mechanisms and might be related to lifespan-related processes. In particular, timing oscillators in the fast (seconds–minutes) and medium (circadian) frequencies might share some properties, including common steps in molecular pathways that lead to the neurochemical basis of such mechanisms. There is evidence suggesting that circadian pacemakers may influence the rate of the interval timer; however, these relationships have not been elucidated, neither at the behavioral nor the molecular level. The major terms relevant to this discussion are defined in the glossary provided in **Table 1**.

CIRCADIAN TIMING

The circadian clock is a self-sustained biological oscillator with a period close to 24 h in constant conditions. Circadian clocks in nature are, however, rarely subjected to the constant conditions that allow a free-running oscillation. On the contrary, they are normally exposed to a rhythmic environment, so that appropriate signals (called *Zeitgebers*, from German *Zeit*, "time"; *geben*, "to give"), such as light, temperature, or food, synchronize its oscillation (Golombek and Rosenstein, 2010). Thus, the circadian system consists of three main components: (i) an input pathway integrating external signals to adjust circadian phase and period, (ii) a central oscillator that generates the circadian signal, and (iii) an output pathway driving circadian periodicity of biological processes as illustrated in **Figure 1A**. Nevertheless, entrainment of the endogenous clock is not the only mechanism controlling the output rhythm. Most Zeitgebers not only entrain circadian rhythms by controlling the phase and period of the pacemaker, but also affect them directly; as a result, they "mask" the behavior of the pacemaker. Masking signals are able to bypass the central oscillator and to directly affect physiology and behavior (Mrosovsky, 1999). There could also be an adjustment of the rate of cycling by neural or endocrine output signals, which define a feedback pathway from rhythms to the clock. This behavioral feedback occurs, for example, with spontaneous locomotor activity (Mistlberger and Holmes, 2000).

MOLECULAR MECHANISMS OF CIRCADIAN OSCILLATION

The molecular mechanism of the endogenous circadian clock is comprised of interlocking feedback loops composed of cycling gene products that control transcription by means of negative and positive regulation of clock genes and proteins (Reppert and Weaver, 2002; Takahashi et al., 2008). Post-transcriptional regulation of clock proteins plays an important role in rhythm generation and entrainment; mutations in key protein kinases have been shown to affect the circadian machinery (Lowrey et al., 2000; Gallego and Virshup, 2007). This cycling molecular framework can also control the transcription of other genes by acting upon specific elements in their promoter regions, such as E-boxes.

In mammals, the transcription factors CLOCK and BMAL1 have been described as positive regulators whereas PERIOD (PER1 and 2) as well as CRYPTOCHROME (CRY1 and 2) proteins provide negative regulatory functions (Reppert and Weaver, 2002). The transcription of PER and CRY is stimulated by the CLOCK–BMAL1 heterodimer bound to the E-box enhancer as illustrated in **Figure 1B**. In turn, PER and CRY proteins are translocated into the nucleus, bind to the BMAL1–CLOCK heterodimer thereby inhibiting their own transcription. The controlled degradation of PER and CRY proteins by the ubiquitin pathway (signaled by

Table 1 | Glossary of timing terms.

Interval timing	Typically defined at the discrimination of durations in the seconds-to-minutes range, but can be extended to both shorter (e.g., milliseconds) and longer (e.g., hours) ranges. Interval timing is less precise than circadian timing, but has an advantage in increased flexibility in that it can run, stop/pause, and reset on command (Gibbon et al., 1997; Buhusi and Meck, 2005). Although the suprachiasmatic nucleus appears unnecessary for interval timing (Lewis et al., 2003), time-of-day effects have been observed for the timing of auditory and visual signals in the seconds-to-minutes range (Meck, 1991; Lustig and Meck, 2001; Agostino et al., 2011). To date, five main types of cognitive and affective factors have been identified that influence interval timing: attention, modality, arousal, affective valence, and linguistic factors (Gibbon et al., 1997; Buhusi and Meck, 2005), all of which can be modulated by circadian rhythms (Shurtleff et al., 1990; Hinton and Meck, 1997; Buonomano, 2007).
Scalar property/Weber's law	The scalar property is one of the hallmark signatures of interval timing. It describes the linear relationship between target durations and the standard deviation (SD) of duration judgments, indicating that variability in timing behavior grows proportional to the mean of the interval being estimated. In this sense, duration discrimination is relative rather than absolute, i.e., time perception is like a rubber band that can be stretched in order to produce time scale invariance across different durations (Gibbon et al., 1997; Matell and Meck, 2000; Bateson, 2003; Buhusi and Meck, 2005; Cheng and Meck, 2007; Buhusi et al., 2009).
Circadian rhythms	The circadian clock is a self-sustained biological oscillator with a period near to 24 h. In mammals, the circadian pacemaker is located in the suprachiasmatic nuclei (SCN) of the hypothalamus, and the principal signal that adjusts its activity is the light–dark cycle (Morin and Allen, 2006; Golombek and Rosenstein, 2010).
Clock genes	The so-called *clock genes* generate a molecular oscillation of gene expression, which is regulated transcriptionally and posttranslationally by positive and negative feedback loops. Within these loops positive factors induce the transcription of E-box-containing clock genes, which in turn down regulate the activity of the positive factors.

phosphorylation through casein kinase Iε/δ) decreases their protein levels and contributes to the oscillation of their mRNA and protein levels. Other posttranslational regulations (e.g., acetylation) also undergo circadian changes (Hirayama et al., 2007). The consequences of protein modification include alterations in activity, subcellular localization, protein–protein interactions, and protein stability. Moreover, additional stabilizing feedback loops, including inhibition of Bmal1 transcription by REV-ERBα (Preitner et al., 2002) further contribute to the timing and robustness of the cycle.

The output of circadian rhythms is coordinated by the expression of another set of genes called clock-controlled genes (CCGs). The pathways that control circadian rhythmicity in mammals have been closely studied using genetically modified animals (see **Table 2** for a description of the behavioral phenotypes of different mutant mice).

THE LIGHT-ENTRAINABLE OSCILLATOR

In mammals, many daily physiological and behavioral rhythms are generated by a master pacemaker located in the suprachiasmatic nuclei (SCN) of the hypothalamus. The most powerful synchronizer or Zeitgeber known is the daily light/dark cycle which entrains and modulates the light-entrainable oscillator (LEO). Light stimulates a group of photosensitive retinal ganglion cells that contain the photopigment melanopsin (Panda et al., 2002) and project to the SCN through the retinohypothalamic tract. Glutamate and pituitary adenylate cyclase activating polypeptide (PACAP) are the primary neurotransmitters responsible for mediating the synchronizing properties of light, and act upon NMDA, AMPA/kainate receptors for glutamate, and the PACAP-specific receptor (PAC1). This leads to an increase of the intracellular concentrations of Ca^{2+}, which initiates a signal transduction cascade in SCN neurons that ultimately results in a phase shift of the circadian system (Golombek et al., 2003, 2004; Morin and Allen, 2006; Golombek and Rosenstein, 2010). Moreover, the mGluR5 and mGluR2/3 metabotropic glutamate receptors have been shown to exert both positive and negative modulation of circadian activity rhythms as a function of the phase of the light/dark cycle (Gannon and Millan, 2011).

Exposure to light pulses at night synchronizes the LEO by inducing phase delays during the early night and phase advances during the late subjective night (i.e., when under constant conditions the animal behaves as if it were the night), led by diverse signal transduction pathways which ultimately rely on the activation of transcription factors such as CREB and clock genes (Lowrey and Takahashi, 2000). During the late night, when light induces phase advances of behavioral rhythms, photic stimulation specifically activates the guanylyl cyclase (GC)/cGMP/cGMP-dependent kinase (PKG) pathway (Golombek et al., 2004; Agostino et al., 2007). Therefore, the accessibility of specific signaling pathways is fundamental for regulation of circadian timing.

FOOD-ENTRAINABLE OSCILLATORS

The discovery of clock gene expression in brain regions outside of the SCN has suggested the temporal control of motivated behaviors independent of such nuclei. In nocturnal rodents, for example, natural feeding occurs principally during the night. In experimental conditions, when access to food is restricted to a few hours during the day, animals become active in anticipation of mealtime. In response to food stimulation, there are also phase advances of the circadian rhythms of gene expression in the liver, kidney, heart, pancreas, and other tissues, as well as in some brain structures, uncoupling them from the control by the SCN whose entrainment to light remains intact (Mendoza, 2007). All these data suggest that peripheral clocks within and outside of the brain are affected by restricted feeding schedules (Feillet et al., 2006a; Balsam et al., 2009).

It has been shown that food-anticipatory activity (FAA) is still present in SCN-ablated animals (Stephan, 2002). FAA is expressed in wheel running, general activity, feeder approaches,

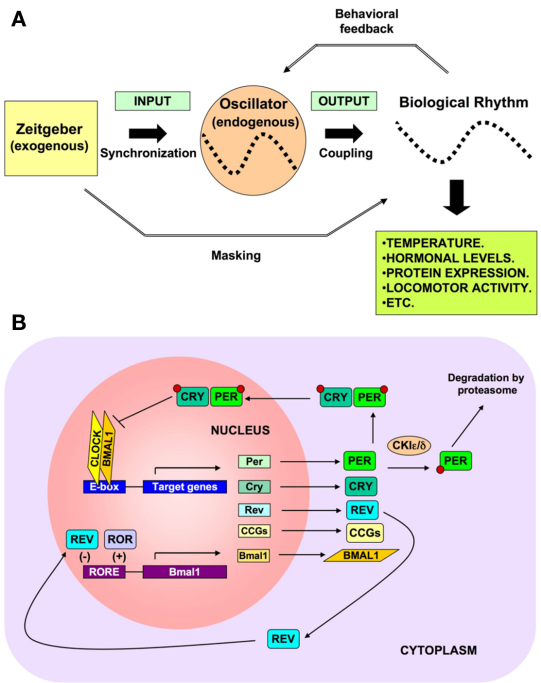

FIGURE 1 | (A) Main components of the circadian timing system. Circadian rhythms consists of three main components: (i) an input pathway integrating exogenous signals to synchronize circadian phase and period, (ii) a central oscillator that generates the endogenous circadian signal, and (iii) an output pathway driving circadian periodicity and coupling of biological processes. **(B)** Molecular mechanisms of circadian timing. The molecular mechanisms of circadian rhythms can be illustrated by the transcription of the Period (Per1and Per2) and Cryptochrome (Cry1, Cry2) genes that are activated by heteromeric complexes containing CLOCK and BMAL1 proteins that act through the E-box regulatory sequences of their target genes. The newly synthesized PER and CRY proteins are translocated into the nucleus, where they inhibit BMAL1–CLOCK activity, and therefore, their own transcription. Clock and Bmal1 both contain basic helix–loop–helix (bHLH) motifs for DNA binding at their N-terminus and Per–Arnt–Sim (PAS) domains. The controlled degradation of PER and CRY proteins by the ubiquitin pathway decreases their protein levels and results in an oscillation of their mRNA and protein levels. During this negative transcriptional feedback loop many of the clock proteins become posttranslationally modified by phosphorylation and ubiquitination (Reppert and Weaver, 2002). This core oscillation is augmented and stabilized by a secondary loop involving two orphan nuclear receptor proteins, REV-ERBα and RORA. Both are activated in phase with the Per and Cry genes by CLOCK and BMAL1, but in turn they affect Bmal1 expression (Preitner et al., 2002). While RORA has a positive role, REV-ERBα is a suppressor of Bmal1, and they coordinate action through RORE regulatory sequences. A positive feedback loop is built by the stimulated transcription of BMAL1 by PER2. Protein phosphorylation events are essential contributors to these feedback loops. Two members of the casein kinase I family (CKIε and CKIδ) phosphorylate PER proteins in order to (i) target them for ubiquitin-mediated proteasomal degradation, and (ii) modulate their nuclear import. A mutation of CKIε shortens rhythm in hamsters (Lowrey et al., 2000) and a mutation of CKIδ shortens rhythm in humans (Xu et al., 2005). The result of these complex regulatory pathways is that the mRNA and protein levels of most circadian genes – except Clock and CKIε – oscillate with a 24-h period. Importantly, the CLOCK–BMAL1 heterodimer regulates the transcription of many clock-controlled genes (CCGs), which in turn influence a wide array of physiological functions external to the oscillatory mechanism. This mediates the output function of the clock, thereby controlling food intake, hormonal synthesis and release, body temperature, metabolism, and many other functions.

and unreinforced bar pressing in an operant chamber. Moreover, some physiological parameters entrained to restricted feeding are still present after SCN lesions, suggesting the presence of an additional circadian oscillator. The food-entrainable oscillator (FEO) displays clear circadian characteristics. One of the most important of these is that its behavioral output (FAA) persists in the absence of food, suggesting that the FEO is able to generate a sustained free-running rhythm (Stephan, 2002).

The circadian mechanism of the FEO at the molecular level is not clear. Moreover, mice with mutations of clock genes are able to entrain activity rhythms to restricted feeding, suggesting there are alternative molecular pathways related to this kind of non-photic entrainment (Mendoza, 2007; see **Table 2**). On the other hand, the reward value of food and its motivational properties are important in entrainment. Mendoza et al. (2005) have observed entrainment of the rat SCN by a palatable meal (chocolate) without food deprivation. This entrainment effect was evident in the circadian rhythm of locomotor activity, a relevant output of the SCN. Their results indicate that the SCN can be entrained by palatable food without undergoing a chronic energy deprivation, probably due to the high level of arousal produced in such conditions.

A crucial role of the dorsomedial hypothalamic (DMH) nucleus has been reported for the FAA expression. In mice, the DMH exhibits little or no mPer1 or mPer2 expression when food is freely available, but strong circadian expression when food is restricted to a limited time of day (Mieda et al., 2006). In rats, neurotoxic lesions destroying 75% to 90% of DMH neurons strongly attenuate food-anticipatory rhythms of locomotion and EEG-defined waking, as well as eliminate the pre-meal rise in core body temperature evident in intact animals (Gooley et al., 2006). However, it was found that rats sustaining complete ablation of the DMH were capable of essentially normal FAA rhythms (Landry et al., 2007). Therefore, it remains to be elucidated which brain structures are necessary for the generation and persistence of food-anticipatory circadian behavioral rhythms. Interestingly, it was recently suggested that the functional model for the FEO is a network of interconnected brain structures entrained by fluctuation of different humoral factors (Carneiro and Araujo, 2009; Aguilar-Roblero and Diaz-Muñoz, 2010). In this sense, a distributed system arranged in a non-hierarchical manner to control FAA has been proposed. Moreover, it has also been reported that regulators of G protein signaling are involved in both the LEO and FEO circadian systems, suggesting a common mechanism of interaction (Hayasaka et al., 2011).

THE CIRCADIAN INFLUENCE ON REWARD-RELATED BEHAVIOR

Results from Roybal et al. (2007) indicate that the central transcriptional activator of molecular rhythms, CLOCK, has an important role in the ventral tegmental area (VTA) in regulating dopaminergic activity, locomotor activity, and anxiety. Moreover, several genes involved in dopaminergic signaling are differentially regulated in the VTA of the *Clock* mutant mice, suggesting that CLOCK affects the transcription of these genes through its actions in this brain region. Several findings support a role for the SCN in controlling distal reward circuitry, perhaps via its influence on rhythmic dopaminergic neurotransmission within mesolimbic structures. Indeed, dopamine (DA) and its related metabolites and receptors exhibit daily fluctuations in their levels in different

Table 2 | Phenotypes of different mutant mice.

Genotype	Physiological and behavioral alterations	Circadian phenotype	FAA[a]	Interval timing
Clock$^{-/-}$ mice	Metabolic and sleep patterns; drugs sensitization	Longer period/arrhythmic (Vitaterna et al., 1994)	Normal (Pitts et al., 2003)	Normal (Cordes and Gallistel, 2008)
Per1$^{-/-}$ mice	Drug sensitization; cancer development	Shorter period (Zheng et al., 2001)	Normal (Feillet et al., 2006b)	Unknown
Per2$^{-/-}$ mice	Drugs sensitization and alcohol consumption; cancer development	Shorter period/arrhythmic (Zheng et al., 2001)	Absent (Feillet et al., 2006b)	Unknown
Cry1$^{-/-}$/Cry2$^{-/-}$ mice	Without phenotypic abnormalities (van der Horst et al., 1999)	Arrhythmic under constant conditions (van der Horst et al., 1999)	Altered (Iijima et al., 2005)	Normal (Papachristos et al., 2011)
NPAS2$^{-/-}$ mice	Sleep and memory patterns	Shorter period (Dudley et al., 2003)	Delayed (Dudley et al., 2003)	Unknown
Bmal1$^{-/-}$ mice	Sleep and metabolic patterns; infertility	Arrhythmic (Bunger et al., 2000)	Absent (Mendoza, 2007)	Unknown
DAT$^{-/-}$ mice	Hyperactivity and learning impairment; insensitive to psychostimulants	Normal photoentrainment, altered amplitude in circadian body temperature (Vincent et al., 2007)	Unknown	Complete loss of temporal control (Meck et al., 2011)
DAT$^{+/-}$ mice	Insensitive to psychostimulants	Unknown	Unknown	Reduced sensitivity to clock-speed effects of MAP[e] (Meck et al., 2011); overestimation of duration (Cevik, 2003)
Knockdown DAT$^{-/-}$ mice	Hyperactivity; impaired response habituation in novel environments	Unknown	Unknown	Overestimation of duration (Balci et al., 2009, 2010)
D2R transgenic mice	Impairment in tasks that require working memory and behavioral flexibility	Unknown	Unknown	Impairment in timing accuracy and precision (Drew et al., 2007)
Vipr2$^{-/-}$ mice[b]	No differences from wild-type littermates	Arrhythmic (Sheward et al., 2007)	Normal (Sheward et al., 2007)	Unknown
NET$^{-/-}$ mice	Reduced spontaneous locomotor activity; supersensitive to psychostimulants	Unknown	Unknown	Normal (Drew et al., 2007)
Orexin$^{-/-}$ mice	Abnormal sleep homeostasis	Normal entrainment of activity and temperature to a restricted feeding schedule (Kaur et al., 2008)	Reduced (Kaur et al., 2008)	Unknown
PROT$^{-/-}$ mice[c]	Normal motor ability; impairment in spatial memory (Meck, 2001)	Unknown	Unknown	Impairment in timing accuracy and precision (Meck, 2001)
GRPR$^{-/-}$ mice[d]	Enhanced fear conditioning (Shumyatsky et al., 2002)	Unknown	Unknown	Normal (Balci et al., 2008)

[a] *FAA, food-anticipatory activity.*

[b] *Vipr2, gene encoding the VIP (vasoactive intestinal peptide) receptor VPAC2.*

[c] *PROT, proline transporter.*

[d] *GRPR, gastrin-releasing peptide receptor.*

[e] *MAP, methamphetamine.*

brain regions (Kafka et al., 1986). Furthermore, most elements of dopaminergic transmission have a diurnal rhythm in striatal regions, including the expression of the DA transporter (DAT), DA receptors, and the rate-limiting enzyme in DA synthesis, tyrosine hydroxylase (TH; McClung, 2007). Administration of haloperidol has been found to increase expression levels of clock genes involved in the transcriptional feedback loop responsible for circadian rhythms, both *in vivo* and in cultured SCN cells (Viyoch

et al., 2005). McClung et al. (2005) reported that *Clock* mutant mice reveal increased dopaminergic function, suggesting that the CLOCK protein plays a part in regulating the transmission of DA in the brain.

The role of the SCN as a synchronizer or driver of oscillators outside the hypothalamus is well established, and many brain regions implicated in cocaine-seeking behavior also contain molecular clocks. Circadian fluctuations in extracellular DA levels in the striatum and nucleus accumbens have been described (Castaneda et al., 2004). Furthermore, identification of specific clock binding elements (E-boxes) within the promoter regions of the DAT, D1A receptor, and TH genes supports the existence of an interaction between circadian clocks and dopaminergic neurotransmission. Indeed, it was recently discovered that the SCN is at least partially responsible for the presence of normal day/night differences in DAT and TH protein expression in the nucleus accumbens, mPFC, and caudate (Sleipness et al., 2007a), as well as for the day/night variation in cocaine-seeking behavior in rats (Sleipness et al., 2007b).

INTERVAL TIMING

The perception of time in the seconds-to-minutes range, referred to as interval timing, is involved in foraging, decision making and multiple-step arithmetic, and has been demonstrated in birds, fish, rodents, primates, and human infants and adults. The psychophysics of interval timing in humans and other animals has been studied extensively (Gibbon, 1977; Gibbon et al., 1984a, 1997; Allen and Gibbon, 1991; Penney et al., 2008). One consistent feature of the behavioral data is that the variability in timed responses increases in direct proportion to the duration of the interval timed, such that the coefficient of variation (the ratio of the SD to the mean response) is a constant, i.e., variability exhibits a scalar property (Gibbon et al., 1997; Buhusi and Meck, 2005). Much closer examinations of timing data across a broad range of closely spaced intervals however, reveal occasional yet systematic departures from scalar variability. These findings have led some to argue that interval timing depends not on a linear accumulator, but rather on a series of biological oscillators with different periods (Crystal, 2003; Crystal and Baramidze, 2007). If it is the case that multiple biological oscillators are responsible for interval timing, then the molecular mechanisms underlying these oscillators may share components with the circadian oscillator. In fact, a Multiple-Oscillator model of interval timing in which entrainment and selection of an appropriate range of oscillators from a series with periods potentially spanning milliseconds to years has been proposed. In this case, time is represented by the phase of the selected oscillators and non-linearities will occur to the extent that these oscillators are non-overlapping (Church and Broadbent, 1990).

Recent neurophysiological modeling of interval timing proposes that temporally coding neural inputs arise from the electrical activity of large areas of the cortex (Buhusi and Meck, 2005; Coull et al., 2011; Oprisan and Buhusi, 2011). The frontal cortex in particular contains neurons that oscillate at different rates (5–15 Hz) and striatal spiny neurons that receive their synaptic input from the cortex can monitor the oscillatory patterns of cortical neural activity. According to the striatal beat frequency (SBF) model of interval timing (Matell and Meck, 2004; Lustig et al., 2005; Allman and Meck, 2011; Coull et al., 2011), coincidence detection in the striatum results in the identification of a pattern of oscillatory firings or beats (i.e., similar to a musical chord) among other beats that represent noise or unrelated information. The probability that a particular "chord" will be identified as a signal increases as the number of detectors that simultaneously respond to such beats increases. In the SBF model, signal durations are translated into a particular cortical pattern or "chord" formed by the firing of multiple neurons with different rates of oscillations. Such a coding scheme ensures that a large number of specific supra-second intervals can be produced by the integration of a limited number of primitives represented by different sub-second oscillation frequencies in the cortex. The relevant anatomical connections, neurotransmitters systems, and signal transduction pathways specified by the SBF model of interval timing are illustrated in **Figure 2A**. In comparison with traditional pacemaker/accumulator models of interval timing (Meck, 1996; Matell and Meck, 2000) where DA is assumed to be the neurobiological substrate of the pacemaker pulses, in the SBF model the role of DA is assumed to act as a "start gun" by indicating the onset of a relevant signal – leading to the synchronization of cortical oscillations and the resetting of the membrane properties of the striatal spiny neurons. Consequently, this initial DA pulse coincides with the "closing of the switch" to begin timing and later, at the end of the interval, a second DA pulse co-occurring with the delivery of reward serves to strengthen synaptic connections that are active within the striatum at the time of feedback – thereby building a "coincidence detector" for a specific signal duration (Matell et al., 2003; Matell and Meck, 2004).

MOLECULAR BASIS OF INTERVAL TIMING

The molecular mechanisms supporting the various ways in which humans and other animals time intervals measured in seconds-to-minutes remain poorly understood (Buonomano, 2007).

Some of the mechanisms believed to be involved in interval timing, including neurotransmitter receptors and signal transduction pathways, are outlined in **Figure 2B**. Signaling by DA, which activates both D1- and D2-like receptors, is involved in the regulation of the timing speed, since DA receptor agonists or antagonists are able to shift the perception of the signal duration (Meck, 1996; Williamson et al., 2008; Coull et al., 2011). Strong activation of cortical glutamate-releasing afferent axons results in release of glutamate in the striatum, postsynaptic depolarization, and elevation of intracellular Ca^{2+} levels in the medium spiny neurons. Activation of NMDA-type glutamate receptors (NMDARs) is also important for interval timing mechanisms (Cheng et al., 2006, 2007a; Coull et al., 2011; Hata, 2011). These signaling pathways might lead to the activation of the cAMP-regulated phosphoprotein of 32 kDa (DARPP-32) and the cyclic-AMP-response element binding protein (CREB), which in turn interact with specific substrates to regulate temporal control of behavior. It has been proposed that a shift from subcortical-DA-dependent mechanisms to cortical-Glu-dependent mechanisms occurs as a function of the amount of training and mGluR2/3 activation (Cheng et al., 2006, 2007a,b; Bhave et al., 2008). Moreover, a postsynaptically released endocannabinoid (EC) could act as a retrograde messenger, and

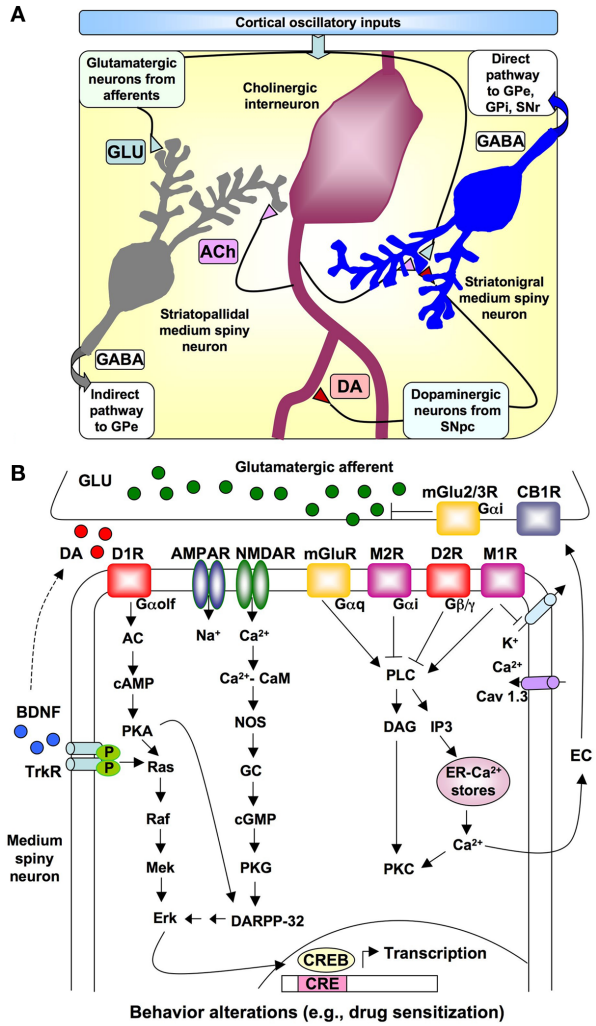

FIGURE 2 | Relationships of different neurons in the striatum and neurotransmitter signaling involved in interval timing. (A) Schematic representation of the relationship among oscillatory cortical inputs, medium spiny neurons, cholinergic interneurons, glutamatergic afferents, and dopaminergic axons projecting from the substantia nigra pars compacta (SNpc) to the striatum as specified by the Striatal Beat Frequency model of interval timing. The direct output pathway to the globus pallidus – external (GPe) and internal (GPi) segments, and substantia nigra reticulata (SNr) as well as the indirect pathway to the GPe are indicated. Relevant neurotransmitters = acetylcholine (ACh), dopamine (DA), γ-aminobutyric acid (GABA), glutamate (GLU). **(B)** Detail of dopaminergic, glutamatergic, and cholinergic input to a striatonigral medium spiny neuron as well as the principal signal transduction pathways modulating the contribution of striatal spiny neurons to interval timing. Abbreviations: AC, adenyl cyclase; ACh, acetylcholine; AMPAR, AMPA receptor; CB1, cannabinoid receptor type 1; CRE, cyclic-AMP-response element; CREB, CRE binding protein; DA, dopamine; DAG, 1,2-diacylglycerol; DARPP-32, camp-regulated phosphoprotein of 32 kDa; D1R, dopamine D1 receptor; D2R, dopamine D2 receptor; EC, endocannabinoids; GABA, γ-aminobutyric acid; Glu, glutamate; GP, globus pallidus; IP3, inositol 1,4,5 trisphosphate; M1R, muscrinic acetylcholine receptor 1; M2R, muscarinic acetylcholine receptor 2; mGluR, metabotropic glutamate receptor; NMDAR, *N*-methyl-D-aspartic acid receptor; NOS, nitric oxide synthase; PKA, protein kinase A; PKC, protein kinase C; SNpc, substantia nigra pars compacta; SNr, substantia nigra pars reticulata; STN, subthalamic nucleus; TrKR, tyrosine kinase receptor.

lead CB1 cannabinoid receptor inhibition of synaptic release of glutamate in the dorsolateral striatum (Gerdeman and Lovinger, 2001; Hilário et al., 2007).

In addition, recent studies of molecular genetics have demonstrated the importance of specific DA regulators on cognitive functioning. Among them, promising candidates are the DRD2/ANKK1-Taq1a, which is a D2 receptor polymorphism associated with decreased D2 density in the striatum, and the genes regulating the Catechol-*O*-methyltransferase (COMT) enzyme, – which degrades catecholamines in the frontal cortex (reviewed in Savitz et al., 2006). The most frequently studied of these COMT-related genes is COMT Val158Met, due to its natural allelic variation in humans. The Val158Met polymorphism is a valine-to-methionine conversion that occurs within the COMT gene, affecting the enzymatic activity of the COMT enzyme. Importantly, these polymorphisms – DRD2/ANKK1-Taq1a and COMT Val158Met – have been shown to be correlated with the variability for the timing of specific durations (e.g., 500 and 2,000 ms standards) as well as the determination of preferred tempos (Wiener et al., 2011). In another study related to the COMT Val158Met polymorphism and timing, it was found that subjects carrying the VAL allele (VAL/VAL, VAL/MET) showed a significant speed up of the internal clock in comparison to carriers without the VAL allele (MET/MET) in a second production task (Reuter et al., 2005). Moreover, a study conducted on synchronous swimmers showed that individual differences in the COMT polymorphism were associated with the reproduction of short time intervals (<2 s). Thus, the carriers of MET/MET polymorphism over-reproduced 1–2 s durations in a duration reproduction task (Portnova et al., 2007). Furthermore, polymorphisms in genes coding for serotonin (5-HT) availability in the cell (5HTT, MOAO, and 5HT2a) showed association with the "loss rate" of duration representations (Sysoeva et al., 2010), which can be related to the properties of interval timing, such as clock-speed and/or rate of decay of the clock reading (Buhusi and Meck, 2009a; Coull et al., 2011).

WHAT TYPES OF CIRCADIAN INFLUENCE ARE THERE ON INTERVAL TIMING?

There are a variety of similarities between interval and circadian timing at the behavioral level to suggest a possible shared molecular basis. As described above, animals use both interval and circadian timing in complementary ways to anticipate the temporal regularity of daily feedings (Terman et al., 1984); as a particular example, such mechanisms are needed to estimate the amount of time that a female ringdove spends sitting on its nest and when it is time for the male ringdove to take over (Gibbon et al., 1984b). Time-of-day effects have been observed for the timing of auditory and visual signals in the seconds-to-minutes range (Aschoff, 1985; Chandrashekaran et al., 1991; Meck, 1991; Pati and Gupta, 1994; Kuriyama et al., 2005). For example, the accuracy for the reproduction of short durations varies with the circadian cycle, such that reproductions are longer at night and in the morning than in the middle of the day (Aschoff, 1998b), while the differential allocation of attention to auditory and visual signal durations covaries as a function, among other variables, of circadian phase (Lustig and Meck, 2001). When humans live in isolation with no external time cues, their perception of the

duration of an hour is highly correlated with τ (tau), their mean circadian period (Aschoff, 1984). In contrast, the production of short intervals within the range of 10- to 20-s is neither correlated with the subject's 1-h time estimates or with the duration of wake time (Aschoff, 1985, 1998a). Nevertheless, the remembered time of reinforcement in the peak-interval procedure using target durations in the seconds-to-minutes range has been shown to exhibit photoperiodic variation in a manner similar to that previously observed for reproductive function in rodents (MacDonald et al., 2007). Consistent with this finding, a circadian rhythm in time estimates was documented in control subjects, but was found to be disrupted in shift workers (Pati and Gupta, 1994). It has also been reported that sleep deprivation influences diurnal variation of time estimation in humans (Soshi et al., 2010). In *Drosophila melanogaster*, for example, the timing of short intervals is disrupted in circadian mutants (Kyriacou and Hall, 1980). Moreover, rats exhibit circadian variations in time perception similar to those that have been demonstrated in humans (Shurtleff et al., 1990; Meck, 1991). Recently, significant differences in the estimation of 24-s intervals at different times of day were reported in mice (Agostino et al., 2011). These differences were maintained under constant dark (DD) conditions. Interval timing was also impaired in mice under constant light (LL) conditions, which abolish circadian rhythmicity. Taken together, these results suggest that time estimation in the seconds-to-minutes range may be modulated by the circadian clock (Meck, 1991; Hinton and Meck, 1997). It is important to note that circadian effects on interval timing might also be mediated not directly through the endogenous clock, but also by changes in external stimulation [such as the light–dark (LD) cycle, access to food, temperature, etc.]. In particular, alterations of time perception in shift workers (as well as what could happen in other conditions of circadian disruption) might also be related to changes in anxiety and stress, as well as the relative sleep deprivation state that accompanies these types of work schedules (Åkerstedt, 2003).

An obvious question is whether the orchestration of interval timing with circadian rhythms shares at least part of their molecular machinery. The accurate timing in seconds, minutes, hours, and days allows foraging animals not only to calculate their rate of return and gage a safe length of time before competitors or predators appear, but also to set a temporal horizon before going to sleep or making decisions about future events (Bateson, 2003; Rosati et al., 2007). Two recent studies using mutant and *knockout* mice, however, indicate that interval and circadian timing are relatively independent at the molecular level (Cordes and Gallistel, 2008; Papachristos et al., 2011). Cordes and Gallistel (2008) have reported intact interval timing in *Clock* mutant mice, which have previously been shown to have a point mutation in the *Clock* gene leading to inactive CLOCK proteins and impaired circadian timing. When housed in a 12:12-h LD cycle, *Clock* mutant mice entrain to the light cycle and maintain rhythmicity like their wild-type littermates. In complete darkness, however, heterozygotes have a longer rhythm than wild types (∼24.4 h, as compared with ∼23.3 h) while homozygotes maintain an even longer period (∼27.3 h), before losing rhythmicity within the first 5–15 cycles (Vitaterna et al., 1994). Consequently, Cordes and Gallistel (2008) trained *Clock* mutant mice and controls in a peak-interval timing procedure using 10 and 20-s visual signal durations in order to determine if expression of the *Clock* gene was necessary for normal interval timing. The results indicated no impairments in the timing of the 10- and 20-s signal durations across the three *Clock* genotypes. If anything, the data suggest that homozygous *Clock* mice are both more accurate and precise in timing short intervals as compared with their wild-type littermates – possibly due to an increased clock-speed resulting from enhanced dopaminergic function (McClung et al., 2005). It should be noted, however, that under the experimental conditions utilized by Cordes and Gallistel (2008), *Clock* mutant mice were constantly entrained to the LD cycle and therefore maintained normal rhythmicity much like their wild-type littermates. Because of this LD entrainment, it would be important to study the effects of a *Clock* mutation on interval timing either under DD or LL conditions during which the circadian clocks in heterozygous and homozygous mice could "free run" differentially as a function of the *Clock* genotype (see Vitaterna et al., 1994). Recently, Papachristos et al. (2011) trained Cry1/Cry2 double *knockout* mice on an interval timing task with durations that ranged between 3 and 27 s. Homozygous *knockouts* displayed an accurate and precise temporal memory similar to that of the control mice, suggesting that the Cry1 and Cry2 genes are not an important component of the interval timer. However, it should be noted that in this study interval timing was assessed in a different group of mice than the one used for the evaluation of circadian rhythmicity and, in addition, mice were fed once a day at the same time of day, therefore providing a potential temporal cue that might mask circadian rhythmicity and influence time perception in the seconds-to-minutes range (see Challet et al., 2003; Feillet et al., 2006a; Challet, 2007; Balsam et al., 2009; Steinman et al., 2011).

In general, these results suggest that expression of the *Clock* or *Cry* genes is not necessary for normal interval timing in the mouse. Although these findings suggest that interval and circadian timing are independent at the molecular level, other genes need to be explored in this regard, (e.g., *Period*). Moreover, more strict circadian paradigms need to be applied in order to clearly dissect the behaviors under study (including experiments under constant light or constant dark situations, as well as testing for additional memory tasks).

Rather than relying on common oscillatory mechanisms, the behavioral correlations observed between interval and circadian timing may be indicative of a different sort of relationship. Diverse lines of evidence suggest functional links among mesolimbic, nigrostriatal, and mesocortical dopaminergic systems (Meck, 1983, 1996, 2006a,b; Gu et al., 2011). For example, pharmacological manipulations indicate that cortico-striatal DA levels regulate the speed of the interval timer, as administration of indirect DA agonists such as cocaine and methamphetamine produce a proportional leftward shift of timing functions (i.e., speeds up the interval timer; Meck, 1983, 1996; Matell et al., 2004, 2006), while DA receptor blockers such as haloperidol and raclopride produce the opposite effect (Meck, 1983, 1986, 1996; Drew et al., 2003; MacDonald and Meck, 2004, 2005, 2006). The D2 receptor has been identified as being critical to the mediation of these pharmacological effects (Meck, 1986; MacDonald and Meck, 2006) and transient overexpression of striatal D2 receptors impairs the

acquisition of temporal control in a 24-s peak-interval procedure (Drew et al., 2007). In addition, deletion of the DAT gene, but not the norepinephrine transporter (NET) gene, abolishes the ability to discriminate supra-second durations in homozygous mice and leads to a decreased sensitivity to the clock-speed enhancing effects of methamphetamine in the heterozygous mice, indicating that excess levels of DA "flood" the temporal integration process and impair interval timing (Meck et al., 2011). Likewise, lesions of the DA/DAT rich areas such as the substantia nigra pars compacta and dorsal striatum lead to decreased levels of DA and impairments in supra-second timing in both humans and rats (Malapani et al., 1998; Meck, 2006b; Coull et al., 2011). Moreover, electrophysiological recordings from striatal spiny neurons that receive both dopaminergic and glutaminergic inputs show them to be involved in the coding of durations in the seconds-to-minutes range (Matell et al., 2003; Cheng et al., 2007a; Chiba et al., 2008; Meck et al., 2008). The dopaminergic–glutamatergic pathways that modulate interval timing in mammals are outlined in **Figure 2A**, whereas studies using genetically modified mice to explore the molecular basis of circadian and interval timing are outlined in **Table 2**.

OPEN QUESTIONS ABOUT TIMING MECHANISMS

Behaviorally, interval timing and reward prediction have been demonstrated across various vertebrate models of learning, including humans, primates, rodents, birds, and fish, as well as invertebrate models, such as *Drosophila melanogaster* and *Caenorhabditis elegans* (Lejeune and Wearden, 1991; Hills, 2003; Penney et al., 2008). One structure of particular interest with regard to interval timing and reward prediction in vertebrates is the habenula, a well-conserved component of the epithalamus and a prominent structure in a model system such as zebrafish (Lee et al., 2010; Cheng et al., 2011). Importantly, zebrafish have an interesting asymmetry in habenula input, i.e., only the right habenula receives input from the forebrain (Hendricks and Jesuthasan, 2007). This asymmetry may provide an ideal situation for localizing timing and reward prediction mechanisms (Bromberg-Martin et al., 2010a,b). Investigation of the role of the habenula in neural circuits for the anticipation of reward has yet to be extended to zebrafish, and should prove worthwhile considering the emerging recognition of the importance of the habenula to cognition and behavior. Moreover, memory of time intervals in the order of seconds, for durations up to 20-s, has been observed in zebrafish larvae (Sumbre et al., 2008). Given that robust circadian rhythms in the locomotor activity of larval (10- to 15-day-old) zebrafish have been observed in constant lighting conditions, this model is likely to prove useful for mutational analyses of both vertebrate interval and circadian timing. In this and other animal models (certainly including mammals and, in particular, rodents), there are still some of outstanding questions to be addressed. For example, the exact molecular mechanisms underlying interval timing remain to be established. Moreover, the circadian modulation of interval timing is lacking a mechanistic explanation and a neuroanatomical substrate (or substrates). Finally, the neurochemical common nature of both processes and their interaction is also matter of controversy.

PERSPECTIVES ON FUTURE DIRECTIONS

While circadian modulation of interval timing may involve a variety of brain regions including the SCN, recent evidence suggests that this structure alone does not directly mediate the timing of short durations (Lewis et al., 2003). However, the SCN may nevertheless modulate circadian changes in interval timing. This modulation can be interpreted in terms of adaptation requirements, given that the same accuracy of time estimation might not be needed at all times throughout the daily cycle. Consistent with this account are the observations that time judgments in humans co-vary with normal circadian rhythms (Kuriyama et al., 2005) and are disrupted in shift workers (Pati and Gupta, 1994). Moreover, rats and mice exhibit circadian variations in time perception similar to those that have been demonstrated in humans (Shurtleff et al., 1990; Meck, 2001; Agostino et al., 2011).

In addition, both timing mechanisms might share a common link in terms of the regulation of arousal or motivational states. Indeed, acquisition of operant cycles of reinforcement, frequently used for the evaluation of interval timing, requires the activation of reward pathways in the brain, usually driven by food stimulation in partially deprived animals (Church and Lacourse, 2001). It is worth noting that at least some features of circadian entrainment (such as non-photic synchronization induced by forced locomotion, feeding or neurochemical stimulation by methamphetamine, and other agents) also depend upon reward-related mechanisms, including dopaminergic activation. Consequently, a common molecular basis related to dopaminergic function in cortico-striatal pathways appears to be the most promising link between interval and circadian timing.

In summary, it is clear that timing and time perception have been instrumental for adaptation to a cyclic and somewhat predictable environment. Endogenous timing mechanisms cover several orders of magnitude of event frequencies and could be interpreted as a continuum that extends from duration estimation in the seconds range to developmental and lifespan experiences on the order of years. Unwinding the molecular basis for these relationships should lead to a better understanding of the intricate labyrinths of cognitive and neural timing systems.

REFERENCES

Agostino, P. V., do Nascimento, M., Bussi, I. L., Eguía, M. C., and Golombek, D. A. (2011). Circadian modulation of interval timing in mice. *Brain Res.* 1370, 154–163.

Agostino, P. V., Plano, S. A., and Golombek, D. A. (2007). Sildenafil accelerates reentrainment of circadian rhythms after advancing light schedules. *Proc. Natl. Acad. Sci. U.S.A.* 104, 9834–9839.

Aguilar-Roblero, R., and Diaz-Muñoz, M. (2010). Chronostatic adaptation in the liver to restricted feeding: the FEO as an emergent oscillator. *Sleep Biol. Rhythms* 8, 9–17.

Åkerstedt, T. (2003). Shift work and disturbed sleep/wakefulness. *Occup. Med.* 53, 89–94.

Allen, L. G., and Gibbon, J. (1991). Human bisection at the geometric mean. *Learn. Motiv.* 22, 39–58.

Allman, M. J., and Meck, W. H. (2011). Pathophysiological distortions in time perception and timed performance. *Brain* doi:10.1093/brain/awr21

Aschoff, J. (1984). Circadian timing. *Ann. N. Y. Acad. Sci.* 423, 442–468.

Aschoff, J. (1985). On the perception of time during prolonged temporal isolation. *Hum. Neurobiol.* 4, 41–52.

Aschoff, J. (1998a). Carcadian parameters as individual characteristics. *J. Biol. Rhythms* 13, 123–131.

Aschoff, J. (1998b). Human perception of short and long time intervals: its correlation with body temperature and the duration of wake time. *J. Biol. Rhythms* 13, 437–442.

Balci, F., Ludvig, E. A., Abner, R., Zhuang, X., Poon, P., and Brunner, D. (2010). Motivational effects on interval timing in dopamine transporter (DAT) knockdown mice. *Brain Res.* 1325, 89–99.

Balci, F., Meck, W. H., Moore, H., and Brunner, D. (2009). "Timing deficits in aging and neuropathology," in *Animal Models of Human Cognitive Aging,* eds J. L. Bizon and A. Wood (Totowa, NJ: Humana Press), 161–201.

Balci, F., Papachristos, E. B., Gallistel, C. R., Brunner, D., Gibson, J., and Shumyatsky, G. P. (2008). Interval timing in genetically modified mice: a simple paradigm. *Genes Brain Behav.* 7, 373–384.

Balsam, P., Sanchez-Castillo, H., Taylor, K., van Volkinburg, H., and Ward, R. D. (2009). Timing and anticipation: conceptual and methodological approaches. *Eur. J. Neurosci.* 30, 1749–1755.

Bateson, M. (2003). "Interval timing and optimal foraging," in *Functional and Neural Mechanisms of Interval Timing*, ed. W. H. Meck (Boca Raton, FL: CRC Press), 113–141.

Bhave, S. R., Cheng, R. K., and Meck, W. H. (2008). "The metabotropic glutamate 2/3 receptor agonist LY379268 counteracts the clock-speed enhancing effects of cocaine," in *Society for Neuroscience*, Washington, 877.20.

Bromberg-Martin, E. S., Matsumoto, M., and Hikosaka, O. (2010a). Distinct tonic and phasic anticipatory activity in lateral habenula and dopamine neurons. *Neuron* 67, 114–155.

Bromberg-Martin, E. S., Matsumoto, M., Nakahara, H., and Hikosaka, O. (2010b). Multiple timescales of memory in lateral habenula and dopamine neurons. *Neuron* 67, 499–510.

Buhusi, C. V., Aziz, D., Winslow, D., Carter, R. E., Swearington, J. E., and Buhusi, M. C. (2009). Interval timing accuracy and scalar timing in c57BL/6 mice. *Behav. Neurosci.* 123, 1102–1113.

Buhusi, C. V., and Meck, W. H. (2005). What makes us tick? Functional and neural mechanisms of interval timing. *Nat. Rev. Neurosci.* 6, 755–765.

Buhusi, C. V., and Meck, W. H. (2009a). Relative time sharing: New findings and an extension of the resource allocation model of temporal processing. *Philos. Trans. R. Soc. Lond. B Biol. Sci.* 364, 1875–1885.

Buhusi, C. V., and Meck, W. H. (2009b). Relativity theory and time perception: single or multiple clocks? *PLoS ONE* 4, e6268. doi:10.1371/journal.pone.0006268

Bunger, M. K., Wilsbacher, L. D., Moran, S. M., Clendenin, C., Radcliffe, L. A., Hogenesch, J. B., Simon, M. C., Takahashi, J. S., and Bradfield, C. A. (2000). Mop3 is an essential component of the master circadian pacemaker in mammals. *Cell* 103, 1009–1017.

Buonomano, D. V. (2007). The biology of time across different scales. *Nat. Chem. Biol.* 3, 594–597.

Buonomano, D. V., and Laje, R. (2010). Population clocks: motor timing with neural dynamics. *Trends Cogn. Sci. (Regul. Ed.)* 14, 520–527.

Carneiro, B. T., and Araujo, J. F. (2009). The foo-entrainable oscillator: a network of interconnected brain structures entrained by humoral signal? *Chronobiol. Int.* 26, 1273–1289.

Castaneda, T. R., de Prado, B. M., Prieto, D., and Mora, F. (2004). Circadian rhythms of dopamine, glutamate and GABA in the striatum and nucleus accumbens of the awake rat: modulation by light. *J. Pineal Res.* 36, 177–185.

Cevik, M. O. (2003). "Neurogenetics of interval timing," in *Functional and Neural Mechanisms of Interval Timing,* ed. W. H. Meck (CRC Press), 297–316.

Challet, E. (2007). Clock genes, circadian rhythms and food intake. *Pathol. Biol.* 55, 176–177.

Challet, E., Caldelas, I., Graff, C., and Pévet, P. (2003). Synchronization of the molecular clockwork by light- and food-related cues in mammals. *Biol. Chem.* 384, 711–719.

Chandrashekaran, M. K., Marimuthu, G., Subbaraj, R., Kumarasamy, P., Ramkumar, M. S., and Sripathi, K. (1991). Direct correlation between the circadian sleep-wakefulness rhythm and time estimation in humans under social and temporal isolation. *J. Biosci.* 16, 97–101.

Cheng, R., Jesuthasan, S., and Penney, T. B. (2011). Time for Zebrafish. *Front. Integr. Neurosci.* 5:40. doi:10.3389/fnint.2011.00040

Cheng, R. K., Ali, Y. M., and Meck, W. H. (2007a). Ketamine "unlocks" the reduced clock-speed effects of cocaine following extended training: evidence for dopamine-glutamate interactions in timing and time perception. *Neurobiol. Learn. Mem.* 88, 149–159.

Cheng, R. K., Hakak, O. L., and Meck, W. H. (2007b). Habit formation and the loss of control of an internal clock: inverse relationship between the level of baseline training and the clock-speed enhancing effects of methamphetamine. *Psychopharmacology (Berl.)* 193, 351–362.

Cheng, R. K., MacDonald, C. J., and Meck, W. H. (2006). Differential effects of cocaine and ketamine on time estimation: implications for neurobiological models of interval timing. *Pharmacol. Biochem. Behav.* 85, 114–122.

Cheng, R. K., and Meck, W. H. (2007). Prenatal choline supplementation increases sensitivity to time by reducing non-scalar sources of variance in adult temporal processing. *Brain Res.* 1186, 242–254.

Chiba, A., Oshio, K., and Inase, M. (2008). Striatal neurons encoded temporal information in duration discrimination task. *Exp. Brain Res.* 186, 671–676.

Church, R. M., and Broadbent, H. A. (1990). Alternative representations of time, number, and rate. *Cognition* 37, 55–81.

Church, R. M., and Lacourse, D. M. (2001). Temporal memory of interfood interval distributions with the same mean and variance. *Learn. Motiv.* 32, 2–21.

Cordes, S., and Gallistel, C. R. (2008). Interval timing in circadian CLOCK mutants. *Brain Res.* 1227, 120–127.

Coull, J. T., Cheng, R. K., and Meck, W. H. (2011). Neuroanatomical and neurochemical substrates of timing. *Neuropsychopharmacology* 36, 3–25.

Crystal, J. D. (2003). "Nonlinearities in sensitivity to time: implications for oscillator-based representations of interval circadian clocks," in *Functional and Neural Mechanisms of Interval Timing*, ed. W. H. Meck (Boca Raton, FL: CRC Press), 61–76.

Crystal, J. D., and Baramidze, G. T. (2007). Endogenous oscillations in short-interval timing. *Behav. Processes* 74, 152–158.

Drew, M. R., Fairhurst, S., Malapani, C., Horvitz, J. C., and Balsam, P. D. (2003). Effects of dopamine antagonists on the timing of two intervals. *Pharmacol. Biochem. Behav.* 75, 9–15.

Drew, M. R., Simpson, E. H., Kellendonk, C., Herzberg, W. G., Lipatova, O., Fairhurst, S., Kandel, E. R., Malapani, C., and Balsam, P. D. (2007). Transient overexpression of striatal D2 receptors impairs operant motivation and interval timing. *J. Neurosci.* 27, 7731–7739.

Dudley, C. A., Erbel-Sieler, C., Estill, S. J., Reick, M., Franken, P., Pitts, S., and McKnight, S. L. (2003). Altered patterns of sleep and behavioral adaptability in NPAS2-deficient mice. *Science* 301, 379–383.

Feillet, C. A., Albrecht, U., and Challet, E. (2006a). "Feeding time" for the brain: a matter of clocks. *J. Physiol. Paris* 100, 252–260.

Feillet, C. A., Ripperger, J. A., Magnone, M. C., Dulloo, A., Albrecht, U., and Challet, E. (2006b). Lack of food anticipation in Per2 mutant mice. *Curr. Biol.* 16, 2016–2022.

Gallego, M., and Virshup, D. M. (2007). Post-translational modifications regulate the ticking of the circadian clock. *Nat. Rev. Mol. Cell Biol.* 8, 139–148.

Gannon, R. L., and Millan, M. J. (2011). Positive and negative modulation of circadian activity rhythms by mGluR5 and mGluR2/3 metabotropic glutamate receptors. *Neuropharmacology* 60, 209–215.

Gerdeman, G., and Lovinger, D. M. (2001). CB1 cannabinoid receptor inhibits synaptic release of glutamate in rat dorsolateral striatum. *J. Neurophysiol.* 85, 468–471.

Gibbon, J. (1977). Scalar expectancy and Weber's law in animal timing. *Psychol. Rev.* 84, 279–325.

Gibbon, J., Church, R. M., and Meck, W. H. (1984a). Scalar timing in memory. *Ann. N. Y. Acad. Sci.* 423, 52–77.

Gibbon, J., Morrell, M., and Silver, R. (1984b). Two kinds of timing in circadian incubation rhythm of ring doves. *Am. J. Physiol.* 247, R1083–R1087.

Gibbon, J., Malapani, C., Dale, C. L., and Gallistel, C. (1997). Toward a neurobiology of temporal cognition: advances and challenges. *Curr. Opin. Neurobiol.* 7, 170–184.

Golombek, D. A., Agostino, P. V., Plano, S. A., and Ferreyra, G. A. (2004). Signaling in the mammalian circadian clock: the NO/cGMP pathway. *Neurochem. Int.* 45, 929–936.

Golombek, D. A., Ferreyra, G. A., Agostino, P. V., Murad, A. D., Rubio, M. F., Pizzio, G. A., Katz, M. E., Marpegan, L., and Bekinschtein, T. A. (2003). From light to genes: moving the hands of the circadian clock. *Front. Biosci.* 8, s285–s293.

Golombek, D. A., and Rosenstein, R. E. (2010). The physiology of circadian entrainment. *Physiol. Rev.* 90, 1063–1102.

Gooley, J. J., Schomer, A., and Saper, C. B. (2006). The dorsomedial hypothalamic nucleus is critical for the expression of food-entrainable circadian rhythms. *Nat. Neurosci.* 9, 398–407.

Gu, B. M., Yin, B., Cheng, R. K., and Meck, W. H. (2011). Quinpirole-induced sensitization to noisy/sparse periodic input: temporal synchronization as a component of obsessive-compulsive disorder. *Neuroscience* 179, 143–150.

Hata, T. (2011). Glutamate – a forgotten target for interval timing. *Front. Integr. Neurosci.* 5:27. doi:10.3389/fnint.2011.00027

Hayasaka, N., Aoki, K., Kinoshita, S., Yamaguchi, S., Wakefield, J. K., Tsuji-Kawahara, S., Horikawa, K., Ikegami, H., Wakana, S., Murakami, T., Ramabhadran, R., Miyazawa, M., and Shibata, S. (2011). Attenuated food anticipatory activity and abnormal circadian locomotor rhythms in Rgs16 knockdown mice. *PLoS ONE* 6, e17655. doi:10.1371/journal.pone.0017655

Hendricks, M., and Jesuthasan, S. (2007). Asymmetric innervation of the habenula in zebrafish. *J. Comp. Neurol.* 502, 611–619.

Hilário, M. R. F., Clouse, E., Yin, H. H., and Costa, R. M. (2007). Endocannabiniod signaling is critical for habit formation. *Front. Integr. Neurosci.* 1:6 doi:10.3389/neuro.07/006.2007

Hills, T. T. (2003). "Toward a unified theory of animal event timing," in *Functional and Neural Mechanisms of Interval Timing*, ed. W. H. Meck (Boca Raton, FL: CRC Press), 77–111.

Hinton, S. C., and Meck, W. H. (1997). The 'internal clocks' of circadian and interval timing. *Endeavour* 21, 82–87.

Hirayama, J., Sahar, S., Grimaldi, B., Tamaru, T., Takamatsu, K., Nakahata, Y., and Sassone-Corsi, P. (2007). CLOCK-mediated acetylation of BMAL1 controls circadian function. *Nature* 450, 1086–1090.

Iijima, M., Yamaguchi, S., van der Horst, G. T., Bonnefont, X., Okamura, H., and Shibata, S. (2005). Altered food-anticipatory activity rhythm in cryptochrome-deficient mice. *Neurosci. Res.* 52, 166–173.

Kafka, M. S., Benedito, M. A., Roth, R. H., Steele, L. K., Wolfe, W. W., and Catravas, G. N. (1986). Circadian rhythms in catecholamine metabolites and cyclic nucleotide production. *Chronobiol. Int.* 3, 101–115.

Kaur, S., Thankachan, S., Begum, S., Blanco-Centurion, C., Sakurai, T., Yanagisawa, M., and Shiromani, P. J. (2008). Entrainment of temperature and activity rhythms to restricted feeding in orexin knock out mice. *Brain Res.* 1205, 47–54.

Kuriyama, K., Uchiyama, M., Suzuki, H., Tagaya, H., Ozaki, A., Aritake, S., Shibui, K., Xin, T., Lan, L., Kamei, Y., and Takahashi, K. (2005). Diurnal fluctuation of time perception under 30-h sustained wakefulness. *Neurosci. Res.* 53, 123–128.

Kyriacou, C. P., and Hall, J. (1980). Circadian rhythm mutations in *Drosophila melanogaster* affect short-term fluctuations in the male's courtship song. *Proc. Natl. Acad. Sci. U.S.A.* 77, 6729–6733.

Landry, G. J., Yamakawa, G. R., Webb, I. C., Mear, R. J., and Mistlberger, R. E. (2007). The dorsomedial hypothalamic nucleus is not necessary for the expression of circadian food-anticipatory activity in rats. *J. Biol. Rhythms* 22, 467–478.

Lee, A., Mathuru, A. S., The, C., Kibat, C., Korzh, V., Penney, T. B., and Jesuthasan, S. (2010). The habenula prevents helpless behavior in larval zebrafish. *Curr. Biol.* 20, 2211–2216.

Lejeune, H., and Wearden, J. H. (1991). The comparative psychology of fixed-interval responding: some quantitative analyses. *Learn. Motiv.* 22, 84–111.

Lewis, P. A., Miall, R. C., Daan, S., and Kacelnik, A. (2003). Interval timing in mice does not rely upon the circadian pacemaker. *Neurosci. Lett.* 348, 131–134.

Lowrey, P. L., Shimomura, K., Antoch, M. P., Yamazaki, S., Zemenides, P. D., Ralph, M. R., Menaker, M., and Takahashi, J. S. (2000). Positional syntenic cloning and functional characterization of the mammalian circadian mutation tau. *Science* 288, 483–492.

Lowrey, P. L., and Takahashi, J. S. (2000). Genetics of the mammalian circadian system: photic entrainment, circadian pacemaker mechanisms, and posttranslational regulation. *Annu. Rev. Genet.* 34, 533–562.

Lustig, C., Matell, M. S., and Meck, W. H. (2005). Not "just" a coincidence: frontal-striatal interactions in working memory and interval timing. *Memory* 13, 441–448.

Lustig, C., and Meck, W. H. (2001). Paying attention to time as one gets older. *Psychol. Sci.* 12, 478–484.

MacDonald, C. J., Cheng, R. K., Williams, C. L., and Meck, W. H. (2007). Combined organizational and activational effects of short and long photoperiods on spatial and temporal memory in rats. *Behav. Processes* 74, 226–233.

MacDonald, C. J., and Meck, W. H. (2004). Systems-level integration of interval timing and reaction time. *Neurosci. Biobehav. Rev.* 28, 747–769.

MacDonald, C. J., and Meck, W. H. (2005). Differential effects of clozapine and haloperidol on interval timing in the supra seconds range. *Psychopharmacology (Berl.)* 182, 232–244.

MacDonald, C. J., and Meck, W. H. (2006). Interaction of raclopride and preparatory-interval effects on simple reaction-time performance. *Behav. Brain Res.* 175, 62–74.

Malapani, C., Rakitin, B., Levy, R., Meck, W. H., Deweer, B., Dubois, B., and Gibbon, J. (1998). Coupled temporal memories in Parkinson's disease: a dopamine-related dysfunction. *J. Cogn. Neurosci.* 10, 316–331.

Matell, M. S., Bateson, M., and Meck, W. H. (2006). Single-trials analyses demonstrate that increases in clock speed contribute to the methamphetamine-induced horizontal shifts in peak-interval timing functions. *Psychopharmacology (Berl.)* 188, 201–212.

Matell, M. S., King, G. R., and Meck, W. H. (2004). Differential adjustment of interval timing by the chronic administration of intermittent or continuous cocaine. *Behav. Neurosci.* 118, 150–156.

Matell, M. S., and Meck, W. H. (2000). Neuropsychological mechanisms of interval timing behavior. *Bioessays* 22, 94–103.

Matell, M. S., and Meck, W. H. (2004). Cortico-striatal circuits and interval timing: coincidence detection of oscillatory processes. *Brain. Res. Cogn. Brain Res.* 21, 139–170.

Matell, M. S., Meck, W. H., and Nicolelis, M. A. (2003). Interval timing and the encoding of signal duration by ensembles of cortical and striatal neurons. *Behav. Neurosci.* 117, 760–773.

McClung, C. A. (2007). Circadian rhythms, the mesolimbic dopaminergic circuit, and drug addiction. *ScientificWorldJournal* 7, 194–202.

McClung, C. A., Sidiropoulou, K., Vitaterna, M., Takahashi, J. S., White, F. J., Cooper, D. C., and Nestler, E. J. (2005). Regulation of dopaminergic transmission and cocaine reward by the Clock gene. *Proc. Natl. Acad. Sci. U.S.A.* 102, 9377–9381.

Meck, W. H. (1983). Selective adjustment of the speed of internal clock and memory processes. *J. Exp. Psychol. Anim. Behav. Process.* 9, 171–201.

Meck, W. H. (1986). Affinity for the dopamine D2 receptor predicts neuroleptic potency in decreasing the speed of an internal clock. *Pharmacol. Biochem. Behav.* 25, 1185–1189.

Meck, W. H. (1991). Modality-specific circadian rhythmicities influence mechanisms of attention and memory for interval timing. *Learn. Motiv.* 22, 153–179.

Meck, W. H. (1996). Neuropharmacology of timing and time perception. *Brain. Res. Cogn. Brain Res.* 3, 227–242.

Meck, W. H. (2001). Interval timing and genomics: what makes mutant mice tick? *Int. J. Comp. Psychol.* 14, 211–231.

Meck, W. H. (2006a). Frontal cortex lesions eliminate the clock speed effect of dopaminergic drugs on interval timing. *Brain Res.* 1108, 157–167.

Meck, W. H. (2006b). Neuroanatomical localization of an internal clock: a functional link between mesolimbic, nigrostriatal, and mesocortical dopaminergic systems. *Brain Res.* 1109, 93–107.

Meck, W. H., Cheng, R. K., Macdonald, C. J., Gainetdinov, R. R., Caron, M. G., and Cevik, M. O. (2011). Gene-dose dependent effects of methamphetamine on interval timing in dopamine-transporter knockout mice. *Neuropharmacology*. doi:10.1016/j.neuropharm.2011.01.042. [Epub ahead of print].

Meck, W. H., Penney, T. B., and Pouthas, V. (2008). Cortico-striatal representation of time in animals and humans. *Curr. Opin. Neurobiol.* 18, 145–152.

Mendoza, J. (2007). Circadian clocks: setting time by food. *J. Neuroendocrinol.* 19, 127–137.

Mendoza, J., Angeles-Castellanos, M., and Escobar, C. (2005). A daily palatable meal without food deprivation entrains the suprachiasmatic nucleus of rats. *Eur. J. Neurosci.* 22, 2855–2862.

Mieda, M., Williams, S. C., Richardson, J. A., Tanaka, K., and Yanagisawa, M. (2006). The dorsomedial hypothalamic nucleus as a putative food-entrainable circadian pacemaker. *Proc. Natl. Acad. Sci. U.S.A.* 103, 12150–12155.

Mistlberger, R. E., and Holmes, M. M. (2000). Behavioral feedback regulation of circadian rhythm phase angle in light-dark entrained mice. *Am. J. Physiol. Regul. Integr. Comp. Physiol.* 279, R813–R821.

Morin, L. P., and Allen, C. N. (2006). The circadian visual system. *Brain Res. Rev.* 51, 1–60.

Mrosovsky, N. (1999). Masking: history, definitions, and measurement. *Chronobiol. Int.* 16, 415–429.

Oprisan, S. A., and Buhusi, C. V. (2011). Modeling pharmacological clock and memory patterns of interval timing in a striatal beat-frequency model of realistic, noisy neurons. *Front. Integr. Neurosci.* 5:52. doi:10.3389/fnint.2011.00052

Panda, S., Sato, T. K., Castrucci, A. M., Rollag, M. D., DeGrip, W. J., Hogenesch, J. B., Provencio, I., and Kay, S. A. (2002). Melanopsin (Opn4) requirement for normal light-induced circadian phase shifting. *Science* 298, 2213–2216.

Papachristos, E. B., Jacobs, E. H., and Elgersma, Y. (2011). Interval timing is intact in arrhythmic cry1/cry2-deficient mice. *J. Biol. Rhythms* 26, 305–313.

Pati, A. K., and Gupta, S. (1994). Time estimation circadian rhythm in shift workers and diurnally active humans. *J. Biosci.* 19, 325–330.

Penney, T. B., Gibbon, J., and Meck, W. H. (2008). Categorical scaling of duration bisection in pigeons (*Columba livia*), mice (*Mus musculus*), and humans (*Homo sapiens*). *Psychol. Sci.* 19, 1103–1109.

Pitts, S., Perone, E., and Silver, R. (2003). Food-entrained circadian rhythms are sustained in arrhythmic Clk/Clk mutant mice. *Am. J. Physiol. Regul. Integr. Comp. Physiol.* 285, R57–67.

Portnova, G. V., Sysoeva, O. V., Maliuchenko, N. V., Timofeeva, M. A., Kulikova, M. A., Tonevitskii, A. G., Kirpichnikov, M. P., and Ivanitskii, A. M. (2007). Genetic basis of time perception in athletes. *Zh. Vyssh. Nerv. Deiat. Im. I P Pavlova.* 57, 450–460.

Preitner, N., Damiola, F., Lopez-Molina, L., Zakany, J., Duboule, D., Albrecht, U., and Schibler, U. (2002). The orphan nuclear receptor REV-ERBalpha controls circadian transcription within the positive limb of the mammalian circadian oscillator. *Cell* 110, 251–260.

Reppert, S. M., and Weaver, D. R. (2002). Coordination of circadian timing in mammals. *Nature* 418, 935–941.

Reuter, M., Peters, K., Schroeter, K., Koebke, W., Lenardon, D., Bloch, B., and Hennig, J. (2005). The influence of the dopaminergic system on cognitive functioning: a molecular genetic approach. *Behav. Brain Res.* 164, 93–99.

Rosati, A. G., Stevens, J. R., Hare, B., and Hauser, M. D. (2007). The evolutionary origins of human patience: temporal preferences in chimpanzees, bonobos, and human adults. *Curr. Biol.* 17, 1663–1668.

Roybal, K., Theobold, D., Graham, A., DiNieri, J. A., Russo, S. J., Krishnan, V., Chakravarty, S., Peevey, J., Oehrlein, N., Birnbaum, S., Vitaterna, M. H., Orsulak, P., Takahashi, J. S., Nestler, E. J., Carlezon, W. A. Jr., and McClung, C. A. (2007). Mania-like behavior induced by disruption of CLOCK. *Proc. Natl. Acad. Sci. U.S.A.* 104, 6406–6411.

Savitz, J., Solms, M., and Ramesar, R. (2006). The molecular genetics of cognition: dopamine, COMT and BDNF. *Genes Brain Behav.* 5, 311–328.

Sheward, W. J., Maywood, E. S., French, K. L., Horn, J. M., Hastings, M. H., Seckl, J. R, Holmes, M. C., and Harmar, A. J. (2007). Entrainment to feeding but not to light: circadian phenotype of VPAC2 receptor-null mice. *J. Neurosci.* 27, 4351–4358.

Shumyatsky, G. P., Tsvetkov, E., Malleret, G., Vronskaya, S., Hatton, M., Hampton, L., Battey, J. F., Dulac, C., Kandel, E. R., and Bolshakov, V. Y. (2002). Identification of a signaling network in lateral nucleus of amygdala important for inhibiting memory specifically related to learned fear. *Cell* 111, 905–918.

Shurtleff, D., Raslear, T. G., and Simmons, L. (1990). Circadian variations in time perception in rats. *Physiol. Behav.* 47, 931–939.

Sleipness, E. P., Sorg, B. A., and Jansen, H. T. (2007a). Diurnal differences in dopamine transporter and tyrosine hydroxylase levels in rat brain: dependence on the suprachiasmatic nucleus. *Brain Res.* 1129, 34–42.

Sleipness, E. P., Sorg, B. A., and Jansen, H. T. (2007b). Contribution of the suprachiasmatic nucleus to day:night variation in cocaine-seeking behavior. *Physiol. Behav.* 91, 523–530.

Soshi, T., Kuriyama, K., Aritake, S., Enomoto, M., Hida, A., Tamura, M., Kim, Y., and Mishima, K. (2010). Sleep deprivation influences diurnal variation of human time perception with prefrontal activity change: a functional near-infrared spectroscopy study. *PLoS ONE* 5, e8395. doi:10.1371/journal.pone.0008395

Steinman, M. Q., Crean, K. K., and Trainor, B. C. (2011). Photoperiod interacts with food restriction in performance in the Barnes maze in female California mice. *Eur. J. Neurosci.* 33, 361–370.

Stephan, F. K. (2002). The "other" circadian system: food as a Zeitgeber. *J. Biol. Rhythms* 17, 284–292.

Sumbre, G., Muto, A., Baier, H., and Poo, M. M. (2008). Entrained rhythmic activities of neuronal ensembles as perceptual memory of time interval. *Nature* 456, 102–106.

Sysoeva, O. V., Tonevitsky, A. G., and Wackermann, J. (2010). Genetic determinants of time perception mediated by the serotonergic system. *PLoS ONE* 5, e12650. doi:10.1371/journal.pone.0012650

Takahashi, J. S., Hong, H. K., Ko, C. H., and McDearmon, E. L. (2008). The genetics of mammalian circadian order and disorder: implications for physiology and disease. *Nat. Rev. Genet.* 9, 764–775.

Terman, M., Gibbon, J., Fairhurst, S., and Waring, A. (1984). Daily meal anticipation: interaction of circadian and interval timing. *Ann. N. Y. Acad. Sci.* 423, 470–487.

van der Horst, G. T., Muijtjens, M., Kobayashi, K., Takano, R., Kanno, S., Takao, M., de Wit, J., Verkerk, A., Eker, A. P., van Leenen, D., Buijs, R., Bootsma, D., Hoeijmakers, J. H., and Yasui, A. (1999). Mammalian Cry1 and Cry2 are essential for maintenance of circadian rhythms. *Nature* 398, 627–630.

Vincent, S. G., Waddell, A. E., Caron, M. G., Walker, J. K., and Fisher, J. T. (2007). A murine model of hyperdopaminergic state displays altered respiratory control. *FASEB J.* 21, 1463–1471.

Vitaterna, M. H., King, D. P., Chang, A. M., Kornhauser, J. M., Lowrey, P. L., McDonald, J. D., Dove, W. F., Pinto, L. H., Turek, F. W., and Takahashi, J. S. (1994). Mutagenesis and mapping of a mouse gene, Clock, essential for circadian behavior. *Science* 264, 719–725.

Viyoch, J., Matsunaga, N., Yoshida, M., To, H., Higuchi, S., and Ohdo, S. (2005). Effect of haloperidol on mPer1 gene expression in mouse suprachiasmatic nuclei. *J. Biol. Chem.* 280, 6309–6315.

Wiener, M., Lohoff, F. W., and Coslett, H. B. (2011). Double dissociation of dopamine genes and timing in humans. *J. Cogn. Neurosci.* 23, 2811–2821.

Williamson, L. L., Cheng, R. K., Etchegaray, M., and Meck, W. H. (2008). "Speed" warps time: methamphetamine's interactive roles in drug abuse, habit formation, and the biological clocks of circadian and interval timing. *Curr. Drug Abuse Rev.* 1, 203–212.

Xu, Y., Padiath, Q. S., Shapiro, R. E., Jones, C. R., Wu, S. C., Saigoh, N., Saigoh, K., Ptácek, L. J., and Fu, Y. H. (2005). Functional consequences of a CKIdelta mutation causing familial advanced sleep phase syndrome. *Nature* 434, 640–644.

Zheng, B., Albrecht, U., Kaasik, K., Sage, M., Lu, W., Vaishnav, S., Li, Q., Sun, Z. S., Eichele, G., Bradley, A., and Lee, C. C. (2001). Nonredundant roles of the mPer1 and mPer2 genes in the mammalian circadian clock. *Cell* 105, 683–694.

Conflict of Interest Statement: The authors declare that the research was conducted in the absence of any commercial or financial relationships that could be construed as a potential conflict of interest.

Received: 06 August 2011; accepted: 30 September 2011; published online: 18 October 2011.

Citation: Agostino PV, Golombek DA and Meck WH (2011) Unwinding the molecular basis of interval and circadian timing. Front. Integr. Neurosci. ***5****:64. doi: 10.3389/fnint.2011.00064*

frontiers in
INTEGRATIVE NEUROSCIENCE

OPINION ARTICLE
published: 18 August 2011
doi: 10.3389/fnint.2011.00040

Time for zebrafish

Ruey-Kuang Cheng[1]*, Suresh Jesuthasan[1,2,3] and Trevor B. Penney[4]

[1] *Biomedical Sciences Institutes, Neuroscience Research Partnership, Singapore*
[2] *Department of Physiology, National University of Singapore, Singapore*
[3] *Neuroscience and Behavioral Disorders Program, Duke-National University of Singapore Graduate Medical School, Singapore*
[4] *Department of Psychology, National University of Singapore, Singapore*
**Correspondence: cheng.ruey-kuang@nrp.a-star.edu.sg*

A key challenge for identifying cellular bases of cognitive functions is to distinguish the contributions of different cell subtypes within complex circuits in a brain. Functional magnetic resonance imaging (fMRI) can reflect what brain areas are activated and electrophysiological recording can record neural activities adjacent to the electrodes, but neither can specify which and how neural subtypes *in vivo* contribute to a cognitive function, nor can they identify glial cells that support cognition (Pereira and Furlan, 2010). In the field of interval timing, considerable work has been done using the above two methods in organisms such as humans, primates, and rodents, yielding information on specific areas of the brain involved (Coull et al., 2011). However, a systems-level understanding from genetics to behaviors in the same organism is lacking. One way in which this can be achieved is to use a genetic system where specific neuronal ensembles or cell populations can be imaged and manipulated, while the resulting behaviors can be observed accordingly. One such system is the zebrafish (*Danio rerio*). The importance of zebrafish as a vertebrate model organism in neuroscience has been steadily increasing as more neural subtype-specific genetic markers and experimental tools become available. Although the rich behavioral repertoire of zebrafish has been characterized recently (Levin and Cerutti, 2009; Fero et al., 2010), its higher cognitive abilities, such as interval timing and time-based decision making, are relatively unknown compared with other species (Buhusi and Meck, 2005; Cheng et al., 2006; Penney et al., 2008). Here, we review some of the latest progress in optical imaging, zebrafish brain development, and timing behaviors to support the claim that the use of zebrafish model will extend our understanding of how different types of neurons work together in a vertebrate brain to generate the sense of time and determine complex time-based behaviors.

A major advantage of using zebrafish in neuroscience research is its transparent skull and brain during the larval stage of development, which enables *in vivo* fluorescence imaging of activity in large populations of cells. This can be done either by injecting calcium-sensitive dyes into the target brain areas, or by generating transgenic lines that express genetically encoded calcium indicators (GECIs, see Wilms and Hausser, 2009) in specific subsets of neurons. These fluorescent indicators report intracellular calcium concentration change triggered by action potentials, thus reflecting neural activity (Tian et al., 2009). From the calcium signals, neural firing rate information can be derived by de-convolution (Yaksi and Friedrich, 2006). With the neural populations identified and visible under the microscope, one can study how these defined neurons react to external stimuli (Dreosti et al., 2009, 2011), to internal stimuli (e.g., the sense of time) and during associative learning (Aizenberg and Schuman, 2011) by measuring the calcium signal change. Under the microscope, it is also possible to reconstruct a 3D functional map of the defined neurons after scanning multiple depths of the target area. This non-invasive imaging technique allows monitoring of neural activities across multiple sessions, which is critical for studying learning and memory (Aizenberg and Schuman, 2011). Interestingly, in addition to capturing images, two-photon microscopy allows ablations at single-cell resolution. This optical lesion technique enables examination of the functional consequences of loss of highly specific neural populations compared with surgical lesions. Besides, due to abundant neurogenesis persisting into adulthood in zebrafish (reviewed in Kizil, et al., 2011), functional recovery naturally occurs after brain lesions in the same fish. This provides excellent reversible brain lesions at single-cell level, which is difficult to conduct in mammalian models. In sum, it is now possible to effectively examine neural substrates underlying interval timing in zebrafish at single-cell resolution and in 3D.

Sumbre et al. (2008) recently demonstrated that larval zebrafish (between 5 and 14 days post fertilization, or dpf) could follow temporal patterns of rhythmic stimuli both at the neuronal level in the optic tectum (a visual area), as well as at the behavioral level in its tail flips. The temporal rhythm was established by repeatedly presenting a 200 ms visual (light flash) conditioned stimulus (CS) at a fixed inter-stimulus interval (ISI) of 4, 6, or 10 s. It was found that the tectal neurons entrained to the CS, such that the calcium signals increased transiently and, more importantly, in synchrony with the ISI. Moreover, this synchronous neural activity pattern continued for several cycles even after the flashing CS terminated. The same study also revealed that the tectal neurons in a fish that is as young as 4 days (one out of seven tested fish), but not 3 days old, was able to keep repeating a temporal pattern established by the ISI. From a developmental perspective, it is intriguing that a 4–5 days old zebrafish brain is sophisticated enough to react to a visual stimulus and to follow its temporal patterns. In general, zebrafish embryos start hatching after 2–3 dpf (henceforth called larvae) and the larvae need to hunt for food after their yolk is depleted at 5 dpf. Therefore, it is reasonable to assume that the developing zebrafish brain is mature enough and ready to function after 5 dpf, with timing external stimuli a part of its abilities. During development, dopamine (DA) neurons in the zebrafish brain mature at different time points ranging from 1 dpf in the diencephalon to 3 dpf in the telencephalon (Mahler et al., 2010). The zebrafish telencephalon is composed of the pallium and the subpallium, which is teleost analog of cortico-basal-ganglia circuits in mammals (Rink and Wullimann, 2002). The DA neurotransmitter systems, especially the ones in cortico-striatal

circuits, play a critical role in interval timing both in animals and humans (reviewed in Meck et al., 2008). Studying the potential timing functions of the DA neurons in the telencephalon may be a good place to start in zebrafish. A Gal4 driver that is active in DA neurons will allow us to label DA neurons in larval zebrafish for optical imaging, or to manipulate it, before, during, and after training on a timing task.

The behavior (rhythmic tail flips) shown by Sumbre et al. (2008) is driven by a flashing CS with the temporal patterns established by the ISI. It will be important to determine next whether larval zebrafish can associate the CS with biologically significant stimuli, such as food or danger (as an unconditioned stimulus, US), by guiding behaviors based on their sense of time between the CS and the US. This is a more sophisticated form of sensorimotor coordination than a simple reflex and is critical for associative learning (Balsam et al., 2010) and for survival. It was recently reported that larval zebrafish (20–35 dpf) could be conditioned to a 5-s light CS with a mild electrical shock as the US (Lee et al., 2010). In the study, after 10 CS–US conditioning trials that required the fish to swim to the non-CS side of a chamber to evade the full impact of the US, the fish showed a significant increase in swim speed at the 5th second of the 5-s CS in the probe trial (i.e., no US presented). This suggests that the fish adjusted their swimming behavior according to their expected time of the US delivery, which is consistent with previous findings in adult goldfish (Drew et al., 2005). To further explore interval timing in larval zebrafish, one can implement a subjective timing component in the task requirement, such as a trace interval between the CS offset and the US onset. Trace conditioning requires the animal to subjectively "bridge" the two stimuli by its own sense of time, because there is no external stimulus (i.e., CS free) to follow during the trace interval. An intact dorsal pallium is found to be critical in learning trace conditioning in adult goldfish (Vargas et al., 2009). In addition, the caudate nucleus (Flores and Disterhoft, 2009) and the hippocampus (Cheng et al., 2008) are also critically involved in trace conditioning in mammals. The analog of both regions can be found in the fish telencephalon (the caudate nucleus in the fish subpallium and the hippocampus in the fish lateral pallium; see Portavella and Vargas, 2005).

In conclusion, the highly conserved neurotransmitter systems and brain anatomy in the vertebrate brain allow us to investigate neural mechanisms of interval timing in zebrafish. We propose two critical experiments here. First, neural substrates of interval timing can be obtained by observing calcium signal change in specific neural populations in the zebrafish telencephalon as a function of the trace interval in a trace conditioning paradigm. Second, it is also crucial to observe how interval timing is affected when a particular set of neurons is disrupted, either by femtosecond laser ablation or optogenetics. Once the fundamentals of interval timing are established, the zebrafish will open a new window for research on interval timing and time-based decision making, especially as it can also be used for genetic or chemical screens (Lieschke and Currie, 2007).

REFERENCES

Aizenberg, M., and Schuman, E. M. (2011). Cerebellar-dependent learning in larval zebrafish. *J. Neurosci.* 31, 8708–8712.

Balsam, P. D., Drew, M. R., and Gallistel, C. R. (2010). Time and associative learning. *Comp. Cogn. Behav. Rev.* 5, 1–22.

Buhusi, C. V., and Meck, W. H. (2005). What makes us tick? Functional and neural mechanisms of interval timing. *Nat. Rev. Neurosci.* 6, 755–765.

Cheng, D. T., Disterhoft, J. F., Power, J. M., Ellis, D. A., and Desmond, J. E. (2008). Neural substrates underlying human delay and trace eyeblink conditioning. *Proc. Natl. Acad. Sci.* U.S.A. 105, 8108–8113.

Cheng, R. K., MacDonald, C. J., and Meck, W. H. (2006). Differential effects of cocaine and ketamine on time estimation: implications for neurobiological models of interval timing. *Pharmacol. Biochem. Behav.* 85, 114–122.

Coull, J. T., Cheng, R. K., and Meck, W. H. (2011). Neuroanatomical and neurochemical substrates oftiming. *Neuropsychopharmacol. Rev.* 36, 3–25.

Dreosti, E., Esposti, F., Baden, T., and Lagnado, L. (2011). In vivo evidence that retinal bipolar cells generate spikes modulated by light. *Nat. Neurosci.* 14, 951–952.

Dreosti, E., Odermatt, B., Dorostkar, M. M., and Lagnado, L. (2009). Agenetically encoded reporter of synaptic activity in vivo. *Nat. Methods* 6, 883–889.

Drew, M. R., Zupan, B., Cooke, A., Couvillon, P. A., and Balsam, P. D. (2005). Temporal control of conditioned responding in goldfish. *J. Exp. Psychol. Anim. Behav. Process* 31, 31–39.

Fero, K., Yokogawa, T., and Burgess, H. A. (2010). "The behavioral repertoire of larval zebrafish," in Zebrafish *Models in Neurobehavioral Research Neuromethods,* ed. A. V. Kalueff, and J. M. Cachat (Totowa, NJ: Humana Press), 249–291.

Flores, L. C., and Disterhoft, J. F. (2009). Caudate nucleus is critically involved in trace eyeblink conditioning. *J. Neurosci.* 29, 14511–14520.

Kizil, C., Kaslin, J., Kroehne, V., and Brand, M. (2011). Adult neurogenesis and brain regeneration in zebrafish. *Dev. Neurobiol.* doi: 10.1002/dneu.20918. [Epub ahead of print].

Lee, A., Mathuru, A. S., The, C., Kibat, C., Korzh, V., Penney, T. B., and Jesuthasan, S. (2010). The habenula prevents helpless behavior in larval zebrafish. *Curr. Biol.* 20, 2211–2216.

Levin, E. D., and Cerutti, D. T. (2009). "Behavioral neuroscience of zebrafish," in *Methods of Behavior Analysis in Neuroscience,* Chap. 15, 2nd Edn, ed. J. J. Buccafusco (Boca Raton, FL: CRC Press).

Lieschke, G. J., and Currie, P. D. (2007). Animal models of human disease: zebrafish swim into view. *Nat. Rev. Genet.* 8, 353–367.

Mahler, J., Filippi, A., and Driever, W. (2010). DeltaA/DeltaD regulate multiple and temporally distinct phases of notch signaling during dopaminergic neurogenesis in zebrafish. *J. Neurosci.* 30, 16621–16635.

Meck, W. H., Penney, T. B., and Pouthas, V. (2008). Cortico-striatal representation of time in animals and humans. *Curr. Opin. Neurobiol.* 18, 145–152.

Penney, T. B., Gibbon, J., and Meck, W. H. (2008). Categorical scaling of duration bisection in pigeons (*Columba livia*), mice (*Mus musculus*), and humans (*Homo sapiens*). *Psychol. Sci.* 19, 1103–1109.

Pereira, A. Jr., and Furlan, F. A. (2010). Astrocytes and human cognition: modeling information integration and modulation of neuronal activity. *Prog. Neurobiol.* 92, 405–420.

Portavella, M., and Vargas, J. P. (2005). Emotional and spatial learning in goldfish is dependent on different telecephalic pallial systems. *Eur. J. Neurosci.* 21, 2800–2806.

Rink, E., and Wullimann, M. F. (2002). Connections of the ventral telencephalon and tyrosine hydroxylase distribution in the zebrafish brain (Danio rerio) lead to identification of an ascending dopaminergic system in a teleost. *Brain Res. Bull.* 57, 385–387.

Sumbre, G., Muto, A., Baier, H., and Poo, M. M. (2008). Entrained rhythmic activities of neuronal ensembles as perceptual memory of time interval. *Nature* 456, 102–107.

Tian, L., Hires, S. A., Mao, T., Huber, D., Chiappe, M. E., Chalasani, S. H., Petreanu, L., Akerboom, J., McKinney, S. A., Schreiter, E. R., Bargmann, C. I., Jayaraman, V., Svoboda, K., and Looger, L. L. (2009). Imaging neural activity in worms, flies and mice with improved GCaMP calcium indicators. *Nat. Methods* 6, 875–881.

Vargas, J. P., Lopez, J. C., and Portavella, M. (2009). What are the functions of fish brain pallium? *Brain Res. Bull.* 79, 436–440.

Wilms, C. D., and Hausser, M. (2009). Lighting up neural networks using a new generation of genetically encoded calcium sensors. *Nat. Methods* 6, 871–872.

Yaksi, E., and Friedrich, R. W. (2006). Reconstruction of firing rate changes across neuronal populations by temporally deconvolved Ca2+ imaging. *Nat. Methods* 3, 377–383.

Received: 01 August 2011; accepted: 01 August 2011; published online: 18 August 2011.

Citation: Cheng R-K, Jesuthasan S and Penney TB (2011) Time for zebrafish. Front. Integr. Neurosci. 5:40. doi: 10.3389/fnint.2011.00040

frontiers in
INTEGRATIVE NEUROSCIENCE

OPINION ARTICLE
published: 23 December 2011
doi: 10.3389/fnint.2011.00087

Using DREADDs to isolate internal clocks

Martilias S. Farrell*

Department of Pharmacology, University of North Carolina School of Medicine, Chapel Hill, NC, USA
**Correspondence: martilias_farrell@med.unc.edu*

Although much is known about the psychophysics of timing and time perception, the ability to selectively modulate discrete neuronal populations subserving interval timing could advance the field in unprecedented ways (see Buhusi and Meck, 2005; Allman and Meck, 2011; Cheng et al., 2011). Current approaches used to delineate the neuronal correlates of timing are often restricted to pharmacological (Meck, 1996; Coull et al., 2011) or ablative approaches, both physical (Meck, 2006a,b; Wiener et al., 2008) and genetic (Sysoeva et al., 2010; Agostino et al., 2011; Meck et al., 2011; Wiener et al., 2011). Most, if not all, of the ablative approaches are limited to loss of function-type hypothesis testing and frequently have unintended off-target effects. The pharmacologic approach has inherent confounds in the non-specificity of small molecule ligands. One way to overcome these confounds is to use a system in which a designer receptor exclusively activated by designer drug (DREADD) is expressed in a cell-type specific manner via transgenic expression. This chemicogenetic approach is further described by the acronym of the first tool of its type: receptor activated solely by synthetic ligand (RASSL). In short, a receptor is engineered such that it is no longer activated by any endogenous ligands and instead activated by an otherwise inert exogenous ligand. The various RASSLs and DREADDs have been reviewed elsewhere (Pei et al., 2008). In short, there are three DREADDs available with proven functionality in neuronal environments – hM3Dq (Gq-coupled, promotes neuronal excitability), hM4Di (Gi-coupled, promotes neuronal inhibition), and the rM3Ds (Gs-coupled, promotes cAMP production). Here, we discuss this technology's potential in the field of interval timing.

Cell-type specificity of signaling has been a hurdle for delineating the neuroanatomical substrates of timing (Cheng et al., 2011). Using the chemicogenetic approach, it is possible to express a receptor in a select population of neurons and then turn that receptor on via peripheral administration of clozapine-N-oxide (CNO). The cell-type specificity is dependent upon the transgenic approach used, though the current genetic toolkit appears to be more than adequate for the study of interval timing. To date, there has been success expressing DREADDs using virally mediated approaches (Ferguson et al., 2011; Krashes et al., 2011; Sasaki et al., 2011), single-transgenic approaches (Guettier et al., 2009), and intersectional transgenic approaches (Alexander et al., 2009; Ray et al., 2011). With these approaches, it should be possible to place a DREADD into a subpopulation of neurons and then determine how this population modulates interval timing. Furthermore, the identical signaling-type initiated via the DREADDs in various subpopulations would allow us to piece together the circuitry by expressing the DREADD in multiple subpopulations either simultaneously or separately (**Figure 1**).

In addition to the cell-type specificity possible with DREADDs, this approach also affords us the ability to silently and independently modulate neuronal signaling. An inherent confound in the pharmacologic approach to neuronal modulation is the intrinsic interference with the endogenous tone of the system being investigated. By definition, any agonist interacting with a receptor competes with the endogenous ligand for that receptor. Thus, the experimental modulation is no longer limited to the modulation of the neuronal population induced by the ligand–receptor pair, but instead also includes interference in the homeostatic, basal signaling state of the system. As it is hypothesized that information is encoded in patterns of neuronal firing and the subsequent phasic neurotransmitter presence (Johnson, 2000), it can be seen that interfering with the temporal signaling nature of the basal state can be detrimental in our quest to determine the neuronal correlates of time (**Figure 2**). The DREADD overcomes this confound by the use of a non-native receptor which has no basal tone. Take, for example, the neurons of the striatum, a well renowned candidate for the epicenter of interval timing circuitry (Matell et al., 2003; Meck et al., 2008). In addition to the technical difficulty of selectively manipulating these neurons through pharmacological means (local microinjections), the key confound is that any pharmacological manipulation will interfere with the afferent tone on the striatal synapses (**Figure 2B**). Thus, the experimental manipulation is no longer limited to striatal medium spiny neuron (MSN) modulation, but instead now includes modulation of the afferent tone associated with the neurotransmitter of the targeted receptor. Thus, the experimental manipulation is affecting both the hypothetical integrator of information (the MSN) and the information itself (the phasic, temporally encoded presynaptic release of neurotransmitter). With the DREADD approach, it is possible to modulate the activity of the MSNs independent of the endogenous tone, leaving the theoretical temporally encoded information in place (**Figure 2C**). This provides us the unique opportunity to reductively piece together each component of the neuronal substrates of timing.

Finally, the usability of the chemicogenetic approach is another salient aspect when considering its application in the field of interval timing. Indeed, other approaches for cell-type specific control of neuronal signaling exist, most notably that of optogenetics (Yizhar et al., 2011). The optogenetic approach has many features that lend well to interval timing research – namely, the exclusive control of neuronal firing in the subsecond range. Both optogenetics and chemicogenetics achieve cell-type specific control of signaling through transgenic expression of a non-native receptor, so both approaches leave the endogenous tone intact. The chemicogenetic approach, in its simplest form (a single-transgenic mouse), requires a simple peritoneal injection of CNO to modulate cell-type specific neuronal signaling. This simplicity is an experimental aspect that cannot be ignored considering the exclusive use of behavior paradigms in the study of interval timing.

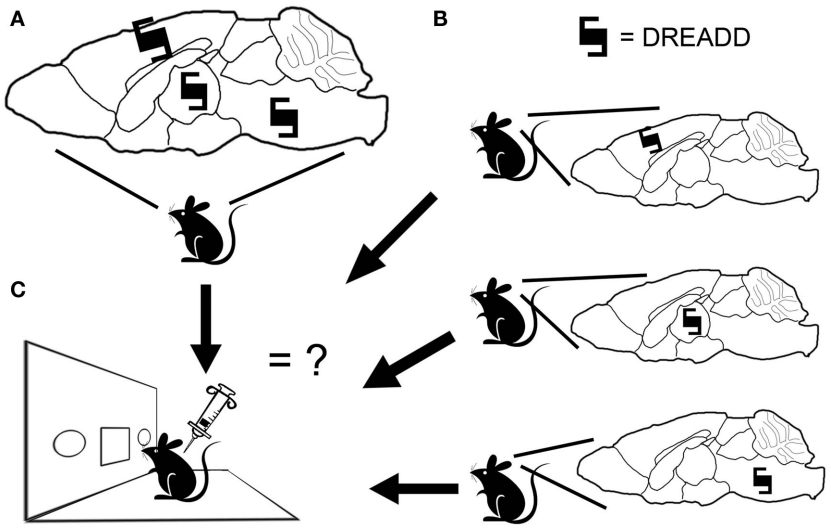

FIGURE 1 | Designer receptor exclusively activated by designer drug (DREADD) expression and behavior. (A) A DREADD can be expressed in multiple brain nuclei, permitting a global modulation of neuronal activity. **(B)** Alternatively, a DREADD can be placed in restricted cell populations. **(C)** By activating the DREADD via CNO injection and administering interval timing tests, it will be possible to compare the effect of selective neuronal modulation in different nuclei, or in multiple nuclei compared to individual nuclei, and thus determine the cell populations necessary for interval timing or sufficient to modulate these processes.

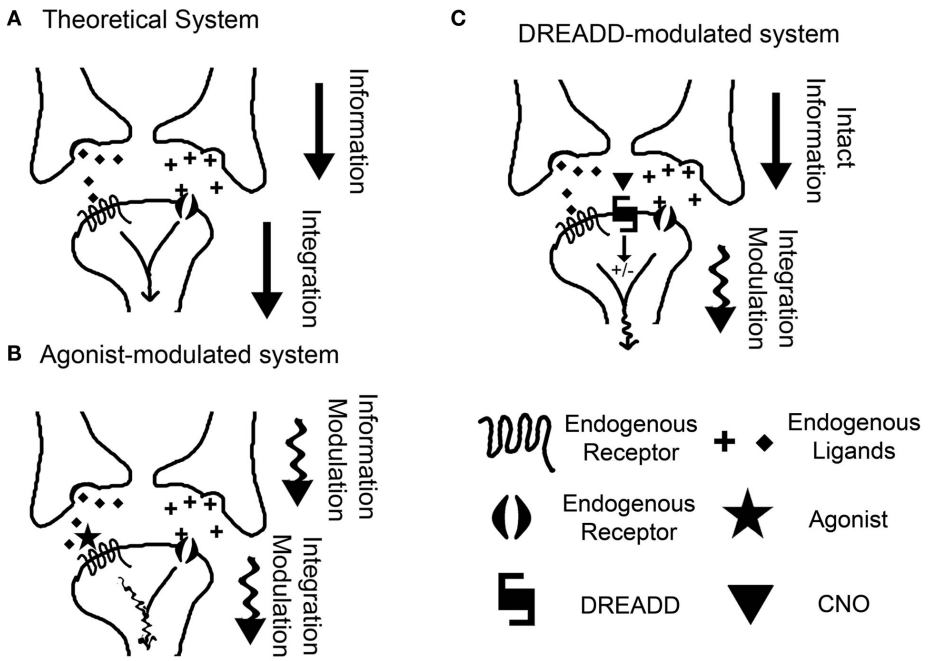

FIGURE 2 | The benefit of non-invasive neuronal modulation. (A) A theoretical model for the neuronal correlate of interval timing, in which a post-synaptic neuron integrates information from multiple inputs. **(B)** In a classical pharmacological manipulation, an agonist is administered with the intent to modulate the post-synaptic neuron responsible for the integration of information. Instead, the agonist simultaneously interferes with the endogenous neurotransmitter tone, thus manipulating the information itself. **(C)** Using a DREADD, modulation of the post-synaptic neuron is achieved exclusively, leaving the information intact. This allows direct investigation of the mechanisms of information integration.

In conclusion, it can be seen that by combining DREADDs and transgenic technology in the chemicogenetic approach it will be possible to further delineate the neuronal substrates of interval timing. The cell-type specific control in combination with the independent modulation of neuronal signaling afford a level of precision that is almost requisite in the investigation of such

an intertwined neuronal process as that of interval timing. We propose an initial experiment here: investigating the functional role of the MSNs in temporal integration (see Matell and Meck, 2004; Oprisan and Buhusi, 2011). It can be seen that this technology is well suited for use in this field, and will hopefully advance our understanding of the neural basis of timing and time perception (Gibbon et al., 1997; Gu et al., 2011).

REFERENCES

Agostino, P. V., Golombek, D. A., and Meck, W. H. (2011). Unwinding the molecular basis of interval and circadian timing. *Front. Integr. Neurosci.* 5:64. doi: 10.3389/fnint.2011.00064

Alexander, G. M., Rogan, S. C., Abbas, A. I., Armbruster, B. N., Pei, Y., Allen, J. A., Nonneman, R. J., Hartmann, J., Moy, S. S., Nicolelis, M. A., McNamara, J. O., and Roth, B. L. (2009). Remote control of neuronal activity in transgenic mice expressing evolved G protein-coupled receptors. *Neuron* 63, 27–39.

Allman, M. J., and Meck, W. H. (2011). Pathophysiological distortions in time perception and timed performance. *Brain*. doi: 10.1093/brain/awr21

Buhusi, C. V., and Meck, W. H. (2005). What makes us tick? Functional and neural mechanisms of interval timing. *Nat. Rev. Neurosci.* 6, 755–765.

Cheng, R. K., Jesuthasan, S., and Penney, T. B. (2011). Time for zebrafish. *Front. Integr. Neurosci.* 5:40. doi: 10.3389/fnint.2011.00040

Coull, J. T., Cheng, R. K., and Meck, W. H. (2011). Neuroanatomical and neurochemical substrates of timing. *Neuropsychopharmacology* 36, 3–25.

Ferguson, S. M., Eskenazi, D., Ishikawa, M., Wanat, M. J., Phillips, P. E., Dong, Y., Roth, B. L., and Neumaier, J. F. (2011). Transient neuronal inhibition reveals opposing roles of indirect and direct pathways in sensitization. *Nat. Neurosci.* 14, 22–24.

Gibbon, J., Malapani, C., Dale, C. L., and Gallistel, C. (1997). Toward a neurobiology of temporal cognition: advances and challenges. *Curr. Opin. Neurobiol.* 7, 170–184.

Gu, B. M., Cheng, R. K., Yin, B., and Meck, W. H. (2011). Quinpirole-induced sensitization to noisy/sparse periodic input: temporal synchronization as a component of obsessive-compulsive disorder. *Neuroscience* 179, 143–150.

Guettier, J. M., Gautam, D., Scarselli, M., de Azua, I. R., Li, J. H., Rosemond, E., Ma, X., Gonzalez, F. J., Armbruster, B. N., Lu, H., Roth, B. L., and Wess, J. (2009). A chemical-genetic approach to study G protein regulation of beta cell function in vivo. *Proc. Natl. Acad. Sci. U.S.A.* 106, 19197–19202.

Johnson, K. O. (2000). Neural coding. *Neuron* 26, 563–566.

Krashes, M. J., Koda, S., Ye, C., Rogan, S. C., Adams, A. C., Cusher, D. S., Maratos-Flier, E., Roth, B. L., and Lowell, B. B. (2011). Rapid, reversible activation of AgRP neurons drives feeding behavior in mice. *J. Clin. Invest.* 121, 1424–1428.

Matell, M. S., and Meck, W. H. (2004). Cortico-striatal circuits and interval timing: coincidence detection of oscillatory processes. *Cogn. Brain Res.* 21, 139–170.

Matell, M. S., Meck, W. H., and Nicolelis, M. A. L. (2003). Interval timing and the encoding of signal duration by ensembles of cortical and striatal neurons. *Behav. Neurosci.* 117, 760–773.

Meck, W. H. (1996). Neuropharmacology of timing and time perception. *Cogn. Brain Res.* 3, 227–242.

Meck, W. H. (2006a). Frontal cortex lesions eliminate the clock speed effect of dopaminergic drugs on interval timing. *Brain Res.* 1108, 157–167.

Meck, W. H. (2006b). Neuroanatomical localization of an internal clock: a functional link between mesolimbic, nigrostriatal, and mesocortical dopaminergic systems. *Brain Res.* 1109, 93–107.

Meck, W. H., Cheng, R. K., Macdonald, C. J., Gainetdinov, R. R., Caron, M. G., and Cevik, M. O. (2011). Gene-dose dependent effects of methamphetamine on interval timing in dopamine-transporter knockout mice. *Neuropharmacology*. doi: 10.1016.j.neuropharm.2011.01.042. [Epub ahead of print].

Meck, W. H., Penney, T. B., and Pouthas, V. (2008). Cortico-striatal representation of time in animals and humans. *Curr. Opin. Neurobiol.* 18, 145–152.

Oprisan, S. A., and Buhusi, C. V. (2011). Modeling pharmacological clock and memory patterns of interval timing in a striatal beat-frequency model with realistic, noisy neurons. *Front. Integr. Neurosci.* 5:52. doi: 10.3389/fnint.2011.00052

Pei, Y., Rogan, S. C., Yan, F., and Roth, B. L. (2008). Engineered GPCRs as tools to modulate signal transduction. *Physiology* 23, 313–321.

Ray, R. S., Corcoran, A. E., Brust, R. D., Kim, J. C., Richerson, G. B., Nattie, E., and Dymecki, S. M. (2011). Impaired respiratory and body temperature control upon acute serotonergic neuron inhibition. *Science* 333, 637–642.

Sasaki, K., Suzuki, M., Mieda, M., Tsujino, N., Roth, B., and Sakurai, T. (2011). Pharmacogenetic modulation of orexin neurons alters sleep/wakefulness states in mice. *PLoS ONE* 6, e20360. doi: 10.1371/journal.pone.0020360

Sysoeva, O. V., Tonevitsky, A. G., and Wackermann, J. (2010). Genetic determinants of time perception mediated by the serotonergic system. *PLoS ONE* 5, e12650. doi: 10.1371/journal.pone.0012650

Wiener, M., Lohoff, F. W., and Coslett, H. B. (2011). Double dissociation of dopamine genes and timing in humans. *J. Cogn. Neurosci.* 23, 2811–2821.

Wiener, M., Magaro, C. M., and Matell, M. S. (2008). Accurate timing but increased impulsivity following excitotoxic lesions of the subthalamic nucleus. *Neurosci. Lett.* 440, 176–180.

Yizhar, O., Fenno, L. E., Davidson, T. J., Mogri, M., and Deisseroth, K. (2011). Optogenetics in neural systems. *Neuron* 71, 9–34.

Received: 01 December 2011; accepted: 02 December 2011; published online: 23 December 2011.

Citation: Farrell MS (2011) Using DREADDs to isolate internal clocks. Front. Integr. Neurosci. ***5****:87. doi: 10.3389/fnint.2011.00087*

frontiers in
INTEGRATIVE NEUROSCIENCE

OPINION ARTICLE
published: 04 January 2012
doi: 10.3389/fnint.2011.00092

Sleep, circadian rhythms, and interval timing: evolutionary strategies to time information

Valter Tucci*

Department of Neuroscience and Brain Technologies, Istituto Italiano di Tecnologia, Genova, Italy
**Correspondence: valter.tucci@iit.it*

A crucial property of the brain is to integrate temporal information with accurate physiological responses (Hinton and Meck, 1997; Buhusi and Meck, 2005; Coull et al., 2011). Evolution has favored biological clocks that dictate homeostatic processes (e.g., the circadian timing of sleep) and, on a smaller time-scale, timed behavioral responses (e.g., interval timing). The interplay between such time-keeping mechanisms is intriguing but biologically complex. Moreover, in biology, analogous problems can be successfully solved by multiple computations. In this article I will discuss of sleep, circadian rhythms, and interval timing by delineating several aspects that suggest a common evolutionary role in providing neurobiological mechanisms for temporal information processing.

Neither interval timing nor the homeostatic regulation of sleep are currently as well-understood, at the molecular level, as the circadian clock. This has triggered a scientific interest in linking these phenomena to the circadian molecular machinery. On one hand, sleep homeostasis has been investigated in genetic and lesion studies of the circadian "master" clock (Franken and Dijk, 2009) to test whether the two processes (homeostatic and circadian) were independent. On the other hand, it has been questioned whether interval timing and circadian clock share similar oscillatory mechanisms, although with a different time-scale (Crystal, 2001, 2006a,b; Crystal and Baramidze, 2007), and whether circadian rhythms affect interval timing. Whilst the research in sleep and circadian clock over the last few years resulted in some interesting positive associations (reviewed in Tucci and Nolan, 2010), the question whether interval timing is related to the circadian clock has not a clear unanimous conclusion yet.

SLEEP AND INTERVAL TIMING

As in conditioning behaviors, in which a brief time interval itself may embody the proper information to be learned, sleep behavior is phase-locked in the 24-h (circadian) rhythms of the organism. However, while the circadian process is self-sustained, sleep is homeostatically regulated and varies according to the previous wakefulness. Back in evolution, single-cell organisms became entrained to environmental rest-activity stimuli (light and temperature changes caused by the earth's rotation) in order to set the time of their metabolic processes (Krueger, 2010). Sleep evolved from rest-activity cycles and it is still debated whether a sleep-like phenotype occurs within single neurons and how this is affected by environmental (extracellular) stimuli. Nevertheless, it is reasonable to envisage that sleep has developed, in multicellular organisms, based on the same biology of a primordial rest state.

In understanding the brain mechanisms of interval timing it is becoming pivotal to define whether the coding of interval timing depends on targeted neuronal mechanisms and their associated sub-cellular signaling pathways or on the states of neuronal networks. There is no doubt that the two mechanisms (single neuronal signaling and networks) are intimately connected but it is fundamental to understand what sets the time for timed responses such as a motor action or an endocrine oscillation.

It appears that sleep and interval timing share a common destiny as they are often studied as emerging properties of neuronal networks. For this reason, it is not surprising that the function of sleep, is thought to be associated to synaptic plasticity, as theorized by the latest functional model of sleep (Tononi and Cirelli, 2006). In both sleep (Tononi and Cirelli, 2006) and interval timing (Buonomano and Laje, 2010) the output units of the network rely on the development and stabilization of proper synaptic weights. Yet, the synaptic interplay between frontal cortex and subcortical neurons, such as striatal neurons, is important in both sleep-related memory consolidation and interval timing. Besides, these phenomena rely on specific patterns of "slow" oscillatory firings (Diekelmann and Born, 2010).

A number of studies has shown that sleep benefits memory consolidation (see Diekelmann and Born, 2010 for an extensive review). Beneficial effects of sleep on memory occur after a few minutes (Lahl et al., 2008), a few hours (Mednick et al., 2003; Tucker et al., 2006a,b; Korman et al., 2007; Nishida and Walker, 2007), or after a proper night of sleep (Pace-Schott et al., 2005; Stickgold, 2005; Stickgold and Walker, 2005a,b; Walker et al., 2005a,b; Marshall and Born, 2007). Of all the memory tasks that have been used in investigating learning and memory aspects of sleep, almost none of them have manipulated temporal variables, until recently. Lewis et al. (2011) and Lewis and Meck, (2011), by using a combination of psychophysics and neuroimaging techniques in human participants, have tested the hypothesis that sleep promotes consolidation of temporal information. The authors differentiated motor and perceptual timing in their task. Interestingly, they reported that brain sleep-wake states during retention modulates motor learning in motor areas, such as the supplementary motor area, the striatum, and the cerebellum, while perceptual timing activates the posterior hippocampus zone (Lewis et al., 2011). This new evidence is in agreement with an influential model of a sleep-dependent memory mechanism that involves slow-wave sleep (SWS; Diekelmann and Born, 2010). Cortical slow oscillations (<1 Hz) provide a timed electrophysiological mechanism of *up*- and *down*-states that pass memories from hippocampal temporary storage to neocortical long-term storage (Cheng et al., 2008, 2009; Molle and Born, 2011).

CIRCADIAN CLOCK AND INTERVAL TIMING

The circadian clock is represented, at the cellular level, by a well-known negative transcription/translation-based feedback

loop that sets the oscillation of the so called "core clock genes." The brain contains a pacemaker-like structure, the suprachiasmatic nuclei (SCN) of the hypothalamus, that provides circadian rhythmicity to other peripheral organs.

Core clock elements in the cell are transcriptional factors that regulate interlocking positive/negative feedback loops (Ko and Takahashi, 2006; Reppert, 2006). In mammals, the positive loop starts when CLOCK and BMAL1 (two members of the bHLH–PAS transcriptional factor family), form heterodimers and then translocate to the nucleus. Here this CLOCK:BMAL1 complex binds to E-box enhancers and promote the transcription of the *Period* (*PER1-3*) and the *Cryptochrome* (*CRY1* and *CRY2*) genes. The resulting proteins form PER:CRY heterodimers that initiate the negative feedback loop. These PER:CRY complexes move back to the nucleus and inhibit the activity of CLOCK:BMAL1 resulting, then, in the repression of their own transcription. However, these are not the only regulatory loops. CLOCK:BMAL1 activates also the transcription of two retinoic acid-related orphan receptors (REV-ERBs and RORs) which regulate positively (RORs) and negatively (REV-ERBs) *Bmal1*. To increase the complexity of the circadian clock, a number of post-translational mechanisms were shown to regulate clock genes (Lopez-Molina et al., 1997; Lowrey and Takahashi, 2000; Lowrey et al., 2000). This whole clock mechanism of activators and repressors represent an oscillatory mechanism that is necessary to coordinate circadian rhythms. However, a remarkable causal relation exists between molecular oscillations and neural activity. An important property of neurons in the SCN of the hypothalamus is their ability to generate, endogenously, action potentials which oscillate throughout day and night (Albus et al., 2002; Schaap et al., 2003; Yamaguchi et al., 2003; Kuhlman and McMahon, 2006; Ko et al., 2009). Neurons are active for 4–6 h during the day and inactive during the night. During the daily active state their responses to excitatory inputs are remarkably reduced while at night they become responsive again. A combination of ion channels regulates membrane currents that maintain the spontaneous circadian activity of SCN neurons (Colwell, 2011). The silencing of SCN neuronal firing, at night, depends on a difference in membrane potential and this is mainly mediated by a hyperpolarizing potassium mechanisms (Kuhlman and McMahon, 2006).

A series of important studies, that have investigated the relation between neuronal activity and circadian molecular clock (Nitabach and Blau, 2002; Nitabach et al., 2002; Sheeba et al., 2008; Choi et al., 2009), has shown that synaptic activity and membrane potential are responsible for the oscillation of core clock genes. This has dramatically changed the general assumption that a molecular clock drives the activity of clock neurons. Nitabach et al. (2002) were able to show, in *Drosophila*, that chronic hyperpolarization silenced circadian neurons and interrupted the circadian behavioral rhythmicity and the expression of PER and TIM proteins. This testifies that neural activity regulates circadian molecular clock. Another component that plays a crucial role in clock gene expression is represented by the levels of Ca^{2+}. The resting levels of Ca^{2+} during the day, when the SCN neurons are more active, are doubled if compared with the night inactivity (Colwell, 2000). Ca^{2+} is thought to be responsible also for another important aspect of circadian rhythms: the phase–response curve (Colwell, 2011). Indeed, the response to an environmental input (e.g., light stimulation) differs according to the specific phase of the circadian cycle.

There are several reasons to investigate associations between interval timing and circadian rhythms. A series of studies contravenes the assumption that interval timing depends on a linear accumulator but, instead, indicates an oscillatory-like mechanisms (Crystal, 1999, 2003; Crystal and Baramidze, 2007; Gu et al., 2011). Thus, it is reasonable to investigate if shared mechanisms between short (seconds-to-minutes) and long (circadian) timed responses occur. Several studies have concluded for a close relationship between interval timing and circadian rhythms. For example, it has been shown that circadian rhythms change the perception for short intervals (Pfaff, 1968; Aschoff, 1998a,b; Nakajima et al., 1998; Morofushi et al., 2001) and that in conditions of temporal isolation (Aschoff, 1998) the time estimation co-varies with their circadian period. Furthermore, in drosophila circadian mutants it is present a deficit for short-interval timing (Kyriacou and Hall, 1980). Yet, dopamine (DA) mechanisms and motivated behaviors are strongly associated with both interval timing (Meck, 2006a,b; Agostino et al., 2011) and circadian clock (Albrecht, 2011). SCN projects toward brain areas within the DA circuitries and which mediate reward-related behaviors.

Other studies, instead, suggested that circadian clock mechanisms are independent of interval timing. This conclusion was driven by SCN lesion studies (Lewis et al., 2003) and by investigations of interval timing in circadian mutants (Cordes and Gallistel, 2008; Papachristos et al., 2011). I shall argue that conclusions driven by lesions restricted to SCN should not be generalized to the molecular level. For example, studies in mice of SCN lesions that lead to arrhythmic circadian behaviors, but did not affect sleep homeostasis (Easton et al., 2004; Larkin et al., 2004), have supported, for a long time, the idea that the two processes (circadian and homeostatic) were independent. However, at a molecular level, we now know that several circadian genes play a role in sleep (Tucci and Nolan, 2010).

Regarding the phenotyping of interval timing in circadian mouse mutants, Cordes and Gallistel (2008) have reported that Clock has no abnormal consequences in the peak-interval procedure in mice. In this study CLOCK-KO mice were used instead of the CLOCK mutants that carry the single point mutations. Similar negative results in interval timing were obtained by Papachristos et al. (2011) in Cry1 and Cry2 KO mice. Our critical argument to these studies is that, due to functional genomic redundancy, gene deletion models may not be able to reveal all the important functions of the gene. Paralog compensation among several clock functional genes has been reported (Debruyne et al. 2006; DeBruyne et al., 2007). It was shown that CLOCK-deficient mice present only mild circadian alterations and, thus, it is not essential for the circadian rhythms (Debruyne et al., 2006). A paralog of CLOCK, NSPAS2, has been proposed to dimerize with BIMAL1 and to work in the mouse forebrain as the clock molecular loop (Reick et al., 2001). NSPAS2 is particularly expressed in the cortex, hippocampus, striatum, amygdala, and thalamus (Garcia et al., 2000) and exerts an important role in sleep and behavior (Dudley et al., 2003). For all these reasons, I believe that further investigations in interval timing and circadian rhythms is required before we can roll out the hypothesis of an independency among these phenomena.

EPIGENETICS AND BIOLOGICAL CLOCKS

Ultimately, the investigation of the genetic determinants that regulate biological clocks is growing in complexity. Epigenetic mechanisms set a number of temporal determinants for gene expression. The action of the genome seems to respond to a principle of modularity (Litvin et al., 2009) that refers to a functional model in which cellular states, determined by genetic variations and by extracellular stimulations, affect transcriptional responses (Litvin et al., 2009). In particular, a primary locus controls the states of the cell and then a secondary locus has an effect only in particular states. This is a very interesting model that implies a timed expression of specific gene-driven phenotypes. The temporal coding of genetic information depends on chromatin states that regulate gene transcription and functioning. Epigenetic marks can vary over periods of minutes to hours and they constitute fundamental mechanisms for learning and memory consolidation (Akbarian and Huang, 2009). Since approximately 10% of all mammalian transcripts present a circadian rhythmicity (Panda et al., 2002), an efficient chromatin remodeling must exist to ensure this rhythmic gene expression (Borrelli et al., 2008). A number of studies has demonstrated that methylation oscillates at clock gene promoters (Etchegaray et al., 2006) and rhythmic histone modification arises at promoter of clock-controlled genes (Etchegaray et al., 2003; Naruse et al., 2004; Ripperger and Schibler, 2006). Although these studies do not proof that specific epigenetic mechanisms, such as those involved in chromatin remodeling, are necessary for clock control, they demonstrate that transcription-permissive chromatin states occur at specific circadian times (Borrelli et al., 2008).

CONCLUSION AND FUTURE DIRECTIONS

Molecular elements play an important role in sleep, circadian rhythms, and interval timing. Thus, timing is coded at behavioral, physiological, genetic, and epigenetic level. An integrated investigation of these mechanisms represents the next frontier in developing models of coding and retaining of temporal information. The choice of animal models (e.g., the mouse), which carry single nucleotides mutations that translate into abnormal circadian phenotypes is preferred to deletion models. In future, it could be envisaged that interval-timing phenotypes will be largely employed in phenotype-based mutagenesis program (Nolan et al., 2000) and would have the potential to promote a new era of molecular discoveries, in interval timing, as we had for circadian clock. However, cognitive tests in mice present a number of restraints that make them unfeasible for such large-scale functional genomics enterprises. An easy solution to this impasse is the development of automated tests in home-cage. They have the advantage to increase the sample of observations, to reduce the time for training and to leave the animals undisturbed. Last, but not least, 24-h home-cage screens allow the integrated investigation of timing phenotypes at different time-scales.

ACKNOWLEDGMENTS

I thank Glenda Lassi for critical reading of the manuscript and for discussions. Support (to Valter Tucci) was provided by the European Commission FP7 Programme under project 223263 (PhenoScale).

REFERENCES

Agostino, P. V., Golombek, D. A., and Meck, W. H. (2011). Unwinding the molecular basis of interval and circadian timing. *Front. Integr. Neurosci.* 5:64. doi: 10.3389/fnint.2011.00064

Akbarian, S., and Huang, H. S. (2009). Epigenetic regulation in human brain-focus on histone lysine methylation. *Biol. Psychiatry* 65, 198–203.

Albrecht, U. (2011). The circadian clock, reward, and memory. *Front. Mol. Neurosci.* 4:41. doi: 10.3389/fnmol.2011.00041

Albus, H., Bonnefont, X., Chaves, I., Yasui, A., Doczy, J., van der Horst, G. T., and Meijer, J. H. (2002). Cryptochrome-deficient mice lack circadian electrical activity in the suprachiasmatic nuclei. *Curr. Biol.* 12, 1130–1133.

Aschoff, J. (1998a). Circadian parameters as individual characteristics. *J. Biol. Rhythms* 13, 123–131.

Aschoff, J. (1998b). Human perception of short and long time intervals: its correlation with body temperature and the duration of wake time. *J. Biol. Rhythms* 13, 437–442.

Borrelli, E., Nestler, E. J., Allis, C. D., and Sassone-Corsi, P. (2008). Decoding the epigenetic language of neuronal plasticity. *Neuron* 60, 961–974.

Buhusi, C. V., and Meck, W. H. (2005). What makes us tick? Functional and neural mechanisms of interval timing. *Nat. Rev. Neurosci.* 6, 755–765.

Buonomano, D. V., and Laje, R. (2010). Population clocks: motor timing with neural dynamics. *Trends Cogn. Sci. (Regul. Ed.)* 14, 520–527.

Cheng, R. K., Williams, C. L., and Meck, W. H. (2008). Oscillatory bands, neuronal synchrony and hippocampal function: implications of the effects of prenatal choline supplementation for sleep-dependent memory consolidation. *Brain Res.* 1237, 176–194.

Cheng, R. K., Williams, C. L., and Meck, W. H. (2009). Neurophysiological mechanisms of sleep-dependent memory consolidation and its facilitation by prenatal choline supplementation. *Chin. J. Physiol.* 52, 223–235.

Choi, C., Fortin, J. P., McCarthy, E., Oksman, L., Kopin, A. S., and Nitabach, M. N. (2009). Cellular dissection of circadian peptide signals with genetically encoded membrane-tethered ligands. *Curr. Biol.* 19, 1167–1175.

Colwell, C. S. (2000). Circadian modulation of calcium levels in cells in the suprachiasmatic nucleus. *Eur. J. Neurosci.* 12, 571–576.

Colwell, C. S. (2011). Linking neural activity and molecular oscillations in the SCN. *Nat. Rev. Neurosci.* 12, 553–569.

Cordes, S., and Gallistel, C. R. (2008). Intact interval timing in circadian CLOCK mutants. *Brain Res.* 1227, 120–127.

Coull, J. T., Cheng, R. K., and Meck, W. H. (2011). Neuroanatomical and neurochemical substrates of timing. *Neuropsychopharmacology* 36, 3–25.

Crystal, J. D. (1999). Systematic nonlinearities in the perception of temporal intervals. *J. Exp. Psychol. Anim. Behav. Process.* 25, 3–17.

Crystal, J. D. (2001). Circadian time perception. *J. Exp. Psychol. Anim. Behav. Process.* 27, 68–78.

Crystal, J. D. (2003). "Nonlinearities in sensitivity to time: implications for oscillator-based representations of interval circadian clocks," in *Functional and Neural Mechanisms of Interval Timing*, ed. W. H. Meck (Boca Raton, FL: CRC Press), 61–76.

Crystal, J. D. (2006a). Animal behavior: timing in the wild. *Curr. Biol.* 16, R252–R253.

Crystal, J. D. (2006b). Long-interval timing is based on a self-sustaining endogenous oscillator. *Behav. Processes* 72, 149–160.

Crystal, J. D., and Baramidze, G. T. (2007). Endogenous oscillations in short-interval timing. *Behav. Processes* 74, 152–158.

Debruyne, J. P., Noton, E., Lambert, C. M., Maywood, E. S., Weaver, D. R., and Reppert, S. M. (2006). A clock shock: mouse CLOCK is not required for circadian oscillator function. *Neuron* 50, 465–477.

DeBruyne, J. P., Weaver, D. R., and Reppert, S. M. (2007). CLOCK and NPAS2 have overlapping roles in the suprachiasmatic circadian clock. *Nat. Neurosci.* 10, 543–545.

Diekelmann, S., and Born, J. (2010). The memory function of sleep. *Nat. Rev. Neurosci.* 11, 114–126.

Dudley, C. A., Erbel-Sieler, C., Estill, S. J., Reick, M., Franken, P., Pitts, S., and McKnight, S. L. (2003). Altered patterns of sleep and behavioral adaptability in NPAS2-deficient mice. *Science* 301, 379–383.

Easton, A., Meerlo, P., Bergmann, B., and Turek, F. W. (2004). The suprachiasmatic nucleus regulates sleep timing and amount in mice. *Sleep* 27, 1307–1318.

Etchegaray, J. P., Lee, C., Wade, P. A., and Reppert, S. M. (2003). Rhythmic histone acetylation underlies transcription in the mammalian circadian clock. *Nature* 421177–421182.

Etchegaray, J. P., Yang, X., DeBruyne, J. P., Peters, A. H., Weaver, D. R., Jenuwein, T., and Reppert, S. M. (2006). The polycomb group protein EZH2 is required for mammalian circadian clock function. *J. Biol. Chem.* 281, 21209–21215.

Franken, P., and Dijk, D. J. (2009). Circadian clock genes and sleep homeostasis. *Eur. J. Neurosci.* 29, 1820–1829.

Garcia, J. A., Zhang, D., Estill, S. J., Michnoff, C., Rutter, J., Reick, M., Scott, K., Diaz-Arrastia, R., and McKnight, S. L. (2000). Impaired cued and contextual memory in NPAS2-deficient mice. *Science* 288, 2226–2230.

Gu, B. M., Yin, B., Cheng, R. K., and Meck, W. H. (2011). Quinpirole-induced sensitization to noisy/sparse periodic input: temporal synchronization as a component of obsessive-compulsive disorder. *Neuroscience* 179, 143–150.

Hinton, S. C., and Meck, W. H. (1997). The 'internal clocks' of circadian and interval timing. *Endeavour* 21, 82–87.

Ko, C. H., and Takahashi, J. S. (2006). Molecular components of the mammalian circadian clock. *Hum. Mol. Genet.* 15 Spec No 2, R271–R277.

Ko, G. Y., Shi, L., and Ko, M. L. (2009). Circadian regulation of ion channels and their functions. *J. Neurochem.* 110, 1150–1169.

Korman, M., Doyon, J., Doljansky, J., Carrier, J., Dagan, Y., and Karni, A. (2007). Daytime sleep condenses the time course of motor memory consolidation. *Nat. Neurosci.* 10, 1206–1213.

Krueger, J. M. (2010). "What exactly is it that sleeps? The evolution, regulation and organization of an emergent network property," in *Evolution of Sleep: Phylogenetic and Functional Perspectives*, eds P. McNamara, R. A. Barton, and C. L. Nunn (New York: Cambridge University Press), 86–106.

Kuhlman, S. J., and McMahon, D. G. (2006). Encoding the ins and outs of circadian pacemaking. *J. Biol. Rhythms* 21, 470–481.

Kyriacou, C. P., and Hall, J. C. (1980). Circadian rhythm mutations in *Drosophila melanogaster* affect short-term fluctuations in the male's courtship song. *Proc. Natl. Acad. Sci. U.S.A.* 77, 6729–6733.

Lahl, O., Wispel, C., Willigens, B., and Pietrowsky, R. (2008). An ultra short episode of sleep is sufficient to promote declarative memory performance. *J. Sleep Res.* 17, 3–10.

Larkin, J. E., Yokogawa, T., Heller, H. C., Franken, P., and Ruby, N. F. (2004). Homeostatic regulation of sleep in arrhythmic Siberian hamsters. *Am. J. Physiol. Regul. Integr. Comp. Physiol.* 287, R104–R111.

Lewis, P. A., Couch, T. J., and Walker, M. P. (2011). Keeping time in your sleep: overnight consolidation of temporal rhythm. *Neuropsychologia* 49, 115–123.

Lewis, P. A., and Meck, W. H. (2011). Does sleep contribute to degeneracy in neural timing? *Psychologist* (in press).

Lewis, P. A., Miall, R. C., Daan, S., and Kacelnik, A. (2003). Interval timing in mice does not rely upon the circadian pacemaker. *Neurosci. Lett.* 348, 131–134.

Litvin, O., Causton, H. C., Chen, B. J., and Pe'er, D. (2009). Modularity and interactions in the genetics of gene expression. *Proc. Natl. Acad. Sci. U.S.A.* 106, 6441–6446.

Lopez-Molina, L., Conquet, F., Dubois-Dauphin, M., and Schibler, U. (1997). The DBP gene is expressed according to a circadian rhythm in the suprachiasmatic nucleus and influences circadian behavior. *EMBO J.* 16, 6762–6771.

Lowrey, P. L., Shimomura, K., Antoch, M. P., Yamazaki, S., Zemenides, P. D., Ralph, M. R., Menaker, M., and Takahashi, J. S. (2000). Positional syntenic cloning and functional characterization of the mammalian circadian mutation tau. *Science* 288, 483–492.

Lowrey, P. L., and Takahashi, J. S. (2000). Genetics of the mammalian circadian system: photic entrainment, circadian pacemaker mechanisms, and posttranslational regulation. *Annu. Rev. Genet.* 34, 533–562.

Marshall, L., and Born, J. (2007). The contribution of sleep to hippocampus-dependent memory consolidation. *Trends Cogn. Sci. (Regul. Ed.)* 11, 442–450.

Meck, W. H. (2006a). Frontal cortex lesions eliminate the clock speed effect of dopaminergic drugs on interval timing. *Brain Res.* 1108, 157–167.

Meck, W. H. (2006b). Neuroanatomical localization of an internal clock: a functional link between mesolimbic, nigrostriatal, and mesocortical dopaminergic systems. *Brain Res.* 1109, 93–107.

Mednick, S., Nakayama, K., and Stickgold, R. (2003). Sleep-dependent learning: a nap is as good as a night. *Nat. Neurosci.* 6, 697–698.

Molle, M., and Born, J. (2011). Slow oscillations orchestrating fast oscillations and memory consolidation. *Prog. Brain Res.* 193, 93–110.

Morofushi, M., Shinohara, K., and Kimura, F. (2001). Menstrual and circadian variations in time perception in healthy women and women with premenstrual syndrome. *Neurosci. Res.* 41, 339–344.

Nakajima, T., Uchiyama, M., Enomoto, T., Shibui, K., Ishibashi, K., Kanno, O., and Okawa, M. (1998). Human time production under constant routine. *Psychiatry Clin. Neurosci.* 52 240–241.

Naruse, Y., Oh-Hashi, K., Iijima, N., Naruse, M., Yoshioka, H., and Tanaka, M. (2004). Circadian and light-induced transcription of clock gene Per1 depends on histone acetylation and deacetylation. *Mol. Cell Biol.* 24, 6278–6287.

Nishida, M., and Walker, M. P. (2007). Daytime naps, motor memory consolidation and regionally specific sleep spindles. *PLoS ONE* 2, e341. doi: 10.1371/journal.pone.0000341

Nitabach, M. N., and Blau, J. (2002). Cellular clockwork. *Nat. Genet.* 32, 559–560.

Nitabach, M. N., Blau, J., and Holmes, T. C. (2002). Electrical silencing of *Drosophila* pacemaker neurons stops the free-running circadian clock. *Cell* 109, 485–495.

Nolan, P. M., Peters, J., Strivens, M., Rogers, D., Hagan, J., Spurr, N., Gray, I. C., Vizor, L., Brooker, D., Whitehill, E., Washbourne, R., Hough, T., Greenaway, S., Hewitt, M., Liu, X., McCormack, S., Pickford, K., Selley, R., Wells, C., Tymowska-Lalanne, Z., Roby, P., Glenister, P., Thornton, C., Thaung, C., Stevenson, J. A., Arkell, R., Mburu, P., Hardisty, R., Kiernan, A., Erven, A., Steel, K. P., Voegeling, S., Guenet, J. L., Nickols, C., Sadri, R., Nasse, M., Isaacs, A., Davies, K., Browne, M., Fisher, E. M., Martin, J., Rastan, S., Brown, S. D., and Hunter, J. (2000). A systematic, genome-wide, phenotype-driven mutagenesis programme for gene function studies in the mouse. *Nat. Genet.* 25, 440–443.

Pace-Schott, E. F., Stickgold, R., Muzur, A., Wigren, P. E., Ward, A. S., Hart, C. L., Walker, M., Edgar, C., and Hobson, J. A. (2005). Cognitive performance by humans during a smoked cocaine binge-abstinence cycle. *Am. J. Drug Alcohol Abuse* 31, 571–591.

Panda, S., Antoch, M. P., Miller, B. H., Su, A. I., Schook, A. B., Straume, M., Schultz, P. G., Kay, S. A., Takahashi, J. S., and Hogenesch, J. B. (2002). Coordinated transcription of key pathways in the mouse by the circadian clock. *Cell* 109, 307–320.

Papachristos, E. B., Jacobs, E. H., and Elgersma, Y. (2011). Interval timing is intact in arrhythmic Cry1/Cry2-deficient mice. *J. Biol. Rhythms* 26, 305–313.

Pfaff, D. (1968). Effects of temperature and time of day on time judgments. *J. Exp. Psychol.* 76, 419–422.

Reick, M., Garcia, J. A., Dudley, C., and McKnight, S. L. (2001). NPAS2: an analog of clock operative in the mammalian forebrain. *Science* 293, 506–509.

Reppert, S. M. (2006). A colorful model of the circadian clock. *Cell* 124, 233–236.

Ripperger, J. A., and Schibler, U. (2006). Rhythmic CLOCK-BMAL1 binding to multiple E-box motifs drives circadian Dbp transcription and chromatin transitions. *Nat. Genet.* 38, 369–374.

Schaap, J., Albus, H., VanderLeest, H. T., Eilers, P. H., Détári, L., and Meijer, J. H. (2003). Heterogeneity of rhythmic suprachiasmatic nucleus neurons: implications for circadian waveform and photoperiodic encoding. *Proc. Natl. Acad. Sci. USA* 100, 15994–15999.

Sheeba, V., Gu, H., Sharma, V. K., O'Dowd, D. K., and Holmes, T. C. (2008). Circadian- and light-dependent regulation of resting membrane potential and spontaneous action potential firing of *Drosophila* circadian pacemaker neurons. *J. Neurophysiol.* 99, 976–988.

Stickgold, R. (2005). Sleep-dependent memory consolidation. *Nature* 437, 1272–1278.

Stickgold, R., and Walker, M. P. (2005a). Memory consolidation and reconsolidation: what is the role of sleep? *Trends Neurosci.* 28, 408–415.

Stickgold, R., and Walker, M. P. (2005b). Sleep and memory: the ongoing debate. *Sleep* 28, 1225–1227.

Tononi, G., and Cirelli, C. (2006). Sleep function and synaptic homeostasis. *Sleep Med. Rev.* 10, 49–62.

Tucci, V., and Nolan, P. M. (2010). "Toward an understanding of the function of sleep: new insights from mouse genetics," in *Evolution of Sleep: Phylogenetic and Functional Perspectives*, eds P. McNamara, R. A. Barton, and C. L. Nunn (New York: Cambridge University Press), 218–237.

Tucker, M. A., Hirota, Y., Wamsley, E. J., Lau, H., Chaklader, A., and Fishbein, W. (2006a). A daytime nap containing solely non-REM sleep enhances declarative but not procedural memory. *Neurobiol. Learn. Mem.* 86, 241–247.

Tucker, P., Lombardi, D., Smith, L., and Folkard, S. (2006b). The impact of rest breaks on temporal trends in injury risk. *Chronobiol. Int.* 23, 1423–1434.

Walker, M. P., Stickgold, R., Alsop, D., Gaab, N., and Schlaug, G. (2005a). Sleep-dependent motor memory plasticity in the human brain. *Neuroscience* 133, 911–917.

Walker, M. P., Stickgold, R., Jolesz, F. A., and Yoo, S. S. (2005b). The functional anatomy of sleep-dependent visual skill learning. *Cereb. Cortex* 15, 1666–1675.

Yamaguchi, S., Isejima, H., Matsuo, T., Okura, R., Yagita, K., Kobayashi, M., and Okamura, H. (2003). Synchronization of cellular clocks in the suprachiasmatic nucleus. *Science* 302, 1408–1412.

Received: 15 December 2011; accepted: 15 December 2011; published online: 04 January 2012.

Citation: Tucci V (2012) Sleep, circadian rhythms, and interval timing: evolutionary strategies to time information. Front. Integr. Neurosci. 5:92. doi: 10.3389/fnint.2011.00092

frontiers in
INTEGRATIVE NEUROSCIENCE

OPINION ARTICLE
published: 01 July 2011
doi: 10.3389/fnint.2011.00028

Interval timing by long-range temporal integration

Patrick Simen[1]*, Fuat Balci[1,2], Laura deSouza[1], Jonathan D. Cohen[1] and Philip Holmes[1]

[1] Princeton Neuroscience Institute, Princeton University, Princeton, NJ, USA
[2] Psychology Department, Koç University, Istanbul, Turkey
*Correspondence: psimen@math.princeton.edu

Classic psychological models of interval timing track time by counting – or *integrating* – pulses emitted by a stochastic pulse generator. However, the neural plausibility of this approach has frequently been questioned, despite the key role played by neural integrators in well-supported models of perceptual decision-making. Although response times on the order of 1–2 s are routinely observed in the decision-making domain, tuning an integrator's parameters precisely enough to time intervals of much greater duration strikes many researchers as implausible. Behavioral and physiological data from timing tasks nonetheless frequently appear consistent with such precision. In this article, we propose that chains of integrators constructed from mechanisms exhibiting a range of intrinsic time constants (ranging from slow protein synthesis processes to rapidly ramping neural firing rates) may be used collectively to perform robust interval timing over a broad range of durations.

Since the 1960s, many psychological models have exploited Poisson-like firing rates of cortical neurons to account for variability in measured behavior Luce (1986). They have also typically applied counters to these spike trains to achieve behavioral functionality (e.g., counting spikes up to a threshold to trigger a timed behavior). In this respect, such models embody the notion that counting, or integration, is as easy for the brain as it is for a digital timer – a notion that strikes many neuroscientists as implausible. We hypothesize that the level of robust integration needed to model interval timing in this way over many orders of temporal magnitude (from fractions of a second to many minutes) can be achieved by physical spike generators and counters with a range of intrinsic spike rates and time constants.

Unlike perfect integration, leaky integration is known to be a fundamental feature of brain function: for example, it is exhibited by voltage dynamics on an individual neuron's capacitive membrane. Equation 1 is a stochastic differential equation that decomposes how a leaky integrator with time constant τ and output $x(t)$ responds to deterministic inputs $I(t)$ (the dt term) combined with additive white noise (the dW term):

$$\tau \cdot dx = (I - x) \cdot dt + c \cdot dW. \quad (1)$$

The x-value of a deterministic ($c = 0$) leaky integrator jumps at the time of a large transient input I, then decays exponentially back to 0 as $e^{-t/\tau}$ if I remains 0 thereafter. Small τ implies large jumps and rapid decay in $x(t)$; x is likewise highly responsive to noise when it is included ($c > 0$).

Although individual membrane potentials reset to a baseline level after conversion into an action potential, *populations* of neurons are thought capable of continuously representing a leaky integrator's state using a firing rate code Shadlen and Newsome (1994). Recurrent connections within such a model population produce reverberating activity that emulates a leaky integrator with a large time constant. Any leaky integrator's leakiness can in fact be completely canceled by recurrent self-excitation, in which the output of a leaky integrator is added to its inputs. In this way, x disappears from the first term on the righthand side of Equation 1, implying that $x(t)$ is the integral of $I(t)$. This balancing is the basis of one form of neural integrator model e.g., Seung (1996), and it is fundamental to the design of analog electronic integrators. When noise is included, Equation 1 defines a stochastic integrator, implying that $x(t)$ is a drift–diffusion process – a process that forms the basis of an influential model of two-alternative decision-making (Ratcliff and Rouder, 1998).

What troubles some researchers is the level of precision-tuning required for self-excitation to cancel the leak: if self-excitation replaces x in the righthand side of Equation 1, not by zero, but by kx, with $k \neq 0$, then the system will remain leaky ($k > 0$) or become unstable ($k < 0$). The impact of non-zero k, however, can be reduced by increasing τ to $\tau' = \alpha\tau$, $\alpha \gg 1$, and increasing I to $I' = \alpha I$ in Equation 1. By using a drift–diffusion process with a large intrinsic value of τ' – say, a process that models protein synthesis within neurons – the impact of failures to balance exactly is relatively minor, since x will now integrate $(I' - kx)/\tau' = (\alpha I - kx)/(\alpha\tau) \approx I/\tau$. Shorter time intervals can be timed with larger values of I', but this entails increasing energetic costs. Thus, pressure to use larger time constants to enhance performance may trade off against pressure to conserve energy.

A number of other robust integration schemes have been proposed in the literature, but we propose a particularly simple solution: using a chain of leaky integrators with a decreasing sequence of intrinsic time constants to implement our feedback-based integrators (other time constant orderings would produce identical results). Each element in this chain triggers the subsequent timing process when it crosses its threshold. With this approach, one can model robust timing and decision-making functionality that obeys the law of time scale invariance so often observed in interval timing tasks: response time distributions superimpose when the response times are divided by the mean response time Gibbon (1977).

We have shown Simen et al. (2011) that a time-scale-invariant drift–diffusion model of timing arises from counting up the spikes of a Poisson process (rate λ_1), and subtracting off the spikes of an opponent Poisson process with proportionally lower rate $\gamma\lambda_1$, $\gamma < 1$. When the net spike count exceeds a fixed threshold, responses are generated; adjusting λ_1 allows different intervals to be timed. The net spike count variance equals the sum of individual spike count variances, which implies a drift–diffusion approximation with $(I - x)$ in Eq. 1 replaced by a constant drift term $A = (1-\gamma)\lambda_1$ and $c = \sqrt{(1+\gamma)/(1-\gamma)A}$. Scale invariance occurs because $c = m\sqrt{A}$ for a constant $m = \sqrt{(1+\gamma)/(1-\gamma)}$, the expected response time is z/A for a constant threshold z, and the variance is $m^2 z/A^2$ (Rivest and Bengio, 2011; Simen et al., 2011).

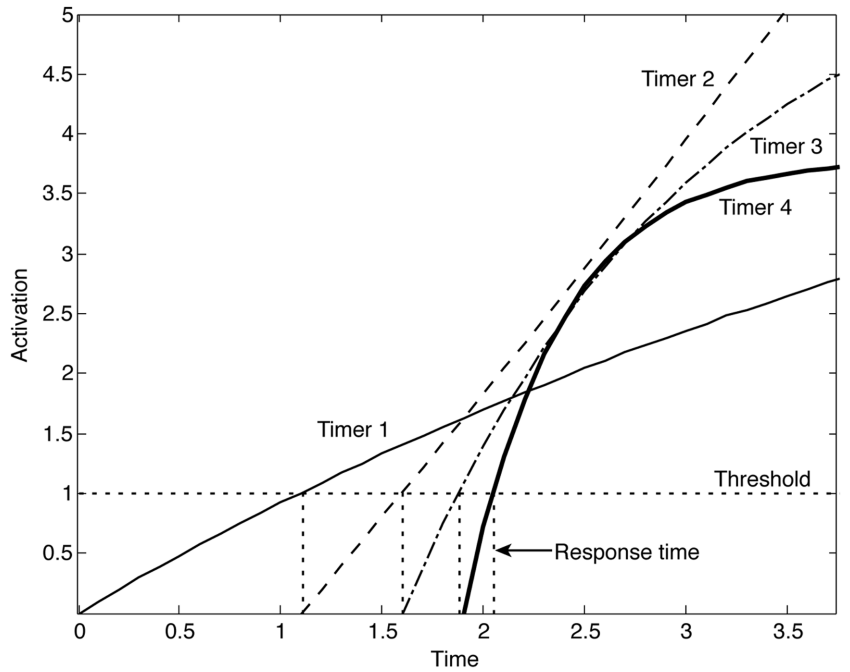

FIGURE 1 | Activation time histories for four sequentially triggered interval timers, based on imperfectly balanced integrators (for each timer, *k* is selected from a normal distribution with mean and SD of 0.1). Here $\tau_1 = 1$, $\tau_2 = 0.5$, $\tau_3 = 0.25$, $\tau_4 = 0.125$. Below threshold, these activations are approximately linear.

If we then add the threshold-crossing times of sequential drift–diffusion processes with different intrinsic time constants, but with drift values inversely proportional to the timed duration (see **Figure 1**), we find that the coefficient of variation (CV) of the summed threshold-crossing times is constant for changing durations (here C_i and C_i' are proportionality constants):

$$\mathrm{Var}(t_i) = C_i / A^2 \text{ and } E(t_i) = C_i' / A$$

$$\Rightarrow \mathrm{CV}\left(\sum_i t_i\right) = \sqrt{\frac{\sum_i C_i}{A^2}} \cdot \frac{A}{\sum_i C_i'} = \text{const.}$$

The mystery of robust temporal integration may therefore reduce to distributing integration tasks to a suite of mechanisms with a range of intrinsic time constants. Each integrator in this scheme triggers the next integrator (with a smaller τ) to ramp up over a time span most appropriate for it. Within each time span, deviations from perfect integration thus remain within tolerable levels. Robust integration may therefore require less in the way of special mechanisms than is sometimes thought, suggesting that theories of timing and perceptual decision-making based on perfect integration are not neurally implausible *a priori*.

ACKNOWLEDGMENTS

This work was supported by the National Institute of Mental Health (P50 MH062196, Cognitive and Neural Mechanisms of Conflict and Control, Silvio M. Conte Center), by the Air Force Research Laboratory (FA9550-07-1-0537), and by an FP7 Marie Curie IRG 277015 to Fuat Balci.

REFERENCES

Gibbon, J. (1977). Scalar expectancy theory and Weber's law in animal timing. *Psychol. Rev.* 84, 279–325.

Luce, R. D. (1986). *Response Times: Their Role in Inferring Elementary Mental Organization*. New York: Oxford University Press.

Ratcliff, R., and Rouder, J. N. (1998). Modeling response times for two-choice decisions. *Psychol. Sci.* 9, 347–356.

Rivest, F., and Bengio, Y. (2011). Adaptive drift-diffusion process to learn time intervals. *arXiv*, 1103.2382v1.

Seung, H. S. (1996). How the brain keeps the eyes still. *Proc. Natl. Acad. Sci. U.S.A.* 93, 13339–13344.

Shadlen, M. N., and Newsome, W. T. (1994). Noise, neural codes and cortical organization. *Curr. Opin. Neurobiol.* 4, 569–579.

Simen, P. A., Balci, F., deSouza, L., Cohen, J. D., and Holmes, P. (2011). A model of interval timing by neural integration. *J. Neurosci.* 31, 9238–9253.

Received: 01 June 2011; accepted: 13 June 2011; published online: 01 July 2011.

Citation: Simen P, Balci F, deSouza L, Cohen JD and Holmes P (2011) Interval timing by long-range temporal integration. Front. Integr. Neurosci. 5:28. doi: 10.3389/fnint.2011.00028

frontiers in
INTEGRATIVE NEUROSCIENCE

OPINION ARTICLE
published: 18 August 2011
doi: 10.3389/fnint.2011.00041

Defining the contributions of network clock models to millisecond timing

Uma R. Karmarkar*

Harvard Business School, Boston, MA USA
**Correspondence: ukarmarkar@hbs.edu*

Our ability to measure time extends from microseconds to days (Buonomano and Karmarkar, 2002; Buhusi and Meck, 2005). Given the wealth of experimental support for a number of different models of timing, it has been recently suggested that multiple mechanisms act in concert to transition smoothly between both temporal ranges and modalities (Wiener et al., 2011). This underscores the importance of determining the specific contributions of individual mechanisms to better understand these transitions and any relevant idiosyncrasies of timing in a particular context.

We focus here on interval discrimination in the range of tens to hundreds of milliseconds, which plays an important role in a variety of tasks, such as speech processing, motion detection, and fine motor coordination. It has been proposed that such timing can emerge directly from the temporal properties intrinsic to neural circuits (Buonomano and Mauk, 1994; Buonomano and Merzenich, 1995; Karmarkar and Buonomano, 2007; for review see Ivry and Schlerf, 2008). Broadly, this class of mechanisms can be described as population or network clocks, as the timing of incoming stimuli is coded as the changes they effect in a population of neurons. This can also be thought of as the change in the overall state of the network. Compared to models of millisecond timing based on a single centralized mechanism (Treisman, 1963; Church, 1984; Gibbon et al., 1997; Ivry and Spencer, 2004) network clock models imply that timing is being done in multiple loci across the cortex. This is interesting because it means that the dynamics of timing are dependent on the properties of the underlying local circuitry, which could vary across modalities.

To understand the behavior of network clocks, it is useful to examine a particular instantiation, referred to as a state-dependent network (SDN), which has been developed in the context of sensory processing (Karmarkar and Buonomano, 2007). For SDNs an incoming stimulus changes the network state not only by causing some population of neurons to fire, but also by engaging a number of intrinsic properties such as short-term plasticity, that change with specific time constants on the millisecond scale. As a result, the response of the network to a particular piece of temporal information is dependent on its recent history. Thus instead of marking each interval separately, timing is done continuously, with the network linking multiple signals together as a temporal object. The SDN can only measure information independently, or *reset*, when the interval between stimuli has been sufficiently long to allow the network to return to its baseline state. This makes two predictions about interval discrimination, the first being that a variable context (or "distractor" stimulus) should have a greater impact or disruption on timing than a fixed one. The second prediction is that when comparing two intervals, timing of the second will be influenced by the first if they are not separated by more time than the reset threshold. These predictions can be tested psychophysically to distinguish the extent to which various types of timing arise from network clocks.

In the auditory system, multiple studies examining interval discrimination with reset tasks have shown results consistent with an SDN model (Karmarkar and Buonomano, 2007; Buonomano et al., 2009; Spencer et al., 2009). Based on this data, the influence of the SDN appears to fall off somewhere between intervals above 250 but below 500 ms (Buonomano et al., 2009). This limit is potentially as restrictive as 300 ms, since stimuli including that interval do not show the expected pattern of impairment due to a variable context (Spencer et al., 2009). However, a secondary analysis of the data from that study might suggest that distractor signals prior to the target interval do appear to exert some bias on discrimination as long as the whole stimulus sequence, or temporal object, does not significantly exceed 400 ms (Figures 3 and 5, Spencer et al., 2009). A threshold in this vicinity is consistent with the assumptions of the SDN model since it is dependent on the time constants of short-term plasticity, which are on the order of a few hundreds of milliseconds (e.g. Zucker, 1989).

Such a restriction in range could be perceived as a challenge to the relevance of SDNs, or network clocks in general, to other sensory modalities. Though intervals of less than 300–400 ms can be useful for somatosensory timing, the visual system appears to operate on a fundamentally slower timescale. Experiments in which individuals had to reproduce durations represented by visual stimuli showed that participants' lowest estimated duration was 300 ms, even when the target interval was less than 100 ms, suggesting difficulty in accurately perceiving those shorter times (Lewis and Miall, 2009). In addition, visual discrimination of intervals has been shown to be less precise, that is, to have a higher variance, than auditory perception of the same durations (Merchant et al., 2008), which could prevent effective measurement of time spans less than 200 ms. Based on this data, the range over which the SDN operates for auditory stimuli might appear to render it inconsequential for visual ones.

It should be noted though, that previous studies have revealed some visual discriminatory capabilities for intervals in the 100 to 200-ms range (e.g. Mattes and Ulrich, 1998; Westheimer, 1999). Furthermore, interval timing in the visual system is spatially localized (Johnston et al., 2006; Burr et al., 2007), suggesting that the mechanism is specific to early visual cortices, consistent with the idea of a local network clock. As such, it is possible that some of the reduction in precision for interval timing is due to the inherent variance of the basic response time in primary visual cortex. This could be considered a time-independent issue that influences the system by adding noise rather than indicating a non-SDN mechanism.

Vision has been considered a difficult modality for defining or studying temporal processing mechanisms. This is because visual timing is extremely sensitive to a number of atemporal stimulus characteristics (Eagleman, 2008), and is generally tightly linked to spatial information, as in motion detection. However, we propose that it is key in determining whether the SDN can be considered a general model of sensory timing.

Finally, it is important to recognize that there are other network clock models based on differing circuitry (e.g. Buonomano and Mauk, 1994; Medina et al., 2000; Fiete et al., 2010). This reflects the broader concept of an intrinsic timer, that temporal processing is dependent on the specific properties of the neural locus in question. The differences in the structure of these models also lead to differences in the range of times they can process, and their ability to integrate spatial and temporal information. For example, it has been proposed that population clock models that leverage recurrent excitatory connections with strong weights can account for motor timing that extends from milliseconds into seconds (Buonomano and Laje, 2010). Despite this diversity, network clock models largely show the same phenotype of continuous temporal processing, in which sequences are treated as temporal objects, making reset-type tasks a general diagnostic tool for this class of timers. As a result, using psychophysical measures to investigate timing directly across modalities is an important first step in defining the contribution of network clock models to human interval discrimination.

REFERENCES

Buhusi, C. V., and Meck, W. H. (2005). What makes us tick? Functional and neural mechanisms of interval timing. *Nat. Rev. Neurosci.* 6, 755–765.

Buonomano, D. V., Bramen, J., and Khodadadifar, M. (2009). Influence of the interstimulus interval on temporal processing and learning: testing the state-dependent model. *Philos. Trans. R. Soc. Lond. B Biol. Sci.* 364, 1865–1873.

Buonomano, D. V., and Karmarkar, U. R. (2002). How do we tell time? *Neuroscientist* 8, 42–51.

Buonomano, D. V., and Laje, R. (2010). Population clocks: motor timing with neural dynamics. *Trends Cogn. Sci. (Regul. Ed.)* 14, 520–527.

Buonomano, D. V., and Mauk, M. D. (1994). Neural network model of the cerebellum: temporal discrimination and the timing of motor responses. *Neural Comput.* 6, 38–55.

Buonomano, D. V., and Merzenich, M. M. (1995). Temporal information transformed into a spatial code by a neural network with realistic properties. *Science* 267, 1028–1030.

Burr, D., Tozzi, A., and Morrone, M. C. (2007). Neural mechanisms for timing visual events are spatially selective in real-world coordinates. *Nat. Neurosci.* 10, 423–425.

Church, R. M. (1984). "Properties of the internal clock," in *Annals of the New York Academy of Sciences*, Vol. 423, *Timing and Time Perception*, eds J. Gibbon and L. Allan (New York: New York Academy of Sciences), 556–582.

Eagleman, D. M. (2008). Human time perception and its illusions. *Curr. Opin. Neurobiol.* 18, 131–136.

Fiete, I. R., Senn, W., Wang, C. Z. H., and Hahnloser, R. H. R. (2010). Spike-time-dependent plasticity and heterosynaptic competition organize networks to produce long scale-free sequences of neural activity. *Neuron* 65, 563–576.

Gibbon, J., Malapani, C., Dale, C. L., and Gallistel, C. R. (1997). Toward a neurobiology of temporal cognition: advances and challenges. *Curr. Opin. Neurobiol.* 7, 170–184.

Ivry, R. B., and Schlerf, J. E. (2008). Dedicated and intrinsic models of time perception. *Trends Cogn. Sci. (Regul. Ed.)* 12, 273–280.

Ivry, R. B., and Spencer, R. M. C. (2004). The neural representation oftime. *Curr. Opin. Neurobiol.* 14, 225–232.

Johnston, A., Arnold, D. H., and Nishida, S. (2006). Spatially localized distortions of event time. *Curr. Biol.* 16, 472–479.

Karmarkar, U. R., and Buonomano, D. V. (2007). Timing in the absence of clocks: encoding time in neural network states. *Neuron* 53, 427–438.

Lewis, P. A., and Miall, R. C. (2009). The precision of temporal judgement: milliseconds, many minutes, and beyond. *Philos. Trans. R. Soc. Lond. B Biol. Sci.* 364, 1897–1905.

Mattes, S., and Ulrich, R. (1998). Directed attention prolongs the perceived brief duration of a stimulus. *Percept. Psychophys.* 60, 1305–1317.

Medina, J. F., Garcia, K. S., Nores, W. L., Taylor, N. M., and Mauk, M. D. (2000). Timing mechanisms in the cerebellum: testing predictions of a large-scale computer simulation. *J. Neurosci.* 20, 5516–5525.

Merchant, H., Zarco, W., and Prado, L. (2008). Do we have a common mechanism for measuring time in the hundreds of millisecond range? Evidence from multiple-interval timing tasks. *J. Neurophysiol.* 99, 939–949.

Spencer, R. M. C., Karmarkar, U. R., and Ivry, R. B. (2009). Evaluating dedicated and intrinsic models of temporal encoding by varying context. *Philos. Trans. R. Soc. Lond. B Biol. Sci.* 364, 1853–1863.

Treisman, M. (1963). Temporal discrimination and the indifference interval: implications for a model of the "internal clock." *Psychol. Monogr.* 77, 1–31.

Westheimer, G. (1999). Discrimination of short time intervals by the human observer. *Exp. Brain Res.* 129, 121–126.

Wiener, M., Matell, M. S., and Coslett, H. B. (2011). Multiple mechanisms for temporal processing. *Front. Integr. Neurosci.* 5:31. doi: 10.3389/fnint.2011.00031

Zucker, R. S. (1989). Short-term synaptic plasticity. *Annu. Rev. Neurosci.* 12, 13–31.

Received: 01 August 2011; accepted: 01 August 2011; published online: 18 August 2011.

Citation: Karmarkar UR (2011) Defining the contributions of network clock models to millisecond timing. Front. Integr. Neurosci. 5:41. doi: 10.3389/fnint.2011.00041

frontiers in
INTEGRATIVE NEUROSCIENCE

OPINION ARTICLE
published: 12 August 2011
doi: 10.3389/fnint.2011.00037

Neural representation of temporal duration: coherent findings obtained with the "lossy integration" model

Olga V. Sysoeva[1,3]*, Marc Wittmann[2] and Jiří Wackermann[2]

[1] Washington University School of Medicine, Saint Louis, MO, USA
[2] Department of Empirical and Analytical Psychophysics, Institute for Frontier Areas of Psychology and Mental Health, Freiburg i. Br., Germany
[3] Institute of Higher Nervous Activity and Neurophysiology, Russian Academy of Sciences, Moscow, Russia
*Correspondence: sysoevao@psychiatry.wustl.edu

Establishing links between experimental data, their models, and the neural substrates presents a permanent challenge for research in timing and time perception. This applies particularly to the problem of internal representation of temporal duration and its neural implementation. In this short communication we will report on progress achieved with the "lossy integration" model (also known as "klepsydra" model; Wackermann and Ehm, 2006) in interpretation of time perception data in the context of neurophysiological and neurobiological findings.

In the pacemaker–gate–accumulator model (Zakay and Block, 1997), which is still considered as the standard model in the literature (Grondin, 2010), temporal durations are internally represented by cumulative pulse counts,

$$A = t \cdot f$$

(t is the interval duration, f the effective pulse train frequency, and A is the number of pulses accumulated in the counter). Consequently, all variations in timing behavior or in a time perception task response can be accounted for by a change of the frequency f of pulses entering the counter. This gives the model its apparent elegance and universality, but is also its main weakness. Since the two hypothetical components, pacemaker and gate, are arranged serially, it is impossible to disentangle their effects. The effective frequency f may vary due to a change of the pacemaker fundamental frequency f_p (e.g., in response to organismic, physiological factors), or due to a change of the gate throughput g (e.g., attentional, cognitive effects):

$$f = f_p \cdot g$$

(where g is a real number in the range from 0 to 1).

By contrast, in the "klepsydra" model, (Wackermann and Ehm, 2006), temporal durations are represented by states of a lossy integrator; written in a differential form

$$\frac{dA}{dt} = f - \kappa \cdot A.$$

The inflow rate f corresponds to the pulse train frequency in the "standard" model (that the states are here continuous, rather than discrete quantities, is unimportant). The outflow rate, however, is determined by the momentary state of the accumulator A and a proportionality factor κ. Therefore, there are two loci of possible effects on internal time representation, the inflow and the outflow. The inflows can be studied only in relative terms, e.g., as inflow ratios between different experimental conditions; however, the loss rate κ can be determined numerically in given physical units (sec^{-1}).

To apply the model to the two tasks mostly used in our experimental studies – duration reproduction and duration discrimination in the supra-second range – we assume two such inflow–outflow units, each one allocated to one of the two temporal intervals to be compared. [Hence the name "dual klepsydra model" under which the model is known (Wackermann and Ehm, 2006).] Numerical procedures are available for estimating the value of κ directly from (individual or group-based) response functions in the reproduction task (Wackermann and Ehm, 2006), or indirectly, from points of subjective indifference determined by psychometric functions fitted to the data from the discrimination task (Wackermann and Späti, 2006). The lossy character of internal time representation is revealed by the progressive shortening of the reproduction response, or by the presentation order effect in the discrimination response (generally known as "subjective shortening" of past durations).

Recent experiments supported the notion of the "loss rate" parameter κ as a stable individual characteristic of the subject, evidenced by the high test–retest reliability of the parameter κ obtained from duration discrimination data (Sysoeva et al., 2010) and duration reproduction data. Moreover, it was shown (Sysoeva et al., 2010) that carriers of genotypic variants related to the activity of the serotonergic (5-HT) transmitter system significantly differ in the "loss rate" parameter κ. These results suggest genetic determination of dynamic parameters of neural representation of time. Higher values of κ were found for the carriers of genotypes characterized by higher potential for 5-HT transmission: (1) lower 5-HT reuptake, known for the 5-HTTLPR SS polymorphism compared with LL, (2) lower 5-HT degradation, described for the "low expression" variant of MAOA VNTR gene compared with "high expression" variant, and (3) higher 5-HT2a receptor density, proposed for the TT polymorphism of 5-HT2a T102C gene compared with CC. Also, they fit well with findings in studies on effects of psychotropic substances affecting the serotonin subsystem. In a double-blind, placebo-controlled study, psilocybin – a serotonin (5-HT) 2A/1A receptor agonist – significantly increased parameter κ which is indicative of a higher "loss rate" of duration representation, observable by a stronger under-reproduction of temporal intervals (Wackermann et al., 2008). These convergent findings suggest an action path from 5-HT activity-related genes, via activity of 5-HT in the brain, to time perception. The psychopharmacological data also indicate that although the loss rate parameter is genetically determined, it can be temporally modified by influencing the 5-HT system.

In a fMRI study, it was shown that parameter κ and the degree of self-rated impulsivity were associated with brain activation during the reproduction phase of the duration reproduction task; the activated brain areas were those related to motor execution as well as to the "core control network." In particular, activation in these regions was positively correlated with the "loss rate" parameter κ (i.e., more pronounced

under-reproduction of intervals), and with the subject's degree of impulsivity (Wittmann et al., 2011). During the encoding of duration in the reproduction task brain activation within bilateral posterior insula showed an accumulating pattern over time which peaked at the end of the interval (Wittmann et al., 2010). Based on the knowledge about insular cortex functioning it has been suggested that the integration of ascending body signals forms the basis for the representation of duration (Craig, 2009; Wittmann, 2009). This hypothesis is supported by recent observations of an association between the decrease of heart-beat frequency – indicative of an increase in parasympathetic activity – during the encoding of duration in individuals performing the duration reproduction task (Meissner and Wittmann, 2011). Interpreting these empirical findings in term of the klepsydra model, the flux of bodily signals into the posterior insular cortex could be interpreted as constituting the inflow component of the model. A more widespread network encompassing the "core control network" (Cole and Schneider, 2007) which would be associated with maintaining the representation of duration over time, can be related to the outflow component of the model, thus representing the "loss rate" of the leaky accumulator.

The work reported above focused on effects of the loss component of the klepsydra model, as the "subjective shortening" is a striking phenomenon seen in duration reproduction or duration discrimination data in the supra-second region. Since these effects are omnipresent in the data (whether they are subject matter of study or not) they have to be taken into account to distinguish net effects of experimental manipulations. The klepsydraic model not only disentangles the inflow (accumulation) and outflow (loss) effects conceptually, but it also allows to separate these effects operationally. An example of this analytic strategy is given in the study of brightness–duration interaction in a duration discrimination task (Wackermann and Meyer-Blankenburg, 2009), where the net effect caused by the stimulus variation is superimposed on the main stimulus-independent effect of subjective shortening. Similar strategies should be applicable in studies intending to manipulate the hypothetical "inflows" by varying somatosensory or proprioceptive stimuli to test the "bodily signals flux" hypothesis.

Summarizing: in the reported studies effects of natural variations or experimental manipulations on time perception were evaluated by means of a simple "lossy integration" model, which conceptually distinguishes between two components of the mechanism underlying internal representation of temporal durations: accumulation of internal "inflow" in the integrator, and a parallel "loss" of accumulated representation ("outflow"). It is suggested that the inflow is primarily derived from the ongoing stream of intero- and proprioceptive neural signals, while the outflow is related to low-level (synaptic?) mechanisms of neural signals transfer. Converging findings on neurophysiological or neurochemical effectors or correlates of time perception provide cumulative evidence for these working hypotheses. Therefore, we wish to draw the attention of the research community to this fruitful methodology, which promises to obtain new insights into human timing and time perception in experimental research as well as in studies of clinical populations.

REFERENCES

Cole, M. W., and Schneider, W. (2007). The cognitive control network: integrated cortical regions with dissociable functions. *Neuroimage* 37, 343–360.

Craig, A. D. (2009). Emotional moments across time: a possible neural basis for time perception in the anterior insula. *Philos. Trans. R. Soc. Lond., B, Biol. Sci.* 364, 1933–1942.

Grondin, S. (2010). Timing and time perception: a review of recent behavioral and neuroscience findings and theoretical directions. *Atten. Percept. Psychophys.* 72, 561–582.

Meissner, K., and Wittmann, M. (2011). Body signals, cardiac awareness, and the perception of time. *Biol. Psychol.* 86, 289–297.

Sysoeva, O. V., Tonevitsky, A., and Wackermann, J. (2010). Genetic determinants of time perception mediated by the serotonergic system. *PLoS ONE* 5, e12650. doi: 10.1371/journal.pone.0012650

Wackermann, J., and Ehm, W. (2006). The dual klepsydra model of internal time representation and time reproduction. *J. Theor. Biol.* 239, 482–493.

Wackermann, J., and Meyer-Blankenburg, N. (2009). "Differential effect of stimulus brightness in visual duration discrimination," in *Fechner Day 2009,* eds M. A. Elliott, S. Antonijevic, S. Berthaud, P. Mulcahy, B. Bargary, C. Martyn, and H. Schmidt (Galway: International Society for Psychophysics), 459–464.

Wackermann, J., and Späti, J. (2006). Asymmetry of the discrimination function for temporal durations in human subjects. *Acta Neurobiol. Exp. (Wars)* 66, 245–254.

Wackermann, J., Wittmann, M., Hasler, F., and Vollenweider, F. X. (2008). Effects of varied doses of psilocybin on time interval reproduction in human subjects. *Neurosci. Lett.* 435, 51–55.

Wittmann, M. (2009). The inner sense of time. *Philos. Trans. R. Soc. Lond., B, Biol. Sci.* 364, 1955–1967.

Wittmann, M., Simmons, A. N., Aron, J., and Paulus, M. P. (2010). Accumulation of neural activity in the posterior insula encodes the passage of time. *Neuropsychologia* 48, 3110–3120.

Wittmann, M., Simmons, A. N., Flagan, T., Lane, S. D., Wackermann, J., and Paulus, M. P. (2011). Neural substrates of time perception and impulsivity. *Brain Res.* 1406, 43–58.

Zakay, D., and Block, R. A. (1997). Temporal cognition. *Curr. Dir. Psychol. Sci.* 6, 12–16.

Received: 28 July 2011; accepted: 29 July 2011; published online: 12 August 2011.

*Citation: Sysoeva OV, Wittmann M and Wackermann J (2011) Neural representation of temporal duration: coherent findings obtained with the "lossy integration" model. Front. Integr. Neurosci. **5**:37. doi: 10.3389/fnint.2011.00037*

frontiers in
INTEGRATIVE NEUROSCIENCE

PERSPECTIVE ARTICLE
published: 03 January 2012
doi: 10.3389/fnint.2011.00090

A unified model of time perception accounts for duration-based and beat-based timing mechanisms

Sundeep Teki[1]*, Manon Grube[2] and Timothy D. Griffiths[1,2]

[1] Wellcome Trust Centre for Neuroimaging, University College London, London, UK
[2] Institute of Neuroscience, Newcastle University, Newcastle-upon-Tyne, UK

Edited by:
Warren H. Meck, Duke University, USA

Reviewed by:
Warren H. Meck, Duke University, USA
Michael Schwartze, Max Planck Society, Germany

***Correspondence:**
Sundeep Teki, Wellcome Trust Centre for Neuroimaging, University College London, 12 Queen Square, London WC1N 3BG, UK.
e-mail: sundeep.teki.10@ucl.ac.uk

Accurate timing is an integral aspect of sensory and motor processes such as the perception of speech and music and the execution of skilled movement. Neuropsychological studies of time perception in patient groups and functional neuroimaging studies of timing in normal participants suggest common neural substrates for perceptual and motor timing. A timing system is implicated in core regions of the motor network such as the cerebellum, inferior olive, basal ganglia, pre-supplementary, and supplementary motor area, pre-motor cortex as well as higher-level areas such as the prefrontal cortex. In this article, we assess how distinct parts of the timing system subserve different aspects of perceptual timing. We previously established brain bases for absolute, duration-based timing and relative, beat-based timing in the olivocerebellar and striato-thalamo-cortical circuits respectively (Teki et al., 2011). However, neurophysiological and neuroanatomical studies provide a basis to suggest that timing functions of these circuits may not be independent. Here, we propose a unified model of time perception based on coordinated activity in the core striatal and olivocerebellar networks that are interconnected with each other and the cerebral cortex through multiple synaptic pathways. Timing in this unified model is proposed to involve serial beat-based striatal activation followed by absolute olivocerebellar timing mechanisms.

Keywords: interval timing, time perception, timing mechanisms, cerebellum, striatum

> *"No clock mechanism fulfills its purpose as a clock unless its activity is perceived by an observer, who understands the manner in which the clock possesses the attributes of the timekeeper."*
> (Gooddy, 1958)

Human brain function is rhythmically organized at several timescales, from low frequency delta waves to high frequency gamma oscillations (Basar et al., 2001; Cheng et al., 2008). Based on such observations, Gooddy (1958) first proposed that the nervous system possesses the anatomical bases and physiological mechanisms for representing time, and may function as a clock. Indeed, recent research suggests that neural ensembles have inherent capacity to decode time encoded in the underlying neural dynamics (Matell et al., 2003; Karmarkar and Buonomano, 2007; Sumbre et al., 2008; Jin et al., 2009; Buonomano and Laje, 2010; Karmarkar, 2011; MacDonald et al., 2011; Merchant et al., 2011).

Complementary to this, is the view that postulates a dedicated internal timekeeper (Treisman, 1963; Wing and Kristofferson, 1973; Church, 1984; Gibbon et al., 1984, 1997; Matell and Meck, 2000; Ivry and Schlerf, 2008). Neuropsychological and neuroimaging work has found evidence for timing mechanisms in several brain areas such as the cerebellum (Ivry and Keele, 1989; Ivry, 1993; Nichelli et al., 1996; Penhune et al., 1998; Xu et al., 2006; Lee et al., 2007; Gooch et al., 2010; Grube et al., 2010a,b; Teki et al., 2011), basal ganglia (Artieda et al., 1992; Pastor et al., 1992; Harrington et al., 1998; Grahn and Brett, 2007; Teki et al., 2011), pre-supplementary and supplementary motor area (pre-SMA/SMA; Halsband et al., 1993; Shima and Tanji, 2000; Macar et al., 2004, 2006; Kotz and Schwartze, 2011), and premotor and prefrontal cortex (Oshio, 2011; for reviews see: Ivry et al., 2002; Lewis and Miall, 2003; Ivry and Spencer, 2004; Meck and Malapani, 2004; Buhusi and Meck, 2005; Meck, 2005; Grahn, 2009; Grondin, 2010; Wiener et al., 2010; Coull et al., 2011). Thus, motor areas might contain specialized timekeeping mechanisms necessary to coordinate temporally precise and structured movements (e.g., handwriting, typing, talking, and walking) as well as perceptual timing.

In this article, we consider the notion that "*movement is time, expressed*": motor structures must have access to timing information and accumulating evidence suggests that the motor structures themselves also act as "*observers*" of time (Gooddy, 1958). We specifically discuss how the neural architecture of the olivocerebellar and striato-thalamo-cortical networks might allow these to observe cortical dynamics and read out "auditory" time in the sub-second range.

TIMING MECHANISMS

Two distinct timing mechanisms in the human brain are suggested by a consideration of the coordination and timing of movements. Lesions of the cerebellum are known to impair the timing of voluntary movements and adversely affect the production of skilled movements (e.g., tapping to a rhythm) and perceptual tasks such as duration discrimination (Ivry et al., 1988, 2002). In an elegant series of experiments, Spencer et al. (2003) showed that patients

with cerebellar damage were selectively impaired in producing discontinuous movements (intermittent circle drawing) without any impairment in producing rhythmic movements (continuous circle drawing). This dissociation was attributed to the inability of the patients to form an explicit representation of absolute time between successive events. Continuous movements lack an event structure and are suggested to depend on temporal regularities that reflect emergent activity in distinct brain areas such as the basal ganglia or the cortex (Spencer et al., 2003; Ivry and Spencer, 2004).

DURATION-BASED VS. BEAT-BASED TIMING

In line with this dissociation in motor timing mechanisms, we posited the existence of analogous mechanisms for perceptual timing: *absolute, duration-based* timing and *relative, beat-based* timing (Grube et al., 2010a,b; Teki et al., 2011). The perceptual distinction has been suggested by previous behavioral work (Monahan and Hirsch, 1990; Yee et al., 1994; Pashler, 2001; McAuley and Jones, 2003; Grahn and McAuley, 2009). Absolute, duration-based timing refers to the measurement of the absolute duration of discrete time intervals (ΔT_i), while relative, beat-based timing refers to the measurement of the duration of time intervals relative to a temporal regularity such as beats ($\Delta T_i / T_{beat}$; Teki et al., 2011).

The concept of beat-based perception of time can be traced back to William James who wrote that "subdividing the time by *beats of sensation* aids our accurate knowledge of the amount of it that elapses" (James, 1890, Vol. 1, p. 619). Improved accuracy of time perception based on beat-based stimuli has been demonstrated in a number of studies (Essens and Povel, 1985; Palmer and Krumhansl, 1990; Parncutt, 1994; Grube and Griffiths, 2009). Several studies have further demonstrated improved timing for regular compared to irregular sequences (e.g., Sakai et al., 1999; Patel et al., 2005; Grahn and Brett, 2007; Teki et al., 2011).

NEURAL SUBSTRATES OF DURATION-BASED AND BEAT-BASED TIMING

Here, we discuss the neural networks that mediate duration-based and beat-based timing mechanisms respectively.

Previous neuropsychological studies of patients with cerebellar damage established the role of the cerebellum in discrete encoding of time intervals (Ivry et al., 1988; Ivry and Keele, 1989; Nichelli et al., 1996). Recently, Grube et al. (2010a) developed a test-battery of stimuli and timing tasks that measured duration-based and beat-based perception of time. A group of patients with Spinocerebellar Ataxia type-6 (SCA-6) were tested. Unlike previous studies of patients with stroke, this patient group has a stereotyped pattern of cerebellar degeneration affecting the superior part of the cerebellum first. The patients showed a specific impairment on the duration-based timing tasks, which involved a comparison of the absolute duration of a test interval to a reference interval of fixed or variable duration. However, they showed no deficits on the tasks comprising rhythmic sequences with a regular beat. This dissociation specifically implicated the cerebellum in the explicit encoding of the absolute duration of time intervals. These results motivated a follow-up study based on the same experimental stimuli in normal participants with temporary impairment of superior medial cerebellar function produced by continuous transcranial magnetic theta-burst stimulation (TBS; Grube et al., 2010b). The comparison of post- vs. pre-stimulation thresholds revealed a similar deficit only for the absolute timing task and not the rhythmic timing tasks.

Perception of rhythmic sequences with a regular beat has been studied in Parkinson's patients with an impaired nigrostriatal dopaminergic system, implicating the striatum in beat-based perception of time (Artieda et al., 1992; Pastor et al., 1992; Harrington et al., 1998). Functional magnetic resonance imaging (fMRI) studies of normal participants have further implicated the basal ganglia and pre-SMA/SMA in rhythm and beat perception. Grahn and Brett (2007) developed a test-battery of rhythmic sequences based on simple metrical, complex metrical or irregular, non-metrical ratios. A rhythm reproduction task revealed significantly better performance for the simple metrical sequences and functional imaging demonstrated bilateral increases in activity in the putamen during the simple metrical task. Subsequent work examining differences in functional activations between a beat and no-beat condition confirmed the role of the putamen and the SMA in the perception of rhythmic sequences with a regular beat (Grahn, 2009; Grahn and Rowe, 2009). Greater activity in the putamen associated with less salient beat markers was interpreted in terms of an internal beat prediction mechanism (Grahn and Rowe, 2009).

FUNCTIONAL DISSOCIATION OF NETWORKS MEDIATING DURATION-BASED AND BEAT-BASED TIMING

Previous work focused on either duration-based or beat-based timing mechanisms in isolation and did not directly compare the two mechanisms using a common perceptual timing task. The stimuli for the duration-based and beat-based timing tasks used by Grube et al. (2010a,b) were not matched for the total number of intervals and stimulus duration, while the beat-based timing work by Grahn and colleagues did not involve an explicit timing task (Grahn and Brett, 2007; Grahn and Rowe, 2009).

In order to resolve these issues, and to examine the contribution of the cerebellar and striatal networks to timing, we developed a novel stimulus and timing task (Teki et al., 2011; stimuli available online at: http://www.fil.ion.ucl.ac.uk/∼steki). Stimuli (**Figure 1A**) consisted of a sequence of intervals that induced a varying temporal context that was either regular (isochronous) or irregular (incorporating 15% jitter). Participants were required to compare the duration of the last to the second-to-last interval for both sequences. The time difference between the last and second-to-last intervals was adjusted to obtain similar accuracy for the regular and irregular sequences. We hypothesized that the timing of intervals in irregular sequences would recruit duration-based timing mechanisms as each interval has to be measured anew to perform the task. In contrast, the timing of regular sequences with a regular beat was predicted to involve beat-based timing mechanisms. The results revealed a clear functional dissociation such that an olivocerebellar network comprising the inferior olive and the cerebellum, including the dentate nucleus and vermis, was more active for duration-based timing and a striato-thalamo-cortical network comprising the putamen, caudate, thalamus, pre-SMA/SMA, premotor, and dorsolateral prefrontal cortex was more active for beat-based timing (Teki et al., 2011).

These results are consistent with previous work implicating the inferior olive (Xu et al., 2006; Liu et al., 2008; Wu et al., 2011),

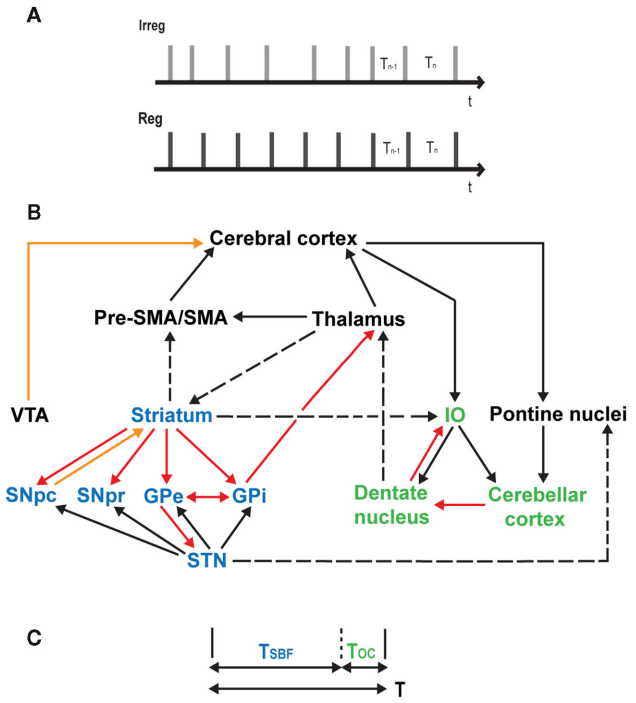

FIGURE 1 | (A) Absolute and relative timing task. Irreg: a sequence of clicks with an average of 15% jitter was used to study absolute, duration-based timing. Participants were required to compare the duration of the final interval, T_n to the penultimate interval, $T_n - 1$ where the final interval, T_n incorporates a difference (ΔT) of 30% of the inter-onset interval (range: 440–560 ms) from that of the preceding interval such that $T_n = T_n - 1 \pm \Delta T_{30\%}$. Reg: a sequence of clicks with no jitter is used to study relative, beat-based timing. Participants were required to compare the duration of the final interval, T_n to the penultimate interval, $T_n - 1$ where the final interval, T_n incorporates a difference (ΔT) of 15% of the inter-onset interval from that of the preceding interval such that $T_n = T_n - 1 \pm \Delta T_{15\%}$ (cf. Teki et al., 2011 for further stimulus details). **(B)** A unified model of time perception. The striatal network (in blue) and the olivocerebellar network (in green) are connected to each other via multiple loops, and with the thalamus, pre-SMA/SMA, and the cerebral cortex. Dopaminergic pathways are shown in orange, inhibitory projections in red, excitatory and known anatomical connections in solid and dashed black lines respectively. IO, inferior olive; VTA, ventral tegmental area; GPe, globus pallidus external; GPi, globus pallidus internal; STN, subthalamic nucleus; SNpc, substantia nigra pars compacta; SNpr, substantia nigra pars reticulata. **(C)** Timing mechanism underlying the unified model. To estimate an interval of duration *T*, both the striato-thalamo-cortical networks and olivocerebellar networks act in parallel to produce timing signals T_{SBF} and T_{OC} respectively such that the combined output of the system approximates the length of the criterion time interval, *T*.

the cerebellum (reviewed above), and the striato-thalamo-cortical system (Matell and Meck, 2000, 2004; MacDonald and Meck, 2004; Buhusi and Meck, 2005; Meck, 2006a,b; Meck et al., 2008) in timing and time perception.

NEUROPHYSIOLOGICAL BASES OF OLIVOCEREBELLAR AND STRIATAL TIMING SIGNALS

In this section, we review the neurophysiological bases for the timing signals that are measured in the two different parts of the timing system.

The inferior olive represents the sole source of climbing fiber input to the Purkinje cells of the cerebellar cortex. Olivary cells possess unique cellular characteristics such as voltage-gated conductances that display rhythmic sub-threshold membrane-potential oscillations at 5–15 Hz (Llinás and Yarom, 1981) as well as electrical gap-junctions. This electrical coupling helps to synchronize the membrane-potential oscillations and results in clusters of neurons in which activity is temporally coherent (Llinas et al., 1974). The deep cerebellar nuclei including the dentate nucleus, which represents the main output of the cerebellum, modulate the electrical coupling coefficient by inhibiting and decoupling the olivary cells into dynamic cell assemblies. The feed-forward inhibitory loop is closed by the Purkinje cells which inhibit the deep cerebellar nuclei. This unique organization in the olivo-cerebellar system results in the formation of a dynamic network capable of generating accurate absolute timing signals (Welsh et al., 1995; Yarom and Cohen, 2002; Jacobson et al., 2008; Mathy et al., 2009).

A possible physiological basis for a timing signal generated by the striato-thalamo-cortical circuits is described by the Striatal Beat Frequency (SBF) model which posits that the medium spiny neurons (MSNs) in the dorsal striatum monitor oscillatory activity (5–15 Hz) in the cerebral cortex and act as coincidence detectors (Miall, 1989; Matell and Meck, 2000, 2004; Meck et al., 2008; Agostino et al., 2011; Oprisan and Buhusi, 2011). Phasic dopamine release from the ventral tegmental area synchronizes the cortical oscillators at interval onset, while the dorsal striatum is modulated by dopaminergic input from the substantia nigra (Buhusi and Meck, 2005; Allman and Meck, 2011). Experience-dependent modulation of cortico-striatal synapses via mechanisms of long-term potentiation and long-term depression improves the reliability of coincidental activation of MSNs. Over repeated stimulus presentations in the form of a regular sequence of time intervals, the MSNs might learn to reliably predict the offset of the criterion interval and encode its duration via mechanisms of dopamine-mediated reinforcement signals: a specialized mechanism for timing analysis in a predictable, beat-based context (see Gu et al., 2011; Jones and Jahanshahi, 2011).

A UNIFIED MODEL OF TIME PERCEPTION

The current state of time perception research suggests that time is represented in a distributed manner and that time may be encoded in the population dynamics in each brain area or by a dedicated internal clock. The results from our fMRI study (Teki et al., 2011) support the notion that time is represented in a context-sensitive manner and depending on the temporal structure of time intervals, the olivocerebellar system or the striato-thalamo-cortical system may mediate timing functions.

The immediate question the work raises is whether there is one timing system or two and can the striatal and olivocerebellar systems be incorporated into a unified system? We attempt such a synthesis here: a unified model can be based on coordinated timing processes (as described above) in the striato-thalamo-cortical and olivocerebellar networks which are strongly connected with each other and the cortex through multi-synaptic loops and may act in parallel to improve the precision of the timing signal (see Meck, 2005; Allman and Meck, 2011 for a review).

The unified model is illustrated in **Figure 1B** and shows the connections between the core striatal and olivocerebellar networks and the cerebral cortex. The basal ganglia and the cerebellum are connected through multiple loops with disynaptic projections from the dentate nucleus to the striatum via the thalamus and from the subthalamic nucleus to the cerebellar cortex via the pontine nuclei (Hoshi et al., 2005; Bostan and Strick, 2010; Bostan et al., 2010). The inferior olive receives auditory input from the cochlear nucleus (Kandler and Herbert, 1991) and bilateral afferents from the striatum (Walberg, 1956). The dentate nucleus sends projections to the premotor/motor cortex, and to the prefrontal and posterior parietal cortex via anatomically segregated "motor" and "cognitive" output channels (Middleton and Strick, 2001). The internal segment of the globus pallidus, which represents the output of the basal ganglia also sends segregated projections to the motor and prefrontal cortex (Middleton and Strick, 2002). Furthermore, pre-SMA and SMA receive connections from the striatum (Jürgens, 1984) and the dentate nucleus (Akkal et al., 2007) and may serve as a temporal accumulator (Casini and Vidal, 2011 – but see Kononowicz and van Rijn, 2011; van Rijn et al., 2011).

TIMING IN THE UNIFIED MODEL

We assume that the coincidental activation of striatal MSNs as established by the SBF model represents the timing signal of the beat-based clock, and that the olivocerebellar system generates a timing signal corresponding to the duration-based clock. Furthermore, concordant with the fMRI results (Teki et al., 2011), the beat-based clock is assumed to be activated more when the stimuli are embedded in a predictable beat-based context and the duration-based clock is assumed to be more active for stimuli in an irregular or isolated context.

Suppose a single time interval of duration T is to be timed as shown in **Figure 1C**. The beat-based clock is assumed to be the default clock of the brain and generates a timing signal which encodes a duration T_{SBF} such that $T = T_{SBF} + \Delta T$, where T_{SBF} is the time corresponding to the SBF model and ΔT represents the error in time measurement. Complementary to its role in monitoring and optimizing movements, we propose that the olivocerebellar system possesses the neural architecture to provide a similar error–correction function for perceptual timing by encoding the duration T_{OC} (where, $T_{OC} = \Delta T$) so that the output of the combined system approximates the original time interval, T. There are a number of auditory inputs to the striatum (Hikosaka et al., 1989; Bordi and LeDoux, 1992; Bordi et al., 1993; Yeterian and Pandya, 1998) and the cerebellum (Snider and Stowell, 1944; Azizi et al., 1985; Huang and Liu, 1985; Schmahmann, 1997; Petacchi et al., 2005; Kotz and Schwartze, 2010) which might allow direct comparison of the internally represented time interval and the actual time interval presented and this information may be fed to the cortex where attention and memory demands may modulate the timing signals.

Here, we extend the unified model to consider responses to a sequence of time intervals. If the interval T is presented in a regular sequence of intervals, the estimates of T_{SBF} may improve with reinforcement resulting in smaller errors in encoding T, thereby minimizing the role of the olivocerebellar system. This is congruent with greater activation of the striato-thalamo-cortical network in the timing of beat-based sequences (Teki et al., 2011). On the other hand, if random jitter is incorporated into the interval T on each occurrence, and repeated through an irregular sequence of intervals, estimates of T_{SBF} in this unpredictable context would be less accurate and result in larger errors in estimation of T. This may result in enhanced activation of the olivocerebellar system to encode the timing errors and is consistent with greater activity in this network for timing of irregular sequences (Teki et al., 2011). Such coordinated activity between the interconnected striato-thalamo-cortical and olivocerebellar networks could form the bases of an optimal timing system that can read out accurate time.

Lastly, we consider the predictions of the model vis-à-vis neuropsychological work based on both duration-based and beat-based timing tasks. The default mode of the unified model is based on relative timing mechanisms in the striatum. According to this prediction, disruption of cerebellar mechanisms should leave relative timing intact; this is consistent with unimpaired relative timing performance observed in acute (TBS over medial cerebellum; Grube et al., 2010b) and chronic (SCA-6; Grube et al., 2010a) cases of cerebellar disruption. The unified model is asymmetrical in that the absolute timing mechanisms in the cerebellum finesse the more adaptive relative timing mechanisms in the striatum. The question that arises, then, is whether a double dissociation is possible and relative timing mechanisms might exist in isolation. The model developed here suggests that "pure" striatal lesions should result in deficits on both absolute and relative timing tasks, and this prediction is consistent with initial results from timing tests on patients with Parkinson's disease (Grube et al., 2010c), Huntington's Disease, and the striatal form of Multiple System Atrophy (Cope et al., 2011).

CONCLUSION

The unified timing model, based on the common activation of the striato-thalamo-cortical and olivocerebellar networks is consistent with their role in time perception as well as the specific motor and perceptual timing deficits observed in clinical populations. The model assumption of serial beat-based striatal activation followed by absolute olivocerebellar timing mechanisms shares some formal similarity to models of pitch and melody perception in which contour is processed before absolute pitch value in a serial fashion (Dowling et al., 1995). The two connected networks possess the mechanisms to mediate timing as proposed but the exact nature and time course of information flow through the inter-connected network remains to be elucidated. A systems-level investigation of these circuits using techniques such as simultaneous recording from olivocerebellar and striatal populations and targeted stimulation using two-photon fluorescence imaging or optogenetics (Cheng et al., 2011; Yizhar et al., 2011) at the cellular level, or analysis of effective connectivity between these brain networks using dynamic causal modeling of functional imaging data (Friston et al., 2003) may help obtain a better understanding of the neural mechanisms and substrates underlying timing and time perception.

ACKNOWLEDGMENTS

Sundeep Teki and Timothy D. Griffiths are supported by the Wellcome Trust, UK.

REFERENCES

Agostino, P. V., Golombek, D. A., and Meck, W. H. (2011). Unwinding the molecular basis of interval and circadian timing. *Front. Integr. Neurosci.* 5:64. doi:10.3389/fnint.2011.00064

Akkal, D., Dum, R. P., and Strick, P. L. (2007). Supplementary motor area and presupplementary motor area: targets of basal ganglia and cerebellar output. *J. Neurosci.* 27, 10659–10673.

Allman, M. J., and Meck, W. H. (2011). Pathophysiological distortions in time perception and timed performance. *Brain* (in press). doi:10.1093/brain/awr210

Artieda, J., Pastor, M. A., Lacruz, F., and Obeso, J. A. (1992). Temporal discrimination is abnormal in Parkinson's disease. *Brain* 115, 199–210.

Azizi, S. A., Burne, R. A., and Woodward, D. J. (1985). The auditory corticopontocerebellar projection in the rat: inputs to the paraflocculus and midvermis. An anatomical and physiological study. *Exp. Brain Res.* 59, 36–49.

Basar, E., Basar-Eroglu, C., Karakas, S., and Schurmann, M. (2001). Gamma, alpha, delta, and theta oscillations govern cognitive processes. *Int. J. Psychophysiol.* 39, 241–248.

Bordi, F., and LeDoux, J. (1992). Sensory tuning beyond the sensory system: an initial analysis of auditory response properties of neurons in the lateral amygdaloid nucleus and overlying areas of the striatum. *J. Neurosci.* 12, 2493–2503.

Bordi, F., LeDoux, J., Clugnet, M. C., and Pavlides, C. (1993). Single-unit activity in the lateral nucleus of the amygdala and overlying areas of the striatum in freely behaving rats: rates, discharge patterns, and responses to acoustic stimuli. *Behav. Neurosci.* 107, 757–769.

Bostan, A. C., Dum, R. P., and Strick, P. L. (2010). The basal ganglia communicate with the cerebellum. *Proc. Natl. Acad. Sci. U.S.A.* 107, 8452–8456.

Bostan, A. C., and Strick, P. L. (2010). The cerebellum and basal ganglia are interconnected. *Neuropsychol. Rev.* 20, 261–270.

Buhusi, C. V., and Meck, W. H. (2005). What makes us tick? Functional and neural mechanisms of interval timing. *Nat. Rev. Neurosci.* 6, 755–765.

Buonomano, D. V., and Laje, R. (2010). Population clocks: motor timing with neural dynamics. *Trends Cogn. Sci. (Regul. Ed.)* 14, 520–527.

Casini, L., and Vidal, F. (2011). The SMAs: neural substrate of the temporal accumulator? *Front. Integr. Neurosci.* 5:35. doi:10.3389/fnint.2011.00035

Cheng, R., Jesuthasan, S., and Penney, T. B. (2011). Time for zebrafish. *Front. Integr. Neurosci.* 5:40. doi:10.3389/fnint.2011.00040

Cheng, R. K., Williams, C. L., and Meck, W. H. (2008). Oscillatory bands, neuronal synchrony and hippocampal function: implications of the effects of prenatal choline supplementation for sleep-dependent memory consolidation. *Brain Res.* 1237, 176–194.

Church, R. M. (1984). Properties of the internal clock. *Ann. N. Y. Acad. Sci.* 423, 566–582.

Cope, T. E., Grube, M., Singh, B., Burn, D. J., and Griffiths, T. D. (2011). The basal ganglia in perceptual timing: timing performance in multiple systems atrophy. *Abstr. Soc. Neurosci.* 476.07.

Coull, J. T., Cheng, R.-K., and Meck, W. H. (2011). Neuroanatomical and neurochemical substrates of timing. *Neuropsychopharmacology* 36, 3–25.

Dowling, W. J., Kwak, S., and Andrews, M. W. (1995). The time course of recognition of novel melodies. *Percept. Psychophys.* 57, 136–149.

Essens, P. J., and Povel, D. J. (1985). Metrical and nonmetrical representations of temporal patterns. *Percept. Psychophys.* 37, 1–7.

Friston, K. J., Harrison, L., and Penny, W. (2003). Dynamic causal modelling. *Neuroimage* 19, 1273–1302.

Gibbon, J., Church, R. M., and Meck, W. H. (1984). Scalar timing in memory. *Ann. N. Y. Acad. Sci.* 423, 52–77.

Gibbon, J., Malapani, C., Dale, C. L., and Gallistel, C. (1997). Toward a neurobiology of temporal cognition: advances and challenges. *Curr. Opin. Neurobiol.* 7, 170–184.

Gooch, C. M., Wiener, M., Wencil, E. B., and Coslett, H. B. (2010). Interval timing disruptions in subjects with cerebellar lesions. *Neuropsychologia* 48, 1022–1031.

Gooddy, W. (1958). Time and the nervous system: the brain as a clock. *Lancet* 1, 1139–1144.

Grahn, J. A. (2009). The role of the basal ganglia in beat perception: neuroimaging and neuropsychological investigations. *Ann. N. Y. Acad. Sci.* 1169, 35–45.

Grahn, J. A., and Brett, M. (2007). Rhythm and beat perception in motor areas of the brain. *J. Cogn. Neurosci.* 19, 893–906.

Grahn, J. A., and McAuley, J. D. (2009). Neural bases of individual differences in beat perception. *Neuroimage* 47, 1894–1903.

Grahn, J. A., and Rowe, J. B. (2009). Feeling the beat: premotor and striatal interactions in musicians and nonmusicians during beat perception. *J. Neurosci.* 29, 7540–7548.

Grondin, S. (2010). Timing and time perception: a review of recent behavioral and neuroscience findings and theoretical directions. *Atten. Percept. Psychophys.* 72, 561–582.

Grube, M., Cooper, F. E., Chinnery, P. F., and Griffiths, T. D. (2010a). Dissociation of duration-based and beat-based auditory timing in cerebellar degeneration. *Proc. Natl. Acad. Sci. U.S.A.* 107, 11597–11601.

Grube, M., Lee, K.-H., Griffiths, T. D., Barker, A. T., and Woodruff, P. W. (2010b). Transcranial magnetic theta-burst stimulation of the human cerebellum distinguishes absolute, duration-based from relative, beat-based perception of subsecond time intervals. *Front. Psychol.* 1:171. doi:10.3389/fpsyg.2010.00171

Grube, M., Cooper, F. E., Mandal, A., Cope, T., Burn, D. J., and Griffiths, T. D. (2010c). The basal ganglia in perceptual timing: the effects of Parkinson's disease and deep-brain stimulation. *Abst. Soc. Neurosci.* 324.6.

Grube, M., and Griffiths, T. D. (2009). Metricality-enhanced temporal encoding and the subjective perception of rhythmic sequences. *Cortex* 45, 72–29.

Gu, B. M., Yin, B., Cheng, R. K., and Meck, W. H. (2011). Quinpirole-induced sensitization to noisy/sparse periodic input: temporal synchronization as a component of obsessive-compulsive disorder. *Neuroscience* 179, 143–150.

Halsband, U., Ito, N., Tanji, J., and Freund, H. J. (1993). The role of premotor cortex and the supplementary motor area in the temporal control of movement in man. *Brain* 116, 243–266.

Harrington, D. L., Haaland, K. Y., and Hermanowicz, N. (1998). Temporal processing in the basal ganglia. *Neuropsychology* 12, 3–12.

Hikosaka, O., Sakamoto, M., and Usui, S. (1989). Functional properties of monkey caudate neurons. II. Visual and auditory responses. *J. Neurophysiol.* 61, 799–813.

Hoshi, E., Tremblay, L., Féger, J., Carras, P. L., and Strick, P. L. (2005). The cerebellum communicates with the basal ganglia. *Nat. Neurosci.* 8, 1491–1493.

Huang, C.-M., and Liu, G. (1985). Electrophysiological mapping of the auditory areas in the cerebellum of the cat. *Brain Res.* 335, 121–129.

Ivry, R. (1993). Cerebellar involvement in the explicit representation of temporal information. *Ann. N. Y. Acad. Sci.* 682, 214–230.

Ivry, R. B., and Keele, S. W. (1989). Timing functions of the cerebellum. *J. Cogn. Neurosci.* 1, 136–152.

Ivry, R. B., Keele, S. W., and Diener, H. C. (1988). Dissociation of the lateral and medial cerebellum in movement timing and movement execution. *Exp. Brain Res.* 73, 167–180.

Ivry, R. B., and Schlerf, J. E. (2008). Dedicated and intrinsic models of time perception. *Trends Cogn. Sci. (Regul. Ed.)* 12, 273–280.

Ivry, R. B., Spencer, R. M., Zelaznik, H. N., and Diedrichsen, J. (2002). The cerebellum and event timing. *Ann. N. Y. Acad. Sci.* 978, 302–317.

Ivry, R. B., and Spencer, R. M. C. (2004). The neural representation of time. *Curr. Opin. Neurobiol.* 14, 225–232.

Jacobson, G. A., Rokni, D., and Yarom, Y. (2008). A model of the olivo-cerebellar system as a temporal pattern generator. *Trends Neurosci.* 31, 617–625.

James, W. (1890). *The Principles of Psychology*, Vol. 1. New York: Henry Holt.

Jin, D. Z., Fujii, N., and Graybiel, A. M. (2009). Neural representation of time in cortico-basal ganglia circuits. *Proc. Natl. Acad. Sci. U.S.A.* 106, 19156–19161.

Jones, C. R. G., and Jahanshahi, M. (2011). Dopamine modulates striato-frontal functioning during temporal processing. *Front. Integr. Neurosci.* 5:70. doi:10.3389/fnint.2011.00070

Jürgens, U. (1984). The efferent and afferent connections of the supplementary motor area. *Brain Res.* 300, 63–81.

Kandler, K., and Herbert, H. (1991). Auditory projections from the cochlear nucleus to pontine and mesencephalic reticular nuclei in the rat. *Brain Res.* 562, 230–242.

Karmarkar, U. R. (2011). Defining the contributions of network clock models to millisecond timing. *Front. Integr. Neurosci.* 5:41. doi:10.3389/fnint.2011.00041

Karmarkar, U. R., and Buonomano, D. V. (2007). Timing in the absence of clocks: encoding time in neural network states. *Neuron* 53, 427–438.

Kononowicz, T. W., and van Rijn, H. (2011). Slow potentials in time estimation: the role of temporal accumulation and habituation. *Front. Integr. Neurosci.* 5:48. doi:10.3389/fnint.2011.00048

Kotz, S. A., and Schwartze, M. (2010). Cortical speech processing unplugged: a timely subcortico-cortical framework. *Trends Cogn. Sci. (Regul. Ed.)* 14, 392–399.

Kotz, S. A., and Schwartze, M. (2011). Differential input of the supplementary motor area to a dedicated temporal processing network: functional and clinical implications. *Front. Integr. Neurosci.* 5:86. doi:10.3389/fnint.2011.00086

Lee, K.-H., Egleston, P. N., Brown, W. H., Gregory, A. N., Barker, A. T., and Woodruff, P. W. R. (2007). The role of the cerebellum in subsecond time perception: evidence from repetitive transcranial magnetic stimulation. *J. Cogn. Neurosci.* 19, 147–157.

Lewis, P. A., and Miall, R. C. (2003). Distinct systems for automatic and cognitively controlled time measurement: evidence from neuroimaging. *Curr. Opin. Neurobiol.* 13, 250–255.

Liu, T., Xu, D., Ashe, J., and Bushara, K. (2008). Specificity of inferior olive response to stimulus timing. *J. Neurophysiol.* 100, 1557–1561.

Llinas, R., Baker, R., and Sotelo, C. (1974). Electrotonic coupling between neurons in cat inferior olive. *J. Neurophysiol.* 37, 560–571.

Llinás, R., and Yarom, Y. (1981). Electrophysiology of mammalian inferior olivary neurones in vitro. Different types of voltage-dependent ionic conductances. *J. Physiol. (Lond.)* 315, 549–567.

Macar, F., Anton, J.-L., Bonnet, M., and Vidal, F. (2004). Timing functions of the supplementary motor area: an event-related fMRI study. *Brain Res. Cogn. Brain Res.* 206–215.

Macar, F., Coull, J., and Vidal, F. (2006). The supplementary motor area in motor and perceptual timing: fMRI studies. *Cogn. Process.* 7, 89–94.

MacDonald, C. J., Lepage, K. Q., Eden, U. T., and Eichenbaum, H. (2011). Hippocampal "time cells" bridge the gap in memory for discontiguous events. *Neuron* 71, 737–749.

MacDonald, C. J., and Meck, W. H. (2004). Systems-level integration of interval timing and reaction time. *Neurosci. Biobehav. Rev.* 28, 747–769.

Matell, M. S., and Meck, W. H. (2000). Neuropsychological mechanisms of interval timing behavior. *Bioessays* 22, 94–103.

Matell, M. S., and Meck, W. H. (2004). Cortico-striatal circuits and interval timing: coincidence detection of oscillatory processes. *Brain Res. Cogn. Brain Res.* 21, 139–170.

Matell, M. S., Meck, W. H., and Nicolelis, M. A. L. (2003). Interval timing and the encoding of signal duration by ensembles of cortical and striatal neurons. *Behav. Neurosci.* 117, 760–773.

Mathy, A., Ho, S. S. N., Davie, J. T., Duguid, I. C., Clark, B. A., and Häusser, M. (2009). Encoding of oscillations by axonal bursts in inferior olive neurons. *Neuron* 62, 388–399.

McAuley, J. D., and Jones, M. R. (2003). Modeling effects of rhythmic context on perceived duration: a comparison of interval and entrainment approaches to short-interval timing. *J. Exp. Psychol. Hum. Percept. Perform.* 29, 1102–1125.

Meck, W. H. (2005). Neuropsychology of timing and time perception. *Brain Cogn.* 58, 1–8.

Meck, W. H. (2006a). Frontal cortex lesions eliminate the clock speed effect of dopaminergic drugs on interval timing. *Brain Res.* 1108, 157–167.

Meck, W. H. (2006b). Neuroanatomical localization of an internal clock: a functional link between mesolimbic, nigrostriatal, and mesocortical dopaminergic systems. *Brain Res.* 1109, 93–107.

Meck, W. H., and Malapani, C. (2004). Neuroimaging of interval timing. *Brain Res. Cogn. Brain Res.* 21, 133–137.

Meck, W. H., Penney, T. B., and Pouthas, V. (2008). Cortico-striatal representation of time in animals and humans. *Curr. Opin. Neurobiol.* 18, 145–152.

Merchant, H., Zarco, W., Pérez, O., Prado, L., and Bartolo, R. (2011). Measuring time with different neural chronometers during a synchronization-continuation task. *Proc. Natl. Acad. Sci. U.S.A.* (in press). doi: 10.1073/pnas.1112933108

Miall, R. C. (1989). The storage of time intervals using oscillating neurons. *Neural Comput.* 1, 359–371.

Middleton, F. A., and Strick, P. L. (2001). Cerebellar projections to the prefrontal cortex of the primate. *J. Neurosci.* 21, 700–712.

Middleton, F. A., and Strick, P. L. (2002). Basal-ganglia "projections" to the prefrontal cortex of the primate. *Cereb. Cortex* 12, 926–935.

Monahan, C. B., and Hirsch, I. J. (1990). Studies in auditory timing: 2. rhythm patterns. *Percept. Psychophys.* 47, 227–242.

Nichelli, P., Alway, D., and Grafman, J. (1996). Perceptual timing in cerebellar degeneration. *Neuropsychologia* 34, 863–871.

Oprisan, S. A., and Buhusi, C. V. (2011). Modeling pharmacological clock and memory patterns of interval timing in a striatal beat-frequency model with realistic, noisy neurons. *Front. Integr. Neurosci.* 5:52. doi:10.3389/fnint.2011.00052

Oshio, K.-I. (2011). Possible functions of prefrontal cortical neurons in duration discrimination. *Front. Integr. Neurosci.* 5:25. doi:10.3389/fnint.2011.00025

Palmer, C., and Krumhansl, C. L. (1990). Mental representations for musical meter. *J. Exp. Psychol. Hum. Percept. Perform.* 16, 728–741.

Parncutt, R. (1994). A perceptual model of pulse salience and metrical accent in musical rhythm. *Music Percept.* 11, 409–464.

Pashler, H. (2001). Perception and production of brief durations: beat-based versus interval-based timing. *J. Exp. Psychol. Hum. Percept. Perform.* 27, 485–493.

Pastor, M. A., Artieda, J., Jahanshahi, M., and Obeso, J. A. (1992). Time estimation and reproduction is abnormal in Parkinson's disease. *Brain* 115, 211–225.

Patel, A. D., Iversen, J. R., Chen, Y., and Repp, B. H. (2005). The influence of metricality and modality on synchronization with a beat. *Exp. Brain Res.* 163, 226–238.

Penhune, V. B., Zattore, R. J., and Evans, A. C. (1998). Cerebellar contributions to motor timing: a PET study of auditory and visual rhythm reproduction. *J. Cogn. Neurosci.* 10, 752–765.

Petacchi, A., Laird, A. R., Fox, P. T., and Bower, J. M. (2005). Cerebellum and auditory function: an ALE meta-analysis of functional neuroimaging studies. *Hum. Brain Mapp.* 25, 118–128.

Sakai, K., Hikosaka, O., Miyauchi, S., Takino, R., Tamada, T., Iwata, N. K., and Nielsen, M. (1999). Neural representation of a rhythm depends on its interval ratio. *J. Neurosci.* 19, 10074–10081.

Schmahmann, J. D. (1997). *The Cerebellum and Cognition*. New York: Academic Press.

Shima, K., and Tanji, J. (2000). Neuronal activity in the supplementary and presupplementary motor area for temporal organization of multiple movements. *J. Neurophysiol.* 84, 2148–2160.

Snider, R. S., and Stowell, A. (1944). Receiving areas of tactile, auditory, and visual systems in the cerebellum. *J. Neurophysiol.* 7, 331–358.

Spencer, R. M. C., Zelaznik, H. N., Diedrichsen, J., and Ivry, R. B. (2003). Disrupted timing of discontinuous but not continuous movements by cerebellar lesions. *Science* 300, 1437–1439.

Sumbre, G., Muto, A., Baier, H., and Poo, M.-M. (2008). Entrained rhythmic activities of neuronal ensembles as perceptual memory of time interval. *Nature* 456, 102–106.

Teki, S., Grube, M., Kumar, S., and Griffiths, T. D. (2011). Distinct neural substrates of duration-based and beat-based auditory timing. *J. Neurosci.* 31, 3805–3812.

Treisman, M. (1963). Temporal discrimination and the indifference interval: implications for a model of the "internal clock." *Pyschol. Monogr.* 77, 1–31.

van Rijn, H., Kononowicz, T. W., Meck, W. H., Ng, K., and Penney, T. B. (2011). Contingent negative variation and its relation to time estimation: a theoretical evaluation. *Front. Integr. Neurosci.* 5:91. doi: 10.3389/fnint.2011.00091

Walberg, F. (1956). Descending connections to the inferior olive. An experimental study in the cat. *J. Comp. Neurol.* 104, 77–173.

Welsh, J. P., Lang, E. J., Sugihara, I., and Llinás, R. (1995). Dynamic organization of motor control within the olivocerebellar system. *Nature* 374, 453–457.

Wiener, M., Turkeltaub, P., and Coslett, H. B. (2010). The image of time: a voxel-wise meta-analysis. *Neuroimage* 49, 1728–1740.

Wing, A. M., and Kristofferson, A. B. (1973). The timing of interresponse intervals. *Percept. Psychophys.* 13, 455–460.

Wu, X., Ashe, J., and Bushara, K. O. (2011). Role of olivocerebellar system in timing without awareness. *Proc. Natl. Acad. Sci. U.S.A.* 108, 13818–13822.

Xu, D., Liu, T., Ashe, J., and Bushara, K. O. (2006). Role of the olivocerebellar system in timing. *J. Neurosci.* 26, 5990–5995.

Yarom, Y., and Cohen, D. (2002). The olivocerebellar system as a generator of temporal patterns. *Ann. N. Y. Acad. Sci.* 978, 122–134.

Yee, W., Holleran, S., and Jones, M. R. (1994). Sensitivity to event timing in regular and irregular sequences: influences of musical skill. *Percept. Psychophys.* 56, 461–471.

Yeterian, E. H., and Pandya, D. N. (1998). Corticostriatal connections of the superior temporal region in rhesus monkeys. *J. Comp. Neurol.* 399, 384–402.

Yizhar, O., Fenno, L. E., Davidson, T. J., Mogri, M., and Deisseroth, K. (2011). Optogenetics in neural systems. *Neuron* 71, 9–34.

Conflict of Interest Statement: The authors declare that the research was conducted in the absence of any commercial or financial relationships that could be construed as a potential conflict of interest.

Received: 02 December 2011; paper pending published: 07 December 2011; accepted: 13 December 2011; published online: 03 January 2012.
*Citation: Teki S, Grube M and Griffiths TD (2012) A unified model of time perception accounts for duration-based and beat-based timing mechanisms. Front. Integr. Neurosci. **5**:90. doi: 10.3389/fnint.2011.00090*

frontiers in
INTEGRATIVE NEUROSCIENCE

OPINION ARTICLE
published: 12 July 2011
doi: 10.3389/fnint.2011.00031

Multiple mechanisms for temporal processing

Martin Wiener[1]*, Matthew S. Matell[2] and H. Branch Coslett[3]

[1] Department of Psychology, University of Pennsylvania, Philadelphia, PA, USA
[2] Department of Psychology, Villanova University, Villanova, PA, USA
[3] Department of Neurology, University of Pennsylvania, Philadelphia, PA, USA
*Correspondence: wimartin@psych.upenn.edu

Many models suggest that time perception is mediated by a unitary mechanism. For example, scalar expectancy theory (SET), the dominant model of timing for the past 30 years, suggests that temporal processing is mediated by a centralized clock-counter module in which elapsed time is measured by the summation of pacemaker pulses (Gibbon et al., 1984). A number of alternative, neurally plausible models have been proposed with clock processes that incorporate either the pacemaker-counter elements of SET, or other neural dynamics such as decay processes or state-dependent network activity (Staddon and Higa, 1999; Karmarkar and Buonomano, 2007; Simen et al., 2011a,b). While these models differ in the mechanisms utilized for the temporal control of behavior, they all suggest that timing is accomplished by a single, amodal process. Support for the hypothesis that timing is mediated by a single mechanism comes from several sources. A number of studies demonstrate that performance is independent of whether the task utilizes motor or "perceptual" temporal representations (Ivry and Hazeltine, 1995; Meegan et al., 2000). Additionally, although an effect of interval duration has been postulated for over a hundred years, such an effect has not been consistently identified; Lewis and Miall (2009), for example, failed to identify a fundamental change in timing performance or "breakpoint" using stimuli ranging from 68 ms to 16.7 min.

We suggest the alternative hypothesis that timing functions are mediated by multiple, overlapping neural systems, which may be flexibly engaged depending on the task requirements. These systems may function independently of one another and may be adaptively engaged *pro re nata*, such that single or multiple systems may be active during any one timing task, depending on environmental conditions and behavioral requirements. One line of support for this hypothesis comes from a quantitative meta-analysis of 41 neuroimaging studies of time perception in which we found that different neural structures were engaged depending on stimulus duration and the "motor" or "perceptual" nature of the task (Wiener et al., 2010a). Of particular interest in this context, however, is the fact that the meta-analysis also demonstrated two areas engaged across all tasks: supplementary motor area (SMA) and right inferior frontal gyrus (rIFG). In subsequent analyses of this dataset, however, we found that even in regions active across several conditions there is evidence of multiple timing mechanisms at work. Consider the SMA for example. Recent observations suggest that the SMA is a heterogeneous structure that may be functionally divided into the SMA "proper" and pre-SMA (Nachev et al., 2008). A rostrocaudal gradient in the SMA has been proposed according to which SMA and pre-SMA subserve motor and cognitive processes, respectively. Consistent with this finding, we found evidence for a functional gradient in the SMA, wherein perceptual timing tasks are more likely to activate voxels within the pre-SMA while motor timing tasks are associated with SMA proper activation-likelihood (**Figure 1A**).

Fractionation of temporal processing may also be evident in the basal ganglia, a brain region often implicated in studies of time perception and with high connectivity to the SMA. **Figure 1B** depicts voxels from SMA and basal ganglia regions with significant activation-likelihood. Once again, different patterns of activation-likelihood were noted as a function of the duration of the stimulus and nature of the task. For example, there was a greater propensity for the basal ganglia to be activated during sub-second timing tasks. However, it is crucial to note that the basal ganglia interact with numerous other regions, and so these activation patterns must be considered in the larger context of interactive networks.

Additional work beyond neuroimaging also argues for multiple timing systems. For example, we recently adopted a behavioral genetics paradigm to look at single-nucleotide polymorphisms in genes associated with different aspects of the dopamine system (Wiener et al., 2011). We found that a polymorphism affecting the expression of striatal D^2 receptors was associated with poorer performance on a perceptual timing task, but only when the intervals tested were below 1 s. In contrast, subjects with a polymorphism affecting the expression of the enzyme catechol-*O*-methyltransferase (COMT), which is known to regulate prefrontal dopamine tone, were impaired during supra-second, but not sub-second timing. This work suggests that different dopaminergic systems may underlie distinct timing procedures.

Another line of data supporting the claim that multiple mechanisms mediate timing comes from the fact that at least under some circumstances timing mechanisms appear to be both modality-specific and mediated by local neural structures. For example, adaptation to focal regions of the visual field produces duration distortions that are localized to that spatial region (Burr et al., 2007). Interestingly, modality-specific regions appear to be invoked for temporal expectations even in the absence of the stimuli themselves (Bueti and Macaluso, 2010), suggesting that the process may be mediated by simulation.

The fact that subject strategies influence the neural circuits recruited for timing is also consistent with the hypothesis that multiple distinct procedures underlie timing. For example, a recent study demonstrated that subjects recruited different

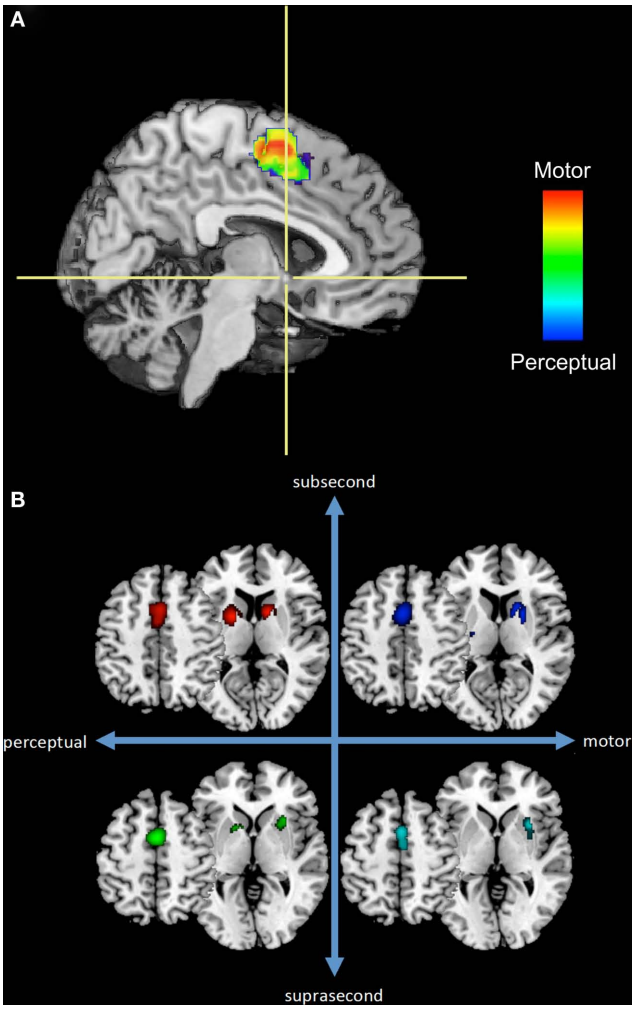

FIGURE 1 | A subset of the results from our previous meta-analysis of neuroimaging timing studies. **(A)** Sagittal section of a rendered brain including SMA voxels from perceptual or motor timing tasks (regardless of duration length) and their overlap. Crosshairs are located at the anterior commissure with the vertical axis dividing the SMA and pre-SMA. **(B)** Separate ALE results for SMA and basal ganglia regions across four temporal contexts.

neural networks depending on whether they implicitly used a beat-based or duration-based strategy (Grahn and McAuley, 2009). Similarly, recordings from rodent striatum demonstrate that patterns of temporally varying neural activity may reflect an integration of the passage of time with its associated action (Portugal et al., 2011), further suggesting that the computations contributing to temporal control may critically depend on both environmental and behavioral context.

The hypothesis that timing may be mediated by multiple distinct procedures also accounts for the puzzling lack of neurologic disorders characterized by a profound and selective impairment in temporal processing. Although syndromes characterized by selective deficits in vision, audition, language, attention, and multiple other faculties have been identified, we are unaware of a similar disorder involving temporal processing. Additionally, studies of patients and animals with brain lesions often demonstrate relatively mild deficits in temporal processing.

The above discussion is not intended to be exhaustive. Differences in performance on tasks assessing timing for synchronized or syncopated beat timing (Jantzen et al., 2004), as well as explicit or implicit timing to temporal intervals (Coull and Nobre, 2008; Wiener et al., 2010b) have also been identified. A challenge for future research will be to identify these different timing networks and to clarify the functional relationship between them.

ACKNOWLEDGMENTS

The authors would like to acknowledge that this article contains the separate opinions of all three authors. At the recommendation of the editors, these opinions were combined into a single article.

REFERENCES

Bueti, D., and Macaluso, E. (2010). Auditory temporal expectations modulate activity in visual cortex. *Neuroimage* 51, 1168–1183.

Burr, D., Tozzi, A., and Morrone, M. C. (2007). Neural mechanisms for timing visual events are spatially selective in real-world coordinates. *Nat. Neurosci.* 10, 423–425.

Coull, J. T., and Nobre, A. (2008). Dissociating explicit timing from temporal expectation with fMRI. *Curr. Opin. Neurobiol.* 18, 137–144.

Gibbon, J., Church, R. M., and Meck, W. H. (1984). Scalar timing in memory. *Ann. N. Y. Acad. Sci.* 423, 52–77.

Grahn, J. A., and McAuley, J. D. (2009). Neural bases of individual differences in beat perception. *Neuroimage* 47, 1894–1903.

Ivry, R. B., and Hazeltine, R. E. (1995). Perception and production of temporal intervals across a range of durations: evidence for a common timing mechanism. *J. Exp. Psychol. Hum. Percept. Perform.* 21, 3–18.

Jantzen, K. J., Steinberg, F. L., and Kelso, J. A. (2004). Brain networks underlying human timing behavior are influenced by prior context. *Proc. Natl. Acad. Sci. U.S.A.* 101, 6815–6820.

Karmarkar, U. R., and Buonomano, D. V. (2007). Timing in the absence of clocks: encoding time in neural network states. *Neuron* 53, 427–438.

Lewis, P. A., and Miall, R. C. (2009). The precision of temporal judgement: milliseconds, many minutes, and beyond. *Philos. Trans. R. Soc. Lond. B Biol. Sci.* 364, 1897–1905.

Meegan, D. V., Aslin, R. N., and Jacobs, R. A. (2000). Motor timing learned without motor training. *Nat. Neurosci.* 3, 860–862.

Nachev, P., Kennard, C., and Husain, M. (2008). Functional role of the supplementary and pre-supplementary motor areas. *Nat. Rev. Neurosci.* 9, 856–869.

Portugal, G., Wilson, A. G., and Matell, M. S. (2011). Behavioral sensitivity of temporally modulated striatal neurons. *Front. Integr. Neurosci.* 5:30. doi: 10.3389/fnint.2011.00030

Simen, P., Balci, F., deSouza, L., Cohen, J., and Holmes, P. (2011a). A model of interval timing by neural integration. *J. Neurosci.* 31, 9238–9253.

Simen, P., Balci, F., deSouza, L., Cohen, J. D., and Holmes, P. (2011b). Interval timing by long-range temporal integration. *Front. Integr. Neurosci.* 5:28. doi: 10.3389/fnint.2011.00028

Staddon, J. E., and Higa, J. J. (1999). Time and memory: towards a pacemaker-free theory of interval timing. *J. Exp. Anal. Behav.* 71, 215–251.

Wiener, M., Lohoff, F. W., and Coslett, H. B. (2011). Double dissociation of dopamine genes and timing in humans. *J. Cogn. Neurosci.* doi: 10.1162/jocn.2011.21626. [Epub ahead of print].

Wiener, M., Turkeltaub, P. E., and Coslett, H. B. (2010a). The image of time: a voxel-wise meta-analysis. *Neuroimage* 49, 1728–1740.

Wiener, M., Turkeltaub, P. E., and Coslett, H. B. (2010b). Implicit timing activates the left inferior parietal cortex. *Neuropsychologia* 48, 3967–3971.

Received: 01 June 2011; accepted: 28 June 2011; published online: 12 July 2011.

*Citation: Wiener M, Matell MS and Coslett HB (2011) Multiple mechanisms for temporal processing. Front. Integr. Neurosci. **5**:31. doi: 10.3389/fnint.2011.00031*

frontiers in
INTEGRATIVE NEUROSCIENCE

OPINION ARTICLE
published: 11 August 2011
doi: 10.3389/fnint.2011.00036

Exploring the 4th dimension: hippocampus, time, and memory revisited

Bin Yin[1]* and Andrew B. Troger[2]

[1] Department of Psychology and Neuroscience, Duke University, Durham, NC, USA
[2] Department of Neurobiology, Harvard University, Cambridge, MA, USA
*Correspondence: bin.yin@duke.edu

Accurate and reliable timing is an essential component of nearly every purposeful behavior. Just as the brain contains mechanisms to track and orient the body in space, so too must it be able to orient itself in time. Coincidence detection – the integration of simultaneous activation of multiple inputs – is a proposed solution to the question of how the brain tracks the duration of events in the seconds-to-minutes range using millisecond-scale neural processes (Matell and Meck, 2000). The striatal beat-frequency (SBF) model is one of the most successful attempts at explaining the neural basis of interval timing in terms of coincidence detection of oscillatory processes (Matell and Meck, 2004; Lustig et al., 2005; Harrington et al., 2010; Oprisan and Buhusi, 2011, submitted). The SBF model involves a set of cortical timekeeper neurons that oscillate at regular, but distinct frequencies, allowing a unique pattern of activation to occur at each point in time. These activation patterns project onto striatal integrators that combine their information with feedback (e.g., reward input) and form the basis of interval timing.

Independent lines of research appear to converge on the conclusion that functional circuits composed of the prefrontal cortex, striatum, and thalamus are instrumental to both time perception and timed performance (Coull et al., 2004, 2011; Hinton and Meck, 2004; Buhusi and Meck, 2005; Meck, 2006a,b; Yin, 2009; Allman and Meck, 2011). This frontal–striatal system is hypothesized to correspond to the functional components of the SBF model (Meck, 1996, 2006a,b; Meck and Benson, 2002; Matell et al., 2003; Matell and Meck, 2004; Meck et al., 2008), wherein cortical oscillatory neurons, and reward input from the substantia nigra are integrated by striatal medium spiny neurons (MSNs). These neurons can hold temporal "memories" via dopamine-facilitated long-term potentiation and long-term depression that, possibly via α-amino-3-hydroxy-5-methyl-4-isoxazolepropionic acid receptor (AMPAR) trafficking (Centonze et al., 2001), modulate synaptic weights. Later, when the same signal duration is timed again, these neurons compare the current pattern of cortical activation with the stored "memories"; if coincidence is detected, then the spiny neurons fire to indicate the target duration has elapsed.

These neural structures contained within cortico-striatal circuits may not be the only ones involved in interval timing, however. The role of the hippocampus in timing and time perception for durations in the supra-seconds range was initially explored by Meck et al. (1984). Since then, numerous studies have demonstrated reliable changes in the accuracy and precision of interval timing following a variety of techniques impacting hippocampal function (e.g., transection of the fimbria fornix, lesions of the medial septal area, resection of the temporal lobe, selective lesions of the dorsal hippocampus, and destruction of the entire hippocampus – see Balci et al., 2009 for a review). Nevertheless, an explanation of the effects of hippocampal damage within the context of a theoretical model of interval timing has been elusive (Grossberg and Merrill, 1992, 1996; Lytton and Lipton, 1999; Onoda et al., 2003; Matell and Meck, 2004; Sakata, 2006; Lewis et al., 2011). As a consequence, the primary goal of this opinion article is to outline mechanisms by which the hippocampus could have specific effects on the modulation of the neural circuits specified by the SBF model of interval timing.

Rats and mice with lesions of the hippocampus and related areas demonstrate a proportional "leftward" shift in distributions of timing judgments for intervals in the range of 2–8 s for temporal bisection procedures and 10–40 s for peak-interval timing procedures – that is, when faced with tasks requiring them to estimate or reproduce a specific duration, they respond earlier on average than normal subjects indicating an over estimation/under production of duration proportional to the anchor durations or target duration(s) being timed (Meck et al., 1984, 1987; Olton et al., 1987, 1988; Buhusi et al., 2004; Balci et al., 2009). Similar effects on timing have also been observed in human participants with hippocampal damage following temporal lobe resection for anchor durations spanning the ranges of 50 vs. 200 ms, 1 vs. 2 s, and 2 vs. 8 s in temporal bisection procedures and 0.5–8 s for temporal reproduction procedures (Vidalaki et al., 1999; Melgire et al., 2005). Interestingly, in both rodents and humans, an increase in the precision of timing often accompanies the distortion in the accuracy of the temporal representations (Meck et al., 1984; Vidalaki et al., 1999; Meck, 2002, 2005; Melgire et al., 2005). These "classic" effects of hippocampal lesions on the performance of rats in the peak-interval procedure are illustrated in **Figure 1**.

Though there have been a number of studies that suggest a lack of any effect on peak-interval timing procedures in hippocampally lesioned animals (Dietrich et al., 1997; Dietrich and Allen, 1998), these experiments included extensive post-lesion training with explicit reinforcement contingencies for probe trials. Evidence suggests that, with extensive training, it is possible for timing behavior to become habitual and to enter a "locked" state where the "classic" horizontal shifts of response functions to pharmacological challenges are no longer apparent (Yin and Knowlton, 2006; Cheng et al., 2007a,b; Yin et al., 2009). It is also known that in cases of extensive training, hippocampal function can be transferred to other brain areas such as the cortex (Wiltgen and Silva, 2007; Wiltgen et al., 2010).

There are several important roles that the hippocampus could play in the SBF timing circuit. Firstly, it could function as a feedback control mediator (Meck, 1988), participating in the determination of temporal expectancy,

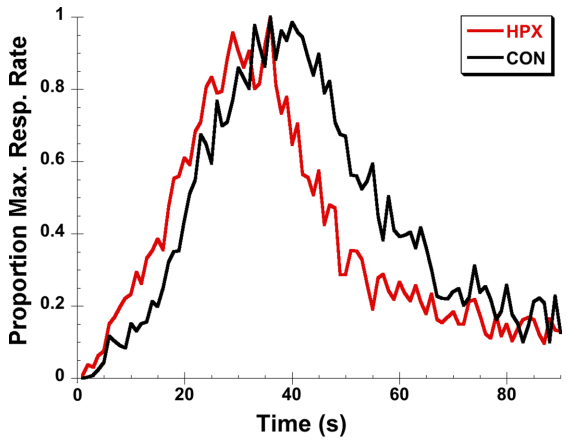

FIGURE 1 | An illustration of the "classic" effects of post-training hippocampal lesions for rats trained on a 40-s peak-interval procedure. The peak functions of rats with hippocampal lesions (HPX) rats are shifted leftward relative to control (CON) rats and are sharper with less spread around the observed peak time. Data are replotted from Buhusi et al. (2004).

which is a continuously updated function of memory, and clock-reading that supports the anticipation of outcomes tied to specific durations. Separate cortical areas exist that participate in the cortico-striatal and fronto-hippocampal circuits, respectively. The former is the basis of the "clock" stage while the latter may modulate the "memory" stage, updating temporal expectancy on a trial-by-trial basis. This memory-modulating cortical area also sends input to the striatal MSNs. Given that hippocampal lesions produce a progressive leftward shift (under production/over estimation) and frontal lesions produce a more or less symmetrical progressive rightward shift (over production/under estimation), it is possible that the hippocampus works in tandem with this frontal–temporal regulatory circuit to update temporal expectancy on a trial-by-trial basis (Meck et al., 1987; MacDonald and Meck, 2004; Lustig et al., 2005).

A second function that the hippocampus might serve in timing and time perception is as a regulator of the dynamic firing threshold of striatal MSNs (Matell and Meck, 2004). Hippocampal–striatal interactions have been previously documented (Devan and White, 1999; Poldrack and Packard, 2003; Lee et al., 2008; Graham et al., 2009). The MSN is essentially a two-state system with a "down-state" that does not allow neural firing and an "up-state" that facilitates firing. State transitions are driven by excitatory inputs. The interspike interval varies because the sub-threshold membrane potential fluctuates (Stern et al., 1997). Properties of sub-threshold signal integration in MSNs are determined by the distribution of synaptic inputs and differential activation of multiple postsynaptic conductances (Carter et al., 2007).

On this basis, we can suggest two possible ways that hippocampal input could directly contribute to modulating striatal neuron firing: phasic excitation and tonic inhibition. The hippocampus could desensitize membrane AMPARs on MSNs with its phasic excitatory output when it detects minor environmental changes, such as at the beginning of a new "to be timed" signal. This would render a varying set of MSNs unable to use "memories" of the previous signal duration. These MSNs must then update their "memories" on a trial-by-trial basis. This would produce more trial-by-trial variation, and would be expected to contribute to the Gaussian-like noise that generates scalar timing (see Matell and Meck, 2004; Oprisan and Buhusi, 2011, submitted).

The hippocampus could also tonically inhibit, and thus lower the sub-threshold membrane potential of striatal neurons such that firing is delayed by a small duration in some proportion of MSNs. Such an effect would be more pronounced in heavily weighted synapses of MSNs corresponding with the "representation" of the previous trial's temporal sequence of responding and reward outcome. In this case, striatal neurons could display "overexcitement" in the absence of hippocampal inhibition followed by habituation, resulting in a leftward shift of the timing function in early trials followed by a return to a more normal response distribution following repeated testing, again possibly explaining the lack of an observed shift in lesioned animals with extensive training.

A third possibility is that the hippocampus might function in a downstream decision-making process that controls motor output. It has been suggested that the decision-making processes downstream of the "clock stage" deserve further investigation (Harrington et al., 2004, 2011; Wearden, 2004; Meck, 2005). A subject's selection and execution of motor action based on the clock's output (which in the SBF model is determined by striatal firing rates) may depend on a "threshold gating" mechanism located in another brain region (Gibbon et al., 1997; Jin et al., 2009; Höhn, et al., 2011). This would predict variation in timing behavior between subjects that have identical perceptions of duration. For example, in a peak-interval procedure, an "impulsive" subject may press the lever well before its perception of the time in the current trial matches a sample taken from its memory distribution of times of reinforcement on previous trials. Conversely, a "less impulsive" subject demonstrating a higher degree of "self control" may be reluctant to press a lever until the time on the current time is much closer to the remembered target duration – or even past this duration (Church et al., 1994).

Regions that might be involved in this subsequent action–selection process are the ventral and dorsomedial striatum, orbitofrontal cortex, and possibly the hippocampus (Johnson et al., 2007; MacDonald et al., 2011). Indeed, it has been reported that the hippocampus may have a role in controlling impulsivity (Cheung and Cardinal, 2005; McHugh et. al., 2008; Sala et al., 2011). On the other hand, it has been shown that ventral/medial striatal neurons are entrained to the hippocampal theta rhythm (Berke et al., 2004). Therefore, it seems reasonable to speculate that the hippocampus might interfere with the downstream temporal control of action sequences (most likely via inhibitory control) in tandem with the ventral/medial striatal neurons. Lesions of the hippocampus may diminish this inhibitory control, thereby resulting in earlier start times, leading to leftward horizontal

shifts of the peak function in the peak-interval procedure (Meck et al., 1984, 1987; Balci et al., 2009; MacDonald et al., 2011). These three possibilities for the mapping of functional hippocampal connectivity within the SBF timing model are illustrated in **Figure 2**.

Further understanding of the hippocampus's role in interval timing could be achieved by examining the differences between pre- and post-hippocampal lesion training on a single-trial level (Church et al., 1994). This would allow us to narrow the range of possible roles the hippocampus might play in either attention, feedback, or memory consolidation mechanisms on a trial-by-trial basis (Meck, 1988; Buhusi and Meck, 2002; Buhusi et al., 2003, 2004). It could also provide us with clues as to whether or not the "clock stage" itself is affected, which would be reflected by a proportional horizontal shift of the response states (see Church et al., 1994; Matell et al., 2006, and MacDonald et al., 2011). Conversely, if the horizontal (e.g., leftward) shift in timing functions resulting from hippocampal damage is due to a change (e.g., decrease) in the latency to start timing rather than in the centering of the distribution of responses around the target duration, then it might suggest the third possibility discussed above. Furthermore, in order to examine the interaction between the hippocampus and either the cortex or the striatum, one could employ a cross-lesioning technique wherein one of each structure would be compromised contralaterally in addition to a transection of the corpus callosum (e.g., Christakou et al., 2001; Chudasama et al., 2003). Moreover, future studies would benefit from the use of optogenetic techniques (Yizhar et al., 2011) in terms of identifying the functional "connectome" among the hippocampus, striatum, and cortex (Chuhma et al., 2011). This would provide regions of interest for more traditional electrophysiological and pharmacological mapping studies of the role of the hippocampus and other brain structures in time – the fourth dimension of neural function (Coull et al., 2011).

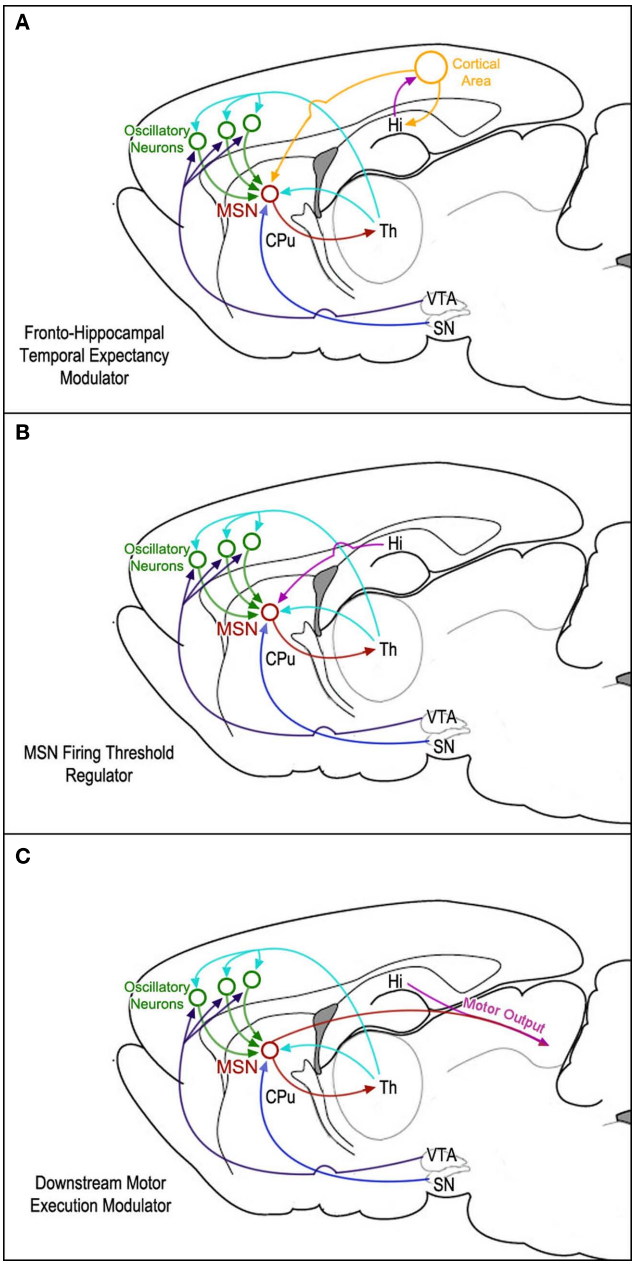

FIGURE 2 | Diagrams of three possible mappings of functional hippocampal connectivity within the neural circuits proposed by the striatal beat-frequency (SBF) model of interval timing: (A) the hippocampus is involved in a feedback mechanism designed to update temporal expectancy with a separate cortical area. This area's output is then integrated with clock and reward information by striatal medium spiny neurons (MSNs). **(B)** The hippocampus modulates MSN firing thresholds via either tonic inhibition or phasic excitation. **(C)** Hippocampal regulation downstream of the MSNs affects translation of temporal information into motor output.

REFERENCES

Allman, M. J., and Meck, W. H. (2011). Pathophysiological distortions in time perception and timed performance. *Brain* (in press).

Balci, F., Meck, W. H., Moore, H., and Brunner, D. (2009). "Timing deficits in aging and neuropathology," in *Animal Models of Human Cognitive Aging*, eds J. L. Bizon and A. Wood (Totowa, NJ: Humana Press), 161–201.

Berke, J. D., Okatan, M., Skurski, J., and Eichenbaum, H. B. (2004). Oscillatory entrainment of striatal neurons in freely moving rats. *Neuron* 43, 883–896.

Buhusi, C. V., Buhusi, M. C., Scripal, I., Maness, P., Schachner, M., and Meck, W. H. (2003). Impaired attentional control of temporal and spatial information in CHL1 KO mice. *Abstr. Soc. Neurosci.* 860, 11.

Buhusi, C. V., and Meck, W. H. (2002). Ibotenic lesions of the hippocampus disrupt attentional control of interval timing. *Abstr. Soc. Neurosci.* 183, 1.

Buhusi, C. V., and Meck, W. H. (2005). What makes us tick? Functional and neural mechanisms of interval timing. *Nat. Rev. Neurosci.* 6, 755–765.

Buhusi, C. V., Mocanu, M., and Meck, W. H. (2004). Abnormal memory consolidation of intevral timing

in rats with ibotenic lesions of the hippocampus. *Abstr. Soc. Neurosci.* 550, 18.

Carter, A. G., Soler-Llavina, G. J., and Sabatini, B. L. (2007). Timing and location of synaptic inputs determine modes of subthreshold integration in striatal medium spiny neurons. *J. Neurosci.* 27, 8967–8977.

Centonze, D., Picconi, B., Gubellini, P., Bernardi, G., and Calabresi, P. (2001). Dopaminergic control of synaptic plasticity in the dorsal striatum. *Eur. J. Neurosci.* 13, 1071–1077.

Cheng, R. K., Ali, Y. M., and Meck, W. H. (2007a). Ketamine "unlocks" the reduced clock-speed effects of cocaine following extended training: evidence for dopamine – glutamate interactions in timing and time perception. *Neurobiol. Learn. Mem.* 88, 149–159.

Cheng, R. K., Hakak, O. L., and Meck, W. H. (2007b). Habit formation and the loss of control of an internal clock: inverse relationship between the level of baseline training and the clock-speed enhancing effects of methamphetamine. *Psychopharmacology (Berl.)* 193, 351–362.

Cheung, T. H. C., and Cardinal, R. N. (2005). Hippocampal lesions facilitate instrumental learning with delayed reinforcement but induce impulsive choice in rats. *BMC Neurosci.* 6, 36. doi: 10.1186/1471-2202-6-36

Christakou, A., Robbins, T. W., and Everitt, B. J. (2001). Functional disconnection of a prefrontal cortical-dorsal striatal system disrupts choice reaction time performance: implications for attentional function. *Behav. Neurosci.* 115, 812–825.

Chudasama, Y., Baunez, C., and Robbins, T. W. (2003). Functional disconnection of the medial prefrontal cortex and subthalamic nucleus in attentional performance: evidence for corticosubthalamic interaction. *J. Neurosci.* 23, 5477–5485.

Chuhma, N., Tanaka, K. F., Hen, R., and Rayport, S. (2011). Functional connectome of the striatal medium spiny neuron. *J. Neurosci.* 31, 1183–1192.

Church, R. M., Meck, W. H., and Gibbon, J. (1994). Application of scalar timing theory to individual trials. *J. Exp. Psychol. Anim. Behav. Process.* 20, 135–155.

Coull, J. T., Cheng, R. K., and Meck, W. H. (2011). Neuroanatomical and neurochemical substrates of timing. *Neuropsychopharmacology* 36, 3–25.

Coull, J. T., Vidal, F., Nazarian, B., and Macar, F. (2004). Functional anatomy of the attentional modulation of time estimation. *Science* 303, 1506–1508.

Devan, B. D., and White, N. M. (1999). Parallel information processing in the dorsal striatum: relation to hippocampal function. *J. Neurosci.* 19, 2789–2798.

Dietrich, A., and Allen, J. D. (1998). Functional dissociation of the prefrontal cortex and the hippocampus in timing behavior. *Behav. Neurosci.* 112, 1043–1047.

Dietrich, A., Allen, J. D., and Bunnell, B. N. (1997). Is the hippocampus involved in temporal discrimination and the memory of short intervals? Int. *J. Neurosci.* 90, 255–269.

Gibbon, J., Malapani, C., Dale, C. L., and Gallistel, C. R. (1997). Toward a neurobiology of temporal cognition: advances and challenges. *Curr. Opin. Neurobiol.* 7, 170–184.

Graham, S., Phua, E., Soon, C. S., Oh, T., Au, C., Shuter, B., Wang, S. C., and Yeh, I. B. (2009). Role of medial cortical, hippocampal and striatal interactions during cognitive set-shifting. *Neuroimage* 45, 1359–1367.

Grossberg, S., and Merrill, J. (1992). A neural network model of adaptively timed reinforcement learning and hippocampal dynamics. *Brain Res. Cogn. Brain Res.* 1, 3–38.

Grossberg, S., and Merrill, J. (1996). The hippocampus and cerebellum in adaptively timed learning, recognition, and movement. *J. Cogn. Neurosci.* 8, 257–277.

Harrington, D. L., Boyd, L. A., Mayer, A. R., Sheltraw, D. M., Lee, R. R., Huang, M., and Rao, S. M. (2004). Neural representation of interval encoding and decision making. *Brain Res. Cogn. Brain Res.* 21, 193–205.

Harrington, D. L., Castillo, G. N., Fong, C. H., and Reed, J. D. (2011). Neural underpinnings of distortions in the experience of time across senses. *Front. Integr. Neurosci.* 5:32. doi: 10.3389/fnint.2011.00032

Harrington, D. L., Zimbelman, J. L., Hinton, S. C., and Rao, S. M. (2010). Neural modulation of temporal encoding, maintenance, and decision processes. *Cereb. Cortex* 20, 1274–1285.

Hinton, S. C., and Meck, W. H. (2004). Frontal-striatal circuitry activated by human peak-interval timing in the supra-seconds range. *Brain Res. Cogn. Brain Res.* 21, 171–182.

Höhn, S., Dallérac, G., Faure, A., Urbach, Y., Nguyen, H. P., Riess, O., von Hörsten, S., Le Blanc, P., Desvignes, N., El Massioui, N., Brown, B. L., and Doyère, V. (2011). Behavioral and in vivo electrophysiological evidence for presymptomatic alteration of prefronto-striatal processing in the transgenic rat model for Huntington disease. *J. Neurosci.* 31, 8986–8997.

Jin, D. Z., Fujii, N., and Graybiel, A. M. (2009). Neural representation of time in cortico-basal ganglia circuits. *Proc. Natl. Acad. Sci. U.S.A.* 106, 19156–19161.

Johnson, A., van der Meer, M. A., and Redish, A. D. (2007). Integrating hippocampus and striatum in decision-making. *Curr. Opin. Neurobiol.* 17, 692–697.

Lee, A. S., Duman, R. S., and Pittenger, C. (2008). A double dissociation revealing bidirectional competition between striatum and hippocampus during learning. *Proc. Natl. Acad. Sci. U.S.A.* 105, 17163–17168.

Lewis, P. A., Couch, T. J., and Walker, M. P. (2011). Keeping time in your sleep: overnight consolidation of temporal rhythm. *Neuropsychologia* 49, 115–123.

Lustig, C., Matell, M. S., and Meck, W. H. (2005). Not "just" a coincidence: Frontal-striatal synchronization in working memory and interval timing. *Memory* 13, 441–448.

Lytton, W. W., and Lipton, P. (1999). Can the hippocampus tell time? The temporo-septal engram shift model. *Neuroreport* 10, 2301–2306.

MacDonald, C. J., Cheng, R. K., and Meck, W. H. (2011). Interval timing and time-based decision making requires differential protein synthesis in the dorsal and ventral striatum for the setting of "start" and "stop" response thresholds. *Front. Integr. Neurosci.* (in press).

MacDonald, C. J., and Meck, W. H. (2004). Systems-level integration of interval timing and reaction time. *Neurosci. Biobehav. Rev.* 28, 747–769.

Matell, M. S., Bateson, M., and Meck, W. H. (2006). Single-trials analyses demonstrate that increases in clock speed contribute to the methamphetamine-induced horizontal shifts in peak-interval timing functions. *Psychopharmacology (Berl.)* 188, 201–212.

Matell, M. S., and Meck, W. H. (2000). Neuropsychological mechanisms of interval timing behavior. *Bioessays* 22, 94–103.

Matell, M. S., and Meck, W. H. (2004). Cortico-striatal circuits and interval timing: coincidence detection of oscillatory processes. *Brain Res. Cogn. Brain Res.* 21, 139–170.

Matell, M. S., Meck, W. H., and Nicolelis, M. A. (2003). Interval timing and the encoding of signal duration by ensembles of cortical and striatal neurons. *Behav. Neurosci.* 117, 760–773.

McHugh, S. B., Campbell, T. G., Taylor, A. M., Rawlins, J. N., and Bannerman, D. M. (2008). A role for dorsal and ventral hippocampus in inter-temporal choice cost-benefit decision making. *Behav. Neurosci.* 122, 1–8.

Meck, W. H. (1988). Hippocampal function is required for feedback control of an internal clock's criterion. *Behav. Neurosci.* 102, 54–60.

Meck, W. H. (1996). Neuropharmacology of timing and time perception. *Brain Res. Cogn. Brain Res.* 3, 227–242.

Meck, W. H. (2005). Neuropsychology of timing and time perception. *Brain Cogn.* 58, 1–8.

Meck, W. H. (2006a). Frontal cortex lesions eliminate the clock speed effect of dopaminergic drugs on interval timing. *Brain Res.* 1108, 157–167.

Meck, W. H. (2006b). Neuroanatomical localization of an internal clock: a functional link between mesolimbic, nigrostriatal, and mesocortical dopaminergic systems. *Brain Res.* 1109, 93–107.

Meck, W. H., and Benson, A. M. (2002). Dissecting the brain's internal clock: how frontal-striatal circuitry keeps time and shifts attention. *Brain Cogn.* 48, 195–211.

Meck, W. H., Church, R. M., and Olton, D. S. (1984). Hippocampus, time, and memory. *Behav. Neurosci.* 98, 3–22.

Meck, W. H., Church, R. M., Wenk, G. L., and Olton, D. S. (1987). Nucleus basalis magnocellularis and medial septal area lesions differentially impair temporal memory. *J. Neurosci.* 7, 3505–3511.

Meck, W. H., Penney, T. B., and Pouthas, V. (2008). Cortico-striatal representation of time in animals and humans. *Curr. Opin. Neurobiol.* 18, 145–152.

Melgire, M., Ragot, R., Samson, S., Penney, T. B., Meck, W. H., and Pouthas, V. (2005). Auditory/visual duration bisection in patients with left or right medial-temporal lobe resection. *Brain Cogn.* 58, 119–124.

Olton, D. S., Meck, W. H., and Church, R. M. (1987). Separation of hippocampal and amygdaloid involvement in temporal memory dysfunctions. *Brain Res.* 404, 180–188.

Olton, D. S., Wenk, G. L., Church, R. M., and Meck, W. H. (1988). Attention and the frontal cortex as examined by simultaneous temporal processing. *Neuropsychologia* 26, 307–318.

Onoda, K., Takahashi, E., and Sakata, S. (2003). Event-related potentials in the frontal cortex, hippocampus, and cerebellum during a temporal discrimination task in rats. *Brain Res. Cogn. Brain Res.* 17, 380–387.

Oprisan, S. A., and Buhusi, C. V. (2011). Modelling pharmacological clock and memory patterns of interval timing in a striatal beat-frequency model with realistic, noisy neurons. *Front. Integr. Neurosci.* (in press).

Poldrack, R. A., and Packard, M. G. (2003). Competition among multiple memory systems: converging evidence from animal and human brain studies. *Neuropsychologia* 41, 245–251.

Sakata, S. (2006). Timing and hippocampal theta in animals. *Rev. Neurosci.* 17, 157–162.

Sala, M., Caverzasi, E., Lazzaretti, M., Morandotti, N., De Vidovich, G., Marraffini, E., Gambini, F., Isola, M., De Bona, M., Rambaldelli, G., d'Allio, G., Barale, F., Zappoli, F., and Brambilla, P. (2011). Dorsolateral prefrontal cortex and hippocampus sustain impulsivity and aggressiveness in borderline personality disorder. *J. Affect. Disord.* 131, 417–421.

Stern, E. A., Kincaid, A. E., and Wilson, C. J. (1997). Spontaneous subthreshold membrane potential fluctuations and action potential variability of rat corticostriatal and striatal neurons in vivo. *J. Neurophysiol.* 77, 1697–1715.

Vidalaki, V. N., Ho, M. Y., Bradshaw, C. M., and Szabadi, E. (1999). Interval timing performance in temporal lobe epilepsy: differences between patients with left and right hemisphere foci. *Neuropsychologia* 37, 1061–1070.

Wearden, J. H. (2004). Decision processes in models of timing. *Acta Neurobiol. Exp. (Wars)* 64, 303–317.

Wiltgen, B. J., and Silva, A. J. (2007). Memory for context becomes less specific with time. *Learn. Mem.* 14, 313–317.

Wiltgen, B. J., Zhou, M., Cai, Y., Balaji, J., Karlsson, M. G., Parivash, S. N., Li, W., and Silva, A. J. (2010). The hippocampus plays a selective role in the retrieval of detailed contextual memories. *Curr. Biol.* 20, 1336–1344.

Yin, H. H. (2009). The role of the murine motor cortex in action duration and order. *Front. Integr. Neurosci.* 3:23. doi: 10.3389/neuro.07.023.2009

Yin, H. H., and Knowlton, B. J. (2006). The role of the basal ganglia in habit formation. *Nat. Neurosci. Rev.* 7, 464–476.

Yin, H. H., Mulcare, S. P., Hilario, M. R., Clouse, E., Holloway, T., Davis, M. I., Hansson, A. C., Lovinger, D. M., and Costa, R. M. (2009). Dynamic reorganization of striatal circuits during the acquisition and consolidation of a skill. *Nat. Neurosci.* 12, 333–341.

Yizhar, O., Fenno, L. E., Davidson, T. J., Mogri, M., and Deisseroth, K. (2011). Optogenetics in neural systems. *Neuron* 71, 9–34.

Received: 26 July 2011; accepted: 29 July 2011; published online: 11 August 2011.

*Citation: Yin B and Troger AB (2011) Exploring the 4th dimension: hippocampus, time, and memory revisited. Front. Integr. Neurosci. **5**:36. doi: 10.3389/fnint.2011.00036*